average bulk temperature and μ_0 is the viscosity at the arithmetic average wall temperature.[1] Then we may write

$$\mathrm{Nu} = \mathrm{Nu}(\mathrm{Re}, \mathrm{Pr}, L/D, \mu_b/\mu_0) \tag{14.3-15}$$

This type of correlation seems to have first been presented by Sieder and Tate.[2] If, in addition, the density varies significantly, then some free convection may occur. This effect can be accounted for in correlations by including the Grashof number along with the other dimensionless groups. This point is pursued further in §14.6.

Let us now pause to reflect on the significance of the above discussion for constructing heat transfer correlations. The heat transfer coefficient h depends on *eight* physical quantities (D, $\langle v \rangle$, ρ, μ_0, μ_b, $\hat{C}_p$, k, L). However, Eq. 14.3-15 tells us that this dependence can be expressed more concisely by giving Nu as a function of only *four* dimensionless groups (Re, Pr, L/D, μ_b/μ_0). Thus, instead of taking data on h for 5 values of each of the eight individual physical quantities (5^8 tests), we can measure h for 5 values of the dimensionless groups (5^4 tests)—a rather dramatic saving of time and effort.

A good global view of heat transfer in circular tubes with nearly constant wall temperature can be obtained from the Sieder and Tate[2] correlation shown in Fig. 14.3-2. This is of the form of Eq. 14.3-15. It has been found empirically[2,3] that transition to turbulence usually begins at about Re = 2100, even when the viscosity varies appreciably in the radial direction.

For *highly turbulent flow*, the curves for $L/D > 10$ converge to a single curve. For Re > 20,000 this curve is described by the equation

$$\mathrm{Nu}_{\mathrm{ln}} = 0.026\,\mathrm{Re}^{0.8}\,\mathrm{Pr}^{1/3}\left(\frac{\mu_b}{\mu_0}\right)^{0.14} \tag{14.3-16}$$

This equation reproduces available experimental data within about ±20% in the ranges $10^4 < \mathrm{Re} < 10^5$ and $0.6 < \mathrm{Pr} < 100$.

For *laminar flow*, the descending lines at the left are given by the equation

$$\mathrm{Nu}_{\mathrm{ln}} = 1.86\left(\mathrm{RePr}\,\frac{D}{L}\right)^{1/3}\left(\frac{\mu_b}{\mu_0}\right)^{0.14} \tag{14.3-17}$$

---

[1] One can arrive at the viscosity ratio by inserting into the equations of change a temperature-dependent viscosity, described, for example, by a Taylor expansion about the wall temperature:

$$\mu = \mu_0 + \left.\frac{\partial \mu}{\partial T}\right|_{T=T_0}(T - T_0) + \cdots \tag{14.3-15a}$$

When the series is truncated and the differential quotient is approximated by a difference quotient, we get

$$\mu \cong \mu_0 + \left(\frac{\mu_b - \mu_0}{T_b - T_0}\right)(T - T_0) \tag{14.3-15b}$$

or, with some rearrangement,

$$\frac{\mu}{\mu_0} \cong 1 + \left(\frac{\mu_b}{\mu_0} - 1\right)\left(\frac{T - T_0}{T_b - T_0}\right) \tag{14.3-15c}$$

Thus, the viscosity ratio appears in the equation of motion and hence in the dimensionless correlation.

[2] E. N. Sieder and G. E. Tate, *Ind. Eng. Chem.*, **28**, 1429–1435 (1936).

[3] A. P. Colburn, *Trans. AIChE*, **29**, 174–210 (1933). **Alan Philip Colburn** (1904–1955), provost at the University of Delaware (1950–1955), made important contributions to the fields of heat and mass transfer, including the "Chilton–Colburn relations."

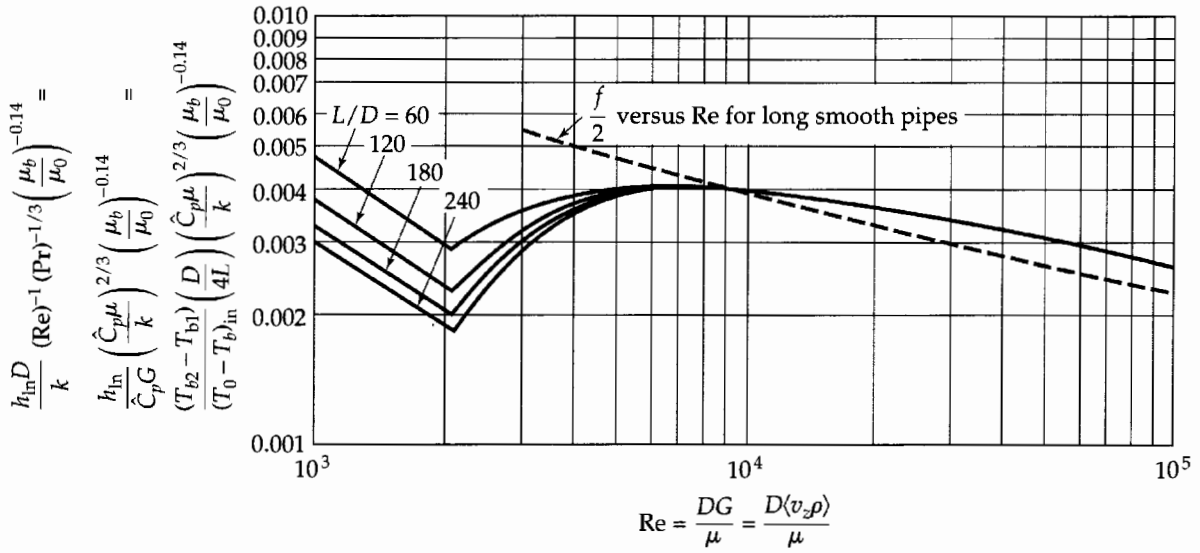

Fig. 14.3-2. Heat transfer coefficients for fully developed flow in smooth tubes. The lines for laminar flow should not be used in the range $\mathrm{RePr}D/L < 10$, which corresponds to $(T_0 - T_b)_2/(T_0 - T_b)_1 < 0.2$. The laminar curves are based on data for $\mathrm{RePr}D/L >> 10$ and nearly constant wall temperature; under these conditions h_a and $h_{\ln}$ are indistinguishable. We recommend using $h_{\ln}$, as opposed to the h_a suggested by Sieder and Tate, because this choice is conservative in the usual heat-exchanger design calculations [E. N. Sieder and G. E. Tate, *Ind. Eng. Chem.*, **28**, 1429–1435 (1936)].

which is based on Eq. (C) of Table 14.2-1[4] and Problem 12D.4. The numerical coefficient in Eq. (C) has been multiplied by a factor of $\frac{3}{2}$ to convert from h_{loc} to $h_{\ln}$, and then further modified empirically to account for the deviations due to variable physical properties. This illustrates how a satisfactory empirical correlation can be obtained by modifying the result of an analytical derivation. Equation 14.3-17 is good within about 20% for $\mathrm{RePr}\,D/L > 10$, but at lower values of $\mathrm{RePr}\,D/L$ it underestimates $h_{\ln}$ considerably. The occurrence of $\mathrm{Pr}^{1/3}$ in Eqs. 14.3-16 and 17 is consistent with the large Prandtl number asymptote found in §§13.6 and 12.4.

The *transition region*, roughly $2100 < \mathrm{Re} < 8000$ in Fig. 14.3-2, is not well understood and is usually avoided in design if possible. The curves in this region are supported by experimental measurements[2] but are less reliable than the rest of the plot.

The general characteristics of the curves in Fig. 14.3-2 deserve careful study. Note that for a heated section of given L and D and a fluid of given physical properties, the ordinate is proportional to the dimensionless temperature rise of the fluid passing through—that is, $(T_{b2} - T_{b1})/(T_0 - T_b)_{\ln}$. Under these conditions, as the flow rate (or Reynolds number) is increased, the exit fluid temperature will first decrease until Re reaches about 2100, then increase until Re reaches about 8000, and then finally decrease again. The influence of L/D on $h_{\ln}$ is marked in laminar flow but becomes insignificant for $\mathrm{Re} > 8000$ with $L/D > 60$.

[4] Equation (C) is an asymptotic solution of the *Graetz problem*, one of the classic problems of heat convection: L. Graetz, *Ann. d. Physik*, **13**, 79–94 (1883), **25**, 337–357 (1885); see J. Lévêque, *Ann. Mines* (Series 12), **13**, 201–299, 305–362, 381–415 (1928) for the asymptote in Eq. (C). An extensive summary can be found in M. A. Ebadian and Z. F. Dong, Chapter 5 of *Handbook of Heat Transfer*, 3rd edition, (W. M. Rohsenow, J. P. Hartnett, and Y. I. Cho, eds.), McGraw-Hill, New York (1998).

Note also that Fig. 14.3-2 somewhat resembles the friction-factor plot in Fig. 6.2-2, although the physical situation is quite different. In the highly turbulent range (Re > 10,000) the heat transfer ordinate agrees approximately with $f/2$ for the long smooth pipes under consideration. This was first pointed out by Colburn,[3] who proposed the following empirical analogy for long, smooth tubes:

$$j_{H,\ln} \approx \tfrac{1}{2}f \qquad \{\mathrm{Re} > 10{,}000\} \tag{14.3-18}$$

in which

$$j_{H,\ln} = \frac{\mathrm{Nu}_{\ln}}{\mathrm{RePr}^{1/3}} = \frac{h_{\ln}}{\langle \rho v \rangle \hat{C}_p}\left(\frac{\hat{C}_p\mu}{k}\right)^{2/3} = \frac{h_{\ln}S}{w\hat{C}_p}\left(\frac{\hat{C}_p\mu}{k}\right)^{2/3} \tag{14.3-19}$$

where S is the area of the tube cross section, w is the mass rate of flow through the tube, and $f/2$ is obtainable from Fig. 6.2-2 using $\mathrm{Re} = Dw/S\mu = 4w/\pi D\mu$. Clearly the analogy of Eq. 14.3-18 is not valid below Re = 10,000. For rough tubes with fully developed turbulent flow the analogy breaks down completely, because f is affected more by roughness than j_H is.

One additional remark about the use of Fig. 14.3-2 has to do with the application to conduits of noncircular cross section. For *highly turbulent* flow, one may use the mean hydraulic radius of Eq. 6.2-16. To apply that empiricism, D is replaced by $4R_h$ everywhere in the Reynolds and Nusselt numbers.

EXAMPLE 14.3-1

Design of a Tubular Heater

Air at 70°F and 1 atm is to be pumped through a straight 2-in. i.d. tube at a rate of 70 lb_m/hr. A section of the tube is to be heated to an inside wall temperature of 250°F to raise the air temperature to 230°F. What heated length is required?

SOLUTION

The arithmetic average bulk temperature is T_{ba} = 150°F, and the film temperature is $T_f = \frac{1}{2}(150 + 250) = 200$°F. At this temperature the properties of air are $\mu = 0.052$ $\mathrm{lb}_m/\mathrm{ft}\cdot\mathrm{hr}$, $\hat{C}_p = 0.242$ $\mathrm{Btu}/\mathrm{lb}_m\cdot\mathrm{F}$, $k = 0.0180$ $\mathrm{Btu}/\mathrm{hr}\cdot\mathrm{ft}\cdot\mathrm{F}$, and $\mathrm{Pr} = \hat{C}_p\mu/k = 0.70$. The viscosities of air at 150°F and 250°F are 0.049 and 0.055 $\mathrm{lb}_m/\mathrm{ft}\cdot\mathrm{hr}$, respectively, so that the viscosity ratio is $\mu_b/\mu_0 = 0.049/0.055 = 0.89$.

The Reynolds number, evaluated at the film temperature, 200°F, is then

$$\mathrm{Re} = \frac{Dw}{S\mu} = \frac{4w}{\pi D\mu} = \frac{4(70)}{\pi(2/12)(0.052)} = 1.02 \times 10^4 \tag{14.3-20}$$

From Fig. 14.3-1 we obtain

$$\frac{(T_{b2} - T_{b1})}{(T_0 - T_b)_{\ln}}\frac{D}{4L}\mathrm{Pr}^{2/3}\left(\frac{\mu_b}{\mu_0}\right)^{-0.14} = 0.0039 \tag{14.3-21}$$

When this is solved for L/D we get

$$\begin{aligned}\frac{L}{D} &= \frac{1}{4(0.0039)}\frac{(T_{b2} - T_{b1})}{(T_0 - T_b)_{\ln}}\mathrm{Pr}^{2/3}\left(\frac{\mu_b}{\mu_0}\right)^{-0.14} \\ &= \frac{1}{4(0.0039)}\frac{(230 - 70)}{72.2}(0.70)^{2/3}(0.89)^{-0.14} \\ &= \frac{1}{4(0.0039)}\frac{160}{72.8}(0.788)(1.02) = 113\end{aligned} \tag{14.3-22}$$

Hence the required length is

$$L = 113D = (113)(2/12) = 19 \text{ ft} \tag{14.3-23}$$

If Re_b had been much smaller, it would have been necessary to estimate L/D before reading Fig. 14.3-2, thus initiating a trial-and-error process.

Note that in this problem we did not have to calculate h. Numerical evaluation of h is necessary, however, in more complicated problems such as heat exchange between two fluids with an intervening wall.

§14.4 HEAT TRANSFER COEFFICIENTS FOR FORCED CONVECTION AROUND SUBMERGED OBJECTS

Another topic of industrial importance is the transfer of heat to or from an object around which a fluid is flowing. The object may be relatively simple, such as a single cylinder or sphere, or it may be more complex, such as a "tube bundle" made up of a set of cylindrical tubes with a stream of gas or liquid flowing between them. We examine here only a few selected correlations for simple systems: the flat plate, the sphere, and the cylinder. Many additional correlations may be found in the references cited in the introduction to the chapter.

Flow Along a Flat Plate

We first examine the flow along a flat plate, oriented parallel to the flow, with its surface maintained at T_0 and the approaching stream having a uniform temperature T_∞ and a uniform velocity v_∞. The heat transfer coefficient $h_{\text{loc}} = q_0/(T_0 - T_\infty)$ and the friction factor $f_{\text{loc}} = \tau_0/\frac{1}{2}\rho v_\infty^2$ are shown in Fig. 14.1-1. For the laminar region, which normally exists near the leading edge of the plate, the following theoretical expressions are obtained (see Eq. 4.4-30 as well as Eqs. 12.4-12, 12.4-15, and 12.4-16):

$$\tfrac{1}{2} f_{\text{loc}} = +\frac{\mu(\partial v_x/\partial y)|_{y=0}}{\rho v_\infty^2} = f''(0)\sqrt{\frac{\mu}{2xv_\infty\rho}} = 0.332\,\text{Re}_x^{-1/2} \tag{14.4-1}$$

$$\text{Nu}_{\text{loc}} = \frac{h_{\text{loc}}x}{k} = \frac{x}{(T_\infty - T_0)}\left.\frac{\partial T}{\partial y}\right|_{y=0} = 2\sqrt{\frac{37}{1260}}\,\text{Re}_x^{1/2}\text{Pr}^{1/3} \tag{14.4-2}$$

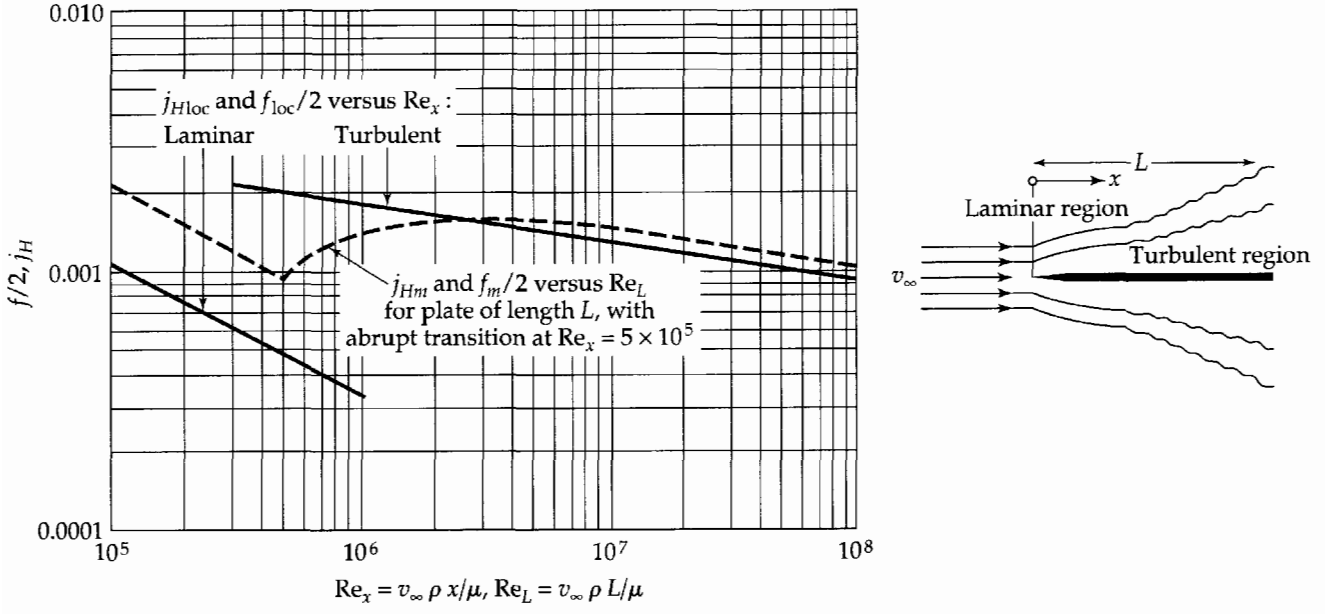

Fig. 14.4-1. Transfer coefficients for a smooth flat plate in tangential flow. Adapted from H. Schlichting, *Boundary-Layer Theory*, McGraw-Hill, New York (1955), pp. 438–439.

As shown in Table 12.4-1, a more accurate value of the numerical coefficient in Eq. 14.4-2 is that of Pohlhausen—namely, 0.332. If we use this value, then Eq. 14.4-2 gives

$$j_{H,\text{loc}} = \frac{\text{Nu}_{\text{loc}}}{\text{RePr}^{1/3}} = \frac{h_{\text{loc}}}{\rho \hat{C}_p v_\infty} \left(\frac{\hat{C}_p \mu}{k} \right)^{2/3} = 0.332\ \text{Re}_x^{-1/2} \tag{14.4-3}$$

Since the numerical coefficient in Eq. 14.4-3 is the same as that in Eq. 14.4-1, we then get

$$j_{H,\text{loc}} = \tfrac{1}{2} f_{\text{loc}} = 0.332\ \text{Re}_x^{-1/2} \tag{14.4-4}$$

for the Colburn analogy between heat transfer and fluid friction. This was to be expected, because there is no "form drag" in this flow geometry.

Equation 14.4-4 was derived for fluids with constant physical properties.[1] When the physical properties are evaluated at the film temperature $T_f = \frac{1}{2}(T_0 + T_\infty)$, Eq. 14.4-3 is known to work well for gases.[2] The analogy of Eq. 14.4-4 is accurate within 2% for Pr > 0.6, but becomes inaccurate at lower Prandtl numbers.

For highly turbulent flows, the Colburn analogy still holds with fair accuracy, with f_{loc} given by the empirical curve in Fig. 14.4-1. The transition between laminar and turbulent flow resembles that for pipes in Fig. 14.3-1, but the limits of the transition region are harder to predict. For smooth, sharp-edged flat plates in an isothermal flow the transition usually begins at a Reynolds number $\text{Re}_x = xv_\infty\rho/\mu$ of 100,000 to 300,000 and is almost complete at a 50% higher Reynolds number.

Flow Around a Sphere

In Problem 10B.1 it is shown that the Nusselt number for a sphere in a stationary fluid is 2. For the sphere with constant surface temperature T_0 in a flowing fluid approaching with a uniform velocity v_∞, the mean Nusselt number is given by the following empiricism[3]

$$\text{Nu}_m = 2 + 0.60\ \text{Re}^{1/2}\ \text{Pr}^{1/3} \tag{14.4-5}$$

This result is useful for predicting the heat transfer to or from droplets or bubbles.

Another correlation that has proven successful[4] is

$$\text{Nu}_m = 2 + (0.4\ \text{Re}^{1/2} + 0.06\text{Re}^{2/3})\text{Pr}^{0.4}\left(\frac{\mu_\infty}{\mu_0}\right)^{1/4} \tag{14.4-6}$$

in which the physical properties appearing in Nu_m, Re, and Pr are evaluated at the approaching stream temperature. This correlation is recommended for $3.5 < \text{Re} < 7.6 \times 10^4$, $0.71 < \text{Pr} < 380$, and $1.0 < \mu_\infty/\mu_0 < 3.2$. In contrast to Eq. 14.4-5, it is not valid in the limit that $\text{Pr} \to \infty$.

---

[1] The result in Eq. 14.4-1 was first obtained by H. Blasius, *Z. Math. Phys.*, **56**, 1–37 (1908), and that in Eq. 14.4-3 by E. Pohlhausen, *Z. angew. Math. Mech.*, **1**, 115–121 (1921).

[2] E. R. G. Eckert, *Trans. ASME*, **56**, 1273–1283 (1956). This article also includes high-velocity flows, for which compressibility and viscous dissipation become important.

[3] W. E. Ranz and W. R. Marshall, Jr., *Chem. Eng. Prog.*, **48**, 141–146, 173–180 (1952). N. Frössling, *Gerlands Beitr. Geophys.*, **52**, 170–216 (1938), first gave a correlation of this form, with a coefficient of 0.552 in lieu of 0.60 in the last term.

[4] S. Whitaker, *Fundamental Principles of Heat Transfer*, Krieger Publishing Co., Malabar, Fla. (1977), pp. 340–342; *AIChE Journal*, **18**, 361–371 (1972).

Flow Around a Cylinder

A cylinder in a stationary fluid of infinite extent does not admit a steady-state solution. Therefore the Nusselt number for a cylinder does not have the same form as that for a sphere. Whitaker recommends for the mean Nusselt number[4]

$$\mathrm{Nu}_m = (0.4\,\mathrm{Re}^{1/2} + 0.06\,\mathrm{Re}^{2/3})\mathrm{Pr}^{0.4}\left(\frac{\mu_\infty}{\mu_0}\right)^{1/4} \tag{14.4-7}$$

in the range $1.0 < \mathrm{Re} < 1.0 \times 10^5$, $0.67 < \mathrm{Pr} < 300$, and $0.25 < \mu_\infty/\mu_0 < 5.2$. Here, as in Eq. 14.4-6, the values of viscosity and thermal conductivity in Re and Pr are those at the approaching stream temperature. Similar results are available for banks of cylinders, which are used in certain types of heat exchangers.[4]

Another correlation,[5] based on a curve-fit of McAdams' compilation of heat transfer coefficient data,[6] and on the low-Re asymptote in Problem 12B.6, is

$$\mathrm{Nu}_m = (0.376\,\mathrm{Re}^{1/2} + 0.057\,\mathrm{Re}^{2/3})\mathrm{Pr}^{1/3} + 0.92\left[\ln\left(\frac{7.4055}{\mathrm{Re}}\right) + 4.18\,\mathrm{Re}\right]^{-1/3}\mathrm{Re}^{1/3}\mathrm{Pr}^{1/3} \tag{14.4-8}$$

This correlation has the proper behavior in the limit that $\mathrm{Pr} \to \infty$, and also behaves properly for small values of the Reynolds number. This result can be used for analyzing the steady-state performance of hot-wire anemometers, which typically operate at low Reynolds numbers.

Flow Around Other Objects

We learn from the preceding three discussions that, for the flow around objects of shapes other than those described above, a fairly good guess for the heat transfer coefficients can be obtained by using the relation

$$\mathrm{Nu}_m - \mathrm{Nu}_{m,0} = 0.6\,\mathrm{Re}^{1/2}\,\mathrm{Pr}^{1/3} \tag{14.4-9}$$

in which $\mathrm{Nu}_{m,0}$ is the mean Nusselt number at zero Reynolds number. This generalization, which is shown in Fig. 14.4-2, is often useful in estimating the heat transfer from irregularly shaped objects.

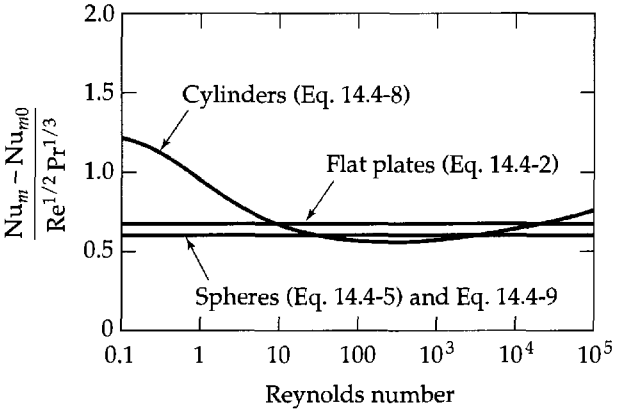

Fig. 14.4-2. Graph comparing the Nusselt numbers for flow around flat plates, spheres, and cylinders with Eq. 14.4-9.

[5] W. E. Stewart (to be published).

[6] W. H. McAdams, *Heat Transmission*, 3rd edition, McGraw-Hill, New York (1954), p. 259.

§14.5 HEAT TRANSFER COEFFICIENTS FOR FORCED CONVECTION THROUGH PACKED BEDS

Heat transfer coefficients between particles and fluid in packed beds are important in the design of fixed-bed catalytic reactors, absorbers, driers, and pebble-bed heat exchangers. The velocity profiles in packed beds exhibit a strong maximum near the wall, attributable partly to the higher void fraction there and partly to the more ordered interstitial passages along this smooth boundary. The resulting segregation of the flow into a fast outer stream and a slower interior one, which mix at the exit of the bed, leads to complicated behavior of mean Nusselt numbers in deep packed beds,[1] unless the tube-to-particle diameter ratio D_t/D_p is very large or close to unity. Experiments with wide, shallow beds show simpler behavior and are used in the following discussion.

We define h_{loc} for a representative volume Sdz of particles and fluid by the following modification of Eq. 14.1-5:

$$dQ = h_{\text{loc}}(aSdz)(T_0 - T_b) \tag{14.5-1}$$

Here a is the outer surface area of particles per unit bed volume, as in §6.4. Equations 6.4-5 and 6 give the effective particle size D_p as $6/a_v = 6(1-\varepsilon)/a$ for a packed bed with void fraction ε.

Extensive data on forced convection for the flow of gases[2] and liquids[3] through shallow packed beds have been critically analyzed[4] to obtain the following local heat transfer correlation,

$$j_H = 2.19\,\text{Re}^{-2/3} + 0.78\,\text{Re}^{-0.381} \tag{14.5-2}$$

and an identical formula for the mass transfer function j_D defined in §22.3. Here the Chilton–Colburn j_H factor and the Reynolds number are defined by

$$j_H = \frac{h_{\text{loc}}}{\hat{C}_p G_0}\left(\frac{\hat{C}_p\mu}{k}\right)^{2/3} \tag{14.5-3}$$

$$\text{Re} = \frac{D_p G_0}{(1-\varepsilon)\mu\psi} = \frac{6G_0}{a\mu\psi} \tag{14.5-4}$$

In this equation the physical properties are all evaluated at the film temperature $T_f = \frac{1}{2}(T_0 - T_b)$, and $G_0 = w/S$ is the superficial mass flux introduced in §6.4. The quantity ψ is a particle-shape factor, with a defined value of 1 for spheres and a fitted value[4] of 0.92 for cylindrical pellets. A related shape factor was used by Gamson[5] in Re and j_H; the present factor ψ is used in Re only.

For small Re, Eq. 14.5-2 yields the asymptote

$$j_H = 2.19\,\text{Re}^{-2/3} \tag{14.5-5}$$

or

$$\text{Nu}_{\text{loc}} = \frac{h_{\text{loc}}D_p}{k(1-\varepsilon)\psi} = 2.19(\text{RePr})^{1/3} \tag{14.5-6}$$

---

[1] H. Martin, *Chem. Eng. Sci.*, **33**, 913–919 (1978).

[2] B. W. Gamson, G. Thodos, and O. A. Hougen, *Trans. AIChE*, **39**, 1–35 (1943); C. R. Wilke and O. A. Hougen, *Trans. AIChE*, **41**, 445–451 (1945).

[3] L. K. McCune and R. H. Wilhelm, *Ind. Eng. Chem.*, **41**, 1124–1134 (1949); J. E. Williamson, K. E. Bazaire, and C. J. Geankoplis, *Ind. Eng. Chem. Fund.*, **2**, 126–129 (1963); E. J. Wilson and C. J. Geankoplis, *Ind. Eng. Chem. Fund.*, **5**, 9–14 (1966).

[4] W. E. Stewart, to be submitted.

[5] B. W. Gamson, *Chem. Eng. Prog.*, **47**, 19–28 (1951).

consistent with boundary layer theory[6] for creeping flow with RePr >> 1. The latter restriction gives Nu >> 1 corresponding to a thin thermal boundary layer relative to $D_p/(1-\varepsilon)\psi$. This asymptote represents the creeping-flow mass-transfer data for liquids[3] very well.

The exponent $\frac{2}{3}$ in Eq. 14.5-3 is a high-Pr asymptote given by boundary layer theory for steady laminar flows[6] and for steadily driven turbulent flows.[7] This dependence is consistent with the cited data over the full range Pr > 0.6 and the corresponding range of the dimensionless group Sc for mass transfer.

§14.6 HEAT TRANSFER COEFFICIENTS FOR FREE AND MIXED CONVECTION[1]

Here we build on Example 11.4-5 to summarize the behavior of some important systems in the presence of appreciable buoyant forces, first by rephrasing the results obtained there in terms of Nusselt numbers and then by extension to other situations: (1) small buoyant forces, where the thin-boundary-layer assumption of Example 11.4-5 may not be valid; (2) very large buoyant forces, where turbulence can occur in the boundary layer, and (3) mixed forced and free convection. We shall confine ourselves to heat transfer between solid bodies and a large quiescent volume of surrounding fluid, and to the constant-temperature boundary conditions of Example 11.4-5. Discussions of other situations, including transient behavior and duct and cavity flows, are available elsewhere.[1]

In Example 11.4-5 we saw that for the free convection near a vertical flat plate, the principal dimensionless group is GrPr, which is often called the *Rayleigh number*, Ra. If we define the area mean Nusselt number as $\mathrm{Nu}_m = hH/k = q_{\mathrm{avg}}H/k(T_0 - T_1)$, then Eq. 11.4-51 may be written as

$$\mathrm{Nu}_m = C(\mathrm{GrPr})^{1/4} \tag{14.6-1}$$

where C was found to be a weak function of Pr. The heat transfer behavior at moderate values of Ra = GrPr is governed, for many shapes of solids, by laminar boundary layers of the type described in Example 11.4-5, and the results of those discussions are normally used directly.

However, at small values of GrPr direct heat conduction to the surroundings may invalidate the boundary layer result, and at sufficiently high values of GrPr the mechanism of heat transfer shifts toward random local eruptions or plumes of fluid, producing turbulence within the boundary layer. Then the Nusselt number becomes independent of the system size. The case of combined forced and free convection (normally referred to as *mixed convection*) is more complex: one must now consider Pr, Gr, and Re as independent variables, and also whether the forced and free convection effects are in the same or different directions. Only the former seems to be at all well understood. The description of the behavior is further complicated by lack of abrupt transitions between the various flow regimes.

---

[6] W. E. Stewart, *AIChE Journal*, **9**, 528–535 (1963); R. Pfeffer, *Ind. Eng. Chem. Fund.*, **3**, 380–383 (1964); J. P. Sørensen and W. E. Stewart, *Chem. Eng. Sci.*, **29**, 833–837 (1974). See also Example 12.4-3.

[7] W. E. Stewart, *AIChE Journal*, **33**, 2008–2016 (1987); corrigenda **34**, 1030 (1988).

[1] G. D. Raithby and K. G. T. Hollands, Chapter 4 in W. M. Rohsenow, J. P. Hartnett, and Y. I. Cho, eds., *Handbook of Heat Transfer*, 3rd edition, McGraw-Hill, New York (1998).

It has been shown, however, that simple and reliable predictions of heat transfer rates (expressed as area mean Nusselt numbers Nu_m) may be obtained for this wide variety of flow regimes by empirical combinations of asymptotic expressions:

a. Nu_m^{cond}, for conduction in the absence of buoyant forces or forced convection

b. Nu_m^{lam}, for thin laminar boundary layers, as in Example 11.4-5

c. Nu_m^{turb}, for turbulent boundary layers

d. Nu_m^{forced}, for pure forced convection

These are dealt with in the following subsections.

No Buoyant Forces

The limiting Nusselt number for vanishingly small free and forced convection is obtained by solving the heat conduction equation (the Laplace equation, $\nabla^2 T = 0$) for constant, uniform temperature over the solid surface and a different constant temperature at infinity. The mean Nusselt number then has the general form

$$Nu_m^{cond} = K(\text{shape}) \tag{14.6-2}$$

With K equal to zero for all objects with at least one infinite dimension (e.g., infinitely long cylinders or infinitely wide plates). For finite bodies K is nonzero, and an important case is that of the sphere for which, according to Problem 10B.1,

$$Nu_m^{cond} = 2 \tag{14.6-3}$$

with the characteristic length taken to be the sphere diameter. Oblate ellipsoids of revolution and circular disks are discussed in Problem 14D.1.

Thin Laminar Boundary Layers

For thin laminar boundary layers, the isothermal vertical flat plate is a representative system, conforming to Eq. 14.6-1. This equation may be generalized to

$$Nu_m^{lam} = C(\text{Pr, shape})(\text{GrPr})^{1/4} \tag{14.6-4}$$

Moreover, the function of Pr and shape can be factored into the product

$$C = C_1(\text{shape})C_2(\text{Pr}) \tag{14.6-5}$$

with[2]

$$C_2 \approx \frac{0.671}{[1 + (0.492/\text{Pr})^{9/16}]^{4/9}} \tag{14.6-6}$$

Representative values[1,3] of C_1 and C_2 are given in Tables 14.6-1 and 2, respectively. Shape factors for a wide variety of other shapes are available.[3,4] For heated horizontal flat surfaces facing downward and cooled horizontal flat surfaces facing upward, the following correlation[5] is recommended:

$$Nu_m^{lam} = \frac{0.527}{[1 + (1.9/\text{Pr})^{9/10}]^{2/9}} (\text{GrPr})^{1/5} \tag{14.6-7}$$

---

[2] S. W. Churchill and R. Usagi, *AIChE Journal*, **23**, 1121–1128 (1972).

[3] W. E. Stewart, *Int. J. Heat and Mass Transfer*, **14**, 1013–1031 (1971).

[4] A. Acrivos, *AIChE Journal*, **6**, 584–590 (1960).

[5] T. Fujii, M. Honda, and I. Morioka, *Int. J. Heat and Mass Transfer*, **15**, 755–767 (1972).

Table 14.6-1 The Factor C_1 in Eq. 14.6-5, and the D in the Nusselt Number, for Several Representative Shapes[a]

Shape →	Vertical plate	Horizontal plate[a]	Horizontal cylinder	Sphere
C_1	1.0	0.835	0.772	0.878
"D" in Nu	Height H	Width W	Diameter D	Diameter D

[a] For a hot upper surface and an insulated lower one, or the reverse for cold surfaces.

Table 14.6-2 The Factor C_2 as a Function of the Prandtl Number

	Hg	Gases	Water				Oils		
Pr	0.022	0.71	1.0	2.0	4.0	6.0	50	100	2000
C_2	0.287	0.515	0.534	0.568	0.595	0.608	0.650	0.656	0.668

For the vertical plate with a constant-heat-flux boundary condition, the recommended power on GrPr is also 1/5.

Laminar free-convection heat fluxes tend to be small, and a conduction correction is often necessary for accurate predictions. The conduction limit is determined by solving the equation $\nabla^2 T = 0$ for the given geometry, and this leads to the calculation of a "conduction Nusselt number," $\mathrm{Nu}_m^{\mathrm{cond}}$. Then the combined Nusselt number, $\mathrm{Nu}_m^{\mathrm{comb}}$, is estimated by combining the two contributing Nusselt numbers by an equation of the form[1]

$$\mathrm{Nu}_m^{\mathrm{comb}} \cong [(\mathrm{Nu}_m^{\mathrm{lam}})^n + (\mathrm{Nu}_m^{\mathrm{cond}})^n]^{1/n} \tag{14.6-8}$$

Optimum values of n are shape-dependent, but 1.07 is a suggested rough estimate in the absence of specific information.

Turbulent Boundary Layers

The effects of turbulence increase gradually, and it is common practice to combine the laminar and turbulent contributions as follows:[1]

$$\mathrm{Nu}_m^{\mathrm{free}} = [(\mathrm{Nu}_m^{\mathrm{comb}})^m + (\mathrm{Nu}_m^{\mathrm{turb}})^m]^{1/m} \tag{14.6-9}$$

Thus for the vertical isothermal flat plate, one writes[1]

$$\mathrm{Nu}_m^{\mathrm{turb}} = \frac{C_3(\mathrm{GrPr})^{1/3}}{1 + (1.4 \times 10^9/\mathrm{Gr})} \tag{14.6-10}$$

with

$$C_3 = \frac{0.13\mathrm{Pr}^{0.22}}{(1 + 0.61\mathrm{Pr}^{0.81})^{0.42}} \tag{14.6-11}$$

and $m = 6$. The values of m in Eq. 14.6-9 are heavily geometry-dependent.

Mixed Free and Forced Convection

Finally, one must deal with the problem of simultaneous free and forced convection, and this is again done through the use of an empirical combining rule:[6]

$$\mathrm{Nu}_m^{\text{total}} = [\mathrm{Nu}_m^{\text{free}})^3 + (\mathrm{Nu}_m^{\text{forced}})^3]^{1/3} \tag{14.6-12}$$

This rule appears to hold reasonably well for all geometries and situations, provided only that the forced and free convection have the *same* primary flow direction.

EXAMPLE 14.6-1

Heat Loss by Free Convection from a Horizontal Pipe

Estimate the rate of heat loss by free convection from a unit length of a long horizontal pipe, 6 in. in outside diameter, if the outer surface temperature is 100°F and the surrounding air is at 1 atm and 80°F.

SOLUTION

The properties of air at 1 atm and a film temperature $T_f = 90°\mathrm{F} = 550°\mathrm{R}$ are

$$\begin{aligned}
\mu &= 0.0190 \text{ cp} = 0.0460 \text{ lb}_m/\text{ft} \cdot \text{hr} \\
\rho &= 0.0723 \text{ lb}_m/\text{ft}^3 \\
\hat{C}_p &= 0.241 \text{ Btu}/\text{lb}_m \cdot \text{R} \\
k &= 0.0152 \text{ Btu}/\text{hr} \cdot \text{ft} \cdot \text{R} \\
\beta &= 1/T_f = (1/550)\text{R}^{-1}
\end{aligned}$$

Other relevant values are $D = 0.5$ ft, $\Delta T = 20°\mathrm{R}$, and $g = 4.17 \times 10^8$ ft/hr^2. From these data we obtain

$$\begin{aligned}
\mathrm{GrPr} &= \left(\frac{(0.5)^3(0.0723)^2(4.17 \times 10^8)(20/550)}{(0.0460)^2}\right)\left(\frac{(0.241)(0.0460)}{0.0152}\right) \\
&= (4.68 \times 10^6)(0.729) = 3.4 \times 10^6
\end{aligned} \tag{14.6-13}$$

Then from Eqs. 14.6-4 to 6 and Table 14.6-1 we get

$$\begin{aligned}
\mathrm{Nu}_m &= 0.772\left(\frac{0.671}{[1 + (0.492/0.729)^{9/16}]^{4/9}}\right)(3.4 \times 10^6)^{1/4} \\
&= 0.772\left(\frac{0.671}{1.30}\right)(42.9) = 17.1
\end{aligned} \tag{14.6-14}$$

The heat transfer coefficient is then

$$h_m = \mathrm{Nu}_m \frac{k}{D} = 17.1\left(\frac{0.0152}{0.5}\right) = 0.52 \text{ Btu}/\text{hr} \cdot \text{ft}^2 \cdot \text{F} \tag{14.6-15}$$

The rate of heat loss per unit length of the pipe is

$$\begin{aligned}
\frac{Q}{L} &= \frac{h_m A \Delta T}{L} = h_m \pi D \Delta T \\
&= (0.52)(3.1416)(0.5)(20) = 16 \text{ Btu}/\text{hr} \cdot \text{ft}
\end{aligned} \tag{14.6-16}$$

This is the heat loss by convection only. The radiation loss for the same problem is obtained in Example 16.5-2.

---

[6] E. Ruckenstein, *Adv. in Chem. Eng.*, **13**, 11–112 (1987) E. Ruckenstein and R. Rajagopalan, *Chem. Eng. Communications*, **4**, 15–29 (1980).

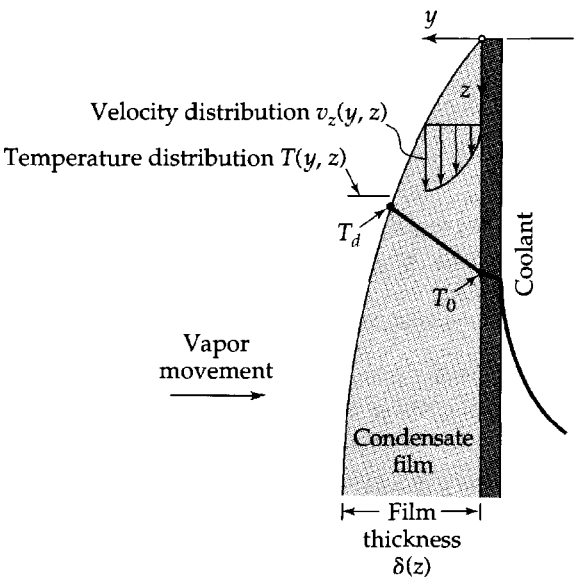

Fig. 14.7-1. Film condensation on a vertical surface (interfacial temperature discontinuity exaggerated).

§14.7 HEAT TRANSFER COEFFICIENTS FOR CONDENSATION OF PURE VAPORS ON SOLID SURFACES

The condensation of a pure vapor on a solid surface is a particularly complicated heat transfer process, because it involves two flowing fluid phases: the vapor and the condensate. Condensation occurs industrially in many types of equipment; for simplicity, we consider here only the common cases of condensation of a slowly moving vapor on the outside of horizontal tubes, vertical tubes, and vertical flat walls.

The condensation process on a vertical wall is illustrated schematically in Fig. 14.7-1. Vapor flows over the condensing surface and is moved toward it by the small pressure gradient near the liquid surface.[1] Some of the molecules from the vapor phase strike the liquid surface and bounce off; others penetrate the surface and give up their latent heat of condensation. The heat thus released must then move through the condensate to the wall, thence to the coolant on the other side of the wall. At the same time, the condensate must drain from the surface by gravity flow.

The condensate on the wall is normally the sole important resistance to heat transfer on the condensing wall. If the solid surface is clean, the condensate will usually form a continuous film over the surface, but if traces of certain impurities are present, (such as fatty acids in a steam condenser), the condensate will form in droplets. "Dropwise condensation"[2] gives much higher rates of heat transfer than "film condensation," but is difficult to maintain, so that it is common practice to assume film condensation in condenser design. The correlations that follow apply only to film condensation.

The usual definition of h_m for condensation of a pure vapor on a solid surface of area A and uniform temperature T_0 is

$$Q = h_m A(T_d - T_0) = w\Delta\hat{H}_{\text{vap}} \tag{14.7-1}$$

in which Q is the rate of heat flow into the solid surface, and T_d is the *dew point* of the vapor approaching the wall surface—that is, the temperature at which the vapor would

[1] Note that there occur small but abrupt changes in pressure and temperature at an interface. These discontinuities are essential to the condensation process, but are generally of negligible magnitude in engineering calculations for pure fluids. For mixtures, they may be important. See R. W. Schrage, *Interphase Mass Transfer*, Columbia University Press (1953).

[2] Dropwise condensation and boiling are discussed at length by J. G. Collier and J. R. Thome, *Convective Boiling and Condensation*, 3rd edition, Oxford University Press (1996).

condense if cooled slowly at the prevailing pressure. This temperature is very nearly that of the liquid at the liquid–gas interface. Therefore h_m may be regarded as a heat transfer coefficient for the liquid film.

Expressions for h_m have been derived[3] for *laminar nonrippling* condensate flow by approximate solution of the equations of energy and motion for a falling liquid film (see Problem 14C.1). For film condensation on a horizontal tube of diameter D, length L, and constant surface temperature T_0, the result of Nusselt[3] may be written as

$$h_m = 0.954\left(\frac{k^3\rho^2 gL}{\mu w}\right)^{1/3} \tag{14.7-2}$$

Here w/L is the mass rate of condensation per unit length of tube, and it is understood that all the physical properties of the condensate are to be calculated at the film temperature, $T_f = \frac{1}{2}(T_d + T_0)$.

For moderate temperature differences, Eq. 14.7-2 may be rewritten with the aid of an energy balance on the condensate to give

$$h_m = 0.725\left(\frac{k^3\rho^2 g\Delta\hat{H}_{\text{vap}}}{\mu D(T_d - T_0)}\right)^{1/4} \tag{14.7-3}$$

Equations 14.7-2 and 3 have been confirmed experimentally within ±10% for single horizontal tubes. They also seem to give satisfactory results for bundles of horizontal tubes,[4] in spite of the complications introduced by condensate dripping from tube to tube.

For film condensation on *vertical tubes* or *vertical walls* of height L, the theoretical results corresponding to Eqs. 14.7-2 and 3 are

$$h_m = \frac{4}{3}\left(\frac{k^3\rho^2 g}{3\mu\Gamma}\right)^{1/3} \tag{14.7-4}$$

and

$$h_m = \frac{2\sqrt{2}}{3}\left(\frac{k^3\rho^2 g\Delta\hat{H}_{\text{vap}}}{\mu L(T_d - T_0)}\right)^{1/4} \tag{14.7-5}$$

respectively. The quantity Γ in Eq. 14.7-4 is the total rate of condensate flow from the bottom of the condensing surface per unit width of that surface. For a vertical tube, $\Gamma = w/\pi D$, where w is the total mass rate of condensation on the tube. For *short vertical tubes* ($L < 0.5$ ft), the experimental values of h_m confirm the theory well, but the measured values for *long vertical tubes* ($L > 8$ ft) may exceed the theory for a given $T_d - T_0$ by as much as 70%. This discrepancy is attributed to ripples that attain greatest amplitude on long vertical tubes.[5]

We now turn to the empirical expressions for *turbulent* condensate flow. Turbulent flow begins, on *vertical tubes or walls*, at a Reynolds number $\text{Re} = \Gamma/\mu$ of about 350. For higher Reynolds numbers, the following empirical formula has been proposed:[6]

$$h_m = 0.003\left(\frac{k^3\rho^2 g(T_d - T_0)L}{\mu^3\Delta\hat{H}_{\text{vap}}}\right)^{1/2} \tag{14.7-6}$$

This equation is equivalent, for small $T_d - T_0$, to the formula

$$h_m = 0.021\left(\frac{k^3\rho^2 g\Gamma}{\mu^3}\right)^{1/3} \tag{14.7-7}$$

---

[3] W. Nusselt, Z. *Ver. deutsch. Ing.*, **60**, 541–546, 596–575 (1916).

[4] B. E. Short and H. E. Brown, *Proc. General Disc. Heat Transfer*, London (1951), pp. 27–31. See also D. Butterworth, in *Handbook of Heat Exchanger Design* (G. F. Hewitt, ed.), Oxford University Press, London (1977), pp. 426–462.

[5] W. H. McAdams, *Heat Transmission*, 3rd edition, McGraw-Hill, New York (1954) p. 333.

[6] U. Grigull, *Forsch. Ingenieurwesen*, **13**, 49–57 (1942); Z. *Ver. dtsch. Ing.*, **86**, 444–445 (1942).

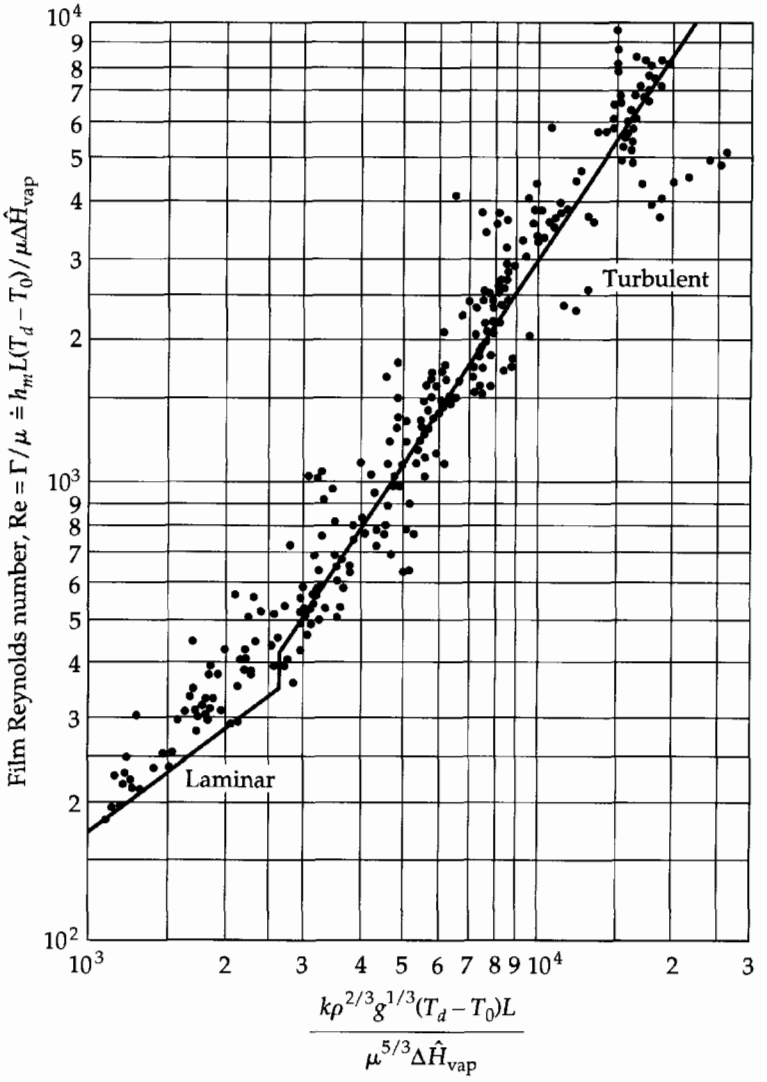

Fig. 14.7-2. Correlation of heat transfer data for film condensation of pure vapors on vertical surfaces. [H. Gröber, S. Erk, and U. Grigull, *Die Grundgesetze der Wärmeübertragung*, 3rd edition, Springer-Verlag, Berlin (1955), p. 296.]

Equations 14.7-4 to 7 are summarized in Fig. 14.7-2, for convenience of making calculations and to show the extent of agreement with the experimental data. Somewhat better agreement could have been obtained by using a family of lines in the turbulent range to represent the effect of Prandtl number. However, in view of the scattering of the data, a single line is adequate.

Turbulent condensate flow is very difficult to obtain on horizontal tubes, unless the tube diameters are very large or high temperature differences are encountered. Equations 14.7-2 and 3 are believed to be satisfactory up to the estimated transition Reynolds number, $\mathrm{Re} = w_T/L\mu$, of about 1000, where w_T is the *total condensate flow* leaving a given tube, including the condensate from the tubes above.[7]

The inverse process of vaporization of a pure fluid is considerably more complicated than condensation. We do not attempt to discuss heat transfer to boiling liquids here, but refer the reader to some reviews.[2,8]

---

[7] W. H. McAdams, *Heat Transmission*, 3rd edition, McGraw-Hill, New York (1954), pp. 338–339.

[8] H. D. Baehr and K Stephan, *Heat and Mass Transfer*, Springer, Berlin (1998), Chapter 4.

EXAMPLE 14.7-1

Condensation of Steam on a Vertical Surface

A boiling liquid flowing in a vertical tube is being heated by condensation of steam on the outside of the tube. The steam-heated tube section is 10 ft high and 2 in. in outside diameter. If saturated steam is used, what steam temperature is required to supply 92,000 Btu/hr of heat to the tube at a tube-surface temperature of 200°F? Assume film condensation.

SOLUTION

The fluid properties depend on the unknown temperature T_d. We make a *guess* of $T_d = T_0 = 200°F$. Then the physical properties at the film temperature (also 200°F) are

$$\Delta\hat{H}_{vap} = 978 \text{ Btu/lb}_m$$
$$k = 0.393 \text{ Btu/hr} \cdot \text{ft} \cdot \text{F}$$
$$\rho = 60.1 \text{ lb}_m/\text{ft}^3$$
$$\mu = 0.738 \text{ lb}_m/\text{ft} \cdot \text{hr}$$

Assuming that the steam gives up only latent heat (the assumption $T_d = T_0 = 200°F$ implies this), an energy balance around the tube gives

$$Q = w\Delta\hat{H}_{vap} = \pi D\Gamma\Delta\hat{H}_{vap} \tag{14.7-8}$$

in which Q is the heat flow into the tube wall. The film Reynolds number is

$$\frac{\Gamma}{\mu} = \frac{Q}{\pi D\mu\Delta\hat{H}_{vap}} = \frac{92{,}000}{\pi(2/12)(0.738)(978)} = 244 \tag{14.7-9}$$

Reading Fig. 14.7-2 at this value of the ordinate, we find that the flow is laminar. Equation 14.7-2 is applicable, but it is more convenient to use the line based on this equation in Fig. 14.7-2, which gives

$$\frac{k\rho^{2/3}g^{1/3}(T_d - T_0)L}{\mu^{5/3}\Delta\hat{H}_{vap}} = 1700 \tag{14.7-10}$$

from which

$$T_d - T_0 = 1700\frac{\mu^{5/3}\Delta\hat{H}_{vap}}{k\rho^{2/3}g^{1/3}L}$$
$$= 1700\frac{(0.738)^{5/3}(978)}{(0.393)(60.1)^{2/3}(4.17 \times 10^8)^{1/3}(10)}$$
$$= 22°F \tag{14.7-11}$$

Therefore, the first approximation to the steam temperature is $T_d = 222°F$. This result is close enough; evaluation of the physical properties in accordance with this result gives $T_d = 220$ as a second approximation. It is apparent from Fig. 14.7-2 that this result represents an upper limit. On account of rippling, the temperature drop through the condensate film may be as little as half that predicted here.

QUESTIONS FOR DISCUSSION

1. Define the heat transfer coefficient, the Nusselt number, the Stanton number, and the Chilton-Colburn j_H. How can each of these be "decorated" to indicate the type of temperature-difference driving force that is being used?
2. What are the characteristic dimensionless groups that arise in the correlations for Nusselt numbers for forced convection? For free convection? For mixed convection?
3. To what extent can Nusselt numbers be calculated a priori from analytical solutions?
4. Explain how one develops an experimental correlation for Nusselt numbers as a function of the relevant dimensionless groups.
5. To what extent can empirical correlations be developed in which the Nusselt number is given as the product of the relevant dimensionless groups, each raised to a characteristic power?

6. In addition to the Nusselt number, we have met up with the Reynolds number Re, the Prandtl number Pr, the Grashof number Gr, the Péclet number Pé, and the Rayleigh number Ra. Define each of these and explain their meaning and usefulness.
7. Discuss the concept of wind-chill temperature.

PROBLEMS

14A.1. Average heat transfer coefficients (Fig. 14A.1). Ten thousand pounds per hour of an oil with a heat capacity of 0.6 Btu/lb$_m$ · F are being heated from 100°F to 200°F in the simple heat exchanger shown in the accompanying figure. The oil is flowing through the tubes, which are copper, 1 in. in outside diameter, with 0.065-in. walls. The combined length of the tubes is 300 ft. The required heat is supplied by condensation of saturated steam at 15.0 psia on the outside of the tubes. Calculate h_1, h_a, and $h_{\ln}$ for the oil, assuming that the inside surfaces of the tubes are at the saturation temperature of the steam, 213°F.

Answers: 78, 139, 190 Btu/hr · ft^2 · F

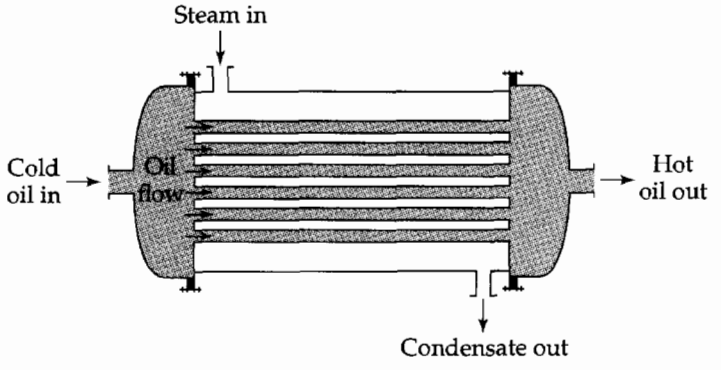

Fig. 14A.1. A single-pass "shell-and-tube" heat exchanger.

14A.2. Heat transfer in laminar tube flow. One hundred pounds per hour of oil at 100°F are flowing through a 1-in. i.d. copper tube, 20 ft long. The inside surface of the tube is maintained at 215°F by condensing steam on the outside surface. Fully developed flow may be assumed through the length of the tube, and the physical properties of the oil may be considered constant at the following values: ρ = 55 lb$_m$/ft^3, $\hat{C}_p$ = 0.49 Btu/lb$_m$ · F, μ = 1.42 lb$_m$/hr · ft, k = 0.0825 Btu/hr · ft · F.

(a) Calculate Pr.

(b) Calculate Re.

(c) Calculate the exit temperature of the oil.

Answers: **(a)** 8.44; **(b)** 1075; **(c)** 155°F

14A.3. Effect of flow rate on exit temperature from a heat exchanger.

(a) Repeat parts **(b)** and **(c)** of Problem 14A.2 for oil flow rates of 200, 400, 800, 1600, and 3200 lb$_m$/hr.

(b) Calculate the total heat flow through the tube wall for each of the oil flow rates in (a).

14A.4. Local heat transfer coefficient for turbulent forced convection in a tube. Water is flowing in a 2-in. i.d. tube at a mass flow rate w = 15,000 lb$_m$/hr. The inner wall temperature at some point along the tube is 160°F, and the bulk fluid temperature at that point is 60°F. What is the local heat flux q_r at the pipe wall? Assume that h_{loc} has attained a constant asymptotic value.

Answer: -7.8×10^4 Btu/hr · ft^2

14A.5. Heat transfer from condensing vapors.

(a) The outer surface of a vertical tube 1 in. in outside diameter and 1 ft long is maintained at 190°F. If this tube is surrounded by saturated steam at 1 atm, what will be the total rate of heat transfer through the tube wall?

(b) What would the rate of heat transfer be if the tube were horizontal?

Answers: **(a)** 8400 Btu/hr; **(b)** 12,000 Btu/hr

14A.6. Forced-convection heat transfer from an isolated sphere.

(a) A solid sphere 1 in. in diameter is placed in an otherwise undisturbed air stream, which approaches at a velocity of 100 ft/s, a pressure of 1 atm, and a temperature of 100°F. The sphere surface is maintained at 200°F by means of an imbedded electric heating coil. What must be the rate of electrical heating in cal/s to maintain the stated conditions? Neglect radiation, and use Eq. 14.4-5.

(b) Repeat the problem in **(a)**, but use Eq. 14.4-6.

Answer: **(a)** 12.9W = 3.1cal/s; **(b)** 16.8W = 4.0 cal/s

14A.7. Free convection heat transfer from an isolated sphere. If the sphere of Problem 14A.6 is suspended in still air at 1 atm pressure and 100°F ambient air temperature, and if the sphere surface is again maintained at 200°F, what rate of electrical heating would be needed? Neglect radiation.

Answer: 0.80W = 0.20 cal/s

14A.8. Heat loss by free convection from a horizontal pipe immersed in a liquid. Estimate the rate of heat loss by free convection from a unit length of a long horizontal pipe, 6 in. in outside diameter, if the outer surface temperature is 100°F and the surrounding water is at 80°F. Compare the result with that obtained in Example 14.6-1, in which air is the surrounding medium. The properties of water at a film temperature of 90°F (or 32.3°C) are μ =

0.7632 cp, $\hat{C}_p = 0.9986$ cal/g · C and $k = 0.363$ Btu/hr · ft · F. Also, the density of water in the neighborhood of 90°F is

T(C)	30.3	31.3	32.3	33.3	34.3
ρ(g/cm^3)	0.99558	0.99528	0.99496	0.99463	0.99430

Answer: $Q/L = 1930$ Btu/hr · ft

14A.9. The ice-fisherman on Lake Mendota. Compare the rates of heat loss of an ice-fisherman, when he is fishing in calm weather (wind velocity zero) and when the wind velocity is 20 mph out of the north. The ambient air temperature is −10°F. Assume that a bundled-up ice-fisherman can be approximated as a sphere 3 ft in diameter.

14B.1. Limiting local Nusselt number for plug flow with constant heat flux.

(a) Equation 10B.9-1 gives the asymptotic temperature distribution for heating a fluid of constant physical properties in plug flow in a long tube with constant heat flux at the wall. Use this temperature profile to show that the limiting Nusselt number for these conditions is Nu = 8.

(b) The asymptotic temperature distribution for the analogous problem for plug flow in a plane slit is given in Eq. 10B.9-2. Use this to show that the limiting Nusselt number is Nu = 12.

14B.2. Local overall heat transfer coefficient. In Problem 14A.1 the thermal resistances of the condensed steam film and wall were neglected. Justify this neglect by calculating the actual inner-surface temperature of the tubes at that cross section in the exchanger at which the oil bulk temperature is 150°F. You may assume that for the oil h_{loc} is constant throughout the exchanger at 190 Btu/hr · ft^2 · F. The tubes are horizontal.

14B.3. The hot-wire anemometer.[1] A hot-wire anemometer is essentially a fine wire, usually made of platinum, which is heated electrically and inserted into a flowing fluid. The wire temperature, which is a function of the fluid temperature, fluid velocity, and the rate of heating, may be determined by measuring its electrical resistance.

(a) A straight cylindrical wire 0.5 in. long and 0.01 in. in diameter is exposed to a stream of air at 70°F flowing past the wire at 100 ft/s. What must the rate of energy input be in watts to maintain the wire surface at 600°F? Neglect radiation as well as heat conduction along the wire.

(b) It has been reported[2] that for a given fluid and wire at given fluid and wire temperatures (hence a given wire resistance)

$$I^2 = B\sqrt{v_\infty} + C \qquad \text{(14B.3-1)}$$

in which I is the current required to maintain the desired temperature, v_∞ is the velocity of the approaching fluid, and C is a constant. How well does this equation agree with the predictions of Eq. 14.4-7 or Eq. 14.4-8 for the fluid and wire of (a) over a fluid velocity range of 100 to 300 ft/s? What is the significance of the constant C in Eq. 14B.3-1?

14B.4. Dimensional analysis. Consider the flow system described in the first paragraph of §14.3, for which dimensional analysis has already given the dimensionless velocity profile (Eq. 6.2-7) and temperature profile (Eq. 14.3-9).

(a) Use Eqs. 6.2-7 and 14.3-9 and the definition of cup-mixing temperature to get the time-averaged expression.

$$\frac{T_{b2} - T_{b1}}{T_0 - T_{b1}} = \text{a function of Re, Pr, } L/D \qquad \text{(14B.4-1)}$$

(b) Use the result just obtained and the definitions of the heat transfer coefficients to derive Eqs. 14.3-12, 13, and 14.

14B.5. Relation between h_{loc} and h_{ln}. In many industrial tubular heat exchangers (see Example 15.4-2) the tube-surface temperature T_0 varies linearly with the bulk fluid temperature T_b. For this common situation h_{loc} and h_{ln} may be simply interrelated.

(a) Starting with Eq. 14.1-5, show that

$$h_{\text{loc}}(\pi D dz)(T_b - T_0) = -(\tfrac{1}{4}\pi D^2)(\rho \hat{C}_p \langle v \rangle dT_b) \qquad \text{(14B.5-1)}$$

and therefore that

$$\int_0^L h_{\text{loc}} dz = \tfrac{1}{4}\rho \hat{C}_p D \langle v \rangle \frac{T_b(L) - T_b(0)}{(T_0 - T_b)_{\text{ln}}} \qquad \text{(14B.5-2)}$$

(b) Combine the result in (a) with Eq. 14.1-4 to show that

$$h_{\text{ln}} = \frac{1}{L}\int_0^L h_{\text{loc}} dz \qquad \text{(14B.5-3)}$$

in which L is the total tube length, and therefore that (if $(\partial h_{\text{loc}}/\partial L)_z = 0$, which is equivalent to the statement that axial heat conduction is neglected)

$$h_{\text{loc}}\big|_{z=L} = h_{\text{ln}} + L\frac{dh_{\text{ln}}}{dL} \qquad \text{(14B.5-4)}$$

14B.6. Heat loss by free convection from a pipe. In Example 14.6-1, would the heat loss be higher or lower if the pipe-surface temperature were 200°F and the air temperature were 180°F?

14C.1. The Nusselt expression for film condensation heat transfer coefficients (Fig. 14.7-1). Consider a laminar film of condensate flowing down a vertical wall, and assume that this liquid film constitutes the sole heat transfer resistance on the vapor side of the wall. Further assume that (i) the shear stress between liquid and vapor may be neglected; (ii) the physical properties in the film may be evaluated at the arithmetic mean of vapor and cooling-surface temperatures and that the cooling-surface temperature may be assumed constant; (iii) acceleration of fluid elements in the film may be neglected compared to the

[1] See, for example, G. Comte-Bellot, Chapter 34 in *The Handbook of Fluid Dynamics* (R. W. Johnson, ed.), CRC Press, Boca Raton, Fla. (1999).

[2] L. V. King, *Phil. Trans. Roy. Soc.* (London), **A214**, 373–432 (1914).

gravitational and viscous forces; (iv) sensible heat changes, $C_p dT$, in the condensate film are unimportant compared to the latent heat transferred through it; and (v) the heat flux is very nearly normal to the wall surface.

(a) Recall from §2.2 that the average velocity of a film of constant thickness δ is $\langle v_z \rangle = \rho g \delta^2 / 3\mu$. Assume that this relation is valid for any value of z.

(b) Write the energy equation for the film, neglecting film curvature and convection. Show that the heat flux through the film toward the cold surface is

$$-q_y = k\left(\frac{T_d - T_0}{\delta}\right) \qquad \text{(14C.1-1)}$$

(c) As the film proceeds down the wall, it picks up additional material by the condensation process. In this process, heat is liberated to the extent of $\Delta\hat{H}_{vap}$ per unit mass of material that undergoes the change in state. Show that equating the heat liberation by condensation with the heat flowing through the film in a segment dz of the film leads to

$$\rho \Delta\hat{H}_{vap} d(\langle v_z \rangle \delta) = k\left(\frac{T_d - T_0}{\delta}\right) dz \qquad \text{(14C.1-2)}$$

(d) Insert the expression for the average velocity from (*a*) into Eq. 14C.1-2 and integrate from $z = 0$ to $z = L$ to obtain

$$\delta(L) = \left(\frac{4k(T_d - T_0)\mu L}{\rho^2 g \Delta\hat{H}_{vap}}\right)^{1/4} \qquad \text{(14C.1-3)}$$

(e) Use the definition of the heat transfer coefficient and the result in (*d*) to obtain Eq. 14.7-5.

(f) Show that Eqs. 14.7-4 and 5 are equivalent for the conditions of this problem.

14C.2. Heat transfer correlations for agitated tanks (Fig. 14C.2). A liquid of essentially constant physical properties is being continuously heated by passage through an agitated tank, as shown in the accompanying figure. Heat is supplied by condensation of steam on the outer wall of the tank. The thermal resistance of the condensate film and the tank wall may be considered small compared to that of the fluid in the tank, and the unjacketed portion of the tank may be assumed to be well insulated. The rate of liquid flow through the tank has a negligible effect on the flow pattern in the tank.

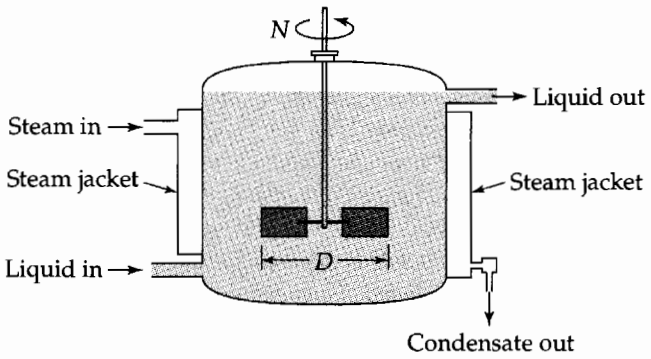

Fig. 14C.2. Continuous heating of a liquid in an agitated tank.

Develop a general form of dimensionless heat transfer correlation for the tank corresponding to the correlation for tube flow in §14.3. Choose the following reference quantities: reference length, D, the impeller diameter; reference velocity, ND, where N is the rate of shaft rotation in revolutions per unit time; reference pressure, $\rho N^2 D^2$, where ρ is the fluid density.

14D.1. Heat transfer from an oblate ellipsoid of revolution. Systems of this sort are best described in oblate ellipsoidal coordinates (ξ, η, ψ)[1] for which

ξ = constant describes oblate ellipsoids $(0 \le \xi < \infty)$

η = constant describes hyperboloids of revolution $(0 \le \eta \le \pi)$

ψ = constant describes half planes $(0 \le \psi < 2\pi)$

Note that $\xi = \xi_0$ can describe oblate ellipsoids, with $\xi_0 = 0$ being a limiting case of the two-sided disk, and the limit as $\xi_0 \to \infty$ being a sphere. In this problem we investigate the corresponding two limiting values of the Nusselt number.

(a) First use Eq. A.7-13 to get the scale factors from the relation between oblate ellipsoidal coordinates and Cartesian coordinates:

$$x = a \cosh\xi \sin\eta \cos\psi \qquad \text{(14D.1-1)}$$

$$y = a \cosh\xi \sin\eta \sin\psi \qquad \text{(14D.1-2)}$$

$$z = a \sinh\xi \cos\eta \qquad \text{(14D.1-3)}$$

in which a is one-half the distance between the foci. Show that

$$h_\xi = h_\eta = a\sqrt{\cosh^2\xi - \sin^2\eta} \qquad \text{(14D.1-4)}$$

$$h_\psi = a \cosh\xi \sin\eta \qquad \text{(14D.1-5)}$$

Equations A.7-13 and 14 can then be used to get any of the ∇-operations that are needed.

(b) Next obtain the temperature profile outside of an oblate ellipsoid with surface temperature T_0, which is embedded in an infinite medium with the temperature T_∞ far from the ellipsoid. Let $\Theta = (T - T_0)/(T_\infty - T_0)$ be a dimensionless temperature, and show that Laplace's equation describing the heat conduction exterior to the ellipsoid is

$$\frac{1}{a^2(\cosh^2\xi - \sin^2\eta)}\left[\frac{\partial}{\partial\xi}\left(\cosh\xi \frac{\partial\Theta}{\partial\xi}\right) + \cdots\right] = 0 \qquad \text{(14D.1-6)}$$

[1] For a discussion of oblate ellipsoidal coordinates, see P. Moon and D. E. Spencer, *Field Theory Handbook*, Springer, Berlin (1961), pp. 31–34. See also J. Happel and H. Brenner, *Low Reynolds Number Hydrodynamics*, Prentice-Hall, Englewood Cliffs, N.J. (1965), pp. 512–516; note that their scale factors are the reciprocals of those defined in this book.

The terms involving derivatives with respect to η and ψ have been omitted because they are not needed. Show that this equation may be solved with the boundary conditions that $\Theta(\xi_0) = 0$ and $\Theta(\infty) = 1$ to obtain

$$\Theta = 1 - \frac{\frac{1}{2}\pi - \arctan(\sinh \xi)}{\frac{1}{2}\pi - \arctan(\sinh \xi_0)} \qquad (14D.1\text{-}7)$$

(c) Next, specialize this result for the two-sided disk (that is, the limiting case that $\xi_0 = 0$), and show that the normal temperature gradient at the surface is

$$(\mathbf{n} \cdot \nabla\Theta)|_{\text{surf}} = \left(\mathbf{n}_\xi \cdot \mathbf{n}_\xi \frac{1}{h_\xi} \frac{\partial\Theta}{\partial\xi}\right)\bigg|_{\xi=0} = \frac{2}{\pi} \frac{1}{R \cos \eta} \qquad (14D.1\text{-}8)$$

where a has been expressed as R, the disk radius. Show further that the total heat loss through both sides of the disk is

$$\begin{aligned} Q &= -2k\int(\mathbf{n} \cdot \nabla T)\, dS \\ &= +2k(T_0 - T_\infty)\int(\mathbf{n} \cdot \nabla\Theta)\, dS \\ &= 2k(T_0 - T_\infty)\int_0^{2\pi}\int_0^{\pi/2}\left(\frac{2}{\pi R \cos \eta}\right)R^2 \cos \eta \sin \eta\, d\eta\, d\psi \\ &= 8kR(T_0 - T_\infty) \end{aligned} \qquad (14D.1\text{-}9)$$

and that the Nusselt number is given by $\text{Nu} = 16/\pi = 5.09$. Since $\text{Nu} = 2$ for the analogous sphere problem, we see that the Nusselt number for any oblate ellipsoid must lie somewhere between 2 and 5.09.

(d) By dimensional analysis show that, without doing any detailed derivation (such as the above), one can predict that the heat loss from the ellipsoid must be proportional to the linear dimension a rather than to the surface area. Is this result limited to ellipsoids? Discuss.

Chapter 15

Macroscopic Balances for Nonisothermal Systems

In Chapter 7 we discussed the macroscopic mass, momentum, angular momentum, and mechanical energy balances. The treatment there was restricted to systems at constant temperature. Actually this restriction is somewhat artificial, since in real flow systems mechanical energy is always being converted into thermal energy by viscous dissipation. What we really assumed in Chapter 7 is that any heat so produced is either too small to change the fluid properties or is immediately conducted away through the walls of the system containing the fluid. In this chapter we extend the previous results to describe the overall behavior of nonisothermal macroscopic flow systems.

For a nonisothermal system there are five macroscopic balances that describe the relations between the inlet and outlet conditions of the stream. They may be derived by integrating the equations of change over the macroscopic system:

$$\int_{V(t)} (\text{eq. of continuity})\, dV = \text{macroscopic mass balance}$$

$$\int_{V(t)} (\text{eq. of motion})\, dV = \text{macroscopic momentum balance}$$

$$\int_{V(t)} (\text{eq. of angular momentum})\, dV = \text{macroscopic angular momentum balance}$$

$$\int_{V(t)} (\text{eq. of mechanical energy})\, dV = \text{macroscopic mechanical energy balance}$$

$$\int_{V(t)} (\text{eq. of (total) energy})\, dV = \text{macroscopic (total) energy balance}$$

The first four of these were discussed in Chapter 7, and their derivations suggest that they can be applied to nonisothermal systems just as well as to isothermal systems. In this chapter we add the fifth balance—namely, that for the total energy. This is derived in §15.1, not by performing the integration above, but rather by applying the law of conservation of total energy directly to the system shown in Fig. 7.0-1. Then in §15.2 we revisit the mechanical energy balance and examine it in the light of the discussion of the

(total) energy balance. Next in §15.3 we give the simplified versions of the macroscopic balances for steady-state systems and illustrate their use.

In §15.4 we give the differential forms (*d*-forms) of the steady-state balances. In these forms, the entry and exit planes 1 and 2 are taken to be only a differential distance apart. The "*d*-forms" are frequently useful for problems involving flow in conduits in which the velocity, temperature, and pressure are continually changing in the flow direction.

Finally, in §15.5 we present several illustrations of unsteady-state problems that can be solved by the macroscopic balances.

This chapter will make use of nearly all the topics we have covered so far and provides an excellent opportunity to review the preceding chapters. Once again we take this opportunity to remind the reader that in using the macroscopic balances, it may be necessary to omit some terms and to estimate the values of others. This requires good intuition or some extra experimental data.

§15.1 THE MACROSCOPIC ENERGY BALANCE

We consider the system sketched in Fig. 7.0-1 and make the same assumptions that were made in Chapter 7 with regard to quantities at the entrance and exit planes:

(i) The time-smoothed velocity is perpendicular to the relevant cross section.

(ii) The density and other physical properties are uniform over the cross section.

(iii) The forces associated with the stress tensor $\boldsymbol{\tau}$ are neglected.

(iv) The pressure does not vary over the cross section.

To these we add (likewise at the entry and exit planes):

(v) The energy transport by conduction $\mathbf{q}$ is small compared to the convective energy transport and can be neglected.

(vi) The work associated with $[\boldsymbol{\tau} \cdot \mathbf{v}]$ can be neglected relative to $p\mathbf{v}$.

We now apply the statement of conservation of energy to the fluid in the macroscopic flow system. In doing this, we make use of the concept of potential energy to account for the work done against the external forces (this corresponds to using Eq. 11.1-9, rather than Eq. 11.1-7, as the equation of change for energy).

The statement of the law of conservation of energy then takes the form:

$$\underbrace{\frac{d}{dt}(U_{tot} + K_{tot} + \Phi_{tot})}_{\substack{\text{rate of increase of}\\ \text{internal, kinetic, and}\\ \text{potential energy in}\\ \text{the system}}} = \underbrace{(\rho_1\hat{U}_1\langle v_1\rangle + \tfrac{1}{2}\rho_1\langle v_1^3\rangle + \rho_1\hat{\Phi}_1\langle v_1\rangle)S_1}_{\substack{\text{rate at which internal, kinetic, and}\\ \text{potential energy enter the system}\\ \text{at plane 1 by flow}}}$$

$$\underbrace{- (\rho_2\hat{U}_2\langle v_2\rangle + \tfrac{1}{2}\rho_2\langle v_2^3\rangle + \rho_2\hat{\Phi}_2\langle v_2\rangle)S_2}_{\substack{\text{rate at which internal, kinetic, and}\\ \text{potential energy leave the system}\\ \text{at plane 2 by flow}}} \qquad (15.1\text{-}1)$$

$$\underbrace{+ Q}_{\substack{\text{rate at which}\\ \text{heat is added}\\ \text{to the system}\\ \text{across boundary}}} \quad \underbrace{+ W_m}_{\substack{\text{rate at which work is done on}\\ \text{the system by the surroundings}\\ \text{by means of the moving}\\ \text{surfaces}}} \quad \underbrace{+ (p_1\langle v_1\rangle S_1 - p_2\langle v_2\rangle S_2)}_{\substack{\text{rate at which work is}\\ \text{done on the system by the}\\ \text{surroundings at planes 1}\\ \text{and 2}}}$$

Here $U_{tot} = \int\rho\hat{U}dV$, $K_{tot} = \int\frac{1}{2}\rho v^2 dV$, and $\Phi_{tot} = \int\rho\hat{\Phi}dV$ are the total internal, kinetic, and potential energy in the system, the integrations being performed over the entire volume of the system.

This equation may be written in a more compact form by introducing the mass rates of flow $w_1 = \rho_1\langle v_1\rangle S_1$ and $w_2 = \rho_2\langle v_2\rangle S_2$, and the total energy $E_{tot} = U_{tot} + K_{tot} + \Phi_{tot}$. We thus get for the *unsteady state macroscopic energy balance*

$$\boxed{\frac{d}{dt}E_{tot} = -\Delta\left[\left(\hat{U} + p\hat{V} + \frac{1}{2}\frac{\langle v^3\rangle}{\langle v\rangle} + \hat{\Phi}\right)w\right] + Q + W_m} \tag{15.1-2}$$

It is clear, from the derivation of Eq. 15.1-1, that the "work done on the system by the surroundings" consists of two parts: (1) the work done by the moving surfaces W_m, and (2) the work done at the ends of the system (planes 1 and 2), which appears as $-\Delta(p\hat{V}w)$ in Eq. 15.1-2. Although we have combined the pV terms with the internal, kinetic, and potential energy terms in Eq. 15.1-2, it is inappropriate to say that "pV energy enters and leaves the system" at the inlet and outlet. The pV terms originate as work terms and should be thought of as such.

We now consider the situation where the system is operating at steady state so that the total energy E_{tot} is constant, and the mass rates of flow in and out are equal ($w_1 = w_2 = w$). Then it is convenient to introduce the symbols $\hat{Q} = Q/w$ (the heat addition per unit mass of flowing fluid) and $\hat{W}_m = W_m/w$ (the work done on a unit mass of flowing fluid). Then the *steady state macroscopic energy balance* is

$$\Delta\left(\hat{H} + \frac{1}{2}\frac{\langle v^3\rangle}{\langle v\rangle} + gh\right) = \hat{Q} + \hat{W}_m \tag{15.1-3}$$

Here we have written $\hat{\Phi}_1 = gh_1$ and $\hat{\Phi}_2 = gh_2$, where h_1 and h_2 are heights above an arbitrarily chosen datum plane (see the discussion just before Eq. 3.3-2). Similarly, $\hat{H}_1 = \hat{U}_1 + p_1\hat{V}_1$ and $\hat{H}_2 = \hat{U}_2 + p_2\hat{V}_2$ are enthalpies per unit mass measured with respect to an arbitrarily specified reference state. The explicit formula for the enthalpy is given in Eq. 9.8-8.

For many problems in the chemical industry the kinetic energy, potential energy, and work terms are negligible compared with the thermal terms in Eq. 15.1-3, and the energy balance simplifies to $\hat{H}_2 - \hat{H}_1 = \hat{Q}$, often called an "enthalpy balance." However this relation should not be construed as a conservation equation for enthalpy.

§15.2 THE MACROSCOPIC MECHANICAL ENERGY BALANCE

The macroscopic mechanical energy balance, given in §7.4 and derived in §7.8, is repeated here for comparison with Eqs. 15.1-2 and 3. The *unsteady-state macroscopic mechanical energy balance*, as given in Eq. 7.4-2, is

$$\boxed{\frac{d}{dt}(K_{tot} + \Phi_{tot}) = -\Delta\left(\frac{1}{2}\frac{\langle v^3\rangle}{\langle v\rangle} + \hat{\Phi} + \frac{p}{\rho}\right)w + W_m - E_c - E_v} \tag{15.2-1}$$

where E_c and E_v are defined in Eqs. 7.4-3 and 4. An approximate form of the *steady-state macroscopic mechanical balance*, as given in Eq. 7.4-7, is

$$\Delta\left(\frac{1}{2}\frac{\langle v^3\rangle}{\langle v\rangle}\right) + g\Delta h + \int_1^2 \frac{1}{\rho}\,dp = \hat{W}_m - \hat{E}_v \tag{15.2-2}$$

The details of the approximation introduced here are explained in Eqs. 7.8-9 to 12.

The integral in Eq. 15.2-2 must be evaluated along a "representative streamline" in the system. To do this, one must know the equation of state $\rho = \rho(p, T)$ and also how T changes with p along the streamline. In Fig. 15.2-1 the surface $\hat{V} = \hat{V}(p, T)$ for an ideal gas is shown. In the pT-plane there is shown a curve beginning at p_1, T_1 (the inlet stream conditions) and ending at p_2, T_2 (the outlet stream conditions). The curve in the pT-plane indicates the succession of states through which the gas passes in going from the initial

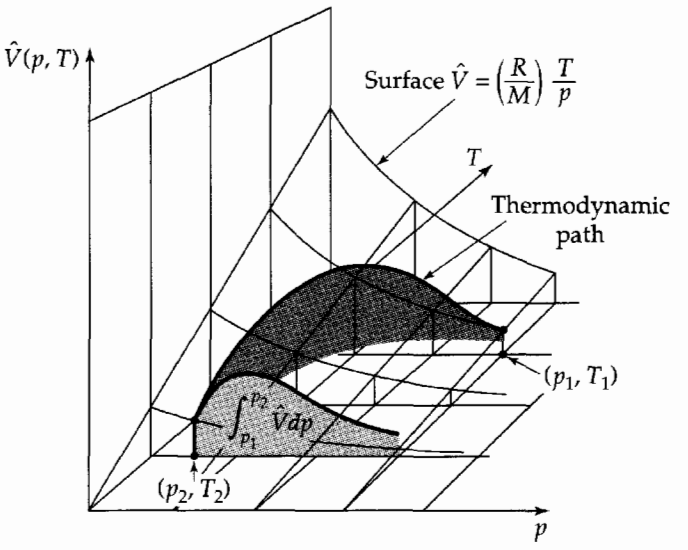

Fig. 15.2-1. Graphical representation of the integral in Eq. 15.2-2. The ruled area is $\int_{p_1}^{p_2} \hat{V}dp = \int_{p_1}^{p_2} (1/\rho)dp$. Note that the value of this integral is negative here, because we are integrating from right to left.

state to the final state. The integral $\int_1^2 (1/\rho)\, dp$ is then the projection of the shaded area in Fig. 15.2-1 onto the $p\hat{V}$-plane. It is evident that the value of this integral changes as the "thermodynamic path" of the process from plane 1 to 2 is altered. If one knows the path and the equation of state then one can compute $\int_1^2 (1/\rho)\, dp$.

In several special situations, it is not difficult to evaluate the integral:

a. For *isothermal systems,* the integral is evaluated by prescribing the isothermal equation of state—that is, by giving a relation for ρ as a function of p. For example, for ideal gases $\rho = pM/RT$ and

$$\int_1^2 \frac{1}{\rho}\, dp = \frac{RT}{M}\int_{p_1}^{p_2} \frac{1}{p}\, dp = \frac{RT}{M} \ln \frac{p_2}{p_1} \qquad \text{(ideal gases)} \qquad (15.2\text{-}3)$$

b. For *incompressible liquids,* ρ is constant so that

$$\int_1^2 \frac{1}{\rho}\, dp = \frac{1}{\rho}(p_2 - p_1) \qquad \text{(incompressible liquids)} \qquad (15.2\text{-}4)$$

c. For frictionless *adiabatic flow of ideal gases* with constant heat capacity, p and ρ are related by the expression $p\rho^{-\gamma}$ = constant, in which $\gamma = \hat{C}_p/\hat{C}_V$ as shown in Example 11.4-6. Then the integral becomes

$$\int_1^2 \frac{1}{\rho}\, dp = \frac{p_1^{1/\gamma}}{\rho_1}\int_{p_1}^{p_2} \frac{1}{p^{1/\gamma}}\, dp = \frac{p_1}{\rho_1}\frac{\gamma}{\gamma - 1}\left[\left(\frac{p_2}{p_1}\right)^{(\gamma-1)/\gamma} - 1\right]$$
$$= \frac{p_1}{\rho_1}\frac{\gamma}{\gamma - 1}\left[\left(\frac{\rho_2}{\rho_1}\right)^{\gamma-1} - 1\right] \qquad (15.2\text{-}5)$$

Hence for this special case of nonisothermal flow, the integration can be performed analytically.

We now conclude with several comments involving both the mechanical energy balance and the total energy balance. We emphasized in §7.8 that Eq. 7.4-2 (same as Eq. 15.2-1) is derived by taking the dot product of $\mathbf{v}$ with the equation of motion and then integrating the result over the volume of the flow system. Since we start with the equation of motion—which is a statement of the law of conservation of linear momentum—the mechanical energy balance contains information different from that of the (total) energy

balance, which is a statement of the law of conservation of energy. Therefore, in general, both balances are needed for problem solving. The mechanical energy balance is not "an alternative form" of the energy balance.

In fact, if we subtract the mechanical energy balance in Eq. 15.2-1 from the total energy balance in Eq. 15.1-2 we get the *macroscopic balance for the internal energy*

$$\boxed{\frac{dU_{tot}}{dt} = -\Delta\hat{U}w + Q + E_c + E_v} \tag{15.2-6}$$

This states that the total internal energy in the system changes because of the difference in the amount of internal energy entering and leaving the system by fluid flow, because of the heat entering (or leaving) the system through walls of the system, because of the heat produced (or consumed) within the fluid by compression (or expansion), and because of the heat produced in the system because of viscous dissipation heating. Equation 15.2-6 cannot be written a priori, since there is no conservation law for internal energy. It can, however, be obtained by integrating Eq. 11.2-1 over the entire flow system.

§15.3 USE OF THE MACROSCOPIC BALANCES TO SOLVE STEADY-STATE PROBLEMS WITH FLAT VELOCITY PROFILES

The most important applications of the macroscopic balances are to steady-state problems. Furthermore, it is usually assumed that the flow is turbulent so that the variation of the velocity over the cross section can be safely neglected (see "Notes" after Eqs. 7.2-3 and 7.4-7). The five macroscopic balances, with these additional restrictions, are summarized in Table 15.3-1. They have been generalized to multiple inlet and outlet ports to accommodate a larger set of problems.

Table 15.3-1 Steady-State Macroscopic Balances for Turbulent Flow in Nonisothermal Systems

Mass:	$\sum w_1 - \sum w_2 = 0$	(A)
Momentum:	$\sum(v_1 w_1 + p_1 S_1)\mathbf{u}_1 - \sum(v_2 w_2 + p_2 S_2)\mathbf{u}_2 + m_{\text{tot}}\mathbf{g} = \mathbf{F}_{f\to s}$	(B)
Angular momentum:	$\sum(v_1 w_1 + p_1 S_1)[\mathbf{r}_1 \times \mathbf{u}_1] - \sum(v_2 w_2 + p_2 S_2)[\mathbf{r}_2 \times \mathbf{u}_2] + \mathbf{T}_{\text{ext}} = \mathbf{T}_{f\to s}$	(C)
Mechanical energy:	$\sum\left(\frac{1}{2}v_1^2 + gh_1 + \frac{p_1}{\rho_1}\right)w_1 - \sum\left(\frac{1}{2}v_2^2 + gh_2 + \frac{p_2}{\rho_2}\right)w_2 = -W_m + E_c + E_v$	(D)
(Total) energy:	$\sum(\frac{1}{2}v_1^2 + gh_1 + \hat{H}_1)w_1 - \sum(\frac{1}{2}v_2^2 + gh_2 + \hat{H}_2)w_2 = -W_m - Q$	(E)

Notes:

[a] All formulas here imply flat velocity profiles.

[b] $\Sigma w_1 = w_{1a} + w_{1b} + w_{1c} + \cdots$, where $w_{1a} = \rho_{1a} v_{1a} S_{1a}$, and so on.

[c] h_1 and h_2 are elevations above an arbitrary datum plane.

[d] $\hat{H}_1$ and $\hat{H}_2$ are enthalpies per unit mass relative to some arbitrarily chosen reference state (see Eq. 9.8-8).

[e] All equations are written for compressible flow; for incompressible flow, $E_c = 0$. The quantities E_c and E_v are defined in Eqs. 7.3-3 and 4.

[f] $\mathbf{u}_1$ and $\mathbf{u}_2$ are unit vectors in the direction of flow.

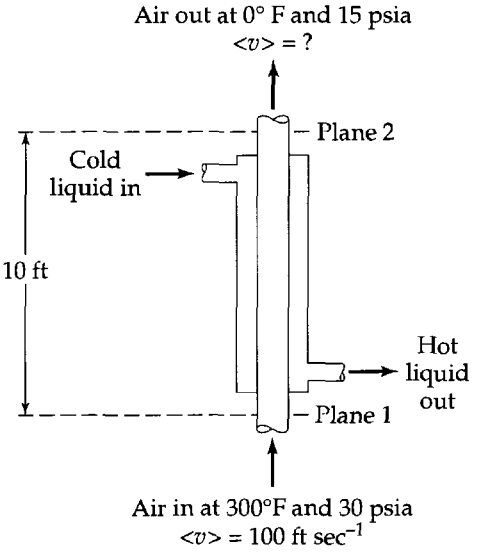

Fig. 15.3-1. The cooling of air in a countercurrent heat exchanger.

EXAMPLE 15.3-1

The Cooling of an Ideal Gas

Two hundred pounds per hour of dry air enter the inner tube of the heat exchanger shown in Fig. 15.3-1 at 300°F and 30 psia, with a velocity of 100 ft/sec. The air leaves the exchanger at 0°F and 15 psia, at 10 ft above the exchanger entrance. Calculate the rate of energy removal across the tube wall. Assume turbulent flow and ideal gas behavior, and use the following expression for the heat capacity of air:

$$\tilde{C}_p = 6.39 + (9.8 \times 10^{-4})T - (8.18 \times 10^{-8})T^2 \tag{15.3-1}$$

where $\tilde{C}_p$ is in Btu/(lb-mole · R) and T is in degrees R.

SOLUTION

For this system, the macroscopic energy balance, Eq. 15.1-3, becomes

$$(\hat{H}_2 - \hat{H}_1) + \tfrac{1}{2}(v_2^2 - v_1^2) + g(h_2 - h_1) = \hat{Q} \tag{15.3-2}$$

The enthalpy difference may be obtained from Eq. 9.8-8, and the velocity may be obtained as a function of temperature and pressure with the aid of the macroscopic mass balance $\rho_1 v_1 = \rho_2 v_2$ and the ideal gas law $p = \rho RT/M$. Hence Eq. 15.3-2 becomes

$$\frac{1}{M}\int_{T_1}^{T_2} \tilde{C}_p dT + \frac{1}{2}v_1^2\left[\left(\frac{p_1 T_2}{p_2 T_1}\right)^2 - 1\right] + g(h_2 - h_1) = \hat{Q} \tag{15.3-3}$$

The explicit expression for $\tilde{C}_p$ in Eq. 15.3-1 may then be inserted into Eq. 15.3-3 and the integration performed. Next substitution of the numerical values gives the heat removal per pound of fluid passing through the heat exchanger:

$$\begin{aligned} -\hat{Q} &= \tfrac{1}{29}[(6.39)(300) + \tfrac{1}{2}(9.8 \times 10^{-4})(5.78 - 2.12)(10^5) \\ &\quad -\tfrac{1}{3}(8.18 \times 10^{-8})(4.39 - 0.97)(10^8)] \\ &\quad +\frac{1}{2}\left(\frac{10^4}{(32.2)(778)}\right)[1 - (1.21)^2] - \left(\frac{10}{778}\right) \\ &= 72.0 - 0.093 - 0.0128 \\ &= 71.9 \text{ Btu/hr} \end{aligned} \tag{15.3-4}$$

The rate of heat removal is then

$$-\hat{Q}w = 14{,}380 \text{ Btu/hr} \tag{15.3-5}$$

Note, in Eq. 15.3-4, that the kinetic and potential energy contributions are negligible in comparison with the enthalpy change.

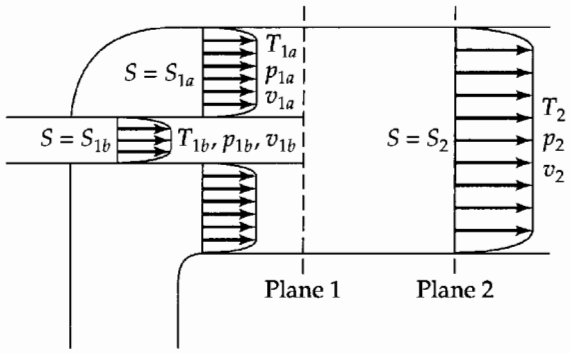

Fig. 15.3-2. The mixing of two ideal gas streams.

EXAMPLE 15.3-2

Mixing of Two Ideal Gas Streams

Two steady, turbulent streams of the same ideal gas flowing at different velocities, temperatures, and pressures are mixed as shown in Fig. 15.3-2. Calculate the velocity, temperature, and pressure of the resulting stream.

SOLUTION

The fluid behavior in this example is more complex than that for the incompressible, isothermal situation discussed in Example 7.6-2, because here changes in density and temperature may be important. We need to use the steady-state macroscopic energy balance, Eq. 15.2-3, and the ideal gas equation of state, in addition to the mass and momentum balances. With these exceptions, we proceed as in Example 7.6-2.

We choose the inlet planes (1a and 1b) to be cross sections at which the fluids first begin to mix. The outlet plane (2) is taken far enough downstream that complete mixing has occurred. As in Example 7.6-2 we assume flat velocity profiles, negligible shear stresses on the pipe wall, and no changes in the potential energy. In addition, we neglect the changes in the heat capacity of the fluid and assume adiabatic operation. We now write the following equations for this system with two entry ports and one exit port:

Mass:
$$w_1 = w_{1a} + w_{1b} = w_2 \tag{15.3-6}$$

Momentum:
$$v_2 w_2 + p_2 S_2 = v_{1a} w_{1a} + p_{1a} S_{1a} + v_{1b} w_{1b} + p_{1b} S_{1b} \tag{15.3-7}$$

Energy:
$$w_2[\hat{C}_p(T_2 - T_{\text{ref}}) + \tfrac{1}{2}v_2^2] = w_{1a}[\hat{C}_p(T_{1a} - T_{\text{ref}}) + \tfrac{1}{2}v_{1a}^2] + w_{1b}[\hat{C}_p(T_{1b} - T_{\text{ref}}) + \tfrac{1}{2}v_{1b}^2] \tag{15.3-8}$$

Equation of state:
$$p_2 = \rho_2 R T_2 / M \tag{15.3-9}$$

In this set of equations we know all the quantities at 1a and 1b, and the four unknowns are p_2, T_2, ρ_2, and v_2. T_{ref} is the reference temperature for the enthalpy. By multiplying Eq. 15.3-6 by $\hat{C}_p T_{\text{ref}}$ and adding the result to Eq. 15.3-8 we get

$$w_2[\hat{C}_p T_2 + \tfrac{1}{2}v_2^2] = w_{1a}[\hat{C}_p T_{1a} + \tfrac{1}{2}v_{1a}^2] + w_{1b}[\hat{C}_p T_{1b} + \tfrac{1}{2}v_{1b}^2] \tag{15.3-10}$$

The right sides of Eqs. 15.3-6, 7, and 10 contain known quantities and we designate them by w, P, and E, respectively. Note that w, P, and E are not independent, because the pressure, temperature, and density of each inlet stream must be related by the equation of state.

We now solve Eq. 15.3-7 for v_2 and eliminate p_2 by using the ideal gas law. In addition we write w_2 as $\rho_2 v_2 S_2$. This gives

$$v_2 + \frac{RT_2}{Mv_2} = \frac{P}{w} \tag{15.3-11}$$

This equation can be solved for T_2, which is inserted into Eq. 15.3-10 to give

$$v_2^2 - \left[2\left(\frac{\gamma}{\gamma+1}\right)\frac{P}{w}\right]v_2 + 2\left(\frac{\gamma-1}{\gamma+1}\right)\frac{E}{w} = 0 \tag{15.3-12}$$

in which $\gamma = C_p/C_V$, a quantity which varies from about 1.1 to 1.667 for gases. Here we have used the fact that $C_p/R = \gamma/(\gamma - 1)$ for an ideal gas. When Eq. 15.3-12 is solved for v_2 we get

$$v_2 = \left(\frac{\gamma}{\gamma+1}\right)\frac{P}{w}\left[1 \pm \sqrt{1 - 2\left(\frac{\gamma^2-1}{\gamma^2}\right)\frac{wE}{P^2}}\right] \tag{15.3-13}$$

On physical grounds, the radicand cannot be negative. It can be shown (see Problem 15B.4) that, when the radicand is zero, the velocity of the final stream is sonic. Therefore, in general one of the solutions for v_2 is supersonic and one is subsonic. Only the lower (subsonic) solution can be obtained in the turbulent mixing process under consideration, since supersonic duct flow is unstable. The transition from supersonic to subsonic duct flow is illustrated in Example 11.4-7.

Once the velocity v_2 is known, the pressure and temperature may be calculated from Eqs. 15.3-7 and 11. The mechanical energy balance can be used to get $(E_c + E_v)$.

§15.4 THE *d*-FORMS OF THE MACROSCOPIC BALANCES

The estimation of E_v in the mechanical energy balance and Q in the total energy balance often presents some difficulties in nonisothermal systems.

For example, for E_v, consider the following two nonisothermal situations:

a. For liquids, the average flow velocity in a tube of constant cross section is nearly constant. However, the viscosity may change markedly in the direction of the flow because of the temperature changes, so that f in Eq. 7.5-9 changes with distance. Hence Eq. 7.5-9 cannot be applied to the entire pipe.

b. For gases, the viscosity does not change much with pressure, so that the local Reynolds number and local friction factor are nearly constant for ducts of constant cross section. However, the average velocity may change considerably along the duct as a result of the change in density with temperature. Hence Eq. 7.5-9 cannot be applied to the entire duct.

Similarly for pipe flow with the wall temperature changing with distance, it may be necessary to use local heat transfer coefficients. For such a situation, we can write Eq. 15.1-3 on an incremental basis and generate a differential equation. Or the cross sectional area of the conduit may be changing with downstream distance, and this situation also results in a need for handling the problem on an incremental basis.

It is therefore useful to rewrite the steady-state macroscopic mechanical energy balance and the total energy balance by taking planes 1 and 2 to be a differential distance dl apart. We then obtain what we call the "*d*-forms" of the balances:

The *d*-Form of the Mechanical Energy Balance

If we take planes 1 and 2 to be a differential distance apart, then we may write Eq. 15.2-2 in the following differential form (assuming flat velocity profiles):

$$d(\tfrac{1}{2}v^2) + gdh + \frac{1}{\rho}dp = d\hat{W} - d\hat{E}_v \tag{15.4-1}$$

Then using Eq. 7.5-9 for a differential length dl, we write

$$vdv + gdh + \frac{1}{\rho}dp = d\hat{W} - \tfrac{1}{2}v^2\frac{f}{R_h}dl \tag{15.4-2}$$

in which f is the local friction factor, and R_h is the local value of the mean hydraulic radius. In most applications we omit the $d\hat{W}$ term, since work is usually done at isolated points along the flow path. The term $d\hat{W}$ would be needed in tubes with extensible walls, magnetically driven flows, or systems with transport by rotating screws.

The *d*-Form of the Total Energy Balance

If we write Eq. 15.1-3 in differential form, we have (with flat velocity profiles)

$$d(\tfrac{1}{2}v^2) + gdh + d\hat{H} = d\hat{Q} + d\hat{W} \tag{15.4-3}$$

Then using Eq. 9.8-7 for $d\hat{H}$ and Eq. 14.1-8 for $d\hat{Q}$ we get

$$vdv + gdh + \hat{C}_p dT + \left[\hat{V} - T\left(\frac{\partial \hat{V}}{\partial T}\right)_p\right]dp = \frac{U_{loc} Z \Delta T}{w} dl + d\hat{W} \tag{15.4-4}$$

in which U_{loc} is the local overall heat transfer coefficient, Z is the corresponding local conduit perimeter, and ΔT is the local temperature difference between the fluids inside and outside of the conduit.

The examples that follow illustrate applications of Eqs. 15.4-2 and 15.4-4.

EXAMPLE 15.4-1

Parallel- or Counter-Flow Heat Exchangers

It is desired to describe the performance of the simple double-pipe heat exchanger shown in Fig. 15.4-1 in terms of the heat transfer coefficients of the two streams and the thermal resistance of the pipe wall. The exchanger consists essentially of two coaxial pipes with one fluid stream flowing through the inner pipe and another in the annular space; heat is transferred across the wall of the inner pipe. Both streams may flow in the same direction, as indicated in the figure, but normally it is more efficient to use counter flow—that is, to reverse the direction of one stream so that either w_h or w_c is negative. Steady-state turbulent flow may be assumed, and the heat losses to the surroundings may be neglected. Assume further that the local overall heat transfer coefficient is constant along the exchanger.

SOLUTION

(a) Macroscopic energy balance for each stream as a whole. We designate quantities referring to the hot stream with a subscript h and the cold stream with subscript c. The steady-state energy balance in Eq. 15.1-3 becomes, for negligible changes in kinetic and potential energy,

$$w_h(\hat{H}_{h2} - \hat{H}_{h1}) = Q_h \tag{15.4-5}$$

$$w_c(\hat{H}_{c2} - \hat{H}_{c1}) = Q_c \tag{15.4-6}$$

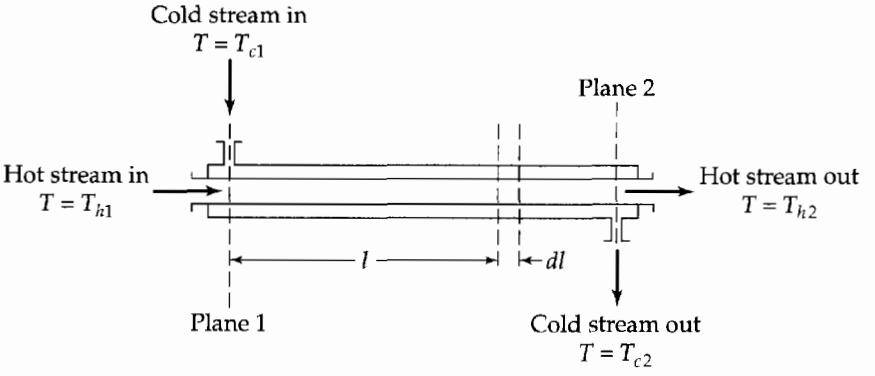

Fig. 15.4-1. A double-pipe heat exchanger.

Because there is no heat loss to the surroundings, $Q_h = -Q_c$. For incompressible liquids with a pressure drop that is not too large, or for ideal gases, Eq. 9.8-8 gives for constant $\hat{C}_p$ the relation $\Delta\hat{H} = \hat{C}_p\Delta T$. Hence Eqs. 15.4-5 and 6 can be rewritten as

$$w_h\hat{C}_{ph}(T_{h2} - T_{h1}) = Q_h \tag{15.4-7}$$

$$w_c\hat{C}_{pc}(T_{c2} - T_{c1}) = Q_c = -Q_h \tag{15.4-8}$$

(b) d-form of the macroscopic energy balance. Application of Eq. 15.4-4 to the hot stream gives

$$\hat{C}_{ph}dT_h = \frac{U_0(2\pi r_0)(T_c - T_h)}{w_h}dl \tag{15.4-9}$$

where r_0 is the outside radius of the inner tube, and U_0 is the overall heat transfer coefficient based on the radius r_0 (see Eq. 14.1-8).

Rearrangement of Eq. 15.4-9 gives

$$\frac{dT_h}{T_c - T_h} = U_0\frac{(2\pi r_0)dl}{w_h\hat{C}_{ph}} \tag{15.4-10}$$

The corresponding equation for the cold stream is

$$-\frac{dT_c}{T_c - T_h} = U_0\frac{(2\pi r_0)dl}{w_c\hat{C}_{pc}} \tag{15.4-11}$$

Adding Eqs. 15.4-10 and 11 gives a differential equation for the temperature difference of the two fluids as a function of l:

$$-\frac{d(T_h - T_c)}{T_h - T_c} = U_0\left(\frac{1}{w_h\hat{C}_{ph}} + \frac{1}{w_c\hat{C}_{pc}}\right)(2\pi r_0)dl \tag{15.4-12}$$

By assuming that U_0 is independent of l and integrating from plane 1 to plane 2, we get

$$\ln\left(\frac{T_{h1} - T_{c1}}{T_{h2} - T_{c2}}\right) = U_0\left(\frac{1}{w_h\hat{C}_{ph}} + \frac{1}{w_c\hat{C}_{pc}}\right)(2\pi r_0)L \tag{15.4-13}$$

This expression relates the terminal temperatures to the stream rates and exchanger dimensions, and it can thus be used to describe the performance of the exchanger. However, it is conventional to rearrange Eq. 15.4-13 by taking advantage of the steady-state energy balances in Eq. 15.4-7 and 8. We solve each of these equations for $w\hat{C}_p$ and substitute the results into Eq. 15.4-13 to obtain

$$Q_c = U_0(2\pi r_0L)\left(\frac{(T_{h2} - T_{c2}) - (T_{h1} - T_{c1})}{\ln[(T_{h2} - T_{c2})/(T_{h1} - T_{c1})]}\right) \tag{15.4-14}$$

or

$$Q_c = U_0A_0(T_h - T_c)_{\ln} \tag{15.4-15}$$

Here A_0 is the total outer surface of the inner tube, and $(T_h - T_c)_{\ln}$ is the "logarithmic mean temperature difference" between the two streams. Equations 15.4-14 and 15 describe the rate of heat exchange between the two streams and find wide application in engineering practice. Note that the stream rates do not appear explicitly in these equations, which are valid for both parallel-flow and counter-flow exchangers (see Problem 15A.1).

From Eqs. 15.4-10 and 11 we can also get the stream temperatures as functions of l if desired. Considerable care must be used in applying the results of this example to laminar flow, for which the variation of the overall heat transfer coefficient may be quite large. An example of a problem with variable U_0 is Problem 15B.1.

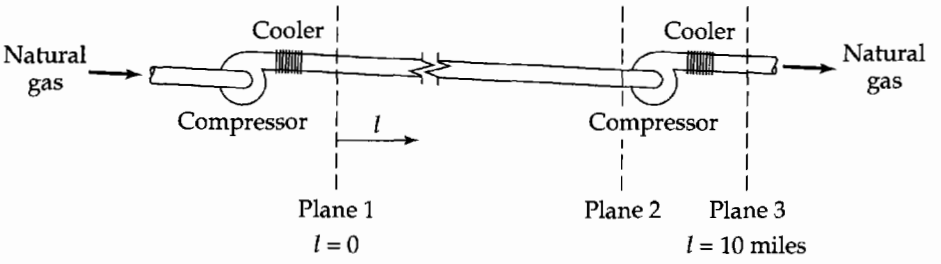

Fig. 15.4-2. Pumping a compressible fluid through a pipeline.

EXAMPLE 15.4-2

Power Requirement for Pumping a Compressible Fluid through a Long Pipe

A natural gas, which may be considered to be pure methane, is to be pumped through a long, smooth pipeline with a 2-ft inside diameter. The gas enters the line at 100 psia with a velocity of 40 ft/s and at the ambient temperature of 70°F. Pumping stations are provided every 10 miles along the line, and at each of these stations the gas is recompressed and cooled to its original temperature and pressure (see Fig. 15.4-2). Estimate the power that must be expended on the gas at each pumping station, assuming ideal gas behavior, flat velocity profiles, and negligible changes in elevation.

SOLUTION

We find it convenient to consider the pipe and compressor separately. First we apply Eq. 15.4-2 to a length dl of the pipe. We then integrate this equation between planes 1 and 2 to obtain the unknown pressure p_2. Once this is known, we may apply Eq. 15.2-2 to the system between planes 2 and 3 to obtain the work done by the pump.

(a) Flow through the pipe. For this portion of the system, Eq. 15.4-2 simplifies to

$$vdv + \frac{1}{\rho}dp + \frac{2v^2 f}{D}dl = 0 \tag{15.4-16}$$

where D is the pipe diameter. Since the pipe is quite long, we assume that the fluid is isothermal at 70°F. We may then eliminate both v and ρ from Eq. 15.4-16 by use of the assumed equation of state, $p = \rho RT/M$, and the macroscopic mass balance, which may be written $\rho v = \rho_1 v_1$. With ρ and v written in terms of the pressure, Eq. 15.4-16 becomes

$$-\frac{1}{p}dp + \frac{RT_1}{M(p_1 v_1)^2}pdp + \frac{2f}{D}dl = 0 \tag{15.4-17}$$

We pointed out in §1.3 that the viscosity of ideal gases is independent of the pressure. From this it follows that the Reynolds number of the gas, $\mathrm{Re} = Dw/S\mu$, and hence the friction factor f, must be constants. We may then integrate Eq. 15.4-17 to obtain

$$-\ln\frac{p_2}{p_1} + \frac{1}{2}\left[\left(\frac{p_2}{p_1}\right)^2 - 1\right]\frac{RT_1}{Mv_1^2} + \frac{2fL}{D} = 0 \tag{15.4-18}$$

This equation gives p_2 in terms of quantities that are already known, except for f, which is easily calculated: the kinematic viscosity of methane at 100 psi and 70 F is about 2.61×10^{-5} ft^2/s, and therefore $\mathrm{Re} = Dv/\nu = (200\text{ ft})(40\text{ ft/s})/(2.61\text{ ft}^2/\text{s}) = 3.07 \times 10^6$. The friction factor can then be estimated to be 0.0025 (see Fig. 6.2-2).

Substituting numerical values into Eq. 15.4-18, we get

$$-\ln\frac{p_2}{p_1} + \frac{1}{2}\left[\left(\frac{p_2}{p_1}\right)^2 - 1\right]\frac{(1545)(530)(32.2)}{(16.04)(40)^2} + \frac{(2)(0.0025)(52{,}800)}{(2.00)} = 0 \tag{15.4-19}$$

or

$$-\ln\frac{p_2}{p_1}+513\left[\left(\frac{p_2}{p_1}\right)^2-1\right]+132=0 \tag{15.4-20}$$

By solving this equation with $p_1 = 100$ psia, we obtain $p_2 = 86$ psia.

(b) Flow through the compressor. We are now ready to apply the mechanical energy balance to the compressor. We start by putting Eq. 15.2-2 into the form

$$\hat{W}_m=\tfrac{1}{2}(v_3^2-v_2^2)+\int_{p_2}^{p_3}\frac{1}{\rho}dp+\hat{E}_v \tag{15.4-21}$$

To evaluate the integral in this equation, we assume that the compression is adiabatic and further that $\hat{E}_v$ between planes 2 and 3 can be neglected. We may use Eq. 15.2-5 to rewrite Eq. 15.2-21 as

$$\begin{aligned}\hat{W}_m&=\tfrac{1}{2}(v_3^2-v_2^2)+\frac{p_2^{1/\gamma}}{\rho_2}\int_{p_2}^{p_3}p^{-1/\gamma}dp\\&=\frac{v_1^2}{2}\left[1-\left(\frac{p_1}{p_2}\right)^2\right]+\frac{RT_2}{M}\frac{\gamma}{\gamma-1}\left[\left(\frac{p_1}{p_2}\right)^{(\gamma-1)/\gamma}-1\right]\end{aligned} \tag{15.4-22}$$

in which $\hat{W}_m$ is the energy required of the compressor. By substituting numerical values into Eq. 15.4-22, we get

$$\begin{aligned}\hat{W}_m&=\frac{(40)^2}{2(32.2)}[1-(1.163)^2]+\frac{(1545)(530)}{16}\frac{1.3}{0.3}(1.163^{0.3/1.3}-1)\\&=-9+7834=7825\text{ ft lb}_f/\text{lb}_m\end{aligned} \tag{15.4-23}$$

The power required to compress the fluid is

$$\begin{aligned}w\hat{W}_m&=\left(\frac{\pi D^2}{4}\right)\left(\frac{p_1M}{RT_1}\right)v_1\hat{W}_m\\&=\frac{\pi(100)(16.04)(40)}{(10.73)(530)}(7825)\text{ ft lb}_f/\text{s}\\&=277{,}000\text{ ft lb}_f/\text{s}=504\text{ hp}\end{aligned} \tag{15.4-24}$$

The power required would be virtually the same if the flow in the pipeline were adiabatic (see Problem 15A.2).

The assumptions used here—assuming the compression to be adiabatic and neglecting the viscous dissipation—are conventional in the design of compressor–cooler combinations. Note that the energy required to run the compressor is greater than the calculated work, $\hat{W}_m$, by (i) $\hat{E}_v$ between planes 2 and 3, (ii) mechanical losses in the compressor itself, and (iii) errors in the assumed p–ρ path. Normally the energy required at the pump shaft is at least 15 to 20% greater than $\hat{W}_m$.

§15.5 USE OF THE MACROSCOPIC BALANCES TO SOLVE UNSTEADY-STATE PROBLEMS AND PROBLEMS WITH NONFLAT VELOCITY PROFILES

In Table 15.5-1 we summarize all five macroscopic balances for unsteady state and nonflat velocity profiles, and for systems with multiple entry and exit ports. One practically never needs to use these balances in this degree of completeness, but it is convenient to have the entire set of equations collected in one place. We illustrate their use in the examples that follow.

Table 15.5-1 Unsteady-State Macroscopic Balances for Flow in Nonisothermal Systems

Mass:	$\frac{d}{dt} m_{\text{tot}} = \sum w_1 - \sum w_2 = \sum \rho_1 \langle v_1 \rangle S_1 - \sum \rho_2 \langle v_2 \rangle S_2$	(A)
Momentum:	$\frac{d}{dt} \mathbf{P}_{\text{tot}} = \sum \left(\frac{\langle v_1^2 \rangle}{\langle v_1 \rangle} w_1 + p_1 S_1 \right) \mathbf{u}_1 - \sum \left(\frac{\langle v_2^2 \rangle}{\langle v_2 \rangle} w_2 + p_2 S_2 \right) \mathbf{u}_2 + m_{\text{tot}} \mathbf{g} - \mathbf{F}_{f \to s}$	(B)
Angular momentum:	$\frac{d}{dt} \mathbf{L}_{\text{tot}} = \sum \left(\frac{\langle v_1^2 \rangle}{\langle v_1 \rangle} w_1 + p_1 S_1 \right) [\mathbf{r}_1 \times \mathbf{u}_1] - \sum \left(\frac{\langle v_2^2 \rangle}{\langle v_2 \rangle} w_2 + p_2 S_2 \right) [\mathbf{r}_2 \times \mathbf{u}_2] + \mathbf{T}_{\text{ext}} - \mathbf{T}_{f \to s}$	(C)
Mechanical energy:	$\frac{d}{dt} (K_{\text{tot}} + \Phi_{\text{tot}}) = \sum \left(\frac{1}{2} \frac{\langle v_1^3 \rangle}{\langle v_1 \rangle} + g h_1 + \frac{p_1}{\rho_1} \right) w_1 - \sum \left(\frac{1}{2} \frac{\langle v_2^3 \rangle}{\langle v_2 \rangle} + g h_2 + \frac{p_2}{\rho_2} \right) w_2 + W_m - E_c - E_v$	(D)
(Total) energy:	$\frac{d}{dt} (K_{\text{tot}} + \Phi_{\text{tot}} + U_{\text{tot}}) = \sum \left(\frac{1}{2} \frac{\langle v_1^3 \rangle}{\langle v_1 \rangle} + g h_1 + \hat{H}_1 \right) w_1 - \sum \left(\frac{1}{2} \frac{\langle v_2^3 \rangle}{\langle v_2 \rangle} + g h_2 + \hat{H}_2 \right) w_2 + W_m + Q$	(E)

Notes:

[a] $\Sigma w_1 = w_{1a} + w_{1b} + w_{1c} + \cdots$, where $w_{1a} = \rho_{1a} v_{1a} S_{1a}$, and so on.

[b] h_1 and h_2 are elevations above an arbitrary datum plane.

[c] $\hat{H}_1$ and $\hat{H}_2$ are enthalpies per unit mass relative to some arbitrarily chosen reference state; the formula for $\hat{H}$ is given in Eq. 9.8-8.

[d] All equations are written for compressible flow; for incompressible flow, $E_c = 0$. The quantities E_c and E_v are defined in Eqs. 7.3-3 and 4.

[e] $\mathbf{u}_1$ and $\mathbf{u}_2$ are unit vectors in the direction of flow.

EXAMPLE 15.5-1

Heating of a Liquid in an Agitated Tank[1]

A cylindrical tank capable of holding 1000 ft^3 of liquid is equipped with an agitator having sufficient power to keep the liquid contents at a uniform temperature (see Fig. 15.5-1). Heat is transferred to the contents by means of a coil arranged in such a way that the area available for heat transfer is proportional to the quantity of liquid in the tank. This heating coil consists of 10 turns, 4 ft in diameter, of 1-in. o.d. tubing. Water at 20°C is fed into this tank at a rate of 20 lb/min, starting with no water in the tank at time $t = 0$. Steam at 105°C flows through the

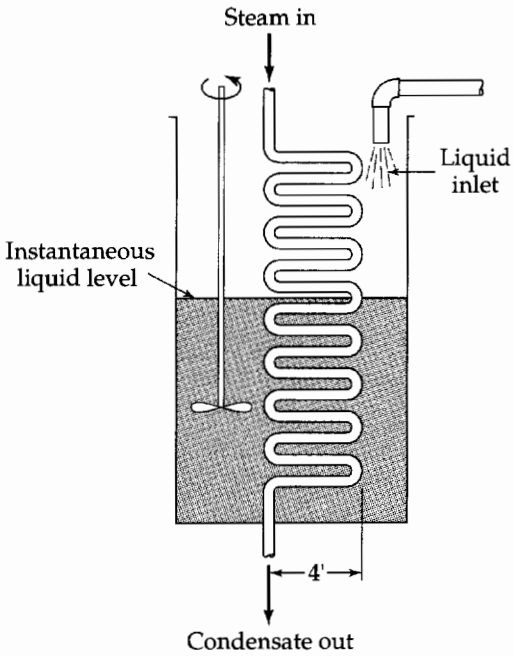

Fig. 15.5-1. Heating of a liquid in a tank with a variable liquid level.

[1] This problem is taken in modified form from W. R. Marshall, Jr., and R. L. Pigford, *Applications of Differential Equations to Chemical Engineering Problems*, University of Delaware Press, Newark, Del. (1947), pp. 16–18.

heating coil, and the overall heat transfer coefficient is 100 Btu/hr · ft² · F. What is the temperature of the water when the tank is filled?

SOLUTION

We shall make the following assumptions:

a. The steam temperature is uniform throughout the coil.

b. The density and heat capacity do not change very much with temperature.

c. The fluid is approximately incompressible so that $\hat{C}_p \approx \hat{C}_V$.

d. The agitator maintains uniform temperature throughout the liquid.

e. The heat transfer coefficient is independent of position and time.

f. The walls of the tank are perfectly insulated so that no heat loss occurs.

We select the fluid within the tank as the system to be considered, and we make a time-dependent energy balance over this system. Such a balance is provided by Eq. (E) of Table 15.5-1. On the left side of the equation the time rates of change of kinetic and potential energies can be neglected relative to that of the internal energy. On the right side we can normally omit the work term, and the kinetic and potential energy terms can be discarded, since they will be small compared with the other terms. Inasmuch as there is no outlet stream, we can set w_2 equal to zero. Hence for this system the total energy balance simplifies to

$$\frac{d}{dt} U_{\text{tot}} = w_1 \hat{H}_1 + Q \tag{15.5-1}$$

This states that the internal energy of the system increases because of the enthalpy added by the incoming fluid, and because of the addition of heat through the steam coil.

Since U_{tot} and $\hat{H}_1$ cannot be given absolutely, we now select the inlet temperature T_1 as the thermal datum plane. Then $\hat{H}_1 = 0$ and $U_{\text{tot}} = \rho\hat{C}_V V(T - T_1) \approx \rho\hat{C}_p V(T - T_1)$, where T and V are the instantaneous temperature and volume of the liquid. Furthermore, the rate of heat addition to the liquid Q is given by $Q = U_0 A(T_s - T)$, in which T_s is the steam temperature, and A is the instantaneous heat transfer area. Hence Eq. 15.5-1 becomes

$$\rho\hat{C}_p \frac{d}{dt} V(T - T_1) = U_0 A(T_s - T) \tag{15.5-2}$$

The expressions for $V(t)$ and $A(t)$ are

$$V(t) = \frac{w_1}{\rho} t \qquad A(t) = \frac{V}{V_0} A_0 = \frac{w_1 t}{\rho V_0} A_0 \tag{15.5-3}$$

in which V_0 and A_0 are the volume and heat transfer area when the tank is full. Hence the energy balance equation becomes

$$w_1\hat{C}_p t \frac{d}{dt}(T - T_1) + w_1\hat{C}_p(T - T_1) = \frac{w_1 t}{\rho V_0} U_0 A_0 (T_s - T) \tag{15.5-4}$$

which is to be solved with the initial condition that $T = T_1$ at $t = 0$.

The equation is more easily solved in dimensionless form. We divide both sides by $w_1\hat{C}_p(T_s - T_1)$ to get

$$t \frac{d}{dt}\left(\frac{T - T_1}{T_s - T_1}\right) + \left(\frac{T - T_1}{T_s - T_1}\right) = \frac{U_0 A_0 t}{\rho\hat{C}_p V_0}\left(\frac{T_s - T}{T_s - T_1}\right) \tag{15.5-5}$$

This equation suggests that suitable definitions of dimensionless temperature and time are

$$\Theta = \left(\frac{T - T_1}{T_s - T_1}\right) \quad \text{and} \quad \tau = \frac{U_0 A_0 t}{\rho\hat{C}_p V_0} \tag{15.5-6, 7}$$

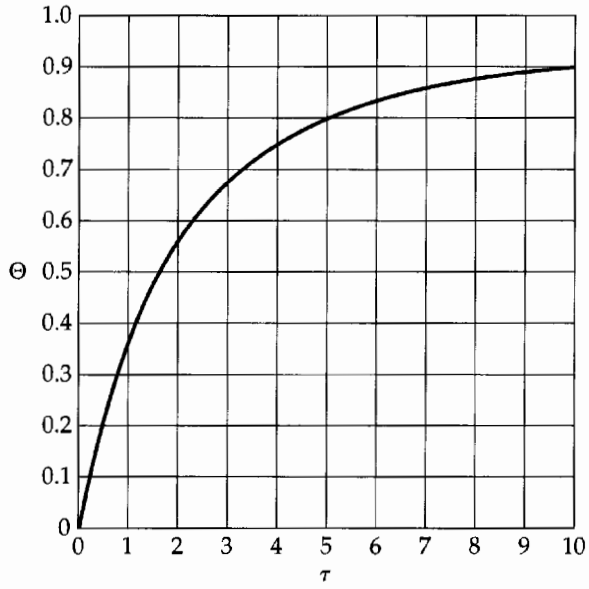

Fig. 15.5-2. Plot of dimensionless temperature, $\Theta = (T - T_1)/(T_s - T_1)$, versus dimensionless time, $\tau = (U_0A_0/\rho\hat{C}_pV_0)t$, according to Eq. 15.5-10. [W. R. Marshall and R. L. Pigford, *Application of Differential Equations to Chemical Engineering*, University of Delaware Press, Newark, Del. (1947), p. 18.]

Then the equation in Eq. 15.5-5 becomes after some rearranging

$$\frac{d\Theta}{d\tau} + \left(1 + \frac{1}{\tau}\right)\Theta = 1 \tag{15.5-8}$$

and the initial condition requires that $\Theta = 0$ at $\tau = 0$.

This is a first-order linear differential equation whose solution is (see Eq. C.1-2)

$$\Theta = 1 - \frac{1 - Ce^{-\tau}}{\tau} \tag{15.5-9}$$

The constant of integration, C, can be obtained from the initial condition after first multiplying Eq. 15.5-9 by τ. In that way it is found that $C = 1$, so that the final solution is

$$\Theta = 1 - \frac{1 - e^{-\tau}}{\tau} \tag{15.5-10}$$

This function is shown in Fig. 15.5-2.

Finally, the temperature T_0 of the liquid in the tank, when it has been filled, is given by Eq. 15.5-10 when $t = \rho V_0/w_1$ (from Eq. 15.5-3) or $\tau = U_0A_0/w_1\hat{C}_p$ (from Eq. 15.5-7). Therefore, in terms of the original variables,

$$\frac{T_0 - T_1}{T_s - T_1} = 1 - \frac{1 - \exp(-U_0A_0/w_1\hat{C}_p)}{U_0A_0/w_1\hat{C}_p} \tag{15.5-11}$$

Thus it can be seen that the final liquid temperature is determined entirely by the dimensionless group $U_0A_0/w_1\hat{C}_p$ which, for this problem, has the value of 2.74. Knowing this we can find from Eq. 15.5-11 that $(T_0 - T_1)/(T_s - T_1) = 0.659$, whence $T_0 = 76°C$.

EXAMPLE 15.5-2

Operation of a Simple Temperature Controller

A well-insulated agitated tank is shown in Fig. 15.5-3. Liquid enters at a temperature $T_1(t)$, which may vary with time. It is desired to control the temperature, $T_2(t)$, of the fluid leaving the tank. It is presumed that the stirring is sufficiently thorough that the temperature in the tank is uniform and equal to the exit temperature. The volume of the liquid in the tank, V, and the mass rate of liquid flow, w, are both constant.

To accomplish the desired control, a metallic electric heating coil of surface area A is placed in the tank, and a temperature-sensing element is placed in the exit steam to measure $T_2(t)$. These devices are connected to a temperature controller that supplies energy to the heating coil at a rate $Q_e = b(T_{max} - T_2)$, in which T_{max} is the maximum temperature for which the controller is designed to operate, and b is a known parameter. It may be assumed that the

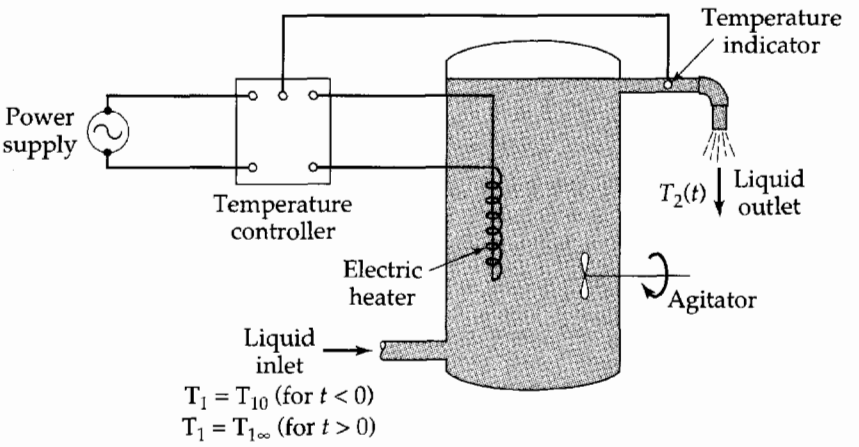

Fig. 15.5-3. An agitated tank with a temperature controller.

liquid temperature $T_2(t)$ is always less than T_{max} in normal operation. The heating coil supplies energy to the liquid in the tank at a rate $Q = UA(T_c - T_2)$, where U is the overall heat transfer coefficient between the coil and the liquid, and T_c is the instantaneous coil temperature, considered to be uniform.

Up to time $t = 0$, the system has been operating at steady state with liquid inlet temperature $T_1 = T_{10}$ and exit temperature $T_2 = T_{20}$. At time $t = 0$, the inlet stream temperature is suddenly increased to $T_1 = T_{1\infty}$ and held there. As a consequence of this disturbance, the tank temperature will begin to rise, and the temperature indicator in the outlet stream will signal the controller to decrease the power supplied to the heating coil. Ultimately, the liquid temperature in the tank will attain a new steady-state value $T_{2\infty}$. It is desired to describe the behavior of the liquid temperature $T_2(t)$. A qualitative sketch showing the various temperatures is given in Fig. 15.5-4.

SOLUTION

We first write the unsteady-state macroscopic energy balances [Eq. (E) of Table 15.5-1] for the liquid in the tank and for the heating coil:

(liquid)
$$\rho\hat{C}_pV\frac{dT_2}{dt} = w\hat{C}_p(T_1 - T_2) + UA(T_c - T_2) \tag{15.5-12}$$

(coil)
$$\rho_c\hat{C}_{pc}V_c\frac{dT_c}{dt} = b(T_{max} - T_2) - UA(T_c - T_2) \tag{15.5-13}$$

Note that in applying the macroscopic energy balance to the liquid, we have neglected kinetic and potential energy changes as well as the power input to the agitator.

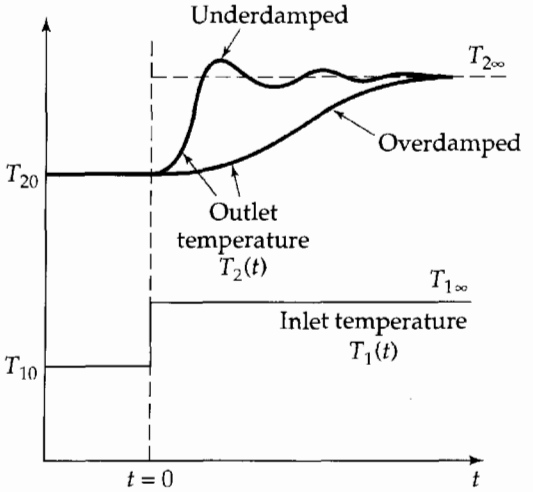

Fig. 15.5-4. Inlet and outlet temperatures as functions of time.

(a) ***Steady-state behavior for $t < 0$.*** When the time derivatives in Eqs. 15.5-12 and 13 are set equal to zero and the equations added, we get for $t < 0$, where $T_1 = T_{10}$:

$$T_{20} = \frac{w\hat{C}_p T_{10} + bT_{\max}}{w\hat{C}_p + b} \tag{15.5.14}$$

Then from Eq. 15.5-13 we can get the initial temperature of the coil

$$T_{c0} = T_{20}\left(1 - \frac{b}{UA}\right) + \frac{bT_{\max}}{UA} \tag{15.5-15}$$

(b) ***Steady-state behavior for $t \to \infty$.*** When similar operations are performed with $T_1 = T_{1\infty}$, we get

$$T_{2\infty} = \frac{w\hat{C}_p T_{1\infty} + bT_{\max}}{w\hat{C}_p + b} \tag{15.5-16}$$

and

$$T_{c\infty} = T_{2\infty}\left(1 - \frac{b}{UA}\right) + \frac{bT_{\max}}{UA} \tag{15.5-17}$$

for the final temperature of the coil.

(c) ***Unsteady state behavior for $t > 0$.*** It is convenient to define dimensionless variables using the steady-state quantities for $t < 0$ and $t \to \infty$:

$$\Theta_2 = \frac{T_2 - T_{2\infty}}{T_{20} - T_{2\infty}} = \text{dimensionless liquid temperature} \tag{15.5-18}$$

$$\Theta_c = \frac{T_c - T_{c\infty}}{T_{c0} - T_{c\infty}} = \text{dimensionless coil temperature} \tag{15.5-19}$$

$$\tau = \frac{UAt}{\rho\hat{C}_p V} = \text{dimensionless time} \tag{15.5-20}$$

In addition we define three dimensionless parameters:

$$R = \rho\hat{C}_p V/\rho_c\hat{C}_{pc}V_c = \text{ratio of thermal capacities} \tag{15.5-21}$$

$$F = w\hat{C}_p/UA = \text{flow-rate parameter} \tag{15.5-22}$$

$$b/UA = \text{controller parameter} \tag{15.5-23}$$

In terms of these quantities, the unsteady-state balances in Eqs. 15.5-12 and 13 become (after considerable manipulation):

$$\frac{d\Theta_2}{d\tau} = -(1 + F)\Theta_2 + (1 - B)\Theta_c \tag{15.5-24}$$

$$\frac{d\Theta_c}{d\tau} = R(\Theta_2 - \Theta_c) \tag{15.5-25}$$

elimination of Θ_c between this pair of equations gives a single second-order linear ordinary differential equation for the exit liquid temperature as a function of time:

$$\frac{d^2\Theta_2}{d\tau^2} + (1 + R + F)\frac{d\Theta_2}{d\tau} + R(B + F)\Theta_2 = 0 \tag{15.5-26}$$

This equation has the same form as that obtained for the damped manometer in Eq. 7.7-21 (see also Eq. C.1-7). The general solution is then of the form of Eq. 7.7-23 or 24:

$$\Theta_2 = C_+ \exp(m_+\tau) + C_- \exp(m_-\tau) \qquad (m_+ \neq m_-) \tag{15.5-27}$$

$$\Theta_2 = C_1 \exp m\tau + C_2\tau \exp m\tau \qquad (m_+ = m_- = m) \tag{15.5-28}$$

where

$$m_{\pm} = \tfrac{1}{2}[-(1 + R + F) \pm \sqrt{(1 + R + F)^2 - 4R(B + F)}] \tag{15.5-29}$$

Thus by analogy with Example 7.7-2, the fluid exit temperature may approach its final value as a monotone increasing function (overdamped or critically damped) or with oscillations (underdamped). The system parameters appear in the dimensionless time variable, as well as in the parameters B, F, and R. Therefore, numerical calculations are needed to determine whether in a particular system the temperature will oscillate or not.

EXAMPLE 15.5-3

Flow of Compressible Fluids Through Head Meters

Extend the development of Example 7.6-5 to the steady flow of compressible fluids through orifice meters and Venturi tubes.

SOLUTION

We begin, as in Example 7.6-5, by writing the steady-state mass and mechanical energy balances between reference planes 1 and 2 of the two flow meters shown in Fig. 15.5-5. For compressible fluids, these may be expressed as

$$w = \rho_1\langle v_1\rangle S_1 = \rho_2\langle v_2\rangle S_2 \tag{15.5-30}$$

$$\frac{\langle v_2\rangle^2}{2\alpha_2} - \frac{\langle v_1\rangle^2}{2\alpha_1} + \int_1^2 \frac{1}{\rho}\,dp + \tfrac{1}{2}\langle v_2\rangle^2 e_v = 0 \tag{15.5-31}$$

in which the quantities $\alpha_i = \langle v_i\rangle^3/\langle v_i^3\rangle$ are included to allow for the replacement of the average of the cube by the cube of the average.

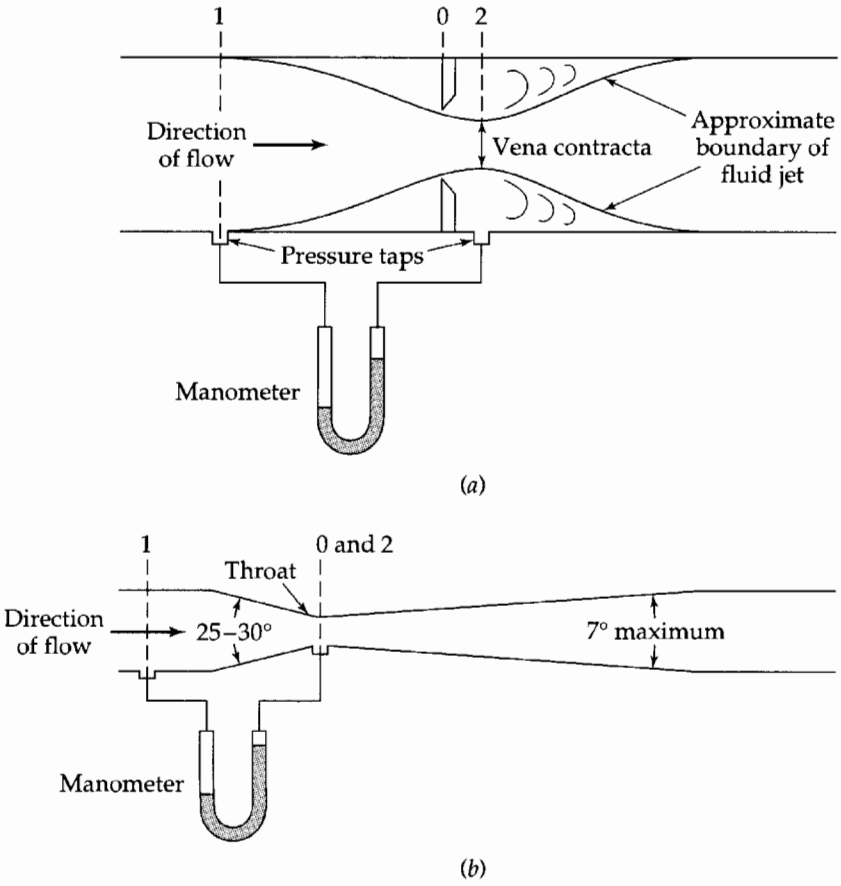

Fig. 15.5-5. Measurement of mass flow rate by use of (*a*) an orifice meter, and (*b*) a Venturi tube.

We next eliminate $\langle v_1 \rangle$ and $\langle v_2 \rangle$ from the above two equations to get an expression for the mass flow rate:

$$w = \rho_2 S_2 \sqrt{\frac{-2\alpha_2 \int_1^2 (1/\rho) dp}{1 - (\alpha_2/\alpha_1)(\rho_2 S_2/\rho_1 S_1)^2 + \alpha_2 e_v}} \tag{15.5-32}$$

We now repeat the assumptions of Example 7.6-5: (i) $e_v = 0$, (ii) $\alpha_1 = 1$, and (iii) $\alpha_2 = (S_0/S_2)^2$. Then Eq. 15.5-32 becomes

$$w = C_d \rho_2 S_0 \sqrt{\frac{-2 \int_1^2 (1/\rho) dp}{1 - (\rho_2 S_0/\rho_1 S_1)^2}} \tag{15.5-33}$$

The empirical "discharge coefficient," C_d, is included in this equation to permit correction of this expression for errors introduced by the three assumptions and must be determined experimentally.

For *Venturi meters*, it is convenient to put plane 2 at the point of minimum cross section of the meter so that $S_2 = S_0$. Then α_2 is very nearly unity, and it has been found experimentally that C_d is almost the same for compressible and incompressible fluids—that is, about 0.98 for well designed Venturi meters. For *orifice meters*, the degree of contraction of a compressible fluid stream at plane 2 is somewhat less than for incompressible fluids, especially at high flow rates, and a different discharge coefficient[2] is required.

In order to use Eq. 15.5-33, the fluid density must be known as a function of pressure. That is, one must know both the path of the expansion and the equation of state of the fluid. In most cases the assumption of frictionless adiabatic behavior appears to be acceptable. For ideal gases, one may write $p\rho^{-\gamma} =$ constant, where $\gamma = C_p/C_V$ (see Eq. 15.2-5). Then Eq. 15.5-33 becomes

$$w = C_d \rho_2 S_0 \sqrt{\frac{2(p_1/\rho_1)[\gamma/(\gamma-1)][1 - (p_2/p_1)^{(\gamma-1)/\gamma}]}{1 - (S_0/S_1)^2 (p_2/p_1)^{2/\gamma}}} \tag{15.5-34}$$

This formula expresses the mass flow rate as a function of measurable quantities and the discharge coefficient. Values of the latter may be found in engineering handbooks.[2]

EXAMPLE 15.5-4

Free Batch Expansion of a Compressible Fluid

A compressible gas, initially at $T = T_0$, $p = p_0$, and $\rho = \rho_0$, is discharged from a large stationary insulated tank through a small convergent nozzle, as shown in Fig. 15.5-6. Show how the fractional remaining mass of fluid in the tank, ρ/ρ_0, may be determined as a function of time. Develop working equations, assuming that the gas is ideal.

SOLUTION

For convenience, we divide the tank into two parts, separated by the surface 1 as shown in the figure. We assume that surface 1 is near enough to the tank exit that essentially all of the fluid mass is to left of it, but far enough from the exit that the fluid velocity through the surface 1 is negligible. We further assume that the average fluid properties to the left of 1 are identical with those at surface 1. We now consider the behavior of these two parts of the system separately.

(a) ***The bulk of the fluid in the tank.*** For the region to the left of surface 1, the unsteady state mass balance in Eq. (A) of Table 15.5-1 is

$$\frac{d}{dt}(\rho_1 V) = -w_1 \tag{15.5-35}$$

[2] R. H. Perry, D. W. Green, and J. O. Maloney, *Chemical Engineers' Handbook*, 7th Edition, McGraw-Hill, New York (1997); see also, Chapter 15 of *Handbook of Fluid Dynamics and Fluid Machinery* (J. A. Schertz and A. E. Fuhs, eds.), Wiley, New York (1996).

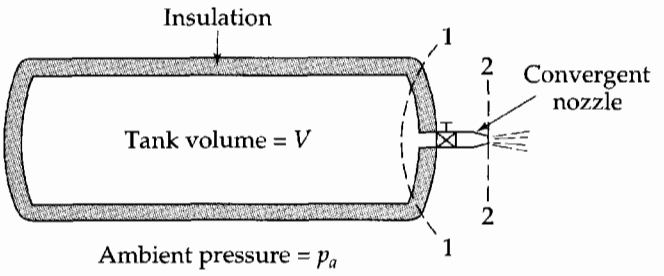

Fig. 15.5-6. Free batch expansion of a compressible fluid. The sketch shows the locations of surfaces 1 and 2.

For the same region, the energy balance of Eq. (E) of Table 15.5-1 becomes

$$\frac{d}{dt}(\rho_1 V(\hat{U}_1 + \hat{\Phi}_1)) = -w_1\left(\hat{U} + \frac{p_1}{\rho_1} + \hat{\Phi}_1\right) \tag{15.5-36}$$

in which V is the total volume in the system being considered, and w_1 is the mass rate of flow of gas leaving the system. In writing this equation, we have neglected the kinetic energy of the fluid.

Substituting the mass balance into both sides of the energy equation gives

$$\rho_1\left(\frac{d\hat{U}_1}{dt} + \frac{d\hat{\Phi}_1}{dt}\right) = \frac{p_1}{\rho_1}\frac{d\rho_1}{dt} \tag{15.5-37}$$

For a stationary system under the influence of no external forces other than gravity, $d\hat{\Phi}_1/dt = 0$, so that Eq. 15.5-37 becomes

$$\frac{d\hat{U}_1}{d\rho_1} = \frac{p_1}{\rho_1^2} \tag{15.5-38}$$

This equation may be combined with the thermal and caloric equations of state for the fluid in order to obtain $p_1(\rho_1)$ and $T_1(\rho_1)$. We find, thus, that the condition of the fluid in the tank depends only on the degree to which the tank has been emptied and not on the rate of discharge. For the special case of an ideal gas with constant $\hat{C}_V$, for which $d\hat{U} = \hat{C}_V dT$ and $p = \rho RT/M$, we may integrate Eq. 15.5-38 to obtain

$$p_1\rho_1^{-\gamma} = p_0\rho_0^{-\gamma} \tag{15.5-39}$$

in which $\gamma = C_p/C_V$. This result also follows from Eq. 11.4-57.

(b) ***Discharge of the gas through the nozzle.*** For the sake of simplicity we assume here that the flow between surfaces 1 and 2 is both frictionless and adiabatic. Also, since w_1 is not far different from w_2, it is also appropriate to consider at any one instant that the flow is quasi-steady-state. Then we can use the macroscopic mechanical energy balance in the form of Eq. 15.2-2 with the second, fourth, and fifth terms omitted. That is,

$$\tfrac{1}{2}v_2^2 + \int_1^2 \frac{1}{\rho}\,dp = 0 \tag{15.5-40}$$

Since we are dealing with an ideal gas, we may use the result in Eq. 15.5-34 to get the instantaneous discharge rate. Since in this problem the ratio S_2/S_1 is very small and its square is even smaller, we can replace the denominator under the square root sign in Eq. 15.5-34 by unity. Then the ρ_2 outside the square root sign is moved inside and use is made of Eq. 15.5-39. This gives

$$w_2 = -V\frac{d\rho_1}{dt} = S_2\sqrt{2p_1\rho_1[\gamma/(\gamma-1)][(p_2/p_0)^{2/\gamma} - (p_2/p_0)^{(\gamma+1)/\gamma}]} \tag{15.5-41}$$

in which S_2 is the cross-sectional area of the nozzle opening.

Now we use Eq. 15.5-39 to eliminate p_1 from Eq. 15.5-41. Then we have a first-order differential equation for ρ_1, which may be integrated to give

$$t = \frac{V/S_2}{\sqrt{2(p_0/\rho_0)[\gamma/(\gamma-1)]}} \int_{\rho_1/\rho_0}^{1} \frac{d(\rho_1/\rho_0)}{\sqrt{(p_2/p_0)^{2/\gamma}(\rho_1/\rho_0)^{\gamma-1} - (p_2/\rho_0)^{(\gamma-1)/\gamma}}} \tag{15.5-42}$$

From this equation we can obtain the time required to discharge any given fraction of the original gas.

At low flow rates the pressure p_2 at the nozzle opening is equal to the ambient pressure. However, examination of Eq. 15.5-41 shows that, as the ambient pressure is reduced, the calculated mass rate of flow reaches a maximum at a critical pressure ratio

$$r \equiv \left(\frac{p_2}{p_1}\right)_{\text{crit}} = \left(\frac{2}{\gamma+1}\right)^{\gamma/(\gamma-1)} \tag{15.5-43}$$

For air ($\gamma = 1.4$), this critical pressure ratio is 0.53. If the ambient pressure is further reduced, the pressure just inside the nozzle will remain at the value of p_2 calculated from Eq. 15.5-43, and the mass rate of flow will become independent of ambient pressure p_a. Under these conditions, the discharge rate is

$$w_{\max} = S_2\sqrt{p_1\rho_1\gamma\left(\frac{2}{\gamma+1}\right)^{(\gamma+1)/(\gamma-1)}} \tag{15.5-44}$$

Then, for $p_a/p_1 < r$, we may write Eq. 15.5-42 more simply:

$$t = \frac{V/S_2}{\sqrt{(p_0/\rho_0)\gamma(2/(\gamma+1))^{(\gamma+1)/(\gamma-1)}}} \int_{\rho_1/\rho_0}^{1} \frac{dx}{x^{(\gamma+1)/2}} \tag{15.5-45}$$

or

$$t = \frac{V/S_2}{\sqrt{(\gamma RT_0/M)(2/(\gamma+1))^{(\gamma+1)/(\gamma-1)}}} \left(\frac{2}{\gamma-1}\right)\left[\left(\frac{\rho_1}{\rho_0}\right)^{(1-\gamma)/2} - 1\right] \qquad (p_a/p_1 < r) \tag{15.5-46}$$

If p_a/p_1 is initially less than r, both Eqs. 15.5-46 and 42 will be useful for calculating the total discharge time.

QUESTIONS FOR DISCUSSION

1. Give the physical significance of each term in the five macroscopic balances.
2. How are the equations of change related to the macroscopic balances?
3. Does each of the four terms within the parentheses in Eq. 15.1-2 represent a form of energy? Explain.
4. How is the macroscopic (total) energy balance related to the first law of thermodynamics, $\Delta U = Q + W$?
5. Explain how the averages $\langle v \rangle$ and $\langle v^3 \rangle$ arise in Eq. 15.1-1.
6. What is the physical significance of E_c and E_v? What sign do they have? How are they related to the velocity distribution? How can they be estimated?
7. How is the macroscopic balance for internal energy derived?
8. What information can be obtained from Eq. 15.2-2 about a fluid at rest?

PROBLEMS

15A.1. Heat transfer in double-pipe heat exchangers.

(a) Hot oil entering the heat exchanger in Example 15.4-1 at surface 2 is to be cooled by water entering at surface 1. That is, the exchanger is being operated in *countercurrent* flow. Compute the required exchanger area A, if the heat transfer coefficient U is 200 Btu/hr · ft^2 · F and the fluid streams have the following properties:

	Mass flow rate (lb_m/hr)	Heat capacity (Btu/lb_m · F)	Temperature entering (°F)	leaving (°F)
Oil	10,000	0.60	200	100
Water	5,000	1.00	60	—

(b) Repeat the calculation of part (a) if $U_1 = 50$ and $U_2 = 350$ Btu/hr · ft^2 · F. Assume that U varies linearly with the water temperature, and use the results of Problem 15B.1.

(c) What is the minimum amount of water that can be used in (a) and (b) to obtain the desired temperature change for the oil? What is the minimum amount of water that can be used in parallel flow?

(d) Calculate the required heat exchanger area for parallel flow operation, if the mass rate of flow of water is 15,500 lb_m/hr and U is constant at 200 Btu/hr · ft^2 ·F.

Answers: **(a)** 104 ft^2; **(b)** 122 ft^2; **(c)** 4290 lb_m/hr, 15,000 lb_m/hr; **(d)** about 101 ft^2

15A.2. Adiabatic flow of natural gas in a pipeline. Recalculate the power requirement $w\hat{W}$ in Example 15.4-2 if the flow in the pipeline were adiabatic rather than isothermal.

(a) Use the result of Problem 15B.3(d) to determine the density of the gas at plane 2.

(b) Use your answer to (a), along with the result of Problem 15B.3(e), to obtain p_2.

(c) Calculate the power requirement, as in Example 15.4-2.

Answers: **(a)** 0.243 lb_m/ft^3; **(b)** 86 psia; **(c)** 504 hp

15A.3. Mixing of two ideal-gas streams.

(a) Calculate the resulting velocity, temperature, and pressure when the following two air streams are mixed in an apparatus such as that described in Example 15.3-2. The heat capacity $\hat{C}_p$ of air may be considered constant at 6.97 Btu/lb-mole · F. The properties of the two streams are:

	w (lb_m/hr)	v (ft/s)	T (°F)	p (atm)
Stream 1a:	1000	1000	80	1.00
Stream 1b:	10,000	100	80	1.00

Answer: **(a)** 11,000 lb_m/hr; about 110 ft/s; 86.5 °F; 1.00 atm

(b) What would the calculated velocity be, if the fluid density were treated as constant?

(c) Estimate $\hat{E}_v$ for this operation, basing your calculation on the results of part (b).

Answers: **(b)** 109 ft/s; **(c)** 1.4×10^3 ft lb_f/lb_m

15A.4. Flow through a Venturi tube. A Venturi tube, with a throat 3 in. in diameter, is placed in a circular pipe 1 ft in diameter carrying dry air. The discharge coefficient C_d of the meter is 0.98. Calculate the mass flow rate of air in the pipe if the air enters the Venturi at 70°F and 1 atm and the throat pressure is 0.75 atm.

(a) Assume adiabatic frictionless flow and $\gamma = 1.4$.

(b) Assume isothermal flow.

(c) Assume incompressible flow at the entering density.

Answers: **(a)** 2.07 lb_m/s; **(b)** 1.96 lb_m/s; **(c)** 2.43 lb_m/s

15A.5. Free batch expansion of a compressible fluid. A tank with volume $V = 10$ ft^3 (see Fig. 15.5-6) is filled with air ($\gamma = 1.4$) at $T_0 = 300$K and $p_0 = 100$ atm. At time $t = 0$ the valve is opened, allowing the air to expand to the ambient pressure of 1 atm through a convergent nozzle, with a throat cross section $S_2 = 0.1$ ft^2.

(a) Calculate the pressure and temperature at the throat of the nozzle, just after the start of the discharge.

(b) Calculate the pressure and temperature within the tank when p_2 attains its final value of 1 atm.

(c) How long will it take for the system to attain the state described in (*b*)?

15A.6. Heating of air in a tube. A horizontal tube of 20 ft length is heated by means of an electrical heating element wrapped uniformly around it. Dry air enters at 5°F and 40 psia at a velocity 75 ft/s and 185 lb_m/hr. The heating element provides heat at a rate of 800 Btu/hr per foot of tube. At what temperature will the air leave the tube, if the exit pressure is 15 psia? Assume turbulent flow and ideal gas behavior. For air in the range of interest the heat capacity at constant pressure in Btu/lb-mole · F is

$$\tilde{C}_p = 6.39 + (9.8 \times 10^{-4})T - (8.18 \times 10^{-8})T^2 \qquad \text{(15A.6-1)}$$

where T is expressed in degrees Rankine.

Answer: $T_2 = 354$°F

15A.7. Operation of a simple double-pipe heat exchanger. A cold-water stream, 5400 lb_m/hr at 70°F, is to be heated by 8100 lb_m/hr of hot water at 200°F in a simple double-pipe heat exchanger. The cold water is to flow through the inner pipe, and the hot water through the annular space between the pipes. Two 20-ft lengths of heat exchanger are available, and also all the necessary fittings.

(a) By means of a sketch, show the way in which the two double-pipe heat exchangers should be connected in order to get the most effective heat transfer.

(b) Calculate the exit temperature of the cold stream for the arrangement decided on in (a) for the following situation:

(i) The heat-transfer coefficient for the annulus, based on the heat transfer area of the inner surface of the inner pipe is 2000 Btu/hr · ft^2 · F.

(ii) The inner pipe has the following properties: total length, 40 ft; inside diameter 0.0875 ft; heat transfer surface per foot, 0.2745 ft^2; capacity at average velocity of 1 ft/s is 1345 lb_m/hr.

(iii) The average properties of the water in the inner pipe are:

$$\mu = 0.45 \text{ cp} = 1.09 \text{ lb}_m/\text{hr} \cdot \text{ft}$$
$$\hat{C}_p = 1.00 \text{ Btu}/\text{lb}_m \cdot \text{F}$$
$$k = 0.376 \text{ Btu}/\text{hr} \cdot \text{ft} \cdot \text{F}$$
$$\rho = 61.5 \text{ lb}_m/\text{ft}^3$$

(iv) The combined resistance of the pipe wall and encrustations is 0.001 hr · ft^2 · F/Btu based on the inner pipe surface area.

(c) Sketch the temperature profile in the exchanger.

Answer: **(b)** 136°F

15B.1. Performance of a double-pipe heat exchanger with variable overall heat transfer coefficient. Develop an expression for the amount of heat transferred in an exchanger of the type discussed in Example 15.4-1, if the overall heat transfer coefficient U varies linearly with the temperature of either stream.

(a) Since $T_h - T_c$ is a linear function of both T_h and T_c, show that

$$\frac{U - U_1}{U_2 - U_1} = \frac{\Delta T - \Delta T_1}{\Delta T_2 - \Delta T_1} \qquad \text{(15B.1-1)}$$

in which $\Delta T = T_h - T_c$, and the subscripts 1 and 2 refer to the conditions at control surfaces 1 and 2.

(b) Substitute the result in (a) for $T_h - T_c$ into Eq. 15.4-12, and integrate the equation thus obtained over the length of the exchanger. Use this result to show that[1]

$$Q_c = A\frac{U_1\Delta T_2 - U_2\Delta T_1}{\ln(U_1\Delta T_2/U_2\Delta T_1)} \tag{15B.1-2}$$

15B.2. Pressure drop in turbulent flow in a slightly converging tube (Fig. 15B.2). Consider the turbulent flow of an incompressible fluid in a circular tube with a diameter that varies linearly with distance according to the relation

$$D = D_1 + (D_2 - D_1)\frac{z}{L} \tag{15B.2-1}$$

At $z = 0$, the velocity is v_1 and may be assumed to be constant over the cross section. The Reynolds number for the flow is such that f is given approximately by the Blasius formula of Eq. 6.2-13,

$$f = \frac{0.0791}{\mathrm{Re}^{1/4}} \tag{15B.2-2}$$

Obtain the pressure drop $p_1 - p_2$ in terms of v_1, D_1, D_2, ρ, L, and $\nu = \mu/\rho$.

(a) Integrate the d-form of the mechanical energy balance to get

$$\frac{1}{\rho}(p_1 - p_2) = \frac{1}{2}(v_2^2 - v_1^2) + 2\int_0^L \frac{v^2 f}{D}\,dz \tag{15B.2-3}$$

and then eliminate v_2 from the equation.

(b) Show that both v and f are functions of D:

$$v = v_1\left(\frac{D_1}{D}\right)^2; \qquad f = \frac{0.0791}{(D_1v_1/\nu)^{1/4}}\left(\frac{D}{D_1}\right)^{1/4} \tag{15B.2-4}$$

Of course, D is a function of z according to Eq. 15B.2-1.

(c) Make a change of variable in the integral in Eq. 15B.2-3 and show that

$$\int_0^L \frac{v^2 f}{D}\,dz = \frac{L}{D_2 - D_1}\int_{D_1}^{D_2} \frac{v^2 f}{D}\,dD \tag{15B.2-5}$$

(d) Combine the results of (b) and (c) to get finally

$$\frac{1}{\rho}(p_1 - p_2) = \frac{1}{2}v_1^2\left[\left(\frac{D_1}{D_2}\right)^4 - 1\right] + \frac{2Lv_1^2}{D_1 - D_2}\frac{\frac{4}{15}(0.0791)}{(D_1v_1/\nu)^{1/4}}\left[\left(\frac{D_1}{D_2}\right)^{15/4} - 1\right] \tag{15B.2-6}$$

(e) Show that this result simplifies properly for $D_1 = D_2$.

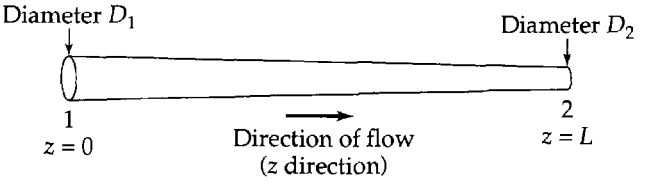

Fig. 15B.2. Turbulent flow in a horizontal, slightly tapered tube (D_1 is slightly greater than D_2).

[1] A. P. Colburn, *Ind. Eng. Chem.*, **25**, 873 (1933).

15B.3. Steady flow of ideal gases in ducts of constant cross section.

(a) Show that, for the horizontal flow of any fluid in a circular duct of uniform diameter D, the d-form of the mechanical energy balance, Eq. 15.4-1, may be written as

$$v\,dv + \frac{1}{\rho}\,dp + \tfrac{1}{2}v^2 de_v = 0 \tag{15B.3-1}$$

in which $de_v = (4f/D)dL$. Assume flat velocity profiles.

(b) Show that Eq. 15B.3-1 may be rewritten as

$$v\,dv + d\left(\frac{p}{\rho}\right) + \left(\frac{p}{\rho^2}\right)d\rho + \tfrac{1}{2}v^2 de_v = 0 \tag{15B.3-2}$$

Show further that, when use is made of the d-form of the mass balance, Eq. 15B.3-2 becomes for *isothermal flow* of an ideal gas

$$de_v = \frac{2RT}{M}\frac{dv}{v^3} - 2\frac{dv}{v} \tag{15B.3-3}$$

(c) Integrate Eq. 15B.3-3 between any two pipe cross sections 1 and 2 enclosing a total pipe length L. Make use of the ideal gas equation of state and the macroscopic mass balance to show that $v_2/v_1 = \rho_1/\rho_2 = p_1/p_2$, so that the "mass velocity" G can be put in the form

$$G \equiv \rho_1 v_1 = \sqrt{\frac{\rho_1 p_1 (1-r)}{e_v - \ln r}} \qquad (\textit{isothermal} \text{ flow of ideal gases}) \tag{15B.3-4}$$

in which $r = (p_2/p_1)^2$. Show that, for any given value of e_v and conditions at section 1, the quantity G reaches its maximum possible value at a critical value of r defined by $\ln r_c + (1 - r_c)/r_c = e_v$. See also Problem 15B.4.

(d) Show that, for the *adiabatic flow* of an ideal gas with constant $\hat{C}_p$ in a horizontal duct of constant cross section, the d-form of the total energy balance (Eq. 15.4-4) simplifies to

$$p\hat{V} + \left(\frac{\gamma - 1}{\gamma}\right)\tfrac{1}{2}v^2 = \text{constant} \tag{15B.3-5}$$

where $\gamma = C_p/C_V$. Combine this result with Eq. 15B.3-2 to get

$$\frac{\gamma + 1}{\gamma}\frac{dv}{v} - 2\left(\frac{p_1}{\rho_1} + \left(\frac{\gamma - 1}{\gamma}\right)\tfrac{1}{2}v_1^2\right)\frac{dv}{v^3} = -de_v \tag{15B.3-6}$$

Integrate this equation between sections 1 and 2 enclosing the resistance e_v, assuming γ constant. Rearrange the result with the aid of the macroscopic mass balance to obtain the following relation for the mass flux G.

$$G \equiv \rho_1 v_1 = \sqrt{\frac{\rho_1 p_1}{\dfrac{e_v - [(\gamma+1)/2\gamma]\ln s}{1 - s} - \dfrac{\gamma - 1}{2\gamma}}} \qquad (\textit{adiabatic} \text{ flow of ideal gases}) \tag{15B.3-7}$$

in which $s = (\rho_2/\rho_1)^2$.

(e) Show by use of the macroscopic energy and mass balances that for horizontal adiabatic flow of ideal gases with constant γ,

$$\frac{p_2}{p_1} = \frac{\rho_2}{\rho_1}\left[1 + \frac{[1 - (\rho_1/\rho_2)^2]G^2}{\rho_1 p_1}\left(\frac{\gamma - 1}{2\gamma}\right)\right] \tag{15B.3-8}$$

This equation can be combined with Eq. 15B.3-7 to show that, as for isothermal flow, there is a critical pressure ratio p_2/p_1 corresponding to the maximum possible mass flow rate.

15B.4. The Mach number in the mixing of two fluid streams.

(a) Show that when the radicand in Eq. 15.3-13 is zero, the Mach number of the final stream is unity. Note that the Mach number, Ma, which is the ratio of the local fluid velocity to the velocity of sound at the local conditions, may be written for an ideal gas as $v/v_s = v/\sqrt{\gamma RT/M}$ (see Problem 11C.1).

(b) Show how the results of Example 15.3-2 may be used to predict the behavior of a gas passing through a sudden enlargement of duct cross section.

15B.5. Limiting discharge rates for Venturi meters.

(a) Starting with Eq. 15.5-34 (for *adiabatic flow*), show that as the throat pressure in a Venturi meter is reduced, the mass rate of flow reaches a maximum when the ratio $r = p_2/p_1$ of throat pressure to entrance pressure is defined by the expression

$$\frac{\gamma+1}{r^{2/\gamma}} - \frac{2}{r^{(\gamma+1)/\gamma}} - \frac{\gamma-1}{(S_1/S_0)^2} = 0 \tag{15B.5-1}$$

(b) Show that for $S_1 >> S_0$ the mass flow rate under these limiting conditions is

$$w = C_d p_1 S_0 \sqrt{\frac{\gamma M}{RT_1}\left(\frac{2}{\gamma+1}\right)^{(\gamma+1)/(\gamma-1)}} \tag{15B.5-2}$$

(c) Obtain results analogous to Eqs. 15B.5-1 and 2 for *isothermal flow.*

15B.6. Flow of a compressible fluid through a convergent–divergent nozzle (Fig. 15B.6). In many applications, such as steam turbines or rockets, hot compressed gases are expanded through nozzles of the kind shown in the accompanying figure in order to convert the gas enthalpy into kinetic energy. This operation is in many ways similar to the flow of gases through orifices. Here, however, the purpose of the expansion is to produce power—for example, by the impingement of the fast-moving fluid on a turbine blade, or by direct thrust, as in a rocket engine.

To explain the behavior of such a system and to justify the general shape of the nozzle described, follow the path of expansion of an ideal gas. Assume that the gas is initially in a very large reservoir at essentially zero velocity and that it expands through an adiabatic frictionless nozzle to zero pressure. Further assume flat velocity profiles, and neglect changes in elevation.

(a) Show, by writing the macroscopic mechanical energy balance or the total energy balance between planes 1 and 2, that

$$\tfrac{1}{2}v_2^2 = \frac{RT_1}{M}\frac{\gamma}{\gamma-1}\left[1 - \left(\frac{p_2}{p_1}\right)^{(\gamma-1)/\gamma}\right] \tag{15B.6-1}$$

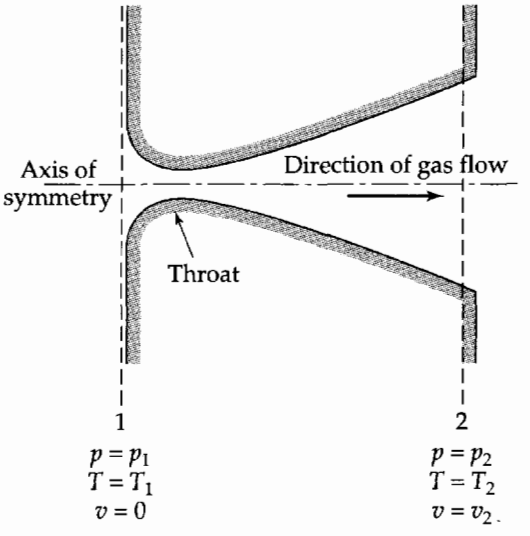

Fig. 15B.6. Schematic cross section of a convergent–divergent nozzle.

(b) Show, by use of the ideal gas law, the steady-state macroscopic mass balance, and Eq. 15B.6-1, that the cross section S of the expanding stream goes through a minimum at a critical pressure

$$p_{2,\text{crit}} = p_1\left(\frac{2}{\gamma+1}\right)^{\gamma/(\gamma-1)} \tag{15B.6-2}$$

(c) Show that the Mach number, $\text{Ma} = v_2/v_s(T_2)$, of the fluid at this minimum cross section is unity (v_s for low-frequency sound waves is derived in Problem 11C.1). How does the result of part (a) above compare with that in Problem 15B.5?

(d) Calculate fluid velocity v, fluid temperature T, and stream cross section S as a function of the local pressure p for the discharge of 10 lb-moles of air per second from 560°R and 10 atm to zero pressure. Discuss the significance of your results.

Answer:

p, atm	10	9	8	7	6	5.28	5	4	3	2	1	0
v, ft sec^{-1}	0	449	645	807	956	1058	1099	1245	1398	1574	1798	2591
T, °R	560	543	525	506	484	466	459	431	397	353	290	0
S, ft^2	∞	0.977	0.739	0.650	0.613	0.606	0.607	0.628	0.688	0.816	1.171	∞

15B.7. Transient thermal behavior of a chromatographic device (Fig. 15B.7). You are a consultant to an industrial concern that is experimenting, among other things, with transient thermal phenomena in gas chromatography. One of the employees first shows you some reprints of a well-known researcher and says that he is trying to apply some of the researcher's new approaches, but that he is currently stuck on a heat transfer problem. Although the problem is only ancillary to the main study, it must nonetheless be understood in connection with his interpretation of the data and the application of the new theories.

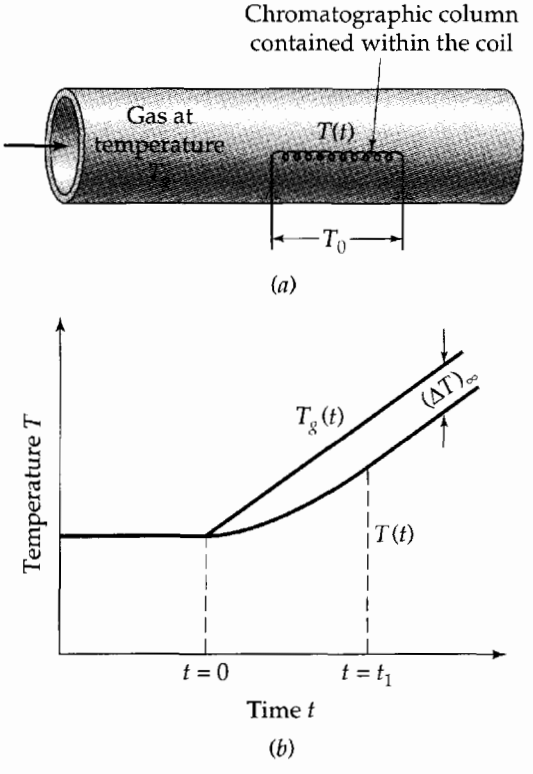

Fig. 15B.7. (*a*) Chromatographic device; (*b*) temperature response of the chromatographic system.

A very tiny chromatographic column is contained within a coil, which is in turn inserted into a pipe through which a gas is blown to control the temperature (see Fig. 15B.7a). The gas temperature will be called $T_g(t)$. The temperature at the ends of the coil (outside the pipe) is T_0, which is not very much different from the initial value of T_g. The actual temperature within the chromatographic column (i.e., within the coil) will be called $T(t)$. Initially the gas and the coil are both at the temperature T_{g0}. Then beginning at time $t = 0$, the gas temperature is increased linearly according to the equation

$$T_g(t) = T_{g0}\left(1 + \frac{t}{t_0}\right) \tag{15B.7-1}$$

where t_0 is a known constant with dimensions of time.

You are told that, by inserting thermocouples into the column itself, the people in the lab have obtained temperature curves that look like those in Fig. 15B.7(b). The $T(t)$ curve seems to become parallel to the $T_g(t)$ curves for large t. You are asked to explain the above pair of curves by means of some kind of theory. Specifically you are asked to find out the following:

(a) At any time t, what will $T_g - T$ be?

(b) What will the limiting value of $T_g - T$ be when $t \rightarrow \infty$? Call this quantity $(\Delta T)_\infty$.

(c) What time interval t_1 is required for $T_g - T$ to come within, say, 1% of $(\Delta T)_\infty$?

(d) What assumptions had to be made to model the system?

(e) What physical constants, physical properties, and so on, have to be known in order to make a comparison between the measured and theoretical values of $(\Delta T)_\infty$?

Devise the simplest possible theory to account for the temperature curves and to answer the above five questions.

15B.8. Continuous heating of a slurry in an agitated tank (Fig. 15B.8). A slurry is being heated by pumping it through a well-stirred heating tank. The inlet temperature of the slurry is T_i and the temperature of the outer surface of the steam coil is T_s. Use the following symbols:

V = volume of the slurry in the tank
$\rho, \hat{C}_p$ = density and heat capacity of the slurry
w = mass rate of flow of slurry through the tank
U = overall heat transfer coefficient of heating coil
A = total heat transfer area of the coil

Assume that the stirring is sufficiently thorough that the fluid temperature in the tank is uniform and the same as the outlet fluid temperature.

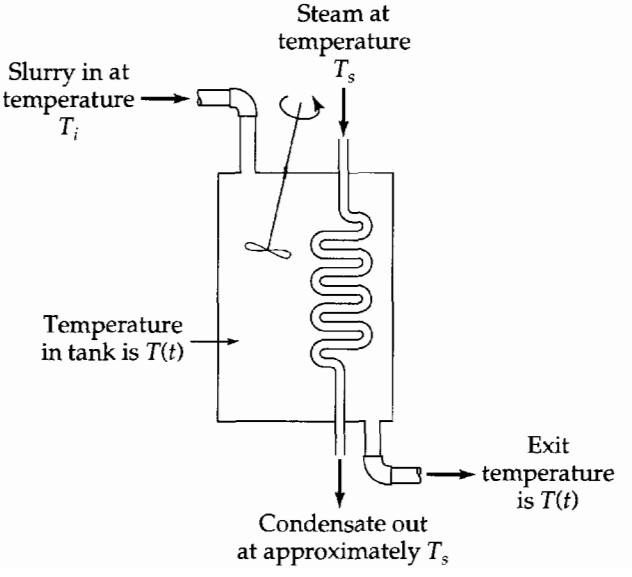

Fig. 15B.8. Heating of a slurry in an agitated tank.

(a) By means of an energy balance, show that the slurry temperature $T(t)$ is described by the differential equation

$$\frac{dT}{dt} = \left(\frac{UA}{\rho\hat{C}_pV}\right)(T_s - T) - \left(\frac{w}{\rho V}\right)(T - T_i) \tag{15B.8-1}$$

The variable t is the time since the start of heating.

(b) Rewrite this differential equation in terms of the dimensionless variables

$$\tau = \frac{wt}{\rho V} \qquad \Theta = \frac{T - T_\infty}{T_i - T_\infty} \tag{15B.8-2, 3}$$

where

$$T_\infty = \frac{(UA/w\hat{C}_p)T_s + T_i}{(UA/w\hat{C}_p) + 1} \tag{15B.8-4}$$

What is the physical significance of τ, Θ, and T_∞?

(c) Solve the dimensionless equation obtained in (b) for the initial condition that $T = T_i$ at $t = 0$.

(d) Check the solution to see that the differential equation and initial condition are satisfied. How does the system behave at large time? Is this limiting behavior in agreement with your intuition?

(e) How is the temperature at infinite time affected by the flow rate? Is this reasonable?

Answer: **(c)** $\dfrac{T - T_\infty}{T_i - T_\infty} = \exp\left[-\left(\dfrac{UA}{\rho\hat{C}_pV} + \dfrac{w}{\rho V}\right)t\right]$

15C.1. Parallel–counterflow heat exchangers (Fig. 15C.1). In the heat exchanger shown in the accompanying figure, the "tube fluid" (fluid A) enters and leaves at the same end of the heat exchanger, whereas the "shell fluid" (fluid B) always moves in the same direction. Thus there are both parallel flow and counterflow in the same apparatus. This flow arrangement is one of the simplest examples of "mixed flow," often used in practice to reduce exchanger length.[2]

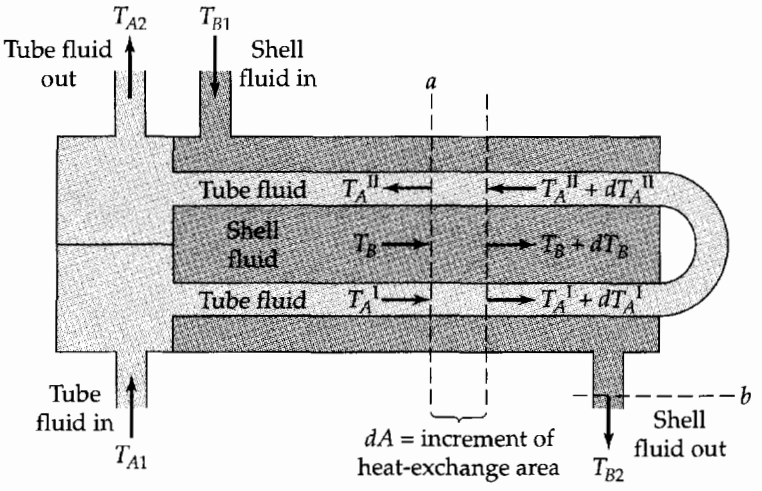

Fig. 15C.1. A parallel–counterflow heat exchanger.

[2] See D. Q. Kern, *Process Heat Transfer*, McGraw-Hill, New York (1950), pp. 127–189; J. H. Perry, *Chemical Engineers' Handbook*, 3rd edition, McGraw-Hill, New York, (1950), pp. 464–465; W. M. Rohsenow, J. P. Hartnett, and Y. I. Cho, *Handbook of Heat Transfer*, 3rd edition, McGraw-Hill, New York (1998), Chapter 17; S. Whitaker, *Fundamentals of Heat Transfer*, corrected edition, Krieger Publishing Company, Malabar, Fla., (1983), Chapter 11.

The behavior of this kind of equipment may be simply analyzed by making the following assumptions:

(i) Steady-state conditions exist.

(ii) The overall heat transfer coefficient U and the heat capacities of the two fluids are constants.

(iii) The shell-fluid temperature T_B is constant over any cross section perpendicular to the flow direction.

(iv) There is an equal amount of heating area in each tube fluid "pass"—that is, for streams I and II in the figure.

(a) Show by an energy balance over the portion of the system between planes a and b that

$$T_B - T_{B2} = R(T_A^{II} - T_A^{I}) \qquad \text{where } R = |w_A\hat{C}_{pA}/w_B\hat{C}_{pB}| \tag{15C.1-1}$$

(b) Show that over a differential section of the exchanger, including a *total* heat exchange surface dA,

$$\frac{dT_A^{I}}{d\alpha} = \frac{1}{2}(T_B - T_A^{I}) \tag{15C.1-2}$$

$$\frac{dT_A^{II}}{d\alpha} = \frac{1}{2}(T_A^{II} - T_B) \tag{15C.1-3}$$

$$\frac{1}{R}\frac{dT_B}{d\alpha} = -\left[T_B - \frac{1}{2}(T_A^{I} + T_A^{II})\right] \tag{15C.1-4}$$

in which $d\alpha = (U/w_A\hat{C}_{pA})dA$, and w_A and $\hat{C}_{pA}$ are defined as in Example 15.4-1.

(c) Show that when T_A^{I} and T_A^{II} are eliminated between these three equations, a differential equation for the shell fluid can be obtained:

$$\frac{d^2\Theta}{d\alpha^2} + R\frac{d\Theta}{d\alpha} - \frac{1}{4}\Theta = 0 \tag{15C.1-5}$$

in which $\Theta(\alpha) = (T_B - T_{B2})/(T_{B1} - T_{B2})$. Solve this equation (see Eq. C.1-7) with the boundary conditions

B.C. 1: at $\alpha = 0$, $\Theta = 1$ (15C.1-6)

B.C. 2: at $\alpha = (UA_T/w_A\hat{C}_{pA})$, $\Theta = 0$ (15C.1-7)

in which A_T is the total heat-exchange surface of the exchanger.

(d) Use the result of part (c) to obtain an expression for $dT_B/d\alpha$. Eliminate $dT_B/d\alpha$ from this expression with the aid of Eq. 15C.1-4 and evaluate the resulting equation at $\alpha = 0$ to obtain the following relation for the performance of the exchanger:

$$\alpha_T = \frac{UA_T}{w_A\hat{C}_{pA}} = \frac{1}{\sqrt{R^2+1}}\ln\left[\frac{2 - \Psi(R + 1 - \sqrt{R^2+1})}{2 - \Psi(R + 1 + \sqrt{R^2+1})}\right] \tag{15C.1-8}$$

in which $\Psi = (T_{A2} - T_{A1})/(T_{B1} - T_{A1})$.

(e) Use this result to obtain the following expression for the rate of heat transfer in the exchanger:

$$Q = UA(\Delta T)_{ln} \cdot Y \tag{15C.1-9}$$

in which

$$(\Delta T)_{ln} = \frac{(T_{B1} - T_{A2}) - (T_{B2} - T_{A1})}{\ln[(T_{B1} - T_{A2})/(T_{B2} - T_{A1})]} \tag{15C.1-10}$$

$$Y = \frac{\sqrt{R^2+1}\,\ln[(1 - \Psi)/(1 - R\Psi)]}{(R-1)\ln\left[\dfrac{2 - \Psi(R + 1 - \sqrt{R^2+1})}{2 - \Psi(R + 1 + \sqrt{R^2+1})}\right]} \tag{15C.1-11}$$

The quantity Y represents the ratio of the heat transferred in the "1–2 parallel–counterflow exchanger" shown to that transferred in a true counterflow exchanger of the same area and terminal fluid temperatures. Values of $Y(R, \Psi)$ are given graphically in Perry's handbook.[2] It may be seen that $Y(R, \Psi)$ is always less than unity.

15C.2. Discharge of air from a large tank. It is desired to withdraw 5 lb_m/s from a large storage tank through an equivalent length of 55 ft of new steel pipe 2.067 in. in diameter. The air undergoes a sudden contraction on entering the pipe, and the accompanying contraction loss is not included in the equivalent length of the pipe. Can the desired flow rate be obtained if the air in the tank is at 150 psig and 70°F and the pressure at the downstream end of the pipe is 50 psig?

The effect of the sudden contraction may be estimated with reasonable accuracy by considering the entrance to consist of an ideal nozzle converging to a cross section equal to that of the pipe, followed by a section of pipe with $e_v = 0.5$ (see Table 7.5-1). The behavior of the nozzle can be determined from Eq. 15.5-34 by assuming the cross sectional area S_1 to be infinite and C_d to be unity.

Answer: Yes. The calculated discharge rate is about 6 lb_m/s if *isothermal* flow is assumed (see Problem 15B.3) and about 6.3 lb_m/s for *adiabatic* flow. The actual rate should be between these limits for an ambient temperature of 70°F.

15C.3. Stagnation temperature (Fig. 15C.3). A "total temperature probe," as shown in the figure, is inserted in a steady stream of an ideal gas at a temperature T_1 and moving with a velocity v_1. Part of the moving gas enters the open end of the probe and is decelerated to nearly zero velocity before slowly leaking out of the bleed holes. This deceleration results in a temperature rise, which is measured by the thermocouple. Since the deceleration is rapid, it is nearly adiabatic.

(a) Develop an expression for the temperature registered by the thermocouple in terms of T_1 and v_1 by using the steady-state macroscopic energy balance, Eq. 15.1-3. Use as your system a representative stream of fluid entering the probe. Draw reference plane 1 far enough upstream that conditions may be assumed unaffected by the probe, and reference plane 2 in the probe itself. Assume zero velocity at plane 2, neglect radiation, and neglect conduction of heat from the fluid as it passes between the reference planes.

(b) What is the function of the bleed holes?

Answer: **(a)** $T_2 - T_1 = v_1^2/2\hat{C}_p$. Temperature rises within about 2% of those given by this expression and may be obtained with well-designed probes.

15D.1. The macroscopic entropy balance.

(a) Show that integration of the equation of change for entropy (Eq. 11D.1-3) over the flow system of Fig. 7.0-1 leads to

$$\frac{d}{dt} S_{\text{tot}} = -\Delta\left(\hat{S} + \frac{q}{\rho v T}\right)w + g_{S,\text{tot}} + Q_S \tag{15D.1-1}$$

in which

$$S_{\text{tot}} = \int_V \rho \hat{S} dV \tag{15D.1-2}$$

$$g_{S,\text{tot}} = -\int_V \frac{1}{T}((\mathbf{q} \cdot \boldsymbol{\nabla} \ln T) + (\boldsymbol{\tau}:\boldsymbol{\nabla}\mathbf{v}))dV \tag{15D.1-3}$$

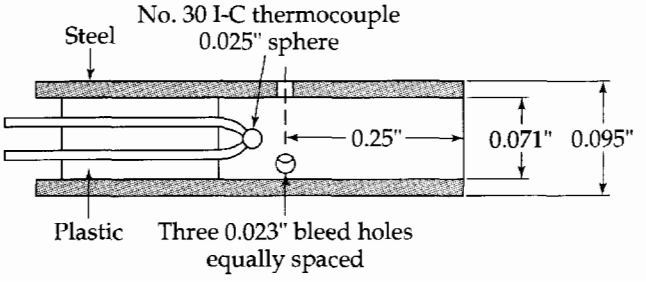

Fig. 15C.3. A "total temperature probe." [H. C. Hottel and A. Kalitinsky, *J. Appl. Mech.*, **12**, A25 (1945).]

(b) Give a term-by-term interpretation of the equations in (a).

(c) Is the term in $g_{s,\text{tot}}$ involving the stress tensor the same as the energy dissipation by viscous heating?

15D.2. Derivation of the macroscopic energy balance. Show how to integrate Eq. (N) of Table 11.4-1 over the entire volume V of a flow system, which, because of moving parts, may be a function of time. With the help of the Gauss divergence theorem and the Leibniz formula for differentiating an integral, show that this gives the macroscopic total energy balance Eq. 15.1-2. What assumptions are made in the derivation? How is W_m to be interpreted? (*Hint:* Some suggestions on solving this problem may be obtained by studying the derivation of the macroscopic mechanical energy balance in §7.8.)

15D.3. Operation of a heat-exchange device (Fig. 15D.3). A hot fluid enters the circular tube of radius R_1 at position $z = 0$ and moves in the positive z direction to $z = L$, where it leaves the tube and flows back along the outside of that tube in the annular space. Heat is exchanged between the fluid in the tube and that in the annulus. Also heat is lost from the annulus to the air outside, which is at the ambient air temperature T_a (a constant). Assume that the density and heat capacity are constant. Use the following notation:

U_1 = overall heat transfer coefficient between the fluid in the tube and the fluid in the annular space

U_2 = overall heat transfer coefficient between the fluid in the annulus and the air at temperature T_a

$T_1(z)$ = temperature of the fluid in the tube

$T_2(z)$ = temperature of the fluid in the annular space

w = mass flow rate through the system (a constant)

If the fluid enters at the inlet temperature T_i, what will be the outlet temperature T_o? It is suggested that the following dimensionless quantities be used: $\Theta_1 = (T_1 - T_a)/(T_i - T_a)$, $N_1 = 2\pi R_1 U_1 L/w\,\hat{C}_p$, and $\zeta = z/L$.

15D.4. Discharge of a gas from a moving tank (Fig. 15.5-6). Equation 15.5-38 in Example 15.5-4 was obtained by setting $d\hat{\Phi}/dt$ equal to zero, a procedure justified only because the tank was said to be stationary. It is nevertheless true that Eq. 15.5-38 is correct for moving tanks as well. This statement can be proved as follows:

(a) Consider a tank such as that pictured in Fig. 15.5-6, but moving at a velocity $\mathbf{v}$ that is much larger than the relative velocity of fluid and tank in the region to the left of surface 1. Show that for this region of the tank the macroscopic momentum balance becomes

$$-\left(\mathbf{F}_{f\to s} + \mathbf{u}_2 \int_{S_1} p_1 dS\right) = m_{\text{tot}}\left(\frac{d\mathbf{v}}{dt} - \mathbf{g}\right) \qquad \text{(15D.4-1)}$$

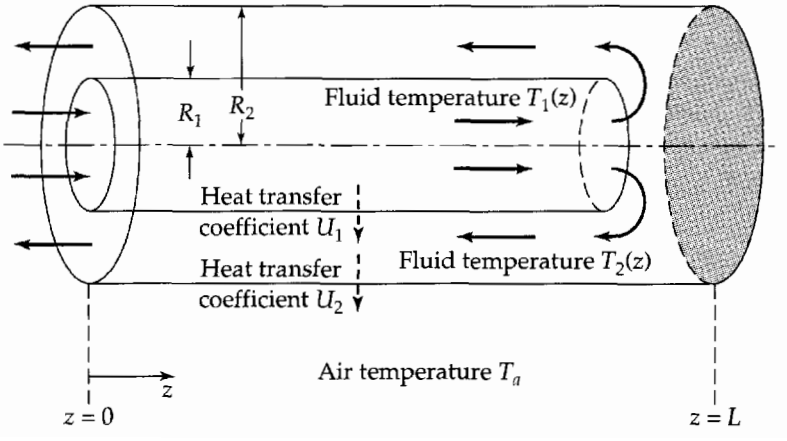

Fig. 15D.3. A heat-exchange device.

in which the fluid velocity is assumed to be uniform and equal to **v**. Then take the dot product of both sides of Eq. 15D.4-1 with **v** to obtain

$$W_m = m_{\text{tot}}\left(\frac{d\hat{K}}{dt} + \frac{d\hat{\Phi}}{dt}\right) \tag{15D.4-2}$$

where $\partial\hat{\Phi}/\partial t$ is neglected.

(b) Substitute this result into the macroscopic energy balance, and continue as in Example 15.5-4.

15D.5. The classical Bernoulli equation. Below Eq. 15.2-5 we have emphasized that the mechanical energy balance and the total energy balance contain different information, since the first is a consequence of conservation of momentum, whereas the second is a consequence of conservation of energy.

For the steady-state flow of a compressible fluid with zero transport properties, both balances lead to the classical Bernoulli equation. The derivation based on the equation of motion was given in Example 3.5-1. Make a similar derivation for the steady state energy equation, assuming zero transport properties, that is, for isentropic flow.[3]

[3] R. B. Bird and M. D. Graham, in *Handbook of Fluid Dynamics* (R. W. Johnson, ed.), CRC Press, Boca Raton, Fla. (1998), p. 3-13.

Chapter 16

Energy Transport by Radiation

We concluded Part I of this book with a chapter about fluids that cannot be described by Newton's law of viscosity, but that require various kinds of nonlinear and time-dependent expressions. We now end Part II with a brief discussion of radiative energy transport, which cannot be described by Fourier's law.

In Chapters 9 to 15 the transport of energy by conduction and by convection has been discussed. Both modes of transport rely on the presence of a material medium. For *heat conduction* to occur, there must be temperature inequalities between neighboring points. For *heat convection* to occur, there must be a fluid that is free to move and transport energy with it. In this chapter, we turn our attention to a third mechanism for energy transport—namely, *radiation*. Radiation is basically an electromagnetic mechanism, which allows energy to be transported with the speed of light through regions of space that are devoid of matter. The rate of energy transport between two "black" bodies in a vacuum is proportional to the difference of the fourth powers of their absolute temperatures. This mechanism is qualitatively very different from the three transport mechanisms considered elsewhere in this book: momentum transport in Newtonian fluids, proportional to the velocity gradient; energy transport by heat conduction, proportional to a temperature gradient; and mass transport by diffusion, proportional to a concentration gradient. Because of the uniqueness of radiation as a means of transport and because of the importance of radiant heat transfer in industrial calculations, we have devoted a separate chapter to this subject.

A thorough understanding of the physics of radiative transport requires the use of several different disciplines:[1,2] electromagnetic theory is needed to describe the essentially wavelike nature of radiation, in particular the energy and pressure associated with electromagnetic waves; thermodynamics is useful for obtaining some relations among

[1] M. Planck, *Theory of Heat*, Macmillan, London (1932), Parts III and IV. Nobel Laureate **Max Karl Ernst Ludwig Planck** (1858–1947) was the first to hypothesize the quantization of energy and thereby introduce a new fundamental constant h (Planck's constant); his name is also associated with the "Fokker–Planck" equation of stochastic dynamics.

[2] W. Heitler, *Quantum Theory of Radiation*, 2nd edition, Oxford University Press (1944).

the "bulk properties" of an enclosure containing radiation; quantum mechanics is necessary in order to describe in detail the atomic and molecular processes that occur when radiation is produced within matter and when it is absorbed by matter; and statistical mechanics is needed to describe the way in which the energy of radiation is distributed over the wavelength spectrum. All we can do in this elementary discussion is define the key quantities and set forth the results of theory and experiment. We then show how some of these results can be used to compute the rate of heat transfer by radiant processes in simple systems.

In §16.1 and §16.2 we introduce the basic concepts and definitions. Then in §16.3 some of the principal physical results concerning black-body radiation are given. In the following section, §16.4, the rate of heat exchange between two black bodies is discussed. This section introduces no new physical principles, the basic problems being those of geometry. Next, §16.5 is devoted to an extension of the preceding section to nonblack surfaces. Finally, in the last section, there is a brief discussion of radiation processes in absorbing media.[3]

§16.1 THE SPECTRUM OF ELECTROMAGNETIC RADIATION

When a solid body is heated—for example, by an electric coil—the surface of the solid emits radiation of wavelength primarily in the range 0.1 to 10 microns. Such radiation is usually referred to as *thermal radiation*. A quantitative description of the atomic and molecular mechanisms by which the radiation is produced is given by quantum mechanics and is outside the scope of this discussion. A qualitative description, however, is possible: When energy is supplied to a solid body, some of the constituent molecules and atoms are raised to "excited states." There is a tendency for the atoms or molecules to return spontaneously to lower energy states. When this occurs, energy is emitted in the form of electromagnetic radiation. Because the emitted radiation results from changes in the electronic, vibrational, and rotational states of the atoms and molecules, the radiation will be distributed over a range of wavelengths.

Actually, thermal radiation represents only a small part of the total spectrum of electromagnetic radiation. Figure 16.1-1 shows roughly the kinds of mechanisms that are responsible for the various parts of the radiation spectrum. The various kinds of radiation are distinguished from one another only by the range of wavelengths they include. In a vacuum, all these forms of radiant energy travel with the speed of light c. The wavelength λ, characterizing an electromagnetic wave, is then related to its frequency ν by the equation

$$\lambda = \frac{c}{\nu} \tag{16.1-1}$$

in which $c = 2.998 \times 10^8$ m/s. In the visible part of the spectrum, the various wavelengths are associated with the "color" of the light.

For some purposes, it is convenient to think of electromagnetic radiation from a corpuscular point of view. Then we associate with an electromagnetic wave of frequency ν a *photon*, which is a particle with charge zero and mass zero with an energy given by

$$\varepsilon = h\nu \tag{16.1-2}$$

---

[3] For additional information on radiative heat transfer and engineering applications, see the comprehensive textbook by R. Siegel and J. R. Howell, *Thermal Radiation Heat Transfer*, 3rd edition, Hemisphere Publishing Co., New York (1992). See also J. R. Howell and M. P. Mengöç, in *Handbook of Heat Transfer*, 3rd edition, (W. M. Rohsenow, J. P. Hartnett, and Y. I. Cho, eds.), McGraw-Hill, New York (1998), Chapter 7.

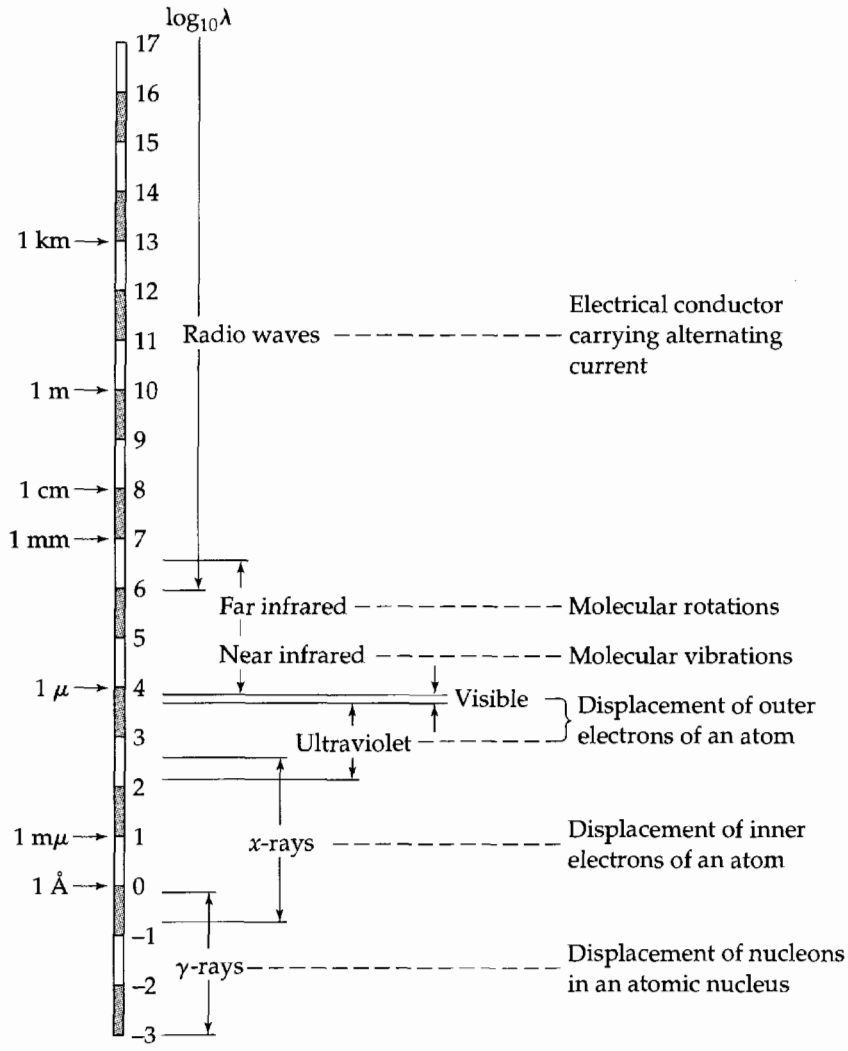

Fig. 16.1-1. The spectrum of electromagnetic radiation, showing roughly the mechanisms by which various wavelengths of radiation are produced (1 Å = Ångström unit = 10^{-8} cm = 0.1 nm; 1 μ = 1 micron = 10^{-6} m).

Here $h = 6.626 \times 10^{-34}$ J·s is Planck's constant. From these two equations and the information from Fig. 16.1-1, we see that decreasing the wavelength of electromagnetic radiation corresponds to increasing the energy of the corresponding photons. This fact ties in with the various mechanisms that produce the radiation. For example, relatively small energies are released when a molecule decreases its speed of rotation, and the associated radiation is in the infrared. On the other hand, relatively large energies are released when an atomic nucleus goes from a high energy state to a lower one, and the associated radiation is either gamma- or x-radiation. The foregoing statements also make it seem reasonable that the radiant energy emitted from heated objects will tend toward shorter wavelengths (higher energy photons) as the temperature of the body is raised.

Thus far we have sketched the phenomenon of the *emission* of radiant energy or photons when a molecular or atomic system goes from a high to a low energy state. The reverse process, known as absorption, occurs when the addition of radiant energy to a molecular or atomic system causes the system to go from a low to a high energy state. The latter process is then what occurs when radiant energy impinges on a solid surface and causes its temperature to rise.

§16.2 ABSORPTION AND EMISSION AT SOLID SURFACES

Having introduced the concepts of absorption and emission in terms of the atomic picture, we now proceed to the discussion of the same processes from a macroscopic viewpoint. We restrict the discussion here to opaque solids.

Radiation impinging on the surface of an opaque solid is either absorbed or reflected. The fraction of the incident radiation that is absorbed is called the *absorptivity* and is given the symbol a. Also the fraction of the incident radiation with frequency ν that is absorbed is designated by a_ν. That is, a and a_ν are defined as

$$a = \frac{q^{(a)}}{q^{(i)}} \qquad a_\nu = \frac{q_\nu^{(a)}}{q_\nu^{(i)}} \tag{16.2-1, 2}$$

in which $q_\nu^{(a)}d\nu$ and $q_\nu^{(i)}d\nu$ are the absorbed and incident radiation per unit area per unit time in the frequency range ν to $\nu + d\nu$. For any *real body*, a_ν will be less than unity and will vary considerably with the frequency. A hypothetical body for which a_ν is a constant, less than unity, over the entire frequency range and at all temperatures is called a *gray body*. That is, a gray body always absorbs the same fraction of the incident radiation of all frequencies. A limiting case of the gray body is that for which $a_\nu = 1$ for all frequencies and all temperatures. This limiting behavior defines a *black body*.

All solid surfaces emit radiant energy. The total radiant energy emitted per unit area per unit time is designated by $q^{(e)}$, and that emitted in the frequency range ν to $\nu + d\nu$ is called $q_\nu^{(e)}d\nu$. The corresponding rates of energy emission from a black body are given the symbols $q_b^{(e)}$ and $q_{b\nu}^{(e)}d\nu$. In terms of these quantities, the *emissivity* for the total radiant-energy emission as well as that for a given frequency are defined as

$$e = \frac{q^{(e)}}{q_b^{(e)}} \qquad e_\nu = \frac{q_\nu^{(e)}}{q_{b\nu}^{(e)}} \tag{16.2-3, 4}$$

The emissivity is also a quantity less than unity for real, nonfluorescing surfaces and is equal to unity for black bodies. At any given temperature the radiant energy emitted by a black body represents an upper limit to the radiant energy emitted by real, nonfluorescing surfaces.

We now consider the radiation within an evacuated enclosure or "cavity" with isothermal walls. We imagine that the entire system is at equilibrium. Under this condition, there is no net flux of energy across the interfaces between the solid and the cavity. We now show that the radiation in such a cavity is independent of the nature of the walls and dependent solely on the temperature of the walls of the cavity. We connect two cavities, the walls of which are at the same temperature, but are made of two different materials, as shown in Fig. 16.2-1. If the radiation intensities in the two cavities were different, there would be a net transport of radiant energy from one cavity to the other. Because such a flux would violate the second law of thermodynamics, the radiation intensities in the two cavities must be equal, regardless of the compositions of the cavity surfaces. Furthermore, it can be shown that the radiation is uniform and unpolarized throughout the cavity. This *cavity radiation* plays an important role in the development

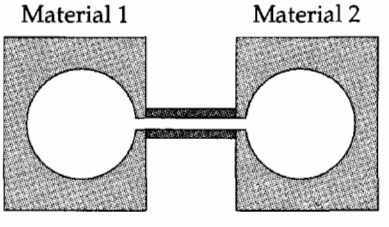

Fig. 16.2-1. Thought experiment for proof that cavity radiation is independent of the wall materials.

of Planck's law. We designate the intensity of the radiation as $q^{(\text{cav})}$. This is the radiant energy that would impinge on a solid surface of unit area placed anywhere within the cavity.

We now perform two additional thought experiments. In the first, we put into a cavity a small black body at the same temperature as the walls of the cavity. There will be no net interchange of energy between the black body and the cavity walls. Hence the energy impinging on the black-body surface must equal the energy emitted by the black body:

$$q^{(\text{cav})} = q_b^{(e)} \tag{16.2-5}$$

From this result, we draw the important conclusion that the radiation emitted by a black body is the same as the equilibrium radiation intensity within a cavity at the same temperature.

In the second thought experiment, we put a small nonblack body into the cavity, once again specifying that its temperature be the same as that of the cavity walls. There is no net heat exchange between the nonblack body and the cavity walls. Hence we can state that the energy absorbed by the nonblack body will be the same as that radiating from it:

$$aq^{(\text{cav})} = q^{(e)} \tag{16.2-6}$$

Comparison of Eqs. 16.2-5 and 6 leads to the result

$$a = \frac{q^{(e)}}{q_b^{(e)}} \tag{16.2-7}$$

The definition of the emissivity e in Eq. 16.2-3 allows us to conclude that

$$\boxed{e = a} \tag{16.2-8}$$

This is *Kirchhoff's law*,[1] which states that at a given temperature the emissivity and absorptivity of any solid surface are the same when the radiation is in equilibrium with the solid surface. It can be shown that Eq. 16.2-8 is also valid for each wavelength separately:

$$\boxed{e_\nu = a_\nu} \tag{16.2-9}$$

Values of the total emissivity e for some solids are given in Table 16.2-1. Actually, e depends also on the frequency and on the angle of emission, but the averaged values given there have found widespread use. The tabulated values are, with a few exceptions, for emission normal to the surface, but they may be used for hemispheric emissivity, particularly for rough surfaces. Unoxidized, clean, metallic surfaces have very low emissivities, whereas most nonmetals and metallic oxides have emissivities above 0.8 at room temperature or higher. Note that emissivity increases with increasing temperature for nearly all materials.

We have indicated that the radiant energy emitted by a black body is an upper limit to the radiant energy emitted by real surfaces and that this energy is a function of the temperature. It has been shown experimentally that the total emitted energy flux from a *black* surface is

$$\boxed{q_b^{(e)} = \sigma T^4} \tag{16.2-10}$$

---

[1] G. Kirchhoff, *Monatsber. d. preuss. Akad. d. Wissenschaften*, p. 783 (1859); *Poggendorffs Annalen*, **109**, 275–301 (1860). **Gustav Robert Kirchhoff** (1824–1887) published his famous laws for electrical circuits while still a graduate student; he taught at Breslau, Heidelberg, and Berlin.

Table 16.2-1 The Total Emissivities of Various Surfaces for Perpendicular Emission[a]

	T(°R)	e	T(°R)	e
Aluminum				
Highly polished,98.3% pure	900	0.039	1530	0.057
Oxidized at 1110°F	850	0.11	1570	0.19
Al-coated roofing	560	0.216		
Copper				
Highly polished, electrolytic	636	0.018		
Oxidized at 1110°F	850	0.57	1570	0.57
Iron				
Highly polished, electrolytic	810	0.052	900	0.064
Completely rusted	527	0.685		
Cast iron, polished	852	0.21		
Cast iron, oxidized at 1100°F	850	0.64	1570	0.78
Asbestos paper	560	0.93	1160	0.945
Brick				
Red, rough	530	0.93		
Silica, unglazed, rough	2292	0.80		
Silica, glazed, rough	2472	0.85		
Lampblack, 0.003 in. or thicker	560	0.945	1160	0.945
Paints				
Black shiny lacquer on iron	536	0.875		
White lacquer	560	0.80	660	0.95
Oil paints, 16 colors	672	0.92–0.96		
Aluminum paints, varying age and lacquer content	672	0.27–0.67		
Refractories, 40 different				
Poor radiators	1570	0.65–0.70	2290	0.75
Good radiators	1570	0.80–0.85	2290	0.85–0.90
Water, liquid, thick layer[b]	492	0.95	672	0.963

[a] Selected values from the table compiled by H. C. Hottel for W. H. McAdams, *Heat Transmission*, 3rd edition, McGraw-Hill, New York (1954), pp. 472–479.

[b] Calculated from spectroscopic data.

in which T is the absolute temperature. This is known as the *Stefan–Boltzmann law*.[2] The Stefan–Boltzmann constant σ has been found to have the value of 0.1712×10^{-8} Btu/hr · ft^2 · R or 1.355×10^{-12} cal/s · cm^2 · K. In the next section we indicate two routes by which this important formula has been obtained theoretically. For *nonblack* surfaces at temperature T the emitted energy flux is

$$\boxed{q^{(e)} = e\sigma T^4} \tag{16.2-11}$$

[2] J. Stefan, *Sitzber. Akad. Wiss. Wien*, **79**, part 2, 391–428 (1879); L. Boltzmann, *Ann. Phys.* (*Wied. Ann.*), Ser. 2, **22**, 291–294 (1884). Slovenian-born **Josef Stefan** (1835–1893), rector of the University of Vienna (1876–1877), in addition to being known for the law of radiation that bears his name, also contributed to the theory of multicomponent diffusion and to the problem of heat conduction with phase change. **Ludwig Eduard Boltzmann** (1844–1906), who held professorships in Vienna, Graz, Munich, and Leipzig, developed the basic differential equation for gas kinetic theory (see Appendix D) and the fundamental entropy-probability relation, $S = \kappa \ln W$, which is engraved on his tombstone in Vienna; κ is called the Boltzmann constant.

in which e must be evaluated at temperature T. The use of Eqs. 16.2-10 and 11 to calculate radiant heat transfer rates between heated surfaces is discussed in §§16.4 and 5.

We have mentioned that the Stefan–Boltzmann constant has been experimentally determined. This implies that we have a true black body at our disposal. Solids with perfectly black surfaces do not exist. However, we can get an excellent approximation to a black surface by piercing a very small hole in the wall of an isothermal cavity. The hole itself is then very nearly a black surface. The extent to which this is a good approximation may be seen from the following relation, which gives the effective emissivity of the hole, e_{hole}, in a rough-walled enclosure in terms of the actual emissivity e of the cavity walls and the fraction f of the total internal cavity area that is cut away by the hole:

$$e_{\text{hole}} \cong \frac{e}{e + f(1 - e)} \tag{16.2-12}$$

If $e = 0.8$ and $f = 0.001$, then $e_{\text{hole}} = 0.99975$. Therefore, 99.975% of the radiation that falls on the hole will be absorbed. The radiation that emerges from the hole will then be very nearly black-body radiation.

§16.3 PLANCK'S DISTRIBUTION LAW, WIEN'S DISPLACEMENT LAW, AND THE STEFAN–BOLTZMANN LAW[1,2,3]

The Stefan–Boltzmann law may be deduced from thermodynamics, provided that certain results of the theory of electromagnetic fields are known. Specifically, it can be shown that for cavity radiation the energy density (that is, the energy per unit volume) within the cavity is

$$u^{(r)} = \frac{4}{c} q_b^{(e)} \tag{16.3-1}$$

Since the radiant energy emitted by a black body depends on temperature alone, the energy density $u^{(r)}$ must also be a function of temperature only. It can further be shown that the electromagnetic radiation exerts a pressure $p^{(r)}$ on the walls of the cavity given by

$$p^{(r)} = \tfrac{1}{3} u^{(r)} \tag{16.3-2}$$

The preceding results for cavity radiation can also be obtained by considering the cavity to be filled with a gas made up of photons, each endowed with an energy $h\nu$ and momentum $h\nu/c$. We now apply the thermodynamic formula

$$\left(\frac{\partial U}{\partial V}\right)_T = T\left(\frac{\partial p}{\partial T}\right)_V - p \tag{16.3-3}$$

to the photon gas or radiation in the cavity. Insertion of $U^{(r)} = Vu^{(r)}$ and $p^{(r)} = \frac{1}{3}u^{(r)}$ into this relation gives the following ordinary differential equation for $u^{(r)}(T)$:

$$u^{(r)} = \tfrac{1}{3} T \frac{du^{(r)}}{dT} - \tfrac{1}{3} u^{(r)} \tag{16.3-4}$$

---

[1] J. de Boer, Chapter VII in *Leerboek der Natuurkunde*, 3rd edition, (R. Kronig, ed.), Scheltema and Holkema, Amsterdam (1951).

[2] H. B. Callen, *Thermodynamics and an Introduction to Thermostatistics*, 2nd edition, Wiley, New York (1985), pp. 78–79.

[3] M. Planck, *Vorlesungen über die Theorie der Wärmestrahlung*, 5th edition, Barth, Leipzig (1923); *Ann. Phys.*, **4**, 553–563, 564–566 (1901).

This equation can be integrated to give

$$u^{(r)} = bT^4 \tag{16.3-5}$$

in which b is a constant of integration. Combination of this result with Eq. 16.3-1 gives the radiant energy emitted from the surface of a black body per unit area per unit time:

$$q_b^{(e)} = \frac{c}{4} u^{(r)} = \frac{cb}{4} T^4 = \sigma T^4 \tag{16.3-6}$$

This is the Stefan–Boltzmann law. Note that the thermodynamic development does not predict the numerical value of σ.

The second way of deducing the Stefan–Boltzmann law is by integrating the *Planck distribution law*. This famous equation gives the radiated energy flux $q_{b\lambda}^{(e)}$ from a black surface in the wavelength range λ to $\lambda + d\lambda$:

$$\boxed{q_{b\lambda}^{(e)} = \frac{2\pi c^2 h}{\lambda^5} \frac{1}{e^{ch/\lambda \kappa T} - 1}} \tag{16.3-7}$$

Here h is Planck's constant. The result can be derived by applying quantum statistics to a photon gas in a cavity, the photons obeying Bose–Einstein statistics.[4,5] The Planck distribution, which is shown in Fig. 16.3-1, correctly predicts the entire energy versus wavelength curve and the shift of the maximum toward shorter wavelengths at higher temperatures. When Eq. 16.3-7 is integrated over all wavelengths, we get

$$\begin{aligned} q_b^{(e)} &= \int_0^\infty q_{b\lambda}^{(e)} d\lambda \\ &= 2\pi c^2 h \int_0^\infty \frac{\lambda^{-5}}{e^{ch/\lambda \kappa T} - 1} d\lambda \\ &= \frac{2\pi \kappa^4 T^4}{c^2 h^3} \int_0^\infty \frac{x^3}{e^x - 1} dx \\ &= \frac{2\pi \kappa^4 T^4}{c^2 h^3} \left(6 \sum_{n=1}^{\infty} \frac{1}{n^4} \right) \\ &= \frac{2\pi \kappa^4 T^4}{c^2 h^3} \left(\frac{\pi^4}{15} \right) \end{aligned} \tag{16.3-8}$$

In the above integration we changed the variable of integration from λ to $x = ch/\lambda \kappa T$. Then the integration over x was performed by expanding $1/(e^x - 1)$ in a Taylor series in e^x (see §C.2) and integrating term by term. The quantum statistical approach thus gives the details of the spectral distribution of the radiation and also the expression for the Stefan–Boltzmann constant,

$$\boxed{\sigma = \frac{2}{15} \frac{\pi^5 \kappa^4}{c^2 h^3}} \tag{16.3-9}$$

having the value 1.355×10^{-12} cal/s · cm^2 · K, which is confirmed within experimental uncertainty by direct radiation measurements. Equation 16.3-9 is an amazing formula, interrelating as it does the σ from radiation, the κ from statistical mechanics, the speed of light c from electromagnetism, and the h from quantum mechanics.

In addition to obtaining the Stefan–Boltzmann law from the Planck distribution, we can get an important relation pertaining to the maximum in the Planck distribution. First

[4] J. E. Mayer and M. G. Mayer, *Statistical Mechanics*, Wiley, New York (1940), pp. 363–374.

[5] L. D. Landau and E. M. Lifshitz, *Statistical Physics*, 3rd edition, Part 1, Pergamon, Oxford (1980), §63.

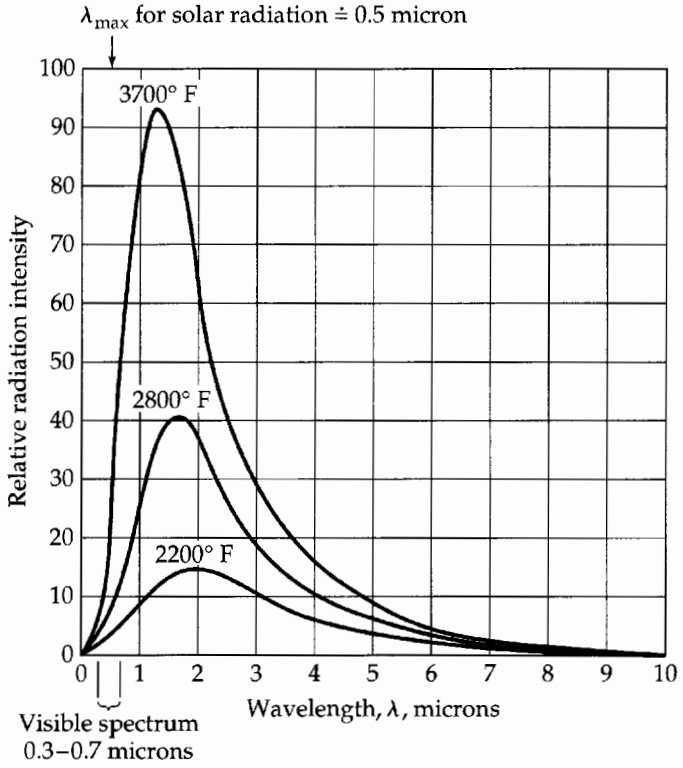

Fig. 16.3-1. The spectrum of equilibrium radiation as given by Planck's law. [M. Planck, *Verh. der deutschen physik. Gesell.*, **2**, 202, 237 (1900); *Ann. der Physik*, **4**, 553–563, 564–566 (1901).

we rewrite Eq. 16.3-7 in terms of x and then set $dq_{b\lambda}^{(e)}/dx = 0$. This gives the following equation for x_{max}, which is the value of x for which the Planck distribution shows a maximum:

$$x_{max} = 5(1 - e^{-x_{max}}) \tag{16.3-10}$$

The solution to this equation is found numerically to be $x_{max} = 4.9651\ldots$. Hence at a given temperature T

$$\lambda_{max}T = \frac{ch}{\mathrm{K}x_{max}} \tag{16.3-11}$$

Inserting the values of the universal constants and the value for x_{max}, we then get

$$\lambda_{max}T = 0.2884 \text{ cm K} \tag{16.3-12}$$

This result, originally found experimentally,[6] is known as *Wien's displacement law*. It is useful primarily for estimating the temperature of remote objects. The law predicts, in agreement with experience, that the apparent color of radiation shifts from red (long wavelengths) toward blue (short wavelengths) as the temperature increases.

Finally, we may reinterpret some of our previous remarks in terms of the Planck distribution law. In Fig. 16.3-2 we have sketched three curves: the Planck distribution law for a hypothetical black body, the distribution curve for a hypothetical gray body, and a distribution curve for some real body. It is thus clear that when we use the total emissivity values, such as those in Table 16.2-1, we are just accounting empirically for the deviations from Planck's law over the entire spectrum.

We should not leave the subject of the Planck distribution without pointing out that Eq. 16.3-7 was presented at the October 1900 meeting of the German Physical Society as

[6] W. Wien, *Sitzungsber. d. kglch. preuss. Akad. d. Wissenschaften*, (VI), p. 55–62 (1893).

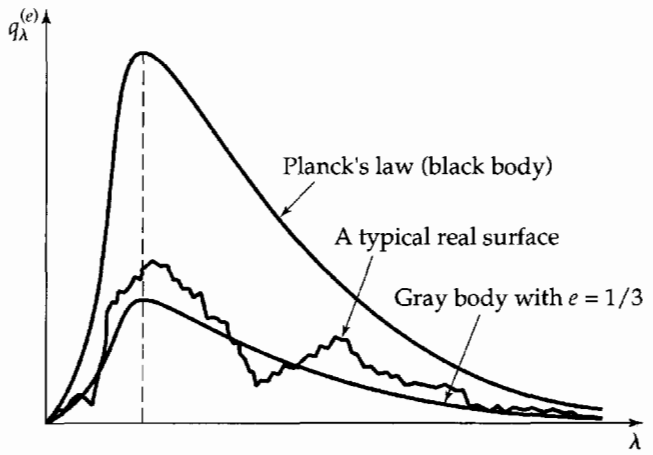

Fig. 16.3-2. Comparison of the emitted radiation from black, gray, and real surfaces.

an *empiricism* that fitted the available data.[7] However, before the end of the year,[8] Planck succeeded in *deriving* the equation, but at the expense of introducing the radical notion of the quantization of energy, an idea that was met with little enthusiasm. Planck himself had misgivings, as clearly stated in his textbook.[9] In a letter in 1931, he wrote: ". . . what I did can be described as an act of desperation. . . . I had been wrestling unsuccessfully for six years. . . with the problem of equilibrium between radiation and matter, and I knew that the problem was of fundamental importance . . ." Then Planck went on to say that he was "ready to sacrifice every one of my previous convictions about physical laws" except for the first and second laws of thermodynamics.[10] Planck's radical proposal ushered in a new and exciting era of physics, and quantum mechanics penetrated into chemistry and other fields in the twentieth century.

EXAMPLE 16.3-1

Temperature and Radiant-Energy Emission of the Sun

For approximate calculations, the sun may be considered a black body, emitting radiation with a maximum intensity at $\lambda = 0.5$ microns (5000 Å). With this information, estimate **(a)** the surface temperature of the sun, and **(b)** the emitted heat flux at the sun's surface.

SOLUTION

(a) From Wien's displacement law, Eq. 16.3-12,

$$T = \frac{0.2884}{\lambda_{max}} = \frac{0.2884 \text{ cm K}}{0.5 \times 10^{-4} \text{ cm}} = 5760\text{K} = 10{,}400 \text{ R} \tag{16.3-13}$$

(b) From the Stefan–Boltzmann law, Eq. 16.2-10,

$$q_b^{(e)} = \sigma T^4 = (0.1712 \times 10^{-8})(10{,}400)^4$$
$$= 2.0 \times 10^7 \text{ Btu/hr} \cdot \text{ft}^2 \tag{16.3-14}$$

---

[7] O. Lummer and E. Pringsheim, *Wied. Ann.*, **63**, 396 (1897); *Ann. der Physik*, **3**, 159 (1900).

[8] M. Planck, *Verhandl. d. deutsch. physik. Ges.*, **2**, 202 and 237 (1900); *Ann. Phys.*, **4**, 553–563, 564–566 (1901).

[9] M. Planck, *The Theory of Heat Radiation*, Dover, New York (1991), English translation of *Vorlesungen über die Theorie der Wärmestrahlung* (1913), p. 154.

[10] A. Hermann, *The Genesis of Quantum Theory*, MIT Press (1971), pp. 23–24.

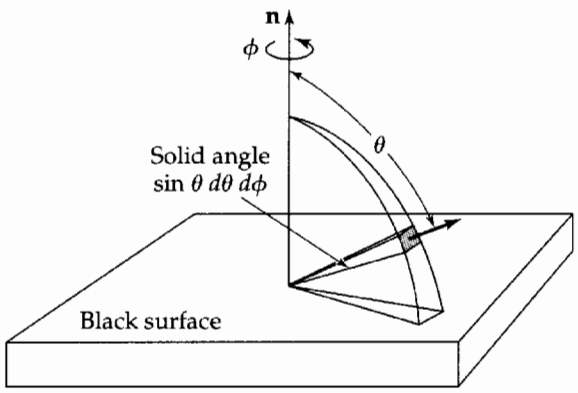

Fig. 16.4-1. Radiation at an angle θ from the normal to the surface into a solid angle $\sin\theta d\theta d\phi$.

§16.4 DIRECT RADIATION BETWEEN BLACK BODIES IN VACUO AT DIFFERENT TEMPERATURES

In the preceding sections we have given the Stefan–Boltzmann law, which describes the total radiant-energy emission from a perfectly black surface. In this section we discuss the radiant-energy transfer between two black bodies of arbitrary geometry and orientation. Hence we need to know how the radiant energy emanating from a black body is distributed with respect to angle. Because black-body radiation is isotropic, the following relation, known as *Lambert's cosine law*,[1] can be deduced:

$$q_{b\theta}^{(e)} = \frac{q_b^{(e)}}{\pi} \cos\theta = \frac{\sigma T^4}{\pi} \cos\theta \tag{16.4-1}$$

in which $q_{b\theta}^{(e)}$ is the energy emitted per unit area per unit time per unit solid angle in a direction θ (see Fig. 16.4-1). The energy emitted through the shaded solid angle is then $q_{b\theta}^{(e)} \sin\theta\, d\theta\, d\phi$ per unit area of black solid surface. Integration of the foregoing expression for $q_{b\theta}^{(e)}$ over the entire hemisphere gives the known total energy emission:

$$\int_0^{2\pi}\int_0^{\pi/2} q_{b\theta}^{(e)} \sin\theta\, d\theta\, d\phi = \frac{\sigma T^4}{\pi}\int_0^{2\pi}\int_0^{\pi/2} \cos\theta \sin\theta\, d\theta\, d\phi$$
$$= \sigma T^4 = q_b^{(e)} \tag{16.4-2}$$

This justifies the inclusion of the factor of $1/\pi$ in Eq. 16.4-1.

We are now in a position to get the net heat transfer rate from body 1 to body 2, where these are black bodies of any shape and orientation (see Fig. 16.4-2). We do this by getting the net heat transfer rate between a pair of surface elements dA_1 and dA_2 that can "see" each other, and then integrating over all such possible pairs of areas. The elements dA_1 and dA_2 are joined by a straight line of length r_{12}, which makes an angle θ_1 with the normal to dA_1 and an angle θ_2 with the normal to dA_2.

We start by writing an expression for the energy radiated from dA_1 into a solid angle $\sin\theta_1\, d\theta_1\, d\phi_1$ about r_{12}. We choose this solid angle large enough that dA_2 will lie entirely within the "beam" (see Fig. 16.4-2). According to Lambert's cosine law, the energy radiated per unit time will be

$$\left(\frac{\sigma T_1^4}{\pi}\cos\theta_1\right) dA_1 \sin\theta_1\, d\theta_1\, d\phi_1 \tag{16.4-3}$$

[1] H. Lambert, *Photometria*, Augsburg (1760).

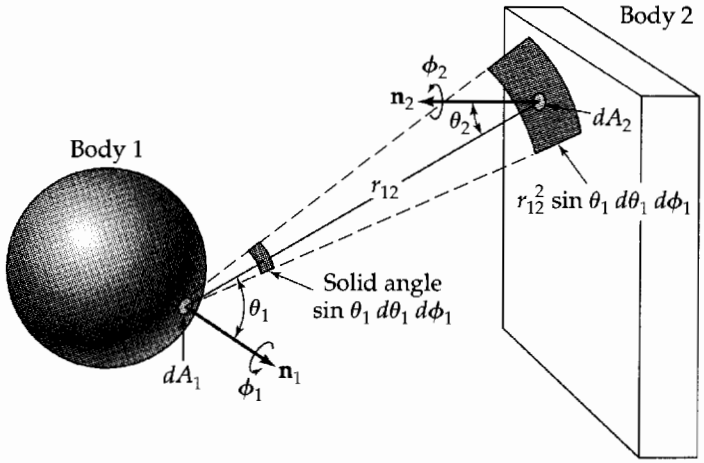

Fig. 16.4-2. Radiant interchange between two black bodies.

Of the energy leaving dA_1 at an angle θ_1, only the fraction given by the following ratio will be intercepted by dA_2:

$$\frac{\begin{pmatrix}\text{area of } dA_2 \text{ projected onto a}\\ \text{plane perpendicular to } r_{12}\end{pmatrix}}{\begin{pmatrix}\text{area formed by the intersection}\\ \text{of the solid angle } \sin\theta_1\, d\theta_1\, d\phi_1\\ \text{with a sphere of radius } r_{12} \text{ with}\\ \text{center at } dA_1\end{pmatrix}} = \frac{dA_2 \cos\theta_2}{r_{12}^2 \sin\theta_1\, d\theta_1\, d\phi_1} \tag{16.4-4}$$

Multiplication of these last two expressions then gives

$$dQ_{\overrightarrow{12}} = \frac{\sigma T_1^4}{\pi} \frac{\cos\theta_1 \cos\theta_2}{r_{12}^2} dA_1 dA_2 \tag{16.4-5}$$

This is the radiant energy emitted by dA_1 and intercepted by dA_2 per unit time. In a similar way we can write

$$dQ_{\overrightarrow{21}} = \frac{\sigma T_2^4}{\pi} \frac{\cos\theta_1 \cos\theta_2}{r_{12}^2} dA_1 dA_2 \tag{16.4-6}$$

which is the radiant energy emitted by dA_2 that is intercepted by dA_1 per unit time. The net rate of energy transport from dA_1 to dA_2 is then

$$\begin{aligned} dQ_{12} &= dQ_{\overrightarrow{12}} - dQ_{\overrightarrow{21}} \\ &= \frac{\sigma}{\pi}(T_1^4 - T_2^4) \frac{\cos\theta_1 \cos\theta_2}{r_{12}^2} dA_1 dA_2 \end{aligned} \tag{16.4-7}$$

Therefore, the net rate of energy transfer from an isothermal black body 1 to another isothermal black body 2 is

$$Q_{12} = \frac{\sigma}{\pi}(T_1^4 - T_2^4) \int\int \frac{\cos\theta_1 \cos\theta_2}{r_{12}^2} dA_1 dA_2 \tag{16.4-8}$$

Here it is understood that the integration is restricted to those pairs of areas dA_1 and dA_2 that are in full view of each other. This result is conventionally written in the form

$$Q_{12} = A_1 F_{12} \sigma (T_1^4 - T_2^4) = A_2 F_{21} \sigma (T_1^4 - T_2^4) \tag{16.4-9}$$

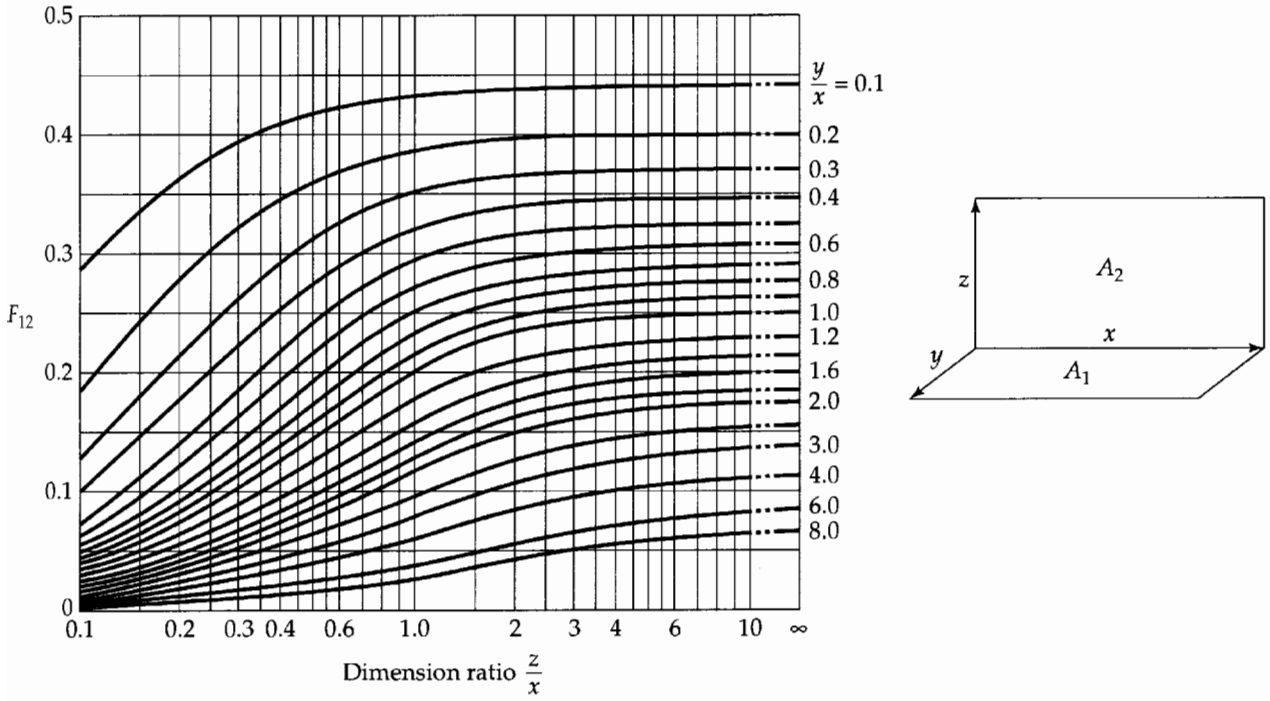

Fig. 16.4-3. View factors for direct radiation between adjacent rectangles in perpendicular planes [H. C. Hottel, Chapter 3 in W. H. McAdams, *Heat Transmission*, McGraw-Hill, New York (1954), p. 68].

where A_1 and A_2 are usually chosen to be the total areas of bodies 1 and 2. The dimensionless quantities F_{12} and F_{21}, called *view factors* (or *angle factors* or *configuration factors*), are given by

$$F_{12} = \frac{1}{\pi A_1} \int\int \frac{\cos\,\theta_1\,\cos\,\theta_2}{r_{12}^2}\, dA_1 dA_2 \tag{16.4-10}$$

$$F_{21} = \frac{1}{\pi A_2} \int\int \frac{\cos\,\theta_1\,\cos\,\theta_2}{r_{12}^2}\, dA_1 dA_2 \tag{16.4-11}$$

and the two view factors are related by $A_1 F_{12} = A_2 F_{21}$. The view factor F_{12} represents the fraction of radiation leaving body 1 that its directly intercepted by body 2.

The actual calculation of view factors is a difficult problem, except for some very simple situations. In Fig. 16.4-3 and Fig. 16.4-4 some view factors for direct radiation are shown.[2,3,4] When such charts are available, the calculations of energy interchanges by Eq. 16.4-9 are easy.

In the above development, we have assumed that Lambert's law and the Stefan–Boltzmann law may be used to describe the nonequilibrium transport process, in spite of the fact that they are strictly valid only for radiative equilibrium. The errors thus introduced do not seem to have been studied thoroughly, but apparently the resulting formulas give a good quantitative description.

---

[2] H. C. Hottel and A. F. Sarofim, *Radiative Transfer*, McGraw-Hill, New York (1967).

[3] H.C. Hottel, Chapter 4 in W. H. McAdams, *Heat Transmission*, McGraw-Hill, New York (1954).

[4] R. Siegel and J. R. Howell, *Thermal Radiation Heat Transfer*, 3rd edition, Hemisphere Publishing Co., New York (1992).

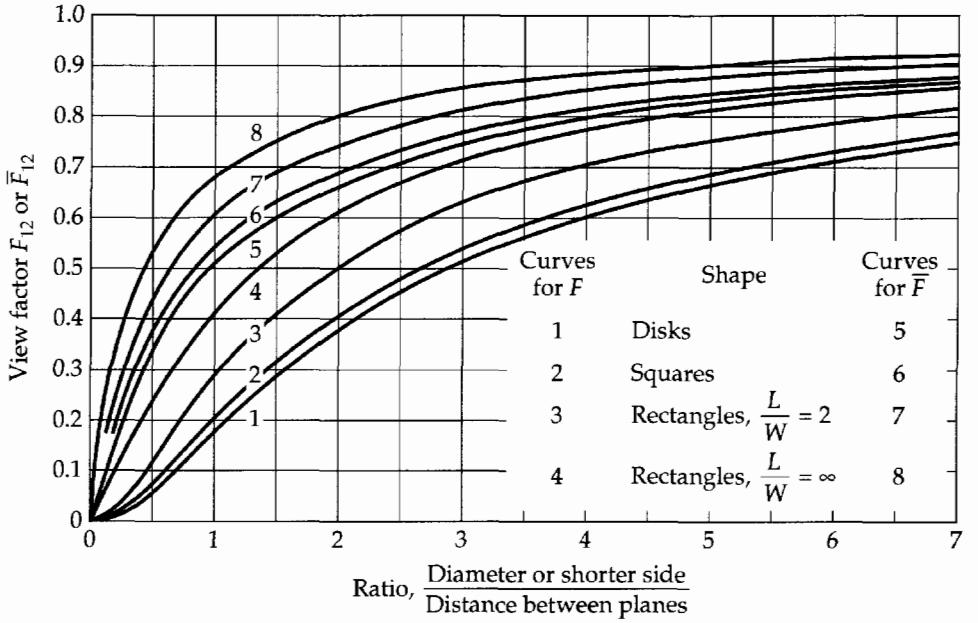

Fig. 16.4-4. View factors for direct radiation between opposed identical shapes in parallel planes. [H. C. Hottel, Chapter 3 in W. H. McAdams *Heat Transmission*, McGraw-Hill, New York (1954), Third Edition, p. 69.]

Thus far we have concerned ourselves with the radiative interactions between two black bodies. We now wish to consider a set of black surfaces 1, 2, . . . , n, which form the walls of a complete enclosure. The surfaces are maintained at temperatures T_1, T_2, . . . , T_n, respectively. The net heat flow from any surface i to the enclosure surfaces is

$$Q_{ie} = \sigma A_i \sum_{j=1}^{n} F_{ij}(T_i^4 - T_j^4) \qquad i = 1, 2, \ldots, n \tag{16.4-12}$$

or

$$Q_{ie} = \sigma A_i \left(T_i^4 - \sum_{j=1}^{n} F_{ij} T_j^4 \right) \qquad i = 1, 2, \ldots, n \tag{16.4-13}$$

In writing the second form, we have used the relations

$$\sum_{j=1}^{n} F_{ij} = 1 \qquad i = 1, 2, \ldots, n \tag{16.4-14}$$

The sums in Eqs. 16.4-13 and 14 include the term F_{ii}, which is zero for any object that intercepts none of its own rays. The set of n equations given in Eq. 16.4-12 (or Eq. 16.4-13) may be solved to get the temperatures or heat flows according to the data available.

A simultaneous solution of Eqs. 16.4-13 and 14 of special interest is that for which $Q_3 = Q_4 = \cdots = Q_n = 0$. Surfaces such as 3, 4, . . . , n are here called "adiabatic." In this situation one can eliminate the temperatures of all surfaces except 1 and 2 from the heat flow calculation and obtain an exact solution for the net heat flow from surface 1 to surface 2:

$$Q_{12} = A_1 \bar{F}_{12} \sigma (T_1^4 - T_2^4) = A_2 \bar{F}_{21} \sigma (T_1^4 - T_2^4) \tag{16.4-15}$$

Values of $\bar{F}_{12}$ for use in this equation are given in Fig. 16.4-4. These values apply only when the adiabatic walls are formed from line elements perpendicular to surfaces 1 and 2.

The use of these view factors F and $\bar{F}$ greatly simplifies the calculations for blackbody radiation, when the temperatures of surfaces 1 and 2 are known to be uniform. The

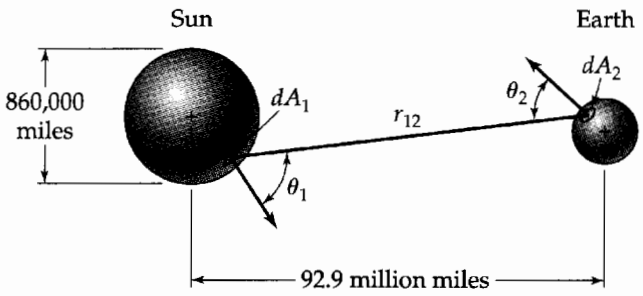

Fig. 16.4-5. Estimation of the solar constant.

reader wishing further information on radiative heat exchange in enclosures is referred to the literature.[4]

EXAMPLE 16.4-1

Estimation of the Solar Constant

The radiant heat flux entering the earth's atmosphere from the sun has been termed the "solar constant" and is important in solar energy utilization as well as in meteorology. Designate the sun as body 1 and the earth as body 2, and use the following data to calculate the solar constant: $D_1 = 8.60 \times 10^5$ miles; $r_{12} = 9.29 \times 10^7$ miles; $q_{b1}^{(e)} = 2.0 \times 10^7$ Btu/hr · ft^2 (from Example 16.3-1).

SOLUTION

In the terminology of Eq. 16.4-5 and Fig. 16.4-5,

$$\text{solar constant} = \frac{d\dot{Q}_{12}}{\cos\theta_2 dA_2} = \frac{\sigma T_1^4}{\pi r_{12}^2}\int \cos\theta_1 dA_1$$

$$= \frac{\sigma T_1^4}{\pi r_{12}^2}\left(\frac{\pi D_1^2}{4}\right) = \frac{q_{b1}^{(e)}}{4}\left(\frac{D_1}{r_{12}}\right)^2$$

$$= \frac{2.0 \times 10^7}{4}\left(\frac{8.60 \times 10^5}{9.29 \times 10^7}\right)^2$$

$$= 430 \text{ Btu/hr} \cdot \text{ft}^2 \qquad (16.4\text{-}16)$$

This is in satisfactory agreement with other estimates that have been made. The treatment of r_{12}^2 as a constant in the integrand is permissible here because the distance r_{12} varies by less than 0.5% over the visible surface of the sun. The remaining integral, $\int \cos\theta_1 dA_1$, is the projected area of the sun as seen from the earth, or very nearly $\pi D_1^2/4$.

EXAMPLE 16.4-2

Radiant Heat Transfer Between Disks

Two black disks of diameter 2 ft are placed directly opposite one another at a distance of 4 ft. Disk 1 is maintained at 2000°R, and disk 2 at 1000°R. Calculate the heat flow between the two disks **(a)** when no other surfaces are present, and **(b)** when the two disks are connected by an adiabatic right-cylindrical black surface.

SOLUTION

(a) From Eq. 16.4-9 and curve 1 of Fig. 16.4-4,

$$Q_{12} = A_1 F_{12}\sigma(T_1^4 - T_2^4)$$

$$= \pi(0.06)(0.1712 \times 10^{-8})[(2000)^4 - (1000)^4]$$

$$= 4.83 \times 10^3 \text{ Btu/hr} \qquad (16.4\text{-}17)$$

(b) From Eq. 16.4-15 and curve 5 of Fig. 16.4-4,

$$Q_{12} = A_1 \bar{F}_{12}\sigma(T_1^4 - T_2^4)$$

$$= \pi(0.34)(0.1712 \times 10^{-8})[(2000)^4 - (1000)^4]$$

$$= 27.4 \times 10^3 \text{ Btu/hr} \qquad (16.4\text{-}18)$$

§16.5 RADIATION BETWEEN NONBLACK BODIES AT DIFFERENT TEMPERATURES

In principle, radiation between nonblack surfaces can be treated by differential analysis of emitted rays and their successive reflected components. For nearly black surfaces this is feasible, as only one or two reflections need be considered. For highly reflecting surfaces, however, the analysis is complicated, and the distributions of emitted and reflected rays with respect to angle and wavelength are not usually known with enough accuracy to justify a detailed calculation.

A reasonably accurate treatment is possible for a small convex surface in a large, nearly isothermal enclosure (i.e., a "cavity"), such as a steam pipe in a room with walls at constant temperature. The rate of energy emission from a nonblack surface 1 to the surrounding enclosure 2 is given by

$$Q_{1\dot{2}} = e_1 A_1 \sigma T_1^4 \tag{16.5-1}$$

and the rate of energy absorption from the surroundings by surface 1 is

$$Q_{\dot{2}1} = a_1 A_1 \sigma T_2^4 \tag{16.5-2}$$

Here we have made use of the fact that the radiation impinging on surface 1 is very nearly cavity radiation or black-body radiation corresponding to temperature T_2. Since A_1 is convex, it intercepts none of its own rays; hence F_{12} has been set equal to unity. The net radiation rate from A_1 to the surroundings is therefore

$$Q_{12} = \sigma A_1 (e_1 T_1^4 - a_1 T_2^4) \tag{16.5-3}$$

In Eq. 16.5-3, e_1 is the value of the emissivity of surface 1 at T_1. The absorptivity a_1 is usually *estimated* as the value of e at T_2.

Next we consider an enclosure formed by n gray, opaque, diffuse-reflecting surfaces $A_1, A_2, A_3, \ldots, A_n$ at temperatures $T_1, T_2, T_3, \ldots, T_n$. Following Oppenheim[1] we define the *radiosity* J_i for each surface A_i as the sum of the fluxes of reflected and emitted radiant energy from A_i. Then the net radiant flow from A_i to A_k is expressed as

$$Q_{ik} = A_i F_{ik} (J_i - J_k) \qquad i, k = 1, 2, 3, \ldots, n \tag{16.5-4}$$

that is, by Eq. 16.4-9 with substitution of radiosities J_i in place of the black-body emissive powers σT_i^4.

The definition of J_i gives, for an opaque surface,

$$J_i = (1 - e_i) I_i + e_i \sigma T_i^4 \tag{16.5-5}$$

in which I_i is the incident radiant flux on A_i. Elimination of I_i in favor of the net radiant flux Q_{ie}/A_i from A_i into the enclosure gives

$$\frac{Q_{ie}}{A_i} = J_i - I_i = J_i - \frac{J_i - e_i \sigma T_i^4}{1 - e_i} \tag{16.5-6}$$

whence

$$\frac{Q_{ie}}{A_i} = \frac{e_i}{1 - e_i} A_i (\sigma T_i^4 - J_i) \tag{16.5-7}$$

Finally, a steady-state energy balance on each surface gives

$$Q_i = Q_{ie} = \sum_{k=1}^{n} Q_{ik} \tag{16.5-8}$$

Here Q_i is the rate of heat addition to surface A_i by nonradiative means.

---

[1] A. K. Oppenheim, *Trans. ASME*, **78**, 725–735 (1956); for earlier work, see G. Poljak, *Tech. Phys. USSR*, **1**, 555–590 (1935).

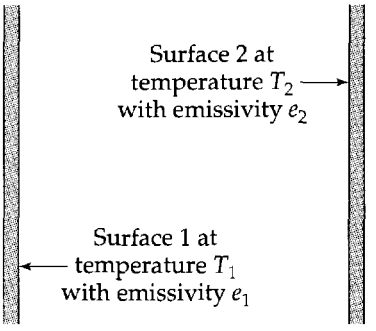

Fig. 16.5-1. Radiation between two infinite, parallel gray surfaces.

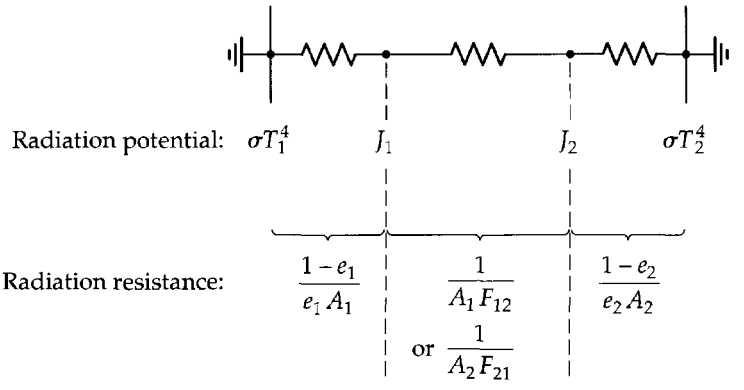

Fig. 16.5-2. Equivalent circuit for system shown in Fig. 16.5-1.

Equations analogous to Eqs. 16.5-4, 7, and 8 arise in the analysis of direct-current circuits, from Ohm's law of conduction and Kirchhoff's law of charge conservation. Hence we have the following analogies:

Electrical	*Radiative*
Current	Q
Voltage	J or σT^4
Resistance	$(1 - e_i)/e_i A_i$ or $1/A_i F_{ij}$

This analogy allows easy diagramming of equivalent circuits for visualization of simple enclosure radiation problems. For example, the system in Fig. 16.5-1 gives the equivalent circuit shown in Fig. 16.5-2 so that the net radiant heat transfer rate is

$$Q_{12} = \frac{\sigma(T_1^4 - T_2^4)}{\dfrac{1 - e_1}{e_1 A_1} + \dfrac{1}{A_1 F_{12}} + \dfrac{1 - e_2}{e_2 A_2}} \tag{16.5-9}$$

The shortcut solution summarized in Eq. 16.4-15 has been similarly generalized to non-black-walled enclosures giving

$$Q_{12} = A_1 \bar{F}_{12}(J_1 - J_2) \tag{16.5-10}$$

in place of Eq. 16.5-8, for an enclosure with $Q_i = 0$ for $i = 2, 3, \ldots, n$. The result is like that in Eq. 16.5-9, except that $\bar{F}_{12}$ must be used instead of F_{12} to include indirect paths from A_1 to A_2, thus giving a larger heat transfer rate.

EXAMPLE 16.5-1

Radiation Shields

Develop an expression for the reduction in radiant heat transfer between two infinite parallel gray planes having the same area, A, when a thin parallel gray sheet of very high thermal conductivity is placed between them as shown in Fig. 16.5-3.

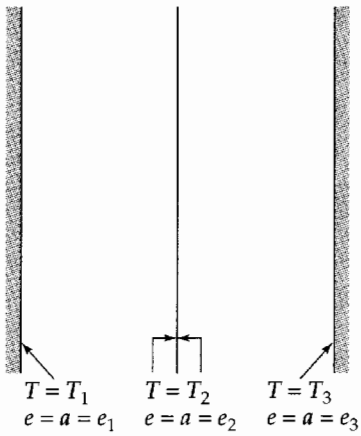

Fig. 16.5-3. Radiation shield.

SOLUTION

The radiation rate between planes 1 and 2 is given by

$$Q_{12} = \frac{A\sigma(T_1^4 - T_2^4)}{\dfrac{1 - e_1}{e_1} + 1 + \dfrac{1 - e_2}{e_2}} = \frac{A\sigma(T_1^4 - T_2^4)}{\dfrac{1}{e_1} + \dfrac{1}{e_2} - 1} \tag{16.5-11}$$

since both planes have the same area A and the view factor is unity. Similarly the heat transfer between planes 2 and 3 is

$$Q_{23} = \frac{A\sigma(T_2^4 - T_3^4)}{\dfrac{1 - e_2}{e_2} + 1 + \dfrac{1 - e_3}{e_3}} = \frac{A\sigma(T_2^4 - T_3^4)}{\dfrac{1}{e_2} + \dfrac{1}{e_3} - 1} \tag{16.5-12}$$

These last two equations may be combined to eliminate the temperature of the radiation shield, T_2, giving

$$Q_{12}\left(\frac{1}{e_1} + \frac{1}{e_2} - 1\right) + Q_{23}\left(\frac{1}{e_2} + \frac{1}{e_3} - 1\right) = A\sigma(T_1^4 - T_3^4) \tag{16.5-13}$$

Then, since $Q_{12} = Q_{23} = Q_{13}$, we get

$$Q_{13} = \frac{A\sigma(T_1^4 - T_3^4)}{\left(\dfrac{1}{e_1} + \dfrac{1}{e_2} - 1\right) + \left(\dfrac{1}{e_2} + \dfrac{1}{e_3} - 1\right)} \tag{16.5-14}$$

Finally, the ratio of radiant energy transfer with a shield to that without one is

$$\frac{(Q_{13})_{\text{with}}}{(Q_{13})_{\text{without}}} = \frac{\left(\dfrac{1}{e_1} + \dfrac{1}{e_3} - 1\right)}{\left(\dfrac{1}{e_1} + \dfrac{1}{e_2} - 1\right) + \left(\dfrac{1}{e_2} + \dfrac{1}{e_3} - 1\right)} \tag{16.5-15}$$

EXAMPLE 16.5-2

Radiation and Free-Convection Heat Losses from a Horizontal Pipe

Predict the total rate of heat loss, by radiation and free convection, from a unit length of horizontal pipe covered with asbestos. The outside diameter of the insulation is 6 in. The outer surface of the insulation is at 560°R, and the walls and air in the room are at 540°R.

SOLUTION

Let the outer surface of the insulation be surface 1 and the walls of the room be surface 2. Then Eq. 16.15-3 gives

$$Q_{12} = \sigma A_1 F_{12}(e_1 T_1^4 - a_1 T_2^4) \tag{16.5-16}$$

Since the pipe surface is convex and completely enclosed by surface 2, F_{12} is unity. From Table 16.2-1, we find $e_1 = 0.93$ at 560°R and $a_1 = 0.93$ at 540 R. Substitution of numerical values into Eq. 16.5-12 then gives for 1 ft of pipe:

$$Q_{12} = (0.1712 \times 10^{-8})(\pi/2)(1.00)[0.93(560)^4 - 0.93(540)^4] \quad (16.5\text{-}17)$$
$$= 32 \text{ Btu/hr}$$

By adding the convection heat loss from Example 14.5-1, we obtain the total heat loss:

$$Q = Q^{(\text{conv})} + Q^{(\text{rad})} = 21 + 32 = 53 \text{ Btu/hr} \quad (16.5\text{-}18)$$

Note that in this situation radiation accounts for more than half of the heat loss. If the fluid were *not* transparent, the convection and radiation processes would not be independent, and the convective and radiative contributions could not be added directly.

EXAMPLE 16.5-3

Combined Radiation and Convection

A body directly exposed to a clear night sky will be cooled below ambient temperature by radiation to outer space. This effect can be used to freeze water in shallow trays well insulated from the ground. Estimate the maximum air temperature for which freezing is possible, neglecting evaporation.

SOLUTION

As a first approximation, the following assumptions may be made:

a. All heat received by the water is by free convection from the surrounding air, which is assumed to be quiescent.

b. The heat effect of evaporation or condensation of water is not significant.

c. Steady state has been achieved.

d. The pan of water is square in cross section.

e. Back radiation from the atmosphere is neglected.

The maximum permitted air temperature at the water surface is $T_1 = 492$°R. The rate of *heat loss by radiation* is

$$Q^{(\text{rad})} = \sigma A_1 e_1 T_1^4 = (0.1712 \times 10^{-8})(L^2)(0.95)(402)^4$$
$$= 95L^2 \text{ Btu/hr} \cdot \text{ft}^2 \quad (16.5\text{-}19)$$

in which L is the length of one edge of the pan.

To get the *heat gain by convection*, we use the relation

$$Q^{(\text{conv})} = hL^2(T_{\text{air}} - T_{\text{water}}) \quad (16.5\text{-}20)$$

in which h is the heat transfer coefficient for free convection. For cooling atmospheric air by a horizontal square facing upward, the heat transfer coefficient is given by[2]

$$h = 0.2(T_{\text{air}} - T_{\text{water}})^{1/4} \quad (16.5\text{-}21)$$

in which h is expressed in Btu/hr · ft² · F and the temperature is given in degrees Rankine.

When the foregoing expressions for heat loss by radiation and heat gain by free convection are equated, we get

$$95L^2 = 0.2L^2(T_{\text{air}} - 492)^{5/4} \quad (16.5\text{-}22)$$

From this we find that the maximum ambient air temperature is 630°R or 170°F. Except under desert conditions, back radiation and moisture condensation from the surrounding air greatly lower the required air temperature.

---

[2] W. H. McAdams, in *Chemical Engineers' Handbook* (J. H. Perry, Ed.), McGraw-Hill, New York (1950), 3rd edition, p. 474.

§16.6 RADIANT ENERGY TRANSPORT IN ABSORBING MEDIA[1]

The methods given in the preceding sections are applicable only to materials that are completely transparent or completely opaque. To describe energy transport in nontransparent media, we write differential equations for the local rate of change of energy as viewed from both the material and radiation standpoint. That is, we regard a material medium traversed by electromagnetic radiation as two coexisting "phases": a "material phase," consisting of all the mass in the system, and a "photon phase," consisting of the electromagnetic radiation.

In Chapter 11 we have already given an energy balance equation for a system containing no radiation. Here we extend Eq. 11.2-1 for the material phase to take into account the energy that is being interchanged with the photon phase by emission and absorption processes:

$$\frac{\partial}{\partial t}\rho\hat{U} = -(\nabla \cdot \rho\hat{U}\mathbf{v}) - (\nabla \cdot \mathbf{q}) - (\nabla \cdot p\mathbf{v}) - (\boldsymbol{\tau}:\nabla\mathbf{v}) - (\mathscr{E} - \mathscr{A}) \tag{16.6-1}$$

Here we have introduced $\mathscr{E}$ and $\mathscr{A}$, which are the local rates of photon emission and absorption per unit volume, respectively. That is, $\mathscr{E}$ represents the energy lost by the material phase resulting from the emission of photons by molecules, and $\mathscr{A}$ represents the local gain of energy by the material phase resulting from photon absorption by the molecules (see Fig. 16.6-1). The $\mathbf{q}$ in Eq. 16.6-1 is the conduction heat flux given by Fourier's law.

For the "photon phase," we may write an equation describing the local rate of change of radiant energy density $u^{(r)}$:

$$\frac{\partial}{\partial t}u^{(r)} = -(\nabla \cdot \mathbf{q}^{(r)}) + (\mathscr{E} - \mathscr{A}) \tag{16.6-2}$$

in which $\mathbf{q}^{(r)}$ is the radiant energy flux. This equation may be obtained by writing a radiant energy balance on an element of volume fixed in space. Note that there is no convec-

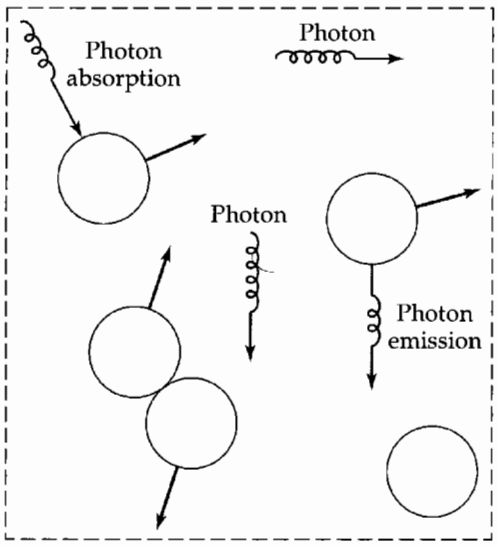

Fig. 16.6-1. Volume element over which energy balances are made; circles represent molecules.

[1] G. C. Pomraning, *Radiation Hydrodynamics*, Pergamon Press, New York (1973); R. Siegel and J. R. Howell, *Thermal Radiation Heat Transfer*, 3rd edition, Hemisphere Publishing Co., New York (1992).

tive term in Eq. 16.6-2, since the photons move independently of the local material velocity. Note further that the term $(\mathscr{E} - \mathscr{A})$ appears with opposite signs in Eqs. 16.6-1 and 2, indicating that a net gain of radiant energy occurs at the expense of molecular energy. Equation 16.6-2 can also be written for the radiant energy within a frequency range ν to $\nu + d\nu$:

$$\frac{\partial}{\partial t} u_\nu^{(r)} = -(\nabla \cdot \mathbf{q}_\nu^{(r)}) + (\mathscr{E}_\nu - \mathscr{A}_\nu) \tag{16.6-3}$$

This expression is obtained by differentiating Eq. 16.6-2 with respect to ν.

For the purpose of simplifying the discussion, we consider a steady-state nonflow system in which the radiation travels only in the positive z direction. Such a system can be closely approximated by passing a collimated light beam through a solution at temperatures sufficiently low that the emission by the solution is unimportant. (If emissions were important, it would be necessary to consider radiation in all directions.) These are the conditions commonly encountered in spectrophotometry. For such a system, Eqs. 16.6-1 and 2 become

$$0 = -\frac{d}{dz} q_z + \mathscr{A} \tag{16.6-4}$$

$$0 = -\frac{d}{dz} q_z^{(r)} - \mathscr{A} \tag{16.6-5}$$

In order to use these equations, we need information about the volumetric absorption rate $\mathscr{A}$. For a unidirectional beam a conventional expression is

$$\mathscr{A} = m_a q_z^{(r)} \tag{16.6-6}$$

in which m_a is known as the *extinction coefficient*. Basically, this states that the rate of photon absorption is proportional to the concentration of photons.

EXAMPLE 16.6-1

Absorption of a Monochromatic Radiant Beam

A monochromatic radiant beam of frequency ν, focused parallel to the z-axis, passes through an absorbing fluid. The local rate of energy absorption is given by $m_{a\nu} q_\nu^{(r)}$, in which $m_{a\nu}$ is the extinction coefficient for radiation of frequency ν. Determine the distribution of the radiant flux $q_\nu^{(r)}(z)$ in the system.

SOLUTION

We neglect refraction and scattering of the incident beam. Also, we assume that the liquid is cooled so that re-radiation can be neglected. Then Eq. 16.6-5 becomes for steady state

$$0 = -\frac{d}{dz} q_\nu^{(r)} - m_{a\nu} q_\nu^{(r)} \tag{16.6-7}$$

Integration with respect to z gives

$$q_\nu^{(r)}(z) = q_\nu^{(r)}(0) \exp(-m_{a\nu} z) \tag{16.6-8}$$

This is *Lambert's law of absorption*,[2] widely used in spectrophotometry. For any given pure material, $m_{a\nu}$ depends in a characteristic way on ν. The shape of the absorption spectrum is therefore a useful tool for qualitative analysis.

---

[2] J. H. Lambert, *Photometria*, Augsburg (1760).

QUESTIONS FOR DISCUSSION

1. The "named laws" in this chapter are important. What is the physical content of the laws associated with the following scientists' names: Stefan and Boltzmann, Planck, Kirchhoff, Lambert, Wien?
2. How are the Stefan–Boltzmann law and the Wien displacement law related to the Planck black-body distribution law?
3. Do black bodies exist? Why is the concept of a black body useful?
4. In specular (mirrorlike) reflection, the angle of incidence equals the angle of reflection. How are these angles related for diffuse reflection?
5. What is the physical significance of the view factor, and how can it be calculated?
6. What are the units of $q^{(e)}$, $q_\nu^{(e)}$, and $q_\lambda^{(e)}$?
7. Under what conditions is the effect of geometry on radiant heat interchange completely expressible in terms of view factors?
8. Which of the equations in this chapter show that the apparent brightness of a black body with a uniform surface temperature is independent of the position (distance and direction) from which it is viewed through a transparent medium?
9. What relation is analogous to Eq. 16.3-2 for an ideal monatomic gas?
10. Check the dimensional consistency of Eq. 16.3-9.

PROBLEMS

16A.1. Approximation of a black body by a hole in a sphere. A thin sphere of copper, with its internal surface highly oxidized, has a diameter of 6 in. How small a hole must be made in the sphere to make an opening that will have an absorptivity of 0.99?

Answer: Radius = 0.70 in.

16A.2. Efficiency of a solar engine. A device for utilizing solar energy, developed by Abbot,[1] consists of a parabolic mirror that focuses the impinging sunlight onto a Pyrex tube containing a high-boiling, nearly black liquid. This liquid is circulated to a heat exchanger in which the heat energy is transferred to superheated water at 25 atm pressure. Steam may be withdrawn and used to run an engine. The most efficient design requires a mirror 10 ft in diameter to generate 2 hp, when the axis of the mirror is pointed directly toward the sun. What is the overall efficiency of the device?

Answer: 15%

16A.3. Radiant heating requirement. A shed is rectangular in shape, with the floor 15 ft by 30 ft and the roof 7.5 ft above the floor. The floor is heated by hot water running through coils. On cold winter days the exterior walls and roof are about −10°F. At what rate must heat be supplied through the floor in order to maintain the floor temperature at 75°F? (Assume that all surfaces of the system are black.)

16A.4. Steady-state temperature of a roof. Estimate the maximum temperature attained by a level roof at 45° north latitude on June 21 in clear weather. Radiation from sources other than the sun may be neglected, and a convection heat transfer coefficient of 2.0 Btu/hr · ft² · F may be assumed. A maximum temperature of 100°F may be assumed for the surrounding air. The solar constant of Example 16.4-1 may be used, and the absorption and scattering of the sun's rays by the atmosphere may be neglected.

(a) Solve for a perfectly black roof.

(b) Solve for an aluminum-coated roof, with an absorptivity of 0.3 for solar radiation and an emissivity of 0.07 at the temperature of the roof.

16A.5. Radiation errors in temperature measurements. The temperature of an air stream in a duct is being measured by means of a thermocouple. The thermocouple wires and junction are cylindrical, 0.05 in. in diameter, and extend across the duct perpendicular to the flow with the junction in the center of the duct. Assuming a junction emissivity $e = 0.8$, estimate the temperature of the gas stream from the following data obtained under steady conditions:

Thermocouple junction temperature	= 500°F
Duct wall temperature	= 300°F
Convection heat transfer coefficient from wire to air	= 50 Btu/hr · ft² · F

The wall temperature is constant at the value given for 20 duct diameters upstream and downstream of the thermocouple installation. The thermocouple leads are positioned so that the effect of heat conduction along them on the junction temperature may be neglected.

16A.6. Surface temperatures on the Earth's moon.

(a) Estimate the surface temperature of our moon at the point nearest the sun by a quasi-steady-state radiant energy balance, regarding the lunar surface as a gray sphere.

[1] C. G. Abbot, in *Solar Energy Research* (F. Daniels and J. A. Duffie, eds.), University of Wisconsin Press, Madison (1955), pp. 91–95; see also U.S. Patent No. 2,460,482 (Feb. 1, 1945).

Neglect radiation and reflection from the planets. The solar constant at Earth is given in Example 16.4-1.

(b) Extend part (a) to give the lunar surface temperature as a function of angular displacement from the hottest point.

16B.1. Reference temperature for effective emissivity. Show that, if the emissivity increases linearly with the temperature, Eq. 16.5-3 may be written as

$$Q_{12} = e_1^\circ \sigma A_1 (T_1^4 - T_2^4) \qquad \text{(16B.1-1)}$$

in which e_1° is the emissivity of surface 1 evaluated at a reference temperature T° given by

$$T^\circ = \frac{T_1^5 - T_2^5}{T_1^4 - T_2^4} \qquad \text{(16B.1-2)}$$

16B.2. Radiation across an annular gap. Develop an expression for the radiant heat transfer between two long, gray coaxial cylinders 1 and 2. Show that

$$Q_{12} = \frac{\sigma(T_1^4 - T_2^4)}{\frac{1}{A_1 e_1} + \frac{1}{A_2}\left(\frac{1}{e_2} - 1\right)} \qquad \text{(16B.2-1)}$$

where A_1 is the surface area of the inner cylinder.

16B.3. Multiple radiation shields.

(a) Develop an equation for the rate of radiant heat transfer through a series of n very thin, flat, parallel metal sheets, each having a different emissivity e, when the first sheet is at temperature T_1 and the nth sheet is at temperature T_n. Give your result in terms of the radiation resistances

$$R_{i,i+1} = \frac{\sigma(T_i^4 - T_{i+1}^4)}{Q_{i,i+1}} \qquad \text{(16B.3-1)}$$

for the successive pairs of planes. Edge effects and conduction across the air gaps between the sheets are to be neglected.

(b) Determine the ratio of the radiant heat transfer rate for n identical sheets to that for two identical sheets.

(c) Compare your results for three sheets with that obtained in Example 16.5-1.

The marked reduction in heat transfer rates produced by a number of radiation shields in series has led to the use of multiple layers of metal foils for high-temperature insulation.

16B.4. Radiation and conduction through absorbing media. A glass slab, bounded by planes $z = 0$ and $z = \delta$, is of infinite extent in the x and y directions. The temperatures of the surfaces at $z = 0$ and $z = \delta$ are maintained at T_0 and T_δ, respectively. A uniform monochromatic radiant beam of intensity $q_0^{(r)}$ in the z direction impinges on the face at $z = 0$. Emission within the slab, reflection, and incident radiation in the negative z direction can be neglected.

(a) Determine the temperature distribution in the slab, assuming m_a and k to be constants.

(b) How does the distribution of the conductive heat flux q_z depend on m_a?

16B.5. Cooling of a black body in vacuo. A thin black body of very high thermal conductivity has a volume V, surface area A, density ρ, and heat capacity $\hat{C}_p$. At time $t = 0$, this body at temperature T_1 is placed in a black enclosure, the walls of which are maintained permanently at temperature T_2 (with $T_2 < T_1$). Derive an expression for the temperature T of the black body as a function of time.

16B.6. Heat loss from an insulated pipe. A Schedule 40 two-inch horizontal steel pipe (inside diameter 2.067 in., wall thickness 0.154 in.; k = 26 Btu/hr · ft · F) carrying steam is insulated with 2 in. of 85% magnesia (k = 0.35 Btu/hr · ft · F) and tightly wrapped with a layer of clean aluminum foil (e = 0.05). The pipe is surrounded by air at 1 atm and 80°F and its inner surface is at 250°F.

(a) Compute the conductive heat flow per unit length, $Q^{(\text{cond})}/L$, through the pipe wall and insulation for assumed temperatures, T_0, of 100°F and 250°F at the outer surface of the aluminum foil.

(b) Compute the radiative and free-convective heat losses, $Q^{(\text{rad})}/L$ and $Q^{(\text{conv})}/L$, for the same assumed outer surface temperatures T_0.

(c) Plot or interpolate the foregoing results to obtain the steady-state values of T_0 and $Q^{(\text{cond})}/L = Q^{(\text{rad})}/L + Q^{(\text{conv})}/L$.

16C.1. Integration of the view-factor integral for a pair of disks (Fig. 16C.1). Two parallel, perfectly black disks of radius R are placed a distance H apart. Evaluate the view-factor integrals for this case and show that

$$F_{12} = F_{21} = \frac{1 + 2B^2 - \sqrt{1 + 4B^2}}{2B^2} \qquad \text{(16.1-1)}^2$$

in which $B = R/H$.

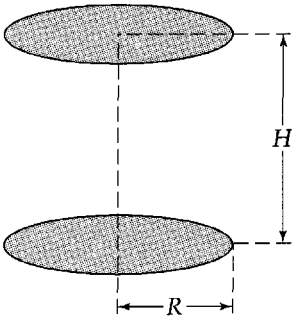

Fig. 16.C-1. Two perfectly black disks.

16D.1. Heat loss from a wire carrying an electric current.[3] An electrically heated wire of length L loses heat to the surroundings by radiative heat transfer. If the ends of the wire are maintained at a constant temperature T_0, obtain an expression for the axial variation in wire temperature. The wire can be considered to be radiating into a black enclosure at temperature T_0.

---

[2] C. Christiansen, *Wiedemann's Ann. d. Physik*, **19**, 267–283 (1883); see also M. Jakob, *Heat Transfer*, Vol. II, Wiley, New York (1957), p. 14.

[3] H. S. Carslaw and J. C. Jaeger, *Conduction of Heat in Solids*, 2nd edition, Oxford University Press (1959), pp. 154–156.

This Page Intentionally Left Blank

Part Three

Mass Transport

This Page Intentionally Left Blank

Chapter 17

Diffusivity and the Mechanisms of Mass Transport

In Chapter 1 we began by stating Newton's law of viscosity, and in Chapter 9 we began with Fourier's law of heat conduction. In this chapter we start by giving Fick's law of diffusion, which describes the movement of one chemical species A through a binary mixture of A and B because of a concentration gradient of A.

The movement of a chemical species from a region of high concentration to a region of low concentration can be observed by dropping a small crystal of potassium permanganate into a beaker of water. The $KMnO_4$ begins to dissolve in the water, and very near the crystal there is a dark purple, concentrated solution of $KMnO_4$. Because of the concentration gradient that is established, the $KMnO_4$ diffuses away from the crystal. The progress of the diffusion can then be followed by observing the growth of the dark purple region.

In §17.1 we give Fick's law for binary diffusion and define the diffusivity $\mathscr{D}_{AB}$ for the pair A–B. Then we discuss briefly the temperature and pressure dependence of the diffusivity. After that we give a summary of the theories available to predict the diffusivity for gases, liquids, colloids, and polymers. At the end of the chapter we discuss the transport of mass of a chemical species by convection, thus paralleling the treatments in Chapters 1 and 9 for momentum and heat transfer. We also introduce molar units and the notation needed for describing diffusion in these units. Finally, we give the Maxwell–Stefan equations for multicomponent gases at low densities.

Before starting the discussion we establish the following conventions. For *multicomponent diffusion*, we designate the species with lower-case Greek letters α, β, γ, ... and their concentrations with the corresponding subscripts. For *binary diffusion* we use the capital italic letters A and B. For *self-diffusion* (diffusion of chemically identical species)

we label the species A and A^*. The "tagged" species A^* may differ physically from A by virtue of radioactivity or other nuclear properties such as the mass, magnetic moment, or spin.[1] The use of this system of notation enables one to see at a glance the type of system to which a given formula applies.

§17.1 FICK'S LAW OF BINARY DIFFUSION (MOLECULAR MASS TRANSPORT)

Consider a thin, horizontal, fused-silica plate of area A and thickness Y. Suppose that initially (for time $t < 0$) both horizontal surfaces of the plate are in contact with air, which we regard as completely insoluble in silica. At time $t = 0$, the air below the plate is suddenly replaced by pure helium, which is appreciably soluble in silica. The helium slowly penetrates into the plate by virtue of its molecular motion and ultimately appears in the gas above. This molecular transport of one substance relative to another is known as *diffusion* (also known as *mass diffusion, concentration diffusion,* or *ordinary diffusion*). The air above the plate is being replaced rapidly, so that there is no appreciable buildup of helium there. We thus have the situation represented in Fig. 17.1-1; this process is analogous to those described in Fig. 1.1-1 and Fig. 9.1-1 where viscosity and thermal conductivity were defined.

In this system, we will call helium "species A" and silica "species B." The concentrations will be given by the "mass fractions" ω_A and ω_B. The mass fraction ω_A is the mass of helium divided by the mass of helium plus silica in a given microscopic volume element. The mass fraction ω_B is defined analogously.

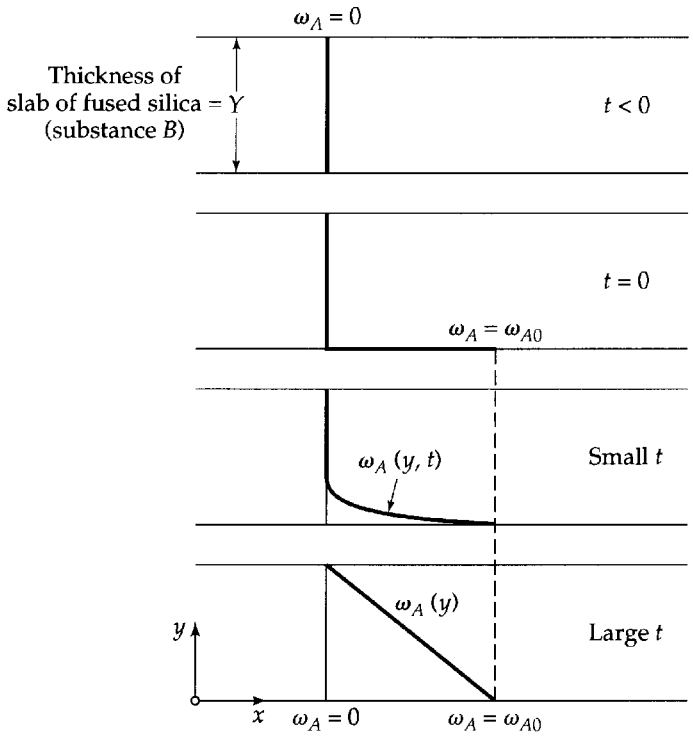

Fig. 17.1-1. Build-up to the steady-state concentration profile for the diffusion of helium (substance A) through fused silica (substance B). The symbol ω_A stands for the mass fraction of helium, and ω_{A0} is the solubility of helium in fused silica, expressed as the mass fraction. See Figs. 1.1-1 and 9.1-1 for the analogous momentum and heat transport situations.

[1] E. O. Stejskal and J. E. Tanner, *J. Chem. Phys.*, **42**, 288–292 (1965); P. Stilbs, *Prog. NMR Spectros*, **19**, 1–45 (1987); P. T. Callaghan and J. Stepišnik, *Adv. Magn. Opt. Reson.* **19**, 325–388 (1996).

For time t less than zero, the mass fraction of helium, ω_A, is everywhere equal to zero. For time t greater than zero, at the lower surface, $y = 0$, the mass fraction of helium is equal to ω_{A0}. This latter quantity is the solubility of helium in silica, expressed as mass fraction, just inside the solid. As time proceeds the mass fraction profile develops, with $\omega_A = \omega_{A0}$ at the bottom surface of the plate and $\omega_A = 0$ at the top surface of the plate. As indicated in Fig. 17.1-1, the profile tends toward a straight line with increasing t.

At steady state, it is found that the mass flow w_{Ay} of helium in the positive y direction can be described to a very good approximation by

$$\frac{w_{Ay}}{A} = \rho \mathcal{D}_{AB} \frac{\omega_{A0} - 0}{Y} \tag{17.1-1}$$

That is, the mass flow rate of helium per unit area (or *mass flux*) is proportional to the mass fraction difference divided by the plate thickness. Here ρ is the density of the silica–helium system, and the proportionality factor $\mathcal{D}_{AB}$ is the *diffusivity* of the silica–helium system. We now rewrite Eq. 17.1-1 for a differential element within the slab:

$$j_{Ay} = -\rho \mathcal{D}_{AB} \frac{d\omega_A}{dy} \tag{17.1-2}$$

Here w_{Ay}/A has been replaced by j_{Ay}, the *molecular mass flux* of helium in the positive y direction. Note that the first index, A, designates the chemical species (in this case, helium), and the second index indicates the direction in which diffusive transport is taking place (in this case, the y direction).

Equation 17.1-2 is the one-dimensional form of *Fick's first law of diffusion*.[1] It is valid for any binary solid, liquid, or gas solution, provided that j_{Ay} is defined as the mass flux relative to the mixture velocity v_y. For the system examined in Fig. 17.1-1, the helium is moving rather slowly and its concentration is very small, so that v_y is negligibly different from zero during the diffusion process.

In general, for a binary mixture

$$v_y = \omega_A v_{Ay} + \omega_B v_{By} \tag{17.1-3}$$

Thus $\mathbf{v}$ is an average in which the species velocities, $\mathbf{v}_A$ and $\mathbf{v}_B$, are weighted according to the mass fractions. This kind of velocity is referred to as the *mass average velocity*. The species velocity $\mathbf{v}_A$ is not the instantaneous molecular velocity of a molecule of A, but rather the arithmetic average of the velocities of all the molecules of A within a tiny volume element.

The mass flux j_{Ay} is then defined, in general, as

$$j_{Ay} = \rho \omega_A (v_{Ay} - v_y) \tag{17.1-4}$$

The mass flux of B is defined analogously. As the two chemical species interdiffuse there is, locally, a shifting of the center of mass in the y direction if the molecular weights of A and B differ. The mass fluxes j_{Ay} and j_{By} are so defined that $j_{Ay} + j_{By} = 0$. In other words, the fluxes j_{Ay} and j_{By} are measured with respect to the motion of the center of mass. This point will be discussed in detail in §§17.7 and 8.

If we write equations similar to Eq. 17.1-2 for the x and z directions and then combine all three equations, we get the vector form of Fick's law:

$$\mathbf{j}_A = -\rho \mathcal{D}_{AB} \nabla \omega_A \tag{17.1-5}$$

---

[1] A. Fick, *Ann. der Physik*, **94**, 59–86 (1855). Fick's second law, the diffusional analog of the heat conduction equation in Eq. 11.2-10, is given in Eq. 19.1-18. **Adolf Eugen Fick** (1829–1901) was a medical doctor who taught in Zürich and Marburg, and later became the Rector of the University of Würzburg. He postulated the laws of diffusion by analogy with heat conduction, not by experiment.

A similar relation can be written for species B:

$$\mathbf{j}_B = -\rho \mathscr{D}_{BA} \nabla \omega_B \tag{17.1-6}$$

It is shown in Example 17.1-2 that $\mathscr{D}_{BA} = \mathscr{D}_{AB}$. Thus for the pair A–B, there is just one diffusivity; in general it will be a function of pressure, temperature, and composition.

The mass diffusivity $\mathscr{D}_{AB}$, the thermal diffusivity $\alpha = k/\rho\hat{C}_p$, and the momentum diffusivity (kinematic viscosity) $\nu = \mu/\rho$ all have dimensions of (length)^2/time. The ratios of these three quantities are therefore dimensionless groups:

The Prandtl number:
$$\mathrm{Pr} = \frac{\nu}{\alpha} = \frac{\hat{C}_p \mu}{k} \tag{17.1-7}$$

The Schmidt number:[2]
$$\mathrm{Sc} = \frac{\nu}{\mathscr{D}_{AB}} = \frac{\mu}{\rho \mathscr{D}_{AB}} \tag{17.1-8}$$

The Lewis number:[2]
$$\mathrm{Le} = \frac{\alpha}{\mathscr{D}_{AB}} = \frac{k}{\rho \hat{C}_p \mathscr{D}_{AB}} \tag{17.1-9}$$

These dimensionless groups of fluid properties play a prominent role in dimensionless equations for systems in which competing transport processes occur. (*Note:* Sometimes the Lewis number is defined as the inverse of the expression above.)

In Tables 17.1-1, 2, 3, and 4 some values of $\mathscr{D}_{AB}$ in cm^2/s are given for a few gas, liquid, solid, and polymeric systems. These values can be converted easily to m^2/s by multiplication by 10^{-4}. Diffusivities of gases at low density are almost independent of ω_A, increase with temperature, and vary inversely with pressure. Liquid and solid diffusivities are strongly concentration-dependent and generally increase with temperature. There are numerous experimental methods for measuring diffusivities, and some of these are described in subsequent chapters.[3]

For *gas mixtures*, the Schmidt number can range from about 0.2 to 3, as can be seen in Table 17.1-1. For *liquid mixtures*, values up to 40,000 have been observed.[4]

Up to this point we have been discussing isotropic fluids, in which the speed of diffusion does not depend on the orientation of the fluid mixture. For some solids and structured fluids, the diffusivity will have to be a tensor rather than a scalar, so that Fick's first law has to be modified thus:

$$\mathbf{j}_A = -[\rho \boldsymbol{\Delta}_{AB} \cdot \nabla \omega_A] \tag{17.1-10}$$

in which $\boldsymbol{\Delta}_{AB}$ is the (symmetric) *diffusivity tensor*.[5,6] According to this equation, the mass flux is not necessarily collinear with the mass fraction gradient. We do not pursue this subject further here.

---

[2] These groups were named for: **Ernst Heinrich Wilhelm Schmidt** (1892–1975), who taught at the universities in Gdansk, Braunschweig, and Munich (where he was the successor to Nusselt); **Warren Kendall Lewis** (1882–1975), who taught at MIT and was a coauthor of a pioneering textbook, W. H. Walker, W. K. Lewis, and W. H. McAdams, *Principles of Chemical Engineering*, McGraw-Hill, New York (1923).

[3] For an extensive discussion, see W. E. Wakeham, A. Nagashima, and J. V. Sengers, *Measurement of the Transport Properties of Fluids: Experimental Thermodynamics, Vol. III*, CRC Press, Boca Raton, Fla. (1991).

[4] D. A. Shaw and T. J. Hanratty, *AIChE Journal*, **23**, 28–37, 160–169 (1977); P. Harriott and R. M. Hamilton, *Chem. Eng. Sci.*, **20**, 1073–1078 (1965).

[5] For flowing polymers, theoretical expressions for the diffusion tensor have been derived using kinetic theory; see H. C. Öttinger, *AIChE Journal*, **35**, 279–286 (1989), and C. F. Curtiss and R. B. Bird, *Adv. Polym. Sci.*, 1–101 (1996), §§6 and 15.

[6] M. E. Glicksman, *Diffusion in Solids: Field Theory, Solid State Principles, and Applications*, Wiley, New York (2000).

Table 17.1-1 Experimental Diffusivities[a] and Limiting Schmidt Numbers[b] of Gas Pairs at 1 Atmosphere Pressure

Gas pair A–B	*Temperature* (K)	$\mathscr{D}_{AB}$ (cm^2/s)	Sc $x_A \to 1$	Sc $x_B \to 1$
CO_2–N_2O	273.2	0.096	0.73	0.72
CO_2–CO	273.2	0.139	0.50	0.96
CO_2–N_2	273.2	0.144	0.48	0.91
	288.2	0.158	0.49	0.92
	298.2	0.165	0.50	0.93
N_2–C_2H_6	298.2	0.148	1.04	0.51
N_2–nC_4H_{10}	298.2	0.0960	1.60	0.33
N_2–O_2	273.2	0.181	0.72	0.74
H_2–SF_6	298.2	0.420	3.37	0.055
H_2–CH_4	298.2	0.726	1.95	0.23
H_2–N_2	273.2	0.674	1.40	0.19
NH_3–H_2[c]	263	0.58	0.19[e]	1.53
NH_3–N_2[c]	298	0.233	0.62[e]	0.65
H_2O–N_2[c]	308	0.259	0.58[e]	0.62
H_2O–O_2[c]	352	0.357	0.56[e]	0.59
C_3H_8–nC_4H_{10}[d]	378.2	0.0768	0.95	0.66
	437.7	0.107	0.91	0.63
C_3H_8–iC_4H_{10}[d]	298.0	0.0439	1.04	0.73
	378.2	0.0823	0.89	0.63
	437.8	0.112	0.87	0.61
C_3H_8–neo-C_5H_{12}[d]	298.1	0.0431	1.06	0.56
	378.2	0.0703	1.04	0.55
	437.7	0.0945	1.03	0.55
nC_4H_{10}–neo-C_5H_{12}[d]	298.0	0.0413	0.76	0.59
	378.2	0.0644	0.78	0.61
	437.8	0.0839	0.80	0.62
iC_4H_{10}–neo-C_5H_{12}[d]	298.1	0.0362	0.89	0.67
	378.2	0.0580	0.89	0.67
	437.7	0.0786	0.87	0.66

[a] Unless otherwise indicated, the values are taken from J. O. Hirschfelder, C. F. Curtiss, and R. B. Bird, *Molecular Theory of Gases and Liquids*, 2nd corrected printing, Wiley, New York (1964), p. 579. All values are given for 1 atmosphere pressure.

[b] Calculated using the Lennard-Jones parameters of Table E.1. The parameters for sulfur hexafluoride were obtained from second virial coefficient data.

[c] Values of $\mathscr{D}_{AB}$ for the water and ammonia mixtures are taken from the tabulation of R. C. Reid, J. M. Prausnitz, and B. E. Poling, *The Properties of Gases and Liquids*, 4th edition, McGraw-Hill, New York (1987).

[d] Values of $\mathscr{D}_{AB}$ for the hydrocarbon–hydrocarbon pairs are taken from S. Gotoh, M. Manner, J. P. Sørensen, and W. E. Stewart, *J. Chem. Eng. Data*, **19**, 169–171 (1974).

[e] Values of μ for water and ammonia were calculated from functions provided by T. E. Daubert, R. P. Danner, H. M. Sibul, C. C. Stebbins, J. L. Oscarson, R. L. Rowley, W. V. Wilding, M. E. Adams, T. L. Marshall, and N. A. Zundel, *DIPPR®, Data Compilation of Pure Compound Properties*, Design Institute for Physical Property Data®, AIChE, New York, N.Y. (2000).

Table 17.1-2 Experimental Diffusivities in the Liquid State[a,b]

A	B	T(°C)	x_A	$\mathscr{D}_{AB} \times 10^5$ (cm^2/s)
Chlorobenzene	Bromobenzene	10.10	0.0332	1.007
			0.2642	1.069
			0.5122	1.146
			0.7617	1.226
			0.9652	1.291
		39.92	0.0332	1.584
			0.2642	1.691
			0.5122	1.806
			0.7617	1.902
			0.9652	1.996
Water	*n*-Butanol	30	0.131	1.24
			0.222	0.920
			0.358	0.560
			0.454	0.437
			0.524	0.267
Ethanol	Water	25	0.026	1.076
			0.266	0.368
			0.408	0.405
			0.680	0.743
			0.880	1.047
			0.944	1.181

[a] The data for the first two pairs are taken from a review article by P. A. Johnson and A. L. Babb, *Chem. Revs.*, **56**, 387–453 (1956). Other summaries of experimental results may be found in: P. W. M. Rutten, *Diffusion in Liquids*, Delft University Press, Delft, The Netherlands (1992); L. J. Gosting, *Adv. in Protein Chem.*, Vol. XI, Academic Press, New York (1956); A. Vignes, *I. E. C. Fundamentals*, **5**, 189–199 (1966).

[b] The ethanol–water data were taken from M. T. Tyn and W. F. Calus, *J. Chem. Eng. Data*, **20**, 310–316 (1975).

Table 17.1-3 Experimental Diffusivities in the Solid State[a]

A	B	T(°C)	$\mathscr{D}_{AB}$ (cm^2/s)
He	SiO_2	20	$2.4\text{–}5.5 \times 10^{-10}$
He	Pyrex	20	4.5×10^{-11}
		500	2×10^{-8}
H_2	SiO_2	500	$0.6\text{–}2.1 \times 10^{-8}$
H_2	Ni	85	1.16×10^{-8}
		165	10.5×10^{-8}
Bi	Pb	20	1.1×10^{-16}
Hg	Pb	20	2.5×10^{-15}
Sb	Ag	20	3.5×10^{-21}
Al	Cu	20	1.3×10^{-30}
Cd	Cu	20	2.7×10^{-15}

[a] It is presumed that in each of the above pairs, component A is present only in very small amounts. The data are taken from R. M. Barrer, *Diffusion in and through Solids*, Macmillan, New York (1941), pp. 141, 222, and 275.

Table 17.1-4 Experimental Diffusivities of Gases in Polymers.[a] Diffusivities, $\mathscr{D}_{AB}$, are given in units of 10^{-6} (cm^2/s). The values for N_2 and O_2 are for 298K, and those for CO_2 and H_2 are for 198K.

	N_2	O_2	CO_2	H_2
Polybutadiene	1.1	1.5	1.05	9.6
Silicone rubber	15	25	15	75
Trans-1,4-polyisoprene	0.50	0.70	0.47	5.0
Polystyrene	0.06	0.11	0.06	4.4

[a] Excerpted from D. W. van Krevelen, *Properties of Polymers*, 3rd edition, Elsevier, Amsterdam (1990), pp. 544–545. Another relevant reference is S. Pauly, in *Polymer Handbook*, 4th edition (J. Brandrup and E. H. Immergut, eds.), Wiley-Interscience, New York (1999), Chapter VI.

In this section we have discussed the diffusion that occurs as a result of a concentration gradient in the system. We refer to this kind of diffusion as *concentration diffusion* or *ordinary diffusion*. There are, however, other kinds of diffusion: *thermal diffusion*, which results from a temperature gradient; *pressure diffusion*, resulting from a pressure gradient; and *forced diffusion*, which is caused by unequal external forces acting on the chemical species. For the time being, we consider only concentration diffusion, and we postpone discussion of the other mechanisms to Chapter 24. Also, in that chapter we discuss the use of activity, rather than concentration, as the driving force for ordinary diffusion.

EXAMPLE 17.1-1

Diffusion of Helium through Pyrex Glass

Calculate the steady-state mass flux j_{Ay} of helium for the system of Fig. 17.1-1 at 500K. The partial pressure of helium is 1 atm at $y = 0$ and zero at the upper surface of the plate. The thickness Y of the pyrex plate is 10^{-2} mm, and its density $\rho^{(B)}$ is 2.6 g/cm^3. The solubility and diffusivity of helium in pyrex are reported[7] as 0.0084 volumes of gaseous helium per volume of glass, and $\mathscr{D}_{AB} = 0.2 \times 10^{-7}$ cm^2/s, respectively. Show that the neglect of the mass average velocity implicit in Eq. 17.1-1 is reasonable.

SOLUTION

The mass concentration of helium in the glass at the lower surface is obtained from the solubility data and the ideal gas law:

$$\rho_{A0} = (0.0084)\frac{p_{A0}M_A}{RT}$$

$$= (0.0084)\frac{(1.0 \text{ atm})(4.00 \text{ g/mole})}{(82.05 \text{ cm}^3 \text{ atm/mole K})(773\text{K})}$$

$$= 5.3 \times 10^{-7} \text{ g/cm}^3 \tag{17.1-11}$$

The mass fraction of helium in the solid phase at the lower surface is then

$$\omega_{A0} = \frac{\rho_{A0}}{\rho_{A0} + \rho_{B0}} = \frac{5.3 \times 10^{-7}}{5.3 \times 10^{-7} + 2.6} = 2.04 \times 10^{-7} \tag{17.1-12}$$

[7] C. C. Van Voorhis, *Phys. Rev.* **23**, 557 (1924), as reported by R. M. Barrer, *Diffusion in and through Solids*, corrected printing, Cambridge University Press (1951).

We may now calculate the flux of helium from Eq. 17.1-1 as

$$j_{Ay} = (2.6\ \text{g/cm}^3)(2.0 \times 10^{-8}\ \text{cm}^2/\text{s})\frac{2.04 \times 10^{-7}}{10^{-3}\ \text{cm}}$$
$$= 1.05 \times 10^{-11}\ \text{g/cm}^2\text{s} \tag{17.1-13}$$

Next, the velocity of the helium can be obtained from Eq. 17.1-4:

$$v_{Ay} = \frac{j_{Ay}}{\rho_A} + v_y \tag{17.1-14}$$

At the lower surface of the plate ($y = 0$) this velocity has the value

$$v_{Ay}\big|_{y=0} = \frac{1.05 \times 10^{-11}\ \text{g/cm}^2\,\text{s}}{5.3 \times 10^{-7}\ \text{g/cm}^3} + v_{y0} = 1.98 \times 10^{-5}\ \text{cm/s} + v_{y0} \tag{17.1-15}$$

The corresponding value v_{y0} of the mass average velocity of the glass–helium system at $y = 0$ is then obtained from Eq. 17.1-3

$$v_{y0} = (2.04 \times 10^{-7})(1.98 \times 10^{-5}\ \text{cm/s} + v_{y0}) + (1 - 2.04 \times 10^{-7})\,(0) \tag{17.1-16}$$
$$v_{y0} = \frac{(2.04 \times 10^{-7})(1.98 \times 10^{-5}\ \text{cm/s})}{1 - (2.04 \times 10^{-7})}$$
$$= 4.04 \times 10^{-12}\ \text{cm/s}$$

Thus it is safe to neglect v_y in Eq. 17.1-14, and the analysis of the experiment in Fig. 17.1-1 at steady state is accurate.

EXAMPLE 17.1-2

The Equivalence of $\mathscr{D}_{AB}$ and $\mathscr{D}_{BA}$

Show that only one diffusivity is needed to describe the diffusional behavior of a binary mixture.

SOLUTION

We begin by writing Eq. 17.1-6 as follows:

$$\mathbf{j}_B = -\rho\mathscr{D}_{BA}\nabla\omega_B = +\rho\mathscr{D}_{BA}\nabla\omega_A \tag{17.1-17}$$

The second form of this equation follows from the fact that $\omega_A + \omega_B = 1$. We next use the vector equivalents of Eqs. 17.1-3 and 4 to write

$$\mathbf{j}_A = \rho\omega_A(\mathbf{v}_A - \omega_A\mathbf{v}_A - \omega_B\mathbf{v}_B)$$
$$= \rho\omega_A((1 - \omega_A)\mathbf{v}_A - \omega_B\mathbf{v}_B)$$
$$= \rho\omega_A\omega_B(\mathbf{v}_A - \mathbf{v}_B) \tag{17.1-18}$$

Interchanging A and B in this expression shows that $\mathbf{j}_A = -\mathbf{j}_B$. Combining this with the second form of Eq. 17.1-17 then gives

$$\mathbf{j}_A = -\rho\mathscr{D}_{BA}\nabla\omega_A \tag{17.1-19}$$

Comparing this with Eq. 17.1-5 gives $\mathscr{D}_{BA} = \mathscr{D}_{AB}$. We find that the order of subscripts is unimportant for a binary system and that only one diffusivity is required to describe the diffusional behavior.

However, it may well be that the diffusivity for a dilute solution of A in B and that for a dilute solution of B in A are *numerically* different. The reason for this is that the diffusivity is concentration-dependent, so that the two limiting values mentioned above are the values of the diffusivity $\mathscr{D}_{BA} = \mathscr{D}_{AB}$ at two different concentrations.

§17.2 TEMPERATURE AND PRESSURE DEPENDENCE OF DIFFUSIVITIES

In this section we discuss the prediction of the diffusivity $\mathscr{D}_{AB}$ for binary systems by corresponding-states methods. These methods are also useful for extrapolating existing data. Comparisons of many alternative methods are available in the literature.[1,2]

For binary gas mixtures at low pressure, $\mathscr{D}_{AB}$ is inversely proportional to the pressure, increases with increasing temperature, and is almost independent of the composition for a given gas pair. The following equation for estimating $\mathscr{D}_{AB}$ at low pressures has been developed[3] from a combination of kinetic theory and corresponding-states arguments:

$$\frac{p\mathscr{D}_{AB}}{(p_{cA}p_{cB})^{1/3}(T_{cA}T_{cB})^{5/12}(1/M_A + 1/M_B)^{1/2}} = a\left(\frac{T}{\sqrt{T_{cA}T_{cB}}}\right)^b \tag{17.2-1}$$

Here $\mathscr{D}_{AB}$ [=] cm^2/s, p [=] atm, and T [=] K. Analysis of experimental data gives the dimensionless constants $a = 2.745 \times 10^{-4}$ and $b = 1.823$ for nonpolar gas pairs, excluding helium and hydrogen, and $a = 3.640 \times 10^{-4}$ and $b = 2.334$ for pairs consisting of H_2O and a nonpolar gas. Equation 17.2-1 fits the experimental data at atmospheric pressure within an average deviation of 6 to 8%. If the gases A and B are nonpolar and their Lennard-Jones parameters are known, the kinetic-theory method described in the next section usually gives somewhat better accuracy.

At high pressures, and in the liquid state, the behavior of $\mathscr{D}_{AB}$ is more complicated. The simplest and best understood situation is that of self-diffusion (interdiffusion of labeled molecules of the same chemical species). We discuss this case first and then extend the results approximately to binary mixtures.

A corresponding-states plot of the self-diffusivity $\mathscr{D}_{AA^*}$ for nonpolar substances is given in Fig. 17.2-1.[4] This plot is based on self-diffusion measurements, supplemented by molecular dynamics simulations and by kinetic theory for the low-pressure limit. The ordinate is $c\mathscr{D}_{AA^*}$ at pressure p and temperature T, divided by $c\mathscr{D}_{AA^*}$ at the critical point. This quantity is plotted as a function of the reduced pressure $p_r = p/p_c$ and the reduced temperature $T_r = T/T_c$. Because of the similarity of species A and the labeled species A^*, the critical properties are all taken as those of species A.

From Fig. 17.2-1 we see that $c\mathscr{D}_{AA^*}$ increases strongly with temperature, especially for liquids. At each temperature $c\mathscr{D}_{AA^*}$ decreases toward zero with increasing pressure. With decreasing pressure, $c\mathscr{D}_{AA^*}$ increases toward a low-pressure limit, as predicted by kinetic theory (see §17.3). The reader is warned that this chart is tentative, and that the lines, except for the low-density limit, are based on data for a very few substances: Ar, Kr, Xe, and CH_4.

The quantity $(c\mathscr{D}_{AA^*})_c$ may be estimated by one of the following three methods:

(i) Given $c\mathscr{D}_{AA^*}$ at a known temperature and pressure, one can read $(c\mathscr{D}_{AA^*})_r$ from the chart and get $(c\mathscr{D}_{AA^*})_c = c\mathscr{D}_{AA^*}/(c\mathscr{D}_{AA^*})_r$.

---

[1] R. C. Reid, J. M. Prausnitz, and B. E. Poling, *The Properties of Gases and Liquids*, 4th edition, McGraw-Hill, New York (1987), Chapter 11.

[2] E. N. Fuller, P. D. Shettler, and J. C. Giddings, *Ind. Eng. Chem.*, **58**, No. 5, 19–27 (1966); Erratum: *ibid.* **58**, No. 8, 81 (1966). This paper gives a useful method for predicting binary gas diffusivities from the molecular formulas of the two species.

[3] J. C. Slattery and R. B. Bird, *AIChE Journal*, **4**, 137–142 (1958).

[4] Other correlations for self-diffusivity at elevated pressures have appeared in Ref. 3 and in L. S. Tee, G. F. Kuether, R. C. Robinson, and W. E. Stewart, *API Proceedings, Division of Refining*, 235–243 (1966); R. C. Robinson and W. E. Stewart, *IEC Fundamentals*, **7**, 90–95 (1968); J. L. Bueno, J. Dizy, R. Alvarez, and J. Coca, *Trans. Inst. Chem. Eng.*, **68**, Part A, 392–397 (1990).

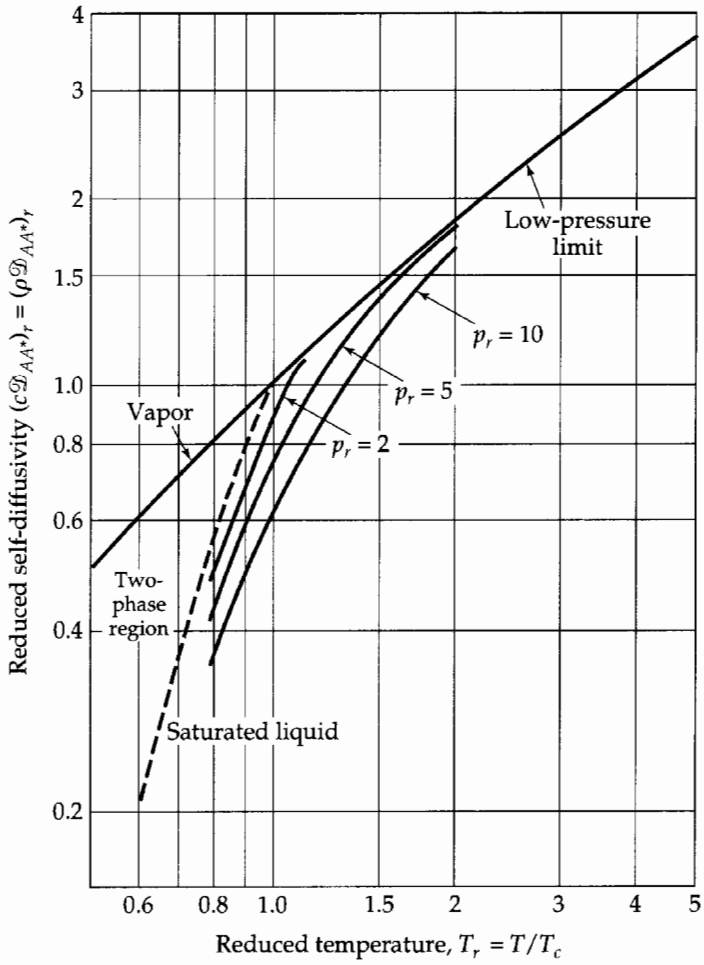

Fig. 17.2-1. A corresponding-states plot for the reduced self-diffusivity. Here $(c\mathscr{D}_{AA^*})_r = (\rho\mathscr{D}_{AA^*})_r$ for Ar, Kr, Xe, and CH_4 is plotted as a function of reduced temperature for several values of the reduced pressure. This chart is based on diffusivity data of J. J. van Loef and E. G. D. Cohen, *Physica A*, **156**, 522–533 (1989), the compressibility function of B. I. Lee and M. G. Kesler, *AIChE Journal*, **21**, 510–527 (1975), and Eq. 17.3-11 for the low-pressure limit.

(ii) One can predict a value of $c\mathscr{D}_{AA^*}$ in the low-density region by the methods given in §17.3 and then proceed as in (i).

(iii) One can use the empirical formula (see Problem 17A.9):

$$(c\mathscr{D}_{AA^*})_c = 2.96 \times 10^{-6}\left(\frac{1}{M_A} + \frac{1}{M_{A^*}}\right)^{1/2} \frac{p_{cA}^{2/3}}{T_{cA}^{1/6}} \tag{17.2-2}$$

This equation, like Eq. 17.2-1, should not be used for helium or hydrogen isotopes. Here c [=] g-mole/cm^3, $\mathscr{D}_{AA^*}$ [=] cm^2/s, T_c [=] K, and p_c [=] atm.

Thus far the discussion of high-density behavior has been concerned with self-diffusion. We turn now to the binary diffusion of chemically dissimilar species. In the absence of other information it is suggested that Fig. 17.2-1 may be used for crude estimation of $c\mathscr{D}_{AB}$, with p_{cA} and T_{cA} replaced everywhere by $\sqrt{p_{cA}p_{cB}}$ and $\sqrt{T_{cA}T_{cB}}$ respectively (see Problem 17A.9 for the basis for this empiricism). The ordinate of the plot is then interpreted as $(c\mathscr{D}_{AB})_r = c\mathscr{D}_{AB}/(c\mathscr{D}_{AB})_c$ and Eq. 17.2-2 is replaced by

$$(c\mathscr{D}_{AB})_c = 2.96 \times 10^{-6}\left(\frac{1}{M_A} + \frac{1}{M_B}\right)^{1/2} \frac{(p_{cA}p_{cB})^{1/3}}{(T_{cA}T_{cB})^{1/12}} \tag{17.2-3}$$

With these substitutions, accurate results are obtained in the low-pressure limit. At higher pressures, very few data are available for comparison, and the method must be regarded as provisional.

The results in Fig. 17.2-1, and their extensions to binary systems, are expressed in terms of $c\mathscr{D}_{AA^*}$ and $c\mathscr{D}_{AB}$ rather than $\mathscr{D}_{AA^*}$ and $\mathscr{D}_{AB}$. This is done because the c-multiplied diffusion coefficients are more frequently required in mass transfer calculations, and their dependence on pressure and temperature is simpler.

EXAMPLE 17.2-1

Estimation of Diffusivity at Low Density

Estimate $\mathscr{D}_{AB}$ for the system CO–CO_2 at 296.1K and 1 atm total pressure.

SOLUTION

The properties needed for Eq. 17.2-1 are (see Table E.1):

Label	Species	M	T_c (K)	p_c (atm)
A	CO	28.01	133	34.5
B	CO_2	44.01	304.2	72.9

Therefore,

$$(p_{cA}p_{cB})^{1/3} = (34.5 \times 72.9)^{1/3} = 13.60$$

$$(T_{cA}T_{cB})^{5/12} = (133 \times 304.2)^{5/12} = 83.1$$

$$\left(\frac{1}{M_A} + \frac{1}{M_B}\right)^{1/2} = \left(\frac{1}{28.01} + \frac{1}{44.01}\right)^{1/2} = 0.2417$$

$$a\left(\frac{T}{\sqrt{T_{cA}T_{cB}}}\right)^{b} = 2.745 \times 10^{-4}\left(\frac{296.1}{\sqrt{133 \times 304.2}}\right)^{1.823} = 5.56 \times 10^{-4}$$

Substitution of these values into Eq. 17.2-1 gives

$$(1.0)\mathscr{D}_{AB} = (5.56 \times 10^{-4})(13.60)(83.1)(24.17) \tag{17.2-4}$$

This gives $\mathscr{D}_{AB} = 0.152$ cm^2/s, in agreement with the experimental value.[5] This is unusually good agreement.

This problem can also be solved by means of Fig. 17.2-1 and Eq. 17.2-3, together with the ideal gas law $p = cRT$. The result is $\mathscr{D}_{AB} = 0.140$ cm^2/s, in fair agreement with the data.

EXAMPLE 17.2-2

Estimation of Self-Diffusivity at High Density

Estimate $c\mathscr{D}_{AA^*}$ for $C^{14}O_2$ in ordinary CO_2 at 171.7 atm and 373K. It is known[6] that $\mathscr{D}_{AA^*} = 0.113$ cm^2/s at 1.00 atm and 298K, at which condition $c = p/RT = 4.12 \times 10^{-5}$ g-mole/cm^3.

SOLUTION

Since a measured value of $\mathscr{D}_{AA^*}$ is given, we use method (i). The reduced conditions of the measurement are $T_r = 298/304.2 = 0.980$ and $p_r = 1.00/72.9 = 0.014$. Then from Fig. 17.2-1 we get the value $(c\mathscr{D}_{AA^*})_r = 0.98$. Hence

$$(c\mathscr{D}_{AA^*})_c = \frac{c\mathscr{D}_{AA^*}}{(c\mathscr{D}_{AA^*})_r} = \frac{(4.12 \times 10^{-5})(0.113)}{0.98}$$

$$= 4.75 \times 10^{-6} \text{ g-mol/cm} \cdot \text{s} \tag{17.2-5}$$

At the conditions of prediction ($T_r = 373/304.2 = 1.23$ and $p_r = 171.7/72.9 = 2.36$), we read $(c\mathscr{D}_{AA^*})_r = 1.21$. The predicted value is then

$$c\mathscr{D}_{AA^*} = (c\mathscr{D}_{AA^*})_r(c\mathscr{D}_{AA^*})_c = (1.21)(4.75 \times 10^{-6})$$

$$= 5.75 \times 10^{-6} \text{ g-mole/cm} \cdot \text{s} \tag{17.2-6}$$

The data of O'Hern and Martin[7] give $c\mathscr{D}_{AA^*} = 5.89 \times 10^{-6}$ g-mole/cm · s at these conditions. This good agreement is not unexpected, inasmuch as their low-pressure data were used in the estimation of $(c\mathscr{D}_{AA^*})_c$.

---

[5] B. A. Ivakin, P. E. Suetin, *Sov. Phys. Tech. Phys.* (English translation), **8**, 748–751 (1964).

[6] E. B. Wynn, *Phys. Rev.*, **80**, 1024–1027 (1950).

[7] H. A. O'Hern and J. J. Martin, *Ind. Eng. Chem.*, **47**, 2081–2086 (1955).

This problem can also be solved by method (iii) without an experimental value of $c\mathscr{D}_{AA^*}$. Equation 17.4-2 gives directly

$$(c\mathscr{D}_{AA^*})_c = 2.96 \times 10^{-6}\left(\frac{1}{44.01} + \frac{1}{46}\right)^{1/2} \frac{(72.9)^{2/3}}{(304.2)^{1/6}}$$
$$= 4.20 \times 10^{-6} \text{ g-mole/cm} \cdot \text{s} \qquad (17.2\text{-}7)$$

The resulting predicted value of $c\mathscr{D}_{AA^*}$ is 5.1×10^{-6} g-mole/cm · s.

EXAMPLE 17.2-3

Estimation of Binary Diffusivity at High Density

Estimate $c\mathscr{D}_{AB}$ for a mixture of 80 mole% CH_4 and 20 mole% C_2H_6 at 136 atm and 313K. It is known that, at 1 atm and 293K, the molar density is $c = 4.17 \times 10^{-5}$ g-mole/cm^3 and $\mathscr{D}_{AB} = 0.163$ cm^2/s.

SOLUTION

Figure 17.2-1 is used, with method (i). The reduced conditions for the known data are

$$T_r = \frac{T}{\sqrt{T_{cA}T_{cB}}} = \frac{293}{\sqrt{(190.7)(305.4)}} = 1.22 \qquad (17.2\text{-}8)$$

$$p_r = \frac{p}{\sqrt{p_{cA}p_{cB}}} = \frac{1.0}{\sqrt{(45.8)(48.2)}} = 0.021 \qquad (17.2\text{-}9)$$

From Fig. 17.2-1 at these conditions we obtain $(c\mathscr{D}_{AB})_r = 1.21$. The critical value $(c\mathscr{D}_{AB})_c$ is therefore

$$(c\mathscr{D}_{AB})_c = \frac{c\mathscr{D}_{AB}}{(c\mathscr{D}_{AB})_r} = \frac{(4.17 \times 10^{-5})(0.163)}{1.21}$$
$$= 5.62 \times 10^{-6} \text{ g-mol/cm} \cdot \text{s} \qquad (17.2\text{-}10)$$

Next we calculate the reduced conditions for the prediction ($T_r = 1.30$, $p_r = 2.90$) and read the value $(c\mathscr{D}_{AB})_r = 1.31$ from Fig. 17.2-1. The predicted value of $c\mathscr{D}_{AB}$ is therefore

$$c\mathscr{D}_{AB} = (c\mathscr{D}_{AB})_r(c\mathscr{D}_{AB})_c = (1.31)(5.62 \times 10^{-6})$$
$$= 7.4 \times 10^{-6} \text{ g-mole/cm} \cdot \text{s} \qquad (17.2\text{-}11)$$

Experimental measurements[8] give $c\mathscr{D}_{AB} = 6.0 \times 10^{-6}$, so that the predicted value is 23% high. Deviations of this magnitude are not unusual in the estimation of $c\mathscr{D}_{AB}$ at high densities.

An alternative solution may be obtained by method (iii). Substitution into Eq. 17.4-3 gives

$$(c\mathscr{D}_{AB})_c = 2.96 \times 10^{-6}\left(\frac{1}{16.04} + \frac{1}{30.07}\right)^{1/2} \frac{(45.8 \times 48.2)^{1/3}}{(190.7 \times 305.4)^{1/12}}$$
$$= 4.78 \times 10^{-6} \text{ g-mole/cm} \cdot \text{s} \qquad (17.2\text{-}12)$$

Multiplication by $(c\mathscr{D}_{AB})_r$ at the desired condition gives

$$c\mathscr{D}_{AB} = (4.78 \times 10^{-6})(1.31)$$
$$= 6.26 \times 10^{-6} \text{ g-mole/cm} \cdot \text{s} \qquad (17.2\text{-}13)$$

This is in closer agreement with the measured value.[8]

---

[8] V. J. Berry, Jr., and R. C. Koeller, *AIChE Journal*, **6**, 274–280 (1960).

§17.3 THEORY OF DIFFUSION IN GASES AT LOW DENSITY

The mass diffusivity $\mathscr{D}_{AB}$ for binary mixtures of nonpolar gases is predictable within about 5% by kinetic theory. As in the earlier kinetic theory discussions in §§1.4 and 9.3, we start with a simplified derivation to illustrate the mechanisms involved and then present the more accurate results of the Chapman–Enskog theory.

Consider a large body of gas containing molecular species A and A^*, which are identical except for labeling. We wish to determine the self-diffusivity $\mathscr{D}_{AA^*}$ in terms of the molecular properties on the assumption that the molecules are rigid spheres of equal mass m_A and diameter d_A.

Since the properties of A and A^* are nearly the same, we can use the following results of the kinetic theory for a pure rigid-sphere gas at low density in which the gradients of temperature, pressure, and velocity are small:

$$\bar{u} = \sqrt{\frac{8\kappa T}{\pi m}} \quad = \text{mean molecular speed relative to } \mathbf{v} \tag{17.3-1}$$

$$Z = \tfrac{1}{4} n\bar{u} \quad = \text{wall collision frequency per unit area in a stationary gas} \tag{17.3-2}$$

$$\lambda = \frac{1}{\sqrt{2}\pi d^2 n} \quad = \text{mean free path} \tag{17.3-3}$$

The molecules reaching any plane in the gas have, on the average, had their last collision at a distance a from the plane, where

$$a = \tfrac{2}{3}\lambda \tag{17.3-4}$$

In these equations n is the number density (total number of molecules per unit volume).

To predict the self-diffusivity $\mathscr{D}_{AA^*}$, we consider the motion of species A in the y direction under a mass fraction gradient $d\omega_A/dy$ (see Fig. 17.3-1), where the fluid mixture moves in the y direction at a finite velocity mass average velocity v_y throughout. The temperature T and the total molar mass concentration ρ are considered constant. We assume that Eqs. 17.3-1 to 4 remain valid in this nonequilibrium situation. The net mass flux of species A crossing a unit area of any plane of constant y is found by writing an expression for the mass of A crossing the plane in the positive y direction and subtracting the mass of A crossing in the negative y direction:

$$(\rho\omega_A v_y)\big|_y + [(\tfrac{1}{4}\rho\omega_A\bar{u})\big|_{y-a} - (\tfrac{1}{4}\rho\omega_A\bar{u})\big|_{y+a}] \tag{17.3-5}$$

Here the first term is the mass transport in the y direction because of the mass motion of the fluid—that is, the convective transport—and the last two terms give the molecular transport relative to v_y.

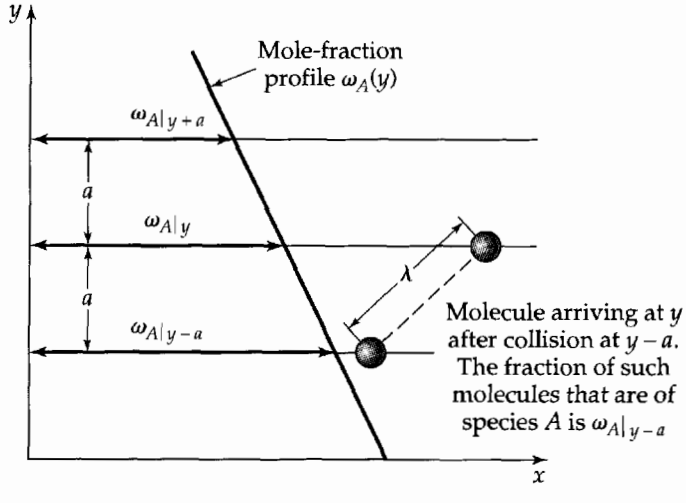

Fig. 17.3-1. Molecular transport of species A from the plane at $(y - a)$ to the plane at y.

It is assumed that the concentration profile $\omega_A(y)$ is very nearly linear over distances of several mean free paths. Then we may write

$$\omega_A|_{y\pm a} = \omega_A|_y \pm \tfrac{2}{3}\lambda \frac{d\omega_A}{dy} \tag{17.3-6}$$

Combination of the last two equations then gives for the *combined mass flux* at plane y:

$$\begin{aligned} n_{Ay} &= \rho\omega_A v_y - \tfrac{1}{3}\rho\bar{u}\lambda \frac{d\omega_A}{dy} \\ &\equiv \rho\omega_A v_y - \rho\mathscr{D}_{AA^*}\frac{d\omega_A}{dy} \end{aligned} \tag{17.3-7}$$

This is the *convective mass flux* plus the *molecular mass flux*, the latter being given by Eq. 17.1-1. Therefore we get the following expression for the self-diffusivity:

$$\mathscr{D}_{AA^*} = \tfrac{1}{3}\bar{u}\lambda \tag{17.3-8}$$

Finally, making use of Eqs. 17.3-1 and 3, we get

$$\mathscr{D}_{AA^*} = \frac{2}{3}\frac{\sqrt{\kappa T/\pi m_A}}{\pi d_A^2}\frac{1}{n} = \frac{2}{3\pi}\frac{\sqrt{\pi m_A \kappa T}}{\pi d_A^2}\frac{1}{\rho} \tag{17.3-9}$$

which can be compared with Eq. 1.4-9 for the viscosity and Eq. 9.3-12 for the thermal conductivity.

The development of a formula for $\mathscr{D}_{AB}$ for rigid spheres of unequal masses and diameters is considerably more difficult. We simply quote the result[1] here:

$$\mathscr{D}_{AB} = \frac{2}{3}\sqrt{\frac{\kappa T}{\pi}}\sqrt{\frac{1}{2}\left(\frac{1}{m_A}+\frac{1}{m_B}\right)}\frac{1}{\pi(\frac{1}{2}(d_A+d_B))^2}\frac{1}{n} \tag{17.3-10}$$

That is, $1/m_A$ is replaced by the arithmetic average of $1/m_A$ and $1/m_B$, and d_A by the arithmetic average of d_A and d_B.

The preceding discussion shows how the diffusivity can be obtained by mean free path arguments. For accurate results the Chapman–Enskog kinetic theory should be used. The Chapman–Enskog results for viscosity and thermal conductivity were given in §§1.4 and 9.3, respectively. The corresponding formula for $c\mathscr{D}_{AB}$ is:[2,3]

$$\begin{aligned} c\mathscr{D}_{AB} &= \frac{3}{16}\sqrt{\frac{2RT}{\pi}\left(\frac{1}{M_A}+\frac{1}{M_B}\right)}\frac{1}{\tilde{N}\sigma_{AB}^2\Omega_{\mathscr{D},AB}} \\ &= 2.2646\times 10^{-5}\sqrt{T\left(\frac{1}{M_A}+\frac{1}{M_B}\right)}\frac{1}{\sigma_{AB}^2\Omega_{\mathscr{D},AB}} \end{aligned} \tag{17.3-11}$$

Or, if we approximate c by the ideal gas law $p = cRT$, we get for $\mathscr{D}_{AB}$

$$\begin{aligned} \mathscr{D}_{AB} &= \frac{3}{16}\sqrt{\frac{2(RT)^3}{\pi}\left(\frac{1}{M_A}+\frac{1}{M_B}\right)}\frac{1}{\tilde{N}p\sigma_{AB}^2\Omega_{\mathscr{D},AB}} \\ &= 0.0018583\sqrt{T^3\left(\frac{1}{M_A}+\frac{1}{M_B}\right)}\frac{1}{p\sigma_{AB}^2\Omega_{\mathscr{D},AB}} \end{aligned} \tag{17.3-12}$$

In the second line of Eqs. 17.3-11 and 12, $\mathscr{D}_{AB}$ [=] cm^2/s, σ_{AB} [=] Å, T [=] K, and p [=] atm.

---

[1] A similar result is given by R. D. Present, *Kinetic Theory of Gases*, McGraw-Hill, New York (1958), p. 55.

[2] S. Chapman and T. G. Cowling, *The Mathematical Theory of Non-Uniform Gases*, 3rd edition, Cambridge University Press (1970), Chapters 10 and 14.

[3] J. O. Hirschfelder, C. F. Curtiss, and R. B. Bird, *Molecular Theory of Gases and Liquids*, 2nd corrected printing, Wiley, New York (1964), p. 539.

The dimensionless quantity $\Omega_{\mathscr{D},AB}$—the "collisional integral" for diffusion—is a function of the dimensionless temperature $\kappa T/\varepsilon_{AB}$. The parameters σ_{AB} and ε_{AB} are those appearing in the Lennard-Jones potential between one molecule of A and one of B (cf. Eq. 1.4-10):

$$\varphi_{AB}(r) = 4\varepsilon_{AB}\left[\left(\frac{\sigma_{AB}}{r}\right)^{12} - \left(\frac{\sigma_{AB}}{r}\right)^{6}\right] \tag{17.3-13}$$

This function $\Omega_{\mathscr{D},AB}$ is given in Table E.2 and Eq. E.2-2. From these results one can compute that $\mathscr{D}_{AB}$ increases roughly as the 2.0 power of T at low temperatures and as the 1.65 power of T at very high temperatures; see the $p_r \to 0$ curve in Fig. 17.2-1. For rigid spheres, $\Omega_{\mathscr{D},AB}$ would be unity at all temperatures and a result analogous to Eq. 17.3-10 would be obtained.

The parameters σ_{AB} and ε_{AB} could, in principle, be determined directly from accurate measurements of $\mathscr{D}_{AB}$ over a wide range of temperatures. Suitable data are not yet available for many gas pairs, and one may have to resort to using some other measurable property, such as the viscosity[4] of a binary mixture of A and B. In the event that there are no such data, then we can estimate σ_{AB} and ϵ_{AB} from the following combining rules:[5]

$$\sigma_{AB} = \tfrac{1}{2}(\sigma_A + \sigma_B); \qquad \varepsilon_{AB} = \sqrt{\varepsilon_A \varepsilon_B} \tag{17.3-14, 15}$$

for nonpolar gas pairs. Use of these combining rules enables us to predict values of $\mathscr{D}_{AB}$ within about 6% by use of viscosity data on the pure species A and B, or within about 10% if the Lennard-Jones parameters for A and B are estimated from boiling point data by use of Eq. 1.4-12.[6]

For isotopic pairs, $\sigma_{AA^*} = \sigma_A = \sigma_{A^*}$ and $\varepsilon_{AA^*} = \varepsilon_A = \varepsilon_{A^*}$; that is, the intermolecular force fields for the various pairs A–A^*, A^*–A^*, and A–A are virtually identical, and the parameters σ_A and ε_A may be obtained from viscosity data on pure A. If, in addition, M_A is large, Eq. 17.3-11 simplifies to

$$c\mathscr{D}_{AA^*} = 3.2027 \times 10^{-5}\sqrt{\frac{T}{M_A}}\frac{1}{\sigma_A^2 \Omega_{\mathscr{D},AA^*}} \tag{17.3-16}$$

The corresponding equation for the rigid-sphere model is given in Eq. 17.3-9.

Comparison of Eq. 17.3-16 with Eq. 1.4-14 shows that the self-diffusivity $\mathscr{D}_{AA^*}$ and the viscosity μ (or kinematic viscosity ν) are related as follows for heavy isotopic gas pairs at low density:

$$\frac{\mu}{\rho\mathscr{D}_{AA^*}} = \frac{\nu}{\mathscr{D}_{AA^*}} = \frac{5}{6}\frac{\Omega_{\mathscr{D},AA^*}}{\Omega_\mu} \tag{17.3-17}$$

in which $\Omega_\mu \approx 1.1\Omega_{\mathscr{D},AA^*}$ over a wide range of $\kappa T/\varepsilon_A$, as may be seen in Table E.2. Thus $\mathscr{D}_{AA^*} \approx 1.32\nu$ for the *self-diffusivity*. The relation between ν and the *binary diffusivity* $\mathscr{D}_{AB}$ is not so simple, because ν may vary considerably with the composition. The Schmidt number $\mathrm{Sc} = \mu/\rho\mathscr{D}_{AB}$ is in the range from 0.2 to 5.0 for most gas pairs.

Equations 17.3-11, 12, 16, and 17 were derived for monatomic nonpolar gases but have been found useful for polyatomic nonpolar gases as well. In addition, these equations may be used to predict $\mathscr{D}_{AB}$ for interdiffusion of a polar gas and a nonpolar gas by using combining laws different[7] from those given in Eq. 17.3-14 and 15.

---

[4] S. Weissman and E. A. Mason, *J. Chem. Phys.*, **37**, 1289–1300 (1962); S. Weissman, *J. Chem. Phys.*, **40**, 3397–3406 (1964).

[5] J. O. Hirschfelder, R. B. Bird, and E. L. Spotz, *Chem. Revs.*, **44**, 205–231 (1949); S. Gotoh, M. Manner, J. P. Sørensen, and W. E. Stewart, *J. Chem. Eng. Data*, **19**, 169–171 (1974).

[6] R. C. Reid, J. M. Prausnitz, and B. E. Poling, *The Properties of Gases and Liquids*, 4th edition, McGraw-Hill, New York (1987).

[7] J. O. Hirschfelder, C. F. Curtiss, and R. B. Bird, *Molecular Theory of Gases and Liquids*, 2nd corrected printing, Wiley, New York (1964), §8.6*b* and p. 1201. Polar gases and gas mixtures are discussed by E. A. Mason and L. Monchick, *J. Chem. Phys.* **36**, 2746–2757 (1962).

EXAMPLE 17.3-1

Computation of Mass Diffusivity for Low-Density Gases

Predict the value of $\mathscr{D}_{AB}$ for the system CO–CO_2 at 296.1K and 1.0 atm total pressure.

SOLUTION

From Table E.1 we obtain the following parameters:

CO:	$M_A = 28.01$	$\sigma_A = 3.590$ Å	$\varepsilon_A/\kappa = 100$K
CO_2:	$M_B = 44.01$	$\sigma_B = 3.996$ Å	$\varepsilon_B/\kappa = 190$K

The mixture parameters are then estimated from Eqs. 17.3-14 and 15:

$$\sigma_{AB} = \tfrac{1}{2}(3.590 + 3.996) = 3.793 \text{ Å} \tag{17.3-18}$$

$$\varepsilon_{AB}/\kappa = \sqrt{(110)(190)} = 144.6\text{K} \tag{17.3-19}$$

The dimensionless temperature is then $\kappa T/\varepsilon_{AB} = (296.1)/(144.6) = 2.048$. From Table E.2 we can find the collision integral for diffusion, $\Omega_{\mathscr{D},AB} = 1.067$. Substitution of the preceding values in Eq. 17.3-12 gives

$$\mathscr{D}_{AB} = 0.0018583\sqrt{(296.1)^3\left(\frac{1}{28.01} + \frac{1}{44.01}\right)}\frac{1}{(1.0)(3.793)^2(1.067)}$$

$$= 0.149 \text{ cm}^2/\text{s} \tag{17.3-20}$$

§17.4 THEORY OF DIFFUSION IN BINARY LIQUIDS

The kinetic theory for diffusion in simple liquids is not as well developed as that for dilute gases, and it cannot presently give accurate analytical predictions of diffusivities.[1-3] As a result our understanding of liquid diffusion depends primarily on the rather crude hydrodynamic and activated-state models. These in turn have spawned a number of empirical correlations, which provide the best available means for prediction. These correlations permit estimation of diffusivities in terms of more easily measured properties such as viscosity and molar volume.

The *hydrodynamic theory* takes as its starting point the Nernst–Einstein equation,[4] which states that the diffusivity of a single particle or solute molecule A through a stationary medium B is given by

$$\mathscr{D}_{AB} = \kappa T(u_A/F_A) \tag{17.4-1}$$

in which u_A/F_A is the "mobility" of a particle A (that is, the steady-state velocity attained by the particle under the action of a unit force). The origin of Eq. 17.4-1 is discussed in §17.5 in connection with the Brownian motion of colloidal suspensions. If the shape and size of A are known, the mobility can be calculated by the solution of the creeping-flow equation of motion[5] (Eq. 3.5-8). Thus, if A is spherical and if one takes into account the possibility of "slip" at the fluid–solid interface, one obtains[6]

$$\frac{u_A}{F_A} = \left(\frac{3\mu_B + R_A\beta_{AB}}{2\mu_B + R_A\beta_{AB}}\right)\frac{1}{6\pi\mu_B R_A} \tag{17.4-2}$$

---

[1] R. J. Bearman and J. G. Kirkwood, *J. Chem. Phys.*, **28**, 136–145 (1958).

[2] R. J. Bearman, *J. Phys. Chem.*, **65**, 1961–1968 (1961).

[3] C. F. Curtiss and R. B. Bird, *J. Chem. Phys.*, **111**, 10362–10370 (1999).

[4] See §17.7 and E. A. Moelwyn-Hughes, *Physical Chemistry*, 2nd edition, corrected printing, Macmillan, New York (1964), pp. 62–74. See also R. J. Silbey and R. A. Alberty, *Physical Chemistry*, 3rd edtion, Wiley, New York (2001), §20.2. Apparently the Nernst–Einstein equation cannot be generalized to polymeric fluids with appreciable velocity gradients, as has been noted by H. C. Öttinger, *AIChE Journal*, **35**, 279–286 (1989).

[5] S. Kim and S. J. Karrila, *Microhydrodynamics: Principles and Selected Applications*, Butterworth-Heinemann, Boston (1991).

[6] H. Lamb, *Hydrodynamics*, 6th edition, Cambridge University Press (1932), reprinted (1997), §337.

in which μ_B is the viscosity of the pure solvent, R_A is the radius of the solute particle, and β_{AB} is the "coefficient of sliding friction" (formally the same as the μ/ζ of problem 2B.9). The limiting cases of $\beta_{AB} = \infty$ and $\beta_{AB} = 0$ are of particular interest:

a. $\beta_{AB} = \infty$ (no-slip condition)

In this case Eq. 17.4-2 becomes Stokes' law (Eq. 2.6-15) and Eq. 17.4-1 becomes

$$\frac{\mathscr{D}_{AB}\mu_B}{\kappa T} = \frac{1}{6\pi R_A} \tag{17.4-3}$$

which is usually called the *Stokes–Einstein equation*. This equation applies well to the diffusion of very large spherical molecules in solvents of low molecular weight[7] and to suspended particles. Analogous expressions developed for nonspherical particles have been used for estimating the shapes of protein molecules.[8,9]

b. $\beta_{AB} = 0$ (complete slip condition)

In this case Eq. 17.4-1 leads to (see Eq. 4B.3-4)

$$\frac{\mathscr{D}_{AB}\mu_B}{\kappa T} = \frac{1}{4\pi R_A} \tag{17.4-4}$$

If the molecules A and B are identical (that is, for *self-diffusion*) and if they can be assumed to form a cubic lattice with the adjacent molecules just touching, then $2R_A = (\tilde{V}_A/\tilde{N}_A)^{1/3}$ and

$$\frac{\mathscr{D}_{AA}\mu_A}{\kappa T} = \frac{1}{2\pi}\left(\frac{\tilde{N}_A}{\tilde{V}_A}\right)^{1/3} \tag{17.4-5}$$

Equation 17.4-5 has been found[10] to agree with self-diffusion data for a number of liquids, including polar and associated substances, liquid metals, and molten sulfur, to within about 12%. The hydrodynamic model has proven less useful for binary diffusion (that is, for A not identical to B) although the predicted temperature and viscosity dependences are approximately correct.

Keep in mind that the above formulas apply only to dilute solutions of A in B. Some attempts have been made, however, to extend the hydrodynamic model to solutions of finite concentrations.[11]

The *Eyring activated-state theory* attempts to explain transport behavior via a quasi-crystalline model of the liquid state.[12] It is assumed in this theory that there is some unimolecular rate process in terms of which diffusion can be described, and it is further assumed that in this process there is some configuration that can be identified as the "activated state." The Eyring theory of reaction rates is applied to this elementary process in a manner analogous to that described in §1.5 for estimation of liquid viscosity. A modifi-

---

[7] A. Polson, *J. Phys. Colloid Chem.*, **54**, 649–652 (1950).

[8] H. J. V. Tyrrell, *Diffusion and Heat Flow in Liquids*, Butterworths, London (1961), Chapter 6.

[9] Creeping motion around finite bodies in a fluid of infinite extent has been reviewed by J. Happel and H. Brenner, *Low Reynolds Number Hydrodynamics*, Prentice-Hall, Englewood Cliffs, N.J. (1965); see also S. Kim and S. J. Karrila, *Microhydrodynamics: Principles and Selected Applications*, Butterworth-Heinemann, Boston (1991). G. K. Youngren and A. Acrivos, *J. Chem. Phys.* **63**, 3846–3848 (1975) have calculated the rotational friction coefficient for benzene, supporting the validity of the no-slip condition at molecular dimensions.

[10] J. C. M. Li and P. Chang, *J. Chem. Phys.*, **23**, 518–520 (1955).

[11] C. W. Pyun and M. Fixman, *J. Chem. Phys.*, **41**, 937–944 (1964).

[12] S. Glasstone, K. J. Laidler, and H. Eyring, *Theory of Rate Processes*, McGraw-Hill, New York (1941), Chapter IX.

cation of the original Eyring model by Ree, Eyring, and coworkers[13] yields an expression similar to Eq. 17.4-5 for traces of A in solvent B:

$$\frac{\mathscr{D}_{AB}\mu_B}{\kappa T} = \frac{1}{\xi}\left(\frac{\tilde{N}_A}{\tilde{V}_B}\right)^{1/3} \tag{17.4-6}$$

Here ξ is a "packing parameter," which in the theory represents the number of nearest neighbors of a given solvent molecule. For the special case of self-diffusion, ξ is found to be very close to 2π, so that Eqs. 17.4-5 and 6 are in good agreement despite the difference between the models from which they were developed.

The Eyring theory is based on an oversimplified model of the liquid state, and consequently the conditions required for its validity are not clear. However, Bearman has shown[2] that the Eyring model gives results consistent with statistical mechanics for "regular solutions," that is, for mixtures of molecules that have similar size, shape, and intermolecular forces. For this limiting situation, Bearman also obtains an expression for the concentration dependence of the diffusivity,

$$\frac{\mathscr{D}_{AB}\mu_B}{(\mathscr{D}_{AB}\mu_B)_{x_A\to 0}} = \left[1 + x_A\left(\frac{\overline{V}_A}{\overline{V}_B} - 1\right)\right]\left(\frac{\partial \ln a_A}{\partial \ln x_A}\right)_{T,p} \tag{17.4-7}$$

in which $\mathscr{D}_{AB}$ and μ_B are the diffusivity and viscosity of the mixture at the composition x_A, and a_A is the thermodynamic activity of species A. For regular solutions, the partial molar volumes, $\overline{V}_A$ and $\overline{V}_B$, are equal to the molar volumes of the pure components. Bearman suggests on the basis of his analysis that Eq. 17.4-7 should be limited to regular solutions, and it has in fact been found to apply well only to nearly ideal solutions.

Because of the unsatisfactory nature of the theory for diffusion in liquids, it is necessary to rely on *empirical* expressions. For example, the Wilke–Chang equation[14] gives the diffusivity for small concentrations of A in B as

$$\mathscr{D}_{AB} = 7.4 \times 10^{-8}\frac{\sqrt{\psi_B M_B}T}{\mu \tilde{V}_A^{0.6}} \tag{17.4-8}$$

Here $\tilde{V}_A$ is the molar volume of the solute A in cm^3/g-mole as liquid at its normal boiling point, μ is the viscosity of the solution in centipoises, ψ_B is an "association parameter" for the solvent, and T is the absolute temperature in K. Recommended values of ψ_B are: 2.6 for water; 1.9 for methanol; 1.0 for benzene, ether, heptane, and other unassociated solvents. Equation 17.4-8 is good only for dilute solutions of nondissociating solutes. For such solutions, it is usually good within ±10%.

Other empiricisms, along with their relative merits, have been summarized by Reid, Prausnitz, and Poling.[15]

EXAMPLE 17.4-1

Estimation of Liquid Diffusivity

Estimate $\mathscr{D}_{AB}$ for a dilute solution of TNT (2,4,6-trinitrotoluene) in benzene at 15°C.

SOLUTION

Use the equation of Wilke and Chang, taking TNT as component A and benzene as component B. The required data are

$$\mu = 0.705\text{cp (the viscosity for pure benzene)}$$
$$\tilde{V}_A = 140\ \text{cm}^3\text{/g-mole (for TNT)}$$

---

[13] H. Eyring, D. Henderson, B. J. Stover, and E. M. Eyring, *Statistical Mechanics and Dynamics*, Wiley, New York (1964), §16.8.

[14] C. R. Wilke, *Chem. Eng. Prog.*, **45**, 218–224 (1949); C. R. Wilke and P. Chang, *AIChE Journal*, **1**, 264–270 (1955).

[15] R. C. Reid, J. M. Prausnitz, and B. E. Poling, *The Properties of Gases and Liquids*, 4th edition, McGraw-Hill, New York (1987), Chapter 11.

$$\psi_B = 1.0 \text{ (for benzene)}$$
$$M_B = 78.11 \text{ (for benzene)}$$

Substitution into Eq. 17.4-8 gives

$$\mathscr{D}_{AB} = 7.4 \times 10^{-8} \frac{\sqrt{(1.0)(78.11)}(273 + 15)}{(0.705)(140)^{0.6}}$$
$$= 1.38 \times 10^{-5} \text{ cm}^2/\text{s} \tag{17.4-9}$$

This result compares well with the measured value of 1.39×10^{-5} cm^2/s.

§17.5 THEORY OF DIFFUSION IN COLLOIDAL SUSPENSIONS[1,2,3]

Next we turn to the movement of small colloidal particles in a liquid. Specifically we consider a finely divided, dilute suspension of spherical particles of material A in a stationary liquid B. When the spheres of A are sufficiently small (but still large with respect to the molecules of the suspending medium), the collisions between the spheres and the molecules of B will result in an erratic motion of the spheres. This random motion is referred to as *Brownian motion*.[4]

The movement of each sphere can be described by an equation of motion, called the *Langevin equation*:

$$m \frac{d\mathbf{u}_A}{dt} = -\zeta \mathbf{u}_A + \mathbf{F}(t) \tag{17.5-1}$$

in which $\mathbf{u}_A$ is the instantaneous velocity of the sphere of mass m. The term $-\zeta \mathbf{u}_A$ gives the Stokes' law drag force,[5] $\zeta = 6\pi\mu_B R_A$ being the "friction coefficient." Finally $\mathbf{F}(t)$ is the rapidly oscillating, irregular Brownian motion force. Equation 17.5-1 cannot be "solved" in the usual sense, since it contains the randomly fluctuating force $\mathbf{F}(t)$. Equations such as Eq. 17.5-1 are called "stochastic differential equations."

If it is assumed that (i) $\mathbf{F}(t)$ is independent of $\mathbf{u}_A$ and that (ii) the variations in $\mathbf{F}(t)$ are much more rapid than those of $\mathbf{u}_A$, then it is possible to extract from Eq. 17.5-1 the probability $W(\mathbf{u}_A,t;\mathbf{u}_{A0})d\mathbf{u}_A$ that at time t the particle will have a velocity in the range of $\mathbf{u}_A$ to $\mathbf{u}_A + d\mathbf{u}_A$. Physical reasoning requires that the probability density $W(\mathbf{u}_A,t;\mathbf{u}_{A0})$ approach a Maxwellian (equilibrium) distribution as $t \to \infty$:

$$W(\mathbf{u}_A,t;\mathbf{u}_{A0}) \to \left(\frac{m}{2\pi\kappa T}\right)^{3/2} \exp(-mu_A^2/2\kappa T) \tag{17.5-2}$$

Here, T is the temperature of the fluid in which the particles are suspended.

---

[1] A. Einstein, *Ann. d. Phys*, **17**, 549–560 (1905), **19**, 371–381 (1906); *Investigations on the Theory of the Brownian Movement*, Dover, New York (1956).

[2] S. Chandrasekhar, *Rev. Mod. Phys.*, **15**, 1–89 (1943).

[3] W. B. Russel, D. A. Saville, and W. R. Schowalter, *Colloidal Dispersions*, Cambridge University Press (1989); H. C. Öttinger, *Stochastic Processes in Polymeric Fluids*, Springer, Berlin (1996).

[4] Named after the botanist R. Brown, *Phil. Mag.* (4), p. 161 (1828); *Ann. d. Phys. u. Chem.*, **14**, 294–313 (1828). Actually the phenomenon had been discovered and reported earlier in 1789 by Jan Ingenhousz (1730–1799) in the Netherlands.

[5] As can be seen from Example 4.2-1, Stokes' law is valid only for the steady, unidirectional motion of a sphere through a fluid. For a sphere moving in an arbitrary manner, there are, in addition to the Stokes' contribution, an inertial term and a memory-integral term (the Basset force). See A. B. Basset, *Phil. Trans.*, **179**, 43–63 (1887); H. Lamb, *Hydrodynamics*, 6th edition, Cambridge University Press (1932), reprinted (1997), p. 644; H. Villat and J. Kravtchenko, *Leçons sur les Fluides Visqueux*, Gauthier-Villars, Paris (1943), p. 213, Eq. (62); L. Landau and E. M. Lifshitz, *Fluid Mechanics*, 2nd edition, Pergamon, New York (1987), p. 94. In applying the Langevin equation to polymer kinetic theory, the role of the Basset force has been investigated by J. D. Schieber, *J. Chem. Phys.*, **94**, 7526–7533 (1991).

Another quantity of interest that can be obtained from the Langevin equation is the probability, $W(\mathbf{r},t;\mathbf{r}_0,\mathbf{u}_{A0})d\mathbf{r}$, that at time t the particle will have a position in the range $\mathbf{r}$ to $\mathbf{r} + d\mathbf{r}$ if its initial position and velocity were $\mathbf{r}_0$ and $\mathbf{u}_{A0}$. For long times, specifically $t >> m/\zeta$, this probability is given by

$$W(\mathbf{r},t;\mathbf{r}_0,\mathbf{u}_{A0})d\mathbf{r} = \left(\frac{\zeta}{4\pi\kappa Tt}\right)^{3/2} \exp(-\zeta(r - r_0)^2/4\kappa Tt)d\mathbf{r} \tag{17.5-3}$$

However, this expression turns out to have just the same form as the solution of Fick's second law of diffusion (see Eq. 19.1-18 and Problem 20B.5) for the diffusion from a point source. One simply has to identify W with the concentration c_A, and $\kappa T/\zeta$ with $\mathscr{D}_{AB}$. In this way Einstein (see Ref. 1 on page 531) arrived at the following expression for the diffusivity of a dilute suspension of spherical colloid particles:

$$\mathscr{D}_{AB} = \frac{\kappa T}{\zeta} = \frac{\kappa T}{6\pi\mu_B R_A} \tag{17.5-4}$$

Thus, $\mathscr{D}_{AB}$ is related to the temperature and the friction coefficient ζ (the reciprocal of the friction coefficient is called the "mobility"). Equation 17.5-4 was already given in Eq. 17.4-3 for the interdiffusion of liquids.

§17.6 THEORY OF DIFFUSION OF POLYMERS

For a *dilute solution* of a polymer A in a low-molecular-weight solvent B, there is a detailed theory,[1] in which the polymer molecules are modeled as bead–spring chains (see Fig. 8.6-2). Each chain is a linear arrangement of N beads and $N - 1$ Hookean springs. The beads are characterized by a friction coefficient ζ, which describes the Stokes' law resistance to the bead motion through the solvent. The model further takes into account the fact that, as a bead moves around, it disturbs the solvent in the neighborhood of all the other beads; this is referred to as *hydrodynamic interaction*. The theory ultimately predicts that the diffusivity should be proportional to $N^{-1/2}$ for large N. Since the number of beads is proportional to the polymer molecular weight M, the following result is obtained:

$$\mathscr{D}_{AB} \sim \frac{1}{\sqrt{M}} \tag{17.6-1}$$

The inverse square-root dependence is rather well borne out by experiment.[2] If hydrodynamic interaction among beads were not included, then one would predict $\mathscr{D}_{AB} \sim 1/M$.

The theory of *self-diffusion* in an undiluted polymer has been studied from several points of view.[3,4] These theories, which are rather crude, lead to the result that

$$\mathscr{D}_{AA^*} \sim \frac{1}{M^2} \tag{17.6-2}$$

---

[1] J. G. Kirkwood, *Macromolecules*, Gordon and Breach, New York (1967), pp. 13, 41, 76–77, 95, 101–102. The original Kirkwood theory has been reexamined and slightly improved by H. C. Öttinger, *J. Chem. Phys.*, **87**, 3156–3165 (1987).

[2] R. B. Bird, C. F. Curtiss, R. C. Armstrong, and O. Hassager, *Dynamics of Polymeric Liquids, Vol. 2, Kinetic Theory*, 2nd edition, Wiley, New York (1987), pp. 174–175.

[3] P.-G. de Gennes and L. Léger, *Ann. Rev. Phys. Chem.*, 49–61 (1982); P.-G. de Gennes, *Physics Today*, **36**, 33–39 (1983). De Gennes introduced the notion of *reptation*, according to which the polymer molecules move back and forth along their backbones in a snake-like Brownian motion.

[4] R. B. Bird, C. F. Curtiss, R. C. Armstrong, and O. Hassager, *Dynamics of Polymeric Liquids, Vol. 2, Kinetic Theory*, 2nd edition, Wiley, New York (1987), pp. 326–327; C. F. Curtiss and R. B. Bird, *Proc. Nat. Acad. Sci.*, **93**, 7440–7445 (1996).

Experimental data agree more or less with this result,[5] but the exponent on the molecular weight may be as great as 3 for some polymers.

Although a very general theory for diffusion of polymers has been developed,[6] not very much has been done with it. So far it has been used to show that, in flowing dilute solutions of flowing polymers, the diffusivity tensor (see Eq. 17.1-10) becomes anisotropic and dependent on the velocity gradients. It has also been shown how to generalize the Maxwell–Stefan equations (see §17.9 and §24.1) for multicomponent polymeric liquids. Further advances in this subject can be expected through use of molecular simulations.[7]

§17.7 MASS AND MOLAR TRANSPORT BY CONVECTION

In §17.1, the discussion of Fick's (first) law of diffusion was given in terms of *mass units*: mass concentration, mass flux, and the mass average velocity. In this section we extend the previous discussion to include *molar units*. Thus most of this section deals with questions of notation and definitions. One might reasonably wonder whether or not this dual set of notation is really necessary. Unfortunately, it really is. When chemical reactions are involved, molar units are usually preferred. When the diffusion equations are solved together with the equation of motion, mass units are usually preferable. Therefore it is necessary to acquire familiarity with both. In this section we also introduce the concept of the *convective flux* of mass or moles.

Mass and Molar Concentrations

Earlier we defined the *mass concentration* ρ_α as the mass of species α per unit volume of solution. Now we define the *molar concentration* $c_\alpha = \rho_\alpha/M_\alpha$ as the number of moles of α per unit volume of solution.

Similarly, in addition to the *mass fraction* $\omega_\alpha = \rho_\alpha/\rho$, we will use the *mole fraction* $x_\alpha = c_\alpha/c$. Here $\rho = \Sigma_\alpha \rho_\alpha$ is the total mass of all species per unit volume of solution, and $c = \Sigma_\alpha c_\alpha$ is the total number of moles of all species per unit volume of solution. By the word "solution" we mean a one-phase gaseous, liquid, or solid mixture. In Table 17.7-1 we summarize these concentration units and their interrelation for multicomponent systems.

It is necessary to emphasize that ρ_α is the mass concentration of species α in a mixture. We use the notation $\rho^{(\alpha)}$ for the density of pure species α when the need arises.

Mass Average and Molar Average Velocity

In a diffusing mixture, the various chemical species are moving at different velocities. By $\mathbf{v}_\alpha$, the "velocity of species α," we do *not* mean the velocity of an individual molecule of species α. Rather, we mean the average of all the velocities of molecules of species α within a small volume. Then, for a mixture of N species, the local *mass average velocity* $\mathbf{v}$ is defined as

$$\mathbf{v} = \frac{\sum_{\alpha=1}^{N} \rho_\alpha \mathbf{v}_\alpha}{\sum_{\alpha=1}^{N} \rho_\alpha} = \frac{\sum_{\alpha=1}^{N} \rho_\alpha \mathbf{v}_\alpha}{\rho} = \sum_{\alpha=1}^{N} \omega_\alpha \mathbf{v}_\alpha \tag{17.7-1}$$

---

[5] P. F. Green, in *Diffusion in Polymers* (P. Neogi, ed.), Dekker, New York (1996), Chapter 6. According to T. P. Lodge, *Phys. Rev. Letters*, **86**, 3218–3221 (1999), measurements on undiluted polymers show that the exponent on the molecular weight should be about 2.3.

[6] C. F. Curtiss and R. B. Bird, *Adv. Polym. Sci.*, **125**, 1–101 (1996) and *J. Chem. Phys.*, **111**, 10362–10370 (1999).

[7] D. N. Theodorou, in *Diffusion in Polymers* (P. Neogi, ed.), Dekker, New York (1996), Chapter 2.

Table 17.7-1 Notation for Concentrations

Basic definitions:

ρ_α = mass concentration of species α (A)

$\rho = \sum_{\alpha=1}^{N} \rho_\alpha$ = mass density of solution (B)

$\omega_\alpha = \rho_\alpha/\rho$ = mass fraction of species α (C)

c_α = molar concentration of species α (D)

$c = \sum_{\alpha=1}^{N} c_\alpha$ = molar density of solution (E)

$x_\alpha = c_\alpha/c$ = mole fraction of species α (F)

$M = \rho/c$ = molar mean molecular weight of solution (G)

Algebraic relations:

$c_\alpha = \rho_\alpha/M_\alpha$ (H)

$\rho_\alpha = c_\alpha M_\alpha$ (I)

$\sum_{\alpha=1}^{N} x_\alpha = 1$ (J)

$\sum_{\alpha=1}^{N} \omega_\alpha = 1$ (K)

$\sum_{\alpha=1}^{N} x_\alpha M_\alpha = M$ (L)

$\sum_{\alpha=1}^{N} \omega_\alpha/M_\alpha = 1/M$ (M)

$x_\alpha = \dfrac{\omega_\alpha/M_\alpha}{\sum_{\beta=1}^{N} (\omega_\beta/M_\beta)}$ (N)

$\omega_\alpha = \dfrac{x_\alpha M_\alpha}{\sum_{\beta=1}^{N} (x_\beta M_\beta)}$ (O)

Differential relations:

$$\nabla x_\alpha = -\frac{M^2}{M_\alpha} \sum_{\substack{\gamma=1 \\ \gamma\neq\alpha}}^{N} \left[\frac{1}{M} + \omega_\alpha\left(\frac{1}{M_\gamma} - \frac{1}{M_\alpha}\right)\right]\nabla\omega_\gamma \qquad (P)^a$$

$$\nabla\omega_\alpha = -\frac{M_\alpha}{M^2} \sum_{\substack{\gamma=1 \\ \gamma\neq\alpha}}^{N} [M + x_\alpha(M_\gamma - M_\alpha)]\nabla x_\gamma \qquad (Q)^a$$

[a]Equations (P) and (Q), simplified for binary ystems, are

$$\nabla x_A = \frac{\frac{1}{M_A M_B}\nabla\omega_A}{\left(\frac{\omega_A}{M_A} + \frac{\omega_B}{M_B}\right)^2} \qquad (P') \qquad\qquad \nabla\omega_A = \frac{M_A M_B \nabla x_A}{(x_A M_A + x_B M_B)^2} \qquad (Q')$$

Note that $\rho\mathbf{v}$ is the local rate at which mass passes through a unit cross section placed perpendicular to the velocity $\mathbf{v}$. This is the local velocity one could measure by means of a Pitot tube or by laser-Doppler velocimetry, and corresponds to the $\mathbf{v}$ used in the equation of motion and in the energy equation in the preceding chapters for pure fluids.

Similarly, one may define a local *molar average velocity* $\mathbf{v}^*$ by

$$\mathbf{v}^* = \frac{\sum_{\alpha=1}^{N} c_\alpha \mathbf{v}_\alpha}{\sum_{\alpha=1}^{N} c_\alpha} = \frac{\sum_{\alpha=1}^{N} c_\alpha \mathbf{v}_\alpha}{c} = \sum_{\alpha=1}^{N} x_\alpha \mathbf{v}_\alpha \qquad (17.7\text{-}2)$$

Note that $c\mathbf{v}^*$ is the local rate at which moles pass through a unit cross section placed perpendicular to the molar velocity $\mathbf{v}^*$. Both the mass average velocity and the molar average velocity will be used extensively throughout the remainder of this book. Still

Table 17.7-2 Notation for Velocities in Multicomponent Systems

Basic definitions:		
$\mathbf{v}_\alpha$	velocity of species α with respect to fixed coordinates	(A)
$\mathbf{v} = \sum_{\alpha=1}^{N} \omega_\alpha \mathbf{v}_\alpha$	mass average velocity	(B)
$\mathbf{v}^* = \sum_{\alpha=1}^{N} x_\alpha \mathbf{v}_\alpha$	molar average velocity	(C)
$\mathbf{v}_\alpha - \mathbf{v}$	diffusion velocity of species α with respect to the mass average velocity $\mathbf{v}$	(D)
$\mathbf{v}_\alpha - \mathbf{v}^*$	diffusion velocity of species α with respect to the molar average velocity $\mathbf{v}^*$	(E)
Additional relations:		
$\mathbf{v} - \mathbf{v}^* = \sum_{\alpha=1}^{N} \omega_\alpha(\mathbf{v}_\alpha - \mathbf{v}^*)$	(F)	
$\mathbf{v}^* - \mathbf{v} = \sum_{\alpha=1}^{N} x_\alpha(\mathbf{v}_\alpha - \mathbf{v})$	(G)	

other average velocities are sometimes used, such as the *volume average velocity* (see Problem 17C.1). In Table 17.7-2 we give a summary of the various relations among these velocities.

Molecular Mass and Molar Fluxes

In §17.1 we defined the molecular mass flux of α as the flow of mass of α through a unit area per unit time: $\mathbf{j}_\alpha = \rho_\alpha(\mathbf{v}_\alpha - \mathbf{v})$. That is, we include only the velocity of species α relative to the mass average velocity $\mathbf{v}$. Similarly, we define the molecular molar flux of species α as the number of moles of α flowing through a unit area per unit time: $\mathbf{J}_A^* = c_A(\mathbf{v}_A - \mathbf{v}^*)$. Here we include only the velocity of species α relative to the molar average velocity $\mathbf{v}^*$.

Then in §17.1 we presented Fick's (first) law of diffusion, which describes how the mass of species A in a binary mixture is transported by means of molecular motions. This law can also be expressed in molar units. Hence we have the pair of relations for *binary* systems:

Mass units: $$\mathbf{j}_A = \rho_A(\mathbf{v}_A - \mathbf{v}) = -\rho\mathscr{D}_{AB}\nabla\omega_A \tag{17.7-3}$$

Molar units: $$\mathbf{J}_A^* = c_A(\mathbf{v}_A - \mathbf{v}^*) = -c\mathscr{D}_{AB}\nabla x_A \tag{17.7-4}$$

The differences $\mathbf{v}_A - \mathbf{v}$ and $\mathbf{v}_A - \mathbf{v}^*$ are sometimes referred to as *diffusion velocities*. Equation 17.7-4 can be derived from Eq. 17.7-3 by using some of the relations in Tables 17.7-1 and 2.

Convective Mass and Molar Fluxes

In addition to transport by molecular motion, mass may also be transported by the bulk motion of the fluid. In Fig. 9.7-1 we show three mutually perpendicular planes of area dS at a point P where the fluid *mass average velocity* is $\mathbf{v}$. The volume rate of flow across the plane perpendicular to the surface element dS perpendicular to the x-axis is $v_x dS$. The rate at which mass of species α is being swept across the same surface element is then $\rho_\alpha v_x dS$. We can write similar expressions for the mass flows of species α across the surface elements perpendicular to the y- and z-axes as $\rho_\alpha v_y dS$ and $\rho_\alpha v_z dS$, respectively. If we

now multiply each of these expressions by the corresponding unit vector, add them, and divide by dS, we get

$$\rho_\alpha \boldsymbol{\delta}_x v_x + \rho_\alpha \boldsymbol{\delta}_y v_y + \rho_\alpha \boldsymbol{\delta}_z v_z = \rho_\alpha \mathbf{v} \tag{17.7-5}$$

as the *convective mass flux vector*, which has units of $\text{kg}/\text{m}^2 \cdot \text{s}$.

If one goes back and repeats the story of the preceding paragraph, but using everywhere molar units and the *molar average velocity* $\mathbf{v}^*$, then we get

$$c_\alpha \boldsymbol{\delta}_x v_x^* + c_\alpha \boldsymbol{\delta}_y v_y^* + c_\alpha \boldsymbol{\delta}_z v_z^* = c_\alpha \mathbf{v}^* \tag{17.7-6}$$

as the *convective molar flux vector*, which has units of $\text{kg-mole}/\text{m}^2 \cdot \text{s}$.

To get the convective mass and molar fluxes across a unit surface whose normal unit vector is $\mathbf{n}$, we form the dot products $(\mathbf{n} \cdot \rho_\alpha \mathbf{v})$ and $(\mathbf{n} \cdot c_\alpha \mathbf{v}^*)$, respectively.

§17.8 SUMMARY OF MASS AND MOLAR FLUXES

In Chapters 1 and 9 we introduced the *combined momentum flux* tensor $\boldsymbol{\phi}$ and the *combined energy flux* vector $\mathbf{e}$, which we found useful in setting up the shell balances and equations of change. We give the corresponding definitions here for the mass and molar flux vectors. We add together the molecular mass flux vector and the convective mass flux vector to get the *combined mass flux* vector, and similarly for the *combined molar flux* vector:

Combined mass flux: $$\mathbf{n}_\alpha = \mathbf{j}_\alpha + \rho_\alpha \mathbf{v} \tag{17.8-1}$$

Combined molar flux: $$\mathbf{N}_\alpha = \mathbf{J}_\alpha^* + c_\alpha \mathbf{v}^* \tag{17.8-2}$$

In the first three lines of Table 17.8-1 we summarize the definitions of the mass and molar fluxes discussed so far. In the shaded squares we also give the definitions of the fluxes $\mathbf{j}_\alpha^*$ (*mass* flux with respect to the *molar* average velocity) and $\mathbf{J}_\alpha$ (*molar* flux with respect to *mass* average velocity). These "hybrid" fluxes should normally not be used.

In the remainder of Table 17.8-1 we give a summary of other useful relations, such as the sums of the fluxes and the interrelations among the fluxes. By using Eqs. (J) and (M) we can rewrite Eqs. 17.8-1 and 2 as

$$\mathbf{j}_\alpha = \mathbf{n}_\alpha - \omega_\alpha \sum_{\beta=1}^{N} \mathbf{n}_\beta \tag{17.8-3}$$

$$\mathbf{J}_\alpha^* = \mathbf{N}_\alpha - x_\alpha \sum_{\beta=1}^{N} \mathbf{N}_\beta \tag{17.8-4}$$

When simplified for binary systems, these relations can be combined with Eqs. 17.7-3 and 17.7-4, to get Eqs. (C) and (D) of Table 17.8-2, which are equivalent forms of Fick's (first) law. The forms given in Eqs. (E) and (F) of Table 17.8-2, in terms of the relative velocities of the species, are interesting because they involve neither $\mathbf{v}$ nor $\mathbf{v}^*$.

In Chapter 18 we will write Fick's law exclusively in the form of Eq. (D) of Table 17.8-2. It is this form that has generally been used in chemical engineering. In many problems something is known about the relation between $\mathbf{N}_A$ and $\mathbf{N}_B$ from the stoichiometry or from boundary conditions. Therefore $\mathbf{N}_B$ can be eliminated from Eq. (D), giving a direct relation between $\mathbf{N}_A$ and ∇x_A for the particular problem.

In §1.7 we pointed out that the total molecular momentum flux through a surface of orientation $\mathbf{n}$ is the vector $[\mathbf{n} \cdot \boldsymbol{\pi}]$. In §9.7 we mentioned the analogous quantity for the molecular heat flux—namely, the scalar $(\mathbf{n} \cdot \mathbf{q})$. The analogous mass transport quantities are the scalars $(\mathbf{n} \cdot \mathbf{j}_\alpha)$ and $(\mathbf{n} \cdot \mathbf{J}_\alpha^*)$, which give the total mass and molar fluxes through a surface of orientation $\mathbf{n}$. Similarly, for the combined fluxes through a surface of orientation $\mathbf{n}$, we have for momentum $[\mathbf{n} \cdot \boldsymbol{\phi}]$, for energy $(\mathbf{n} \cdot \mathbf{e})$, and for species $(\mathbf{n} \cdot \mathbf{n}_\alpha)$ and $(\mathbf{n} \cdot \mathbf{N}_\alpha)$.

Table 17.8-1 Notation for Mass and Molar Fluxes*

Quantity	With respect to stationary axes		With respect to mass average velocity $\mathbf{v}$		With respect to molar average velocity $\mathbf{v}^*$	
Velocity of species α (cm/s)	$\mathbf{v}_\alpha$	(A)	$\mathbf{v}_\alpha - \mathbf{v}$	(B)	$\mathbf{v}_\alpha - \mathbf{v}^*$	(C)
Mass flux of species α (g/cm^2 s)	$\mathbf{n}_\alpha = \rho_\alpha \mathbf{v}_\alpha$	(D)	$\mathbf{j}_\alpha = \rho_\alpha(\mathbf{v}_\alpha - \mathbf{v})$	(E)	$\mathbf{j}_\alpha^* = \rho_\alpha(\mathbf{v}_\alpha - \mathbf{v}^*)$	(F)
Molar flux of species α (g-moles/cm^2 s)	$\mathbf{N}_\alpha = c_\alpha \mathbf{v}_\alpha$	(G)	$\mathbf{J}_\alpha = c_\alpha(\mathbf{v}_\alpha - \mathbf{v})$	(H)	$\mathbf{J}_\alpha^* = c_\alpha(\mathbf{v}_\alpha - \mathbf{v}^*)$	(I)
Sums of mass fluxes	$\sum_{\alpha=1}^{N} \mathbf{n}_\alpha = \rho\mathbf{v}$	(J)	$\sum_{\alpha=1}^{N} \mathbf{j}_\alpha = 0$	(K)	$\sum_{\alpha=1}^{N} \mathbf{j}_\alpha^* = \rho(\mathbf{v} - \mathbf{v}^*)$	(L)
Sums of molar fluxes	$\sum_{\alpha=1}^{N} \mathbf{N}_\alpha = c\mathbf{v}^*$	(M)	$\sum_{\alpha=1}^{N} \mathbf{J}_\alpha = c(\mathbf{v}^* - \mathbf{v})$	(N)	$\sum_{\alpha=1}^{N} \mathbf{J}_\alpha^* = 0$	(O)
Relations between mass and molar fluxes	$\mathbf{n}_\alpha = M_\alpha \mathbf{N}_\alpha$	(P)	$\mathbf{j}_\alpha = M_\alpha \mathbf{J}_\alpha$	(Q)	$\mathbf{j}_\alpha^* = M_\alpha \mathbf{J}_\alpha^*$	(R)
Interrelations among mass fluxes	$\mathbf{n}_\alpha = \mathbf{j}_\alpha + \rho_\alpha \mathbf{v}$	(S)	$\mathbf{j}_\alpha = \mathbf{n}_\alpha - \omega_\alpha \sum_{\beta=1}^{N} \mathbf{n}_\beta$	(T)	$\mathbf{j}_\alpha^* = \mathbf{n}_\alpha - x_\alpha \sum_{\beta=1}^{N} \frac{M_\alpha}{M_\beta} \mathbf{n}_\beta$	(U)
Interrelations among molar fluxes	$\mathbf{N}_\alpha = \mathbf{J}_\alpha^* + c_\alpha \mathbf{v}^*$	(V)	$\mathbf{J}_\alpha = \mathbf{N}_\alpha - \omega_\alpha \sum_{\beta=1}^{N} \frac{M_\beta}{M_\alpha} \mathbf{N}_\beta$	(W)	$\mathbf{J}_\alpha^* = \mathbf{N}_\alpha - x_\alpha \sum_{\beta=1}^{N} \mathbf{N}_\beta$	(X)

* Entries in the shaded boxes, involving the "hybrid fluxes" $\mathbf{j}_\alpha^*$ and $\mathbf{J}_\alpha$, are seldom needed; they are included only for the sake of completeness.

Table 17.8-2 Equivalent Forms of Fick's (First) Law of Binary Diffusion

Flux	Gradient	Form of Fick's Law	
$\mathbf{j}_A$	$\nabla\omega_A$	$\mathbf{j}_A = -\rho\mathscr{D}_{AB}\nabla\omega_A$	(A)
$\mathbf{J}_A^*$	∇x_A	$\mathbf{J}_A^* = -c\mathscr{D}_{AB}\nabla x_A$	(B)
$\mathbf{n}_A$	$\nabla\omega_A$	$\mathbf{n}_A = \omega_A(\mathbf{n}_A + \mathbf{n}_B) - \rho\mathscr{D}_{AB}\nabla\omega_A = \rho_A\mathbf{v} - \rho\mathscr{D}_{AB}\nabla\omega_A$	(C)
$\mathbf{N}_A$	∇x_A	$\mathbf{N}_A = x_A(\mathbf{N}_A + \mathbf{N}_B) - c\mathscr{D}_{AB}\nabla x_A = c_A\mathbf{v}^* - c\mathscr{D}_{AB}\nabla x_A$	(D)
$\rho(\mathbf{v}_A - \mathbf{v}_B)$	$\nabla\omega_A$	$\rho(\mathbf{v}_A - \mathbf{v}_B) = -\frac{\rho\mathscr{D}_{AB}}{\omega_A\omega_B}\nabla\omega_A$	(E)
$c(\mathbf{v}_A - \mathbf{v}_B)$	∇x_A	$c(\mathbf{v}_A - \mathbf{v}_B) = -\frac{c\mathscr{D}_{AB}}{x_A x_B}\nabla x_A$	(F)

§17.9 THE MAXWELL–STEFAN EQUATIONS FOR MULTICOMPONENT DIFFUSION IN GASES AT LOW DENSITY

For *multicomponent diffusion* in *gases at low density* it has been shown[1,2] that to a very good approximation

$$\nabla x_\alpha = -\sum_{\beta=1}^{N} \frac{x_\alpha x_\beta}{\mathscr{D}_{\alpha\beta}} (\mathbf{v}_\alpha - \mathbf{v}_\beta) = -\sum_{\beta=1}^{N} \frac{1}{c\mathscr{D}_{\alpha\beta}} (x_\beta \mathbf{N}_\alpha - x_\alpha \mathbf{N}_\beta) \qquad \alpha = 1, 2, 3, \ldots, N \qquad (17.9\text{-}1)$$

The $\mathscr{D}_{\alpha\beta}$ here are the *binary* diffusivities calculated from Eq. 17.3-11 or Eq. 17.3-12. Therefore, for an N-component system, $\frac{1}{2}N(N-1)$ binary diffusivities are required.

Equations 17.9-1 are referred to as the *Maxwell–Stefan equations*, since Maxwell[3] suggested them for binary mixtures on the basis of kinetic theory, and Stefan[4] generalized them to describe the diffusion in a gas mixture with N species. Later Curtiss and Hirschfelder obtained Eqs. 17.9-1 from the multicomponent extension of the Chapman–Enskog theory.

For dense gases, liquids, and polymers it has been shown that the Maxwell–Stefan equations are still valid, but that the strongly concentration-dependent diffusivities appearing therein are *not* the binary diffusivities.[5]

There is an important difference between binary diffusion and multicomponent diffusion.[6] In binary diffusion the movement of species A is always proportional to the negative of the concentration gradient of species A. In multicomponent diffusion, however, other interesting situations can arise: (i) *reverse diffusion*, in which a species moves against its own concentration gradient; (ii) *osmotic diffusion*, in which a species diffuses even though its concentration gradient is zero; (iii) *diffusion barrier*, when a species does not diffuse even though its concentration gradient is nonzero. In addition, the flux of a species is not necessarily collinear with the concentration gradient of that species.

QUESTIONS FOR DISCUSSION

1. How is the binary diffusivity defined? How is self-diffusion defined? Give typical orders of magnitude of diffusivities for gases, liquids, and solids.
2. Summarize the notation for the molecular, convective, and total fluxes for the three transport processes. How does one calculate the flux of mass, momentum, and energy across a surface with orientation **n**?
3. Define the Prandtl, Schmidt, and Lewis numbers. What ranges of Pr and Sc can one expect to encounter for gases and liquids?
4. How can you estimate the Lennard-Jones potential for a binary mixture, if you know the parameters for the two components of the mixture?
5. Of what value are the hydrodynamic theories of diffusion?
6. What is the Langevin equation? Why is it called a "stochastic differential equation"? What information can be obtained from it?

---

[1] C. F. Curtiss and J. O. Hirschfelder, *J. Chem. Phys.*, **17**, 550–555 (1949).

[2] For applications to engineering, see E. L. Cussler, *Diffusion: Mass Transfer in Fluid Systems*, 2nd edition, Cambridge University Press (1997); R. Taylor and R. Krishna, *Multicomponent Mass Transfer*, Wiley, New York (1993).

[3] J. C. Maxwell, *Phil. Mag.*, **XIX**, 19–32 (1860); **XX**, 21–32, 33–36 (1868).

[4] J. Stefan, *Sitzungsber. Kais. Akad. Wiss. Wien*, **LXIII**(2), 63–124 (1871); **LXV**(2), 323–363 (1872).

[5] C. F. Curtiss and R. B. Bird, *Ind. Eng. Chem. Res.*, **38**, 2515–2522 (1999); **40**, 1791 (2001); *J. Chem. Phys.*, **111**, 10362–10370 (1999).

[6] H. L. Toor, *AIChE Journal*, **3**, 198–207 (1959).

7. Compare and contrast the relation between binary diffusivity and viscosity for gases and for liquids.
8. How are the Maxwell–Stefan equations for multicomponent diffusion in gases related to the Fick equations for binary systems?
9. In a multicomponent mixture, does the vanishing of $\mathbf{N}_\alpha$ imply the vanishing of ∇x_α?

PROBLEMS

17A.1. Prediction of a low-density binary diffusivity. Estimate $\mathscr{D}_{AB}$ for the system methane–ethane at 293K and 1 atm by the following methods:

(a) Equation 17.2-1.

(b) The corresponding-states chart in Fig. 17.2-1 along with Eq. 17.2-3.

(c) The Chapman–Enskog relation (Eq. 17.3-12) with Lennard-Jones parameters from Appendix E.

(d) The Chapman–Enskog relation (Eq. 17.3-12) with the Lennard-Jones parameters estimated from critical properties.

Answers (all in cm^2/s): **(a)** 0.152; **(b)** 0.138; **(c)** 0.146; **(d)** 0.138.

17A.2. Extrapolation of binary diffusivity to a very high temperature. A value of $\mathscr{D}_{AB} = 0.151\ cm^2/s$ has been reported[1] for the system CO_2–air at 293K and 1 atm. Extrapolate $\mathscr{D}_{AB}$ to 1500K by the following methods:

(a) Equation 17.2-1.

(b) Equation 17.3-10.

(c) Equations 17.3-12 and 15, with Table E.2.

What do you conclude from comparing these results with the experimental value[1] of $2.45\ cm^2/s$?

Answers (all in cm^2/s): **(a)** 2.96; **(b)** 1.75; **(c)** 2.51

17A.3. Self-diffusion in liquid mercury. The diffusivity of Hg^{203} in normal liquid Hg has been measured,[2] along with viscosity and volume per unit mass. Compare the experimentally measured $\mathscr{D}_{AA^*}$ with the values calculated with Eq. 17.4-5.

T (K)	$\mathscr{D}_{AA^*}$ (cm^2/s)	μ (cp)	$\hat{V}$ (cm^3/g)
275.7	1.52×10^{-5}	1.68	0.0736
289.6	1.68×10^{-5}	1.56	0.0737
364.2	2.57×10^{-5}	1.27	0.0748

17A.4. Schmidt numbers for binary gas mixtures at low density. Use Eq. 17.3-11 and the data given in Problem 1A.4 to compute $Sc = \mu/\rho\mathscr{D}_{AB}$ for binary mixtures of hydrogen and Freon-12 at $x_A = 0.00, 0.25, 0.50, 0.75$, and 1.00, at 25°C and 1 atm.

Sample answers: At $x_A = 0.00$, $Sc = 3.43$; at $x_A = 1.00$, $Sc = 0.407$

17A.5. Estimation of diffusivity for a binary mixture at high density. Predict $c\mathscr{D}_{AB}$ for an equimolar mixture of N_2 and C_2H_6 at 288.2K and 40 atm.

(a) Use the value of $\mathscr{D}_{AB}$ at 1 atm from Table 17.1-1, along with Fig. 17.2-1.

(b) Use Eq. 17.2-3 and Fig. 17.2-1.

Answers: **(a)** 5.8×10^{-6} g-mole/cm · s; **(b)** 5.3×10^{-6} g-mole/cm · s

---

[1] Ts. M. Klibanova, V. V. Pomerantsev, and D. A. Frank-Kamenetskii, *J. Tech. Phys. (USSR)*, **12**, 14–30 (1942), as quoted by C. R. Wilke and C. Y. Lee, *Ind. Eng. Chem.*, **47**, 1253 (1955).

[2] R. E. Hoffman, *J. Chem. Phys.*, **20**, 1567–1570 (1952).

17A.6. Diffusivity and Schmidt number for chlorine–air mixtures.

(a) Predict $\mathscr{D}_{AB}$ for chlorine–air mixtures at 75°F and 1 atm. Treat air as a single substance with Lennard-Jones parameters as given in Appendix E. Use the Chapman–Enskog theory results in §17.3.

(b) Repeat (a) using Eq. 17.2-1.

(c) Use the results of (a) and of Problem 1A.5 to estimate Schmidt numbers for chlorine–air mixtures at 297K and 1 atm for the following mole fractions of chlorine: 0, 0.25, 0.50, 0.75, and 1.00.

Answers: **(a)** 0.121 cm^2/s; **(b)** 0.124 cm^2/s; **(c)** Sc = 1.27, 0.832, 0.602, 0.463, 0.372

17A.7. The Schmidt number for self-diffusion.

(a) Use Eqs. 1.3-1b and 17.2-2 to predict the self-diffusion Schmidt number $Sc = \mu/\rho\mathscr{D}_{AA^*}$ at the critical point for a system with $M_A \approx M_{A^*}$.

(b) Use the above result, along with Fig. 1.3-1 and Fig. 17.2-1, to predict $Sc = \mu/\rho\mathscr{D}_{AA^*}$ at the following states:

Phase	Gas	Gas	Gas	Liquid	Gas	Gas
T_r	0.7	1.0	5.0	0.7	1.0	2.0
p_r	0.0	0.0	0.0	saturation	1.0	1.0

17A.8. Correction of high-density diffusivity for temperature. The measured value[3] of $c\mathscr{D}_{AB}$ for a mixture of 80 mole% CH_4 and 20 mole% C_2H_6 at 313K and 136 atm is 6.0×10^{-6} g-mol/cm · s (see Example 17.2-3). Predict $c\mathscr{D}_{AB}$ for the same mixture at 136 atm and 351K, using Fig. 17.2-1.

Answer: 6.3×10^{-6} g-mole/cm · s
Observed:[3] 6.33×10^{-6} g-mol/cm · s

17A.9. Prediction of critical $c\mathscr{D}_{AB}$ values. Figure 17.2-1 gives the low-pressure limit $(c\mathscr{D}_{AA^*})_r = 1.01$ at $T_r = 1$ and $\rho_r \to 0$. At this limit, Eq. 17.2-13 gives

$$1.01(c\mathscr{D}_{AA^*})_c = 2.2646 \times 10^{-5} \sqrt{T_{cA}\left(\frac{1}{M_A} + \frac{1}{M_{A^*}}\right)} \frac{1}{\sigma^2_{AA^*}\,\Omega_{\mathscr{D},AA^*}} \qquad \text{(17A.9-1)}$$

Here the argument $\kappa T_{cA}/\varepsilon_{AA^*}$ of $\Omega_{\mathscr{D},AA^*}$ is reported[4] as = 1.225 for Ar, Kr, and Xe. We use the value 1/0.77 from Eq. 1.4-11a as a representative average over many fluids.

(a) Combine Eq. 17A.9-1 with the relations

$$\sigma_{AA^*} = 2.44(T_{cA}/p_{cA})^{1/3} \qquad \varepsilon_{AA^*}/\kappa = 0.77T_{cA} \qquad \text{(17A.9-2, 3)}$$

and Table E.2 to obtain Eq. 17.2-2 for $(c\mathscr{D}_{AA^*})_c$

(b) Show that the approximations

$$\sigma_{AB} = \sqrt{\sigma_A\sigma_B} \qquad \varepsilon_{AB} = \sqrt{\varepsilon_A\varepsilon_B} \qquad \text{(17A.9-4, 5)}$$

for Lennard-Jones parameters for the A–B interaction give

$$\sigma_{AB} = 2.44\left(\frac{T_{cA}T_{cB}}{p_{cA}p_{cB}}\right)^{1/6} \qquad \frac{\varepsilon_{AB}}{\kappa} = 0.77\sqrt{T_{cA}T_{cB}} \qquad \text{(17A.9-6, 7)}$$

when the molecular parameters of each species are predicted according to Eqs. 1.4-11a, c. Combine these expressions with Eq. 17A.9-1 (with A^* replaced by B and T_{cA} by $\sqrt{T_{cA}T_{cB}}$) to obtain Eq. 17.2-3 for $(c\mathscr{D}_{AB})_c$. The corresponding replacement of p_c and T_c in Fig. 17.2-1 by $\sqrt{p_{cA}p_{cB}}$ and $\sqrt{T_{cA}T_{cB}}$ amounts to regarding the A–B collisions as dominant over collisions of like molecules in determining the value of $c\mathscr{D}_{AB}$.

---

[3] V. J. Berry and R. C. Koeller, *AIChE Journal*, **6**, 274–280 (1960).
[4] J. J. van Loef and E. G. D. Cohen, *Physica A*, **156**, 522–533 (1989).

17A.10. Estimation of liquid diffusivities.

(a) Estimate the diffusivity for a dilute aqueous solution of acetic acid at 12.5°C, using the Wilke–Chang equation. The density of pure acetic acid is 0.937 g/cm^3 at its boiling point.

(b) The diffusivity of a dilute aqueous solution of methanol at 15°C is about 1.28×10^{-5} cm/s. Estimate the diffusivity for the same solution at 100°C.

Answer: **(b)** 6.7×10^{-5} cm/s

17B.1. Interrelation of composition variables in mixtures.

(a) Using the basic definitions in Eqs. (A) to (G) of Table 17.7-1, verify the algebraic relations in Eqs. (H) to (O).

(b) Verify that, in Table 17.7-1, Eqs. (P) and (Q) simplify to Eqs. (P′) and (Q′) for binary mixtures.

(c) Derive Eqs. (P′) and (Q′) from Eqs. (N) and (O).

17B.2. Relations among fluxes in multicomponent systems. Verify Eqs. (K), (O), (T), and (X) of Table 17.8-1 using only the definitions of concentrations, velocities, and fluxes.

17B.3. Relations between fluxes in binary systems. The following equation is useful for interrelating expressions in mass units and those in molar units in two-component systems:

$$\frac{\mathbf{j}_A}{\rho\omega_A\omega_B} = \frac{\mathbf{J}_A^*}{cx_Ax_B} \tag{17B.3-1}$$

Verify the correctness of this relation.

17B.4. Equivalence of various forms of Fick's law for binary mixtures.

(a) Starting with Eq. (A) of Table 17.8-2, derive Eqs. (B), (D), and (F).

(b) Starting with Eq. (A) of Table 17.8-2, derive the folowing flux expressions:

$$\mathbf{j}_A = -\rho(M_AM_B/M^2)\mathscr{D}_{AB}\nabla x_A \tag{17B.4-1}$$

$$\nabla x_A = \frac{1}{c\mathscr{D}_{AB}}(x_A\mathbf{N}_B - x_B\mathbf{N}_A) \tag{17B.4-2}$$

What conclusions can be drawn from these two equations?

(c) Show that Eq. (F) of Table 17.8-2 can be written as

$$\mathbf{v}_A - \mathbf{v}_B = -\mathscr{D}_{AB}\nabla \ln \frac{x_A}{x_B} \tag{17B.4-3}$$

17C.1. Mass flux with respect to volume average velocity. Let the *volume average velocity* in an N-component mixture be defined by

$$\mathbf{v}^{\blacksquare} = \sum_{\alpha=1}^{N} \rho_\alpha(\bar{V}_\alpha/M_\alpha)\mathbf{v}_\alpha = \sum_{\alpha=1}^{N} c_\alpha\bar{V}_\alpha\mathbf{v}_\alpha \tag{17C.1-1}$$

in which $\bar{V}_\alpha$ is the partial molar volume of species α. Then define

$$\mathbf{j}_\alpha^{\blacksquare} = \rho_\alpha(\mathbf{v}_\alpha - \mathbf{v}^{\blacksquare}) \tag{17C.1-2}$$

as the mass flux with respect to the volume average velocity.

(a) Show that for a binary system of A and B,

$$\mathbf{j}_A^{\blacksquare} = \rho(\bar{V}_B/M_B)\mathbf{j}_A \tag{17C.1-3}$$

To do this you will need to use the identity $c_A\bar{V}_A + c_B\bar{V}_B = 1$. Where does this come from?

(b) Show that Fick's first law then assumes the form

$$\mathbf{j}_A^{\blacksquare} = -\mathscr{D}_{AB}\nabla\rho_A \tag{17C.1-4}$$

To verify this you will need the relation $\bar{V}_A\nabla c_A + \bar{V}_B\nabla c_B = 0$. What is the origin of this?

17C.2. Mass flux with respect to the solvent velocity.

(a) In a system with N chemical species, choose component N to be the solvent. Then define

$$\mathbf{j}_\alpha^N = \rho_\alpha(\mathbf{v}_\alpha - \mathbf{v}_N) \tag{17C.2-1}$$

to be the mass flux with respect to the solvent velocity. Verify that

$$\mathbf{j}_\alpha^N = \mathbf{j}_\alpha - (\rho_\alpha/\rho_N)\mathbf{j}_N \tag{17C.2-2}$$

(b) For a binary system (labeling B as the solvent), show that

$$\mathbf{j}_A^B = (\rho/\rho_B)\mathbf{j}_A = -(\rho^2/\rho_B)\mathscr{D}_{AB}\nabla\omega_A \tag{17C.2-3}$$

How does this result simplify for a very dilute solution of A in solvent B?

17C.3. Determination of Lennard-Jones potential parameters from diffusivity data of a binary gas mixture.

(a) Use the following data[5] for the system H_2O–O_2 at 1 atm pressure to determine σ_{AB} and $\varepsilon_{AB}/\text{K}$:

T (K)	400	500	600	700	800	900	1000	1100
$\mathscr{D}_{AB}$ (cm^2/s)	0.47	0.69	0.94	1.22	1.52	1.85	2.20	2.58

One way to do this is as follows: (i) Plot the data as $\log(T^{3/2}/\mathscr{D}_{AB})$ versus $\log T$ on a thin sheet of graph paper. (ii) Plot $\Omega_{\mathscr{D},AB}$ versus $\text{K}T/\varepsilon_{AB}$ on a separate sheet of graph paper to the same scale. (iii) Superpose the first plot on the second, and from the scales of the two overlapping plots, determine the numerical ratios $(T/(\text{K}T/\varepsilon_{AB}))$ and $((T^{3/2}/\mathscr{D}_{AB})/\Omega_{\mathscr{D},AB})$. (iv) Use these two ratios and Eq. 17.3-11 to solve for the two parameters σ_{AB} and $\varepsilon_{AB}/\text{K}$.

[5] R. E. Walker and A. A. Westenberg, *J. Chem. Phys.*, **32**, 436–442 (1960); R. M. Fristrom and A. A. Westenberg, *Flame Structure*, McGraw-Hill, New York (1965), p. 265.

Chapter 18

Concentration Distributions in Solids and in Laminar Flow

In Chapter 2 we saw how a number of steady-state viscous flow problems can be set up and solved by making a *shell momentum balance*. In Chapter 9 we saw further how steady-state heat-conduction problems can be handled by means of a *shell energy balance*. In this chapter we show how steady-state diffusion problems may be formulated by *shell mass balances*. The procedure used here is virtually the same as that used previously:

a. A mass balance is made over a thin shell perpendicular to the direction of mass transport, and this shell balance leads to a first-order differential equation, which may be solved to get the mass flux distribution.

b. Into this expression we insert the relation between mass flux and concentration gradient, which results in a second-order differential equation for the concentration profile. The integration constants that appear in the resulting expression are determined by the boundary conditions on the concentration and/or mass flux at the bounding surfaces.

In Chapter 17 we pointed out that several kinds of mass fluxes are in common use. For simplicity, we shall in this chapter use the combined flux $\mathbf{N}_A$—that is, the number of moles of A that go through a unit area in unit time, the unit area being fixed in space. We shall relate the molar flux to the concentration gradient by Eq. (D) of Table 17.8-2, which for the z-component is

$$N_{Az} = -c\mathscr{D}_{AB}\frac{\partial x_A}{\partial z} + x_A(N_{Az} + N_{Bz}) \tag{18.0-1}$$

combined flux | molecular flux | convective flux

Before Eq. 18.0-1 is used, we usually have to eliminate N_{Bz}. This can be done only if something is known beforehand about the ratio N_{Bz}/N_{Az}. In each of the binary diffusion

problems discussed in this chapter, we begin by specifying this ratio by physical or chemical reasoning.

In this chapter we study diffusion in both *nonreacting* and *reacting* systems. When chemical reactions occur, we distinguish between two reaction types: *homogeneous*, in which the chemical change occurs in the entire volume of the fluid, and *heterogeneous*, in which the chemical change takes place only in a restricted region, such as the surface of a catalyst. Not only is the physical picture different for homogeneous and heterogeneous reactions, but there is also a difference in the way the two types of reactions are described mathematically. The rate of production of a chemical species by *homogeneous* reaction appears as a source term in the differential equation obtained from the shell balance, just as the thermal source term appears in the shell energy balance. The rate of production by a *heterogeneous* reaction, on the other hand, appears not in the differential equation, but rather in the boundary condition at the surface on which the reaction occurs.

In order to set up problems involving chemical reactions, some information has to be available about the rate at which the various chemical species appear or disappear by reaction. This brings us to the vast subject of *chemical kinetics*, that branch of physical chemistry that deals with the mechanisms of chemical reactions and the rates at which they occur.[1] In this chapter we assume that the reaction rates are described by means of simple functions of the concentrations of the reacting species.

At this point we need to mention the notation to be used for the chemical rate constants. For homogeneous reactions, the molar rate of production of species A may be given by an expression of the form

Homogeneous reaction:
$$R_A = k_n''' c_A^n \tag{18.0-2}$$

in which R_A [=] moles/cm^3 · s and c_A [=] moles/cm^3. The index n indicates the "order" of the reaction;[2] for a first-order reaction, k_1''' [=] 1/s. For heterogeneous reactions, the molar rate of production at the reaction surface may often be specified by a relation of the form

Heterogeneous reaction:
$$N_{Az}|_{\text{surface}} = k_n'' c_A^n|_{\text{surface}} \tag{18.0-3}$$

in which N_{Az} [=] moles/cm^2 · s and c_A [=] moles/cm^3. Here k_1'' [=] cm/s. Note that the triple prime on the rate constant indicates a volume source and the double prime a surface source.

We begin in §18.1 with a statement of the shell balance and the kinds of boundary conditions that may arise in solving diffusion problems. In §18.2 a discussion of diffusion through a stagnant film is given, this topic being necessary to the understanding of the film models of diffusional operations in chemical engineering. Then, in §§18.3 and 18.4 we given some elementary examples of diffusion with chemical reaction—both heterogeneous and homogeneous. These examples illustrate the role that diffusion plays in chemical kinetics and the important fact that diffusion can significantly affect the rate of a chemical reaction. In §§18.5 and 6 we turn our attention to forced-convection mass transfer—that is, diffusion superimposed on a flow field. Although we have not in-

---

[1] R. J. Silbey and R. A. Alberty, *Physical Chemistry*, 3rd edition, Wiley, New York (2001), Chapter 18.

[2] Not all rate expressions are of the simple form of Eq. 18.0-2. The reaction rate may depend in a complicated way on the concentration of all species present. Similar remarks hold for Eq. 18.0-3. For detailed information on reaction rates see *Table of Chemical Kinetics, Homogeneous Reactions*, National Bureau of Standards, Circular 510 (1951), Supplement No. 1 to Circular 510 (1956). This reference is now being supplemented by a data base maintained by NIST at "http://kinetics.nist.gov/." For heterogeneous reactions, see R. Mezaki and H. Inoue, *Rate Equations of Solid-Catalyzed Reactions*, U. of Tokyo Press, Tokyo (1991). See also C. G. Hill, *Chemical Engineering Kinetics and Reactor Design: An Introduction*, Wiley, New York (1977).

cluded an example of free-convection mass transfer, it would have been possible to parallel the discussion of free-convection heat transfer given in §10.9. Next, in §18.7 we discuss diffusion in porous catalysts. Finally, in the last section we extend the evaporation problem of §18.2 to a three-component system.

§18.1 SHELL MASS BALANCES; BOUNDARY CONDITIONS

The diffusion problems in this chapter are solved by making mass balances for one or more chemical species over a thin shell of solid or fluid. Having selected an appropriate system, the law of conservation of mass of species A in a binary system is written over the volume of the shell in the form

$$\left\{\begin{array}{l}\text{rate of}\\ \text{mass of}\\ A \text{ in}\end{array}\right\} - \left\{\begin{array}{l}\text{rate of}\\ \text{mass of}\\ A \text{ out}\end{array}\right\} + \left\{\begin{array}{l}\text{rate of production of}\\ \text{mass of } A \text{ by}\\ \text{homogeneous reaction}\end{array}\right\} = 0 \qquad (18.1\text{-}1)$$

The conservation statement may, of course, be expressed in terms of moles. The chemical species A may enter or leave the system by diffusion (i.e., by molecular motion) and also by virtue of the overall motion of the fluid (i.e., by convection), both of these being included in $\mathbf{N}_A$. In addition, species A may be produced or consumed by homogeneous chemical reactions.

After a balance is made on a shell of finite thickness by means of Eq. 18.1-1, we then let the thickness become infinitesimally small. As a result of this process a differential equation for the mass (or molar) flux is generated. If, into this equation, we substitute the expression for the mass (or molar) flux in terms of the concentration gradient, we get a differential equation for the concentration.

When this differential equation has been integrated, constants of integration appear, and these have to be determined by the use of boundary conditions. The boundary conditions are very similar to those used in heat conduction (see §10.1):

a. The concentration at a surface can be specified; for example, $x_A = x_{A0}$.

b. The mass flux at a surface can be specified; for example, $N_{Az} = N_{A0}$. If the ratio N_{Bz}/N_{Az} is known, this is equivalent to giving the concentration gradient.

c. If diffusion is occurring in a solid, it may happen that at the solid surface substance A is lost to a surrounding stream according to the relation

$$N_{A0} = k_c(c_{A0} - c_{Ab}) \qquad (18.1\text{-}2)$$

in which N_{A0} is the molar flux at the surface, c_{A0} is the surface concentration, c_{Ab} is the concentration in the bulk fluid stream, and the proportionality constant k_c is a "mass transfer coefficient." Methods of correlating mass transfer coefficients are discussed in Chapter 22. Equation 18.1-2 is analogous to "Newton's law of cooling" given in Eq. 10.1-2.

d. The rate of chemical reaction at the surface can be specified. For example, if substance A disappears at a surface by a first-order chemical reaction, then $N_{A0} = k_1'' c_{A0}$. That is, the rate of disappearance at a surface is proportional to the surface concentration, the proportionality constant k_1'' being a first-order chemical rate coefficient.

§18.2 DIFFUSION THROUGH A STAGNANT GAS FILM

Let us now analyze the diffusion system shown in Fig. 18.2-1 in which liquid A is evaporating into gas B. We imagine there is some device that maintains the liquid level at $z = z_1$. Right at the liquid–gas interface, the gas-phase concentration of A, expressed as mole

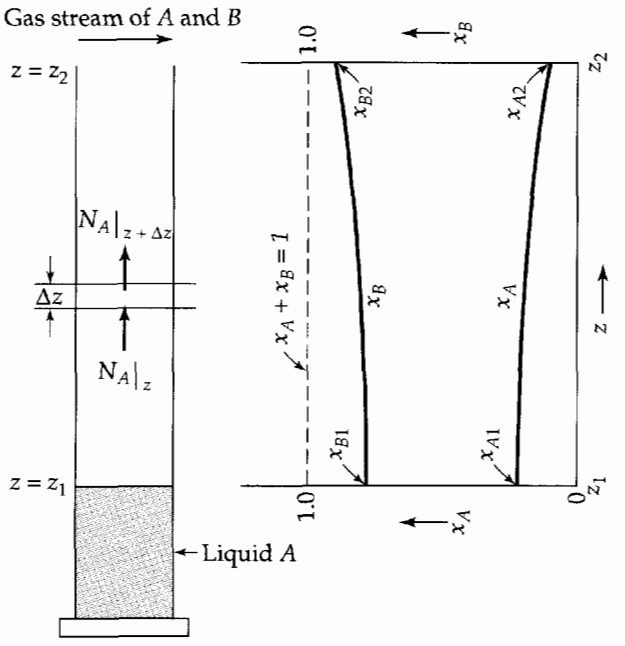

Fig. 18.2-1. Steady-state diffusion of A through stagnant B with the liquid-vapor interface maintained at a fixed position. The graph shows how the concentration profiles deviate from straight lines because of the convective contribution to the mass flux.

fraction, is x_{A1}. This is taken to be the gas-phase concentration of A corresponding to equilibrium[1] with the liquid at the interface. That is, x_{A1} is the vapor pressure of A divided by the total pressure, p_A^{vap}/p, provided that A and B form an ideal gas mixture and that the solubility of gas B in liquid A is negligible.

A stream of gas mixture A–B of concentration x_{A2} flows slowly past the top of the tube, to maintain the mole fraction of A at x_{A2} for $z = z_2$. The entire system is kept at constant temperature and pressure. Gases A and B are assumed to be ideal.

We know that there will be a net flow of gas upward from the gas–liquid interface, and that the gas velocity at the cylinder wall will be smaller than that in the center of the tube. To simplify the problem, we neglect this effect and assume that there is no dependence of the z-component of the velocity on the radial coordinate.

When this evaporating system attains a steady state, there is a net motion of A away from the interface and the species B is stationary. Hence the molar flux of A is given by Eq. 17.0-1 with $N_{Bz} = 0$. Solving for N_{Az}, we get

$$N_{Az} = -\frac{c\mathcal{D}_{AB}}{1 - x_A}\frac{dx_A}{dz} \tag{18.2-1}$$

A steady-state mass balance (in molar units) over an increment Δz of the column states that the amount of A entering at plane z equals the amount of A leaving at plane $z + \Delta z$:

$$SN_{Az}|_z - SN_{Az}|_{z+\Delta z} = 0 \tag{18.2-2}$$

Here S is the cross-sectional area of the column. Division by $S\Delta z$ and taking the limit as $\Delta z \to 0$ gives

$$-\frac{dN_{Az}}{dz} = 0 \tag{18.2-3}$$

[1] L. J. Delaney and L. C. Eagleton [*AIChE Journal*, **8**, 418–420 (1962)] conclude that, for evaporating systems, the interfacial equilibrium assumption is reasonable, with errors in the range of 1.3 to 7.0% possible.

Substitution of Eq. 18.2-1 into Eq. 18.2-3 gives

$$\frac{d}{dz}\left(\frac{c\mathscr{D}_{AB}}{1-x_A}\frac{dx_A}{dz}\right)=0 \tag{18.2-4}$$

For an ideal gas mixture the equation of state is $p = cRT$, so that at constant temperature and pressure c must be a constant. Furthermore, for gases $\mathscr{D}_{AB}$ is very nearly independent of the composition. Therefore, $c\mathscr{D}_{AB}$ can be moved to the left of the derivative operator to get

$$\frac{d}{dz}\left(\frac{1}{1-x_A}\frac{dx_A}{dz}\right)=0 \tag{18.2-5}$$

This is a second-order differential equation for the concentration profile expressed as mole fraction of A. Integration with respect to z gives

$$\frac{1}{1-x_A}\frac{dx_A}{dz}=C_1 \tag{18.2-6}$$

A second integration then gives

$$-\ln(1-x_A)=C_1z+C_2 \tag{18.2-7}$$

If we replace C_1 by $-\ln K_1$ and C_2 by $-\ln K_2$, Eq. 18.2-7 becomes

$$1-x_A=K_1^zK_2 \tag{18.2-8}$$

The two constants of integration, K_1 and K_2, may then be determined from the boundary conditions

B.C. 1: at $z = z_1$, $x_A = x_{A1}$ (18.2-9)

B.C. 2: at $z = z_2$, $x_A = x_{A2}$ (18.2-10)

When the constants have been obtained, we get finally

$$\boxed{\left(\frac{1-x_A}{1-x_{A1}}\right)=\left(\frac{1-x_{A2}}{1-x_{A1}}\right)^{\frac{z-z_1}{z_2-z_1}}} \tag{18.2-11}$$

The profiles for gas B are obtained by using $x_B = 1 - x_A$. The concentration profiles are shown in Fig. 18.2-1. It can be seen there that the slope dx_A/dz is not constant although N_{Az} is; this could have been anticipated from Eq. 18.2-1.

Once the concentration profiles are known, we can get average values and mass fluxes at surfaces. For example, the average concentration of B in the region between z_1 and z_2 is obtained as follows:

$$\frac{x_{B,\text{avg}}}{x_{B1}}=\frac{\int_{z_1}^{z_2}(x_B/x_{B1})dz}{\int_{z_1}^{z_2}dz}=\frac{\int_0^1(x_{B2}/x_{B1})^{\zeta}\,d\zeta}{\int_0^1 d\zeta}=\frac{(x_{B2}/x_{B1})^{\zeta}}{\ln(x_{B2}/x_{B1})}\Bigg|_0^1 \tag{18.2-12}$$

in which $\zeta = (z - z_1)/(z_2 - z_1)$ is a dimensionless length variable. This average may be rewritten as

$$x_{B,\text{avg}}=\frac{x_{B2}-x_{B1}}{\ln(x_{B2}/x_{B1})} \tag{18.2-13}$$

That is, the average value of x_B is the logarithmic mean, $(x_B)_{\ln}$, of the terminal concentrations.

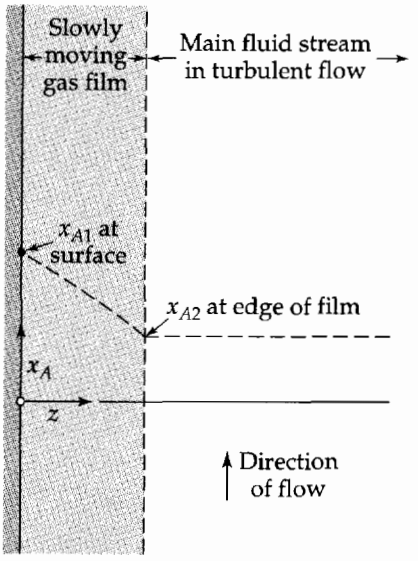

Fig. 18.2-2. Film model for mass transfer; component A is diffusing from the surface into the gas stream through a hypothetical stagnant gas film.

The rate of mass transfer at the liquid–gas interface—that is, the rate of evaporation—may be obtained from Eq. 18.2-1 as follows:

$$N_{Az}|_{z=z_1} = -\frac{c\mathscr{D}_{AB}}{1-x_{A1}}\frac{dx_A}{dz}\bigg|_{z=z_1} = +\frac{c\mathscr{D}_{AB}}{x_{B1}}\frac{dx_B}{dz}\bigg|_{z=z_1} = \frac{c\mathscr{D}_{AB}}{z_2-z_1}\ln\left(\frac{x_{B2}}{x_{B1}}\right) \tag{18.2-14}$$

By combining Eqs. 18.2-13 and 14 we get finally

$$N_{Az}|_{z=z_1} = \frac{c\mathscr{D}_{AB}}{(z_2-z_1)(x_B)_{\ln}}(x_{A1}-x_{A2}) \tag{18.2-15}$$

This expression gives the evaporation rate in terms of the characteristic driving force $x_{A1} - x_{A2}$.

By expanding the solution in Eq. 18.2-15 in a Taylor series, we can get (see §C.2 and Problem 18B.18)

$$N_{Az}|_{z=z_1} = \frac{c\mathscr{D}_{AB}(x_{A1}-x_{A2})}{(z_2-z_1)}\left[1+\tfrac{1}{2}(x_{A1}+x_{A2})+\tfrac{1}{3}(x_{A1}^2+x_{A1}x_{A2}+x_{A2}^2)+\cdots\right] \tag{18.2-16}$$

The expression in front of the bracketed expansion is the result that one would get if the convection term were entirely omitted in Eq. 18.0-1. The bracketed expansion then gives the correction resulting from including the convection term. Another way of interpreting this expression is that the simple result corresponds to joining the end points of the x_A curve in Fig. 18.2-1 by a straight line, and the complete result corresponds to using the curve of x_A versus z. If the terminal mole fractions are small, the correction term in brackets in Eq. 18.2-16 is only slightly greater than unity.

The results of this section have been used for experimental determinations of gas diffusivities.[2] Furthermore, these results find use in the "film models" of mass transfer. In Fig. 18.2-2 a solid or liquid surface is shown along which a gas is flowing. Near the surface is a slowly moving film through which A diffuses. This film is bounded by the surfaces $z = z_1$ and $z = z_2$. In this "model" it is assumed that there is a sharp transition from a stagnant film to a well-mixed fluid in which the concentration gradients are negligible. Although this model is physically unrealistic, it has nevertheless proven useful as a simplified picture for correlating mass transfer coefficients.

[2] C. Y. Lee and C. R. Wilke, *Ind. Eng. Chem.*, **46**, 2381–2387 (1954).

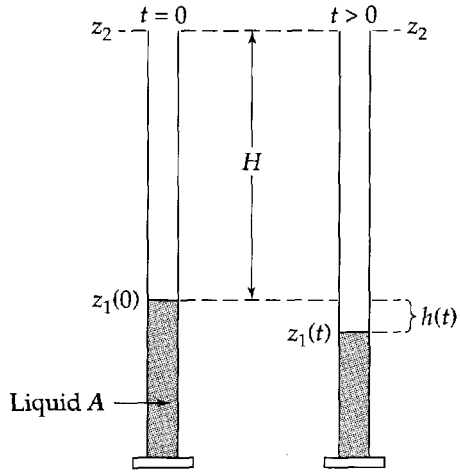

Fig. 18.2-3. Evaporation with quasi-steady-state diffusion. The liquid level goes down very slowly as the liquid evaporates. A gas mixture of composition x_{A2} flows across the top of the tube.

EXAMPLE 18.2-1

Diffusion with a Moving Interface

We want now to examine a problem that is slightly different from the one just discussed. Instead of maintaining the liquid–gas interface at a constant height, we allow the liquid level to subside as the evaporation proceeds, as shown in Fig. 18.2-3. Since the liquid retreats very slowly, we can use a quasi-steady state method with confidence.

SOLUTION

First we equate the molar rate of evaporation of A from the liquid phase with the rate at which moles of A enter the gas phase:

$$-S\frac{\rho^{(A)}}{M_A}\frac{dz_1}{dt} = \frac{c\mathscr{D}_{AB}}{(z_2 - z_1(t))(x_B)_{\ln}}(x_{A1} - x_{A2})S \tag{18.2-17}$$

Here $\rho^{(A)}$ is the density of pure liquid A and M_A is the molecular weight. On the right side of Eq. 18.2-17 we have used the steady-state evaporation rate evaluated at the current liquid column height (this is the quasi-steady-state approximation). This equation can be integrated to give

$$\int_0^h (H + h)dh = \frac{c\mathscr{D}_{AB}(x_{A1} - x_{A2})}{(\rho^{(A)}/M_A)(x_B)_{\ln}}\int_0^t dt \tag{18.2-18}$$

in which $h(t) = z_1(0) - z_1(t)$ is the distance that the interface has descended in time t, and $H = z_2 - z_1(0)$ is the initial height of the gas column. When we abbreviate the right side of Eq. 18.2-18 by $\frac{1}{2}Ct$, the equation can be integrated and then solved for h to give

$$h(t) = H(\sqrt{1 + (Ct/H^2)} - 1) \tag{18.2-19}$$

One can use this experiment to get the diffusivity from measurements of the liquid level as a function of time.

EXAMPLE 18.2-2

Determination of Diffusivity

The diffusivity of the gas pair O_2–CCl_4 is being determined by observing the steady-state evaporation of carbon tetrachloride into a tube containing oxygen, as shown in Fig. 18.2-1. The distance between the CCl_4 liquid level and the top of the tube is $z_2 - z_1 = 17.1$ cm. The total pressure on the system is 755 mm Hg, and the temperature is 0°C. The vapor pressure of CCl_4 at that temperature is 33.0 mm Hg. The cross-sectional area of the diffusion tube is 0.82 cm^2. It is found that 0.0208 cm^3 of CCl_4 evaporate in a 10-hour period after steady state has been attained. What is the diffusivity of the gas pair O_2–CCl_4?

SOLUTION

Let A stand for CCl_4 and B for O_2. The molar flux of A is then

$$N_A = \frac{(0.0208\text{ cm}^3)(1.59\text{ g/cm}^3)}{(154\text{ g/g-mole})(0.82\text{ cm}^2)(3.6 \times 10^4\text{ s})}$$
$$= 7.26 \times 10^{-9}\text{ g-mole/cm}^2 \cdot \text{s} \tag{18.2-20}$$

Then from Eq. 18.2-14 we get

$$\mathscr{D}_{AB} = \frac{(N_A|_{z=z_1})(z_2 - z_1)}{c \ln(x_{B2}/x_{B1})}$$
$$= \frac{(N_A|_{z=z_1})(z_2 - z_1)RT}{p \ln(p_{B2}/p_{B1})}$$
$$= \frac{(7.26 \times 10^{-9})(17.1)(82.06)(273)}{(755/760)(2.303 \log_{10}(755/722))}$$
$$= 0.0636 \text{ cm}^2/\text{s} \tag{18.2-21}$$

This method of determining gas-phase diffusivities suffers from several defects: the cooling of the liquid by evaporation, the concentration of nonvolatile impurities at the interface, the climbing of the liquid up the walls of the tube, and the curvature of the meniscus.

EXAMPLE 18.2-3

Diffusion through a Nonisothermal Spherical Film

(a) Derive expressions for diffusion through a spherical shell that are analogous to Eq. 18.2-11 (concentration profile) and Eq. 18.2-14 (molar flux). The system under consideration is shown in Fig. 18.2-4.

(b) Extend these results to describe the diffusion in a nonisothermal film in which the temperature varies radially according to

$$\frac{T}{T_1} = \left(\frac{r}{r_1}\right)^n \tag{18.2-22}$$

where T_1 is the temperature at $r = r_1$. Assume as a *rough* approximation that $\mathscr{D}_{AB}$ varies as the $\frac{3}{2}$-power of the temperature:

$$\frac{\mathscr{D}_{AB}}{\mathscr{D}_{AB,1}} = \left(\frac{T}{T_1}\right)^{3/2} \tag{18.2-23}$$

in which $\mathscr{D}_{AB,1}$ is the diffusivity at $T = T_1$. Problems of this kind arise in connection with drying of droplets and diffusion through gas films near spherical catalyst pellets.

The temperature distribution in Eq. 18.2-22 has been chosen solely for mathematical simplicity. This example is included to emphasize that, in nonisothermal systems, Eq. 18.0-1 is the correct starting point rather than $N_{Az} = -\mathscr{D}_{AB}(dc_A/dz) + x_A(N_{Az} + N_{Bz})$, as has been given in some textbooks.

SOLUTION

(a) A steady-state mass balance on a spherical shell leads to

$$\frac{d}{dr}(r^2 N_{Ar}) = 0 \tag{18.2-24}$$

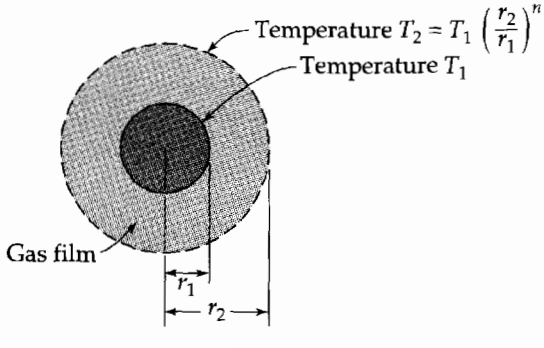

Fig. 18.2-4. Diffusion through a hypothetical spherical stagnant gas film surrounding a droplet of liquid A.

We now substitute into this equation the expression for the molar flux N_{Ar}, with N_{Br} set equal to zero, since B is insoluble in liquid A. This gives

$$\frac{d}{dr}\left(r^2 \frac{c\mathscr{D}_{AB}}{1-x_A}\frac{dx_A}{dr}\right) = 0 \tag{18.2-25}$$

For *constant temperature* the product $c\mathscr{D}_{AB}$ is constant, and Eq. 18.2-25 may be integrated to give the concentration distribution

$$\left(\frac{1-x_A}{1-x_{A1}}\right) = \left(\frac{1-x_{A2}}{1-x_{A1}}\right)^{\frac{(1/r_1)-(1/r)}{(1/r_1)-(1/r_2)}} \tag{18.2-26}$$

From Eq. 18.2-26 we can then get

$$W_A = 4\pi r_1^2 N_{Ar}|_{r=r_1} = \frac{4\pi c\mathscr{D}_{AB}}{(1/r_1)-(1/r_2)} \ln\left(\frac{1-x_{A2}}{1-x_{A1}}\right) \tag{18.2-27}$$

which is the molar flow of A across any spherical surface of radius r between r_1 and r_2.

(b) For the nonisothermal problem, combination of Eqs. 18.2-22 and 23 gives the variation of diffusivity with position:

$$\frac{\mathscr{D}_{AB}}{\mathscr{D}_{AB,1}} = \left(\frac{r}{r_1}\right)^{3n/2} \tag{18.2-28}$$

When this expression is inserted into Eq. 18.2-25 and c is set equal to p/RT, we get

$$\frac{d}{dr}\left(r^2 \frac{p\mathscr{D}_{AB,1}/RT_1}{1-x_A}\left(\frac{r}{r_1}\right)^{n/2}\frac{dx_A}{dr}\right) = 0 \tag{18.2-29}$$

After integrating between r_1 and r_2, we obtain (for $n \neq -2$)

$$W_A = 4\pi r_1^2 N_{Ar}|_{r=r_1} = \frac{4\pi(p\mathscr{D}_{AB,1}/RT_1)[1+(n/2)]}{[(1/r_1)^{1+(n/2)} - (1/r_2)^{1+(n/2)}]r_1^{n/2}} \ln\left(\frac{1-x_{A2}}{1-x_{A1}}\right) \tag{18.2-30}$$

For $n = 0$, this result simplifies to that in Eq. 18.2-27.

§18.3 DIFFUSION WITH A HETEROGENEOUS CHEMICAL REACTION

Let us now consider a simple model for a catalytic reactor, such as that shown in Fig. 18.3-1a, in which a reaction $2A \rightarrow B$ is being carried out. An example of a reaction of this type would be the solid-catalyzed dimerization of $CH_3CH = CH_2$.

We imagine that each catalyst particle is surrounded by a stagnant gas film through which A has to diffuse to reach the catalyst surface, as shown in Fig. 18.3-1b At the catalyst surface we assume that the reaction $2A \rightarrow B$ occurs instantaneously, and that the product B then diffuses back out through the gas film to the main turbulent stream composed of A and B. We want to get an expression for the local rate of conversion from A to B when the effective gas-film thickness and the main stream concentrations x_{A0} and x_{B0} are known. We assume that the gas film is isothermal, although in many catalytic reactions the heat generated by the reaction cannot be neglected.

For the situation depicted in Fig. 18.3-1b, there is *one* mole of B moving in the *minus* z direction for every *two* moles of A moving in the *plus* z direction. We know this from the stoichiometry of the reaction. Therefore we know that at steady state

$$N_{Bz} = -\tfrac{1}{2}N_{Az} \tag{18.3-1}$$

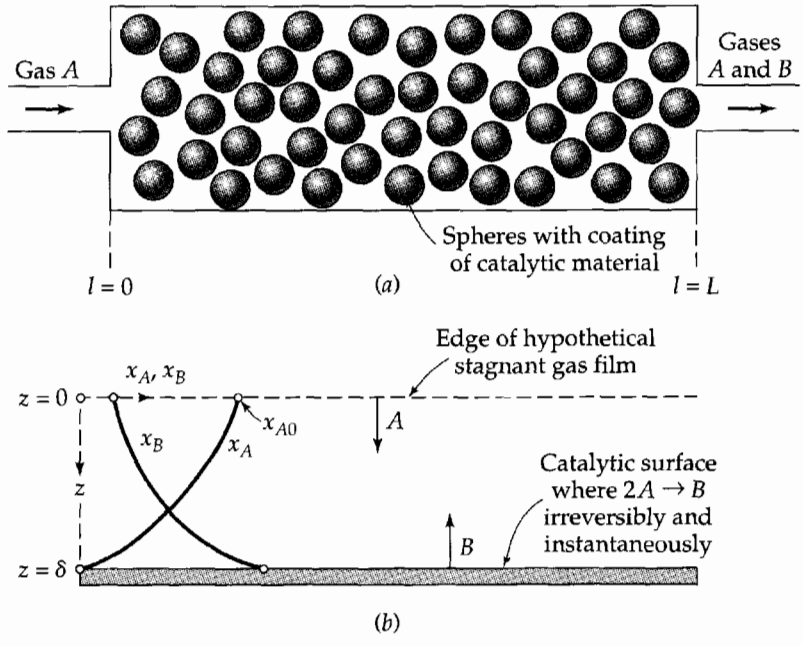

Fig. 18.3-1. (*a*) Schematic diagram of a catalytic reactor in which A is being converted to B. (*b*) Idealized picture (or "model") of the diffusion problem near the surface of a catalyst particle.

at any value of z. This relation may be substituted into Eq. 18.0-1, which may then be solved for N_{Az} to give

$$N_{Az} = -\frac{c\mathcal{D}_{AB}}{1 - \frac{1}{2}x_A}\frac{dx_A}{dz} \tag{18.3-2}$$

Hence, Eq. 18.0-1 plus the stoichiometry of the reaction have led to an expression for N_{Az} in terms of the concentration gradient.

We now make a mass balance on species A over a thin slab of thickness Δz in the gas film. This procedure is exactly the same as that used in connection with Eqs. 18.2-2 and 3 and leads once again to the equation

$$\frac{dN_{Az}}{dz} = 0 \tag{18.3-3}$$

Insertion of the expression for N_{Az}, developed above, into this equation gives (for constant $\mathcal{D}_{AB}$)

$$\frac{d}{dz}\left(\frac{1}{1 - \frac{1}{2}x_A}\frac{dx_A}{dz}\right) = 0 \tag{18.3-4}$$

Integration twice with respect to z gives

$$-2\ln(1 - \tfrac{1}{2}x_A) = C_1 z + C_2 = -(2\ln K_1)z - (2\ln K_2) \tag{18.3-5}$$

It is somewhat easier to find the integration constants K_1 and K_2 than C_1 and C_2. The boundary conditions are

B.C. 1: at $z = 0$, $x_A = x_{A0}$ (18.3-6)

B.C. 2: at $z = \delta$, $x_A = 0$ (18.3-7)

The final result is then

$$\boxed{(1 - \tfrac{1}{2}x_A) = (1 - \tfrac{1}{2}x_{A0})^{1-(z/\delta)}} \tag{18.3-8}$$

for the concentration profile in the gas film. Equation 18.3-2 may now be used to get the molar flux of reactant through the film:

$$N_{Az} = \frac{2c\mathscr{D}_{AB}}{\delta} \ln\left(\frac{1}{1 - \frac{1}{2}x_{A0}}\right) \tag{18.3-9}$$

The quantity N_{Az} may also be interpreted as the local rate of reaction per unit area of catalytic surface. This information can be combined with other information about the catalytic reactor sketched in Fig. 18.3-1(*a*) to get the overall conversion rate in the entire reactor.

One point deserves to be emphasized. Although the chemical reaction occurs instantaneously at the catalytic surface, the conversion of A to B proceeds at a finite rate because of the diffusion process, which is "in series" with the reaction process. Hence we speak of the conversion of A to B as being *diffusion controlled.*

In the example above we have assumed that the reaction occurs instantaneously at the catalytic surface. In the next example we show how to account for finite reaction kinetics at the catalytic surface.

EXAMPLE 18.3-1

Diffusion with a Slow Heterogeneous Reaction

Rework the problem just considered when the reaction $2A \rightarrow B$ is not instantaneous at the catalytic surface at $z = \delta$. Instead, assume that the rate at which A disappears at the catalyst-coated surface is proportional to the concentration of A in the fluid at the interface,

$$N_{Az} = k_1'' c_A = k_1'' c x_A \tag{18.3-10}$$

in which k_1'' is a rate constant for the pseudo-first-order surface reaction.

SOLUTION

We proceed exactly as before, except that B.C. 2 in Eq. 18.3-7 must be replaced by

$$\text{B.C. 2':} \qquad \text{at } z = \delta, \qquad x_A = \frac{N_{Az}}{k_1'' c} \tag{18.3-11}$$

N_{Az} being, of course, a constant at steady state. The determination of the integration constants from B.C. 1 and B.C. 2' leads to

$$(1 - \tfrac{1}{2}x_A) = \left(1 - \frac{1}{2}\frac{N_{Az}}{k_1'' c}\right)^{z/\delta} (1 - \tfrac{1}{2}x_{A0})^{1-(z/\delta)} \tag{18.3-12}$$

From this we evaluate $(dx_A/dz)|_{z=0}$ and substitute it into Eq. 18.3-2, to get

$$N_{Az} = \frac{2c\mathscr{D}_{AB}}{\delta} \ln\left(\frac{1 - \frac{1}{2}(N_{Az}/k_1'' c)}{1 - \frac{1}{2}x_{A0}}\right) \tag{18.3-13}$$

This is a transcendental equation for N_{Az} as a function of x_{A0}, k_1'', $c\mathscr{D}_{AB}$, and δ. When k_1'' is large, the logarithm of $1 - \frac{1}{2}(N_{Az}/k_1'' c)$ may be expanded in a Taylor series and all terms discarded but the first. We then get

$$N_{Az} = \frac{2c\mathscr{D}_{AB}/\delta}{1 + \mathscr{D}_{AB}/k_1''\delta} \ln\left(\frac{1}{1 - \frac{1}{2}x_{A0}}\right) \quad (k_1 \text{ large}) \tag{18.3-14}$$

Note once again that we have obtained the rate of the *combined* reaction and diffusion process. Note also that the dimensionless group $\mathscr{D}_{AB}/k_1''\delta$ describes the effect of the surface reaction kinetics on the overall diffusion-reaction process. The reciprocal of this group is known as the *second Damköhler number*[1] $\mathrm{Da}^{\mathrm{II}} = k_1''\delta/\mathscr{D}_{AB}$. Evidently we get the result in Eq. 18.3-9 in the limit as $\mathrm{Da}^{\mathrm{II}} \rightarrow \infty$.

[1] G. Damhöhler, Z. *Elektrochem.*, **42**, 846–862 (1936).

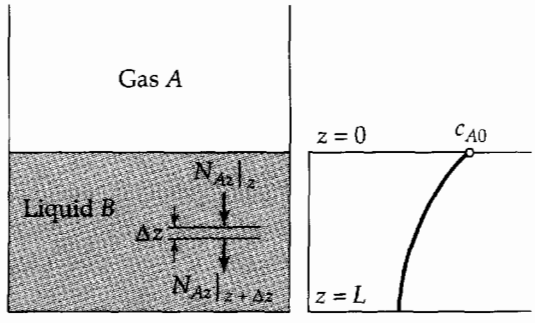

Fig. 18.4-1. Absorption of A by B with a homogeneous reaction in the liquid phase.

§18.4 DIFFUSION WITH A HOMOGENEOUS CHEMICAL REACTION

As the next illustration of setting up a mass balance, we consider the system shown in Fig. 18.4-1. Here gas A dissolves in liquid B in a beaker and diffuses isothermally into the liquid phase. As it diffuses, A also undergoes an irreversible first-order homogeneous reaction: $A + B \rightarrow AB$. An example of such a system is the absorption of CO_2 by a concentrated aqueous solution of NaOH.

We treat this as a binary solution of A and B, ignoring the small amount of AB that is present (the *pseudobinary assumption*). Then the mass balance on species A over a thickness Δz of the liquid phase becomes

$$N_{Az}|_z S - N_{Az}|_{z+\Delta z} S - k_1''' c_A S \Delta z = 0 \tag{18.4-1}$$

in which k_1''' is a first-order rate constant for the chemical decomposition of A, and S is the cross-sectional area of the liquid. The product $k_1''' c_A$ represents the moles of A consumed by the reaction per unit volume per unit time. Division of Eq. 18.4-1 by $S\Delta z$ and taking the limit as $\Delta z \rightarrow 0$ gives

$$\frac{dN_{Az}}{dz} + k_1''' c_A = 0 \tag{18.4-2}$$

If the concentration of A is small, then we may to a good approximation write Eq. 18.0-1 as

$$N_{Az} = -\mathcal{D}_{AB} \frac{dc_A}{dz} \tag{18.4-3}$$

since the total molar concentration c is virtually uniform throughout the liquid. Combining the last two equations gives

$$\mathcal{D}_{AB} \frac{d^2 c_A}{dz^2} - k_1''' c_A = 0 \tag{18.4-4}$$

This is to be solved with the following boundary conditions:

B.C. 1: at $z = 0$, $c_A = c_{A0}$ (18.4-5)

B.C. 2: at $z = L$, $N_{Az} = 0$ (or $dc_A/dz = 0$) (18.4-6)

The first boundary condition asserts that the concentration of A at the surface in the liquid remains at a fixed value c_{A0}. The second states that no A diffuses through the bottom of the container at $z = L$.

If Eq. 18.4-4 is multiplied by $L^2/c_{A0}\mathcal{D}_{AB}$, then it can be written in dimensionless variables in the form of Eq. C.1-4

$$\frac{d^2\Gamma}{d\zeta^2} - \phi^2 \Gamma = 0 \tag{18.4-7}$$

where $\Gamma = c_A/c_{A0}$ is a dimensionless concentration, $\zeta = z/L$ is a dimensionless length, and $\phi = \sqrt{k_1''' L^2/\mathcal{D}_{AB}}$ is a dimensionless group, known as the *Thiele modulus*.[1] This group represents the relative influence of the chemical reaction $k_1''' c_{A0}$ and diffusion $c_{A0}\mathcal{D}_{AB}/L^2$. Equation 18.4-7 is to be solved with the dimensionless boundary conditions that at $\zeta = 0$, $\Gamma = 1$, and at $\zeta = 1$, $d\Gamma/d\zeta = 0$. The general solution is

$$\Gamma = C_1 \cosh \phi\zeta + C_2 \sinh \phi\zeta \tag{18.4-8}$$

When the constants of integration are evaluated, we get

$$\Gamma = \frac{\cosh \phi \cosh \phi\zeta - \sinh \phi \sinh \phi\zeta}{\cosh \phi} = \frac{\cosh[\phi(1-\zeta)]}{\cosh \phi} \tag{18.4-9}$$

Then reverting to the original notation

$$\boxed{\frac{c_A}{c_{A0}} = \frac{\cosh[\sqrt{k_1''' L^2/\mathcal{D}_{AB}}(1-(z/L))]}{\cosh\sqrt{k_1''' L^2/\mathcal{D}_{AB}}}} \tag{18.4-10}$$

The concentration profile thus obtained is plotted in Fig. 18.4-1.

Once we have the complete concentration profile, we may evaluate other quantities, such as the average concentration in the liquid phase

$$\frac{c_{A,\text{avg}}}{c_{A0}} = \frac{\int_0^L (c_A/c_{A0})dz}{\int_0^L dz} = \frac{\tanh \phi}{\phi} \tag{18.4-11}$$

Also, the molar flux at the plane $z = 0$ can be found to be

$$N_{Az}|_{z=0} = -\mathcal{D}_{AB}\left.\frac{dc_A}{dz}\right|_{z=0} = \left(\frac{c_{A0}\mathcal{D}_{AB}}{L}\right)\phi \tanh \phi \tag{18.4-12}$$

This result shows how the chemical reaction influences the rate of absorption of gas A by liquid B.

The reader may wonder how the solubility c_{A0} and the diffusivity $\mathcal{D}_{AB}$ can be determined experimentally if there is a chemical reaction taking place. First, k_1''' can be measured in a separate experiment in a well-stirred vessel. Then, in principle, c_{A0} and $\mathcal{D}_{AB}$ can be obtained from the measured absorption rates for various liquid depths L.

EXAMPLE 18.4-1

Gas Absorption with Chemical Reaction in an Agitated Tank[2]

Estimate the effect of chemical reaction rate on the rate of gas absorption in an agitated tank (see Fig. 18.4-2). Consider a system in which the dissolved gas A undergoes an irreversible first order reaction with the liquid B; that is, A disappears within the liquid phase at a rate proportional to the local concentration of A. An example of such a system is the absorption of SO_2 or H_2S in aqueous NaOH solutions.

---

[1] E. W. Thiele, *Ind. Eng. Chem.*, **31**, 916–920 (1939). **Ernest William Thiele** (pronounced "tee-lee") (1895–1993) is noted for his work on catalyst effectiveness factors and his part in the development of the "McCabe-Thiele" diagram. After 35 years with Standard Oil of Indiana, he taught for a decade at Notre Dame University.

[2] E. N. Lightfoot, *AIChE Journal*, **4**, 499–500 (1958), **8**, 710–712 (1962).

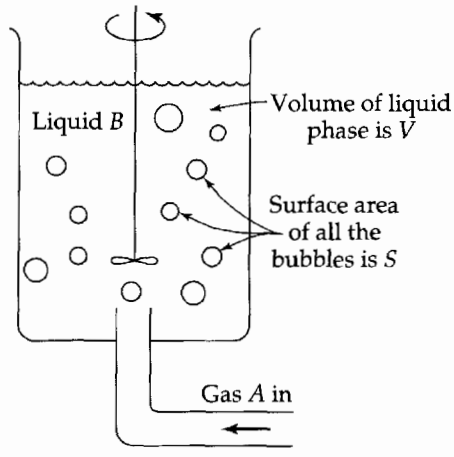

Fig. 18.4-2. Gas-absorption apparatus.

SOLUTION

An exact analysis of this situation is not possible because of the complexity of the gas-absorption process. However, a useful semiquantitative understanding can be obtained by the analysis of a relatively simple model. The model we use involves the following assumptions:

a. Each gas bubble is surrounded by a stagnant liquid film of thickness δ, which is small relative to the bubble diameter.

b. A quasi-steady concentration profile is quickly established in the liquid film after the bubble is formed.

c. The gas A is only sparingly soluble in the liquid, so that we can neglect the convection term in Eq. 18.0-1.

d. The liquid outside the stagnant film is at a concentration $c_{A\delta}$, which changes so slowly with respect to time that it can be considered constant.

The differential equation describing the diffusion with chemical reaction is the same as that in Eq. 18.4-4, but the boundary conditions are now

B.C. 1: at $z = 0$, $c_A = c_{A0}$ (18.4-13)

B.C. 2: at $z = \delta$, $c_A = c_{A\delta}$ (18.4-14)

The concentration c_{A0} is the interfacial concentration of A in the liquid phase, which is assumed to be at equilibrium with the gas phase at the interface, and $c_{A\delta}$ is the concentration of A in the main body of the liquid. The solution of Eq. 18.4-4 with these boundary conditions is

$$\frac{c_A}{c_{A0}} = \frac{\sinh\phi\cosh\phi\zeta + (B - \cosh\phi\sinh\phi\zeta)}{\sinh\phi} \tag{18.4-15}$$

in which $\zeta = z/\delta$, $B = c_{A\delta}/c_{A0}$, and $\phi = \sqrt{k_1'''\delta^2/\mathcal{D}_{AB}}$. This result is plotted in Fig. 18.4-3.

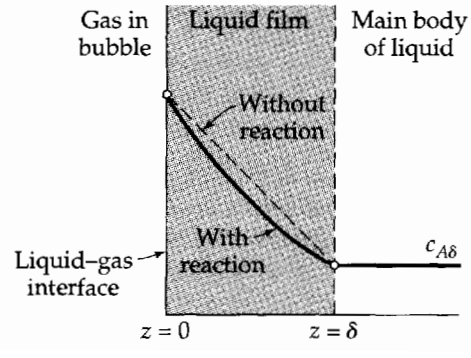

Fig. 18.4-3. Predicted concentration profile in the liquid film near a bubble.

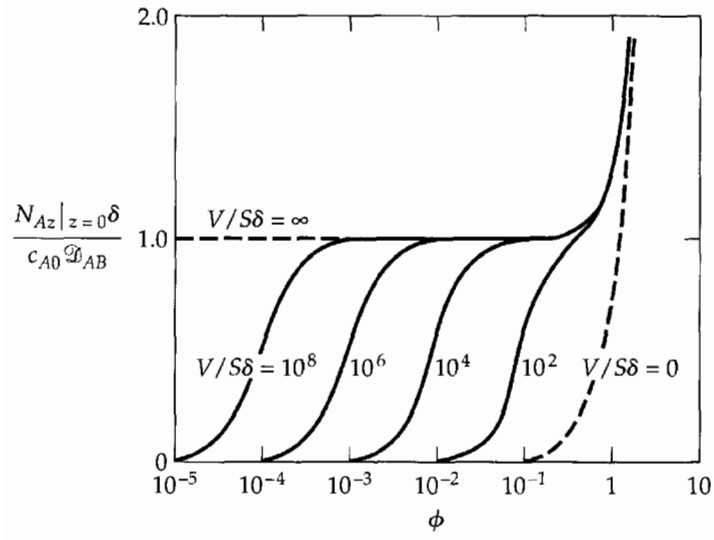

Fig. 18.4-4. Gas absorption accompanied by an irreversible first-order reaction.

Next we use assumption (d) above and equate the amount of A entering the main body of liquid at $z = \delta$ over the total bubble surface S in the tank to the amount of A consumed in the bulk of the liquid by chemical reaction:

$$-S\mathscr{D}_{AB}\left.\frac{dc_A}{dz}\right|_{z=\delta} = Vk_1'''c_{A\delta} \tag{18.4-16}$$

Substitution of c_A from Eq. 18.4-15 into Eq. 18.4-16 gives an expression for B:

$$B = \frac{1}{\cosh\phi + (V/S\delta)\phi\sinh\phi} \tag{18.4-17}$$

When this result is substituted into Eq. 18.4-15, we obtain an expression for c_A/c_{A0} in terms of ϕ and $V/S\delta$.

From this expression for the concentration profile we can then get the total rate of absorption with chemical reaction from $N_{Az} = -\mathscr{D}_{AB}(dc_A/dz)$ evaluated at $z = 0$, thus:

$$\breve{N} = \frac{N_{Az}|_{z=0}\delta}{c_{A0}\mathscr{D}_{AB}} = \frac{\phi}{\sinh\phi}\left(\cosh\phi - \frac{1}{\cosh\phi + (V/S\delta)\phi\sinh\phi}\right) \tag{18.4-18}$$

The result is plotted in Fig. 18.4-4.

It is seen here that the dimensionless absorption rate per unit area of interface, $\breve{N}$, increases with ϕ for all finite values of $V/S\delta$. At very low values of ϕ—that is, for very slow reactions—$\breve{N}$ approaches zero. For this limiting situation the liquid is nearly saturated with dissolved gas, and the "driving force" for absorption is very small. At large values of ϕ the dimensionless surface mass flux $\breve{N}$ increases rapidly with ϕ and becomes very nearly independent of $V/S\delta$. Under the latter circumstances, the reaction is so rapid that almost all of the dissolving gas is consumed within the film. Then B is very nearly zero, and the bulk of the liquid plays no significant role. In the limit as ϕ becomes very large, $\breve{N}$ approaches ϕ.

Somewhat more interesting behavior is observed for intermediate values of ϕ. It may be noted that, for moderately large $V/S\delta$, there is a considerable range of ϕ for which $\breve{N}$ is very nearly unity. In this region the chemical reaction is fast enough to keep the bulk of the solution almost solute free, but slow enough to have little effect on solute transport in the film. Such a situation will arise when the ratio $V/S\delta$ of bulk to film volume is sufficient to offset the higher volumetric reaction rate in the film. The absorption rate is then equal to the physical absorption rate (that is, the rate for $k_1''' = 0$) for a solute-free tank. This behavior is frequently observed in practice, and operation under such conditions has proven a useful means of characterizing the mass transfer behavior of a variety of gas absorbers.[2]

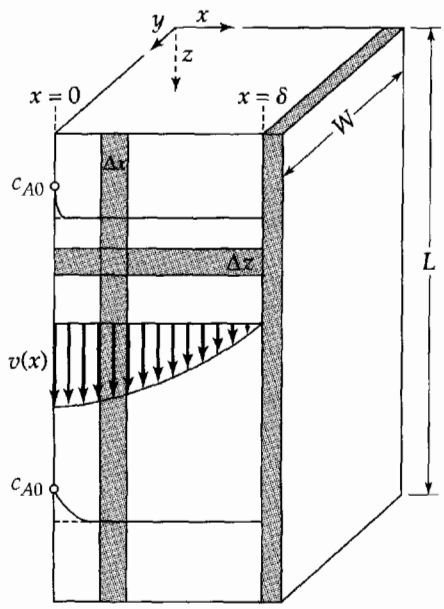

Fig. 18.5-1. Absorption of A into a falling film of liquid B.

§18.5 DIFFUSION INTO A FALLING LIQUID FILM (GAS ABSORPTION)[1]

In this section we present an illustration of *forced-convection* mass transfer, in which viscous flow and diffusion occur under such conditions that the velocity field can be considered virtually unaffected by the diffusion. Specifically, we consider the absorption of gas A by a laminar falling film of liquid B. The material A is only slightly soluble in B, so that the viscosity of the liquid is unaffected. We shall make the further restriction that the diffusion takes place so slowly in the liquid film that A will not "penetrate" very far into the film—that is, that the penetration distance will be small in comparison with the film thickness. The system is sketched in Fig. 18.5-1. An example of this kind of system occurs in the absorption of O_2 in H_2O.

Let us now set up the differential equations describing the diffusion process. First, we have to solve the momentum transfer problem to obtain the velocity profile $v_z(x)$ for the film; this has already been worked out in §2.2 in the absence of mass transfer at the fluid surface, and we know that the result is

$$v_z(x) = v_{\max}\left[1 - \left(\frac{x}{\delta}\right)^2\right] \tag{18.5-1}$$

provided that "end effects" are ignored.

Next we have to establish a mass balance on component A. We note that c_A will be changing with both x and z. Hence, as the element of volume for the mass balance, we select the volume formed by the intersection of a slab of thickness Δz with a slab of thickness Δx. Then the mass balance on A over this segment of a film of width W becomes

$$N_{Az}|_z\, W\Delta x - N_{Az}|_{z+\Delta z}\, W\Delta x + N_{Ax}|_x\, W\Delta z - N_{Ax}|_{x+\Delta x}\, W\Delta z = 0 \tag{18.5-2}$$

Dividing by $W\,\Delta x\,\Delta z$ and performing the usual limiting process as the volume element becomes infinitesimally small, we get

$$\frac{\partial N_{Az}}{\partial z} + \frac{\partial N_{Ax}}{\partial x} = 0 \tag{18.5-3}$$

[1] S. Lynn, J. R. Straatemeier, and H. Kramers, *Chem. Engr. Sci.*, **4**, 49–67 (1955).

Into this equation we now insert the expression for N_{Az} and N_{Ax}, making appropriate simplifications of Eq. 18.0-1. For the molar flux in the z direction, we write, assuming constant c,

$$N_{Az} = \underline{-\mathcal{D}_{AB}\frac{\partial c_A}{\partial z}} + x_A(N_{Az} + N_{Bz}) \approx c_A v_z(x) \tag{18.5-4}$$

We discard the dashed-underlined term, since the transport of A in the z direction will be primarily by convection. We have made use of Eq. (M) in Table 17.8-1 and the fact that $\mathbf{v}$ is almost the same as $\mathbf{v}^*$ in dilute solutions. The molar flux in the x direction is

$$N_{Ax} = -\mathcal{D}_{AB}\frac{\partial c_A}{\partial x} + \underline{x_A(N_{Ax} + N_{Bx})} \approx -\mathcal{D}_{AB}\frac{\partial c_A}{\partial x} \tag{18.5-5}$$

Here we neglect the dashed-underlined term because in the x direction A moves predominantly by diffusion, there being almost no convective transport normal to the wall on account of the very slight solubility of A in B. Combining the last three equations, we then get for constant $\mathcal{D}_{AB}$

$$v_z\frac{\partial c_A}{\partial z} = \mathcal{D}_{AB}\frac{\partial^2 c_A}{\partial x^2} \tag{18.5-6}$$

Finally, insertion of Eq. 18.5-1 for the velocity distribution gives

$$v_{\max}\left[1 - \left(\frac{x}{\delta}\right)^2\right]\frac{\partial c_A}{\partial z} = \mathcal{D}_{AB}\frac{\partial^2 c_A}{\partial x^2} \tag{18.5-7}$$

as the differential equation for $c_A(x, z)$.

Equation 18.5-7 is to be solved with the following boundary conditions:

B.C. 1: at $z = 0$, $c_A = 0$ (18.5-8)

B.C. 2: at $x = 0$, $c_A = c_{A0}$ (18.5-9)

B.C. 3: at $x = \delta$, $\frac{\partial c_A}{\partial x} = 0$ (18.5-10)

The first boundary condition corresponds to the fact that the film consists of pure B at the top ($z = 0$), and the second indicates that at the liquid–gas interface the concentration of A is determined by the solubility of A in B (that is, c_{A0}). The third boundary condition states that A cannot diffuse through the solid wall. This problem has been solved analytically in the form of an infinite series,[2] but we do not give that solution here. Instead, we seek only a limiting expression valid for "short contact times," that is, for small values of $L/v_{\max}$.

If, as indicated in Fig. 18.5-1, the substance A has penetrated only a short distance into the film, then the species A "has the impression" that the film is moving throughout with a velocity equal to $v_{\max}$. Furthermore if A does not penetrate very far, it does not "sense" the presence of the solid wall at $x = \delta$. Hence, if the film were of infinite thickness moving with the velocity $v_{\max}$, the diffusing material "would not know the difference." This physical argument suggests (correctly) that we will get a very good result if we replace Eq. 18.5-7 and its boundary conditions by

$$v_{\max}\frac{\partial c_A}{\partial z} = \mathcal{D}_{AB}\frac{\partial^2 c_A}{\partial x^2} \tag{18.5-11}$$

B.C. 1: at $z = 0$, $c_A = 0$ (18.5-12)

B.C. 2: at $x = 0$, $c_A = c_{A0}$ (18.5-13)

B.C. 3: at $x = \infty$, $c_A = 0$ (18.5-14)

[2] R. L. Pigford, PhD thesis, University of Illinois (1941).

An exactly analogous problem occurred in Example 4.1-1, which was solved by the method of combination of variables. It is therefore possible to take over the solution to that problem just by changing the notation. The solution is[3]

$$\frac{c_A}{c_{A0}} = 1 - \frac{2}{\sqrt{\pi}} \int_0^{x/\sqrt{4\mathscr{D}_{AB}z/v_{max}}} \exp(-\xi^2)\, d\xi \tag{18.5-15}$$

or

$$\boxed{\frac{c_A}{c_{A0}} = 1 - \operatorname{erf} \frac{x}{\sqrt{4\mathscr{D}_{AB}z/v_{\max}}} = \operatorname{erfc} \frac{x}{\sqrt{4\mathscr{D}_{AB}z/v_{\max}}}} \tag{18.5-16}$$

In these expressions "erf x" and "erfc x" are the "error function" and the "complementary error function" of x, respectively. They are discussed in §C.6 and tabulated in standard reference works.[4]

Once the concentration profiles are known, the local mass flux at the gas–liquid interface may be found as follows:

$$N_{Ax}|_{x=0} = -\mathscr{D}_{AB} \frac{\partial c_A}{\partial x}\bigg|_{x=0} = c_{A0} \sqrt{\frac{\mathscr{D}_{AB} v_{\max}}{\pi z}} \tag{18.5-17}$$

Then the total molar flow of A across the surface at $x = 0$ (i.e., being absorbed by a liquid film of length L and width W) is

$$\begin{aligned} W_A &= \int_0^W \int_0^L N_{Ax}|_{x=0}\, dz\, dy \\ &= W c_{A0} \sqrt{\frac{\mathscr{D}_{AB} v_{\max}}{\pi}} \int_0^L \frac{1}{\sqrt{z}}\, dz \\ &= W L c_{A0} \sqrt{\frac{4\mathscr{D}_{AB} v_{\max}}{\pi L}} \end{aligned} \tag{18.5-18}$$

The same result is obtained by integrating the product $v_{\max} c_A$ over the flow cross section at $z = L$ (see Problem 18C.3).

Equation 18.5-18 shows that the mass transfer rate is directly proportional to the square root of the diffusivity and inversely proportional to the square root of the "exposure time," $t_{\text{exp}} = L/v_{\max}$. This approach for studying gas absorption was apparently first proposed by Higbie.[5]

The problem discussed in this section illustrates the "penetration model" of mass transfer. This model is discussed further in Chapters 20 and 22.

EXAMPLE 18.5-1

Gas Absorption from Rising Bubbles

Estimate the rate at which gas bubbles of A are absorbed by liquid B as the gas bubbles rise at their terminal velocity v_t through a clean quiescent liquid.

---

[3] The solution is worked out in detail by the method of combination of variables in Example 4.1-1.

[4] M. Abramowitz and I. A. Stegun, *Handbook of Mathematical Functions*, Dover, New York, 9th printing (1973), pp. 310 et seq.

[5] R. Higbie, *Trans. AIChE*, **31**, 365–389 (1935). **Ralph Wilmarth Higbie** (1908–1941), a graduate of the University of Michigan, provided the basis for the "penetration model" of mass transfer. He worked at E. I. du Pont de Nemours & Co., Inc., and also at Eagle-Picher Lead Co.; then he taught at the University of Arkansas and the University of North Dakota.

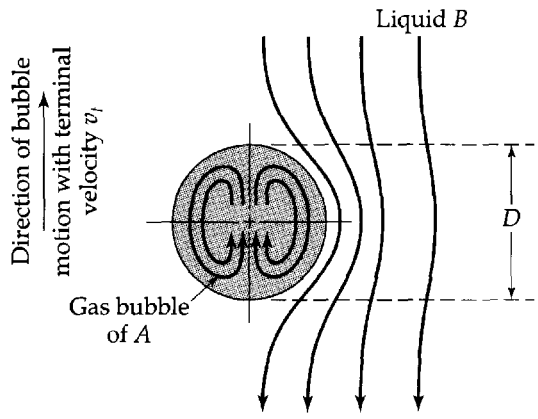

Fig. 18.5-2. Absorption of gas A into liquid B.

SOLUTION

Gas bubbles of moderate size, rising in liquids free of surface-active agents, undergo a toroidal circulation (Rybczynski–Hadamard circulation) as shown in Fig. 18.5-2. The liquid moves downward relative to each rising bubble, enriched in species A near the interface in the manner of the falling film in Fig. 18.5-1. The depth of penetration of the dissolved gas into the liquid is slight over the major part of the bubble, because of the motion of the liquid relative to the bubble and because of the smallness of the liquid-phase diffusivity $\mathscr{D}_{AB}$. Thus, as a rough approximation, we can use Eq. 18.5-18 to estimate the rate of gas absorption, replacing the exposure time $t_{\text{exp}} = L/v_{\text{max}}$ for the falling film by D/v_t for the bubble, where D is the instantaneous bubble diameter. This gives an estimate[5] of the molar absorption rate, averaged over the bubble surface, as

$$(N_A)_{\text{avg}} = \sqrt{\frac{4\mathscr{D}_{AB}v_t}{\pi D}}\, c_{A0} \tag{18.5-19}$$

Here c_{A0} is the solubility of gas A in liquid B at the interfacial temperature and partial pressure of gas A. Interestingly, the result in Eq. 18.5-19 turns out to be correct for potential flow of the liquid around the bubble (see Problem 4B.5). This equation has been approximately confirmed[6] for gas bubbles 0.3 to 0.5 cm in diameter rising through carefully purified water.

This system has also been analyzed for creeping flow[7] and the result is (see Example 20.3-1)

$$(N_A)_{\text{avg}} = \sqrt{\frac{4\mathscr{D}_{AB}v_t}{3\pi D}}\, c_{A0} \tag{18.5-20}$$

instead of Eq. 18.5-19.

Trace amounts of surface-active agents cause a marked decrease in absorption rates from small bubbles, by forming a "skin" around each bubble and thus effectively preventing internal circulation. The molar absorption rate in the small-diffusivity limit then becomes proportional to the $\frac{1}{3}$ power of the diffusivity, as for a solid sphere (see §§22.2 and 3).

A similar approach has been used successfully for predicting mass transfer rates during drop formation at a capillary tip.[8]

---

[6] D. Hammerton and F. H. Garner, *Trans. Inst. Chem. Engrs. (London)*, **32**, S18-S24 (1954).

[7] V. G. Levich, *Physicochemical Hydrodynamics*, Prentice-Hall, Englewood Cliffs, N.J. (1962), p. 408, Eq. 72.9. This reference gives many additional results, including liquid–liquid mass transfer and surfactant effects.

[8] H. Groothuis and H. Kramers, *Chem. Eng. Sci.*, **4**, 17–25 (1955).

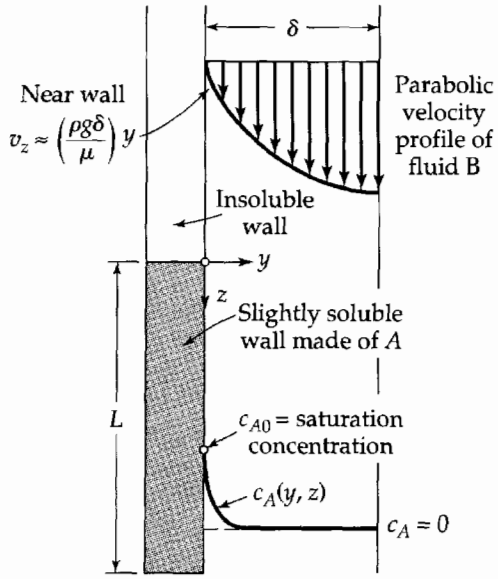

Fig. 18.6-1. Solid A dissolving into a falling film of liquid B, moving with a fully developed parabolic velocity profile.

§18.6 DIFFUSION INTO A FALLING LIQUID FILM (SOLID DISSOLUTION)[1]

We now turn to a falling film problem that is different from the one discussed in the previous section. Liquid B is flowing in laminar motion down a vertical wall as shown in Fig. 18.6-1. The film begins far enough up the wall so that v_z depends only on y for $z \geq 0$. For $0 < z < L$ the wall is made of a species A that is slightly soluble in B.

For short distances downstream, species A will not diffuse very far into the falling film. That is, A will be present only in a very thin boundary layer near the solid surface. Therefore the diffusing A molecules will experience a velocity distribution that is characteristic of the falling film right next to the wall, $y = 0$. The velocity distribution is given in Eq. 2.2-18. In the present situation $\cos\theta = 1$, and $x = \delta - y$, and

$$v_z = \frac{\rho g \delta^2}{2\mu}\left[1 - \left(1 - \frac{y}{\delta}\right)^2\right] = \frac{\rho g \delta^2}{2\mu}\left[2\left(\frac{y}{\delta}\right) - \left(\frac{y}{\delta}\right)^2\right] \tag{18.6-1}$$

At and adjacent to the wall $(y/\delta)^2 << (y/\delta)$, so that for this problem the velocity is, to a very good approximation, $v_z = (\rho g \delta/\mu)y \equiv ay$. This means that Eq. 18.5-6, which is applicable here, becomes for short distances downstream

$$ay\frac{\partial c_A}{\partial z} = \mathcal{D}_{AB}\frac{\partial^2 c_A}{\partial y^2} \tag{18.6-2}$$

where $a = \rho g \delta/\mu$. This equation is to be solved with the boundary conditions

B.C. 1: at $z = 0$, $c_A = 0$ (18.6-3)

B.C. 2: at $y = 0$, $c_A = c_{A0}$ (18.6-4)

B.C. 3: at $y = \infty$, $c_A = 0$ (18.6-5)

In the second boundary condition, c_{A0} is the solubility of A in B. The third boundary condition is used instead of the correct one ($\partial c_A/\partial y = 0$ at $y = \delta$), since for short contact times we feel intuitively that it will not make any difference. After all, since the mole-

[1] H. Kramers and P. J. Kreyger, *Chem. Eng. Sci.*, **6**, 42–48 (1956); see also R. L. Pigford, *Chem. Eng. Prog. Symposium Series* No. 17, Vol. 51, pp. 79–92 (1955) for the analogous heat-conduction problem.

cules of A penetrate only slightly into the film, they cannot get far enough to "see" the outer boundary of the film, and hence they cannot distinguish between the true boundary condition and the approximate boundary condition that we use. The same kind of reasoning was encountered in Example 12.2-2 and Problem 12B.4.

The form of the boundary conditions in Eqs. 18.6-3 to 5 suggests the method of combination of variables. Therefore we try $c_A/c_{A0} = f(\eta)$, where $\eta = y(a/9\mathscr{D}_{AB}z)^{1/3}$. This combination of the independent variables can be shown to be dimensionless, and the factor of "9" is included to make the solution look neater.

When this change of variable is made, the partial differential equation in Eq. 18.6-2 reduces to an ordinary differential equation

$$\frac{d^2f}{d\eta^2} + 3\eta^2\frac{df}{d\eta} = 0 \tag{18.6-6}$$

with the boundary conditions $f(0) = 1$ and $f(\infty) = 0$.

This second-order equation, which is of the form of Eq. C.1-9, has the solution

$$f = C_1\int_0^\eta \exp(-\bar{\eta}^3)\,d\bar{\eta} + C_2 \tag{18.6-7}$$

The constants of integration can then be evaluated using the boundary conditions, and one obtains finally

$$\boxed{\frac{c_A}{c_{A0}} = \frac{\displaystyle\int_\eta^\infty \exp(-\bar{\eta}^3)\,d\bar{\eta}}{\displaystyle\int_0^\infty \exp(-\bar{\eta}^3)\,d\bar{\eta}} = \frac{\displaystyle\int_\eta^\infty \exp(-\bar{\eta}^3)\,d\bar{\eta}}{\Gamma(\frac{4}{3})}} \tag{18.6-8}$$

for the concentration profiles, in which $\Gamma(\frac{4}{3}) = 0.8930\ldots$ is the gamma function of $\frac{4}{3}$. Next the local mass flux at the wall can be obtained as follows

$$\begin{aligned} N_{Ay}|_{y=0} &= -\mathscr{D}_{AB}\frac{\partial c_A}{\partial y}\bigg|_{y=0} = -\mathscr{D}_{AB}c_{A0}\left[\frac{d}{d\eta}\left(\frac{c_A}{c_{A0}}\right)\frac{\partial\eta}{\partial y}\right]\bigg|_{y=0} \\ &= -\mathscr{D}_{AB}c_{A0}\left[-\frac{\exp(-\eta^3)}{\Gamma(\frac{4}{3})}\left(\frac{a}{9\mathscr{D}_{AB}z}\right)^{1/3}\right]\bigg|_{y=0} = +\frac{\mathscr{D}_{AB}c_{A0}}{\Gamma(\frac{4}{3})}\left(\frac{a}{9\mathscr{D}_{AB}z}\right)^{1/3} \end{aligned} \tag{18.6-9}$$

Then the molar flow of A across the entire mass transfer surface at $y = 0$ is

$$W_A = \int_0^W\int_0^L N_{Ay}|_{y=0}\,dz\,dx = \frac{2\mathscr{D}_{AB}c_{A0}WL}{\Gamma(\frac{7}{3})}\left(\frac{a}{9\mathscr{D}_{AB}L}\right)^{1/3} \tag{18.6-10}$$

where $\Gamma(\frac{7}{3}) = \frac{4}{3}\Gamma(\frac{4}{3}) = 1.1907\ldots$.

The problem discussed in §18.5 and the one discussed here are examples of two types of asymptotic solutions that are discussed further in §20.2 and §20.3 and again in Chapter 22. It is therefore important that these two problems be thoroughly understood. Note that in §18.5, $W_A \propto (\mathscr{D}_{AB}L)^{1/2}$, whereas in this section $W_A \propto (\mathscr{D}_{AB}L)^{2/3}$. The differences in the exponents reflect the nature of the velocity gradient at the mass transfer interface: in §18.5, the velocity gradient was zero, whereas in this section, the velocity gradient is nonzero.

§18.7 DIFFUSION AND CHEMICAL REACTION INSIDE A POROUS CATALYST

Up to this point we have discussed diffusion in gases and liquids in systems of simple geometry. We now wish to apply the shell mass balance method and Fick's first law to describe diffusion within a porous catalyst pellet. We make no attempt to describe the

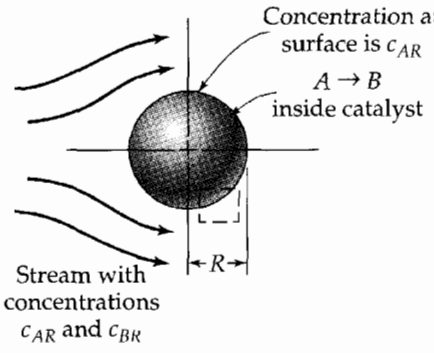

Fig. 18.7-1. A spherical catalyst that is porous. For a magnified version of the inset, see Fig. 18.7-2.

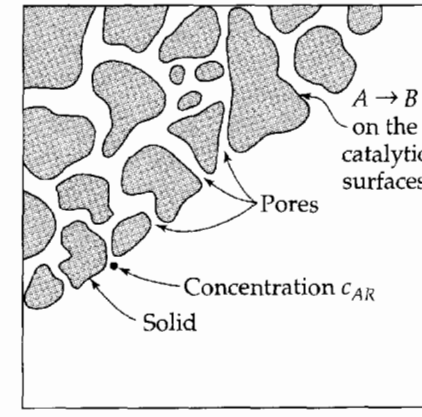

Fig. 18.7-2. Pores in the catalyst, in which diffusion and chemical reaction occur.

diffusion inside the tortuous void passages in the pellet. Instead, we describe the "averaged" diffusion of the reactant in terms of an "effective diffusivity."[1,2,3]

Specifically, we consider a spherical porous catalyst particle of radius R, as shown in Fig. 18.7-1. This particle is in a catalytic reactor, where it is submerged in a gas stream containing the reactant A and the product B. In the neighborhood of the surface of the particular catalyst particle under consideration, we presume that the concentration is c_{AR} moles of A per unit volume. Species A diffuses through the tortuous passages in the catalyst and is converted to B on the catalytic surfaces, as sketched in Fig. 18.7-2.

We start by making a mass balance for species A on a spherical shell of thickness Δr within a single catalyst particle:

$$N_{Ar}|_r \cdot 4\pi r^2 - N_{Ar}|_{r+\Delta r} \cdot 4\pi(r + \Delta r)^2 + R_A \cdot 4\pi r^2 \Delta r = 0 \tag{18.7-1}$$

Here $N_{Ar}|_r$ is the number of moles of A passing in the r direction through an imaginary spherical surface at a distance r from the center of the sphere. The source term $R_A \cdot 4\pi r^2 \Delta r$ is the molar rate of production of A by chemical reaction in the shell of thickness Δr. Dividing by $4\pi\,\Delta r$ and letting $\Delta r \rightarrow 0$ gives

$$\lim_{\Delta r \rightarrow 0} \frac{(r^2 N_{Ar})|_{r+\Delta r} - (r^2 N_{Ar})|_r}{\Delta r} = r^2 R_A \tag{18.7-2}$$

or, using the definition of the first derivative,

$$\frac{d}{dr}(r^2 N_{Ar}) = r^2 R_A \tag{18.7-3}$$

This limiting process is clearly in conflict with the fact that the porous medium is granular rather than continuous. Consequently, in Eq. 18.7-3 the symbols N_{Ar} and R_A cannot be interpreted as quantities having a meaningful value at a point. Rather we have to interpret them as quantities averaged over a small neighborhood of the point in question—a neighborhood small with respect to the dimension R, but large with respect to the dimensions of the passages within the porous particle.

---

[1] E. W. Thiele, *Ind. Eng. Chem.*, **31**, 916–920 (1939).
[2] R. Aris, *Chem. Eng. Sci.*, **6**, 265–268 (1957).
[3] A. Wheeler, *Advances in Catalysis*, Academic Press, New York (1950), Vol. 3, pp. 250–326.

We now *define* an "effective diffusivity" for species A in the porous medium by

$$N_{Ar} = -\mathscr{D}_A \frac{dc_A}{dr} \tag{18.7-4}$$

in which c_A is the concentration of the gas A contained within the pores. The effective diffusivity $\mathscr{D}_A$ must be measured experimentally. It depends generally on pressure and temperature and also on the catalyst pore structure. The actual mechanism for diffusion in pores is complex, since the pore dimensions may be smaller than the mean free path of the diffusing molecules. We do not belabor the question of mechanism here but assume only that Eq. 18.7-4 can adequately represent the diffusion process (see §24.6).

When the preceding expression is inserted into Eq. 18.7-3, we get, for constant diffusivity

$$\mathscr{D}_A \frac{1}{r^2}\frac{d}{dr}\left(r^2 \frac{dc_A}{dr}\right) = -R_A \tag{18.7-5}$$

We now consider the situation where species A disappears according to a first-order chemical reaction on the catalytic surfaces that form all or part of the "walls" of the winding passages. Let a be the available catalytic surface per unit volume (of solids + voids). Then $R_A = -k_1'' a c_A$, and Eq. 18.7-5 becomes (see Eq. C.1-6)

$$\mathscr{D}_A \frac{1}{r^2}\frac{d}{dr}\left(r^2 \frac{dc_A}{dr}\right) = k_1'' a c_A \tag{18.7-6}$$

This equation is to be solved with the boundary conditions that $c_A = c_{AR}$ at $r = R$, and that c_A is finite at $r = 0$.

Equations containing the operator $(1/r^2)(d/dr)[r^2(d/dr)]$ can frequently be solved by using a "standard trick"—namely, a change of variable $c_A/c_{AR} = (1/r)f(r)$. The equation for $f(r)$ is then

$$\frac{d^2 f}{dr^2} = \left(\frac{k_1'' a}{\mathscr{D}_A}\right) f \tag{18.7-7}$$

This is a standard second-order differential equation, which can be solved in terms of exponentials or hyperbolic functions. When it is solved and the result divided by r we get the following solution of Eq. 18.7-6 in terms of hyperbolic functions (see §C.5):

$$\frac{c_A}{c_{AR}} = \frac{C_1}{r}\cosh\sqrt{\frac{k_1'' a}{\mathscr{D}_A}}\, r + \frac{C_2}{r}\sinh\sqrt{\frac{k_1'' a}{\mathscr{D}_A}}\, r \tag{18.7-8}$$

Application of the boundary conditions gives finally

$$\boxed{\frac{c_A}{c_{AR}} = \left(\frac{R}{r}\right)\frac{\sinh\sqrt{k_1'' a/\mathscr{D}_A}\, r}{\sinh\sqrt{k_1'' a/\mathscr{D}_A}\, R}} \tag{18.7-9}$$

In studies on chemical kinetics and catalysis one is frequently interested in the molar flux N_{AR} or the molar flow W_{AR} at the surface $r = R$:

$$W_{AR} = 4\pi R^2 N_{AR} = -4\pi R^2 \mathscr{D}_A \left.\frac{dc_A}{dr}\right|_{r=R} \tag{18.7-10}$$

When Eq. 18.7-9 is used in this expression, we get

$$W_{AR} = 4\pi R \mathscr{D}_A c_{AR}\left(1 - \sqrt{\frac{k_1'' a}{\mathscr{D}_A}}\, R \coth\sqrt{\frac{k_1'' a}{\mathscr{D}_A}}\, R\right) \tag{18.7-11}$$

This result gives the rate of conversion (in moles/sec) of A to B in a single catalyst particle of radius R in terms of the parameters describing the diffusion and reaction processes.

If the catalytically active surface were all exposed to the stream of concentration c_{AR}, then the species A would not have to diffuse through the pores to a reaction site. The molar rate of conversion would then be given by the product of the available surface and the surface reaction rate:

$$W_{AR,0} = (\tfrac{4}{3}\pi R^3)(a)(-k_1'' c_{AR}) \tag{18.7-12}$$

Taking the ratio of the last two equations, we get

$$\eta_A = \frac{W_{AR}}{W_{AR,0}} = \frac{3}{\phi^2}(\phi \coth \phi - 1) \tag{18.7-13}$$

in which $\phi = \sqrt{k_1'' a/\mathcal{D}_A} R$ is the *Thiele modulus*,[1] encountered in §18.4. The quantity η_A is called the *effectiveness factor*.[1-4] It is the quantity by which $W_{AR,0}$ has to be multiplied to account for the intraparticle diffusional resistance to the overall conversion process.

For nonspherical catalyst particles, the foregoing results may be applied approximately by reinterpreting R. We note that for a sphere of radius R the ratio of volume to external surface is $R/3$. For nonspherical particles, we redefine R in Eq. 18.7-13 as

$$R_{\text{nonsph}} = 3\left(\frac{V_P}{S_P}\right) \tag{18.7-14}$$

where V_P and S_P are the volume and external surface of a single catalyst particle. The absolute value of the conversion rate is then given approximately by

$$|W_{AR}| \approx V_P a k_1'' c_{AR} \eta_A \tag{18.7-15}$$

where

$$\eta_A = \frac{1}{3\Lambda^2}(3\Lambda \coth 3\Lambda - 1) \tag{18.7-16}$$

in which the quantity $\Lambda = \sqrt{k_1'' a/\mathcal{D}_A}(V_P/S_P)$ is a generalized modulus.[2,3]

The particular utility of the quantity Λ may be seen in Fig. 18.7-3. It is clear that when the exact theoretical expressions for η_A are plotted as functions of Λ, the curves

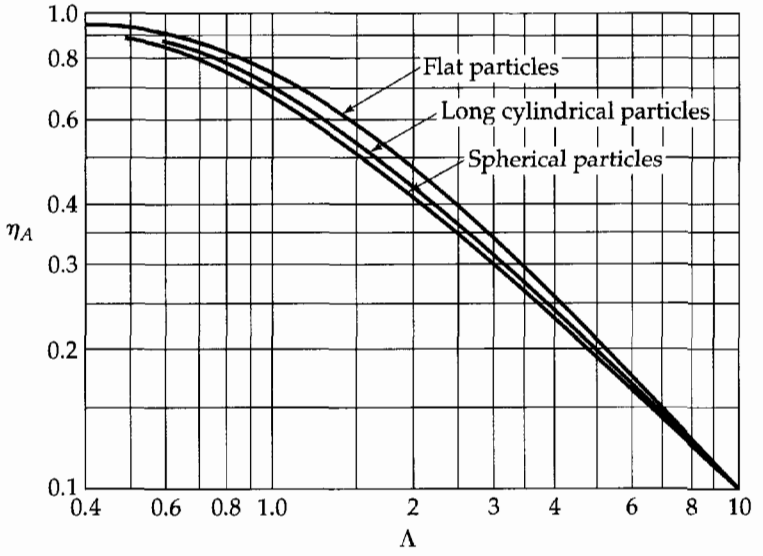

Fig. 18.7-3. Effectiveness factors for porous solid catalysts of various shapes [R. Aris, *Chem. Eng. Sci.*, **6**, 262–268 (1957)].

[4] O. A. Hougen and K. M. Watson, *Chemical Process Principles*, Wiley, New York (1947), Part III, Chapter XIX. See also *CPP Charts*, by O. A. Hougen, K. M. Watson, and R. A. Ragatz, Wiley, New York (1960), Fig. E.

have common asymptotes for large and small Λ and do not differ from one another very much for intermediate values of Λ. Thus Fig. 18.7-3 provides a justification for the use of Eq. 18.7-16 to estimate η_A for nonspherical particles.

§18.8 DIFFUSION IN A THREE-COMPONENT GAS SYSTEM

Up to this point the systems we have discussed have been binary systems, or ones that could be approximated as two-component systems. To illustrate the setting up of multicomponent diffusion problems for gases, we rework the initial evaporation problem of §18.2 when liquid water (species 1) is evaporating into air, regarded as a binary mixture of nitrogen (2) and oxygen (3) at 1 atm and 352K. We take the air–water interface to be at $z = 0$ and the top end of the diffusion tube to be at $z = L$. We consider the vapor pressure of water to be known, so that x_1 is known at $z = 0$ (that is, $x_{10} = 341/760 = 0.449$), and the mole fractions of all three gases are known at $z = L$: $x_{1L} = 0.10$, $x_{2L} = 0.75$, $x_{3L} = 0.15$. The diffusion tube has a length $L = 11.2$ cm.

The conservation of mass leads, as in §18.2, to the following expressions:

$$\frac{dN_{\alpha z}}{dz} = 0 \qquad \alpha = 1, 2, 3 \tag{18.8-1}$$

From this it may be concluded that the molar fluxes of the three species are all constants at steady state. Since species 2 and 3 are not moving, we conclude that N_{2z} and N_{3z} are both zero.

Next we need the expressions for the molar fluxes from Eq. 17.9-1. Since $x_1 + x_2 + x_3 = 1$, we need only two of the three available equations, and we select the equations for species 2 and 3. Since $N_{2z} = 0$ and $N_{3z} = 0$, these equations simplify considerably:

$$\frac{dx_2}{dz} = \frac{N_{1z}}{c\mathscr{D}_{12}} x_2; \qquad \frac{dx_3}{dz} = \frac{N_{1z}}{c\mathscr{D}_{13}} x_3 \tag{18.8-2, 3}$$

Note that the diffusivity $\mathscr{D}_{23}$ does not appear here, because there is no relative motion of species 2 and 3. These equations can be integrated from an arbitrary height z to the top of the tube at L, to give for constant $c\mathscr{D}_{\alpha\beta}$

$$\int_{x_2}^{x_{2L}} \frac{dx_2}{x_2} = \frac{N_{1z}}{c\mathscr{D}_{12}} \int_z^L dz; \qquad \int_{x_3}^{x_{3L}} \frac{dx_3}{x_3} = \frac{N_{1z}}{c\mathscr{D}_{13}} \int_z^L dz \tag{18.8-4, 5}$$

Integration then gives

$$\frac{x_2}{x_{2L}} = \exp\left(-\frac{N_{1z}(L-z)}{c\mathscr{D}_{12}}\right); \qquad \frac{x_3}{x_{3L}} = \exp\left(-\frac{N_{1z}(L-z)}{c\mathscr{D}_{13}}\right) \tag{18.8-6, 7}$$

and the mole fraction profile of water vapor in the diffusion column will be

$$\boxed{x_1 = 1 - x_{2L} \exp\left(-\frac{N_{1z}(L-z)}{c\mathscr{D}_{12}}\right) - x_{3L} \exp\left(-\frac{N_{1z}(L-z)}{c\mathscr{D}_{13}}\right)} \tag{18.8-8}$$

When we apply the boundary condition at $z = 0$, we get

$$x_{10} = 1 - x_{2L} \exp\left(-\frac{N_{1z}L}{c\mathscr{D}_{12}}\right) - x_{3L} \exp\left(-\frac{N_{1z}L}{c\mathscr{D}_{13}}\right) \tag{18.8-9}$$

which is a transcendental equation for N_{1z}.

According to Reid, Prausnitz, and Poling,[1] $\mathscr{D}_{12} = 0.364$ cm^2/s and $\mathscr{D}_{13} = 0.357$ cm^2/s at 352K and 1 atm. At these conditions $c = 3.46 \times 10^{-5}$ g-moles/cm^3. To get a quick solution to Eq. 18.8-9, we take both diffusivities to be equal[2] to 0.36 cm^2/s. Then we get

$$0.449 = 1 - 0.90 \exp\left(- \frac{N_{1z}(11.2)}{(3.462 \times 10^{-5})(0.36)} \right) \tag{18.8-10}$$

from which we find that $N_{1z} = 5.523 \times 10^{-7}$ g-moles/cm^2 ·s. This can be used as a first guess in solving Eq. 18.8-9 more exactly, if desired. Then the entire profiles can be calculated from Eqs. 18.8-6 to 8.

QUESTIONS FOR DISCUSSION

1. What arguments are used in this chapter for eliminating N_B from Eq. 18.0-1?
2. Suggest ways in which the diffusivity $\mathscr{D}_{AB}$ could be measured by means of the examples in this chapter. Summarize possible sources of error.
3. In what limit do the concentration curves in Fig. 18.2-1 become straight lines?
4. Distinguish between homogeneous and heterogeneous reactions. Which ones are described by boundary conditions and which ones manifest themselves in the differential equations?
5. Discuss the term "diffusion-controlled reaction."
6. What kind of "device" would you suggest in the first sentence of §18.2 for maintaining the level of the interface constant?
7. Why is the left-hand term in Eq. 18.2-15 called the "evaporation rate"?
8. Explain carefully how Eq. 18.2-19 is set up.
9. Criticize Example 18.2-3. To what extent is it "just a schoolbook problem"? What do you learn from the problem?
10. In what sense can the quantity N_{Az} in Eq. 18.3-9 be interpreted as a local rate of chemical reaction?
11. How does the size of a bubble change as it moves upward in a liquid?
12. In what connection have you encountered Eq. 18.5-11 before?
13. What happens if you try to solve Eq. 18.7-8 by using exponentials instead of hyperbolic functions? How can we make the simpler choice ahead of time?
14. Compare and contrast the systems discussed in §§18.5 and 6 as regards the physical problems, the mathematical methods used to solve them, and the final expressions for the molar fluxes.

PROBLEMS

18A.1 Evaporation rate. For the system shown in Fig. 18.2-1, what is the evaporation rate in g/hr of CCl_3NO_2 (chloropicrin) into air at 25°C? Make the customary assumption that air is a "pure substance."

Total pressure	770 mm Hg
Diffusivity (CCl_3NO_2–air)	0.088 cm^2/s
Vapor pressure of CCl_3NO_2	23.81 mm Hg
Distance from liquid level to top of tube	11.14 cm
Density of CCl_3NO_2	1.65 g/cm^3
Surface area of liquid exposed for evaporation	2.29 cm^2

Answer: 0.0139 g/hr

---

[1] R. C. Reid, J. M. Prausnitz, and B. E. Poling, *The Properties of Gases and Liquids*, 4th edition, McGraw-Hill, New York (1987), p. 591.

[2] The solution to ternary diffusion problems in which two of the binary diffusivities are equal was discussed by H. L. Toor, *AIChE Journal*, **3**, 198–207 (1957).

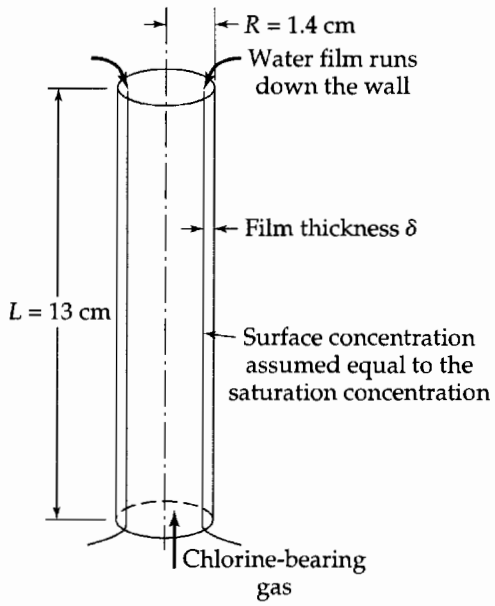

Fig. 18A.4. Schematic drawing of a wetted-wall column.

18A.2. Sublimation of small iodine spheres in still air. A sphere of iodine, 1 cm in diameter, is placed in still air at 40°C and 747 mm Hg pressure. At this temperature the vapor pressure of iodine is about 1.03 mm Hg. We want to determine the diffusivity of the iodine–air system by measuring the sublimation rate. To help determine reasonable experimental conditions,

(a) Estimate the diffusivity for the iodine–air system at the temperature and pressure given above, using the intermolecular force parameters in Table E.1.

(b) Estimate the rate of sublimation, basing your calculations on Eq. 18.2-27. (*Hint:* Assume r_2 to be very large.)

This method has been used for measuring the diffusivity, but it is open to question because of the possible importance of free convection.

Answer: **(a)** $\mathscr{D}_{I_2\text{-air}} = 0.0888$ cm^2/s; **(b)** $W_{I_2} = 1.06 \times 10^{-4}$ g-mole/hr

18A.3. Estimating the error in calculating the absorption rate. What is the maximum possible error in computing the absorption rate from Eq. 18.5-18, if the solubility of A in B is known within ±5% and the diffusivity of A in B is known within ±15%? Assume that the geometric quantities and the velocity are known very accurately.

18A.4. Chlorine absorption in a falling film (Fig. 18A.4). Chlorine is being absorbed from a gas in a small experimental wetted-wall tower as shown in the figure. The absorbing fluid is water, which is moving with an average velocity of 17.7 cm/s. What is the absorption rate in g-moles/hr, if the liquid-phase diffusivity of the chlorine–water system is 1.26×10^{-5} cm^2/s, and if the saturation concentration of chlorine in water is 0.823 g chlorine per 100 g water (these are the experimental values at 16°C). The dimensions of the column are given in the figure. (*Hint:* Ignore the chemical reaction between chlorine and water.)

Answer: 0.273 g-moles/hr

18A.5. Measurement of diffusivity by the point-source method (Fig. 18C.1).[1] We wish to design a flow system to utilize the results of Problem 18C.1 for the measure of $\mathscr{D}_{AB}$. The approaching

[1] This is the most precise method yet developed for measurements of diffusivity at high temperatures. For a detailed description of the method, see R. E. Walker and A. A. Westenberg, *J. Chem. Phys.*, **29**, 1139–1146, 1147–1153 (1958). For a summary of measured values and comparisons with the Chapman–Enskog theory, see R. M. Fristrom and A. A. Westenberg, *Flame Structure*, McGraw-Hill, New York (1965), Chapter XIII.

stream of pure B will be directed vertically upward, and the gas composition will be measured at several points along the z-axis.

(a) Calculate the gas-injection rate W_A in g-moles/s required to produce a mole fraction $x_A \approx 0.01$ at a point 1 cm downstream of the source, in an ideal gaseous system at 1 atm and 800°C, if $v_0 = 50$ cm/s and $\mathscr{D}_{AB} \approx 5$ cm^2/s.

(b) What is the maximum permissible error in the radial position of the gas-sampling probe, if the measured composition x_A is to be within 1% of the centerline value?

18A.6. Determination of diffusivity for ether–air system. The following data on the evaporation of ethyl ether, with liquid density of 0.712 g/cm^3, have been tabulated by Jost.[2] The data are for a tube of 6.16 mm diameter, a total pressure of 747 mm Hg, and a temperature of 22°C.

Decrease of the ether level (measured from the open end of the tube), in mm	Time, in seconds, required for the indicated decrease of level
from 9 to 11	590
from 14 to 16	895
from 19 to 21	1185
from 24 to 26	1480
from 34 to 36	2055
from 44 to 46	2655

The molecular weight of ethyl ether is 74.12, and its vapor pressure at 22°C is 480 mm Hg. It may be assumed that the ether concentration at the open end of the tube is zero. Jost has given a value of $\mathscr{D}_{AB}$ for the ether–air system of 0.0786 cm^2/s at 0°C and 760 mm Hg.

(a) Use the evaporation data to find $\mathscr{D}_{AB}$ at 747 mm Hg and 22°C, assuming that the arithmetic average gas-column lengths may be used for $z_2 - z_1$ in Fig. 18.2-1. Assume further that the ether–air mixture is ideal and that the diffusion can be regarded as binary.

(b) Convert the result to $\mathscr{D}_{AB}$ at 760 mm Hg and 0°C using Eq. 17-2-1.

18A.7. Mass flux from a circulating bubble.

(a) Use Eq. 18.5-20 to estimate the rate of absorption of CO_2 (component A) from a carbon dioxide bubble 0.5 cm in diameter rising through pure water (component B) at 18°C and at a pressure of 1 atm. The following data[3] may be used: $\mathscr{D}_{AB} = 1.46 \times 10^{-5}$ cm^2/s, $c_{A0} = 0.041$ g-mole/liter, $v_t = 22$ cm/s.

(b) Recalculate the rate of absorption, using the experimental results of Hammerton and Garner,[4] who obtained a surface-averaged k_c of 117 cm/hr (see Eq. 18.1-2).

Answers: **(a)** 1.17×10^{-6} g-mol/cm^2 s; **(b)** 1.33×10^{-6} g-mol/cm^2 s.

18B.1. Diffusion through a stagnant film—alternate derivation. In §18.2 an expression for the evaporation rate was obtained in Eq. 18.2-14 by differentiating the concentration profile found a few lines before. Show that the same results may be derived without finding the concentration profile. Note that at steady state, N_{Az} is a constant according to Eq. 18.2-3. Then Eq. 18.2-1 can be integrated directly to get Eq. 18.2-14.

---

[2] W. Jost, *Diffusion*, Academic Press, New York (1952), pp. 411–413.

[3] G. Tammann and V. Jessen, *Z. anorg. allgem. Chem.*, **179**, 125–144 (1929); F. H. Garner and D. Hammerton, *Chem. Eng. Sci.*, **3**, 1–11 (1954).

[4] D. Hammerton and F. H. Garner, *Trans. Inst. Chem. Engrs.* (London), **32**, S18-S24 (1954).

18B.2. Error in neglecting the convection term in evaporation.

(a) Rework the problem in the text in §18.2 by neglecting the term $x_A(\mathbf{N}_A + \mathbf{N}_B)$ in Eq. 18.0-1. Show that this leads to

$$N_{Az} = \frac{c\mathscr{D}_{AB}}{z_2 - z_1}(x_{A1} - x_{A2}) \tag{18B.2-1}$$

This is a useful approximation if A is present only in very low concentrations.

(b) Obtain the result in (a) from Eq. 18.2-14 by making the appropriate approximation.

(c) What error is made in the determination of $\mathscr{D}_{AB}$ in Example 18.2-2 if the result in (a) is used?

Answer: 0.78%

18B.3. Effect of mass transfer rate on the concentration profiles.

(a) Combine the result in Eq. 18.2-11 with that in Eq. 18.2-14 to get

$$\frac{1 - x_A}{1 - x_{A1}} = \exp\left(\frac{N_{Az}(z - z_1)}{c\mathscr{D}_{AB}}\right) \tag{18B.3-1}$$

(b) Obtain the same result by integrating Eq. 18.2-1 directly, using the fact that N_{Az} is constant.

(c) Note what happens when the mass transfer rate becomes small. Expand Eq. 18B.3-1 in a Taylor series and keep two terms only, as is appropriate for small N_{Az}. What happens to the slightly curved lines in Fig. 18.2-1 when N_{Az} is very small?

18B.4. Absorption with chemical reaction.

(a) Rework the problem discussed in the text in §18.4, but take $z = 0$ to be the bottom of the beaker and $z = L$ at the gas–liquid interface.

(b) In solving Eq. 18.4-7, we took the solution to be of the sum of two hyperbolic functions. Try solving the problem by using the equally valid solution $\Gamma = C_1 \exp(\phi\zeta) + C_2 \exp(-\phi\zeta)$.

(c) In what way do the results in Eqs. 18.4-10 and 12 simplify for very large L? For very small L? Interpret the results physically.

18B.5. Absorption of chlorine by cyclohexene. Chlorine can be absorbed from Cl_2–air mixtures by olefins dissolved in CCl_4. It was found[5] that the reaction of Cl_2 with cyclohexene (C_6H_{10}) is second order with respect to Cl_2 and zero order with respect to C_6H_{10}. Hence the rate of disappearance of Cl_2 per unit volume is $k_2''' c_A^2$ (where A designates Cl_2).

Rework the problem of §18.4 where B is a C_6H_{10}–CCl_4 mixture, assuming that the diffusion can be treated as pseudobinary. Assume that the air is essentially insoluble in the C_6H_{10}–CCl_4 mixture. Let the liquid phase be sufficiently deep that L can be taken to be infinite.

(a) Show that the concentration profile is given by

$$\frac{c_{A0}}{c_A} = \left[1 + \sqrt{\frac{k_2''' c_{A0}}{6\mathscr{D}_{AB}}}\, z\right]^2 \tag{18B.5-1}$$

(b) Obtain an expression for the rate of absorption of Cl_2 by the liquid.

(c) Suppose that a substance A dissolves in and reacts with substance B so that the rate of disappearance of A per unit volume is some arbitrary function of the concentration, $f(c_A)$. Show that the rate of absorption of A is given by

$$N_{Az}|_{z=0} = \sqrt{2\mathscr{D}_{AB}\int_0^{c_{A0}} f(c_A)\,dc_A} \tag{18B.5-2}$$

Use this result to check the result of (b).

---

[5] G. H. Roper, *Chem. Eng. Sci.*, **2**, 18–31, 247–253 (1953).

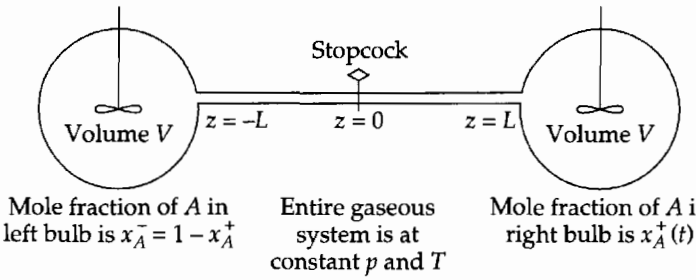

Fig. 18B.6. Sketch of a two-bulb apparatus for measuring gas diffusivities. The stirrers in the two bulbs maintain uniform concentration in the bulbs.

18B.6. Two-bulb experiment for measuring gas diffusivity—quasi-steady-state analysis[6] (Fig. 18B.6). One way of measuring gas diffusivities is by means of a two-bulb experiment. The left bulb and the tube from $z = -L$ to $z = 0$ are filled with gas A. The right bulb and the tube from $z = 0$ to $z = +L$ are filled with gas B. At time $t = 0$ the stopcock is opened, and diffusion begins; then the concentrations of A in the two well-stirred bulbs change. One measures x_A^+ as a function of time, and from this deduces $\mathscr{D}_{AB}$. We wish to derive the equations describing the diffusion.

Since the bulbs are large compared with the tube, x_A^+ and x_A^- change *very slowly* with time. Hence the diffusion in the tube can be treated as a quasi-steady-state problem, with the boundary conditions that $x_A = x_A^-$ and $z = -L$, and that $x_A = x_A^+$ at $z = +L$.

(a) Write a molar balance on A over a segment Δz of the tube (of cross-sectional area S), and show that $N_{Az} = C_1$, a constant.

(b) Show that Eq. 18.0-1 simplifies, for this problem, to

$$N_{Az} = -c\mathscr{D}_{AB}\frac{dx_A}{dz} \tag{18B.6-1}$$

(c) Integrate this equation, using (a). Call the constant of integration C_2.

(d) Evaluate the constant by requiring that $x_A = x_A^i$ at $z = +L$.

(e) Next set $x_A = x_A^-$ (or $1 - x_A^+$) at $z = -L$, and solve for N_{Az} to get finally

$$N_{Az} = (\tfrac{1}{2} - x_A^+)\frac{c\mathscr{D}_{AB}}{L} \tag{18B.6-2}$$

(f) Make a mass balance on substance A over the right bulb to obtain

$$S(\tfrac{1}{2} - x_A^+)\frac{c\mathscr{D}_{AB}}{L} = Vc\frac{dx_A^+}{dt} \tag{18B.6-3}$$

(g) Integrate the equation in (f) to get an expression for x_A^+ which contains $\mathscr{D}_{AB}$:

$$\ln\left(\frac{\frac{1}{2} - x_A^+}{\frac{1}{2}}\right) = -\frac{S\mathscr{D}_{AB}t}{LV} \tag{18B.6-4}$$

(h) Suggest a method of plotting the experimental data to evaluate $\mathscr{D}_{AB}$.

18B.7. Diffusion from a suspended droplet (Fig. 18.2-4). A droplet of liquid A, of radius r_1, is suspended in a stream of gas B. We postulate that there is a spherical stagnant gas film of radius r_2 surrounding the droplet. The concentration of A in the gas phase is x_{A1} at $r = r_1$ and x_{A2} at the outer edge of the film, $r = r_2$.

(a) By a shell balance, show that for steady-state diffusion r^2N_{Ar} is a constant within the gas film, and set the constant equal to $r_1^2N_{Ar1}$, the value at the droplet surface.

(b) Show that Eq. 18.0-1 and the result in (a) lead to the following equation for x_A:

$$r_1^2N_{Ar1} = -\frac{c\mathscr{D}_{AB}}{1 - x_A}r^2\frac{dx_A}{dr} \tag{18B.7-1}$$

---

[6] S. P. S. Andrew, *Chem. Eng. Sci.*, **4**, 269–272 (1955).

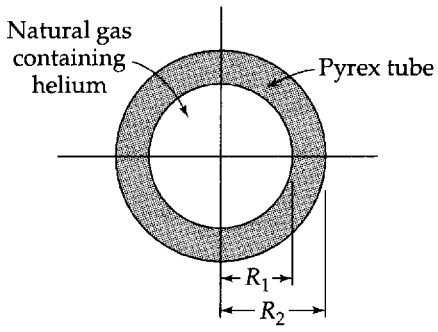

Fig. 18B.8. Diffusion of helium through pyrex tubing. The length of the tubing is L.

(c) Integrate this equation between the limits r_1 and r_2 to get

$$N_{Ar1} = \frac{c\mathcal{D}_{AB}}{r_2 - r_1}\left(\frac{r_2}{r_1}\right)\ln\frac{x_{B2}}{x_{B1}} \tag{18B.7-2}$$

What is the limit of this expression when $r_2 \rightarrow \infty$?

18B.8. Method for separating helium from natural gas (Fig. 18B.8). Pyrex glass is almost impermeable to all gases but helium. For example, the diffusivity of He through pyrex is about 25 times the diffusivity of H_2 through pyrex, hydrogen being the closest "competitor" in the diffusion process. This fact suggests that a method for separating helium from natural gas could be based on the relative diffusion rates through pyrex.[7]

Suppose a natural gas mixture is contained in a pyrex tube with dimensions shown in the figure. Obtain an expression for the rate at which helium will "leak" out of the tube, in terms the diffusivity of helium through pyrex, the interfacial concentrations of the helium in the pyrex, and the dimensions of the tube.

Answer: $W_{He} = 2\pi L \dfrac{\mathcal{D}_{\text{He-Pyrex}}(c_{\text{He},1} - c_{\text{He},2})}{\ln (R_2/R_1)}$

18B.9. Rate of leachng (Fig. 18B.9). In studying the rate of leaching of a substance A from solid particles by a solvent B, we may postulate that the rate-controlling step is the diffusion of A from the particle surface through a stagnant liquid film thickness δ out into the main stream. The molar solubility of A in B is c_{A0}, and the concentration in the main stream is $c_{A\delta}$.

(a) Obtain a differential equation for c_A as a function of z by making a mass balance on A over a thin slab of thickness Δz. Assume that $\mathcal{D}_{AB}$ is constant and that A is only slightly soluble in B. Neglect the curvature of the particle.

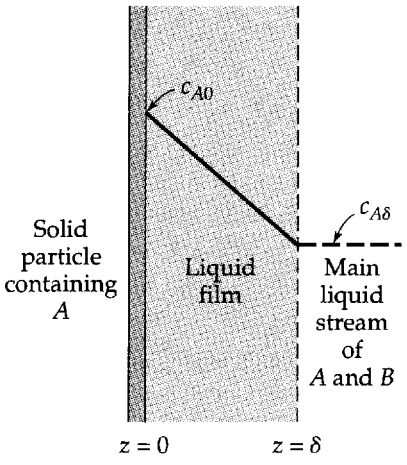

Fig. 18B.9. Leaching of A by diffusion into a stagnant liquid film of B.

[7] *Scientific American*, **199**, 52 (1958) describes briefly the method developed by K. B. McAfee of Bell Telephone Laboratories.

(b) Show that, in the absence of chemical reaction in the liquid phase, the concentration profile is linear.

(c) Show that the rate of leaching is given by

$$N_{Az} = \mathscr{D}_{AB}(c_{A0} - c_{A\delta})/\delta \tag{18B.9-1}$$

18B.10 Constant-evaporating mixtures. Toluene (1) and ethanol (2) are evaporating at $z = 0$ in a vertical tube, from a binary liquid mixture of uniform composition x_1 through stagnant nitrogen (3), with pure nitrogen at the top. The unequal diffusivities of toluene and ethanol through nitrogen shift the relative evaporation rates in favor of ethanol. Analyze this effect for an isothermal system at 60 F and 760 mm Hg total pressure, if the predicted[8] diffusivities at 60° F are $c\mathscr{D}_{12} = 1.53 \times 10^{-6}$, $c\mathscr{D}_{13} = 2.98 \times 10^{-6}$, $c\mathscr{D}_{23} = 4.68 \times 10^{-6}$ g-moles/cm · s.

(a) Use the Maxwell-Stefan equations to obtain the steady-state vapor-phase mole fraction profiles $y_\alpha(z)$ in terms of the molar fluxes $N_{\alpha z}$ in this ternary system. The molar fluxes are known to be constants from the equations of continuity for the three species. Since nitrogen has a negligible solubility in the liquid at the conditions given, $N_{3z} = 0$. As boundary conditions, set $y_1 = y_2 = 0$ at $z = L$, and let $y_1 = y_{10}$ and $y_2 = y_{20}$ at $z = 0$; the latter values remain to be determined. Show that

$$y_3(z) = e^{-A(L-z)}; \qquad y_1(z) = \frac{D}{A-B}e^{-A(L-z)} - \left(\frac{C}{B} + \frac{D}{A-B}\right)e^{-B(L-z)} + \frac{C}{B} \tag{18B.10-1}$$

$$A = \frac{N_{1z}}{c\mathscr{D}_{13}} + \frac{N_{2z}}{c\mathscr{D}_{23}}; \qquad B = \frac{N_{1z} + N_{2z}}{c\mathscr{D}_{12}}; \qquad C = \frac{N_{1z}}{c\mathscr{D}_{12}}; \qquad D = \frac{N_{1z}}{c\mathscr{D}_{12}} - \frac{N_{1z}}{c\mathscr{D}_{13}} \tag{18B.10-2}$$

(b) A constant evaporating liquid mixture is one whose composition is the same as that of the evaporated material, that is, for which $N_{1z}/(N_{1z} + N_{2z}) = x_1$. Use the results of part (a) along with the equilibrium data in the table below to calculate the constant-evaporating liquid composition at a total pressure of 760 mm Hg. In the table, row I gives liquid-phase compositions. Row II gives vapor-phase compositions in two-component experiments; these are expressed as nitrogen-free values $y_1/(y_1 + y_2)$ for the ternary system. Row III gives the sum of the partial pressures of toluene and ethanol.

I:	x_1	0.096	0.155	0.233	0.274	0.375
II:	$y_1/(y_1 + y_2)$	0.147	0.198	0.242	0.256	0.277
III:	$p_1 + p_2$ (mm Hg)	388	397	397	395	390

A suggested strategy for the calculation is as follows: (i) guess a liquid composition x_1; (ii) calculate y_{10}, y_{20}, and y_{30} using lines 2 and 3 of the table; (iii) calculate A from Eq. 18B.10-1, with $z = 0$; (iv) use the result of iii to calculate LN_{2z}, LB, LC, and LD, and finally y_1 (0) for assumed values of LN_{1z}; (v) interpolate the results of iv to y_1 (0) = y_{10} to obtain the correct LN_{1z} and LN_{2z} for the guessed x_1. Repeat steps i–v with improved guesses for x_1 until $N_{1z}/(N_{1z} + N_{2z})$ converges to x_1. The final x_1 is the constant evaporating composition.

18B.11. Diffusion with fast second-order reaction (Figs. 18.2-2 and 18B.11). A solid A is dissolving in a flowing liquid stream S in a steady-state, isothermal flow system. Assume in accordance with the film model that the surface of A is covered with a stagnant liquid film of thickness δ and that the liquid outside the film is well mixed (see Fig. 18.2-2).

(a) Develop an expression for the rate of dissolution of A into the liquid if the concentration of A in the main liquid stream is negligible.

(b) Develop a corresponding expression for the dissolution rate if the liquid contains a substance B, which, at the plane $z = \kappa\delta$, reacts instantaneously and irreversibly with A: $A + B \rightarrow P$. (An example of such a system is the dissolution of benzoic acid in an aqueous NaOH solution.) The main liquid stream consists primarily of B and S, with B at a mole fraction of $x_{B\infty}$.

---

[8] L. Monchick and E. A. Mason, *J. Chem. Phys.*, **35**, 1676–1697 (1961), with δ read as δ_{max} in Table IV; E. A. Mason and L. Monchick, *J. Chem. Phys.*, **36**, 2746–2757 (1962); L. S. Tee, S. Gotoh, and W. E. Stewart, *Ind. Eng. Chem. Fundam.*, **5**, 356–362 (1966).

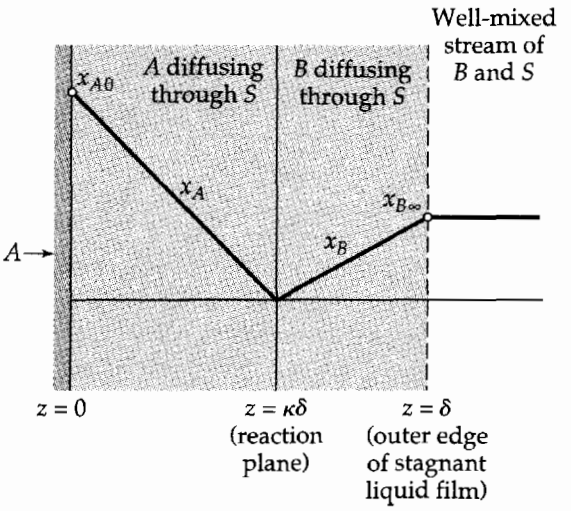

Fig. 18B.11. Concentration profiles for diffusion with rapid second-order reaction. The concentration of product P neglected.

(*Hint:* It is necessary to recognize that species A and B both diffuse toward a thin reaction zone as shown in Fig. 18B.11.)

Answers: **(a)** $N_{Az}|_{z=0} = \left(\frac{c\mathscr{D}_{AS}x_{A0}}{\delta}\right)$; **(b)** $N_{Az}|_{z=0} = \left(\frac{c\mathscr{D}_{AS}x_{A0}}{\delta}\right)\left(1 + \frac{x_{B\infty}\mathscr{D}_{BS}}{x_{A0}\mathscr{D}_{AS}}\right)$

18B.12. A sectioned-cell experiment[9] for measuring gas-phase diffusivity (Fig. 18B.12). Liquid A is allowed to evaporate through a stagnant gas B at 741 mm Hg total pressure and 25°C. At that temperature, the vapor pressure of A is known to be 600 mm Hg. After steady state has been

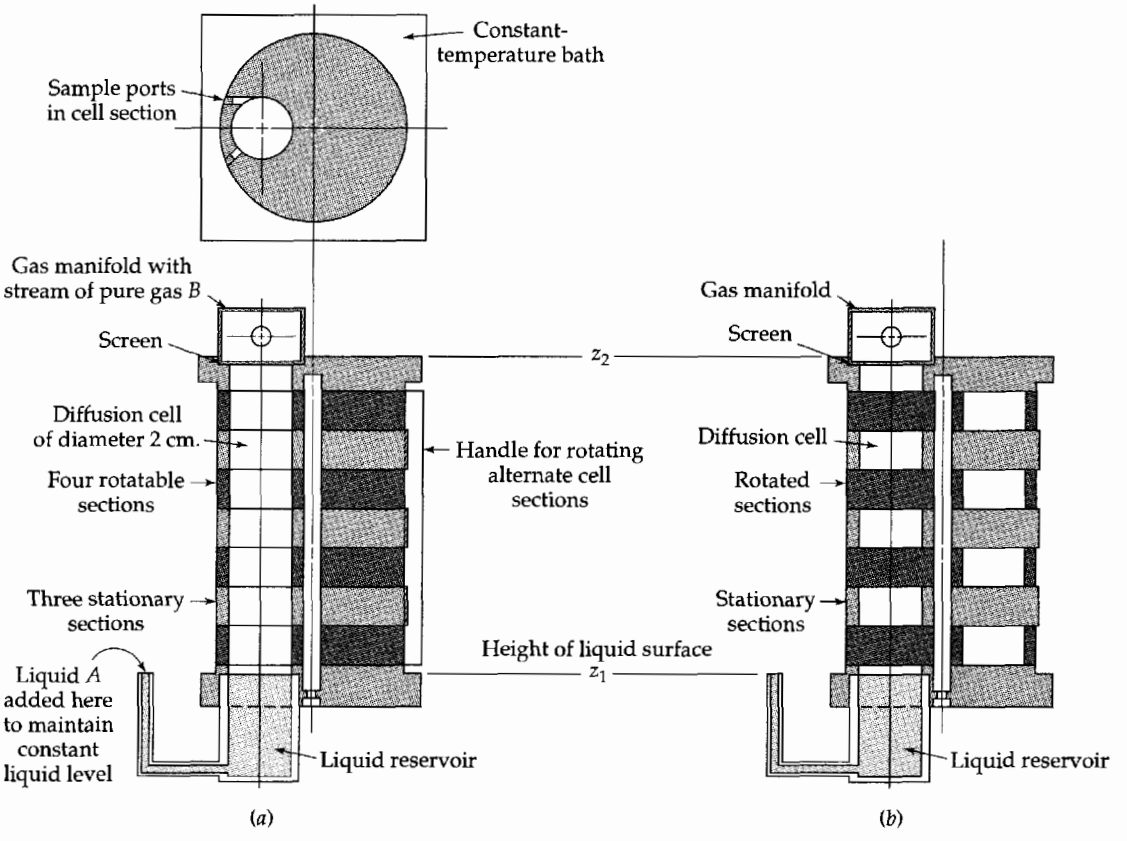

Fig. 18B.12. A sectioned-cell experiment for measuring gas diffusivities. (*a*) Cell configuration during the approach to steady-state. (*b*) Cell configuration for gas sampling at the end of the experiment.

[9] E. J. Crosby, *Experiments in Transport Phenomena*, Wiley, New York (1961), Experiment 10.a.

attained, the cylindrical column of gas is divided into sections as shown. For a 4-section apparatus with total height 4.22 cm, the analysis of the gas samples thus obtained gives the following results:

	$(z - z_1)$ in cm		
Section	Bottom of section	Top of section	Mole fraction of A
I	0.10	1.10	0.757
II	1.10	2.10	0.641
III	2.10	3.10	0.469
IV	3.10	4.10	0.215

The measured evaporation rate of A at steady state is 0.0274 g-moles/hr. Ideal gas behavior may be assumed.

(a) Verify the following expression for the concentration profile at steady state:

$$\ln \frac{x_{B2}}{x_B} = \frac{N_{Az}(z_2 - z)}{c\mathscr{D}_{AB}} \tag{18B.12-1}$$

(b) Plot the mole fraction x_B in each cell versus the value of z at the midplane of the cell on semilogarithmic graph paper. Is a straight line obtained? What are the intercepts at z_1 and z_2? Interpret these results.

(c) Use the concentration profile of Eq. 18B.12-1 to find analytical expressions for the average concentrations in each section of the tube.

(d) Find the best value of $\mathscr{D}_{AB}$ from this experiment.

Answer: **(d)** 0.155 cm^2/s

18B.13. Tarnishing of metal surfaces. In the oxidation of most metals (excluding the alkali and alkaline-earth metals) the volume of oxide produced is greater than that of the metal consumed. This oxide thus tends to form a compact film, effectively insulating the oxygen and metal from each other. For the derivations that follow, it may be assumed that

(a) For oxidation to proceed, oxygen must diffuse through the oxide film and that this diffusion follows Fick's law.

(b) The free surface of the oxide film is saturated with oxygen from the surrounding air.

(c) Once the film of oxide has become reasonably thick, the oxidation becomes diffusion controlled; that is, the dissolved oxygen concentration is essentially zero at the oxide-metal surface.

(d) The rate of change of dissolved oxygen content of the film is small compared to the rate of reaction. That is, quasi-steady-state conditions may be assumed.

(e) The reaction involved is $\frac{1}{2}xO_2 + M \rightarrow MO_x$.

We wish to develop an expression for rate of tarnishing in terms of oxygen diffusivity through the oxide film, the densities of the metal and its oxide, and the stoichiometry of the reaction. Let c_O be the solubility of oxygen in the film, c_f the molar density of the film, and z_f the thickness of the film. Show that the film thickness is

$$z_f = \sqrt{\frac{2\mathscr{D}_{O_2-MO_x}t}{x}\frac{c_O}{c_f}} \tag{18B.13-1}$$

This result, the so-called "quadratic law," gives a satisfactory empirical correlation for a number of oxidation and other tarnishing reactions.[10] Most such reactions are, however, much more complex than the mechanism given above.[11]

---

[10] G. Tammann, Z. *anorg. allgem. Chemie*, **124**, 25–35 (1922).

[11] W. Jost, Diffusion, *Academic Press*, New York (1952), Chapter IX. For a discussion of the oxidation of silicon, see R. Ghez, *A Primer of Diffusion Problems*, Wiley, New York (1988), §2.3.

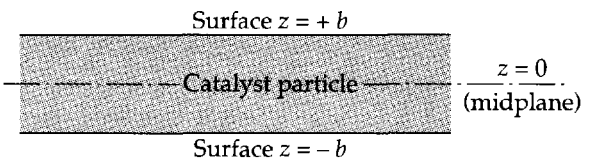

Fig. 18B.14. Side view of a disk-shaped catalyst particle.

18B.14. Effectiveness factors for thin disks (Fig. 18B.14). Consider porous catalyst particles in the shape of thin disks, such that the surface area of the edge of the disk is small in comparison with that of the two circular faces. Apply the method of §18.7 to show that the steady-state concentration profile is

$$\frac{c_A}{c_{As}} = \frac{\cosh\sqrt{k_1''a/\mathcal{D}_A}\,z}{\cosh\sqrt{k_1''a/\mathcal{D}_A}\,b} \tag{18B.14-1}$$

where z and b are described in the figure. Show that the total mass transfer rate at the surfaces $z = \pm b$ is

$$|W_A| = 2\pi R^2 c_{As}\mathcal{D}_A\lambda \tanh \lambda b \tag{18B.14-2}$$

in which $\lambda = \sqrt{k_1''a/\mathcal{D}_A}$. Show that, if the disk is sliced parallel to the xy-plane into n slices, the total mass transfer rate becomes

$$|W_A^{(n)}| = 2\pi R^2 c_{As}\mathcal{D}_A\lambda n \tanh(\lambda b/n) \tag{18B.14-3}$$

Obtain the expression for the effectiveness factor by taking the limit

$$\eta_A = \lim_{n\to\infty} \frac{|W_A|}{|W_A^{(n)}|} = \frac{\tanh \lambda b}{\lambda b} \tag{18B.14-4}$$

Express this result in terms of the parameter Λ defined in §18.6.

18B.15. Diffusion and heterogeneous reaction in a slender cylindrical tube with a closed end (Fig. 18B.15). A slender cylindrical pore of length L, cross-sectional area S, and perimeter P, is in contact at its open end with a large body of well-mixed fluid, consisting of species A and B. Species A, a minor constituent of this fluid, disappears into the pore, diffuses in the z direction and reacts on its walls. The rate of this reaction may be expressed as $(\mathbf{n}\cdot\mathbf{n}_A)|_{\text{surface}} = f(\omega_{A0})$; that is, at the wall the mass flux normal to the surface is some function of the mass fraction, ω_{A0}, of A in the fluid adjacent to the solid surface. The mass fraction ω_{A0} depends on z, the distance from the inlet. Because A is present in low concentration, the fluid temperature and density may be considered constant, and the diffusion flux is adequately described by $\mathbf{j}_A = -\rho\mathcal{D}_{AB}\nabla\omega_A$,

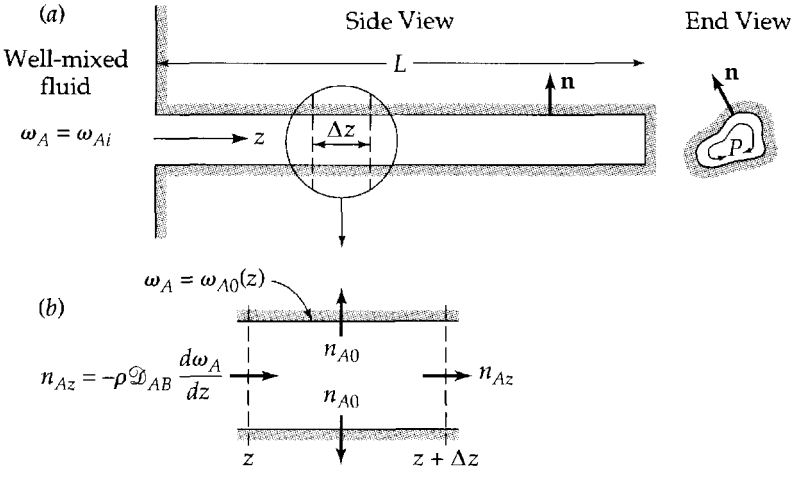

Fig. 18B.15. (*a*) Diffusion and heterogeneous reaction in a long, noncircular cylinder. (*b*) Region of thickness Δz over which the mass balance is made.

where the diffusivity may be regarded as a constant. Because the pore is long compared to its lateral dimension, concentration gradients in the lateral directions may be neglected. Note the similarity with the problem discussed in §10.7.

(a) Show by means of a shell balance that, at steady state,

$$-\frac{dn_{Az}}{dz} = \frac{P}{S} f(\omega_{A0}) \tag{18B.15-1}$$

(b) Show that the steady-state mass average velocity v_z is zero for this system.

(c) Substitute the appropriate form of Fick's law into Eq. 18.15-1, and integrate the resulting differential equation for the special case that $f(\omega_{A0}) = k_1''\omega_{A0}$. To obtain a boundary condition at $z = L$, neglect the rate of reaction on the closed end of the cylinder; why is this a reasonable approximation?

(d) Develop an expression for the total rate w_A of disappearance of A in the cylinder.

(e) Compare the results of parts (c) and (d) with those of §10.7 both from the standpoint of the mathematical development and the nature of the assumptions made.

Answers: **(c)** $\dfrac{\omega_A}{\omega_{Ai}} = \dfrac{\cosh N[1 - (z/L)]}{\cosh N}$, where $N = \sqrt{\dfrac{PL^2k_1''}{S\rho\mathscr{D}_{AB}}}$; **(d)** $w_A = (S\rho\mathscr{D}_{AB}\omega_{Ai}/L)N \tanh N$

18B.16. Effect of temperature and pressure on evaporation rate.

(a) In §18.2 what is the effect of a change of temperature and pressure on the quantity x_{A1}?

(b) If the pressure is doubled, how is the evaporation rate in Eq. 18.2-14 affected?

(c) How does the evaporation rate change when the system temperature is raised from T to T'?

18B.17. Reaction rates in large and small particles.

(a) Obtain the following limits for Eq. 18.7-11:

$$R \to 0: \qquad W_{AR} = -(\tfrac{4}{3}\pi R^3)(k_1''a)c_{AR} \tag{18B.17-1}$$

$$R \to \infty: \qquad W_{AR} = -(4\pi R^2)(k_1''a\mathscr{D}_A)^{1/2}c_{AR} \tag{18B.17-2}$$

Interpret these results physically.

(b) Obtain the corresponding asymptotes for the system discussed in Problem 18B.14. Compare them with the results in (a).

18B.18. Evaporation rate for small mole fraction of the volatile liquid. In Eq. 18.2-15, expand

$$\frac{1}{(x_B)_{\ln}} = \left(\frac{1}{x_{A1} - x_{A2}}\right)\left(\ln \frac{1 - x_{A2}}{1 - x_{A1}}\right) \tag{18B.18-1}$$

in a Taylor series appropriate for small mole fractions of A. First rewrite the logarithm of the quotient as the difference of the logarithms. Then expand $\ln(1 - x_{A1})$ and $\ln(1 - x_{A2})$ in Taylor series about $x_{A1} = 1$ and $x_{A2} = 1$, respectively. Verify that Eq. 18.2-16 is correct.

18B.19. Oxygen uptake by a bacterial aggregate. Under suitable circumstances the rate of oxygen metabolism by bacterial cells is very nearly zero order with respect to oxygen concentration. We examine such a case here and focus our attention on a spherical aggregate of cells, which has a radius R. We wish to determine the total rate of oxygen uptake by the aggregate as a function of aggregate size, oxygen mass concentration ρ_0 at the aggregate surface, the metabolic activity of the cells, and the diffusional behavior of the oxygen. For simplicity we consider the aggregate to be homogeneous. We then approximate the metabolic rate by an effective volumetric reaction rate $r_{O_2} = -k_0'''$ and the diffusional behavior by Fick's law, with an effective pseudobinary diffusivity $\mathscr{D}_{O_2m}$. Because the solubility of oxygen is very low in this system, both convective oxygen transport and transient effects may be neglected.[12]

---

[12] J. A. Mueller, W. C. Boyle, and E. N. Lightfoot, *Biotechnol. and Bioengr.*, **10**, 331–358 (1968).

(a) Show by means of a shell mass balance that the quasi-steady-state oxygen concentration profile is described by the differential equation

$$\frac{1}{\xi^2}\frac{d}{d\xi}\left(\xi^2\frac{d\chi}{d\xi}\right) = N \tag{18B.19-1}$$

where $\chi = \rho_{O_2}/\rho_0$, $\xi = r/R$, and $N = k_0'''R^2/\rho_0\mathcal{D}_{O_2m}$.

(b) There may be an oxygen-free core in the aggregate, if N is sufficiently large, such that $\chi = 0$ for $\xi < \xi_0$. Write sufficient boundary conditions to integrate Eq. 18B.19-1 for this situation. To do this, it must be recognized that both χ and $d\chi/d\xi$ are zero at $\xi = \xi_0$. What is the physical significance of this last statement?

(c) Perform the integration of Eq. 18B.19-1 and show how ξ_0 may be determined.

(d) Sketch the total oxygen uptake rate and ξ_0 as functions of N, and discuss the possibility that no oxygen-free core exists.

Answer: **(c)** $\chi = 1 - \frac{N}{6}(1-\xi^2) + \frac{N}{3}\xi_0^3\left(\frac{1}{\xi} - 1\right)$ for $\xi \geq \xi_0 \geq 0$, where ξ_0 is determined as a function of N from

$$\xi_0^3 - \frac{3}{2}\xi_0^2 + \left(\frac{1}{2} - \frac{3}{N}\right) = 0$$

18C.1. Diffusion from a point source in a moving stream (Fig. 18C.1). A stream of fluid B in laminar motion has a uniform velocity v_0. At some point in the stream (taken to be the origin of coordinates) species A is injected at a small rate W_A g-moles/s. This rate is assumed to be sufficiently small that the mass average velocity will not deviate appreciably from v_0. Species A is swept downstream (in the z direction), and at the same time it diffuses both axially and radially.

(a) Show that a steady-state mass balance on species A over the indicated ring-shaped element leads to the following partial differential equation if $\mathcal{D}_{AB}$ is assumed to be constant:

$$v_0\frac{\partial c_A}{\partial z} = \mathcal{D}_{AB}\left[\frac{1}{r}\frac{\partial}{\partial r}\left(r\frac{\partial c_A}{\partial r}\right) + \frac{\partial^2 c_A}{\partial z^2}\right] \tag{18C.1-1}$$

(b) Show that Eq. 18C.1-1 can also be written as

$$v_0\left(\frac{z}{s}\frac{\partial c_A}{\partial s} + \frac{\partial c_A}{\partial z}\right) = \mathcal{D}_{AB}\left[\frac{1}{s^2}\frac{\partial}{\partial s}\left(s^2\frac{\partial c_A}{\partial s}\right) + \frac{\partial^2 c_A}{\partial z^2} + 2\frac{z}{s}\frac{\partial^2 c_A}{\partial s\partial z}\right] \tag{18C.1-2}$$

in which $s^2 = r^2 + z^2$.

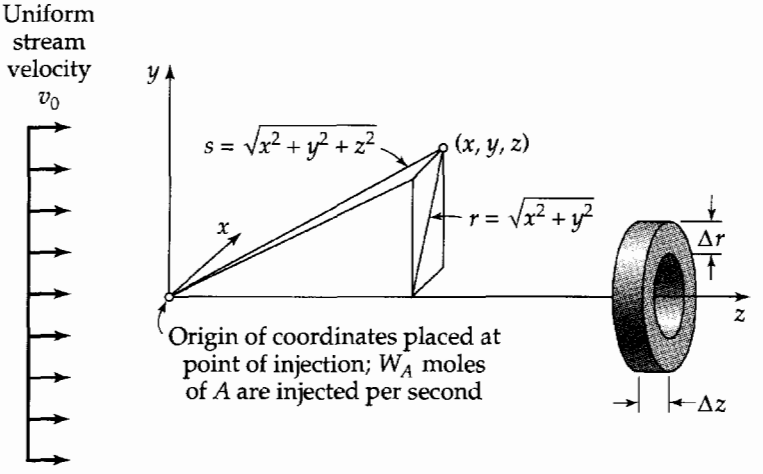

Fig. 18C.1. Diffusion of A from a point source into a stream of B that moves with a uniform velocity.

(c) Verify (lengthy!) that the solution

$$c_A = \frac{W_A}{4\pi \mathscr{D}_{AB} s} \exp[-(v_0/2\mathscr{D}_{AB})(s - z)] \tag{18C.1-3}$$[13]

satisfies the differential equation above.

(d) Show further that the following boundary conditions are also satisfied by Eq. 18C.1-3:

B.C. 1: $\quad$ at $s = \infty$, $\quad c_A = 0$ (18C.1-4)

B.C. 2: $\quad$ as $s \to 0$, $\quad -4\pi s^2 \mathscr{D}_{AB} \frac{\partial c_A}{\partial s} \to W_A$ (18C.1-5)

B.C. 3: $\quad$ at $r = 0$, $\quad \frac{\partial c_A}{\partial r} = 0$ (18C.1-6)

Explain the physical meaning of each of these boundary conditions.

(e) Show how data on $c_A(r, z)$ for given v_0 and $\mathscr{D}_{AB}$ may be plotted, when the preceding solution applies, to give a straight line with slope $v_0/2\mathscr{D}_{AB}$ and intercept $\ln \mathscr{D}_{AB}$.

18C.2. Diffusion and reaction in a partially impregnated catalyst. Consider a catalytic sphere like that in §18.7, except that the active ingredient of the catalyst is present only in the annular region between $r = \kappa R$ and $r = R$:

In region I $(0 < r < \kappa R)$, $\quad k_1'' a = 0$ (18C.2-1)

In region II $(\kappa R < r < R)$, $\quad k_1'' a = \text{constant} > 0$ (18C.2-2)

Such a situation may arise when the active ingredient is put on the particles after pelleting, as is done for many commercial catalysts.

(a) Integrate Eq. 18.7-6 separately for the active and inactive regions. Then apply the appropriate boundary conditions to evaluate the integration constants, and solve for the concentration profile in each region. Give qualitative sketches to illustrate the forms of the profiles.

(b) Evaluate W_{AR}, the total molar rate of conversion of A in a single particle.

18C.3. Absorption rate in a falling film. The result in Eq. 18.5-18 may be obtained by an alternative procedure.

(a) According to an overall mass balance on the film, the total moles of A transferred per unit time across the gas–liquid interface must be the same as the total molar rate of flow of A across the plane $z = L$. The latter rate is calculated as follows:

$$W_A = \lim_{\delta \to \infty} (W\delta v_{\max}) \left(\frac{1}{\delta} \int_0^{\delta} c_A|_{z=L} \, dx \right) = W v_{\max} \int_0^{\infty} c_A|_{z=L} \, dx \tag{18C.3-1}$$

Explain this procedure carefully.

(b) Insert the solution for c_A in Eq. 18.5-15 into the result of (a) to obtain:

$$\begin{aligned} W_A &= W v_{\max} c_{A0} \frac{2}{\sqrt{\pi}} \int_0^{\infty} \left(\int_{x/\sqrt{4\mathscr{D}_{AB}L/v_{\max}}}^{\infty} \exp(-\xi^2) \, d\xi \right) dx \\ &= W v_{\max} c_{A0} \frac{2}{\sqrt{\pi}} \sqrt{\frac{4\mathscr{D}_{AB}L}{v_{\max}}} \int_0^{\infty} \left(\int_u^{\infty} \exp(-\xi^2) \, d\xi \right) du \end{aligned} \tag{18C.3-2}$$

In the second line, the new variable $u = x/\sqrt{4\mathscr{D}_{AB}L/v_{\max}}$ has been introduced.

(c) Change the order of integration in the double integral, to get

$$W_A = W L c_{A0} \sqrt{\frac{4\mathscr{D}_{AB} v_{\max}}{\pi L}} \cdot 2 \int_0^{\infty} \exp(-\xi^2) \left(\int_0^{\xi} du \right) d\xi \tag{18C.3-3}$$

Explain by means of a carefully drawn sketch how the limits are chosen for the integrals The integrals may now be done analytically to get Eq. 18.5-18.

18C.4. Estimation of the required length of an isothermal reactor (Fig. 18.3-1). Let a be the area of catalyst surface per unit volume of a packed-bed catalytic reactor and S be the cross-sectional area of the reactor. Suppose that the rate of mass flow through the reactor is w (in lb_m/hr, for example).

(a) Show that a steady-state mass balance on substance A over a length dl of the reactor leads to

$$\frac{d\omega_{A0}}{dl} = -\frac{SaN_AM_A}{w} \tag{18C.4-1}$$

(b) Use the result of (a) and Eq. 18.3-9, with the assumptions of constant δ and $\mathscr{D}_{AB}$, to obtain an expression for the reactor length L needed to convert an inlet stream of composition $x_A(0)$ to an outlet stream of composition $x_A(L)$.

(*Hint:* Equation (P) of Table 17.8-1 may be useful.)

Answer: **(b)** $L = \left(\frac{w\delta M_B}{2Sac\,\mathscr{D}_{AB}}\right)\int_{x_A(0)}^{x_A(L)} \frac{dx_{A0}}{[M_Ax_{A0} + M_B(1 - x_{A0})]^2 \ln(1 - \frac{1}{2}x_{A0})}$

18C.5. Steady-state evaporation. In a study of the evaporation of a mixture of methanol (1) and acetone (2) through air (3), the concentration profiles of the three species in the tube were measured[14] after attainment of steady state. In this situation, species 3 is not moving, and species 1 and 2 are diffusing upward, with the molar fluxes N_{z1} and N_{z2}, measured in the experiments. The interfacial concentrations of these two species, x_{10} and x_{20}, were also measured. In addition, the three binary diffusion coefficients were known. The interface was located at $z = 0$ and the upper end of the diffusion tube was at $z = L$.

(a) Show that the Maxwell–Stefan equation for species 3 can be solved to get

$$x_3 = x_{30}e^{A\zeta} \tag{18C.5-1}$$

in which $A = \nu_{113} + \nu_{223}$, with $\nu_{\alpha\beta\gamma} = N_\alpha L/c\mathscr{D}_{\beta\gamma}$ and $\zeta = z/L$.

(b) Next verify that the equation for species 2 can be solved to get

$$x_2 = x_{20}e^{B\zeta} + \frac{\nu_{212}}{B}(1 - e^{B\zeta}) + \frac{Cx_{30}}{A - B}(e^{A\zeta} - e^{B\zeta}) \tag{18C.5-2}$$

where $B = \nu_{112} + \nu_{212}$ and $C = \nu_{212} - \nu_{223}$.

(c) Compare the above equations with the published results.

(d) How well do Eqs. 18C.5-1 and 2 fit the experimental data?

18D.1. Effectiveness factors for long cylinders. Derive the expression for η_A for long cylinders analogous to Eq. 18.7-16. Neglect the diffusion through the ends of the cylinders.

Answer: $\eta_A = \frac{I_1(2\Lambda)}{\Lambda I_0(2\Lambda)}$, where I_0 and I_1 are "modified Bessel functions"

18D.2. Gas absorption in a falling film with chemical reaction. Rework the problem discussed in §18.5 and described in Fig. 18.5-1, when gas A reacts with liquid B by a first-order irreversible chemical reaction in the liquid phase, with rate constant k_1'''. Specifically, find the expression for the total absorption rate analogous to that given in Eq. 18.5-18. Show that the result for absorption with reaction properly simplifies to that for absorption without reaction.

Answer: $W_A = Wc_{A0}v_{max}\sqrt{\frac{\mathscr{D}_{AB}}{k_1'''}}\left[(\tfrac{1}{2} + u)\,\mathrm{erf}\sqrt{u} + \sqrt{\frac{u}{\pi}}e^{-u}\right]$ in which $u = k_1'''L/v_{max}$

---

[13] H. A. Wilson, *Proc. Camb. Phil. Soc.*, **12**, 406–423 (1904).

[14] R. Carty and T. Schrodt, *Ind. Eng. Chem.*, **14**, 276–278 (1975).

Chapter 19

Equations of Change for Multicomponent Systems

In Chapter 18, problems in diffusion were formulated by making shell mass balances on one or more of the diffusing species. In this chapter we start by making a mass balance over an arbitrary differential fluid element to establish the equation of continuity for the various species in a multicomponent mixture. Then insertion of mass flux expressions gives the diffusion equations in a variety of forms. These diffusion equations can be used to set up any of the problems in Chapter 18 and more complicated ones as well.

Then we summarize all of the equations of change for mixtures: the equations of continuity, the equation of motion, and the equation of energy. These include the equations of change that were given in Chapters 3 and 11. Next we summarize the flux expressions for mixtures. All these equations are given in general form, although for problem solving we generally use simplified versions of them.

The remainder of the chapter is devoted to analytical solutions and dimensional analyses of mass transfer systems.

§19.1 THE EQUATIONS OF CONTINUITY FOR A MULTICOMPONENT MIXTURE

In this section we apply the law of conservation of mass to each species α in a mixture, where $\alpha = 1, 2, 3, \ldots, N$. The system we consider is a volume element $\Delta x\, \Delta y\, \Delta z$ fixed in space, through which the fluid mixture is flowing (see Fig. 3.1-1). Within this mixture, reactions among the various chemical species may be occurring, and we use the symbol r_α to indicate the rate at which species α is being produced, with dimensions of mass/volume · time.

The various contributions to the mass balance are

rate of increase of mass of α in the volume element	$(\partial \rho_\alpha / \partial t)\Delta x\, \Delta y\, \Delta z$	(19.1-1)
rate of addition of mass of α across face at x	$n_{\alpha x}\vert_x\, \Delta y\, \Delta z$	(19.1-2)

rate of removal of mass of α across face at $x + \Delta x$ $\quad n_{\alpha x}|_{x+\Delta x}\, \Delta y\, \Delta z$ (19.1-3)

rate of production of mass of α by chemical reactions $\quad r_\alpha \Delta x\, \Delta y\, \Delta z$ (19.1-4)

The combined mass flux $n_{\alpha x}$ includes both the molecular flux and the convective flux. There are also addition and removal terms in the y and z directions. When the entire mass balance is written down and divided by $\Delta x\, \Delta y\, \Delta z$, one obtains, after letting the size of the volume element decrease to zero,

$$\frac{\partial \rho_\alpha}{\partial t} = -\left(\frac{\partial n_{\alpha x}}{\partial x} + \frac{\partial n_{\alpha y}}{\partial y} + \frac{\partial n_{\alpha z}}{\partial z}\right) + r_\alpha \qquad \alpha = 1, 2, 3, \ldots, N \tag{19.1-5}$$

This is the *equation of continuity for species* α in a multicomponent reacting mixture. It describes the change in mass concentration of species α with time at a fixed point in space by the diffusion and convection of α, as well as by chemical reactions that produce or consume α. The quantities $n_{\alpha x}$, $n_{\alpha y}$, $n_{\alpha z}$ are the Cartesian components of the mass flux vector $\mathbf{n}_\alpha = \rho_\alpha \mathbf{v}_\alpha$ given in Eq. (D) of Table 17.8-1.

Equation 19.1-5 may be rewritten in vector notation as

$$\frac{\partial \rho_\alpha}{\partial t} = -(\nabla \cdot \mathbf{n}_\alpha) + r_\alpha \qquad \alpha = 1, 2, 3, \ldots, N \tag{19.1-6}$$

Alternatively we can use Eq. (S) of Table 17.8-1 to write

$$\frac{\partial \rho_\alpha}{\partial t} = -(\nabla \cdot \rho_\alpha \mathbf{v}) - (\nabla \cdot \mathbf{j}_\alpha) + r_\alpha \qquad \alpha = 1, 2, 3, \ldots, N \tag{19.1-7}$$[1]

rate of increase of mass of A per unit volume	net rate of addition of mass of A per unit volume by convection	net rate of addition of mass of A per unit volume by diffusion	rate of production of mass of A per unit volume by reaction

Addition of all N equations in either Eq. 19.1-6 or 7 gives

$$\frac{\partial \rho}{\partial t} = -(\nabla \cdot \rho \mathbf{v}) \tag{19.1-8}$$

which is the *equation of continuity for the mixture*. This equation is identical to the equation of continuity for a pure fluid given in Eq. 3.1-4. In obtaining Eq. 19.1-8 we had to use Eq. (J) of Table 17.8-1 and also the fact that the law of conservation of total mass gives $\Sigma_\alpha r_\alpha = 0$. Finally we note that Eq. 19.1-8 becomes

$$(\nabla \cdot \mathbf{v}) = 0 \tag{19.1-9}$$

for a fluid mixture of *constant mass density* ρ.

In the preceding discussion we used mass units. However, a corresponding derivation is also possible in molar units. The equation of continuity for species α in molar quantities is

$$\frac{\partial c_\alpha}{\partial t} = -(\nabla \cdot \mathbf{N}_\alpha) + R_\alpha \qquad \alpha = 1, 2, 3, \ldots, N \tag{19.1-10}$$

[1] J. Crank, *The Mathematics of Diffusion*, 2nd edition, Oxford University Press (1975).

where R_α is the molar rate of production of α per unit volume. This equation can be rewritten by use of Eq. (V) of Table 17.8-1 to give

$$\frac{\partial c_\alpha}{\partial t} = -(\nabla \cdot c_\alpha \mathbf{v}^*) - (\nabla \cdot \mathbf{J}_\alpha^*) + R_\alpha \qquad \alpha = 1, 2, 3, \ldots, N \tag{19.1-11}$$

rate of increase in moles of A per unit volume	net rate of addition in moles of A per unit volume by convection	rate of addition of moles of A per unit volume by diffusion	rate of production of moles of A per unit volume by reaction

When all N equations in Eq. 19.1-10 or 11 are added we get

$$\frac{\partial c}{\partial t} = -(\nabla \cdot c\mathbf{v}^*) + \sum_{\alpha=1}^{N} R_\alpha \tag{19.1-12}$$

for the equation of continuity for the mixture. To get this we used Eq. (M) of Table 17.8-1. We also note that the chemical reaction term does not drop out because the number of moles is not necessarily conserved in a chemical reaction. Finally we note that

$$(\nabla \cdot \mathbf{v}^*) = \frac{1}{c} \sum_{\alpha=1}^{N} R_\alpha \tag{19.1-13}$$

for a fluid mixture of constant *molar density* c.

We have thus seen that the equation of continuity for species α may be written in two forms, Eq. 19.1-7 and Eq. 19.1-11. Using the continuity relations in Eqs. 19.1-8 and 19.1-12 the reader may verify that the equation of continuity for species α can be put into two additional, equivalent forms:

$$\rho\left(\frac{\partial \omega_\alpha}{\partial t} + (\mathbf{v} \cdot \nabla \omega_\alpha)\right) = -(\nabla \cdot \mathbf{j}_\alpha) + r_\alpha \qquad \alpha = 1, 2, 3, \ldots, N \tag{19.1-14}$$

$$c\left(\frac{\partial x_\alpha}{\partial t} + (\mathbf{v}^* \cdot \nabla x_\alpha)\right) = -(\nabla \cdot \mathbf{J}_\alpha^*) + R_\alpha - x_\alpha \sum_{\beta=1}^{N} R_\beta \qquad \alpha = 1, 2, 3, \ldots, N \tag{19.1-15}$$

These two equations express exactly the same physical content, but they are written in two different sets of notation—the first in mass quantities and the second in molar quantities. To use these equations we have to insert the appropriate expressions for the fluxes and the chemical reaction terms. In this chapter we give only the results for *binary systems* with constant $\rho\mathscr{D}_{AB}$, with constant $c\mathscr{D}_{AB}$, or with zero velocity.

Binary Systems with Constant $\rho\mathscr{D}_{AB}$

For this assumption, Eq. 19.1-14 becomes, after inserting Fick's law from Eq. (A) of Table 17.8-2,

$$\rho\left(\frac{\partial \omega_A}{\partial t} + (\mathbf{v} \cdot \nabla \omega_A)\right) = \rho\mathscr{D}_{AB}\nabla^2\omega_A + r_A \tag{19.1-16}$$

with a corresponding equation for species B. This equation is appropriate for describing the diffusion in *dilute liquid solutions* at constant temperature and pressure. The left side can be written as $\rho D\omega_A/Dt$. Equation 9.1-16 without the r_A term is of the same form as Eq. 11.2-8 or 9. This similarity is quite important, since it is the basis for the analogies that are frequently drawn between heat and mass transport in flowing fluids with constant physical properties.

Binary Systems with Constant $c\mathscr{D}_{AB}$

For this assumption, Eq. 19.1-15 becomes, after inserting Fick's law from Eq. (B) of Table 17.8-2,

$$c\left(\frac{\partial x_A}{\partial t} + (\mathbf{v}^* \cdot \nabla x_A)\right) = c\mathscr{D}_{AB}\nabla^2 x_A + (x_B R_A - x_A R_B) \tag{19.1-17}$$

with a corresponding equation for species B. This equation is useful for *low-density gases* at constant temperature and pressure. The left side can *not* be written as cDx_α/Dt because of the appearance of $\mathbf{v}^*$ rather than $\mathbf{v}$.

Binary Systems with Zero Velocity

If there are no chemical reactions occurring, then the chemical production terms are all zero. If, in addition $\mathbf{v}$ is zero and ρ constant in Eq. 19.1-16, or $\mathbf{v}^*$ is zero and c constant in Eq. 19.1-17, then we get

$$\frac{\partial c_A}{\partial t} = \mathscr{D}_{AB}\nabla^2 c_A \tag{19.1-18}$$

which is called *Fick's second law of diffusion*, or sometimes simply *the diffusion equation*. This equation is usually used for diffusion in *solids* or *stationary liquids* (that is, $\mathbf{v} = 0$ in Eq. 19.1-16) and for *equimolar counter-diffusion* in gases (that is, $\mathbf{v}^* = 0$ in Eq. 19.1-17). By equimolar counter-diffusion we mean that the net molar flux with respect to stationary coordinates is zero; in other words, that for every mole of A that moves, say, in the positive z direction, there is a mole of B that moves in the negative z direction.

Note that Eq. 19.1-18 has the same form as the *heat conduction equation* in Eq. 11.2-10. This similarity is the basis for analogies between many heat conduction and diffusion problems in solids. Keep in mind that many hundreds of problems described by Fick's second law have been solved. Solutions are tabulated in the monographs of Crank[1] and of Carslaw and Jaeger.[2]

In Tables B-10 and 11 we give Eq. 19.1-14 (multicomponent equation of continuity in terms of $\mathbf{j}_\alpha$) and Eq. 19.1-16 (binary diffusion equation for constant ρ and $\mathscr{D}_{AB}$) in the three standard coordinate systems. Other forms of the equation of continuity can be patterned after these.

EXAMPLE 19.1-1

Diffusion, Convection, and Chemical Reaction[3]

In Fig. 19.1-1 we show a system in which a liquid, B, moves slowly upward through a slightly soluble porous plug of A. Then A slowly disappears by a first-order reaction after it has dissolved. Find the steady-state concentration profile $c_A(z)$, where z is the coordinate upward from the plug. Assume that the velocity profile is approximately flat across the tube. Assume further that c_{A0} is the solubility of unreacted A in B. Neglect temperature effects associated with the heat of reaction.

SOLUTION

Equation 19.1-16 is appropriate for dilute liquid solutions. Dividing this equation by the molecular weight M_A and specializing for the one-dimensional steady-state problem at hand, we get for constant ρ:

$$v_0 \frac{dc_A}{dz} = \mathscr{D}_{AB}\frac{d^2 c_A}{dz^2} - k_1''' c_A \tag{19.1-19}$$

---

[2] H. S. Carslaw and J. C. Jaeger, *Conduction of Heat in Solids*, 2nd edition, Oxford University Press (1959).

[3] W. Jost, *Diffusion*, Academic Press, New York (1952), pp. 58–59.

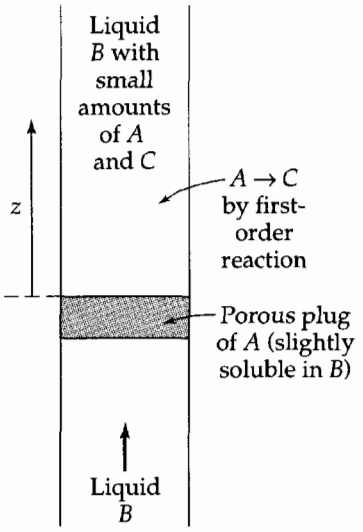

Fig. 19.1-1. Simultaneous diffusion, convection, and chemical reaction.

This is to be solved with the boundary conditions that $c_A = c_{A0}$ at $z = 0$ and $c_A = 0$ at $z = \infty$. Equation 19.1-19 is a standard second-order linear differential equation (Eq. C.7) for which there is a well-known method of solution.

A trial function $c_A = e^{az}$ leads to two values of a, one of which violates the boundary condition at $z = \infty$. The final solution is then

$$\frac{c_A}{c_{A0}} = \exp[-(\sqrt{1 + (4k_1'''\mathcal{D}_{AB}/v_0^2)} - 1)(v_0 z/2\mathcal{D}_{AB})] \tag{19.1-20}$$

This example illustrates the use of the equation of continuity of A for setting up a diffusion problem with convection and chemical reaction.

§19.2 SUMMARY OF THE MULTICOMPONENT EQUATIONS OF CHANGE

In the three main parts of this book we have by stages introduced the conservation laws known as the equations of change. In Chapter 3 conservation of mass and conservation of momentum in pure fluids were presented. In Chapter 11 we added the conservation of energy in pure fluids. In §19.1 we added mass conservation equations for the various species present. We now want to summarize the conservation equations for multicomponent systems.

We start, in Table 19.2-1, by giving the equations of change for a mixture of N chemical species in terms of the combined fluxes with respect to stationary axes. The equation numbers indicate where each equation first appeared. By tabulating the equations of change in this way, we can gain an appreciation for the unity of the subject. The only assumption made here is that all the species are acted on by the same external force per unit mass, $\mathbf{g}$; note (b) of Table 19.2-1 explains the modifications needed when this is not the case.

The important feature of these equations is that they are all of the form

$$\left\{\begin{matrix}\text{rate of}\\ \text{increase of}\\ \text{entity}\end{matrix}\right\} = \left\{\begin{matrix}\text{net rate}\\ \text{of addition}\\ \text{of entity}\end{matrix}\right\} + \left\{\begin{matrix}\text{rate of}\\ \text{production}\\ \text{of entity}\end{matrix}\right\} \tag{19.2-1}$$

in which "entity" stands for mass, momentum, or energy, respectively. In each equation the net rate of addition of the entity per unit volume is the negative of a divergence term. The "rates of production" arise from chemical reactions in the first equation and from the external force field in the other two. Each equation is a statement of a *conservation law*. Usually we think of the conservation statements as laws that have gradually

Table 19.2-1 Equations of Change for Multicomponent Mixtures in Terms of the Combined Fluxes

Mass of α: ($\alpha = 1, 2, \ldots, N$)	$\frac{\partial}{\partial t}\rho\omega_\alpha = -(\nabla \cdot \mathbf{n}_\alpha) + r_\alpha$	(A)[a] (Eq. 19.1-6)
Momentum:	$\frac{\partial}{\partial t}\rho\mathbf{v} = -[\nabla \cdot \boldsymbol{\phi}] + \rho\mathbf{g}$	(B)[b] (Eq. 3.2-8)
Energy:	$\frac{\partial}{\partial t}\rho(\hat{U} + \frac{1}{2}v^2) = -(\nabla \cdot \mathbf{e}) + (\rho\mathbf{v} \cdot \mathbf{g})$	(C)[b] (Eq. 11.1-6)

[a] When all N equations of continuity are added, the equation of continuity for the fluid mixture

$$\frac{\partial}{\partial t}\rho = -(\nabla \cdot \rho\mathbf{v}) \qquad \text{(D) (Eq. 3.1-4)}$$

is obtained. Here $\mathbf{v}$ is the mass average velocity defined in Eq. 17.7-1.

[b] If species α is acted on by a force per unit volume given by $\mathbf{g}_\alpha$, then $\rho\mathbf{g}$ has to be replaced by $\Sigma_\alpha\rho_\alpha\mathbf{g}_\alpha$ in Eq. (B), and $(\rho\mathbf{v} \cdot \mathbf{g})$ has to be replaced by $\Sigma_\alpha(\mathbf{n}_\alpha \cdot \mathbf{g}_\alpha)$ in Eq. (C). These replacements are required, for example, if some of the species are ions with different charges on them, acted on by an electric field. Problems of this sort are discussed in Chapter 24.

evolved by experience and experiment and therefore are generally accepted by the scientific community.[1]

The three "combined fluxes," which appear in Eqs. (A) to (C) of Table 19.2-1, can be written as the *convective fluxes* plus the *molecular* (or *diffusive*) *fluxes*. These various fluxes are displayed in Table 19.2-2, where the equation numbers corresponding to their first appearance are given.

When the flux expressions of Table 19.2-2 are substituted into the conservation equations of Table 19.2-1 and then converted to the D/Dt form by means of Eqs. 3.5-4 and 5, we get the multicomponent equations of change in their usual forms. These are tabulated in Table 19.2-3.

In addition to these conservation equations, one needs also to have the expressions for the fluxes in terms of the gradients and the transport properties (the latter being functions of temperature, density, and composition). Finally one needs also the thermal equation of state, $p = p(\rho, T, x_\alpha)$, and the caloric equation of state, $\hat{U} = \hat{U}(\rho, T, x_\alpha)$, and information about the rates of any homogeneous chemical reactions occurring.[2]

[1] Actually the conservation laws for energy, momentum, and angular momentum follow from Lagrange's equation of motion, together with the homogeneity of time, the homogeneity of space, and the isotropy of space, respectively (*Noether's theorem*). Thus there is something very fundamental about these conservation laws, more than is apparent at first sight. For more on this, see L. Landau and E. M. Lifshitz, *Mechanics*, Addison-Wesley, Reading, Mass. (1960), Chapter 2, and Emmy Noether, *Nachr. Kgl. Ges. Wiss. Göttingen (Math.-phys. Kl.)* (1918), pp. 235–257. **Amalie Emmy Noether** (1882–1935), after doing the doctorate at the University of Erlangen, was a protégée of Hilbert in Göttingen until Hitler's purge of 1933 forced her to move to the United States, where she became a professor of mathematics at Bryn Mawr College; a crater on the moon is named after her.

[2] One might wonder whether or not we need separate equations of motion and energy for species α. Such equations can be derived by continuum arguments, but the species momentum and energy fluxes are not measurable quantities and molecular theory is required in order to clarify their meanings. These separate species equations are not needed for solving transport problems. However, the species equations of motion have been helpful for deriving kinetic expressions for the mass fluxes in multicomponent systems [see C. F. Curtiss and R. B. Bird, *Proc. Nat. Acad. Sci. USA*, **93**, 7440–7445 (1996) and *J. Chem. Phys.*, **111**, 10362–10370 (1999)].

Table 19.2-2 The Combined, Molecular, and Convective Fluxes for Multicomponent Mixtures (all with the same sign convention)

Entity	Combined flux	=	Molecular flux	+	Convective flux	
Mass ($\alpha = 1, 2, \ldots, N$)	$\mathbf{n}_\alpha$	=	$\mathbf{j}_\alpha$	+	$\rho \mathbf{v} \omega_\alpha$	(A)[a] (Eq. 17.8-1)
Momentum	$\boldsymbol{\phi}$	=	$\boldsymbol{\pi}$	+	$\rho \mathbf{v}\mathbf{v}$	(B)[b] (Eq. 1.7-1)
Energy	$\mathbf{e}$	=	$\mathbf{q} + [\boldsymbol{\pi} \cdot \mathbf{v}]$	+	$\rho \mathbf{v}(\hat{U} + \frac{1}{2}v^2)$	(C)[c] (Eq. 9.8-5)

[a] The velocity $\mathbf{v}$ appearing in all these expressions is the mass average velocity, defined in Eq. 17.7-1.

[b] The molecular momentum flux consists of two parts: $\boldsymbol{\pi} = p\boldsymbol{\delta} + \boldsymbol{\tau}$.

[c] The molecular energy flux is made up of the heat flux vector $\mathbf{q}$ and the work flux vector $[\boldsymbol{\pi} \cdot \mathbf{v}] = p\mathbf{v} + [\boldsymbol{\tau} \cdot \mathbf{v}]$, the latter occurring only in flow systems.

Table 19.2-3 Equations of Change for Multicomponent Mixtures in Terms of the Molecular Fluxes

Total mass:	$\dfrac{D\rho}{Dt} = -\rho(\nabla \cdot \mathbf{v})$	(A) (Eq. (A) of Table 3.5-1)
Species mass: ($\alpha = 1, 2, \cdots, N$)	$\rho \dfrac{D\omega_\alpha}{Dt} = -(\nabla \cdot \mathbf{j}_\alpha) + r_\alpha$	(B)[a] (Eq. 19.1-7a)
Momentum:	$\rho \dfrac{D\mathbf{v}}{Dt} = -\nabla p - [\nabla \cdot \boldsymbol{\tau}] + \rho \mathbf{g}$	(C)[b] (Eq. (B) of Table 3.5-1)
Energy:	$\rho \dfrac{D}{Dt}(\hat{U} + \frac{1}{2}v^2) = -(\nabla \cdot \mathbf{q}) - (\nabla \cdot p\mathbf{v}) - (\nabla \cdot [\boldsymbol{\tau} \cdot \mathbf{v}]) + (\rho \mathbf{v} \cdot \mathbf{g})$	(D)[b] (Eq. (E) of Table 11.4-1)

[a] Only $N - 1$ of these equations are independent, since the sum of the N equations gives $0 = 0$.

[b] See note (*b*) of Table 19.2-1 for the modifications needed when the various species are acted on by different forces.

We conclude this discussion with a few remarks about special forms of the equations of motion and energy. In §11.3 it was pointed out that the *equation of motion* as presented in Chapter 3 is in suitable form for setting up forced-convection problems, but that an alternate form (Eq. 11.3-2) is desirable for displaying explicitly the buoyant forces resulting from temperature inequalities in the system. In binary systems with concentration inequalities as well as temperature inequalities, we write the equation of motion as in Eq. (B) of Table 3.5-1 and use an approximate equation of state formed by making a double Taylor expansion of $\rho(T, \omega_A)$ about the state $\overline{T}, \overline{\omega}_A$:

$$\begin{aligned} \rho(T, \omega_A) &= \overline{\rho} + \left.\frac{\partial \rho}{\partial T}\right|_{\overline{T}, \overline{\omega}_A} (T - \overline{T}) + \left.\frac{\partial \rho}{\partial \omega_A}\right|_{\overline{T}, \overline{\omega}_A} (\omega_A - \overline{\omega}_A) + \cdots \\ &\approx \overline{\rho} - \overline{\rho}\overline{\beta}(T - \overline{T}) - \overline{\rho}\overline{\zeta}(\omega_A - \overline{\omega}_A) \end{aligned} \tag{19.2-2}$$

Table 19.2-4 The Equations of Energy for Multicomponent Systems, with Gravity as the Only External Force[a,b]

$$\rho \frac{D}{Dt}(\hat{U} + \hat{\Phi} + \tfrac{1}{2}v^2) = -(\nabla \cdot \mathbf{q}) - (\nabla \cdot [\boldsymbol{\pi} \cdot \mathbf{v}]) \tag{A}^c$$

$$\rho \frac{D}{Dt}(\hat{U} + \tfrac{1}{2}v^2) = -(\nabla \cdot \mathbf{q}) - (\nabla \cdot [\boldsymbol{\pi} \cdot \mathbf{v}]) + (\mathbf{v} \cdot \rho\mathbf{g}) \tag{B}$$

$$\rho \frac{D}{Dt}(\tfrac{1}{2}v^2) = -(\mathbf{v} \cdot [\nabla \cdot \boldsymbol{\pi}]) + (\mathbf{v} \cdot \rho\mathbf{g}) \tag{C}$$

$$\rho \frac{D\hat{U}}{Dt} = -(\nabla \cdot \mathbf{q}) - (\boldsymbol{\pi}:\nabla\mathbf{v}) \tag{D}$$

$$\rho \frac{D\hat{H}}{Dt} = -(\nabla \cdot \mathbf{q}) - (\boldsymbol{\tau}:\nabla\mathbf{v}) + \frac{Dp}{Dt} \tag{E}$$

$$\rho\hat{C}_p \frac{DT}{Dt} = -(\nabla \cdot \mathbf{q}) - (\boldsymbol{\tau}:\nabla\mathbf{v}) + \left(\frac{\partial \ln \hat{V}}{\partial \ln T}\right)_{p,x_\alpha} \frac{Dp}{Dt} + \sum_{\alpha=1}^{N} \overline{H}_\alpha[(\nabla \cdot \mathbf{J}_\alpha) - R_\alpha] \tag{F}^d$$

$$\rho\hat{C}_V \frac{DT}{Dt} = -(\nabla \cdot \mathbf{q}) - (\boldsymbol{\pi}:\nabla\mathbf{v}) + \left(1 - \left(\frac{\partial \ln p}{\partial \ln T}\right)_{\rho,x_\alpha}\right)p(\nabla \cdot \mathbf{v}) + \sum_{\alpha=1}^{N}\left(\overline{U}_\alpha + \left(1 - \left(\frac{\partial \ln p}{\partial \ln T}\right)_{\rho,x_\alpha}\right)p\overline{V}_\alpha\right)[(\nabla \cdot \mathbf{J}_\alpha) - R_\alpha] \tag{G}$$

$$\frac{\partial}{\partial t}\sum_{\alpha=1}^{N} c_\alpha \overline{H}_\alpha + \left(\nabla \cdot \sum_{\alpha=1}^{N} \mathbf{N}_\alpha \overline{H}_\alpha\right) = (\nabla \cdot k\nabla T) - (\boldsymbol{\tau}:\nabla\mathbf{v}) + \frac{Dp}{Dt} \tag{H}^e$$

[a] For multicomponent mixtures $\mathbf{q} = -k\nabla T + \sum_{\alpha=1}^{N} \frac{\overline{H}_\alpha}{M_\alpha}\mathbf{j}_\alpha + \mathbf{q}^{(x)}$, where $\mathbf{q}^{(x)}$ is a usually negligible term associated with the diffusion-thermo effect (see Eq. 24.2-6).

[b] The equations in this table are valid only if the same external force is acting on all species. If this is not the case, then $\Sigma_\alpha(\mathbf{j}_\alpha \cdot \mathbf{g}_\alpha)$ must be added to Eq. (A) and Eqs. (D–H), the last term in Eq. (B) has to be replaced by $\Sigma_\alpha(\mathbf{n}_\alpha \cdot \mathbf{g}_\alpha)$, and the last term in Eq. (C) has to be replaced by $\Sigma_\alpha(\mathbf{v} \cdot \rho_\alpha\mathbf{g}_\alpha)$.

[c] Exact only if $\partial\hat{\Phi}/\partial t = 0$.

[d] L. B. Rothfeld, PhD thesis, University of Wisconsin (1961); see also Problem 19D.2.

[e] The contribution of $\mathbf{q}^{(x)}$ to the heat flux vector has been omitted in this equation.

Here the coefficient $\bar{\zeta} = -(1/\rho)(\partial\rho/\partial\omega_A)$ evaluated at $\overline{T}$ and $\overline{\omega}_A$ relates the density to the composition. This coefficient is the mass transfer analog of the coefficient $\bar{\beta}$ introduced in Eq. 11.3-1. When this approximate equation of state is substituted into the $\rho\mathbf{g}$ term (but not into the $\rho D\mathbf{v}/Dt$ term) of the equation of motion, we get the *Boussinesq equation of motion* for a binary mixture, with gravity as the only external force:

$$\rho \frac{D\mathbf{v}}{Dt} = (-\nabla p + \bar{\rho}\mathbf{g}) - [\nabla \cdot \boldsymbol{\tau}] - \bar{\rho}\mathbf{g}\bar{\beta}(T - \overline{T}) - \bar{\rho}\mathbf{g}\bar{\zeta}(\omega_A - \overline{\omega}_A) \tag{19.2-3}$$

The last two terms in this equation describe the buoyant force resulting from the temperature and composition variations within the fluid.

Next we turn to the *equation of energy*. Recall that in Table 11.4-1 the energy equation for pure fluids was given in a variety of forms. The same can be done for mixtures, and a representative selection of the many possible forms of this equation is given in Table 19.2-4. Note that it is not necessary to add a term S_c (as we did in Chapter 10) to describe the thermal energy released by homogeneous chemical reactions. This information is included implicitly in the functions $\hat{H}$ and $\hat{U}$, and appears explicitly as $-\Sigma_\alpha\overline{H}_\alpha R_\alpha$ and $-\Sigma_\alpha\overline{U}_\alpha R_\alpha$ in Eqs. (F) and (G). Remember that in calculating $\hat{H}$ and $\hat{U}$, the energies of formation and mixing of the various species must be included (see Example 23.5-1).

§19.3 SUMMARY OF THE MULTICOMPONENT FLUXES

The equations of change have been given in terms of the fluxes of mass, momentum, and energy. To solve these equations, we have to replace the fluxes by expressions involving the transport properties and the gradients of concentration, velocity, and temperature. Here we summarize the flux expressions for mixtures:

Mass: $$\mathbf{j}_A = -\rho\mathscr{D}_{AB}\nabla\omega_A \qquad \text{binary only} \tag{19.3-1}$$

Momentum: $$\boldsymbol{\tau} = -\mu[\nabla\mathbf{v} + (\nabla\mathbf{v})^\dagger] + (\tfrac{2}{3}\mu - \kappa)(\nabla\cdot\mathbf{v})\boldsymbol{\delta} \tag{19.3-2}$$

Energy: $$\mathbf{q} = -k\nabla T + \sum_{\alpha=1}^{N}\frac{\overline{H}_\alpha}{M_\alpha}\mathbf{j}_\alpha \tag{19.3-3}$$

Now we append a few words of explanation:

a. The *mass flux* expression given here is for binary mixtures only. For multicomponent gas mixtures at moderate pressures, we can use the Maxwell–Stefan equations of Eq. 17.9-1. There are additional contributions to the mass flux corresponding to driving forces other than the concentration gradients: *forced diffusion*, which occurs when the various species are subjected to different external forces; *pressure diffusion*, proportional to ∇p; and *thermal diffusion*, proportional to ∇T. These other diffusion mechanisms, the first two of which can be quite important, are covered in Chapter 24.

b. The *momentum flux* expression is the same for multicomponent mixtures as for pure fluids. Once again we point out that the contribution containing the dilatational viscosity κ is seldom important. Of course, for polymers and other viscoelastic fluids, Eq. 19.3-2 has to be replaced by more complex models, as explained in Chapter 8.

c. The *energy-flux* expression given here for multicomponent fluids consists of two terms: the first term is the heat transport by conduction which was given for pure materials in Eq. 9.1-4, and the second term describes the heat transport by each of the diffusing species. The quantity $\overline{H}_\alpha$ is the partial molar enthalpy of species α. There is actually one further contribution to the energy flux, related to a concentration driving force—usually quite small—and this *diffusion-thermo effect* will be discussed in Chapter 24. The thermal conductivity of a mixture—the k in Eq. 19.3-3—is defined as the proportionality constant between the heat flux and the temperature gradient in the absence of any mass fluxes.

We conclude this discussion with a few comments about the combined energy flux $\mathbf{e}$. By substituting Eq. 19.3-3 into Eq. (C) of Table 19.2-2, we get after some minor rearranging:

$$\begin{aligned}\mathbf{e} &= \rho(\hat{U} + \tfrac{1}{2}v^2)\mathbf{v} + \mathbf{q} + p\mathbf{v} + [\boldsymbol{\tau}\cdot\mathbf{v}]\\ &= \rho(\hat{U} + \tfrac{1}{2}v^2)\mathbf{v} - k\nabla T + \sum_{\alpha=1}^{N}\frac{\overline{H}_\alpha}{M_\alpha}\mathbf{j}_\alpha + p\mathbf{v} + [\boldsymbol{\tau}\cdot\mathbf{v}]\\ &= -k\nabla T + \sum_{\alpha=1}^{N}\overline{H}_\alpha\mathbf{J}_\alpha + \rho(\hat{U} + p\hat{V})\mathbf{v} + \underline{\tfrac{1}{2}\rho v^2\mathbf{v} + [\boldsymbol{\tau}\cdot\mathbf{v}]}\end{aligned} \tag{19.3-4}$$

In some situations, notably in films and low-velocity boundary layers, the contributions $\frac{1}{2}\rho v^2\mathbf{v}$ and $[\boldsymbol{\tau}\cdot\mathbf{v}]$ are negligible. Then the dashed-underlined terms may be discarded. This leads to

$$\begin{aligned}\mathbf{e} &= -k\nabla T + \sum_{\alpha=1}^{N}\overline{H}_\alpha\mathbf{J}_\alpha + \rho\hat{H}_\alpha\mathbf{v}\\ &= -k\nabla T + \sum_{\alpha=1}^{N}\overline{H}_\alpha\mathbf{J}_\alpha + \sum_{\alpha=1}^{N}c_\alpha\overline{H}_\alpha\mathbf{v}\end{aligned} \tag{19.3-5}$$

Then use of Eqs. (G) and (H) of Table 17.8-1 leads finally to

$$\mathbf{e} = -k\nabla T + \sum_{\alpha=1}^{N} \overline{H}_\alpha \mathbf{N}_\alpha \tag{19.3-6}$$

Finally, for ideal gas mixtures, this expression can be further simplified by replacing the partial molar enthalpies $\overline{H}_\alpha$ by the molar enthalpies $\tilde{H}_\alpha$. Equation 19.3-6 provides a standard starting point for solving one-dimensional problems in simultaneous heat and mass transfer.[1]

EXAMPLE 19.3-1

The Partial Molar Enthalpy

The partial molar enthalpy $\overline{H}_\alpha$, which appears in Eqs. 19.3-3 and 19.3-6, is defined for a multicomponent mixture as

$$\overline{H}_\alpha = \left(\frac{\partial H}{\partial n_\alpha}\right)_{T,p,n_\beta} \tag{19.3-7}$$

in which n_α is the number of moles of species α in the mixture, and the subscript n_β indicates that the derivative is to be taken holding the number or moles of each species other than α constant. The enthalpy $H(n_1, n_2, n_3, \ldots)$ is an "extensive property," since, if the number of moles of each component is multiplied by k, the enthalpy itself will be multiplied by k:

$$H(kn_1, kn_2, kn_3, \cdots) = kH(n_1, n_2, n_3, \cdots) \tag{19.3-8}$$

Mathematicians refer to this kind of function as being "homogeneous of degree 1." For such functions Euler's theorem[2] can be used to conclude that

$$H = \sum_\alpha n_\alpha \overline{H}_\alpha \tag{19.3-9}$$

(a) Prove that, for a binary mixture, the partial molar enthalpies at a given mole fraction can be determined by plotting the enthalpy per mole as a function of mole fraction, and then determining the intercepts of the tangent drawn at the mole fraction in question (see Fig. 19.3-1). This shows one way to get the partial molar enthalpy from data on the enthalpy of the mixture.

(b) How else could one get the partial molar enthalpy?

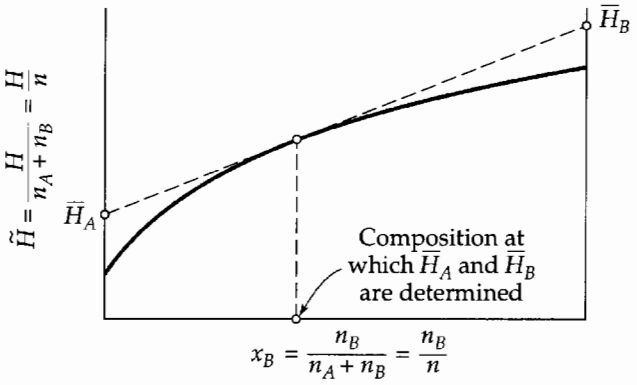

Fig. 19.3-1. The "method of intercepts" for determining partial molar quantities in a binary mixture.

[1] T. K. Sherwood, R. L. Pigford, and C. R. Wilke, *Mass Transfer*, McGraw-Hill, New York (1975), Chapter 7. **Thomas Kilgore Sherwood** (1903–1976) was a professor at MIT for nearly 40 years, and then taught at the University of California in Berkeley. Because of his many contributions to the field of mass transfer, the Sherwood number (Sh) was named after him.

[2] M. D. Greenberg, *Foundations of Applied Mathematics*, Prentice-Hall, Englewood Cliffs, N.J. (1978), p. 128; R. J. Silbey and R. A. Alberty, *Physical Chemistry*, 3rd edition, Wiley, New York (2001), §§1.10, 4.9, and 6.10.

SOLUTION

(a) Throughout this example, for brevity we omit the subscripts p, T indicating that these quantities are held constant. First we write expressions for the intercepts as follows:

$$\overline{H}_A = \tilde{H} - x_B\left(\frac{\partial \tilde{H}}{\partial x_B}\right)_n; \qquad \overline{H}_B = \tilde{H} + x_A\left(\frac{\partial \tilde{H}}{\partial x_B}\right)_n \tag{19.3-10, 11}$$

in which $\tilde{H} = H/(n_A + n_B) = H/n$. To verify the correctness of Eq. 19.3-10, we rewrite the expression in terms of H:

$$\overline{H}_A = \frac{H}{n} - \frac{x_B}{n}\left(\frac{\partial H}{\partial x_B}\right)_n \tag{19.3-12}$$

Now the expression $\overline{H}_A = (\partial H/\partial n_A)_{n_B}$ implies that H is a function of n_A and n_B, whereas $(\partial H/\partial x_A)_n$ implies that H is a function of x_A and n. The relation between these kinds of derivatives is given by the chain rule of partial differentiation. To apply this rule we need the relation between the independent variables, which, in this problem, are

$$n_A = (1 - x_B)n; \qquad n_B = x_B n \tag{19.3-13, 14}$$

Therefore we may write

$$\left(\frac{\partial H}{\partial x_B}\right)_n = \left(\frac{\partial H}{\partial n_A}\right)_{n_B}\left(\frac{\partial n_A}{\partial x_B}\right)_n + \left(\frac{\partial H}{\partial n_B}\right)_{n_A}\left(\frac{\partial n_B}{\partial x_B}\right)_n$$
$$= \overline{H}_A(-n) + \overline{H}_B(+n) \tag{19.3-15}$$

Substitution of this into Eq. 19.3-12 and use of Euler's theorem ($H = n_A\overline{H}_A + n_B\overline{H}_B$) then gives an identity. This proves the validity of Eq. 19.3-10, and the correctness of Eq. 19.3-11 can be proved similarly.

(b) One can also get $\overline{H}_A$ by using the definition in Eq. 19.3-7 and measuring the slope of the curve of H versus n_A, holding n_B constant. One can also get $\overline{H}_A$ by measuring the enthalpy of mixing and using

$$H = n_A\overline{H}_A + n_B\overline{H}_B = n_A\tilde{H}_A + n_B\tilde{H}_B + \Delta H_{\text{mix}} \tag{19.3-16}$$

Often the enthalpy of mixing is neglected and the enthalpies of the pure substances are given as $\tilde{H}_A \approx \tilde{C}_{pA}(T - T^o)$ and a similar expression for $\tilde{H}_B$. This is a standard assumption for gas mixtures at low to moderate pressures.

Other methods for evaluating partial molar quantities may be found in current textbooks on thermodynamics.

§19.4 USE OF THE EQUATIONS OF CHANGE FOR MIXTURES

The equations of change in §19.2 can be used to solve all the problems of Chapter 18, and more difficult ones as well. Unless the problems are idealized or simplified, mixture transport phenomena are quite complicated and usually numerical techniques are required. Here we solve a few introductory problems by way of illustration.

EXAMPLE 19.4-1

Simultaneous Heat and Mass Transport[1]

(a) Develop expressions for the mole fraction profile $x_A(y)$ and the temperature profile $T(y)$ for the system pictured in Fig. 19.4-1, given the mole fractions and temperatures at both film boundaries ($y = 0$ and $y = \delta$). Here a hot condensable vapor, A, is diffusing at steady state through a stagnant film of noncondensable gas, B, to a cold surface at $y = 0$, where A condenses. Assume ideal gas behavior and uniform pressure. Furthermore assume the physical

[1] A. P. Colburn and T. B. Drew, *Trans. Am. Inst. Chem. Engrs.*, **38**, 197–212 (1937).

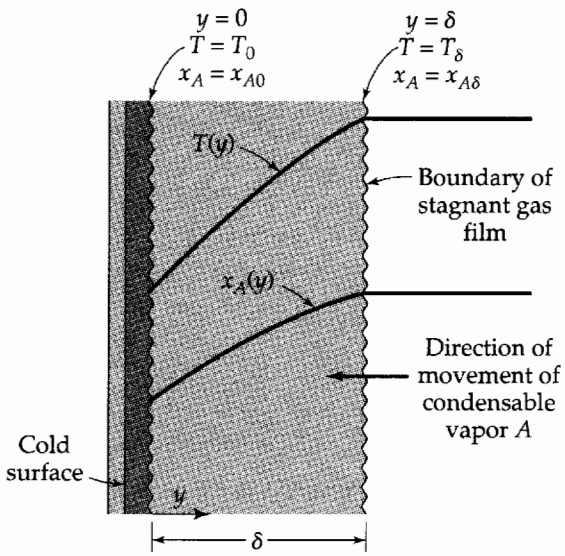

Fig. 19.4-1. Condensation of a hot vapor A on a cold surface in the presence of a non-condensable gas B.

properties to be constant, evaluated at some mean temperature and composition. Neglect radiative heat transfer.

(b) Generalize the result for the situation where both A and B are condensing on the wall, and allow for unequal film thicknesses for heat and mass transport.

SOLUTION

(a) To determine the desired quantities, we must solve the equations of continuity and energy for this system. Simplification of Eq. 19.1-10 and Eq. C of Table 19.2-1 for steady, one-dimensional transport, in the absence of chemical reactions and external forces, gives

Continuity of A:
$$\frac{dN_{Ay}}{dy} = 0 \tag{19.4-1}$$

Energy:
$$\frac{de_y}{dy} = 0 \tag{19.4-2}$$

Therefore, both N_{Ay} and e_y are constant throughout the film.

To determine the *mole fraction profile*, we need the molar flux for diffusion of A through stagnant B:

$$N_{Ay} = -\frac{c\mathscr{D}_{AB}}{1 - x_A}\frac{dx_A}{dy} \tag{19.4-3}$$

Insertion of Eq. 19.4-3 into Eq. 19.4-1 and integration gives the mole fraction profile (see §18.2)

$$\left(\frac{1 - x_A}{1 - x_{A0}}\right) = \left(\frac{1 - x_{A\delta}}{1 - x_{A0}}\right)^{y/\delta} \tag{19.4-4}$$

Here we have taken $c\mathscr{D}_{AB}$ to be constant, at the value for the mean film temperature. We can then evaluate the constant flux N_{Ay} from Eqs. 19.4-3 and 4:

$$N_{Ay} = \frac{c\mathscr{D}_{AB}}{\delta}\ln\frac{1 - x_{A\delta}}{1 - x_{A0}} \tag{19.4-5}$$

Note that N_{Ay} is negative because species A is condensing. The last two expressions may be combined to put the concentration profiles in an alternative form:

$$\frac{x_A - x_{A0}}{x_{A\delta} - x_{A0}} = \frac{1 - \exp[(N_{Ay}/c\mathscr{D}_{AB})y]}{1 - \exp[(N_{Ay}/c\mathscr{D}_{AB})\delta]} \tag{19.4-6}$$

To get the *temperature profile*, we use the energy flux from Eq. 19.3-6 for an ideal gas along with Eq. 9.8-8:

$$e_y = -k\frac{dT}{dy} + (\tilde{H}_A N_{Ay} + \tilde{H}_B N_{By})$$
$$= -k\frac{dT}{dy} + N_{Ay}\tilde{C}_{pA}(T - T_0) \tag{19.4-7}$$

Here we have chosen T_0 as the reference temperature for the enthalpy. Insertion of this expression for e_y into Eq. 19.4-2 and integration between the limits $T = T_0$ at $y = 0$, and $T = T_\delta$ at $y = \delta$ gives

$$\frac{T - T_0}{T_\delta - T_0} = \frac{1 - \exp[(N_{Ay}\tilde{C}_{pA}/k)y]}{1 - \exp[(N_{Ay}\tilde{C}_{pA}/k)\delta]} \tag{19.4-8}$$

It can be seen that the temperature profile is not linear for this system except in the limit as $N_{Ay}\tilde{C}_{pA}/k \to 0$. Note the similarity between Eqs. 19.4-6 and 8.

The conduction energy flux at the wall is greater here than in the absence of mass transfer. Thus, using a superscript zero to indicate the conditions in the absence of mass transfer, we may write

$$\frac{-k(dT/dy)|_{y=0}}{-k(dT/dy)^0|_{y=0}} = \frac{-(N_{Ay}\tilde{C}_{pA}/k)\delta}{1 - \exp[(N_{Ay}\tilde{C}_{pA}/k)\delta]} \tag{19.4-9}$$

We see then that the rate of heat transfer is directly affected by simultaneous mass transfer, whereas the mass flux is not directly affected by simultaneous heat transfer. In applications at temperatures below the normal boiling point of species A, the quantity $N_{Ay}\tilde{C}_{pA}/k$ is small, and the right side of Eq. 19.4-9 is very nearly unity (see Problem 19A.1). The interaction between heat and mass transfer is further discussed in Chapter 22.

(b) If both A and B are condensing at the wall, then Eqs. 19.4-1 and 2, when integrated, lead to $N_{Ay} = N_{A0}$ and $e_y = e_0$, where the subscript "0" quantities are evaluated at $y = 0$. We also integrate the analog of Eq. 19.4-1 for B to get $N_{By} = N_{B0}$ and obtain

$$-c\mathcal{D}_{AB}\frac{dx_A}{dy} + x_A(N_{A0} + N_{B0}) = N_{A0} \tag{19.4-10}$$

$$-k\frac{dT}{dy} + (N_{A0}\overline{H}_A + N_{B0}\overline{H}_B) = e_0 \tag{19.4-11}$$

In the second of these equations, we replace $\overline{H}_A$ by $\tilde{C}_{pA}(T - T_0)$ and $\overline{H}_B$ by $\tilde{C}_{pB}(T - T_0)$, and since the reference temperature is T_0, we may replace e_0 by q_0, the conductive heat flux at the wall. In the first equation, we subtract $x_{A0}(N_{A0} + N_{B0})$ from both sides to make the equation similar in form to the temperature equation just obtained. Thus

$$-c\mathcal{D}_{AB}\frac{dx_A}{dy} + (N_{A0} + N_{B0})(x_A - x_{A0}) = N_{A0} - x_{A0}(N_{A0} + N_{B0}) \tag{19.4-12}$$

$$-k\frac{dT}{dy} + (N_{A0}\tilde{C}_{pA} + N_{B0}\tilde{C}_{pB})(T - T_0) = q_0 \tag{19.4-13}$$

Integration with respect to y and application of the boundary conditions at $y = 0$ gives

$$\frac{(N_{A0} + N_{B0})(x_A - x_{A0})}{N_{A0} - x_{A0}(N_{A0} + N_{B0})} = 1 - \exp\left[(N_{A0} + N_{B0})\frac{y}{c\mathcal{D}_{AB}}\right] \tag{19.4-14}$$

$$\frac{(N_{A0}\tilde{C}_{pA} + N_{B0}\tilde{C}_{pB})(T - T_0)}{q_0} = 1 - \exp\left[(N_{A0}\tilde{C}_{pA} + N_{B0}\tilde{C}_{pB})\frac{y}{k}\right] \tag{19.4-15}$$

These are the concentration and temperature profiles in terms of the mass and heat fluxes. Applications of the boundary conditions at the outer edges of the films—that is, at $y = \delta_x$ and $y = \delta_T$, respectively—give

$$\frac{(N_{A0} + N_{B0})(x_{A\delta} - x_{A0})}{N_{A0} - x_{A0}(N_{A0} + N_{B0})} = 1 - \exp\left[(N_{A0} + N_{B0})\frac{\delta_x}{c\mathscr{D}_{AB}}\right] \tag{19.4-16}$$

$$\frac{(N_{A0}\tilde{C}_{pA} + N_{B0}\tilde{C}_{pB})(T_\delta - T_0)}{q_0} = 1 - \exp\left[(N_{A0}\tilde{C}_{pA} + N_{B0}\tilde{C}_{pB})\frac{\delta_T}{k}\right] \tag{19.4-17}$$

These equations relate the fluxes to the film thicknesses and the transport properties. When Eq. 19.4-14 is divided by Eq. 19.4-16 and Eq. 19.4-15 is divided by Eq. 19.4-17, we get the concentration profiles in terms of the transport coefficients (analogously to Eqs. 19.4-6 and 8). Equations 19.4-16 and 17 will be encountered again in §22.8.

EXAMPLE 19.4-2

Concentration Profile in a Tubular Reactor

A catalytic tubular reactor is shown in Fig. 19.4-2. A dilute solution of solute A in a solvent S is in fully developed, laminar flow in the region $z < 0$. When it encounters the catalytic wall in the region $0 \le z \le L$, solute A is instantaneously and irreversibly rearranged to an isomer B. Write the diffusion equation appropriate for this problem, and find the solution for short distances into the reactor. Assume that the flow is isothermal and neglect the presence of B.

SOLUTION

For the conditions stated above, the flowing liquid will always be very nearly pure solvent S. The product $\rho\mathscr{D}_{AS}$ can be considered constant, and the diffusion of A in S can be described by the steady-state version of Eq. 19.1-14 (ignoring the presence of a small amount of the reaction product B). The relevant equations of change for the system are then

Continuity of A:

$$v_z\frac{\partial c_A}{\partial z} = \mathscr{D}_{AS}\left[\frac{1}{r}\frac{\partial}{\partial r}\left(r\frac{\partial c_A}{\partial r}\right) + \underline{\frac{\partial^2 c_A}{\partial z^2}}\right] \tag{19.4-18}$$

Motion:

$$0 = -\frac{d\mathscr{P}}{dz} + \mu\frac{1}{r}\frac{d}{dr}\left(r\frac{dv_z}{dr}\right) \tag{19.4-19}$$

We make the usual assumption that axial diffusion can be neglected with respect to axial convection, and therefore delete the dashed-underlined term (compare with Eqs. 10.8-11 and 12). Equation 19.4-19 can be solved to give the parabolic velocity profile $v_z(r) = v_{z,\max}[1 - (r/R)^2]$. When this result is substituted into Eq. 19.4-18, we get

$$v_{z,\max}\left[1 - \left(\frac{r}{R}\right)^2\right]\frac{\partial c_A}{\partial z} = \mathscr{D}_{AS}\frac{1}{r}\frac{\partial}{\partial r}\left(r\frac{\partial c_A}{\partial r}\right) \tag{19.4-20}$$

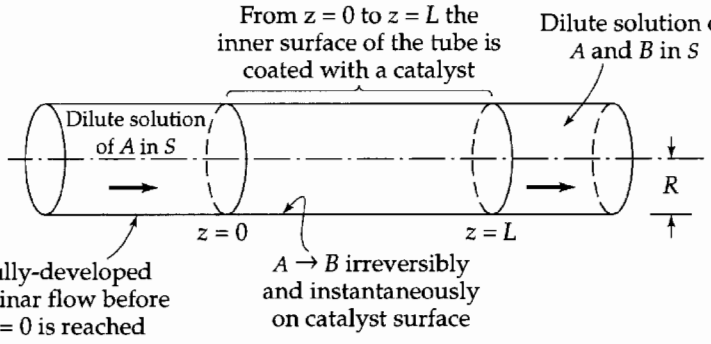

Fig. 19.4-2. Boundary conditions for a tubular reactor.

This is to be solved with the boundary conditions

$$\text{B.C. 1:} \qquad \text{at } z = 0, \qquad c_A = c_{A0} \tag{19.4-21}$$

$$\text{B.C. 2:} \qquad \text{at } r = R, \qquad c_A = 0 \tag{19.4-22}$$

$$\text{B.C. 3:} \qquad \text{at } r = 0, \qquad c_A = \text{finite} \tag{19.4-23}$$

For short distances z into the reactor, the concentration c_A differs from c_{A0} only near the wall, where the velocity profile is practically linear. Hence we can introduce the variable $y = R - r$, neglect curvature terms, and replace B.C. 3 by a fictitious boundary condition at $y = \infty$ (see Example 12.2-2 for a detailed discussion of this method of treating the entrance region of the tube).

The reformulated problem statement is then

$$2v_{z,\max}\frac{y}{R}\frac{\partial c_A}{\partial z} = \mathscr{D}_{AS}\frac{\partial^2 c_A}{\partial y^2} \tag{19.4-24}$$

with the boundary conditions

$$\text{B.C. 1:} \qquad \text{at } z = 0, \qquad c_A = c_{A0} \tag{19.4-25}$$

$$\text{B.C. 2:} \qquad \text{at } y = 0, \qquad c_A = 0 \tag{19.4-26}$$

$$\text{B.C. 3:} \qquad \text{at } y = \infty, \qquad c_A = c_{A0} \tag{19.4-27}$$

This problem can be solved by the method of combination of independent variables by seeking a solution of the form $c_A/c_{A0} = f(\eta)$, where $\eta = (y/R)(2v_{z,\max}R^2/9\mathscr{D}_{AS}z)^{1/3}$. One thus obtains the ordinary differential equation $f'' + 3\eta^2 f' = 0$, which can be integrated to give (see Eq. C.1-9)

$$\frac{c_A}{c_{A0}} = \frac{\int_0^\eta \exp(-\bar{\eta}^3)\,d\bar{\eta}}{\int_0^\infty \exp(-\bar{\eta}^3)\,d\bar{\eta}} = \frac{\int_0^\eta \exp(-\bar{\eta}^3)\,d\bar{\eta}}{\Gamma(\frac{4}{3})} \tag{19.4-28}$$

This problem is mathematically analogous to the Graetz problem of Problem 12D.4, Θ of that problem being analogous to $1 - (c_A/c_{A0})$ here.

Experiments of the type described here have proved useful for obtaining mass transfer data at high Schmidt numbers.[2] A particularly attractive reaction is the reduction of ferricyanide ions on metallic surfaces according to the reaction

$$Fe(CN)_6^{-3} + e^{-1} \rightarrow Fe(CN)_6^{-4} \tag{19.4-29}$$

in which ferricyanide and ferrocyanide take the place of A and B in the above development. This electrochemical reaction is quite rapid under properly chosen conditions. Furthermore, since it involves only electron transfer, the physical properties of the solution are almost entirely unaffected. The forced diffusion effects neglected here may be suppressed by the addition of an indifferent electrolyte in excess.[3,4]

EXAMPLE 19.4-3

Catalytic Oxidation of Carbon Monoxide

Figure 19.4-3 shows schematically how oxygen and carbon monoxide combine at a catalytic surface (palladium) to make carbon dioxide, according to the technologically important reaction[5]

$$O_2 + 2CO \rightarrow 2CO_2 \tag{19.4-30}$$

---

[2] D. W. Hubbard and E. N. Lightfoot, *Ind. Eng. Chem. Fundam.*, **5**, 370–379 (1966).

[3] J. S. Newman, *Electrochemical Systems*, 2nd edition, Prentice-Hall, Englewood Cliffs, N.J. (1991), §1.10.

[4] J. R. Selman and C. W. Tobias, *Advances in Chemical Engineering*, **10**, Academic Press, New York, N.Y. (1978), pp. 212–318.

[5] B. C. Gates, *Catalytic Chemistry*, Wiley, New York (1992), pp. 356–362; C. N. Satterfield, *Heterogeneous Catalysis in Industrial Practice*, McGraw-Hill, New York, 2nd edition (1991), Chapter 8.

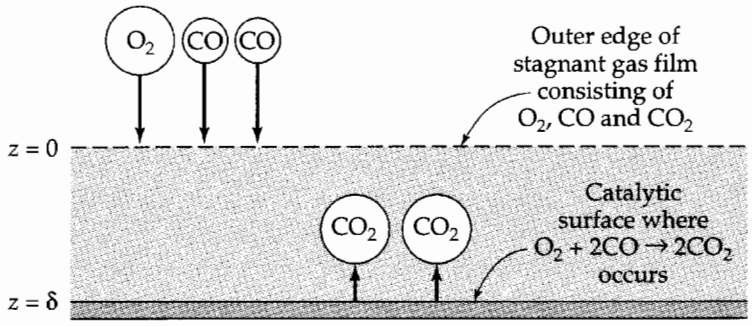

Fig. 19.4-3. Three-component system with a catalytic chemical reaction.

For this analysis, the reaction is assumed to occur instantaneously and irreversibly at the catalytic surface. The gas composition at the outer edge of the film (at $z = 0$) is presumed known, and the catalyst surface is at $z = \delta$. The temperature and pressure are assumed to be independent of position throughout the film. We label the chemical species by: $O_2 = 1$, $CO = 2$, $CO_2 = 3$.

SOLUTION

For steady-state, one-dimensional diffusion without homogeneous reactions, Eq. 19.1-10 gives

$$\frac{dN_{1z}}{dz} = 0; \qquad \frac{dN_{2z}}{dz} = 0; \qquad \frac{dN_{3z}}{dz} = 0 \tag{19.4-31}$$

which tells us that all of the molar fluxes are constants across the film. From boundary conditions provided by the stoichiometry of the problem we further know that

$$N_{1z} = \tfrac{1}{2}N_{2z} = -\tfrac{1}{2}N_{3z} \tag{19.4-32}$$

The Maxwell–Stefan equations of Eq. 17.9-1 then give:

$$\begin{aligned}\frac{dx_3}{dz} &= -\frac{1}{c\mathscr{D}_{13}}(x_1N_{3z} - x_3N_{1z}) - \frac{1}{c\mathscr{D}_{23}}(x_2N_{3z} - x_3N_{2z}) \\ &= -\frac{N_{3z}}{c\mathscr{D}_{13}}(1 + \tfrac{1}{2}x_3)\end{aligned} \tag{19.4-33}$$

$$\begin{aligned}\frac{dx_1}{dz} &= -\frac{1}{c\mathscr{D}_{12}}(x_2N_{1z} - x_1N_{2z}) - \frac{1}{c\mathscr{D}_{13}}(x_3N_{1z} - x_1N_{3z}) \\ &= \frac{N_{3z}}{2c\mathscr{D}_{12}}(1 - 3x_1 - x_3) + \frac{N_{3z}}{2c\mathscr{D}_{13}}(2x_1 + x_3)\end{aligned} \tag{19.4-34}$$

These equations have been simplified by using Eq. 19.4-32, and by using the fact that $\mathscr{D}_{23} \approx \mathscr{D}_{13}$ over a wide range of temperature. The latter may be seen by using Appendix E to show that $\sigma_{23} = 3.793$Å and $\sigma_{13} = 3.714$Å, and that $\varepsilon_{23}/\kappa = 145$K and $\varepsilon_{13}/\kappa = 146$K. Since only the mole fraction x_3 appears in Eq. 19.4-33, this equation may be integrated[6] at once to give

$$x_3 = -2 + (x_{30} + 2)\exp\left(-\frac{N_{3z}z}{2c\mathscr{D}_{13}}\right) \tag{19.4-35}$$

Combination of the last two equations then gives, after integration

$$x_1 = 1 - \frac{1}{3}(x_{30} + 2)\exp\left(-\frac{N_{3z}z}{2c\mathscr{D}_{13}}\right) - \left(\frac{1}{3} - x_{10} - \frac{1}{3}x_{30}\right)\exp\left[-\left(\frac{3}{2}\frac{\mathscr{D}_{13}}{\mathscr{D}_{12}} - 1\right)\left(\frac{N_{3z}z}{c\mathscr{D}_{13}}\right)\right] \tag{19.4-36}$$

[6] Three-component problems with two diffusivities equal have been discussed by H. L. Toor, *AIChE Journal*, **3**, 198–207 (1957).

From this equation and a similar one for x_2, we can get x_3 at $z = \delta$. Then from Eq. 19.4-35 we get

$$N_{3z} = -\frac{c\mathscr{D}_{13}}{\delta}\ln\left(\frac{x_{3\delta}+2}{x_{30}+2}\right) \tag{19.4-37}$$

which gives the rate of production of carbon dioxide at the catalytic surface. This result can then be substituted into Eqs. 19.4-35 and 36 and the three mole fractions can be calculated as functions of z.

EXAMPLE 19.4-4

Thermal Conductivity of a Polyatomic Gas

In §9.3 we pointed out that the thermal conductivities of polyatomic gases deviate from the formula for monatomic gases, because of the effects of the internal degrees of freedom in the complex molecules. When the Eucken formula for polyatomic gases (Eq. 9.3-15) is divided by the formula for monatomic gases (Eq. 9.3-14) and use is made of the ideal gas law, one can write the ratio of the polyatomic gas thermal conductivity to that of a monatomic gas as

$$\frac{k_{\text{poly}}}{k_{\text{mon}}} = \frac{3}{5} + \frac{4}{15}\frac{\tilde{C}_v}{R} \tag{19.4-38}$$

Derive a result of this form by modeling the polyatomic gas as an interacting gas mixture, in which the various "species" are the polyatomic gas molecules in the various rotational and vibrational states.

SOLUTION

The heat flux for a gas mixture is given in Eq. 19.3-3. All "species" will have the same thermal conductivity because they differ only in their internal quantum states. Therefore we expect each k_α to be k_{mon}. Similarly, the mass flux for each "species" should be given by Fick's law for a pure gas $\mathbf{j}_\alpha = -\rho\mathscr{D}_{\alpha\alpha}\nabla\omega_\alpha$, with all the $\mathscr{D}_{\alpha\alpha}$ having a common value $\mathscr{D}_{\text{mon}}$. Thus we get

$$\begin{aligned}\mathbf{q}_{\text{poly}} &= -k_{\text{mon}}\nabla T - \sum_{\alpha=1}^{N}\frac{\tilde{H}_\alpha}{M_\alpha}\rho\mathscr{D}_{\alpha\alpha}\nabla\omega_\alpha \\ &= -k_{\text{mon}}\nabla T - c\mathscr{D}_{\text{mon}}\sum_{\alpha=1}^{N}\tilde{H}_\alpha\nabla x_\alpha\end{aligned} \tag{19.4-39}$$

since the molecular weights of all the "species" are the same.

If now it is postulated that the distribution over the various quantum states is in equilibrium with the local temperature, then $\nabla x_\alpha = (dx_\alpha/dT)\nabla T$. Then we can define the *effective thermal conductivity* of the mixture by

$$\mathbf{q}_{\text{poly}} = -k_{\text{mon}}\nabla T - c\mathscr{D}_{\text{mon}}\sum_{\alpha=1}^{N}\tilde{H}_\alpha(dx_\alpha/dT)\nabla T \equiv -k_{\text{poly}}\nabla T \tag{19.4-40}$$

and write

$$\begin{aligned}\frac{k_{\text{poly}}}{k_{\text{mon}}} &= 1 + \left(\frac{c\mathscr{D}_{\text{mon}}}{k_{\text{mon}}}\right)\left(\frac{d}{dT}\sum_{\alpha=1}^{N}\tilde{H}_\alpha x_\alpha - \sum_{\alpha=1}^{N}x_\alpha\left(\frac{d\tilde{H}_\alpha}{dT}\right)\right) \\ &= 1 + \left(\frac{c\mathscr{D}_{\text{mon}}}{k_{\text{mon}}}\right)(\tilde{C}_{p,\text{poly}} - \tilde{C}_{p,\text{mon}}) \\ &= 1 + \tfrac{4}{5}A[(\tilde{C}_{p,\text{poly}}/\tilde{C}_{p,\text{mon}}) - 1]\end{aligned} \tag{19.4-41}$$

Here the temperature-dependent quantity

$$A = \tfrac{5}{4}(c\mathscr{D}_{\text{mon}}\tilde{C}_{p,\text{mon}}/k_{\text{mon}}) \tag{19.4-42}$$

can be calculated from the kinetic theory of gases at low density. It varies only very slowly with temperature, and a suitable mean value is 1.106. The quantity $\tilde{C}_{p,\text{poly}} = d\tilde{H}/dT$ is the heat capacity for a gas in which the equilibrium among the various quantum states is maintained

during the change of temperature, whereas $\tilde{C}_{p,\text{mon}}$ is the heat capacity for a gas in which transitions between quantum states are not allowed, so that $\tilde{C}_{p,\text{mon}} = \frac{5}{2}R$. When the numerical value $A = 1.106$ is inserted in Eq. 19.4-41, we get finally

$$\frac{k_{\text{poly}}}{k_{\text{mon}}} = 0.115 + 0.354\left(\frac{\tilde{C}_{p,\text{poly}}}{R}\right) = 0.469 + 0.354\left(\frac{\tilde{C}_{V,\text{poly}}}{R}\right) \tag{19.4-43}$$

which is the formula recommended by Hirschfelder.[7] Although the predictions of Eq. 19.4-43 are not much better than those of the older Eucken formula, the above development does at least give some feel for the role of the internal degrees of freedom in heat conduction.[8,9]

§19.5 DIMENSIONAL ANALYSIS OF THE EQUATIONS OF CHANGE FOR NONREACTING BINARY MIXTURES

In this section we dimensionally analyze the equations of change summarized in §19.2, using special cases of the flux expressions of §19.3. The discussion parallels that of §11.5 and serves analogous purposes: to identify the controlling dimensionless parameters of representative mass transfer problems, and to provide an introduction to the mass transfer correlations of Chapter 22.

Once again we restrict the discussion primarily to systems of constant physical properties. The equation of continuity for the mixture then takes the familiar form

Continuity: $$(\nabla \cdot \mathbf{v}) = 0 \tag{19.5-1}$$

The equation of motion may be approximated in the manner of Boussinesq (see §11.3) by putting Eqs. 19.3-2 and 19-5.1 into Eq. 19.2-3, and replacing $-\nabla p + \bar{\rho}\mathbf{g}$ by $-\nabla\mathcal{P}$. For a constant-viscosity Newtonian fluid this gives

Motion: $$\bar{\rho}\frac{D\mathbf{v}}{Dt} = \mu\nabla^2\mathbf{v} - \nabla\mathcal{P} - \bar{\rho}\mathbf{g}\bar{\beta}(T - \bar{T}) - \bar{\rho}\mathbf{g}\bar{\zeta}(\omega_A - \bar{\omega}_A) \tag{19.5-2}$$

The energy equation, in the absence of chemical reactions, viscous dissipation, and external forces other than gravity, is obtained from Eq. (F) of Table 19.2-4, with Eq. 19.3-3. In using the latter we further neglect the diffusional transport of energy relative to the mass average velocity. For constant thermal conductivity this leads to

Energy: $$\frac{DT}{Dt} = \alpha\nabla^2 T \tag{19.5-3}$$

in which $\alpha = k/\rho\tilde{C}_p$ is the thermal diffusivity. For nonreacting binary mixtures with constant ρ and $\mathcal{D}_{AB}$, Eq. 19.1-14 takes the form

Continuity of A: $$\frac{D\omega_A}{Dt} = \mathcal{D}_{AB}\nabla^2\omega_A \tag{19.5-4}$$

For the assumptions that have been made, the analogy between Eqs. 19.5-3 and 4 is clear.

---

[7] J. O. Hirschfelder, *J. Chem. Phys.*, **26**, 274–281 (1957); see also D. Secrest and J. O. Hirschfelder, *Physics of Fluids*, **4**, 61–73 (1961) for further development of the theory, in which equilibrium among the various quantum states is not assumed.

[8] For a comparison of the two formulas with experimental data, see Reid, Prausnitz, and Poling, op. cit., p. 497. The Hirschfelder formula in Eq. 19.4-42 and the Eucken formula of Eq. 9.3-15 tend to bracket the observed conductivity values.

[9] J. H. Ferziger and H. G. Kaper, *Mathematical Theory of Transport Processes in Gases*, North Holland, Amsterdam (1977), §§11.2 and 3.

We now introduce the reference quantities l_0, v_0, and $\mathcal{P}_0$, used in §3.7 and §11.5, the reference temperatures T_0 and T_1 of §11.5, and the analogous reference mass fractions ω_{A0} and ω_{A1}. Then the dimensionless quantities we will use are

$$\check{x} = \frac{x}{l_0} \qquad \check{y} = \frac{y}{l_0} \qquad \check{z} = \frac{z}{l_0} \qquad \check{t} = \frac{v_0 t}{l_0} \tag{19.5-5}$$

$$\check{\mathbf{v}} = \frac{\mathbf{v}}{v_0} \qquad \check{\nabla} = l_0 \nabla \qquad \frac{D}{D\check{t}} = \left(\frac{l_0}{v_0}\right)\frac{D}{Dt} \qquad \check{\mathcal{P}} = \frac{\mathcal{P} - \mathcal{P}_0}{\bar{\rho} v_0^2} \tag{19.5-6}$$

$$\check{T} = \frac{T - T_0}{T_1 - T_0} \qquad \check{\omega}_A = \frac{\omega_A - \omega_{A0}}{\omega_{A1} - \omega_{A0}} \tag{19.5-7}$$

Here it is understood that $\mathbf{v}$ is the mass average velocity of the mixture. It should be recognized that for some problems other choices of dimensionless variables may be preferable.

In terms of the dimensionless variables listed above, the equations of change may be expressed as

Continuity:
$$(\check{\nabla} \cdot \check{\mathbf{v}}) = 0 \tag{19.5-8}$$

Motion:
$$\frac{D\check{\mathbf{v}}}{D\check{t}} = \frac{1}{\mathrm{Re}}\check{\nabla}^2\check{\mathbf{v}} - \check{\nabla}\check{\mathcal{P}} - \frac{\mathrm{Gr}}{\mathrm{Re}^2}\frac{\mathbf{g}}{g}(\check{T} - \bar{\check{T}}) - \frac{\mathrm{Gr}_\omega}{\mathrm{Re}^2}\frac{\mathbf{g}}{g}(\check{\omega}_A - \bar{\check{\omega}}_A) \tag{19.5-9}$$

Energy:
$$\frac{D\check{T}}{D\check{t}} = \frac{1}{\mathrm{RePr}}\check{\nabla}^2\check{T} \tag{19.5-10}$$

Continuity of A:
$$\frac{D\check{\omega}_A}{D\check{t}} = \frac{1}{\mathrm{ReSc}}\check{\nabla}^2\check{\omega}_A \tag{19.5-11}$$

The Reynolds, Prandtl, and thermal Grashof numbers have been given in Table 11.5-1. The other two numbers are new:

$$\mathrm{Sc} = \left[\!\left[\frac{\mu}{\rho\mathcal{D}_{AB}}\right]\!\right] = \left[\!\left[\frac{\nu}{\mathcal{D}_{AB}}\right]\!\right] = \text{Schmidt number} \tag{19.5-12}$$

$$\mathrm{Gr}_\omega = \left[\!\left[\frac{g\bar{\zeta}(\omega_{A1} - \omega_{A0})l_0^3}{\nu^2}\right]\!\right] = \text{diffusional Grashof number} \tag{19.5-13}$$

The Schmidt number is the ratio of momentum diffusivity to mass diffusivity and represents the relative ease of molecular momentum and mass transfer. It is analogous to the Prandtl number, which represents the ratio of the momentum diffusivity to the thermal diffusivity. The diffusional Grashof number arises because of the buoyant force caused by the concentration inhomogeneities. The products RePr and ReSc in Eqs. 19.5-10 and 11 are known as Péclet numbers, Pé and $\mathrm{Pé}_{AB}$, respectively.

The dimensional analysis of mass transfer problems parallels that for heat transfer problems. We illustrate the technique by three examples: (i) The strong similarity between Eqs. 19.5-10 and 11 permits the solution of many mass transfer problems by analogy with previously solved heat transfer problems; such an analogy is used in Example 19.5-1. (ii) Frequently the transfer of mass requires or releases energy, so that the heat and mass transfer must be considered simultaneously, as is illustrated in Example 19.5-2. (iii) Sometimes, as in many industrial mixing operations, diffusion plays a subordinate role in mass transfer and need not be given detailed consideration; this situation is illustrated in Example 19.5-3.

We shall see then that, just as for heat transfer, the use of dimensional analysis for the solution of practical mass transfer problems is an art. This technique is normally most useful when the effects of at least some of the many dimensionless ratios can be neglected. Estimation of the relative importance of pertinent dimensionless groups normally requires considerable experience.

EXAMPLE 19.5-1

Concentration Distribution about a Long Cylinder

We wish to predict the concentration distribution about a long isothermal cylinder of a volatile solid A, immersed in a gaseous stream of a species B, which is insoluble in solid A. The system is similar to that pictured in Fig. 11.5-1, except that here we consider the transfer of mass rather than heat. The vapor pressure of the solid is small compared to the total pressure in the gas, so that the mass transfer system is virtually isothermal.

Can the results of Example 11.5-1 be used to make the desired prediction?

SOLUTION

The results of Example 11.5-1 are applicable if it can be shown that suitably defined dimensionless concentration profiles in the mass transfer system are identical to the temperature profiles in the heat transfer system:

$$\check{\omega}_A(\check{x}, \check{y}, \check{z}) = \check{T}(\check{x}, \check{y}, \check{z}) \tag{19.5-14}$$

This equality will be realized if the differential equations and boundary conditions for the two systems can be put into identical form.

We therefore begin by choosing the same reference length, velocity, and pressure as in Example 11.5-1, and an analogous composition function: $\check{\omega}_A = (\omega_A - \omega_{A0})/(\omega_{A\infty} - \omega_{A0})$. Here ω_{A0} is the mass fraction of A in the gas adjacent to the interface, and $\omega_{A\infty}$ is the value far from the cylinder. We also specify that $\overline{\omega}_A = \omega_{A0}$ so that $\overline{\check{\omega}}_A = 0$. The equations of change needed here are then Eqs. 19.5-8, 9, and 11. Thus the differential equations here and in Problem 11.5-1 are analogous except for the viscous heating term in Eq. 11.5-3.

As for the boundary conditions, we have here:

B.C. 1: as $\check{x}^2 + \check{y}^2 \to \infty$, $\quad \check{\mathbf{v}} \to \boldsymbol{\delta}_x \quad \check{\omega}_A \to 1$ (19.5-15)

B.C. 2: at $\check{x}^2 + \check{y}^2 = \frac{1}{4}$, $\quad \check{\mathbf{v}} = \dfrac{1}{\text{ReSc}} \dfrac{(\omega_{A0} - \omega_{A\infty})}{(1 - \omega_{A0})} \check{\nabla}\check{\omega}_A \quad \check{\omega}_A = 0$ (19.5-16)

B.C. 3: at $\check{x}^2 + \check{y}^2 = \infty$ and $\check{y} = 0$, $\quad \check{\mathcal{P}} = 0$ (19.5-17)

The boundary condition on $\check{\mathbf{v}}$, obtained with the help of Fick's first law, states that there is an interfacial radial velocity resulting from the sublimation of A.

If we compare the above description with that for heat transfer in Example 11.5-1, we see that there is no mass transfer counterpart of the viscous dissipation term in the energy equation and no heat transfer counterpart to the interfacial radial velocity component in the boundary condition of Eq. 19.5-16. The descriptions are otherwise analogous, however, with $\check{\omega}_A$, Sc, and Gr_ω taking the places of $\check{T}$, Pr, and Gr.

When the Brinkman number is sufficiently small, viscous dissipation will be unimportant, and that term in the energy equation can be neglected. Neglecting the Brinkman number term is appropriate, except for flows of very viscous fluids with large velocity gradients, or in hypersonic boundary layers (§10.4). Similarly, when $(1/\text{ReSc})[(\omega_{A0} - \omega_{A\infty})/(1 - \omega_{A0})]$ is very small, it may be set equal to zero without introducing appreciable error. If these limiting conditions are met, analogous behavior will be obtained for heat and mass transfer. More precisely, the dimensionless concentration $\check{\omega}_A$ will have the same dependence on $\check{x}$, $\check{y}$, $\check{z}$, $\check{t}$, Re, Pr, and Gr_ω as the dimensionless temperature $\check{T}$ will have on $\check{x}$, $\check{y}$, $\check{z}$, $\check{t}$, Re, Pr, and Gr. The concentration and temperature profiles will then be identical at a given Re whenever Sc = Pr and Gr_ω = Gr.

The thermal Grashof number can, at least in principle, be varied at will by changing $T_0 - T_\infty$. Hence it is likely that the desired Grashof numbers can be obtained. However, it can be seen from Tables 9.1-1 and 17.1-1 that Schmidt numbers for gases can vary over a considerably wide range than can the Prandtl numbers. Hence it may be difficult to obtain a satisfactory thermal model of the mass transfer process, except in a limited range of the Schmidt number.

Another possibly serious obstacle to achieving similar heat and mass transfer behavior is the possible nonuniformity of the surface temperature. The heat of sublimation must be obtained from the surrounding gas, and this in turn will cause the solid temperature to become lower than that of the gas. Hence it is necessary to consider both heat and mass transfer simultaneously. A very simple analysis of simultaneous heat and mass transfer is discussed in the next example.

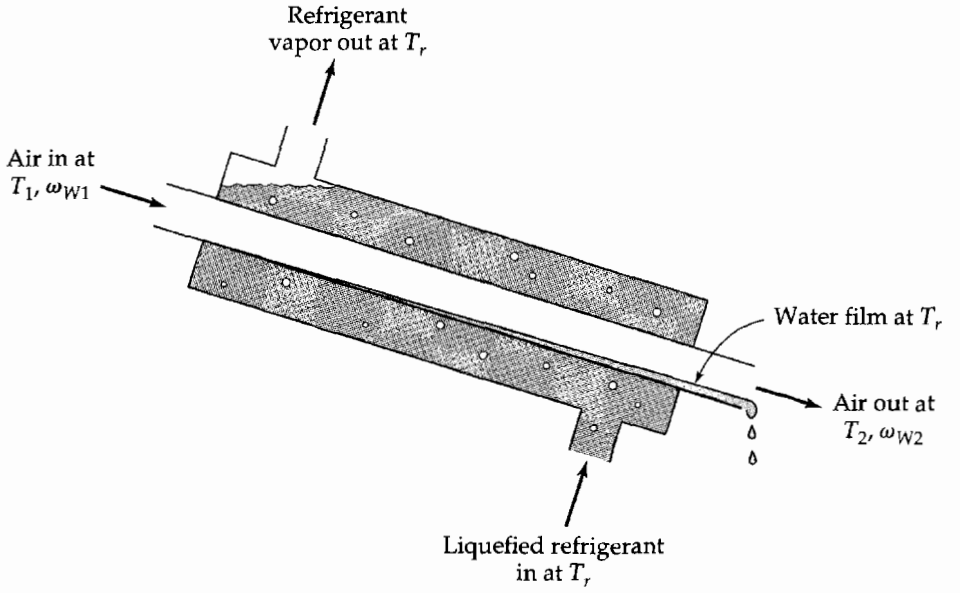

Fig. 19.5-1. Schematic representation of a dehumidifier. Air enters with inlet temperature T_1 and humidity ω_{W1} (the mass fraction of water vapor). It leaves with outlet temperature T_2 and humidity ω_{W2}. Because the heat transfer to the refrigerant is very effective, the temperature at the air-condensate interface is close to the refrigerant temperature T_r.

EXAMPLE 19.5-2

Fog Formation during Dehumidification

Wet air is being simultaneously cooled and dehumidified by passage through a metal tube chilled by the boiling of a liquid refrigerant. The tube surface is below the dew point of the entering air and therefore becomes covered with a water film. Heat transfer from the refrigerant to this condensate layer is sufficiently effective that the free water surface may be considered isothermal and at the boiling point of the refrigerant. This system is shown in Fig. 19.5-1.

We wish to determine the range of refrigerant temperatures that may be used without danger of fog formation. Fog is undesirable, because most of the tiny water droplets constituting the fog will pass through the cooling tube along with the air unless special collectors are provided. Fog can form if the wet air become supersaturated at any point in the system.

SOLUTION

Let species A be air and W be water. It is convenient here to choose the dimensionless variables

$$\check{T} = \frac{T - T_r}{T_1 - T_r}; \qquad \check{\omega}_W = \frac{\omega_W - \omega_{Wr}}{\omega_{W1} - \omega_{Wr}} \tag{19.5-18}$$

The subscripts are further defined in Fig. 19.5-1.

For the air–water system at moderate temperatures, the assumption of constant ρ and $\mathscr{D}_{AW}$ is reasonable, with air regarded as a single species. The heat capacities of water vapor and air are unequal, but the diffusional transport of energy is expected to be small. Hence Eqs. 19.5-9 to 11 provide a reasonably reliable description of the dehumidification process. The boundary conditions needed to integrate these equations include $\check{\omega}_W = \check{T} = 1$ at the tube inlet, $\check{\omega}_W = \check{T} = 0$ at the gas–liquid boundary, and no-slip and inlet conditions on the velocity $\check{\mathbf{v}}$.

We find then that the dimensionless profiles are related by

$$\check{\omega}_W(\check{x}, \check{y}, \check{z}, \text{Re}, \text{Gr}_\omega, \text{Gr}, \text{Sc}, \text{Pr}) = \check{T}(\check{x}, \check{y}, \check{z}, \text{Re}, \text{Gr}, \text{Gr}_\omega, \text{Pr}, \text{Sc}) \tag{19.5-19}$$

Thus $\check{\omega}_W$ is the same function of its arguments as $\check{T}$ is of its arguments *in the exact order given.* Since in general Gr_ω is not equal to Gr and Sc is not equal to Pr, the two profiles are not similar. This general result is too complex to be of much value.

However, for the air–water system, at moderate temperatures and near-atmospheric pressure, Sc is about 0.6 and Pr is about 0.71.

If we assume for the moment that Sc and Pr are equal, the dimensional analysis becomes much simpler. For this special situation, the energy and species continuity equations are iden-

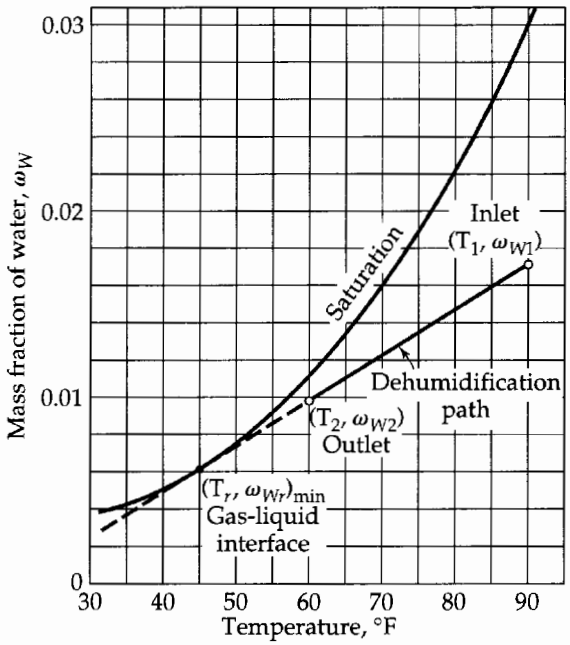

Fig. 19.5-2. A representative dehumidification path. The dehumidification path shown here corresponds to $T_{r,min}$, the lowest refrigerant temperature ensuring the absence of fog. The dehumidification path for this situation is a tangent to the saturation curve through the point (ω_{W1}, T_1), representing the given inlet-air conditions. Calculated dehumidification paths for lower refrigerant temperatures would cross the saturation curve. Saturation water vapor concentrations would then be exceeded, making fog formation possible.

tration and temperature profiles are then identical. It should be noted that equality of Gr_ω and Gr is not required. This is because the Grashof numbers affect the concentration and temperature profiles only by way of the velocity **v**, which appears in both the continuity equation and the energy equation in the same way.

Therefore, with the assumption that Sc = Pr, we have

$$\breve{\omega}_W = \breve{T} \tag{19.5-20}$$

at each point in the system. This means, in turn, that *every* concentration-temperature pair in the tube lies on a straight line between (ω_{W1}, T_1) and (ω_{Wr}, T_r) on a psychrometric chart. This is shown graphically in Fig. 19.5-2 for a representative set of conditions. Note that (ω_{Wr}, T_r) must lie on the saturation curve, since equilibrium is very closely approximated.

It follows that there can be no fog formation if a straight line drawn between (ω_{W1}, T_1) and (ω_{Wr}, T_r) does not cross the saturation curve. Then the lowest refrigerant temperature that cannot produce fog is represented by the point of tangency of a straight line through (ω_{W1}, T_1) with the saturation curve.

It should be noted that *all* of the conditions along the line from the inlet (ω_{W1}, T_1) to (ω_{Wr}, T_r) will occur in the gas even though the bulk or cup-mixing conditions vary only from (ω_{W1}, T_1) to (ω_{W2}, T_2). Thus some fog can form even if saturation is not reached in the bulk of the flowing gas. For air entering at 90°F and 50% relative humidity, the minimum safe refrigerant temperature is about 45°F. It may also be seen from Fig. 19.5-2 that it is not necessary to bring all of the wet air to its dew point in order to dehumidify it. It is only necessary that the air be saturated at the cooling surface. The exit bulk conditions (ω_{W2}, T_2) can be anywhere along the dehumidification path between (ω_{W1}, T_1) and (ω_{Wr}, T_r), depending on the effectiveness of the apparatus used. Calculations based on the assumed equality of Sc and Pr have proven very useful for the air–water system.

In addition, it can be seen, by considering the physical significance of the Schmidt and Prandtl numbers, that the above-outlined calculation procedure is conservative. Since the Schmidt number is slightly smaller than the Prandtl number, dehumidification will proceed proportionally faster than cooling, and concentration–temperature pairs will lie slightly below the dehumidification path drawn in Fig. 19.5-2. In condensing organic vapors from air, the reverse situation often occurs. Then the Schmidt numbers tend to be higher than the Prandtl numbers, and cooling proceeds faster than condensation. Conditions then lie above the straight line of Fig. 19.5-2, and the danger of fog formation is increased.

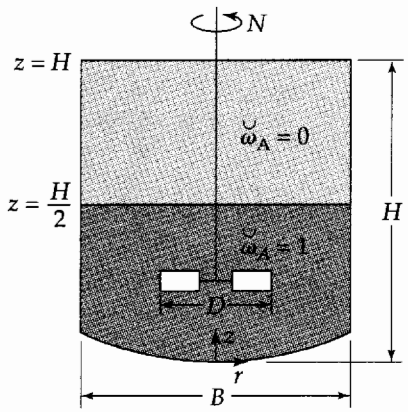

Fig. 19.5-3. Blending of miscible fluids. At zero time, the upper half of this tank is solute free, and the lower half contains a uniform distribution of solute at a dimensionless concentration of unity, and the fluid is motionless. The impeller is caused to turn at a constant rate of rotation N for all time greater than zero. Positions in the tank are given by the coordinates r, θ, z, with r measured radially from the impeller axis, and z upward from the bottom of the tank.

EXAMPLE 19.5-3

Blending of Miscible Fluids

Develop by dimensional analysis the general form of a correlation for the time required to blend two miscible fluids in an agitated tank. Consider a tank of the type described in Fig. 19.5-3, and assume that the two fluids and their mixtures have essentially the same physical properties.

SOLUTION

It will be assumed that the achievement of "equal degrees of blending" in any two mixing operations means obtaining the same dimensionless concentration profile in each. That is, the dimensionless solute concentration $\breve{\omega}_A$ is the same function of suitable dimensionless coordinates $(\breve{r}, \theta, \breve{z})$ of the two systems when the degrees of blending are equal. These concentration profiles will depend on suitably defined dimensionless groups appearing in the pertinent conservation equations and their boundary conditions, and on a dimensionless time.

In this problem we select the following definitions for the dimensionless variables:

$$\breve{r} = \frac{r}{D} \qquad \breve{z} = \frac{z}{D} \qquad \breve{\mathbf{v}} = \frac{\mathbf{v}}{ND} \qquad \breve{t} = Nt \qquad \breve{p} = \frac{p - p_0}{\rho N^2 D^2} \tag{19.5-21}$$

Here D is the impeller diameter, N is the rate of rotation of the impeller in revolutions per unit time, and p_0 is the prevailing atmospheric pressure. The dimensionless pressure $\breve{p}$ is used here rather than the quantity $\breve{\mathcal{P}}$ defined in §3.7; the formulation with $\breve{p}$ is simpler and gives equivalent results. Note that $\breve{t}$ is equal to the total number of turns of the impeller since the start of mixing.

The conservation equations describing this system are Eqs. 19.5-8, 9, and 11 with zero Grashof numbers. The dimensionless groups arising in these equations are Re, Fr, and Sc. The boundary conditions include the vanishing of $\mathbf{v}$ on the tank wall and of p on the free liquid surface. In addition we have to specify the initial conditions

$$\text{C. 1:} \qquad \text{at } \breve{t} \le 0, \qquad \breve{\omega}_A = 0 \qquad \text{for } \frac{1}{2}\frac{H}{D} < \breve{z} < \frac{H}{D} \tag{19.5-22}$$

$$\text{C. 2:} \qquad \text{at } \breve{t} \le 0, \qquad \breve{\omega}_A = 1 \qquad \text{for } 0 < \breve{z} < \frac{1}{2}\frac{H}{D} \tag{19.5-23}$$

$$\text{C. 3:} \qquad \text{at } \breve{t} \le 0, \qquad \breve{\mathbf{v}} = 0 \qquad \text{for } 0 < \breve{z} < \frac{H}{D} \text{ and } 0 < \breve{r} < \frac{1}{2}\frac{B}{D} \tag{19.5-24}$$

and the requirement of no slip on the impeller (see Eq. 3.7-34).

We find then that the concentration profiles are functions of Re, Sc, Fr, the dimensionless time $\breve{t}$, the tank geometry (via H/D and B/D), and the relative proportions of the two fluids. That is,

$$\breve{\omega}_A = f(\text{Re, Fr, Sc, } \breve{t}\text{, geometry, initial conditions}) \tag{19.5-25}$$

It is frequently possible to reduce the number of variables to be investigated.

It has been observed that, if the tank is properly baffled,[1] no vortices of importance occur; that is, the free liquid surface is effectively level. Under these circumstances, or in the absence of a free liquid surface, the Froude number does not appear in the system description, as we found in §3.7.

It is further found, in most operations on low-viscosity liquids, that the rate-limiting step is the creation of a finely divided dispersion of one fluid in the other. In such a dispersion, the diffusional processes take place over very small distances. As a result, molecular diffusion is not rate limiting, and the Schmidt number (Sc) has little importance. It is further found that the effect of the Reynolds number (Re) is negligible under most commonly encountered conditions. This is because most of the mixing takes place in the interior of the tank where viscous effects are small, rather than in the boundary layers adjacent to the tank and impeller surfaces, where they are large.[2]

For most impeller–tank combinations in common use, the Reynolds number (Re) is unimportant when its value is above about 10^4. This behavior has been substantiated by a number of investigators.[3]

We thus arrive, *after extensive experimentation*, at a surprisingly simple result. When all of the assumptions above are valid, the concentration profile depends only on $\check{t}$. Hence *the dimensionless time required to produce any desired degree of mixing is a constant* for a given system geometry. In other words, the total number of turns of the impeller during the mixing process determines the degree of blending, independently of Re, Fr, Sc, and tank size—provided, of course, that the tanks and impellers are geometrically similar.

For the same reasons, in a properly baffled tank, the dimensionless velocity distribution and the volumetric pumping efficiency of the impeller are nearly independent of the Froude number (Fr) and of the Reynolds number (Re), when $\mathrm{Re} > 10^4$.

QUESTIONS FOR DISCUSSION

1. How do the various equations of change given in Chapters 3 and 11 have to be modified for reacting mixtures?
2. What modifications in the flux expressions given in Chapters 3 and 11 are needed to describe chemically reacting mixtures?
3. Under what conditions is $(\nabla \cdot \mathbf{v}) = 0$? $(\nabla \cdot \mathbf{v}^*) = 0$?
4. Equations 19.1-14 and 15 are physically equivalent. For what kinds of problems is there a preference for one form over the other?
5. Interpret physically each term in the equations in Table 19.2-3.
6. The thermal conductivity of a mixture is defined as the ratio of the heat flux to the negative of the temperature gradient when all the diffusional mass fluxes are zero. Interpret this statement in terms of Eq. 19.3-3.

[1] A common and effective baffling arrangement for vertical cylindrical tanks with axially mounted impellers is a set of four evenly spaced strips along the tank wall, with their flat surfaces in planes through the tank axis, extending from the top to the bottom of the tank and at least two-tenths of the distance to the tank center.

[2] The insensitivity of the required mixing time to the Reynolds number can be seen intuitively from the fact that the term $(1/\mathrm{Re})\check{\nabla}^2\check{\mathbf{v}}$ in Eq. 19.5-9 becomes small compared to the acceleration term $D\check{\mathbf{v}}/D\check{t}$ at large Re. Such intuitive arguments are dangerous, however, and the effect of Re is always important in the immediate neighborhood of solid surfaces. Here the amount of mixing taking place in the immediate neighborhood of solid surfaces is small and can be neglected.

The insensitivity of the required mixing time to the Schmidt number can be seen from the time-averaged equation of continuity in Chapter 21. At large Re, the turbulent mass flux is much greater than that due to molecular diffusion, except in the immediate neighborhood of the solid surfaces.

[3] E. A. Fox and V. E. Gex, *AIChE Journal*, **2**, 539–544 (1956); H. Kramers, G. M. Baars, and W. H. Knoll, *Chem. Eng Sci*, **2**, 35–42 (1955); J. G. van de Vusse, *Chem. Eng. Sci.*, **4**, 178–200, 209–220 (1955).

7. Discuss the similarities and differences between heat transfer and mass transfer.
8. Go through all the steps in converting Eq. 19.3-4 into Eq. 19.3-6. Why is the latter (approximate) result important?
9. Comment on the statement at the end of Example 19.4-1 that the rate of heat transfer is directly affected by simultaneous mass transfer, whereas the reverse is not true.

PROBLEMS

19A.1. Dehumidification of air (Fig. 19.4-1). For the system of Example 19.4-1, let the vapor be H_2O and the stagnant gas be air. Assume the following conditions (which are representative in air conditioning): (i) at $y = \delta$, $T = 80°F$ and $x_{H_2O} = 0.018$; (ii) at $y = 0$, $T = 50°F$.

(a) For $p = 1$ atm, calculate the right side of Eq. 19.4-9.

(b) Compare the conductive and diffusive heat flux at $y = 0$. What is the physical significance of your answer?

Answer: **(a)** 1.004

19B.1. Steady-state evaporation (Fig. 18.2-1). Rework the problem solved in §18.2, dealing with the evaporation of liquid A into gas B, starting from Eq. 19.1-17.

(a) First obtain an expression for $\mathbf{v}^*$, using Eq. (M) of Table 17.8-1, as well as Fick's law in the form of Eq. (D) of Table 17.8-2.

(b) Show that Eq. 19.1-17 then becomes the following nonlinear second-order differential equation:

$$\frac{d^2x_A}{dz^2} + \frac{1}{1 - x_A}\left(\frac{dx_A}{dz}\right)^2 = 0 \tag{19B.1-1}$$

(c) Solve this equation to get the mole fraction profile given in Eq. 18.2-11.

19B.2. Gas absorption with chemical reaction (Fig. 18.4-1). Rework the problem solved in §18.4, by starting with Eq. 19.1-16. What assumptions do you have to make in order to get Eq. 18.4-4?

19B.3. Concentration-dependent diffusivity. A stationary liquid layer of B is bounded by planes $z = 0$ (a solid wall) and $z = b$ (a gas–liquid interface). At these planes the concentration of A is c_{A0} and c_{Ab} respectively. The diffusivity $\mathscr{D}_{AB}$ is a function of the concentration of A.

(a) Starting from Eq. 19.1-5 derive a differential equation for the steady-state concentration distribution.

(b) Show that the concentration distribution is given by

$$\frac{\int_{c_A}^{c_{A0}} \mathscr{D}_{AB} dc_A}{\int_{c_{Ab}}^{c_{A0}} \mathscr{D}_{AB} dc_A} = \frac{z}{b} \tag{19B.3-1}$$

(c) Show that the molar flux at the solid–liquid surface is

$$N_{Az}|_{z=0} = \frac{1}{b}\int_{c_{Ab}}^{c_{A0}} \mathscr{D}_{AB}(c_A) dc_A \tag{19B.3-2}$$

(d) Now assume that the diffusivity can be expressed as a Taylor series in the concentration

$$\mathscr{D}_{AB}(c_A) = \overline{\mathscr{D}}_{AB}[1 + \beta_1(c_A - \bar{c}_A) + \beta_2(c_A - \bar{c}_A)^2 + \cdots] \tag{19B.3-3}$$

in which $\bar{c}_A = \frac{1}{2}(c_{A0} + c_{Ab})$ and $\overline{\mathscr{D}}_{AB} = \mathscr{D}_{AB}(\bar{c}_A)$. Then, show that

$$N_{Az}|_{z=0} = \frac{\overline{\mathscr{D}}_{AB}}{b}(c_{A0} - c_{Ab})[1 + \tfrac{1}{12}\beta_2(c_{A0} - c_{Ab})^2 + \cdots] \tag{19B.3-4}$$

(e) How does this result simplify if the diffusivity is a linear function of the concentration?

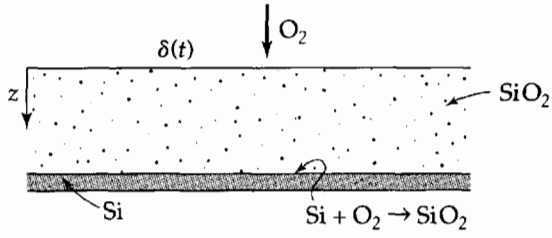

Fig. 19B.4. Oxidation of silicon.

19B.4. Oxidation of silicon (Fig. 19B.4).[1] A slab of silicon is exposed to gaseous oxygen (species A) at pressure p, producing a layer of silicon dioxide (species B). The layer extends from the surface $z = 0$, where the oxygen dissolves with concentration $c_{A0} = Kp$, to the surface at $z = \delta(t)$, where the oxygen and silicon undergo a first-order reaction with rate coefficient k_1''. The thickness $\delta(t)$ of the growing oxide layer is to be predicted. A quasi-steady-state method is useful here, inasmuch as the advancement of the reaction front is very slow.

(a) First solve the diffusion equation of Eq. 19.1-18, with the term $\partial c_A/\partial t$ neglected, and apply the boundary conditions to obtain

$$c_A = c_{A0} - (c_{A0} - c_{A\delta})\frac{z}{\delta} \tag{19B.4-1}$$

in which the concentration $c_{A\delta}$ at the reaction plane is as yet unknown.

(b) Next use an unsteady-state molar O_2 balance on the region $0 < z < \delta(t)$ to obtain, with the aid of the Leibniz formula of §C.3,

$$c_{A\delta}\frac{d\delta}{dt} = -\mathscr{D}_{AB}\frac{dc_A}{dz} - k_1'' c_{A\delta} \tag{19B.4-2}$$

(c) Now write an unsteady-state molar balance on SiO_2 in the same region to obtain

$$+k_1'' c_{A\delta} = \frac{1}{\tilde{V}_B}\frac{d\delta}{dt} \tag{19B.4-3}$$

(d) In Eq. 19B.4-2, evaluate $d\delta/dt$ from Eq. 19B.4-3 and dc_A/dz from Eq. 19B.4-1. This will yield an equation for $c_{A\delta}$:

$$\frac{k_1''\delta\tilde{V}_B}{\mathscr{D}_{AB}}c_{A\delta}^2 + \left(1 + \frac{k_1''\delta}{\mathscr{D}_{AB}}\right)c_{A\delta} = c_{A0} \tag{19B.4-4}$$

Inserting numerical values into Eq. 19B.4-4 shows that the quadratic term can safely be neglected.[1]

(e) Combine Eqs. 19B.4-3 and 19B.4-4 (without the quadratic term) to get a differential equation for $\delta(t)$. Show that this leads to

$$\frac{\delta^2}{2\mathscr{D}_{AB}} + \frac{\delta}{k_1''} = \tilde{V}_B c_{A0} t \tag{19B.4-5}$$

which agrees with experimental data.[1] Interpret the result.

19B.5. The Maxwell–Stefan equations for multicomponent gas mixtures. In Eq. 17.9-1 the Maxwell-Stefan equations for the mass fluxes in a multicomponent gas system are given. Show that these equations simplify for a binary system to Fick's first law, as given in Eq. 17.1-5.

19B.6. Diffusion and chemical reaction in a liquid.

(a) A solid sphere of substance A is suspended in a liquid B in which it is slightly soluble, and with which A undergoes a first-order chemical reaction with rate constant k_1'''. At steady

[1] R. Ghez, *A Primer of Diffusion Problems*, Wiley-Interscience, New York (1988), pp. 46–55; this book discusses a number of problems that arise in the microelectronics field.

state the diffusion is exactly balanced by the chemical reaction. Show that the concentration profile is

$$\frac{c_A}{c_{A0}} = \frac{R}{r}\frac{e^{-br/R}}{e^{-b}} \tag{19B.6-1}$$

in which R is the radius of the sphere, c_{A0} is the molar solubility of A in B, and $b^2 = k_1'''R^2/\mathcal{D}_{AB}$.

(b) Show by quasi-steady-state arguments how to calculate the gradual decrease in diameter of the sphere as A dissolves and reacts. Show that the radius of the sphere is given by

$$\sqrt{\frac{k_1'''}{\mathcal{D}_{AB}}}(R - R_0) - \ln\frac{1 + \sqrt{k_1'''/\mathcal{D}_{AB}}R}{1 + \sqrt{k_1'''/\mathcal{D}_{AB}}R_0} = -\frac{k_1'''c_{A0}M_A}{\rho_{sph}}(t - t_0) \tag{19B.6-2}$$

in which R_0 is the sphere radius at time t_0, and ρ_{sph} is the density of the sphere.

19B.7. Various forms of the species continuity equation.

(a) In this chapter the species equation of continuity is given in three different forms: Eq. 19.1-7, Eq. (A) of Table 19.2-1, and Eq. (B) in Table 19.2-3. Show that these three equations are equivalent.

(b) Show how to get Eq. 19.1-15 from Eq. 19.1-11.

19C.1. Alternate form of the binary diffusion equation. In the absence of chemical reactions, Eq. 19.1-17 can be written in terms of $\mathbf{v}$ rather than $\mathbf{v}^*$ by using a different measure of concentration—namely, the logarithm of the mean molecular weight:[2]

$$\frac{\partial}{\partial t}\ln M + (\mathbf{v}\cdot\nabla\ln M) = \mathcal{D}_{AB}\nabla^2\ln M \tag{19C.1-1}$$

in which $M = x_AM_A + x_BM_B$. (*Caution:* Solution is lengthy.)

Equation 19C.1-1 is difficult to solve even for the stagnant gas film of §18.2, because of the variable mass density ρ that appears in the continuity equation (Eq. A of Table 19.2-3).

19D.1. Derivation of the equation of continuity. In §19.1 the species equation of continuity is derived by making a mass balance on a small rectangular volume $\Delta x\,\Delta y\,\Delta z$ fixed in space.

(a) Repeat the derivation for an arbitrarily shaped volume element V with a sufficiently smooth fixed boundary S. Show that the species mass balance can be written as

$$\frac{d}{dt}\int_V \rho_A dV = -\int_S (\mathbf{n}\cdot\mathbf{n}_A)dS + \int_V r_A dV \tag{19D.1-1}$$

Use the Gauss divergence theorem to convert the surface integral to a volume integral, and then obtain Eq. 19.1-6.

(b) Repeat the derivation using a region of fluid contained within a surface, each point of which is moving with local mass average velocity.

19D.2. Derivation of the equation of change for temperature for a multicomponent system. Derive Eq. (F) in Table 19.2-4 from Eq. (E). We suggest the following sequence of steps:

(a) Since the enthalpy is an extensive thermodynamic property, we can write

$$H(m_1, m_2, m_3, \ldots, m_N) = m\hat{H}(\omega_1, \omega_2, \omega_3, \ldots, \omega_{N-1}) \tag{19D.2-1}$$

in which the m_α are the masses of the various species, m is the sum of the m_α, and the $\omega_\alpha = m_\alpha/m$ are the corresponding mass fractions. Both H and $\hat{H}$ are understood to be functions of T and p as well as of composition. Use the chain rule of partial differentiation to show that

$$(\alpha \neq N) \qquad \left(\frac{\partial H}{\partial m_\alpha}\right)_{m_\gamma} = \sum_{\beta=1}^{N-1}\left(\frac{\partial \hat{H}}{\partial \omega_\beta}\right)_{\omega_\gamma}\left(\delta_{\alpha\beta} - \frac{m_\beta}{m}\right) + \hat{H} \tag{19D.2-2}$$

---

[2] C. H. Bedingfield, Jr., and T. B. Drew, *Ind. Eng. Chem.*, **42**, 1164–1173 (1950).

$$(\alpha = N) \qquad \left(\frac{\partial H}{\partial m_N}\right)_{m_\gamma} = \sum_{\beta=1}^{N-1}\left(\frac{\partial \hat{H}}{\partial \omega_\beta}\right)_{\omega_\gamma}\left(-\frac{m_\beta}{m}\right) + \hat{H} \tag{19D.2-3}$$

Subtraction then gives for $\alpha \neq N$

$$\left(\frac{\partial H}{\partial m_\alpha}\right)_{m_\gamma} - \left(\frac{\partial H}{\partial m_N}\right)_{m_\gamma} = \left(\frac{\partial \hat{H}}{\partial \omega_\alpha}\right)_{\omega_\gamma} \tag{19D.2-4}$$

The subscript ω_γ means "holding all other mass fractions constant."

(b) The left side of Eq. (E) can be expanded by regarding the enthalpy per unit mass to be a function of p, T, and the first $(N-1)$ mass fractions:

$$\rho\frac{D\hat{H}}{Dt} = \rho\left(\frac{\partial \hat{H}}{\partial p}\right)_{T,\omega_\gamma}\frac{Dp}{Dt} + \rho\left(\frac{\partial \hat{H}}{\partial T}\right)_{p,\omega_\gamma}\frac{DT}{Dt} + \rho\sum_{\alpha=1}^{N-1}\left(\frac{\partial \hat{H}}{\partial \omega_\alpha}\right)_{p,T,\omega_\gamma}\frac{D\omega_\alpha}{Dt} \tag{19D.2-5}$$

Next, verify that the coefficients of the substantial derivatives can be identified as

$$\rho\left(\frac{\partial \hat{H}}{\partial p}\right)_{T,\omega_\gamma} = 1 - \left(\frac{\partial \ln \hat{V}}{\partial \ln T}\right)_{p,\omega_\gamma} \tag{19D.2-6}$$

$$\rho\left(\frac{\partial \hat{H}}{\partial T}\right)_{p,\omega_\gamma} = \rho\hat{C}_p \tag{19D.2-7}$$

The coefficient of $\rho(D\omega_\alpha/Dt)$ has already been given in Eq. 19D.2-4.

(c) Substitute the coefficients into Eq. 19D.2-5, and then use Eq. 19.1-14 to eliminate $\rho(D\omega_\alpha/Dt)$, and verify that $(\partial H/\partial m_\alpha)_{p,T,m_\gamma}$ is the same as $(\bar{H}_\alpha/M_\alpha)$. The summation on α, which goes from 1 to $N-1$, now has to be appropriately rewritten as a summation from 0 to N, by using Eq. (K) of Table 17.8-1 and the fact that $\Sigma_\alpha r_\alpha = 0$.

(d) Then combine the results of (a), (b), and (c) with Eq. (E) to get Eq. (F).

19D.3. Gas separation by atmolysis or "sweep diffusion" (Fig. 19D.3). When two gases A and B are forced to diffuse through a third gas C, there is a tendency of A and B to separate because of the difference in their diffusion rates. This phenomenon was first studied by Hertz,[3] and later by Maier.[4] Benedict and Boas[5] studied the economics of the process particularly with regard to isotope separation. Keyes and Pigford[6] contributed further to both theory and experiment.

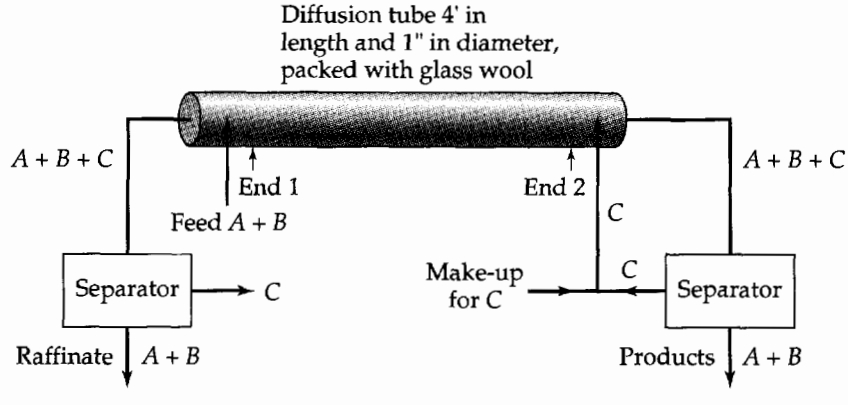

Fig. 19D.3. The Keyes–Pigford experiment for studying atmolysis.

---

[3] G. Hertz, *Zeits. f. Phys.*, **91**, 810–815 (1934).

[4] G. G. Maier, *Mechanical Concentration of Gases*, U.S. Bureau of Mines Bulletin 431 (1940).

[5] M. Benedict and A. Boas, *Chem. Eng. Prog.*, **47**, 51–62, 111–122 (1951).

[6] J. J. Keys, Jr., and R. L. Pigford, *Chem. Eng. Sci.*, **6**, 215–226 (1957).

In their experimental arrangement, C was a condensable vapor, which could be separated from A and B by lowering the temperature so that C would be liquefied.

We want to study the details of the three-component diffusion taking place in the diffusion tube of length L, when the apparatus is operated at steady state. Obtain an expression relating the concentrations x_{A1} and x_{B1} at the feed end of the tube to the concentrations x_{A2} and x_{B2} at the product end. This expression will contain the molar fluxes of the three species, which are controlled by the rates of addition of materials in the two entering streams.

Use the following notation for dimensionless quantities: $\zeta = z/L$ for the distance down the tube from the feed entrance; $r_A = \mathscr{D}_{AB}/\mathscr{D}_{AC}$ and $r_B = \mathscr{D}_{AB}/\mathscr{D}_{BC}$ for the diffusivity ratios; and $\nu_\alpha = N_{\alpha z}L/c\mathscr{D}_{AB}$ for the molar fluxes (with $\alpha = A, B, C$).

(a) Shows that, in terms of these dimensionless quantities, the Maxwell–Stefan equations for the diffusion are

$$\frac{dx_A}{d\zeta} = Y_{AA}x_A + Y_{AB}x_B + Y_A \tag{19D.3-1}$$

$$\frac{dx_B}{d\zeta} = Y_{BA}x_A + Y_{BB}x_B + Y_B \tag{19D.3-2}$$

where $Y_{AA} = \nu_B^* + r_A(\nu_A + \nu_C)$, $Y_{AB} = \nu_A(r_A - 1)$, and $Y_A = -r_A\nu_A$, and the remaining quantities are obtained by interchanging A and B.

(b) By using Laplace transforms, solve Eqs. 19D.3-1 and 2 to get the concentration profiles for A and B in the tube.

(c) Show that the terminal concentrations are interrelated thus,

$$x_{A2} = \frac{X_A(x_{A1}, x_{B1}; 0)}{p_+p_-} + \frac{X_A(x_{A1}, x_{B1}; p_+)\exp p_+}{p_+(p_+ - p_-)} + \frac{X_A(x_{A1}, x_{B1}; p_-)\exp p_-}{p_-(p_- - p_+)} \tag{19D.3-3}$$

in which

$$p_\pm = \tfrac{1}{2}[(Y_{AA} + Y_{BB}) \pm \sqrt{(Y_{AA} + Y_{BB})^2 + 4Y_{AB}Y_{BA}}] \tag{19D.3-4}$$

$$X_A(x_{A1}, x_{B1}, p) = p^2x_{A1} + p(Y_A - x_{A1}Y_{BB} + x_{B1}Y_{AB}) + (Y_{AB}Y_B - Y_{BB}Y_A) \tag{19D.3-5}$$

A similar expression may be obtained for x_{B2}. Keyes and Pigford[6] give further results for special cases.

19D.4. Steady-state diffusion from a rotating disk.[7] A large disk is rotating with an angular velocity Ω in an infinite expanse of liquid B. The surface is coated with a material A that is slightly soluble in B. Find the rate at which A dissolves in B. (The solution to this problem can be applied to a disk of finite radius R with negligible error.)

The fluid dynamics of this problem was developed by von Kármán[8] and later corrected by Cochran.[9] It was found that the velocity components can be expressed, except near the edge, as

$$v_r = \Omega r F(\zeta); \qquad v_\theta = \Omega r G(\zeta); \qquad v_z = \sqrt{\Omega\nu}H(\zeta) \tag{19D.4-1}$$

in which $\zeta = z\sqrt{\Omega/\nu}$. The functions F, G, and H have the following expansions,[8]

$$F = a\zeta - \tfrac{1}{2}\zeta^2 - \tfrac{1}{3}b\zeta^3 - \tfrac{1}{12}b^2\zeta^4 - \cdots \tag{19D.4-2}$$

$$G = 1 + b\zeta + \tfrac{1}{2}a\zeta^3 + \tfrac{1}{12}(ab - 1)\zeta^4 - \cdots \tag{19D.4-3}$$

$$H = -a\zeta^2 + \tfrac{1}{3}\zeta^3 + \tfrac{1}{6}\zeta^4 + \cdots \tag{19D.4-4}$$

in which $a = 0.510$ and $b = -0.616$. It is further known that, in the limit as $\zeta \to \infty$, $H \to -0.886$, and F, G, F', and G' all approach zero. Also it is known that the boundary layer thickness is proportional to $\sqrt{\nu/\Omega}$, except near the edge of the disk.

---

[7] V. G. Levich, *Physicochemical Hydrodynamics*, Prentice-Hall, Englewood Cliffs, N.J. (1962), §11.

[8] T. von Kármán, *Zeits. f. angew. Math. u. Mech.*, **1**, 244–247 (1921).

[9] W. G. Cochran, *Proc. Camb. Phil. Soc.*, **30**, 365–375 (1934).

The diffusion equation of Eq. 19.1-16 with the known velocity components is to be solved under the boundary conditions that: $\rho_A = \rho_{A0}$ at $z = 0$; $\rho_A = 0$ at $z = \infty$; and $\partial\rho_A/\partial r = 0$ at $r = 0, \infty$. Since there can be but one solution to this linear problem, it may be seen that a solution of the form $\rho_A(z)$ can be found that satisfies the differential equation and all the boundary conditions. Thus, the solution for ρ_A does not depend on the radial coordinate in the region considered.

(a) Show that at steady-state Eq. 19.1-16 gives

$$H(\zeta)\frac{d\rho_A}{d\zeta} = \frac{1}{\mathrm{Sc}}\frac{d^2\rho_A}{d\zeta^2} \tag{19D.4-5}$$

(b) Solve Eq. 19D.4-5 to get, for large Schmidt number,

$$\frac{\rho_A}{\rho_{A0}} = 1 - \frac{(\frac{1}{3}a\mathrm{Sc})^{1/3}}{\Gamma(\frac{4}{3})}\int_0^\zeta \exp(-\tfrac{1}{3}a\mathrm{Sc}\bar{\zeta}^3)d\bar{\zeta} \tag{19D.4-6}$$

(c) Show that the mass flux at the surface of the disk is[7]

$$j_{Az}|_{z=0} = 0.620\frac{\rho_{A0}\mathscr{D}_{AB}^{2/3}\Omega^{1/2}}{\nu^{1/6}} \tag{19D.4-7}$$

for large Schmidt number. Clearly, if desired, one could use higher terms in the series expansion for H and extend the Schmidt-number range.[10] This system has been used for studying the removal of solid behenic acid from stainless-steel surfaces.[11]

---

[10] D. Schuhmann, *Physicochemical Hydrodynamics (V. G. Levich Fextschrift)*, Vol. 1 (D. B. Spalding ed.), Advance Publications Ltd., London (1977), pp. 445–459; see also K.-T. Liu and W. E. Stewart, *Intl. Jnl. Heat and Mass Trf.*, **15**, 187–189 (1972).

[11] C. S. Grant, A. T. Perka, W. D. Thomas, and R. Caton, *AIChE Journal*, **42**, 1465–1476 (1996).

Chapter 20

Concentration Distributions with More Than One Independent Variable

Most of the diffusion problems discussed in the preceding two chapters led to ordinary differential equations for the concentration profiles. In this chapter we use the general equations of Chapter 19 to set up and solve some diffusion problems that lead to partial differential equations.

A large number of diffusion problems can be solved by simply looking up the solutions to the analogous problems in heat conduction. When the differential equations and the boundary and initial conditions for the diffusion process are of exactly the same form as those for the heat conduction process, then the heat conduction solution may be taken over with appropriate changes in notation. In Table 20.0-1 the three main heat transport equations used in Chapter 12 are shown along with their mass transport analogs. Many solutions to the nonflow equations may be found in the monographs of Carslaw and Jaeger[1] and of Crank.[2]

Because the diffusion problems described by the equations in Table 20.0-1 are analogous to the problems of Chapter 12, we do not discuss them extensively here. Instead, we focus primarily on problems involving diffusion with chemical reactions, diffusion with a moving interface, and diffusion with rapid mass transfer.

In §20.1 we discuss a variety of time-dependent diffusion problems. In §20.2 we present some steady-state boundary layer problems involving binary mixtures. This is followed by two boundary layer analyses for more complicated systems: the diffusion in steady flow around arbitrary objects in §20.3, and the diffusion in flows with complex interfacial motion in §20.4. Finally, in §20.5 we explore an asymptotic solution to the "Taylor dispersion" problem.

[1] H. S. Carslaw and J. C. Jaeger, *Conduction of Heat in Solids*, 2nd edition, Oxford University Press (1959).

[2] J. Crank, *The Mathematics of Diffusion*, 2nd edition, Clarendon Press, Oxford (1975).

Table 20.0-1 Analogies Between Special Forms of the Heat Conduction and Diffusion Equations

	Process	Unsteady-state nonflow	Steady-state flow	Steady-state nonflow
	Solution Given in	§12.1—Exact solutions	§12.2—Exact solutions §12.4—Boundary layer solutions	§12.3—Exact solutions in two dimensions by analytic functions
Heat conduction	Equations	$\frac{\partial T}{\partial t} = \alpha\nabla^2 T$	$(\mathbf{v}\cdot\nabla T) = \alpha\nabla^2 T$	$\nabla^2 T = 0$
	Applications	Heat conduction in solids	Heat conduction in laminar incompressible flow	Steady heat conduction solids
	Assumptions	1. k = constant 2. $\mathbf{v} = 0$	1. k, ρ = constants 2. No viscous dissipation 3. Steady state	1. k = constant 2. $\mathbf{v} = 0$ 3. Steady state
Diffusion	Equations	$\frac{\partial c_A}{\partial t} = \mathscr{D}_{AB}\nabla^2 c_A$	$(\mathbf{v}\cdot\nabla c_A) = \mathscr{D}_{AB}\nabla^2 c_A$	$\nabla^2 c_A = 0$
	Applications	Diffusion of traces of A through B	Diffusion in laminar flow (dilute solutions of A in B)	Steady diffusion in solids
	Assumptions	1. $\mathscr{D}_{AB}, \rho$ = constants 2. $\mathbf{v} = 0$ 3. No chemical reactions	1. $\mathscr{D}_{AB}, \rho$ = constants 2. Steady state 3. No chemical reactions	1. $\mathscr{D}_{AB}, \rho$ = constants 2. Steady state 3. No chemical reactions 4. $\mathbf{v} = 0$
	Applications	OR Equimolar counter-diffusion in low density gases		
	Assumptions	1. $\mathscr{D}_{AB}, c$ = constants 2. $\mathbf{v}^* = 0$ 3. No chemical reactions		

§20.1 TIME-DEPENDENT DIFFUSION

In this section we give four examples of time-dependent diffusion. The first deals with evaporation of a volatile liquid and illustrates the deviations from Fick's second law that arise at high mass-transfer rates. The second and third examples deal with unsteady-state diffusion with chemical reactions. In the last example we examine the role of interfacial-area changes in diffusion. The method of combination of variables is used in Examples 20.1-1, 2, and 4, and Laplace transforms are used in Example 20.1-3.

EXAMPLE 20.1-1

Unsteady-State Evaporation of a Liquid (the "Arnold Problem")

We wish to predict the rate at which a volatile liquid A evaporates into pure B in a tube of infinite length. The liquid level is maintained at $z = 0$ at all times. The temperature and pressure are assumed constant, and the vapors of A and B form an ideal gas mixture. Hence the molar density c is constant throughout the gas phase, and $\mathscr{D}_{AB}$ may be considered to be constant. It is further assumed that species B is insoluble in liquid A, and that the molar average velocity in the gas phase does not depend on the radial coordinate.

SOLUTION

For this system the equation of continuity for the mixture, given in Eq. 19.1-12, becomes

$$\frac{\partial v_z^*}{\partial z} = 0 \tag{20.1-1}$$

in which v_z^* is the z-component of the molar average velocity. Integration with respect to z gives

$$v_z^* = v_{z0}^*(t) \tag{20.1-2}$$

Here and elsewhere in this problem, the subscript "0" indicates a quantity evaluated at $z = 0$. According to Eq. (M) of Table 17.8-1, this velocity can be written in terms of the molar fluxes of A and B as

$$v_z^* = \frac{N_{Az0} + N_{Bz0}}{c} \tag{20.1-3}$$

However, N_{Bz0} is zero because of the insolubility of species B in liquid A. Then use of Eq. (D) of Table 17.8-2 gives finally

$$v_z^* = -\frac{\mathscr{D}_{AB}}{1 - x_{A0}} \frac{\partial x_A}{\partial z}\bigg|_{z=0} \tag{20.1-4}$$

in which x_{A0} is the interfacial gas-phase concentration, evaluated here on the assumption of interfacial equilibrium. For an ideal gas mixture this is just the vapor pressure of pure A divided by the total pressure.

The equation of continuity of Eq. 19.1-17 then becomes

$$\frac{\partial x_A}{\partial t} - \left(\frac{\mathscr{D}_{AB}}{1 - x_{A0}} \frac{\partial x_A}{\partial z}\bigg|_{z=0}\right) \frac{\partial x_A}{\partial z} = \mathscr{D}_{AB} \frac{\partial^2 x_A}{\partial z^2} \tag{20.1-5}$$

This is to be solved with the initial and boundary conditions:

I.C.:	at $t = 0$,	$x_A = 0$	(20.1-6)
B.C. 1:	at $z = 0$,	$x_A = x_{A0}$	(20.1-7)
B.C. 2:	at $z = \infty$,	$x_A = 0$	(20.1-8)

We can try the same kind of combination of variables used in Example 4.1-1; namely, $X = x_A/x_{A0}$ and $Z = z/\sqrt{4\mathscr{D}_{AB}t}$. However, since Eq. 20.1-5 contains the parameter x_{A0}, we can anticipate that X will depend not only on Z but also parametrically on x_{A0}.

In terms of these dimensionless variables, Eq. 20.1-5 can be written as

$$\frac{d^2X}{dZ^2} + 2(Z - \varphi)\frac{dX}{dZ} = 0 \tag{20.1-9}$$

Here the quantity

$$\varphi(x_{A0}) = -\frac{1}{2}\frac{x_{A0}}{1 - x_{A0}} \frac{dX}{dZ}\bigg|_{Z=0} \tag{20.1-10}$$

is a dimensionless molar average velocity, $\varphi = v_z^*\sqrt{t/\mathscr{D}_{AB}}$, as can be seen by comparing Eqs. 20.1-10 and 20.1-4. The initial and boundary conditions in Eqs. 20.1-6 to 8 now become

B.C. 1:	at $Z = 0$,	$X = 1$	(20.1-11)
B.C. 2 and I.C.:	at $Z = \infty$,	$X = 0$	(20.1-12)

Equation 20.1-9 can be attacked by first letting $dX/dZ = Y$. This gives a first-order differential equation for Y that can be solved to obtain

$$Y = C_1 \exp[-(Z - \varphi)^2] \equiv \frac{dX}{dZ} \tag{20.1-13}$$

This gives on integration

$$X = C_1 \int_0^Z \exp[-(\bar{Z} - \varphi)^2] d\bar{Z} + C_2 \tag{20.1-14}$$

Combining this result with Eqs. 20.1-11 and 12, we get

$$X(Z) = 1 - \frac{\int_0^Z \exp[-(\bar{Z} - \varphi)^2] d\bar{Z}}{\int_0^\infty \exp[-(\bar{Z} - \varphi)^2] d\bar{Z}} = 1 - \frac{\int_{-\varphi}^{Z-\varphi} \exp(-W^2) dW}{\int_{-\varphi}^{\infty} \exp(-W^2) dW} \tag{20.1-15}$$

Then we use the definition of the error function and some of the properties of this function, in particular, $-\text{erf}(-\varphi) = \text{erf}\,\varphi$ and $\text{erf}\,\infty = 1$ (see §C.6). This leads to the final expression for the mole fraction distribution:[1]

$$X(Z) = 1 - \frac{\text{erf}(Z - \varphi) + \text{erf}\,\varphi}{\text{erf}\,\infty + \text{erf}\,\varphi} = \frac{1 - \text{erf}(Z - \varphi)}{1 + \text{erf}\,\varphi} \tag{20.1-16}$$

To get the function $\varphi(x_{A0})$, this mole fraction distribution has to be substituted into Eq. 20.1-10. This gives

$$\varphi = \frac{1}{\sqrt{\pi}} \frac{x_{A0}}{1 - x_{A0}} \frac{\exp(-\varphi^2)}{1 + \text{erf}\,\varphi} \tag{20.1-17}$$

Rather than solving this to get φ as a function of x_{A0}, it is easier to evaluate x_{A0} as a function of φ:

$$x_{A0} = \frac{1}{1 + [\sqrt{\pi}(1 + \text{erf}\,\varphi)\varphi \exp \varphi^2]^{-1}} \tag{20.1-18}$$

A small table of $\varphi(x_{A0})$ is given in Table 20.1-1, and the concentration profiles are shown in Fig. 20.1-1.

We can now calculate the rate of production of vapor from a surface of area S. If V_A is the volume of A produced by evaporation up to time t, then

$$\frac{dV_A}{dt} = \frac{N_{Az0}S}{c} = S\varphi\sqrt{\frac{\mathcal{D}_{AB}}{t}} \tag{20.1-19}$$

Table 20.1-1 Table[1] of $\varphi(x_{A0})$ and $\psi(x_{A0})$

x_{A0}	φ	$\psi = \varphi\sqrt{\pi}/x_{A0}$
0.00	0.0000	1.000
0.25	0.1562	1.108
0.50	0.3578	1.268
0.75	0.6618	1.564
1.00	∞	∞

[1] J. H. Arnold, *Trans. AIChE*, **40**, 361–378 (1944). **Jerome Howard Arnold** (1907–1974) taught at MIT, the University of Minnesota, the University of North Dakota, and the University of Iowa; he worked for Standard Oil of California (1944–1948) and was the director of the Contra Costa Transit District (1956–1960).

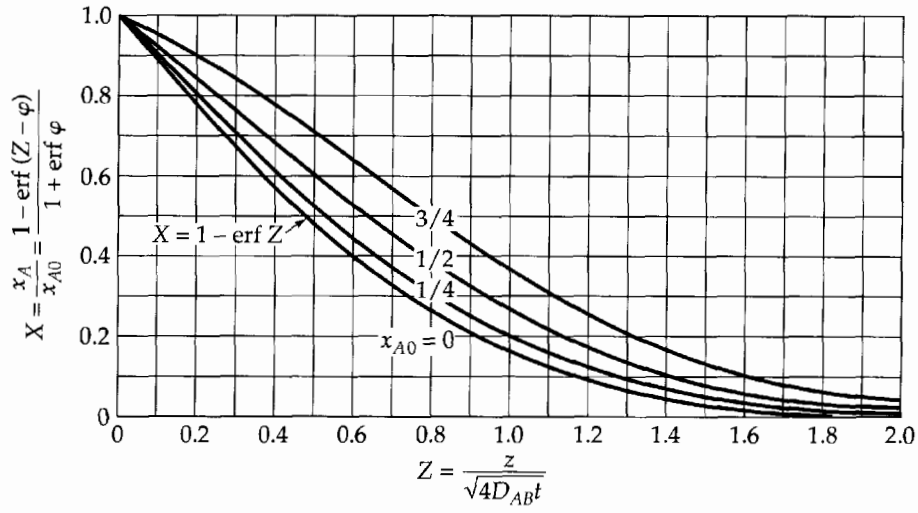

Fig. 20.1-1. Concentration profiles in time-dependent evaporation, showing that the deviation from Fick's law increases with the volatility of the evaporating liquid.

Integration with respect to t then gives

$$V_A = S\varphi\sqrt{4\mathscr{D}_{AB}t} \tag{20.1-20}$$

This relation can be used to calculate the diffusivity from the rate of evaporation (see Problem 20A.1).

We can now assess the importance of including the convective transport of species A in the tube. If Fick's second law (Eq. 19.1-18) had been used to determine X, we would have obtained

$$V_A^{\text{Fick}} = Sx_{A0}\sqrt{\frac{4\mathscr{D}_{AB}t}{\pi}} \tag{20.1-21}$$

Thus we can rewrite Eq. 20.1-20 as

$$V_A = Sx_{A0}\sqrt{\frac{4\mathscr{D}_{AB}t}{\pi}} \cdot \psi \tag{20.1-22}$$

The factor $\psi = \varphi\sqrt{\pi}/x_{A0}$, tabulated in Table 20.1-1, is a correction for the deviation from the Fick's second law results caused by the nonzero molar average velocity. We see that the deviation becomes especially significant when x_{A0} is large—that is, for liquids with large volatility.

In the preceding analysis it is assumed that the system is isothermal. Actually, the interface will be cooled by the evaporation, particularly at large values of x_{A0}. This effect can be minimized by using a small-diameter tube made of a good thermal conductor. For application to other mass transfer systems, however, the analysis given here needs to be extended by including the solution to the energy equation, so that the interfacial temperature and compositions can be calculated (see Problem 20B.2).

This analysis can be extended[2] to include interphase transfer of both species, with any time-independent flux ratio N_{Az0}/N_{Bz0} and any initial gas composition $x_{A\infty}$. A simple example of such a system is the diffusion-controlled reaction $2A \rightarrow B$ on a catalytic solid at $z = 0$, with

[2] W. E. Stewart, J. B. Angelo, and E. N. Lightfoot, *AIChE Journal*, **16**, 771–786 (1970), have generalized this example and the following one to forced convection in three-dimensional flows, including turbulent systems.

the heat of reaction removed through the solid. The concentration profile is a generalization of that in Eq. 20.1-16:

$$\Pi \equiv \frac{x_A - x_{A0}}{x_{A\infty} - x_{A0}} = \frac{\text{erf}(Z - \varphi) + \text{erf}\,\varphi}{1 + \text{erf}\,\varphi} \tag{20.1-23}$$

The dimensionless flux φ now depends on x_{A0}, $x_{A\infty}$, and the ratio N_{Bz0}/N_{Az0}:

$$\varphi = \frac{1}{2}\frac{(x_{A0} - x_{A\infty})(N_{Az0} + N_{Bz0})}{N_{Az0} - x_{A0}(N_{Az0} + N_{Bz0})}\frac{d\Pi}{dZ}\bigg|_{Z=0} \tag{20.1-24}$$

The relation between the interfacial fluxes and the terminal compositions is

$$\frac{(x_{A0} - x_{A\infty})(N_{Az0} + N_{Bz0})}{N_{Az0} - x_{A0}(N_{Az0} + N_{Bz0})} = \sqrt{\pi}(1 + \text{erf}\,\varphi)\varphi \exp \varphi^2 \tag{20.1-25}$$

Equations 20.1-16, 10, and 18 are included as special cases of the last three equations. The last one is a key result for mass transfer calculations (see §22.8).

EXAMPLE 20.1-2

Gas Absorption with Rapid Reaction[3,4]

Gas A is absorbed by a stationary liquid solvent S, the latter containing solute B. Species A reacts with B in an instantaneous irreversible reaction according to the equation $aA + bB \rightarrow$ Products. It may be assumed that Fick's second law adequately describes the diffusion processes, since A, B, and the reaction products are present in S in low concentrations. Obtain expressions for the concentration profiles.

SOLUTION

Because of the instantaneous reaction of A and B, there will be a plane parallel to the liquid–vapor interface at a distance z_R from it, which separates the region containing no A from that containing no B. The distance z_R is a function of t, since the boundary between A and B retreats as B is used up in the chemical reaction.

The differential equations for c_A and c_B are then

$$\frac{\partial c_A}{\partial t} = \mathcal{D}_{AS}\frac{\partial^2 c_A}{\partial z^2} \qquad \text{for } 0 \le z \le z_R(t) \tag{20.1-26}$$

$$\frac{\partial c_B}{\partial t} = \mathcal{D}_{BS}\frac{\partial^2 c_B}{\partial z^2} \qquad \text{for } z_R(t) \le z < \infty \tag{20.1-27}$$

These are to be solved with the following initial and boundary conditions:

I.C.:	at $t = 0$,	$c_B = c_{B\infty}$	for $z > 0$	(20.1-28)
B.C. 1:	at $z = 0$,	$c_A = c_{A0}$		(20.1-29)
B.C. 2, 3:	at $z = z_R(t)$,	$c_A = c_B = 0$		(20.1-30)
B.C. 4:	at $z = z_R(t)$,	$-\frac{1}{a}\mathcal{D}_{AS}\frac{\partial c_A}{\partial z} = +\frac{1}{b}\mathcal{D}_{BS}\frac{\partial c_B}{\partial z}$		(20.1-31)
B.C. 5:	at $z = \infty$,	$c_B = c_{B\infty}$		(20.1-32)

Here c_{A0} is the interfacial concentration of A, and $c_{B\infty}$ is the original concentration of B. The fourth boundary condition is the stoichiometric requirement that a moles of A consume b moles of B (see Problem 20B.2).

---

[3] T. K. Sherwood, R. L. Pigford, and C. R. Wilke, *Absorption and Extraction*, 3rd edition, McGraw-Hill, New York (1975), Chapter 8. See also G. Astarita, *Mass Transfer with Chemical Reaction*, Elsevier, Amsterdam (1967), Chapter 5.

[4] For related problems with moving boundaries associated with phase changes, see H. S. Carslaw and J. C. Jaeger, *Conduction of Heat in Solids*, 2nd edition, Oxford University Press (1959). See also S. G. Bankoff, *Advances in Chemical Engineering*, Academic Press, New York (1964), Vol. 5, pp. 76–150; J. Crank, *Free and Moving Boundary Problems*, Oxford University Press (1984).

The absence of a characteristic length in this problem, and the fact that $c_B = c_{B\infty}$ both at $t = 0$ and $z = \infty$, suggests trying a combination of variables. Comparison with the previous example (without the v_z^* term) suggests the following trial solutions:

$$\frac{c_A}{c_{A0}} = C_1 + C_2 \operatorname{erf} \frac{z}{\sqrt{4\mathscr{D}_{AS}t}} \qquad \text{for } 0 \le z \le z_R(t) \tag{20.1-33}$$

$$\frac{c_B}{c_{B\infty}} = C_3 + C_4 \operatorname{erf} \frac{z}{\sqrt{4\mathscr{D}_{BS}t}} \qquad \text{for } z_R(t) \le z < \infty \tag{20.1-34}$$

These functions satisfy the differential equations, and if the constants of integration, C_1 to C_4, can be so chosen that the initial and boundary conditions are satisfied, we will have the complete solution to the problem.

Application of the initial condition and the first three boundary conditions permits the evaluation of the integration constants in terms of $z_R(t)$, thereby giving

$$\frac{c_A}{c_{A0}} = 1 - \frac{\operatorname{erf}(z/\sqrt{4\mathscr{D}_{AS}t})}{\operatorname{erf}(z_R/\sqrt{4\mathscr{D}_{AS}t})} \qquad \text{for } 0 \le z \le z_R(t) \tag{20.1-35}$$

$$\frac{c_B}{c_{B\infty}} = 1 - \frac{1 - \operatorname{erf}(z/\sqrt{4\mathscr{D}_{BS}t})}{1 - \operatorname{erf}(z_R/\sqrt{4\mathscr{D}_{BS}t})} \qquad \text{for } z_R(t) \le z < \infty \tag{20.1-36}$$

B.C. 5 is then automatically satisfied. Finally, insertion of these solutions into B.C. 4 gives the following implicit equation from which $z_R(t)$ can be obtained:

$$1 - \operatorname{erf}\sqrt{\frac{\gamma}{\mathscr{D}_{BS}}} = \frac{ac_{B\infty}}{bc_{A0}} \sqrt{\frac{\mathscr{D}_{BS}}{\mathscr{D}_{AS}}} \operatorname{erf}\sqrt{\frac{\gamma}{\mathscr{D}_{AS}}} \exp\left(\frac{\gamma}{\mathscr{D}_{AS}} - \frac{\gamma}{\mathscr{D}_{BS}}\right) \tag{20.1-37}$$

Here γ is a constant equal to $z_R^2/4t$. Thus z_R increases as $\sqrt{t}$.

To calculate the concentration profiles, one first solves Eq. 20.1-37 for $\sqrt{\gamma}$, and then inserts this value for $z_R/\sqrt{4t}$ in Eqs. 20.1-35 and 36. Some calculated concentration profiles are shown in Fig. 20.1-2 (for $a = b$), to illustrate the rate of movement of the reaction zone.

From the concentration profiles we can calculate the rate of mass transfer at the interface:

$$N_{Az0} = -\mathscr{D}_{AS} \frac{\partial c_A}{\partial z}\bigg|_{z=0} = \frac{c_{A0}}{\operatorname{erf}\sqrt{\gamma/\mathscr{D}_{AS}}} \sqrt{\frac{\mathscr{D}_{AS}}{\pi t}} \tag{20.1-38}$$

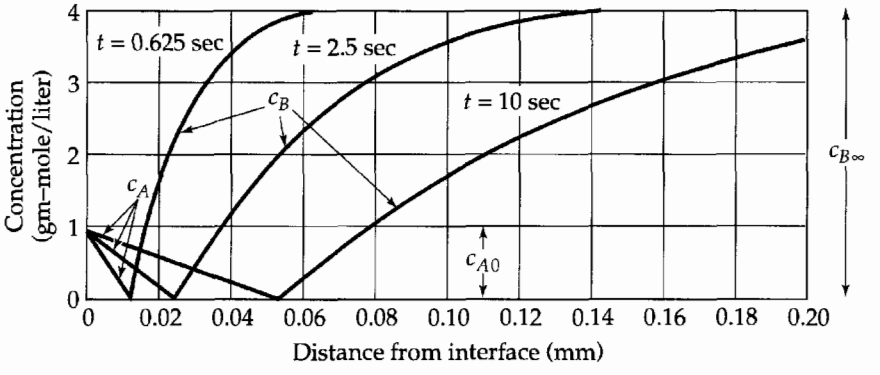

Fig. 20.1-2. Gas absorption with rapid chemical reaction, with concentration profiles given by Eqs. 20.1-35 to 37 (for $a = b$). This calculation was made for $\mathscr{D}_{AS} = 3.9 \times 10^{-5}$ ft^2/hr and $\mathscr{D}_{BS} = 1.95 \times 10^{-5}$ ft^2/hr [T. K. Sherwood and R. L. Pigford, *Absorption and Extraction*, McGraw-Hill, New York (1952), p. 336].

The average rate of absorption up to time t is then

$$N_{Az0,\text{avg}} = \frac{1}{t}\int_0^t N_{Az0}dt = 2\frac{c_{A0}}{\text{erf}\sqrt{\gamma/\mathcal{D}_{AS}}}\sqrt{\frac{\mathcal{D}_{AS}}{\pi t}} \tag{20.1-39}$$

Hence the average rate up to time t is just twice the instantaneous rate.

EXAMPLE 20.1-3

Unsteady Diffusion with First-Order Homogeneous Reaction[5–8]

When species A diffuses in a liquid medium B and reacts with it irreversibly ($A + B \rightarrow C$) according to a pseudo-first-order reaction, then the process of diffusion plus reaction is described by

$$\frac{\partial \omega_A}{\partial t} + (\mathbf{v}\cdot\nabla\omega_A) = \mathcal{D}_{AB}\nabla^2\omega_A - k_1'''\omega_A \tag{20.1-40}$$

provided that the solution of A is dilute and that not much C is produced. Here k_1''' is the rate constant for the homogeneous reaction. Equation 20.1-40 is frequently encountered with the initial and boundary conditions

I.C. at $t = 0$: $$\omega_A = \omega_{AI}(x, y, z) \tag{20.1-41}$$

B.C. at bounding surfaces: $$\omega_A = \omega_{A0}(x, y, z) \tag{20.1-42}$$

and with a velocity profile independent of time. For such problems show that the solution is

$$\omega_A = g\exp(-k_1'''t) + \int_0^t \exp(-k_1'''t)\frac{\partial}{\partial t'}f(x, y, z, t')dt' \tag{20.1-43}$$

Here f is the solution of Eqs. 20.1-40 to 42 with $k_1''' = 0$ and $\omega_{AI} = 0$, whereas g is the solution with $k_1''' = 0$ and $\omega_{A0} = 0$.

SOLUTION

This problem is linear in ω_A. It may, therefore, be solved by a superposition of two simpler problems:

$$\omega_A = \omega_A^{(1)} + \omega_A^{(2)} \tag{20.1-44}$$

with $\omega_A^{(1)}$ described by the equations

P.D.E.: $$\frac{\partial \omega_A^{(1)}}{\partial t} + (\mathbf{v}\cdot\nabla\omega_A^{(1)}) = \mathcal{D}_{AB}\nabla^2\omega_A^{(1)} - k_1'''\omega_A^{(1)} \tag{20.1-45}$$

I.C. at $t = 0$: $$\omega_A^{(1)} = \omega_{AI}(x, y, z) \tag{20.1-46}$$

B.C. at surfaces: $$\omega_A^{(1)} = 0 \tag{20.1-47}$$

---

[5] P. V. Danckwerts, *Trans. Faraday Soc.*, **47**, 1014–1023 (1951). **Peter Victor Danckwerts** (1916–1984) was bomb disposal officer for the Port of London during "the Blitz" and was wounded in a mine field in Italy during WWII; while teaching at Imperial College in London and at Cambridge University he directed research on residence-time distribution, diffusion and chemical reaction, and the role of diffusion in gas absorption.

[6] A. Giuliani and F. P. Foraboschi, *Atti. Acad. Sci. Inst. Bologna*, **9**, 1–16 (1962); F. P. Foraboschi, *ibid.*, **11**, 1–14 (1964); F. P. Foraboschi, *AIChE Journal*, **11**, 752–768 (1965).

[7] E. N. Lightfoot, *AIChE Journal*, **10**, 278–284 (1964).

[8] W. E. Stewart, *Chem. Eng. Sci.*, **23**, 483–487 (1968); corrigenda, *ibid.*, **24**, 1189–1190 (1969). There this approach was generalized to time-dependent flows with homogeneous and heterogeneous first-order reactions.

and $\omega_A^{(2)}$ described by

P.D.E.: $$\frac{\partial \omega_A^{(2)}}{\partial t} + (\mathbf{v} \cdot \nabla \omega_A^{(2)}) = \mathscr{D}_{AB} \nabla^2 \omega_A^{(2)} - k_1''' \omega_A^{(2)} \tag{20.1-48}$$

I.C. at $t = 0$: $$\omega_A^{(2)} = 0 \tag{20.1-49}$$

B.C. at surfaces: $$\omega_A^{(2)} = \omega_{A0}(x, y, z) \tag{20.1-50}$$

We now proceed to solve these two auxiliary problems by means of Laplace transform.

Taking the Laplace transform of the equations for $\omega_A^{(1)}$ gives

P.D.E. + I.C.: $$(p + k_1''')\overline{\omega}_A^{(1)} - \omega_{AI}(x, y, z) + (\mathbf{v} \cdot \nabla \overline{\omega}_A^{(1)}) = \mathscr{D}_{AB} \nabla^2 \overline{\omega}_A^{(1)} \tag{20.1-51}$$

B.C. at surfaces: $$\overline{\omega}_A^{(1)} = 0 \tag{20.1-52}$$

Now, the function g in Eq. 20.1-43 is the solution for $\omega_A^{(1)}$ with k_1''' replaced by zero. Correspondingly the Laplace transform $\bar{g}$ satisfies Eqs. 20.1-51 and 52 with $p + k_1'''$ replaced by p:

$$\overline{\omega}_A^{(1)}(p, x, y, z) = \bar{g}(p + k_1''', x, y, z) \tag{20.1-53}$$

Hence by taking the inverse Laplace transform we get

$$\omega_A^{(1)} = g \exp(-k_1''' t) \tag{20.1-54}$$

which is the first part of the solution.

Next, taking the Laplace transform of Eqs. 20.1-48 to 50 gives

P.D.E. + I.C.: $$(p + k_1''')\overline{\omega}_A^{(2)} + (\mathbf{v} \cdot \nabla \overline{\omega}_A^{(2)}) = \mathscr{D}_{AB} \nabla^2 \overline{\omega}_A^{(2)} \tag{20.1-55}$$

B.C. at surfaces: $$\overline{\omega}_A^{(2)} = \frac{1}{p} \omega_{A0}(x, y, z) \tag{20.1-56}$$

The Laplace transform $\bar{f}$ satisfies the same two equations with k_1''' replaced by zero. That is, if we now use s for the transform variable in lieu of p, we have

P.D.E. + I.C.: $$s\bar{f} + (\mathbf{v} \cdot \nabla \bar{f}) = \mathscr{D}_{AB} \nabla^2 \bar{f} \tag{20.1-57}$$

B.C. at surfaces: $$\bar{f} = \frac{1}{s} \omega_{A0}(x, y, z) \tag{20.1-58}$$

We see that the function $s\bar{f}$ satisfies the same boundary condition as $p\overline{\omega}_A^{(2)}$ and that the differential equations for $s\bar{f}$ and $p\overline{\omega}_A^{(2)}$ are identical when $s = p + k'''$. Hence

$$p\overline{\omega}_A^{(2)}\big|_p = (s\bar{f})\big|_{s=p+k_1'''} \tag{20.1-59}$$

or

$$\overline{\omega}_A^{(2)}(p, x, y, z) = \frac{p + k_1'''}{p} \bar{f}(p + k_1''', x, y, z) \tag{20.1-60}$$

Taking the inverse transform then gives

$$\omega_A^{(2)} = \int_0^t \exp(-k_1''' t') \frac{\partial}{\partial t'} f(x, y, z, t') dt' \tag{20.1-61}$$

as the second part of the solution. Addition of the two parts of the solution, $\omega_A^{(1)}$ and $\omega_A^{(2)}$, then gives Eq. 20.1-43 directly.

Equation 20.1-43 provides a means for predicting concentration profiles in reacting systems from calculations or experiments on nonreacting systems at the same flow conditions. Several extensions of this treatment are available, including multicomponent systems,[9] turbulent flow,[8,9] and more general boundary conditions.[7–9]

---

[9] Y.-H. Pao, *AIAA Journal*, **2**, 1550–1559 (1964); *Chem. Eng. Sci.*, **19**, 694–696 (1964); *ibid.*, **20**, 665–669 (1965).

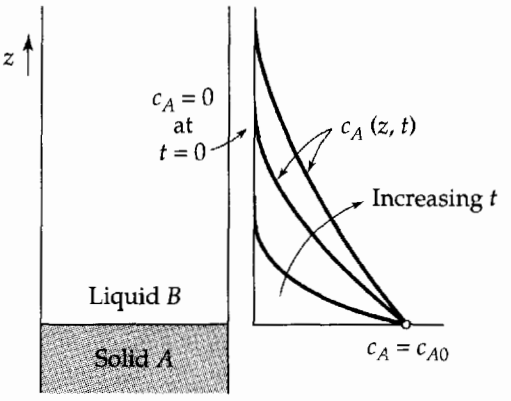

Fig. 20.1-3. Time-dependent diffusion from a soluble wall of A into a semi-infinite column of liquid B.

EXAMPLE 20.1-4

Influence of Changing Interfacial Area on Mass Transfer at an Interface[10,11]

Figure 20.1-3 shows schematically the concentration profiles for the diffusion of A from a slightly soluble wall into a semi-infinite body of liquid above it. If the density and diffusivity are constants, then this problem is the mass transfer analog of the problems discussed in §§4.1 and 12.1. The diffusion is described by the one-dimensional version of Fick's second law, Eq. 19.1-18,

$$\frac{\partial c_A}{\partial t} = \mathscr{D}_{AB}\frac{\partial^2 c_A}{\partial z^2} \tag{20.1-62}$$

along with the initial condition that $c_A = 0$ throughout the liquid, and the boundary conditions that $c_A = c_{A0}$ at the solid–liquid interface and $c_A = 0$ infinitely far from the interface. The solution to this problem is

$$\frac{c_A}{c_{A0}} = 1 - \operatorname{erf}\frac{z}{\sqrt{4\mathscr{D}_{AB}t}} \tag{20.1-63}$$

from which we can get the interfacial flux

$$N_{Az0} = c_{A0}\sqrt{\frac{\mathscr{D}_{AB}}{\pi t}} \tag{20.1-64}$$

Equation 20.1-63 is the mass transfer analog of Eqs. 4.1-15 and 12.1-8.

In Fig. 20.1-4 we depict a similar problem in which the interfacial area is changing with time as the liquid spreads out in the x and y directions, so that the interfacial area is a function of time, $S(t)$. The initial and boundary conditions for the concentration are kept the same. We wish to know the function $c_A(z, t)$ for this system.

SOLUTION

The velocity distribution for this varying interfacial area problem is $v_x = +\frac{1}{2}ax$, $v_y = +\frac{1}{2}ay$, $v_z = -az$, where $a = d \ln S/dt$. Then the diffusion equation for this system is

$$\frac{\partial c_A}{\partial t} - \left(\frac{d}{dt}\ln S\right)z\frac{\partial c_A}{\partial z} = \mathscr{D}_{AB}\frac{\partial^2 c_A}{\partial z^2} \tag{20.1-65}$$

---

[10] D. Ilkovič, *Collec. Czechoslov. Chem. Comm.*, **6**, 498–513 (1934). The final result in this section was obtained by Ilkovič in connection with his work on the dropping-mercury electrode.

[11] V. G. Levich, *Physicochemical Hydrodynamics*, 2nd edition (English translation), Prentice-Hall, Englewood Cliffs N.J. (1962), §108. This book contains a wealth of theoretical and experimental results on diffusion and flow phenomena in liquids and two-phase systems.

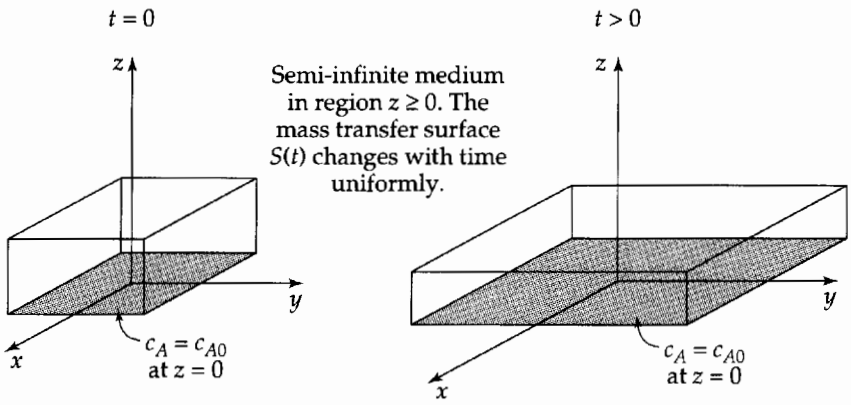

Fig. 20.1-4. Time-dependent diffusion across a mass transfer interface $S(t)$ that is changing with time. The liquid B, in the region above the plane $z = 0$, has a velocity distribution $v_x = +\frac{1}{2}ax$, $v_y = +\frac{1}{2}ay$, and $v_z = -az$, where $a = d \ln S/dt$.

Since Eq. 20.1-62 is solved by the method of combination of variables, the same technique can be tried here. We postulate

$$\frac{c_A}{c_{A0}} = g(\zeta) \qquad \text{with } \zeta = \frac{z}{\delta(t)} \tag{20.1-66}$$

Substitution of this trial solution into Eq. 20.1-65 gives

$$\frac{d^2g}{d\zeta^2} + 2\left[\frac{\delta^2}{2\mathscr{D}_{AB}}\left(\frac{d}{dt}\ln(S\delta)\right)\right]\zeta\frac{dg}{d\zeta} = 0 \tag{20.1-67}$$

If we set the expression within the brackets equal to unity, then we accomplish two things: (i) we obtain an equation for g that has the same form as Eq. 4.1-9, to which the solution is known; (ii) we get an equation for δ as a function of t:

$$\frac{d}{dt}\ln(S\delta) = \frac{2\mathscr{D}_{AB}}{\delta^2} \tag{20.1-68}$$

This equation may be integrated to give

$$\int_0^{S(t)\delta(t)} d(S\delta)^2 = 4\mathscr{D}_{AB}\int_0^t S^2(\bar{t})d\bar{t} \tag{20.1-69}$$

The lower limit on the left side is chosen so as to ensure that $c_A = 0$ initially throughout the fluid. This choice then leads to

$$\delta(t) = \sqrt{4\mathscr{D}_{AB}\int_0^t [S(\bar{t})/S(t)]^2 d\bar{t}} \tag{20.1-70}$$

and we get finally for the concentration profiles

$$\frac{c_A}{c_{A0}} = 1 - \operatorname{erf}\frac{z}{\sqrt{4\mathscr{D}_{AB}\int_0^t [S(\bar{t})/S(t)]^2 d\bar{t}}} \tag{20.1-71}$$

The interfacial mass flux is then obtained by differentiating Eq. 20.1-71 to get

$$N_{Az0} = c_{A0}\sqrt{\frac{\mathscr{D}_{AB}}{\pi t}}\left(\frac{1}{t}\int_0^t [S(\bar{t})/S(t)]^2 d\bar{t}\right)^{-1/2} \tag{20.1-72}$$

The total number of moles of A that have crossed the interface at time t through the surface $S(t)$ can be obtained from integration of Eq. 20.1-71 as follows:

$$\begin{aligned} M_A(t) &= \int\int\int_0^\infty c_A dz\, dy\, dx = S(t)c_{A0}\int_0^\infty (1 - \text{erf}(z/\delta))dz \\ &= S(t)c_{A0}\frac{2}{\sqrt{\pi}}\int_0^\infty \int_{z/\delta}^\infty \exp(-\zeta^2)\, d\zeta\, dz \\ &= S(t)c_{A0}\frac{2}{\sqrt{\pi}}\delta\int_0^\infty \exp(-\zeta^2)\,\zeta\, d\zeta \\ &= S(t)c_{A0}\frac{1}{\sqrt{\pi}}\sqrt{4\mathscr{D}_{AB}\int_0^t [S(\bar{t})/S(t)]^2 d\bar{t}} \\ &= c_{A0}\sqrt{\frac{4\mathscr{D}_{AB}}{\pi}\int_0^t [S(\bar{t})]^2 d\bar{t}} \end{aligned} \tag{20.1-73}$$

An equivalent expression can be obtained by integrating Eq. 20.1-72:

$$\begin{aligned} M_A(t) &= \int_0^t S(\bar{t})N_{Az0}(\bar{t})d\bar{t} \\ &= c_{A0}\sqrt{\frac{\mathscr{D}_{AB}}{\pi}}\int_0^t \frac{[S(\bar{t})]^2}{\sqrt{\int_0^{\bar{t}} [S(\bar{\bar{t}})/S(\bar{t})]^2 d\bar{\bar{t}}}}\, d\bar{t} \end{aligned} \tag{20.1-74}$$

Both Eq. 21.1-73 and Eq. 21.1-74 can be checked by verifying that $dM_A/dt = N_{Az0}(t)S(t)$.

If $S(t) = at^n$, where a is a constant, the above results simplify to

$$N_{Az0}(t) = c_{A0}\sqrt{\frac{(2n+1)\mathscr{D}_{AB}}{\pi t}} \tag{20.1-75}$$

$$M_A(t) = c_{A0}a\sqrt{\frac{4\mathscr{D}_{AB}t^{2n+1}}{(2n+1)\pi}} \tag{20.1-76}$$

For the diffusion into the surrounding liquid from a gas bubble whose volume is increasing linearly with time, $n = \frac{2}{3}$ and $2n + 1 = \frac{7}{3}$. This is of course an approximate result, in which curvature has been neglected, and is therefore valid only for short contact times. Related results have been obtained for interfaces of arbitrary shapes,[2,12] and experimentally verified for several laminar and turbulent systems.[2,13]

§20.2 STEADY-STATE TRANSPORT IN BINARY BOUNDARY LAYERS

In §12.4 we discussed the application of boundary layer analysis to nonisothermal flow of pure fluids. The equations of continuity, motion, and energy were presented in boundary layer form and were solved for some simple situations. In this section we extend the set of boundary layer equations to binary reacting mixtures, adding the equation of continuity for species A so that the concentration profiles can be evaluated. Then we analyze three examples for the flat-plate geometry: one on forced convection with a homogeneous reaction, one on rapid mass transfer, and one on analogies for small mass-transfer rates.

[12] J. B. Angelo, E. N. Lightfoot, and D. W. Howard, *AIChE Journal*, **12**, 751–760 (1966).

[13] W. E. Stewart, in *Physicochemical Hydrodynamics* (D. B. Spalding, ed.), Advance Publications Ltd., London, Vol. 1 (1977), pp. 22–63.

Consider the steady, two-dimensional flow of a binary fluid around a submerged object, such as that in Fig. 4.4-1. In the vicinity of the solid surface, the equations of change given in §§18.2 and 3 may be simplified as follows, provided that ρ, μ, k, $\hat{C}_p$, and $\mathscr{D}_{AB}$ are essentially constant (except in the $\rho\mathbf{g}$ term), and that viscous dissipation can be neglected:

Continuity:
$$\frac{\partial v_x}{\partial x} + \frac{\partial v_y}{\partial y} = 0 \tag{20.2-1}$$

Motion:
$$\rho\left(v_x\frac{\partial v_x}{\partial x} + v_y\frac{\partial v_x}{\partial y}\right) = \rho v_e\frac{dv_e}{dx} + \mu\frac{\partial^2 v_x}{\partial y^2} + \bar{\rho}g_x\bar{\beta}(T - T_\infty) + \bar{\rho}g_x\bar{\zeta}(\omega_A - \omega_{A\infty}) \tag{20.2-2}$$

Energy:
$$\rho\hat{C}_p\left(v_x\frac{\partial T}{\partial x} + v_y\frac{\partial T}{\partial y}\right) = k\frac{\partial^2 T}{\partial y^2} - \left(\frac{\overline{H}_A}{M_A} - \frac{\overline{H}_B}{M_B}\right)r_A \tag{20.2-3}$$

Continuity of A:
$$\rho\left(v_x\frac{\partial \omega_A}{\partial x} + v_y\frac{\partial \omega_A}{\partial y}\right) = \rho\mathscr{D}_{AB}\frac{\partial^2 \omega_A}{\partial y^2} + r_A \tag{20.2-4}$$

The equation of continuity is the same as Eq. 12.4-1. The equation of motion, obtained from Eq. 19.2-3, differs from Eq. 12.4-2 by the addition of the binary buoyant force term $\bar{\rho}g_x\bar{\zeta}(\omega_A - \omega_{A\infty})$. The energy equation, obtained from Eq. (F) of Table 19.2-4, differs from Eq. 12.4-3 by the addition of the chemical heat-source term $-[(\overline{H}_A/M_A) - (\overline{H}_B/M_B)]r_A$. Equation 20.2-4 is obtained from Eq. 19.1-16 by setting $\omega_A = \omega_A(x, y)$ and neglecting the diffusion in the x direction. More complete equations, valid for high-velocity, variable-property boundary layers, are available elsewhere.[1]

The usual boundary conditions on v_x are that $v_x = 0$ at the solid surface, and $v_x = v_e(x)$ at the outer edge of the *velocity boundary layer*. The usual boundary conditions on T in Eq. 20.2-3 are that $T = T_0(x)$ at the solid surface, and $T = T_\infty$ at the outer edge of the *thermal boundary layer*. The corresponding boundary conditions on ω_A in Eq. 20.2-4 are that $\omega_A = \omega_{A0}(x)$ at the surface and $\omega_A = \omega_{A\infty}$ at the outer edge of the *diffusional boundary layer*. Thus there are now three boundary layers to consider, each with its own thickness. In fluids with constant physical properties and large Prandtl and Schmidt numbers, the thermal and diffusional boundary layers usually lie within the velocity boundary layer, whereas for $\mathrm{Pr} < 1$ and $\mathrm{Sc} < 1$ they may extend beyond it.

For mass transfer systems the velocity v_y at the surface is usually not zero, but depends on x. Hence we set $v_y = v_0(x)$ at $y = 0$. This boundary condition is appropriate whenever there is a net mass flux between the surface and the stream, as in melting, drying, sublimation, combustion of the wall, or transpiration of the fluid through a porous wall. Clearly, some of these processes are possible with pure fluids, but for simplicity we have deferred their consideration to this chapter (see also §§18.3 and 22.8 for related analyses).

With the help of the equation of continuity, Eqs. 20.2-1 to 4 can be formally integrated, with the boundary conditions just given, to obtain the following set of boundary layer balances:

Continuity + motion:
$$\mu\left.\frac{\partial v_x}{\partial y}\right|_{y=0} = \frac{d}{dx}\int_0^\infty \rho v_x(v_e - v_x)dy + \frac{dv_e}{dx}\int_0^\infty \rho(v_e - v_x)dy - \int_0^\infty \rho g_x\beta(T - T_\infty)dy - \int_0^\infty \rho g_x\zeta(\omega_A - \omega_{A\infty})dy + \rho v_0 v_e \tag{20.2-5}$$

Continuity + energy:
$$k\left.\frac{\partial T}{\partial y}\right|_{y=0} = \frac{d}{dx}\int_0^\infty \rho v_x\hat{C}_p(T_\infty - T)\,dy - \int_0^\infty \left(\frac{\overline{H}_A}{M_A} - \frac{\overline{H}_B}{M_B}\right)r_A dy - \rho v_0\hat{C}_p(T_\infty - T_0) \tag{20.2-6}$$

[1] See, for example, W. H. Dorrance, *Viscous Hypersonic Flow*, McGraw-Hill, New York (1962), and K. Stewartson, *The Theory of Laminar Boundary Layers in Compressible Fluids*, Oxford University Press (1964).

Continuity + continuity of A:

$$\rho\mathcal{D}_{AB}\left.\frac{\partial\omega_A}{\partial y}\right|_{y=0} = \frac{d}{dx}\int_0^\infty \rho v_x(\omega_{A\infty} - \omega_A)\,dy + \int_0^\infty r_A dy - \rho v_0(\omega_{A\infty} - \omega_{A0}) \qquad (20.2\text{-}7)$$

These equations are extensions of the *von Kármán balances* of §§4.4 and 12.4 and may be similarly applied, as shown in Example 20.2-1.

Boundary layer techniques have been of considerable value in developing the theory of high-speed flight, separations processes, chemical reactors, and biological mass transfer systems. A few of the interesting problems that have been studied are chemical reactions in hypersonic boundary layers,[1] mass transfer from droplets,[2] electrode polarization in forced convection[2] and free convection,[3] reverse-osmosis water desalination,[4] and interphase transfer in packed-bed reactors and distillation columns.[5]

EXAMPLE 20.2-1

Diffusion and Chemical Reaction in Isothermal Laminar Flow Along a Soluble Flat Plate

An appropriate mass transfer analog to the problem discussed in Example 12.4-1 would be the flow along a flat plate that contains a species A slightly soluble in the fluid B. The concentration at the plate surface would be c_{A0}, the solubility of A in B, and the concentration of A far from the plate would be $c_{A\infty}$. In this example we let $c_{A\infty} = 0$ and break the analogy with Example 12.4-1 by letting A react with B by an nth order homogeneous reaction, so that $R_A = -k_n''' c_A^n$. The concentration of dissolved A is assumed to be small, so that the physical properties μ, ρ, and $\mathcal{D}_{AB}$ are virtually constant throughout the fluid. We wish to analyze the system, sketched in Fig. 20.2-1, by the von Kármán method.

SOLUTION

We begin by postulating forms for the velocity and concentration profiles. To minimize the algebra and still illustrate the method, we select simple functions (clearly one can suggest more realistic functions):

$$\begin{cases} \dfrac{v_x}{v_\infty} = \dfrac{y}{\delta} & y \le \delta(x) \\ \dfrac{v_x}{v_\infty} = 1 & y \ge \delta(x) \end{cases} \qquad (20.2\text{-}8)$$

$$\begin{cases} \dfrac{c_A}{c_{A0}} = 1 - \dfrac{y}{\delta_c} & y \le \delta_c(x) \\ \dfrac{c_A}{c_{A0}} = 0 & y \ge \delta_c(x) \end{cases} \qquad (20.2\text{-}9)$$

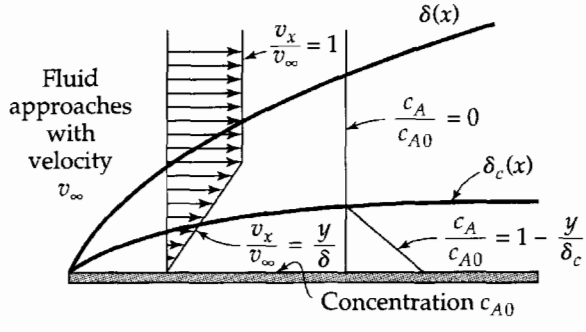

Fig. 20.2-1. Assumed velocity and concentration profiles for the laminar boundary layer with homogeneous chemical reaction.

[2] V. G. Levich, *Physicochemical Hydrodynamics*, 2nd edition (English translation), Prentice-Hall, Englewood Cliffs, N.J. (1962).

[3] C. R. Wilke, C. W. Tobias, and M. Eisenberg, *Chem. Eng. Prog.*, **49**, 663–674 (1953).

[4] W. N. Gill, D. Zeh, and C. Tien, *Ind. Eng. Chem. Fund.*, **4**, 433–439 (1965); *ibid.*, **5**, 367–370 (1966). See also P. L. T. Brian, *ibid.*, **4**, 439–445 (1965).

[5] J. P. Sørensen and W. E. Stewart, *Chem. Eng. Sci.*, **29**, 833–837 (1974); W. E. Stewart and D. L. Weidman, *ibid.*, **45**, 2155–2160 (1990); T. C. Young and W. E. Stewart, *AIChE Journal*, **38**, 592–602, 1302 (1992).

Note that we use different thicknesses, δ and δ_c, for the velocity and concentration boundary layers. In order to relate this problem to that of Example 12.4-1, we introduce the quantity $\Delta = \delta_c/\delta$, which in this case is a function of x because of the chemical reaction occurring. We restrict the discussion to $\Delta \leq 1$, for which the concentration boundary layer lies entirely within the velocity boundary layer. We can also neglect the interfacial velocity $v_0 = v_y|_{y=0}$, which is small here because of the small solubility of A. Insertion of these expressions into Eqs. 20.2-5 and 7 then gives the differential equations

$$\frac{\mu v_\infty}{\delta} = \frac{d}{dx}\left(\tfrac{1}{6}\rho v_\infty^2 \delta\right) \tag{20.2-10}$$

$$-\frac{\mathscr{D}_{AB} c_{A0}}{\delta\Delta} = \frac{d}{dx}\left(-\tfrac{1}{6} c_{A0} v_\infty \delta\Delta^2\right) - \frac{k_n''' c_{A0}^n \delta\Delta}{n+1} \tag{20.2-11}$$

for the boundary layer thicknesses δ and $\delta_c = \delta\Delta$.

Equation 20.2-10 is readily integrated to give

$$\delta = \sqrt{12\frac{\nu x}{v_\infty}} \tag{20.2-12}$$

Insertion of this result into Eq. 20.2-11 and multiplication by $-\delta\Delta/\nu c_{A0}$ gives

$$\frac{1}{\mathrm{Sc}} = \frac{4}{3} x \frac{d}{dx}\Delta^3 + \Delta^3 + 12\left[\frac{k_n''' c_{A0}^{n-1} x}{(n+1)v_\infty}\right]\Delta^2 \tag{20.2-13}$$

as the differential equation for Δ. Thus Δ depends on the Schmidt number, $\mathrm{Sc} = \mu/\rho\mathscr{D}_{AB}$, and on the dimensionless position coordinate shown in the square brackets. The bracketed quantity is $1/(n+1)$ times the *first Damköhler number*[6] based on the distance x.

When *no reaction* is occurring, k_n''' is zero, and Eq. 20.2-13 becomes a linear first-order reaction for Δ^3. When that equation is integrated, we get

$$\Delta^3 = \frac{1}{\mathrm{Sc}} + \frac{C}{x^{3/4}} \tag{20.2-14}$$

in which C is a constant of integration. Because Δ does not become infinite as $x \to 0$, we obtain in the absence of chemical reaction (cf. Eq. 12.4-15):

$$\Delta = \mathrm{Sc}^{-1/3} \qquad \Delta < 1 \tag{20.2-15}$$

That is, when there is no reaction and $\mathrm{Sc} > 1$, the concentration and velocity boundary layer thicknesses bear a constant ratio to one another, dependent only on the value of the Schmidt number.

When a *slow reaction* occurs (or when x is small), a series solution to Eq. 20.2-13 can be obtained:

$$\Delta = \mathrm{Sc}^{-1/3}(1 + a_1\xi + a_2\xi^2 + \cdots) \tag{20.2-16}$$

in which

$$\xi = 12\left[\frac{k_n''' c_{A0}^{n-1} x}{(n+1)v_\infty}\right] \tag{20.2-17}$$

Substitution of this expression into Eq. 20.2-13 gives

$$a_1 = -\tfrac{1}{7}\mathrm{Sc}^{1/3}, \qquad a_2 = +\tfrac{3}{539}\mathrm{Sc}^{2/3}, \qquad \text{etc.} \tag{20.2-18}$$

Because a_1 is negative, the concentration boundary layer thickness is diminished by the chemical reaction.

---

[6] G. Damköhler, *Zeits. f. Electrochemie*, **42**, 846–862 (1936); W. E. Stewart, *Chem. Eng. Prog. Symp. Series*, #58, **61**, 16–27 (1965).

When a *fast reaction* occurs (or when x is very large), a series solution in $1/\xi$ is more appropriate. For large ξ, we assume that the dominant term is of the form $\Delta = \text{const.} \cdot \xi^m$ where $m < 0$. Substitution of this trial function into Eq. 20.2-13 then shows that

$$\Delta = (\text{Sc}\xi)^{-1/2} \qquad \text{for large } \xi \tag{20.2-19}$$

Combination of Eqs. 20.2-12 and 19 shows that, at large distances from the leading edge, the concentration boundary layer thickness $\delta_c = \delta\Delta$ becomes a constant independent of v_∞ and ν.

Once $\Delta(\xi, \text{Sc})$ is known, then the concentration profiles and the mass transfer rate at the surface may be found. A more refined treatment of this problem has been given elsewhere.[7]

EXAMPLE 20.2-2

Forced Convection from a Flat Plate at High Mass-Transfer Rates

The laminar boundary layer on a flat plate (see Fig. 20.2-2) has been a popular system for heat and mass transfer studies. In this example, we give an analysis of subsonic forced convection in this geometry at high mass-transfer rates, and discuss the analogies that hold in this situation. This example is an extension of Example 4.4-2.

SOLUTION

Consider the nonisothermal, steady, two-dimensional flow of a binary fluid in the system of Fig. 20.2-2. The fluid properties ρ, μ, $\hat{C}_p$, k, and $\mathcal{D}_{AB}$ are considered constant, viscous dissipation is neglected, and there are no homogeneous chemical reactions. The Prandtl boundary layer equations for the laminar region are

Continuity:
$$\frac{\partial v_x}{\partial x} + \frac{\partial v_y}{\partial y} = 0 \tag{20.2-20}$$

Motion:
$$v_x \frac{\partial v_x}{\partial x} + v_y \frac{\partial v_x}{\partial y} = \nu \frac{\partial^2 v_x}{\partial y^2} \tag{20.2-21}$$

Energy:
$$v_x \frac{\partial T}{\partial x} + v_y \frac{\partial T}{\partial y} = \alpha \frac{\partial^2 T}{\partial y^2} \tag{20.2-22}$$

Continuity of A:
$$v_x \frac{\partial \omega_A}{\partial x} + v_y \frac{\partial \omega_A}{\partial y} = \mathcal{D}_{AB} \frac{\partial^2 \omega_A}{\partial y^2} \tag{20.2-23}$$

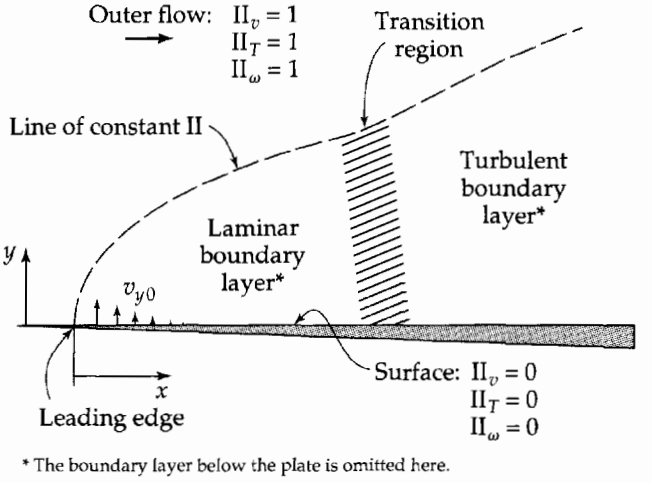

Fig. 20.2-2. Tangential flow along a sharp-edged semi-infinite flat plate with mass transfer into the stream. The laminar-turbulent transition usually occurs at a length Reynolds number $(xv_\infty/\nu)_{\text{crit}}$ on the order of 10^5 to 10^6.

[7] P. L. Chambré and J. D. Young, *Physics of Fluids*, **1**, 48–54 (1958). Catalytic surface reactions in boundary layers have been studied by P. L. Chambré and A. Acrivos, *J. Appl. Phys.*, **27**, 1322–1328 (1956).

The boundary conditions are taken to be:

$$\text{at } x \leq 0 \text{ or } y = \infty, \qquad v_x = v_\infty \tag{20.2-24}$$
$$T = T_\infty$$
$$\omega_A = \omega_{A\infty}$$
$$\text{at } y = 0, \qquad v_x = 0 \tag{20.2-25}$$
$$T = T_0$$
$$\omega_A = \omega_{A0}$$
$$\text{at } y = 0, \qquad v_y = v_0(x) \tag{20.2-26}$$

Here the function $v_0(x)$ stands for $v_y(x, y)$ evaluated at $y = 0$ and describes the distribution of mass transfer rate along the surface. This function will be specified later.

Equation 20.2-20 can be integrated, with the boundary condition of Eq. 20.2-26, to give

$$v_y = v_0(x) - \frac{\partial}{\partial x}\int_0^y v_x dy \tag{20.2-27}$$

This expression is to be inserted for v_y into Eqs. 20.2-21 to 23.

To capitalize on the analogous form of Eqs. 20.2-21 to 23 and the first six boundary conditions, we define the dimensionless profiles

$$\Pi_v = \frac{v_x}{v_\infty} \qquad \Pi_T = \frac{T - T_0}{T_\infty - T_0} \qquad \Pi_\omega = \frac{\omega_A - \omega_{A0}}{\omega_{A\infty} - \omega_{A0}} \tag{20.2-28}$$

and the dimensionless physical property ratios

$$\Lambda_v = \frac{\nu}{\nu} = 1 \qquad \Lambda_T = \frac{\nu}{\alpha} = \mathrm{Pr} \qquad \Lambda_\omega = \frac{\nu}{\mathscr{D}_{AB}} = \mathrm{Sc} \tag{20.2-29}$$

With these definitions, and the above equation for v_y, Eqs. 20.2-21 to 23 all take the form

$$\Pi_v \frac{\partial \Pi}{\partial x} + \left(\frac{v_0(x)}{v_\infty} - \frac{\partial}{\partial x}\int_0^y \Pi_v dy\right)\frac{\partial \Pi}{\partial y} = \frac{\nu}{v_\infty \Lambda}\frac{\partial^2 \Pi}{\partial y^2} \tag{20.2-30}$$

and the boundary conditions on the dependent variables reduce to the following:

$$\text{at } x \leq 0 \text{ or } y = \infty, \qquad \Pi = 1 \tag{20.2-31}$$
$$\text{at } y = 0, \qquad \Pi = 0 \tag{20.2-32}$$

Thus the dimensionless velocity, temperature, and composition profiles all satisfy the same equation, but with their individual values of Λ.

The form of the boundary conditions on Π suggests that a combination of variables be tried. By analogy with Eq. 4.4-20 we select the combination:

$$\eta = y\sqrt{\frac{1}{2}\frac{v_\infty}{\nu x}} \tag{20.2-33}$$

Then by treating Π and Π_v as functions of η (see Problem 20B.3), we obtain the differential equation

$$\left(\frac{v_0(x)}{v_\infty}\sqrt{2\frac{v_\infty x}{\nu}} - \int_0^\eta \Pi_v d\eta\right)\frac{d\Pi}{d\eta} = \frac{1}{\Lambda}\frac{d^2\Pi}{d\eta^2} \tag{20.2-34}$$

with the boundary conditions

$$\text{at } \eta = \infty, \qquad \Pi = 1 \tag{20.2-35}$$
$$\text{at } \eta = 0, \qquad \Pi = 0 \tag{20.2-36}$$

From the last three equations we conclude that the profiles will be expressible in terms of the single coordinate η, if and only if the interfacial velocity $v_0(x)$ is of the form

$$\frac{v_0(x)}{v_\infty}\sqrt{2\frac{v_\infty x}{\nu}} = K = \text{const.} \tag{20.2-37}$$

Any other functional form for $v_0(x)$ would cause the left side of Eq. 20.2-34 to depend on both x and η, so that a combination of variables would not be possible. The boundary layer equations would then require integration in two dimensions, and the calculations would become more difficult. Equation 20.2-37 specifies that $v_0(x)$ vary as $1/\sqrt{x}$, and thus, inversely with the boundary layer thickness δ of Eq. 4.4-17.This equation has the same range of validity as Eq. 20.2-34, that is, $1 << (v_\infty x/\nu) < (v_\infty x/\nu)_{\text{crit}}$ (see Fig. 20.2-2).

Fortunately the condition in Eq. 20.3-37 is a useful one. It corresponds to a direct proportionality of ρv_0 to the interfacial fluxes τ_0, q_0, and j_{A0}. Conditions of this type arise naturally in diffusion-controlled surface reactions, and also in certain cases of drying and transpiration cooling. The determination of K for these situations is considered at the end of this example. Until then we treat K as given.

With the specification of $v_0(x)$ according to Eq. 20.2-37, the problem statement is complete, and we are ready to discuss the calculation of the profiles. This is best done by numerical integration, with specified values of the parameters Λ and K.

The first step in the solution is to evaluate the velocity profile Π_v. For this purpose it is convenient to introduce the function

$$f = -K + \int_0^\eta \Pi_v d\eta \tag{20.2-38}$$

which is a generalization of the dimensionless stream function f used in Example 4.4-2. Then setting $\Lambda = 1$ in Eq. 20.2-34 and making the substitutions $f' = df/d\eta = \Pi_v$, $f'' = d^2f/d\eta^2 = d\Pi_v/d\eta$, and so on, gives the equation of motion in the form

$$-ff'' = f''' \tag{20.2-39}$$

and Eqs. 20.2-35, 36, and 38 give the boundary conditions

$$\text{at } \eta = \infty, \quad f' = 1 \tag{20.2-40}$$

$$\text{at } \eta = 0, \quad f' = 0 \tag{20.2-41}$$

$$\text{at } \eta = 0, \quad f = -K \tag{20.2-42}$$

Equation 20.2-39 can be solved numerically with these boundary conditions to obtain f as a function of η for various values of K.

Once the function $f(\eta, K)$ has been evaluated, we can integrate Eq. 20.2-34 with the boundary conditions in Eqs. 20.2-35 and 36 to obtain

$$\Pi(\eta, \Lambda, K) = \frac{\displaystyle\int_0^\eta \exp\left(-\Lambda \int_0^{\bar{\eta}} f(\bar{\bar{\eta}}, K)d\bar{\bar{\eta}}\right) d\bar{\eta}}{\displaystyle\int_0^\infty \exp\left(-\Lambda \int_0^{\bar{\eta}} f(\bar{\bar{\eta}}, K)d\bar{\bar{\eta}}\right) d\bar{\eta}} \tag{20.2-43}$$

Some profiles calculated from this equation by numerical integration are given in Fig. 20.2-3. The velocity profiles are given by the curves for $\Lambda = 1$. The temperature and composition profiles for various Prandtl and Schmidt numbers are given by the curves for the corresponding values of Λ. Note that the velocity, temperature, and composition boundary layers get thicker when K is positive (as in evaporation) and thinner when K is negative (as in condensation).

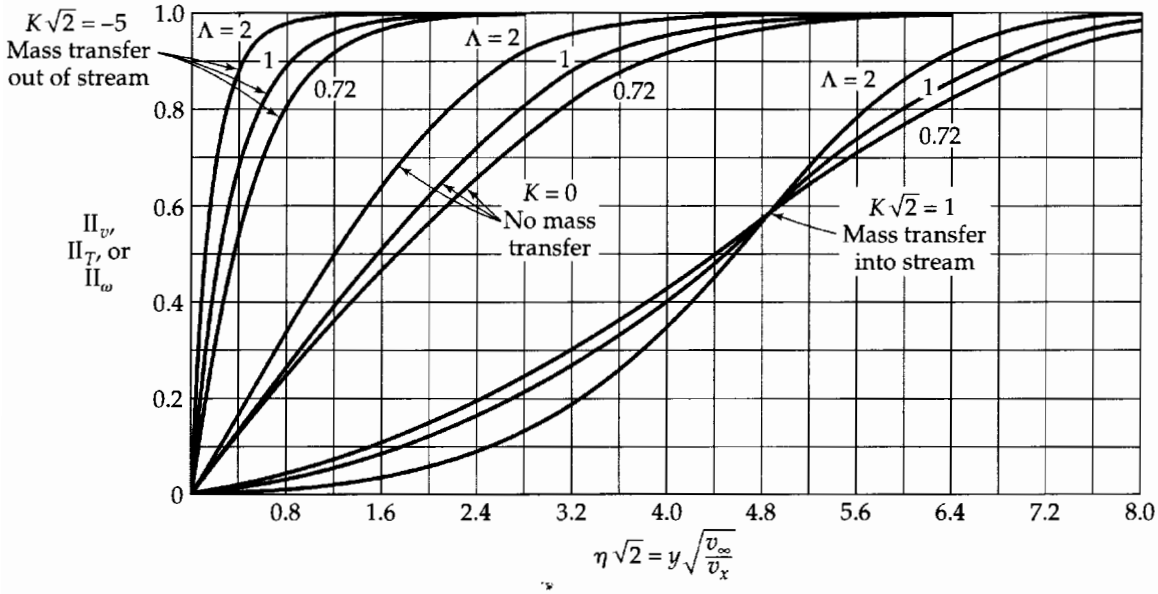

Fig. 20.2-3. Velocity, temperature, and composition profiles in the laminar boundary layer on a flat plate with mass transfer at the wall [H. S. Mickley, R. C. Ross, A. L. Squyers, and W. E. Stewart, *NACA Technical Note 3208* (1954).]

The gradients of the velocity, temperature, and composition at the wall are obtainable from the derivative of Eq. 20.2-43:

$$\Pi'(0, \Lambda, K) = \left.\frac{d\Pi(\eta, \Lambda, K)}{d\eta}\right|_{\eta=0} = \frac{1}{\int_0^\infty \exp\left(-\Lambda \int_0^\eta f(\bar{\eta}, K) d\bar{\eta}\right) d\eta} \tag{20.2-44}$$

Some values computed from this formula by numerical integration are then given in Table 20.2-1.

Table 20.2-1 Dimensionless Gradients of Velocity, Temperature, and Composition in Laminar Flow Along a Flat Plate[a]

K	$\Lambda = 0.1$	$\Lambda = 0.2$	$\Lambda = 0.4$	$\Lambda = 0.6$	$\Lambda = 0.7$	$\Lambda = 0.8$	$\Lambda = 1.0$	$\Lambda = 1.4$	$\Lambda = 2.0$	$\Lambda = 5.0$
−3.0	0.4491	0.7681	1.3722	1.9648	2.2600	2.5550	3.1451	4.3273	6.1064	15.0567
−2.0	0.3664	0.5956	1.0114	1.4100	1.6070	1.8032	2.1945	2.9764	4.1524	10.0863
−1.0	0.2846	0.4282	0.6658	0.8799	0.9829	1.0842	1.2836	1.6754	2.2568	5.1747
−0.5	0.2427	0.3452	0.4999	0.6291	0.6890	0.7468	0.8579	1.0688	1.3707	2.8194
−0.2	0.2165	0.2948	0.4024	0.4849	0.5213	0.5555	0.6190	0.7333	0.8861	1.5346
0.0	0.1980	0.2604	0.3380	0.3917	0.4139	0.4340	0.4696	0.5281	0.5972	0.8156
0.2	0.1783	0.2246	0.2736	0.3011	0.3108	0.3187	0.3305	0.3439	0.3496	0.3015
0.5	0.1441	0.1657	0.1751	0.1701	0.1656	0.1603	0.1485	0.1240	0.09096	0.01467
0.75	0.1032	0.1023	0.0840	0.0638	0.0549	0.0471	0.0340	0.0172	0.00571	0.0000152
0.87574[b]	**0**	**0**	**0**	**0**	**0**	**0**	**0**	**0**	**0**	**0**

[a] Taken from the following sources: E. Elzy and R. M. Sisson, *Engineering Experiment Station Bulletin No. 40*, Oregon State University, Corvallis, Or. (1967); H. L. Evans, *Int. J. Heat and Mass Transfer*, **3**, 321–339 (1961); W. E. Stewart and R. Prober, *Int. J. Heat and Mass Transfer*, **5**, 1149–1163 (1962) and **6**, 872 (1963). More complete results, and reviews of earlier work, are given in these references.

[b] The value K = 0.87574 is the largest positive mass transfer rate attainable in this geometry with steady laminar flow. See H. W. Emmons and D. C. Leigh, *Interim Technical Report No. 9*, Combustion Aerodynamics Laboratory, Harvard University (1953).

The molecular fluxes of momentum, energy, and mass at the wall are then given by the dimensionless expressions

$$\frac{\tau_0}{\rho v_\infty (v_\infty - 0)} = \Pi'(0, 1, K)\sqrt{\frac{\nu}{2v_\infty x}} \tag{20.2-45}$$

$$\frac{q_0}{\rho \hat{C}_p v_\infty (T_0 - T_\infty)} = \frac{\Pi'(0, \mathrm{Pr}, K)}{\mathrm{Pr}}\sqrt{\frac{\nu}{2v_\infty x}} \tag{20.2-46}$$

$$\frac{j_{A0}}{\rho v_\infty (\omega_{A0} - \omega_{A\infty})} = \frac{\Pi'(0, \mathrm{Sc}, K)}{\mathrm{Sc}}\sqrt{\frac{\nu}{2v_\infty x}} \tag{20.2-47}$$

with the tabulated values of $\Pi'(0, \Lambda, K)$. Thus the fluxes can be computed directly when K is known. These expressions are obtained from the flux expressions of Newton, Fourier, and Fick, and the profiles as given in Eq. 20.2-43. The energy flux q_0 here corresponds to the conduction term $-k\nabla T$ of Eq. 19.3-3; the diffusive flux j_{A0} is obtained by using Eq. 20.2-47 above.

The fluid properties ρ, μ, $\hat{C}_p$, k, and $\mathscr{D}_{AB}$ have been treated as constants in this development. However, Eqs. 20.2-45 to 47 have been found to agree closely with the corresponding variable-property calculations,[8–10] provided that K is generalized as follows,

$$K = \frac{\rho_0 v_0(x)}{\rho v_\infty}\sqrt{2\frac{v_\infty x}{\nu}} \tag{20.2-48}$$

and that ρ, μ, $\hat{C}_p$, k, and $\mathscr{D}_{AB}$ are evaluated at the "reference conditions" $T_f = \frac{1}{2}(T_0 + T_\infty)$ and $\omega_{Af} = \frac{1}{2}(\omega_{A0} + \omega_{A\infty})$.

In many situations, one of the following dimensionless quantities

$$R_v = \frac{(n_{A0} + n_{B0})(v_\infty - 0)}{\tau_0} \tag{20.2-49}$$

$$R_T = \frac{(n_{A0} + n_{B0})\hat{C}_p(T_0 - T_\infty)}{q_0} \tag{20.2-50}$$

$$R_\omega = \frac{(n_{A0} + n_{B0})(\omega_{A0} - \omega_{A\infty})}{j_{A0}} = \frac{(\omega_{A0} - \omega_{A\infty})(n_{A0} + n_{B0})}{n_{A0} - \omega_{A0}(n_{A0} + n_{B0})} \tag{20.2-51}$$

is known or readily computed. These flux ratios, R, are independent of x under the present boundary conditions and are related to Λ and K as follows,

$$R = \frac{K\Lambda}{\Pi'(0, \Lambda, K)} \tag{20.2-52}$$

according to Eqs. 20.2-45 to 51. From Eq. 20.2-52 we see that the dimensionless interfacial mass flux K can be tabulated as a function of R and Λ, by use of the results in Table 20.2-1. Then K can be found by interpolation if the numerical values of R and Λ are given for one of the three profiles (i.e., if we can specify R_v, or R_T and Pr, or R_ω and Sc.) Convenient plots of these relations are given in Figures 22.8-5 to 7.

As a simple illustration, suppose that the flat plate is porous and is saturated with liquid A, which vaporizes into a gaseous stream of A and B. Suppose also that gas B is noncondensable and insoluble in liquid A, and that ω_{A0} and $\omega_{A\infty}$ are given. Then R_ω can be calculated from

---

[8] For calculations of momentum and energy transfer in gas flows with $K \neq 0$, see E. R. G. Eckert, *Trans. A.S.M.E.*, **78**, 1273–1283 (1956).

[9] For calculations of momentum and mass transfer in binary and multicomponent gas mixtures, see W. E. Stewart and R. Prober, *Ind. Eng. Chem. Fundamentals*, **3**, 224–235 (1964); improved reference conditions are provided by T. C. Young and W. E. Stewart, *ibid.*, **25**, 276–482 (1986), as noted in §22.9.

[10] For other methods of applying Eq. 20.2-47 to variable-property fluids, see O. T. Hanna, *AIChE Journal*, **8**, 278–279 (1962); **11**, 706–712 (1965).

Table 20.2-2 Coefficients for the Approximate Flat-Plate Formulas,[a] Eqs. 20.2-54 and 55

Λ	0	0.1	0.2	0.5	0.7	1.0	2	5	10	100	∞
$a(\Lambda)$	$\left(\frac{2}{\pi}\right)^{1/2}\Lambda^{1/6}$	0.4266	0.4452	0.4620	0.4662	0.4696	0.4740	0.4769	0.4780	0.4789	0.4790
$b(\Lambda)$	1.308	0.948	0.874	0.783	0.752	0.723	0.676	0.632	0.610	0.577	0.566

[a] Taken from H. J. Merk, *Appl. Sci. Res.*, **A8**, 237–277 (1959), and R. Prober and W. E. Stewart, *Int. J. Heat and Mass Transfer*, **6**, 221–229, 872 (1963).

Eq. 20.2-51 with $n_{B0} = 0$, and K can be found by interpolating the function $K(R, \Lambda)$ to $R = R_\omega$ and $\Lambda = \mu/\rho\mathcal{D}_{AB}$.

For moderate values of K, the calculations can be simplified by representing $\Pi'(0, \Lambda, K)$ as a truncated Taylor series in the parameter K:

$$\Pi'(0, \Lambda, K) = \Pi'(0, \Lambda, 0) + K\frac{\partial}{\partial K}\Pi'(0, \Lambda, K)\Big|_{K=0} \tag{20.2-53}$$

This expansion can be written more compactly as

$$\Pi'(0, \Lambda, K) = a\Lambda^{1/3} - bK\Lambda \tag{20.2-54}$$

in which a and b are slowly varying functions of Λ, given in Table 20.2-2. Insertion of Eq. 20.2-54 into Eq. 20.2-52 gives the convenient expression for the dimensionless interfacial mass flux K

$$K = a\Lambda^{-2/3}\frac{R}{1 + bR} \tag{20.2-55}$$

for calculations with unknown parameter K. This result is easy to use and fairly accurate. The predicted function $K(R, \Lambda)$ is within 1.6% of that found from Table 20.2-1 for $|R| < 0.25$ and $\Lambda > 0.1$.

This example illustrates the related effects of the interfacial velocity v_0 on the velocity, temperature, and composition profiles. The effect of v_0 on a given profile, Π, is small if $R << 1$ for that profile (as in most separation processes) and large if $R \geq 1$ (as in many combustion and transpiration cooling processes). Some applications are given in Chapter 22.

EXAMPLE 20.2-3

Approximate Analogies for the Flat Plate at Low Mass-Transfer Rates

Pohlhausen[11] solved the energy equation for the system of Example 12.1-2 and curve-fitted his results for the heat transfer rate Q (see third line of Table 12.4-1). Compare his result with Eq. 20.2-46, and derive the corresponding results for the momentum and mass fluxes.

SOLUTION

By inserting the coefficient 0.664 in place of $\sqrt{148/315}$ in Eq. 12.4-17, and setting $2Wq_0(x) = (dQ/dL)|_{L=x}$, we get

$$\frac{q_0}{\hat{\rho C}_p v_\infty(T_0 - T_\infty)} \cong 0.332\,\mathrm{Pr}^{2/3}\sqrt{\frac{\nu}{v_\infty x}} \tag{20.2-56}$$

This result is subject to the boundary condition $v_0(x) = 0$, which corresponds to $K = 0$ in the system of Example 20.2-2.

[11] E. Pohlhausen, *Zeits. f. angew. Math. Mech.*, **1**, 115–121 (1921).

Equation 20.2-56 is obtainable from Eq. 20.2-46 when $K = 0$ by setting $\Pi'(0, \mathrm{Pr}, 0) \cong 0.4696\mathrm{Pr}^{1/3}$; this agrees with Table 20.2-2 at $\Lambda = 1$. Making comparable substitutions in Eqs. 20.2-45 and 46, we get the convenient analogy

$$\frac{\tau_0}{\rho v_\infty(v_\infty - 0)} \cong \frac{q_0}{\rho \hat{C}_p v_\infty(T_0 - T_\infty)} \mathrm{Pr}^{2/3} \cong \frac{j_{A0}}{\rho v_\infty(\omega_{A0} - \omega_{A\infty})} \mathrm{Sc}^{2/3}$$

$$\cong 0.332\sqrt{\frac{\nu}{v_\infty x}} \tag{20.2-57}$$

which has been recommended by Chilton and Colburn[12] for this flow situation (cf. §§14.3 and 22.3). The expression for τ_0 agrees with the exact solution at $K = 0$, and the results for q_0 and j_{A0} are accurate within ±2% at $K = 0$ for $\Lambda > 0.5$.

§20.3 STEADY-STATE BOUNDARY LAYER THEORY FOR FLOW AROUND OBJECTS

In §§18.5 and 6 we discussed two related mass transfer problems of boundary layer type. Now we want to enlarge[1-7] on the ideas presented there and consider the flow around objects of other shapes such as the one shown in Fig. 12.4-2. Although we present the material in this section in terms of mass transfer, it is understood that the results can be taken over directly for the analogous heat transfer problem by appropriate changes of notation. The concentration boundary layer is presumed to be very thin, which means that the results are restricted either to small diffusivity or to short exposure times. The results are applicable only to the region between the forward stagnation locus (from which x is measured) and the region of separation or turbulence, if any, as indicated in Figure 12.4-2.

The concentration of the diffusing species is called c_A, and its concentration at the surface of the object is c_{A0}. Outside the concentration boundary layer, the concentration of A is zero.

Proceeding as in Example 12.4-3, we adopt an orthogonal coordinate system for the concentration boundary layer, in which x is measured along the surface everywhere in the direction of the streamlines. The y-coordinate is perpendicular to the surface, and the z-coordinate is measured along the surface perpendicular to the streamlines. These are "general orthogonal coordinates," as described in Eqs. A.7-10 to 18, but with $h_y = 1$, and $h_x = h_x(x, z)$ and $h_z = h_z(x, z)$. Since the flow near the interface does not have a velocity component in the z direction, the equation of continuity there is

$$\frac{\partial}{\partial x}(h_z v_x) + h_x h_z \frac{\partial}{\partial y} v_y = 0 \tag{20.3-1}$$

[12] T. H. Chilton and A. P. Colburn, *Ind. Eng. Chem.*, **26**, 1183–1187 (1934).

[1] A. Acrivos, *Chem. Eng. Sci.*, **17**, 457–465 (1962).

[2] W. E. Stewart, *AIChE Journal*, **9**, 528–535 (1963).

[3] D. W. Howard and E. N. Lightfoot, *AIChE Journal*, **14**, 458–467 (1968).

[4] W. E. Stewart, J. B. Angelo, and E. N. Lightfoot, *AIChE Journal*, **16**, 771–786 (1970).

[5] E. N. Lightfoot, in *Lectures in Transport Phenomena*, American Institute of Chemical Engineers, New York (1969).

[6] E. Ruckenstein, *Chem. Eng. Sci.*, **23**, 363–371 (1968).

[7] W. E. Stewart, in *Physicochemical Hydrodynamics*, Vol. 1 (D. B. Spalding, ed.), Advance Publications, Ltd., London (1977), pp. 22–63.

according to Eq. A.7-16. The diffusion equation for the concentration boundary layer is then

$$v_x \frac{1}{h_x}\frac{\partial c_A}{\partial x} + v_y \frac{\partial c_A}{\partial y} = \mathscr{D}_{AB}\frac{\partial^2 c_A}{\partial y^2} \tag{20.3-2}$$

where Eqs. A.7-15 and 17 have been used. In writing these equations it has been assumed that: (i) the x- and z-components of the diffusion flux are negligible, (ii) the boundary layer thickness is small compared to the local interfacial radii of curvature, and (iii) the density and diffusivity are constant. We now want to get formal expressions for the concentration profiles and mass fluxes for two cases that are generalizations of the problems solved in §18.5 and §18.6. When we get the expressions for the local molar flux at the interface, we will find that the dependences on the diffusivity ($\frac{1}{2}$-power in §18.5 and the $\frac{2}{3}$-power in §18.6) correspond to cases (a) and (b) below. This turns out to be of great importance in the establishment of dimensionless correlations for mass transfer coefficients, as we shall see in Chapter 22.

Zero Velocity Gradient at the Mass Transfer Surface

This situation arises in a surfactant-free liquid flowing around a gas bubble. Here v_x does not depend on y, and v_y can be obtained from the equation of continuity given above. Therefore, for small mass-transfer rates we can write general expressions for the velocity components as

$$v_x = v_s(x, z) \tag{20.3-3}$$

$$v_y = -\frac{y}{h_x h_z}\frac{\partial}{\partial x}(h_z v_s) \equiv -\gamma y \tag{20.3-4}$$

where γ depends on x and z. When this is used in Eq. 20.3-2, we get for the diffusion in the liquid phase

$$v_s \frac{1}{h_x}\frac{\partial c_A}{\partial x} - \gamma y \frac{\partial c_A}{\partial y} = \mathscr{D}_{AB}\frac{\partial^2 c_A}{\partial y^2} \tag{20.3-5}$$

which is to be solved with the boundary conditions

B.C. 1: at $x = 0$, $c_A = 0$ (20.3-6)

B.C. 2: at $y = 0$, $c_A = c_{A0}$ (20.3-7)

B.C. 3: as $y \to \infty$, $c_A \to 0$ (20.3-8)

The nature of the boundary conditions suggests that a combination of variables treatment might be appropriate. However, it is far from obvious how to construct an appropriate dimensionless combination. Hence we try the following: let $c_A/c_{A0} = f(\eta)$, where $\eta = y/\delta_A(x, z)$, and $\delta_A(x, z)$ is the boundary layer thickness for species A, to be determined later.

When the indicated combination of variables is introduced into Eq. 20.3-5, the equation becomes

$$\frac{d^2 f}{d\eta^2} + \frac{1}{\mathscr{D}_{AB}}\left(\frac{v_s}{h_x}\delta_A\frac{\partial \delta_A}{\partial x} + \gamma\delta_A^2\right)\eta\frac{df}{d\eta} = 0 \tag{20.3-9}$$

with the boundary conditions: $f(0) = 1$ and $f(\infty) = 0$. If, now, the coefficient of the $\eta(df/d\eta)$ term were a constant, then Eq. 20.3-9 would have the same form as Eq. 4.1-9, which we know how to solve. For convenience we specify the constant as

$$\frac{1}{\mathscr{D}_{AB}}\left(\frac{v_s}{h_x}\delta_A\frac{\partial \delta_A}{\partial x} + \gamma\delta_A^2\right) = 2 \tag{20.3-10}$$

Next we insert the expression for γ from Eq. 20.3-4 and rearrange the equation thus:

$$\frac{\partial}{\partial x}\delta_A^2 + \left(\frac{\partial}{\partial x}\ln(h_z v_s)^2\right)\delta_A^2 = \frac{4\mathscr{D}_{AB}h_x}{v_s} \tag{20.3-11}$$

This is a linear, first-order equation for δ_A^2, which has to be solved with the boundary condition $\delta_A = 0$ at $x = 0$. Integration of Eq. 20.3-11 gives

$$\delta_A(x, z) = 2\sqrt{\frac{\mathscr{D}_{AB}\int_0^x h_x h_z^2 v_s x}{h_z^2 v_s^2}} \tag{20.3-12}$$

as the thickness function for the diffusional boundary layer. Since Eq. 20-3-9 and the boundary conditions then contain η as the only independent variable, the postulated combination of variables is valid, and the concentration profiles are given by the solution of Eq. 20.3-9:

$$f(\eta) = 1 - \frac{2}{\sqrt{\pi}}\int_0^\eta \exp(-\bar{\eta}^2)\, d\bar{\eta} = 1 - \operatorname{erf}\eta \tag{20.3-13}$$

Equations 20.3-12 and 13 are the solution to the problem at hand.

Next, we combine this solution with Fick's first law to evaluate the molar flux of species A at the interface:

$$N_{Ay}|_{y=0} = -\mathscr{D}_{AB}\frac{\partial c_A}{\partial y}\bigg|_{y=0} = -\mathscr{D}_{AB}c_{A0}\left(\frac{df}{d\eta}\frac{\partial \eta}{\partial y}\right)\bigg|_{y=0}$$

$$= +\mathscr{D}_{AB}c_{A0}\frac{2}{\sqrt{\pi}}\left(\exp(-\eta^2)\frac{1}{\delta_A}\right)\bigg|_{y=0} = c_{A0}\sqrt{\frac{\mathscr{D}_{AB}}{\pi}\frac{h_z^2 v_s^2}{\int_0^x h_x h_z^2 v_s d\bar{x}}} \tag{20.3-14}$$

This result shows the same dependence of the mass flux on the $\frac{1}{2}$-power of the diffusivity that arose in Eq. 18.5-17, for the much simpler gas absorption problem solved there. In fact, if we set the scale factors h_x and h_z equal to unity and replace v_s by v_{max}, we recover Eq. 18.5-17 exactly.

Linear Velocity Profile Near the Mass-Transfer Surface

This velocity function is appropriate for mass transfer at a solid surface (see Example 12.4-3) when the concentration boundary layer is very thin. Here v_x depends linearly on y within the concentration boundary layer, and v_y can be obtained from the equation of continuity. Consequently, when the net mass flux through the interface is small, the velocity components in the concentration boundary layer are

$$v_x = \beta(x, z)y \tag{20.3-15}$$

$$v_y = -\frac{y^2}{2h_x h_z}\frac{\partial}{\partial x}(h_z\beta) \equiv -\gamma y^2 \tag{20.3-16}$$

in which γ depends on x and z. Substituting these expressions into Eq. 20.3-2 gives the diffusion equation for the liquid phase

$$\frac{\beta y}{h_x}\frac{\partial c_A}{\partial x} - \gamma y^2\frac{\partial c_A}{\partial y} = \mathscr{D}_{AB}\frac{\partial^2 c_A}{\partial y^2} \tag{20.3-17}$$

which is to be solved with the boundary conditions

B.C. 1: at $x = 0$, $c_A = 0$ (20.3-18)

B.C. 2: at $y = 0$, $c_A = c_{A0}$ (20.3-19)

B.C. 3: as $y \to \infty$, $c_A \to 0$ (20.3-20)

Once again, we use the method of combination of variables, by setting $c_A/c_{A0} = f(\eta)$, where $\eta = y/\delta_A(x, z)$.

When the change of variables is made, the diffusion equation becomes

$$\frac{d^2 f}{d\eta^2} + \frac{1}{\mathscr{D}_{AB}}\left(\frac{\beta}{h_x}\delta_A^2\frac{\partial \delta_A}{\partial x} + \gamma\delta_A^3\right)\eta^2\frac{df}{d\eta} = 0 \tag{20.3-21}$$

with the boundary conditions: $f(0) = 1$ and $f(\infty) = 0$. A solution of the form $f(\eta)$ is possible only if the factor in parentheses is a constant. Setting the constant equal to 3 reduces Eq. 20.3-21 to Eq. 18.6-6, for which the solution is known. Therefore we now get the boundary layer thickness by requiring that

$$\frac{1}{\mathscr{D}_{AB}}\left(\frac{\beta}{h_x}\delta_A^2\frac{\partial\delta_A}{\partial x}+\gamma\delta_A^3\right)=3 \tag{20.3-22}$$

or

$$\frac{\partial}{\partial x}\delta_A^3+\left(\frac{\partial}{\partial x}\ln(h_z\beta)^{3/2}\right)\delta_A^3=\frac{9\mathscr{D}_{AB}h_x}{\beta} \tag{20.3-23}$$

The solution of this first-order, linear equation for δ_A^3 is

$$\delta_A=\frac{1}{\sqrt{h_z\beta}}\sqrt[3]{9\mathscr{D}_{AB}\int_0^x\sqrt{h_z\beta}\,h_xh_z\,dx} \tag{20.3-24}$$

Hence the solution to the problem in this subsection is

$$\frac{c_A}{c_{A0}}=f(\eta)=\frac{\int_\eta^\infty\exp(-\bar{\eta}^3)\,d\bar{\eta}}{\Gamma(\frac{4}{3})} \tag{20.3-25}$$

which reduces to Eq. 18.6-10 for the system considered there.

Finally, we get the expression for the molar flux at the interface, which is

$$\begin{aligned}N_{Ay}|_{y=0}&=-\mathscr{D}_{AB}\frac{\partial c_A}{\partial y}\bigg|_{y=0}=-\mathscr{D}_{AB}c_{A0}\left(\frac{df}{d\eta}\frac{\partial\eta}{\partial y}\right)\bigg|_{y=0}\\&=\frac{\mathscr{D}_{AB}c_{A0}}{\Gamma(\frac{4}{3})}\frac{\sqrt{h_z\beta}}{\sqrt[3]{9\mathscr{D}_{AB}\int_0^x\sqrt{h_z\beta}\,h_xh_z\,dx}}\end{aligned} \tag{20.3-26}$$

For a plane surface, with $h_x = h_z = 1$ and β = constant, Eq. 20.3-26 reduces to Eq. 18.6-11.

EXAMPLE 20.3-1

Mass Transfer for Creeping Flow Around a Gas Bubble

A liquid B is flowing very slowly around a spherical bubble of gas A of radius R. Find the rate of mass transfer of A into the surrounding fluid, if the solubility of gas A in liquid B is c_{A0}. **(a)** Show how to use Eq. 20.3-14 to get the mass flux at the gas–liquid interface for this system. **(b)** Then get the average mass flux over the entire spherical surface.

SOLUTION

(a) Select as the origin of coordinates the upstream stagnation point, and define the coordinates x and z as follows: $x = R\theta$ and $z = R(\sin\theta)\phi$, in which θ and ϕ are the usual spherical coordinates. The y direction is then the same as the r direction of spherical coordinates. The interfacial velocity is obtained from Eq. 4B.3-3 as $v_s = \frac{1}{2}v_\infty\sin\theta$, where v_∞ is the approach velocity.

When these quantities are inserted into Eq. 20.3-14 we get

$$\begin{aligned}N_{Ay}|_{y=0}&=c_{A0}\sqrt{\frac{\mathscr{D}_{AB}}{\pi}\frac{(R\sin\theta)^2(\frac{1}{2}v_\infty\sin\theta)^2}{\int_0^{R\theta}(R)(R\sin\theta)^2(\frac{1}{2}v_\infty\sin\theta)d(R\theta)}}\\&=c_{A0}\sin^2\theta\sqrt{\frac{\mathscr{D}_{AB}v_\infty}{2\pi R}\frac{1}{\int_0^\theta\sin^3\theta\,d\theta}}\\&=c_{A0}\sin^2\theta\sqrt{\frac{3\mathscr{D}_{AB}v_\infty}{2\pi R}}\frac{1}{\sqrt{\cos^3\theta-3\cos\theta+2}}\end{aligned} \tag{20.3-27}$$

(b) To get the surface-averaged value of the mass flux, we integrate the above expression over all θ and ϕ and divide by the sphere surface:

$$\begin{aligned} N_{A0,\text{avg}} &= \frac{1}{4\pi R^2}\int_0^{2\pi}\int_0^{\pi} N_{Ay}\Big|_{y=0} R\,\sin\theta\,d\theta\,d\phi \\ &= \frac{2\pi R^2 c_{A0}}{4\pi R^2}\sqrt{\frac{3\mathscr{D}_{AB}v_\infty}{2\pi R}}\int_0^{\pi}\frac{\sin^3\theta\,d\theta}{\sqrt{\cos^3\theta - 3\cos\theta + 2}} \\ &= \frac{c_{A0}}{2}\sqrt{\frac{3\mathscr{D}_{AB}v_\infty}{2\pi R}}\int_{-1}^{+1}\frac{(1-u^2)du}{\sqrt{u^3 - 3u + 2}} \\ &= \frac{c_{A0}}{2}\sqrt{\frac{3\mathscr{D}_{AB}v_\infty}{2\pi R}}\int_{-1}^{+1}\frac{(1+u)du}{\sqrt{2+u}} \\ &= \frac{c_{A0}}{2}\sqrt{\frac{3\mathscr{D}_{AB}v_\infty}{2\pi R}}\left(\frac{4}{3}\right) = \sqrt{\frac{4\mathscr{D}_{AB}v_\infty}{3\pi D}}\,c_{A0} \end{aligned} \tag{20.3-28}$$

In going from the second to the third line, we made the change of variable $\cos\theta = u$, and to get the fourth line, we factored out $(1 - u)$ from the numerator and denominator. Equation 20.3-28 was cited in Eq. 18.5-20 in connection with absorption from gas bubbles.[8] This equation is referred to again in Chapter 22 in connection with the subject of mass transfer coefficients.

§20.4 BOUNDARY LAYER MASS TRANSPORT WITH COMPLEX INTERFACIAL MOTION[1-3]

Time-dependent interfacial motions and turbulence are common in fluid–fluid transfer operations. Boundary layer theory gives useful insight and asymptotic relations for these systems, utilizing the thinness of the concentration boundary layers for small $\mathscr{D}_{AB}$ (as in liquids) or for flows with frequent boundary layer separation (as at rippling or oscillating interfaces). Mass transfer with simple interfacial motions has been discussed in §18.5 for a laminar falling film and a circulating bubble, and in Example 20.1-4 for a uniformly expanding interface. Here we consider mass transfer with more general interfacial motions.

Consider the time-dependent transport of species A between two fluid phases, with initially uniform but different compositions. We start with the binary continuity equation for constant ρ and $\mathscr{D}_{AB}$ (Eq. 19.1-16, divided by ρ):

$$\frac{D\omega_A}{Dt} = \mathscr{D}_{AB}\nabla^2\omega_A + \frac{1}{\rho}r_A \tag{20.4-1}$$

We now want to reduce this to boundary layer form for small $\mathscr{D}_{AB}$, and then present solutions for various forced-convection problems with controlling resistance in one phase.

We use the following boundary layer approximations:

(i) that the diffusive mass flux is collinear with the unit vector **n** normal to the nearest interfacial element. (This approximation is used throughout the boundary layer sections of this book. Higher-order approximations,[4] not treated here, are appropriate for describing boundary layer diffusion near edges, wakes, and separation loci.)

---

[8] V. G. Levich, *Physicochemical Hydrodynamics*, Prentice-Hall, Englewood Cliffs, N.J. (1962), p. 408, Eq. 72.9.

[1] J. B. Angelo, E. N. Lightfoot, and D. W. Howard, *AIChE Journal*, **12**, 751–760 (1966).

[2] W. E. Stewart, J. B. Angelo, and E. N. Lightfoot, *AIChE Journal*, **16**, 771–786 (1970).

[3] W. E. Stewart, *AIChE Journal*, **33**, 2008–2016 (1987); **34**, 1030 (1988).

[4] J. Newman, *Electroanal. Chem. and Interfacial Electrochem.*, **6**, 187–352 (1973).

(ii) that the tangential fluid velocity relative to the interface is negligible within the concentration boundary layer. (This approximation is satisfactory for fluid–fluid systems free of surfactants, when the interfacial drag is not too large.)

(iii) that the concentration boundary layer along each interface is thin relative to the local radii of interfacial curvature.

(iv) that the concentration boundary layers on nonadjacent interfacial elements do not overlap.

Each of these approximations is asymptotically valid for small $\mathscr{D}_{AB}$ in nonrecirculating flows with nonrigid interfaces and nonzero $D\omega_A/Dt$—that is, with time-dependent concentration as viewed by an observer moving with the fluid. The systems considered in part (a) of §20.3 are thus included, because they are time-dependent for such an observer (though steady for a stationary one).

Interfacially embedded coordinates are used in this discussion, with a piecewise smooth interfacial grid as in Fig. 20.4-1. Each interfacial element in the system is permanently labeled with surface coordinates (u, w), and its position vector is $\mathbf{r}_s(u, w, t)$. Each point in a boundary layer is identified by its distance y from the nearest interfacial point, together with the surface coordinates (u, w) of that point. The instantaneous position vector of each point (u, w, y) at time t is then

$$\mathbf{r}(u, w, y, t) = \mathbf{r}_s(u, w, t) + y\mathbf{n}(u, w, t) \tag{20.4-2}$$

relative to a stationary origin, as illustrated in Fig. 20.4-2. The function $\mathbf{r}_s(u, w, t)$ gives the trajectory of each interfacial point $(u, w, 0)$, and the associated function $\mathbf{n}(u, w, t) = (\partial/\partial y)\mathbf{r}$ gives the instantaneous normal vector from each surface element toward its positive side. These functions are computable from fluid mechanics for simple flows, and provide a framework for analyzing experiments in complex flows.

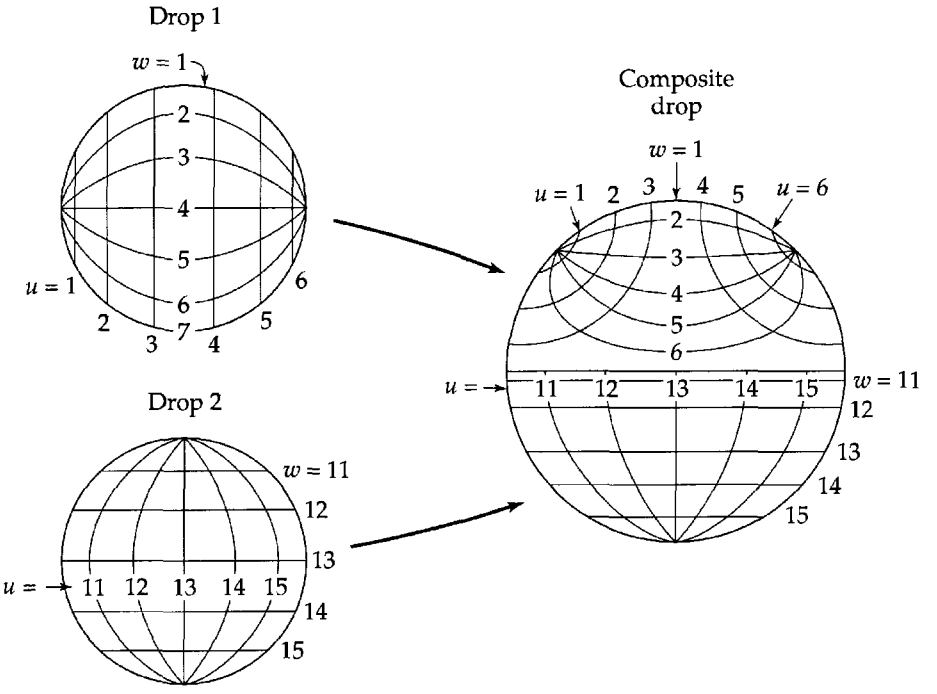

Fig. 20.4-1. Schematic illustration of embedded coordinates in a simple coalescence process. W.E. Stewart, J.B. Angelo, and E.N. Lightfoot, AIChE Journal, **14**, 458–467 (1968).

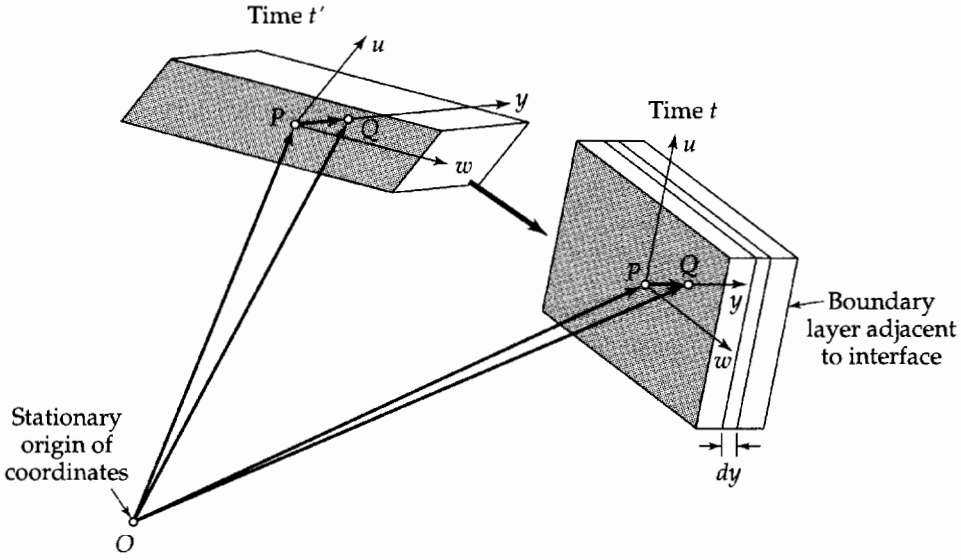

Fig. 20.4-2. Element dS (shaded) of a deforming interfacial area shown at two different times, t' and t, with the adjacent boundary layer. The vectors are (at time t):

$\vec{OP} = \mathbf{r}_s(u, w, t)$ = position vector of a point on the interface

$\vec{PQ} = y\mathbf{n}(u, w, t)$ = vector of length y normal to the interface locating a point in the boundary layer

$\vec{OQ} = \mathbf{r}(u, w, y, t)$ = position vector for a point in the boundary layer

The element of interfacial area consists of the same material particles as it moves through space. The magnitude of the area changes with time and is given by $dS = \left| \frac{\partial \mathbf{r}_s}{\partial u} du \times \frac{\partial \mathbf{r}_s}{\partial w} dw \right|$ Similarly, the magnitude of the volume of that part of the boundary layer between y and $y + dy$ is $dV = \left| \left[\frac{\partial \mathbf{r}_s}{\partial u} du \times \frac{\partial \mathbf{r}_s}{\partial w} dw \right] \cdot \mathbf{n}\, dy \right|$.

The instantaneous volume of a spatial element $du\, dw\, dy$ in the boundary layer (see Fig. 20.4-2) is

$$dV = \sqrt{g(u, w, y, t)}\, du\, dw\, dy \tag{20.4-3}$$

in which $\sqrt{g(u, w, y, t)}$ is the following product of the local interfacial base vectors, $(\partial/\partial u)\mathbf{r}_s$ and $(\partial/\partial v)\mathbf{r}_s$, and the normal unit vector $(\partial/\partial y)\mathbf{r}_s = \mathbf{n}$,

$$\sqrt{g} = \left| \left[\frac{\partial \mathbf{r}_s}{\partial u} \times \frac{\partial \mathbf{r}_s}{\partial w} \right] \cdot \mathbf{n} \right| = \left| \left[\frac{\partial \mathbf{r}_s}{\partial u} \times \frac{\partial \mathbf{r}_s}{\partial w} \right] \right| \tag{20.4-4}$$

and is considered nonnegative in this discussion. The second equality follows because $\mathbf{n}$ is collinear with the vector product of the local interfacial base vectors, which lie in the plane of the interface. Correspondingly, the instantaneous area of the interfacial element $du\, dw$ in Fig. 20.4-2 is

$$dS = s(u, w, t)du\, dw \tag{20.4-5}$$

in which $s(u, w, t)$ is the following product of the interfacial basis vectors:

$$s(u, w, t) = \sqrt{g(u, w, 0, t)} = \left| \left[\frac{\partial \mathbf{r}_s}{\partial u} \times \frac{\partial \mathbf{r}_s}{\partial w} \right] \right| \tag{20.4-6}$$

In these interfacially embedded coordinates, the mass average velocity **V** relative to stationary coordinate axes takes the form

$$\mathbf{V}(u, w, y, t) = \mathbf{v}(u, w, y, t) + \frac{\partial}{\partial t}\mathbf{r}(u, w, y, t) \tag{20.4-7}$$

In this section, **v** is the mass average fluid velocity relative to an observer at (u, w, y), and $(\partial/\partial t)\mathbf{r}(u, w, y, t)$ is the velocity of that observer relative to the stationary origin. Taking the divergence of this equation gives the corollary[2] (see Problem 20D.5)

$$(\nabla \cdot \mathbf{V}(\mathbf{r}, t)) = (\nabla \cdot \mathbf{v}(u, w, y, t)) + \frac{\partial \ln \sqrt{g(u, w, y, t)}}{\partial t} \tag{20.4-8}$$

This equation states that the divergence of **V** differs from that of **v** by the local rate of expansion or contraction of the embedded coordinate frame.

The last term in Eq. 20.4-8 arises when interfacial deformation occurs. Its omission in such problems gives inaccurate predictions, which Higbie[5] and Danckwerts[6,7] then adjusted by introducing hypothetical surface residence times[5,6] or surface rejuvenation.[7] Such hypotheses are not needed in the present analysis.

Application of Eq. 20.4-8 at $y = 0$ and use of the constant-density condition

$$(\nabla \cdot \mathbf{V}) = 0 \tag{20.4-9}$$

along with the no-slip condition on the tangential part of **v**, gives the derivative

$$\left.\frac{\partial v_y}{\partial y}\right|_{y=0} = -\frac{\partial \ln s(u, w, t)}{\partial t} \tag{20.4-10}$$

Hence, the truncated Taylor expansion

$$v_y = v_{y0} - y\frac{\partial \ln s(u, w, t)}{\partial t} + O(y^2) \tag{20.4-11}$$

describes the normal component of **v** in an incompressible fluid near a deforming interface.

The corresponding expansion for the tangential part of **v** gives

$$\mathbf{v}_{\parallel} = y\mathbf{B}_{\parallel}(u, w, t) + O(y^2) \tag{20.4-12}$$

in which $\mathbf{B}_{\parallel}(u, w, t)$ is the interfacial y-derivative of $\mathbf{v}_{\parallel}$. With these results (neglecting the $O(y^2)$ terms) and approximation (i), we can write Eq. 20.4-1 for $\omega_A(u, w, y, t)$ as

$$\frac{\partial \omega_A}{\partial t} + (y\mathbf{B}_{\parallel} \cdot \nabla\omega_A) + \left(v_{y0} - y\frac{\partial \ln s}{\partial t}\right)\frac{\partial \omega_A}{\partial y} = \mathcal{D}_{AB}(\nabla \cdot \mathbf{n}\nabla\omega_A) + \frac{1}{\rho}r_A$$
$$= \mathcal{D}_{AB}\left[\frac{\partial^2 \omega_A}{\partial y^2} + (\nabla_0 \cdot \mathbf{n})\frac{\partial \omega_A}{\partial y} + \cdots\right] + \frac{1}{\rho}r_A \tag{20.4-13}$$

Here $(\nabla_0 \cdot \mathbf{n})$ is the surface divergence of **n** at the nearest interfacial point and is the sum of the principal curvatures of the surface there. The $+\cdots$ stands for terms of higher order, which are here neglected.

To select the dominant terms in Eq. 20.4-13, we introduce a dimensionless coordinate

$$Y = y/\kappa(\mathcal{D}_{AB}) \tag{20.4-14}$$

---

[5] R. Higbie, *Trans. AIChE*, **31**, 365–389 (1935).

[6] P. V. Danckwerts, *Ind. Eng. Chem.*, **43**, 1460–1467 (1951).

[7] P. V. Danckwerts, *AIChE Journal*, **1**, 456–463 (1955).

in which κ is an average thickness of the concentration boundary layer. When Eq. 20.4-14 is written in terms of this new variable, we get

$$\frac{\partial \omega_A}{\partial t} + \kappa(Y\mathbf{B}_{\|} \cdot \nabla\omega_A) + \left(\frac{v_{y0}}{\kappa} - Y\frac{\partial \ln s}{\partial t}\right)\frac{\partial \omega_A}{\partial Y} = \frac{\mathscr{D}_{AB}}{\kappa^2}\left[\frac{\partial^2 \omega_A}{\partial Y^2} + \kappa(\nabla_0 \cdot \mathbf{n})\frac{\partial \omega_A}{\partial Y} + \cdots\right] + \frac{1}{\rho}r_A \tag{20.4-15}$$

for ω_A in terms of u, w, Y, and t. Since, on physical grounds, κ will decrease with decreasing $\mathscr{D}_{AB}$, the dominant terms for small $\mathscr{D}_{AB}$ are those of lowest order in κ—namely, all but the $\mathbf{B}_{\|}$ and $(\nabla_0 \cdot \mathbf{n})$ contributions. The subdominance of the latter terms confirms the asymptotic validity of approximations (ii) and (iii) in non-recirculating flows.

Now, the coefficients of all the dominant terms must be proportional over the range of $\mathscr{D}_{AB}$, in order that these terms remain of comparable size in the small-$\mathscr{D}_{AB}$ limit. Such a "dominant balance principle" was applied previously in §13.6. Here it gives the orders of magnitude

$$\mathscr{D}_{AB}/\kappa^2 = O(1) \qquad \text{and} \qquad v_{y0}/\kappa = O(1) \tag{20.4-16, 17}$$

for the terms of the lowest order with respect to κ. Equation 20.4-16 is consistent with the previous examples of $\frac{1}{2}$-power dependence of the diffusional boundary layer thickness on $\mathscr{D}_{AB}$ in free-surface flows. It also confirms the asymptotic correctness of assumption (iv) for small values of $\mathscr{D}_{AB}$. Equation 20.4-17 is consistent with the proportionality of v_z^* to $\sqrt{\mathscr{D}_{AB}}$ shown under Eq. 20.1-10 for the Arnold problem. Thus, the boundary layer equation for ω_A in either phase near a deforming interface is

$$\frac{\partial \omega_A}{\partial t} + \left(v_{y0} - y\frac{\partial \ln s}{\partial t}\right)\frac{\partial \omega_A}{\partial y} = \mathscr{D}_{AB}\frac{\partial^2 \omega_A}{\partial y^2} + \frac{1}{\rho}r_A \tag{20.4-18}$$

to lowest order in κ. At the next order of approximation, terms proportional to κ would appear, and these involve the tangential velocity $y\mathbf{B}_{\|}$ and the interfacial curvature $(\nabla_0 \cdot \mathbf{n})$. The latter term appears in Problems 20C.1 and 20C.2.

Multiplication of Eq. 20.4-18 by ρ/M_A (a constant for the assumptions made here), and use of z as the coordinate normal to the interface as in Example 20.1-1, give the corresponding equation for the molar concentration $c_A(u, w, z, t)$

$$\frac{\partial c_A}{\partial t} + \left(v_{z0} - z\frac{\partial \ln s}{\partial t}\right)\frac{\partial c_A}{\partial z} = \mathscr{D}_{AB}\frac{\partial^2 c_A}{\partial z^2} + R_A \tag{20.4-19}$$

which allows convenient extension of several earlier examples. Another useful corollary is the binary boundary layer equation in terms of x_A and $\mathbf{v}^*$

$$\frac{\partial x_A}{\partial t} + \left(v_{z0}^* - z\frac{\partial \ln s}{\partial t}\right)\frac{\partial x_A}{\partial z} = \mathscr{D}_{AB}\frac{\partial^2 x_A}{\partial z^2} + \frac{1}{c}[R_A - x_A(R_A + R_B)] \tag{20.4-20}$$

in which c and $\mathscr{D}_{AB}$ have been treated as constants, as in Example 20.1-1.

EXAMPLE 20.4-1

Mass Transfer with Nonuniform Interfacial Deformation

Equation 20.4-19 readily gives a generalized form of Eq. 20.1-65, by omitting the reaction source term R_A and neglecting the normal velocity term v_{z0} (thus assuming the interfacial net mass flux to be small). The equation thus obtained has the form of Eq. 20.1-65, except that the total surface growth rate $d \ln S/dt$ is replaced by the local growth rate, given by $\partial \ln s(u, w, t)/\partial t$. The resulting partial differential equation has two additional space variables (u and w), but is solvable in the same manner, since no derivatives with respect to the added variables appear.

SOLUTION

Rewriting Eq. 20.1-66 with a boundary layer thickness function $\delta(u, w, t)$ leads by analogous steps to the relation

$$\delta(u, w, t) = \sqrt{4\mathscr{D}_{AB} \int_0^t [s(u, w, \bar{t})/s(u, w, t)]^2 \, d\bar{t}} \tag{20.4-21}$$

and the corresponding generalizations of Eqs. 20.1-71 and 72:

$$\frac{c_A}{c_{A0}} = 1 - \operatorname{erf} \frac{z}{\sqrt{4\mathscr{D}_{AB} \int_0^t [s(u, w, \bar{t})/s(u, w, t)]^2 \, d\bar{t}}} \tag{20.4-22}$$

$$N_{Az0} = c_{A0} \sqrt{\frac{\mathscr{D}_{AB}}{\pi t}} \left(\frac{1}{t} \int_0^t [s(u, w, \bar{t})/s(u, w, t)]^2 \, d\bar{t} \right)^{-1/2} \tag{20.4-23}$$

These solutions, unlike Eq. 20.1-71 and Eq. 20.1-72, include the spatial variations of the boundary layer thickness and interfacial molar flux N_{Az0} that occur in nonuniform flows. Local stretching of the interface (as at stagnation loci) thins the boundary layer and enhances N_{Az0}. Local interfacial shrinkage (at separation loci) diminishes N_{Az0}, but also ejects stale fluid from the boundary layer, allowing its mixing into the interior of the same phase. Observations of mass transfer enhancement by such mixing have been interpreted by some workers as "surface renewal," even though creation of new surface elements in an existing surface is not permitted in continuum fluid mechanics.

These results, and others for negligible v_{z0}, are obtainable conveniently by introducing the following new variables into Eq. 20.4-19:

$$Z = zs(u, w, t) \quad \text{and} \quad \tau = \int_0^t s^2(u, w, \bar{t}) d\bar{t} \tag{20.4-24, 25}$$

In the absence of chemical reactions, the resulting differential equation for the concentration function $c_A(u, w, Z, \tau)$ becomes

$$\frac{\partial c_A}{\partial \tau} = \mathscr{D}_{AB} \frac{\partial^2 c_A}{\partial Z^2} \tag{20.4-26}$$

This is a generalization of Fick's second law to an asymptotic relation for forced convection in free-surface flows.

EXAMPLE 20.4-2

Gas Absorption with Rapid Reaction and Interfacial Deformation

Show how to generalize Example 20.1-2 to flow systems, by using Eq. 20.4-26 for the two reaction-free zones.

SOLUTION

Using Eq. 20.4-26, we get the following replacements for Eqs. 20.1-26 and 27:

$$\frac{\partial c_A}{\partial \tau} = \mathscr{D}_{AS} \frac{\partial^2 c_A}{\partial Z^2} \qquad \text{for } 0 \le Z \le Z_R \tag{20.4-27}$$

$$\frac{\partial c_B}{\partial \tau} = \mathscr{D}_{BS} \frac{\partial^2 c_B}{\partial Z^2} \qquad \text{for } Z_R \le Z < \infty \tag{20.4-28}$$

Now the reaction *plane* $z = z_R$ of the original example is a *time-dependent surface*, $Z = Z_R$, or $z_R(u, w, t) = Z_R/s(u, w, t)$. The initial and boundary conditions remain as before, subject to this generalization of the reaction-front location.

The solutions for c_A and c_B then take the forms in Eqs. 20.1-35 and 36, with $z/\sqrt{t}$ replaced by $Z/\sqrt{\tau}$, and $z_R/\sqrt{t}$ by $\sqrt{\gamma}$. The latter constant is again given by Eq. 20.1-37. The enhancement of the absorption rate by the chemical reaction accordingly parallels the expressions that will be given in Eq. 22.5-10, and simplified in Eqs. 22.5-11 through 13.

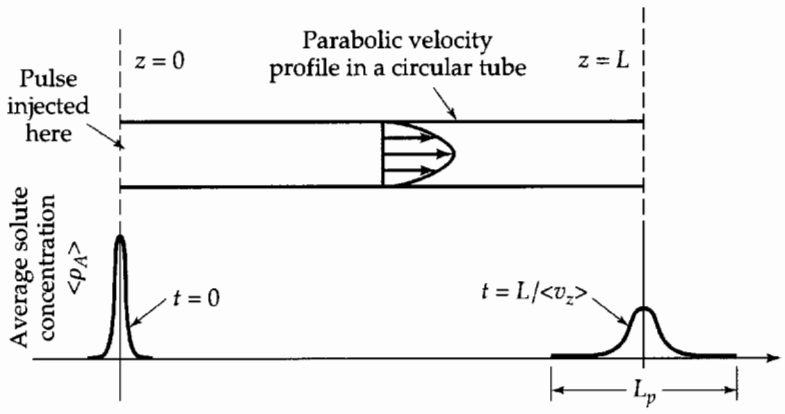

Fig. 20.5-1. Sketch showing the axial spreading of a concentration pulse in Taylor dispersion in a circular tube.

§20.5 "TAYLOR DISPERSION" IN LAMINAR TUBE FLOW

Here we discuss the transport and spreading of a solute "pulse" of material A introduced into fluid B in steady laminar flow through a long, straight tube of radius R, as shown in Fig. 20.5-1. A pulse of mass m_A is introduced at the inlet $z = 0$ over a very short period near time $t = 0$, and its progress through the tube is to be analyzed in the long-time limit. Problems of this type arise frequently in process control (see Problem 20C.4), medical diagnostic procedures,[1] and in a variety of environmental applications.[2]

A short distance downstream from the inlet, the θ-dependence of the mass fraction distribution will die out. Then the diffusion equation for $\omega_A(r, z, t)$ in Poiseuille flow with constant μ, ρ, and $\mathscr{D}_{AB}$ takes the form

$$\frac{\partial \omega_A}{\partial t} + v_{z,\max}\left[1 - \left(\frac{r}{R}\right)^2\right]\frac{\partial \omega_A}{\partial z} = \mathscr{D}_{AB}\left(\frac{1}{r}\frac{\partial}{\partial r}\left(r\frac{\partial \omega_A}{\partial r}\right) + \frac{\partial^2 \omega_A}{\partial z^2}\right) \tag{20.5-1}$$

This equation is to be solved with the boundary conditions

$$\text{B.C. 1 and 2:} \qquad \text{at } r = 0 \text{ and at } r = R, \qquad \frac{\partial \omega_A}{\partial r} = 0 \tag{20.5-2}$$

which express the radial symmetry of the mass fraction profile and the impermeability of the tube wall to diffusion. For this long-time analysis it is not necessary to specify the exact shape of the pulse injected at $t = 0$. No exact analytical solution is available for the mass fraction profile $\omega_A(r, z, t)$—even if an initial condition were clearly formulated—but Taylor[3,4] gave a useful approximate analysis that we summarize here. This involves getting from Eq. 20.5-1 a partial differential equation for the cross-sectional average mass fraction

$$\langle \omega_A \rangle = \frac{\int_0^{2\pi}\int_0^R \omega_A r\, dr\, d\theta}{\int_0^{2\pi}\int_0^R r\, dr\, d\theta} = \frac{2}{R^2}\int_0^R \omega_A r\, dr \tag{20.5-3}$$

which can then be solved to describe the behavior at long times.

---

[1] J. B. Bassingthwaighte and C. A. Goresky, in Section 2, Volume 3 of *Handbook of Physiology*, 2nd edition, American Physiological Society, Bethesda, Md. (1984).

[2] P. C. Chatwin and C. M. Allen, *Ann. Rev. Fluid Mech.*, **17**, 119–150 (1985); B. E. Logan, *Environmental Transport Processes*, Wiley-Interscience, New York (1999), Chapters 10 and 11; J. H. Seinfeld, *Advances in Chemical Engineering*, Academic Press, New York (1983), pp. 209–299.

[3] G. I. Taylor, *Proc. Roy. Soc.* **A219**, 186–203 (1953).

[4] G. I. Taylor, *Proc. Roy. Soc.*, **A225**, 473–477 (1954).

Taylor began by neglecting the axial molecular diffusion term (dashed underlined term in Eq. 20.5-1), and subsequently showed[4] that this is permissible if the Péclet number $\text{Pé}_{AB} = R\langle v_z\rangle/\mathscr{D}_{AB}$ is of the order of 70 or greater, and if the length $L_p(t)$ of the region occupied by the pulse, measured visually in Taylor's experiments,[3] is of the order of $170R$ or greater. Here $\langle v_z\rangle = \frac{1}{2}v_{z,\max}$ is the mean speed of the flow.

Taylor sought a solution valid for long times. He estimated the condition for the validity of his result to be

$$\frac{L_p}{v_{z,\max}} >> \frac{R^2}{(3.8)^2\mathscr{D}_{AB}} \tag{20.5-4}$$

When the pulse length L_p attains this range, enough time has elapsed that the initial shape of the pulse no longer matters.

In order to follow the development of the concentration profile as the fluid moves downstream, it is useful to introduce the shifted axial coordinate

$$\bar{z} = z - \langle v_z\rangle t \tag{20.5-5}$$

When this is used in Eq. 20.5-1 (without the dashed-underlined term), we get the following diffusion equation for $\omega_A(r, \bar{z}, t)$,

$$\frac{\partial \omega_A}{\partial t} + v_{z,\max}(\tfrac{1}{2} - \xi^2)\frac{\partial \omega_A}{\partial \bar{z}} = \frac{\mathscr{D}_{AB}}{R^2}\frac{1}{\xi}\frac{\partial}{\partial \xi}\left(\xi\frac{\partial \omega_A}{\partial \xi}\right) \tag{20.5-6}$$

in which $\xi = r/R$ is the dimensionless radial coordinate. The time derivative here is understood to be taken at constant $\bar{z}$, and, under the condition of Eq. 20.5-4, it may be neglected relative to the radial diffusion term. As a result we have a quasi-steady-state equation

$$\frac{1}{\xi}\frac{\partial}{\partial \xi}\left(\xi\frac{\partial \omega_A}{\partial \xi}\right) = \frac{R^2 v_{z,\max}}{\mathscr{D}_{AB}}(\tfrac{1}{2} - \xi^2)\frac{\partial \omega_A}{\partial \bar{z}} \tag{20.5-7}$$

For the condition of Eq. 20.5-4, the mass fraction can be expressed as

$$\omega_A(\xi, \bar{z}, t) = \langle \omega_A\rangle + \omega_A'(\xi, \bar{z}, t) \qquad \text{with } |\omega_A'| << \langle \omega_A\rangle \tag{20.5-8}$$

where $\langle \omega_A\rangle$ is a function of $\bar{z}$ and t. Substituting this expression into the right side of Eq. 20.5-7, and accordingly neglecting ω_A', we then get

$$\frac{1}{\xi}\frac{\partial}{\partial \xi}\left(\xi\frac{\partial \omega_A}{\partial \xi}\right) = \frac{R^2 v_{z,\max}}{\mathscr{D}_{AB}}(\tfrac{1}{2} - \xi^2)\frac{\partial \langle \omega_A\rangle}{\partial \bar{z}} \tag{20.5-9}$$

from which the radial dependence of the mass fraction can be obtained under the condition of Eq. 20.5-4.

Integration of Eq. 20.5-9 with the boundary conditions of Eq. 20.5-2 then yields

$$\omega_A(\xi, \bar{z}) = \frac{R^2 v_{z,\max}}{8\mathscr{D}_{AB}}\frac{\partial \langle \omega_A\rangle}{\partial \bar{z}}(\xi^2 - \tfrac{1}{2}\xi^4) + \omega_A(0, \bar{z}) \tag{20.5-10}$$

The average of this profile over the cross section is

$$\langle \omega_A\rangle = \frac{\int_0^1 \omega_A \xi d\xi}{\int_0^1 \xi d\xi} = \frac{R^2 v_{z,\max}}{24\mathscr{D}_{AB}}\frac{\partial \langle \omega_A\rangle}{\partial \bar{z}} + \omega_A(0, \bar{z}) \tag{20.5-11}$$

Subtracting this equation from the previous one, and replacing $v_{z,\max}$ by $2\langle v_z\rangle$, gives finally

$$\omega_A - \langle \omega_A\rangle = \frac{R^2\langle v_z\rangle}{2\mathscr{D}_{AB}}\frac{\partial \langle \omega_A\rangle}{\partial \bar{z}}(-\tfrac{1}{3} + \xi^2 - \tfrac{1}{2}\xi^4) \tag{20.5-12}$$

as Taylor's approximate solution of Eq. 20.5-6.

The total mass flow of A through a plane of constant $\bar{z}$ (that is, the flow relative to the average velocity $\langle v_z \rangle$) is

$$\pi R^2 \rho \langle \omega_A (v_z - \langle v_z \rangle) \rangle = \frac{\pi R^4 \rho \langle v_z \rangle^2}{\mathscr{D}_{AB}} \frac{\partial \langle \omega_A \rangle}{\partial \bar{z}} \int_0^1 (-\tfrac{1}{3} + \xi^2 - \tfrac{1}{2}\xi^4)(\tfrac{1}{2} - \xi^2)\xi \, d\xi$$
$$= -\frac{\pi R^4 \rho \langle v_z \rangle^2}{48 \mathscr{D}_{AB}} \frac{\partial \langle \omega_A \rangle}{\partial \bar{z}} \tag{20.5-13}$$

Next we note that, with the assumption of ρ = constant, $\rho \langle \omega_A \langle v_z \rangle \rangle = \langle \rho_A \rangle \langle v_z \rangle$ and $\rho \langle \omega_A v_z \rangle \approx \langle \rho_A v_{Az} \rangle = \langle n_{Az} \rangle$. (Replacing v_z by v_{Az} is allowed here because, with axial molecular diffusion neglected, species A and B are moving with the same axial speed). Therefore when Eq. 20.5-13 is divided by πR^2, we obtain the averaged mass flux expression

$$\langle n_{Az} \rangle = \langle \rho_A \rangle \langle v_z \rangle - K \frac{\partial \langle \rho_A \rangle}{\partial \bar{z}} = \langle \rho_A \rangle \langle v_z \rangle - K \frac{\partial \langle \rho_A \rangle}{\partial z} \tag{20.5-14}$$

relative to stationary coordinates. Here K is an *axial dispersion coefficient*, given by Taylor's analysis as

$$K = \frac{R^2 \langle v_z \rangle^2}{48 \mathscr{D}_{AB}} = \frac{1}{48} \mathscr{D}_{AB} \mathrm{Pé}_{AB}^2 \tag{20.5-15}$$

This formula indicates that axial dispersion (in the range Pé >> 1 considered so far) is enhanced by the radial variation of v_z and reduced by radial molecular diffusion.

Although Eq. 20.5-14 has the form of Fick's law in Eq. (C) of Table 17.8-2, the present equation does not include any axial molecular diffusion. Also it should be emphasized that K is not a property of the fluid mixture, but depends on R and $\langle v_z \rangle$ as well as on $\mathscr{D}_{AB}$.

Next we write the equation of continuity of Eq. 19.1-6, averaged over the tube cross section, as

$$\frac{\partial}{\partial t} \langle \rho_A \rangle = -\frac{\partial}{\partial z} \langle n_{Az} \rangle \tag{20.5-16}$$

When the expression for the mass flux of A from Eq. 20.5-14 is inserted, we get the following *axial dispersion equation*:

$$\frac{\partial}{\partial t} \langle \rho_A \rangle + \langle v_z \rangle \frac{\partial}{\partial z} \langle \rho_A \rangle = K \frac{\partial^2}{\partial z^2} \langle \rho_A \rangle \tag{20.5-17}$$

This equation can be solved to get the shape of the traveling pulse resulting from a δ-function input of a mass m_A of solute A into a stream of otherwise pure B:

$$\langle \rho_A \rangle = \frac{m_A}{2\pi R^2 \sqrt{\pi K t}} \exp\left(-\frac{(z - \langle v_z \rangle t)^2}{4Kt} \right) \tag{20.5-18}$$

This can be used along with Eq. 20.5-15 to extract $\mathscr{D}_{AB}$ from data on the concentrations in the traveling pulse. In fact, this is probably the best method for reasonably quick measurements of liquid diffusivities.

Taylor's development laid the foundation for an extensive literature on convective dispersion. However, it remained to study the approximations made and to determine their range of validity. Aris[5] gave a detailed treatment of dispersion in tubes and ducts, covering the full range of t and including diffusion in the z and θ directions. His long-time asymptote

$$K = \mathscr{D}_{AB} + \frac{R^2 \langle v_z \rangle^2}{48 \mathscr{D}_{AB}} = \mathscr{D}_{AB} \left(1 + \frac{1}{48} \mathrm{Pé}_{AB}^2 \right) \tag{20.5-19}$$

---

[5] R. Aris, *Proc. Roy. Soc.*, **A235**, 67–77 (1956).

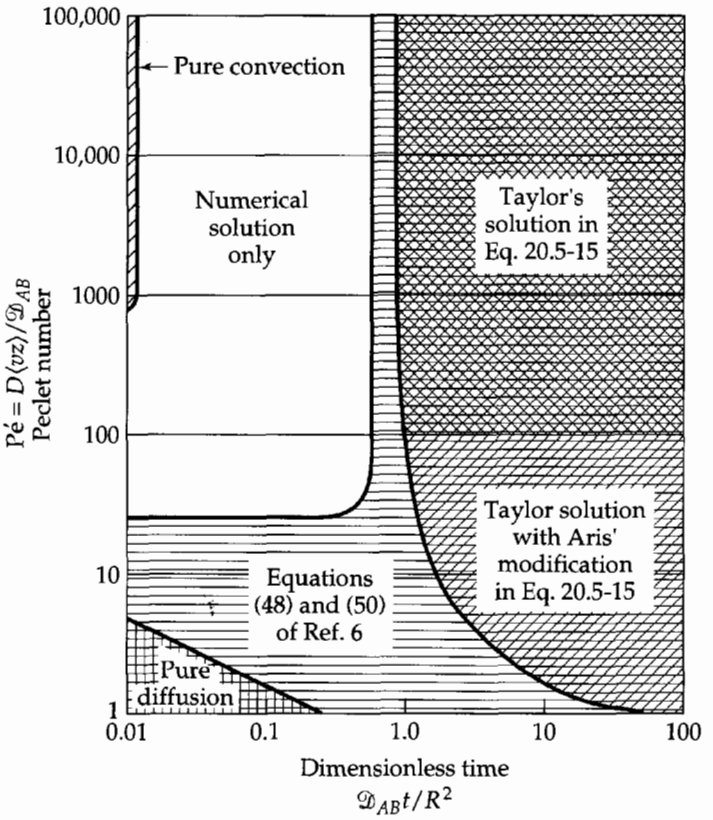

Fig. 20.5-2. Sketch showing the limits of the Taylor (Eq. 20.3-15) and Aris (Eq. 20.5-19) expressions for the axial dispersion coefficient. This figure is patterned after one in Ref. 6.

is an important extension of Eq. 20.5-15. From this result, we see that molecular diffusion enhances the axial dispersion when the Péclet number Pé = $R\langle v_z\rangle/\mathscr{D}_{AB}$ is less than $\sqrt{48}$ and inhibits axial dispersion at larger Péclet numbers, where Taylor's mode of transport predominates.

The ranges of validity of the Taylor and Aris dispersion formulas have been studied thoroughly by finite difference calculations[6] and by orthogonal collocation.[7] Figure 20.5-2 shows the useful ranges of Eq. 20.5-15 and 19. The latter formula has been widely used for measurements of binary diffusivities, and an extension of it[8] has been used to measure ternary diffusivities in liquids.

Several further investigations on convective dispersion will be mentioned here. *Coiled tubes* give reduced longitudal dispersion, as shown by the experiments of Koutsky and Adler[9] and analyzed for laminar flow by Nunge, Lin, and Gill.[10] This effect is important in chemical reactor design and in diffusivity measurements, where coiling is often necessary to get enough tube length into a compact apparatus.

Extra-column dispersion, caused by the pump and connecting tubing of chromatographic systems, was investigated by Shankar and Lenhoff[11] with detailed predic-

---

[6] V. Ananthakrishnan, W. N. Gill, and A. J. Barduhn, *AIChE Journal*, **11**, 1063–1072 (1965).
[7] J. C. Wang and W. E. Stewart, *AIChE Journal*, **29**, 493–497 (1983).
[8] Ph. W. M. Rutten, *Diffusion in Liquids*, Delft University Press, Delft, The Netherlands (1992).
[9] J. A. Koutsky and R. J. Adler, *Can. J. Chem. Eng.*, **42**, 239–246 (1964).
[10] R. J. Nunge, T. S. Lin, and W. N. Gill, *J. Fluid Mech.*, **51**, 363–382 (1972).
[11] A. Shankar and A. M. Lenhoff, *J. Chromatography*, **556**, 235–248 (1991).

tions and precise experiments. Their experiments showed that the form of radial averaging is important at times shorter than the recommended range shown in Fig. 20.5-2 for the Taylor–Aris formula. Depending on the type of analyzer used, the data may be better described either by a cup-mixing average ρ_{Ab} or by the area average $\langle \rho_A \rangle$ used above.

Hoagland and Prud'homme[12] have analyzed laminar longitudinal dispersion in *tubes of sinusoidally varying radius*, $R(z) = R_0(1 + \varepsilon \sin(2\pi z/\lambda))$, to model dispersion in packed-bed processes. Their results parallel Eq. 20.5-19, when the variations have small relative amplitude ε and long relative wavelength λ/R_0. One might think that the axial dispersion in a packed column would be similar to that in tubes of sinusoidally varying radius, but that is not the case. Instead of Eq. 20.3-19, one finds $K \approx 2.5\mathscr{D}_{AB}\text{Pé}_{AB}$, with the first power of the Péclet number appearing, instead of the second power and with K independent of $\mathscr{D}_{AB}$.[13] Brenner and Edwards[14] have given analyses of convective dispersion and reaction in various geometries, including tubes and spatially periodic packed beds.

Dispersion has also been investigated in more complex flows. For *turbulent flows* in straight tubes, Taylor[15] derived and experimentally verified the axial dispersion formula $K/Rv^* = 10.1$, where v^* is the friction velocity used in Eq. 5.3-2. Bassingthwaighte and Goresky[1] investigated models of solute and water exchange in the cardiovascular system, and Chatwin and Allen[2] give mathematical models of turbulent dispersion in rivers and estuaries.

Equations 20.5-1 and 19 are limited to the conditions of Eqs. 20.5-2 and 4. Therefore, they are *not* appropriate for describing entrance regions of steady-state reactor operations or systems with heterogeneous reactions. Equation 20.5-1 is a better starting point for laminar flows.

QUESTIONS FOR DISCUSSION

1. What experimental difficulties might be encountered in using the system in Example 20.1-1 to measure gas-phase diffusivities?
2. What problems do you foresee in using the Taylor dispersion technique of §20.5 for measuring liquid-phase diffusivities?
3. Show that Eq. 20.1-16 satisfies the partial differential equation as well as the initial and boundary conditions.
4. What do you conclude from Table 20.1-1?
5. Why are Laplace transforms useful in solving the problem in Example 20.1-3? Could Laplace transforms be used to solve the problem in Example 20.1-1?
6. How is the velocity distribution in Example 20.1-4 obtained?
7. Describe the method of solving the variable surface area problem in Example 20.1-4.
8. Perform the check suggested after Eq. 20.1-74.
9. What effects do chemical reactions have on the boundary layer?
10. Discuss the Chilton–Colburn expressions in Eq. 20.2-57. Would you expect these same relations to be valid for flows around cylinders and spheres?

---

[12] D. A. Hoagland and R. K. Prud'homme, *AIChE Journal*, **31**, 236–244 (1985).

[13] A. M. Athalye, J. Gibbs, and E. N. Lightfoot, *J. Chromatog.* **589**, 71–85 (1992).

[14] H. Brenner and D. A. Edwards, *Macrotransport Processes*, Butterworth-Heinemann, Boston (1993).

[15] G. I. Taylor, *Proc. Roy. Soc.*, **A223**, 446–467 (1954).

PROBLEMS

20A.1. Measurement of diffusivity by unsteady-state evaporation. Use the following data to determine the diffusivity of ethyl propionate (species *A*) into a mixture of 20 mole% air and 80 mole% hydrogen (this mixture being treated as a pure gas *B*).[1]

Increase in vapor volume (cm^3)	$\sqrt{t}$ ($s^{1/2}$)
0.01	15.5
0.11	19.4
0.22	23.4
0.31	26.9
0.41	30.5
0.50	34.0
0.60	37.5
0.70	41.5

These data were obtained[1] by using a glass tube 200 cm long, with an inside diameter 1.043 cm; the temperature was 27.9°C and the pressure 761.2 mm Hg. The vapor pressure of ethyl propionate at this temperature is 41.5 mm Hg. Note that t is the actual time from the start of the evaporation, whereas the volume increase is measured from $t \approx 240$ s.

20A.2. Absorption of oxygen from a growing bubble (Fig. 20A.2). Oxygen is being injected into pure water from a capillary tube. The system is virtually isothermal and isobaric at 25°C and 1 atm. The solubility of oxygen in the liquid phase is $\omega_{A0} = 7.78 \times 10^{-4}$, and the liquid-phase diffusivity for the oxygen–water pair is $\mathcal{D}_{AB} = 2.60 \times 10^{-5}$ cm^2/s. Calculate the instantaneous total absorption rate in g/s, for a bubble of 1 mm diameter and age $t = 2$ s, assuming

(a) Constant volumetric growth rate

(b) Constant radial growth rate dr_s/dt

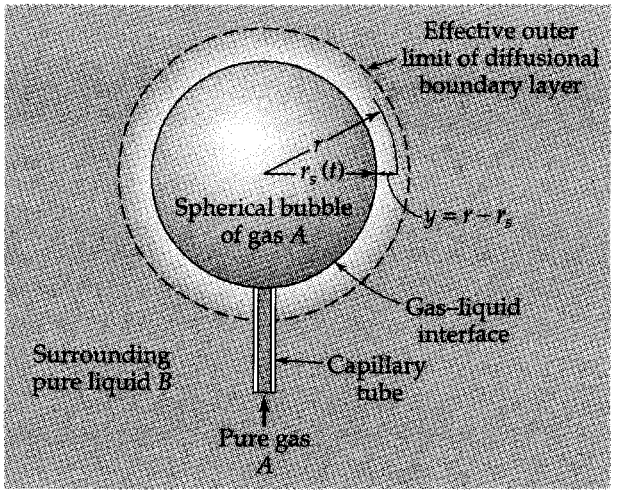

Fig. 20A.2. Gas absorption from a growing bubble, idealized as a sphere.

Answers: **(a)** 7.6×10^{-8} g/s; **(b)** 1.11×10^{-7} g/s

20A.3. Rate of evaporation of *n*-octane. At 20°C, how many grams of liquid *n*-octane will evaporate into N_2 in 24.5 hr in a system such as that studied in Example 20.1-1 at system pressures of **(a)** 1 atm, and **(b)** 2 atm? The area of the liquid surface is 1.29 cm^2, and the vapor pressure of *n*-octane at 20°C is 10.45 mm Hg.

Answer: **(a)** 6.71 mg

[1] D. F. Fairbanks and C. R. Wilke, *Ind. Eng. Chem.* **42**, 471–475 (1950).

20A.4. Effect of bubble size on interfacial composition (Fig. 20A.2). Here we examine the assumption of time-independent interfacial composition, ω_{A0}, for the system in Fig. 20A.2. We note that, because of the interfacial tension, the gas pressure p_A depends on the instantaneous bubble radius r_s. The equilibrium expression

$$p_A = p_\infty + \frac{2\sigma}{r_s} \tag{20A.4-1}$$

is adequate unless dr_s/dt is very large. Here p_∞ is the ambient liquid pressure at the mean elevation of the bubble, and σ is the interfacial tension.

For a sparingly soluble solute, the interfacial liquid composition ω_{A0} depends on p_A according to Henry's law

$$\omega_{A0} = Hp_A \tag{20A.4-2}$$

in which the Henry's law constant, H, depends on the two species and on the liquid temperature and pressure. This expression may be combined with Eq. 20A.4-1 to obtain the dependence of ω_{A0} on r_s.

For a gas bubble dissolving in liquid water to $T = 25°C$ and $p_\infty = 1$ atm, how small must the bubble be in order to obtain a 10% increase in ω_{A0} above the value for a very large bubble? Assume $\sigma = 72$ dyn/cm over the relevant composition range.

Answer: 1.4 microns

20A.5. Absorption with rapid second-order reaction (Fig. 20.1-2). Make the following calculations for the reacting system depicted in the figure:

(a) Verify the location of the reaction zone, using Eq. 20.1-37.

(b) Calculate N_{A0} at $t = 2.5$ s.

20A.6. Rapid forced-convection mass transfer into a laminar boundary layer. Calculate the evaporation rate $n_{A0}(x)$ for the system described under Eq. 20.2-52, given that $\omega_{A0} = 0.9$, $\omega_{A\infty} = 0.1$, $n_{B0}(x) = 0$ and Sc = 2.0. Use Fig. 22.8-5 with R calculated as R_ω from Eq. 20.2-51, to find the dimensionless mass flux ϕ (denoted by ϕ_ω for diffusional calculations with mass fractions). Then use Eq. 22.8-21 and Table 20.2-1 to calculate K, and Eq. 20.2-48 to calculate $n_{A0}(x)$.

Answer: $n_{A0}(x) = 0.33\sqrt{\rho v_\infty \mu / x}$

20A.7. Slow forced-convection mass transfer into a laminar boundary layer. This problem illustrates the use of Eqs. 20.2-55 and 57 and tests their accuracy against that of Eq. 20.2-47.

(a) Estimate the local evaporation rate, n_{A0}, as a function of x for the drying of a porous water-saturated slab, shaped as in Fig. 20.2-2. The slab is being dried in a rapid current of air, under conditions such that $\omega_{A0} = 0.05$, $\omega_{A\infty} = 0.01$, and Sc = 0.6. Use Eq. 20.2-55 for the calculation.

(b) Make an alternate calculation of n_{A0} using Eq. 20.2-57.

(c) For comparison with the preceding approximate results, calculate n_{A0} from Eq. 20.2-47 and Table 20.2-1. The K values found in (a) will be sufficiently accurate for looking up $\Pi'(0, \text{Sc}, K)$.

Answers: **(a)** $n_{A0}(x) = 0.0188\sqrt{\rho v_\infty \mu / x}$; **(b)** $n_{A0}(x) = 0.0196\sqrt{\rho v_\infty \mu / x}$;
(c) $n_{A0}(x) = 0.0188\sqrt{\rho v_\infty \mu / x}$

20B.1. Extension of the Arnold problem to account for interphase transfer of both species. Show how to obtain Eqs. 20.1-23, 24, and 25 starting with the equations of continuity for species A and B (in molar units) and the appropriate initial and boundary conditions.

20B.2. Extension of the Arnold problem to nonisothermal diffusion. In the situation described in Problem 20B.1, find the analogous result for the temperature distribution $T(z, t)$.

(a) Show that the energy equation [Eq. (H) of Table 19.2-4] reduces to

$$\frac{\partial T}{\partial t} + v_z^* \frac{\partial T}{\partial z} = \alpha \frac{\partial^2 T}{\partial z^2} \tag{20B.2-1}$$

provided that k, p, and c (or ρ) are essentially constant, and that $\overline{H}_\alpha = \tilde{H}_\alpha(p, T)$ and $\tilde{C}_{pA} = \tilde{C}_{pB} =$ constant; consequently α is then a constant. Here the dissipation term $(\boldsymbol{\tau}:\nabla\mathbf{v})$ and the work term $\Sigma_\alpha(\mathbf{j}_\alpha \cdot \mathbf{g}_\alpha)$ are appropriately neglected. (*Hint:* Use the species equation of continuity of Eq. 19.1-10.)

(b) Show that the solution of Eq. 20B.2-1, with the initial condition that $T = T_\infty$ at $t = 0$, and the boundary conditions that $T = T_0$ at $z = 0$ and $T = T_\infty$ at $z = \infty$, is

$$\frac{T - T_0}{T_\infty - T_0} = \Pi_T(Z_T) = \frac{\text{erf}(Z_T - \varphi_T) + \text{erf}\varphi_T}{1 + \text{erf}\varphi_T} \tag{20B.2-2}$$

with

$$Z_T = \frac{z}{\sqrt{4\alpha t}} \quad \text{and} \quad \varphi_T = v_z^* \sqrt{\frac{t}{\alpha}} \tag{20B.2-3}$$

(c) Show that the interfacial mass and energy fluxes are related to T_0 and T_∞ by

$$\frac{N_{A0} + N_{B0}}{[q_0/\tilde{C}_p(T_0 - T_\infty)]} = \sqrt{\pi}(1 + \text{erf}\ \varphi_T)\varphi_T \exp \varphi_T^2 \tag{20B.2-4}$$

so that N_{A0}/q_0 and N_{B0}/q_0 are constant for $t > 0$. This nifty result arises because there is no characteristic length or time in the mathematical model of the system.

20B.3. Stoichiometric boundary condition for rapid irreversible reaction. The reactant fluxes in Example 20.1-2 must satisfy the stoichiometric relation

$$\text{at } z = z_R(t), \qquad \frac{1}{a} c_A(v_{Az} - v_R) = -\frac{1}{b} c_B(v_{Bz} - v_R) \tag{20B.3-1}$$

in which $v_R = dz_R/dt$. Show that this relation leads to Eq. 20.1-31 when use is made of Fick's first law, with the assumptions of constant c and instantaneous irreversible reaction.

20B.4. Taylor dispersion in slit flow (Fig. 2B.3). Show that, for laminar flow in a plane slit of width $2B$ and length L, the Taylor dispersion coefficient is

$$K = \frac{2B^2\langle v_z\rangle^2}{105\mathscr{D}_{AB}} \tag{20B.4-1}$$

20B.5. Diffusion from an instantaneous point source. At time $t = 0$, a mass m_A of species A is injected into a large body of fluid B. Take the point of injection to be the origin of coordinates. The material A diffuses radially in all directions. The solution may be found in Carslaw and Jaeger:[2]

$$\rho_A = \frac{m_A}{(4\pi\mathscr{D}_{AB}t)^{3/2}} \exp\left(-r^2/4\mathscr{D}_{AB}t\right) \tag{20B.5-1}$$

(a) Verify that Eq. 20B.5-1 satisfies Fick's second law.

(b) Verify that Eq. 20B.5-1 satisfies the boundary conditions at $r = \infty$.

(c) Show that Eq. 20B.5-1, when integrated over all space, gives m_A, as required.

(d) What happens to Eq. 20B.5-1 when $t \to 0$?

20B.6. Unsteady diffusion with first-order chemical reaction. Use Eq. 20.1-43 to obtain the concentration profile for the following situations:

---

[2] H. S. Carslaw and J. C. Jaeger, *Conduction of Heat in Solids*, 2nd edition, Oxford University Press (1959), p. 257.

(a) The catalyst particle of Problem 18B.14, in time-dependent operation with the boundary conditions as given before, but with the initial condition that $c_A = 0$ at $t = 0$. The differential equation for c_A is

$$\varepsilon \frac{\partial c_A}{\partial t} = \mathcal{D}_A \frac{\partial^2 c_A}{\partial z^2} - k_1'' a c_A \tag{20B.6-1}$$

where ε is the interior void fraction for the particle. The necessary solution with $k_1'' a = 0$ may be found from the result of Example 12.1-2.

(b) Diffusion and reaction of a solute, A, injected at $t = 0$ at the point $r = 0$ (in spherical coordinates) in an infinite stationary medium. Here the function g of Eq. 20.1-43 is given as

$$g = \frac{1}{(4\pi \mathcal{D}_{AB} t)^{3/2}} \exp(-r^2/4\mathcal{D}_{AB}t) \tag{20B.6-2}$$

and the function f vanishes.

20B.7. Simultaneous momentum, heat, and mass transfer: alternate boundary conditions (Fig. 20B.7). The dimensionless profiles $\Pi(\eta, \Lambda, K)$ in Eq. 20.2-43 are applicable to a variety of situations. Use Eqs. 20.2-49 to 52 to obtain implicit equations for the evaluation of the dimensionless net mass flux K for the following steady-state operations:

(a) Evaporation of pure liquid A from a saturated porous plate into a gaseous stream of A and B. Substance B is insoluble in liquid A.

(b) Instantaneous irreversible reaction of gas A with a solid plate of C to give gaseous B, according to the reaction $A + C \rightarrow 2B$. The molecular weights of A and B are equal.

(c) Transpiration cooling of a porous-walled hollow plate, as shown in the figure. The fluid is pure A throughout, and the injected fluid is distributed so as to maintain the whole outer surface of the plate at a uniform temperature T_0.

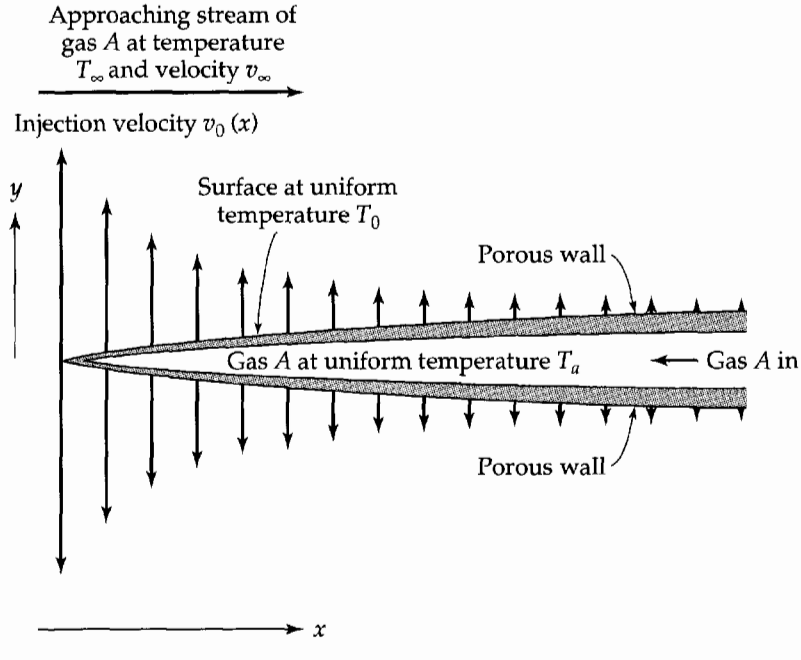

Fig. 20B.7. A transpiration-cooled porous plate.

Answers: **(a)** $K = \frac{1}{\text{Sc}}\left(\frac{\omega_{A0} - \omega_{A\infty}}{1 - \omega_{A0}}\right)\Pi'(0, \text{Sc}, K)$; **(b)** $K = \frac{1}{\text{Sc}}\omega_{A\infty}\,\Pi'(0, \text{Sc}, K)$

(c) $K = \frac{1}{\text{Pr}}\left(\frac{T_0 - T_\infty}{T_a - T_0}\right)\Pi'(0, \text{Pr}, K)$

20B.8. Absorption from a pulsating bubble. Use the results of Example 20.1-4 to calculate $\delta(t)$ and $N_{A0}(t)$ for a bubble whose radius undergoes a square-wave pulsation:

$$r_s = R_1 \quad \text{for } 2n < \omega t < 2n + 1$$
$$r_s = R_2 \quad \text{for } 2n + 1 < \omega t < 2n + 2 \tag{20B.10-1}$$

Here ω is a characteristic frequency, and $n = 0, 1, 2, \ldots$.

20B.9. Verification of the solution of the Taylor-dispersion equation. Show that the solution to Eq. 20.5-17, given in Eq. 20.5-18, satisfies the differential equation, the initial condition, and the boundary conditions.[3] The latter are that at $z = \pm\infty$,

$$\langle \rho_A \rangle = 0 \quad \text{and} \quad \frac{\partial}{\partial z}\langle \rho_A \rangle = 0 \tag{20B.9-1}$$

The initial condition is that, at $t = 0$, the solute pulse, of mass m_A, is concentrated at $z = 0$, with no solute anywhere else in the tube, so that for all times,

$$\pi R^2 \int_{-\infty}^{+\infty} \langle \rho_A \rangle dz = m_A \tag{20B.9-2}$$

(a) Show that Eq. 20.5-17 can be reduced to the one-dimensional form of Fick's second law by the coordinate transformation

$$\bar{z} = z - \langle v_z \rangle t \tag{20B.9-3}$$

(b) Show that Eq. 20.5-18 satisfies the equation derived in (a).

(c) Show that Eqs. 20B.9-1 and 2 are also satisfied.

20C.1. Order-of-magnitude analysis of gas absorption from a growing bubble (Fig. 20A.2).

(a) For the growth of the spherical bubble of Problem 20A.2(*a*) in a liquid of constant density, show that in the liquid phase the radial velocity is $v_r = C_0/r^2$ according to the equation of continuity. Then use the boundary condition that $v_r = dr_s/dt$ at $r = r_s(t)$ to obtain

$$v_r = \frac{r_s^2}{r^2}\frac{dr_s}{dt} \tag{20C.1-1}$$

(b) Next, using the species equation of continuity in spherical coordinates with diffusion in the radial direction only, show that

$$\frac{\partial \omega_A}{\partial t} + \left(\frac{r_s^2}{r^2}\frac{dr_s}{dt}\right)\frac{\partial \omega_A}{\partial r} = \mathcal{D}_{AB}\frac{1}{r^2}\frac{\partial}{\partial r}\left(r^2\frac{\partial \omega_A}{\partial r}\right) \qquad (r > r_s(t)) \tag{20C.1-2}$$

and indicate suitable initial and boundary conditions.

(c) For short contact times, the effective diffusion zone is a relatively thin layer, so that it is convenient to introduce a variable $y = r - r_s(t)$. Show that this leads to

$$\overset{(1)}{\frac{\partial \omega_A}{\partial t}} + \left(\overset{(2)}{-\frac{2y}{r_s}} + \overset{(3)}{\frac{3y^2}{r_s^2}} + \cdots\right)\frac{dr_s}{dt}\frac{\partial \omega_A}{\partial y} = \mathcal{D}_{AB}\left[\overset{(4)}{\frac{\partial^2 \omega_A}{\partial y^2}} + \frac{2}{r_s}\left(\overset{(5)}{1} - \overset{(6)}{\frac{y}{r_s}} + \overset{(7)}{\frac{y^2}{r_s^2}} - \cdots\right)\frac{\partial \omega_A}{\partial y}\right] \tag{20C.1-3}$$

(d) From Example 20.1-4 we can see that the contributions of terms (1), (2), and (4) are all of the same order of magnitude in the concentration boundary layer, that is, at $y = O(\delta_\omega) = O(\sqrt{\mathcal{D}_{AB}t})$. Taking these terms to be of order O(1), estimate the orders of magnitude of the remaining terms shown in Eq. 20C.1-3.

---

[3] See, for example, H. S. Carslaw and J. C. Jaeger, *Heat Conduction in Solids*, 2nd edition, Oxford University Press (1959), §10.3. For the effects of finite tube length, see H. Brenner, *Chem. Eng. Sci.*, **17**, 229–243 (1961).

(e) Show that the terms of the two leading orders in Eq. 20C.1-3 give

$$\frac{\partial \omega_A}{\partial t} + \left[-\frac{2y}{r_s} + \underline{\frac{3y^2}{r_s^2}} \right] \frac{dr_s}{dt} \frac{\partial \omega_A}{\partial r} = \mathcal{D}_{AB} \left[\frac{\partial^2 \omega_A}{\partial y^2} + \underline{\frac{2}{r_s} \frac{\partial \omega_A}{\partial y}} \right] \tag{20C.1-4}$$

the second-order terms being designated by dashed underlines.

(e) This equation has been analyzed thoroughly in the electrochemical literature.[4] The results for n_{A0} are further considered in Problem 20C.2.

20C.2. Effect of surface curvature on absorption from a growing bubble (Fig. 20A.2). Pure gas A is flowing from a small capillary into a large reservoir of initially pure liquid B at a constant molar flow rate W_A. The interfacial molar flux of A into the liquid is predictable from the *Levich-Koutecký-Newman equation*

$$N_{A0} = c_{A0} \sqrt{\frac{7\mathcal{D}_{AB}}{3\pi t}} \left(1 + \frac{16}{11} \sqrt{\frac{3}{7}} \frac{\Gamma(\frac{15}{14})}{\Gamma(\frac{11}{7})} \frac{\mathcal{D}_{AB}^{1/2} t^{1/6}}{\gamma} \right) \tag{20C.2-1}$$

in which

$$\gamma = \frac{r(t)}{t^{1/3}} = \left(\frac{3W_A}{4\pi c} \right)^{1/3} \tag{20C.2-2}$$

for purely radial motion and a spherical bubble. Equation 20C.2-1 is a consequence of Eq. 20C.1-4.

(a) Give an expression for the number of moles of A absorbed over a bubble lifetime t_0.

(b) Use Eq. 20C.2-1 to obtain more accurate results for the absorption rates in Problem 20A.2.

20C.3. Absorption with chemical reaction in a semi-infinite medium. A semi-infinite medium of material B extends from the plane boundary $x = 0$ to $x = \infty$. At time $t = 0$ substance A is brought into contact with this medium at the plane $x = 0$, the surface concentration being c_{A0} (for absorption of gas A by liquid B, for example, c_{A0} would be the saturation concentration). Substances A and B react to produce C according to the irreversible first-order reaction $A + B \rightarrow C$. It is assumed that A is present in such a small concentration that the equation describing the diffusion plus chemical reaction process is

$$\frac{\partial c_A}{\partial t} = \mathcal{D}_{AB} \frac{\partial^2 c_A}{\partial x^2} - k_1''' c_A \tag{20C.3-1}$$

in which k_1''' is the first-order rate constant. This equation has been solved for the initial condition that $c_A = 0$ at $t = 0$, and the boundary conditions that $c_A = c_{A0}$ at $x = 0$, and $c_A = 0$ at $x = \infty$. The solution is[5]

$$\frac{c_A}{c_{A0}} = \frac{1}{2} \exp\left(-\sqrt{\frac{k_1''' x^2}{\mathcal{D}_{AB}}} \right) \operatorname{erfc}\left(\frac{x}{\sqrt{4\mathcal{D}_{AB} t}} - \sqrt{k_1''' t} \right) + \frac{1}{2} \exp\left(\sqrt{\frac{k_1''' x^2}{\mathcal{D}_{AB}}} \right) \operatorname{erfc}\left(\frac{x}{\sqrt{4\mathcal{D}_{AB} t}} + \sqrt{k_1''' t} \right) \tag{20C.3-2}$$

(a) Verify that Eq. 20C.3-2 satisfies the differential equation and the boundary conditions.

(b) Show that the molar flux at the interface $x = 0$ is

$$N_{Ax}|_{x=0} = c_{A0} \sqrt{\mathcal{D}_{AB} k_1'''} \left(\operatorname{erf} \sqrt{k_1''' t} + \frac{\exp(-k_1''' t)}{\sqrt{\pi k_1''' t}} \right) \tag{20C.3-3}$$

---

[4] J. Koutecký, *Czech. J. Phys.*, **2**, 50–55 (1953). See also V. Levich, *Physicochemical Hydrodynamics*, 2nd edition, Prentice-Hall, Englewood Cliffs, N.J. (1962). The right sides of Levich's Eqs. 108.17 and 108.18 should be multiplied by $t^{2/3}$. See also J. S. Newman, *Electrochemical Systems*, 2nd edition, Prentice-Hall, Englewood Cliffs, N.J. (1991).

[5] P. V. Danckwerts, *Trans. Faraday Soc.*, **46**, 300–304 (1950).

(c) Show further that the total moles absorbed across area A up to time t is

$$M_A = Ac_{A0}\sqrt{\mathscr{D}_{AB}t}\left[\left(\sqrt{k_1'''t} + \frac{1}{2\sqrt{k_1'''t}}\right)\operatorname{erf}\sqrt{k_1'''t} + \frac{\exp(-k_1'''t)}{\sqrt{\pi}}\right] \tag{20C.3-4}$$

(d) Show that, for large values of $k_1'''t$, the expression in (c) reduces asymptotically to

$$M_A = Ac_{A0}\sqrt{\mathscr{D}_{AB}k_1'''}\left(t + \frac{1}{2k_1'''}\right) \tag{20C.3-5}$$

This result[6] is good within 2% for values of $k_1'''t$ greater than 4.

20C.4. Design of fluid control circuits. It is desired to control a reactor via continuous analysis of a side stream. Calculate the maximum frequency of concentration changes that can be detected as a function of the volumetric withdrawal rate, if the stream is drawn through a 10 cm length of tubing with an internal diameter of 0.5 mm. *Suggestion:* Use as a criterion that the standard deviation of a pulse duration be no more than 5% of the cycle time $t_0 = 2\pi/\omega$, where ω is the frequency it is desired to detect.

20C.5. Dissociation of a gas caused by a temperature gradient. A dissociating gas (for example, $Na_2 \rightleftarrows 2Na$) is enclosed in a tube, sealed at both ends, and the two ends are maintained at different temperatures. Because of the temperature gradient established, there will be a continuous flow of Na_2 molecules from the cold end to the hot end, where they dissociate into Na atoms, which in turn flow from the hot end to the cold end. Set up the equations to find the concentration profiles. Check your results against those of Dirac.[7]

20D.1. Two-bulb experiment for measuring gas diffusivities—analytical solution (Fig. 18B.6). This experiment, described in Problem 18B.6, is analyzed there by a quasi-steady-state method. The method of separation of variables gives the exact solution[8] for the compositions in the two bulbs as

$$x_A^{\pm} = \tfrac{1}{2}\left[1 \pm \sum_{n=1}^{\infty}(-1)^{n+1}\left(\frac{2N}{\gamma_n}\right)\frac{\sqrt{\gamma_n^2 + N^2}}{\gamma_n^2 + N^2 + N}\exp\left(-\frac{\gamma_n^2\mathscr{D}_{AB}t}{L^2}\right)\right] \tag{20D.1-1}$$

in which γ_n is the nth root of $\gamma \tan \gamma = N$, and $N = SL/V$. Here the $\pm$ sign corresponds to the reservoirs attached at $\pm L$. Make a numerical comparison between Eq. 20D.1-1 and the experimental measurements of Andrew.[9] Also compare Eq. 20D.1-1 with the simpler result in Eq. 18B.6-4.

20D.2. Unsteady-state interphase diffusion. Two immiscible solvents I and II are in contact at the plane $z = 0$. At time $t = 0$ the concentration of A is $c_{\mathrm{I}} = c_{\mathrm{I}}^{\circ}$ in phase I and $c_{\mathrm{II}} = c_{\mathrm{II}}^{\circ}$ in phase II. For $t > 0$ diffusion takes place across the liquid–liquid interface. It is to be assumed that the solute is present only in small concentration in both phases, so that Fick's second law of diffusion is applicable. We therefore have to solve the equations

$$\frac{\partial c_{\mathrm{I}}}{\partial t} = \mathscr{D}_{\mathrm{I}}\frac{\partial^2 c_{\mathrm{I}}}{\partial z^2} \qquad -\infty < z < 0 \tag{20D.2-1}$$

$$\frac{\partial c_{\mathrm{II}}}{\partial t} = \mathscr{D}_{\mathrm{II}}\frac{\partial^2 c_{\mathrm{II}}}{\partial z^2} \qquad 0 < z < +\infty \tag{20D.2-2}$$

---

[6] R. A. T. O. Nijsing, *Absorptie van gassen in vloeistoffen, zonder en met chemische reactie*, Academisch Proefschrift, Technische Universiteit Delft (1957).

[7] P. A. M. Dirac, *Proc. Camb. Phil. Soc.*, **22**, Part II, 132–137 (1924). This was Dirac's first publication, written while he was a graduate student.

[8] R. B. Bird, *Advances in Chemical Engineering*, Vol. 1, Academic Press, New York (1956), pp. 156–239; errata, Vol. 2 (1958), p. 325. The result at the bottom of p. 207 is in error, since the factor of $(-1)^{n+1}$ is missing. See also H. S. Carslaw and J. C. Jaeger, *Conduction of Heat in Solids*, 2nd edition, Oxford University Press (1959), p. 129.

[9] S. P. S. Andrew, *Chem. Eng. Sci.*, **4**, 269–272 (1955).

in which c_I and c_{II} are the concentrations of A in phases I and II, and $\mathscr{D}_I$ and $\mathscr{D}_{II}$ are the corresponding diffusivities. The initial and boundary conditions are:

I. C. 1:	at $t = 0$,	$c_I = c_I^o$	(20D.2-3)
I. C. 2:	at $t = 0$,	$c_{II} = c_{II}^o$	(20D.2-4)
B. C. 1:	at $z = 0$,	$c_{II} = mc_I$	(20D.2-5)
B. C. 2:	at $z = 0$,	$-\mathscr{D}_I \frac{\partial c_I}{\partial z} = -\mathscr{D}_{II} \frac{\partial c_{II}}{\partial z}$	(20D.2-6)
B. C. 3:	at $z = -\infty$,	$c_I = c_I^o$	(20D.2-7)
B. C. 4:	at $z = +\infty$,	$c_{II} = c_{II}^o$	(20D.2-8)

The first boundary condition at $z = 0$ is the statement of equilibrium at the interface, m being the "distribution coefficient" or "Henry's law constant." The second boundary condition is a statement that the molar flux calculated at $z = 0^-$ is the same as that at $z = 0^+$; that is, there is no loss of A at the liquid–liquid interface.

(a) Solve the equations simultaneously by Laplace transform or other appropriate means to obtain:

$$\frac{c_I - c_I^o}{c_{II}^o - mc_I^o} = \frac{1 + \text{erf}(z/\sqrt{4\mathscr{D}_I t})}{m + \sqrt{\mathscr{D}_I/\mathscr{D}_{II}}} \tag{20D.2-9}$$

$$\frac{c_{II} - c_{II}^o}{c_I^o - (1/m)c_{II}^o} = \frac{1 - \text{erf}(z/\sqrt{4\mathscr{D}_{II} t})}{(1/m) + \sqrt{\mathscr{D}_{II}/\mathscr{D}_I}} \tag{20D.2-10}$$

(b) Obtain the expression for the mass transfer rate at the interface.

20D.3. Critical size of an autocatalytic system. It is desired to use the result of Example 20.1-3 to discuss the critical size of a system in which an "autocatalytic reaction" is occurring. In such a system the reaction products increase the rate of reaction. If the ratio of the system surface to the system volume is large, then the reaction products tend to escape from the boundaries of the system. If the surface to volume ratio is small, however, the rate of escape may be less than the rate of creation, and the reaction rate will increase rapidly. For a system of a given shape, there will be a critical size for which the rate of production just equals the rate of removal.

One example is that of nuclear fission. In a nuclear pile the rate of fission depends on the local neutron concentration. If neutrons are produced at a rate that exceeds the rate of escape by diffusion, the reaction is self-sustaining and a nuclear explosion occurs.

Similar behavior is also encountered in many chemical systems, although the behavior here is generally more complicated. An example is the thermal decomposition of acetylene gas, which is thermodynamically unstable according to the overall reaction.

$$\text{H} - \text{C} \equiv \text{C} - \text{H} \rightarrow \text{H}_2 + 2\text{C} \tag{20D.3-1}$$

This reaction appears to proceed by a branched-chain, free-radical mechanism, in which the free radicals behave qualitatively as the neutrons in the preceding paragraph, so that the decomposition is autocatalytic.

However, the free radicals are effectively neutralized by contact with an iron surface, so that the free-radical concentration is maintained near zero at such a surface. Acetylene gas can then be stored safely in an iron pipe below a "critical" diameter, which is smaller the higher the pressure or temperature of the gas. If the pipe is too large, the formation of even one free radical is likely to cause a rapidly increasing rate of decomposition, which may result in a serious explosion.

(a) Consider a system enclosed in a long cylinder in which the diffusion and reaction process is described by

$$\frac{\partial c_A}{\partial t} = \mathscr{D}_{AB} \frac{1}{r} \frac{\partial}{\partial r}\left(r \frac{\partial c_A}{\partial r}\right) + k_1''' c_A \tag{20D.3-2}$$

with $c_A = 0$ at $r = R$, and $c_A = f(r)$ at $t = 0$, in which $f(r)$ is some function of r. Use the result of Example 20.1-3 to get a solution for $c_A(r, t)$.

(b) Show that the critical radius for the system is

$$R_{\text{crit}} = \alpha_1 \sqrt{\frac{\mathscr{D}_{AB}}{k_1'''}} \tag{20D.3-3}$$

in which α_1 is the first zero of the zero-order Bessel function J_0.

(c) For a bare cylindrical nuclear reactor core,[10] the effective value of $k_1'''/\mathscr{D}_{AB}$ is 9×10^{-3} cm^{-2}. What is the critical radius?

Answer: **(c)** $R_{\text{crit}} = 25.3$ cm

20D.4. Dispersion of a broad pulse in steady, laminar axial flow in a tube. In the Taylor dispersion problem, consider a distributed solute pulse of substance A introduced into a tube of length L containing a fluid in steady, laminar flow. Now the inlet boundary condition is that

$$\text{at } t = 0, \qquad \frac{d}{dt} m_A = f(t) \tag{20D.4-1}$$

with the same constraints of negligible diffusion across the tube inlet and outlet as in Problem 20B.9. Note now that each element of solute acts independently of all the others.

(a) Using the result of Problem 20B.9, show that the exit concentration is given by

$$\langle \rho_A \rangle|_{z=L} = \frac{1}{\sqrt{4\pi R^4 \mathscr{D}_{AB}}} \int_{-\infty}^{t} f(t') \frac{\exp[-(L - \langle v_z \rangle (t - t'))/\sqrt{4\mathscr{D}_{AB}(t - t')}]}{\sqrt{t'}} dt' \tag{20D.4-2}$$

(b) Specialize this result for a square pulse:

$$f = f_0 \quad \text{for } 0 < t < t_0; \qquad f = 0 \quad \text{for } t > t_0 \tag{20D.4-3}$$

Sketch the result for several values of $\langle v_z \rangle t_0/L$.

20D.5. Velocity divergence in interfacially embedded coordinates. Consider a closed domain $D(u, w, y)$ in the interfacially embedded coordinates of Fig. 20.4-2.

(a) Integrate Eq. 20.4-7 over the boundary surface of D to obtain

$$\int_{S_D} (\mathbf{V} \cdot d\mathbf{S}_D) = \int_{S_D} (\mathbf{v} \cdot d\mathbf{S}_D) + \int_{S_D} \left(\frac{\partial \mathbf{r}(u, w, y, t)}{\partial t} \cdot d\mathbf{S}_D \right) \tag{20D.5-1}$$

in which $d\mathbf{S}_D$ is a vector element of area, having magnitude dS_D and the direction of the outward normal to the boundary of the domain D.

(b) The integrand of the last term is the velocity of the boundary element $d\mathbf{S}_D$. Hence, the last integral is the rate of change of the volume of D. Rewrite this integral accordingly with the aid of Eq. 20.4-3, giving

$$\begin{aligned} \int_{S_D} \left(\frac{\partial \mathbf{r}(u, w, y, t)}{\partial t} \cdot d\mathbf{S}_D \right) &= \frac{d}{dt} \int_D \sqrt{g(u, w, y, t)}\, du\, dw\, dy \\ &= \int_D \frac{\partial \sqrt{g(u, w, y, t)}}{\partial t} du\, dw\, dy \end{aligned} \tag{20D.5-2}$$

The second equality is obtained by the Leibniz rule, noting that u, w, and y are independent of t on each surface element $d\mathbf{S}_D$.

(c) Use the result of (b) and the Gauss–Ostrogradskii divergence theorem of §A.5 to express Eq. 20D.5-1 as the vanishing of a sum of three volume integrals over $D(u, w, y)$. Show that this result, and the arbitrariness of the choice of D, yield Eq. 20.4-8.

---

[10] R. L. Murray, *Nuclear Reactor Physics*, Prentice-Hall, Englewood Cliffs, N.J. (1957), pp. 23, 30, 53.

Chapter 21

Concentration Distributions in Turbulent Flow

In preceding chapters we have derived the equations for diffusion in a fluid or solid, and we have shown how one can obtain expressions for the concentration distribution, provided no fluid turbulence is involved. Next we turn our attention to mass transport in turbulent flow.

The discussion here is quite similar to that in Chapter 13, and much of that material can be taken over by analogy. Specifically, §§13.4, 13.5, and 13.6 can be taken over directly by replacing heat transfer quantities by mass transfer quantities. In fact, the problems discussed in those sections have been tested more meaningfully in mass transfer, since the range of experimentally accessible Schmidt numbers is considerably greater than that for Prandtl numbers.

We restrict ourselves here to isothermal binary systems, and make the assumption of constant mass density and diffusivity. Therefore the partial differential equation describing diffusion in a flowing fluid (Eq. 19.1-16) is of the same form as that for heat conduction in a flowing fluid (Eq. 11.2-9), except for the inclusion of the chemical reaction term in the former.

§21.1 CONCENTRATION FLUCTUATIONS AND THE TIME-SMOOTHED CONCENTRATION

The discussion in §13.1 about temperature fluctuations and time-smoothing can be taken over by analogy for the molar concentration c_A. In a turbulent stream, c_A will be a rapidly oscillating function that can be written as the sum of a time-smoothed value $\bar{c}_A$ and a turbulent concentration fluctuation c'_A

$$c_A = \bar{c}_A + c'_A \tag{21.1-1}$$

which is analogous to Eq. 13.1-1 for the temperature. By virtue of the definition of c'_A we see that $\overline{c'_A} = 0$. However, quantities such as $\overline{v'_x c'_A}$, $\overline{v'_y c'_A}$, and $\overline{v'_z c'_A}$ are not zero, because the local fluctuations in concentration and velocity are not independent of one another.

The time-smoothed concentration profiles $\bar{c}_A(x, y, z, t)$ are those measured, for example, by the withdrawal of samples from the fluid stream at various points and various

times. In tube flow with mass transfer at the wall, one expects that the time-smoothed concentration $\bar{c}_A$ will vary only slightly with position in the turbulent core, where the transport by turbulent eddies predominates. In the slowly moving region near the boundary surface, on the other hand, the concentration $\bar{c}_A$ will be expected to change within a small distance from its turbulent-core value to the wall value. The steep concentration gradient is then associated with the slow molecular diffusion process in the viscous sublayer in contrast to the rapid eddy transport in the turbulent core.

§21.2 TIME-SMOOTHING OF THE EQUATION OF CONTINUITY OF *A*

We begin with the equation of continuity for species A, which we presume is disappearing by an nth-order chemical reaction.[1] Equation 19.1-16 then gives, in rectangular coordinates,

$$\frac{\partial c_A}{\partial t} = -\left(\frac{\partial}{\partial x} v_x c_A + \frac{\partial}{\partial y} v_y c_A + \frac{\partial}{\partial z} v_z c_A\right) + \mathcal{D}_{AB}\left(\frac{\partial^2 c_A}{\partial x^2} + \frac{\partial^2 c_A}{\partial y^2} + \frac{\partial^2 c_A}{\partial z^2}\right) - k_n''' c_A^n \quad (21.2\text{-}1)$$

Here k_n''' is the reaction rate coefficient for the nth-order chemical reaction, and is presumed to be independent of position. In subsequent equations we shall consider $n = 1$ and $n = 2$ to emphasize the difference between reactions of first and higher order.

When c_A is replaced by $\bar{c}_A + c_A'$, and v_i by $\bar{v}_i + v_i'$, we obtain after time-averaging

$$\frac{\partial \bar{c}_A}{\partial t} = -\left(\frac{\partial}{\partial x} \bar{v}_x \bar{c}_A + \frac{\partial}{\partial y} \bar{v}_y \bar{c}_A + \frac{\partial}{\partial z} \bar{v}_z \bar{c}_A\right) - \underline{\left(\frac{\partial}{\partial x} \overline{v_x' c_A'} + \frac{\partial}{\partial y} \overline{v_y' c_A'} + \frac{\partial}{\partial z} \overline{v_z' c_A'}\right)}$$
$$+ \mathcal{D}_{AB}\left(\frac{\partial^2 \bar{c}_A}{\partial x^2} + \frac{\partial^2 \bar{c}_A}{\partial y^2} + \frac{\partial^2 \bar{c}_A}{\partial z^2}\right) - \begin{cases} k_1''' \bar{c}_A \\ k_2'''(\bar{c}_A^2 + \underline{\overline{c_A'^2}}) \end{cases} \text{ or} \quad (21.2\text{-}2)$$

Comparison of this equation with Eq. 21.2-1 indicates that the time-smoothed equation differs in the appearance of some extra terms, marked here with dashed underlines. The terms containing $\overline{v_i' c_A'}$ describe the turbulent mass transport and we designate them by $\bar{j}_{Ai}^{(t)}$, the ith component of the turbulent molar flux vector. We have now met the third of the turbulent fluxes, and we may summarize their components thus:

turbulent molar flux (vector)	$\bar{j}_{Ai}^{(t)} = \overline{v_i' c_A'}$	(21.2-3)
turbulent momentum flux (tensor)	$\bar{\tau}_{ij}^{(t)} = \rho \overline{v_i' v_j'}$	(21.2-4)
turbulent heat flux (vector)	$\bar{q}_i^{(t)} = \rho C_p \overline{v_i' T'}$	(21.2-5)

All of these are defined as fluxes with respect to the mass average velocity.

It is interesting to note that there is an essential difference between the behaviors of chemical reactions of different orders. The first-order reaction has the same form in the time-smoothed equation as in the original equation. The second-order reaction, on the other hand, contributes on time-smoothing an extra term $-k_2''' \overline{c_A'^2}$, this being the manifestation of the interaction between the chemical kinetics and the turbulent fluctuations.

We now summarize all three of the time-smoothed equations of change for turbulent flow of an isothermal, binary fluid mixture with constant ρ, $\mathcal{D}_{AB}$, and μ:

continuity	$(\nabla \cdot \bar{\mathbf{v}}) = 0$	(21.2-6)
motion	$\rho \frac{D\bar{\mathbf{v}}}{Dt} = -\nabla \bar{p} - [\nabla \cdot (\bar{\boldsymbol{\tau}}^{(v)} + \underline{\bar{\boldsymbol{\tau}}^{(t)}})] + \rho \mathbf{g}$	(21.2-7)
continuity of A	$\frac{D\bar{c}_A}{Dt} = -(\nabla \cdot (\bar{\mathbf{j}}_A^{(v)} + \underline{\bar{\mathbf{j}}_A^{(t)}})) - \begin{cases} k_1''' \bar{c}_A \\ k_2'''(\bar{c}_A^2 + \underline{\overline{c_A'^2}}) \end{cases}$ or	(21.2-8)

Here $\bar{\mathbf{j}}_A^{(v)} = -\mathcal{D}_{AB} \nabla \bar{c}_A$, and it is understood that the operator D/Dt is to be written with the time-smoothed velocity $\bar{\mathbf{v}}$ in it.

---

[1] S. Corrsin, *Physics of Fluids*, **1**, 42–47 (1958).

§21.3 SEMI-EMPIRICAL EXPRESSIONS FOR THE TURBULENT MASS FLUX

In the preceding section we showed that the time-smoothing of the equation of continuity of A gives rise to a turbulent mass flux, with components $\bar{j}_{Ai}^{(t)} = \overline{v_i' c_A'}$. To solve mass transport problems in turbulent flow, it may be useful to postulate a relation between $\bar{j}_{Ai}^{(t)}$ and the time-smoothed concentration gradient. A number of empirical expressions can be found in the literature, but we present here only the two most popular ones.

Eddy Diffusivity

By analogy with Fick's first law of diffusion, we may write

$$\bar{j}_{Ay}^{(t)} = -\mathscr{D}_{AB}^{(t)} \frac{d\bar{c}_A}{dy} \tag{21.3-1}$$

as the defining equation for the *turbulent diffusivity* $\mathscr{D}_{AB}^{(t)}$, also called the *eddy diffusivity*. As is the case with the eddy viscosity and the eddy thermal conductivity, the eddy diffusivity is not a physical property characteristic of the fluid, but depends on position, direction, and the nature of the flow field.

The eddy diffusivity $\mathscr{D}_{AB}^{(t)}$ and the eddy kinematic viscosity $\nu^{(t)} = \mu^{(t)}/\rho$ have the same dimensions—namely, length squared divided by time. Their ratio

$$\mathrm{Sc}^{(t)} = \frac{\nu^{(t)}}{\mathscr{D}_{AB}^{(t)}} \tag{21.3-2}$$

is a dimensionless quantity, known as the *turbulent Schmidt number*. As is the case with the turbulent Prandtl number, the turbulent Schmidt number is of the order of unity (see the discussion in §13.3). Thus the eddy diffusivity may be estimated by replacing it by the turbulent kinematic viscosity, about which a fair amount is known. This is done in §21.4, which follows.

The Mixing-Length Expression of Prandtl and Taylor

According to the mixing-length theory of Prandtl, momentum, energy, and mass are all transported by the same mechanism. Hence by analogy with Eqs. 5.4-4 and 13.3-3 we may write

$$\bar{j}_{Ay}^{(t)} = -l^2 \left| \frac{d\bar{v}_x}{dy} \right| \frac{d\bar{c}_A}{dy} \tag{21.3-3}$$

where l is the Prandtl mixing length introduced in Chapter 5. The quantity $l^2|d\bar{v}_x/dy|$ appearing here corresponds to $\mathscr{D}_{AB}^{(t)}$ of Eq. 21.3-1, and to the expressions for $\nu^{(t)}$ and $\alpha^{(t)}$ implied by Eqs. 5.4-4 and 13.3-3. Thus, the mixing-length theory satisfies the *Reynolds analogy* $\nu^{(t)} = \alpha^{(t)} = \mathscr{D}_{AB}^{(t)}$, or $\mathrm{Pr}^{(t)} = \mathrm{Sc}^{(t)} = 1$.

§21.4 ENHANCEMENT OF MASS TRANSFER BY A FIRST-ORDER REACTION IN TURBULENT FLOW[1]

We now examine the effect of the chemical reaction term in the turbulent diffusion equation. Specifically we study the effect of the reaction on the rate of mass transfer at the wall for steadily driven turbulent flow in a tube, where the wall (of material A) is slightly

[1] O. T. Hanna, O. C. Sandall, and C. L. Wilson, *Ind. Eng. Chem. Research*, **26**, 2286–2290 (1987). An analogous problem dealing with falling films is given by O. C. Sandall, O. T. Hanna, and F. J. Valeri, *Chem. Eng. Communications*, **16**, 135–147 (1982).

soluble in the fluid (a liquid B) flowing through the tube. Material A dissolves in liquid B and then disappears by a first-order reaction. We shall be particularly interested in the behavior with high Schmidt numbers and rapid reaction rates.

For tube flow with axial symmetry and with $\bar{c}_A$ independent of time, Eq. 21.2-8 becomes

$$\bar{v}_z \frac{\partial \bar{c}_A}{\partial z} = \frac{1}{r}\frac{\partial}{\partial r}\left(r(\mathcal{D}_{AB} + \mathcal{D}_{AB}^{(t)})\frac{\partial \bar{c}_A}{\partial r}\right) - k_1'''\bar{c}_A \tag{21.4-1}$$

Here we have made the customary assumption that the axial transport by both molecular and turbulent diffusion can be neglected. We want to find the mass transfer rate at the wall

$$+\mathcal{D}_{AB}\frac{\partial \bar{c}_A}{\partial r}\bigg|_{r=R} = k_c(c_{A0} - \bar{c}_{A,\text{axis}}) \tag{21.4-2}$$

where c_{A0} and $\bar{c}_{A,\text{axis}}$ are the concentrations of A at the wall and at the tube axis. As pointed out in the preceding section, the turbulent diffusivity is zero at the wall, and consequently does not appear in Eq. 21.4-2. The quantity k_c is a *mass transfer coefficient*, analogous to the heat transfer coefficient h. The coefficient h was discussed in Chapter 14 and mentioned in Chapter 9 in connection with "Newton's law of cooling." As a first approximation[1] we take $\bar{c}_{A,\text{axis}}$ to be zero, assuming that the reaction is sufficiently rapid that the diffusing species never reaches the tube axis; then $\partial \bar{c}_A/\partial r$ must also be zero at the tube axis. After analyzing the system under this assumption, we will relax the assumption and give computations for a wider range of reaction rates.

We now define the dimensionless reactant concentration $C = \bar{c}_A/c_{A0}$. Then under the further assumption[1] that, for large z, the concentration will be independent of z, Eq. 21.4-1 becomes

$$\frac{1}{r}\frac{\partial}{\partial r}\left(r(\mathcal{D}_{AB} + \mathcal{D}_{AB}^{(t)})\frac{\partial C}{\partial r}\right) = k_1'''C \tag{21.4-3}$$

This equation may now be multiplied by r and integrated from an arbitrary position to the tube wall to give

$$k_cR - r(\mathcal{D}_{AB} + \mathcal{D}_{AB}^{(t)})\frac{\partial C}{\partial r} = k_1'''\int_r^R \bar{r}C(\bar{r})d\bar{r} \tag{21.4-4}$$

Here the boundary conditions at $r = 0$ have been used, as well as the definition of the mass transfer coefficient. Then a second integration from $r = 0$ to $r = R$ gives

$$k_cR\int_0^R \frac{1}{r(\mathcal{D}_{AB} + \mathcal{D}_{AB}^{(t)})}dr - 1 = k_1'''\int_0^R \frac{1}{r(\mathcal{D}_{AB} + \mathcal{D}_{AB}^{(t)})}\left[\int_r^R \bar{r}C(\bar{r})d\bar{r}\right]dr \tag{21.4-5}$$

Here we have used the boundary conditions $C = 0$ at $r = 0$ and $C = 1$ at $r = R$.

Next we introduce the variable $y = R - r$, since the region of interest is right next to the wall. Then we get

$$k_cR\int_0^R \frac{1}{(R-y)(\mathcal{D}_{AB} + \mathcal{D}_{AB}^{(t)})}dy - 1 = k_1'''\int_0^R \frac{1}{(R-y)(\mathcal{D}_{AB} + \mathcal{D}_{AB}^{(t)})}\left[\int_0^y (R-\bar{y})C(\bar{y})d\bar{y}\right]dy \tag{21.4-6}$$

in which $C(\bar{y})$ is not the same function of $\bar{y}$ as $C(\bar{r})$ is of $\bar{r}$. For large Sc the integrands are important only in the region where $y << R$, so that $R - y$ may be safely approximated by R. Furthermore, we can use the fact that the turbulent diffusivity in the neighborhood

of the wall is proportional to the third power of the distance from the wall. When the integrals are rewritten in terms of $\sigma = y/R$, we get the dimensionless equation

$$\frac{1}{2}\left(\frac{k_c D}{\mathscr{D}_{AB}}\right)\left(\frac{\mathscr{D}_{AB}}{\nu}\right)\int_0^1 \frac{1}{(\mathscr{D}_{AB}/\nu) + K\sigma^3}\,d\sigma - 1 = \left(\frac{k_1''' R^2}{\nu}\right)\int_0^1 \frac{1}{(\mathscr{D}_{AB}/\nu) + K\sigma^3}\left[\int_0^\sigma C(\bar{\sigma})\,d\bar{\sigma}\right]d\sigma \tag{21.4-7}$$

This equation contains several dimensionless groupings: the Schmidt number $\mathrm{Sc} = \nu/\mathscr{D}_{AB}$, a dimensionless reaction-rate parameter $\mathrm{Rx} = k_1''' R^2/\nu$, and a dimensionless mass transfer coefficient $\mathrm{Sh} = k_c D/\mathscr{D}_{AB}$ known as the Sherwood number (D being the tube diameter).

In the limit that $\mathrm{Rx} \to \infty$, the solution to Eq. 21.4-3 under the given boundary conditions is $C = \exp(-\mathrm{Sh}\sigma/2)$. Substitution of this solution into Eq. 21.4-7 then gives after straightforward integration

$$\frac{1}{2}\frac{\mathrm{Sh}}{\mathrm{Sc}} I_0 - 1 = 2\frac{\mathrm{Rx}}{\mathrm{Sh}} I_0 - 2\frac{\mathrm{Rx}}{\mathrm{Sh}} I_1 \tag{21.4-8}$$

in which

$$I_0 = \int_0^1 \frac{1}{\mathrm{Sc}^{-1} + K\sigma^3}\,d\sigma \tag{21.4-9}$$

$$I_1 = \int_0^1 \frac{\exp(-\mathrm{Sh}\sigma/2)}{\mathrm{Sc}^{-1} + K\sigma^3}\,d\sigma \tag{21.4-10}$$

This can be solved[1] to give Sh as a function of Sc, Rx, and K.

The foregoing solution of Eq. 21.4-3 is reasonable when Sc, Rx, and z are sufficiently large, and is an improvement over the result given by Vieth, Porter and Sherwood.[2] However, in the absence of chemical reaction, Eq. 21.4-3 fails to describe the downstream increase of C caused by the transfer of species A into the fluid. Thus, the mass-transfer enhancement by the chemical reaction cannot be assessed realistically from the results of either Ref. 1 or Ref. 2.

For a better analysis of the enhancement problem, we use Eq. 21.4-1 to get a more complete differential equation for C:

$$\bar{v}_z \frac{\partial C}{\partial z} = \frac{1}{r}\frac{\partial}{\partial r}\left(r(\mathscr{D}_{AB} + \mathscr{D}_{AB}^{(t)})\frac{\partial C}{\partial r}\right) - k_1''' C \tag{21.4-11}$$

The assumption that $C = 0$ at $r = 0$ is then replaced by the zero-flux condition $\partial C/\partial r = 0$ there. We represent $\mathscr{D}_{AB}^{(t)}$ in this geometry as $l^2|d\bar{v}_z/dr|$ for fully developed flow, by use of a position-dependent mixing length l as in Eq. 21.3-3. Introducing dimensionless notations $v^+ = \bar{v}_z/v_*$, $z^+ = zv_*/\nu$, $r^+ = rv_*/\nu$, and $l^+ = lv_*/\nu$ based on the friction velocity $v_* = \sqrt{\tau_0/\rho}$ of §5.3, we can then express Eq. 21.4-11 in the dimensionless form

$$\begin{aligned} v^+\frac{\partial C}{\partial z^+} &= \frac{1}{r^+}\frac{\partial}{\partial r^+}\left(r^+\left(\frac{\mathscr{D}_{AB} + \mathscr{D}_{AB}^{(t)}}{\nu}\right)\frac{\partial C}{\partial r^+}\right) - \left[\frac{k_1'''\nu}{v_*^2}\right]C \\ &= \frac{1}{r^+}\frac{\partial}{\partial r^+}\left(r^+\left(\frac{1}{\mathrm{Sc}} + (l^+)^2\left|\frac{dv^+}{dr^+}\right|\right)\frac{\partial C}{\partial r^+}\right) - \mathrm{Da}\,C \end{aligned} \tag{21.4-12}$$

in which a Damkohler number $\mathrm{Da} = k_1'''\nu/v_*^2$ has been introduced.

An excellent model for the mixing length l is available in Eq. 5.4-7, developed by Hanna, Sandall, and Mazet[3] by modifying the model given by van Driest.[4] This model

---

[2] W. R. Vieth, J. H. Porter, and T. K. Sherwood, *Ind. Eng. Chem. Fundam.*, **2**, 1–3 (1963).

[3] O. T. Hanna, O. C. Sandall, and P. R. Mazet, *AIChE Journal*, **27**, 693–697 (1981).

[4] E. R. van Driest, *J. Aero. Sci.*, **23**, 1007–1011, 1036 (1956).

will give smooth concentration profiles, provided that we use a velocity function with continuous radial derivative, rather than the piecewise continuous expressions given in Fig. 5.5-3. Such a function is obtainable by integrating the differential equation

$$(l^+)^2\left(\frac{dv^+}{dy^+}\right)^2 + \frac{dv^+}{dy^+} = 1 - \frac{y^+}{R^+} \quad \text{for } 0 \leq y^+ \leq R^+ \tag{21.4-13}$$

in the dimensionless variables $v^+ = \bar{v}_z/v_*$ and $y^+ = yv_*/\nu$ of Fig. 5.5-3, with the boundary conditions $v^+ = 0$ at $y^+ = 0$ (the wall) and $dv^+/dy^+ = 0$ at $y^+ = R^+$ (the centerline). Equation 21.4-13 is obtained (see Problem 21B.5) by combining the cylindrical-coordinate versions of Eqs. 5.5-3 and 5.4-4 with the dimensionless form

$$l^+ = \frac{lv_*}{\nu} = 0.4y^+ \frac{1 - \exp(-y^+/26)}{\sqrt{1 - \exp(-0.26y^+)}} \quad \text{for } 0 \leq y^+ \leq R^+ \tag{21.4-14}$$

of the mixing-length model shown in Eq. 5.4-7. Equation 21.4-13 is solvable via the quadratic formula to give

$$\frac{dv^+}{dy^+} = \begin{cases} \dfrac{-1 + \sqrt{1 + 4(l^+)^2[1 - y^+/R^+]}}{2(l^+)^2} & \text{if } y^+ > 0; \\ 1 & \text{if } y^+ = 0 \end{cases} \tag{21.4-15}$$

and v^+ is then computable by quadrature using, for example, the subroutines trapzd and qtrap of Press et al.[5] The resulting v^+ function closely resembles the plotted line in Fig. 5.5-3, with small changes near $y^+ = 30$ where the plotted line has a slope discontinuity, and near the centerline where the calculated v^+ function attains a maximum value dependent on the dimensionless wall radius R^+ whereas the line in Fig. 5.5-3 improperly does not.

Equations 21.4-12 through 15 were solved numerically[6] for fully developed flow of a fluid of kinematic viscosity $\nu = 0.6581$ cm^2/s in a smooth tube of 3 cm inner diameter, at Re = 10,000, Sc = 200 and various Damkohler numbers Da. These calculations were done with the software package Athena Visual Workbench.[7] The resulting Sherwood numbers $\text{Sh} = k_cD/\mathcal{D}_{AB}$, based on k_c as defined in Eq. 21.4-2, are plotted in Fig. 21.4-1 as

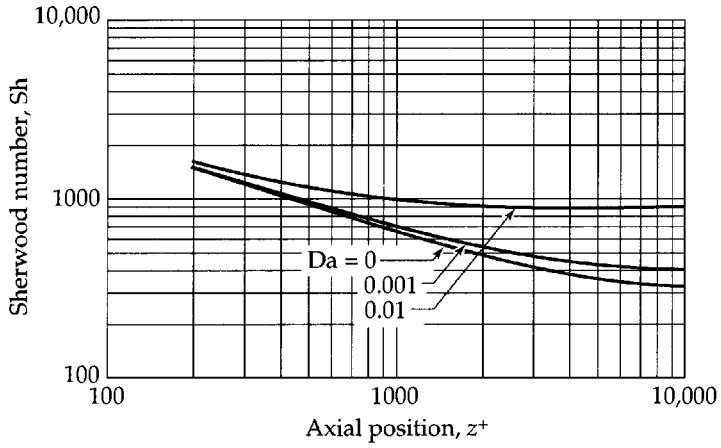

Fig. 21.4-1. Calculated Sherwood numbers, $\text{Sh} = k_cD/\mathcal{D}_{AB}$, for turbulent mass transfer from the wall of a tube, with and without homogeneous first-order chemical reaction. Results calculated at Re = 10,000 and Sc = 200, as functions of axial position $z^+ = zv_*/D$ and Damkohler number $\text{Da} = k_1'''\nu/v_*^2$.

[5] W. H. Press, S. A. Teukolsky, W. T. Vettering, and B. P. Flannery, *Numerical Recipes in FORTRAN*, Cambridge University Press, 2nd edition (1992).

[6] M. Caracotsios, personal communication.

[7] Information on this package is available at www.athenavisual.com and from stewart_associates.msn.com.

functions of z^+ for various values of the Damkohler number Da. These results lead to the following conclusions:

1. In the absence of reaction (that is, when Da = 0), the Sherwood number falls off rapidly with increasing distance into the mass-transfer region. This behavior is consistent with the results of Sleicher and Tribus[8] for a corresponding heat transfer problem, and confirms that the convection term of Eq. 21.4-11 is essential for this system. This term was neglected in References 2 and 3 by regarding the concentration profiles as "fully developed."
2. In the presence of a pseudo-first-order homogeneous reaction of the solute (that is, when Da > 0), the Sherwood number falls off downstream less rapidly, and ultimately attains a constant asymptote that depends on the Damkohler number. Thus, the enhancement factor, defined as Sh (with reaction)/Sh (without reaction), can increase considerably with increasing distance into the mass-transfer region.

§21.5 TURBULENT MIXING AND TURBULENT FLOW WITH SECOND-ORDER REACTION

We now consider processes occurring within turbulent fluid systems, with particular reference to the two mixers shown in Fig. 12.5-1. In Fig. 12.5-1(*a*) is shown a *steady state system*, in which two input streams enter a system of fixed geometry at constant rates, and in Fig. 12.5-1(*b*) an *unsteady state system*, in which two initially stationary, segregated, miscible fluids are mixed by turning an impeller at a constant angular velocity, starting at time $t = 0$. One stream [in (*a*)] or one initial region [in (*b*)] contains solute A in solvent S, and the other contains solute B in solvent S. All solutions are sufficiently dilute that the solutes do not appreciably affect the viscosity, density, or species diffusivities. Then the behavior of the solute (A or B) in either system [(*a*) or (*b*)] is described by the non-time-smoothed diffusion equations

$$\frac{Dc_A}{Dt} = \mathcal{D}_{AS}\nabla^2 c_A + R_A \qquad \frac{Dc_B}{Dt} = \mathcal{D}_{BS}\nabla^2 c_B + R_B \tag{21.5-1, 2}$$

with suitable initial and boundary conditions.

For these systems, we may write that at $z = 0$ [in (*a*)] or $t = 0$ [in (*b*)]

$$c_A = c_{A0} \quad \text{and} \quad c_B = 0 \tag{21.5-3, 4}$$

over the A inlet port [in (*a*)] or the initial region [in (*b*)], and

$$c_B = c_{B0} \quad \text{and} \quad c_A = 0 \tag{21.5-5, 6}$$

over the B inlet port [in (*a*)] or the initial region [in (*b*)]. In addition, we consider all confining surfaces to be inert and impenetrable.[1]

No Reaction Occurring

For this situation, the terms R_A and R_B are identically zero. We now define a single new independent variable

$$\Gamma = \frac{c_{A0} - c_A}{c_{A0}} = \frac{c_B}{c_{B0}} \tag{21.5-7}$$

---

[8] C. A. Sleicher and M. Tribus, *Trans. ASME*, **79**, 789–797 (1957).

[1] In system (*a*), these boundary conditions are only approximations. The indicated values of c_A and c_B are regarded as asymptotic values for $z << 0$.

Then both Eqs. 21.5-1 and 2 take the following form over the whole system:

$$\frac{D\Gamma}{Dt} = \mathcal{D}_{iS}\nabla^2\Gamma \tag{21.5-8}$$

Here the subscript i can represent either solute A or solute B, and

$$\Gamma = 0 \text{ for } (a) \text{ the entering } A\text{-rich stream, or} \quad (b) \text{ initially } A\text{-rich region} \tag{21.5-9}$$

$$\Gamma = 1 \text{ for } (a) \text{ the entering } B\text{-rich stream, or} \quad (b) \text{ initially } B\text{-rich region} \tag{21.5-10}$$

It follows that, for equal diffusivities, the time-smoothed concentration profiles, $\overline{\Gamma}(x, y, z, t)$ are identical for both solutes, where

$$\overline{\Gamma} = \frac{c_{A0} - \overline{c}_A}{c_{A0}} = \frac{\overline{c}_B}{c_{B0}} \tag{21.5-11}$$

However, the fluctuating quantities Γ' are also of interest, as they are measures of "unmixedness." These can be equal only in a statistical sense. To show this, we subtract Eq. 21.5-11 from Eq. 21.5-7, and then square the result and time-smooth it to give

$$\overline{\left(\frac{c'_A}{c_{A0}}\right)^2} = \overline{\left(\frac{c'_B}{c_{B0}}\right)^2} = d^2 \tag{21.5-12}$$

Here $d(x, y, z, t)$ is a dimensionless *decay function*, which decreases toward zero at large z [for the motionless mixer in Fig. 21.5-1(*a*)], or at large t [for the mixing tank of Fig. 21.5-1(*b*)]. Cross-sectional averages of this quantity can be measured, and are shown in Fig. 21.5-2.

It remains to determine the functional dependence of the decay function, and to do this we introduce the dimensionless variables:

$$\check{\mathbf{v}} = \frac{\mathbf{v}}{v_0}; \qquad \check{t} = \frac{v_0 t}{l_0}; \qquad \check{\nabla} = l_0\nabla \tag{21.5-13}$$

Then Eq. 21.5-8 becomes

$$\frac{D\Gamma}{D\check{t}} = \frac{1}{\text{ReSc}}\check{\nabla}^2\Gamma \tag{21.5-14}$$

in which $\text{Re} = l_0 v_0 \rho/\mu$.

In order to be able to draw specific conclusions, we now focus our attention on mixing tanks [see Fig. 21.5(*b*)], and further assume low-viscosity liquids and low-molecular-weight solutes. For these systems l_0 is normally chosen to be the diameter of the impeller, and v_0 to be $l_0 N$, where N is the rate of impeller rotation in revolutions per unit time.

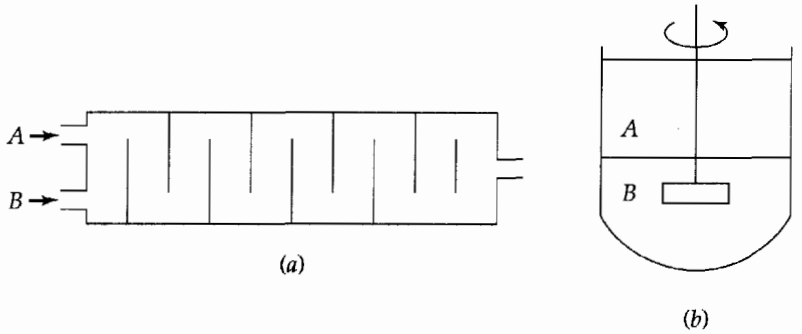

Fig. 21.5-1. Two types of mixers: (*a*) a baffled mixer with no moving parts; (*b*) a batch mixer with a stirrer.

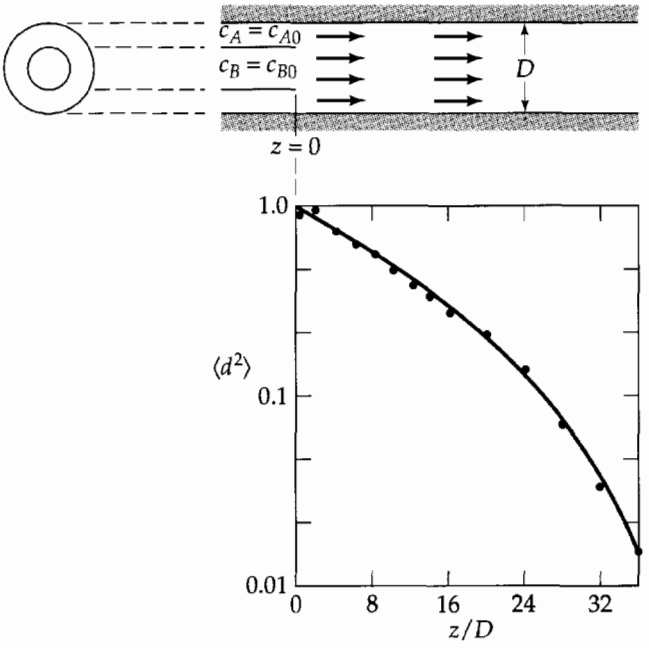

Fig. 21.5-2. The decay function for a specific device for the mixing of two streams emerging from a tube and from an annular region. This figure is patterned after one by E. L. Cussler, *Diffusion: Mass Transfer in Fluid Systems*, Cambridge University Press (1997), p. 422, based on data of R. S. Brodkey, *Turbulence in Mixing Operations*, Academic Press, New York (1975), p. 65, Fig. 6, upper curve. The radius of the outer tube is $\sqrt{2}$ times that of the inner one.

It is now useful to consider experience gained in the study of such systems and to classify the overall mixing process as follows:[2]

(i) *macromixing*, in which large-scale motions spread the *A*-rich and *B*-rich fluids over the entire tank region, into subregions that are large compared to the distances solute molecules have moved by diffusion.

(ii) *micromixing*, in which diffusion provides the final blending over scales of molecular dimensions.

It has been found[1] that macromixing is normally much the slower process, and this observation can be explained in terms of dimensional analysis. This finding is consistent with experience in large-scale mixing.

For industrial systems, Reynolds numbers are normally well over 10^4 and Schmidt numbers on the order of 10^5. The diffusion term in Eq. 21.5-14 thus tends to be small almost everywhere in the system. This term is negligible during the period of macromixing, where diffusion, and hence the Schmidt number, have no significant effect. Then for many practical purposes one may write

$$\frac{D\Gamma}{D\check{t}} \approx 0 \qquad (\mathrm{ReSc} >> 1) \tag{21.5-15}$$

We may then relax the requirement of equal diffusivities in extrapolating experience to a new system. It follows that Reynolds numbers as well as Schmidt numbers should have no significant effect on the macromixing process, and that the effective degree of unmixedness, d^2, depends mainly on the dimensionless time.

For large-scale mixing tanks, this prediction is amply confirmed.[3] These normally operate at large Reynolds numbers (typically greater than 10^4), where the large-scale motions, expressed in terms of $\check{\mathbf{v}}(\check{x}, \check{y}, \check{z}, \check{t})$, are observed to be independent of both Reynolds number and system size. Thus a very large number of investigators have observed using

---

[2] M. L. Hanks and H. L. Toor, *Ind. Eng. Chem. Res.*, **34**, 3252–3256 (1995).

[3] J. Y. Oldshue, *Fluid Mixing Technology*, McGraw-Hill, New York (1983); H. Benkreira, *Fluid Mixing*, Institution of Chemical Engineers, Rugby, UK, Vol. 4 (1990), Vol. 6 (1999); I. Bouwmans and H. E. A. van den Akker, in Vol. 4 of *Fluid Mixing*, Institution of Chemical Engineers, Rugby, UK (1990), pp. 1–12.

many different mixer geometries, that the product of the required mixing time t_{mix} and rotation rate N is a constant independent of mixer size and Reynolds number:

$$Nt_{mix} = K(\text{geometry}) \quad \text{or} \quad t_{mix} = K/N \tag{21.5-16}$$

That is, the required mixing time t_{mix} corresponds, for a given tank geometry, essentially to the required number of turns of the impeller. This expectation is confirmed by experience.

This finding is consistent with observations[2] that both the dimensionless volume flow rate through the impeller, Q/ND^3, and the tank friction factor, $P/\rho N^3 D^5$, are constants, depending only on the tank and impeller geometries (see Problem 6C.3). Here Q is the volumetric flow in the jet produced by the impeller, and P is the power required to turn it.

Similar remarks usually apply to motionless mixers, where increasing the flow velocities typically has little effect on the degree of mixing. However, approximations like this must be tested, and such tests should be considered as first steps in an experimental program. As a practical matter, these approximations are almost always reliable on scale-up, since Reynolds numbers normally increase with equipment size.

Reaction Occurring

We next consider the effects of a homogeneous, irreversible chemical reaction, and for simplicity we write this as $A + B \rightarrow$ products. Again we assume dilute solutions, so that the heat of reaction and the presence of reaction products have no significant effect. In addition, we assume equal diffusivities for the two solutes.

We next define

$$\Gamma_{\text{reaction}} = \frac{c_{A0} - (c_A - c_B)}{c_{A0} + c_{B0}} \tag{21.5-17}$$

Then when we subtract Eq. 21.5-2 from Eq. 21.5-1, we find that the description of Γ_{reaction} is identical to that for its nonreactive counterpart. Hence

$$\left(\frac{c_{A0} - (c_A - c_B)}{c_{A0} + c_{B0}}\right)_{\text{reactive}} = \left(\frac{c_{A0} - c_A}{c_{A0}}\right)_{\text{nonreactive}} \left(\frac{c_B}{c_{B0}}\right)_{\text{nonreactive}} \tag{21.5-18}$$

By subtracting from this its time-smoothed counterpart, we find that an equation like Eq. 21.5-18 must hold for the fluctuations:

$$\left(\frac{c'_A - c'_B}{c_{A0} + c_{B0}}\right)_{\text{reactive}} = \left(\frac{c'_A}{c_{A0}}\right)_{\text{nonreactive}} \tag{21.5-19}$$

The time-smoothed mean square of the quantity on the right side is equal to δ^2, which is measurable as illustrated in Fig. 21.5-2, and therefore we have a way of predicting the corresponding quantity for reacting systems.

Equation 21.5-19 suggests that the fluctuations in c_A and c_B in reactive problems occur on the same time and distance scales as for nonreactive problems. Note that this is true for arbitrary geometry, flow conditions, and reaction kinetics. We are now ready to consider special cases.

We begin with a *fast reaction*, for which the two solutes cannot coexist, and the rate of the reaction is controlled by the diffusion of the species toward each other. Then, for the first (macromixing) stage of the blending process, where diffusion is very slow compared to the larger-scale convective processes, there is no significant reaction. In this, typically dominant, stage of the blending process

$$\left(\frac{c'_A}{c_{A0}}\right)_{\text{reactive}} = \left(\frac{c'_A}{c_{A0}}\right)_{\text{nonreactive}} \tag{21.5-20}$$

It has been suggested[4] that Eq. 21.5-20 is also true for the micromixing stage. Where this can be assumed (e.g., in the common situation where macromixing is rate controlling), it follows that reactive and nonreactive processes lead to identical descriptions of solute fluctuations.

In practice, fast reactions (e.g., neutralization of acids with bases) are often used to determine the effectiveness of mixers, as these are much easier to follow experimentally than nonreactive mixing. Frequently one can use simple macroscopic measures such as temperature rise or an indicator color change. However, the measurement of concentration fluctuations can provide more insight into the nature and the course of the mixing process.

Slow reactions are also important, and we consider the special case of irreversible second-order kinetics, defined by

$$R_A = -k_2''' c_A c_B \tag{21.5-21}$$

When this is time-smoothed, we get

$$\overline{R}_A = -k'''(\bar{c}_A \bar{c}_B + \overline{c_A' c_B'}) \tag{21.5-22}$$

We find, therefore, that the fluctuations in solute concentration increase the time-smoothed reaction rate relative to that when a simple product of time-smoothed concentrations is used. It is, however, difficult to assess the practical importance of this effect.

We illustrate this point by a simple order-of-magnitude analysis, beginning with the definition of a reaction time constant t_A for one of the reactants, here solute A:

$$t_A = c_{A0}/R_A \tag{21.5-23}$$

To a first approximation, we may write

$$t_A \approx 1/k_2''' c_{B0} \tag{21.5-24}$$

Fast and slow reactions may then be defined as those for which

$$t_{\text{mix}} >> t_A \qquad \text{fast reaction} \tag{21.5-25}$$

$$t_{\text{mix}} << t_A \qquad \text{slow reaction} \tag{21.5-26}$$

We have already discussed the case of fast reaction. For slow reactions, turbulence has no significant effect, because fluctuations become negligible before any appreciable reaction has taken place.

If the mixing and reaction time constants are of the same order of magnitude, a deeper analysis than the above is needed. Such an analysis must include a model for the turbulent motion, and does not appear to be presently available.

QUESTIONS FOR DISCUSSION

1. Discuss the similarities and differences between turbulent heat and mass transport.
2. Discuss the behavior of first- and higher-order reactions in the time-smoothing of the equation of continuity for a given species. What are the consequences of this?
3. To what extent are the turbulent momentum flux, heat flux, and mass flux similar in form?
4. What empiricisms are available for describing the turbulent mass flux?
5. How can eddy diffusivities be measured, and on what do they depend?
6. Would you expect to get trustworthy results for mass transfer in turbulent tube flow without chemical reaction just by setting Rx = 0 in Eq. 21.4-8?

[4] K.-T. Li and H. L. Toor, *Ind. Eng. Chem. Fundam.*, **25**, 719–723 (1986).

PROBLEMS

21A.1. Determination of eddy diffusivity (Figs. 18C.1 and 21A.1). In Problem 18C.1 we gave the formula for the concentration profiles in diffusion from a point source in a moving stream. In isotropic highly turbulent flow, Eq. 18C.1-2 may be modified by replacing $\mathscr{D}_{AB}$ by the eddy diffusivity $\mathscr{D}_{AB}^{(t)}$. This equation has been found to be useful for determining the eddy diffusivity. The molar flow rate of carbon dioxide is 1/1000 that of air.

(a) Show that if one plots $\ln sc_A$ versus $s - z$ the slope is $-v_0/2\mathscr{D}_{AB}^{(t)}$.

(b) Use the data on the diffusion of CO_2 from a point source in a turbulent air stream shown in Fig. 21A.1 to get $\mathscr{D}_{AB}^{(t)}$ for these conditions: pipe diameter, 15.24 cm; $v_0 = 1512$ cm/s.

(c) Compare the value of $\mathscr{D}_{AB}^{(t)}$ with the molecular diffusivity $\mathscr{D}_{AB}$ for the system CO_2–air.

(d) List all assumptions made in the calculations.

Answer: **(b)** $\mathscr{D}_{AB}^{(t)} = 19$ cm^2/s

21A.2. Heat and mass transfer analogy. Write the mass transfer analog of Eq. 13.4-19. What are the limitations of the resulting equation?

21B.1. Wall mass flux for turbulent flow with no chemical reactions. Use the diffusional analog of Eq. 13.4-20 for turbulent flow in circular tubes, and the Blasius formula for the friction factor, to obtain the following expression for the Sherwood number,

$$\mathrm{Sh} = 0.0160\,\mathrm{Re}^{7/8}\,\mathrm{Sc}^{1/3} \tag{21B.1-1}$$

valid for large Schmidt numbers.[1]

21B.2. Alternate expressions for the turbulent mass flux. Seek an asymptotic expression for the turbulent mass flux for long circular tubes with a boundary condition of constant wall mass flux. Assume that the net mass transfer across the wall is small.

(a) Parallel the approach to laminar flow heat transfer in §10.8 to write

$$\Pi(\xi, \zeta) = -\frac{\omega_A - \omega_{A1}}{j_{A0}D/\rho\mathscr{D}_{AB}} = C_1\zeta + \Pi_\infty(\xi) + C_2 \tag{21B.2-1}$$

in which $\xi = r/D$, $\zeta = (z/D)/\mathrm{ReSc}$, ω_{A1} is the inlet mass fraction of A, and j_{A0} is the interfacial mass flux of A into the fluid.

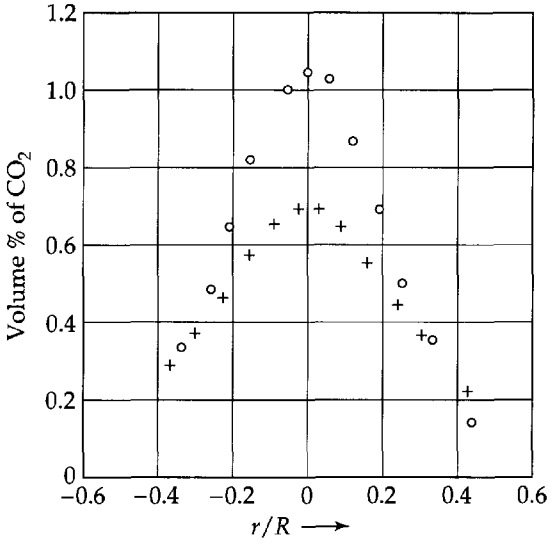

Fig. 21A.1. Concentration traverse data for CO_2 injected into a turbulent air stream with Re = 119,000 in a tube of diameter 15.24 cm. The circles are concentrations at a distance z = 112.5 cm downstream from the injection point, and the crosses are concentrations at z = 152.7 cm. [Experimental data are taken from W. L. Towle and T. K. Sherwood, *Ind. Eng. Chem.*, **31**, 457–462 (1939).]

[1] O. T. Hanna, O. C. Sandall, and C. L. Wilson, *Ind. Eng. Chem. Res.*, **28**, 2286–2290 (1987).

(b) Next use the equation of continuity for species A to obtain

$$-4\frac{v_z}{\langle v_z\rangle} = \frac{1}{\xi}\frac{d}{d\xi}\left[\left(1 + \frac{\mathrm{Sc}}{\mathrm{Sc}^{(t)}}\frac{\mu^{(t)}}{\mu}\right)\xi\frac{d\Pi_\infty}{d\xi}\right] \tag{21B.2-2}$$

in which $\mathrm{Sc}^{(t)} = \mu^{(t)}/\rho\mathscr{D}_{AB}^{(t)}$. This equation is to be integrated with the boundary conditions that Π_∞ is finite at $\xi = 0$ and $d\Pi_\infty/d\xi = -1$ at $\xi = \frac{1}{2}$.

(c) Integrate once with respect to ξ to obtain

$$-\frac{d\Pi_\infty}{d\xi} = \frac{\frac{1}{2} - 4\int_\xi^{1/2}(v_z/\langle v_z\rangle)\xi d\xi}{\xi[1 + (\mathrm{Sc}/\mathrm{Sc}^{(t)})(\mu^{(t)}/\mu)]} \tag{21B.2-3}$$

21B.3. An asymptotic expression for the turbulent mass flux.[1] Start with the final result of Problem 21B.2, and note that for sufficiently high Sc all curvature of the concentration profile will take place very near the wall, where $v_z/\langle v_z\rangle \approx 0$ and $\xi \approx \frac{1}{2}$. Assume that $\mathrm{Sc}^{(t)} = 1$ and use Eq. 5.4-2 to obtain

$$-\frac{d\Pi_\infty}{d\xi} = \frac{1}{[1 + \mathrm{Sc}(\mu^{(t)}/\mu)]} = \frac{1}{1 + \mathrm{Sc}(yv_*/14.5\nu)^3} \tag{21B.3-1}$$

Introduce the new coordinate $\eta = \mathrm{Sc}^{1/3}(yv_*/14.5\nu)$ into Eq. 21B.3-1 to get an equation for $d\Pi/d\eta$ valid within the laminar sublayer. Then integrate from $\eta = 0$ (where $\omega_A = \omega_{A0}$) to $\eta = \infty$ (where $\omega_A \approx \omega_{Ab}$) to obtain an explicit relation for the wall mass flux j_{A0}. Compare with the analog of Eq. 13.4-20 obtained in Problem 21A.2.

21B.4. Deposition of silver from a turbulent stream (Fig. 21B.3). An approximately 0.1 N solution of KNO_3 containing 1.00×10^{-6} g-equiv. $AgNO_3$ per liter is flowing between parallel Ag plates,

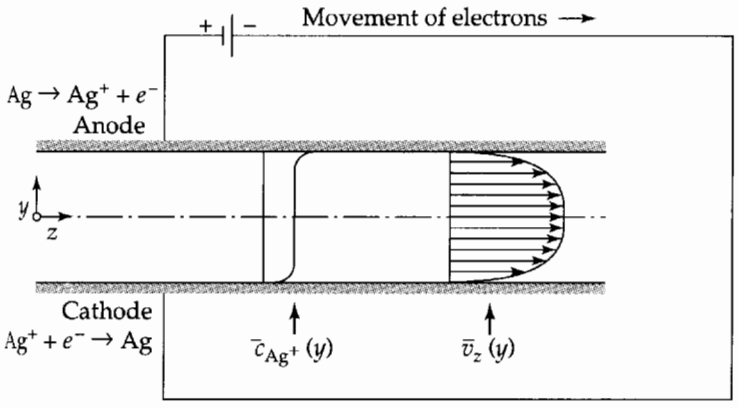

(*a*)

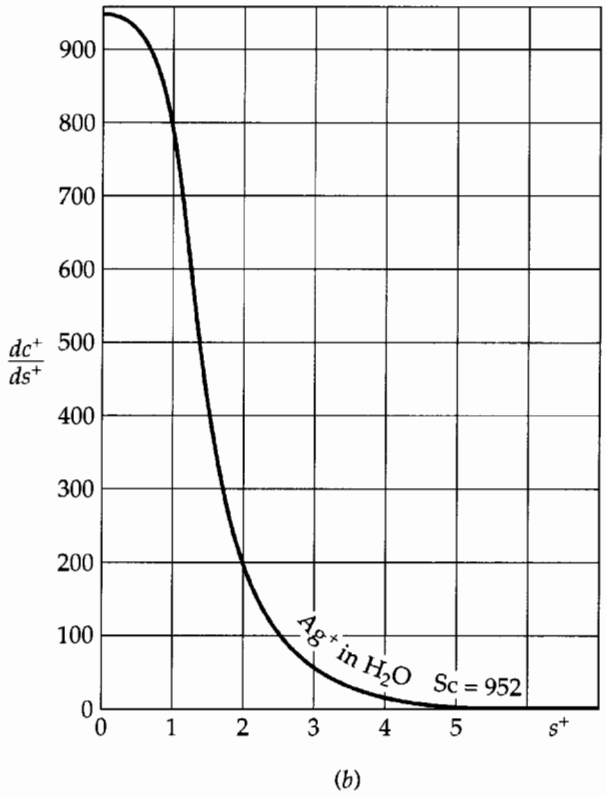

(*b*)

Fig. **21B.3.** (*a*) Electrodeposition of Ag^+ from a turbulent stream flowing in the positive z direction between two parallel plates. (*b*) Concentration gradients in electrodeposition of Ag at an electrode.

[1] C. S. Lin, R. W. Moulton, and G. L. Putnam, *Ind. Eng. Chem.*, **45**, 636 (1953).

as shown in Fig. 21B.3(*a*). A small voltage is applied across the plates to produce a deposition of Ag on the cathode (lower plate) and to polarize the circuit completely (that is, to maintain the Ag^+ concentration at the cathode very nearly zero). Forced diffusion may be ignored, and the Ag^+ may be considered to be moving to the cathode by ordinary (that is, Fickian) diffusion and eddy diffusion only. Furthermore, this solution is sufficiently dilute that the effects of the other ionic species on the diffusion of Ag^+ are negligible.

(a) Calculate the Ag^+ concentration profile, assuming that (i) the effective binary diffusivity of Ag^+ through water is 1.06×10^{-5} cm^2/s; (ii) the truncated Lin, Moulton, and Putnam expression of Eq. 5.4-2 for the turbulent velocity distribution in round tubes is valid for "slit flow" as well, if four times the hydraulic radius is substituted for the tube diameter; (iii) the plates are 1.27 cm apart, and $\sqrt{\tau_0/\rho}$ is 11.4 cm/s.

(b) Estimate the rate of deposition of Ag on the cathode, neglecting all other electrode reactions.

(c) Does the method of calculation in part (a) predict a discontinuous slope for the concentration profile at the center plane of the system? Explain.

Answers: **(a)** See Fig. 21B.3(*b*); **(b)** 6.7×10^{-12} equiv/cm$^2 \cdot$ s

21B.5. Mixing-length expression for the velocity profile.

(a) Start with Eq. 5.5-3, and show that for steadily driven, fully developed turbulent flow in a tube

$$\frac{\bar{\tau}_{rz}}{\tau_0} = \frac{r}{R} = 1 - \frac{y}{R} \tag{21B.5-1}$$

(b) Next set $\bar{\tau}_{rz} = \bar{\tau}_{rz}^{(v)} + \bar{\tau}_{rz}^{(t)}$, where $\bar{\tau}_{rz}^{(v)}$ is given by the cylindrical coordinate analog of Eq. 5.2-9, and $\bar{\tau}_{rz}^{(t)}$ by Eq. 5.5-5. Show that Eq. 21B.5-1 then becomes

$$\rho l^2 \left(\frac{d\bar{v}_z}{dy}\right)^2 + \mu\left(\frac{d\bar{v}_z}{dy}\right) = \tau_0\left(1 - \frac{y}{R}\right) \text{ for } 0 \leq y \leq R \tag{21B.5-2}$$

(c) Obtain Eq. 21.4-13 from Eq. 21B.5-2 by introducing the dimensionless symbols used in the former equation.

Chapter 22

Interphase Transport in Nonisothermal Mixtures

Here we build on earlier discussions of binary diffusion to provide means for predicting the behavior of mass transfer operations such as distillation, absorption, adsorption, extraction, drying, membrane filtrations, and heterogeneous chemical reactions. This chapter has many features in common with Chapters 6 and 14. It is particularly closely related to Chapter 14, because there are many situations where the analogies between heat and mass transfer can be regarded as exact.

There are, however, important differences between heat and mass transfer, and we will devote much of this chapter to exploring these differences. Since many mass transfer operations involve fluid–fluid interfaces, we have to deal with distortions of the interfacial shape by viscous drag and by surface tension gradients resulting from inhomogeneities in temperature and composition. In addition, there may be interactions between heat and mass transfer, and there may be chemical reactions occurring. Furthermore, at high mass transfer rates, the temperature and concentration profiles may be distorted. These effects complicate and sometimes invalidate the neat analogy between heat and mass transfer that one might otherwise expect.

In Chapter 14 the interphase heat transfer involved the movement of heat to or from a solid surface, or the heat transfer between two fluids separated by a solid surface. Here we will encounter heat and mass transfer between two contiguous phases: fluid–fluid or fluid–solid. This raises the question as to how to account for the resistance to diffusion provided by the fluids on both sides of the interface.

We begin the chapter by defining, in §22.1, the mass and heat transfer coefficients for binary mixtures in one phase (liquid or gas). Then in §22.2 we show how analytical solutions to diffusion problems lead to explicit expressions for mass transfer coefficients. In that section we give some analytic expressions for mass transfer coefficients at high

Schmidt numbers for a number of relatively simple systems. We emphasize the different behavior of systems with fluid–fluid and solid–fluid interfaces.

In §22.3 we show how dimensional analysis leads to predictions involving the Sherwood number (Sh) and the Schmidt number (Sc), which are the analogs of the Nusselt number (Nu) and the Prandtl number (Pr) defined in Chapter 14. Here the emphasis is on the analogies between heat transfer in pure fluids and mass transfer in binary mixtures. Then in §22.4 we proceed to the definition of mass transfer coefficients for systems with diffusion in two adjoining phases. We show there how to apply the information about mass transfer in single phases to the understanding of mass transfer between two phases.

Finally, in the last five sections of the chapter, we take up some effects that are peculiar to mass transfer systems: mass transfer with chemical reactions (§22.5), the interaction of heat and mass transfer processes in free convection (§22.6), the complicating factors of interfacial tension forces and Marangoni effects (§22.7), the distortions of temperature and concentration profiles that arise in systems with large net mass transfer rates across the interface (§22.8); and finally the matrix analysis of mass transport in multicomponent systems. In this chapter the emphasis is on the non-analogous behavior of heat and mass transfer systems.

In this chapter we have limited the discussion to a few key topics on mass transfer and transfer coefficient correlations. Further information is available in specialized textbooks on these and related topics.[1–4]

§22.1 DEFINITION OF TRANSFER COEFFICIENTS IN ONE PHASE

In this chapter we relate the rates of mass transfer across phase boundaries to the relevant concentration differences, mainly for binary systems. These relations are analogous to the heat transfer correlations of Chapter 14 and contain *mass transfer coefficients* in place of the heat transfer coefficients of that chapter. The system may have a true phase boundary, as in Fig. 22.1-1, 2, or 4, or an abrupt change in hydrodynamic properties, as in the system of Fig. 22.1-3, containing a porous solid. Figure 22.1-1 shows the evaporation of a volatile liquid, often used in experiments to develop mass transfer correlations. Figure 22.1-2 shows a permselective membrane, in which a selectively permeable surface permits more effective transport of solvent than of a solute that is to be retained, as in ultrafiltration of protein solutions and the desalting of sea water. Figure 22.1-3 shows a macroscopically porous solid, which can serve as a mass transfer surface or can provide sites for adsorption or reaction. Figure 22.1-4 shows an idealized liquid–vapor contactor where the mass transfer interface may be distorted by viscous or surface-tension forces.

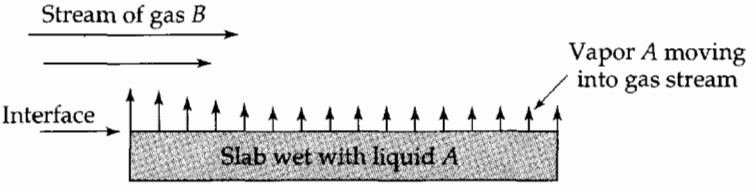

Fig. 22.1-1. Example of mass transfer across a plane boundary: drying of a saturated slab.

[1] T. K. Sherwood, R. L. Pigford, and C. R. Wilke, *Mass Transfer*, McGraw-Hill, New York (1975).

[2] R. E. Treybal, *Mass Transfer Operations*, 3rd edition, McGraw-Hill, New York (1980).

[3] E. L. Cussler, *Diffusion: Mass Transfer in Fluid Systems*, 2nd edition, Cambridge University Press (1997).

[4] D. E. Rosner, *Transport Processes in Chemically Reacting Flow Systems* (Unabridged), Dover, New York (2000).

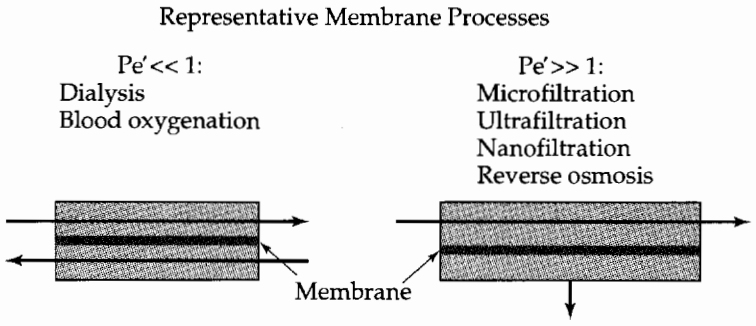

Fig. 22.1-2. Two rather typical kinds of membrane separators, classified here according to a Péclet number, $\text{Pé} = \delta v/\mathcal{D}_{\text{eff}}$, for the flow through the membrane. Here δ is the membrane thickness, v is the velocity at which solvent passes through the membrane, and $\mathcal{D}_{\text{eff}}$ is the effective solute diffusivity through the membrane. The heavy line represents the membrane, and the arrows represent the flow along or through the membrane.

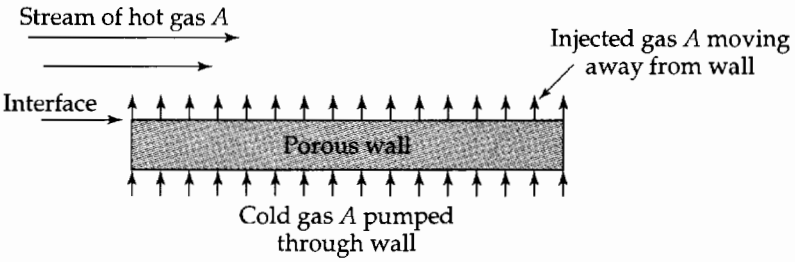

Fig. 22.1-3. Example of mass transfer through a porous wall: transpiration cooling.

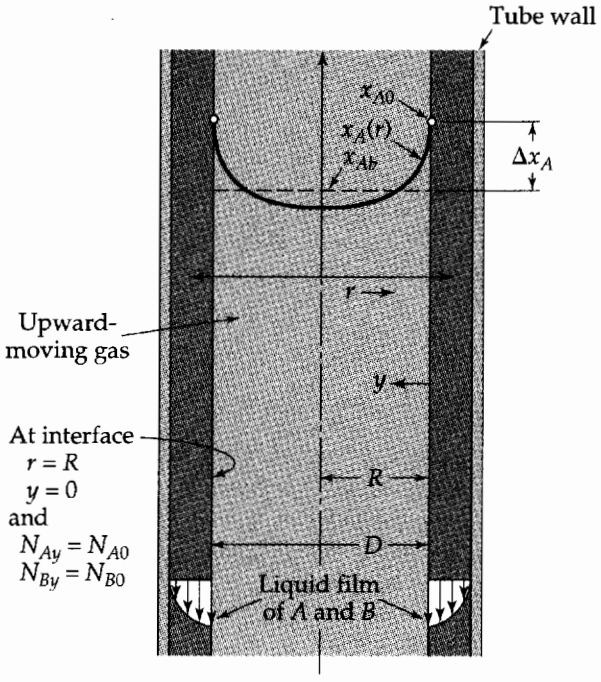

Fig. 22.1-4. Example of a gas–liquid contacting device: the wetted-wall column. Two chemical species A and B are moving from the downward-flowing liquid stream into the upward-flowing gas stream in a cylindrical tube.

In each of these systems, there will be both heat and mass transfer at the interface, and each of these fluxes will have a molecular (diffusive) and a convective term (here we have moved the convective term to the left side of the equation):

$$N_{A0} - x_{A0}(N_{A0} + N_{B0}) = -\left(c\mathscr{D}_{AB}\frac{\partial x_A}{\partial y}\right)\Bigg|_{y=0} \tag{22.1-1}$$

$$e_0 - (N_{A0}\overline{H}_{A0} + N_{B0}\overline{H}_{B0}) = -\left(k\frac{\partial T}{\partial y}\right)\Bigg|_{y=0} \tag{22.1-2}$$

These equations are just Eq. 18.0-1 and Eq. 19.3-6 written at the mass transfer interface ($y = 0$). They describe the interphase molar flux of species A and the interphase flux of energy (excluding the kinetic energy and the contribution from $[\boldsymbol{\tau} \cdot \mathbf{v}]$). Both N_{A0} and e_0 are defined as positive for transfer *into* the local phase except in §22.4 where the fluxes in each phase are defined as positive for transfer toward the liquid.

In Chapter 14 we defined the heat transfer coefficient in the absence of mass transfer by Eq. 14.1-1 ($Q = hA\,\Delta T$). For surfaces with mass and heat transfer, Eqs. 22.1-1 and 2 suggest that the following definitions are appropriate:

$$W_{A0} - x_{A0}(W_{A0} + W_{B0}) = k_{xA}A\,\Delta x_A \tag{22.1-3}$$

$$E_0 - (W_{A0}\overline{H}_{A0} + W_{B0}\overline{H}_{B0}) = hA\,\Delta T \tag{22.1-4}$$

Here W_{A0} is the number of moles of species A per unit time going through the transfer surface at $y = 0$, and E_0 is the total amount of energy going through the surface. The transfer coefficients k_{xA} and h are not defined until the area A and the driving forces Δx_A and ΔT have been specified. All the comments in Chapter 14 regarding these definitions may be taken over in this chapter, with the result that a subscript 1, ln, a, m, or loc can be added to make clear the type of driving force that is used. In this chapter, however, we shall mainly use the local transfer coefficients and occasionally the mean transfer coefficients. Also, in this chapter, molar fluxes of the species will be used, since in chemical engineering this is traditional. The relations between the mass-transfer expressions in molar and mass units are summarized in Table 22.2-1.

Local transfer coefficients are defined by writing Eqs. 22.1-3 and 4 for a differential area. Since $dW_{A0}/dA = N_{A0}$ and $dE_0/dA = e_0$, we get the definitions

$$N_{A0} - x_{A0}(N_{A0} + N_{B0}) = k_{xA,\text{loc}}\Delta x_A \tag{22.1-5}$$

$$e_0 - (N_{A0}\overline{H}_{A0} + N_{B0}\overline{H}_{B0}) = h_{\text{loc}}\Delta T \tag{22.1-6}$$

Next, we note that the left side of Eq. 22.1-5 is J^*_{A0}, and that the left side of a similar equation written for species B is J^*_{B0}. However, since $J^*_{A0} = -J^*_{B0}$ and $\Delta x_A = -\Delta x_B$, we find that $k_{xA,\text{loc}} = k_{xB,\text{loc}}$, and therefore we can write both mass transfer coefficients as $k_{x,\text{loc}}$, which has units of (moles)/(area)(time). Furthermore, if the heat of mixing is zero (as in ideal gas mixtures), we can replace $\overline{H}_{A0}$ by $\tilde{C}_{pA,0}(T_0 - T^\circ)$, where T° is an arbitrarily chosen reference temperature, as explained in Example 19.3-1. A similar replacement may be made for $\overline{H}_{B0}$. With these changes we get

$$N_{A0} - x_{A0}(N_{A0} + N_{B0}) = k_{x,\text{loc}}\Delta x_A \tag{22.1-7}$$

$$e_0 - (N_{A0}\tilde{C}_{pA,0} + N_{B0}\tilde{C}_{pB,0})(T_0 - T^\circ) = h_{\text{loc}}\Delta T \tag{22.1-8}$$

We remind the reader that rapid mass transfer across phase boundaries can distort the velocity, temperature, and concentration profiles, as we have already seen in §18.2 and in Example 19.4-1. The correlations provided in §22.2, as well as their analogs in Chapters 6 and 14, are all for small net mass-transfer rates, that is, for situations in which the convective terms in Eqs. 22.1-7 and 8 are negligible relative to the first term. Such situations are common, and most correlations in the literature suffer from the same limitation. In §22.8 we consider the deviations associated with high net mass-transfer rates and decorate the transfer coefficients at these conditions with a superscript "•" (see §22.8).

In much of the chemical engineering literature, the mass transfer coefficients are defined by

$$N_{A0} = k^0_{x,\text{loc}} \Delta x_A \tag{22.1-9}$$

The relation of this "apparent" mass transfer coefficient to that defined by Eq. 22.1-7 is

$$k^0_{x,\text{loc}} = \frac{k_{x,\text{loc}}}{[1 - x_{A0}(1 + r)]} \tag{22.1-10}$$

in which $r = N_{B0}/N_{A0}$. Other widely used mass transfer coefficients are defined by

$$N_{A0} = k^0_{c,\text{loc}} \Delta c_A \quad \text{and} \quad n_{A0} = k^0_{\rho,\text{loc}} \Delta \rho_A \tag{22.1-11}$$

for liquids and

$$N_{A0} = k^0_{p,\text{loc}} \Delta p_A \tag{22.1-12}$$

for gases. In the limit of low solute concentrations and low net mass transfer rates, for which most correlations have been obtained,

$$\lim_{x_{A0}(1+r)\to 0} \begin{Bmatrix} k^0_{x,\text{loc}} \\ ck^0_{c,\text{loc}} \\ pk^0_{p,\text{loc}} \\ \rho k^0_{\rho,\text{loc}} \end{Bmatrix} = k_{x,\text{loc}} \tag{22.1-13}$$

The superscript 0 indicates that these quantities are applicable only for *small mass-transfer rates* and *small mole fractions of species A*.

In many industrial contactors, the true interfacial area is not known. An example of such a system would be a column containing a random packing of irregular solid particles. In such a situation, one can define a volumetric mass transfer coefficient, $k_x a$, incorporating the interfacial area for a differential region of the column. The rate at which moles of species A are transferred to the interstitial fluid in a volume Sdz of the column is then given by

$$\begin{aligned} dW_{A0} &= (k_x a)(x_{A0} - x_{Ab}) S dz + x_{A0}(dW_{A0} + dW_{B0}) \\ &\approx (k^0_x a)(x_{A0} - x_{Ab}) S dz \end{aligned} \tag{22.1-14}$$

Here the interfacial area, a, per unit volume is combined with the mass transfer coefficient, S is the total column cross section, and z is measured in the primary flow direction. Correlations for predicting values of these coefficients are available, but they should be used with caution. Rarely do they include all the important parameters, and as a result they cannot be safely extrapolated to new systems. Furthermore, although they are usually described as "local," they actually represent a poorly defined average over a wide range of interfacial conditions.[1–5]

We conclude this section by defining a dimensionless group widely used in the mass-transfer literature and in the remainder of this book:

$$\text{Sh} = \frac{k_x l_0}{c\mathscr{D}_{AB}} \tag{22.1-15}$$

which is called the Sherwood number based on the characteristic length l_0. This quantity can be "decorated" with subscripts 1, a, m, ln, and loc in the same manner as h.

---

[1] J. Stichlmair and J. F. Fair, *Distillation Principles and Practice*, Wiley, New York (1998).

[2] H. Z. Kister, *Distillation Design*, McGraw-Hill, New York (1992).

[3] J. C. Godfrey and M. M. Slater, *Liquid–Liquid Extraction Equipment*, Wiley, New York (1994).

[4] R. H. Perry and D. W. Green, *Chemical Engineers' Handbook*, 8th edition, McGraw-Hill, New York (1997).

[5] J. E. Vivian and C. J. King, in *Modern Chemical Engineering* (A. Acrivos, ed.), Reinhold, New York (1963).

§22.2 ANALYTICAL EXPRESSIONS FOR MASS TRANSFER COEFFICIENTS

In the preceding chapters we obtained a number of analytical solutions for concentration profiles and for the associated molar fluxes. From these solutions we can now derive the corresponding mass transfer coefficients. These are usually presented in dimensionless form in terms of Sherwood numbers. We summarize these analytical expressions here for use in later sections of this chapter. All of the results given in this section are for systems with a slightly soluble component A, small diffusivities $\mathscr{D}_{AB}$, and small net mass-transfer rates, as defined in §§22.1 and 8. It may be helpful at this point to refer to Table 22.2-1, where the dimensionless groups for heat and mass transfer have been summarized.

Mass Transfer in Falling Films on Plane Surfaces

For the absorption of a slightly soluble gas A into a falling film of pure liquid B, we can put the result of Eq. 18.5-18 into the form of Eq. 22.1-3 (appropriately modified for molar concentration units in the manner of Eq. 22.1-11), thus

$$W_{A0} = \left(\sqrt{\frac{4\mathscr{D}_{AB}v_{\max}}{\pi L}}\right)(WL)(c_{A0} - 0) \equiv k^0_{c,m}A\Delta c_A \tag{22.2-1}$$

Table 22.2-1 Analogies Among Heat and Mass Transfer at Low Mass-Transfer Rates

	Heat transfer quantities (pure fluids)	Binary mass transfer quantities (isothermal fluids, molar units)	Binary mass transfer quantities (isothermal fluids, mass units)
Profiles	T	x_A	ω_A
Diffusivity	$\alpha = k/\rho\hat{C}_p$	$\mathscr{D}_{AB}$	$\mathscr{D}_{AB}$
Effect of profiles on density	$\beta = -\frac{1}{\rho}\left(\frac{\partial\rho}{\partial T}\right)_p$	$\xi = -\frac{1}{\rho}\left(\frac{\partial\rho}{\partial x_A}\right)_{p,T}$	$\zeta = -\frac{1}{\rho}\left(\frac{\partial\rho}{\partial\omega_A}\right)_{p,T}$
Flux	$\mathbf{q}$	$\mathbf{J}^*_A = \mathbf{N}_A + x_A(\mathbf{N}_A + \mathbf{N}_B)$	$\mathbf{j}_A = \mathbf{n}_A + \omega_A(\mathbf{n}_A + \mathbf{n}_B)$
Transfer rate	Q	$W_{A0} - x_{A0}(W_{A0} + W_{B0})$	$w_{A0} - \omega_{A0}(w_{A0} + w_{B0})$
Transfer coefficient	$h = \frac{Q}{A\,\Delta T}$	$k_x = \frac{W_{A0} - x_{A0}(W_{A0} + W_{B0})}{A\,\Delta x_A}$	$k_\omega = \frac{w_{A0} - \omega_{A0}(w_{A0} + w_{B0})}{A\,\Delta\omega_A}$
Dimensionless groups common to all three correlations	$\mathrm{Re} = l_0v_0\rho/\mu$ $\mathrm{Fr} = v_0^2/gl_0$	$\mathrm{Re} = l_0v_0\rho/\mu$ $\mathrm{Fr} = v_0^2/gl_0$	$\mathrm{Re} = l_0v_0\rho/\mu$ $\mathrm{Fr} = v_0^2/gl_0$
Dimensionless groups that are different	$\mathrm{Nu} = hl_0/k$ $\mathrm{Pr} = \hat{C}_p\mu/k$ $\mathrm{Gr} = l_0^3\rho^2g\beta\Delta T/\mu^2$ $\mathrm{Pé} = \mathrm{RePr} = l_0v_0\hat{C}_p/k$	$\mathrm{Sh} = k_xl_0/c\mathscr{D}_{AB}$ $\mathrm{Sc} = \mu/\rho\mathscr{D}_{AB}$ $\mathrm{Gr}_x = l_0^3\rho^2g\xi\Delta x_A/\mu^2$ $\mathrm{Pé} = \mathrm{ReSc} = l_0v_0/\mathscr{D}_{AB}$	$\mathrm{Sh} = k_\omega l_0/\rho\mathscr{D}_{AB}$ $\mathrm{Sc} = \mu/\rho\mathscr{D}_{AB}$ $\mathrm{Gr}_\omega = l_0^3\rho^2g\zeta\Delta\omega_A/\mu^2$ $\mathrm{Pé} = \mathrm{ReSc} = l_0v_0/\mathscr{D}_{AB}$
Chilton–Colburn j-factors	$j_H = \mathrm{NuRe}^{-1}\mathrm{Pr}^{-1/3} = \frac{h}{\rho\hat{C}_pv_0}\left(\frac{\hat{C}_p\mu}{k}\right)^{2/3}$	$j_D = \mathrm{ShRe}^{-1}\mathrm{Sc}^{-1/3} = \frac{k_x}{cv_0}\left(\frac{\mu}{\rho\mathscr{D}_{AB}}\right)^{2/3}$	$j_D = \mathrm{ShRe}^{-1}\mathrm{Sc}^{-1/3} = \frac{k_\omega}{\rho v_0}\left(\frac{\mu}{\rho\mathscr{D}_{AB}}\right)^{2/3}$

Notes: (a) The subscript 0 on l_0 and v_0 indicates the characteristic length and velocity respectively, whereas the subscript 0 on the mole (or mass) fraction and molar (or mass) flux means "evaluated at the interface." (b) All three of these Grashof numbers can be written as $\mathrm{Gr} = l_0^3\rho g\,\Delta\rho/\mu^2$, provided that the density change is caused only by a difference of temperature or composition.

Then, when the characteristic area is chosen to be the area of the interface WL, we see that

$$\mathrm{Sh}_m = \frac{k_{c,m}^0 L}{\mathscr{D}_{AB}} = \sqrt{\frac{4Lv_{\max}}{\pi \mathscr{D}_{AB}}} = \sqrt{\frac{4}{\pi}\left(\frac{Lv_{\max}\rho}{\mu}\right)\left(\frac{\mu}{\rho\mathscr{D}_{AB}}\right)}$$
$$= 1.128(\mathrm{ReSc})^{1/2} \tag{22.2-2}$$

This equation expresses the Sherwood number (the dimensionless mass transfer coefficient) in terms of the Reynolds number and the Schmidt number, with Re defined in terms of the maximum velocity $v_{\max}$ in the film and the film length L. The Reynolds number could also be defined in terms of the average film velocity with a different numerical coefficient.

Similarly, for the dissolution of a slightly soluble material A from the wall into a falling liquid film of pure B, we can put Eq. 18.6-10 into the form of Eq. 22.1-3 as follows:

$$W_{A0} = \left(\frac{2\mathscr{D}_{AB}}{\Gamma(\frac{7}{3})}\sqrt[3]{\frac{a}{9\mathscr{D}_{AB}L}}\right)(WL)(c_{A0} - 0) \equiv k_{c,m}^0 A\,\Delta c_A \tag{22.2-3}$$

Then, using the definition $a = \rho g\delta/\mu$ given just after Eq. 18.6-1 and the expression for the maximum velocity in the film in Eq. 2.2-19, we find the Sherwood number as follows:

$$\mathrm{Sh}_m = \frac{k_{c,m}^0 L}{\mathscr{D}_{AB}} = \frac{2}{\Gamma(\frac{7}{3})}\sqrt[3]{\frac{(2v_{\max}/\delta)L^2}{9\mathscr{D}_{AB}}} = \frac{1}{\Gamma(\frac{7}{3})}\sqrt[3]{\frac{16}{9}\left(\frac{L}{\delta}\right)\left(\frac{Lv_{\max}\rho}{\mu}\right)\left(\frac{\mu}{\rho\mathscr{D}_{AB}}\right)}$$
$$= 1.017\sqrt[3]{\left(\frac{L}{\delta}\right)}(\mathrm{ReSc})^{1/3} \tag{22.2-4}$$

In this instance we have not only the Reynolds number and Schmidt number appearing, but also the ratio of the film length to the film thickness.

These two problems—gas absorption by a falling film and the dissolution of a solid wall into a falling film—illustrate two important situations. In the first problem, there is no velocity gradient at the gas–liquid interface, and the quantity ReSc appears to the $\frac{1}{2}$-power in the expression for the Sherwood number. In the second problem, there is a velocity gradient at the solid–liquid interface, and the quantity ReSc appears to the $\frac{1}{3}$-power in the Sherwood number expression.

Mass Transfer for Flow Around Spheres

Next we consider the diffusion that occurs in the creeping flow around a spherical gas bubble and around a solid sphere of diameter D. This pair of systems parallels the two systems discussed in the previous subsection.

For the gas absorption from a gas bubble surrounded by a liquid in creeping flow, we can put Eq. 20.3-28 in the form of Eq. 22.1-5 thus:

$$N_{A0,\mathrm{avg}} = \sqrt{\frac{4}{3\pi}\frac{\mathscr{D}_{AB}v_\infty}{D}}\,(c_A - 0) \equiv k_{c,m}^0 \Delta c_A \tag{22.2-5}$$

The Sherwood number is then

$$\mathrm{Sh}_m = \frac{k_{c,m}^0 D}{\mathscr{D}_{AB}} = \sqrt{\frac{4}{3\pi}\frac{Dv_\infty}{\mathscr{D}_{AB}}} = \sqrt{\frac{4}{3\pi}\left(\frac{Dv_\infty\rho}{\mu}\right)\left(\frac{\mu}{\rho\mathscr{D}_{AB}}\right)}$$
$$= 0.6415(\mathrm{ReSc})^{1/2} \tag{22.2-6}$$

Here the Reynolds number is defined using the approach velocity v_∞ of the fluid (or, alternatively, the terminal velocity of the rising bubble).

For the creeping flow around a solid sphere with a slightly soluble coating that dissolves into the approaching fluid, we may modify the result in Eq. 12.4-34 to get

$$N_{A0,\text{avg}} = \frac{(3\pi)^{2/3}}{2^{7/3}\Gamma(\frac{4}{3})}\sqrt[3]{\frac{\mathscr{D}_{AB}^2 v_\infty}{D^2}}(c_A - 0) \equiv k^0_{c,m}\Delta c_A \tag{22.2-7}$$

This result may be rewritten in terms of the Sherwood number as

$$\text{Sh}_m = \frac{k^0_{c,m}D}{\mathscr{D}_{AB}} = \frac{(3\pi)^{2/3}}{2^{7/3}\Gamma(\frac{4}{3})}\sqrt[3]{\frac{Dv_\infty}{\mathscr{D}_{AB}}} = \frac{(3\pi)^{2/3}}{2^{7/3}\Gamma(\frac{4}{3})}\sqrt[3]{\left(\frac{Dv_\infty\rho}{\mu}\right)\left(\frac{\mu}{\rho\mathscr{D}_{AB}}\right)}$$
$$= 0.991(\text{ReSc})^{1/3} \tag{22.2-8}$$

As in the preceding subsection we have ReSc to the $\frac{1}{2}$-power for the gas–liquid system and ReSc to the $\frac{1}{3}$-power for the liquid–solid system.

Both Eq. 22.2-6 and Eq. 22.2-8 are valid only for creeping flow. However, they are not valid in the limit that Re goes to zero. As we know from Problem 10B.1 and Eq. 14.4-5, if there is no flow past the solid sphere or the spherical bubble, $\text{Sh}_m = 2$. It has been found that a satisfactory description of the mass transfer all the way down to Re = 0 can be obtained by using the simple superpositions: $\text{Sh}_m = 2 + 0.6415(\text{ReSc})^{1/2}$ and $\text{Sh}_m = 2 + 0.991(\text{ReSc})^{1/3}$ in lieu of Eqs. 22.2-6 and 8.

Mass Transfer in Steady, Nonseparated Boundary Layers on Arbitrarily Shaped Objects

For systems with a fluid-fluid interface and no velocity gradient at the interface, we found the mass flux at the surface to be given by Eq. 20.3-14:

$$N_{A0} = \sqrt{\frac{\mathscr{D}_{AB}}{\pi}\frac{h_z^2 v_s^2}{\int_0^x h_x h_z^2 v_s d\bar{x}}}(c_{A0} - 0) \equiv k^0_{c,\text{loc}}\Delta c_A \tag{22.2-9}$$

The local Sherwood number is

$$\text{Sh}_{\text{loc}} = \frac{k^0_{c,\text{loc}}l_0}{\mathscr{D}_{AB}} = \frac{1}{\sqrt{\pi}}(\text{ReSc})^{1/2}\sqrt{\frac{h_z^2 v_s^2}{\int_0^x h_x h_z^2 v_s d\bar{x}}\frac{l_0}{v_0}} \tag{22.2-10}$$

in which the constant, $1/\sqrt{\pi}$, is equal to 0.5642 and $\text{Re} = l_0 v_0 \rho/\mu$.

Similarly for systems with fluid–solid interfaces and a velocity gradient at the interface, the mass flux expression is given in Eq. 20.3-26 as

$$N_{A0} = \frac{\mathscr{D}_{AB}}{\Gamma(\frac{4}{3})}\sqrt[3]{\frac{(h_z\beta)^{3/2}}{9\mathscr{D}_{AB}\int_0^x \sqrt{h_z\beta}\, h_x h_z dx}}(c_{A0} - 0) \equiv k^0_{c,\text{loc}}\Delta c_A \tag{22.2-11}$$

The analogous Sherwood number expression is

$$\text{Sh}_{\text{loc}} = \frac{k^0_{c,\text{loc}}l_0}{\mathscr{D}_{AB}} = \frac{1}{9^{1/3}\Gamma(\frac{4}{3})}(\text{ReSc})^{1/3}\sqrt[3]{\frac{(h_z\beta)^{3/2}}{\int_0^x \sqrt{h_z\beta}\, h_x h_z dx}\frac{l_0^2}{v_0}} \tag{22.2-12}$$

where the numerical coefficient has the value 0.5384. In these equations l_0 and v_0 are a characteristic length and a characteristic velocity that can be chosen after the shape of the body has been defined. Here again we see that the $\frac{1}{2}$-power on ReSc appears in the fluid–fluid system, and the $\frac{1}{3}$-power on ReSc appears in the fluid–solid system—regardless of the shape. The radicands of the Sherwood number expressions are dimensionless.

Mass Transfer in the Neighborhood of a Rotating Disk

For a disk of diameter D coated with a slightly soluble material A rotating with angular velocity Ω in a large region of liquid B, the mass flux at the surface of the disk is independent of position. According to Eq. 19D.4-7 we have

$$N_{A0} = 0.620\left(\frac{\mathscr{D}_{AB}^{2/3}\Omega^{1/2}}{\nu^{1/6}}\right)(c_{A0} - 0) \equiv k_{c,m}^{0}\Delta c_A \tag{22.2-13}$$

This may be expressed in terms of the Sherwood number as

$$\mathrm{Sh}_m = \frac{k_{c,m}^{0}D}{\mathscr{D}_{AB}} = 0.620\left(\frac{D\Omega^{1/2}\rho^{1/6}}{\mathscr{D}_{AB}^{1/3}\mu^{1/6}}\right) = 0.620\sqrt{\frac{D(D\Omega)\rho}{\mu}}\sqrt[3]{\frac{\mu}{\rho\mathscr{D}_{AB}}}$$
$$= 0.620\,\mathrm{Re}^{1/2}\mathrm{Sc}^{1/3} \tag{22.2-14}$$

Here the characteristic velocity in the Reynolds number is chosen to be $D\Omega$.

§22.3 CORRELATION OF BINARY TRANSFER COEFFICIENTS IN ONE PHASE

In this section we show that correlations for binary mass transfer coefficients at low mass-transfer rates can be obtained directly from their heat transfer analogs simply by a change of notation. These correspondences are quite useful, and many heat transfer correlations have, in fact, been obtained from their mass transfer analogs.

To illustrate the background of these useful analogies and the conditions under which they apply, we begin by presenting the diffusional analog of the dimensional analysis given in §14.3. Consider the steadily driven, laminar or turbulent isothermal flow of a liquid solution of A in B, in the tube shown in Fig. 22.3-1. The fluid enters the tube at $z = 0$ with velocity uniform out to very near the wall and with a uniform inlet composition x_{A1}. From $z = 0$ to $z = L$, the tube wall is coated with a solid solution of A and B, which dissolves slowly and maintains the interfacial liquid composition constant at x_{A0}. For the moment we assume that the physical properties ρ, μ, c, and $\mathscr{D}_{AB}$ are constant.

The mass transfer situation just described is mathematically analogous to the heat transfer situation described at the beginning of §14.3. To emphasize the analogy, we present the equations for the two systems together. Thus the rate of heat addition by conduction between 1 and 2 in Fig. 14.3-1 and the molar rate of addition of species A by

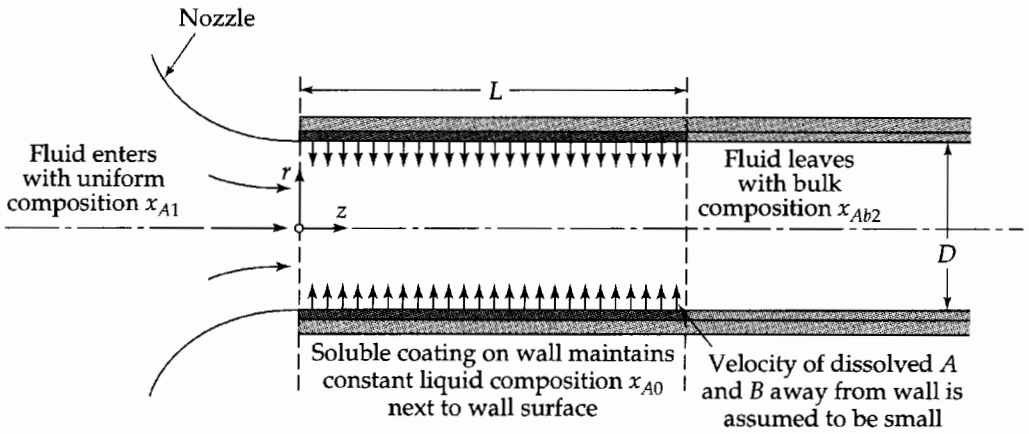

Fig. 22.3-1. Mass transfer in a pipe with a soluble wall.

diffusion between 1 and 2 in Fig. 22.3-1 are given by the following expressions, valid for either laminar or turbulent flow:

heat transfer:
$$Q(t) = \int_0^L \int_0^{2\pi} \left(+k \frac{\partial T}{\partial r}\bigg|_{r=R} \right) R \, d\theta \, dz \tag{22.3-1}$$

mass transfer:
$$W_{A0}(t) - x_{A0}(W_{A0}(t) + W_{B0}(t)) = \int_0^L \int_0^{2\pi} \left(+c\mathcal{D}_{AB} \frac{\partial x_A}{\partial r}\bigg|_{r=R} \right) R \, d\theta \, dz \tag{22.3-2}$$

Equating the left sides of these equations to $h_1(\pi DL)(T_0 - T_1)$ and $k_{x1}(\pi DL)(x_{A0} - x_{A1})$ respectively, we get for the transfer coefficients

heat transfer:
$$h_1(t) = \frac{1}{\pi DL(T_0 - T_1)} \int_0^L \int_0^{2\pi} \left(+k \frac{\partial T}{\partial r}\bigg|_{r=R} \right) R \, d\theta \, dz \tag{22.3-3}$$

mass transfer:
$$k_{x1}(t) = \frac{1}{\pi DL(x_{A0} - x_{A1})} \int_0^L \int_0^{2\pi} \left(+c\mathcal{D}_{AB} \frac{\partial x_A}{\partial r}\bigg|_{r=R} \right) R \, d\theta \, dz \tag{22.3-4}$$

We now introduce the dimensionless variables $\check{r} = r/D$, $\check{z} = z/D$, $\check{T} = (T - T_0)/(T_1 - T_0)$, and $\check{x}_A = (x_A - x_{A0})/(x_{A1} - x_{A0})$ and rearrange to obtain

heat transfer:
$$\mathrm{Nu}_1(t) = \frac{h_1 D}{k} = \frac{1}{2\pi L/D} \int_0^{L/D} \int_0^{2\pi} \left(-\frac{\partial \check{T}}{\partial \check{r}}\bigg|_{\check{r}=\frac{1}{2}} \right) d\theta \, d\check{z} \tag{22.3-5}$$

mass transfer:
$$\mathrm{Sh}_1(t) = \frac{k_{x1} D}{c\mathcal{D}_{AB}} = \frac{1}{2\pi L/D} \int_0^{L/D} \int_0^{2\pi} \left(-\frac{\partial \check{x}_A}{\partial \check{r}}\bigg|_{\check{r}=\frac{1}{2}} \right) d\theta \, d\check{z} \tag{22.3-6}$$

Here Nu is the Nusselt number for heat transfer without mass transfer, and Sh is the Sherwood number for isothermal mass transfer at small mass-transfer rates. The Nusselt number is a dimensionless temperature gradient integrated over the surface, and the Sherwood number is a dimensionless concentration gradient integrated over the surface.

These gradients can, in principle, be evaluated from Eqs. 11.5-7, 8, and 9 (for heat transfer) and Eqs. 19.5-8, 9, and 11 (for mass transfer), under the following boundary conditions (with $\check{\mathbf{v}}$ and $\check{\mathcal{P}}$ defined as in §14.3 and with time averaging of the solutions if the flow is turbulent):

velocity and pressure:

$$\text{at } \check{z} = 0, \check{\mathbf{v}} = \boldsymbol{\delta}_z \qquad \text{for } 0 \le \check{r} < \tfrac{1}{2} \tag{22.3-7}$$
$$\text{at } \check{r} = \tfrac{1}{2}, \check{\mathbf{v}} = 0 \qquad \text{for } \check{z} \ge 0 \tag{22.3-8}$$
$$\text{at } \check{r} = 0 \text{ and } \check{z} = 0, \check{\mathcal{P}} = 0 \tag{22.3-9}$$

temperature:

$$\text{at } \check{z} = 0, \check{T} = 1 \qquad \text{for } 0 \le r < \tfrac{1}{2} \tag{22.3-10}$$
$$\text{at } \check{r} = \tfrac{1}{2}, \check{T} = 0 \qquad \text{for } 0 \le z \le L/D \tag{22.3-11}$$

concentration:

$$\text{at } \check{z} = 0, \check{x}_A = 1 \qquad \text{for } 0 \le r < \tfrac{1}{2} \tag{22.3-12}$$
$$\text{at } \check{r} = \tfrac{1}{2}, \check{x}_A = 0 \qquad \text{for } 0 \le z \le L/D \tag{22.3-13}$$

The boundary condition in Eq. 22.3-8, on the velocity at the wall, is accurate for the heat-transfer system and also for the mass-transfer system provided that $x_{A0}(W_{A0} + W_{B0})$ is small; the latter criterion is discussed in §§22.1 and 8. No boundary conditions are needed at the outlet plane, $z = L/D$, when we neglect the $\partial^2/\partial z^2$ terms of the conservation equations in the manner of §4.4 and §14.3.

If we can neglect the heat production by viscous dissipation in Eq. 11.5-9 and if there is no production of A by chemical reaction as in Eq. 19.5-11, then the differential equations for heat and mass transport are analogous along with the boundary conditions. It follows then that the dimensionless profiles of temperature and concentration (time smoothed, when necessary) are similar,

$$\check{T} = F(\check{r}, \theta, \check{z}, \text{Re}, \text{Pr}); \qquad \check{x}_A = F(\check{r}, \theta, \check{z}, \text{Re}, \text{Sc}) \tag{22.3-14, 15}$$

with the same form of F in both systems. Thus, to get the concentration profiles from the temperature profiles, one replaces $\check{T}$ by $\check{x}_A$ and Pr by Sc.

Finally, inserting the profiles into Eqs. 22.3-5 and 6 and performing the integrations and then time-averaging give for *forced convection*

$$\text{Nu}_1 = G(\text{Re}, \text{Pr}, L/D); \qquad \text{Sh}_1 = G(\text{Re}, \text{Sc}, L/D) \tag{22.3-16, 17}$$

Here G is the same function in both equations. The same formal expression is obtained for Nu_a, Nu_{ln}, Nu_{loc} as well as for the corresponding Sherwood numbers. This important analogy permits one to write down a mass transfer correlation from the corresponding heat transfer correlation merely by replacing Nu by Sh, and Pr by Sc. The same can be done for any geometry and for both laminar and turbulent flow. Note, however, that to get this analogy one has to assume (i) constant physical properties, (ii) small net mass-transfer rates, (iii) no chemical reactions, (iv) no viscous dissipation heating, (v) no absorption or emission of radiant energy, and (vi) no pressure diffusion, thermal diffusion, or forced diffusion. Some of these effects will be discussed in subsequent sections of this chapter; others will be treated in Chapter 24.

For *free convection* around objects of any given shape, a similar analysis shows that

$$\text{Nu}_m = H(\text{Gr}, \text{Pr}); \qquad \text{Sh}_m = H(\text{Gr}_x, \text{Sc}) \tag{22.3-18, 19}$$

Here H is the same function in both cases, and the Grashof numbers for both processes are defined analogously (see Table 22.2-1 for a summary of the analogous quantities for heat and mass transfer).

To allow for the variation of physical properties in mass transfer systems, we extend the procedures introduced in Chapter 14 for heat transfer systems. That is, we generally evaluate the physical properties at some kind of mean film composition and temperature, except for the viscosity ratio μ_b/μ_0.

We now give three illustrations of how to "translate" from heat transfer to mass transfer correlations:

Forced Convection Around Spheres

For forced convection around a solid sphere, Eq. 14.4-5 and its mass-transfer analog are:

$$\text{Nu}_m = 2 + 0.60\,\text{Re}^{1/2}\,\text{Pr}^{1/3}; \qquad \text{Sh}_m = 2 + 0.60\,\text{Re}^{1/2}\,\text{Sc}^{1/3} \tag{22.3-20, 21}$$

Equations 22.3-20 and 21 are valid for constant surface temperature and composition, respectively, and for small net mass-transfer rates. They may be applied to simultaneous heat and mass transfer under restrictions (i)–(vi) given after Eq. 22.3-17.

Forced Convection along a Flat Plate

As another illustration of the use of analogies, we can cite the extension of Eq. 14.4-4 for the laminar boundary layer along a flat plate, to include mass transfer:

$$j_{H,\text{loc}} = j_{D,\text{loc}} = \tfrac{1}{2} f_{\text{loc}} = 0.332\,\text{Re}_x^{-1/2} \tag{22.3-22}$$

The Chilton–Colburn j-factors, one for heat transfer and one for diffusion, are defined as[1]

$$j_{H,\text{loc}} = \frac{\text{Nu}_{\text{loc}}}{\text{RePr}^{1/3}} = \frac{h_{\text{loc}}}{\rho \hat{C}_p v_\infty} \left(\frac{\hat{C}_p \mu}{k} \right)^{2/3} \tag{22.3-23}$$

$$j_{D,\text{loc}} = \frac{\text{Sh}_{\text{loc}}}{\text{ReSc}^{1/3}} = \frac{k_{x,\text{loc}}}{c v_\infty} \left(\frac{\mu}{\rho \mathcal{D}_{AB}} \right)^{2/3} \tag{22.3-24}$$

The three-way analogy in Eq. 22.3-22 is accurate for Pr and Sc near unity (see Table 12.4-1) within the limitations mentioned after Eq. 22.3-17. For flow around other objects, the friction factor part of the analogy is not valid because of the form drag, and even for flow in circular tubes the analogy with $\frac{1}{2} f_{\text{loc}}$ is only approximate (see §14.4).

The Chilton–Colburn Analogy

The more widely applicable empirical analogy

$$j_H = j_D = \text{a function of Re, geometry, and boundary conditions} \tag{22.3-25}$$

has proven to be useful for transverse flow around cylinders, flow through packed beds, and flow in tubes at high Reynolds numbers. For flow in ducts and packed beds, the "approach velocity" v_∞ has to be replaced by the interstitial velocity or the superficial velocity. Equation 22.3-25 is the usual form of the *Chilton–Colburn analogy*. It is evident from Eqs. 22.3-20 and 21, however, that the analogy is valid for flow around spheres only when Nu and Sh are replaced by (Nu − 2) and (Sh − 2).

It would be very misleading to leave the impression that all mass transfer coefficients can be obtained from the analogous heat transfer coefficient correlations. For mass transfer we encounter a much wider variety of boundary conditions and other ranges of the relevant variables. Non-analogous behavior is addressed in §§22.5-8.

EXAMPLE 22.3-1

Evaporation from a Freely Falling Drop

A spherical drop of water, 0.05 cm in diameter, is falling at a velocity of 215 cm/s through dry, still air at 1 atm pressure with no internal circulation. Estimate the instantaneous rate of evaporation from the drop, when the drop surface is at T_0 = 70°F and the air (far from the drop) is at T_∞ = 140°F. The vapor pressure of water at 70°F is 0.0247 atm. Assume quasi-steady state conditions.

SOLUTION

Designate water as species A and air as species B. The solubility of air in water may be neglected, so that $W_{B0} = 0$. Then assuming that the evaporation rate is small, we may write Eq. 22.1-3 for the entire spherical surface as

$$W_{A0} = k_{xm}(\pi D^2) \frac{x_{A0} - x_{A\infty}}{1 - x_{A0}} \tag{22.3-26}$$

The mean mass transfer coefficient, k_{xm}, may be predicted from Eq. 22.3-21 in the assumed absence of internal circulation.

The film conditions needed for estimating the physical properties are obtained as follows:

$$T_f = \tfrac{1}{2}(T_0 + T_\infty) = \tfrac{1}{2}(70 + 140) = 105°\text{F} \tag{22.3-27}$$

$$x_{Af} = \tfrac{1}{2}(x_{A0} + x_{A\infty}) = \tfrac{1}{2}(0.0247 + 0) = 0.0124 \tag{22.3-28}$$

[1] T. H. Chilton and A. P. Colburn, *Ind. Eng. Chem.*, **26**, 1183–1187 (1934).

In computing x_{Af}, we have assumed ideal gas behavior, equilibrium at the interface, and complete insolubility of air in water. The mean mole fraction, x_{Af}, of the water vapor is sufficiently small that it can be neglected in evaluating the physical properties at the film conditions:

$$c = 3.88 \times 10^{-5}\ \text{g-moles/cm}^3$$
$$\rho = 1.12 \times 10^{-3}\ \text{g/cm}^3$$
$$\mu = 1.91 \times 10^{-4}\ \text{g/cm} \cdot \text{s (from Table 1.1-1)}$$
$$\mathscr{D}_{AB} = 0.292\ \text{cm}^2\text{/s (from Eq. 17.2-1)}$$
$$\text{Sc} = \left(\frac{\mu}{\rho \mathscr{D}_{AB}}\right) = \frac{1.91 \times 10^{-4}}{(1.12 \times 10^{-3})(0.292)} = 0.58$$
$$\text{Re} = \left(\frac{Dv_\infty \rho}{\mu}\right) = \frac{(0.05)(215)(1.12 \times 10^{-3})}{1.91 \times 10^{-4}} = 63$$

When these values are used in Eq. 22.3-21 we get

$$\text{Sh}_m = 2 + 0.60(63)^{1/2}(0.58)^{1/3} = 5.96 \tag{22.3-29}$$

and the mean mass transfer coefficient is then

$$k_{xm} = \frac{c\mathscr{D}_{AB}}{D}\text{Sh}_m = \frac{(3.88 \times 10^{-5})(0.292)}{0.05}(5.96)$$
$$= 1.35 \times 10^{-3}\ \text{g-mol/s} \cdot \text{cm}^2 \tag{22.3-30}$$

Then from Eq. 22.3-26 the evaporation rate is found to be

$$W_{A0} = (1.35 \times 10^{-3})(\pi)(0.05)^2 \frac{0.0247 - 0}{1 - 0.0247}$$
$$= 2.70 \times 10^{-7}\ \text{g-mole/s} \tag{22.3-31}$$

This result corresponds to a decrease of 1.23×10^{-3} cm/s in the drop diameter and indicates that a drop of this size will fall a considerable distance before it evaporates completely.

In this example, for simplicity, the velocity and surface temperature of the drop were given. In general, these conditions must be calculated from momentum and energy balances, as discussed in Problem 22B.1.

EXAMPLE 22.3-2

The Wet and Dry Bulb Psychrometer

We next turn to a problem for which the analogy between heat and mass transfer leads to a surprisingly simple and useful, if approximate, result. The system, shown in Fig. 22.3-2, is a pair of thermometers, one of which is covered with a cylindrical wick kept saturated with water. The wick will cool by evaporation into the moving air stream and for steady operation will approach an asymptotic value known as the *wet bulb temperature.* The bare thermometer, on the other hand, will tend to approach the actual temperature of the approaching air, and this value is called the *dry bulb temperature.* Develop an expression for determining the humidity of the air from the wet and dry bulb temperature readings neglecting radiation and assuming that the replacement of the evaporating water has no significant effect on the wet bulb temperature measurement. In Problem 22B.2 we will see how radiation can be taken into account.

SOLUTION

For simplicity, we assume that the fluid velocity is high enough that the thermometer readings are unaffected by radiation and by heat conduction along the thermometer stems, but not so high that viscous dissipation heating effects become significant. These assumptions are usually satisfactory for glass thermometers and for gas velocities of 30 to 100 ft/s. The dry bulb temperature is then the same as the temperature T_∞ of the approaching gas, and the wet bulb temperature is the same as the temperature T_0 of the outside of the wick.

Let species A be water and species B be air. An energy balance is made on a system that contains a length L of the wick (the distance between planes 1 and 2 in the figure). The rate of

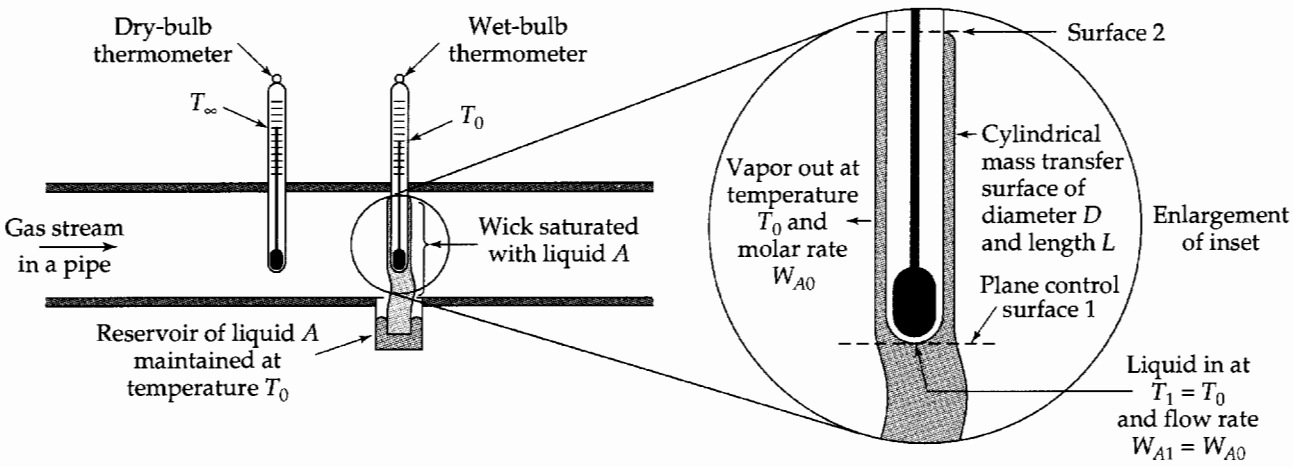

Fig. 22.3-2. Sketch of a wet-bulb and dry-bulb psychrometer installation. It is assumed that no heat or mass moves across plane 2.

heat addition to the system by the gas stream is $h_m(\pi DL)(T_\infty - T_0)$. Enthalpy also enters via plane 1 at a rate $W_{A1}\overline{H}_{A1}$ in the liquid phase and leaves at the mass transfer surface at a rate $W_{A0}\overline{H}_{A0}$, both of these occurring at a temperature T_0. Hence the energy balance gives

$$h_m(\pi DL)(T_\infty - T_0) = W_{A0}(\overline{H}_{A1} - \overline{H}_{A0}) \tag{22.3-32}$$

since the water enters the system at plane 1 at the same rate that it leaves as water vapor at the mass transfer interface 0. To a very good approximation, $\overline{H}_{A1} - \overline{H}_{A0}$ may be replaced by $\Delta\tilde{H}_{\text{vap}}$, the molar heat of vaporization of water.

From the definition of the mass transfer coefficient

$$W_{A0} - x_{A0}(W_{A0} + W_{B0}) = k_{xm}(\pi DL)(x_{A0} - x_{A\infty}) \tag{22.3-33}$$

in which $W_{B0} = 0$ as in the preceding example. Combination of Eqs. 22.2-32 and 33 gives then

$$\frac{(x_{A0} - x_{A\infty})}{(T_\infty - T_0)(1 - x_{A0})} = \frac{h_m}{k_{xm}\Delta\tilde{H}_{\text{vap}}} \tag{22.3-34}$$

Then using the definitions of Nu_m and Sh_m, and noting that $\rho\hat{C}_p = c\tilde{C}_p$, we may rewrite Eq. 22.3-34 as

$$\frac{(x_{A0} - x_{A\infty})}{(T_\infty - T_0)(1 - x_{A0})} = \frac{\text{Nu}_m}{\text{Sh}_m}\left(\frac{\text{Sc}}{\text{Pr}}\right)\frac{\tilde{C}_p}{\Delta\tilde{H}_{\text{vap}}} \tag{22.3-35}$$

Because of the analogy between heat and mass transfer, we can expect that the mean Nusselt and Sherwood numbers will be of the same form:

$$\text{Nu}_m = F(\text{Re})\text{Pr}^n; \qquad \text{Sh}_m = F(\text{Re})\text{Sc}^n \tag{22.3-36, 37}$$

where F is the same function of Re in both expressions. Therefore, knowing the dry and wet bulb temperatures and the mole fraction of the water vapor adjacent to the wick (x_{A0}), we can calculate the upstream composition $x_{A\infty}$ of the air stream from

$$\frac{(x_{A0} - x_{A\infty})}{(T_\infty - T_0)(1 - x_{A0})} = \left(\frac{\text{Sc}}{\text{Pr}}\right)^{1-n}\frac{\tilde{C}_p}{\Delta\tilde{H}_{\text{vap}}} \tag{22.3-38}$$

The exponent n depends to a slight extent on the geometry, but is not far from $\frac{1}{3}$, and the quantity $(\text{Sc}/\text{Pr})^{1-n}$ is not far from unity.[2] Furthermore, the wet bulb temperature is seen to be

[2] A somewhat different equation, with $1 - n = 0.56$, was recommended for measurements in air by C. H. Bedingfield and T. B. Drew, *Ind. Eng. Chem.*, **42**, 1164–1173 (1950).

independent of the Reynolds number under the assumption introduced in Eqs. 22.3-36 and 37. This result would also have been obtained by using the Chilton–Colburn relations, which would give $n = \frac{1}{3}$ directly.

The interfacial gas composition x_{A0} can be accurately predicted, at low mass-transfer rates, by neglecting the heat and mass transfer resistance of the interface itself (see §22.4 for further discussion of this point). One can then represent x_{A0} by the vapor–liquid equilibrium relationship:

$$x_{A0} = x_{A0}(T_0, p) \tag{22.3-39}$$

A relation of this kind will hold for given species A and B if the liquid is pure A as assumed above A commonly used approximation of this relationship is

$$x_{A0} = \frac{p_{A,\text{vap}}}{p} \tag{22.3-40}$$

in which $p_{A,\text{vap}}$ is the vapor pressure of pure A at temperature T_0. This relation assumes tacitly that the presence of B does not alter the partial pressure of A at the interface, and that A and B form an ideal gas mixture.

If an air–water mixture at 1 atm pressure gives a wet bulb temperature of 70°F and a dry bulb temperature of 140°F, then

$$\begin{aligned} p_{A,\text{vap}} &= 0.0247 \text{ atm} \\ x_{A0} &= 0.0247, \text{ from Eq. 22.3-40} \\ \tilde{C}_p &= 6.98 \text{ Btu/lb-mole} \cdot \text{F at 105°F, the film temperature} \\ \Delta\tilde{H}_{\text{vap}} &= 18{,}900 \text{ Btu/lb-mole at 70°F} \\ \text{Sc} &= 0.58 \text{ (see Example 22.2-1)} \\ \text{Pr} &= 0.74, \text{ from Eq. 9.3-16} \end{aligned}$$

Substitution into Eq. 22.3-37, with $n = \frac{1}{3}$, then gives

$$\frac{(0.0247 - x_{A\infty})}{(140 - 70)(1 - 0.0247)} = \left(\frac{0.58}{0.74}\right)^{2/3} \frac{6.98}{18{,}900} \tag{22.3-41}$$

From this the mole fraction of water in the approaching air is

$$x_{A\infty} = 0.0033 \tag{22.3-42}$$

Since we assumed that the film concentration was $x_A = 0$ as a first approximation, we could go back and make a second approximation by using an average film concentration of $\frac{1}{2}(0.0247 + 0.0033) = 0.0140$ in the physical property calculations. The physical properties are not known accurately enough here to justify recalculation.

The calculated result in Eq. 22.3-43 is in only fair agreement with published humidity charts, because these are typically based on the adiabatic saturation temperature rather than the wet bulb temperature.[3]

EXAMPLE 22.3-3

Mass Transfer in Creeping Flow Through Packed Beds

Many important adsorptive operations, from purification of proteins in modern biotechnology to the recovery of solvent vapor by dry-cleaning establishments, occur in dense particulate beds and are typically carried out in steady creeping flow—that is, at $\text{Re} = D_p v_0 \rho / \mu < 20$. Here D_p is the effective particle diameter and v_0 is the superficial velocity, defined as volumetric flow rate divided by the total cross section of the bed (see §6.4). It follows that the dimensionless velocity $\mathbf{v}/v_0$ will have a spatial distribution independent of the Reynolds number. Detailed information is available only for spherical packing particles.

[3] O. A. Hougen, K. M. Watson, and R. A. Ragatz, *Chemical Process Principles*, Part I, 2nd edition, Wiley, New York, (1954), p. 120.

Using the dimensional analysis discussion at the beginning of this section, predict the form of the steady-state mass transfer coefficient correlation for creeping flow.

SOLUTION

The dimensional analysis procedure in §19.5 may be used, with D_p as the characteristic length and v_0 the characteristic velocity. Then, from Eq. 19.5-11, we see that the dimensionless concentration depends only on the product ReSc, in addition to the dimensionless position coordinates and the geometry of the bed.

The most extensive data are for creeping flow at large Péclet numbers. Experimental data on the dissolution of benzoic acid spheres in water[4] have yielded the result

$$\mathrm{Sh}_m = \frac{1.09}{\varepsilon}(\mathrm{ReSc})^{1/3} \qquad \mathrm{ReSc} >> 1 \tag{22.3-43}$$

where ε is the volume fraction of the bed occupied by the flowing fluid. Equation 22.3-43 is reasonably consistent with the relation

$$\mathrm{Sh}_m = 2 + 0.991(\mathrm{ReSc})^{1/3} \tag{22.3-44}$$

which incorporates the creeping flow solution for flow around an isolated sphere[5] ($\varepsilon = 1$) (see §§22.2*b*). This suggests that the flow pattern around an isolated sphere is not much different from that around a sphere surrounded by other spheres, particularly near the sphere surface where most of the mass transport takes place.

No reliable data are available for the limiting behavior at very low values of ReSc, but numerical calculations for a regular packing[6] predict that the Sherwood number asymptotically approaches a constant near 4.0 if based on a local difference between interfacial and bulk compositions.

Behavior within the solid phase is far more complex, and no simple approximation is wholly trustworthy. However, experiments to date[7] show that where intraparticle mass transport is described by Fick's second law, one can use the approximation

$$\mathrm{Sh}_m = \frac{k_{c,s}D_p}{\mathscr{D}_{As}} \approx 10 \tag{22.3-45}$$

where $k_{c,s}$ is the effective mass transfer coefficient within the solid phase and $\mathscr{D}_{As}$ is the diffusivity of A in the solid phase. The equation is for "slow" changes in the solute concentration bathing the particle. This is an asymptotic solution for a linear change of surface concentration with time,[8] and has been justified[9] by calculations. For a Gaussian (bell-shaped) concentration wave, "slow" means that the passage time (temporal standard deviation) of the wave is long relative to the particle diffusional response time, which is of the order of $D_p^2/6\mathscr{D}_{As}$. Fick's second law must be solved with the detailed history of surface concentration when this inequality is not satisfied.

In packed beds, as with tube flow, one must keep in mind the fact that there will be nonuniformities in the concentration as a function of the radial coordinate. This was discussed in §14.5 and §20.3.

---

[4] E. J. Wilson and C. J. Geankopolis, *Ind. Eng. Chem. Fundamentals*, **5**, 9–14 (1966). See also J. R. Selman and C. W. Tobias, *Advances in Chemical Engineering*, **10**, 212–318 (1978), for an extensive summary of mass transfer coefficient correlations obtained by electrochemical measurements.

[5] V. G. Levich, *Physicochemical Hydrodynamics*, Prentice-Hall, Englewood Cliffs, N.J. (1962), §14.

[6] J. P. Sørensen and W. E. Stewart, *Chem. Eng. Sci.*, **29**, 811–837 (1974).

[7] A. M. Athalye, J. Gibbs, and E. N. Lightfoot, *J. Chromatography*, **589**, 71–85 (1992).

[8] H. S. Carslaw and J. C. Jaeger, *Conduction of Heat in Solids*, 2nd edition, Oxford University Press (1959), §9.3, Eqs. 10 and 11.

[9] J. F. Reis, E. N. Lightfoot, P. T. Noble, and A. S. Chiang, *Sep. Sci. Tech.*, **14**, 367–394 (1979).

EXAMPLE 22.3-4

Mass Transfer to Drops and Bubbles

In both gas–liquid[10] and liquid–liquid[11] contactors, sprays of liquid drops or clouds of bubbles are frequently encountered. Contrast their mass transfer behavior with that of solid spheres.

SOLUTION

Many different types of behavior are encountered, and surface forces can play a very important role. We discuss surface forces in some detail in §22.7. Here we consider only some limiting cases and refer readers to the above-cited references.

Very small drops and bubbles behave like solid spheres and can be treated by the correlations in Example 22.3-3 and in Chapter 14. However, if both adjacent phases are free of surfactants and small particulate contaminants, the interior phase circulates and carries the adjacent regions of the exterior phase along. This stress-driven "Hadamard–Rybczinski circulation"[12] increases the mass transfer rates markedly, often by almost an order of magnitude, and the rates can be estimated from extensions[13–16] of the "penetration model" discussed in §18.5. Thus, for a spherical bubble of gas A with diameter D rising through a clean liquid B, the Sherwood number on the liquid side lies in the range[16]

$$\sqrt{\frac{4}{3\pi}\frac{Dv_t}{\mathcal{D}_{AB}}} < \mathrm{Sh}_m < \sqrt{\frac{4}{\pi}\frac{Dv_t}{\mathcal{D}_{AB}}} \tag{22.3-46}$$

where v_t is the terminal velocity (see Eqs. 18.5-19 and 20).

The size at which the transition from the solid-like behavior to circulation occurs depends on degree of surface contamination and is not easily predicted.

Very large drops or bubbles oscillate,[13] and both phases follow a modified penetration model,

$$\mathrm{Sh}_m \approx \sqrt{\frac{4.8D^2\omega}{\pi\mathcal{D}_{AB}}} \tag{22.3-47}$$

with angular frequency of oscillation[17]

$$\omega = \sqrt{\frac{192\sigma}{D^3(3\rho_D + 2\rho_C)}} \tag{22.3-48}$$

where σ is the interfacial tension, and ρ_D and ρ_C are the densities of the drops and the continuous medium.

The success of this model implies that the boundary layer is refreshed once every oscillation, but there is also a small effect of periodic stretching of the surface.

§22.4 DEFINITION OF TRANSFER COEFFICIENTS IN TWO PHASES

Recall that in §10.6 we introduced the concept of an overall heat transfer coefficient, U, to describe the heat transfer between two streams separated from each other by a wall. This overall coefficient accounted for the thermal resistance of the wall itself, as well as the thermal resistance in the fluids on either side of the wall.

---

[10] J. Stichlmair and J. F. Fair, *Distillation Principles and Practice*, Wiley, New York (1998).
[11] J. C. Godfrey and M. M. Slater, *Liquid–Liquid Extraction Equipment*, Wiley, New York (1994).
[12] J. Happel and H. Brenner, *Low Reynolds Number Hydrodynamics*, Martinus Nijhoff, The Hague (1983).
[13] J. B. Angelo, E. N. Lightfoot, and D. W. Howard, *AIChE Journal*, **12**, 751–760 (1966).
[14] J. B. Angelo and E. N. Lightfoot, *AIChE Journal*, **14**, 531–540 (1968).
[15] W. E. Stewart, J. B. Angelo, and E. N. Lightfoot, *AIChE Journal*, **16**, 771–786 (1970).
[16] R. Higbie, *Trans. AIChE*, **31**, 365–389 (1935).
[17] R. R. Schroeder and R. C. Kintner, *AIChE Journal*, **11**, 5–8 (1965).

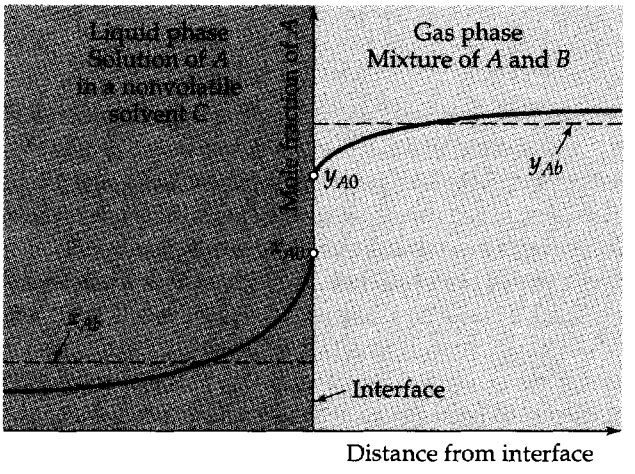

Fig. 22.4-1. Concentration profiles in the neighborhood of a gas–liquid interface

We now treat the analogous situation for mass transfer, except that here we are concerned with two fluids in intimate contact with one another, so that there is no wall resistance or interfacial resistance. This is the situation most commonly met in practice. Since the interface itself contains no significant mass, we may begin by assuming continuity of the total mass flux at the interface for any species being transferred. Then for the system shown in Fig. 22.4-1 we write

$$N_{A0}|_{\text{gas}} = N_{A0}|_{\text{liquid}} = N_{A0} \tag{22.4-1}$$

for the interfacial flux of A toward the liquid phase. Then using the definition given in Eq. 22.1-9, we get

$$N_{A0} = k^0_{y,\text{loc}}(y_{Ab} - y_{A0}) = k^0_{x,\text{loc}}(x_{A0} - x_{Ab}) \tag{22.4-2}$$

in which we are now following the tradition of using x for mole fractions in the liquid phase and y for mole fractions in the gas phase. We now have to interrelate the interfacial compositions in the two phases.

In nearly all situations this can be done by assuming equilibrium across the interface, so that adjacent gas and liquid compositions lie on the equilibrium curve (see Fig. 22.4-2), which is regarded as known from solubility data:

$$y_{A0} = f(x_{A0}) \tag{22.4-3}$$

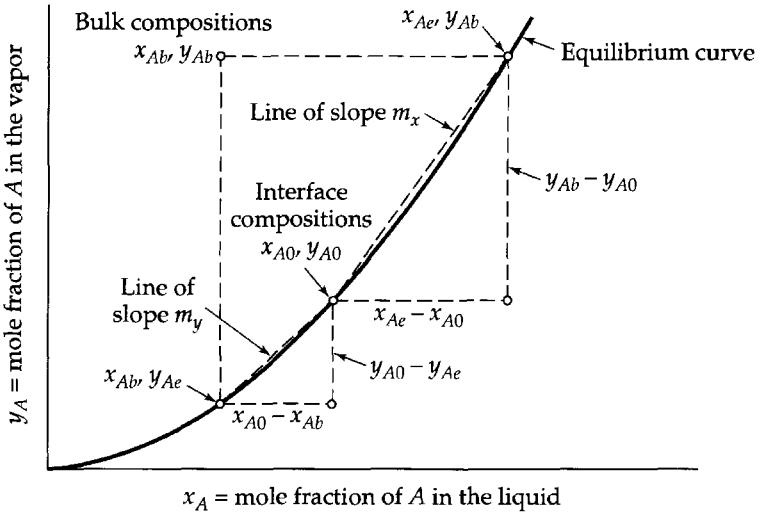

Fig. 22.4-2. Relations among gas- and liquid-phase compositions, and the graphical interpretations of m_x and m_y.

Exceptions to this are: (i) extremely high mass-transfer rates, observed for gas phases at high vacuum, where N_{A0} approaches $p_{A0}/\sqrt{2\pi M_A RT}$, the equilibrium rate at which gas molecules impinge on the interface; and (ii) interfaces contaminated with high concentrations of adsorbed particles or surfactant molecules. Situation (i) is quite rare, and situation (ii) normally acts indirectly by changing the flow behavior rather than causing deviations from equilibrium. In extreme cases surface contamination can provide additional transport resistances.

To describe rates of interphase transport, one can either use Eqs. 22.4-2 and 3 to calculate interface concentrations and then proceed to use the single-phase coefficients, or else work with overall mass transfer coefficients

$$N_{A0} = K^0_{y,\text{loc}}(y_{Ab} - y_{Ae}) = K^0_{x,\text{loc}}(x_{Ae} - x_{Ab}) \tag{22.4-4}$$

Here y_{Ae} is the gas phase composition in equilibrium with a liquid at composition x_{Ab}, and x_{Ae} is the liquid phase composition in equilibrium with a gas at composition y_{Ab}. The quantity $K^0_{y,\text{loc}}$ is the overall mass transfer coefficient "based on the gas phase," and $K^0_{x,\text{loc}}$ is the overall mass transfer coefficient "based on the liquid phase." Here again the molar flux N_{A0} is taken to be positive for transfer to the liquid phase.

Equating the quantities in Eqs. 22.4-2 and 4 gives two relations

$$K^0_{x,\text{loc}}(x_{Ae} - x_{Ab}) = k^0_{x,\text{loc}}(x_{A0} - x_{Ab}) \tag{22.4-5}$$

$$K^0_{y,\text{loc}}(y_{Ab} - y_{Ae}) = k^0_{y,\text{loc}}(y_{Ab} - y_{A0}) \tag{22.4-6}$$

connecting the two-phase coefficients with the single-phase coefficients.

The quantities x_{Ae} and y_{Ae} introduced in the above three relations may be used to define quantities m_x and m_y as follows:

$$m_x = \frac{y_{Ab} - y_{A0}}{x_{Ae} - x_{A0}}; \qquad m_y = \frac{y_{A0} - y_{Ae}}{x_{A0} - x_{Ab}} \tag{22.4-7, 8}$$

As we can see from Fig. 22.4-2, m_x is the slope of the line connecting points (x_{A0}, y_{A0}) and (x_{Ae}, y_{Ab}) on the equilibrium curve, and m_y is the slope of the line from (x_{Ab}, y_{Ae}) to (x_{A0}, y_{A0}).

From the above relations we can then eliminate the concentrations and get relations among the single-phase and two-phase mass transfer coefficients:

$$\frac{k^0_{x,\text{loc}}}{K^0_{x,\text{loc}}} = 1 + \frac{k^0_{x,\text{loc}}}{m_x k^0_{y,\text{loc}}}; \qquad \frac{k^0_{y,\text{loc}}}{K^0_{y,\text{loc}}} = 1 + \frac{m_y k^0_{y,\text{loc}}}{k^0_{x,\text{loc}}} \tag{22.4-9, 10}$$

The first of these was obtained from Eqs. 22.4-5, 2, and 7, and the second from Eqs. 22.4-6, 2, and 8. If the equilibrium curve is nearly linear over the range of interest, then $m_x = m_y = m$, which is the local slope of the curve at the interfacial conditions. We see, then, that the expressions in Eqs. 22.4-9, 10 both contain a ratio of single-phase coefficients weighted with a quantity m. This quantity is of considerable importance:

(i) If $k^0_{x,\text{loc}}/mk^0_{y,\text{loc}} << 1$, the mass-transport resistance of the gas phase has little effect, and it is said that the mass transfer is *liquid-phase controlled.* In practice, this means that the system design should favor liquid-phase mass transfer.

(ii) If $k^0_{x,\text{loc}}/mk^0_{y,\text{loc}} >> 1$, then the mass transfer is *gas-phase controlled.* In a practical situation, this means that the system design should favor gas-phase mass transfer.

(iii) If $0.1 < k^0_{x,\text{loc}}/mk^0_{y,\text{loc}} < 10$, roughly, one must be careful to consider the interactions of the two phases in calculating the two-phase transfer coefficients. Outside this range the interactions are usually unimportant. We return to this point in the example below.

The mean two phase mass transfer coefficients must be defined carefully, and we consider here only the special case where bulk concentrations in the two adjacent phases do not change significantly over the total mass-transfer surface S. We may then define K^0_{xm} by

$$(N_{A0})_m = \frac{1}{S}\int_S K^0_{x,\text{loc}}(x_{Ae} - x_{Ab})dS = K^0_{xm}(x_{Ae} - x_{Ab}) \tag{22.4-11}$$

so that, when Eq. 22.3-9 is used,

$$K^0_{xm} = \frac{1}{S}\int_S \frac{1}{(1/k^0_{x,\text{loc}}) + (1/m_x k^0_{y,\text{loc}})}\,dS \tag{22.4-12}$$

Frequently area mean overall mass transfer coefficients are calculated from area mean coefficients for the two adjoining phases:

$$K^0_{x,\text{approx}} = \frac{1}{(1/k^0_{xm}) + (1/m_x k^0_{ym})} \tag{22.4-13}$$

The two mean values in Eqs. 22.4-12 and 13 can be significantly different (see Example 22.4-3).

EXAMPLE 22.4-1

Determination of the Controlling Resistance

Oxygen is to be removed from water using nitrogen gas at atmospheric pressure and 20°C in the form of bubbles exhibiting internal circulation, as shown in Fig. 22.4-3. Estimate the relative importance of the two mass transfer coefficients $k^0_{x,\text{loc}}$ and $k^0_{y,\text{loc}}$. Let A stand for O_2, B for H_2O, and C for N_2.

SOLUTION

We can do this by assuming that the penetration model (see §18.5) holds in each phase, so that

$$k^0_{x,\text{loc}} \approx k_{x,\text{loc}} = c_l\sqrt{\frac{\mathscr{D}_{AB}}{\pi t_{\text{exp}}}}; \qquad k^0_{y,\text{loc}} \approx k_{y,\text{loc}} = c_g\sqrt{\frac{\mathscr{D}_{AC}}{\pi t_{\text{exp}}}} \tag{22.4-14}$$

where c_l and c_g are the total molar concentrations in the liquid and gas phases, respectively. The effective exposure time, t_{exp}, is the same for each of the phases.

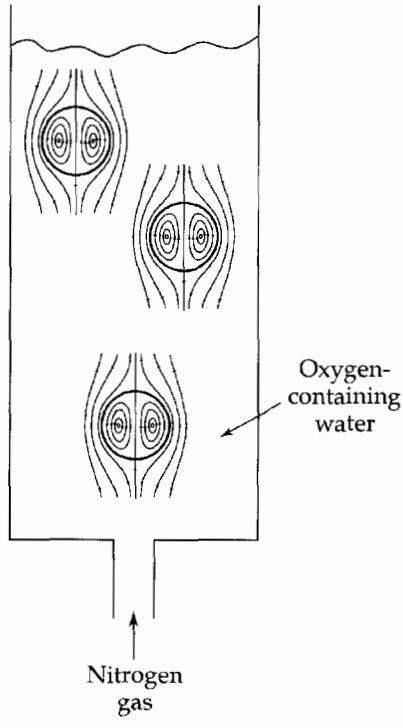

Fig. 22.4-3. Schematic diagram of an oxygen stripper, in which oxygen from the water diffuses into the nitrogen gas bubbles.

The solubility of O_2 in water at 20°C is 1.38×10^{-3} moles per liter at an oxygen partial pressure of 760 mm Hg, the vapor pressure of water is 17.535 mm Hg, and the total pressure in the solubility measurements is 777.5 mm Hg. At 20°C, the diffusivity of O_2 in water is $\mathscr{D}_{AB} = 2.1 \times 10^{-5}$ cm^2/s, and in the gas phase the diffusivity for $O_2 - N_2$ is $\mathscr{D}_{AC} = 0.2$ cm^2/s. We can then write

$$\frac{k^0_{x,\text{loc}}}{mk^0_{y,\text{loc}}} = \frac{c_l}{c_g}\sqrt{\frac{\mathscr{D}_{AB}}{\mathscr{D}_{AC}}} \cdot \frac{1}{m} \tag{22.4-15}$$

Into this we must substitute

$$\frac{c_l}{c_g} = \frac{c_l}{(p/RT)} = \frac{1000/18}{(777.5/760)/(0.08206)(293.5)} = 1308 \tag{22.4-16}$$

$$\sqrt{\frac{\mathscr{D}_{AB}}{\mathscr{D}_{AC}}} = \sqrt{\frac{2.1 \times 10^{-5}}{0.2}} = 0.01 \tag{22.4-17}$$

$$\frac{1}{m} = \frac{1.38 \times 10^{-3}/55.5}{760/777.5} = 2.54 \times 10^{-5} \tag{22.4-18}$$

It follows that

$$\frac{k^0_{x,\text{loc}}}{mk^0_{y,\text{loc}}} = (1308)(0.01)(2.54 \times 10^{-5}) = 3.32 \times 10^{-4} \tag{22.4-19}$$

Therefore, only the liquid-phase resistance is significant, and the assumption of penetration behavior in the gas phase is not critical to the determination of liquid-phase control. It may also be seen that the dominant factor is the low solubility of oxygen in water. One may generalize and state that absorption or desorption of sparingly soluble gases is almost always liquid-phase controlled. Correction of the gas-phase coefficient for net mass transfer is clearly not significant, and the correction for the liquid phase is negligible.

EXAMPLE 22.4-2

Interaction of Phase Resistances

There are many situations for which the one-phase transfer coefficients are not available for the boundary conditions of the two-phase mass transfer problem, and it is common practice to use one-phase models in which interfacial boundary conditions are assumed, without regard to the interaction of the diffusion processes in the two phases. Such a simplification can introduce significant errors. Test this approximate procedure for the leaching of a solute A from a solid sphere of B of radius R in an incompletely stirred fluid C, so large in volume that the bulk fluid concentration of A can be neglected.

SOLUTION

The exact description of the leaching process is given by the solution of Fick's second law written for the concentration of A in the solid in the region $0 < r < R$:

$$\frac{\partial c_{As}}{\partial t} = \mathscr{D}_{AB}\frac{1}{r^2}\frac{\partial}{\partial r}\left(r^2\frac{\partial c_{As}}{\partial r}\right) \tag{22.4-20}$$

The boundary and initial conditions are:

B.C. 1: at $r = 0$, c_{As} is finite (22.4-21)

B.C. 2: at $r = R$, $c_{As} = mc_{Al} + b$ (22.4-22)

I.C.: at $t = 0$, $c_{As} = c_0$ (22.4-23)

The diffusional process on the liquid side of the solid–liquid interface is described in terms of a mass transfer coefficient, defined by

$$-\mathscr{D}_{AB}\left.\frac{\partial c_{As}}{\partial r}\right|_{r=R} = k_c(c_{Al} - 0) \tag{22.4-24}$$

in which $c_{Al}(t)$ is the concentration in the liquid phase adjacent to the interface. The behavior of the diffusion in the two phases is coupled through Eq. 22.4-22, which describes the equilibrium

at the interface. Because of the coupling, it is convenient to use the method of Laplace transform. First, however, we restate the problem in dimensionless form, using $\xi = r/R$, $\tau = \mathcal{D}_{AB}t/R^2$, $C_s = c_{As}/c_0$, $C_l = (mc_{Al} + b)/c_0$, and $N = k_cR/m\mathcal{D}_{AB}$. Eqs. 22.3-20 and 24 become

$$\frac{\partial C_s}{\partial \tau} = \frac{1}{\xi^2}\frac{\partial}{\partial \xi}\left(\xi^2 \frac{\partial C_s}{\partial \xi}\right); \qquad -\frac{\partial C_s}{\partial \xi}\bigg|_{\xi=1} = NC_l \tag{22.4-25, 26}$$

with C_s finite at the sphere center, $C_s = C_l$ at the sphere surface, and $C_s = 1$ throughout the sphere initially.

When we take the Laplace transform of this problem, we get

$$p\overline{C}_s - 1 = \frac{1}{\xi^2}\frac{d}{d\xi}\left(\xi^2 \frac{d\overline{C}_s}{d\xi}\right); \qquad -\frac{\partial \overline{C}_s}{\partial \xi}\bigg|_{\xi=1} = N\overline{C}_l \tag{22.4-27, 28}$$

with $\overline{C}_s$ finite at the sphere center, and $\overline{C}_s = \overline{C}_l$ at the sphere surface. The solution of Eqs. 22.4-27 (which is a nonhomogeneous analog of Eq. C.1-6a) and 28 is

$$\overline{C}_s = -\frac{N}{p[\sqrt{p}\cosh\sqrt{p} - (1-N)\sinh\sqrt{p}]}\frac{\sinh\sqrt{p}\xi}{\xi} + \frac{1}{p} \tag{22.4-29}$$

The Laplace transform of M_A, the total amount of A within the sphere at any time t, is

$$\frac{\overline{M}_A}{4\pi R^3 c_0} = \int_0^1 \overline{C}_s \xi d\xi = \frac{N^2}{p^2(\sqrt{p}\coth\sqrt{p} - (1-N))} - \frac{N}{p^2} + \frac{1}{3p} \tag{22.4-30}$$

Inversion by using the Heaviside partial fractions expansion theorem for repeated roots[1] gives

$$\frac{M_A(t)}{\frac{4}{3}\pi R^3 c_{A0}} = 6\sum_{n=1}^{\infty} B_n \exp(-\lambda_n^2 \mathcal{D}_{AB}t/R^2) \tag{22.4-31}$$

The constants λ_n and B_n are found to be, for finite k_c (or N),

$$\lambda_n \cot\lambda_n - (1-N) = 0; \qquad B_n = \frac{N^2}{\lambda_n^3}\frac{\sin^2\lambda_n}{(\lambda_n - \sin\lambda_n\cos\lambda_n)} \tag{22.4-32, 33}$$

and for infinite k_c (or N),

$$\lambda_n = n\pi; \qquad B_n = \left(\frac{1}{n\pi}\right)^2 \tag{22.4-34, 35}$$

Note that we have succeeded in getting the total amount of A transferred across the interface, $M_A(t)$, without finding the expression for the concentration profile in the system. This is an advantage in using the Laplace transform.

We may now define two overall mass transfer coefficients: (i) the correct overall coefficient for this system based on the solid phase

$$K_s = \frac{N_{Ar}|_{r=R}}{c_{Ab}} = -\frac{R}{3}\frac{1}{M_A}\frac{dM_A}{dt} \tag{22.4-36}$$

where c_{Ab} is the volume-average concentration of A in the solid phase, and (ii) an approximate overall coefficient, based on the separately calculated behavior of the two phases, calculated by Eq. 22.4-13,

$$\frac{1}{K_{s,\text{approx}}} = -\frac{3}{R}\frac{M_A^0}{dM_A^0/dt} + \frac{m}{k_c} \tag{22.4-37}$$

where the superscript 0 indicates "zero external resistance" and k_c is the liquid-phase transfer coefficient.

---

[1] A. Erdélyi, W. Magnus, F. Oberhettinger, and F. G. Tricomi, *Tables of Integral Transforms*, McGraw-Hill (1954), p. 232, Formula 21.

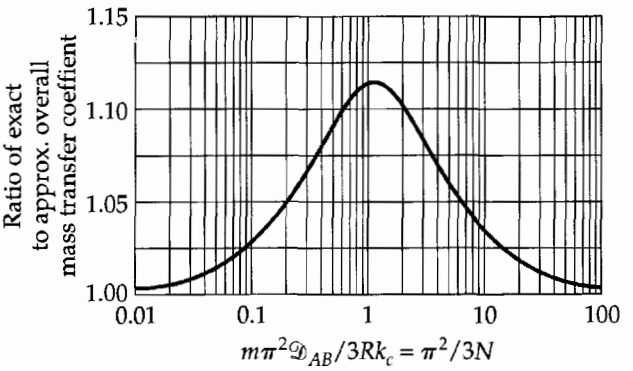

Fig. 22.4-4. Ratio of exact to approximate overall mass transfer coefficient in the leaching of a solute from a solute from a sphere, for large $\mathcal{D}_{AB}t/R^2$, plotted versus the dimensionless ratio $m\pi^2\mathcal{D}_{AB}/3Rk_c$.

We can now make a comparison between K_s and $K_{s,\text{approx}}$. We do this only for large values of $\mathcal{D}_{AB}t/R^2$, for which the leading term of the sum in Eq. 22.4-31 suffices. For this situation, we obtain

$$\frac{1}{K_{s,\text{approx}}} = \frac{3R}{\pi^2\mathcal{D}_{AB}} + \frac{m}{k_c} \tag{22.4-38}$$

and

$$\frac{K_s}{K_{s,\text{approx}}} = \frac{\lambda_1^2}{\pi^2}\left(1 + \frac{\pi^2 m\mathcal{D}_{AB}}{3Rk_c}\right) \tag{22.4-39}$$

where λ_1 is to be calculated for the actual value of k_c; keep in mind that λ_1 is obtained from Eq. 22.4-32, in which $N = k_cR/m\mathcal{D}_{AB}$. A plot of Eq. 22.4-39 is shown in Fig. 22.4-4. There we see that the maximum error in the two-film model occurs near $\pi^2/3N = 1$, and that departures from the two-film theory are appreciable but not very large.

EXAMPLE 22.4-3

***Area Averaging*[2]**

Consider a characteristic section of a packed tower for which the separately measured single-phase mass transfer coefficients yield a calculated ratio

$$\frac{k^0_{xm}}{mk^0_{ym}} = 10 \tag{22.4-40}$$

but in which the liquid phase wets only half of the packing surface. Here the subscript m refers to the mean value over a typical area S of the packing surface. The gas-phase transfer coefficient, on the other hand, is uniform over the entire surface. This hypothetical example is a special case of nonuniform wetting. Calculate the true and approximate values of k^0_{xm}/K^0_{xm} according to Eqs. 12.4-12 and 13.

SOLUTION

We begin with Eq. 22.4-12 and note that for half of the area $k^0_{x,\text{loc}} = 0$, and that over the other half

$$k^0_{x,\text{loc}} = 2k^0_{xm} \tag{22.4-41}$$

whereas, for the gas phase

$$k^0_{y,\text{loc}} = k^0_{ym} \tag{22.4-42}$$

Eq. 22.4-12 thus yields

$$K^0_{xm} = \frac{1}{S}\left[\frac{\frac{1}{2}S}{(1/2k^0_{xm}) + (1/mk^0_{ym})}\right] \tag{22.4-43}$$

[2] C. J. King, *AIChE Journal*, **10**, 671–677 (1964).

From this and Eqs. 22.4-40 and 22.4-9, we find that the correct value for k^0_{xm}/K^0_{xm} is

$$\frac{k^0_{xm}}{K^0_{xm}} = 1 + 2\frac{k^0_{xm}}{mk^0_{ym}} = 21 \tag{22.4-44}$$

whereas the approximate value from Eq. 22.4-13 is

$$\frac{k^0_{xm}}{K^0_{xm}} = 1 + \frac{k^0_{xm}}{mk^0_{ym}} = 11 \tag{22.4-45}$$

Thus the maldistribution of the liquid-phase mass transfer coefficient halves the rate of mass transfer, even though the liquid phase resistance "on the average" is very low. The general unavailability of such detailed information is one more reason for the uncertainty in predicting the behavior of complex contactors.

§22.5 MASS TRANSFER AND CHEMICAL REACTIONS

Many mass transfer operations are accompanied by chemical reactions, and the reaction kinetics can have a profound effect on transport rates. Important examples include absorption of reactive gases and reactive distillation. There are two situations of particular interest:

(i) Absorption of a sparingly soluble substance A into a phase containing a second reactant B in large concentration. Absorption of carbon dioxide into NaOH or amine solutions is an industrially important example, and here the reaction may be considered pseudo-first-order because reactant B is present in great excess:

$$R_A = -(k'''_2 c_B)c_A = -k'''_1 c_A \tag{22.5-1}$$

An example of this type of problem was given in §18.4.

(ii) Absorption of a rapidly reacting solute A into a solution of B. Here to a first approximation it may be assumed that the two species react so rapidly that they cannot coexist. An illustration of this was given in Example 20.1-2.

We shall be particularly interested in liquid boundary layers, and heat-of-reaction effects tend to be modest because the ratio of Sc to Pr is usually very large. Macroscopic heating effects do occur, and these are discussed in Chapter 23. Here we limit ourselves to a few illustrative examples showing how one can use models of absorption with chemical reaction to predict the performance of operating equipment.[1]

EXAMPLE 22.5-1

Estimation of the Interfacial Area in a Packed Column

Mass transfer measurements with irreversible first-order reaction have often been used to estimate interfacial area in complex mass transfer equipment. Show here how this method can be justified.

SOLUTION

The system we consider here is the absorption of carbon dioxide into a caustic solution, which is limited by hydration of dissolved CO_2 according to the reaction

$$CO_2(aq) + H_2O \rightleftarrows H_2CO_3 \tag{22.5-2}$$

[1] T. K. Sherwood, R. L. Pigford, and C. R. Wilke, *Mass Transfer*, McGraw-Hill, New York (1975), Chapter 8.

The carbonic acid then reacts with NaOH at a rate proportional to carbon dioxide concentration. The kinetics of this reaction are well characterized.[1]

The solution of this diffusion problem has been given in Problem 20C.3. From Eq. 20.3-3, we find that for long times[2,3]

$$W_{A0} = Ac_{A0}\sqrt{\mathscr{D}_{AB}k_1'''} \tag{22.5-3}$$

which can be solved for the total surface area. It follows that the total surface area A under consideration is given by

$$A = \frac{1}{c_{A0}\sqrt{\mathscr{D}_{AB}k_1'''}}\frac{dM_{A,\text{tot}}}{dt} \tag{22.5-4}$$

here $M_{A,\text{tot}}$ is the number of moles of carbon dioxide absorbed by time t.

This development is readily extended to a falling film of length L and surface velocity v_s, provided that $k_1L/v_s >> 1$. First-order reaction in mass transfer boundary layers is discussed in Example 18.4-1 for a simple film model and in Example 20.1-3. The development can be further extended to estimate the interfacial area in packed columns, in which the liquid phase is supported as a falling film on solid surfaces, a common design.

EXAMPLE 22.5-2

Estimation of Volumetric Mass Transfer Coefficients

We next consider gas absorption with first-order reaction in an agitated tank and take as a starting point the reaction

$$O_2 + 2Na_2SO_3 \rightarrow 2Na_2SO_4 \tag{22.5-5}$$

already discussed in Example 18.4-1, using a thin stagnant film of liquid as a mass transfer model.

SOLUTION

This is not a realistic model, but the development in Example 18.4-1 can be rephrased in a *model-insensitive form* by writing

$$k_c = \frac{\mathscr{D}_{AB}}{\delta} \tag{22.5-6}$$

so that

$$\phi = \sqrt{\frac{k_1'''\delta^2}{\mathscr{D}_{AB}}} \rightarrow \sqrt{\frac{k_1'''\mathscr{D}_{AB}}{k_c^2}} \quad \text{and} \quad \frac{V}{A\delta} \rightarrow \frac{Vk_c}{A\mathscr{D}_{AB}} \tag{22.5-7}$$

The subscript AB should be changed to O_2S, where S represents the sulfite solution.

One can now test the *model sensitivity* of the system by comparing the film model with the penetration model. This is done in Fig. 22.5-1, where it can be seen that there is no significant difference between the two.[4] Moreover, there is a substantial region of parameter space where the predicted rate of oxygen absorption is identical to that for physical absorption in an oxygen-free tank. This chemical system has therefore proven a popular means for estimating volumetric mass transfer coefficients. It has long been used to characterize the oxygenation effectiveness of aerobic bioreactors.[5]

---

[2] P. V. Danckwerts, *Trans. Faraday Soc.*, **46**, 300–304 (1950).

[3] R. A. T. O. Nijsing, *Absorptie van gassen in vloeistoffen, zonder en met chemische reactie*, Academisch Proefschrift, Delft (1957).

[4] E. N. Lightfoot, *AIChE Journal*, **8**, 710–712 (1962).

[5] A. M. Friedman and E. N. Lightfoot, *Ind. Eng. Chem.*, **49**, 1227–1230 (1957); J. E. Bailey and D. F. Ollis, *Biochemical Engineering Fundamentals*, McGraw-Hill, New York (1986); V. Linek, P. Benes, and J. Sinkule, *Biotechnol.-Bioeng.*, **35**, 766–770 (1990).

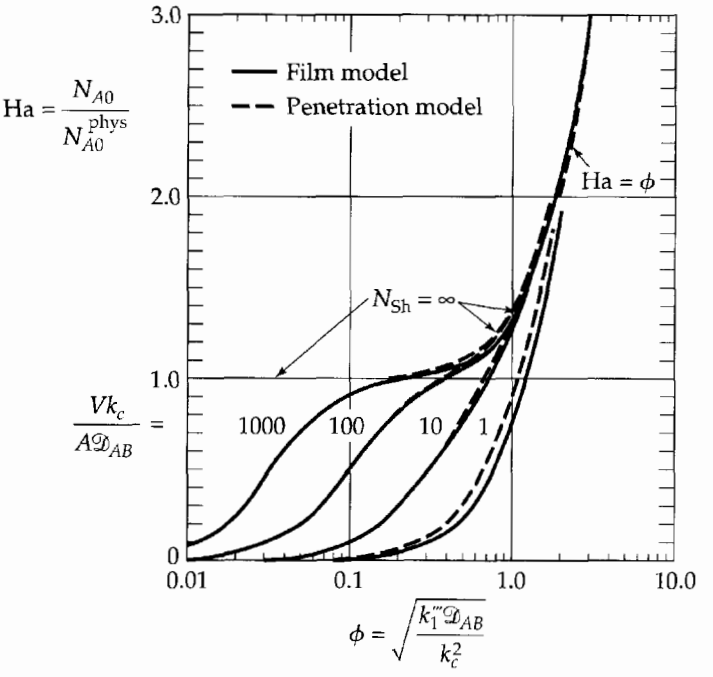

Fig. 22.5-1. Effect of irreversible first-order reaction on pseudosteady-state absorption of a sparingly soluble gas in an agitated tank. Comparison of the penetration and stagnant-film models.

EXAMPLE 22.5-3

Model-Insensitive Correlations for Absorption with Rapid Reaction

Next consider the absorption with rapid irreversible reaction, and seek to simplify and generalize the discussion of Example 20.1-2. Do this in terms of the *Hatta number*[6] defined as

$$\text{Ha} = \frac{N_{A0}}{N_{A0}^{\text{phys}}} \tag{22.5-8}$$

here the superscript phys denotes absorption of solute A in the same system but without reaction. This dimensionless group provides a convenient measure of the promoting effect of chemical reaction on the rate of absorption.

SOLUTION

In the absence of solute B, species A would undergo physical absorption (that is, absorption without reaction) at a rate

$$N_{A0}^{\text{phys}} = c_{A0}\sqrt{\frac{\mathcal{D}_{AS}}{\pi t}} \tag{22.5-9}$$

since $\text{erf}\sqrt{\gamma/\mathcal{D}_{AS}}$ goes to unity with decreasing $c_{B\infty}/c_{A0}$. We now divide the result in Eq. 20.1-39 by Eq. 22.5-9 to get

$$\text{Ha} = \frac{1}{\text{erf}\sqrt{\gamma/\mathcal{D}_{AS}}} \tag{22.5-10}$$

which can be further simplified in the following cases:[7,8]

---

[6] S. Hatta, *Technological Reports of Tôhoku University*, **10**, 613–662 (1932). **Shirôji Hatta** (1895–1973) taught at Tôhoku University from 1925 to 1958 and in 1954 he was appointed Dean of Engineering; after "retiring" he accepted a position at Chiyoda Chemical Engineering and Construction Co. He served as editor-in-chief of *Kagaku Kôgaku* and as president of Kagaku Kôgakkai.

[7] E. N. Lightfoot, *Chem. Eng. Sci.*, **17**, 1007–1011 (1962).

[8] D. H. Cho and W. E. Ranz, *Chem. Eng. Prog. Symposium Series* # 72, **63**, 37–45 and 46–58 (1967).

(i) *For small values of* $c_{B\infty}/c_{A0}$, or *for equal diffusivities,*

$$\text{Ha} = 1 + \frac{ac_{B\infty}}{bc_{A0}} \tag{22.5-11}$$

(ii) *For large values of* $c_{B\infty}/c_{A0}$,

$$\text{Ha} = \left(1 + \frac{ac_{B\infty}\mathcal{D}_{BS}}{bc_{A0}\mathcal{D}_{AS}}\right)\sqrt{\frac{\mathcal{D}_{AS}}{\mathcal{D}_{BS}}} \tag{22.5-12}$$

(iii) *For all values of* $c_{B\infty}/c_{A0}$ (approximate),

$$\text{Ha} \approx 1 + \frac{ac_{B\infty}}{bc_{A0}}\sqrt{\frac{\mathcal{D}_{BS}}{\mathcal{D}_{AS}}} \tag{22.5-13}$$

Equation 22.5-11 is particularly useful, since it is accurate for the common situation of nearly equal diffusivities as well as for small $c_{B\infty}/c_{A0}$. Equation 22.5-13 is useful because it is valid for both large and very small values of $ac_{B\infty}\mathcal{D}_{BS}/bc_{A0}\mathcal{D}_{AS}$. In addition, the exact solution always lies in the space between the curve of Eq. 22.5-13 and those portions of the curves of Eqs. 22.5-11 and 12 that are closest to it. This is shown in Fig. 22.5-2, where these bounding approximations are compared to the exact solution.

We next note that we can replace the diffusivity ratio by the corresponding ratio of nonreactive Sherwood numbers,

$$\sqrt{\frac{\mathcal{D}_{AS}}{\mathcal{D}_{BS}}} = \frac{\text{Sh}_B^0}{\text{Sh}_A^0} \tag{22.5-14}$$

where the superscript 0 denotes the observed Sherwood number in the absence of chemical reaction. We may thus obtain a set of model-insensitive bounding solutions

$$\begin{aligned}\text{Ha} &\approx 1 + \frac{ac_{B\infty}}{bc_{A0}} \\ &\approx \left[1 + \left(\frac{ac_{B\infty}}{bc_{A0}}\right)\left(\frac{\mathcal{D}_{BS}}{\mathcal{D}_{AS}}\right)\right]\frac{\text{Sh}_B^0}{\text{Sh}_A^0} \\ &\approx 1 + \left(\frac{ac_{B\infty}}{bc_{A0}}\right)\frac{\text{Sh}_A^0}{\text{Sh}_B^0}\end{aligned} \tag{22.5-15}$$

These equations have been shown[7] to provide convenient bounds for laminar and turbulent boundary layers as well as the penetration model of Example 20.1-2. They thus form a highly model-insensitive correlation and are widely useful.

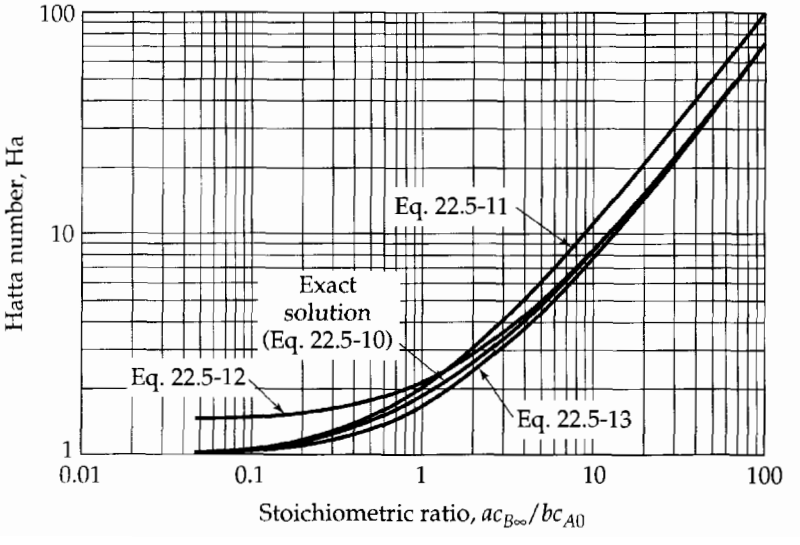

Fig. 22.5-2. Model-insensitive correlations for absorption with rapid chemical reaction, derived from the penetration model, for the case that $\mathcal{D}_{AS} = 2\mathcal{D}_{BS}$.

§22.6 COMBINED HEAT AND MASS TRANSFER BY FREE CONVECTION

In this section we consider briefly some important interactions among the transfer processes, with emphasis on free convection. This is an extension of our earlier discussion of free-convection heat transfer in §14.6 and is reasonably well understood.

Combined heat and mass transfer by free convection is among the simple examples of interaction between all three transport phenomena. The dimensionless equations describing them have been given in Eqs. 19.5-8 to 11. Numerical integration of these equations is possible,[1] but we can obtain simple, useful results via boundary layer theory. We consider two particularly simple problems in the examples that follow.

EXAMPLE 22.6-1

Additivity of Grashof Numbers

Develop an expression for the combined free-convection heat and mass transfer for the special case of equal Prandtl and Schmidt numbers. Assume that transfer is between a surface of constant temperature and composition, and a large uniform surrounding fluid.

SOLUTION

This is a direct extension of the boundary conditions of Example 11.4-5. Then if the dimensionless temperature and composition are defined analogously, it follows that $\check{T} = \check{x}_A$ everywhere within the system under investigation.

It then follows that the solution of this mixed convection problem is identical to that for heat or mass transfer alone, but with Gr or Gr_ω replaced by the sum $(Gr + Gr_\omega)$. This simplification is widely used for the air–water system, where the small difference between the Sc and Pr numbers does not have a significant effect.

Thus for evaporation from a water-wetted vertical plate (with Sc = 0.61 and Pr = 0.73), one may use Eq. 11.4-11 with C = 0.518 to obtain

$$\mathrm{Nu}_m \approx 0.518[0.73(\mathrm{Gr} + \mathrm{Gr}_\omega)]^{1/4} \tag{22.6-1}$$

$$\mathrm{Sh}_m \approx 0.518[0.61(\mathrm{Gr} + \mathrm{Gr}_\omega)]^{1/4} \tag{22.6-2}$$

Note that the $\frac{1}{4}$-th powers of Pr and Sc are 0.92 and 0.88, respectively. This difference is hardly significant in view of the uncertainties of any actual situation and the boundary layer model on which these results are based. Note also that the thermal Grashof number is normally by far the larger, so that neglect of this interaction would greatly underestimate the evaporation rates.

EXAMPLE 22.6-2

Free-Convection Heat Transfer as a Source of Forced-Convection Mass Transfer

There are many situations—for example, the evaporation of solvents with low volatility—where thermal Grashof numbers are much larger than their mass transfer counterparts ($Gr > Gr_\omega$) and the Schmidt numbers exceed the Prandtl numbers (Sc > Pr). Under these conditions, the thermal buoyant forces provide a momentum source, which in turn provides a convective flow to drive mass transfer. It has been shown[2] that the thermally induced gradient of upward velocity at the surface of a vertical flat plate of length L is given by

$$\left.\frac{\partial v_z}{\partial y}\right|_{y=0} \approx 1.08\left(\frac{4}{3}\frac{z}{L}\right)^{1/4}\left(\frac{\mathrm{Gr}}{\mathrm{Pr}}\right)^{1/4}\sqrt{\frac{g\beta\Delta T}{L}} \tag{22.6-3}$$

Here z is the distance measured upward along the plate, y is measured outward into the fluid, and ΔT is the difference between the plate temperature and the temperature of the surroundings. This is an asymptotic expression for large Prandtl number, but is also useful for gases. Develop expressions for the local and mean Sherwood numbers.

---

[1] W. R. Wilcox, *Chem. Eng. Sci.*, **13**, 113–119 (1961).

[2] A. Acrivos, *Phys. Fluids*, **3**, 657–658 (1960).

SOLUTION

The thermal free convection provides a velocity field within which the mass transfer boundary layer develops. Given this velocity field, we may use the mass transfer analog of Eqs. 12.4-30 and 29 along with the definition $\mathrm{Nu}_{\mathrm{loc}} = D/\Gamma(\frac{4}{3})\delta_T$ to obtain a description of the mass transfer rate in two-dimensional flow:

$$\mathrm{Sh}_{\mathrm{loc}} = \frac{(\mathrm{ReSc})^{1/3}}{9^{1/3}\Gamma(\frac{4}{3})} \frac{\sqrt{\Gamma_0}}{\left(\int_0^{z/L} \sqrt{\Gamma_0(u)}du\right)^{1/3}} \tag{22.6-4}$$

Here

$$\Gamma_0 = \frac{l_0}{v_0}\frac{\partial v_z}{\partial y}\bigg|_{y=0} \tag{22.6-5}$$

is the dimensionless velocity gradient at the wall (l_0 and v_0 are arbitrary reference quantities used in the definition of the Reynolds number). For free convection it is convenient to use the plate height L for l_0 and ν/L for v_0. Then the Reynolds number is unity, and the quantity Γ_0 is $\Gamma_0 = (L^2/\nu)(\partial v_z/\partial y)|_{y=0}$. Then Eq. 22.6-4 becomes

$$\begin{aligned}\mathrm{Sh}_{\mathrm{loc}} &= \left(\frac{1.08}{8}\right)^{1/3} \frac{(\frac{4}{3})^{1/12}}{\Gamma(\frac{4}{3})} (\mathrm{GrSc})^{1/4}\left(\frac{\mathrm{Sc}}{\mathrm{Pr}}\right)^{1/12}\left(\frac{L}{z}\right)^{1/4} \\ &\approx 0.59(\mathrm{GrSc})^{1/4}\left(\frac{\mathrm{Sc}}{\mathrm{Pr}}\right)^{1/12}\left(\frac{L}{z}\right)^{1/4}\end{aligned} \tag{22.6-6}$$

The mean Sherwood number, obtained by averaging over the plate surface, is

$$\mathrm{Sh}_m \approx 0.79(\mathrm{GrSc})^{1/4}\left(\frac{\mathrm{Sc}}{\mathrm{Pr}}\right)^{1/12} \tag{22.6-7}$$

Note that these last two equations show features of both free and forced convection in laminar boundary layers: the $\frac{1}{4}$-power of the Grashof number for free convection and the $\frac{1}{3}$-power of the Schmidt number for forced convection.

Moreover, we can now test the effect of Sc/Pr, because we know from the preceding example and Table 14.6-1 that, for Pr = Sc,

$$\mathrm{Sh}_m = 0.67(\mathrm{GrSc})^{1/4} \tag{22.6-8}$$

in which the coefficient is lower than that in Eq. 22.6-7 by the ratio 0.85. The Sherwood number Sh_m will lie between the predictions of Eqs. 22.6-7 and 8 for $\mathrm{Sc} \geq \mathrm{Pr}$ and $\mathrm{Pr} >> 1$.

Arguments similar to those used in Eq. 14.6-6 now suggest the following extension of Eqs. 22.67 and 68,

$$\mathrm{Sh}_m \approx 0.73(1 \pm 0.1)\frac{(\mathrm{GrSc})^{1/4}(\mathrm{Sc/Pr})^{1/12}}{[1 + (0.492/\mathrm{Pr})^{9/16}]^{4/9}} \tag{22.6-9}$$

for $\mathrm{Sc} \geq \mathrm{Pr}$ and $\mathrm{Pr} \geq 0.73$. This result is correct for the limits Pr = 0.73 and Pr = ∞ and hence can include the evaporation of solvents in air. This analysis can also be extended to other shapes.

---

§22.7 EFFECTS OF INTERFACIAL FORCES ON HEAT AND MASS TRANSFER

In this section we consider briefly some important interactions among the three transfer processes, with emphasis on the effects of variable interfacial tension (*Marangoni effects*). The importance of this subject stems from the prevalence of direct fluid–fluid contact in mass transfer systems, but it can also be important in similar heat transfer operations. Still poorly understood diffusional processes permit violation of the no-slip condition on

fluid flow over solid surfaces in the neighborhood of advancing menisci.[1] As for the distorting effects of surface tension gradients on mass and heat transfer in gas–liquid contacting, these will enter through a description of the boundary conditions.

According to Eq. 11C.6-4, if the stresses in the gas (phase II) are ignored, the interfacial tangential stresses acting on an interface with normal unit vector $\mathbf{n}$ are given by[2]

$$[(\boldsymbol{\delta} - \mathbf{nn}) \cdot [\mathbf{n} \cdot \boldsymbol{\tau}]] = -\nabla^s \sigma \tag{22.7-1}$$

where σ is the surface tension ∇^s is the two-dimensional gradient operator in the interface, and $(\boldsymbol{\delta} - \mathbf{nn})$ is a "projection operator" that selects those components of $[\mathbf{n} \cdot \boldsymbol{\tau}]$ that lie in the interfacial tangent plane. For example, if $\mathbf{n}$ is taken to be the unit vector in the z direction, Eq. 22.7-1 gives

$$\tau_{zx} = -\frac{\partial \sigma}{\partial x} \qquad \tau_{zy} = -\frac{\partial \sigma}{\partial y} \tag{22.7-2, 3}$$

which are the interfacial tension forces in the x and y directions acting in the xy-plane.

The surface-tension-induced stresses are typically of the same order as their hydrodynamic counterparts, and the flow phenomena that may result from them are known collectively as *Marangoni effects*.[3] It has been shown[4] that mass transfer rates can be increased up to threefold by Marangoni effects, but can also be reduced in other circumstances.

The nature and extent of Marangoni effects depend strongly on the system geometry and the transport properties, and it will be convenient to consider here four specific examples:

(i) drops and bubbles surrounded by a liquid continuum

(ii) sprays of drops in a gaseous continuum

(iii) supported liquid films in a gaseous or liquid continuum

(iv) foams of gas bubbles in a liquid continuum

These systems, each important in practice, show very different behavior from one another.

For drops and bubbles moving through a liquid continuum, the primary problems are surfactants or microscopic particles that can reduce or eliminate the "Hadamard–Rybczinski circulation" and also hinder the periodic mixing accompanying oscillation in

---

[1] V. Ludviksson and E. N. Lightfoot, *AIChE Journal*, **14**, 674–677 (1968); P. A. Thompson and S. M. Troian, *Phys. Rev. Letters*, **63**, 766–769 (1997); A. Marmur, in *Modern Approach to Wettability: Theory and Applications* (M. E. Schrader and G. Loeb, eds.), Plenum Press (1992); D. Schaeffer and P.-Z. Wong, *Phys. Rev. Letters*, **80**, 3069–3072 (1998).

[2] In Eq. 3.2-6 of D. A. Edwards, H. Brenner, and D. T. Wasan, *Interfacial Transport Processes and Rheology*, Butterworth-Heinemann, Boston (1991), the operator $(\boldsymbol{\delta} - \mathbf{nn})$ is called the "dyadic surface idemfactor"; the same quantity is called the "projection tensor" by J. C. Slattery, *Interfacial Transport Phenomena*, Springer Verlag, New York (1990), p. 1086. Both books contain a wealth of information on surface tension, surface viscosity, surface viscoelasticity, and other properties of interfaces and their methods of measurement.

[3] C. G. M. Marangoni, *Tipographia dei fratelli Fusi*, Pavia (1865); *Ann. Phys.* (Poggendorf), **143**, 337–354 (1871). Historical articles on the Marangoni effects are L. E. Scriven and C. V. Sternling, *Nature*, **187**, 186–188 (1960), and S. Ross and P. Becher, *J. Coll. Interfac. Sci.*, **149**, 575–579 (1992).

[4] A good overview of Marangoni effects and related phenomena, with emphasis on liquid–liquid systems, is provided in J. C. Godfrey and M. J. Slater, *Liquid–Liquid Extraction Equipment*, Wiley, New York (1994), pp. 68–75. A theory offered by C. V. Sternling and L. E. Scriven, *AIChE Journal*, **5**, 514–523 (1959), provides useful insight but is considered too simple to give reliable predictions of the onset of instabilities.

larger drops or bubbles.[5] These are discussed briefly in Example 22.3-4. These situations are important in gas absorbers and liquid extractors. For sprays of drops in a gas, important in large distillation columns, Marangoni forces play no significant role.[6]

Foam beds, important in smaller distillation columns, and supported films, important in a wide variety of packed columns, are particularly interesting. Both are strongly affected by surface-tension gradients resulting from the changes of surface tension with composition of the adjoining streams.

Foam beds are stabilized when the bulk liquid has a lower surface tension than that in equilibrium with the bulk gas, called a "positive system." In such a situation, interfacial tension tends to be higher where bubbles are close together than where they are far apart, and the shrinking of high-surface-tension regions tends to drive the bubbles apart, thus stabilizing the foam. Where there are only small differences in surface tension, or where the direction is reversed, a "negative system," there is no stabilizing effect and the foaming is poor. Concentration of ethanol from water is interesting, because it has strong positive surface tension gradients where the relative volatility is high, but becomes very nearly neutral as the azeotrope is approached. Thus, for a bubble-cap column, stage efficiencies are high where least needed and low as the azeotropic composition is approached.

In packed columns, where the descending liquid is supported on solid surfaces as thin films, the situation is quite different. Here the surface tension of the descending liquid decreases downward for a positive system and is subject to hydrodynamic instability to form narrow rivulets. These markedly decrease interfacial area and mass transfer effectiveness. In negative systems, on the other hand, films are stabilized, and mass transfer is more effective than for neutral systems. No quantitative analysis of this situation appears to be available, but it has been shown that instabilities found by Zuiderweg and Harmens for wetted-wall columns can be predicted by linearized stability analysis.[7] Stability analysis also suggests that the presence of a positive surface-tension gradient should improve the efficiency of condensers. Another study of stability for very small films opens up new possibilities for microfluidic processors.[8]

EXAMPLE 22.7-1

Elimination of Circulation in a Rising Gas Bubble

The presence of surfactants can stop Hadamard–Rybczinski circulation in a rising gas bubble. Explain this phenomenon (see Fig. 22.7-1).

SOLUTION

Circulation results in stretching of the surface at the top of a rising bubble and shrinking of the surface at the bottom. As a result, surfactant accumulates at the bottom, producing a higher than average concentration there, whereas a lower-than-average concentration exists at the top. Since surfactants reduce surface tension, this results in a surface-tension-induced stress (in spherical coordinates)

$$\tau_{r\theta,s}|_{r=R} = \frac{1}{R}\frac{\partial \sigma}{\partial \theta} \tag{22.7-4}$$

tending to oppose the interfacial deformation (see Eq. 22.7-1). If the magnitude of this stress reaches the value that would occur on a rising solid sphere (see Eq. 2.6-6)

$$\tau_{r\theta}|_{r=R} = \frac{3}{2}\frac{\mu v_\infty}{R}\sin\theta \tag{22.7-5}$$

circulation will stop.

---

[5] J. B. Angelo and E. N. Lightfoot, *AIChE Journal*, **12**, 751–760 (1966).

[6] F. J. Zuiderweg and A. Harmens, *Chem. Eng. Sci.*, **9**, 89–103 (1958).

[7] K. H. Wang, V. Ludviksson, and E. N. Lightfoot, *AIChE Journal*, **17**, 1402–1408 (1971).

[8] D. E. Kataoka and M. S. Troian, *Nature*, **402**, 794–797 (16 December 1999).

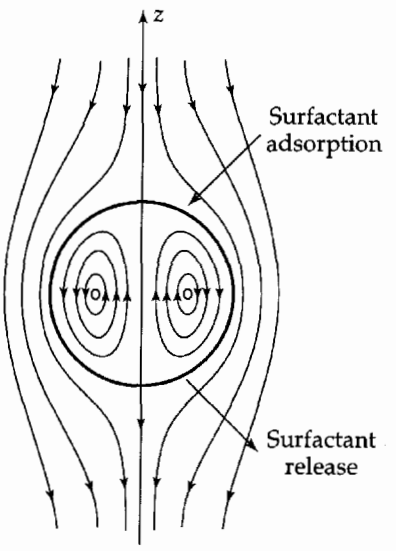

Fig. 22.7-.1 Surfactant transport during Hadamard–Rybczynski circulation

As a practical matter, even small amounts of surfactant prevent circulation. Small concentration of microscopic suspended particulates have a similar effect, being swept to the rear of bubbles and forming a rigid surface.

EXAMPLE 22.7-2

Marangoni Instability in a Falling Film

Among the simplest mass-transfer-induced Marangoni effects is instability in a falling film resulting from counterflow adsorption of vapors with a high heat of solution. An important representative example is the counterflow absorption of HCl vapor into water, which is so inefficient that cocurrent flow is preferable. Explain this effect.

SOLUTION

This situation can be simulated by allowing a film of water to flow down a plate that is colder at the top than at the bottom. If sufficient care is taken, one can obtain a sinusoidally varying film thickness, as shown[9] by interferometry in Fig. 22.7-2(*a*). Here each new dark line represents a line of constant thickness, differing from its neighbors by one-half wavelength of light in the water.

This situation corresponds to a series of parallel *roll cells* of the type pictured in Fig. 22.7-2(*b*), driven by lateral surface tension gradients. These gradients, in turn, result from small variations in film thickness caused by inevitable small spatial variations of surface velocity: the thicker regions move faster and thus tend to be colder than the thin regions. A simple perturbation analysis[1] shows that perturbations of some widths grow faster than others, and the fastest growing ones tend to dominate. The periods of the sinusoidal lines in Fig. 22.7-2(*a*) correspond to these fastest growing disturbances.

Such regularity is, however, seldom observed in practice. More commonly one sees occasional thick rivulets surrounded by large thin regions. These thin regions, taking up most of the available surface, are both slowly moving and quickly saturated and are thus ineffective for mass transfer. Only the rivulets are effective, and their total surface area is very small. Similar behavior is observed for surface-tension gradients caused by vertical variations in composition. However, in that case the behavior is more complicated and requires an analysis of interphase mass transfer.[7]

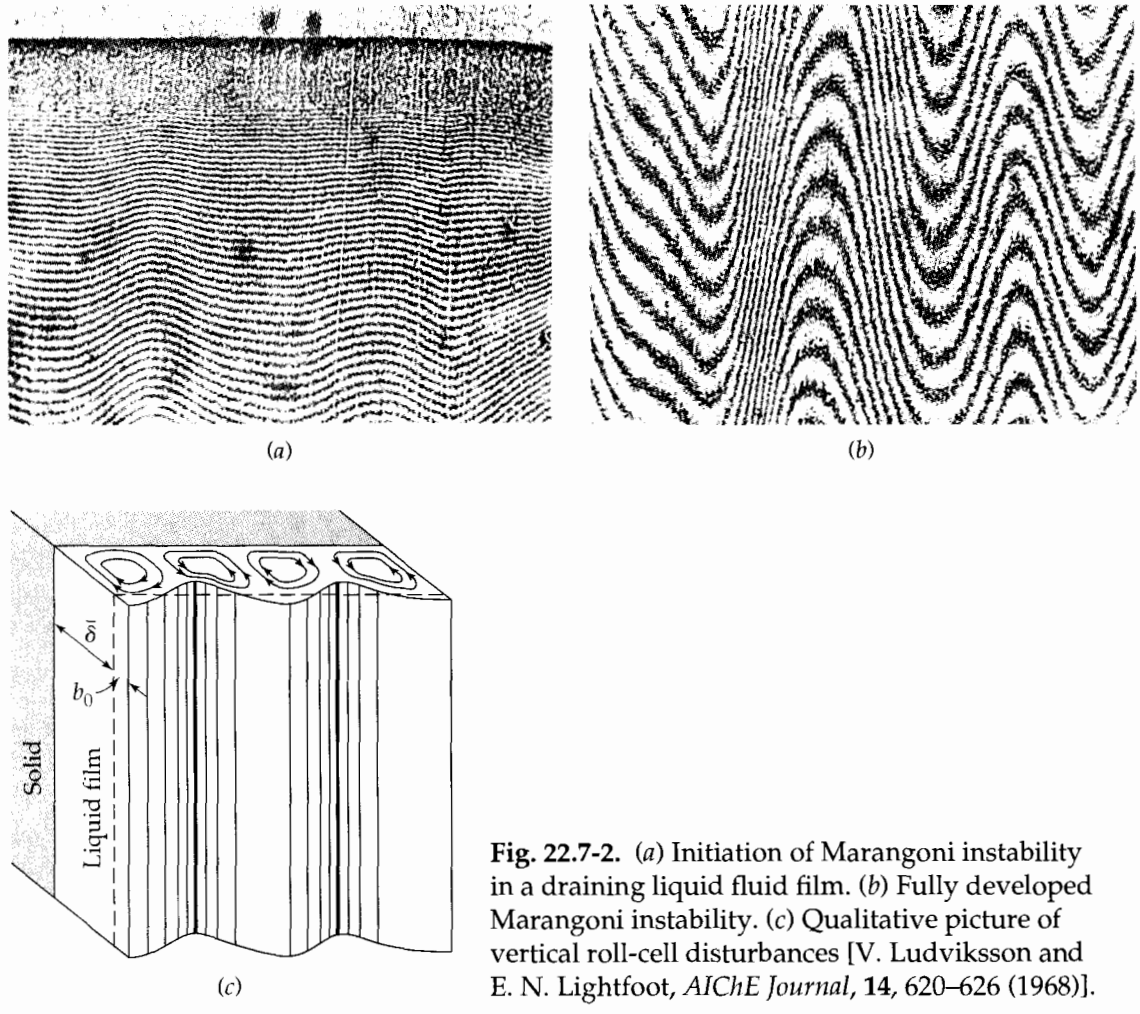

Fig. 22.7-2. (*a*) Initiation of Marangoni instability in a draining liquid fluid film. (*b*) Fully developed Marangoni instability. (*c*) Qualitative picture of vertical roll-cell disturbances [V. Ludviksson and E. N. Lightfoot, *AIChE Journal*, **14**, 620–626 (1968)].

§22.8 TRANSFER COEFFICIENTS AT HIGH NET MASS TRANSFER RATES

High net mass transfer rates across phase boundaries distort the boundary-layer profiles of velocity and temperature as well as species concentration, and they also alter the boundary layer thicknesses. Both of these effects tend to increase friction factors and the heat and mass transfer coefficients, if the mass transfer is toward the boundary, and to reduce them in the reverse situation. These usual trends are reversed, however, in free convection and in flows driven by a rotating surface. The magnitudes of such changes are dependent on the system geometry, boundary conditions, and the magnitudes of the governing parameters such as the Reynolds, Prandtl, and Schmidt numbers, and they are accompanied by the effects of changes in physical properties. They can also either increase or decrease the hydrodynamic stability. Accurate allowance for the effects of net mass transfer thus requires extensive calculation and/or experimentation, but some of the more salient features can be illustrated by using idealized physical models, and this is the approach we follow here.

We begin with the classic *stagnant-film model,* which provides simple estimates of the profile distortion, but is incapable of predicting changes in the effective film thickness. We then discuss the *penetration model* and the flat-plate *laminar boundary layer model.* We conclude with several illustrative examples, the last of which is a complete numerical ex-

ample of boundary layers on a spinning disk. This example will provide a useful appraisal of model sensitivity.

As pointed out in §22.1, when high net mass transfer rates are being considered, we introduce a modified notation for the transfer coefficients:

$$N_{A0} - x_{A0}(N_{A0} + N_{B0}) = k^{\bullet}_{x,\mathrm{loc}}\Delta x_A \tag{22.8-1a}$$

$$e_0 - (N_{A0}\tilde{C}_{pA,0} + N_{B0}\tilde{C}_{pB,0})(T_0 - T^{\circ}) = h^{\bullet}_{\mathrm{loc}}\Delta T \tag{22.8-1b}$$

The black dots in $k^{\bullet}_{x,\mathrm{loc}}$ and $h^{\bullet}_{\mathrm{loc}}$ imply that the distortions of the concentration and temperature profiles resulting from high net mass transfer rates are being included.

The relations between these transfer coefficients and those defined in Eqs. 22.1-7 and 8 are

$$k_{x,\mathrm{loc}} = \lim_{N_{A0}+N_{B0}\to 0} k^{\bullet}_{x,\mathrm{loc}} \tag{22.8-2a}$$

$$h_{\mathrm{loc}} = \lim_{N_{A0}\tilde{C}_{pA,0}+N_{B0}\tilde{C}_{pB,0}\to 0} h^{\bullet}_{\mathrm{loc}} \tag{22.8-2b}$$

This shows explicitly the limiting process that relates the two types of transfer coefficients.

The Stagnant-Film Model[1–4]

We have already discussed this model briefly in §18.2 and more fully in Example 19.4-1. By combining the expressions in Eqs. 19.4-16 and 17 with the definitions in Eqs. 22.8-1a and 1b, we get for the system in Fig. 22.8-1

$$1 + \frac{(N_{A0} + N_{B0})}{k^{\bullet}_{x,\mathrm{loc}}} = \exp\left[(N_{A0} + N_{B0})\frac{\delta_x}{c\mathscr{D}_{AB}}\right] \tag{22.8-3}$$

$$1 + \frac{(N_{A0}\tilde{C}_{pA} + N_{B0}\tilde{C}_{pB})}{h^{\bullet}_{\mathrm{loc}}} = \exp\left[(N_{A0}\tilde{C}_{pA} + N_{B0}\tilde{C}_{pB})\frac{\delta_T}{k}\right] \tag{22.8-4}$$

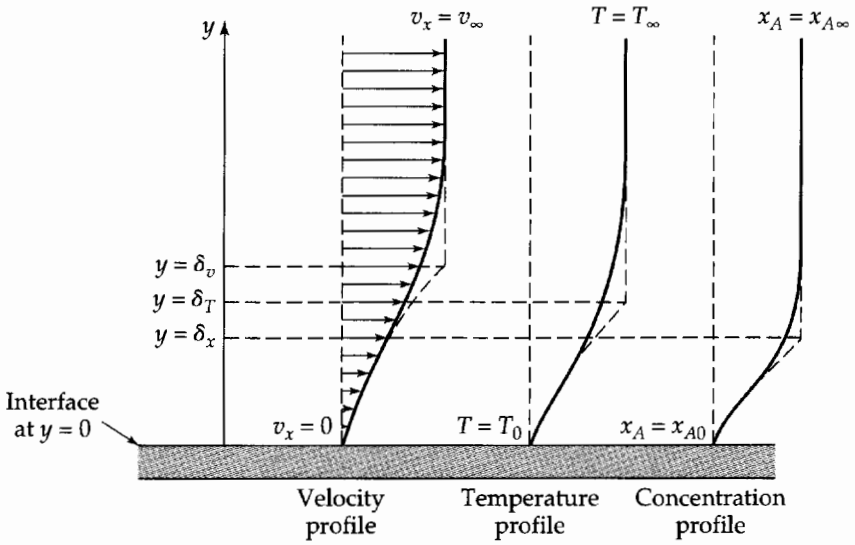

Fig. 22.8-1. Steady flow along a flat surface with rapid mass transfer into the stream. The unbroken curves represent the true profiles, and the broken curves are predicted by the film model.

---

[1] W. K. Lewis and K. C. Chang, *Trans. AIChE*, **21**, 127–136 (1928).
[2] G. Ackerman, *Forschungsheft*, **382**, 1–16 (1937).
[3] A. P. Colburn and T. B. Drew, *Trans. AIChE*, **33**, 197–212 (1937).
[4] H. S. Mickley, R. C. Ross, A. L. Squyers, and W. E. Stewart, *NACA Tech. Note 3208* (1954).

By following the limiting processes indicated in Eqs. 22.8-2a and 2b, we then get expressions for the transfer coefficients in the low net mass transfer limit:

$$\frac{1}{k_{x,\text{loc}}} = \frac{\delta_x}{c\mathscr{D}_{AB}} \tag{22.8-5}$$

$$\frac{1}{h_{\text{loc}}} = \frac{\delta_T}{k} \tag{22.8-6}$$

These limiting values are found by expanding the right sides of Eqs. 22.8-3 and 4 in Taylor series and retaining two terms. Substitution of Eqs. 22.7-5 and 6 into Eqs. 19.4-16 and 17 enables us to eliminate the film thicknesses (which are ill-defined) in favor of the transfer coefficients at low mass-transfer rates (which are measurable):

$$1 + \frac{(N_{A0} + N_{B0})(x_{A0} - x_{A\infty})}{N_{A0} - x_{A0}(N_{A0} + N_{B0})} = \exp\left(\frac{N_{A0} + N_{B0}}{k_{x,\text{loc}}}\right) \tag{22.8-7}$$

$$1 + \frac{(N_{A0}\tilde{C}_{pA} + N_{B0}\tilde{C}_{pB})(T_0 - T_\infty)}{q_0} = \exp\left(\frac{N_{A0}\tilde{C}_{pA} + N_{B0}\tilde{C}_{pB}}{h_{\text{loc}}}\right) \tag{22.8-8}$$

These equations are the principal results of the film model. They show how the conductive energy flux and the diffusion flux at the wall depend on N_{A0} and N_{B0}. In this model, the effects of net mass transfer on the conductive and diffusive interfacial fluxes are clearly analogous. Although these relations were derived for laminar flow and constant physical properties, they are also useful for turbulent flow and for variable physical properties (see Problem 22B.3).

The results for heat and mass transfer can be summarized in two equations:

$$\theta = \frac{\phi}{R} = \frac{\phi}{e^{\phi} - 1} = \frac{\ln(1 + R)}{R} \tag{22.8-9}$$

$$\Pi = \frac{e^{\phi\eta} - 1}{e^{\phi} - 1} = \frac{(1 + R)^{\eta}}{R} \qquad (\eta \leq 1) \tag{22.8-10}$$

Equation 22.8-9 gives the correction factors θ_x and θ_T by which the coefficients $k_{x,\text{loc}}$ and h_{loc} must be multiplied to obtain the coefficients at high net mass transfer rates. Equation 22.8-10 gives the concentration and temperature profiles. The meanings of the symbols are summarized in Table 22.8-1.

Table 22.8-1 Summary of Dimensionless Quantities to be Used for All Models Discussed in §22.8. Mass-based versions appear in §20.2 and §22.9.

θ = correction factors R = flux ratios
ϕ = rate factors Π = profiles
η = dimensionless distance from wall

	Mass transfer	Heat transfer
θ	$\theta_x = \dfrac{k^{\bullet}_{x,\text{loc}}}{k_{x,\text{loc}}}$	$\theta_T = \dfrac{h^{\bullet}_{\text{loc}}}{h_{\text{loc}}}$
ϕ	$\phi_x = \dfrac{N_{A0} + N_{B0}}{k_{x,\text{loc}}}$	$\phi_T = \dfrac{N_{A0}\tilde{C}_{pA} + N_{B0}\tilde{C}_{pB}}{h_{\text{loc}}}$
R	$R_x = \dfrac{(N_{A0} + N_{B0})(x_{A0} - x_{A\infty})}{N_{A0} - x_{A0}(N_{A0} + N_{B0})}$	$R_T = \dfrac{(N_{A0}\tilde{C}_{pA} + N_{B0}\tilde{C}_{pB})(T_0 - T_\infty)}{q_0}$
Π	$\Pi_x = \dfrac{x_A - x_{A0}}{x_{A\infty} - x_{A0}}$	$\Pi_T = \dfrac{T - T_0}{T_\infty - T_0}$
η	$\eta_x = \dfrac{y}{\delta_x} = \dfrac{y}{c\mathscr{D}_{AB}/k_{x,\text{loc}}}$	$\eta_T = \dfrac{y}{\delta_T} = \dfrac{y}{k/h_{\text{loc}}}$

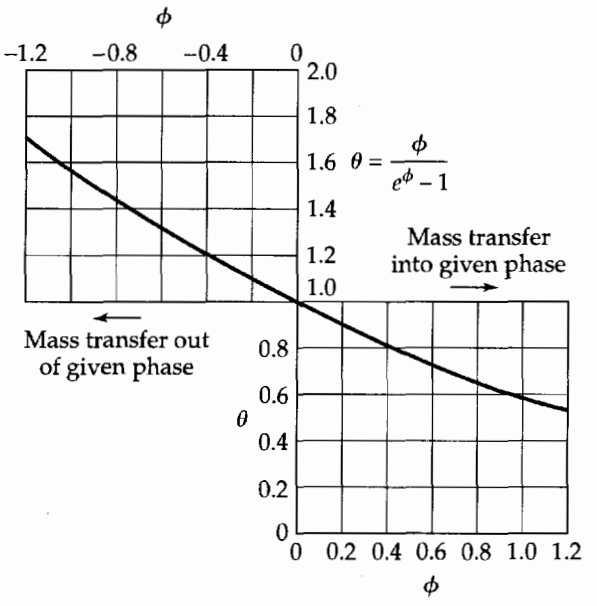

Fig. 22.8-2. The variation of the transfer coefficients with mass transfer rate, as given by the film model (see Eq. 22.8-9).

Equation 22.8-9 is given graphically in Fig. 22.8-2. This shows that for net transfer of A and B into the stream (positive ϕ), the transfer coefficients decrease, whereas net transfer of A and B out of the stream (negative ϕ) causes the transfer coefficients to increase.

Some sample profiles from Eq. 22.8-10 are shown in Fig. 22.8-3. In the limit of small mass-transfer rates (i.e., $\phi \to 0$ or $R \to 0$), Eq. 22.8-10 becomes simply $\Pi = \eta$. The film model regards the region outside the film as perfectly mixed, thus giving a profile that is flat beyond $\eta = 1$.

The Penetration Model

We next turn to the transfer coefficient at large net mass transfer rates for systems in which there is no significant drag at the interface. We have already studied several systems of this type: gas absorption into a falling liquid film and from a rising bubble (§18.5), and unsteady-state evaporation (§20.1). These systems are generally lumped together under the heading of *penetration theory*.

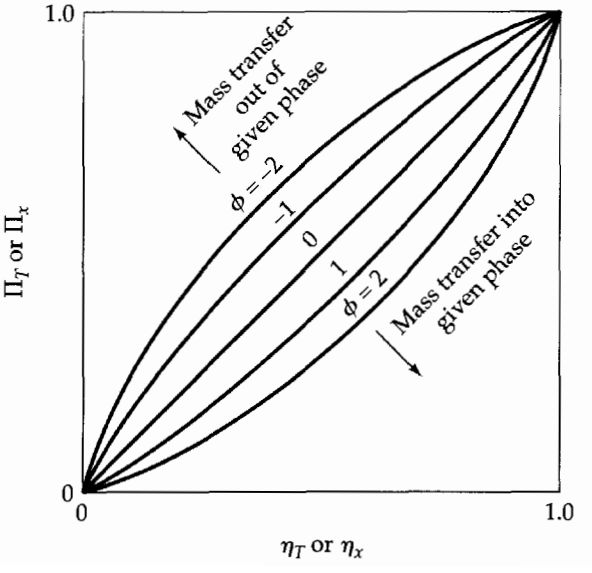

Fig. 22.8-3. Temperature and concentration profiles in a laminar film, as calculated by the film model (see Eq. 22.8-10).

A falling film system is shown in Fig. 22.8-4. The time of travel from the liquid inlet to the liquid outlet (the "exposure time") is sufficiently short that the diffusing species does not penetrate very far into the liquid. In such a situation, we can (from a mathematical point of view) regard the falling film as infinitely thick. We may then take over the results from Example 20.1-1.

Equation 20.1-23 gives the concentration profiles for a corresponding unsteady-state system with large net mass transfer rate, and an analogous equation can be written down for the temperature profiles:

$$\Pi_x \equiv \frac{x_A - x_{A0}}{x_{A\infty} - x_{A0}} = \frac{\text{erf}(\eta_x - \varphi_x) + \text{erf}\,\varphi_x}{1 + \text{erf}\,\varphi_x} \tag{22.8-11}$$

$$\Pi_T \equiv \frac{T - T_0}{T_\infty - T_0} = \frac{\text{erf}(\eta_T - \varphi_T) + \text{erf}\,\varphi_T}{1 + \text{erf}\,\varphi_T} \tag{22.8-12}$$

Here $\eta_x = y/\sqrt{4\mathscr{D}_{AB}t}$ and $\eta_T = y/\sqrt{4\alpha t}$ are dimensionless distances from the interface, and φ in each formula is a dimensionless molar average velocity at the interface:

$$\varphi_x = \frac{N_{A0} + N_{B0}}{c}\sqrt{\frac{t}{\mathscr{D}_{AB}}} \qquad \varphi_T = \frac{N_{A0} + N_{B0}}{c}\sqrt{\frac{t}{\alpha}} \tag{22.8-13a, b}$$

From these results and the definitions for the transfer coefficients in Eqs. 22.8-1 and 2, we may now get the rate factors ϕ, the flux ratios R, and the correction factors θ, defined in the preceding subsection:

$$\phi = \sqrt{\pi}\varphi \tag{22.8-14}$$

$$R = \left(1 + \text{erf}\frac{\phi}{\sqrt{\pi}}\right)\phi\,\exp\left(\frac{\phi^2}{\pi}\right) \tag{22.8-15}$$

$$\theta = \frac{\exp(-\phi^2/\pi)}{1 + \text{erf}(\phi/\sqrt{\pi})} \tag{22.8-16}$$

From the definitions in Eqs. 22.8-1 and 2 and the profiles in Eqs. 22.8-11 and 12, we can also get the expressions for the transfer coefficients at low net mass transfer rates:

$$k_{x,\text{loc}} = c\sqrt{\frac{\mathscr{D}_{AB}}{\pi t}}; \qquad h_{\text{loc}} = \rho\hat{C}_p\sqrt{\frac{\alpha}{\pi t}} \tag{22.8-17, 18}$$

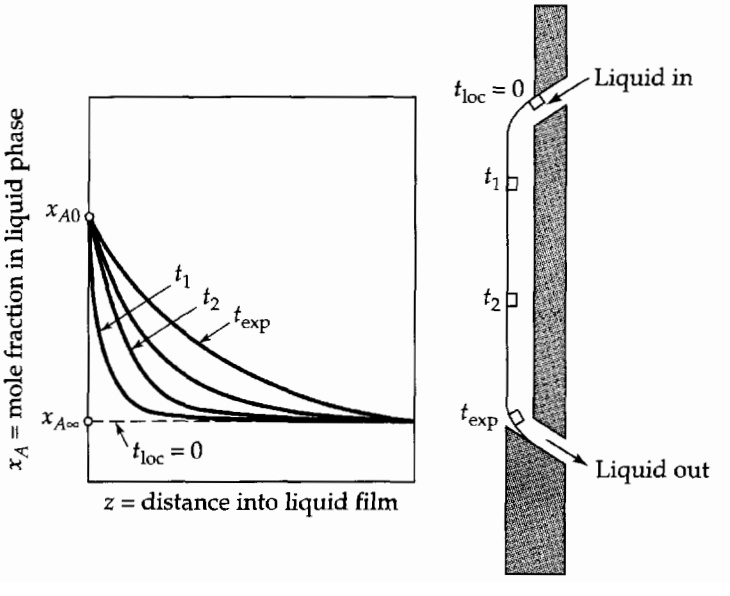

Fig. 22.8-4. Diffusion into a falling liquid film. Here t_{exp} is the total time of exposure of a typical element of volume near the surface.

The corresponding coefficients at high net mass transfer rates can be obtained by multiplying by the correction factor in Eq. 22.8-16.

From the last two equations we get the relation

$$h_{\text{loc}} = k_{x,\text{loc}}\tilde{C}_p\left(\frac{\alpha}{\mathscr{D}_{AB}}\right)^{1/2} \tag{22.8-19}$$

A similar relation, with an exponent of $\frac{2}{3}$ (instead of $\frac{1}{2}$) is obtained from the Chilton–Colburn relations given in Eqs. 22.3-23 to 25. The latter are valid for flows adjacent to rigid boundaries, whereas Eq. 22.8-19 pertains to fluid-fluid systems with no velocity gradient at the interface.

The proportionality of $k_{x,\text{loc}}$ to the square root of the diffusivity, given in Eq. 22.8-17, has been confirmed experimentally for the liquid phase in several gas–liquid mass transfer systems, including short wetted-wall columns, packed columns, and liquids around gas bubbles in certain instances. The penetration model has also been applied to absorption with chemical reactions (see Example 20.1-2).

The Flat-Plate Boundary Layer Model

The steady-state transport in the boundary layer along a flat plate for a fluid with constant physical properties was discussed in §20.2. The general expression for the profiles, $\Pi(\eta, \Lambda, K)$, was given in Eq. 20.2-43. There $\eta = y\sqrt{v_\infty/2\nu x}$ is a dimensionless position coordinate measured from the plate, Λ is the physical property group (i.e., 1, Pr, or Sc), and $K = (v_{y0}/v_\infty)\sqrt{2v_\infty x/\nu}$ is a dimensionless net mass flux from the plate.

Once again we introduce the notations defined in Table 22.8-1. Then for the boundary layer calculation we have

$$R = \frac{K\Lambda}{\Pi'(0, \Lambda, K)} \qquad \phi = \frac{K\Lambda}{\Pi'(0, \Lambda, 0)} \qquad \theta = \frac{\Pi'(0, \Lambda, K)}{\Pi'(0, \Lambda, 0)} \tag{22.8-20, 21, 22}$$

In the boundary layer calculation it was assumed that the heat capacities of both species are identical.

The momentum, heat, and mass fluxes for the flat plate are given in Fig. 22.8-5. Then in the following two figures, Figs. 22.8-6 and 22.8-7, two plots are given, comparing the correction factors, θ, for the film model, the penetration model, and the boundary layer model. The boundary layer model gives a dependence on Λ that is not found in the other models, because this model includes the effect of the tangential velocity profiles on the temperature and concentration profiles. The film model predicts the smallest dependence of the transfer coefficients on net mass-transfer rate.

Correction factors considerably different from 1 arise when either ϕ or R is of magnitude 1 or greater for T or x_A; see Figures 22.8-6, 7 and 8, and the relation $\theta = \phi/R$. Large net interfacial mass fluxes, by these measures, are common when the mass transfer is mechanically driven as in ultrafiltration (Example 22.8-5) and transpiration cooling (Problem 20B.7(c)). Large net mass fluxes can also occur in vaporization, condensation, melting and other changes of state, and in heterogeneous chemical reactions, when accompanied by correspondingly large temperature differences or radiation intensities to transfer the requisite latent heat or energy of reaction. More moderate net fluxes, and correction factors near unity, are common in multistage and packed-column separation processes, where the differences of temperature and composition within a separation stage or flow cross-section are normally rather small. The energy flux ratio R_T is an important criterion for assessing the net-flux corrections, as illustrated in Examples 22.8-2 and 3.

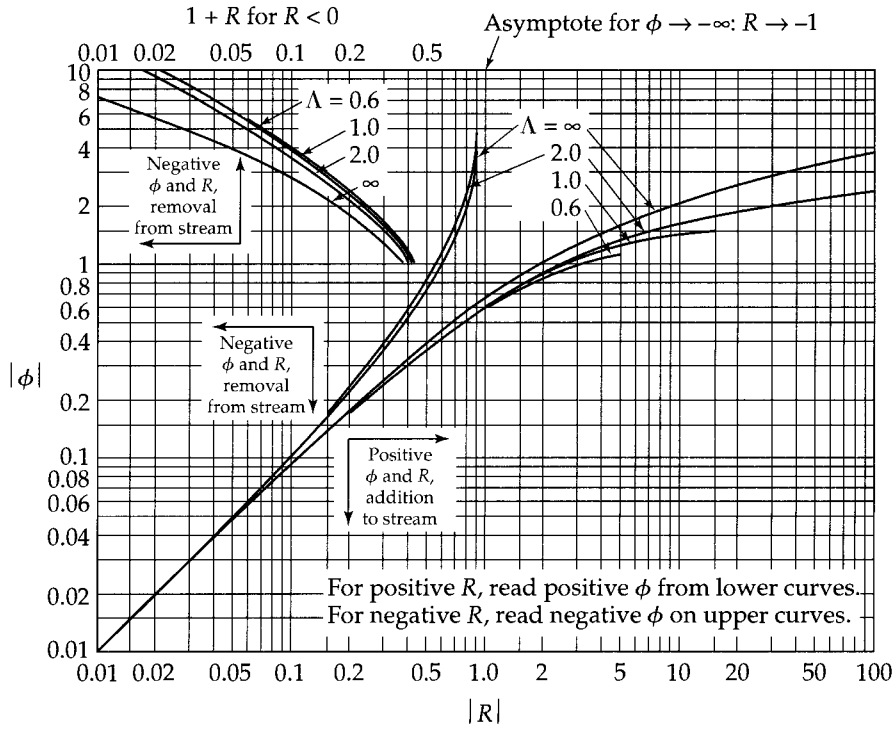

Fig. 22.8-5. Heat and mass fluxes between a flat plate and a laminar boundary layer [W. E. Stewart, ScD thesis, Massachusetts Institute of Technology (1951)].

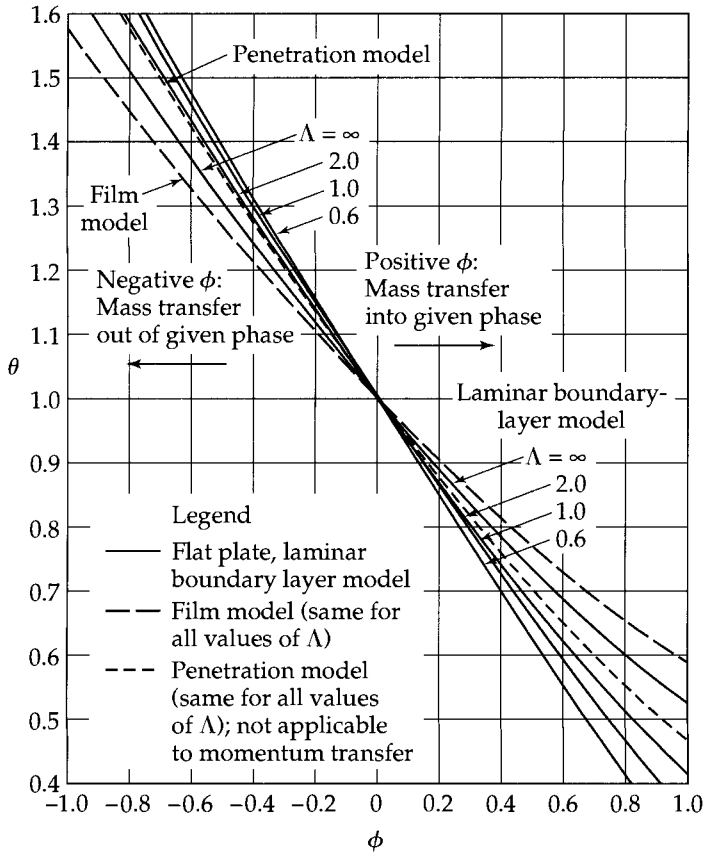

Fig. 22.8-6. The variation of the transfer coefficients with mass transfer rate as predicted by various models. The line for $\Lambda \to \infty$ holds for the nonseparated, steady state boundary-layer regions on rigid surfaces, whatever their geometry.

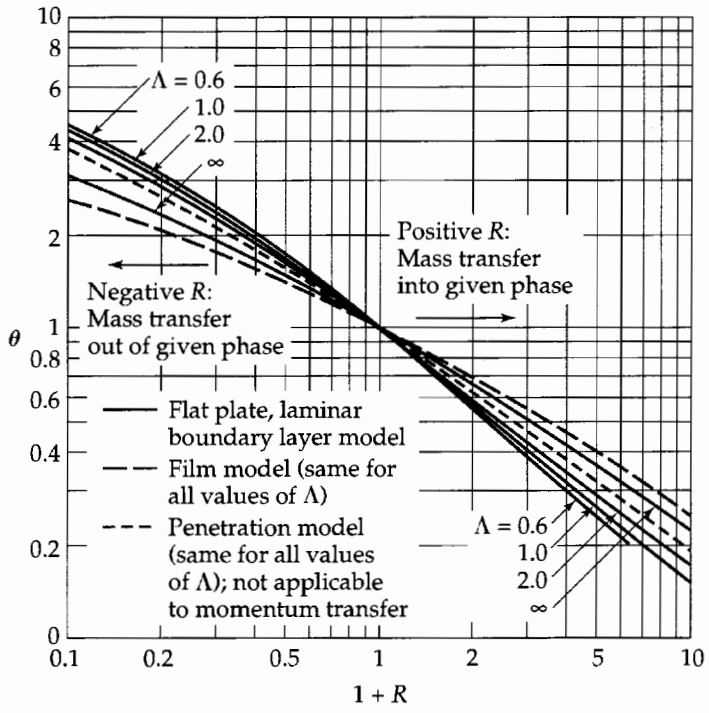

Fig. 22.8-7. The variation of the transfer coefficients with the flux ratio R as predicted by various models. The line for $\Lambda \to \infty$ holds for the nonseparated, steady state boundary-layer regions on smooth rigid surfaces, whatever their geometry.

EXAMPLE 22.8-1

Rapid Evaporation of a Liquid from a Plane Surface

Solvent A is evaporating out of a coat of lacquer on a plane surface exposed to a tangential stream of noncondensable gas B. At a given point on the surface, the gas-phase mass transfer coefficient $k_{x,\text{loc}}$ at the prevailing average fluid properties is given as 0.1 lb-mole/hr · ft^2; the Schmidt number is Sc = 2.0. The interfacial gas composition is $x_{A0} = 0.80$. Estimate the local rate of evaporation, using **(a)** the stagnant film model, **(b)** the flat-plate boundary layer model, and **(c)** the uncorrected mass transfer coefficient $k_{x,\text{loc}}$.

SOLUTION

(a) Since B is noncondensable, $N_{B0} = 0$. Application of Eq. 22.8-7 (which is the same as $1 + R_x = \exp \phi_x$) to the gas phase then gives

$$1 + \frac{(N_{A0} + 0)(0.80 - 0)}{N_{A0} - 0.80(N_{A0} + 0)} = \exp\left(\frac{N_{A0} + 0}{0.1}\right) \tag{22.8-23}$$

From this we get, after taking the logarithm,

$$N_{A0} = 0.1 \ln(1 + 4.0) = 0.161 \text{ lb-mole/hr} \cdot \text{ft}^2 \tag{22.8-24}$$

as the result of the stagnant-film model. This corresponds to a correction factor $\theta_x = \phi_x / R_x = 0.40$.

(b) As in part (a), $R_x = 4.0$. Then from Fig. 22.8-5, at $R_x = 4.0$ and $\Lambda_x = 2.0$, we find that $\phi_x = 1.3$. By setting $N_{B0} = 0$ in the formula for ϕ_x in Table 22.8-1, we get

$$N_{A0} = k_{x,\text{loc}} \phi_x = (0.1)(1.3) = 0.13 \text{ lb-mole/hr} \cdot \text{ft}^2 \tag{22.8-25}$$

as the result of the flat-plate boundary layer model. The corresponding correction factor θ_x is 0.33.

(c) If the mass transfer coefficient $k_{x,\text{loc}}$ is used without correction for the net interfacial flux, we get from Eq. 22.1-5, with $N_{B0} = 0$

$$N_{A0} - 0.80(N_{A0} + 0) = (0.1)(0.80 - 0) \tag{22.8-26}$$

whence $N_{A0} = 0.400$. This result is much too high and shows that the corrections for net molar flux are important at these conditions. The boundary layer solution in part (b) should be accurate if the flow is laminar and the variation in the physical properties is not too great.

EXAMPLE 22.8-2

Correction Factors in Droplet Evaporation

Adjust the results of Example 22.3-1 for the net molar flux by applying the correction factors θ_x and θ_T from the film model and from the flat-plate boundary layer model.

SOLUTION

In Example 22.3-3 the molar flux ratio R_x at any point on the surface of the drop is

$$R_x = \frac{(N_{A0} + N_{B0})(x_{A0} - x_{A\infty})}{N_{A0} - x_{A0}(N_{A0} + N_{B0})} = \frac{(N_{A0} + 0)(0.0247 + 0)}{N_{A0} - 0.0247(N_{A0} + 0)} = \frac{0.0247}{1 - 0.0247} = 0.0253 \tag{22.8-27}$$

From Eq. 22.8-9 (film model) or Fig. 22.8-7 (flat-plate boundary layer model), the predicted correction factor θ_x is about 0.99 at all points on the drop. Hence the corrected mass transfer rate is (by adjustment of Eq. 22.3-31)

$$W_{A0} = \theta_x k_{xm} \pi D^2 \frac{x_{A0} - x_{A\infty}}{1 - x_{A0}} = (0.987)(2.70 \times 10^{-7}) = 2.66 \times 10^{-7}\ \text{g-mole/s} \cdot \text{cm}^2 \tag{22.8-28}$$

This result differs only slightly from that obtained in Example 22.3-1. Thus the assumption of a small mass-transfer rate was satisfactory under the given conditions.

EXAMPLE 22.8-3

Wet-Bulb Performance Corrected for Mass-Transfer Rate

Extend the analysis of Example 22.3-2 to include the corrections for net mass-transfer rate, using the stagnant film model.

SOLUTION

By rewriting the energy balance, Eq. 22.3-32, for any point on the wick, we obtain for finite mass-transfer rate

$$N_{A0}\Delta\tilde{H}_{A,\text{vap}} = h'_{\text{loc}}(T_\infty - T_0) \tag{22.8-29}$$

Multiplication of both sides by $\tilde{C}_{pA}/(\Delta\tilde{H}_{A,\text{vap}}h'_{\text{loc}})$ gives, since $N_{B0} = 0$,

$$R_T = \frac{N_{A0}\tilde{C}_{pA}}{h'_{\text{loc}}} = \frac{\tilde{C}_{pA}(T_\infty - T_0)}{\Delta\tilde{H}_{A,\text{vap}}} \tag{22.8-30}$$

The right-hand member of this equation is easily calculated if T_0, T_∞, and p are given.

Next we write the expression $\phi = \ln(1 + R)$ for both heat and mass transfer, taking into account the fact that $N_{B0} = 0$:

$$\frac{N_{A0}\tilde{C}_{pA}}{h_{\text{loc}}} = \ln(1 + R_T); \qquad \frac{N_{A0}}{k_{x,\text{loc}}} = \ln(1 + R_x) \tag{22.8-31, 32}$$

Solving both equations for N_{A0} and equating the resulting expressions gives

$$\ln(1 + R_x) = \frac{h_{\text{loc}}}{k_{x,\text{loc}}\tilde{C}_{pA}} \ln(1 + R_T) \tag{22.8-33}$$

Then substituting the expressions for R_x and R_T from Table 22.8-1 yields

$$\ln\left(1 + \frac{x_{A0} - x_{A\infty}}{1 - x_{A0}}\right) = \frac{h_{\text{loc}}}{k_{x,\text{loc}}\tilde{C}_{pA}} \ln\left(1 + \frac{\tilde{C}_{pA}(T_\infty - T_0)}{\Delta\tilde{H}_{A,\text{vap}}}\right) \tag{22.8-34}$$

This equation shows that x_{A0} and T_0 will be constant over the surface of the wick if $h_{\text{loc}}/(k_{x,\text{loc}}\tilde{C}_{pA})$ is constant and thus equal to $h_m/(k_{xm}\tilde{C}_{pA})$. This constancy is assumed here for

simplicity. Such an assumption is particularly satisfactory for the water–air system, for which Pr and Sc are nearly equal. With this substitution, Eq. 22.8-34 becomes

$$\ln\left(1 + \frac{x_{A0} - x_{A\infty}}{1 - x_{A0}}\right) = \frac{h_m}{k_{xm}\tilde{C}_{pA}} \ln\left(1 + \frac{\tilde{C}_{pA}(T_\infty - T_0)}{\Delta\tilde{H}_{A,\text{vap}}}\right) \tag{22.8-35}$$

This solution simplifies exactly to Eq. 22.3-35 at low mass-transfer rates.

For the numerical problem in Example 22.3-2, the following values apply:

$$x_{A0} = 0.0247$$

$$\tilde{C}_{pA} = 8.03 \text{ Btu/lb-mole} \cdot \text{F for water vapor at } 105^\circ\text{F}$$

$$h_m/k_{xm} = 5.93 \text{ Btu/lb-mole} \cdot \text{F from the Chilton–Colburn analogy (Eq. 22.3-25)}$$

$$\frac{\tilde{C}_{pA}(T_\infty - T_0)}{\Delta\tilde{H}_{A,\text{vap}}} = \frac{(8.03)(140 - 70)}{18{,}900} = 0.0297$$

Insertion of these values into Eq. 22.8-35 gives

$$\ln\left(1 + \frac{0.0247 - x_{A\infty}}{1 - 0.0247}\right) = \frac{5.93}{8.03} \ln(1.0297) = 0.0216 \tag{22.8-36}$$

Solving this equation, we get

$$x_{A\infty} = 0.0034 \tag{22.8-37}$$

This result differs only slightly from the value 0.0033 obtained in Example 22.3-2 and justifies the previous omission of the correction factors under the given conditions.

Numerical studies indicate that the simple Eq. 22.3-34 gives a close approximation to Eq. 22.8-35 for the air–water system under all likely wet-bulb conditions. Eqs. 22.3-32 and 33 overestimate the mass transfer rate almost equally, and when these equations are combined, the errors largely compensate.

EXAMPLE 22.8-4

Comparison of Film and Penetration Models for Unsteady Evaporation in a Long Tube

Compare the effects of net mass transfer for the unsteady evaporation system described in Example 20.1-1 with the predictions of **(a)** the generalized penetration model, and **(b)** the stagnant-film model introduced above. The latter calculation amounts to a quasi-steady-state treatment of this time-dependent system.

SOLUTION

We begin by noting that for this system $x_{A\infty} = 0$ and $N_{B0} = 0$. It follows from Eq. 22.8-1a and Table 22.8-1 that

$$N_{A0} = \theta_x k_x \frac{x_{A0} - 0}{1 - x_{A0}} \tag{22.8-38}$$

The correction factor θ_x is thus the ratio of the flux corrected for net mass transfer to the uncorrected flux.

(a) ***The penetration model.*** We note that the concentration gradient at the liquid surface can be obtained by differentiating Eq. 20.1-16 and rewriting the result in terms of x_A and z. The result is

$$\left.\frac{\partial x_A}{\partial z}\right|_{z=0} = -\frac{2}{\sqrt{\pi}} \frac{\exp(-\varphi^2)}{1 + \text{erf}\,\varphi} \frac{x_{A0}}{\sqrt{4\mathscr{D}_{AB}t}} \tag{22.8-39}$$

For negligible net mass transfer, $\varphi = 0$. Thus, the ratio of the mass flux in the presence of net mass transfer to the flux in the absence of net mass transfer is

$$\theta_x = \frac{\exp(-\varphi^2)}{1 + \text{erf}\,\varphi} \tag{22.8-40}$$

Table 22.8-2 Comparison of Film and Penetration Models.

x_{A0}	θ_x from penetration model (Eq. 22.8-41)	θ_x from film model (Eq. 22.8-42)
0.00	1.000	1.000
0.25	0.831	0.863
0.50	0.634	0.693
0.75	0.391	0.462
1.00	0.000	0.000

in agreement with Eqs. 22.8-14 and 16. To get θ_x as a function of x_{A0}, we may use Fig. 22.8-7, or use Eq. 20.1-17 to write

$$\theta_x = (1 - x_{A0})\psi(x_{A0}) \qquad \text{(penetration model)} \tag{22.8-41}$$

where $\psi(x_{A0})$ is the quantity defined just after Eq. 20.1-22 and given in Table 20.1-1.

(b) ***The stagnant-film model.*** The film model result may be obtained from Eq. 22.8-9 in the form $\theta = (1/R)\ln(1 + R)$ to obtain

$$\theta_x = \frac{1 - x_{A0}}{x_{A0}} \ln\left(\frac{1}{1 - x_{A0}}\right) \qquad \text{(film model)} \tag{22.8-42}$$

Numerical values for both models are provided in Table 22.8-2 and also in Fig. 22.8-7.

It is seen that the penetration model predicts a stronger correction θ_x for net mass transfer than does the film model. This is in part because the net flow thickens the boundary layer, an effect that the film model does not consider. It may also be noted that this example is a realistic use of the penetration model, as there is little effect of solute concentration on the physical properties in this simple isothermal system. A much different situation is seen in the next example.

EXAMPLE 22.8-5

Concentration Polarization in Ultrafiltration

Ultrafiltration of proteins is a concentration process, in which water from an aqueous protein solution is forced through a membrane impermeable to the protein but permeable to water and small solutes such as inorganic salts. Protein then accumulates in a *polarization layer*, or region of high protein concentration adjacent to the membrane surface, as indicated in Fig. 22.8-8. Determine the relation between water permeation velocity and the transmembrane

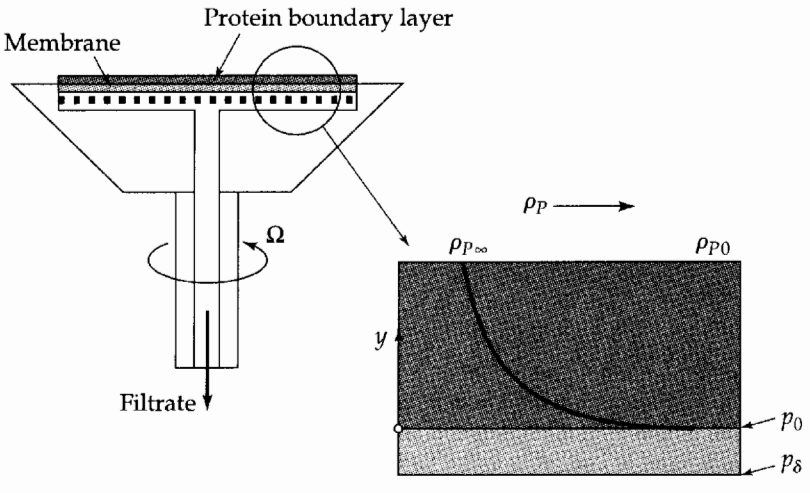

Fig. 22.8-8. A spinning-disk ultrafilter.

pressure difference. Describe the effect of net mass transfer on the mass transfer coefficient for protein transport. Assume that the membrane is completely impermeable to protein so that the net transport of protein across the membrane surface is zero.

SOLUTION

For simplicity we choose a spinning-disk geometry as shown in Fig. 22.8-8, for which the protein concentration will be a function only of the distance y from the disk surface and not of radial position[5] (see Problem 19D.4). However, we will have to consider the dependence of density, viscosity, and protein–water diffusivity on the protein concentration, and we will need the concept of osmotic pressure.[6]

The basis for our solution is the concept of *hydraulic permeability* of the filtration membrane:

$$v_\delta = K_H(p_0 - p_\delta - \pi) \tag{22.8-43}$$

Here v_δ is the velocity, or volumetric flux, of the solvent leaving the downstream surface of the membrane. Equation 22.8-43 defines K_H, the hydraulic permeability of the membrane. The quantities p_0 and p_δ are the hydrodynamic pressures against the membrane as indicated in Fig. 22.8-8, and π is the *osmotic pressure* at the upstream surface of the membrane. The inclusion of π recognizes that it is really the total thermodynamic potential that drives the transmembrane transport (this point will be discussed further in Chapter 24.)

For this situation, the interfacial protein velocity is zero, so that a solvent mass balance across the protein boundary layer gives

$$\rho^{(S)}v_\delta = -(\rho_S v_{Sy})|_{y=0} \tag{22.8-44}$$

in which y is the distance from the upstream membrane surface into the protein boundary layer. The quantity $\rho^{(S)}$ is the density of the pure solvent, and $\rho_{S0} = \rho_S|_{y=0}$ and $v_{S0} = v_{Sy}|_{y=0}$ are the mass concentration and velocity of solvent at the upstream membrane surface.

The osmotic pressure π is a function of the protein concentration ρ_P, and we will provide an example of this in Problem 22C.1. We find then that the water flux across the membrane depends on the protein concentration at the membrane surface as well as the hydrodynamic pressure drop across the membrane. This concentration, in turn, can be related to v_δ through the membrane impermeability condition for the protein and the definition of the mass transfer coefficient. Then at $y = 0$, we describe the impermeability of the membrane to protein by

$$n_{Py} = 0 = k_\rho^\circ(\rho_{P0} - \rho_{P\infty}) + \omega_{P0}(0 + \rho_{S0}v_{S0}) \tag{22.8-45}$$

where k_ρ° has been defined analogously to k_c°. Combination with Eq. 22.8-44 then gives

$$-\rho^{(S)}v_\delta = k_\rho^\circ(\rho_{P0} - \rho_{P\infty})/\omega_{P0} \tag{22.8-46}$$

This equation may now be solved for the filtrate velocity:

$$v_\delta = k_\rho\theta\left(\frac{\rho_0}{\rho^{(S)}}\right)\left(1 - \frac{\rho_{P\infty}}{\rho_{P0}}\right) \tag{22.8-47}$$

Here $\rho_0 = \rho_{P0} + \rho_{S0}$ and $\theta = k_\rho^\circ/k_\rho$ is a mass transfer correction factor, analogous to θ_x, which now must include the effects of property changes as well as the net velocity correction introduced in Table 22.8-1. We return to a discussion of this quantity below (see Eq. 22.8-48). The term ρ_0 is the solution density at the upstream membrane surface.

We can now calculate the desired quantities, v_δ and the transmembrane pressure difference, if we have sufficient information about the transport and equilibrium properties. Here we consider the approaching protein concentration $\rho_{P\infty}$ to be given, and for convenience we

---

[5] D. R. Olander, *J. Heat Transfer*, **84**, 185 (1972).

[6] R. J. Silbey and R. A. Alberty, Physical Chemistry, 3rd edition, Wiley, New York (2001), p. 206.

begin by selecting values of the protein concentration ρ_{P0} at the membrane surface over the range between $\rho_{P\infty}$ and the solubility limit of the protein:

(i) For any chosen value of ρ_{P0}, we can calculate the corresponding value of v_δ from Eq. 22.8-47 with appropriate values for k_p and θ. These values also permit calculation of osmotic pressure π from the appropriate equilibrium relationship.

(ii) We may then calculate the transmembrane pressure difference required for this flow from Eq. 22.8-43 and an appropriate value of K_H.

The strong effects of protein concentration on system properties mean that the solution must be obtained numerically.

We content ourselves here to summarize the results of Kozinski and Lightfoot[7] for bovine serum albumin; they were the first to make such calculations and seem still to have provided the best documentation. In their publications it is shown that the effective mass transfer coefficient can be expressed as the product of two factors, one accounting for the concentration effects and another taking account of the additional effect of property variations:

$$\theta = \theta_c \theta_p \tag{22.8-48}$$

where, over the parameter space investigated,

$$\theta_c = 1.6\left(\frac{\rho_{P0}}{\rho_{P\infty}}\right)^{1/3}; \qquad \theta_p = \mathscr{D}_{\text{rel}}^{2/3}\left(\frac{1}{\nu}\right)_{\text{rel}}^{1/3} \tag{22.8-49, 50}$$

and

$$\mathscr{D}_{\text{rel}} = \frac{1}{2}\left(1 + \frac{\mathscr{D}_{PS}(0)}{\mathscr{D}_{PS}(\infty)}\right); \qquad \left(\frac{1}{\nu}\right)_{\text{rel}} = \frac{1}{2}\left(1 + \frac{\nu(\infty)}{\nu(0)}\right) \tag{22.8-51, 52}$$

Equations 22.8-49 to 52 must be considered empirical. Equation 22.8-47 overpredicts v_δ for small polarization levels, but for that situation the effect of osmotic pressure on flow is small. The subscript rel means "relative to the free-stream value."

The mass transfer coefficient in the limit of slow mass transfer and small property variations is given[7] as

$$\text{Sh}_m = \text{Sh}_{\text{loc}} = \frac{k_p L}{\mathscr{D}_{PS}(\infty)} = 0.6205\left(\frac{L^2\Omega}{\nu(\infty)}\right)^{1/2}\left(\frac{\nu(\infty)}{\mathscr{D}_{PS}(\infty)}\right)^{1/3} \tag{22.8-53}$$

in which L is the disk diameter and Ω is the rate of rotation in radians per unit time. The independence of mass transfer rate on disk size is the reason that this geometry is so popular for careful mass transfer studies. Other geometries are considered briefly by Kozinski and Lightfoot.[7]

A comparison of a priori predictions from the above model with experimental data is shown in Fig. 22.8-9, where we see that the two agree well. This good agreement may result in part because the albumin molecules behave much like incompressible particles at the high solvent ionic strength at which the data were taken. It may also be seen that osmotic effects are negligible below pressure drops of about 5 psi; here the predicted behavior is indistinguishable from that of the protein-free solvent, essentially water. It is only in this unimportant region that Eq. 22.8-48 is unreliable. Details of the calculations are provided in Problem 22C.1.

The effect of increasing pressure difference across the protein boundary layer is quite different from that for a nonselective membrane. At first, the concentration boundary layer gets thinner, as would be expected, and the mass transfer coefficient k_p' increases. However, with

---

[7] A. A. Kozinski, PhD thesis, University of Wisconsin (1971); A. A. Kozinski and E. N. Lightfoot, *AIChE Journal*, **18**, 1030–1040 (1972).

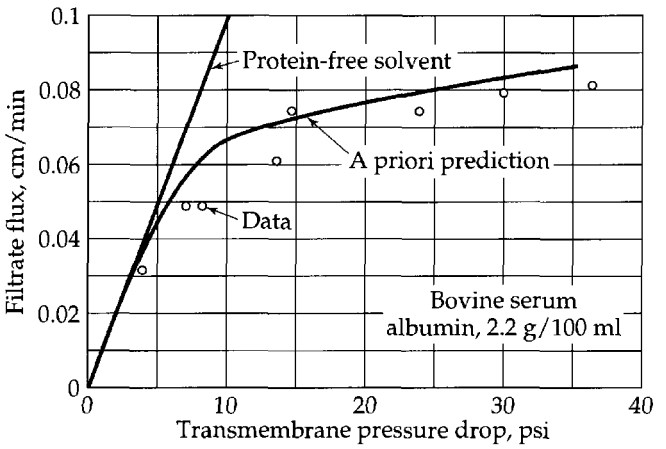

Fig. 22.8-9. Protein ultrafiltration with a spinning disk at 273 rpm.

further increase in the pressure difference the boundary layer thickness, k_ρ^* and θ_c all approach asymptotic limits. In practice, these asymptotes are closely approached before the effect of polarization becomes appreciable, relative to the membrane flow resistance, and these asymptotes suffice to predict the relation between the transmembrane pressure difference and transmembrane flow.

The behavior can be seen more clearly inserting Eq. 22.8-48 and 49 and the approximate formula

$$1.6\left(\frac{\rho_{P0}}{\rho_{P\infty}}\right)^{1/3}\left(1-\frac{\rho_{P\infty}}{\rho_{P0}}\right) \approx 1.39 \ln \frac{\rho_{P0}}{\rho_{P\infty}} \tag{22.8-54}$$

into Eq. 22.8-47. Then, to a surprisingly good approximation, Eq. 22.8-47 takes the form

$$v_\delta = \left(1.39 k_\rho \ln \frac{\rho_{P0}}{\rho_{P\infty}}\right)\left(\frac{\rho_0}{\rho^{(S)}}\right)\theta_p \tag{22.8-55}$$

The quantity in the first set of parentheses has the form of the simple film model, but with k_ρ multiplied by 1.39. It is probably Eq. 22.8-55 that has made the simple film model attractive to many for correlating ultrafiltration and reverse osmosis data. However, neglect of the multiplier 1.39 has caused corresponding underestimation of v_δ, even before addressing the effects of property variations.

§22.9 MATRIX APPROXIMATIONS FOR MULTICOMPONENT MASS TRANSPORT

Multicomponent mass transport occurs widely in chemical, physiological, biological, and environmental processes and is analyzed by various mathematical methods. Here we review some matrix approximation methods for mass transport by convection and ordinary diffusion in multicomponent gases. A fuller treatment, including mass transport in liquids, is given in the text by Taylor and Krishna.[1]

Multicomponent mass transport problems are commonly approximated by linearization—that is, by replacing the variable properties in the governing equations with constant reference values. This approach is a useful complement to purely numerical methods, especially for complex flows, and can give good predictions when the property

[1] R. Taylor and R. Krishna, *Multicomponent Mass Transfer*, Wiley, New York (1993).

variations are not too large. Multicomponent analyses of this sort have been presented by many investigators, for quiescent media[2] and for forced-convection systems.[3–6]

We begin with the species continuity equations as given in Eq. 19.1-15, and apply them to an N-component gas system with $N-1$ independent mole fractions x_α and an equal number of independent diffusion fluxes $\mathbf{J}_\alpha^*$. Let $[x]$ and $[\mathbf{J}^*]$ denote, respectively, the column arrays of independent mole fractions $x_1, \ldots, x_{N-1}$ and independent diffusion fluxes $\mathbf{J}_1^*, \ldots, \mathbf{J}_{N-1}^*$; then approximating the molar density c in Eq. 19.1-15 by a reference value c_{ref} gives the linearized equation system

$$c_{\text{ref}}\left(\frac{\partial}{\partial t}[x] + (\mathbf{v}^* \cdot \nabla[x])\right) = -(\nabla \cdot [\mathbf{J}^*]) \tag{22.9-1}$$

for laminar or turbulent flows free of homogeneous chemical reactions.

For multicomponent ordinary diffusion, the flux expression may be written either as a matrix generalization[2,4] of Fick's first law (Eq. B of Table 17.8-2),

$$[\mathbf{J}^*] = -c[\mathbf{D}]\nabla[x] \tag{22.9-2}$$

or as a matrix statement[3,5] of the Maxwell–Stefan equation (Eq. 17.9-1):

$$c\nabla[x] = -[\mathbf{A}][\mathbf{J}^*] \tag{22.9-3}$$

The matrices $[\mathbf{D}]$ and $[\mathbf{A}]$ must be $(N-1) \times (N-1)$ and nonsingular to give the stated number of independent fluxes (in Eq. 22.9-2), and of independent mole fractions (in Eq. 22.9-3). Consistency of these two equations then requires that $[\mathbf{D}] = [\mathbf{A}]^{-1}$ at any given state.

In the moderate-density gas region, the elements of the matrix $[\mathbf{A}]$ are predictable accurately from Eq. 17.9-1, giving

$$\left.\begin{aligned} A_{\alpha\beta} &= \frac{x_\alpha}{\mathscr{D}_{\alpha N}} - \frac{x_\alpha}{\mathscr{D}_{\alpha\beta}} \quad \text{for } \beta \neq \alpha \\ A_{\alpha\alpha} &= \frac{x_\alpha}{\mathscr{D}_{\alpha N}} + \sum_{\substack{\beta=1 \\ \beta\neq\alpha}}^{N} \frac{x_\alpha}{\mathscr{D}_{\alpha\beta}} \end{aligned}\right\} \tag{22.9-4}$$

in which the divisors $\mathscr{D}_{\alpha\beta}$ are the *binary* diffusivities of the corresponding pairs of species. In the first approximation of the Chapman–Enskog kinetic theory of gases, the coefficient for a given pair α, β depends only on c and T, as in Eq. 17.3-11. These simple expressions lead us to prefer Eq. 22.9-3 over Eq. 22.9-2, unless measurements of $[\mathbf{D}]$ are available at the desired conditions. Formally similar equations may be written in mass- or volume-based compositions and fluxes, after appropriate transformation of the coefficient matrix $[\mathbf{A}]$ or $[\mathbf{D}]$. Mass units are preferred if the equation of motion is included in the problem formulation, since the mass average velocity is then essential as indicated in §19.2.

---

[2] L. Onsager, *Ann. N.Y. Acad. Sci.*, **46**, 241–265 (1948); P. J. Dunlop and L. J. Gosting, *J. Phys. Chem.*, **63**, 86–93 (1959); J. S. Kirkaldy, *Can. J. Phys.*, **37**, 30–34 (1959); S. R. de Groot and P. Mazur, *Non-Equilibrium Thermodynamics*, North-Holland, Amsterdam (1961); J. S. Kirkaldy, D. Weichert, and Zia-Ul-Haq, *Can. J. Phys.*, **41**, 2166–2173 (1963); E. L. Cussler, Jr., and E. N. Lightfoot, *AIChE Journal*, **10**, 702–703, 783–785 (1963); H. T. Cullinan, *Ind. Eng. Chem. Fund.*, **4**, 133–139 (1965).

[3] R. Prober, PhD thesis, Univ. of Wisconsin (1961).

[4] H. L. Toor, *AIChE Journal*, **10**, 460–465 (1964).

[5] W. E. Stewart and R. Prober, *Ind. Eng. Chem. Fund.*, **3**, 224–235 (1964).

[6] V. Tambour and B. Gal-Or, *Physics of Fluids*, **19**, 219–225 (1976).

For multicomponent systems ($N \geq 3$), each of these flux expressions normally has a nondiagonal coefficient matrix, giving a coupled system of diffusion equations. Equation 22.9-3 can be decoupled by use of the transformation

$$[\mathbf{P}]^{-1}[\mathbf{A}][\mathbf{P}] = \begin{bmatrix} \check{A}_1 & & \\ & \ddots & \\ & & \check{A}_{N-1} \end{bmatrix} \tag{22.9-5}$$

in which [**P**] is the matrix of column eigenvectors of [**A**], and $\check{A}_1, \ldots, \check{A}_{N-1}$ are the corresponding eigenvalues. These eigenvalues, the roots of the equation $\det[\mathbf{A} - \lambda\mathbf{I}] = 0$, are positive at any locally stable state of the mixture; they are also invariant to similarity transformations of [**A**] to other composition units. Here **I** is the unit matrix of order $N - 1$. The matrix [**D**], when used, is reducible in like manner with the same matrix [**P**], and its eigenvalues $\check{D}_1, \ldots, \check{D}_{N-1}$ are the reciprocals of $\check{A}_1, \ldots, \check{A}_{N-1}$. For economy of effort, [**A**] (or [**D**]) and the arrays derived therefrom will always be evaluated at reference property values, so will not need the subscript $_{\text{ref}}$; however, a subscript ω will be added in [**A**], [**D**], [**P**], and $[\mathbf{P}]^{-1}$ when these arrays are based on quantities in mass units.

Equation 22.9-5 suggests that the following transformed compositions and transformed diffusion fluxes should be useful:

$$[\check{x}] = [\mathbf{P}]^{-1}[x] = \begin{bmatrix} \check{x}_1 \\ \vdots \\ \check{x}_{N-1} \end{bmatrix}; \qquad \begin{bmatrix} x_1 \\ \vdots \\ x_{N-1} \end{bmatrix} = [\mathbf{P}][\check{x}] \tag{22.9-6, 7}$$

$$[\check{\mathbf{J}}^*] = [\mathbf{P}]^{-1}[\mathbf{J}^*] = \begin{bmatrix} \check{\mathbf{J}}_1^* \\ \vdots \\ \check{\mathbf{J}}_{N-1}^* \end{bmatrix}; \qquad \begin{bmatrix} \mathbf{J}_1^* \\ \vdots \\ \mathbf{J}_{N-1}^* \end{bmatrix} = [\mathbf{P}][\check{\mathbf{J}}^*] \tag{22.9-8, 9}$$

Hereafter, an accent (ˇ) will be placed on such transformed variables and on the corresponding diagonal matrix elements, including the eigenvalues $\check{A}_\alpha$ and $\check{D}_\alpha$. Premultiplication of Eq. 22.9-3 by $[\mathbf{P}]^{-1}$ and use of Eqs. 22.9-5 through 9 then gives uncoupled flux equations

$$c_{\text{ref}}\nabla\check{x}_\alpha = -\check{A}_\alpha\check{\mathbf{J}}_\alpha^* \qquad (\alpha = 1, \ldots, N-1) \tag{22.9-10}$$

formally equivalent to Fick's first law for $N - 1$ binary systems. The multicomponent continuity equation 22.9-1 correspondingly transforms to

$$c_{\text{ref}}\frac{\partial\check{x}_\alpha}{\partial t} + c_{\text{ref}}(\check{\mathbf{v}}^* \cdot \nabla x_\alpha) = -(\nabla \cdot \check{\mathbf{J}}_\alpha^*) \qquad (\alpha = 1, \ldots, N-1) \tag{22.9-11}$$

Thus, the transformed compositions $\check{x}_\alpha$ and fluxes $\check{\mathbf{J}}_\alpha^*$ for each α satisfy the continuity and flux equations of a binary problem with the same $\mathbf{v}^*$ function (laminar or turbulent) as the multicomponent system, and with a diffusivity $\mathscr{D}_{AB}$ equal to the eigenvalue $\check{D}_\alpha = 1/\check{A}_\alpha$.

The initial and boundary conditions on $[\check{x}]$ and $[\check{\mathbf{J}}^*]$ are obtained from those on $[x]$ and $[\mathbf{J}^*]$ by application of Eqs. 22.9-6 and 8. The resulting quasi-binary problems may then be solved, using theory or correlations of experiments, and the results combined[5] via Eqs. 22.9-7 and 9 to get the multicomponent solution in terms of $[x]$ and $[\mathbf{J}^*]$.

Local mass transfer rates in binary systems are expressible in the form

$$N_{A0} - x_{A0}(N_{A0} + N_{B0}) = k_{x,\text{loc}}^{\cdot}(\mathscr{D}_{AB}, \ldots)(x_{A0} - x_{Ab}) \tag{22.9-12}$$

as indicated in Eq. 22.1-7 and §22.8. The notation ... after $\mathscr{D}_{AB}$ stands for any additional variables (such as ϕ_x of §22.8) on which the binary mass transfer coefficient $k_x^{\cdot}$ may depend. The corresponding set of equations in the notation of Eqs. 22.9-10 and 11 is

$$\check{J}_{\alpha 0}^* = \check{k}_{x,\text{loc}}^{\cdot}(\check{D}_\alpha, \ldots)(\check{x}_{\alpha 0} - \check{x}_{\alpha b}) \qquad (\alpha = 1, \ldots, N-1) \tag{22.9-13}$$

or in matrix form,

$$\begin{bmatrix} \check{J}^*_{1,0} \\ \vdots \\ \check{J}^*_{N-1,0} \end{bmatrix} = \begin{bmatrix} \check{k}_x(\check{D}_1, \ldots & & \\ & \ddots & \\ & & \check{k}_x(\check{D}_{N-1}, \ldots) \end{bmatrix} \begin{bmatrix} \check{x}_{1,0} - \check{x}_{1b} \\ \vdots \\ \check{x}_{n-1,0} - \check{x}_{N-1,b} \end{bmatrix} \tag{22.9-14}$$

Transformation of this result into the original variables gives the interfacial diffusion fluxes $J^*_{1,0}, \ldots, J^*_{N-1,0}$ into the gas phase as

$$[J^*_0] = [\mathbf{P}][\check{\mathbf{k}}_x][\mathbf{P}]^{-1}[x_0 - x_b] \tag{22.9-15}$$

or the composition differences for given fluxes $J_{\alpha 0}$ as

$$[x_0 - x_b] = [\mathbf{P}][\check{\mathbf{k}}_x]^{-1}[\mathbf{P}]^{-1}][J^*_0] \tag{22.9-16}$$

Here $[\check{\mathbf{k}}_x]$ is the diagonal matrix shown in Eq. 22.9-14, and $[\check{\mathbf{k}}_x]^{-1}$ is formed from the reciprocals of the same diagonal elements.

As for binary systems, further information is needed to calculate the species fluxes $N_{\alpha 0}$ relative to the interface, which give the local transfer rates. A flux ratio $r = N_{A0}/N_{B0}$ was specified in Eq. 21.1-9 to solve for N_{A0}; analogous specifications are required for multicomponent systems. The calculation of the fluxes $N_{\alpha 0}$ from diffusion fluxes $J^*_{\alpha 0}$ and relative transfer rates is called the "bootstrap problem,"[1,7] and is treated well in Ref. 1. This problem becomes simpler if Eq. 22.9-14 is rewritten as follows, using the array $[N_0]$ of interfacial molar fluxes $N_{1,0}, \ldots, N_{N-1,0}$ relative to the interface,

$$\left[N_0 - x_0 \sum_{\alpha=1}^{N} N_{\alpha 0}\right] = [\mathbf{P}][\check{\mathbf{k}}_x][\mathbf{P}]^{-1}[x_0 - x_b] \tag{22.9-17}$$

to allow direct insertion of relations among the species transfer rates. The corresponding result for the array $[n_0]$ of interfacial mass fluxes $n_{1,0}, \ldots, n_{N-1,0}$ relative to the interface is:

$$\left[n_0 - \omega_0 \sum_{\alpha=1}^{N} n_{\alpha,0}\right] = [\mathbf{P}_\omega][\check{\mathbf{k}}_\omega][\mathbf{P}_\omega]^{-1}[\omega_0 - \omega_\infty] \tag{22.9-18}$$

Several special forms of these results will now be given.

For systems with *no net molar interfacial flux*, the N-term summation in Eq. 22.9-17 vanishes, and this equation takes the convenient form

$$[N_0] = [\mathbf{P}][\check{\mathbf{k}}_x][\mathbf{P}]^{-1}[x_0 - x_b] \tag{22.9-19}$$

in which the diagonal array $[\check{\mathbf{k}}_x]$ needs *no net-flux correction*. This result can be extended to *moderate net molar interfacial flux* by approximating each transfer coefficient $\check{k}_x(\check{D}_\alpha, \check{\phi}_{x\alpha})$ in Eq. 22.9-14 as a linear function of the net molar interfacial flux, using the tangent line at $\phi = 0$ of the θ-curve in Fig. 22.8-2 for the chosen mass transfer model. This gives the linear equation system[8]

$$\left[N_0 - 0.5(x_0 + x_b) \sum_{\alpha=1}^{N} N_{\alpha 0}\right] = [\mathbf{P}][\check{\mathbf{k}}_x][\mathbf{P}]^{-1}[x_0 - x_b] \tag{22.9-20}$$

for the *stagnant-film model* given in §22.8. In the same manner, one obtains

$$\left[N_0 - (0.363x_0 + 0.637x_b) \sum_{\alpha=1}^{N} N_{\alpha 0}\right] = [\mathbf{P}][\check{\mathbf{k}}_x][\mathbf{P}]^{-1}[x_0 - x_b] \tag{22.9-21}$$

---

[7] R. Krishna and G. L. Standart, *Chem. Eng. Commun.*, **3**, 201–275 (1979).

[8] W. E. Stewart, *AIChE Journal*, **19**, 398–400 (1973); Erratum, **25**, 208 (1979).

for the *penetration model* given in §20.4 and §22.8, and

$$\left[N_0 - (0.434x_0 + 0.566x_b)\sum_{\alpha=1}^{N} N_{\alpha 0}\right] = [\mathbf{P}][\check{\mathbf{k}}_x][\mathbf{P}]^{-1}[x_0 - x_b] \tag{22.9-22}$$

for the limit $\Lambda \to \infty$ in *laminar boundary layers*, shown in Figs. 22.8-5, 6 and valid for non-separated boundary layers in three-dimensional steady flows.[9]

In systems with *no net mass interfacial flux*, as in steady-state solid-catalyzed reactions, Eq. 22.9-18 reduces to

$$[n_0] = [\mathbf{P}_\omega][\check{\mathbf{k}}_\omega][\mathbf{P}_\omega]^{-1}[\omega_0 - \omega_b] \tag{22.9-23}$$

The elements of the matrix $\check{k}_\omega$ can be predicted from expressions for the binary Sherwood number or j_D factor as defined for mass-based units in Table 22.2-1, with eigenvalues $\check{D}_\alpha$ inserted in place of binary diffusivities $\mathcal{D}_{AB}$.

For a given flow field, the product $[\mathbf{P}][\check{\mathbf{k}}_x][\mathbf{P}]^{-1}$ in Eqs. 22.9-19 through 22 is a function of the matrix [**A**]. This matrix triple product, here called $[\mathbf{k}_x]$, is non-diagonal for $N \geq 3$ whereas $[\check{\mathbf{k}}_x]$ is diagonal as noted above. A simple, efficient method for approximating such functions has been developed by Alopaeus and Nordén.[10] Let f be a scalar real-valued function defined on the eigenvalues of a matrix [**A**], in which the diagonal elements are dominant as in Eq. 22.9-4. The proposed approximations to the elements of the matrix $[\mathbf{B}] = f[\mathbf{A}]$ are then as follows:

$$\text{for diagonal elements, } B_{ii} = f(A_{ii}) \tag{22.9-24}$$

$$\text{for off-diagonal elements, } B_{ij} = \begin{cases} A_{ii}\dfrac{df(A_{ii})}{dA_{ii}} & \text{if } A_{ii} \approx A_{jj} \\ A_{ij}\dfrac{f(A_{ii}) - f(A_{jj})}{A_{ii} - A_{jj}} & \text{otherwise.} \end{cases} \tag{22.9-25}$$

Alopaeus and Nordén[10] tested these approximations to mass-transfer coefficient matrices $[\mathbf{k}_x]$ of the form $b[\mathbf{D}]^{1-p}$ or the form $b[\mathbf{A}]^{p-1}$, and to the corresponding fluxes $N_{\alpha 0}$, in systems of 3 to 25 gaseous species. Exponents p from 0.25 to 0.66 were used; values from 0 to 0.5 appear in the mass transfer expressions of this chapter. Comparisons were made against exact calculations of elements $k_{x\alpha\beta}$ and $N_{\alpha 0}$ via Eq. 22.9-19, and against a film model given by Krishna and Standart[11] in which each element $k_{x\alpha\beta}$ is calculated independently with the corresponding binary diffusivity $\mathcal{D}_{\alpha\beta}$. The calculations from Eqs. 22.9-24 and 25 were 3 to 5 times quicker than those with Eq. 22.9-19 and proved quite accurate (relative errors typically less than 1% and seldom as large as 10%), especially when done directly from the diagonally dominant Stefan-Maxwell matrix [**A**] rather than from its inverse, [**D**]. Calculations with the Krishna-Standart film model were slower than those with Eqs. 22.9-24 and 25, and the typical errors were several times as large. Therefore, Eqs. 22.9-24 and 25 are recommended as practical approximations to the elements of the product matrix $[\mathbf{B}] = [\mathbf{P}][\check{\mathbf{k}}_x][\mathbf{P}]^{-1}$ in Eqs. 22.9-19 through 22 whenever Eq. 22.9-4 is used. This approximation may be used in Eq. 22.9-23 also, with [**B**] transformed at the end into mass-based units; however, Eq. 22.9-20 or 22 will be more convenient and comparably accurate at the moderate net molar fluxes normally encountered in heterogeneous catalysis.

The accuracy of the linearized solutions depends on the choice of the reference property values, especially when the property variations are large. In the following discussion all properties are evaluated at a common reference state, with composition given as a mole fraction

$$[x_{\text{ref}}] = a_x[x_b] + (1 - a_x)[x_0] \tag{22.9-26}$$

---

[9] W. E. Stewart, *AIChE Journal*, **9**, 528–535 (1963).

[10] V. Alopaeus and H. V. Nordén, *Computers & Chemical Engineering*, **23**, 1177–1182 (1999).

[11] R. Krishna and G. L. Standart, *AIChE Journal*, **22**, 383–389 (1976).

or a mass fraction

$$[\omega_{\text{ref}}] = a_\omega[\omega_b] + (1 - a_\omega)[\omega_0] \tag{22.9-27}$$

Note that $[x_{\text{ref}}]$ remains open to choice even for Eq. 22.9-20, 21, or 22, since the average compositions shown there provide net-flux corrections and not physical property values.

Equations 22.9-17, 18 and several other approximations for multicomponent mass transfer have been tested[12] against detailed variable-property integrations for isothermal systems. The conclusions from this study were as follows:

1. For twenty problems of unsteady-state gaseous diffusion, covering a wide range of net mass transfer rates, linearization in molar units approximated the exact solutions best. Rates of isobutane evaporation and condensation, for the system i-C_4H_{10}-N_2-H_2 in the geometry of Example 20.1-1, were approximated with a standard deviation of 1.6% by Eq. 22.9-17, using reference mole fractions calculated from Eq. 22.9-26 with $a_x = 0.5$. Linearization in mass-based units, via Eq. 22.9-18, proved inferior because of the large variations in ρ and $[\mathbf{A}_\omega]$. This method, with its preferred a_ω value of 0.8, gave a standard deviation of 3.8% for the interfacial fluxes $N_{\alpha 0}$ of the single transferable species (isobutane). Quasi-steady-state film approximations proved less accurate; use of correction factors $\theta_{x\alpha} = \check{\phi}_{x\alpha}/(\exp\check{\phi}_{x\alpha} - 1)$ (as given by Stewart and Prober[5] for the film model of §22.8) gave a standard deviation of 7.88% with a_x optimized to 1.0. The film model of Krishna and Standart,[11] which does not use linearization, gave a standard deviation of 14.3% independent of a_x and a_ω. These results favor the use of Eq. 22.9-17 (or, for moderate transfer rates, Eq. 22.9-21) with $a_x = 0.5$ for the gas phase in transfer operations described by a penetration model.
2. For twenty problems of momentum and mass transfer in laminar gaseous boundary layers of H_2, N_2 and CO_2 on a porous flat plate, solved accurately by Prober,[3] linearization in mass-based units approximated the exact solutions best. The detailed variable-property solutions for $n_{\alpha 0}$ were approximated[12] for all three species with a standard deviation of 0.55% by Eq. 22.9-18, using mass transfer coefficients $\check{k}_\alpha$ predicted via Eq. 20.2-47 and 22.9-27 with a_ω optimized to 0.4. The film models of Stewart and Prober[5] and of Standart and Krishna[12] gave standard deviations of 4.78% (with $a_x = 1.0$) and 8.25%, respectively, for the species transfer rates.

The methods presented here are coming into widespread use in the engineering of multicomponent separation processes. Advances in computing technology have facilitated the use of these methods and stimulated investigations toward better ones, to deal with nonlinear phenomena including complex chemical reactions.

QUESTIONS FOR DISCUSSION

1. Under what conditions can the analogies in Table 22.2-1 be applied? Can they be applied in systems with chemical reaction?
2. Why is the heat transfer coefficient in Eq. 22.1-6 defined differently from that in Eq. 14.1-1—or is it?
3. Some of the mass transfer coefficients in this chapter have a superscript 0 and others have a superscript •. Explain carefully what these superscripts denote.
4. What conclusions can you draw from the analytical calculations of mass transfer coefficients in §22.2?

---

[12] T. C. Young and W. E. Stewart, *Ind. Eng. Chem. Res.*, **25**, 476–482 (1986).

5. What is the significance of the 2 in Eqs. 22.3-20 and 21?
6. What is the meaning of the subscripts 0, e, and b in §22.4?
7. What is meant by the term "model insensitive"?
8. In what way does surface tension have an influence on interphase mass transfer? How is surface tension defined? How does surface tension depend on temperature?
9. Discuss the physical basis for the film model, the penetration model, and the boundary layer model for heat and mass transfer.
10. How are the heat and mass transfer coefficients affected by high mass-transfer rates across the interface?

PROBLEMS

22A.1. Prediction of mass transfer coefficients in closed channels. Estimate the gas-phase mass transfer coefficients for water vapor evaporating into air at 2 atm and 25°C, and a mass flow rate of 1570 lb_m/hr, in the systems that follow. Take $\mathscr{D}_{AB} = 0.130\ cm^2/s$.

(a) A 6-in. i.d. vertical pipe with a falling film of water on the wall. Use the following correlation[1] for gases in a wetted-wall column:

$$Sh_{loc} = 0.023\ Re^{0.83}Sc^{0.44} \quad (Re > 2000) \tag{22A.1-1}$$

(b) a 6-in.-diameter packed bed of water-saturated spheres, with $a = 100\ ft^{-1}$.

22A.2. Calculation of gas composition from psychrometric data. A stream of moist air has a wet-bulb temperature of 80°F and a dry-bulb temperature of 130°F, measured at 800 mm Hg total pressure and high air velocity. Compute the mole fraction of water vapor in the air stream. For simplicity, consider water as a trace component in estimating the film properties.

Answer: $x_{A\infty} = 0.0158$ (using n = 0.44 in Eq. 22.3-38)

22A.3. Calculating the inlet air temperature for drying in a fixed bed. A shallow bed of water-saturated granular solids is to be dried by blowing dry air through it at 1.1 atm pressure and a superficial velocity of 15 ft/s. What air temperature is required initially to keep the solids at a surface temperature of 60°F? Neglect radiation. See §14.5 for forced-convection heat transfer coefficients in fixed beds.

22A.4. Rate of drying of granular solids in a fixed bed. Calculate the initial rate of water removal in the drying operation described in Problem 22A.3, if the solids are cylinders with $a = 180\ ft^{-1}$.

22B.1. Evaporation of a freely falling drop. A drop of water, 1.00 mm in diameter, is falling freely through dry, still air at pressure of 1 atm and a temperature of 100°F with no internal circulation. Assume quasi-steady-state behavior and a small mass-transfer rate to compute **(a)** the velocity of the falling drop, **(b)** the surface temperature of the drop, and **(c)** the rate of change of the drop diameter in cm/s. Assume that the film properties are those of dry air at 80°F.

Answers: **(a)** 390 cm/s; **(b)** 54°F; **(c)** 5.6×10^{-4} cm/s

22B.2. Effect of radiation on psychrometric measurements. Suppose that a wet-bulb and dry-bulb thermometer are installed in a long duct with constant inside surface temperature T_s and that the gas velocity is small. Then the dry-bulb temperature T_{db} and the wet-bulb temperature T_{wb} should be corrected for radiation effects. We assume, as in Example 22.3-2, that the thermometers are so installed that the heat conduction along the glass stems can be neglected.

(a) Make an energy balance on a unit area of the dry bulb to obtain an equation for the gas temperature T_∞ in terms of T_{db}, T_s, h_{db}, e_{db}, and a_{db} (these last two are the emissivity and absorptivity of the dry bulb).

---

[1] E. R. Gilliland and T. K. Sherwood, *Ind. Eng. Chem.*, **26**, 516–523 (1934).

(b) Make an energy balance on a unit area of the wet bulb and obtain an expression for the evaporation rate.

(c) Compute $x_{A\infty}$ for the pressure and thermometer readings of Example 22.3-2, with the additional information that $v_\infty = 15$ ft/s, $T_s = 130°F$, $e_{db} = a_{db} = e_{wb} = a_{wb} = 0.93$, dry-bulb diameter = 0.1 in., and wet-bulb diameter = 0.15 in. including the wick.

Answer: **(c)** $x_{A\infty} = 0.0021$

22B.3. Film theory with variable transport properties.

(a) Show that for systems in which the transport properties are functions of y, Eqs. 19.4-12 and 13 may be integrated to give for $y \leq \delta_x$ or $y \leq \delta_T$, respectively,

$$1 - \frac{(N_{A0} + N_{B0})(x_A - x_A)}{N_{A0} - x_{A0}(N_{A0} + N_B)} = \exp\left[(N_{A0} + N_{B0}) \int_0^y \frac{dy}{c\mathcal{D}_{AB}}\right] \tag{22B.3-1}$$

$$1 - \frac{(N_{A0}\tilde{C}_{pA} + N_{B0}\tilde{C}_{pB})(T - T_0)}{q_0} = \exp\left[(N_{A0}\tilde{C}_{pA} + N_{B0}\tilde{C}_{pB}) \int_0^y \frac{dy}{k}\right] \tag{22B.3-2}$$

(b) Make the corresponding changes in Eqs., 19.4-16 and 17 as well as in Eqs. 22.8-5 and 6. Then verify that Eqs. 22.8-7 and 8 remain valid. Thus it is not necessary to work with the integrals in calculating transfer rates if h_{loc} and $k_{x,\text{loc}}$ can be predicted.

(c) Show that h_{loc} and $k_{x,\text{loc}}$ have to be evaluated in terms of the physical properties and flow regime (laminar or turbulent) that prevail at the conditions for which h^*_{loc} and $k^*_{x,\text{loc}}$ are desired.

22B.4. An evaporative ice maker. Consider a circular shallow dish of water 0.5 m in diameter and filled to the brim, resting on an insulating layer, such as loose straw, and in a windless area. At what air temperature can the water be cooled to freezing if the relative humidity of the air is 30%? Make the following assumptions: (i) neglect radiation, (ii) consider radiation to a night sky of effective temperature 150K, and (iii) assume that the dish has a lip around the edge 2 mm high.

22B.5. Oxygen stripping. Calculate the rate at which oxygen transfers from quiescent oxygen-saturated water at 20°C to a bubble of pure nitrogen 1 mm in diameter, if the bubble acts as a rigid sphere. Note that it will first be necessary to determine the bubble velocity of rise through the water.

22B.6. Controlling diffusional resistance. Water drops 2 mm in diameter are being oxygenated by falling freely through pure oxygen at 20°C and a pressure of 1 atm. Do you need to know the gas-phase diffusivity to calculate the rate of oxygen transport? Why? The solubility of oxygen under these conditions is 1.39 mmols/liter, and its diffusivity in the liquid phase is about 2.1×10^{-5} cm^2/s.

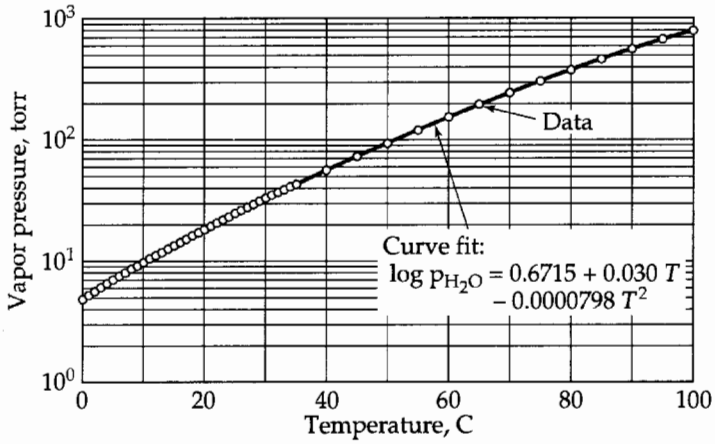

Fig. 22B.7. Water vapor pressure under its own vapor data from *Lange's Handbook of Chemistry* (J. Dean, ed.), 15th edition, McGraw-Hill, New York (1999).

22B.7. Determination of diffusivity (Fig. 22B.7). The diffusivity of water vapor in nitrogen is to be determined at a pressure of 1 atm over the temperature range from 0°C to 100°C by means of the "Arnold experiment" of Example 20.1-1. It will, therefore, be necessary to use the correction factor θ_{AB} to the penetration model. Calculate this factor as a function of temperature. The vapor pressure of water in this range may be obtained from Fig. 22B.7 or calculated from

$$\log_{10} p_{H_2O} = 0.6715 + 0.030T - 0.00008T^2 \qquad \text{(22B.7-1)}$$

where p_{H_2O} is the vapor pressure in mm Hg, and T is the temperature in degrees centigrade.

22B.8. Marangoni effects in condensation of vapors. In many situations the heat transfer coefficient for condensing vapors is given as $h = k/\delta$, where k is the thermal conductivity of the condensate film, and δ is the film thickness. Correlations available in the literature are normally based on the assumption of zero shear stress at the free surface of the film, but if the surface temperature decreases downward, there will be a shear stress $\tau_s = \partial\sigma/\partial z$, where σ is the surface tension, and z is measured downward, that is, in the direction of flow. How much will this effect change a heat transfer coefficient of 5000 kcal/hr · m² · C for a water film? The kinematic viscosity of water may be assumed to be 0.0029 cm²/s, the density is 0.96 g/cm³, the thermal conductivity 0.713 kcal/hr · m · C, and $d\sigma/dT = -0.2$ dynes/cm · C for the purposes of this problem.

Partial Answer: $\rho\langle v_z\rangle = \left(\frac{\rho^2 g\delta^2}{3\mu}\right)\left(1 + \frac{3}{2}\frac{\tau_s}{\rho g\delta}\right)$

The term in τ_s represents the effect of surface tension gradients, and when this term is small, its denominator will be near the value for no gradient. For the conditions of this problem, $\rho g\delta = 14.3$ dyn/cm². Surface tension effects will thus be small for systems such as the one under consideration, where the surface tension increases downward. In the opposite case, however, even small gradients can cause hydrodynamic instabilities and thus can have major effects.

22B.9. Film model for spheres. Derive the results that correspond to Eqs. 22.8-3, 4 for simultaneous heat and mass transfer in a system with spherical symmetry. That is, assume a spherical mass transfer surface and assume that T and x_A depend only on the radial coordinate r. Show that Eqs. 22.8-7 and 8 do not need to be changed. What difficulties would be encountered if one tried to use the film theory to calculate the drag on a sphere?

22B.10. Film model for cylinders. Derive the results that correspond to Eqs. 22.8-3, 4 for a system with cylindrical symmetry. That is, assume a cylindrical mass transfer surface and assume that T and x_A depend only on r. Verify that Eqs. 22.8-7, 8 do not need to be changed.

22C.1. Calculation of ultrafiltration rates. Check the accuracy of the predictions shown in Fig. 22.8-9 for the following data and physical properties:

Physical system:
- Rotation rate of disk filter = 273 rpm
- Bovine serum albumin at $\rho_P = 2.2$ g/100 ml
- Diffusivity in phosphate buffer (at pH 6.7) = 7.1×10^{-7} cm²/s
- Kinematic viscosity of buffer = 0.01 cm²/s
- Partial specific volumes of protein and buffer are 0.75 and 1.00 ml/g, respectively
- Hydraulic permeability, $K_H = 0.0098$ cm/min · psi

Effect of protein concentration:
- Solution density $\rho = 0.997 + 0.224\rho_P$ in g/ml
- Protein-buffer diffusivity ratio $\mathscr{D}_{PS}(0)/\mathscr{D}_{PS}(\rho_P) = 21.3\phi_P/\tanh(21.3\phi_P)$, where $\phi_P = \omega_P\hat{V}_P/(\omega_P\hat{V}_P + \omega_S\hat{V}_S)$ is the volume fraction of protein, with $\hat{V}_P$ and $\hat{V}_S$ being the partial specific volumes of protein and solvent
- Protein-buffer viscosity ratio $\mu(0)/\mu(\rho_P) = 1.11 - 0.054\rho_P + 0.00067\rho_P^2$, with ρ_P in g/100 ml
- Osmotic pressure $\pi = 0.013\rho_P^2$ in psi (100 ml/g)²

The operating data are as follows:

Transmembrane pressure difference, $(p_0 - p_\delta)$, psi	**Percolation velocity v_δ, cm/min**
4.0	0.032
7.1	0.049
8.4	0.049
13.6	0.061
14.7	0.066
23.9	0.074
29.7	0.078
30.0	0.079
36.4	0.081
47.0	0.082

Chapter 23

Macroscopic Balances for Multicomponent Systems

Applications of the laws of the conservation of mass, momentum, and energy to engineering flow systems have been discussed in Chapter 7 (isothermal systems) and Chapter 15 (nonisothermal systems). In this chapter we continue the discussion by introducing three additional factors not encountered in the earlier chapters: (a) the fluid in the system is composed of more than one chemical species; (b) chemical reactions may be occurring, along with changes of composition and production or consumption of heat; and (c) mass may be entering the system through the bounding surfaces (that is, across surfaces other than planes 1 and 2). Various mechanisms by which mass may enter or leave through the bounding surfaces of the system are shown in Fig. 23.0-1.

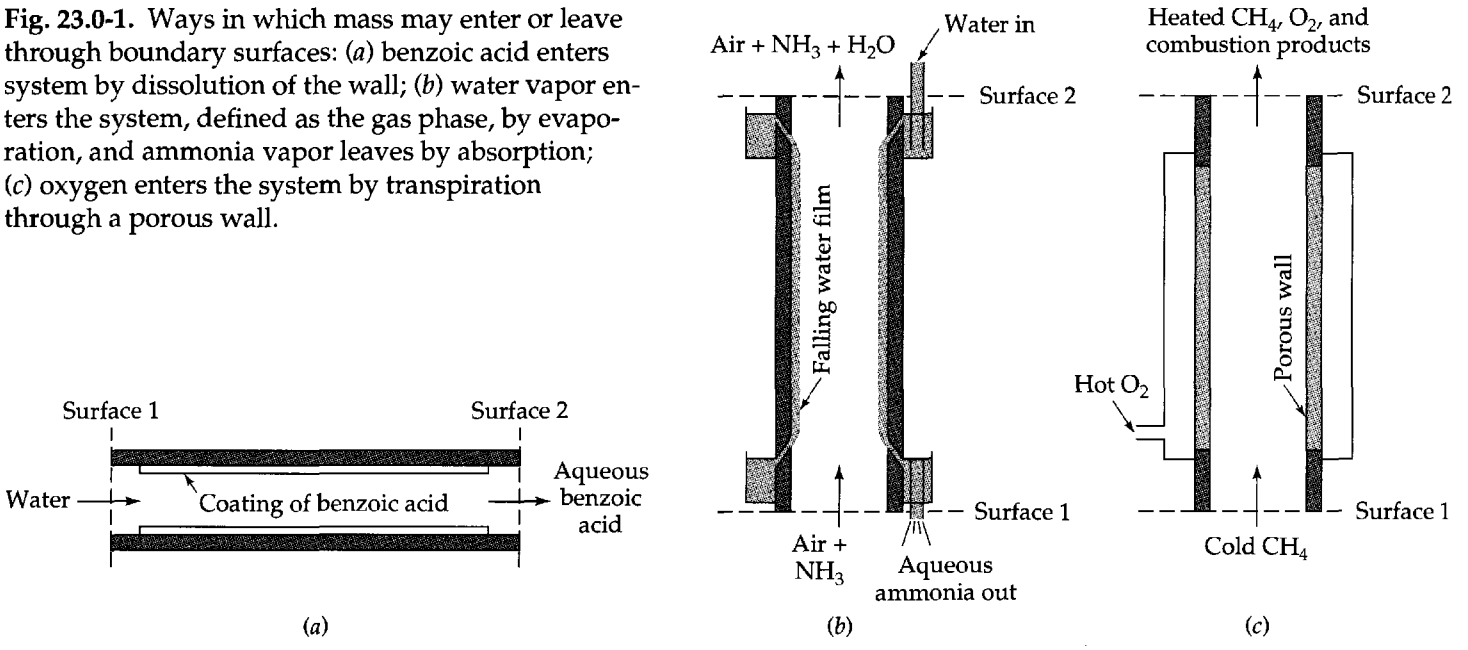

Fig. 23.0-1. Ways in which mass may enter or leave through boundary surfaces: (*a*) benzoic acid enters system by dissolution of the wall; (*b*) water vapor enters the system, defined as the gas phase, by evaporation, and ammonia vapor leaves by absorption; (*c*) oxygen enters the system by transpiration through a porous wall.

In this chapter we summarize the macroscopic balances for the more general situation described above. Each of these balances will now contain one extra term, to account for mass, momentum, or energy transport across the bounding surfaces. The balances thus obtained are capable of describing industrial mass transfer processes, such as absorption, extraction, ion exchange, and selective adsorption. Inasmuch as entire treatises have been devoted to these topics, all we try to do here is to show how the material discussed in the preceding chapters paves the way for the study of mass transfer operations. The reader interested in pursuing these topics further should consult the available textbooks and treatises.[1-8]

The main emphasis on this chapter is on the mass balances for mixtures. For that reason, §23.1 is accompanied by five examples, which illustrate problems arising in environmental science, isotope separation, economic evaluation, and biomedical science. In §§23.2 to 23.4 the other macroscopic balances are given. In Table 23.5-1 they are summarized for systems with multiple inlets and outlets. The last two sections of the chapter illustrate applications of the macroscopic balances to more complex systems.

§23.1 THE MACROSCOPIC MASS BALANCES

The statement of the law of conservation of mass of chemical species α in a multicomponent macroscopic flow system is

$$\boxed{\frac{dm_{\alpha,\text{tot}}}{dt} = -\Delta w_\alpha + w_{\alpha,0} + r_{\alpha,\text{tot}} \qquad \alpha = 1, 2, 3, \ldots, N} \tag{23.1-1}$$

This is a generalization of Eq. 7.1-2. Here $m_{\alpha,\text{tot}}$ is the instantaneous total mass of α in the system, and $-\Delta w_a = w_{\alpha 1} - w_{\alpha 2} = \rho_{\alpha 1}\langle v_1\rangle S_1 - \rho_{\alpha 2}\langle v_2\rangle S_2$ is the difference between the mass rates of flow of species α across planes 1 and 2. The quantity $w_{\alpha,0}$ is the mass rate of addition of species α to the system by mass transfer across the bounding surface. Note that $w_{\alpha,0}$ is positive when mass is *added* to the system, just as Q and W_m are taken to be positive in the total energy balance when heat is added to the system and work is done on the system by moving parts. Finally, the symbol $r_{\alpha,\text{tot}}$ stands for the net rate of production of species α by homogeneous and heterogeneous reactions within the system.[1]

Recall that in Table 15.5-1 the molecular and eddy transport of momentum and energy across surfaces 1 and 2 in the direction of flow were neglected with respect to the convective transport. The same is done everywhere in this chapter—in Eq. 23.1-1 and in the other macroscopic balances presented here.

---

[1] W. L. McCabe, J. C. Smith, and P. Harriot, *Unit Operations of Chemical Engineering*, McGraw-Hill, New York, 6th edition (2000).

[2] T. K. Sherwood, R. L. Pigford, and C. R. Wilke, *Mass Transfer*, McGraw-Hill, New York (1975).

[3] R. E. Treybal, *Mass Transfer Operations*, 3rd edition, McGraw-Hill, New York (1980).

[4] C. J. King, *Separation Processes*, McGraw-Hill, New York (1971).

[5] C. D. Holland, *Multicomponent Distillation*, McGraw-Hill, New York (1963).

[6] T. C. Lo, M. H. I. Baird, and C. Hanson, eds., *Handbook of Solvent Extraction*, Wiley-Interscience, New York (1983).

[7] R. T. Yang, *Gas Separations by Adsorption Processes*, Butterworth, Boston (1987).

[8] J. D. Seader and E. J. Henley, *Separation Process Principles*, Wiley, New York (1998).

[1] The quantities $m_{\alpha,\text{tot}}$, $w_{\alpha,0}$, and $r_{\alpha,\text{tot}}$ may be expressed as integrals:

$$m_{\alpha,\text{tot}} = \int_V \rho_\alpha dV; \qquad w_{\alpha,0} = -\int_{S_0} (\mathbf{n}\cdot\rho_\alpha \mathbf{v}_\alpha) dS; \qquad r_{\alpha,\text{tot}} = \int_V r_\alpha dV + \int_{S_0} r_\alpha^{(s)} dS \tag{23.1-1a, b, c}$$

in which $\mathbf{n}$ is the outwardly directed unit normal vector, and S_0 is that portion of the bounding surface on which mass transfer occurs. The integrands in $r_{\alpha,\text{tot}}$ are the net rates of production of species α by homogeneous and heterogeneous reactions, respectively.

If all N equations in Eq. 23.1-1 are summed, we get

$$\frac{dm_{\text{tot}}}{dt} = -\Delta w + w_0 \tag{23.1-2}$$

in which $w_0 = \Sigma_\alpha w_{\alpha,0}$, and use has been made of the law of conservation of mass in the form $\Sigma_\alpha r_{\alpha,\text{tot}} = 0$.

It is often convenient to write Eq. 23.1-1 in molar units:

$$\boxed{\frac{dM_{\alpha,\text{tot}}}{dt} = -\Delta W_\alpha + W_{\alpha,0} + R_{\alpha,\text{tot}} \qquad \alpha = 1, 2, 3, \ldots, N} \tag{23.1-3}$$

Here the capital letters represent the molar counterparts of the lowercase symbols in Eq. 23.1-1. When Eq. 23.1-3 is summed over all species, the result is

$$\frac{dM_{\text{tot}}}{dt} = -\Delta W + W_0 + \sum_{\alpha=1}^{N} R_{\alpha,\text{tot}} \tag{23.1-4}$$

Note that the last term is not in general zero, because moles are produced or consumed in many reaction systems.

In some applications, such as spatially continuous mass transfer operations, it is customary to rewrite Eq. 23.1-1 or 3 for a differential element of the system (that is, in the "d-form" discussed in §15.4). Then the differentials $dw_{\alpha,0}$ or $dW_{\alpha,0}$ can be expressed in terms of local mass transfer coefficients.

EXAMPLE 23.1-1

Disposal of an Unstable Waste Product

A fluid stream emerges from a chemical plant with a constant mass flow rate w and discharges into a river (Fig. 23.1-1*a*). It contains a waste material A at mass fraction ω_{A0}, which is unstable and decomposes at a rate proportional to its concentration according to the expression $r_A = -k_1''' \rho_A$—that is, by a first-order reaction.

To reduce pollution it is decided to allow the effluent stream to pass through a holding tank of volume V, before discharging into the river (Fig. 23.1-1*b*). The tank is equipped with

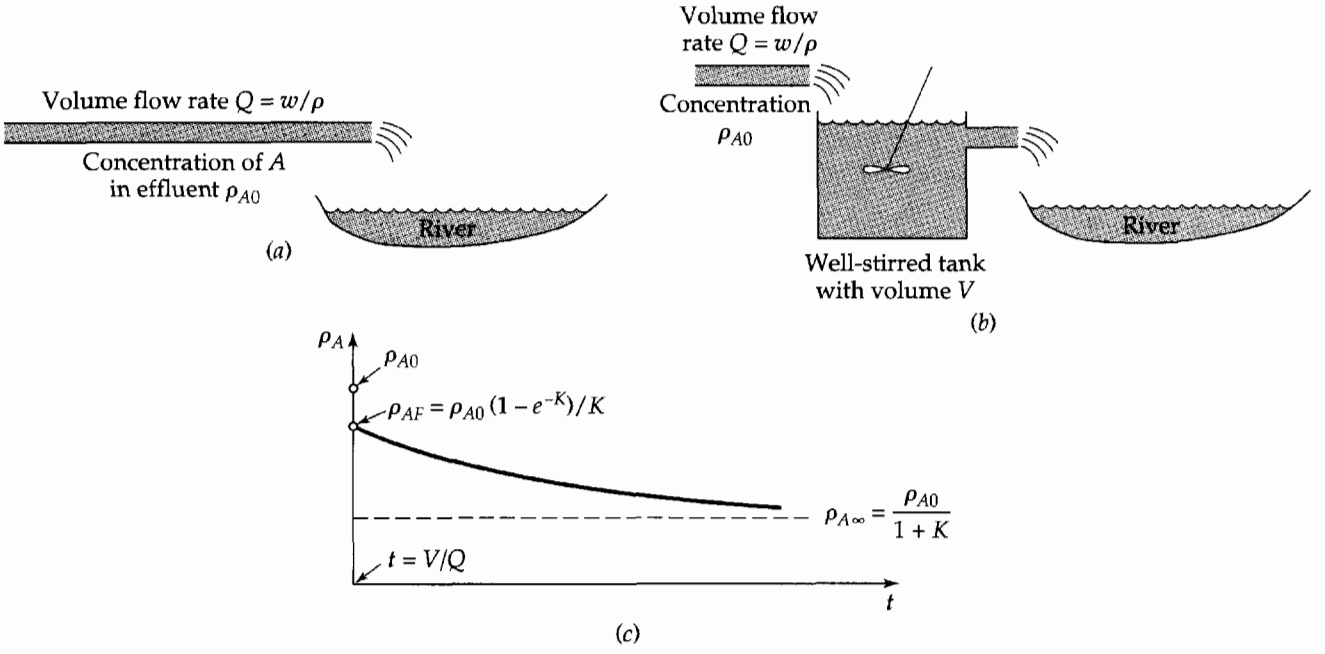

Fig. 23.1-1. (*a*) Waste stream with unstable pollutant emptying directly into a river. (*b*) Waste stream with holding tank that allows the unstable pollutant to decay prior to going into the river. (*c*) Sketch showing the concentration of pollutant being discharged into the river after the holding tank has been filled (the dimensionless quantity K is $k_1'''V/Q$).

an efficient stirrer that keeps the fluid in the tank at very nearly uniform composition. At time $t = 0$ the fluid begins to flow into the empty tank. No liquid flows out until the tank has been filled up to the volume V.

Develop an expression for the concentration of the fluid in the tank as a function of time, both during the tank-filling process and after the tank has been completely filled.

SOLUTION

(a) We begin by considering the period during which the tank is being filled—that is the period $t \leq \rho V/w$, where ρ is the density of the fluid mixture. We apply the macroscopic mass balance of Eq. 23.1-1 to the holding tank. The quantity $m_{A,\text{tot}}$ on the left side is $wt\omega_A$ at time t. The mass rate of flow entering the tank is $w\omega_{A0}$, and there is no outflow during the tank-filling stage. No A is entering or leaving through a mass transfer interface. The mass rate of production of species A is $r_{A,\text{tot}} = (wt/\rho)(-k_1'''\rho_A) = -k_1'''m_{A,\text{tot}}$. Therefore the macroscopic mass balance for species A during the filling period is

$$\frac{d}{dt}m_{A,\text{tot}} = w\omega_{A0} - k_1'''m_{A,\text{tot}} \tag{23.1-5}$$

This first-order differential equation can be solved with the initial condition that $m_{A,\text{tot}} = 0$ at $t = 0$ to give

$$m_{A,\text{tot}} = \frac{w\omega_{A0}}{k_1'''}(1 - \exp(-k_1'''t)) \tag{23.1-6}$$

This may be written in terms of the instantaneous mass fraction of A in the tank by using the relation $m_{A,\text{tot}} = wt\omega_A$:

$$\frac{\omega_A}{\omega_{A0}} = \frac{1 - \exp(-k_1'''t)}{k_1'''t} \qquad \left(t \leq \frac{\rho V}{w}\right) \tag{23.1-7}$$

The mass fraction of A at the instant when the tank is full, ω_{AF}, is then given by

$$\frac{\omega_{AF}}{\omega_{A0}} = \frac{1 - e^{-K}}{K} \tag{23.1-8}$$

in which $K = k_1'''\rho V/w = k_1'''V/Q$.

(b) The mass balance on the tank after it has been filled is

$$\frac{d}{dt}(\rho_A V) = w\omega_{A0} - w\omega_A - k_1'''\rho_A V \tag{23.1-9}$$

or, in dimensionless form, with $\tau = (w/\rho V)t$,

$$\frac{d\omega_A}{d\tau} + (1 + K)\omega_A = \omega_{A0} \tag{23.1-10}$$

This first-order differential equation can be solved with the initial condition that $\omega_A = \omega_{AF}$ at $\tau = 1$ to give

$$\frac{\omega_A - [\omega_{A0}/(1 + K)]}{\omega_{AF} - [\omega_{A0}/(1 + K)]} = e^{-(1+K)(\tau-1)} \qquad \left(t \geq \frac{\rho V}{w}\right) \tag{23.1-11}$$

This shows that as time progresses the mass fraction of the pollutant being discharged into the river decreases exponentially, with a limiting value of

$$\omega_{A\infty} = \frac{\omega_{A0}}{1 + K} = \frac{\omega_{A0}}{1 + (k_1'''\rho V/w)} \tag{23.1-12}$$

The curve for the mass concentration as a function of time after the filling of the tank is shown in Fig. 23.1-1(*c*). This curve can be used to determine conditions such that the effluent concentration will be in the permitted range. Equation 23.1-12 can be used to decide on the size of holding tank that is required.

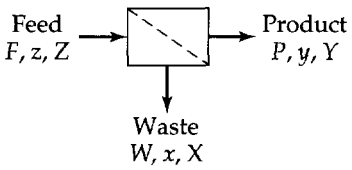

Fig. 23.1-2. Binary splitter, in which a feed stream is split into a product stream and a waste stream.

EXAMPLE 23.1-2

Binary Splitters

Describe the operation of a binary splitter, one of the commonest and simplest separation devices (see Fig. 23.1-2). Here a binary mixture of A and B enters the apparatus in a feed stream at a molar rate F, and by some separation mechanism it is split into a product stream with a molar rate P and a waste stream with molar rate W. The mole fraction of A (the desired component) in the feed stream is z, and the mole fractions in the product and waste streams are y and x, respectively.

SOLUTION

We start by writing the steady-state macroscopic mass balances for component A and for the entire fluid as

$$zF = yP + xW \tag{23.1-13}$$

$$F = P + W \tag{23.1-14}$$

It is customary to define the ratio $\theta = P/F$ of the molar rates of the product and feed streams as the *cut*. Equation 23.1-13 then becomes, after eliminating W by use of Eq. 23.1-14,

$$z = \theta y + (1 - \theta)x \tag{23.1-15}$$

Normally the cut θ and the feed composition z are taken to be known.

We now need a relation between the feed and waste compositions, and it is conventional to write an equation relating the compositions of the two outgoing streams:

$$Y = \alpha X \tag{23.1-16}$$

Here α is known as the *separation factor*, also usually taken as known, and which characterizes the separation capability of the splitter. Here Y and X are the mole ratios defined by

$$X = \frac{y}{1 - y} \quad \text{and} \quad X = \frac{x}{1 - x} \tag{23.1-17, 18}$$

In terms of the mole fractions, Eq. 23.1-16 may be written as

$$y = \frac{\alpha x}{1 + (\alpha - 1)x} \quad \text{or} \quad x = \frac{y}{\alpha - (\alpha - 1)y} \tag{23.1-19, 20}$$

Equations 23.1-15 and 19 (or 20) describe completely the splitter operation.

For vapor–liquid splitting—that is, equilibrium distillation—it is typical to define the *ideal* splitter in terms of an operation in which the product and waste streams are in equilibrium. For this situation, α is the *relative volatility*, and for thermodynamically ideal systems, it is just the ratio of the component vapor pressures. Even for nonideal systems, α changes relatively slowly with composition.

For *real* splitters one can then define α in terms of an empirical correction factor—for example, the *efficiency*—defined by

$$\alpha = E\alpha^* \tag{23.1-21}$$

where α^* is the separation factor for the ideal model, and E is a correction factor that accounts for the failure of the actual system to meet the ideal behavior.

We thus find that, for a given feed composition, the *enrichment* $(y - z)/z$ produced by the splitter is a function of the cut θ and the separation factor α. The enrichment can be calculated from the following equation, which is obtained by combining Eqs. 23.1-15 and 20:

$$z = \theta y + (1 - \theta)\frac{y}{\alpha - (\alpha - 1)y} \tag{23.1-22}$$

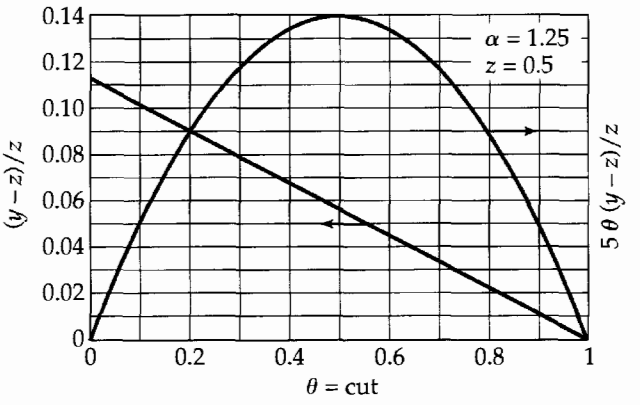

Fig. 23.1-3. Behavior of a binary splitter.

This is a quadratic equation for y that can be solved when z is given, and then the enrichment $(y - z)/z$ is obtained. An example is given in Fig. 23.1-3 where both $(y - z)/z$ and $5\theta(y - z)/z$ are plotted as functions of θ for $z = \frac{1}{2}$ and $\alpha = 1.25$ (a reasonable value for many processes). It may be seen that, whereas the maximum enrichment $(y - z)/z$ is obtained for vanishingly small cuts, the product of enrichment and product rate is greatest at an intermediate θ value. Finding an optimum θ value is a problem that must be addressed on economic grounds.

Simple splitters of the general type pictured in Fig. 23.1-2 are very widely used as building blocks in multistage separation processes. These include evaporators and crystallizers, which typically have a very high separation factor α per stage, and systems for distillation, gas absorption, and liquid extraction, where α can vary widely. All of these applications are well covered in standard texts on unit operations.

Membrane processes are rapidly increasing in importance, and many of the design principles were developed for the isotope fractionation industry.[2] Discussions of modern applications are also available.[3]

EXAMPLE 23.1-3

The Macroscopic Balances and Dirac's "Separative Capacity" and "Value Function"

During the Manhattan Project of World War II, the British physicist Dirac[2,4,5] used the macroscopic mass balances for a binary splitter to develop a criterion for comparing the effectiveness of different separation processes—for example, thermal diffusion and centrifugation. The same criterion has also proven useful in the evaluation of bioseparations.

We imagine the simple separation system shown in Fig. 23.1-2 in which F is the molar rate of flow of the feed stream, which contains a binary mixture of A and B, and P and W are the molar rates of flow of the product and waste streams. The mole fractions of species A in the three streams are z, y, and x, respectively.

In the system there is some mechanism (for example, a membrane) for increasing the concentration of A in the product stream and decreasing it in the waste stream. We then may define a *separation factor* α as in Eqs. 23.1-16 to 18

$$\alpha = \frac{y/(1-y)}{x/(1-x)} = 1 + \frac{y-x}{x(1-y)} \tag{23.1-23}$$

---

[2] E. Von Halle and J. Schacter, *Diffusion Separation Methods*, in Volume 8 of *Kirk-Othmer Encyclopedia of Chemical Technology* (M. Howe-Grant, ed.), 4th edition, Wiley, New York (1993), pp. 149–203.

[3] W. S. W. Ho and K. K. Sirkar, *Membrane Handbook*, Van Nostrand Reinhold, New York (1992), p. 954; R. D. Noble and S. A. Stern, *Membrane Separations Technology*, Elsevier, Amsterdam (1995), p. 718.

[4] P. A. M. Dirac, British Ministry of Supply (1941); this is reprinted in *The Collected Works of P. A. M. Dirac (1924–1948)*, (R. H. Dalitz, ed.) Cambridge University Press (1995). Nobel Laureate **Paul Adrien Maurice Dirac** (1902–1984), one of the leaders in the development of quantum mechanics, developed the relativistic wave equation and predicted the existence of the positron.

[5] K. Cohen, *Theory of Isotope Separation*, McGraw-Hill, New York (1951).

We have written this in a second form, because we will consider only systems in which there is only a slight enrichment of species A, so that $\alpha - 1$ is a very small quantity. When Eq. 23.1-23 is solved for y as a function of x we then get

$$y = \frac{x + (\alpha - 1)x}{1 + (\alpha - 1)x} \approx x + (\alpha - 1)x(1 - x) \tag{23.1-24}$$

Next we define the *Dirac separative capacity* Δ of the system as the net increase in "value" (this could, for example, be the monetary value) of the streams that are participating in the system:

$$\Delta = Pv(y) + Wv(x) - Fv(z) \tag{23.1-25}$$

in which $v(x)$ is the *Dirac value function.* (In the separation science literature, the separative capacity is often given the symbol δU.)

Show how the separative capacity and value function can be obtained by using the definition in Eq. 23.1-25 along with the mass balances for the system.

SOLUTION

The total mass balance and the mass balance for species A are:

$$F = P + W; \qquad Fz = Py + Wx \tag{23.1-26, 27}$$

We now divide Eq. 23.1-27 by F, and then use Eq. 23.1-26 to eliminate W. Then introducing the quantity $\theta = P/F$ (called the "cut"), we get

$$z = \theta y + (1 - \theta)x \quad \text{or} \quad z - x = \theta(y - x) \tag{23.1-28}$$

Next we divide Eq. 23.1-25 by F and introduce θ to get

$$\frac{\Delta}{F} = \theta v(y) + (1 - \theta)v(x) - v(z) \tag{23.1-29}$$

Inasmuch as the differences between the concentrations of the streams are quite small, we can expand $v(y)$ and $v(x)$ about z and get

$$v(x) = v(z) + (x - z)v'(z) + \tfrac{1}{2}(x - z)^2 v''(z) + \cdots \tag{23.1-30}$$

$$v(y) = v(z) + (y - z)v'(z) + \tfrac{1}{2}(y - z)^2 v''(z) + \cdots \tag{23.1-31}$$

where the primes indicate differentiation with respect to z. When these expressions are put into Eq. 23.1-29 and we use Eq. 23.1-28, we get

$$\frac{\Delta}{F} = \tfrac{1}{2}\theta(1 - \theta)(y - z)^2 v''(z) \tag{23.1-32}$$

When we use Eq. 23.1-24, this last equation becomes

$$\frac{\Delta}{F} = \tfrac{1}{2}\theta(1 - \theta)(\alpha - 1)z^2(1 - z)^2 v''(z) \tag{23.1-33}$$

We now assume that the separative capacity of the system is virtually independent of concentration. Therefore we set the concentration-dependent factor in Eq. 23.1-33 equal to unity, so that

$$\frac{\Delta}{F} = \tfrac{1}{2}\theta(1 - \theta)(\alpha - 1) \tag{23.1-34}$$

is the final expression for the separative capacity. According to this expression, the separative capacity has a maximum when the system is operated at $\theta = \frac{1}{2}$.

It remains to obtain the Dirac value function, which must satisfy the differential equation

$$\frac{d^2v}{dz^2} = \frac{1}{z^2(1 - z)^2} \tag{23.1-35}$$

When this equation is integrated, we get

$$v = (2z - 1)\ln\left(\frac{z}{1-z}\right) - 2 + C_1 z + C_2 \tag{23.1-36}$$

The two integration constants may be assigned arbitrarily, and several different choices have been used. However, the most common choice is $v(\frac{1}{2}) = 0$ and $v'(\frac{1}{2}) = 0$. This leads to

$$v = (2z - 1)\ln\left(\frac{z}{1-z}\right) \tag{23.1-37}$$

which is the symmetrical solution, in the sense that $v(1 - z) = v(z)$ and $v'(1 - z) = -v'(z)$.

The value function $v(z)$ and the separative capacity Δ have proven useful in comparing separations made in different kinds of equipment as well as different concentration ranges. From an economic standpoint $v(z)$ as given by Eq. 23.1-37 has been found useful for determining price differences for isotope mixtures of differing purity.

EXAMPLE 23.1-4

Compartmental Analysis

One of the simplest and most useful applications of the species macroscopic mass balance is *compartmental analysis*, in which a complex system is treated as a network of perfect mixers, each of constant volume, connected by ducts of negligible volume, with no dispersion occurring in the connecting ducts. Imagine mixing units, labeled 1, 2, 3, . . . , n, . . . , N, containing various species (labeled with indices $\alpha, \beta, \gamma, \ldots$). Then the mass concentration $\rho_{\alpha n}$ of species α in unit n changes with time according to the equation

$$V_n \frac{d\rho_{\alpha n}}{dt} = \sum_{m=1}^{N} Q_{mn}(\rho_{\alpha m} - \rho_{\alpha n}) + V_n r_{\alpha n} \tag{23.1-38}$$

Here V_n is the volume of unit n, Q_{mn} is the volumetric flow rate of solvent flow from unit m to unit n, and $r_{\alpha n}$ is the rate of formation of species α per unit volume in unit n.

Show how such a model can be specialized to describe the removal of toxic metabolic products (that is, the toxic materials resulting from the human metabolism) from a patient by *hemodialysis*. Hemodialysis is the periodic removal of toxic metabolites achieved by contacting the blood and a dialysis fluid in countercurrent flow, separated by a cellophane membrane that is permeable to the metabolite.

SOLUTION

The simple two-compartment model of Fig. 23.1-4 has been found to be adequate for representing the hemodialysis system. Here the large block, or compartment 1 (labeled "body") represents the combined body fluids, except for those in the blood, which are represented by compartment 2. The blood circulates via a branching system of vessels through compartment 1 at a volumetric rate Q, and in the process extracts solute across the vessel walls. This process is highly efficient, and a single solute is assumed to leave compartment 1 at concentration ρ_1, equal to the concentration throughout that compartment. At the same time, the solute is being formed within the body fluids at a constant rate G, and during dialysis it is being extracted from the blood by the dialyzer at a rate $D\rho_2$. The proportionality constant D is known as the "dialyzer clearance" and is fixed by the dialyzer design and operating conditions.

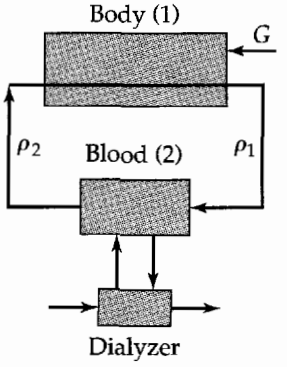

$$V_1 \frac{d\rho_1}{dt} = G - Q(\rho_1 - \rho_2)$$

$$V_2 \frac{d\rho_2}{dt} = Q(\rho_1 - \rho_2) - D\rho_2$$

Fig. 23.1-4. Two-compartment model used to analyze the functioning of a dialyzer.

The very complex process actually taking place is modeled by the two equations

$$V_1 \frac{d\rho_1}{dt} = -Q(\rho_1 - \rho_2) + G \tag{23.1-39}$$

$$V_2 \frac{d\rho_2}{dt} = Q(\rho_1 - \rho_2) - D\rho_2 \tag{23.1-40}$$

with $D = 0$ between the dialysis periods. Because we are considering a single solute, the concentrations have only one subscript to indicate the compartment. We measure the time t from the start of a dialysis procedure, when the blood and body fluids are very nearly in equilibrium with each other, so that we may write the initial conditions as

$$\text{I. C.: at } t = 0, \qquad \rho_1 = \rho_2 = \rho_0 \tag{23.1-41}$$

where ρ_0 is a constant. We now want to get an explicit expression for the toxic metabolite concentration in the blood as a function of time.

We start by adding Eqs. 23.1-39 and 40 and solving for $d\rho_1/dt$. The latter is then substituted into the time derivative of Eq. 23.1-40 to obtain a differential equation for the metabolite concentration in the blood:

$$\frac{d^2\rho_2}{dt^2} + \left(\frac{Q}{V_1} + \frac{Q}{V_2} + \frac{D}{V_2}\right)\frac{d\rho_2}{dt} + \frac{QD}{V_1V_2}\rho_2 = \frac{QG}{V_1V_2} \tag{23.1-42}$$

with

$$\text{I. C.: at } t = 0, \qquad \rho_2 = \rho_0 \quad \text{and} \quad \frac{d\rho_2}{dt} = -\frac{D\rho_0}{V_2} \tag{23.1-43}$$

The second initial condition is obtained by use of Eqs. 23.1-40 and 41.

This equation is now to be solved with the following specific parameter values, which are typical for the removal of creatinine from a 70-kg adult human:

Quantity	V_1 (liters)	V_2 (liters)	Q (liters per min)	D (liters per min)	G (g/min)	ρ_0 (g per liter)
Magnitude	43	4.5	5.4	0.3	0.0024	0.140

The differential equation and initial conditions now take the form:

$$\frac{d^2\rho_2}{dt^2} + (1.3922)\frac{d\rho_2}{dt} + (0.00837)\rho_2 = 6.70 \times 10^{-5} \tag{23.1-44}$$

$$\text{I. C.: at time } t = 0, \qquad \rho_2 = \rho_0 \quad \text{and} \quad \frac{d\rho_2}{dt} = -0.00933 \tag{23.1-45}$$

in which concentration is in grams per liter and time is in minutes. The complementary function that satisfies the associated homogeneous equation is

$$\rho_{2,\text{cf}} = C_1 \exp(0.006043t) + C_2 \exp(1.386t) \tag{23.1-46}$$

and the particular integral is

$$\rho_{2,\text{pi}} = 0.0080 \tag{23.1-47}$$

The complete solution to the nonhomogeneous equation is given by the sum of the complementary function and the particular integral. When the constants of integration are determined from the initial conditions, we get

$$\rho_2 = 0.1258 \exp(0.006043t) + (0.0062 \exp(1.386t) + 0.0080 \tag{23.1-48}$$

$$\frac{d\rho_2}{dt} = -0.000760 \exp(0.006043t) - 0.0086 \exp(1.386t) \tag{23.1-49}$$

during the dialysis period.

For the recovery period following dialysis, we assume here that the patient has no kidney function, so the clearance D is zero. Equation 23.1-42 takes the simpler form

$$\frac{d^2\rho_2'}{dt^2} + Q\left(\frac{V_1 + V_2}{V_1V_2}\right)\frac{d\rho_2'}{dt} = \frac{QG}{V_1V_2} \tag{23.1-50}$$

where ρ' is the concentration during the recovery period. The complementary function and particular integral are

$$\rho_{2,\text{cf}}' = C_3 \exp\left[-Q\left(\frac{V_1 + V_2}{V_1V_2}\right)t'\right] + C_4 \tag{23.1-51}$$

$$\rho_{2,\text{pi}}' = \frac{Gt'}{V_1 + V_2} \tag{23.1-52}$$

in which t' is the time measured from the start of the recovery period. Inserting the numerical values, we then get for the concentration during the recovery period and its time derivative

$$\rho_2' = C_3 \exp(-1.325t') + (5.05 \times 10^{-5})t' + C_4 \tag{23.1-53}$$

$$\frac{d\rho_2'}{dt'} = -1.325C_3 \exp(-1.325t') + (5.05 \times 10^{-5}) \tag{23.1-54}$$

The integration constants are to be determined from the matching conditions at $t' = 0$,

$$\text{at } t' = 0, \qquad \rho_2' = \rho_2 \quad \text{and} \quad \rho_1' = \rho_1 \tag{23.1-55, 56}$$

We need a second initial condition for determining the integration constants in Eq. 23.1-53. This can be obtained from Eq. 23.1-40 and the corresponding equation for ρ_2' (i.e., with $D = 0$), combined with the two relations in Eqs. 23.1-55 and 56. This relation is

$$\text{at } t' = 0, \qquad \frac{d\rho_2'}{dt} = \frac{d\rho_2}{dt} + \frac{D\rho_2}{V_2} \tag{23.1-57}$$

For illustrative purposes, we shall end the dialysis at 50 min, for which

$$\rho_2(t = 50) = 0.099239 = \rho_2' \tag{23.1-58}$$

We now have enough information to determine the constants of integration, and therefore we get for the concentration in the blood during the recovery period

$$\rho_2' = 0.0972 - 0.00422 \exp(-1.325t') + (5.05 \times 10^{-5})t' \tag{23.1-59}$$

Equations 23.1-48 and 59 are plotted in Fig. 23.1-5.

Of perhaps more interest is Fig. 23.1-6, which shows the application of Eqs. 23.1-39 and 40 to an actual patient. Here the points represent data and the lines are the model predictions. Here only the dialyzer clearance and the creatinine concentrations are known, and the data of

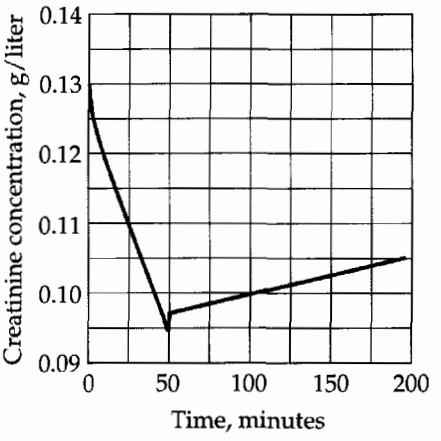

Fig. 23.1-5. Pharmacokinetics of dialysis: model prediction.

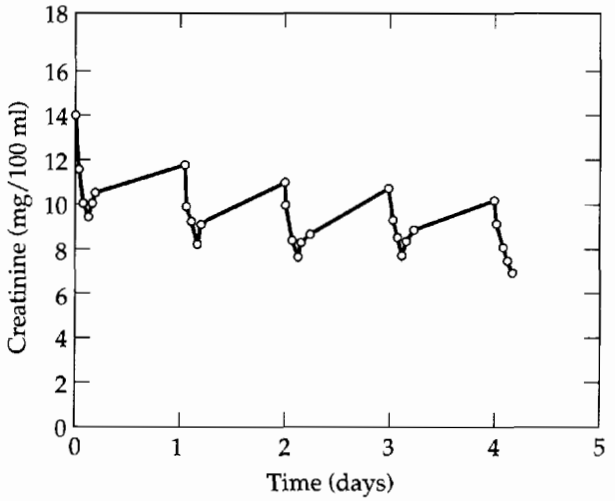

Fig. 23.1-6. Experimental (dots) and simulated creatinine data (solid curve) for a dialysis patient [R. L. Bell, K. Curtiss, and A. L. Babb, *Trans. Amer. Soc. Artificial Internal Organs*, **11**, 183 (1965)].

the first cycle are used to estimate the remaining parameters. The resulting model is then used to predict the next three cycles. We see that this approach does an excellent job of correlating the data and has predictive value. Note that the sudden rise in creatinine concentration at 50 min results from the fact that the dialyzer is no longer removing it from the blood. As a result, the disequilibrium between the blood and the rest of the body then becomes smaller.

Similar compartmental models have wide application in medicine, where they are referred to as *pharmacokinetic models*.[6] A priori pharmacokinetic modeling, where model parameters are determined separately from the process being modeled, was pioneered by Bischoff and Dedrick.[7]

EXAMPLE 23.1-5

Time Constants and Model Insensitivity

In the foregoing example it is clear, even on casual inspection, that neither the body fluids nor the circulating blood have much in common with ideal mixing tanks, and it is therefore of some interest to examine the success of the simple compartmental model critically. To make a start in that direction, compare the response (that is, the output concentration) of two quite different systems in Fig. 23.1-7 to an exponentially decaying solute input: one in which the en-

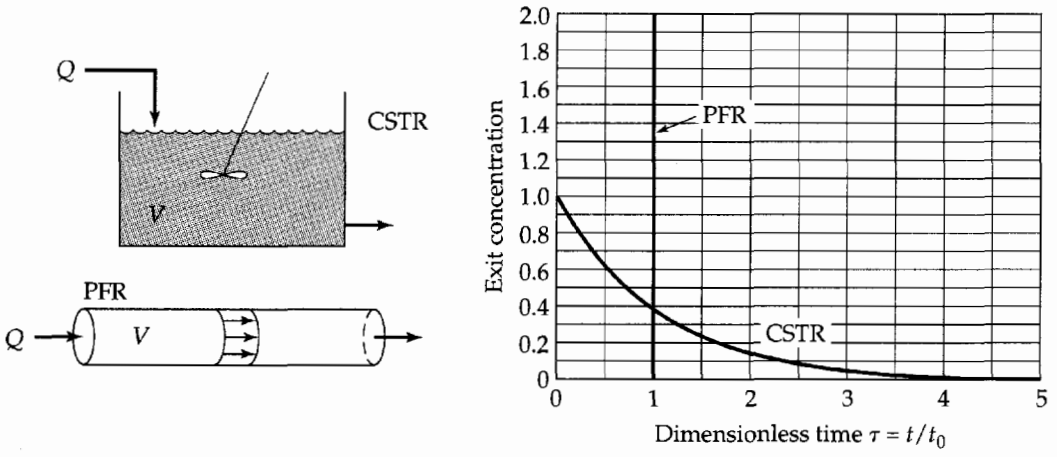

Fig. 23.1-7. Responses of the PFR and the CSTR to a pulse input.

[6] P. G. Welling, *Pharmacokinetics*, American Chemical Society (1997).

[7] K. B. Bischoff and R. L. Dedrick, *J. Pharm. Sci.*, **87**, 1347–1357 (1968); *AIChE Symposium Series*, **64**, 32–44 (1968).

tering fluid moves through in plug flow (*a plug flow reactor*, PFR), and another that acts as a perfect mixer (or *continuous stirred tank reactor*, CSTR). As shown in Fig. 23.1-7, the responses to a pulse input are quite different for the PFR and the CSTR. Assume steady flow at a volumetric flow rate Q through each system, and further assume that the tracer being followed is too dilute to affect the flow behavior of the carrier solvent. Assume that no reaction is occurring.

SOLUTION

For both systems we assume that the concentration is initially zero throughout and that the concentration of species α in the inlet stream is

$$\rho_\alpha = \rho_0 \exp(-t/t_0) \tag{23.1-60}$$

where ρ_0 and t_0 are constants, specific to the problem.

For the PFR, the exit stream concentration shows only a time delay and decay, and we may write at once for $X = \rho_\alpha/\rho_0$

$$X = 0 \qquad \text{for } t < t_{\text{res}} \tag{23.1-61}$$

where $t_{\text{res}} = V/Q$ is the *mean solute residence time*, a second time constant imposed on the system. The result for longer time is

$$X = \exp[-(t - t_{\text{res}})/t_0] \qquad \text{for } t > t_{\text{res}} \tag{23.1-62}$$

which is of more interest to us here.

For the CSTR we begin with the basic differential equation

$$V\frac{dX}{dt} = Q(\exp(-t/t_0) - X) \tag{23.1-63}$$

with the initial condition that $X = 0$ at $t = 0$. This first-order linear differential equation has the solution

$$X = \left(\frac{\alpha}{\alpha - 1}\right)(e^{-\tau} - e^{-\alpha\tau}) \qquad (\alpha \neq 1) \tag{23.1-64}$$

$$X = \tau e^{-\tau} \qquad (\alpha = 1) \tag{23.1-65}$$

in which $\alpha = t_0/t_{\text{res}}$ and $\tau = t/t_0$. Exit concentrations are plotted in Fig. 23.1-8 as functions of the dimensionless time $\tau = t/t_0$ for each reactor and for $1/\alpha = t_{\text{res}}/t_0$ of 0.1 and 1.0.

It may be seen that for $1/\alpha = t_{\text{res}}/t_0 = 1.0$ the two reactors produce much different effluent concentrations, as one might expect. However, for $t_{\text{res}}/t_0 << 1$ and t significantly greater than t_{res}, the effluent curves for the two reactors are virtually indistinguishable. This is the region of validity for compartmental analysis, and we see that in addition to the time constants imposed by the system itself, there is also another time constant t_{obs}, the time at which the ob-

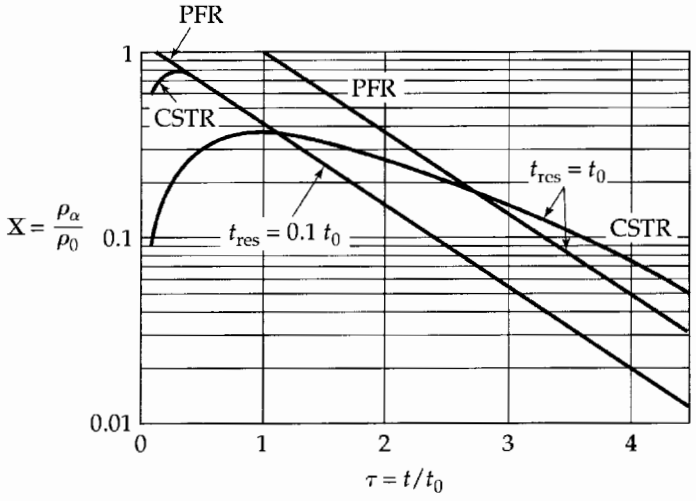

Fig. 23.1-8. Response of the PFR and the CSTR to an exponentially decaying input.

servations of the effluent concentration begin. We may then define the range of validity of compartmental analysis by the inequalities

$$t_0 >> t_{res} \text{ and } t_{obs} \geq t_{res} \tag{23.1-66}$$

Thus, compartmental analysis is most useful as a long-time approximate description of a system that responds slowly relative to solute residence times of its component units. It may immediately be seen that these conditions are met in Example 23.1-4, where the long-time metabolite concentrations are of primary interest.

Equation 23.1-66 summarizes the requirements for pharmacokinetics, which are met in a very wide variety of biological transport-reaction problems. They are also satisfied in a great many environmental situations.[8]

§23.2 THE MACROSCOPIC MOMENTUM AND ANGULAR MOMENTUM BALANCES

The macroscopic statements of the laws of conservation of momentum and angular momentum for a fluid mixture, with gravity as the only external force, are

$$\frac{d\mathbf{P}_{tot}}{dt} = -\Delta\left(\frac{\langle v^2\rangle}{\langle v\rangle} w + pS\right)\mathbf{u} + \mathbf{F}_{s\to f} + \mathbf{F}_0 + m_{tot}\mathbf{g} \tag{23.2-1}$$

$$\frac{d\mathbf{L}_{tot}}{dt} = -\Delta\left(\frac{\langle v^2\rangle}{\langle v\rangle} w + pS\right)[\mathbf{r}\times\mathbf{u}] + \mathbf{T}_{s\to f} + \mathbf{T}_0 + \mathbf{T}_{ext} \tag{23.2-2}$$

These (seldom used) equations are the same as Eqs. 7.2-2 and 7.3-2, except for the addition of the terms $\mathbf{F}_0$ and $\mathbf{T}_0$, which are the net influxes[1] of momentum and angular momentum into the system by mass transfer. For most mass transfer processes these terms are so small that they can be safely neglected.

§23.3 THE MACROSCOPIC ENERGY BALANCE

For a fluid mixture, the macroscopic statement of the law of conservation of energy is

$$\frac{d}{dt}(U_{tot} + K_{tot} + \Phi_{tot}) = -\Delta\left[\left(\hat{U} + p\hat{V} + \frac{1}{2}\frac{\langle v^3\rangle}{\langle v\rangle} + \hat{\Phi}\right)w\right] + Q_0 + Q + W_m \tag{23.3-1}$$

This equation is the same as Eq. 15.1-2, except that an additional term Q_0 has been added.[1] This term accounts for addition of energy to the system as a result of mass trans-

---

[8] F. H. Shair and K. L. Heitner, *Envir. Sci. and Tech.*, **8**, 444–451 (1974).

[1] These terms may be written as integrals,

$$\mathbf{F}_0 = -\int_{S_0}[\mathbf{n}\cdot\rho\mathbf{vv}]\,dS; \qquad \mathbf{T}_0 = -\int_{S_0}[\mathbf{n}\cdot\{\mathbf{r}\times\rho\mathbf{vv}\}]\,dS \tag{23.2-1a, b}$$

in which $\mathbf{n}$ is the outwardly directed unit normal vector.

[1] This term may be written as an integral,

$$Q_0 = -\int_{S_0}\left(\mathbf{n}\cdot\left\{\tfrac{1}{2}\rho v^2\mathbf{v} + \rho\hat{\Phi}\mathbf{v} + \sum_{\alpha=1}^{N} c_\alpha\bar{H}_\alpha\mathbf{v}_\alpha\right\}\right)dS \tag{23.3-1a}$$

in which $\mathbf{n}$ is the outwardly directed unit normal vector. The origin of this term may be seen by referring to Eq. 19.3-5 and Eq. (H) of Table 17-8-1.

fer. It may be of considerable importance, particularly if material is entering through the bounding surface at a much higher or lower temperature than that of the fluid inside the flow system, or if it reacts chemically in the system.

When chemical reactions are occurring, considerable heat may be released or absorbed. This heat of reaction is automatically taken into account in the calculation of the enthalpies of the entering and leaving streams (see Example 23.5-1).

In some applications, in which the energy transfer rates across the surface are functions of position, it is more convenient to rewrite Eq. 23.3-1 in the *d*-form—that is, over a differential portion of the flow system as described in §15.4. Then the increment of heat added, dQ, is expressible in terms of a local heat transfer coefficient.

§23.4 THE MACROSCOPIC MECHANICAL ENERGY BALANCE

A careful examination of the derivation of the mechanical energy balance in §7.8 shows that the result obtained there applies to mixtures as well as to pure fluids. If we now include the surface S_0, then we get

$$\boxed{\frac{d}{dt}(K_{\text{tot}} + \Phi_{\text{tot}}) = -\Delta\left[\left(\frac{1}{2}\frac{\langle v^3\rangle}{\langle v\rangle} + \hat{\Phi} + \frac{p}{\rho}\right)w\right] + B_0 + W_m - E_c - E_v} \tag{23.4-1}$$

This is the same as Eq. 7.4-2, except for the addition of the term B_0, which accounts for the mechanical energy transport across the mass transfer boundary.[1] The use of this equation is illustrated in Example 22.5-3.

§23.5 USE OF THE MACROSCOPIC BALANCES TO SOLVE STEADY-STATE PROBLEMS

The macroscopic balances are summarized in Table 23.5-1 for systems with more than one entry and exit plane. The terms with subscript 0 describe the addition or removal of mass, momentum, angular momentum, energy, and mechanical energy at mass-transfer surfaces. Usually these balances are not used in their entirety, but it is convenient to have a complete listing of them for problem-solving purposes. For steady-state problems, the left sides of the equations may be omitted. As we saw in Chapters 7 and 15, considerable intuition is required in using the macroscopic balances, and sometimes it is necessary to supplement the equations with experimental observations.

EXAMPLE 23.5-1

Energy Balances for a Sulfur Dioxide Converter

Hot gases from a sulfur burner enter a converter, in which the sulfur dioxide present is to be oxidized catalytically to sulfur trioxide, according to the reaction $SO_2 + \frac{1}{2}O_2 \rightleftarrows SO_3$. How much heat must be removed from the converter per hour to permit a 95% conversion of the SO_2 for the conditions shown in Fig. 23.5-1? Assume that the converter is large enough for the components of the exit gas to be in thermodynamic equilibrium with one another. That is, the partial pressures of the exit gases are related by the equilibrium constraint

$$K_p = \frac{p_{SO_3}}{p_{SO_2}p_{O_2}^{1/2}} \tag{23.5-1}$$

[1] In terms of a surface integral, this term is given by

$$B_0 = -\int_{S_0} (\mathbf{n} \cdot [\tfrac{1}{2}\rho v^2 + \rho\hat{\Phi} + p]\mathbf{v})\, dS \tag{23.4-1a}$$

Table 23.5-1 Unsteady-State Macroscopic Balances for Nonisothermal Multicomponent Systems

Mass:

$$\frac{d}{dt}m_{\text{tot}} = \Sigma w_1 - \Sigma w_2 + w_0 = \Sigma \rho_1 \langle v_1 \rangle S_1 - \Sigma \rho_2 \langle v_2 \rangle S_2 + w_0 \tag{A}$$

Mass of species α:

$$\frac{d}{dt}m_{\alpha,\text{tot}} = \Sigma w_{\alpha 1} - \Sigma w_{\alpha 2} + w_{\alpha 0} + r_{\alpha,\text{tot}} \qquad \alpha = 1, 2, 3, \ldots N \tag{B}$$

Momentum:

$$\frac{d}{dt}\mathbf{P}_{\text{tot}} = \Sigma\left(\frac{\langle v_1^2 \rangle}{\langle v_1 \rangle} w_1 + p_1 S_1\right)\mathbf{u}_1 - \Sigma\left(\frac{\langle v_2^2 \rangle}{\langle v_2 \rangle} w_2 + p_2 S_2\right)\mathbf{u}_2 + m_{\text{tot}}\mathbf{g} + \mathbf{F}_0 - \mathbf{F}_{f\to s} \tag{C}$$

Angular momentum:

$$\frac{d}{dt}\mathbf{L}_{\text{tot}} = \Sigma\left(\frac{\langle v_1^2 \rangle}{\langle v_1 \rangle} w_1 + p_1 S_1\right)[\mathbf{r}_1 \times \mathbf{u}_1] - \Sigma\left(\frac{\langle v_2^2 \rangle}{\langle v_2 \rangle} w_2 + p_2 S_2\right)[\mathbf{r}_2 \times \mathbf{u}_2] + \mathbf{T}_{\text{ext}} + \mathbf{T}_0 - \mathbf{T}_{f\to s} \tag{D}$$

Mechanical energy:

$$\frac{d}{dt}(K_{\text{tot}} + \Phi_{\text{tot}}) = \Sigma\left(\frac{1}{2}\frac{\langle v_1^3 \rangle}{\langle v_1 \rangle} + gh_1 + \frac{p_1}{\rho_1}\right)w_1 - \Sigma\left(\frac{1}{2}\frac{\langle v_2^3 \rangle}{\langle v_2 \rangle} + gh_2 + \frac{p_2}{\rho_2}\right)w_2 + W_m + B_0 - E_c - E_v \tag{E}$$

(Total) energy:

$$\frac{d}{dt}(K_{\text{tot}} + \Phi_{\text{tot}} + U_{\text{tot}}) = \Sigma\left(\frac{1}{2}\frac{\langle v_1^3 \rangle}{\langle v_1 \rangle} + gh_1 + \hat{H}_1\right)w_1 - \Sigma\left(\frac{1}{2}\frac{\langle v_2^3 \rangle}{\langle v_2 \rangle} + gh_2 + \hat{H}_2\right)w_2 + W_m + Q_0 + Q \tag{F}$$

Notes:

(a) $\Sigma w_{\alpha 1} = w_{\alpha 1a} + w_{\alpha 1b} + w_{\alpha 1c} + \cdots$, where $w_{\alpha 1a} = \rho_{\alpha 1a} v_{1a} S_{1a}$, and so on; Equations (A) and (B) can be written in molar units by replacing the lowercase symbols by capital letters and adding to Eq. (A) the term $\Sigma_\alpha R_{\alpha,\text{tot}}$ to account for the fact that moles need not be conserved in a chemical reaction.

(b) h_1 and h_2 are elevations above an arbitrary datum plane.

(c) $\hat{H}_1$ and $\hat{H}_2$ are enthalpies per unit mass (for the mixture) relative to some arbitrarily chosen reference state; see Example 19.3-1.

(d) All equations are written for compressible flow; for incompressible flow, $E_c = 0$. The quantities E_c and E_v are defined in Eqs. 7.3-3 and 4.

(e) $\mathbf{u}_1$ and $\mathbf{u}_2$ are unit vectors in the direction of flow.

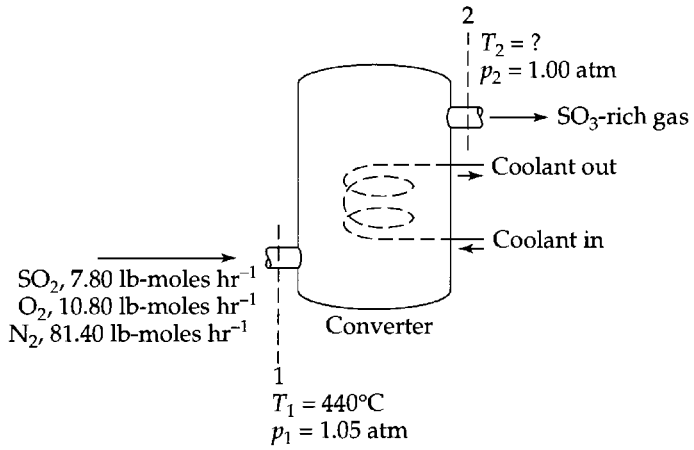

Fig. 23.5-1. Catalytic oxidation of sulfur dioxide.

Approximate values of K_p for this reaction are

T (K)	600	700	800	900
$K_p(\text{atm}^{-1/2})$	9500	880	69.5	9.8

SOLUTION

It is convenient to divide this problem into two parts: **(a)** first we use the mass balance and equilibrium expression to find the desired exit temperature, and then **(b)** we use the energy balance to determine the required heat removal.

(a) ***Determination[1] of T_2.*** We begin by writing the steady-state macroscopic mass balance, Eq. 23.1-3, for the various constituents in the two streams in the form:

$$W_{\alpha 2} = W_{\alpha 1} + R_{\alpha,\text{tot}} \tag{23.5-2}$$

In addition, we take advantage of the two stoichiometric relations

$$R_{SO_2,\text{tot}} = -R_{SO_3,\text{tot}} \tag{23.5-3}$$

$$R_{O_2,\text{tot}} = \tfrac{1}{2}R_{SO_2,\text{tot}} \tag{23.5-4}$$

We can now get the desired molar flow rates through surface 2:

$$W_{SO_2,2} = 7.80 - (0.95)(7.80) = 0.38 \text{ lb-mole/hr} \tag{23.5-5}$$

$$W_{SO_3,2} = 0 + (0.95)(7.80) = 7.42 \text{ lb-mole/hr} \tag{23.5-6}$$

$$W_{O_2,2} = 10.80 - \tfrac{1}{2}(0.95)(7.80) = 7.09 \text{ lb-mole/hr} \tag{23.5-7}$$

$$W_{N_2,2} = W_{N_2,1} = 81.40 \text{ lb-mole/hr} \tag{23.5-8}$$

$$W_2 = 0.38 + 7.42 + 7.09 + 81.40 = 96.29 \text{ lb-mole/hr} \tag{23.5-9}$$

Next, substituting numerical values into the equilibrium expression Eq. 23.5-1 gives

$$K_p = \frac{(7.42/96.29)}{(0.38/96.29)(7.09/96.29)^{1/2}} = 72.0 \text{ atm}^{-1/2} \tag{23.5-10}$$

This value of K_p corresponds to an exit temperature T_2 of about 510°C, according to the equilibrium data given above.

(b) ***Calculation of the required heat removal.*** As indicated by the results of Example 15.3-1, changes in kinetic and potential energy may be neglected here in comparison with changes in enthalpy. In addition, for the conditions of this example, we may assume ideal gas behavior. Then, for each constituent, $\overline{H}_\alpha = \tilde{H}_\alpha(T)$. We may then write the macroscopic energy balance, Eq. 23.3-1, as

$$-Q = \sum_{\alpha=1}^{N} (W_\alpha \tilde{H}_\alpha)_1 - \sum_{\alpha=1}^{N} (W_\alpha \tilde{H}_\alpha)_2 \tag{23.5-11}$$

For each of the individual constituents we may write

$$\tilde{H}_\alpha = \tilde{H}_\alpha^\circ + (\tilde{C}_{p\alpha})_{\text{avg}}(T - T^\circ) \tag{23.5-12}$$

Here $\tilde{H}_\alpha^\circ$ is the standard enthalpy of formation[2] of species α from its constituent elements at the enthalpy reference temperature T°, and $(\tilde{C}_{p\alpha})_{\text{avg}}$ is the enthalpy-mean heat capacity[2] of the species between T and T°. For the conditions of this problem, we may use the

[1] See O. A. Hougen, K. M. Watson, and R. A. Ragatz, *Chemical Process Principles*, Part II, 2nd edition, Wiley, New York (1959), pp. 1017–1018.

[2] See, for example, O. A. Hougen, K. M. Watson, and R. A. Ragatz, *Chemical Process Principles*, Part I, 2nd edition, Wiley, New York (1959), pp. 257, 296.

following[2] numerical values for these physical properties (the last two columns are obtained from Eq. 23.5-12):

Species	$\tilde{H}^0_\alpha$ cal/g-mole at 25°C	$(\tilde{C}_{p\alpha})_{avg}$ [cal/g-mole · C] from 25°C to 440°C	from 25°C to 510°C	$(W_\alpha \tilde{H}_\alpha)_1$ Btu/hr	$(W_\alpha \tilde{H}_\alpha)_2$ Btu/hr
SO_2	−70,960	11.05	11.24	−931,900	−44,800
SO_3	−94,450	—	15.87	0	−1,158,700
O_2	0	7.45	7.53	60,100	46,600
N_2	0	7.12	7.17	433,000	509,500
			Totals	−438,800	−647,400

Substitution of the preceding values into Eq. 23.5-11 gives the required rate of heat removal:

$$-Q = (-438{,}800) - (-647{,}400) = 208{,}600 \text{ Btu/hr} \tag{23.5-13}$$

EXAMPLE 23.5-2

Height of a Packed-Tower Absorber[3]

It is desired to remove a soluble gas A from a mixture of A and an insoluble gas B by contacting the mixture with a nonvolatile liquid solvent L in the apparatus shown in Fig. 23.5-2. The apparatus consists essentially of a vertical pipe filled with a randomly arranged packing of small rings of a chemically inert material. The liquid L is sprayed evenly over the top of the packing and trickles over the surfaces of these small rings. In so doing, it is intimately contacted with the gas mixture that is passing up the tower. This direct contacting between the two streams permits the transfer of A from the gas to the liquid.

The gas and liquid streams enter the apparatus at molar rates of $-W_G$ and W_L, respectively, on an A-free basis. Note that the gas rate is negative, because the gas stream is flowing from plane 2 to plane 1 in this problem. The molar ratio of A to G in the entering gas stream is $Y_{A2} = y_{A2}/(1 - y_{A2})$, and the molar ratio of A to L in the entering liquid stream is $X_{A1} = x_{A1}/(1 - x_{A1})$. Develop an expression for the tower height z required to reduce the molar ratio Y_A in the gas stream from Y_{A2} to Y_{A1}, in terms of the mass transfer coefficients in the two streams and the stream rates and compositions.

Assume that the concentration of A is always small in both streams, so that the operation may be considered isothermal and so that the high mass-transfer rate corrections to the mass transfer coefficients are not needed, and the mass transfer coefficients, k^0_x and k^0_y, defined in the second line of Eq. 22.2-14 can be used.

SOLUTION

Since the behavior of a packed tower is quite complex, we replace the true system by a hypothetical model. We consider the system to be equivalent to two streams flowing side-by-side with no back-mixing, as shown in Fig. 23.5-3, and in contact with one another across an interfacial area a per unit volume of packed column (see Eq. 22.1-14).

We further assume that the fluid velocity and composition of each stream are uniform over the tower cross section, and neglect both eddy and molecular transport in the flow direction. We also consider the concentration profiles in the direction of flow to be continuous curves, not appreciably affected by the placement of the individual packing particles.

The model resulting from these simplifying assumptions is probably not a very satisfactory description of a packed tower. The neglect of back-mixing and fluid-velocity nonuniformity are probably particularly serious. However, the presently available correlations for mass

[3] J. D. Seader and E. J. Henley, *Separation Process Principles*, Wiley, New York (1998).

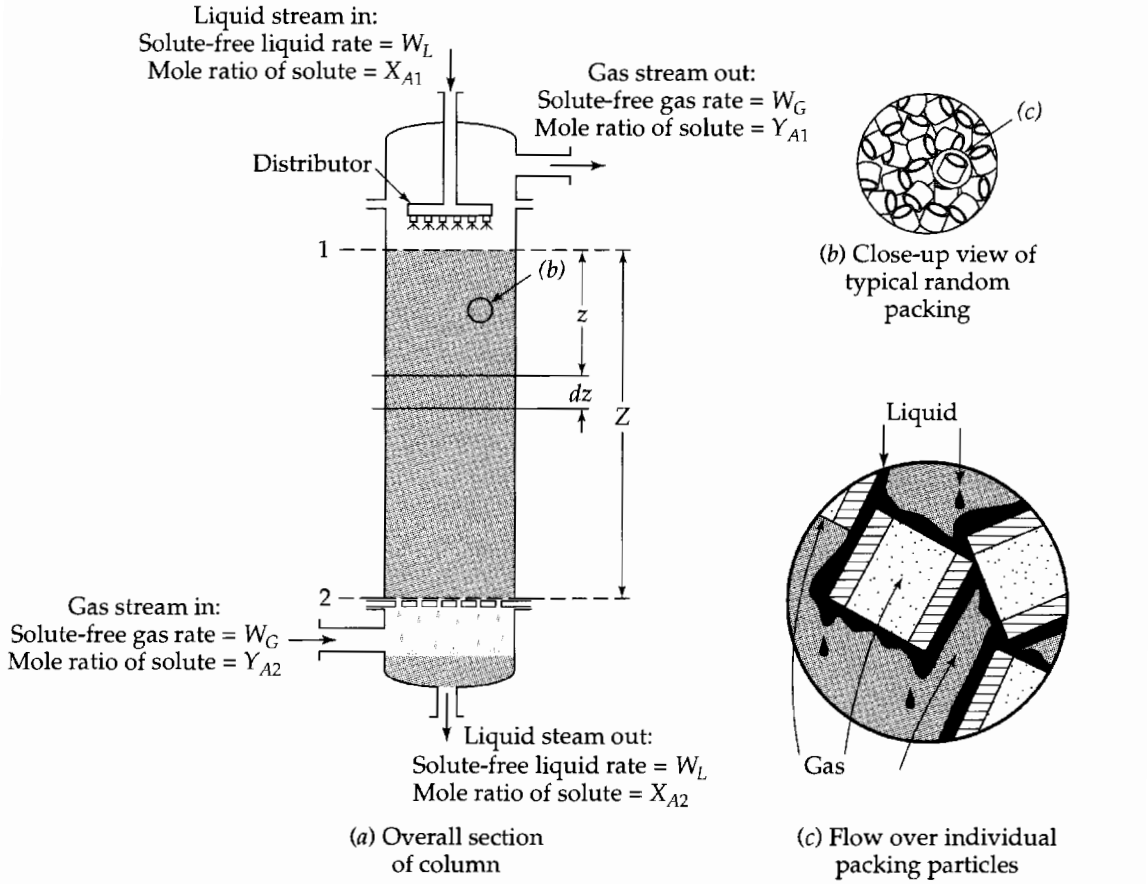

Fig. 23.5-2. A packed-column mass transfer apparatus in which the descending phase is dispersed. Note that in this drawing W_G is negative; that is, the gas is flowing from 2 toward 1.

transfer coefficients have been calculated on the basis of this model, which should therefore be employed when these correlations are used.

We are now in a position to develop an expression for the column height, and we do this in two stages: **(a)** First we use the overall macroscopic mass balance to determine the exit liquid-phase composition and the relation between bulk compositions of the two phases at

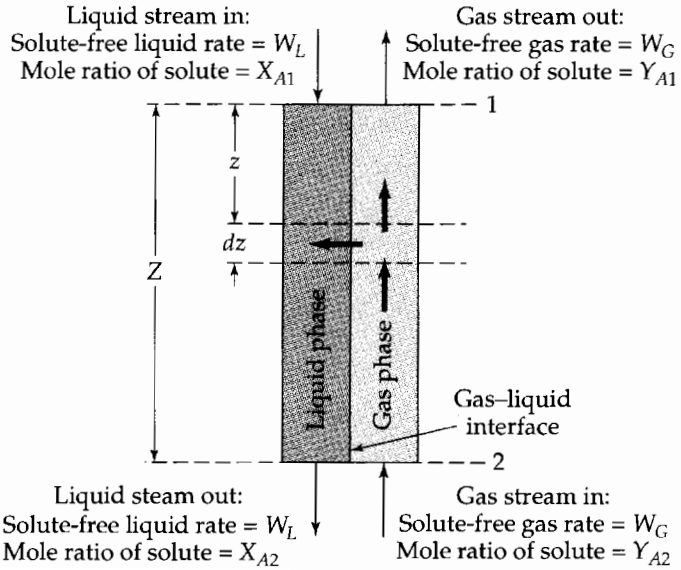

Fig. 23.5-3. Schematic representation of a packed-tower absorber, showing a differential element on which a mass balance is made.

each point in the tower. **(b)** We then use these results along with the differential form of the macroscopic mass balance to determine the interfacial conditions and the required tower height.

(a) ***Overall macroscopic mass balances.*** For the solute A we write the macroscopic mass balance of Eq. 23.1-3 for each stream of the system between planes 1 and 2 as

liquid stream $$W_{Al2} - W_{Al1} = W_{Al,0} \tag{23.5-14}$$

gas stream $$W_{Ag2} - W_{Ag1} = W_{Ag,0} \tag{23.5-15}$$

Here the subscripts Al and Ag refer to the solute A in the liquid and gas streams, respectively. Since the number of moles leaving the liquid stream must enter the gas stream across the interface, $W_{Al,0} = -W_{Ag,0}$, and Eqs. 23.5-14 and 15 may be combined to give

$$W_{Al2} - W_{Al1} = -(W_{Ag2} - W_{Ag1}) \tag{23.5-16}$$

This can now be rewritten in terms of the compositions of the entering and leaving streams by setting $W_{Al2} = W_L X_{A2}$, and so on, and then rearrangement gives

$$X_{A2} = X_{A1} - \frac{W_G}{W_L}(Y_{A2} - Y_{A1}) \tag{23.5-17}$$

Thus we have found the concentration of A in the exit liquid stream.

By replacing plane 2 by a plane at a distance z down the column, Eq. 23.5-17 may be used to obtain an expression relating bulk stream compositions at any point in the tower:

$$X_A = X_{A1} - \frac{W_G}{W_L}(Y_A - Y_{A1}) \tag{23.5-18}$$

Equation 23.5-18 (the "operating line") is shown in Fig. 23.5-4 along with the equilibrium distribution for the conditions of Problem 23A.2.

(b) ***Application of the macroscopic-balances in the d-form.*** We now apply Eq. 23.1-3 to a differential increment dz of the tower, first to estimate the interfacial conditions and then determine the tower height required for a given separation.

(i) ***Determination of interfacial conditions.*** Because only A is transferred across the interface, we may write, according to the second line of Eq. 22.1-14 (which presumes low concentrations of A and small mass-transfer rates):

$$dW_{Al,0} = (k_x^0 a)(x_{A0} - x_A)S dz \tag{23.5-19}$$

$$dW_{Ag,0} = (k_y^0 a)(y_{A0} - y_A)S dz \tag{23.5-20}$$

Here a is the interfacial area per unit volume of the packed bed tower, S is the cross-sectional area of the tower, x_{A0} and y_{A0} are the interfacial mole fractions of A in the liquid and gas phases, respectively, and x_A and y_A are the corresponding bulk concentrations (the index b is being omitted here, so that x_A, y_A, X_A, and Y_A are all bulk compositions).

Then, since (for the dilute solutions considered here) $x_A = X_A/(X_A + 1) \approx X_A$ and $y_A = Y_A/(Y_A + 1) \approx Y_A$, Eqs. 23.5-19 and 20 may be combined to give

$$\frac{Y_A - Y_{A0}}{X_A - X_{A0}} = -\frac{(k_x^0 a)}{(k_y^0 a)} \tag{23.5-21}$$

This equation enables us to determine Y_{A0} as a function of Y_A. For any Y_A, one may locate X_A on the operating line (mass balance). One then draws a straight line of slope $-(k_x^0 a)/(k_y^0 a)$ through the point (Y_A, X_A), as shown in Fig. 23.5-4. The intersection of this line with the equilibrium curve then gives the local interfacial compositions (Y_{A0}, X_{A0}).

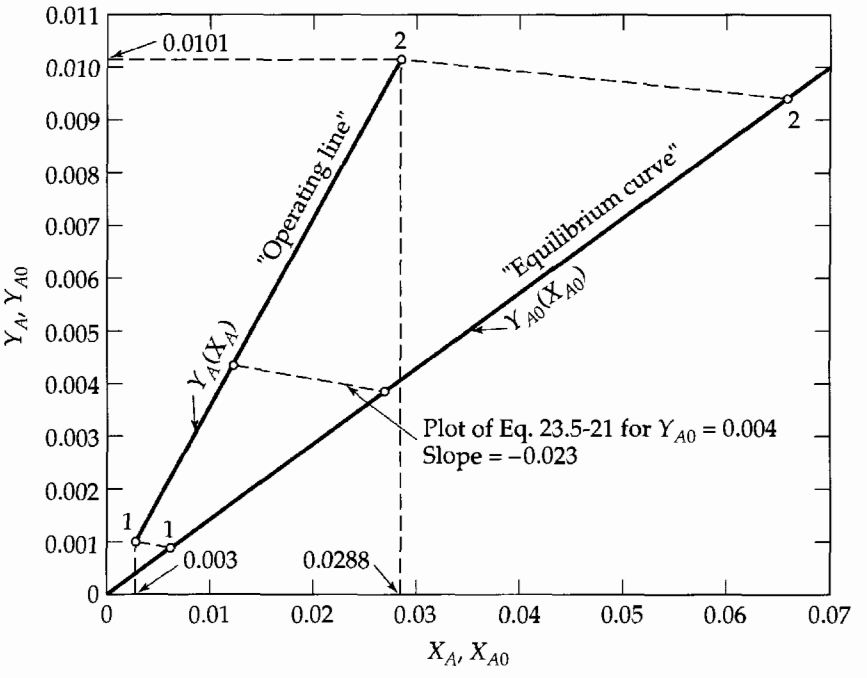

Fig. 23.5-4. Calculation of interfacial conditions in the absorption of cyclohexane from air in a packed column (see Problem 23A.2).

(ii) ***Determination of required column height.*** Application of Eq. 23.1-1 to the gas stream in a volume $S\,dz$ of the tower gives

$$W_G dY_A = dW_{Ag,0} \tag{23.5-22}$$

This expression may be combined with Eq. 23.5-20 for the dilute solutions being considered to obtain

$$-W_G dY_A = (k_y^0 a)(Y_A - Y_{A0})S\,dz \tag{23.5-23}$$

This equation may now be rearranged and integrated from $z = 0$ to $z = Z$:

$$Z = -\frac{W_G}{S(k_y^0 a)} \int_{Y_{A1}}^{Y_{A2}} \frac{dY_A}{Y_A - Y_{A0}} \tag{23.5-24}$$

Equation 23.5-24 is the desired expression for the column height required to effect the specified separation. In writing Eq. 23.5-24 we have neglected the variation of the mass transfer coefficient k_y^0 with composition. This is usually permissible only for dilute solutions.

In general, Eq. 23.5-24 must be integrated by numerical or graphical procedures. However, for dilute solutions, it may frequently be assumed that the operating and equilibrium lines of Fig. 23.5-4 are straight. If, in addition, the ratio k_x^0/k_y^0 is constant, then $Y_A - Y_{A0}$ varies linearly with Y_A. We may then integrate Eq. 23.5-24 to obtain (see Problem 23B.1)

$$Z = \frac{W_G}{S(k_y^0 a)} \frac{Y_{A2} - Y_{A1}}{(Y_{A0} - Y_A)_{\ln}} \tag{23.5-25}$$

where

$$(Y_{A0} - Y_A)_{\ln} = \frac{(Y_{A0} - Y_A)_2 - (Y_{A0} - Y_A)_1}{\ln [(Y_{A0} - Y_A)_2/(Y_{A0} - Y_A)_1]} \tag{23.5-26}$$

Equation 23.5-25 can be rearranged to give

$$W_{Ag,0} = W_G(Y_{A2} - Y_{A1}) = (k_y^0 a)ZS(Y_{A0} - Y_A)_{\ln} \tag{23.5-27}$$

Comparison of Eq. 23.5-27 and Eq. 15.4-15 shows the close analogy between packed towers and simple heat exchangers. Expressions analogous to Eq. 23.5-24 but containing the overall mass transfer coefficient K_y^0 may also be derived (see Problem 23B.1). Again, we may use the final results, Eqs. 23.5-25 or 27, for either cocurrent or countercurrent flow. Keep in mind, however, that the simplified model used to describe the packed tower is not as reliable as the corresponding one used for heat exchangers.

EXAMPLE 23.5-3

Linear Cascades

We saw in Example 23.1-2 that the degree of separation possible in a simple binary splitter can be quite limited, and it is therefore often desirable to combine individual splitters in a countercurrent *cascade* such as that shown in Fig. 23.5-5. Here the feed to any splitter stage is the sum of the waste stream from the splitter immediately above it and the product from the splitter immediately below.

Show how such an arrangement can increase the degree of separation relative to that obtained in a single splitter.

SOLUTION

For the system as a whole we can write a mass balance for the desired product and for the solution as a whole. That is, we treat the entire system as a splitter and write

$$z_F F = y_P P + x_W W \qquad F = P + W \tag{23.5-28, 29}$$

It will be assumed here that all of quantities in these equations are given, so that the problem is specified as far as the overall mass balances are concerned. It remains for us to determine the number of stages required to meet these conditions.

We begin by writing a set of mass balances over the top portion of the column, here the top two stages for illustrative purposes (see Fig. 23.5-5):

$$y_3 U_3 - x_2 D_2 = y_P P \qquad U_3 - D_2 = P \tag{23.5-30, 31}$$

Here U_n and D_n are the upflowing and downflowing streams from stage n, and y_n and x_n are the corresponding mole fractions of the desired solute. When P is eliminated between Eqs. 23.5-3 and 31, we get

$$\frac{y_2 - y_P}{x_2 - y_P} = \frac{D_2}{U_3} \tag{23.5-32}$$

This equation gives the relation between the compositions of the downflowing and upflowing streams passing each other at any column cross section above the feed stage, in terms of the corresponding flow rates. This relation, when shown on an x-y plot (which is called a *McCabe–Thiele diagram*[3,4]) is known as the *operating line* for the system. We concentrate for the moment on compositions and return later to the problem of determining stream rate ratios.

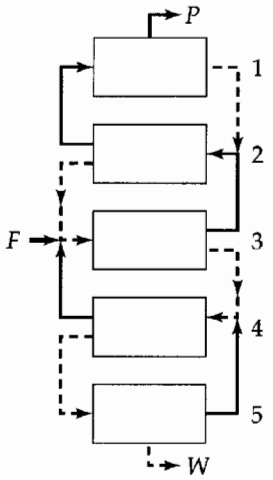

Fig. 23.5-5. A linear cascade. Upward flows are shown by solid lines, and downward flows by dashed lines.

[4] W. L. McCabe and E. W. Thiele, *Ind. Eng. Chem.*, **17**, 605–611 (1925).

The phase compositions in each stage are assumed to satisfy an equilibrium relation such as (see Eq. 23.1-19)

$$y_n = \frac{ax_n}{1 + (\alpha - 1)x_n} \tag{23.5-33}$$

or, more generally, $y_n = f(x_n)$, where $f(x)$ is taken to be a known function.

Equations 23.5-32 and 33 (or its generalization) now permit determination of all compositions in the portion of the column above the feed point, usually known as the *rectifying section*, and similar calculations can be made for the *stripping section*, the portion below the feed point. We may then determine the number of stages required for the separation under consideration and the proper location of the feed stage.

First, however, we need to determine the stream rate ratios required in Eq. 23.5-32, and we consider three special cases here:

(a) ***Total reflux.*** This special mode of operation, in which P and W are zero, is important, as it provides the smallest possible number of stages that can yield the desired output compositions. Here

$$U_n = D_{n-1} \tag{23.5-34}$$

for all n, and the operating line is given by

$$y_n = x_{n-1} \tag{23.5-35}$$

This simple relation holds for all physical systems. The stage compositions are plotted in Fig. 23.5-6 (for a product mole fraction of 0.9 and a waste mole fraction of 0.1), along with an equilibrium curve of the form of Eq. 23.5-33 with $\alpha = 2.5$.

The steplike lines between the equilibrium and operating lines in this figure suggest a graphical method of determining stage compositions: each "step" between the equilibrium and operating lines represents an incremental one-component splitter or stage. The diagram thus suggests that six stages are required for this rather simple separation. However, for the situation of total reflux and constant relative volatility α, it is simplest to recognize that

$$Y_n = Y_{n-1}/\alpha \tag{23.5-36a}$$

so that

$$Y_N = Y_1/\alpha^N \tag{23.5-36b}$$

For the situation pictured in Fig. 23.5-6, we have then

$$\log\left(\frac{0.9/0.1}{0.1/0.9}\right) = (N - 1)\ \log\ 2.5 \tag{23.5-37}$$

or

$$N = 1 + \frac{\log\ 81}{\log\ 2.5} = 5.796 \tag{23.5-38}$$

which is more accurate but virtually equal to the graphical estimate.

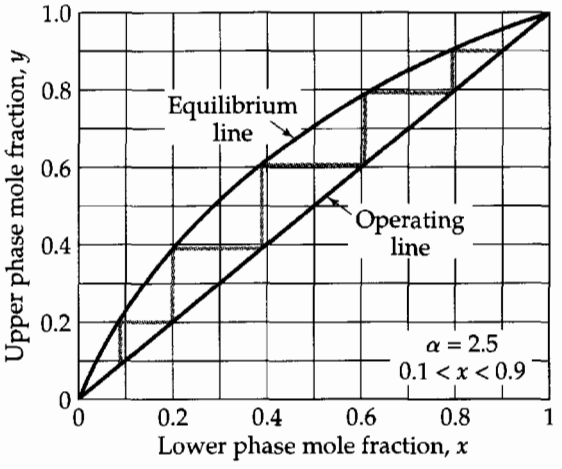

Fig. 23.5-6. McCabe–Thiele diagram for total reflux, with $\alpha = 2.5$ and $0.1 < x < 0.9$.

If products are to be withdrawn, it is necessary to calculate the stream-rate ratios, and the means for doing so vary with the specific operation considered.

(b) ***Thermodynamic constraints: adiabatic cascades and minimum reflux.*** For most of the common stagewise operations, stream ratios are determined by thermodynamic constraints, and these are thoroughly discussed in a wide variety of unit operations texts. We need not repeat this readily accessible information here, but we briefly consider distillation, the most widely used of all, by way of example. In principle, stream ratios in distillation are determined by assuming adiabatic columns and a set of "enthalpy balances" (see last paragraph of §15.1) corresponding to the mass balances just introduced.

However, it is very often permissible to assume equal molar heats of vaporization for the various species and to neglect "sensible heats" (i.e., the $\tilde{C}_p\Delta T$ contributions to $\Delta\tilde{H}$). With these simplifications the stream rates U_n and D_n are constants. We may then write for any position above the feed plate

$$U = D + P \quad \text{and} \quad y_{n-1}U = x_nD + y_PP \tag{23.5-39, 40}$$

and below the feed plate

$$D = U + W \quad \text{and} \quad x_mD = y_{m+1}U + x_WW \tag{23.5-41, 42}$$

Here the stage indices n and m refer respectively to the upper or rectifying section (above the feed point) and to the lower or stripping section of the column (below the feed point).

By way of example we consider the system in part (a) for a saturated liquid feed, equimolar in the two species involved, and operated at minimum reflux: the smallest amount of returning liquid from the top plate that can produce the desired separation. This situation will occur when the operating line touches the equilibrium curve, and in the system being considered, this "pinch" will occur first at the feed plate. The vapor composition on the feed plate is then given by

$$Y_F = 2.5X_F = 2.5 \quad \text{or} \quad y_F = \frac{Y_F}{1 + Y_F} = 0.7143 \tag{23.5-43, 44}$$

The operating line then has two branches, one above and one below the feed plate, as shown in Fig. 23.5-7.

Any real column must operate between the limits of total and minimum reflux, but normal operation is just a few percent above the minimum. This is because the cost of individual plates tends to be much lower than the costs associated with increasing the reflux (the liquid returned to the column by condensation of vapor from the top plate): increasing the steam load required to return vapor from the liquid leaving the bottom plate, the condenser load to return the overhead vapor, and the capital costs of larger column diameter, larger reboiler, to return vapor at the bottom, and condenser, to return liquid at the top.

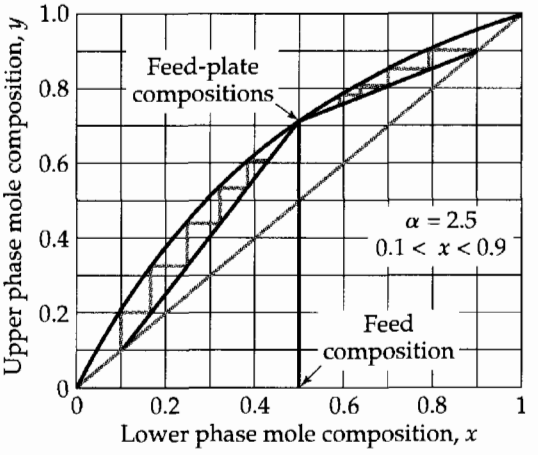

Fig. 23.5-7. McCabe–Thiele diagram for minimum reflux, with $\alpha = 2.5$ and $0.1 < x < 0.9$.

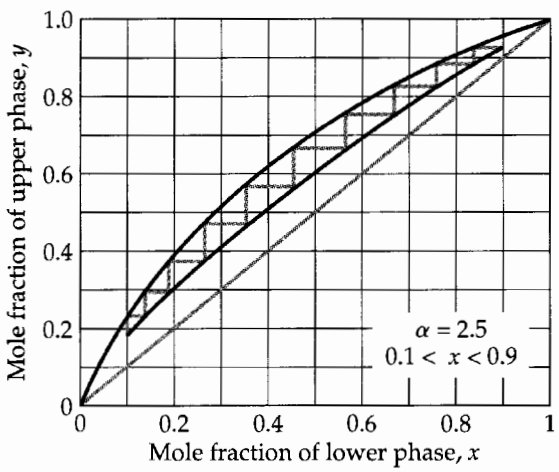

Fig. 23.5-8. McCabe–Thiele diagram for an ideal cascade, with $\alpha = 2.5$ and $0.1 < x < 0.9$.

(c) ***Transport constraints and ideal cascades.*** For separation via selectively permeable membranes, the ratio of the product to waste streams is governed by the pressure exerted across the membrane, and the energy required to produce this pressure must be renewed for every stage of the cascade. This gives the designer an extra degree of freedom and has led to a wide variety of cascade configurations. First developed for isotopes,[5] membrane cascades have now been developed for industrial gas separations[6] and appear promising for many other applications.

We consider here by example *ideal* cascades, which are those in which only streams of identical composition are mixed. In the terms of this example, that means

$$Y_{n+1} = X_{n-1} = \frac{Y_{n-1}}{\alpha} \tag{23.5-45}$$

and, by extension,

$$Y_{n+1} = \frac{Y_n}{\sqrt{\alpha}} \tag{23.5-46}$$

It follows that just twice as many stages are needed as at total reflux, and that the operating line lies halfway between the "equilibrium" curve and the 45° line. As shown in Fig. 23.5-8, the operating line has a continuous derivative across the feed stage.

Ideal cascades provide the smallest possible total stage stream flows, but the flows now vary with position: they are highest at the feed stage and decrease toward the ends of the cascade. For this reason these systems are known as *tapered cascades* (see Problem 23B.6).

EXAMPLE 23.5-4

Expansion of a Reactive Gas Mixture Through a Frictionless Adiabatic Nozzle

An equimolar mixture of CO_2 and H_2 is confined at 1000K and 1.50 atm in the large insulated pressure tank shown in Fig. 15.5-9. Under these conditions the reaction

$$CO_2 + H_2 \Leftrightarrow CO + H_2O \tag{23.5-47}$$

may take place. After being stored in the tank long enough for the reaction to proceed to equilibrium, the gas is allowed to escape through the small converging nozzle shown to the ambient pressure of 1 atm.

---

[5] E. von Halle and J. Schacter, *Diffusion Separation Methods*, in *Kirk-Othmer Encyclopedia of Chemical Technology*, Volume 8, Wiley, New York (1993), pp. 149–203.

[6] R. Agrawal, *Ind. Eng. Chem. Research*, **35**, 3607–3617 (1996); R. Agrawal and J. Xu, *AIChE Journal*, **42**, 2141–2154 (1996).

Estimate the temperature and velocity of the escaping gas through the nozzle throat (*a*) assuming that no appreciable reaction takes place during passage of gas through the nozzle, and (*b*) assuming instant attainment of thermodynamic equilibrium at all points in the nozzle. In each case, assume that the expansion is adiabatic and frictionless.

SOLUTION

We begin by assuming quasi-steady-state operation, flat velocity profiles, and negligible changes in potential energy. We also assume constant heat capacities and ideal gas behavior, and we neglect diffusion in the direction of flow. We may then write the macroscopic energy balance, Eq. 23.3-1, in the form

$$\tfrac{1}{2}v_2^2 = \hat{H}_1 - \hat{H}_2 \tag{23.5-48}$$

Here the subscripts 1 and 2 refer to conditions in the tank and at the nozzle throat, respectively, and, as in Example 15.5-4, the fluid velocity in the tank is assumed to be zero.

To determine the enthalpy change, we equate $d(\frac{1}{2}v^2)$ from the *d*-form of the steady-state energy balance (Eq. 23.3-1) to $d(\frac{1}{2}v^2)$ of the *d*-form of the steady-state mechanical energy balance (Eq. 23.4-1) to get

$$\frac{1}{\rho}dp = d\hat{H} \tag{23.5-49}$$

This result also follows from Eq. E of Table 19.2-4. In addition to Eq. 23.5-49, we use the ideal gas law and an expression for $\hat{H}(T)$, obtained with the help of Table 17.1-1, Eq. 19.3-16, and the relation $\rho\hat{H} = c\tilde{H}$, to get

$$p = cRT = \frac{\rho RT}{M} = \frac{\rho RT}{\sum_{\alpha=1}^{N} x_\alpha M_\alpha} \tag{23.5-50}$$

$$\hat{H} = \frac{\tilde{H}}{\rho/c} = \frac{\sum_{\alpha=1}^{N} x_\alpha \bar{H}_\alpha}{M} = \frac{\sum_{\alpha=1}^{N} x_\alpha[\tilde{H}_\alpha^\circ + \bar{C}_{p\alpha}(T - T^\circ)]}{\sum_{\alpha=1}^{N} x_\alpha M_\alpha} \tag{23.5-51}$$

Here x_α is the mole fraction of the species α at temperature T, and $\tilde{H}_\alpha^\circ$ is the molar enthalpy of species α at the reference temperature T°. The evaluation of $\hat{H}$ is discussed separately for the two approximations.

Approximation (a): Assumption of very slow chemical reaction. Here the x_α are constant at the equilibrium values for 1000K, and we may write Eq. 23.5-51 as

$$d\hat{H} = \left(\frac{\Sigma_\alpha x_\alpha \tilde{C}_{p\alpha}}{\Sigma_\alpha x_\alpha M_\alpha}\right)dT \tag{23.5-52}$$

Hence we may write Eq. 23.5-49 in the form

$$d\ln p = \left(\frac{\Sigma_\alpha x_\alpha \tilde{C}_{p\alpha}}{R}\right)d\ln T \tag{23.5-53}$$

Since x_α and $\tilde{C}_{p\alpha}$ are assumed constant, this equation may be integrated from (p_1, T_1) to (p_2, T_2) to get

$$T_2 = T_1\left(\frac{p_2}{p_1}\right)^{R/\Sigma_\alpha x_\alpha \tilde{C}_{p\alpha}} \tag{23.5-54}$$

We may now combine this expression with Eqs. 23.5-48 and 51 to obtain the desired expression for the gas velocity at plane 2:

$$v_2 = \left\{2T_1\left[1 - \left(\frac{p_2}{p_1}\right)^{R/\Sigma_\alpha x_\alpha \tilde{C}_{p\alpha}}\right]\frac{\Sigma_\alpha x_\alpha \tilde{C}_{p\alpha}}{\Sigma_\alpha x_\alpha M_\alpha}\right\}^{1/2} \tag{23.5-55}$$

By substituting numerical values into Eqs. 23.5-54 and 55, we obtain (see Problem 23A.1) $T_2 = 920\text{K}$ and $v_2 = 1726$ ft/s. It may be seen that this treatment is very similar to that presented in Example 15.5-4. It is also subject to the restriction that the throat velocity must be subsonic; that is, the pressure in the nozzle throat cannot fall below that fraction of p_1 required to produce sonic velocity at the throat (see Eq. 15B.6-2). If the ambient pressure falls below this critical value of p_2, the throat pressure will remain at the critical value, and there will be a shock wave beyond the nozzle exit.

Approximation (b): Assumption of very rapid reaction. We may proceed here as in part ***(a)***, except that the mole fractions x_α must now be considered functions of the temperature defined by the equilibrium relation

$$\frac{(x_{H_2O})(x_{CO})}{(x_{H_2})(x_{CO_2})} = K_x(T) \tag{23.5-56}$$

and the stoichiometric relations

$$x_{H_2O} = x_{CO} \qquad x_{H_2} = x_{CO_2} \qquad \sum_{\alpha=1}^{4} x_\alpha = 1 \tag{23.5-57, 58, 59}$$

The quantity $K_x(T)$ in Eq. 23.5-56 is the known equilibrium constant for the reaction. It may be considered as a function only of temperature, because of the assumed ideal gas behavior and because the number of moles present is not affected by the chemical reaction. Equations 23.5-57 and 58 follow from the stoichiometry of the reaction and the composition of the gas originally placed in the tank.

The expression for the final temperature is now considerably more complicated. For this reaction, where $\Sigma_\alpha x_\alpha M_\alpha$ is constant, Eqs. 23.5-49 and 50 may be combined to give

$$R \ln \frac{p_2}{p_1} = \int_{T_1}^{T_2} \left(\frac{d\tilde{H}}{dT}\right) d \ln T \tag{23.5-60}$$

where, with the heat capacities approximated as constants,

$$\frac{d\tilde{H}}{dT} = \sum_{\alpha=1}^{4} [\tilde{H}_\alpha^\circ + \tilde{C}_{p\alpha}(T - T^\circ)] \frac{dx_\alpha}{dT} + \sum_{\alpha=1}^{4} x_\alpha \tilde{C}_{p\alpha} \tag{23.5-61}$$

In general, the integral in Eq. 23.5-60 must be evaluated numerically, since the x_α and the dx_α/dT are all complicated functions of temperature governed by Eqs. 23.5-56 to 59. Once T_2 has been determined from Eq. 23.5-61, however, v_2 may be obtained by use of Eqs. 23.5-48 and 51. By substituting numerical values into these expressions, we obtain (see Problem 23B.2) $T_2 = 937\text{K}$ and $v_2 = 1752$ ft/s.

We find, then, that both the exit temperature and the velocity from the nozzle are greater when chemical equilibrium is maintained throughout the expansion. The reason for this is that the equilibrium shifts with decreasing temperature in such a way as to release heat of reaction to the system. Such a release of energy will occur with decreasing temperature in any system at chemical equilibrium, regardless of the reactions involved. This is one consequence of the famous rule of Le Châtelier. In this case, the reaction is endothermic as written and the equilibrium constant decreases with falling temperature. As a result, CO and H_2O are partially reconverted to H_2 and CO_2 on expansion, with a corresponding release of energy.

It is interesting that in rocket engines the exhaust velocity, hence the engine thrust, are also increased if rapid equilibration can be obtained, even though the combustion reactions are strongly exothermic. The reason for this is that the equilibrium constants for these reactions increase with falling temperature so that the heat of reaction is again released on expansion. This principle has been suggested as a method for improving the thrust of rocket engines. The increase in thrust potentially obtainable in this way is quite large.

This example was chosen for its simplicity. Note in particular that if a change in the number of moles accompanies the chemical reaction, then the equilibrium constant, and hence the enthalpy, are functions of the pressure. In this case, which is quite common, the variables p

and T implicit in Eq. 23.5-60 cannot be separated, and a step-by-step integration of this equation is required. Such integrations have been performed, for example, for the prediction of the behavior of supersonic wind tunnels and rocket engines, but the calculations involved are too lengthy for presentation here.

§23.6 USE OF THE MACROSCOPIC BALANCES TO SOLVE UNSTEADY-STATE PROBLEMS

In §23.5 the discussion was restricted to steady state. Here we move on to the transient behavior of multicomponent systems. Such behavior is important in a large number of practical operations, such as leaching and drying of solids, chromatographic separations, and chemical reactor operations. In many of these processes heats of reaction as well as mass transfer must be considered. A complete discussion of these topics is outside the scope of this text, and we restrict ourselves to several simple examples. More extensive discussions may be found elsewhere.[1]

EXAMPLE 23.6-1

Start-Up of a Chemical Reactor

It is desired to produce a substance B from a raw material A in a chemical reactor of volume V equipped with a stirrer that is capable of keeping the entire contents of the reactor fairly homogeneous. The formation of B is reversible, and the forward and reverse reactions may be considered first order, with reaction-rate constants k'''_{1B} and k'''_{1A}, respectively. In addition, B undergoes an irreversible first-order decomposition, with a reaction-rate constant k'''_{1C}, to a third component C. The chemical reactions of interest may be represented as

$$A \rightleftarrows B \rightarrow C \tag{23.6-1}$$

At zero time, a solution of A at a concentration c_{A0} is introduced to the initially empty reactor at a constant mass flow rate w.

Develop an expression for the amount of B in the reactor, when it is just filled to its capacity V, assuming that there is no B in the feed solution and neglecting changes of fluid properties.

SOLUTION

We begin by writing the unsteady-state macroscopic mass balances for species A and B. In molar units these may be expressed as

$$\frac{dM_{A,\text{tot}}}{dt} = \frac{wc_{A0}}{\rho} - k'''_{1B}M_{A,\text{tot}} + k'''_{1A}M_{B,\text{tot}} \tag{23.6-2}$$

$$\frac{dM_{B,\text{tot}}}{dt} = -(k'''_{1A} + k'''_{1C})M_{B,\text{tot}} + k'''_{1B}M_{A,\text{tot}} \tag{23.6-3}$$

Next we eliminate $M_{A,\text{tot}}$ from Eq. 23.6-3. First we differentiate this equation with respect to t to get

$$\frac{d^2M_{B,\text{tot}}}{dt^2} = -(k'''_{1A} + k'''_{1C})\frac{dM_{B,\text{tot}}}{dt} + k'''_{1B}\frac{dM_{A,\text{tot}}}{dt} \tag{23.6-4}$$

In this equation, we replace $dM_{A,\text{tot}}/dt$ by the right side of Eq. 23.6-2, and then use Eq. 23.6-3 to eliminate $M_{A,\text{tot}}$. In this way we obtain a linear second-order differential equation for $M_{B,\text{tot}}$ as a function of time:

$$\frac{d^2M_{B,\text{tot}}}{dt^2} + (k'''_{1A} + k'''_{1B} + k'''_{1C})\frac{dM_{B,\text{tot}}}{dt} + k'''_{1B}k'''_{1C}M_{B,\text{tot}} = \frac{k'''_{1B}wc_{A0}}{\rho} \tag{23.6-5}$$

[1] W. R. Marshall, Jr., and R. L. Pigford, *The Application of Differential Equations to Chemical Engineering Problems*, University of Delaware Press, Newark, Del. (1947); B. A. Ogunnaike and W. H. Ray, *Process Dynamics, Modeling, and Control*, Oxford University Press (1994).

This equation is to be solved with the initial conditions

I.C. 1: at $t = 0$, $$M_{B,\text{tot}} = 0 \tag{23.6-6}$$

I.C. 2: at $t = 0$, $$\frac{dM_{B,\text{tot}}}{dt} = 0 \tag{23.6-7}$$

This equation can be integrated to give

$$M_{B,\text{tot}} = \frac{wc_{A0}}{\rho k'''_{1C}} \left(\frac{s_-}{s_+ - s_-} \exp(s_+ t) - \frac{s_+}{s_+ - s_-} \exp(s_- t) + 1 \right) \tag{23.6-8}$$

where

$$2s_\pm = -(k'''_{1A} + k'''_{1B} + k'''_{1C}) \pm \sqrt{(k'''_{1A} + k'''_{1B} + k'''_{1C})^2 - 4\,k'''_{1B}k'''_{1C}} \tag{23.6-9}$$

Equations 23.6-8 and 9 give the total mass of B in the reactor as a function of time, up to the time at which the reactor is completely filled. These expressions are very similar to the equations obtained for the damped manometer in Example 7.7-2 and the temperature controller in Example 15.5-2. It can be shown, however, that s_+ and s_- are both real and negative, and therefore $M_{B,\text{tot}}$ cannot oscillate (see Problem 23B.3).

EXAMPLE 23.6-2

Unsteady Operation of a Packed Column

There are many industrially important processes in which mass transfer takes place between a fluid and a granular porous solid: for example, recovery of organic vapors by adsorption on charcoal, extraction of caffeine from coffee beans, and separation of aromatic and aliphatic hydrocarbons by selective adsorption on silica gel. Ordinarily, the solid is held fixed, as indicated in Fig. 23.6-1, and the fluid is allowed to percolate through it. The operation is thus inherently unsteady, and the solid must be periodically replaced or "regenerated," that is, returned to its original condition by heating or other treatment. To illustrate the behavior of such fixed-bed mass transfer operations, we consider as a physically simple case, the removal of a solute from a solution by passage through an adsorbent bed.

In this operation, a solution containing a single solute A at mole fraction x_{A1} in a solvent B is passed at a constant volumetric flow rate w/ρ through a packed tower. The tower packing consists of a granular solid capable of adsorbing A from the solution. At the start of the

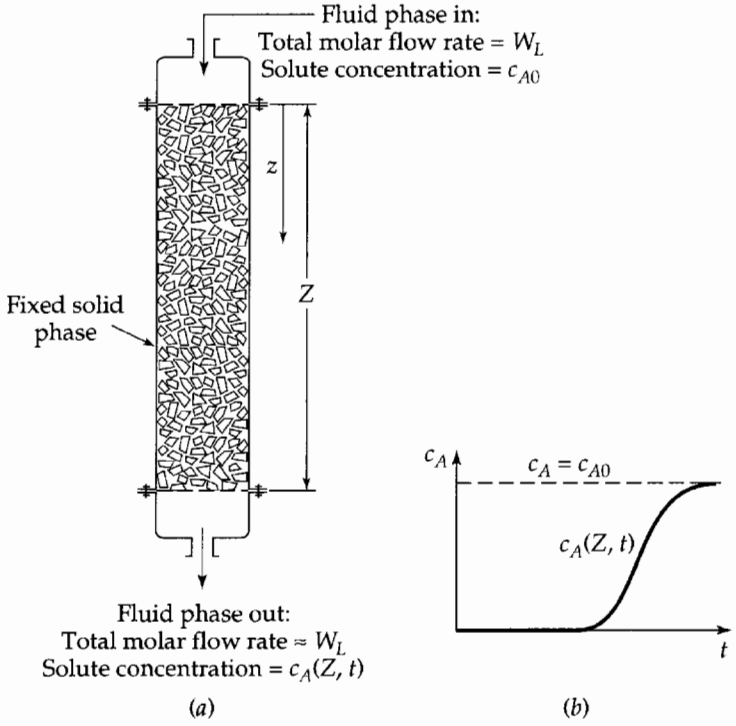

Fig. 23.6-1. A fixed-bed absorber: (*a*) pictorial representation of equipment; (*b*) a typical effluent curve.

percolation, the interstices of the bed are filled with pure liquid B, and the solid is free of A. The percolating fluid displaces this solvent evenly so that the solution concentration of A is always uniform over any cross section. For simplicity, it is assumed that the equilibrium concentration of A adsorbed on the solid is proportional to the local concentration of A in the solution. It is also assumed that the concentration of A in the percolating solution is always small and that the resistance of the porous solid to intraparticle mass transport is negligible.

Develop an expression for the concentration of A in the column as a function of time and of distance down the column.

SOLUTION

Paralleling the treatment of the gas absorber in Example 23.5-2, we think of the two phases as being continuous and existing side by side as pictured in Fig. 23.6-2. We again define the contact area per unit packed volume of column as a. Now, however, one of the phases is stationary, and unsteady-state conditions prevail. Because of this locally unsteady behavior, the macroscopic mass balances are applied locally over a small column increment of height Δz. We may use Eq. 23.1-3 and the assumption of dilute solutions to state that the molar rate of flow of solvent, W_B, is essentially constant over the length of the column and the time of operation. We now proceed to use Eq. 23.1-3 to write the mass conservation relations for species A in each phase for a column increment of height Δz.

For the *solid phase* in this increment of column we may apply Eq. 22.3-3 locally, keeping in mind that now $M_{A,\text{tot}}$ depends on both z and t:

$$\frac{dM_{A,\text{tot}}}{dt} = W_{A0} \tag{23.6-10}$$

or

$$(1 - \varepsilon)S\Delta z \frac{\partial c_{As}}{\partial t} = (k_x^0 a)(x_A - x_{A0})S\Delta z \tag{23.6-11}$$

Here use has been made of Eq. 22.1-14, and the symbols have the following meaning:

ε = volume fraction of column occupied by the liquid

S = cross-sectional area of (empty) column

c_{AS} = moles of adsorbed A per unit volume of the solid phase

x_A = bulk mole fraction of A in the liquid phase

x_{A0} = interfacial mole fraction of A in the fluid phase, assumed to be in equilibrium with c_{As}

k_x^0 = fluid-phase mass transfer coefficient, defined in Eq. 22.1-14, for small mass-transfer rates

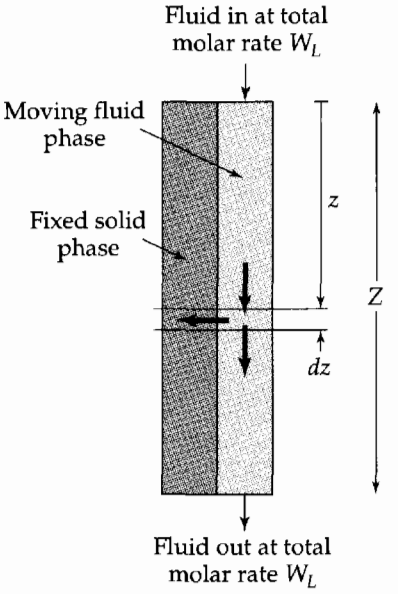

Fig. 23.6-2. Schematic model for a fixed-bed absorber, showing a differential element over which a mass balance is made.

Note that, in writing Eq. 23.6-11, we have neglected convective mass transfer through the solid–fluid interface. This is reasonable if x_{A0} is much smaller than unity. We have also assumed that the particles are small enough so that the concentration of the solution surrounding any given particle is essentially constant over the particle surface.

For the *fluid phase*, in the column increment under consideration, Eq. 23.1-3 becomes

$$\frac{dM_{A,\text{tot}}}{dt} = -\Delta W_A + W_{A0} \tag{23.6-12}$$

or

$$\varepsilon c S \Delta z \frac{\partial x_A}{\partial t} = -W_B \Delta z \frac{\partial x_A}{\partial z} - (k_x^0 a)(x_A - x_{A0}) S \Delta z \tag{23.6-13}$$

Here c is the total molar concentration of the liquid. Equation 23.6-13 may be rewritten by the introduction of a modified time variable, defined by

$$t' = t - \left(\frac{\varepsilon c S}{W_B}\right) z \tag{23.6-14}$$

It may be seen that, for any position in the column, t' is the time measured from the instant that the percolating solvent "front" has reached the position in question. By rewriting Eqs. 23.6-13 and 11 in terms of t', we get

$$\left(\frac{\partial x_A}{\partial z}\right)_{t'} = -\frac{(k_x^0 a) S}{W_B} (x_A - x_{A0}) \tag{23.6-15}$$

$$\left(\frac{\partial c_{As}}{\partial t'}\right)_z = \frac{(k_x^0 a)}{(1 - \varepsilon)} (x_A - x_{A0}) \tag{23.6-16}$$

Equations 23.6-15 and 16 combine the equations of conservation of mass for each phase with the assumed mass transfer rate expression. These two equations are to be solved simultaneously along with the interphase equilibrium distribution, $x_{A0} = mc_{As}$, in which m is a constant. The boundary conditions are

B.C. 1: at $t' = 0$, $\quad c_{As} = 0 \quad$ for all $z > 0$ (23.6-17)

B.C. 2: at $z = 0$, $\quad x_A = x_{A1} \quad$ for all $t' > 0$ (23.6-18)

Before solving these equations, it is convenient to rewrite them in terms of the following dimensionless variables:

$$X(\zeta, \tau) = \frac{x_A}{x_{A1}} \qquad Y(\zeta, \tau) = \frac{mc_{As}}{x_{A1}} \qquad \zeta = \frac{(k_x^0 a) S}{W_B} z \qquad \tau = \frac{(k_x^0 a) m}{(1 - \varepsilon)} t' \tag{23.6-19, 20, 21, 22}$$

In terms of these variables, the differential equations and boundary conditions take the form

$$\frac{\partial X}{\partial \zeta} = -(X - Y); \qquad \frac{\partial Y}{\partial \tau} = +(X - Y) \tag{23.6-23, 24}$$

with the boundary conditions $Y(\zeta, 0) = 0$ and $X(0, \tau) = 1$.

The solution[2] to Eqs. 23.6-23 and 24 for these boundary conditions is

$$X = 1 - \int_0^{\zeta} e^{-(\tau + \bar{\zeta})} J_0(i\sqrt{4\tau\bar{\zeta}}) d\bar{\zeta} \tag{23.6-25}$$

Here $J_0(ix)$ is a zero-order Bessel function of the first kind. This solution is presented graphically in several available references.[3]

---

[2] This result was first obtained by A. Anzelius, *Z. angew. Math. u. Mech.*, **6**, 291–294 (1926), for the analogous problem in heat transfer. One method of obtaining this result is outlined in Problem 23D.1. See also H. Bateman, *Partial Differential Equations of Mathematical Physics*, Dover, New York (1944), pp. 123–125.

[3] See, for example, O. A. Hougen and K. M. Watson, *Chemical Process Principles*, Part III, Wiley, New York (1947), p. 1086. Their y/y_0, $b\tau$, and aZ correspond to our X, τ, and ζ.

EXAMPLE 23.6-3

The Utility of Low-Order Moments

For many complex systems, complete descriptions are either infeasible or unnecessary, and it is sufficient to obtain only a few basic characteristics. Specifically, we may ask how one may determine the system volume V and the volume flow rate Q through it from observations of short tracer pulses of mass m introduced at the inlet and then measured at the outlet. Consider for this purpose the macroscopically steady flow through a closed system of arbitrary geometry, but with a single inlet and outlet, such as that suggested in Fig. 7.0-1, except that there are no moving surfaces. The flow and diffusional behavior are arbitrary, except that the tracer distribution must be described by the diffusion equation (Eq. 19.1-7 with Eq. 17.7-3 inserted for the mass flux)

$$\frac{\partial \rho_T}{\partial t} = -(\nabla \cdot \rho_T \mathbf{v}) + (\nabla \cdot \mathscr{D}_{TS} \nabla \rho_T) \tag{23.6-26}$$

in which ρ_T is the local tracer concentration and $\mathscr{D}_{TS}$ is the pseudobinary diffusivity for the tracer moving through the solution that fills the system. Turbulent systems may be included by using time-smoothed quantities and an effective turbulent diffusivity.

In developing the macroscopic balances we shall need to use the condition that there is no flow or diffusion through the walls of the enclosure

$$(\mathbf{n} \cdot \mathbf{v}) = 0 \quad \text{and} \quad (\mathbf{n} \cdot \nabla \rho_T) = 0 \tag{23.6-27, 28}$$

and that the diffusive flux of the tracer is small compared to the convective flux at the inlet and outlet to the system

$$\mathscr{D}_{TS}(\mathbf{n} \cdot \nabla \rho_T) << \rho_T (\mathbf{n} \cdot \mathbf{v}) \tag{23.6-29}$$

Here $\mathbf{n}$ is the outwardly directed unit normal vector. We take the inlet tracer concentration to be zero up to $t = 0$ and also after some finite time $t = t_0$. In practice the concentration pulse duration should be quite short.

SOLUTION

The analysis[4] is based on the moments $I^{(n)}$ of the tracer concentration with respect to time, defined by:

$$I^{(n)}(\mathbf{r}) = \int_{-\infty}^{-\infty} \rho_T(\mathbf{r}, t) t^n dt \tag{23.6-30}$$

We now multiply Eq. 23.6-26 by t^n and integrate with respect to time over the range of nonzero exit tracer concentration

$$\int_0^\infty \frac{\partial \rho_T}{\partial t} t^n dt + \left(\nabla \cdot \mathbf{v} \int_0^\infty \rho_T t^n dt\right) = \left(\nabla \cdot \mathscr{D}_{TS} \nabla \int_0^\infty \rho_T t^n dt\right) \tag{23.6-31}$$

When the first term is integrated by parts and we make use of the notation introduced in Eq. 23.6-30, we get

$$\begin{cases} -nI^{(n-1)} = -(\nabla \cdot \mathbf{v} I^{(n)}) + (\nabla \cdot \mathscr{D}_{TS} \nabla I^{(n)}) & (n \geq 1) \\ 0 = -(\nabla \cdot \mathbf{v} I^{(n)}) + (\nabla \cdot \mathscr{D}_{TS} \nabla I^{(n)}) & (n = 0) \end{cases} \tag{23.6-32, 33}$$

for all systems that give finite moments. We now have a hierarchy of equations for the $I^{(n)}$ in terms of the lower-order moments, and the structure of these equations is very convenient.

In physical terms, it was first noted by Spalding[5] that Eq. 23.6-32 has the same form as the diffusion equation with chemical reaction, Eq. 19.1-16, but with the concentration replaced by $I^{(n)}$ and the reaction term replaced by $nI^{(n-1)}$. Hence we can integrate these equations over the entire volume of the flow system and thereby develop a new set of macroscopic balances.

---

[4] E. N. Lightfoot, A. M. Lenhoff, and R. I. Rodrigues, *Chem. Eng. Sci.*, **36**, 954–956 (1982).

[5] D. B. Spalding, *Chem. Eng. Sci.*, **9**, 74–77 (1958).

We begin by integrating Eq. 23.6-33, for $n = 0$, over the entire volume of the flow system between planes 1 and 2:

$$0 = -\int_V (\nabla \cdot \mathbf{v}I^{(0)})dV + \int_V (\nabla \cdot \mathscr{D}_{TS}\nabla I^{(0)})dV \tag{23.6-34}$$

The volume integrals may be converted into surface integrals by using the Gauss divergence theorem to get

$$0 = -\int_S (\mathbf{n} \cdot \mathbf{v}I^{(0)})dS + \int_S (\mathbf{n} \cdot \mathscr{D}_{TS}\nabla I^{(0)})dS \tag{23.6-35}$$

where $S = S_f + S_1 + S_2$. The integral over the fixed surface S_f is zero according to Eq. 23.6-27 and 28, and the integrals over the inlet and outlet planes S_1 and S_2 can be simplified, so that we get

$$0 = \int_{S_1} vI^{(0)}dS - \int_{S_2} vI^{(0)}dS \tag{23.6-36}$$

Here we have made use of Eq. 23.6-29 to drop the diffusive terms at planes 1 and 2. If we assume that $I^{(0)}$ is constant over a cross section, we may remove it from the integral, and then we get

$$0 = \langle v_1 \rangle S_1 I_1^{(0)} - \langle v_2 \rangle S_2 I_2^{(0)} \tag{23.6-37}$$

For an incompressible fluid, the volume rate of flow, Q, is constant, so that $\langle v_1 \rangle S_1 = \langle v_2 \rangle S_2$, and

$$I_1^{(0)} = I_2^{(0)} \tag{23.6-38}$$

That is, $I^{(0)}$ evaluated at plane 1 is the same as $I^{(0)}$ at plane 2, and at every point in the system. It is standard notation to abbreviate this quantity as M_0, the zeroth (absolute) moment. Equation 23.6-38 is analogous to Eq. 23.1-2 for a steady-state system with no mass transport across the walls. Next we evaluate $I_1^{(0)}$ for the introduction of a mass m of tracer over a time interval that is very small with respect to the mean tracer residence time $t_{\text{res}} = V/Q$:

$$I_1^{(0)} = \int_0^\infty \rho_T(\mathbf{r}, t)|_{S_1} dt = \left(\frac{Q}{V}\int_0^{Q/V} \rho_T(\mathbf{r}, t)|_{S_1} dt\right)\frac{V}{Q} = \left(\frac{m}{V}\right)\frac{V}{Q} = = \frac{m}{Q} \tag{23.6-39}$$

The replacement, in the second step, of the upper limit by Q/V is permitted by the finite duration of the tracer pulse. From the last two equations we then get

$$Q = \frac{m}{I_2^{(0)}} = \frac{m}{M_0} \tag{23.6-40}$$

This provides the possibility of measuring blood flow rate from the mass of an injected tracer and the value of $I_2^{(0)} = M_0$. The latter can be obtained by means of a catheter inserted into the blood vessel or by NMR techniques.

This simple formula[6] was first introduced in 1829 and has been extensively used since 1897 for measurement of blood-flow rates,[7] including cardiac output.[8] It is also widely used for many environmental systems, such as rivers, and also for systems in the process industries.

Next we turn to Eq. 23.6-32, and integrate it over the volume of the flow system, once again making use of the fact that the diffusive term over the inlet and outlet is much smaller than the convective term. This gives

$$-n\int_V I^{(n-1)}(\mathbf{r}, t)dV = -\int_V (\nabla \cdot \mathbf{v}I^{(n)})\, dV \tag{23.6-41}$$

---

[6] E. Hering, *Zeits. f. Physik*, **3**, 85–126 (1829).

[7] G. N. Stewart, *J. Physiol.* (London), **22**, 159–183 (1897).

[8] K. Zierler, *Ann. Biomed. Eng.*, **28**, 836–848 (2000).

or, if $I^{(n)}$ is assumed constant over a cross-section,

$$-n\left(\frac{1}{V}\int_V I^{(n-1)}(\mathbf{r}, t)dV\right) = \frac{1}{V}\left(\langle v_1\rangle S_1 I_1^{(n)} - \langle v_2\rangle S_2 I_2^{(n)}\right) \tag{23.6-42}$$

Then, defining the quantity in parentheses on the left side as the volume average, we get finally[3]

$$-n[I^{(n-1)}]_{\text{vol avg}} = \frac{Q}{V}\left(I_1^{(n)} - I_2^{(n)}\right) \tag{23.6-43}$$

Now, if we set $n = 1$, we get the following:

$$-I^{(0)} = \frac{Q}{V}\left(I_1^{(1)} - I_2^{(1)}\right) = \frac{1}{t_{\text{res}}}\left(I_1^{(1)} - I_2^{(1)}\right) \tag{23.6-44}$$

If the tracer is injected as a *delta-function input*, so that $I_1^{(1)} = 0$, we can use the notation $I_2^{(1)} = M_1$ (the first moment), and the last equation becomes

$$\frac{I_2^{(1)}}{I^{(0)}} = t_{\text{res}} \quad \text{or} \quad \frac{M_1}{M_0} = t_{\text{res}} \tag{23.6-45}$$

This result, used in conjunction with Eq. 23.6-40, has long been applied by cardiologists for determining blood volume. It has since found many other environmental and process-industry calculations.

Higher moments have also proven useful, in particular the central moments

$$\mu_n = \int_{-\infty}^{\infty} \rho_T(t - t_{\text{res}})^n dt \tag{23.6-46}$$

These are commonly applied for the special case of an impulsive tracer input. Then the normalized second central moment, or variance, is

$$\sigma^2 = \frac{\mu_2}{M_0^2} \tag{23.6-47}$$

This is the square of the standard deviation, when the exit tracer profile is a Gaussian distribution. The third central moment is a measure of the asymmetry about t_{res}, and the fourth a measure of the kurtosis. In practice, the fourth moment is nearly impossible to determine accurately from experimental data, and obtaining even the third proves to be quite difficult.

Use of the second moment has found some very important applications in studying tracer dynamics of biological tissue,[9] and again the large literature in the medical field has been extended to many other applications. It is also interesting to note the additivity relationships in serially connected systems. Thus M_0 is invariant to the number of included subsystems, and M_1, μ_2, and μ_3 are additive, but higher-order moments are not.

QUESTIONS FOR DISCUSSION

1. How are the macroscopic balances for multicomponent mixtures derived? How are they related to the equations of change?
2. In Eq. 23.1-1, how are homogeneous and heterogeneous reactions accounted for? What is the physical meaning of $w_{\alpha 0}$?
3. Give a specific example of a system in which the last term in Eq. 23.1-4 is zero.
4. In using Table 23.5-1 one normally specifies the directions of the streams (that is, whether they are input or output streams). How could one proceed if the flow directions change with time?

[9] F. Chinard, *Ann. Biomed Eng.*, **28**, 849–859 (2000).

5. Summarize the calculation procedures for the enthalpy per unit mass, $\hat{H} = \hat{U} + p\hat{V}$, in Eq. 23.3-1 and the partial molar enthalpy in Eq. 23.3-1a. What are these quantities for ideal gas mixtures?
6. Review the derivation of the mechanical energy balance in §7.8. What would have to be changed in that derivation, if one wishes to apply it to a nonisothermal, reacting mixture in a flow system with no mass transfer surfaces?
7. To what extent does this chapter provide the background for studying unit operations, such as absorption, extraction, distillation, and crystallization?
8. What changes would have to be made in this chapter to describe processes in a space ship or on the surface of the moon?

PROBLEMS

23A.1. Expansion of a gas mixture: very slow reaction rate. Estimate the temperature and velocity of the water–gas mixture at the discharge end of the nozzle in Example 23.5-4 if the reaction rate is very slow. Use the following data: $\log_{10} K_x = -0.15$, $\tilde{C}_{p,H_2} = 7.217$, $\tilde{C}_{p,CO_2} = 12.995$, $\tilde{C}_{p,H_2O} = 9.861$, $\tilde{C}_{p,CO} = 7.932$ (all heat capacities are in Btu/lb-mole · F. Is the nozzle exit pressure equal to the ambient pressure?

Answers: 920K, 1726 ft/s; yes, the nozzle flow is subsonic.

23A.2. Height of a packed-tower absorber. A packed tower of the type described in Example 23.5-2 is to be used for removing 90% of the cyclohexane from a cyclohexane–air mixture by absorption into a nonvolatile light oil. The gas stream enters the bottom of the tower at a volumetric rate of 363 ft^3/min, at 30°C, and at 1.05 atm pressure. It contains 1% cyclohexane by volume. The oil enters the top of the tower at a rate of 20 lb-mol/hr, also at 30°C, and it contains 0.3% cyclohexane on a molar basis. The vapor pressure of cyclohexane at 30°C is 121 mm Hg, and solutions of it in the oil may be considered to follow Raoult's law.

(a) Construct the operating line for the column.

(b) Construct an equilibrium curve for the range of operation encountered here. Assume the operation to be isothermal and isobaric.

(c) Determine the interfacial conditions at each end of the column.

(d) Determine the required tower height using Eq. 23.5-24 if $k_x^0a = 0.32$ moles/hr · ft^3, $k_y^0a = 14.2$ moles/hr · ft^3, and the tower cross section S is 2.00 ft^2.

(e) Repeat part (d), using Eq. 23.5-25.

Answer: **(d)** ca. 62 ft; **(e)** 60 ft

23B.1. Effective average driving forces in a gas absorber. Consider a packed-tower gas absorber of the type discussed in Example 23.5-2. Assume that the solute concentration is always low and that the equilibrium and operating lines are both very nearly straight. Under these conditions, both k_y^0a and k_x^0a may be considered constant over the mass-transfer surface.

(a) Show that $(Y_A - Y_{Ae})$ varies linearly with Y_A. Note that Y_A is the bulk mole ratio of A in the gas phase and Y_{Ae} is the equilibrium gas-phase mole ratio over a liquid of bulk composition X_A (see Fig. 22.4-2).

(b) Repeat part (a) for $(Y_A - Y_{A0})$.

(c) Use the results of parts (a) and (b) to show that

$$W_{Ag,0} = (k_y^0a)ZS(Y_{A0} - Y_A)_{\ln} \tag{23B.1-1}$$

$$W_{Ag,0} = (K_y^0a)ZS(Y_{Ae} - Y_A)_{\ln} \tag{23B.1-2}$$

The overall mass transfer coefficient K_y^0 is defined by Eq. 22.4-4. Note that this part of the problem may be solved by analogy with the development in Example 15.4-1.

23B.2. Expansion of a gas mixture: very fast reaction rate. Estimate the temperature and velocity of the water–gas mixture at the discharge end of the nozzle in Example 23.5-4 if the reaction rate may be considered infinitely fast. Use the data supplied in Problem 23A.1 as well as the following: at 900K, $\log_{10} K_x = -0.34$; $\tilde{H}_{H_2} = +6340$; $\tilde{H}_{H_2O}(g) = -49{,}378$; $\tilde{H}_{CO} = -16{,}636$;

$\tilde{H}_{CO_2} = -83{,}242$ (all enthalpies are given in cal/g-mole). For simplicity, neglect the effect of temperature on heat capacity, and assume that $\log_{10} K_x$ varies linearly with temperature between 900 and 1000K. The following simplified procedure is recommended:

(a) It may be seen in advance that T_2 will be higher than for slow reaction rates, and hence greater than 920K (see Problem 23A.1). Show that, over the temperature range to be encountered, $\tilde{H}$ varies very nearly linearly with the temperature according to the expression $(d\tilde{H}/dT)_{avg} \approx 12.40$ cal/gm-mol·K.

(b) Substitute the result in (a) into Eq. 23.5-41 to show that $T_2 \approx 937$K.

(c) Calculate $\tilde{H}_1$ and $\tilde{H}_2$, and show by use of Eq. 23.5-29 that $v_2 = 1750$ ft/s.

23B.3. Startup of a chemical reactor.

(a) Integrate Eq. 23.6-5 along with the given initial conditions to show that Eq. 23.6-8 correctly describes $M_{B,tot}$ as a function of time.

(b) Show that s_+ and s_- in Eq. 23.6-9 are real and negative. *Hint:* Show that

$$(k'''_{1A} + k'''_{1B} + k'''_{1C})^2 - 4\,k'''_{1B}k'''_{1C} = (k'''_{1A} - k'''_{1B} + k'''_{1C})^2 + 4k'''_{1A}k'''_{1B} \tag{23B.3-1}$$

(c) Obtain expressions for $M_{A,tot}$ and $M_{C,tot}$ as functions of time.

23B.4. Irreversible first-order reaction in a continuous reactor. A well-stirred reactor of volume V is initially completely filled with a solution of solute A in a solvent S at concentration c_{A0}. At time $t = 0$, an identical solution of A in S is introduced at a constant mass flow rate w. A small constant stream of dissolved catalyst is introduced at the same time, causing A to disappear according to an irreversible first-order reaction with rate constant k'''_1 sec^{-1}. The rate constant may be assumed independent of composition and time. Show that the concentration of A in the reactor (assumed isothermal) at any time is

$$\frac{c_A}{c_{A0}} = \left(1 - \frac{wt_0}{\rho V}\right)e^{-t/t_0} + \frac{wt_0}{\rho V} \tag{23B.4-1}$$

in which $t_0^{-1} = [(w/\rho V) + k'''_1]$.

23B.5. Mass and enthalpy balances in an adiabatic splitter. One hundred pounds of 40% by mass of superheated aqueous ammonia with a specific enthalpy of 420 Btu/lb is to be flashed adiabatically to a pressure of 10 atm. Calculate the compositions and masses of the liquid and vapor produced. For the purposes of this problem you may assume that at thermodynamic equilibrium

$$\log_{10} Y_{NH_3} = 1.4 + 1.53 \log_{10} X_{NH_3} \tag{23B.5-1}$$

where Y_{NH_3} and X_{NH_3} are the *mass* ratios of ammonia to water. The enthalpies of saturated liquid and vapor at 10 atm may be assumed to be

$$\hat{H} = 1210 - 465y_{NH_3} - 115y_{NH_3}^{12} \tag{23B.5-2}$$

Btu/lb of saturated vapor, and

$$\hat{h} = 330 - 950x_{NH_3} + 740x_{NH_3}^2 \tag{23B.5-3}$$

Btu/lb of saturated liquid. Here x_{NH_3} and y_{NH_3} are *mass* fractions of ammonia.

Answer: $P = 36.5$ lbs, $y_P = 0.713$, $\hat{H}_p = 877$ Btu/lb$_m$; $W = 63.6$ lb$_m$, $x_W = 0.22$, $\hat{h}_W = 157$ Btu/lb$_m$

23B.6. Flow distribution in an ideal cascade. Determine the upflowing and downflowing stream flows of individual stages for the ideal cascade described in Example 23.5-3. Express your results as fractions of the feed rate, and start from the bottom of the cascade. Use 12 stages as the closest integer providing the desired separation. It is suggested that you begin by calculating the upflowing and downflowing stream compositions and then use the mass balances

$$D_{n-1} = U_n + W; \qquad x_{n-1}D_{n-1} = y_nU_n + x_WW \tag{23B.6-1}$$

below the feed plate and the corresponding balances above it. Use 10 stages with the bottoms (W) composition equal to a mole fraction of 0.1.

23B.7. Isotope separation and the value function. You wish to compare an existing isotope fractionator that processes 50 moles/hr of a feed containing 1.0 mole% of the desired isotope to a product of 90% purity and a waste of 10% with another that processes 50 moles/hr of 10 mole% material to product and waste of 95% and 2%, respectively. Which fractionation is more effective? Assume the Dirac separative capacity to be an accurate measure of effectiveness.

23C.1. Irreversible second-order reaction in an agitated tank. Consider a system similar to that discussed in Problem 23B.4, except that the solute disappears according to a second-order reaction; that is, $R_{A,\text{tot}} = -k_2''' V c_A^2$. Develop an expression for c_A as a function of time by the following method:

(a) Use a macroscopic mass balance for the tank to obtain a differential equation describing the evolution of c_A with time.

(b) Rewrite the differential equation and the accompanying initial condition in terms of the variable

$$u = c_A + \frac{w}{2\rho V k_2'''}\left(1 + \sqrt{1 + \frac{4\rho V k_2''' c_{A0}}{w}}\right) \tag{23C.1-1}$$

The nonlinear differential equation obtained in this way is a *Bernoulli differential equation.*

(c) Now put $v = 1/u$ and perform the integration. Then rewrite the result in terms of the original variable c_A.

23C.2. Protein purification (Fig. 23C.2). It is desired to purify a binary protein mixture using an ideal cascade of individual ultrafiltration stages of the type shown in the figure. The larger of the two membrane units is the source of separation and each protein flux across the membrane is expressed by

$$N_i = c_i v S_i \tag{23C.2-1}$$

where N_i is the transmembrane protein flux of species i, c_i is its concentration in the upstream solution (assumed to be well mixed), v is the transmembrane superficial velocity, and S_i is a protein-specific *sieving factor*. The smaller membrane unit is used solely to maintain a solvent balance and can be ignored for the purposes of this problem.

(a) Show that the enrichment of protein 1 relative to 2 is given by

$$Y_1 = \alpha_{12} X_1 \tag{23C.2-2}$$

where Y_1 and X_1 are the mole ratios of protein 1 to protein 2 in the product and waste streams, respectively, and $\alpha_{12} = S_1/S_2$.

(b) Determine the number of stages required in an ideal cascade to produce 99% pure protein 1 from a 90% feed in 95% yield as a function of α_{12}. It is suggested that α_{12} be varied from 2 to 200.

(c) Calculate the output concentrations, yield, and stream flow rates for a three-stage cascade, with $\alpha_{12} = 40$, and with a feed of 90% purity to the middle stage.

(d) Compare the Dirac separative capacity of this three-stage cascade with that of a single unit with the same molar ratio of product to feed.

23C.3. Physical significance of the zeroth and first moments. Consider some simple flow systems, such as plug flow and well-stirred vessels, individually and in series or parallel arrangements. Show that flow rates and volumes can be obtained from the moments defined in Example 23.6-3.

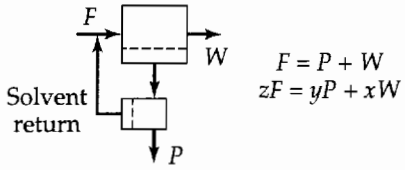

Fig. 23C.2. A membrane-based binary splitter.

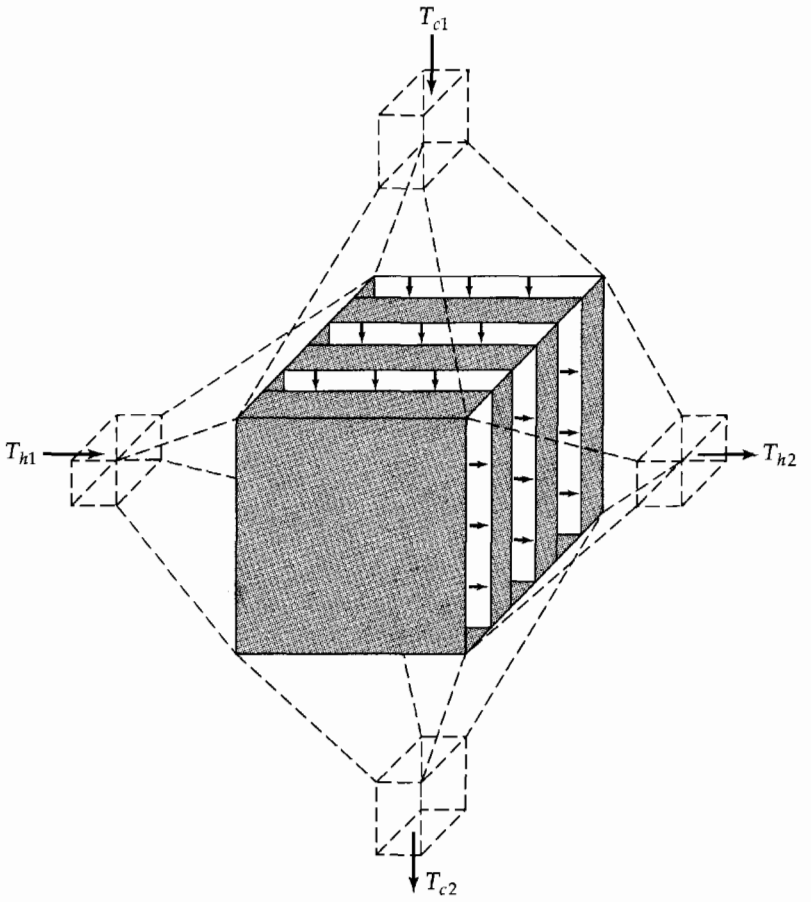

Fig. 23C.4. A schematic representation of a "sandwich-type" cross-flow heat exchanger.

23C.4. Analogy between the unsteady operation of an adsorption column and a cross-flow heat exchanger[1] (Fig. 23C.4). In the heat exchanger shown in the figure, the two fluid streams flow at right angles to one another, and the heat flux parallel to the wall is neglected. Here exchange of heat is clearly less than for a countercurrent exchanger of the same surface and overall heat transfer coefficient under otherwise identical conditions. The heat flow in these exchangers may be expressed for constant U_{loc} as

$$Q = U_{\text{loc}} A \Delta T_{\text{ln}} Y \tag{23C.4-1}$$

Here Q is the total rate of heat transfer, A is the heat transfer surface area, and ΔT_{ln} is the logarithmic mean of $(T_{h1} - T_{c1})$ and $(T_{h1} - T_{c1})$, as defined in the figure. Note that T_{h2} and T_{c2} are the flow-averaged temperatures of the two exit streams. We may then regard Y as the ratio of heat transferred in cross flow to that which would be transferred in counterflow.

Use Eq. 23.6-27 to write an expression for Y as a function of the stream rates, physical properties, heat transfer area, and local overall heat transfer coefficient. Express the result in terms of definite integrals, and assume $\hat{C}_{ph}$, $\hat{C}_{pc}$, and U_{loc} to be constant.

23D.1. Unsteady-state operation of a packed column. Show that Eq. 23.6-25 is a valid solution of Eqs. 23.6-23 and 24. The following approach is recommended:

(a) Take the Laplace transform of Eqs. 23.6-23 and 24 with respect to τ. Eliminate the transform of Y from the resulting expressions. Show that the transform of X may be written for the given boundary conditions as

$$\overline{X} = \frac{1}{s} e^{-[s/(s+1)]\zeta} \tag{23D.1-1}$$

in which $\overline{X}$ is the Laplace transform of X.

---

[1] W. Nusselt, *Tech. Math. Therm.*, **1**, 417 (1930); D. M. Smith, *Engineering*, **138**, 479 (1934).

(b) Rewrite this expression in the form

$$\overline{X} = \frac{1}{s} - \int_0^{\zeta} e^{-\bar{\zeta}} \left(\frac{1}{s+1} \right) e^{[\bar{\zeta}/(s+1)]} d\bar{\zeta} \tag{23D.1-2}$$

Invert this expression to obtain Eq. 23.6-25 by making use of the identity

$$\mathcal{L}\{e^{a\tau} F(\tau)\} = \overline{F}(s-a) \tag{23D.1-3}$$

where $\mathcal{L}\{F(\tau)\} = \overline{F}(s)$.

23D.2. Additivity of the lower moments. Consider a pair of flow systems meeting the requirements of Example 23.6-3 arranged in series. Show that (i) the zeroth moment is the same at the system inlets and outlets of the first and second systems, and (ii) the first absolute moment and the second and third central moments, but not the fourth central moment, are additive. *Suggestion:* For the second and higher moments it is helpful to recognize that the output from the second unit, following a pulse input to the first may be obtained by the use of the convolution integral

$$c(t) = \int_0^t h_1(t-\tau) h_2(\tau) d\tau \equiv h_1 * h_2 \tag{23D.2-1}$$

where h is a system response to a pulse input. A simple way of proceeding is to recognize that the Laplace transform of $c(t)$ may be written as

$$\mathcal{L}\{c(t)\} \equiv F(s) = h_1(s) h_2(s) \tag{23D.2-2}$$

It then follows that

$$F'(s) = h_1'(s) h_2(s) + h_1(s) h_2'(s) \tag{23D.2-3}$$

and similarly for the higher derivatives. Now it may also be shown that

$$M_0 = F(0); \qquad M_1 = -\frac{F'(0)}{F(0)} \tag{23D.2-4, 5}$$

$$\mu_2 = \frac{F''(0)}{F(0)} - \frac{[F'(0)]^2}{[F(0)]^2} \tag{23D.2-6}$$

$$\mu_3 = -\frac{F'''(0)}{F(0)} + 3\frac{F'(0)F''(0)}{[F(0)]^2} - 2\frac{[F'(0)]^3}{[F(0)]^3} \tag{23D.2-7}$$

$$\mu_4 = \frac{F^{(iv)}(0)}{F(0)} - 4\frac{F'(0)F'''(0)}{[F(0)]^2} + 6\frac{F''(0)[F'(0)]^2}{[F(0)]^3} - 3\frac{[F'(0)]^4}{[F(0)]^4} \tag{23D.2-8}$$

23D.3. Start-up of a chemical reactor. Rework Example 23.6-1 by use of Laplace transforms of Eqs. 23.6-2 and 3.

23D.4. Transient behavior of N reactors in series.[2] There are N identical chemical reactors of volume V connected in series, each equipped with a perfect stirrer. Initially, each tank is filled with pure solvent S. At zero time, a solution of A in S is introduced to the first tank at a constant volumetric flow rate Q and a constant concentration $c_A(0)$. This solution also contains a small amount of a dissolved catalyst, introduced just prior to discharge into the first tank, which causes the following first-order reactions to occur:

$$A \underset{k'''_{1BA}}{\overset{k'''_{1AB}}{\rightleftharpoons}} B \underset{k'''_{1CB}}{\overset{k'''_{1BC}}{\rightleftharpoons}} C \tag{23D.4-1}$$

The rate constants in these reactions are assumed constant throughout the system. Let $h = Q/V$, the inverse of the "effective residence time" in each tank. Obtain an expression for $c_\alpha(n)$, the concentration of chemical species α in the nth tank at any time t.

---

[2] A. Acrivos and N. R. Amundson, *Ind. Eng. Chem.*, **47**, 1533–1541 (1955).

Chapter 24

Other Mechanisms for Mass Transport

In Chapter 1 we stated that the molecular transport of momentum is related to the velocity gradient by Newton's law of viscosity. In Chapter 8 we gave Fourier's law, which says that molecular heat transport occurs because of a gradient in temperature. However, when we discussed mixtures in Chapter 19, we pointed out an extra contribution to the molecular heat flux that accounts for the amount of enthalpy transported by the interdiffusion of the various species. In Chapter 17 we gave Fick's (first) law of diffusion, which says that molecular mass transport occurs as the result of a concentration gradient. We indicated there that other driving forces may contribute to the mass flux. The purposes of this chapter are to describe the most important of these additional driving forces and to illustrate some applications.

Important among these forces are the gradients of electrical potential and pressure, which govern the behavior of ionic systems and permselective membranes as well as ultracentrifuges. *Electrokinetic* phenomena in particular are rapidly gaining in importance. Induced dipoles can produce separations, such as *dielectrophoresis* and *magnetophoresis*, which are useful in specialized applications. In addition, we shall find that temperature gradients can cause mass fluxes by a process known as *thermal diffusion*[1] or the *Soret effect*, and that concentration gradients can produce heat transfer by the *diffusion-thermo*,[2] or the *Dufour*, effect. Finally, it is important to realize that in systems containing three or more components, the behavior of any one species is influenced by the concentration gradients of all other species present.

Fortunately the wide range of behavior resulting from these various driving forces can be described compactly via the framework provided by nonequilibrium thermody-

[1] The effect was first observed in liquids by C. Ludwig, *Sitzber. Akad. Wiss. Wien* **20**, 539 (1856), but is named after Ch. Soret, *Arch. Sci. Phys. Nat., Genève*, **2**, 48–61 (1879); **4**, 209–213 (1880); *Comptes Rendus Acad. Sci., Paris*, **91**, 289–291 (1880). The first observations in gases were made by S. Chapman and F. W. Dootson, *Phil. Mag.*, **33**, 248–253 (1917).

[2] L. Dufour, *Arch. Sci. Phys. Nat. Genève*, **45**, 9–12 (1872); *Ann. Phys.* (5) **28**, 490–492 (1873).

namics;[3] this topic is summarized in §§24.1 and 2. This discussion concludes with the generalized Maxwell–Stefan equations. In the remaining sections we show how various specializations of these equations can be used to provide convenient descriptions of selected diffusional processes.

Those who do not wish to read the first two sections can go directly to the later sections, where the essential results of nonequilibrium thermodynamics are summarized.

§24.1 THE EQUATION OF CHANGE FOR ENTROPY

Nonequilibrium thermodynamics makes use of four postulates above and beyond those of equilibrium thermodynamics:[1]

1. The equilibrium thermodynamic relations apply to systems that are not in equilibrium, provided that the gradients are not too large (*quasi-equilibrium postulate*).
2. All fluxes in the system may be written as linear relations involving all the forces (*linearity postulate*).
3. No coupling of fluxes and forces occurs if the difference in tensorial order of the flux and force is an odd number (*Curie's postulate*).[2]
4. In the absence of magnetic fields the matrix of the coefficients in the flux–force relations is symmetric (*Onsager's reciprocal relations*).[3]

In this and the following section we will use these postulates, which arose from a need to describe various observed phenomena and also from kinetic theory developments. Note that the nonequilibrium theory we are using excludes consideration of non-Newtonian fluids.[4]

In Problem 11D.1 we saw how to derive Jaumann's entropy balance equation,

$$\boxed{\rho \frac{D\hat{S}}{Dt} = -(\nabla \cdot \mathbf{s}) + g_S} \tag{24.1-1}$$

in which $\hat{S}$ is the entropy per unit mass of a multicomponent fluid, $\mathbf{s}$ is the entropy-flux vector, and g_S is the rate of entropy production per unit volume. At this point we do not know what $\mathbf{s}$ and g_S are, and hence our first task is to find expressions for these quantities

---

[3] The discussion here is for multicomponent systems. A discussion for binary systems can be found in L. Landau and E. M. Lifshitz, *Fluid Mechanics*, 2nd edition, Pergamon Press (1987), Chapter VI. See also R. B. Bird, *Korean J. Chem. Eng.*, **15**, 105–123 (1998).

[1] S. R. de Groot and P. Mazur, *Non-Equilibrium Thermodynamics*, North-Holland, Amsterdam (1962). See also H. B. Callen, *Thermodynamics and an Introduction to Thermostatistics*, Wiley, New York (1985), Chapter 14.

[2] P. Curie, *Oeuvres*, Paris (1903), p. 129.

[3] Nobel laureate **Lars Onsager** (1903–1976) studied chemical engineering at the Technical University of Trondheim; after working with Peter Debye in Zürich for two years, he held teaching positions at several universities before moving on to Yale University. His contributions to the thermodynamics of irreversible processes are to be found in L. Onsager, *Phys. Rev.*, **37**, 405–426 (1931); **38**, 2265–2279 (1931). A summary of experimental verifications of the Onsager reciprocal relations has been given by D. G. Miller, in *Transport Phenomena in Fluids* (H. J. M. Hanley, ed.), Marcel Dekker, New York (1969), Chapter 11.

[4] To describe nonlinear viscoelastic fluids one has to generalize the thermodynamic theory, as described in A. N. Beris and B. J. Edwards, *Thermodynamics of Flowing Systems with Internal Microstructure*, Oxford University Press (1994); M. Grmela and H. C. Öttinger, *Phys. Rev.*, **E56**, 6620–6632 (1997); H. C. Öttinger and M. Grmela, *Phys. Rev.*, **E56**, 6633–6655 (1997); B. J. Edwards, H. C. Öttinger, and R. J. J. Jongschaap, *J. Non-Equilibrium Thermodynamics*, **27**, 356–373 (1997); H. C. Öttinger, *Phys. Rev.*, **E57**, 1416–1420 (1998); H. C. Öttinger, *Applied Rheology*, **9**, 17–26 (1999).

in terms of the fluxes and gradients in the system. To do this we have to use the assumption that the equations of equilibrium thermodynamics are valid locally (the "quasi-equilibrium postulate"), which means that equations such as

$$d\hat{U} = Td\hat{S} - pd\hat{V} + \sum_{\alpha=1}^{N} \frac{\overline{G}_\alpha}{M_\alpha} d\omega_\alpha \tag{24.1-2}$$

can be used in a system that is not too far from equilibrium. In this equation $\overline{G}_\alpha$ is the partial molar Gibbs free energy and M_α the molecular weight of species α. We now apply this relation to a fluid element moving with the mass average velocity $\mathbf{v}$. Then we can replace the differential operators by substantial derivative operators. In that form, Eq. 24.1-2 enables us to express $D\hat{S}/Dt$ in terms of $D\hat{U}/Dt$, $D(1/\rho)/Dt$, and $D\omega_\alpha/Dt$. Then the equation of change for internal energy [Eq. (D) of Table 19.2-4], the overall equation of continuity [Eq. (A) of Table 19.2-3], and the equation of continuity for species α [Eq. (B) of Table 19.2-3] can be used for the three substantial derivatives that have been introduced. Thus, after considerable rearranging, we find

$$\mathbf{s} = \frac{1}{T}\left(\mathbf{q} - \sum_{\alpha=1}^{N} \frac{\overline{G}_\alpha}{M_\alpha}\mathbf{j}_\alpha\right) \tag{24.1-3}$$

$$g_S = -\left(\mathbf{q}\cdot\frac{1}{T^2}\nabla T\right) - \sum_{\alpha=1}^{N}\left(\mathbf{j}_\alpha\cdot\left[\nabla\left(\frac{1}{T}\frac{\overline{G}_\alpha}{M_\alpha}\right) - \frac{1}{T}\mathbf{g}_\alpha\right]\right) - \left(\boldsymbol{\tau}:\frac{1}{T}\nabla\mathbf{v}\right) - \sum_{\alpha=1}^{N}\frac{1}{T}\frac{\overline{G}_\alpha}{M_\alpha}r_\alpha \tag{24.1-4}$$

The entropy production has been written as a sum of products of fluxes and forces. However, there are only $N-1$ independent mass fluxes $\mathbf{j}_\alpha$, and, because of the Gibbs-Duhem equation, there are also only $N-1$ independent forces. When we take into account this lack of independence,[5] we may rewrite the entropy flux and the entropy production in the following form:

$$\boxed{\mathbf{s} = \frac{1}{T}\mathbf{q}^{(h)} + \sum_{\alpha=1}^{N}\frac{\overline{S}_\alpha}{M_\alpha}\mathbf{j}_\alpha} \tag{24.1-5}$$

$$\boxed{Tg_S = -(\mathbf{q}^{(h)}\cdot\nabla\ln T) - \sum_{\alpha=1}^{N}\left(\mathbf{j}_\alpha\cdot\frac{cRT}{\rho_\alpha}\mathbf{d}_\alpha\right) - (\boldsymbol{\tau}:\nabla\mathbf{v}) - \sum_{\alpha=1}^{N}\frac{\overline{G}_\alpha}{M_\alpha}r_\alpha} \tag{24.1-6}$$

in which $\mathbf{q}^{(h)}$ is the heat flux with the diffusional enthalpy flux subtracted off,

$$\mathbf{q}^{(h)} = \mathbf{q} - \sum_{\alpha=1}^{N}\frac{\overline{H}_\alpha}{M_\alpha}\mathbf{j}_\alpha \tag{24.1-7}$$

and

$$\begin{aligned} cRT\mathbf{d}_\alpha &= c_\alpha T\nabla\left(\frac{\overline{G}_\alpha}{T}\right) + c_\alpha\overline{H}_\alpha\nabla\ln T - \omega_\alpha\nabla p - \rho_\alpha\mathbf{g}_\alpha + \omega_\alpha\sum_{\beta=1}^{N}\rho_\beta\mathbf{g}_\beta \\ &= c_\alpha RT\nabla\ln a_\alpha + (\phi_\alpha - \omega_\alpha)\nabla p - \rho_\alpha\mathbf{g}_\alpha + \omega_\alpha\sum_{\beta=1}^{N}\rho_\beta\mathbf{g}_\beta \end{aligned} \tag{24.1-8}$$

The second form in Eq. 24.1-8 is obtained[5] by using the relation $d\overline{G}_\alpha = RTd\ln a_\alpha$, where a_α is the activity. In the operation $\nabla\ln a_\alpha$, the derivative is to be taken at constant T and p, and the quantity $\phi_\alpha = c_\alpha\overline{V}_\alpha$ is the volume fraction of species α. The $\mathbf{d}_\alpha$ introduced here are called *diffusional driving forces*, and they account for the *concentration diffusion* (term

[5] For the intermediate steps, see C. F. Curtiss and R. B. Bird, *Ind. Eng. Chem. Research*, **38**, 2515–2522 (1999), errata **40**, 1791 (2001).

with $\nabla \ln a_\alpha$), *pressure diffusion* (term with ∇p), and *forced diffusion* (term with $\mathbf{g}_\alpha$). The $\mathbf{d}_\alpha$ are so defined that $\Sigma_\alpha \mathbf{d}_\alpha = 0$.

The entropy production in Eq. 24.1-6, which is a sum of products of fluxes and forces, is the starting point for the nonequilibrium thermodynamics development. According to the "linearity postulate" each of the fluxes in Eq. 24.1-6 ($\mathbf{q}^{(h)}$, $\mathbf{j}_\alpha$, $\boldsymbol{\tau}$, and $\overline{G}_\alpha/M_\alpha$) can be written as a linear function of all the forces (∇T, $\mathbf{d}_\alpha$, $\nabla \mathbf{v}$, and r_α). However, because of "Curie's postulate," each of the $\mathbf{j}_\alpha$ must depend linearly on all of the $\mathbf{d}_\alpha$ as well as on ∇T, and $\mathbf{q}^{(h)}$ must depend linearly on ∇T as well as on all the $\mathbf{d}_\alpha$, but neither $\mathbf{j}_\alpha$ nor $\mathbf{q}^{(h)}$ can depend on $\nabla \mathbf{v}$ or r_α. Similarly the stress tensor $\boldsymbol{\tau}$ will depend on the tensor $\nabla \mathbf{v}$, and also on the scalar driving forces r_α multiplied by the unit tensor. Since the "coupling" between $\boldsymbol{\tau}$ and the chemical reactions has not been studied, we omit any further consideration of it. In the next section we discuss the coupling among all the vector forces and vector fluxes and the consequences of applying the "Onsager reciprocal relations."

§24.2 THE FLUX EXPRESSIONS FOR HEAT AND MASS

We now employ the "linearity postulate" to obtain for the vector fluxes

$$\mathbf{q}^{(h)} = -a_{00}\nabla \ln T - \sum_{\beta=1}^{N} \frac{cRTa_{0\beta}}{\rho_\beta}\mathbf{d}_\beta \tag{24.2-1}$$

$$\mathbf{j}_\alpha = -a_{\alpha 0}\nabla \ln T - \rho_\alpha \sum_{\beta=1}^{N} \frac{cRTa_{\alpha\beta}}{\rho_\alpha\rho_\beta}\mathbf{d}_\beta \qquad \alpha = 1, 2, \ldots, N \tag{24.2-2}$$

In these equations the quantities a_{00}, $a_{0\beta}$, $a_{\alpha 0}$, and $a_{\alpha\beta}$ are the "phenomenological coefficients" (that is, the transport properties). Because the $\mathbf{j}_\alpha$ and $\mathbf{d}_\alpha$ are not all independent, it must be required that $a_{\alpha\beta} + \Sigma_\gamma a_{\alpha\gamma} = 0$, where the sums are over all γ (except $\gamma = \beta$) from 1 to N. Now according to the Onsager reciprocal relations, $a_{\alpha 0} = a_{0\alpha}$ and $a_{\alpha\beta} = a_{\beta\alpha}$ for all values of α and β from 1 to N.

Next we relate the phenomenological coefficients to the transport coefficients. First we relabel $a_{\alpha 0}$ and $a_{0\alpha}$ as D_α^T, the *multicomponent thermal diffusion coefficients*. These have the property that $\Sigma_\alpha D_\alpha^T = 0$. Then we define the *multicomponent Fick diffusivities*,[1] $\mathbb{D}_{\alpha\beta}$, by $\mathbb{D}_{\alpha\beta} = -cRTa_{\alpha\beta}/\rho_\alpha\rho_\beta$. These diffusivities are symmetric ($\mathbb{D}_{\alpha\beta} = \mathbb{D}_{\beta\alpha}$) and obey the relations $\Sigma_\alpha \omega_\alpha \mathbb{D}_{\alpha\beta} = 0$. Then Eq. 24.2-2 becomes

$$\boxed{\mathbf{j}_\alpha = -D_\alpha^T \nabla \ln T + \rho_\alpha \sum_{\beta=1}^{N} \mathbb{D}_{\alpha\beta}\mathbf{d}_\beta \qquad \alpha = 1, 2, \ldots, N} \tag{24.2-3}$$

for the multicomponent mass fluxes. These are the *generalized Fick equations*. When the second form of Eq. 24.1-8 is substituted into Eq. 24.2-3 we see that there are four contributions to the mass-flux vector $\mathbf{j}_\alpha$: the concentration diffusion term (containing the activity gradient), the pressure diffusion term (containing the pressure gradient), the forced diffusion term (containing the external forces), and the thermal diffusion term (proportional to the temperature gradient).

---

[1] C. F. Curtiss, *J. Chem. Phys.*, **49**, 2917–2919 (1968); see also D. W. Condiff, *J. Chem. Phys.*, **51**, 4209–4212 (1969), and C. F. Curtiss and R. B. Bird, *Ind. Eng. Chem. Research*, **39**, 2515–2522 (1999); errata **41**, 1791 (2001). The $\mathbb{D}_{\alpha\beta}$ used here are the negatives of the Curtiss $\tilde{D}_{\alpha\beta}$, which, in turn, are different from the $D_{\alpha\beta}$ used by J. O. Hirschfelder, C. F. Curtiss, and R. B. Bird, *Molecular Theory of Gases and Liquids*, Wiley, New York (1954), second corrected printing (1964), Chapter 11.

Equation 24.2-3 can be turned "wrong-side out"[1,2] and solved for the driving forces $\mathbf{d}_\alpha$:

$$\boxed{\mathbf{d}_\alpha = -\sum_{\beta\neq\alpha}\frac{x_\alpha x_\beta}{\mathcal{D}_{\alpha\beta}}\left(\frac{D_\alpha^T}{\rho_\alpha}-\frac{D_\beta^T}{\rho_\beta}\right)(\nabla \ln T) - \sum_{\beta\neq\alpha}\frac{x_\alpha x_\beta}{\mathcal{D}_{\alpha\beta}}\left(\frac{\mathbf{j}_\alpha}{\rho_\alpha}-\frac{\mathbf{j}_\beta}{\rho_\beta}\right) \quad (\alpha = 1, 2, \ldots, N)} \tag{24.2-4}$$

These are the *generalized Maxwell–Stefan equations*, a special case of which was given in Eq. 17.9-1. The $\mathcal{D}_{\alpha\beta}$ are called the *multicomponent Maxwell-Stefan diffusivities*, and they have been proven to be symmetric;[3] their relation to the $\mathbb{D}_{\alpha\beta}$ will be discussed presently.

When the expression for $\mathbf{d}_\alpha$ in Eq. 24.2-4 is substituted into Eq. 24.2-1, we get

$$\mathbf{q}^{(h)} = -\left[a_{00} + \sum_{\alpha=1}^{N}\sum_{\substack{\beta=1\\\beta\neq\alpha}}^{N}\frac{cRTx_\alpha x_\beta}{\rho_\alpha}\frac{D_\alpha^T}{\mathcal{D}_{\alpha\beta}}\left(\frac{D_\beta^T}{\rho_\beta}-\frac{D_\alpha^T}{\rho_\alpha}\right)\right]\nabla \ln T + \sum_{\alpha=1}^{N}\sum_{\substack{\beta=1\\\beta\neq\alpha}}^{N}\frac{cRTx_\alpha x_\beta}{\rho_\alpha}\frac{D_\alpha^T}{\mathcal{D}_{\alpha\beta}}\left(\frac{\mathbf{j}_\alpha}{\rho_\alpha}-\frac{\mathbf{j}_\beta}{\rho_\beta}\right) \tag{24.2-5}$$

The thermal conductivity of a mixture is defined to be the coefficient of proportionality between the heat-flux vector and the temperature gradient when there are no mass fluxes in the system. Thus, the quantity in brackets is, by general agreement, the thermal conductivity k times the absolute temperature T. If we combine this result with the definition in Eq. 24.1-7, w get for the final expression for the heat flux:[3]

$$\boxed{\mathbf{q} = -k\nabla T + \sum_{\alpha=1}^{N}\frac{\overline{H}_\alpha}{M_\alpha}\mathbf{j}_\alpha + \sum_{\alpha=1}^{N}\sum_{\substack{\beta=1\\\beta\neq\alpha}}^{N}\frac{cRTx_\alpha x_\beta}{\rho_\alpha}\frac{D_\alpha^T}{\mathcal{D}_{\alpha\beta}}\left(\frac{\mathbf{j}_\alpha}{\rho_\alpha}-\frac{\mathbf{j}_\beta}{\rho_\beta}\right)} \tag{24.2-6}$$

We see that the heat flux vector $\mathbf{q}$ consists of three terms: the heat conduction term (containing the thermal conductivity), the heat diffusion term (containing the partial molar enthalpies and the mass fluxes), and finally the Dufour term (containing the thermal diffusion coefficients and the mass fluxes). The heat diffusion term, already encountered in Eq. 19.3-3, is generally important in diffusing systems. The Dufour term is usually small and can usually be neglected.

Equations 24.2-3, 4, and 6 are the principal results of nonequilibrium thermodynamics. We now have the mass- and heat-flux vectors expressed in terms of the transport properties and the fluxes.

Next we discuss the relation between the matrix of Fick diffusivities $\mathbb{D}_{\alpha\beta}$ and that of the Maxwell–Stefan diffusivities $\mathcal{D}_{\alpha\beta}$. Both matrices are symmetric and of order $N \times N$, and both have $\frac{1}{2}N(N-1)$ independent elements. The $\mathcal{D}_{\alpha\beta}$ are obtained thus:[3]

$$\mathcal{D}_{\alpha\beta} = \frac{x_\alpha x_\beta}{\omega_\alpha\omega_\beta}\frac{\sum_{\gamma\neq\alpha}\mathbb{D}_{\alpha\gamma}(\text{adj } B_\alpha)_{\gamma\beta}}{\sum_{\gamma\neq\alpha}(\text{adj } B_\alpha)_{\gamma\beta}} \qquad \alpha, \beta = 1, 2, \ldots, N \tag{24.2-7}$$

in which $(B_\alpha)_{\beta\gamma} = -\mathbb{D}_{\beta\gamma} + \mathbb{D}_{\alpha\gamma}$—that is, the $\beta\gamma$-component of a matrix called B_α, which is of order $(N-1)\times(N-1)$—and adj B_α is the matrix adjoint to B_α. For binary and ternary

---

[2] H. J. Merk, *Appl. Sci. Res.*, **A8**, 73–99 (1959); E. Helfand, *J. Chem. Phys.*, **33**, 319–322 (1960). **Hendrik Jacobus Merk** (1920–1988) performed the inversion of the mass-flux expressions when he was a graduate student in engineering physics at the Technical University of Delft; from 1953 to 1987 he was a professor at the same institution.

[3] C. F. Curtiss and R. B. Bird, *Ind. Eng. Chem. Research*, **38**, 2515–2522 (1999); errata, **40**, 1791 (2001).

Table 24.2-1 Summary[1] of Expressions for the $\mathbb{D}_{\alpha\beta}$ in Terms of the $\mathcal{D}_{\alpha\beta}$. [Note: Additional entries may be generated by cyclic permutation of the indices. Formulas for four-component systems are given in the references.]

Binary:

$$\mathbb{D}_{11} = -\frac{\omega_2^2}{x_1 x_2}\mathcal{D}_{12} \tag{A}$$

$$\mathbb{D}_{22} = -\frac{\omega_1^2}{x_1 x_2}\mathcal{D}_{12} \tag{B}$$

$$\mathbb{D}_{12} = \mathbb{D}_{21} = \frac{\omega_1\omega_2}{x_1 x_2}\mathcal{D}_{12} \tag{C}$$

Ternary:

$$\mathbb{D}_{11} = -\frac{\dfrac{(\omega_2+\omega_3)^2}{x_1\mathcal{D}_{23}} + \dfrac{\omega_2^2}{x_2\mathcal{D}_{13}} + \dfrac{\omega_3^2}{x_3\mathcal{D}_{12}}}{\dfrac{x_1}{\mathcal{D}_{12}\mathcal{D}_{13}} + \dfrac{x_2}{\mathcal{D}_{12}\mathcal{D}_{23}} + \dfrac{x_3}{\mathcal{D}_{13}\mathcal{D}_{23}}} \tag{D}$$

$$\mathbb{D}_{12} = \frac{\dfrac{\omega_1(\omega_2+\omega_3)}{x_1\mathcal{D}_{23}} + \dfrac{\omega_2(\omega_1+\omega_3)}{x_2\mathcal{D}_{13}} - \dfrac{\omega_3^2}{x_3\mathcal{D}_{12}}}{\dfrac{x_1}{\mathcal{D}_{12}\mathcal{D}_{13}} + \dfrac{x_2}{\mathcal{D}_{12}\mathcal{D}_{23}} + \dfrac{x_3}{\mathcal{D}_{13}\mathcal{D}_{23}}} \tag{E}$$

systems, the explicit interrelations are given in Tables 24.2-1 and 2. In Eq. (C) of Table 24.2-1, it can be seen that for a binary mixture the $\mathbb{D}_{\alpha\beta}$ and $\mathcal{D}_{\alpha\beta}$ differ by a factor that is a function of the concentration. However, they do have the same sign, which explains why the plus sign was chosen in Eq. 24.2-3 instead of a minus sign.

We are now in a position to present the three final results of this section that are useful as starting points for solving diffusion problems. For *multicomponent diffusion in gases or liquids*, combining Eqs. 24.1-8 and 24.2-4 gives

$$\sum_{\substack{\beta=1\\ \beta\neq\alpha}}^{N} \frac{x_\alpha x_\beta}{\mathcal{D}_{\alpha\beta}}(\mathbf{v}_\alpha - \mathbf{v}_\beta) = -x_\alpha(\nabla \ln a_\alpha)_{T,p} - \frac{1}{cRT}\left[(\phi_\alpha - \omega_\alpha)\nabla p - \rho_\alpha \mathbf{g}_\alpha + \omega_\alpha \sum_{\beta=1}^{N}\rho_\beta \mathbf{g}_\beta\right]$$
$$- \sum_{\substack{\beta=1\\ \beta\neq\alpha}}^{N} \frac{x_\alpha x_\beta}{\mathcal{D}_{\alpha\beta}}\left(\frac{D_\alpha^T}{\rho_\alpha} - \frac{D_\beta^T}{\rho_\beta}\right)(\nabla \ln T) \quad (\alpha = 1, 2, \ldots, N) \tag{24.2-8}$$

This equation has been written in terms of the difference of molecular velocities, $\mathbf{v}_\alpha - \mathbf{v}_\beta$. Equations (D) to (I) of Table 17.8-1 may then be used to write this equation in terms of any desired mass or molar fluxes.

Table 24.2-2 Summary[1] of Expressions for the $\mathcal{D}_{\alpha\beta}$ in Terms of the $\mathbb{D}_{\alpha\beta}$. [Note: Additional entries can be generated by cyclic permutation of the indices. See the original references for four-component systems.]

Binary:

$$\mathcal{D}_{12} = \frac{x_1 x_2}{\omega_1\omega_2}\mathbb{D}_{12} = -\frac{x_1 x_2}{\omega_2^2}\mathbb{D}_{11} = -\frac{x_1 x_2}{\omega_1^2}\mathbb{D}_{22} \tag{A}$$

Ternary:

$$\mathcal{D}_{12} = \frac{x_1 x_2}{\omega_1\omega_2}\frac{\mathbb{D}_{12}\mathbb{D}_{33} - \mathbb{D}_{13}\mathbb{D}_{23}}{\mathbb{D}_{12} + \mathbb{D}_{33} - \mathbb{D}_{13} - \mathbb{D}_{23}} \tag{B}$$

If one wishes to designate one species γ as being special (for example, the solvent), then Eq. 24.2-8 can be rewritten thus (see Problem 24C.1):

$$\sum_{\substack{\beta=1\\ \text{all } \beta}}^{N} \frac{x_\alpha x_\beta}{D_{\alpha\beta}} (\mathbf{v}_\gamma - \mathbf{v}_\beta) = -x_\alpha(\nabla \ln a_\alpha)_{T,p} - \frac{1}{cRT}\left[(\phi_\alpha - \omega_\alpha)\nabla p - \rho_\alpha \mathbf{g}_\alpha + \omega_\alpha \sum_{\beta=1}^{N} \rho_\beta \mathbf{g}_\beta\right]$$

$$- \sum_{\substack{\beta=1\\ \text{all } \beta}}^{N} \frac{x_\alpha x_\beta}{\mathcal{D}_{\alpha\beta}} \left(\frac{D_\gamma^T}{\rho_\gamma} - \frac{D_\beta^T}{\rho_\beta}\right)(\nabla \ln T) \quad (\alpha = 1, 2, \ldots, N) \tag{24.2-9}$$

Note that in Eq. 24.2-8 there are $N(N-1)/2$ symmetric diffusivities, $\mathcal{D}_{\alpha\beta}$, and that the $\mathcal{D}_{\alpha\alpha}$ do not appear and are hence not defined. However, in Eq. 24.2-9, there are $N(N+1)/2$ symmetric diffusivities, but the $\mathcal{D}_{\alpha\alpha}$ (N of them) now appear, and therefore we have to supply an auxiliary relation $\Sigma_\alpha(x_\alpha/\mathcal{D}_{\alpha\beta}) = 0$, in which the sum is over all α. Equation 24.2-9, with the auxiliary relation, is equivalent to Eq. 24.2-8, and both of these generalized Maxwell–Stefan equations are equivalent to the generalized Fick equations of Eq. 24.2-3, together with its auxiliary relation.

For *multicomponent diffusion in gases at low density*, the activity may be replaced by the mole fraction, and furthermore, to a very good approximation, the $\mathcal{D}_{\alpha\beta}$ may be replaced by $\mathcal{D}_{\alpha\beta}$. These are the *binary* diffusivities for all pairs of species in the mixture. Since the $\mathcal{D}_{\alpha\beta}$ vary only slightly with concentration, whereas the $\mathbb{D}_{\alpha\beta}$ are highly concentration-dependent, it is preferable to use the Maxwell–Stefan form (Eq. 24.2-4) rather than the Fick form (Eq. 24.2-3).

For *binary diffusion in gases or liquids*, Eq. (C) of Table 24.2-1 and Eq. 17B.3-1 may be used to simplify Eq. 24.2-8 as follows:

$$\mathbf{j}_A^* = -c\mathcal{D}_{AB}\left[x_A \nabla \ln a_A + \frac{1}{cRT}[(\phi_A - \omega_A)\nabla p - \rho\omega_A\omega_B(\mathbf{g}_A - \mathbf{g}_B)] + k_T \nabla \ln T\right] \tag{24.2-10}$$

In this equation we have introduced the *thermal diffusion ratio*, defined by $k_T = -D_A^T/\rho\tilde{D}_{AB} = +(D_A^T/\rho\mathcal{D}_{AB})(x_A x_B/\omega_A\omega_B)$. Other quantities encountered are the *thermal diffusion factor* α_T and the *Soret coefficient* σ_T, defined by $k_T = \alpha_T x_A x_B = \sigma_T x_A x_B T$. For gases α_T is almost independent of composition, and σ_T is the quantity preferred for liquids. When k_T is positive, species A moves toward the colder region, and when it is negative, species A moves toward the warmer region. Some sample values of k_T for gases and liquids are given in Table 24.2-3.

For binary mixtures of dilute gases, it is found by experiment that the species with the larger molecular weight usually goes to the colder region. If the molecular weights are about equal, then usually the species with the larger diameter moves to the colder region. In some instances there is a change in the sign of the thermal diffusion ratio as the temperature is lowered.[4]

In the remainder of the chapter, we explore some of the consequences of the mass-flux expressions in Eqs. 24.2-8, 9, and 10.

EXAMPLE 24.2-1

Thermal Diffusion and the Clusius–Dickel Column

In this example we discuss the diffusion of species under the influence of a temperature gradient. To illustrate the phenomenon we consider the system shown in Fig. 24.2-1, two bulbs joined together by an insulated tube of small diameter and filled with a mixture of ideal gases A and B. The bulbs are maintained at constant temperatures T_1 and T_2, respectively, and the diameter of the insulated tube is small enough to eliminate convection currents substantially. Ultimately the system arrives at a steady state, with gas A enriched at one end of the tube and depleted at the other. Obtain an expression for $x_{A2} - x_{A1}$, the difference of the mole fractions at the two ends of the tube.

[4] S. Chapman and T. G. Cowling, *The Mathematical Theory of Non-Uniform Gases*, 3rd edition, Cambridge University Press (1970), p. 274.

Table 24.2-3 Experimental Thermal Diffusion Ratios for Liquids and Low-Density Gas Mixtures

Liquids:[a]

Components *A–B*	*T* (K)	x_A	k_T
$C_2H_2Cl_4$–*n*-C_6H_{14}	298	0.5	1.08
$C_2H_4Br_2$–$C_2H_4Cl_2$	298	0.5	0.225
$C_2H_2Cl_4$–CCl_4	298	0.5	0.060
CBr_4–CCl_4	298	0.09	0.129
CCl_4–CH_3OH	313	0.5	1.23
CH_3OH–H_2O	313	0.5	−0.137
cyclo-C_6H_{12}–C_6H_6	313	0.5	0.100

Gases:

Components *A–B*	*T* (K)	x_A	k_T
Ne–He[b]	330	0.80	0.0531
		0.40	0.1004
N_2–H_2[c]	264	0.706	0.0548
		0.225	0.0663
D_2–H_2[d]	327	0.90	0.0145
		0.50	0.0432
		0.10	0.0166

[a] R. L. Saxton, E. L. Dougherty, and H. G. Drickamer, *J. Chem. Phys.*, **22**, 1166–1168 (1954); R. L. Saxton and H. G. Drickamer, *J. Chem. Phys.*, **22**, 1287–1288 (1954); L. J. Tichacek, W. S. Kmak, and H. G. Drickamer, *J. Phys. Chem.*, **60**, 660–665 (1956).

[b] B. E. Atkins, R. E. Bastick, and T. L. Ibbs, *Proc. Roy. Soc. (London)*, **A172**, 142–158 (1939).

[c] T. L. Ibbs, K. E. Grew, and A. A. Hirst, *Proc. Roy. Soc. (London)*, **A173**, 543–554 (1939).

[d] H. R. Heath, T. L. Ibbs, and N. E. Wild, *Proc. Roy. Soc. (London)*, **A178**, 380–389 (1941).

SOLUTION

After steady state has been achieved, there is no net motion of either *A* or *B*, so that $\mathbf{J}_A^* = 0$. If we take the tube axis to be in the *z* direction, then from Eq. 24.2-10 we get

$$\frac{dx_A}{dz} + \frac{k_T}{T}\frac{dT}{dz} = 0 \tag{24.2-11}$$

Here the activity a_A has been replaced by the mole fraction x_A, as is appropriate for an ideal gas mixture. Usually the degree of separation in an apparatus of this kind is small. We may therefore ignore the effect of composition on k_T and integrate this equation to get

$$x_{A2} - x_{A1} = -\int_{T_1}^{T_2} \frac{k_T}{T}\, dT \tag{24.2-12}$$

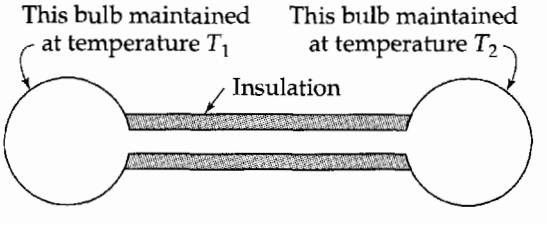

Fig. 24.2-1. Steady-state binary thermal diffusion in a two-bulb apparatus. The mixture of gases *A* and *B* tends to separate under the influence of the thermal gradient.

Because the dependence of k_T on T is rather complicated, it is customary to assume k_T constant at the value for some mean temperature T_m. Equation 24.2-12 then gives (approximately)

$$x_{A2} - x_{A1} = -k_T(T_m) \ln \frac{T_2}{T_1} \tag{24.2-13}$$

The recommended[5] mean temperature is

$$T_m = \frac{T_1 T_2}{T_2 - T_1} \ln \frac{T_2}{T_1} \tag{24.2-14}$$

Equations 23.2-13 and 14 are useful for estimating the order of magnitude of thermal diffusion effects.

Unless the temperature gradient is very large, the separation will normally be quite small. Therefore it has been advantageous to combine the thermal diffusion effect with free convection between two vertical walls, one heated and the other cooled. The heated stream then ascends, and the cooled one descends. The upward stream will be richer in one of the components—say, *A*—and the downward stream will be richer in *B*. This is the principle of the operation of the *Clusius–Dickel column*.[6–8] By coupling many of these columns together in a "cascade" it is possible to perform a separation. During World War II this was one of the methods used for separating the uranium isotopes by using uranium hexafluoride gas. The method has also been used with some success in the separation of organic mixtures, where the components have very nearly the same boiling points, so that distillation is not an option.

The thermal diffusion ratio can also be obtained from the Dufour (diffusion-thermo) effect, but the analysis of the experiment is fraught with problems and experimental errors difficult to avoid.[9]

EXAMPLE 24.2-2

Pressure Diffusion and the Ultra Centrifuge

Next we examine diffusion in the presence of a pressure gradient. If a sufficiently large pressure gradient can be established, then a measurable separation can be effected. One example of this is the ultracentrifuge, which has been used to separate enzymes and proteins. In Fig. 24.2-2 we show a small cylindrical cell in a very high-speed centrifuge. The length of the cell,

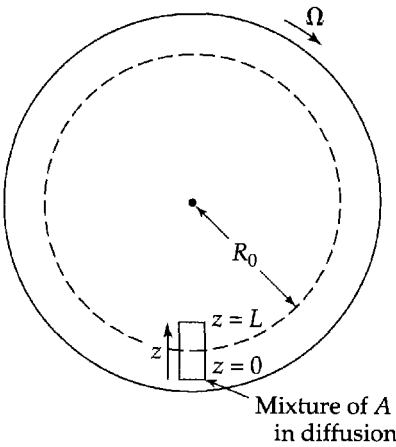

Fig. 24.2-2. Steady-state pressure diffusion in a centrifuge. The mixture in the diffusion cell tends to separate by virtue of the pressure gradient produced in the centrifuge.

[5] H. Brown, *Phys. Rev.*, **58**, 661–662 (1940).

[6] K. Clusius and G. Dickel, *Z. Phys. Chem.*, **B44**, 397–450, 451–473 (1939).

[7] K. E. Grew and T. L. Ibbs, *Thermal Diffusion in Gases*, Cambridge University Press (1952); K. E. Grew, in *Transport Phenomena in Fluids* (H. J. M. Hanley, ed.), Marcel Dekker, New York (1969), Chapter 10.

[8] R. B. Bird, *Advances in Chemical Engineering*, **1**, 155–239 (1956), §4.D.2; *errata*, **2**, 325 (1958).

[9] S. Chapman and T. G. Cowling, *The Mathematical Theory of Nonuniform Gases*, 3rd edition, Cambridge University Press (1970), pp. 268–271.

L, is short with respect to the radius of rotation R_0, and the solution density may be considered a function of composition only. Determine the distribution of the two components at steady state in terms of their partial molar volumes and the pressure gradient. The latter is obtained from the equation of motion as

$$\frac{dp}{dz} = -\rho g_\Omega \approx -\rho \Omega R_0 \tag{24.2-15}$$

For simplicity, we assume that the partial molar volumes and the activity coefficients are constant over the range of conditions existing in the cell.

SOLUTION

At steady state $j_A = 0$, and the relevant terms in Eq. 24.2-10 give for species A

$$\frac{dx_A}{dz} + \frac{M_A x_A}{RT}\left(\frac{\bar{V}_A}{M_A} - \frac{1}{\rho}\right)\frac{dp}{dz} = 0 \tag{24.2-16}$$

Inserting the appropriate expression for the pressure gradient and then multiplying by $(\bar{V}_B/x_A)dz$, we get for species A

$$\bar{V}_B \frac{dx_A}{x_A} = -\bar{V}_B \frac{g_\Omega}{RT}(\rho \bar{V}_A - M_A)dz \tag{24.2-17}$$

Then we write a similar equation for species B, which is

$$\bar{V}_A \frac{dx_B}{x_B} = -\bar{V}_A \frac{g_\Omega}{RT}(\rho \bar{V}_B - M_B)dz \tag{24.2-18}$$

Subtracting Eq. 24.2-18 from Eq. 24.2-17 we get

$$\bar{V}_B \frac{dx_A}{x_A} - \bar{V}_A \frac{dx_B}{x_B} = \frac{g_\Omega}{RT}(M_B \bar{V}_A - M_A \bar{V}_B)dz \tag{24.2-19}$$

We now integrate this equation from $z = 0$ to some arbitrary value of z, taking account of the fact that the mole fractions of A and B at $z = 0$ are x_{A0} and x_{B0}, respectively. This gives

$$\bar{V}_B \int_{x_{A0}}^{x_A} \frac{dx_A}{x_A} - \bar{V}_A \int_{x_{B0}}^{x_B} \frac{dx_B}{x_B} = \frac{M_B \bar{V}_A - M_A \bar{V}_B}{RT} \int_0^z g_\Omega dz \tag{24.2-20}$$

If g_Ω is treated as constant over the range of integration, then we get

$$\bar{V}_B \ln \frac{x_A}{x_{A0}} - \bar{V}_A \ln \frac{x_B}{x_{B0}} = \frac{M_B \bar{V}_A - M_A \bar{V}_B}{RT} g_\Omega z \tag{24.2-21}$$

Then we take the exponential of both sides to find

$$\left(\frac{x_A}{x_{A0}}\right)^{\bar{V}_B}\left(\frac{x_{B0}}{x_B}\right)^{\bar{V}_A} = \exp\left[(M_B \bar{V}_A - M_A \bar{V}_B)\left(\frac{g_\Omega z}{RT}\right)\right] \tag{24.2-22}$$

This describes the steady-state concentration distribution for a binary system in a constant centrifugal force field. Note that, since this result contains no transport coefficients at all, the same result can be obtained by an equilibrium thermodynamics analysis.[10] However, if one wishes to analyze the time-dependent behavior of a centrifugation, then the diffusivity for the mixing A–B will appear in the result, and the problem cannot be solved by equilibrium thermodynamics.

---

[10] E. A. Guggenheim, *Thermodynamics*, North-Holland, Amsterdam (1950), pp. 356–360.

§24.3 CONCENTRATION DIFFUSION AND DRIVING FORCES

In Chapter 17 we wrote Fick's first law by stating that the mass (or molar) flux is proportional to the gradient of the mass (or mole) fraction, as summarized in Table 17.8-2.

On the other hand, in Eq. 24.2-10 it appears that the thermodynamics of irreversible processes dictates using the activity gradient as the driving force for concentration diffusion. In this section we show that either the activity gradient or the mass (or mole) fraction gradient driving force may be used, but that each choice requires a different diffusivity. These two diffusivities are related, and we illustrate this for a binary mixture.

When we drop the pressure-, thermal-, and forced-diffusion terms from Eq. 24.2-10, we get

$$\mathbf{j}_A^* = -c\mathcal{D}_{AB}x_A\nabla \ln a_A \tag{24.3-1}$$

This may be rewritten by making use of the fact that the activity coefficient is a function of x_A to obtain

$$\mathbf{j}_A^* = -c\mathcal{D}_{AB}\left(\frac{\partial \ln a_A}{\partial \ln x_A}\right)_{T,p}\nabla x_A \tag{24.3-2}$$

The activity may be written as the product of the activity coefficient and the mole fraction ($a_A = \gamma_A x_A$) so that

$$\mathbf{j}_A^* = -c\mathcal{D}_{AB}\left[1 + \left(\frac{\partial \ln \gamma_A}{\partial \ln x_A}\right)_{T,p}\right]\nabla x_A \tag{24.3-3}$$

If the mixture is "ideal," then the activity coefficient is equal to unity, Eq. 24.3-3 becomes the same as Eq. (B) of Table 17.8-2, and $\mathcal{D}_{AB} = \mathscr{D}_{AB}$.

If the mixture is "nonideal," one can express the binary diffusivity $\mathscr{D}_{AB}$ as

$$\mathscr{D}_{AB} = \mathcal{D}_{AB}\left(\frac{\partial \ln a_A}{\partial \ln x_A}\right)_{T,p} = \mathcal{D}_{AB}\left(1 + \left(\frac{\partial \ln \gamma_A}{\partial \ln x_A}\right)_{T,p}\right) \tag{24.3-4}$$

then Eq. 24.3-2 and 3 become

$$\mathbf{j}_A^* = -c\mathscr{D}_{AB}\nabla x_A \tag{24.3-5}$$

which is one of the forms of Fick's law (see Eq. (B) of Table 17.8-2). In order to measure $\mathcal{D}_{AB}$, one has to have measurements of the activity as a function of concentration, and for this reason $\mathcal{D}_{AB}$ has not been popular.

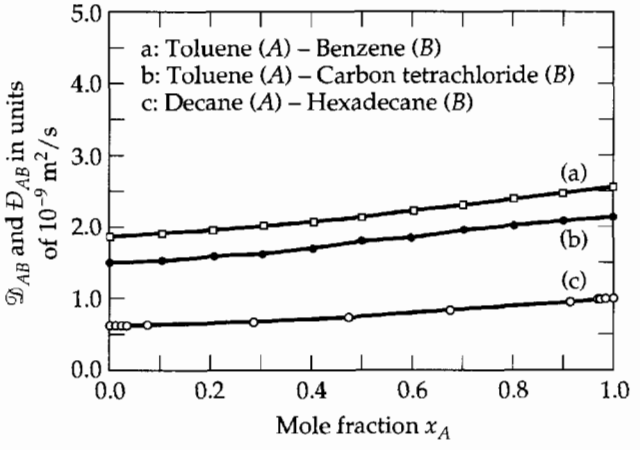

Fig. 24.3-1. Diffusivity in ideal liquid mixtures at 25°C [P. W. M. Rutten, *Diffusion in Liquids*, Delft University Press (1992), p. 31].

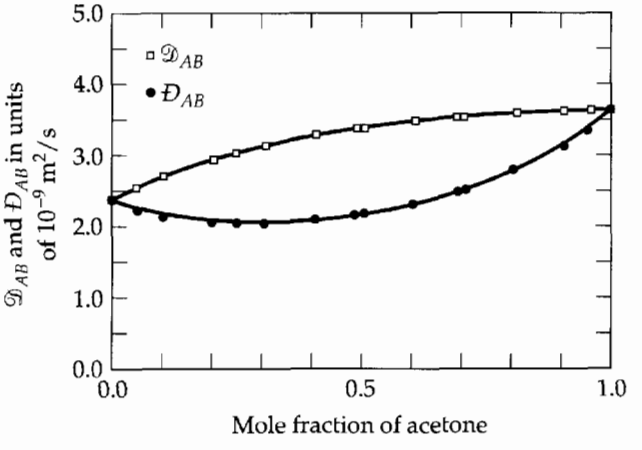

Fig. 24.3-2. Diffusivity in a nonideal liquid mixture (acetone–chloroform (at 25°C) [P. W. M. Rutten, *Diffusion in Liquids*, Delft University Press (1992), p. 32].

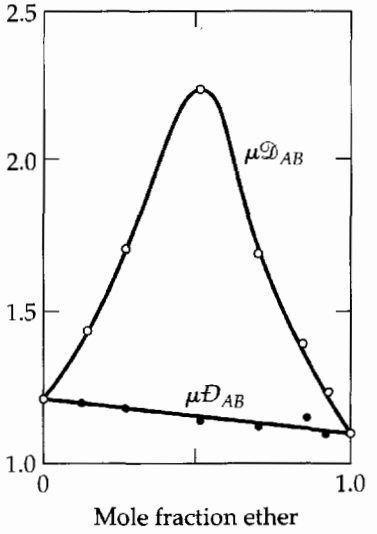

Fig. 24.3-3. Effect of activity on the product of viscosity and diffusivity for liquid mixtures of chloroform and diethyl ether [R. E. Powell, W. E. Roseveare, and H. Eyring, *Ind. Eng. Chem.*, **33**, 430–435 (1941)].

For ideal mixtures $\mathscr{D}_{AB}$ and $\mathscr{D}_{AB}$ are identical, and are nearly linear functions of the mole fraction as shown in Fig. 24.3-1. For nonideal mixtures $\mathscr{D}_{AB}$ and $\mathscr{D}_{AB}$ are different nonlinear functions of the mole fraction; an example is shown in Fig. 24.3-2. However, the product $\mu\mathscr{D}_{AB}$ has been found for *some* nonideal mixtures to be very nearly linear in the mole fraction, whereas $\mu\mathscr{D}_{AB}$ is not (see Fig. 24.3-3). There is no compelling reason to prefer one diffusivity over the other. Most of the diffusivities reported in the literature are $\mathscr{D}_{AB}$ and not $\mathscr{D}_{AB}$.

§24.4 APPLICATIONS OF THE GENERALIZED MAXWELL–STEFAN EQUATIONS

The generalized Maxwell–Stefan equations were given in Eq. 24.2-4 in terms of the diffusional driving forces $\mathbf{d}_\alpha$, and the expression for $\mathbf{d}_\alpha$ was given in Eq. 24.1-8. When these are combined we get the Maxwell–Stefan equations in terms of the activity gradient, the pressure gradient, and the external forces acting on the various species, given (Eqs. 24.2-8 or 9):

$$-\mathbf{d}_\alpha = \sum_{\substack{\beta=1 \\ \text{all } \beta}}^{N} \frac{x_\alpha x_\beta}{\mathscr{D}_{\alpha\beta}} (\mathbf{v}_\gamma - \mathbf{v}_\beta) + \text{thermal diffusion terms}$$

$$= -x_\alpha (\nabla \ln a_\alpha)_{T,p} - \frac{1}{cRT}\left[(\phi_\alpha - \omega_\alpha)\nabla p - \rho_\alpha \mathbf{g}_\alpha + \omega_\alpha \sum_{\beta=1}^{N} \rho_\beta \mathbf{g}_\beta\right]$$

$$\alpha = 1, 2, 3, \ldots, N \qquad (24.4\text{-}1)$$

The thermal diffusion terms have not been displayed here, since they will not be needed in this section. The symbols $\phi_\alpha = c_\alpha \bar{V}_\alpha$ and ω_α designate, respectively, the volume fraction and mass fraction of species α. As explained in §§24.1 and 2, several auxiliary relations have to be kept in mind:

$$\sum_{\alpha=1}^{N} \mathbf{d}_\alpha = 0; \qquad \mathscr{D}_{\alpha\beta} = \mathscr{D}_{\beta\alpha}; \qquad \sum_{\alpha=1}^{N} \frac{x_\alpha}{\mathscr{D}_{\alpha\beta}} = 0 \qquad (24.4\text{-}2, 3, 4)$$

The first of these relations follows from the definition of the $\mathbf{d}_\alpha$, the second is a consequence of the Onsager reciprocal relations, and the third is needed because of the introduction of an especially designated species γ. The choice as to which species is designated as γ is arbitrary; often setting γ equal to α is convenient. The choice depends

on the nature of the system under study, and this point will be illustrated in the examples that follow.

In all previous chapters, the only external force that has been considered has been the gravitational force. In this section we set the external force per unit mass $\mathbf{g}_\alpha$ equal to a sum of forces

$$\mathbf{g}_\alpha = \mathbf{g} - \left(\frac{z_\alpha F}{M_\alpha}\right)\nabla\phi + \delta_{\alpha m}\frac{1}{\rho_m}\nabla p \tag{24.4-5}$$

Here $\mathbf{g}$ is the gravitational acceleration, z_α is the elementary charge on species α (for example, -1 for the chloride ion Cl^-), $F = 96485$ abs.-coulombs/g-equivalent is the Faraday constant, ϕ is the electrostatic potential, and the subscript m on the Kronecker delta $\delta_{\alpha m}$ refers to any mechanically restrained matrix, such as a permselective membrane.

In sum, for solving multicomponent diffusion problems in isothermal systems, we now have N mass-flux equations (of which only $N - 1$ are independent), the species equations of continuity, and the equation of motion. This set of equations has proven to be useful for solving wide classes of mass transfer problems, and we discuss some of these in the following examples.

Of course, in order to solve multicomponent diffusion problems one needs the Maxwell–Stefan diffusivities $Đ_{\alpha\beta}$ that occur in Eq. 24.4-1. Very few measurements have been made of these quantities, which require the simultaneous measurement of the activity as a function of concentration. Among the few examples of such measurements are those made by Rutten.[1]

EXAMPLE 24.4-1

Centrifugation of Proteins

Protein molecules are large enough that they can be concentrated by centrifugation against the dispersive tendencies of Brownian motion, and this process has proven useful for molecular weight determination as well as for small-scale preparative separations. Show how the behavior of protein molecules in a centrifugal field can be predicted, and the kind of information that can be obtained from their behavior in a centrifuge tube (see Fig. 24.4-1). As we shall see in Example 24.4-3, we may treat the protein and its attendant counter-ions as a single large electrically neutral molecule. Choose the protein as species γ and begin with the mass-flux equation for it. The small ionic species needed for protein stability play no significant role in this development and can be ignored.

SOLUTION

We consider here a pseudobinary system of a single globular protein P in a solvent W, which is primarily water, and initially we restrict the discussion to a dilute solution rotating in a tube perpendicular to the axis of rotation (Fig. 24.,4-1*a*) at a constant angular velocity Ω. For such a system $x_W \approx 1$ and the solute flow field with respect to stationary axes will be that of rigid-body rotation—namely, $\mathbf{v}_W = \boldsymbol{\delta}_\theta \Omega r$.

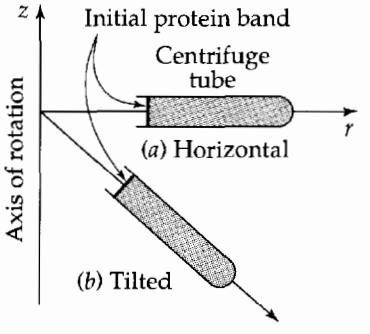

Fig. 24.4-1. Ultracentrifugation of proteins, with two possible orientations of the centrifuge tube.

[1] Ph. W. M. Rutten, *Diffusion in Liquids*, Delft University Press, Delft, The Netherlands (1992).

Then the radial diffusion of the protein is described by the r-component of the simplified Maxwell–Stefan equation

$$\frac{x_P}{\mathcal{D}_{PW}} v_{P_r} = -\left(1 + \frac{\partial \ln \gamma_P}{\partial \ln x_P}\right) \frac{\partial x_P}{\partial r} - \frac{1}{cRT} (\phi_P - \omega_P) \frac{\partial p}{\partial r} \tag{24.4-6}$$

We see immediately that the protein will move in the positive radial direction if its mass fraction is greater than its volume fraction—that is, if it is denser than the solvent. If Eq. 24.4-6 is multiplied through by $c\mathcal{D}_{PW}$, we get

$$\begin{aligned} N_P &= -c\mathcal{D}_{PW}\left[\left(1 + \frac{\partial \ln \gamma_P}{\partial \ln x_P}\right) \frac{\partial x_P}{\partial r} + \frac{1}{cRT} (\phi_P - \omega_P) \frac{\partial p}{\partial r}\right] \\ &= -c\mathscr{D}_{PW} \frac{\partial x_P}{\partial r} - \frac{\mathcal{D}_{PW}}{RT} (\phi_P - \omega_P) \frac{\partial p}{\partial r} \end{aligned} \tag{24.4-7}$$

in which the usual pseudobinary Fickian diffusivity $\mathscr{D}_{PW}$ is introduced. The diffusivity in Eq. 24.4-7 can be estimated from Eq. 17.4-3 as

$$\mathscr{D}_{PW} = \frac{\kappa T}{6\pi \mu_W R_P f_P} \tag{24.4-8}$$

in which R_P is the radius of a sphere having the volume of the protein molecule, μ_W is the solvent (water) viscosity, and f_P is a hydrodynamic shape factor (that is, a correction factor to account for the nonsphericity of the protein molecule).

From the equation of motion for the solution, we get the pressure gradient in terms of the angular velocity of the ultracentrifuge, thus

$$\frac{\partial p}{\partial r} = \rho \frac{v_\theta^2}{r} = \rho \Omega^2 r \tag{24.4-9}$$

The term $\rho\Omega^2 r$ will not vary significantly over the length of the centrifugation tube, which is small compared with the radius of the ultracentrifuge rotor.

Now we want to get an appreciation of the molecular weight dependence of the pressure-gradient term in Eq. 24.4-7. To do that we introduce the following approximations, valid in the dilute solution limit, common in protein processing:

$$\phi_P = c_P \overline{V}_P = x_P c \overline{V}_P \approx x_P \frac{\overline{V}_P}{\overline{V}_W} = x_P \frac{M_P}{M_W} \frac{\hat{V}_P}{\hat{V}_W} \tag{24.4-10a}$$

$$\omega_P = \frac{\rho_P}{\rho} = \frac{c_P M_P}{cM} = x_P \frac{M_P}{(x_P M_P + x_W M_W)} \approx x_P \frac{M_P}{M_W} \tag{24.4-10b}$$

Here $\hat{V}_P = \overline{V}_P / M_P$ is the partial specific volume of the protein. The partial specific volume of the solvent may be taken as 1 ml/g without significant error, and $\hat{V}_P$ for globular proteins is usually in the neighborhood of 0.75 ml/g. We see then that the decisive factor in permitting effective centrifugation is the ratio of molecular weights rather than the specific volumes, as the latter are not greatly different for the two species.

When Eqs. 24.4-7, 8, 10, and 11 are combined, the protein flux takes the form

$$\begin{aligned} N_P &= -c\mathscr{D}_{PW} \frac{\partial x_P}{\partial r} + x_P(N_P + N_W) \\ &= -c\mathscr{D}_{PW} \frac{\partial x_P}{\partial r} + c_P v_{\text{migr}} \end{aligned} \tag{24.4-11}$$

which somewhat resembles Fick's first law. Here, the "migration velocity" for the protein is

$$v_{\text{migr}} = -\frac{\mathcal{D}_{PW}}{cRT}\left[\frac{M_P}{M_W}\left(\frac{\hat{V}_P}{\hat{V}_W} - 1\right)\right] \rho \Omega^2 r \tag{24.4-12}$$

Note that the radial molar flux of water greatly exceeds that of protein, and that the convective protein flux $c_P v_{\text{migr}}$ is very small.

Next we substitute the molar flux of Eq. 24.4-11 into the species equation of continuity

$$\frac{\partial c_P}{\partial t} = -\frac{\partial N_P}{\partial r} \tag{24.4-13}$$

or, for constant $\mathcal{D}_{PW}$

$$\frac{\partial c_P}{\partial t} = \mathcal{D}_{PW}\frac{\partial^2 c_P}{\partial r^2} - c_P v_{\text{migr}} \tag{24.4-14}$$

which is the equation we want to solve for several specific situations.

(a) ***Transient Behavior.*** We first consider migration of a thin protein band under conditions where fractional changes in r are small and no significant amount of protein reaches the far end of the tube. Then we can introduce a new independent variable $u = r - v_{\text{migr}}t$ that enables us to transform $c_P(r, t)$ into $c_P(u, t)$. The diffusion equation becomes

$$\left(\frac{\partial c_P}{\partial t}\right)_u = \mathcal{D}_{PW}\left(\frac{\partial^2 c_P}{\partial u^2}\right)_t \tag{24.4-15}$$

along with the initial condition

$$\text{At } t = 0, \qquad c_P = C\delta(u) \tag{24.4-16}$$

where C is a constant that tells how much protein is contained in the band, and the boundary conditions

$$\text{As } u \to \pm\infty, \qquad c_P \to 0 \tag{24.4-17}$$

Equation 24.4-17 is a long-tube approximation widely used in this application.

Equations 24.4-15 to 17 describe a Gaussian distribution of the protein about its center of mass, resulting from diffusion and moving with the velocity v_{migr}. The migration velocity can be measured, and this measurement yields a product of protein diffusivity and molecular weight. The broadness of the band in turn provides an independent measure of the diffusivity, and thus, combined with knowledge of the migration velocity and specific volumes, the molecular weight.[2] If the molecular weight is known, for example, from mass spectrometry, the shape factor f_P can be determined. This, in turn, is a useful measure of protein shape.

(b) ***Steady Polarization.*** We next consider long-time behavior when the protein has been concentrated at the end of the tube and has attained a steady state. Under these circumstances, there is no radial motion and Eqs. 24.4-6, 9, and 10 give

$$-\left(1 + \frac{\partial \ln \gamma_P}{\partial \ln x_P}\right)\frac{d \ln x_P}{dr} = \frac{1}{cRT}\left(\frac{M_P}{M_W}\right)\left(\frac{\hat{V}_P}{\hat{V}_W} - 1\right)\frac{dp}{dr} \tag{24.4-18}$$

The concentration gradient may be measured, and all other quantities except for M_P may be determined independently of the centrifugation process. Protein activity coefficients may, for example, be obtained from osmotic pressure data. Therefore the molecular weight of the protein may be unambiguously determined. Only mass spectrometry can provide better accuracy, and it is not suitable for all proteins.

(c) ***Preparative Operation.*** The speed of centrifugal separation can be greatly increased by tilting the tube as in Fig. 24.4-1*b*. Here the protein is forced toward the outer boundary of the tube by centrifugal action, and the resulting density gradient causes an axial bulk

---

[2] R. J. Silbey and R. A. Alberty, *Physical Chemistry*, 3rd edition, Wiley, New York (2001), p. 801.

transport by free convection, a process similar to that used for larger particles in disk centrifuges.[3]

EXAMPLE 24.4-2

Proteins as Hydrodynamic Particles

Show that the results of the last example are equivalent to treating the proteins as small hydrodynamic particles.

SOLUTION

If, in the previous example, we had not used the simplifications in Eqs. 24.4-9 and 10, we would have obtained for the migration velocity in steady-state operation

$$v_{\text{migr}} = -\left(\overline{V}_P - \frac{\omega_P}{c_P}\right)\frac{dp}{dr}\frac{\mathcal{D}_{PW}}{RT} \tag{24.4-19}$$

If now we restrict ourselves to dilute solutions so that the activity coefficient is very close to unity, we can set $\mathcal{D}_{PW}$ to $\mathscr{D}_{PW}$ and use Eq. 24.4-8 for the diffusivity and Eq. 24.4-9 for the pressure gradient. Then the migration velocity becomes

$$v_{\text{migr}} = -\left(\overline{V}_P - \frac{\omega_P}{c_P}\right)(\rho_W \Omega^2 r)\frac{1}{RT}\left(\frac{\kappa T}{6\pi\mu_W R_P f_P}\right) \tag{24.4-20}$$

Next we recognize that $\Omega^2 r = g_{\text{eff}}$ (an effective body force per unit mass resulting from the centrifugal field) and that $\kappa/R = \tilde{N}$ (Avogadro's number), and we get

$$v_{\text{migr}} = -\left(\overline{V}_P \rho_W - \frac{\rho_P}{c_P}\right)\frac{g_{\text{eff}}}{\tilde{N}}\left(\frac{1}{6\pi\mu_W R_P f_P}\right) \tag{24.4-21}$$

where we have used the approximation $\omega_P = \rho_P/(\rho_P + \rho_W) \approx \rho_P/\rho_W$ for a dilute protein solution. Next we set $\overline{V}_P \approx (\frac{4}{3}\pi R_P^3)\tilde{N}$, the volume per mole of protein, and $\rho_P/c_P \approx (\frac{4}{3}\pi R_P^3)(\rho^{(P)})\tilde{N}$, the mass per mole of protein; here $\rho^{(P)}$ is the pure protein density. When these quantities are inserted into Eq. 24.4-21 we get

$$v_{\text{migr}} = \frac{2R_P^2(\rho^{(P)} - \rho_W)g_{\text{eff}}}{9\mu_W f_P} \tag{24.4-22}$$

Comparison with Eq. 2.6-17 shows that the migration velocity for a nonspherical protein in a centrifugal field is the same as the terminal velocity for a sphere in a corresponding gravitational field (divided by the factor f_P to account for deviation from sphericity).

One may also start with an equation of motion for a particle P initially at rest in a suspension sufficiently dilute that particle–particle interactions are negligible. Then the particle velocity relative to a large body of quiescent fluid F is

$$\mathbf{v}_P - \mathbf{v}_F = -\mathscr{D}_{PF}\left(\nabla \ln n_P + \frac{1}{\kappa T}\left[V_P\left(1 - \frac{\rho^{(P)}}{\rho}\right)(\nabla p)_\infty - \mathbf{F}_{em}\right.\right.$$
$$\left.\left. + (\rho^{(P)} + \tfrac{1}{2}\rho)V_P\frac{d\mathbf{v}_P}{dt} + 6\sqrt{\pi\mu\rho}R_P^2\int_0^t \frac{d\mathbf{v}_P}{d\tau}\frac{1}{\sqrt{t-\tau}}d\tau\right]\right) \tag{24.4-23}$$

Here n_P is the number concentration of particles, V_P and R_P are the particle volume and radius, and the subscript ∞ refers to the conditions "far" from the particle (that is, outside the hydrodynamic boundary layer). Equation 24.4-23 is the equation of motion with an added term for Brownian motion, which is important, for example, in aerosol collection.[4] The symbol $\mathbf{F}_{em}$ stands for the electromagnetic force per particle.

---

[3] See, for example, *Perry's Chemical Engineers' Handbook*, McGraw-Hill, New York, 7th edition (1997), p. **18**–113.

[4] See L. D. Landau and E. M. Lifshitz, *Fluid Mechanics*, Pergamon Press, Oxford (1987), pp. 90–91, Problem 7.

The diffusivity $\mathscr{D}_{pF}$ in this example corresponds to $\mathscr{D}_{pW}$ of Example 24.4-1, and it may be seen that there is a very close analogy between the molecular and particulate descriptions. There are, in fact, only three significant differences:

1. The thermodynamic activity coefficient is considered to be unity for the particle.
2. The instantaneous acceleration of the molecule is neglected.
3. The effects of past history (that is, the Basset force given by the integral in Eq. 24.4-23) are neglected for the molecule.

In practice, activity coefficients tend to approach unity in dilute solutions, and the Basset forces tend to be small even for large particles. However, the instantaneous effects of acceleration can be appreciable for particles greater than about one micron in diameter.

EXAMPLE 24.4-3

Diffusion of Salts in an Aqueous Solution

Consider now for simplicity a 1-1 electrolyte M^+X^-, such as sodium chloride, diffusing in a system such as that shown in Fig. 24.4-2. Here well-mixed reservoirs at two different salt concentrations are joined by a constriction in which diffusional transfer between the two reservoirs takes place. The potentiometer shown in the figure measures the potential difference $\Delta\phi$ between the electrodes, without drawing any current from the system. Show how the generalized Maxwell–Stefan equations can be used to describe the diffusional behavior.

SOLUTION

The salt (S) is considered to be fully dissociated, so that the system is being regarded as ternary, with M^+, X^-, and water as the three species. We neglect the pressure diffusion term: the reference pressure cRT in Eq. 24.4-1 is approximately 1350 atmospheres under normal ambient conditions, and the pressure differences occurring in systems such as that pictured are of negligible importance.

The assumption of electroneutrality and no current flow provide the following constraints:

$$x_{M^+} = x_{X^-} = x_S = 1 - x_W \tag{24.4-24}$$

$$N_{M^+} = N_X = N_S \tag{24.4-25}$$

Here the mole fractions of the cation M^+ and the anion X^- are equal to that of the salt S.

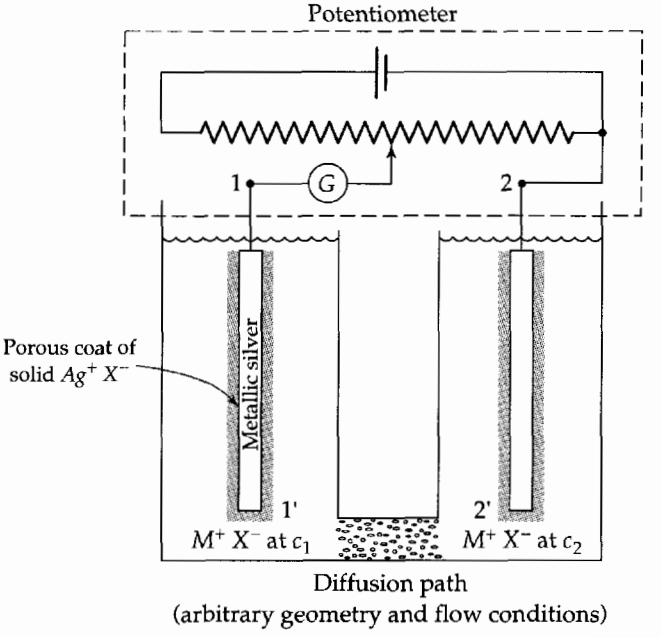

Fig. 24.4-2. Salt diffusion and diffusion potentials. The symbol G denotes a galvonometer.

We may then select species γ in Eq. 24.4-1 to be species α, and use Eqs. 24.4-5 and 24 to obtain for the cation and the anion

$$\frac{1}{c\mathscr{D}_{M^+W}}(x_W N_{M^+} - x_{M^+}N_W) = -x_{M^+}\nabla \ln a_{M^+} + \frac{1}{cRT}\left(\rho_{M^+}\mathbf{g}_{M^+} - \omega_{M^+}\sum_\beta \rho_\beta \mathbf{g}_\beta\right) \tag{24.4-26}$$

$$\frac{1}{c\mathscr{D}_{X^-W}}(x_W N_{X^-} - x_{X^-}N_W) = -x_{X^-}\nabla \ln a_{X^-} + \frac{1}{cRT}\left(\rho_{X^-}\mathbf{g}_{X^-} - \omega_{X^-}\sum_\beta \rho_\beta \mathbf{g}_\beta\right) \tag{24.4-27}$$

Next we use the expression for $\mathbf{g}_\alpha$ in Eq. 24.4-5, as well as Eqs. 24.4-24 and 25, to get:

$$\frac{1}{cD_{M^+W}}(x_W N_S - x_S N_W) = -\left(\frac{\partial \ln a_{M^+}}{\partial \ln x_S}\right)\nabla x_S - \left(\frac{x_S}{RT}\right)F\nabla\phi \tag{24.4-28}$$

$$\frac{1}{c\mathscr{D}_{X^-W}}(x_W N_S - x_S N_W) = -\left(\frac{\partial \ln a_{X^-}}{\partial \ln x_S}\right)\nabla x_S + \left(\frac{x_S}{RT}\right)F\nabla\phi \tag{24.4-29}$$

Note that the ion–ion diffusivity does not appear, because there is no velocity difference between the two ions when there is no current.

The electrostatic potential ϕ may be eliminated between these two equations by adding them together. The resulting flux expression

$$N_S = -\left(\frac{1}{c\mathscr{D}_{M^+W}} + \frac{1}{c\mathscr{D}_{X^-W}}\right)^{-1}\left(\frac{\partial \ln (a_{M^+}a_{X^-})}{\partial \ln x_S}\right)\nabla x_S + x_S(N_S + N_W) \tag{24.4-30}$$

may be put into the form of Fick's law

$$N_S = -c\mathscr{D}_{SW}\nabla x_S + x_S(N_S + N_W) \tag{24.4-31}$$

by introducing the definition of the concentration-based diffusivity

$$\mathscr{D}_{SW} = 2\left(\frac{\mathscr{D}_{M^+W}\mathscr{D}_{X^-W}}{\mathscr{D}_{M^+W} + \mathscr{D}_{X^-W}}\right)\left(1 + \frac{\partial \ln \gamma_S}{\partial \ln x_S}\right) \tag{24.4-32}$$

and, since $a_S = a_{M^+}a_{X^-} = x_S^2\gamma_\pm^2$ and $\gamma_\pm = \sqrt{\gamma_{M^+}\gamma_{X^-}}$,

$$\gamma_S = \gamma_{M^+}\gamma_{X^-} \tag{24.4-33}$$

which is the mean ionic activity coefficient.

The ion-water diffusivities may in turn be estimated from limiting equivalent conductances in the form

$$\lambda_{\alpha\infty} = \lim_{x_\alpha \to 0}\frac{z_\alpha \mathscr{D}_{\alpha W}F^2}{RT} \tag{24.4-34}$$

As a practical matter, diffusivities vary much less with concentration than do conductances, and salt diffusivities can be estimated with fair accuracy up to about 1N concentrations from limiting conductances. A basic reason for this is that ion–ion diffusional interactions, which always occur when a current flows, become appreciable at even modest salt concentrations (see Problem 24C.3).

Eq. 24.4-32 shows that the slower ion tends to dominate in determining the salt diffusivity, and this fact is the justification for treating the protein as a large neutral molecule in Example 24.4-1. Soluble proteins are nearly always charged, but they and their attendant *counter-ions* behave like a neutral salt, and its diffusivity is dominated by the protein moiety, which in turn acts very much like a hydrodynamic particle.

In a concentration gradient, the faster of the two ions tends to get ahead of the slower. However, this results in the formation of a potential gradient tending to speed the slower ion and slow the faster one. It can be shown (see Problem 24B.2) that this so-called *junction potential* is described by

$$\frac{d\phi}{dx_S} = -\frac{RT}{F}\frac{1}{x_S}\left[\frac{(\partial \ln a_{M^+}/\partial \ln x_S)\mathscr{D}_{M^+W} - (\partial \ln a_{X^-}/\partial \ln x_S)\mathscr{D}_{X^-W}}{\mathscr{D}_{M^+W} + \mathscr{D}_{X^-W}}\right] \tag{24.4-35}$$

However, these potentials cannot be measured directly, as the electrodes needed to complete

However, these potentials cannot be measured directly, as the electrodes needed to complete the electric circuit affect the measurement (see Problem 24C.3). One can obtain an approximate value through the use of potassium chloride salt bridges.[5]

This elementary example is only a very bare introduction to a complex and important subject. The interested reader is referred to the large literature on electrochemistry.[6]

EXAMPLE 24.4-4

***Departures from Local Electroneutrality: Electro-Osmosis*[6]**

It is already clear from the preceding discussion of diffusion potential that local departures from electroneutrality do exist in diffusing electrolytes, and they are not always negligible. To examine this situation, consider a long tube of circular cross section containing an electrolyte, at least one component of which is adsorbed on the tube wall. This adsorption results in a fixed surface charge and a region of net charge, the *diffuse double layer*, in the solution adjacent to the tube wall. This net charge will produce an electric field within the tube that varies with radial, but not axial, position. If a potential difference is applied across the ends of the tube, the result will be a fluid flow, known as *electro-osmosis*. Conversely, if a hydrodynamic pressure is used to produce a flow, it will result in a potential difference, known as a *streaming potential*, developing across the ends of the tube. These phenomena are representative of a class known as electrokinetic phenomena. Develop an expression for the electro-osmotic flow developed in the absence of an axial pressure gradient.

SOLUTION

Our first problem is now to develop an expression for the electrostatic potential distribution, after which we can calculate the electro-osmotic flow.

The starting point for the electrostatic potential calculation is the Poisson equation

$$\nabla^2\phi = -\frac{\rho_e}{\varepsilon} \tag{24.4-36}$$

Here ρ_e is the electrical charge density

$$\rho_e = F\sum_{\alpha=1}^{N} z_\alpha c_\alpha \tag{24.4-37}$$

and ε is the dielectric permittivity of the solution. For the problem at hand, Eq. 24.4-36 reduces to

$$\frac{1}{r}\frac{d}{dr}\left(r\frac{d\phi}{dr}\right) = -\frac{\rho_e}{\varepsilon} \tag{24.4-38}$$

Now, following Newman[6] we assume that the concentration of charge follows a Boltzmann distribution

$$\frac{c_\alpha}{c_{\alpha\infty}} = \exp\left(-\frac{z_\alpha F\phi}{RT}\right) \approx 1 - \frac{z_\alpha F\phi}{RT} \tag{24.4-39}$$

and use a truncated Taylor expansion, known as the Debye–Hückel approximation, so that we can obtain an explicit solution. Here the subscript ∞ can be considered to indicate the centerline of the tube, because, as we shall see, the charge density drops off very rapidly with the distance from the tube wall. For the same reason we may neglect the wall curvature and assume that the net charge at the centerline is zero so that

$$\frac{d^2\phi}{dy^2} = \frac{\phi}{\lambda^2} \qquad \text{where } \lambda = \left(\frac{F^2}{\varepsilon RT}\sum_{\alpha=1}^{N} z_\alpha^2 c_{\alpha\infty}\right)^{-1/2} \tag{24.4-40, 41}$$

---

[5] R. A. Robinson and R. H. Stokes, *Electrolyte Solutions*, revised edition, Butterworth, London (1965), p. 571. This venerable reference contains a great detail of useful data.

[6] See, for example, J. S. Newman, *Electrochemical Systems*, 2nd edition, Prentice-Hall, Englewood Cliffs, N.J. (1991). Example 24.4-4 is taken from p. 215.

Here $y = R - r$ is the distance measured into the fluid from the wall, and λ is the *Debye length*, which tends to be very small. Thus for a 1-1 electrolyte

$$\lambda \approx \frac{3.0}{\sqrt{c_S}} \tag{24.4-42}$$

where the units of Debye length λ and the salt concentration c_S are Ångströms and molarity, respectively. Thus for a 0.1 N solution, the Debye length is only about 10 Å. As a result, departures from neutrality can usually be neglected in macroscopic systems. Similarly, concentration imbalances are very small for junction potentials, which are typically no more than tens of millivolts (see also Problem 24C.4).

We now need boundary conditions to integrate Eq. 24.4-38, and the first is just the assumption of electroneutrality at large distances from the wall:

$$\text{B.C. 1:} \quad \text{As } \frac{y}{\lambda} \to \infty, \qquad \phi \to 0 \tag{24.4-43}$$

The second is obtained from Gauss's law (see Newman[6], p. 75), assuming there is no potential gradient within the solid surface itself,

$$\text{B.C. 2:} \quad \text{At } y = 0, \qquad \frac{d\phi}{dy} = -\frac{q_e}{\varepsilon} \tag{24.4-44}$$

where q_e is the surface charge per unit area. Integration of Eq. 24.4-40 then gives

$$\phi = -\frac{q_e}{\lambda} e^{-y/\lambda} \tag{24.4-45}$$

Newman[6] gives a more rigorous development that allows for surface curvature, but for any tube of radius greater than tens of nanometers, this is really not necessary.

We are now ready to put these results into the equation of motion, and we shall here assume steady laminar flow, so that

$$0 = \mu \frac{1}{r} \frac{d}{dr}\left(r \frac{dv_z}{dr}\right) - \frac{dp}{dr} + \rho_e E_z \tag{24.4-46}$$

in which the axial electric field strength is

$$E_z = \frac{\partial \phi}{\partial z} \tag{24.4-47}$$

Neglecting the pressure gradient and using Eq. 24.4-36 to eliminate ρ_e, we find

$$0 = \mu \frac{1}{r} \frac{d}{dr}\left(r \frac{dv_z}{dr}\right) + \varepsilon \frac{1}{r} \frac{d}{dr}\left(r \frac{d\phi}{dr}\right) E_z \tag{24.4-48}$$

Now, if curvature is again neglected, this equation may be integrated to give

$$v_z = \left(\frac{\lambda q_e}{\mu}\right) E_z (1 - e^{-y/\lambda}) \tag{24.4-49}$$

The quantity in the first set of parentheses may be considered to be an experimentally determined property of the system, and $\exp(-y/\lambda)$ is negligible over the bulk of the tube cross section for essentially all tubes. Thus the velocity is uniform except very near the wall.

Such electro-osmotic flows are being widely used in microscopic flow reactors and separators—for example, in diagnostic devices—and they offer the advantage of negligible convective dispersion. Note that the velocity is effectively independent of the tube radius. Thus electro-osmosis especially useful in tubes of small radii, where large pressure gradients would otherwise be required to produce the same flow velocity.

EXAMPLE 24.4-5

Additional Mass Transfer Driving Forces

We have now covered all of the mass transfer mechanisms normally considered in a nonequilibrium thermodynamic framework, but there are other possibilities that have proven significant. Here we consider three: the force on a charged particle moving across a magnetic field, and the forces of electrical or magnetic induction. These contain nonlinear terms—that is, products of species velocities and force fields—and therefore they are, strictly speaking, outside the scope of irreversible thermodynamics. However, it has been found permissible to add them to the body forces appearing in Eq. 24.4-1. Develop a specific form for the resulting equation, and show how it can be used to describe mass transfer processes affected by one or more of these additional forces.

SOLUTION

We begin by defining an extended driving force for mass transfer, $\mathbf{d}_{\alpha,\text{ext}}$, to include these additional forces:

$$\mathbf{d}_{\alpha,\text{ext}} = \mathbf{d}_\alpha + \frac{x_\alpha z_\alpha F}{RT}[\mathbf{v}_\alpha \times \mathbf{B}] + \frac{x_\alpha}{RT}\{\Gamma_\alpha^{\text{el}}[\mathbf{E}\cdot\nabla\mathbf{E}] + \Gamma_\alpha^{\text{mag}}[\mathbf{B}\cdot\nabla\mathbf{B}]\} \tag{24.4-50}$$

Here $\mathbf{B}$ is the magnetic induction, $\mathbf{E} = \nabla\phi$ the electric field, $\Gamma_\alpha^{\text{el}}$ the *electric susceptibility*, and $\Gamma_\alpha^{\text{mag}}$ the *magnetic susceptibility*.

The origin of the terms containing $[\mathbf{v}_\alpha \times \mathbf{B}]$ and $[\mathbf{E}\cdot\nabla\mathbf{E}]$ in Eq. 24.4-50 is in the Lorentz relation

$$\mathbf{F} = q_0(\mathbf{E} + [\mathbf{v}\times\mathbf{B}]) \tag{24.4-51}$$

where q_0 is the electric charge. This is shown explicitly in Eq. 24.4-51 for a charged particle moving through a magnetic field (see Problem 24B.1), but only indirectly for the electric induction $[\mathbf{E}\cdot\nabla\mathbf{E}]$, which is based on the interaction of a *nonuniform field* with an electric dipole.

To show the origin of the $[\mathbf{E}\cdot\nabla\mathbf{E}]$ term in Eq. 24.4-50, consider, for example, the one-dimensional situation pictured in Fig. 24.4-3. An electric field will tend to align dipoles that are normally randomized by Brownian motion, and, if the field is nonuniform, there will be a net force on an aligned dipole of magnitude

$$F_z = q_0\left[\left(E_0 + \frac{l}{2}\frac{\partial E}{\partial z}\right) - \left(E_0 - \frac{l}{2}\frac{\partial E}{\partial z}\right)\right] = q_0 l\frac{\partial E}{\partial z} \tag{24.4-52}$$

where q_0 is the magnitude of the charge at either end of the dipole and l is the distance between the two centers of charge.

In some cases—for example, the zwitterion form of amino acids—one can determine both q_0 and l from molecular theory. However, for particles and most molecules, one finds only *induced dipoles*: a partial charge separation resulting from the presence of the field. Under the conditions of interest here, only a small fraction of intrinsic dipoles is aligned with the field, and both the fractional alignment of these and the strength of the induced dipoles are

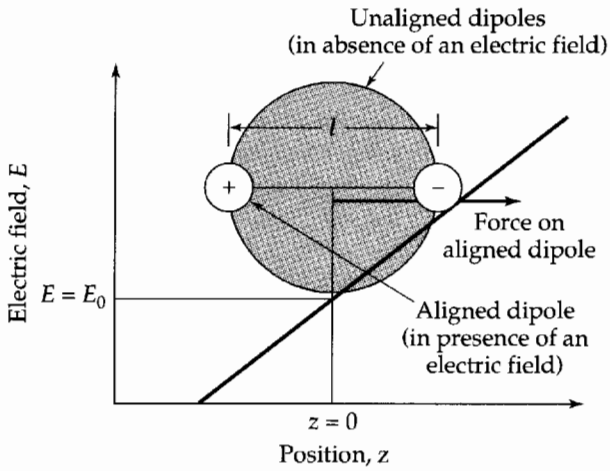

Fig. 24.4-3. Origin of the dielectrophoretic force given in Eq. 24.4-52.

normally assumed to be proportional to the field strength. All these factors are collected into what is usually an experimentally determined quantity, the *electric susceptibility*. The origin of the magnetophoresis term is analogous. We now turn to brief discussions of applications of these new separation mechanisms.

The behavior of ions moving across a magnetic field is the basis of classic mass spectrometry, although time-of-flight mass spectrometers are also in widespread use. Both types of spectrometers are highly developed and find extensive applications for analyzing mixtures from simple inorganic gases to complex nonvolatile biological molecules such as proteins. In fact, where applicable, they provide the most accurate means available for determining protein molecular weight, often within one dalton for a molecular weight typically of the order of tens of thousands.

Both dielectro- and magnetophoresis have long been used on a large process scale for removing small particles suspended in fluids. Nonuniform fields are achieved in the case of dielectrophoresis by using a packing of small dielectric particles, such as glass beads, between electrodes (see, for example, Problem 24B.1). Because particles always move toward the stronger field, one can use alternating current, usually at some tens of kilovolts, and thus avoid electrode reactions. Current flows are extremely small and can normally be neglected. In magnetophoresis, a nonuniform field is achieved by placing ferromagnetic meshes between poles of an electromagnet, which can of course work only with paramagnetic or ferromagnetic materials. A classic example is the removal of color bodies consisting of magnetic iron oxides to whiten clay.

New uses for dielectrophoresis have been developing very rapidly in the fields of biology,[7] advanced materials,[8] including nanotechnology, and environmental monitoring.[9] They include classification, quantitative analysis, and manipulation, including the formation of ordered arrays.

Many of these applications require major extensions of Eq. 24.4-50 to include quadrupolar and even octopolar forces.[10] Moreover, there are strong interactions between electrical forces and hydrodynamics, and both device and particle shape can have profound effects.[11]

§24.5 MASS TRANSFER ACROSS SELECTIVELY PERMEABLE MEMBRANES

Membranes may be viewed physically as thin sheets, usually separating two bulk phases and controlling mass transfer between them. In addition, the membrane is typically kept stationary against external pressure gradients and internal viscous drag by some mechanical constraint, typically a wire mesh or equivalent structure. Membranes consist of

[7] C. Polk, *IEEE Transactions on Plasma Science*, **28**, 6–14 (2000); J. Suehiro et al., *J. Physics D: Applied Physics*, **32**, 2814–2320 (1999); J. P. H. Bert, R. Pethig, and M. S. Talary, *Trans. Inst. Meas. Control*, **20**, 82–91 (1998); A. P. Brown, W. B. Betts, A. B. Harrison, and J. G. O'Neill, *Biosensors and Bioelectronics*, **14**, 341–351 (1999); O. D. Velev and E. W. Kaler, *Langmuir*, **15**, 3693–3698 (1999); T. Yamamoto, et al., *Conference Record, IAS Annual Meeting (IEEE Industry Applications Society)*, **3**, 1933–1940 (1998); M. S. Talary, et al., *Med. and Bio. Eng. and Computing*, **33**, 235–237 (1995); H. Morgan and N. G. Green, *J. Electrostatics*, **42**, 279–293 (1997).

[8] L. Cui and H. Morgan, *J. Micromech. Microeng.*, **10**, 72–79 (2000); M. Hase et al., *Proc. Intl. Soc. Optical Eng.*, **3673**, 133–140 (1999); C. A. Randall, *IEEE Intl. Symp. on Applications of Ferroelectrics*, Piscataway, N.J. (1996).

[9] P. Baron, *ASTM Special Technical Publication*, 147–155 (1999); R. J. Han, O. R. Moss, and B. A. Wong, *Aerosol Sci. Tech.*, 241–258 (1994).

[10] C. Reichle et al., *J. Phys. D: Appl. Phys.*, **32**, 2128–2135 (1999); A. Ramos et al., *J. Electrostatics*, **47**, 71–81 (1999); M Washizu and T. B. Jones, *J. Electrostatics*, **33**, 187–198 (1994); B. Khusid and A. Acrivos, *Phys. Rev. E*, **54**, 5428–5435 (1996).

[11] S. Kim and S. J. Karrila, *Microhydrodynamics*, Butterworth-Heinemann, Boston (1991); D. W. Howard, E. N. Lightfoot, and J. O. Hirschfelder, *AIChE Journal*, **22**, 794–798 (1976).

an insoluble, selectively permeable matrix m and one or more mobile permeating species $\alpha, \beta, \ldots$. Mathematically they are defined by three constraints:

1. Negligible curvature

$$\delta << R_{\text{curv}} \tag{24.5-1}$$

where δ is the membrane thickness, and R_{curv} is the membrane surface radius of curvature. It follows that mass transport is unidirectional and perpendicular to the membrane surface.

2. Immobility of the matrix

$$v_m = 0 \tag{24.5-2}$$

where v_m is the velocity of the matrix, which serves as the coordinate reference.

3. Pseudosteady behavior

$$\frac{\partial c_\alpha}{\partial t} = 0 \tag{25.4-3}$$

where α is any contained species, including the matrix m. This really means that the diffusional response times within the membrane are short compared to those in the adjacent solutions.

We now wish to show how these constraints can be used to specialize the Maxwell–Stefan equations and to produce compact but reliable descriptions of transport in membranes.

We begin by recognizing that the matrix must be considered to be one of the diffusing species, and we choose to use the Maxwell–Stefan equations only for the mobile species. We may then use Eqs. 24.4-1 and 5 and write for a mixture of N mobile species:

$$\sum_{\substack{\beta=1 \\ \beta\neq\alpha}}^{N} \frac{x_\alpha x_\beta}{\mathscr{D}_{\alpha\beta}} (x_\alpha - x_\beta) = -x_\alpha \nabla_{T,p} \ln a_\alpha - x_\alpha \left(\frac{\overline{V}_\alpha}{RT}\right) \nabla p - x_\alpha z_\alpha \left(\frac{F}{RT}\right) \nabla \phi \tag{24.5-4}$$

Note that α has been chosen as the reference species in the equation for each α and that the force holding the membrane stationary—that is, the last term in Eq. 24.4-5—has resulted in the elimination of the mass-fraction term in the expression for pressure diffusion.[1]

We next note that, from a thermodynamic point of view, the number of components is the number of independent *mobile* species in the solutions bathing the membrane, because it is the external solution that determines the state of the membrane at equilibrium. We also recognize that, for most situations, the effective molecular weight of the matrix cannot be determined. We thus define the internal system as including only the mobile species and define mole fractions of these species to sum to unity. However, since the interaction of each species with the membrane is quite significant, we also define $\mathscr{D}'_{\alpha M}$ by

$$\frac{x_M}{\mathscr{D}_{\alpha M}} = \frac{1}{\mathscr{D}'_{\alpha M}} \tag{24.5-5}$$

Equation 24.5-5 completes the specialization of the Maxwell–Stefan equations for membrane transport, but we still have to select a generally applicable set of boundary conditions.

These conditions are obtained by requiring the total "potential" of each species to be continuous across the boundary

$$\left(\frac{\overline{V}_{\alpha,\text{avg}}}{RT}\right)(p_m - p_e) + z_\alpha \left(\frac{F}{RT}\right)(\phi_m - \phi_e) = 0 \tag{24.5-6}$$

---

[1] E. M. Scattergood and E. N. Lightfoot, *Trans. Faraday Soc.*, **64**, 1135–1146 (1968).

Here the subscripts m and e refer to conditions within the membrane and in the external solution, respectively. The activity a_α is to be calculated at the composition of the membrane phase but at the pressure of the external solution, and

$$\overline{V}_{\alpha,\text{avg}} = \frac{1}{p_m - p_e} \int_{p_e}^{p_m} \overline{V}_\alpha dp \tag{24.5-7}$$

In practice, the solutes are normally considered incompressible and $\overline{V}_\alpha$ to be constant across the interface.

Often conditions inside the membrane are very difficult, or even impossible, to determine, and Eq. 24.5-6 is primarily useful under these circumstances to obtain a qualitative understanding of membrane behavior. Partly for this reason complete descriptions of membrane transport are rare (see, however, Scattergood and Lightfoot[1]). Highly simplified, but often directly useful, introductions to membrane transport are available in a variety of sources.[2-4] One venerable approximation, found especially useful by biologists, is that of Kedem and Katchalsky.[5]

However, rapid progress is being made in obtaining fundamental data, and much of this is reported in the *Journal of Membrane Science*. One important area is that of microporous membranes.[6] One can also expect advances in modeling behavior. It has long been known[7] that the generalized Lorentz reciprocal theorem for creeping flows[8] provides a sound basis for extending hydrodynamic diffusion theory of §17.4 to multicomponent diffusion in microporous membranes. Recently developed computational techniques[9] should make the necessary computations tractable enough to provide real predictive power. These techniques can also be used to develop self-assembling structures,[10] which offer new possibilities for highly selective membranes.

This field offers an extremely wide variety of membrane types and of mass transfer processes taking place in them. One can distinguish between biological[11] and synthetic[12] membranes, but there are very wide ranges of composition and behavior within each of these categories. Among the synthetic group there are "homogeneous" membranes, in which the matrix acts as a true solvent for permeating species, and "microporous" membranes, in which the permeating species are confined to matrix-free regions, as well as mixtures of the two types. These factors are important from a materials standpoint, but the formalisms needed to describe their transport behavior are much the same for all.

---

[2] E. L. Cussler, *Diffusion: Mass Transfer in Fluid Systems*, 2nd edition, Cambridge University Press (1997), p. 580.

[3] W. M. Deen, *Analysis of Transport Phenomena*, Oxford University Press (1998), p. 597.

[4] J. D. Seader and E. J. Henley, *Separation Process Principles*, Wiley, New York (1998).

[5] O. Kedem and A. Katchalsky, *Biochem. Biophys. Acta*, **27**, 229 (1958).

[6] K. Kaneko, *J. Membrane Sci.*, **96**, 59–89 (1994); K. Sakai, *J. Membrane Sci.*, **96**, 91–130 (1994); S. Nakao, *J. Membrane Sci.*, **96**, 181–165 (1994).

[7] E. N. Lightfoot, J. B. Bassingthwaighte, and E. F. Grabowski, *Ann. Biomed. Eng.*, **4**, 78–90 (1976).

[8] J. Happel and H. Brenner, *Low Reynolds Number Hydrodynamics*, Prentice-Hall (1965), Martinus Nijhoff (1983), p. 62, p. 85.

[9] S. Kim and S. J. Karrila, *Microhydrodynamics: Principles and Selected Applications*, Butterworth-Heinemann, Boston (1991).

[10] I. Mustakis, S. C. Clear, P. F. Nealey, and S. Kim, *ASME Fluids Engineering Division Summer Meeting*, FEDSM, June 22–26 (1997).

[11] B. Alberts et al., *The Molecular Biology of the Cell*, Garland, New York (1999), Chapters 10 and 11.

[12] W. S. W. Ho and K. K. Sirkar, *Membrane Handbook*, Van Nostrand Reinhold, New York (1992), p. 954; R. D. Noble and S. A. Stern, *Membrane Separations Technology*, Membrane Science and Technology Series, **2**, Elsevier (Amsterdam), p. 718; R. van Reis and A. L. Zydney, "Protein Ultrafiltration" in *Encyclopedia of Bioprocess Technology* (M. C. Flickinger and S. W. Drew, eds.), Wiley, New York (1999), pp. 2197–2214; L. J. Zeman and A. L. Zydney, *Microfiltration and Ultrafiltration*, Marcel Dekker, New York (1996).

There are also a wide variety of process conditions in widespread use. Here we consider only a few examples to illustrate commonly encountered situations.

EXAMPLE 24.5-1

Concentration Diffusion Between Preexisting Bulk Phases

Consider "solute" A diffusing through a membrane placed between binary solutions of solute A in solvent B *under the influence of concentration gradients alone.* This is a commonly encountered situation, including dialysis, blood oxygenation, and many gas-separation systems.[13] There are many variants, including *facilitated diffusion* (see Problem 24C.8). Hemodialysis is a special case, where pressure differences are used to drive water across the membrane, but concentration diffusion of solutes is of primary interest from the present standpoint. Assume for the moment that the flux of solvent, N_B, is already known. Develop an analog to Fick's first law for this system.

SOLUTION

We are primarily concerned here with solute A, and the Maxwell–Stefan equation for it takes the form

$$\frac{x_A v_A}{\mathscr{D}'_{AM}} + \frac{x_A x_B}{\mathscr{D}_{AB}}(v_A - v_B) = -\left[1 + \left(\frac{\partial \ln \gamma_A}{\partial \ln x_A}\right)_{T,p}\right]\frac{dx_A}{dz} \tag{24.5-8}$$

This may be rearranged to give

$$N_A = -c\left(\frac{\mathscr{D}'_{AM}\mathscr{D}_{AB}}{\mathscr{D}'_{AM} + \mathscr{D}_{AB}}\right)\left[1 + \left(\frac{\partial \ln \gamma_A}{\partial \ln x_A}\right)_{T,p}\right]\frac{dx_A}{dz} + x_A(N_A + N_B)\left(\frac{\mathscr{D}'_{AM}}{\mathscr{D}'_{AM} + \mathscr{D}_{AB}}\right) \tag{24.5-9}$$

This is reminiscent of Fick's law, with the first term on the right corresponding to the Fickian diffusive flux and the second to the convective term. However, the effective diffusivity now contains a membrane contribution, and the convective term is now weighted by a ratio of diffusivities. This situation corresponds to the situation pictured in Fig. 24.5-1. The arrow pointing to the right represents the diffusion relative to the solvent, modified by the interaction with the matrix, while the arrow pointing to the left represents the "drag" of the membrane, which tends to reduce the transport relative to the convection occurring in the absence of the membrane matrix—namely, $x_A(N_A + N_B)$. Note that, in general, there are mass transfer boundary layers on both sides of the membrane.

There are several limiting situations of interest. If the membrane interacts only very weakly with the solute, $\mathscr{D}'_{AM} >> \mathscr{D}_{AB}$. Then

$$N_A = -c\mathscr{D}_{AB}\left[1 + \left(\frac{\partial \ln \gamma_A}{\partial \ln x_A}\right)_{T,p}\right]\frac{dx_A}{dz} + x_A(N_A + N_B) \tag{24.5-10}$$

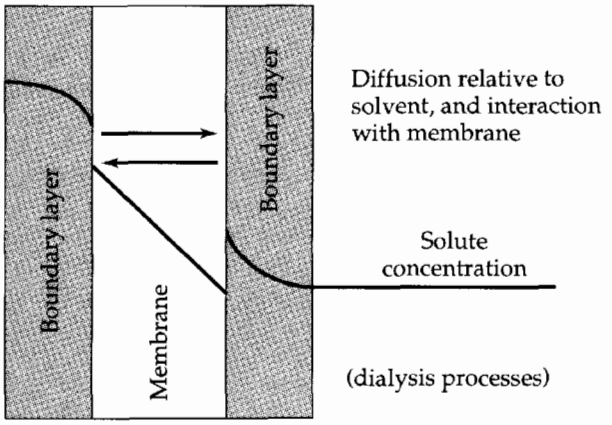

Fig. 24.5-1. Intramembrane mass transport.

[13] W. J. Koros and G. K. Fleming, *J. Membrane Sci.*, **83**, 1–80 (1993).

which is exactly Fick's law. However, it must be remembered that both molar concentration and diffusivity are those in the membrane phase. We next look at a limiting situation, where

$$x_A(N_A + N_B) << N_A \tag{24.5-11}$$

and the distribution between membrane and solution is linear, so that

$$c_{Ae} = K_D c_{Am} \tag{25.5-12}$$

where the subscripts e and m refer to the external solution and membrane phases, respectively, and K_D is the distribution coefficient for the two phases. We may then write

$$N_A = P(c_{Ae0} - c_{Ae\delta}) \tag{24.5-13}$$

where

$$P = K_D D_{A,\text{eff}} \tag{24.5-14}$$

is known as the *membrane permeability*, and

$$D_{A,\text{eff}} = \left(\frac{\mathcal{D}'_{AM}\mathcal{D}_{AB}}{\mathcal{D}'_{AM} + \mathcal{D}_{AB}}\right)\left[1 + \left(\frac{\partial \ln \gamma_A}{\partial \ln x_A}\right)_{T,p}\right] \tag{24.5-15}$$

The subscripts $_{Ae}0$ and $_{Ae}\delta$ refer to the solute concentrations at the "upstream" and "downstream" sides of the membrane.

EXAMPLE 24.5-2

Ultrafiltration and Reverse Osmosis

Now consider the filtration processes, in which it is desired to remove a solvent selectively relative to a solute by pressure-driven flow across a solute-rejecting membrane. Applications include ultrafiltration and reverse osmosis, the former dealing with macromolecular and the latter with small solutes.[14] Microfiltration and nanofiltration are formally similar, but the particulate nature of the entities being removed presents additional complications we do not wish to consider here.[12] Develop a framework for describing solvent flow rate and filtrate composition as functions of driving pressure.

SOLUTION

Inevitably some solute moves through the membrane along with the solvent, as indicated in Fig. 24.5-1, and it will now be necessary to consider the Maxwell–Stefan equations for both species. However, membrane filtration is a complex process requiring a great deal of information to obtain a complete a priori description, and we therefore begin with an overview of characteristic behavior using Fig. 24.5-2 as a point of departure. Here both the flow through the membrane and the composition of the filtrate are shown schematically as functions of the

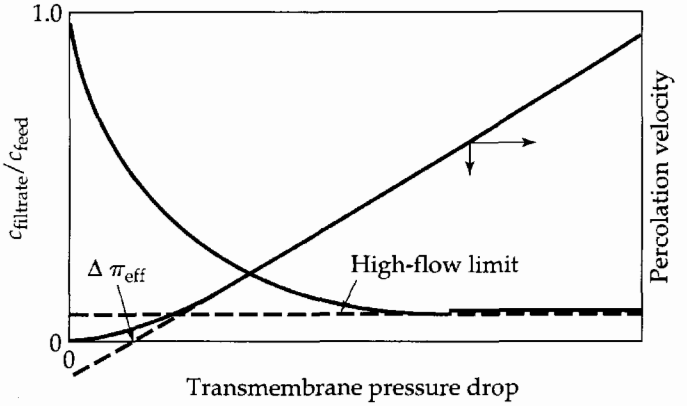

Fig. 24.5-2. Ultrafiltration: flow and solute rejection.

[14] R. J. Petersen, *J. Membrane Sci.*, **83**, 81–150 (1993).

transmembrane pressure drop. First we note that the flow increases with pressure drop, slowly at first, but approaching a linear relation asymptotically, and the asymptote crosses the line of zero velocity at a finite pressure drop, $\Delta\pi_{\text{eff}}$. The ratio of the filtrate solute concentration to the feed concentration drops with increasing pressure drop, from unity toward an asymptote,[15] which is normally much lower than unity. Our main concern in this brief introduction is to explain this characteristic behavior in terms of key thermodynamic and transport behavior.

This situation differs fundamentally from that just described, in that pressure diffusion now comes into play, and in that the downstream solution is produced by the transmembrane mass transfer. Hence the downstream ratio of solute to solvent is the same as the ratio of the corresponding mass transfer rates. There is, therefore, no boundary layer on the downstream side of the membrane, and it is an almost universal practice to use a composite structure. Such composite membranes consist of a very thin selective layer on the upstream face, and a comparatively thick, highly porous, nonselective backing that provides mechanical strength. This backing can be ignored in the present example.

We begin by focusing on the intramembrane behavior for which the Maxwell–Stefan equations, modified from Eq. 24.5-4, assume the forms

$$\frac{x_S x_W}{\mathcal{D}_{SW}}(v_S - v_W) + \frac{x_S v_S}{\mathcal{D}'_{SM}} = -\frac{1}{RT}x_S\nabla_{T,p}(RT\ln a_S) - \frac{c_S\overline{V}_S}{cRT}\nabla p \tag{24.5-16}$$

$$\frac{x_S x_W}{\mathcal{D}_{SW}}(v_W - v_S) + \frac{x_W v_W}{\mathcal{D}'_{WM}} = -\frac{1}{RT}x_W\nabla_{T,p}(RT\ln a_W) - \frac{c_W\overline{V}_W}{cRT}\nabla p \tag{24.5-17}$$

Here the subscripts S and W refer to the partially rejected solute and solvent (usually water) respectively. The terms $x_\alpha\overline{V}_\alpha$ have been replaced by $c_\alpha\overline{V}_\alpha/c$, to make the presence of the volume fractions

$$\phi_\alpha = c_\alpha\overline{V}_\alpha \tag{24.5-18}$$

explicit. In addition, the first term on the right has been rewritten as a reminder that the derivative represents the gradient of the partial molar free energy

$$d\overline{G}_\alpha = RTd\ln a_\alpha \tag{24.5-19}$$

with composition, temperature, and pressure being held constant.

We begin by examining flow behavior, and to do this we add Eqs. 24.5-16 and 17 to get a relation between species transport rates and *intramembrane* pressure gradient

$$\left(\frac{N_S}{c\mathcal{D}'_{SM}} + \frac{N_W}{c\mathcal{D}'_{WM}}\right) = -\frac{1}{cRT}\nabla p_m \tag{24.5-20}$$

The subscript m on pressure is a reminder that we have so far calculated only the pressure drop inside the membrane. Here advantage has been taken of the Gibbs–Duhem equation

$$\sum_\alpha \overline{G}_\alpha dx_\alpha = 0 \tag{24.5-21}$$

and the fact that the volume fractions sum to unity.

To obtain the directly measurable difference between upstream and downstream solution pressures, we must go back to Eq. 24.5-6, which takes the form

$$p_e - p_m = \frac{RT}{\overline{V}_S}\ln\frac{a_{Sm}}{a_{Se}} = \pi_e - \pi_m \tag{24.5-22}$$

---

[15] Actually there is a continuing, very slow drop of filtrate solute concentration even at very high pressure drops, presumably resulting from the compression of the membrane. However, we shall not attempt to deal with this small effect here.

Looking at the upstream side of the membrane, for example, Eq. 24.5-22 states that a finite pressure drop across the membrane interface is required to drive the solute against an increase in the thermodynamic activity. Then the measurable transmembrane pressure drop is

$$\Delta p_{\text{ext}} = \frac{cRT}{\delta}\left(\frac{N_S}{c\mathcal{D}'_{SM}} + \frac{N_W}{c\mathcal{D}'_{WM}}\right) + \Delta\pi_{\text{eff}} \tag{24.5-23}$$

where δ is the membrane thickness, and

$$\Delta\pi_{\text{eff}} = (\pi_{e0} - \pi_{e\delta}) - (\pi_{m0} - \pi_{m\delta}) \tag{24.5-24}$$

where the subscripts 0 and δ refer to the upstream and downstream sides of the membrane, respectively. The intramembrane osmotic pressures are seldom known, but they are substantially smaller than the corresponding solution values (see Problems 24C.7 and 8). At the present state of understanding, Eq. 24.5-24 explains why there is a finite intercept to the asymptotic flow behavior, and an elimination of the membrane contributions provides an upper limit to it. It also provides some insight into intramembrane behavior from experimental observations, but not an a priori prediction of the intercept.

Next we eliminate the pressure gradient from Eq. 24.5-16 with the aid of Eq. 24.5-23

$$N_S\left(\frac{x_W}{c\mathcal{D}_{WS}} - \frac{\phi_S}{c\mathcal{D}'_{SM}}\right) - N_W\left(\frac{x_S}{c\mathcal{D}_{SW}} + \frac{\phi_S}{c\mathcal{D}'_{WM}}\right) = -\left(1 + \frac{\partial \ln \gamma_s}{\partial \ln x_s}\right)\frac{dx_s}{dz} \tag{24.5-25}$$

This expression can be integrated to obtain the solute concentration profile (see, for example, Problems 24C.7 and 8). In general the concentration profile shows an increasingly negative slope in the flow direction, and this feature becomes more pronounced as the flow rate through the membrane increases—that is, as the transmembrane pressure drop becomes larger.

At very low flow rates, N_S and N_W are relatively small and diffusion is relatively fast. There is only a small drop in solute concentration across the membrane, and the result is the poor rejection seen for low pressure drops in Fig. 24.5-2. This behavior is suggested by the zero-flow concentration profile in Fig. 24.5-1.

At very high flow rates, on the other hand, concentration gradients are large and diffusion is weak, except very close to the downstream boundary of the membrane, where a very large negative concentration gradient develops. Near the upstream boundary, the two mass-flux terms are large compared to their difference, and one may neglect concentration gradients in calculating the mass-flux ratio:

$$\frac{N_S}{N_W} \approx \frac{x_S}{x_W}\left(\frac{(1/c\mathcal{D}_{SW}) + (\bar{V}_S/\mathcal{D}'_{WM})}{(1/c\mathcal{D}_{SW}) + (\bar{V}_W/\mathcal{D}'_{SM})}\right) \tag{24.5-26}$$

The bases of solute exclusion now become clear:

1. Thermodynamic exclusion, defined by the ratio x_S/x_W.
2. Frictional differentiation, defined by differences in the interaction terms with the membrane $(\bar{V}_S/\bar{V}_W)(\mathcal{D}'_{SM}/\mathcal{D}'_{WM})$.

Both effects are used in practice and are illustrated in the problems.

EXAMPLE 24.5-3

***Charged Membranes and Donnan Exclusion*[16]**

Consider now membranes containing immobilized charges consisting of polyelectrolyte gels. Such gels contain repeated covalently bound ionic groups, as pictured in Fig. 24.5-3. The membrane interior may then be viewed as a solution containing spatially bound *fixed charges*, mobile *counter-ions*, *invading electrolyte*, and water. For simplicity assume that the fixed

[16] H. Strathmann, "Electrodialysis," Section V in *Membrane Handbook* (W. W. S. Ho and K. K. Sirkar, eds.), Van Nostrand Reinhold, New York (1992).

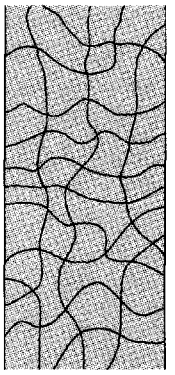

Membrane

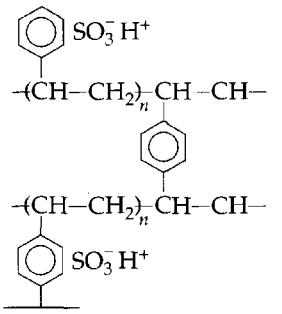

Molecular structure

Fig. 24.5-3. A sulfonic acid based ion-exchange membrane.

charges are anions, written as X^-, and the counter-ions are cations, written as M^+. The external solution is aqueous M^+X^-, and it provides the invading electrolyte M^+X^-. Show how the presence of fixed charges produces an exclusion of invading electrolyte.

SOLUTION

This system is dominated by the behavior at the membrane boundary, and we therefore return to Eq. 24.5-6, written for the water and for the salts S or M^+X^-. The expression for water is

$$\ln \frac{a_{We}}{a_{Wm}} = \frac{\overline{V}_W}{RT}(p_m - p_e) = \frac{\overline{V}_W}{RT}\Delta\pi \tag{24.5-27}$$

where the subscripts e and m refer to the external solution and the membrane, respectively. Since the intramembrane electrolyte concentration is always higher than the external, thus resulting in a lower internal chemical activity for water, the membrane interior is at a higher pressure than the external solution (see, for example, Problem 24B.4).

The corresponding equation for the salt S yields

$$\frac{a_{Se}}{a_{Sm}} = \frac{x_{M^+e}x_{X^-e}}{x_{M^-m}x_{X\ m}}\frac{\gamma_{Se}}{\gamma_{Sm}} = \exp\left(\frac{\overline{V}_S}{RT}\Delta\pi\right) \tag{24.5-28}$$

or

$$\frac{c_{M^+e}c_{X^-e}}{c_{M^+m}c_{X^-m}} = K_D = \frac{\gamma_{Sm}}{\gamma_{Se}}\left(\frac{c_m}{c_e}\right)^2 \exp\left(\frac{\overline{V}_S}{RT}\Delta\pi\right) \tag{24.5-29}$$

It follows that

$$c_{Sm}^2 + c_{Sm}c_{X^-m} = \frac{1}{K_D}c_{Se}^2 \tag{24.5-30}$$

and therefore that the concentration of salt in the membrane phase is less than that in the solution. This suppression of invading electrolyte by the presence of fixed charges is known as *Donnan exclusion* (see Problem 24B.3).

The preponderance of counter-ions, here M^+, inside the membrane, tends to cause them to diffuse out to the external solution, whereas the co-ions, here X^-, tend to diffuse into the membrane. The result is the development of an electrical potential difference between the membrane and external solution. This is normally estimated, by neglecting osmotic effects and assuming activity coefficients of unity, as

$$\phi_m - \phi_e = \left(-\frac{z_{M^+}F}{RT}\right)\ln\frac{x_{M^+m}}{x_{M^+e}} \tag{24.5-31}$$

Equations 24.5-27 to 30 also apply to the relations between solutions on opposite sides of a membrane containing a partially excluded solute on one side, which now corresponds to the membrane phase of the above development. Equation 24.5-31 is often used for lack of knowledge of the neglected effects.

Thus Eq. 24.5-31 is particularly widely used by biologists to explain the origin of the ubiquitous potentials observed across biological membranes.[11] However, the means by which biological membranes can produce and control ion selectivity are extremely sophisticated and are only beginning to be understood.[17]

§24.6 MASS TRANSPORT IN POROUS MEDIA

Porous media are important in many mass transfer applications, some of which, such as catalysis[1] have already been touched on in this text (§18.7), and they exhibit a very wide variety of morphologies.[2,3] Adsorptive processes, such as chromatography, usually take place in granular beds and the absorbent particles themselves are often porous solids. Secondary recovery of crude petroleum typically involves mass transfer in porous rock, and freeze drying, or *lyophilization*, of foods and pharmaceuticals[4] depends on the transport of water vapor through a porous layer of dried solids. Related transport processes occur throughout the large field of particle technology,[5] and, as already indicated in §24.5, some membranes may be considered as microporous structures. Microporous structures abound in living organisms and contribute importantly to both water and solute distribution.[3]

Discussion of porous solids also brings us full circle, back to the discussions of momentum transfer with which this text began. Many of the models used to describe mass transfer in porous media are hydrodynamic in origin, and sometimes the concepts of mass and momentum transfer become blurred.

Predicting the transport of liquids and gases in porous media is a difficult and challenging problem, and no completely satisfactory theory is available. Mass is transported in a porous medium by a variety of mechanisms: (i) by ordinary diffusion, described by the Maxwell–Stefan equations; (ii) by Knudsen diffusion; (iii) by viscous flow according to the Hagen–Poiseuille equation; (iv) by surface diffusion—that is, the creeping of adsorbed molecules along the surfaces of the pores; (v) by thermal transpiration, which is the thermal analog of viscous slip; and (vi) by thermal diffusion. In this discussion, we neglect the last three of these mechanisms.

This problem has been attacked by many investigators,[6] and summarized by others.[7] We give here the principal results of their work. Available models are based either on

---

[17] B. Hill, *Ionic Channels of Excitable Membranes*, Sinauer Associates, Sunderland, Mass. (1992); F. M. Ashcroft, *Ion Channels and Disease: Channelopathies, Academic Press*, New York (1999); D. J. Aidley, *The Physiology of Excitable Cells*, Cambridge University Press (1998).

[1] (a) R. Aris, *The Mathematical Theory of Diffusion and Reaction in Permeable Catalysts*, Vols. 1 and 2 Oxford University Press (1975); (b) O. Levenspiel, *Chemical Reaction Engineering*, 3rd edition, Wiley, New York (1999).

[2] M. Sahimi, *Flow and Transport in Porous Media and Fractured Rock*, Verlagsgesellschaft, Weinheim, Germany (1995); V. Staněk, Fixed Bed Operations, Ellis Horwood, Chichester, England (1994).

[3] F. E. Curry, R. H. Adamson, Bing-Mei Fu, and S. Weinbaum, *Bioengineering Conference* (Sun River, Oregon), ASME, New York (1997).

[4] (a) L. Rey and J. C. May, "Freeze-Drying/Lyophilization of Pharmaceutical and Biological Products" in *Drugs and the Pharmaceutical Sciences* (J. Swarbrick, ed.), Marcel Dekker, New York (1999); (b) P. Sheehan and A. I. Liabis, *Biotech. and Bioeng.*, **60**, 712–728 (1998).

[5] M. Rhodes, *Introduction to Particle Technology*, Wiley, New York (1998).

[6] J. Hoogschagen, *J. Chem. Phys.*, **21**, 2096 (1953), *Ind. Eng. Chem.*, **47**, 906–913 (1955); D. S. Scott and F. A. L. Dullien, *AIChE Journal*, **8**, 113–117 (1962); L. B. Rothfeld, *AIChE Journal*, **9**, 19–24 (1963); P. L. Silveston, *AIChE Journal*, **10**, 132–133 (1964); R. D. Gunn and C. J. King, *AIChE Journal*, **15**, 507–514 (1969); C. Feng and W. E. Stewart, *Ind. Eng. Chem. Fund.*, **12**, 143–147 (1973); C. F. Feng, V. V. Kostrov, and W. E. Stewart, *Ind. Eng. Chem. Fund.*, **13**, 5–9 (1974).

[7] E. A. Mason and R. B. Evans, III, *J. Chem. Ed.*, **46**, 358–364 (1969); R. B. Evans III, L. D. Love, and E. A. Mason, *J. Chem. Ed.*, **46**, 423–427 (1969); R. Jackson, *Transport in Porous Catalysts*, Elsevier, Amsterdam (1977); R. E. Cunningham and R. J. J. Williams, *Diffusion in Gases and Porous Media*, Plenum Press, New York (1980); Chapter 6 of this book gives a summary of the history of the subject of diffusion.

cylindrical channels or aggregates of spheroidal particles, and we shall review a few representative examples here. We shall also restrict the discussion to two limiting situations within the pores of the solid matrix:

(i) *Free-molecule flow of gases*, in which the molecular diameters are short and mean free paths are long relative to the characteristic dimensions of the pores. Under these conditions, there is no significant interaction between the intrapore species.

(ii) *Continuum flow of gases or liquids*, in which both the diameters and the spacing of the intrapore molecules are short compared to the pore dimensions. Here the intrapore fluid can be described by the generalized hydrodynamic theory,[8] and the generalized Maxwell–Stefan equations for multicomponent diffusion can be used.

There are also phenomena for gas transport, known as the *slip-flow* phenomena, in which the mean free paths are comparable to the pore dimensions,[9] but we shall not discuss these here.

Free-Molecule Transport

Transport of rarefied gases is an example of Knudsen flow, already presented in Problem 2B.9. For a long capillary tube of radius a the Knudsen formula takes the form

$$N_A = -\frac{8a}{3}\frac{1}{\sqrt{2\pi M_A RT}}\frac{dp_A}{dz} = -\frac{8a}{3}\sqrt{\frac{RT}{2\pi M_A}}\frac{dc_A}{dz} \tag{24.6-1}$$

Here p_A is the partial pressure of species A in any mixture. Note that Eq. 24.6-1 states that the transport of any individual species under these limiting conditions is unaffected by the presence of others. Thus the total molar flow rate W_A in a tube is proportional to the cube of the tube radius and to the inverse square root of the molecular weight. This dependence on molecular weight is known as *Graham's law*.

Equation 24.6-1 can be rewritten as

$$N_A = -D_{AK}\frac{dc_A}{dz} \tag{24.6-2}$$

which defines the "Knudsen diffusivity" D_{AK}. However, this must be considered as a binary diffusivity for species A relative to the porous medium that is *not* consistent with Fick's law, because the molar flux contains no convective term. As a result D_{AK} is not a state property, containing as it does, the tube radius a. To allow for the tortuous nature of the channels in a porous medium and the limited cross-sectional area available for flow, the flux expression must be further modified by writing

$$\langle N_A \rangle = D_{AK}^{\text{eff}}\frac{dc_A}{dz} \tag{24.6-3}$$

where

$$D_{AK}^{\text{eff}} = (\varepsilon/\tau)D_{AK} \tag{24.6-4}$$

and $\langle N_A \rangle$ is the molar flux based on the total cross section of the porous medium. In this expression ε is the fractional void space in the porous material, and τ is a tortuosity fac-

---

[8] E. N. Lightfoot, J. B. Bassingthwaighte, and E. F. Grabowski, *Ann. Biomed. Eng.*, **4**, 78–90 (1976).

[9] R. Jackson, *Transport in Porous Catalysts*, Elsevier, Amsterdam (1977); R. E. Cunningham and R. J. J. Williams, *Diffusion in Gases and Porous Media*, Plenum Press, New York (1980).

tor. Although models exist[1a,10] for estimating the magnitude of τ, it must normally be determined experimentally.[11]

As an alternative to Eq. 24.6-4 for the effective Knudsen diffusivity, one may treat the aggregate as a collection of large immobile spheres (or "giant gas molecules"), and use the Chapman–Enskog kinetic theory.[12] Problem 24B.6 shows that this approach yields predictions very similar to those of Eq. 24.6-4. There is remarkable model insensitivity.

EXAMPLE 24.6-1

Knudsen Diffusion

Two large well-stirred reservoirs, each of volume V, are joined by a short duct of cross-sectional area S and length L, filled with a porous solid as indicated in Figure 24.6-1. Initially reservoir 1 is filled with hydrogen at uniform pressure p_0 and reservoir 2 with nitrogen, also at p_0. The entire system is maintained at a constant temperature. At time $t = 0$ a small valve in the duct is opened, and the two reservoirs are allowed to equilibrate with each other. Develop an expression for the total pressure in each reservoir as a function of time, assuming that the flow of each gas through the connecting duct follows Eq. 24.6-1, and that the ideal gas law holds throughout the system.

SOLUTION

We begin by assuming quasi-steady-state behavior in the duct so that, for either gas, the rate of transfer from reservoir 1 to reservoir 2 is given by

$$W_A = \frac{(8/3)(\varepsilon/\tau)aS}{L\sqrt{2\pi M_A RT}}(p_{A1} - p_{A2}) \equiv K_A(p_{A1} - p_{A2}) \tag{24.6-5}$$

where W_A is the molar rate of flow of species A (either nitrogen or hydrogen) and a is the effective radius of the pores in the plug joining the two reservoirs. Now a macroscopic mass balance for reservoir 2 gives

$$V\frac{dc_{A2}}{dt} = \frac{V}{RT}\frac{dp_{A2}}{dt} = K_A(p_{A1} - p_{A2}) \tag{24.6-6}$$

or

$$\frac{dp_{A2}}{dt} = \left(K_A\frac{RT}{V}\right)(p_{A1} - p_{A2}) \tag{24.6-7}$$

Now a mass balance over the whole system yields

$$p_{A1} + p_{A2} = p_0 \tag{24.6-8}$$

The initial conditions are that at time $t = 0$,

$$p_{H1} = p_0 \qquad p_{N1} = 0 \qquad p_{H2} = 0 \qquad p_{N2} = p_0 \tag{24.6-9}$$

These initial conditions complete the specification of the system behavior, and we see that the distributions of the two gases are independent of each other.

For *nitrogen* we can define the dimensionless variables $\psi = p_N/p_0$ and $\tau = (RTK_N/V)t$. Then we may write Eq. 24.6-7 for nitrogen in compartment 2

$$\frac{d\psi_{N2}}{d\tau} = 1 - 2\psi_{N2} \tag{24.6-10}$$

with the initial condition $\psi_{N2}(0) = 1$. The solution to this problem is then

$$\psi_{N2} = \tfrac{1}{2}(1 + e^{-2\tau}) \qquad \psi_{N1} = \tfrac{1}{2}(1 - e^{-2\tau}) \tag{24.6-11}$$

---

[10] W. E. Stewart and M. F. L. Johnson, *J. Catalysis*, **4**, 248–252 (1965).

[11] J. B. Butt, *Reaction Kinetics and Reactor Design*, 2nd edition, Marcel Dekker, New York (1999), p. 500, Table 7.4.

[12] R. B. Evans III, G. M. Watson, and E. A. Mason, *J. Chem. Phys.*, **35**, 2076–2083 (1961).

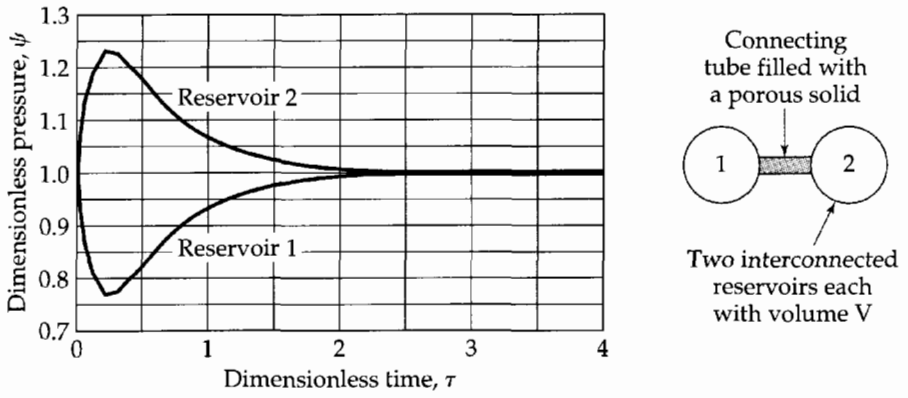

Fig. 24.6-1. Knudsen flow.

For *hydrogen* we note that $K_H = \sqrt{28/2}K_N \approx 3.74K_N$. Hence the differential equation for hydrogen is

$$\frac{d\psi_{H2}}{d\tau} = 3.74(1 - 2\psi_{H2}) \tag{24.6-12}$$

with the initial condition $\psi_{H2}(0) = 0$. The solution to the differential equation is then

$$\psi_{H2} = \tfrac{1}{2}(1 - e^{-7.48\tau}) \qquad \psi_{H1} = \tfrac{1}{2}(1 - e^{-7.48\tau}) \tag{24.6-13}$$

The results are plotted in Fig. 24.6-1.

The ratio $N_A/N_B = -\sqrt{M_B/M_A}$ of molar fluxes obtained here was first observed by Graham[13] in 1833 and rediscovered by Hoogschagen[6] in 1953. Though derived here for Knudsen flow, this relation is valid also for isobaric diffusion well outside the Knudsen region. It has been derived from kinetic theory by several investigators and verified experimentally in tubes and porous media[6,7,13,14] up to very large ratios of passage width to mean free path. Two sets of confirmatory data are shown in Table 24.6-1. In both sets of experiments,[13,14] an apparatus similar to that in Fig. 24.6-1 was used, and various tests gases were used against air. The flux ratios N_{gas}/N_{air} were initial values, when each reservoir contained only air or the test gas.

Continuum Transport

To date, fluid mechanical modeling of intrapore transport has been limited to binary solutions in which molecules of the minor constituent (solute) are large compared to those of the solvent. Models for this situation are based on hydrodynamic diffusion theory extended to porous structures.[8] Descriptions are obtained by solving the creeping flow equations of motion for spheres (representing the solute) through a continuum (representing the solvent) in closed channels.[15] Important effects include partial exclusion of solute at the channel entrance and selective interaction with the channel wall. Result to date are limited to single solutes, but the rapid development of computational techniques[16] should permit extension to more complex systems. Hydrodynamic diffusion

---

[13] T. Graham, *Phil. Mag.*, **2**, 175, 269, 351 (1833). **Thomas Graham** (1805–1869), son of a prosperous manufacturer, attended the University of Glasgow from 1819 to 1826; in 1837, he was named professor of chemistry, University College, London, became a Fellow of the Royal Society in 1834, and in the same year was named Master of the Mint.

[14] E. A. Mason and B. Kronstadt, IMP-ARO(D)-12, University of Maryland, Institute for Molecular Physics, March 20, 1967.

[15] Z.-Y Yan, S. Weinbaum, and R. Pfeffer, *J. Fluid Mech.*, **162**, 415–438 (1986).

[16] S. Kim and S. J. Karrila, *Microhydrodynamics: Principles and Selected Applications*, Butterworth-Heinemann, Boston (1991).

Table 24.6-1 Experimental Verification of Graham's Law [T. Graham, *Phil. Mag.*, **2**, 175, 269, 351 (1833); E. A. Mason and B. Kronstadt, IMP-ARO(D)-12, University of Maryland, Institute for Molecular Physics, March 20, 1967].

	N_{gas}/N_{air}		
Gas	Graham[a]	Mason and Kronstadt[b]	$\left(\frac{M_{air}}{M_{gas}}\right)^{1/2}$
H_2	3.83		3.791
He		2.66 ± 0.01	2.690
CH_4	1.344	1.33 ± 0.01	1.3437
C_2H_4	1.0191		1.0162
CO	1.0149		1.0169
N_2	1.0143	1.02 ± 0.01	1.0168
O_2	0.9487	0.960 ± 0.005	0.9514
H_2S	0.95		0.9219
Ar		0.855 ± 0.011	0.8516
N_2O	0.82		0.8112
CO_2	0.812		0.8113
SO_2	0.68		0.6724

calculations can be used for microporous membranes, but only if there are no significant intermolecular forces between the solutes and the pore walls.

Modeling viscous flow in these systems has already been discussed in §6.4, and it is common practice to describe such a flow, for the low Reynolds numbers of most interest here, by the Blake–Kozeny expression (Eq. 6.4-9) [see however Rhodes[5] (Chapter 5), Sahimi[2] (Chapter 6), Staněk[2] (Chapter 3)]:

$$v_0 = -\frac{D_p^2}{150\mu}\frac{\varepsilon^3}{(1-\varepsilon)^2}\nabla p \tag{24.6-14}$$

Here v_0 is the superficial mass-average velocity. Note from the discussion of §19.2 that the velocity used here is the mass-average velocity of the fluid through the porous material.

To obtain macroscopic descriptions we may use the generalized Maxwell–Stefan equations (Eq. 24.5-4), and we shall restrict ourselves here to concentration- and pressure-driven flow. Moreover, when the mobile species are small relative to pore dimensions, the boundary conditions simplify to continuity of species concentration and pressure at the interface between the external and "intrapore" fluid.

EXAMPLE 24.6-2

Transport from a Binary External Solution

Simplify the Maxwell–Stefan equations for the diffusion of a binary dilute solution, of a large solute species A in a solvent B, through a macroporous medium M, a matrix with pores large compared to the diameters of both mobile species, but small enough that lateral concentration gradients within each pore may be neglected.

SOLUTION

We begin by determining the pressure-flow relationship and note that we have two ways of doing this: the Blake–Kozeny equation (Eq. 24.6-14), and the diffusion-based result (Eq. 24.5-20) of the previous section.

For high velocities through the porous material and pores large relative to molecular dimensions, it is the mass-average velocity that must be proportional to the pressure gradient,

and we may assume that the Blake–Kozeny equation governs the flow. We begin by rewriting Eq. 24.6-14) as

$$\left(\frac{150\mu(1-\varepsilon)^2}{D_p^2\varepsilon^3}\right)(\omega_A v_A + \omega_B v_B) = -\frac{dp}{dz} \tag{24.6-15}$$

and Eq. 24.5-20 as

$$cRT\left(\frac{v_A}{\mathcal{D}'_{AM}} + \frac{v_B}{\mathcal{D}'_{BM}}\right) = -\frac{dp}{dz} \tag{24.6-16}$$

Equating the coefficients of v_A and v_B in these two equations then yields descriptions of $\mathcal{D}'_{AM}$ and $\mathcal{D}'_{BM}$, respectively. If the pores are small relative to the molecular dimensions and the mass-average velocity is not large relative to the diffusional velocities $v_\alpha - v$, one is in a still poorly studied flow region, and one must resort either to experiment or to an appropriate molecular model.[17]

To determine the rate of solute transport, we turn to Eq. 24.5-25 *noting that the diffusivities of that section already include the factor* ε/τ. However, if the pore dimensions are very large with respect to the effective diameters of the solute and solvent molecules, the ratio $\mathcal{D}_{AB}/\mathcal{D}'_{AM}$ will be very small. We can thus obtain

$$N_A x_B - N_B x_A = -c(\varepsilon/\tau)\mathcal{D}_{AB}^{\text{ext}}\nabla x_A \tag{24.6-17}$$

in which

$$\mathcal{D}_{AB}^{\text{ext}} = \mathcal{D}_{AB}^{\text{ext}}\left(1 + \frac{\partial \ln \gamma_A}{\partial \ln x_A}\right) \tag{24.6-18}$$

where the superscript ext refers to conditions in the external solution of the same composition as the pore fluid. Equation 24.6-17 may in turn be rewritten as

$$N_A = -c(\varepsilon/\tau)\mathcal{D}_{AB}^{\text{ext}}\nabla x_A + (N_A + N_B) \tag{24.6-19}$$

which is Fick's first law modified for void fraction and tortuosity. It is widely used.

Exactly as in unconfined fluids, one cannot determine net flow, or pressure drop, from diffusional considerations alone. One needs a flux ratio or equivalent. A specific example is supplied by freeze-drying, where water vapor must diffuse through a porous region of dried solid and where inert gases may be assumed stagnant. This region is also interesting in that conditions can vary from simple continuum diffusion, as here, through the slip-flow region, and on to the Knudsen region.[4b]

It must be remembered that Eq. 24.6-19 and the equations leading up to it represent only the direct effect of molecular diffusion. The convective dispersion resulting from interparticle mixing and local departures from rectilinear flow must be added when using the volume-averaged convective equation (see §20.5, Butt[12] §5.2.5, and Levenspiel[1b] §13.2).

QUESTIONS FOR DISCUSSION

1. How does equilibrium thermodynamics have to be supplemented in order to study non-equilibrium systems, such as those that involve velocity, temperature, and concentration gradients?
2. What new transport coefficients arise in multicomponent mixtures and what do they describe?
3. To what extent does this chapter explain the origin of Eq. 19.3-3? Is that equation completely correct?
4. Is Eq. 24.1-6 really the starting point for the derivation of the complete expressions for the fluxes? Discuss its origin.

---

[17] Z.-Y. Yan, S. Weinbaum, and R. Pfeffer, *J. Fluid Mech.*, **162**, 415–438 (1986).

5. How are the thermal diffusion coefficient, the thermal diffusion ratio, and the Soret coefficient defined? Can the signs of these quantities be predicted a priori?
6. How can one start with Eq. 24.2-8 and obtain Eq. 17.9-1? What restrictions have to be placed on Eq. 17.9-1?
7. What is the proper driving force for diffusion: the gradient of the concentration, the gradient of the activity, or some other quantity?
8. Discuss the Clusius–Dickel column for isotope separation.
9. To describe the steady-state operation of an ultracentrifuge it is not necessary to know any transport properties. Does this seem odd?
10. What various physical phenomena need to be understood in order to describe diffusion in porous media?

PROBLEMS

24A.1. Thermal diffusion.

(a) Estimate the steady-state separation of H_2 and D_2 occurring in the simple thermal diffusion apparatus shown in Fig. 24.2-1 under the following conditions: T_1 is 200K, T_2 is 600K, the mole fraction of deuterium is initially 0.10, and the effective average k_T is 0.0166.

(b) At what temperature should this average k_T have been evaluated?

Answers: **(a)** The mole fraction of H_2 is higher by 0.0183 in the hot bulb
(b) 330K

24A.2. Ultracentrifugation of proteins. Estimate the steady-state concentration profile when a typical albumin solution is subjected to a centrifugal field 50,000 times the force of gravity under the following conditions:

Cell length = 1.0 cm

Molecular weight of albumin = 45,000

Apparent density of albumin in solution = $M_A/\bar{V}_A = 1.34$ g/cm^3

Mole fraction of albumin (at $z = 0$), $x_{A0} = 5 \times 10^{-6}$

Apparent density of water in the solution = 1.00 g/cm^3

Temperature = 75°F

Answer: $x_A = 5 \times 10^{-6} \exp(-22.7z)$, with z in cm

24A.3. Ionic diffusivities. The limiting (that is, at zero concentration) equivalent ionic conductances, in dimensions of cm^2/ohm · g-equiv for the following ions at 25°C are:[1] Na^+, 50.10; K^+, 73.5; Cl^-, 76.35. Calculate the corresponding ionic diffusivities from the definion

$$\mathcal{D}_{iw} = \frac{RT}{F^2}\frac{\lambda_{i0}}{|z_i|} \tag{24A.3-1}$$

Note that F = 96,500 coulombs/g-equiv, RT/F = 25.692 mv at 25°C, and 1 coulomb = 1 ampere · s.

24B.1. The dimensions of the Lorentz force. Show how the Lorentz force on a charge moving through a magnetic field corresponds to the first term added to the linear $\mathbf{d}_\alpha$ of Eq. 25.4-51 and gives a consistent set of units for this quantity. *Suggestion:* Note that $cRT\mathbf{d}_\alpha$ represents the motive force for diffusive motion of species α per unit volume and that the usual dimensions of the magnetic induction are 1 Weber = 1 Newton-second/Coulomb-meter.

24B.2. Junction potentials. Consider two well-mixed reservoirs of aqueous salt at 25°C, as in Fig. 24.4-2, separated by a stagnant region. Salt concentrations are 1.0 N on the left (1) and 0.1 N on the right (2). Estimate junction potentials for NaCl and for KCl using the ion diffusivities

[1] R. A. Robinson and R. H. Stokes, *Electrolyte Solutions*, revised edition, Butterworths, London (1965), Table 6.1.

of Problem 24A.3. Assume constant ion activity coefficients. Which compartment will be the more positive? Why?

24B.3. Donnan exclusion. The sulfonic acid membrane used by Scattergood[2] had the following equilibrium internal composition when immersed in 0.1 N NaCl:

Organic sulfonic acid polymer	$c_{X^-} = 1.03$ g-equiv/liter
Water	$c_w = 13.2$ g-equiv/liter
Chloride ion	$c_{Cl^-} = 0.001$ g-equiv/liter
Sodium ion	$c_{Na^+} = 1.031$ g-equiv/liter

Calculate the distribution coefficient of sodium chloride

$$K_D = \frac{(x_{Na^+}x_{Cl^-})_{\text{external}}}{(x_{Na^+}x_{Cl^-})_{\text{membrane}}} \tag{24B.3-1}$$

Note that the concentration of water in the external solution is about 55.5 g-mol/liter.

Answer: 0.064

24B.4. Osmotic pressure. Typical sea water, containing 3.45% by weight of dissolved salts, has a vapor pressure 1.84% below that of pure water. Estimate the minimum possible transmembrane pressure required to produce pure water, if the membrane is ideally selective.

Answer: about 25 atm

24B.5. Permeability of a perfectly selective filtration membrane. Develop an expression for the hydraulic permeability of the perfectly selective membrane described in Example 22.8-5 in terms of the diffusional parameters introduced in §24.5.

Answer: $K_H = \mathscr{D}'_{wm}/RT\delta$, where δ is the membrane thickness

24B.6. Model insensitivity. In modeling a porous medium as a parallel network of channels one must allow both for the toruous nature ("tortuosity" τ) of real systems and also the restriction of the transport to the fraction ε of the cross section that is available for flow. Equation 24.6-3 then must be modified to

$$\mathbf{N}_A = -\frac{8}{3}\frac{\varepsilon a}{\tau}\frac{1}{\sqrt{2\pi M_A RT}}\nabla p \tag{24B.6-1}$$

An alternate approach is to consider the transport process to be a diffusion of species A through an immobilized set of giant molecules[3] (these particles comprising the porous medium). This model yields the expression

$$\mathbf{N}_A = -\frac{\pi}{4}\left(\frac{1+\frac{1}{8}\pi}{1-\varepsilon}\right)\frac{\varepsilon a}{\tau}\frac{1}{\sqrt{2\pi M_A RT}}\nabla p \tag{24B.6-2}$$

Compare these two equations, noting that the value of ε is often about 0.4.

24C.1. Expressions for the mass flux.

(a) Show how to transform the left side of Eq. 24.2-8 into the left side of Eq. 24.2-9. First rewrite the former as follows:

$$\sum_{\substack{\beta=1\\ \beta\neq\alpha}}^{N}\frac{x_\alpha x_\beta}{\mathscr{D}_{\alpha\beta}}(\mathbf{v}_\gamma - \mathbf{v}_\beta) + x_\alpha(\mathbf{v}_\alpha - \mathbf{v}_\gamma)\sum_{\substack{\beta=1\\ \beta\neq\alpha}}^{N}\frac{x_\beta}{\mathscr{D}_{\alpha\beta}} \tag{24C.1-1}$$

Rewrite the second term as a sum over *all* β, and then add a term to compensate for the modification of the sum. Note that this change has introduced into the sum a term containing $\mathscr{D}_{\alpha\alpha}$,

---

[2] E. M. Scattergood and E. N. Lightfoot, *Trans. Faraday Soc.*, **64**, 1135–1146 (1968).

[3] R. B. Evans, III, G. M. Watson, and E. A. Mason, *J. Chem. Phys.*, **35**, 2076–2083 (1961).

which was not defined because it was not needed. Now, we are at liberty to define $\mathscr{D}_{\alpha\alpha}$ in any way we choose, and the choice we make is

$$\frac{x_\alpha}{\mathscr{D}_{\alpha\alpha}} = -\sum_{\substack{\beta=1\\ \beta\neq\alpha}}^{N} \frac{x_\beta}{\mathscr{D}_{\alpha\beta}} \quad \text{or} \quad \sum_{\substack{\beta=1\\ \text{all } \beta}}^{N} \frac{x_\beta}{\mathscr{D}_{\alpha\beta}} = 0 \tag{24C.1-2, 3}$$

This choice enables us to obtain the left side of Eq. 24.2-9, and also the auxiliary relation given after Eq. 24.2-9 is, in fact, just Eq. 24C.1-3 above.

(b) Next repeat the above derivation by replacing $\mathbf{v}_\beta$ by $[\mathbf{v}_\beta + (D_\beta^T/\rho_\beta)\nabla \ln T]$, and verify that both the diffusion terms and the thermal diffusion terms of Eq. 24.2-8 may be transformed into the corresponding terms in Eq. 24.2-9.

24C.2. Differential centrifugation. The lysing (bursting) of *E. coli* cells has produced a dilute suspension of *inclusion bodies*, hard insoluble aggregates of a desired protein, unlysed cells, and unwanted dissolved proteins. For purposes of this problem all may be considered as spheres with the properties indicated here.

	Cells	Inclusion bodies	Proteins
Mass or equivalent	1.89×10^{-12} g	2.32×10^{-15} g	50 kilodaltons
Density (g/ml)	1.07	1.3	1.3

Can these materials be effectively separated by centrifugation? Explain.

24C.3. Transport characteristics of sodium chloride. In the accompanying table[1] equivalent conductance, diffusivity, and thermodynamic activity coefficients are given for sodium chloride at 25°C. The first two are given as functions of the molarity (M), and the third for molality (m). It may be assumed for the purposes of this problem that $M/m = 1 - 0.019m$. Limiting ionic equivalent conductances (that is, at infinite dilution) are 50.10 and 76.35, respectively. The salt equivalent conductance in turn is defined as

$$\Lambda_S = \lambda_{Na^+} + \lambda_{Cl^-} = K_{sp}/c_S \tag{24C.3-1}$$

where the specific conductance $K_{sp} = L/AR$, where R is the resistance of a volume of solution of length L and cross-sectional area A. Use these data to discuss the sensitivity of the solution behavior to the three diffusivities $\mathscr{D}_{Na^+,W}$, $\mathscr{D}_{Cl^-,W}$, and $\mathscr{D}_{Na^+Cl^-}$ needed to describe this response to solution concentration.

Electrochemical characteristics of aqueous NaCl solution at 25°C

Molar concentration	Equivalent conductance (cm^2/ohm-equiv)	Diffusivity $cm^2/s \times 10^5$	Molal concentration	Activity coefficient
0	126.45	1.61	0	1
0.00055	124.51			
0.001	123.74	1.585		
0.005	120.64			
0.01	118.53			
0.02	115.76			
0.05	111.06	1.507		
0.1	106.74	1.483	0.1	0.778
0.2	101.71	1.475	0.2	0.735
			0.3	0.710
			0.4	0.693
0.5	93.62	1.474	0.5	0.681

Electrochemical characteristics of aqueous NaCl solution at 25°C *(continued)*

Molar concentration	Equivalent conductance (cm^2/ohm-equiv)	Diffusivity $cm^2/s \times 10^5$	Molal concentration	Activity coefficient
			0.6	0.673
			0.7	0.667
			0.8	0.659
			0.9	0.657
1	85.76	1.484	1.0	0.657
			1.2	0.654
			1.4	0.655
1.5	79.86	1.495		
			1.6	0.657
			1.8	0.662
2	74.71	1.516	2.0	0.668
			2.5	0.688
3	65.57	1.563	3.0	0.714
			3.5	0.746
4	57.23		4.0	0.783
			4.5	0.826
5	49.46		5.0	0.874

24C.4. Departures from electroneutrality. Following Newman, estimate the departures from electroneutrality in the stagnant region between the reservoirs of Problem 24B.2 as follows. First calculate the electric field gradient $d^2\phi/dz^2$, where z is the distance measured from reservoir 1 toward reservoir 2, assuming that the salt concentration in g-moles/liter is given by

$$c_s = 1.0 - 0.9\frac{z}{L} \tag{24C.4-1}$$

where L is the length of the stagnant region. Then put the result into Poisson's equation

$$\nabla^2\phi = \frac{F}{\varepsilon}\sum_{i=1}^{N} z_i c_i \tag{24C.4-2}$$

Here ε is the dielectric constant, and F/ε may be taken to be 1.392×10^{16} volt-cm/g-equiv (see Newman[4], pp. 74 and 256), which corresponds to a relative dielectric constant of 78.303. For this problem, the summation reduces to $(c_+ - c_-)$.

24C.5. Dielectrophoretic driving forces. When an electric potential is imposed across an uncharged nonconducting medium, one may write

$$(\nabla \cdot \varepsilon \mathbf{E}) = 0 \tag{24C.5-1}$$

where ε is the dielectric constant.

Show how this equation can be used to calculate the distribution of electric field **E** in the region between two coaxial cylindrical metal electrodes of outer and inner radii R_2 and R_1, respectively. You may neglect variations in the dielectric constant. Toward which electrode will particles of positive susceptibility migrate, and how will their migration velocity vary with position?

[4] J. S. Newman, *Electrochemical Systems*, 2nd edition, Prentice-Hall, New York (1991), p. 256.

24C.6. Effects of small inclusions in a dielectric medium. The production of field nonlinearities by embedded particles can be illustrated by considering the limiting case of a single particle of radius R in an otherwise uniform field. The field distribution in both the external medium and the particle are defined by Laplace's equation, $\nabla^2\phi = 0$, and by the boundary condition on the sphere surface (here the indices s and c stand for sphere and continuum).

$$\varepsilon_s(\boldsymbol{\delta}_r \cdot \nabla\phi_s) = \varepsilon_c(\boldsymbol{\delta}_r \cdot \nabla\phi_c) \tag{24C.6-1}$$

Develop expressions for ϕ_c and ϕ_s, if $\phi_c \rightarrow A r\cos\theta$ for large r.

24C.7. Frictionally induced selective filtration. Describe the glucose rejection behavior of a cellophane[5,6] that shows no thermodynamic rejection. You may assume glucose mole fraction in the feed to the membrane to be 0.01 and the following properties:

$$K_D = 1.0; \qquad \overline{V}_s/\overline{V}_w = 4; \qquad \mathscr{D}'_{wm}/\mathscr{D}'_{gm} = 100; \qquad \mathscr{D}'_{wm}/\mathscr{D}'_{gw} = 25$$

Here the subscripts g, w, and m refer to glucose, water, and the membrane matrix, respectively.
Partial answer: The high-flow-limiting mole fraction of sugar in the filtrate is 0.00242.

24C.8. Thermodynamically induced selective filtration. Describe the behavior of the hypothetical membrane for which $K_D = 1.0$, solute activity coefficients are unity, and $\mathscr{D}'_{sm}/\mathscr{D}'_{wm} = \overline{V}_w/\overline{V}_s$.
Partial answer: The high-flow limiting product solute concentration is 0.1 times that in the feed.

24C.9. Facilitated transport. Consider here the transport of a solute S across a homogeneous membrane from one external solution to another as a complex CS with a carrier C unable to leave the membrane phase. The solute S may be considered to be insoluble in the membrane and convection to be negligible (see Fig. 24C.8). Assume further that:

1. Equilibrium exists at both membrane surfaces according to

$$c_{CS} = K_D c_C c_S \tag{24C.9-1}$$

where the concentration of S is that in the external solution, and those of C and CS are in the membrane.[7]

2. Both C and CS follow the simple rate expression $N_i = D_{im}\Delta c_i$.

Develop a general expression for the transport rate of S in terms of the total amount of carrier plus carrier complex present in the membrane, the solution concentrations of S, the quantity K_D, and the diffusivities. What is the maximum rate of transport of S (that is, as its concentration at the left of the diagram becomes very high and that at the right is zero)?

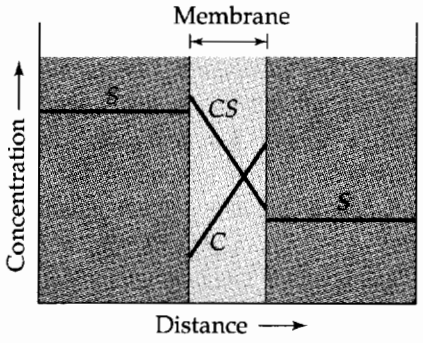

Fig. 24C.8. Elementary facilitated transport. Concentration profiles for the solute (S), the carrier (C), and the complex (CS).

[5] B. Z. Ginzburg and A. Katchalsky, *J. Gen. Physiol.*, **47**, 403–418 (1963).
[6] T. G. Kaufmann and E. F. Leonard, *AIChE Journal*, **14**, 110–117 (1968).
[7] See, however, J. D. Goddard, J. S. Schultz, and R. J. Bassett, *Chem. Eng. Sci.*, **25**, 665–683 (1970), and W. D. Stein, *The Movement of Molecules across Cell Membranes*, Academic Press, New York (1984).

24D.1. Entropy flux and entropy production.

(a) Verify that Eqs. 24.1-3 and 4 follow from Eqs. 24.1-1 and 2.

(b) Show that one can go backward from Eqs. 21.4-5 through 8 to Eqs. 24.1-3 and 4. To do this it may be necessary to use one form of the Gibbs–Duhem equation,

$$\sum_{\alpha=1}^{N} \rho_\alpha \nabla\left(\frac{1}{T}\frac{\overline{G}_\alpha}{M_\alpha}\right) - \frac{1}{T}\nabla p + \sum_{\alpha=1}^{N} \rho_\alpha \frac{\overline{H}_\alpha}{M_\alpha}\frac{1}{T^2}\nabla T = 0 \tag{24D.1-1}$$

Postface

Of all the messages we have tried to convey in this long text, the most important is to recognize the *key role of the equations of change*, developed in Chapters 3, 11, and 19. Written at the microscopic continuum level, they are the key link between the very complex motions of individual molecules and the observable behavior of most systems of engineering interest. They can be used to determine velocity, pressure, temperature, and concentration profile, as well as the fluxes of momentum, energy, and mass, even in complicated time-dependent systems. They are applicable to turbulent systems, and even when complete a priori solutions prove infeasible, simplify the efficient use of data through dimensional analysis. Integrated forms of the equations of change provide the macroscopic balances.

No introductory text can, however, meet the needs of every reader. We have attempted, therefore, to provide *a solid basis in the fundamentals* needed to tackle presently unforeseen applications of transport phenomena in an intelligent way. We have also given extensive references to sources where additional information can be found. Some of these references contain specialized data or introduce powerful problem-solving techniques. Others show how transport analysis can be incorporated into equipment and process design.

We have therefore concentrated on relatively simple examples that illustrate the characteristics of the equations of change and the kinds of questions they are capable of answering. This has required largely neglecting the very powerful numerical techniques available for solving difficult problems. Fortunately, there are now many *monographs on numerical techniques* and packaged programs of greater or lesser generality. Graphics programs are also available, which greatly simplify the presentation of data and simulations.

It should also be recognized that great advances are being made in the molecular theory of transport phenomena, ranging from improved techniques for predicting the transport properties to the development of new materials. *Molecular dynamics and Brownian dynamics simulation techniques* are proving to be very powerful for understanding such varied systems as ultra-low density gases, thin films, small pores, interfaces, colloids, and polymeric liquids.

Simple models of *turbulent transport* have been included, but these are only a modest introduction to a large and important field. Highly sophisticated techniques have been developed for specialized areas, such as predicting the forces and torques on aircraft, the combustion processes in automobiles, and the performance of fluid mixers. It is hoped that the interested reader will not stop with our very limited introductory discussion.

Conversely, we have greatly expanded our coverage of *boundary-layer phenomena*, because its importance and power are now being recognized in many applications. Once primarily the province of aerodynamicists, boundary-layer techniques are now widely used in many fields of heat and mass transfer, as well as in fluid mechanics. Applications abound in such varied fields as catalysis, separation processes, and biology.

Of great and increasing importance is *non-Newtonian behavior*, encountered in the preparation and use of films, lubricants, adhesives, suspensions, and emulsions. Biological examples are exceedingly important, ranging from the operation of the joints to drag-reducing slimes on marine animals, and down to the very basic problem of digesting foodstuffs.

No music and no oral communication would be possible without *compressible flow*, an area we have neglected because of space limitations. Compressible flow is also of critical

importance in the design of airplanes, re-entry vehicles in our space program, and in predicting meteorological phenomena. The awesome destructive power of tornadoes is a challenging example of the latter.

Some problems involving transport phenomena in *chemically reacting systems* have been presented. For simplicity, we have taken the chemical kinetics expressions to be of rather idealized forms. For problems in combustion, flame propagation, and explosion phenomena more realistic descriptions of the kinetics will be needed. The same is true in biological systems, and the understanding of the functioning of the human body will require much more detailed descriptions of the interactions among chemical kinetics, catalysis, diffusion, and turbulence.

In basic terms, each of us is internally powered by the close equivalent of fuel cells, with current carried primarily by cations, in particular protons, rather than electrons. There are also *complex electrical transport phenomena* taking place in the now ubiquitous microelectronic devices such as computers and cellular phones. We have provided a very modest introduction to electrotransport, but again the reader is urged to go on to more specialized sources.

No engineering project can be conceived, let alone completed, purely through use of the descriptive disciplines, such as transport phenomena and thermodynamics. Engineering, in the last analysis, depends heavily on heuristics to supplement incomplete knowledge. Transport phenomena can, however, prove immensely helpful by providing useful approximations, starting with order-of-magnitude estimates, and going on to successively more accurate approximations, such as those provided by boundary-layer theory. It is therefore important, perhaps in a second reading of this text, to seek *shape- and model-insensitive descriptions* by examining the numerical behavior of our model systems.

R. B. B.
W. E. S.
E. N. L.

Appendix A

Vector and Tensor Notation[1]

The physical quantities encountered in transport phenomena fall into three categories: *scalars*, such as temperature, pressure, volume, and time; *vectors*, such as velocity, momentum, and force; and (second-order) *tensors*, such as the stress, momentum flux, and velocity gradient tensors. We distinguish among these quantities by the following notation:

s = scalar (lightface Italic)

$\mathbf{v}$ = vector (boldface Roman)

$\boldsymbol{\tau}$ = second-order tensor (boldface Greek)

In addition, boldface Greek symbols with one subscript (such as $\boldsymbol{\delta}_i$) are vectors.

For vectors and tensors, several different kinds of multiplication are possible. Some of these require the use of special multiplication signs to be defined later: the single dot ($\cdot$), the double dot ($:$), and the cross ($\times$). We enclose these special multiplications, or sums thereof, in different kinds of parentheses to indicate the type of result produced:

( ) = scalar

[ ] = vector

{ } = second-order tensor

No special significance is attached to the kind of parentheses if the only operations enclosed are addition and subtraction, or a multiplication in which $\cdot$, $:$, and $\times$ do not appear. Hence $(\mathbf{v} \cdot \mathbf{w})$ and $(\boldsymbol{\tau}:\nabla\mathbf{v})$ are scalars, $[\nabla \times \mathbf{v}]$ and $[\boldsymbol{\tau} \cdot \mathbf{v}]$ are vectors, and $\{\mathbf{v} \cdot \nabla\boldsymbol{\tau}\}$ and

[1] This appendix is very similar to Appendix A of R. B. Bird, R. C. Armstrong, and O. Hassager, *Dynamics of Polymeric Liquids, Vol. 1, Fluid Mechanics*, 2nd edition, Wiley-Interscience, New York (1987). There, in §8, a discussion of nonorthogonal coordinates is given. Also in Table A.7-4, there is a summary of the del operations for bipolar coordinates.

$\{\boldsymbol{\sigma} \cdot \boldsymbol{\tau} + \boldsymbol{\tau} \cdot \boldsymbol{\sigma}\}$ are second-order tensors. On the other hand, $\mathbf{v} - \mathbf{w}$ may be written as $(\mathbf{v} - \mathbf{w})$, $[\mathbf{v} - \mathbf{w}]$, or $\{\mathbf{v} - \mathbf{w}\}$, since no dot or cross operations appear. Similarly $\mathbf{vw}$, $(\mathbf{vw})$, $[\mathbf{vw}]$, and $\{\mathbf{vw}\}$ are all equivalent.

Actually, scalars can be regarded as zero-order tensors and vectors as first-order tensors. The multiplication signs may be interpreted thus:

Multiplication Sign	Order of Result
None	Σ
$\times$	$\Sigma - 1$
$\cdot$	$\Sigma - 2$
:	$\Sigma - 4$

in which Σ represents the sum of the orders of the quantities being multiplied. For example, $s\boldsymbol{\tau}$ is of the order $0 + 2 = 2$, $\mathbf{vw}$ is of the order $1 + 1 = 2$, $\boldsymbol{\delta}_1\boldsymbol{\delta}_2$ is of the order $1 + 1 = 2$, $[\mathbf{v} \times \mathbf{w}]$ is of the order $1 + 1 - 1 = 1$, $(\boldsymbol{\sigma}:\boldsymbol{\tau})$ is of the order $2 + 2 - 4 = 0$, and $\{\boldsymbol{\sigma} \cdot \boldsymbol{\tau}\}$ is of the order $2 + 2 - 2 = 2$.

The basic operations that can be performed on scalar quantities need not be elaborated on here. However, the laws for the algebra of scalars may be used to illustrate three terms that arise in the subsequent discussion of vector operations:

a. For the multiplication of two scalars, r and s, the order of multiplication is immaterial so that the *commutative* law is valid: $rs = sr$.

b. For the successive multiplication of three scalars, q, r, and s, the order in which the multiplications are performed is immaterial, so that the *associative* law is valid: $(qr)s = q(rs)$.

c. For the multiplication of a scalar s by the sum of scalars p, q, and r, it is immaterial whether the addition or multiplication is performed first, so that the *distributive* law is valid: $s(p + q + r) = sp + sq + sr$.

These laws are not generally valid for the analogous vector and tensor operations described in the following paragraphs.

§A.1 VECTOR OPERATIONS FROM A GEOMETRICAL VIEWPOINT

In elementary physics courses, one is introduced to vectors from a geometrical standpoint. In this section we extend this approach to include the operations of vector multiplication. In §A.2 we give a parallel analytic treatment.

Definition of a Vector and Its Magnitude

A vector $\mathbf{v}$ is defined as a quantity of a given magnitude and direction. The magnitude of the vector is designated by $|\mathbf{v}|$ or simply by the corresponding lightface symbol v. Two vectors $\mathbf{v}$ and $\mathbf{w}$ are equal when their magnitudes are equal and when they point in the same direction; they do not have to be collinear or have the same point of origin. If $\mathbf{v}$ and $\mathbf{w}$ have the same magnitude but point in opposite directions, then $\mathbf{v} = -\mathbf{w}$.

Addition and Subtraction of Vectors

The addition of two vectors can be accomplished by the familiar parallelogram construction, as indicated by Fig. A.1-1a. Vector addition obeys the following laws:

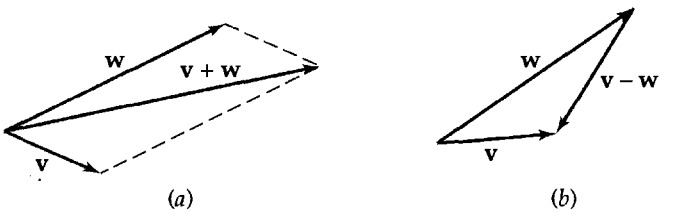

Fig. A.1-1. (*a*) Addition of vectors; (*b*) subtraction of vectors.

Commutative:	$(\mathbf{v} + \mathbf{w}) = (\mathbf{w} + \mathbf{v})$	(A.1-1)
Associative:	$(\mathbf{v} + \mathbf{w}) + \mathbf{u} = \mathbf{v} + (\mathbf{w} + \mathbf{u})$	(A.1-2)

Vector subtraction is performed by reversing the sign of one vector and adding; thus $\mathbf{v} - \mathbf{w} = \mathbf{v} + (-\mathbf{w})$. The geometrical construction for this is shown in Fig. A.1-1b.

Multiplication of a Vector by a Scalar

When a vector is multiplied by a scalar, the magnitude of the vector is altered but its direction is not. The following laws are applicable

Commutative:	$s\mathbf{v} = \mathbf{v}s$	(A.1-3)
Associative:	$r(s\mathbf{v}) = (rs)\mathbf{v}$	(A.1-4)
Distributive	$(q + r + s)\mathbf{v} = q\mathbf{v} + r\mathbf{v} + s\mathbf{v}$	(A.1-5)

Scalar Product (or Dot Product) of Two Vectors

The scalar product of two vectors **v** and **w** is a scalar quantity defined by

$$(\mathbf{v} \cdot \mathbf{w}) = vw \cos \phi_{vw} \tag{A.1-6}$$

in which ϕ_{vw} is the angle between the vectors **v** and **w**. The scalar product is then the magnitude of w multiplied by the projection of **v** on **w**, or vice versa (Fig. A.1-2a). Note that the scalar product of a vector with itself is just the square of the magnitude of the vector

$$(\mathbf{v} \cdot \mathbf{v}) = |\mathbf{v}|^2 = v^2 \tag{A.1-7}$$

The rules governing scalar products are as follows:

Commutative:	$(\mathbf{u} \cdot \mathbf{v}) = (\mathbf{v} \cdot \mathbf{u})$	(A.1-8)
Not Associative:	$(\mathbf{u} \cdot \mathbf{v})\mathbf{w} \neq \mathbf{u}(\mathbf{v} \cdot \mathbf{w})$	(A.1-9)
Distributive:	$(\mathbf{u} \cdot \{\mathbf{v} + \mathbf{w}\}) = (\mathbf{u} \cdot \mathbf{v}) + (\mathbf{u} \cdot \mathbf{w})$	(A.1-10)

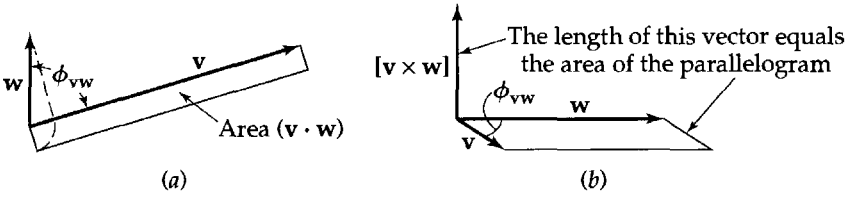

Fig. A.1-2. Products of two vectors: (*a*) the scalar product; (*b*) the vector product.

Vector Product (or Cross Product) of Two Vectors

The vector product of two vectors $\mathbf{v}$ and $\mathbf{w}$ is a vector defined by

$$[\mathbf{v} \times \mathbf{w}] = \{vw \sin \phi_{vw}\}\mathbf{n}_{vw} \tag{A.1-11}$$

in which $\mathbf{n}_{vw}$ is a vector of unit length (a "unit vector") perpendicular to both $\mathbf{v}$ and $\mathbf{w}$ and pointing in the direction that a right-handed screw will move if turned from $\mathbf{v}$ toward $\mathbf{w}$ through the angle ϕ_{vw}. The vector product is illustrated in Fig. A.1-2b. The magnitude of the vector product is just the area of the parallelogram defined by the vectors $\mathbf{v}$ and $\mathbf{w}$. It follows from the definition of the vector product that

$$[\mathbf{v} \times \mathbf{v}] = 0 \tag{A.1-12}$$

Note the following summary of laws governing the vector product operation:

Not Commutative: $$[\mathbf{v} \times \mathbf{w}] = -[\mathbf{w} \times \mathbf{v}] \tag{A.1-13}$$

Not Associative: $$[\mathbf{u} \times [\mathbf{v} \times \mathbf{w}]] \neq [[\mathbf{u} \times \mathbf{v}] \times \mathbf{w}] \tag{A.1-14}$$

Distributive: $$[\{\mathbf{u} + \mathbf{v}\} \times \mathbf{w}] = [\mathbf{u} \times \mathbf{w}] + [\mathbf{v} \times \mathbf{w}] \tag{A.1-15}$$

Multiple Products of Vectors

Somewhat more complicated are multiple products formed by combinations of the multiplication processes just described:

(a) $rs\mathbf{v}$ (b) $s(\mathbf{v} \cdot \mathbf{w})$ (c) $s[\mathbf{v} \times \mathbf{w}]$
(d) $(\mathbf{u} \cdot [\mathbf{v} \times \mathbf{w}])$ (e) $[\mathbf{u} \times [\mathbf{v} \times \mathbf{w}]]$ (f) $([\mathbf{u} \times \mathbf{v}] \cdot [\mathbf{w} \times \mathbf{z}])$
(g) $[[\mathbf{u} \times \mathbf{v}] \times [\mathbf{w} \times \mathbf{z}]]$

The geometrical interpretations of the first three of these are straightforward. The magnitude of $(\mathbf{u} \cdot [\mathbf{v} \times \mathbf{w}])$ can easily be shown to represent the volume of a parallelepiped with edges defined by the vectors $\mathbf{u}$, $\mathbf{v}$, and $\mathbf{w}$.

EXERCISES

1. What are the "orders" of the following quantities: $(\mathbf{v} \cdot \mathbf{w})$, $(\mathbf{v} - \mathbf{u})\mathbf{w}$, $(\mathbf{ab}:\mathbf{cd})$, $[\mathbf{v} \cdot \rho\mathbf{wu}]$, $[[\mathbf{a} \times \mathbf{f}] \times [\mathbf{b} \times \mathbf{g}]]$?
2. Draw a sketch to illustrate the inequality in Eq. A.1-9. Are there any special cases for which it becomes an equality?
3. A mathematical plane surface of area S has an orientation given by a unit normal vector $\mathbf{n}$, pointing downstream of the surface. A fluid of density ρ flows through this surface with a velocity $\mathbf{v}$. Show that the mass rate of flow through the surface is $w = \rho(\mathbf{n} \cdot \mathbf{v})S$.
4. The angular velocity $\mathbf{W}$ of a rotating solid body is a vector whose magnitude is the rate of angular displacement (radians per second) and whose direction is that in which a right-handed screw would advance if turned in the same direction. The position vector $\mathbf{r}$ of a point is the vector from the origin of coordinates to the point. Show that the velocity of any point in a rotating solid body is $\mathbf{v} = [\mathbf{W} \times \mathbf{r}]$, relative to an origin located on the axis of rotation.
5. A constant force $\mathbf{F}$ acts on a body moving with a velocity $\mathbf{v}$, which is not necessarily collinear with $\mathbf{F}$. Show that the rate at which $\mathbf{F}$ does work on the body is $W = (\mathbf{F} \cdot \mathbf{v})$.

§A.2 VECTOR OPERATIONS IN TERMS OF COMPONENTS

In this section a parallel analytical treatment is given to each of the topics presented geometrically in §A.1. In the discussion here we restrict ourselves to rectangular coordinates and label the axes as 1, 2, 3 corresponding to the usual notation of x, y, z; only right-handed coordinates are used.

Many formulas can be expressed compactly in terms of the *Kronecker delta* δ_{ij} and the *permutation symbol* ε_{ijk}. These quantities are defined thus:

$$\begin{cases} \delta_{ij} = +1, & \text{if } i = j \\ \delta_{ij} = 0, & \text{if } i \neq j \end{cases} \tag{A.2-1, A.2-2}$$

$$\begin{cases} \varepsilon_{ijk} = +1, & \text{if } ijk = 123, 231, \text{ or } 312 \\ \varepsilon_{ijk} = -1, & \text{if } ijk = 321, 132, \text{ or } 213 \\ \varepsilon_{ijk} = 0, & \text{if any two indices are alike} \end{cases} \tag{A.2-3, A.2-4, A.2-5}$$

Note also that $\varepsilon_{ijk} = (1/2)(i - j)(j - k)(k - i)$.

Several relations involving these quantities are useful in proving some vector and tensor identities

$$\sum_{j=1}^{3}\sum_{k=1}^{3} \varepsilon_{ijk}\varepsilon_{hjk} = 2\delta_{ih} \tag{A.2-6}$$

$$\sum_{k=1}^{3} \varepsilon_{ijk}\varepsilon_{mnk} = \delta_{im}\delta_{jn} - \delta_{in}\delta_{jm} \tag{A.2-7}$$

Note that a three-by-three determinant may be written in terms of the ε_{ijk}

$$\begin{vmatrix} a_{11} & a_{12} & a_{13} \\ a_{21} & a_{22} & a_{23} \\ a_{31} & a_{32} & a_{33} \end{vmatrix} = \sum_{i=1}^{3}\sum_{j=1}^{3}\sum_{k=1}^{3} \varepsilon_{ijk}a_{1i}a_{2j}a_{3k} \tag{A.2-8}$$

The quantity ε_{ijk} thus selects the necessary terms that appear in the determinant and affixes the proper sign to each term.

The Unit Vectors

Let $\boldsymbol{\delta}_1$, $\boldsymbol{\delta}_2$, $\boldsymbol{\delta}_3$ be the "unit vectors" (i.e., vectors of unit magnitude) in the direction of the 1, 2, 3 axes[1] (Fig. A.2-1). We can use the definitions of the scalar and vector products to tabulate all possible products of each type

$$\begin{cases} (\boldsymbol{\delta}_1 \cdot \boldsymbol{\delta}_1) = (\boldsymbol{\delta}_2 \cdot \boldsymbol{\delta}_2) = (\boldsymbol{\delta}_3 \cdot \boldsymbol{\delta}_3) = 1 \\ (\boldsymbol{\delta}_1 \cdot \boldsymbol{\delta}_2) = (\boldsymbol{\delta}_2 \cdot \boldsymbol{\delta}_3) = (\boldsymbol{\delta}_3 \cdot \boldsymbol{\delta}_1) = 0 \end{cases} \tag{A.2-9, A.2-10}$$

$$\begin{cases} [\boldsymbol{\delta}_1 \times \boldsymbol{\delta}_1] = [\boldsymbol{\delta}_2 \times \boldsymbol{\delta}_2] = [\boldsymbol{\delta}_3 \times \boldsymbol{\delta}_3] = 0 \\ [\boldsymbol{\delta}_1 \times \boldsymbol{\delta}_2] = \boldsymbol{\delta}_3; \quad [\boldsymbol{\delta}_2 \times \boldsymbol{\delta}_3] = \boldsymbol{\delta}_1; \quad [\boldsymbol{\delta}_3 \times \boldsymbol{\delta}_1] = \boldsymbol{\delta}_2 \\ [\boldsymbol{\delta}_2 \times \boldsymbol{\delta}_1] = -\boldsymbol{\delta}_3; \quad [\boldsymbol{\delta}_3 \times \boldsymbol{\delta}_2] = -\boldsymbol{\delta}_1; \quad [\boldsymbol{\delta}_1 \times \boldsymbol{\delta}_3] = -\boldsymbol{\delta}_2 \end{cases} \tag{A.2-11, A.2-12, A.2-13}$$

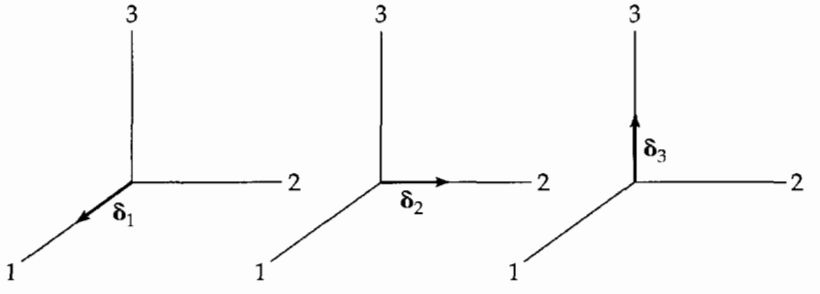

Fig. A.2-1. The unit vectors $\boldsymbol{\delta}_i$; each vector is of unit magnitude and points in the ith direction.

[1] In most elementary texts the unit vectors are called $\boldsymbol{i}$, $\boldsymbol{j}$, $\boldsymbol{k}$. We prefer to use $\boldsymbol{\delta}_1$, $\boldsymbol{\delta}_2$, $\boldsymbol{\delta}_3$ because the components of these vectors are given by the Kronecker delta. That is, the component of $\boldsymbol{\delta}_1$ in the 1-direction is δ_{11} or unity; the component of $\boldsymbol{\delta}_1$ in the 2-direction is δ_{12} or zero.

All of these relations may be summarized by the following two relations:

$$\boxed{(\boldsymbol{\delta}_i \cdot \boldsymbol{\delta}_j) = \delta_{ij}} \tag{A.2-14}$$

$$\boxed{[\boldsymbol{\delta}_i \times \boldsymbol{\delta}_j] = \sum_{k=1}^{3} \varepsilon_{ijk}\boldsymbol{\delta}_k} \tag{A.2-15}$$

in which δ_{ij} is the Kronecker delta, and ε_{ijk} is the permutation symbol defined in the introduction to this section. These two relations enable us to develop analytic expressions for all the common dot and cross operations. In the remainder of this section and in the next section, in developing expressions for vector and tensor operations all we do is to break all vectors up into components and then apply Eqs. A.2-14 and 15.

Expansion of a Vector in Terms of its Components

Any vector **v** can be completely specified by giving the values of its projections v_1, v_2, v_3, on the coordinate axes 1, 2, 3 (Fig. A.2-2). The vector can be constructed by adding vectorially the components multiplied by their corresponding unit vectors:

$$\mathbf{v} = \boldsymbol{\delta}_1 v_1 + \boldsymbol{\delta}_2 v_2 + \boldsymbol{\delta}_3 v_3 = \sum_{i=1}^{3} \boldsymbol{\delta}_i v_i \tag{A.2-16}$$

Note that a *vector associates a scalar with each coordinate direction.*[2] The v_i are called the "components of the vector **v**" and they are scalars, whereas the $\boldsymbol{\delta}_i v_i$ are vectors, which when added together vectorially give **v**.

The magnitude of a vector is given by

$$|\mathbf{v}| = v = \sqrt{v_1^2 + v_2^2 + v_3^2} = \sqrt{\sum_i v_i^2} \tag{A.2-17}$$

Two vectors **v** and **w** are equal if their components are equal: $v_1 = w_1$, $v_2 = w_2$, and $v_3 = w_3$. Also $\mathbf{v} = -\mathbf{w}$, if $v_1 = -w_1$, and so on.

Addition and Subtraction of Vectors

The sum or difference of vectors **v** and **w** may be written in terms of components as

$$\mathbf{v} \pm \mathbf{w} = \sum_i \boldsymbol{\delta}_i v_i \pm \sum_i \boldsymbol{\delta}_i w_i = \sum_i \boldsymbol{\delta}_i (v_i \pm w_i) \tag{A.2-18}$$

Geometrically, this corresponds to adding up the projections of **v** and **w** on each individual axis and then constructing a vector with these new components. Three or more vectors may be added in exactly the same fashion.

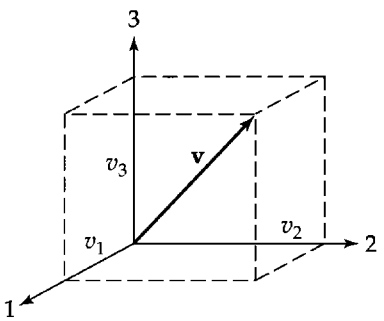

Fig. A.2-2. The components v_i of the vector **v** are the projections of the vector on the coordinate axes 1, 2, and 3.

[2] For a discussion of the relation of this definition of a vector to the definition in terms of the rules for transformation of coordinates, see W. Prager, *Mechanics of Continua*, Ginn, Boston (1961).

Multiplication of a Vector by a Scalar

Multiplication of a vector by a scalar corresponds to multiplying each component of the vector by the scalar:

$$s\mathbf{v} = s\left\{\sum_i \boldsymbol{\delta}_i v_i\right\} = \sum_i \boldsymbol{\delta}_i (s v_i) \tag{A.2-19}$$

Scalar Product (or Dot Product) of Two Vectors

The scalar product of two vectors **v** and **w** is obtained by writing each vector in terms of components according to Eq. A.2-16 and then performing the scalar-product operations on the unit vectors, using Eq. A.2-14

$$\begin{aligned}(\mathbf{v}\cdot\mathbf{w}) &= \left(\left\{\sum_i \boldsymbol{\delta}_i v_i\right\}\cdot\left\{\sum_j \boldsymbol{\delta}_j w_j\right\}\right) = \sum_i\sum_j (\boldsymbol{\delta}_i\cdot\boldsymbol{\delta}_j) v_i w_j \\ &= \sum_i\sum_j \delta_{ij} v_i w_j = \sum_i v_i w_i \end{aligned} \tag{A.2-20}$$

Hence the scalar product of two vectors is obtained by summing the products of the corresponding components of the two vectors. Note that $(\mathbf{v}\cdot\mathbf{v})$ (sometimes written as $\mathbf{v}^2$ or as v^2) is a scalar representing the square of the magnitude of **v**.

Vector Product (or Cross Product) of Two Vectors

The vector product of two vectors **v** and **w** may be worked out by using Eqs. A.2-16 and 15:

$$\begin{aligned}[\mathbf{v}\times\mathbf{w}] &= \left[\left\{\sum_j \boldsymbol{\delta}_j v_j\right\}\times\left\{\sum_k \boldsymbol{\delta}_k w_k\right\}\right] \\ &= \sum_j\sum_k [\boldsymbol{\delta}_j\times\boldsymbol{\delta}_k] v_j w_k = \sum_i\sum_j\sum_k \varepsilon_{ijk}\boldsymbol{\delta}_i v_j w_k \\ &= \begin{vmatrix} \boldsymbol{\delta}_1 & \boldsymbol{\delta}_2 & \boldsymbol{\delta}_3 \\ v_1 & v_2 & v_3 \\ w_1 & w_2 & w_3 \end{vmatrix} \end{aligned} \tag{A.2-21}$$

Here we have made use of Eq. A.2-8. Note that the ith-component of $[\mathbf{v}\times\mathbf{w}]$ is given by $\sum_j\sum_k \varepsilon_{ijk} v_j w_k$; this result is often used in proving vector identities.

Multiple Vector Products

Expressions for the multiple products mentioned in §A.1 can be obtained by using the preceding analytical expressions for the scalar and vector products. For example, the product $(\mathbf{u}\cdot[\mathbf{v}\times\mathbf{w}])$ may be written

$$(\mathbf{u}\cdot[\mathbf{v}\times\mathbf{w}]) = \sum_i u_i [\mathbf{v}\times\mathbf{w}]_i = \sum_i\sum_j\sum_k \varepsilon_{ijk} u_i v_j w_k \tag{A.2-22}$$

Then, from Eq. A.2-8, we obtain

$$(\mathbf{u}\cdot[\mathbf{v}\times\mathbf{w}]) = \begin{vmatrix} u_1 & u_2 & u_3 \\ v_1 & v_2 & v_3 \\ w_1 & w_2 & w_3 \end{vmatrix} \tag{A.2-23}$$

The magnitude of $(\mathbf{u}\cdot[\mathbf{v}\times\mathbf{w}])$ is the volume of a parellelepiped defined by the vectors **u**, **v**, **w** drawn from a common origin. Furthermore, the vanishing of the determinant is a necessary and sufficient condition that the vectors **u**, **v**, and **w** be coplanar.

The Position Vector

The usual symbol for the position vector—that is, the vector specifying the location of a point in space—is **r**. The components of **r** are then x_1, x_2, and x_3, so that

$$\mathbf{r} = \sum_i \boldsymbol{\delta}_i x_i \tag{A.2-24}$$

This is an irregularity in the notation, since the components have a symbol different from that for the vector. The magnitude of **r** is usually called $r = \sqrt{x_1^2 + x_2^2 + x_3^2}$, and this r is the radial coordinate in spherical coordinates (see Fig. A.6-1).

EXAMPLE A.2-1

Proof of a Vector Identity

The analytical expressions for dot and cross products may be used to prove vector identities; for example, verify the relation

$$[\mathbf{u} \times [\mathbf{v} \times \mathbf{w}]] = \mathbf{v}(\mathbf{u} \cdot \mathbf{w}) - \mathbf{w}(\mathbf{u} \cdot \mathbf{v}) \tag{A.2-25}$$

SOLUTION

The i-component of the expression on the left side can be expanded as

$$[\mathbf{u} \times [\mathbf{v} \times \mathbf{w}]]_i = \sum_j \sum_k \varepsilon_{ijk} u_j [\mathbf{v} \times \mathbf{w}]_k = \sum_j \sum_k \varepsilon_{ijk} u_j \left\{ \sum_l \sum_m \varepsilon_{klm} v_l w_m \right\}$$

$$= \sum_j \sum_k \sum_l \sum_m \varepsilon_{ijk} \varepsilon_{klm} u_j v_l w_m = \sum_j \sum_k \sum_l \sum_m \varepsilon_{ijk} \varepsilon_{lmk} u_j v_l w_m \tag{A.2-26}$$

We may now use Eq. A.2-7 to complete the proof

$$[\mathbf{u} \times [\mathbf{v} \times \mathbf{w}]]_i = \sum_j \sum_l \sum_m (\delta_{il}\delta_{jm} - \delta_{im}\delta_{jl}) u_j v_l w_m = v_i \sum_j \sum_m \delta_{jm} u_j w_m - w_i \sum_j \sum_l \delta_{jl} u_j v_l$$

$$= v_i \sum_j u_j w_j - w_i \sum_l u_j v_j = v_i(\mathbf{u} \cdot \mathbf{w}) - w_i(\mathbf{u} \cdot \mathbf{v}) \tag{A.2-27}$$

which is just the i-component of the right side of Eq. A.2-25. In a similar way one may verify such identities as

$$(\mathbf{u} \cdot [\mathbf{v} \times \mathbf{w}]) = (\mathbf{v} \cdot [\mathbf{w} \times \mathbf{u}]) \tag{A.2-28}$$

$$([\mathbf{u} \times \mathbf{v}] \cdot [\mathbf{w} \times \mathbf{z}]) = (\mathbf{u} \cdot \mathbf{w})(\mathbf{v} \cdot \mathbf{z}) - (\mathbf{u} \cdot \mathbf{z})(\mathbf{v} \cdot \mathbf{w}) \tag{A.2-29}$$

$$[[\mathbf{u} \times \mathbf{v}] \times [\mathbf{w} \times \mathbf{z}]] = ([\mathbf{u} \times \mathbf{v}] \cdot \mathbf{z})\mathbf{w} - ([\mathbf{u} \times \mathbf{v}] \cdot \mathbf{w})\mathbf{z} \tag{A.2-30}$$

EXERCISES

1. Write out the following summations:

   (a) $\sum_{k=1}^{3} k^2$ **(b)** $\sum_{k=1}^{3} a_k^2$ **(c)** $\sum_{j=1}^{3} \sum_{k=1}^{3} a_{jk} b_{kj}$ **(d)** $\left(\sum_{j=1}^{3} a_j \right)^2 = \sum_{j=1}^{3} \sum_{k=1}^{3} a_j a_k$

2. A vector **v** has components $v_x = 1$, $v_y = 2$, $v_z = -5$. A vector **w** has components $w_x = 3$, $w_y = -1$, $w_z = 1$. Evaluate:

   (a) $(\mathbf{v} \cdot \mathbf{w})$

   (b) $[\mathbf{v} \times \mathbf{w}]$

   (c) The length of **v**

   (d) $(\boldsymbol{\delta}_1 \cdot \mathbf{v})$

   (e) $[\boldsymbol{\delta}_1 \times \mathbf{w}]$

   (f) $\phi_{\mathbf{vw}}$

   (g) $[\mathbf{r} \times \mathbf{v}]$, where **r** is the position vector.

3. Evaluate: **(a)** $([\boldsymbol{\delta}_1 \times \boldsymbol{\delta}_2] \cdot \boldsymbol{\delta}_3)$ **(b)** $[[\boldsymbol{\delta}_2 \times \boldsymbol{\delta}_3] \times [\boldsymbol{\delta}_1 \times \boldsymbol{\delta}_3]]$.

4. Show that Eq. A.2-6 is valid for the particular case $i = 1, h = 2$.
   Show that Eq. A.2-7 is valid for the particular case $i = j = m = 1, n = 2$.
5. Verify that $\sum_{j=1}^{3} \sum_{k=1}^{3} \varepsilon_{ijk}\alpha_{jk} = 0$ if $\alpha_{jk} = \alpha_{kj}$.
6. Explain carefully the statement after Eq. A.2-21 that the ith component of $[\mathbf{v} \times \mathbf{w}]$ is $\sum_j \sum_k \varepsilon_{ijk} v_j w_k$.
7. Verify that $([\mathbf{v} \times \mathbf{w}] \cdot [\mathbf{v} \times \mathbf{w}]) + (\mathbf{v} \cdot \mathbf{w})^2 = v^2 w^2$ (the "identity of Lagrange").

§A.3 TENSOR OPERATIONS IN TERMS OF COMPONENTS

In the last section we saw that expressions could be developed for all common dot and cross operations for vectors by knowing how to write a vector $\mathbf{v}$ as a sum $\sum_i \boldsymbol{\delta}_i v_i$, and by knowing how to manipulate the unit vectors $\boldsymbol{\delta}_i$. In this section we follow a parallel procedure. We write a tensor $\boldsymbol{\tau}$ as a sum $\sum_i \sum_j \boldsymbol{\delta}_i \boldsymbol{\delta}_j \tau_{ij}$, and give formulas for the manipulation of the unit dyads $\boldsymbol{\delta}_i \boldsymbol{\delta}_j$; in this way, expressions are developed for the commonly occurring dot and cross operations for tensors.

The Unit Dyads

The unit vectors $\boldsymbol{\delta}_i$ were defined in the preceding discussion and then the *scalar products* $(\boldsymbol{\delta}_i \cdot \boldsymbol{\delta}_j)$ and *vector products* $[\boldsymbol{\delta}_i \times \boldsymbol{\delta}_j]$ were given. There is a third kind of product that can be formed with the unit vectors—namely, the *dyadic products* $\boldsymbol{\delta}_i \boldsymbol{\delta}_j$ (written without multiplication symbols). According to the rules of notation given in the introduction to Appendix A, the products $\boldsymbol{\delta}_i \boldsymbol{\delta}_j$ are tensors of the second order. Since $\boldsymbol{\delta}_i$ and $\boldsymbol{\delta}_j$ are of unit magnitude, we will refer to the products $\boldsymbol{\delta}_i \boldsymbol{\delta}_j$ as *unit dyads*. Whereas each unit vector in Fig. A.2-1 represents a single coordinate direction, the unit dyads in Fig. A.3-1 represent *ordered* pairs of coordinate directions.

(In physical problems we often work with quantities that require the simultaneous specification of two directions. For example, the flux of x-momentum across a unit area of surface perpendicular to the y direction is a quantity of this type. Since this quantity is sometimes not the same as the flux of y-momentum perpendicular to the x direction, it is evident that specifying the two directions is not sufficient; we must also agree on the order in which the directions are given.)

The dot and cross products of unit vectors were introduced by means of the geometrical definitions of these operations. The analogous operations for the unit dyads are introduced formally by relating them to the operations for unit vectors

$$(\boldsymbol{\delta}_i \boldsymbol{\delta}_j : \boldsymbol{\delta}_k \boldsymbol{\delta}_l) = (\boldsymbol{\delta}_j \cdot \boldsymbol{\delta}_k)(\boldsymbol{\delta}_i \cdot \boldsymbol{\delta}_l) = \delta_{jk}\delta_{il} \tag{A.3-1}$$

$$[\boldsymbol{\delta}_i \boldsymbol{\delta}_j \cdot \boldsymbol{\delta}_k] = \boldsymbol{\delta}_i (\boldsymbol{\delta}_j \cdot \boldsymbol{\delta}_k) = \boldsymbol{\delta}_i \delta_{jk} \tag{A.3-2}$$

$$[\boldsymbol{\delta}_i \cdot \boldsymbol{\delta}_j \boldsymbol{\delta}_k] = (\boldsymbol{\delta}_i \cdot \boldsymbol{\delta}_j)\boldsymbol{\delta}_k = \delta_{ij}\boldsymbol{\delta}_k \tag{A.3-3}$$

$$\{\boldsymbol{\delta}_i \boldsymbol{\delta}_j \cdot \boldsymbol{\delta}_k \boldsymbol{\delta}_l\} = \boldsymbol{\delta}_i (\boldsymbol{\delta}_j \cdot \boldsymbol{\delta}_k)\boldsymbol{\delta}_l = \delta_{jk}\boldsymbol{\delta}_i \boldsymbol{\delta}_l \tag{A.3-4}$$

$$\{\boldsymbol{\delta}_i \boldsymbol{\delta}_j \times \boldsymbol{\delta}_k\} = \boldsymbol{\delta}_i [\boldsymbol{\delta}_j \times \boldsymbol{\delta}_k] = \sum_{l=1}^{3} \varepsilon_{jkl} \boldsymbol{\delta}_i \boldsymbol{\delta}_l \tag{A.3-5}$$

$$\{\boldsymbol{\delta}_i \times \boldsymbol{\delta}_j \boldsymbol{\delta}_k\} = [\boldsymbol{\delta}_i \times \boldsymbol{\delta}_j]\boldsymbol{\delta}_k = \sum_{l=1}^{3} \varepsilon_{ijk} \boldsymbol{\delta}_l \boldsymbol{\delta}_k \tag{A.3-6}$$

These results are easy to remember: one simply takes the dot (or cross) product of the nearest unit vectors on either side of the dot (or cross); in Eq. A.3-1 two such operations are performed.

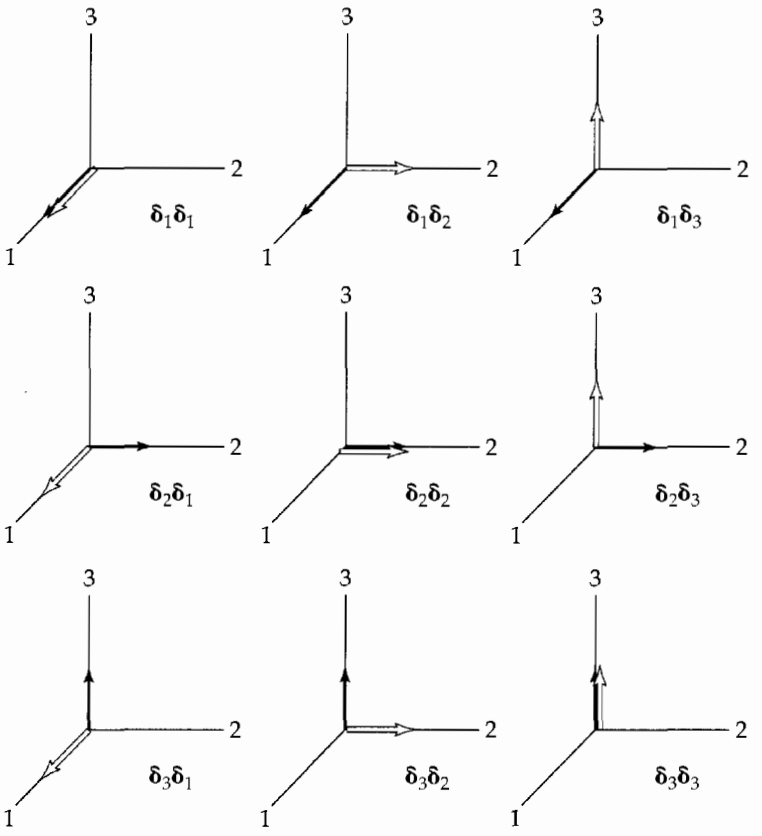

Fig. A.3-1. The unit dyads $\boldsymbol{\delta}_i\boldsymbol{\delta}_j$. The solid arrows represent the first unit vector in the dyadic product, and the hollow vectors the second. Note that $\boldsymbol{\delta}_1\boldsymbol{\delta}_2$ is not the same as $\boldsymbol{\delta}_2\boldsymbol{\delta}_1$.

Expansion of a Tensor in Terms of Its Components

In Eq. A.2-16 we expanded a vector in terms of its components, each component being multiplied by the appropriate unit vector. Here we extend this idea and define[1] a (second-order) tensor as *a quantity that associates a scalar with each ordered pair of coordinate directions* in the following sense:

$$\begin{aligned}\boldsymbol{\tau} &= \boldsymbol{\delta}_1\boldsymbol{\delta}_1\tau_{11} + \boldsymbol{\delta}_1\boldsymbol{\delta}_2\tau_{12} + \boldsymbol{\delta}_1\boldsymbol{\delta}_3\tau_{13} \\ &\quad + \boldsymbol{\delta}_2\boldsymbol{\delta}_1\tau_{21} + \boldsymbol{\delta}_2\boldsymbol{\delta}_2\tau_{22} + \boldsymbol{\delta}_2\boldsymbol{\delta}_3\tau_{23} \\ &\quad + \boldsymbol{\delta}_3\boldsymbol{\delta}_1\tau_{31} + \boldsymbol{\delta}_3\boldsymbol{\delta}_2\tau_{32} + \boldsymbol{\delta}_3\boldsymbol{\delta}_3\tau_{33} \\ &= \sum_{i=1}^{3}\sum_{j=1}^{3}\boldsymbol{\delta}_i\boldsymbol{\delta}_j\tau_{ij}\end{aligned} \tag{A.3-7}$$

The scalars τ_{ij} are referred to as the "components of the tensor $\boldsymbol{\tau}$."

There are several special kinds of second-order tensors worth noting:

1. If $\tau_{ij} = \tau_{ji}$, the tensor is said to be *symmetric*.
2. If $\tau_{ij} = -\tau_{ji}$, the tensor is said to be *antisymmetric*.
3. If the components of a tensor are taken to be the components of $\boldsymbol{\tau}$, but with the indices transposed, the resulting tensor is called the *transpose* of $\boldsymbol{\tau}$ and given the symbol $\boldsymbol{\tau}^\dagger$:

$$\boldsymbol{\tau}^\dagger = \sum_i\sum_j \boldsymbol{\delta}_i\boldsymbol{\delta}_j\tau_{ji} \tag{A.3-8}$$

[1] Tensors are often defined in terms of the transformation rules; the connections between such a definition and that given above is discussed by W. Prager, *Mechanics of Continua*, Ginn, Boston (1961).

4. If the components of the tensor are formed by ordered pairs of the components of two vectors **v** and **w**, the resulting tensor is called the *dyadic product of* **v** and **w** and given the symbol **vw**:

$$\mathbf{vw} = \sum_i \sum_j \boldsymbol{\delta}_i \boldsymbol{\delta}_j v_i w_j \tag{A.3-9}$$

Note that $\mathbf{vw} \neq \mathbf{wv}$, but that $(\mathbf{vw})^\dagger = \mathbf{wv}$.

5. If the components of the tensor are given by the Kronecker delta δ_{ij}, the resulting tensor is called the *unit tensor* and given the symbol $\boldsymbol{\delta}$:

$$\boldsymbol{\delta} = \sum_i \sum_j \boldsymbol{\delta}_i \boldsymbol{\delta}_j \delta_{ij} \tag{A.3-10}$$

The magnitude of a tensor is defined by

$$|\boldsymbol{\tau}| = \tau = \sqrt{\tfrac{1}{2}(\boldsymbol{\tau}:\boldsymbol{\tau}^\dagger)} = \sqrt{\tfrac{1}{2}\sum_i \sum_j \tau_{ij}^2} \tag{A.3-11}$$

Addition of Tensors and Dyadic Products

Two tensors are added thus:

$$\boldsymbol{\sigma} + \boldsymbol{\tau} = \sum_i \sum_j \boldsymbol{\delta}_i \boldsymbol{\delta}_j \sigma_{ij} + \sum_i \sum_j \boldsymbol{\delta}_i \boldsymbol{\delta}_j \tau_{ij} = \sum_i \sum_j \boldsymbol{\delta}_i \boldsymbol{\delta}_j (\sigma_{ij} + \tau_{ij}) \tag{A.3-12}$$

That is, the sum of two tensors is that tensor whose components are the sums of the corresponding components of the two tensors. The same is true for dyadic products.

Multiplication of a Tensor by a Scalar

Multiplication of a tensor by a scalar corresponds to multiplying each component of the tensor by the scalar:

$$s\boldsymbol{\tau} = s\left\{\sum_i \sum_j \boldsymbol{\delta}_i \boldsymbol{\delta}_j \tau_{ij}\right\} = \sum_i \sum_j \boldsymbol{\delta}_i \boldsymbol{\delta}_j \{s\tau_{ij}\} \tag{A.3-13}$$

The same is true for dyadic products.

The Scalar Product (or Double Dot Product) of Two Tensors

Two tensors may be multiplied according to the double dot operation

$$(\boldsymbol{\sigma}:\boldsymbol{\tau}) = \left(\left\{\sum_i \sum_j \boldsymbol{\delta}_i \boldsymbol{\delta}_j \sigma_{ij}\right\}:\left\{\sum_k \sum_l \boldsymbol{\delta}_k \boldsymbol{\delta}_l \tau_{kl}\right\}\right) = \sum_i \sum_j \sum_k \sum_l (\boldsymbol{\delta}_i \boldsymbol{\delta}_j : \boldsymbol{\delta}_k \boldsymbol{\delta}_l) \sigma_{ij} \tau_{kl}$$
$$= \sum_i \sum_j \sum_k \sum_l \delta_{il} \delta_{jk} \sigma_{ij} \tau_{kl} = \sum_i \sum_j \sigma_{ij} \tau_{ji} \tag{A.3-14}$$

in which Eq. A.3-1 has been used. Similarly, we may show that

$$(\boldsymbol{\tau}:\mathbf{vw}) = \sum_i \sum_j \tau_{ij} v_j w_i \tag{A.3-15}$$

$$(\mathbf{uv}:\mathbf{wz}) = \sum_i \sum_j u_i v_j w_j z_i \tag{A.3-16}$$

The Tensor Product (the Single Dot Product) of Two Tensors

Two tensors may also be multiplied according to the single dot operation

$$\{\boldsymbol{\sigma}\cdot\boldsymbol{\tau}\} = \left\{\left(\sum_i\sum_j \boldsymbol{\delta}_i\boldsymbol{\delta}_j\sigma_{ij}\right)\cdot\left(\sum_k\sum_l \boldsymbol{\delta}_k\boldsymbol{\delta}_l\tau_{kl}\right)\right\} = \sum_i\sum_j\sum_k\sum_l [\boldsymbol{\delta}_i\boldsymbol{\delta}_j\cdot\boldsymbol{\delta}_k\boldsymbol{\delta}_l]\sigma_{ij}\tau_{kl}$$
$$= \sum_i\sum_j\sum_k\sum_l \delta_{jk}\boldsymbol{\delta}_i\boldsymbol{\delta}_l\sigma_{ij}\tau_{kl} = \sum_i\sum_l \boldsymbol{\delta}_i\boldsymbol{\delta}_l\left(\sum_j \sigma_{ij}\tau_{jl}\right) \tag{A.3-17}$$

That is, the il-component of $\{\boldsymbol{\sigma}\cdot\boldsymbol{\tau}\}$ is $\sum_j \sigma_{ij}\tau_{jl}$. Similar operations may be performed with dyadic products. It is common practice to write $\{\boldsymbol{\sigma}\cdot\boldsymbol{\sigma}\}$ as $\boldsymbol{\sigma}^2$, $\{\boldsymbol{\sigma}\cdot\boldsymbol{\sigma}^2\}$ as $\boldsymbol{\sigma}^3$, and so on.

The Vector Product (or Dot Product) of a Tensor with a Vector

When a tensor is dotted into a vector, we get a vector

$$[\boldsymbol{\tau}\cdot\mathbf{v}] = \left[\left\{\sum_i\sum_j \boldsymbol{\delta}_i\boldsymbol{\delta}_j\tau_{ij}\right\}\cdot\left\{\sum_k \boldsymbol{\delta}_k v_k\right\}\right] = \sum_i\sum_j\sum_k [\boldsymbol{\delta}_i\boldsymbol{\delta}_j\cdot\boldsymbol{\delta}_k]\tau_{ij}v_k$$
$$= \sum_i\sum_j\sum_k \boldsymbol{\delta}_i\delta_{jk}\tau_{ij}v_k = \sum_i \boldsymbol{\delta}_i\left\{\sum_j \tau_{ij}v_j\right\} \tag{A.3-18}$$

That is, the ith component of $[\boldsymbol{\tau}\cdot\mathbf{v}]$ is $\sum_j \tau_{ij}v_j$. Similarly, the ith component of $[\mathbf{v}\cdot\boldsymbol{\tau}]$ is $\sum_j v_j\tau_{ji}$. Clearly, $[\boldsymbol{\tau}\cdot\mathbf{v}] \neq [\mathbf{v}\cdot\boldsymbol{\tau}]$ unless $\boldsymbol{\tau}$ is symmetric.

Recall that when a vector $\mathbf{v}$ is multiplied by a scalar s, the resultant vector $s\mathbf{v}$ points in the same direction as $\mathbf{v}$ but has a different length. However, when $\boldsymbol{\tau}$ is dotted into $\mathbf{v}$, the resultant vector $[\boldsymbol{\tau}\cdot\mathbf{v}]$ differs from $\mathbf{v}$ in *both* length and direction; that is, the tensor $\boldsymbol{\tau}$ "deflects" or "twists" the vector $\mathbf{v}$ to form a new vector pointing in a different direction.

The Tensor Product (or Cross Product) of a Tensor with a Vector

When a tensor is crossed with a vector, we get a tensor:

$$\{\boldsymbol{\tau}\times\mathbf{v}\} = \left\{\left(\sum_i\sum_j \boldsymbol{\delta}_i\boldsymbol{\delta}_j\tau_{ij}\right)\times\left(\sum_k \boldsymbol{\delta}_k v_k\right)\right\} = \sum_i\sum_j\sum_k [\boldsymbol{\delta}_i\boldsymbol{\delta}_j\times\boldsymbol{\delta}_k]\tau_{ij}v_k$$
$$= \sum_i\sum_j\sum_k\sum_l \varepsilon_{jkl}\boldsymbol{\delta}_i\boldsymbol{\delta}_l\tau_{ij}v_k = \sum_i\sum_l \boldsymbol{\delta}_i\boldsymbol{\delta}_l\left\{\sum_j\sum_k \varepsilon_{jkl}\tau_{ij}v_k\right\} \tag{A.3-19}$$

Hence, the il-component of $\{\boldsymbol{\tau}\times\mathbf{v}\}$ is $\sum_j\sum_k \varepsilon_{jkl}\tau_{ij}v_k$. Similarly the lk-component of $\{\mathbf{v}\times\boldsymbol{\tau}\}$ is $\sum_i\sum_j \varepsilon_{ijl}v_i\tau_{jk}$.

Other Operations

From the preceding results, it is not difficult to prove the following identities:

$$[\boldsymbol{\delta}\cdot\mathbf{v}] = [\mathbf{v}\cdot\boldsymbol{\delta}] = \mathbf{v} \tag{A.3-20}$$
$$[\mathbf{uv}\cdot\mathbf{w}] = \mathbf{u}(\mathbf{v}\cdot\mathbf{w}) \tag{A.3-21}$$
$$[\mathbf{w}\cdot\mathbf{uv}] = (\mathbf{w}\cdot\mathbf{u})\mathbf{v} \tag{A.3-22}$$
$$(\mathbf{uv}:\mathbf{wz}) = (\mathbf{uw}:\mathbf{vz}) = (\mathbf{u}\cdot\mathbf{z})(\mathbf{v}\cdot\mathbf{w}) \tag{A.3-23}$$
$$(\boldsymbol{\tau}:\mathbf{uv}) = ([\boldsymbol{\tau}\cdot\mathbf{u}]\cdot\mathbf{v}) \tag{A.3-24}$$
$$(\mathbf{uv}:\boldsymbol{\tau}) = (\mathbf{u}\cdot[\mathbf{v}\cdot\boldsymbol{\tau}]) \tag{A.3-25}$$

EXERCISES

1. The components of a symmetric tensor $\boldsymbol{\tau}$ are

$$\begin{array}{lll} \tau_{xx} = 3 & \tau_{xy} = 2 & \tau_{xz} = -1 \\ \tau_{yx} = 2 & \tau_{yy} = 2 & \tau_{yz} = 1 \\ \tau_{zx} = -1 & \tau_{zy} = 1 & \tau_{zz} = 4 \end{array}$$

The components of a vector $\mathbf{v}$ are

$$v_x = 5 \qquad v_y = 3 \qquad v_z = -2$$

Evaluate

(a) $[\boldsymbol{\tau} \cdot \mathbf{v}]$ **(b)** $[\mathbf{v} \cdot \boldsymbol{\tau}]$ **(c)** $(\boldsymbol{\tau}:\boldsymbol{\tau})$

(d) $(\mathbf{v} \cdot [\boldsymbol{\tau} \cdot \mathbf{v}])$ **(e)** $\mathbf{vv}$ **(f)** $[\boldsymbol{\tau} \cdot \boldsymbol{\delta}_1]$

2. Evaluate

(a) $[[\boldsymbol{\delta}_1\boldsymbol{\delta}_2 \cdot \boldsymbol{\delta}_2] \times \boldsymbol{\delta}_1]$ **(c)** $(\boldsymbol{\delta}:\boldsymbol{\delta})$

(b) $(\boldsymbol{\delta}:\boldsymbol{\delta}_1\boldsymbol{\delta}_2)$ **(d)** $\{\boldsymbol{\delta} \cdot \boldsymbol{\delta}\}$

3. If $\boldsymbol{\alpha}$ is symmetrical and $\boldsymbol{\beta}$ is antisymmetrical, show that $(\boldsymbol{\alpha}:\boldsymbol{\beta}) = 0$.

4. Explain carefully the statement after Eq. A.3-17 that the il-component of $\{\boldsymbol{\sigma} \cdot \boldsymbol{\tau}\}$ is $\sum_j \sigma_{ij}\tau_{jl}$.

5. Consider a rigid structure composed of point particles joined by massless rods. The particles are numbered 1, 2, 3, . . . , N, and the particle masses are m_ν ($\nu = 1, 2, \ldots, N$). The locations of the particles with respect to the center of mass are $\mathbf{R}_\nu$. The entire structure rotates on an axis passing through the center of mass with an angular velocity $\mathbf{W}$. Show that the angular momentum with respect to the center of mass is

$$\mathbf{L} = \sum_\nu m_\nu[\mathbf{R}_\nu \times [\mathbf{W} \times \mathbf{R}_\nu]] \tag{A.3-26}$$

Then show that the latter expression may be rewritten as

$$\mathbf{L} = [\boldsymbol{\Phi} \cdot \mathbf{W}] \tag{A.3-27}$$

where

$$\boldsymbol{\Phi} = \sum_\nu m_\nu\{(\mathbf{R}_\nu \cdot \mathbf{R}_\nu)\boldsymbol{\delta} - \mathbf{R}_\nu\mathbf{R}_\nu\} \tag{A.3-28}$$

is the *moment-of-inertia tensor*.

6. The kinetic energy of rotation of the rigid structure in Exercise 5 is

$$K = \sum_\nu \tfrac{1}{2}m_\nu(\dot{\mathbf{R}}_\nu \cdot \dot{\mathbf{R}}_\nu) \tag{A.3-29}$$

where $\dot{\mathbf{R}}_\nu = [\mathbf{W} \times \mathbf{R}_\nu]$ is the velocity of the νth particle. Show that

$$K = \tfrac{1}{2}(\boldsymbol{\Phi}:\mathbf{WW}) \tag{A.3-30}$$

§A.4 VECTOR AND TENSOR DIFFERENTIAL OPERATIONS

The vector differential operator ∇, known as "nabla" or "del," is defined in rectangular coordinates as

$$\nabla = \boldsymbol{\delta}_1\frac{\partial}{\partial x_1} + \boldsymbol{\delta}_2\frac{\partial}{\partial x_2} + \boldsymbol{\delta}_3\frac{\partial}{\partial x_3} = \sum_i \boldsymbol{\delta}_i\frac{\partial}{\partial x_i} \tag{A.4-1}$$

in which the $\boldsymbol{\delta}_i$ are the unit vectors and the x_i are the variables associated with the 1, 2, 3 axes (i.e., the x_1, x_2, x_3 are the Cartesian coordinates normally referred to as x, y, z). The symbol ∇ is a vector-operator—it has components like a vector but it cannot stand alone;

it must operate on a scalar, vector, or tensor function. In this section we summarize the various operations of ∇ on scalars, vectors, and tensors. As in §§A.2 and A.3, we decompose vectors and tensors into their components and then use Eqs. A.2-14 and 15, and Eqs. A.3-1 to 6. Keep in mind that in this section equations written out in component form are valid only for rectangular coordinates, for which the unit vectors $\boldsymbol{\delta}_i$ are constants; curvilinear coordinates are discussed in §§A.6 and 7.

The Gradient of a Scalar Field

If s is a scalar function of the variables x_1, x_2, x_3, then the operation of ∇ on s is

$$\nabla s = \boldsymbol{\delta}_1 \frac{\partial s}{\partial x_1} + \boldsymbol{\delta}_2 \frac{\partial s}{\partial x_2} + \boldsymbol{\delta}_3 \frac{\partial s}{\partial x_3} = \sum_i \boldsymbol{\delta}_i \frac{\partial s}{\partial x_i} \tag{A.4-2}$$

The vector thus constructed from the derivatives of s is designated by ∇s (or grad s) and is called the *gradient* of the scalar field s. The following properties of the gradient operation should be noted.

Not Commutative: $$\nabla s \neq s\nabla \tag{A.4-3}$$

Not Associative: $$(\nabla r)s \neq \nabla(rs) \tag{A.4-4}$$

Distributive: $$\nabla(r + s) = \nabla r + \nabla s \tag{A.4-5}$$

The Divergence of a Vector Field

If the vector $\mathbf{v}$ is a function of the space variables x_1, x_2, x_3, then a scalar product may be formed with the operator ∇; in obtaining the final form, we use Eq. A.2-14:

$$\begin{aligned}(\nabla \cdot \mathbf{v}) &= \left(\left\{\sum_i \boldsymbol{\delta}_i \frac{\partial}{\partial x_i}\right\} \cdot \left\{\sum_j \boldsymbol{\delta}_j v_j\right\}\right) = \sum_i \sum_j (\boldsymbol{\delta}_i \cdot \boldsymbol{\delta}_j) \frac{\partial}{\partial x_i} v_j \\ &= \sum_i \sum_j \delta_{ij} \frac{\partial}{\partial x_i} v_j = \sum_i \frac{\partial v_i}{\partial x_i}\end{aligned} \tag{A.4-6}$$

This collection of derivatives of the components of the vector $\mathbf{v}$ is called the *divergence* of $\mathbf{v}$ (sometimes abbreviated div $\mathbf{v}$). Some properties of the divergence operator should be noted

Not Commutative: $$(\nabla \cdot \mathbf{v}) \neq (\mathbf{v} \cdot \nabla) \tag{A.4-7}$$

Not Associative: $$(\nabla \cdot s\mathbf{v}) \neq (\nabla s \cdot \mathbf{v}) \tag{A.4-8}$$

Distributive: $$(\nabla \cdot \{\mathbf{v} + \mathbf{w}\}) = (\nabla \cdot \mathbf{v}) + (\nabla \cdot \mathbf{w}) \tag{A.4-9}$$

The Curl of a Vector Field

A cross product may also be formed between the ∇ operator and the vector $\mathbf{v}$, which is a function of the three space variables. This cross product may be simplified by using Eq. A.2-15 and written in a variety of forms

$$\begin{aligned}[\nabla \times \mathbf{v}] &= \left[\left\{\sum_j \boldsymbol{\delta}_j \frac{\partial}{\partial x_j}\right\} \times \left\{\sum_k \boldsymbol{\delta}_k v_k\right\}\right] \\ &= \sum_j \sum_k [\boldsymbol{\delta}_j \times \boldsymbol{\delta}_k] \frac{\partial}{\partial x_j} v_k = \sum_i \sum_j \sum_k \varepsilon_{ijk} \boldsymbol{\delta}_i \frac{\partial}{\partial x_j} v_k \\ &= \begin{vmatrix} \boldsymbol{\delta}_1 & \boldsymbol{\delta}_2 & \boldsymbol{\delta}_3 \\ \dfrac{\partial}{\partial x_1} & \dfrac{\partial}{\partial x_2} & \dfrac{\partial}{\partial x_3} \\ v_1 & v_2 & v_3 \end{vmatrix} \\ &= \boldsymbol{\delta}_1\left\{\frac{\partial v_3}{\partial x_2} - \frac{\partial v_2}{\partial x_3}\right\} + \boldsymbol{\delta}_2\left\{\frac{\partial v_1}{\partial x_3} - \frac{\partial v_3}{\partial x_1}\right\} + \boldsymbol{\delta}_3\left\{\frac{\partial v_2}{\partial x_1} - \frac{\partial v_1}{\partial x_2}\right\}\end{aligned} \tag{A.4-10}$$

The vector thus constructed is called the *curl* of **v**. Other notations for $[\nabla \times \mathbf{v}]$ are curl **v** and rot **v**, the latter being common in the German literature. The curl operation, like the divergence, is distributive but not commutative or associative. Note that the ith component of $[\nabla \times \mathbf{v}]$ is $\Sigma_j \Sigma_k \varepsilon_{ijk}(\partial/\partial x_j)v_k$.

The Gradient of a Vector Field

In addition to the scalar product $(\nabla \cdot \mathbf{v})$ and the vector product $[\nabla \times \mathbf{v}]$ one may also form the dyadic product $\nabla\mathbf{v}$:

$$\nabla\mathbf{v} = \left\{\sum_i \boldsymbol{\delta}_i \frac{\partial}{\partial x_i}\right\}\left\{\sum_j \boldsymbol{\delta}_j v_j\right\} = \sum_i \sum_j \boldsymbol{\delta}_i\boldsymbol{\delta}_j \frac{\partial}{\partial x_i} v_j \tag{A.4-11}$$

This is called the *gradient* of the vector **v** and is sometimes written grad **v**. It is a second-order tensor whose ij-component[1] is $(\partial/\partial x_i)v_j$. Its transpose is

$$(\nabla\mathbf{v})^\dagger = \sum_i \sum_j \boldsymbol{\delta}_i\boldsymbol{\delta}_j \frac{\partial}{\partial x_j} v_i \tag{A.4-12}$$

whose ij-component is $(\partial/\partial x_j)v_i$. Note that $\nabla\mathbf{v} \neq \mathbf{v}\nabla$ and $(\nabla\mathbf{v})^\dagger \neq \mathbf{v}\nabla$.

The Divergence of a Tensor Field

If the tensor $\boldsymbol{\tau}$ is a function of the space variables x_1, x_2, x_3, then a vector product may be formed with operator ∇; in obtaining the final form we use Eq. A.3-3:

$$\begin{aligned}[\nabla \cdot \boldsymbol{\tau}] &= \left[\left\{\sum_i \boldsymbol{\delta}_i \frac{\partial}{\partial x_i}\right\} \cdot \left\{\sum_j \sum_k \boldsymbol{\delta}_j\boldsymbol{\delta}_k\tau_{jk}\right\}\right] = \sum_i \sum_j \sum_k [\boldsymbol{\delta}_i \cdot \boldsymbol{\delta}_j\boldsymbol{\delta}_k] \frac{\partial}{\partial x_i}\tau_{jk} \\ &= \sum_i \sum_j \sum_k \delta_{ij}\boldsymbol{\delta}_k \frac{\partial}{\partial x_i}\tau_{jk} = \sum_k \boldsymbol{\delta}_k\left\{\sum_i \frac{\partial}{\partial x_i}\tau_{ik}\right\}\end{aligned} \tag{A.4-13}$$

This is called the *divergence* of the tensor $\boldsymbol{\tau}$, and is sometimes written div $\boldsymbol{\tau}$. The kth component of $[\nabla \cdot \boldsymbol{\tau}]$ is $\sum_i (\partial/\partial x_i)\tau_{ik}$. If $\boldsymbol{\tau}$ is the product $s\mathbf{vw}$, then

$$[\nabla \cdot s\mathbf{vw}] = \sum_k \boldsymbol{\delta}_k\left\{\sum_i \frac{\partial}{\partial x_i}(sv_iw_k)\right\} \tag{A.4-14}$$

The Laplacian of a Scalar Field

If we take the divergence of a gradient of the scalar function s, we obtain

$$\begin{aligned}(\nabla \cdot \nabla s) &= \left(\left\{\sum_i \boldsymbol{\delta}_i \frac{\partial}{\partial x_i}\right\} \cdot \left\{\sum_j \boldsymbol{\delta}_j \frac{\partial s}{\partial x_j}\right\}\right) \\ &= \sum_i \sum_j \delta_{ij} \frac{\partial}{\partial x_i}\frac{\partial s}{\partial x_j} = \left\{\sum_i \frac{\partial^2}{\partial x_i^2} s\right\}\end{aligned} \tag{A.4-15}$$

The collection of differential operators operating on s in the last line is given the symbol ∇^2; hence in rectangular coordinates

$$(\nabla \cdot \nabla) = \nabla^2 = \frac{\partial^2}{\partial x_1^2} + \frac{\partial^2}{\partial x_2^2} + \frac{\partial^2}{\partial x_3^2} \tag{A.4-16}$$

This is called the *Laplacian* operator. (Some authors use the symbol Δ for the Laplacian operator, particularly in the older German literature; hence $(\nabla \cdot \nabla s)$, $(\nabla \cdot \nabla)s$, $\nabla^2 s$, and Δs

[1] *Caution:* Some authors define the ij-component of $\nabla\mathbf{v}$ to be $(\partial/\partial x_j)v_i$.

are all equivalent quantities.) The Laplacian operator has only the distributive property, as do the gradient, divergence, and curl.

The Laplacian of a Vector Field

If we take the divergence of the gradient of the vector function $\mathbf{v}$, we obtain

$$\begin{aligned}[\nabla \cdot \nabla \mathbf{v}] &= \left[\left\{\sum_i \boldsymbol{\delta}_i \frac{\partial}{\partial x_i}\right\} \cdot \left\{\sum_j \sum_k \boldsymbol{\delta}_j \boldsymbol{\delta}_k \frac{\partial}{\partial x_j} v_k\right\}\right] \\ &= \sum_i \sum_j \sum_k [\boldsymbol{\delta}_i \cdot \boldsymbol{\delta}_j \boldsymbol{\delta}_k] \frac{\partial}{\partial x_i} \frac{\partial}{\partial x_j} v_k \\ &= \sum_i \sum_j \sum_k \delta_{ij} \boldsymbol{\delta}_k \frac{\partial}{\partial x_i} \frac{\partial}{\partial x_j} v_k = \sum_k \boldsymbol{\delta}_k \left(\sum_i \frac{\partial^2}{\partial x_i^2} v_k\right) \end{aligned} \tag{A.4-17}$$

That is, the kth component of $[\nabla \cdot \nabla \mathbf{v}]$ is, in Cartesian coordinates, just $\nabla^2 v_k$. Alternative notations for $[\nabla \cdot \nabla \mathbf{v}]$ are $(\nabla \cdot \nabla)\mathbf{v}$ and $\nabla^2 \mathbf{v}$.

Other Differential Relations

Numerous identities can be proved using the definitions just given:

$$\nabla rs = r\nabla s + s\nabla r \tag{A.4-18}$$

$$(\nabla \cdot s\mathbf{v}) = (\nabla s \cdot \mathbf{v}) + s(\nabla \cdot \mathbf{v}) \tag{A.4-19}$$

$$(\nabla \cdot [\mathbf{v} \times \mathbf{w}]) = (\mathbf{w} \cdot [\nabla \times \mathbf{v}]) - (\mathbf{v} \cdot [\nabla \times \mathbf{w}]) \tag{A.4-20}$$

$$[\nabla \times s\mathbf{v}] = [\nabla s \times \mathbf{v}] + s[\nabla \times \mathbf{v}] \tag{A.4-21}$$

$$[\nabla \cdot \nabla \mathbf{v}] = \nabla(\nabla \cdot \mathbf{v}) - [\nabla \times [\nabla \times \mathbf{v}]] \tag{A.4-22}$$

$$[\mathbf{v} \cdot \nabla \mathbf{v}] = \tfrac{1}{2}\nabla(\mathbf{v} \cdot \mathbf{v}) - [\mathbf{v} \times [\nabla \times \mathbf{v}]] \tag{A.4-23}$$

$$[\nabla \cdot \mathbf{v}\mathbf{w}] = [\mathbf{v} \cdot \nabla \mathbf{w}] + \mathbf{w}(\nabla \cdot \mathbf{v}) \tag{A.4-24}$$

$$(s\boldsymbol{\delta}{:}\nabla \mathbf{v}) = s(\nabla \cdot \mathbf{v}) \tag{A.4-25}$$

$$[\nabla \cdot s\boldsymbol{\delta}] = \nabla s \tag{A.4-26}$$

$$[\nabla \cdot s\boldsymbol{\tau}] = [\nabla s \cdot \boldsymbol{\tau}] + s[\nabla \cdot \boldsymbol{\tau}] \tag{A.4-27}$$

$$\nabla(\mathbf{v} \cdot \mathbf{w}) = [(\nabla \mathbf{v}) \cdot \mathbf{w}] + [(\nabla \mathbf{w}) \cdot \mathbf{v}] \tag{A.4-28}$$

EXAMPLE A.4-1

Proof of a Tensor Identity

Prove that for *symmetric* $\boldsymbol{\tau}$:

$$(\boldsymbol{\tau}{:}\nabla \mathbf{v}) = (\nabla \cdot [\boldsymbol{\tau} \cdot \mathbf{v}]) - (\mathbf{v} \cdot [\nabla \cdot \boldsymbol{\tau}]) \tag{A.4-29}$$

SOLUTION

First we write out the right side in terms of components:

$$(\nabla \cdot [\boldsymbol{\tau} \cdot \mathbf{v}]) = \sum_i \frac{\partial}{\partial x_i} [\boldsymbol{\tau} \cdot \mathbf{v}]_i = \sum_i \sum_j \frac{\partial}{\partial x_i} \tau_{ij} v_j \tag{A.4-30}$$

$$(\mathbf{v} \cdot [\nabla \cdot \boldsymbol{\tau}]) = \sum_j v_j [\nabla \cdot \boldsymbol{\tau}]_j = \sum_j \sum_i v_j \frac{\partial}{\partial x_i} \tau_{ij} \tag{A.4-31}$$

The left side may be written as

$$(\boldsymbol{\tau}{:}\nabla \mathbf{v}) = \sum_i \sum_j \tau_{ji} \frac{\partial}{\partial x_i} v_j = \sum_i \sum_j \tau_{ij} \frac{\partial}{\partial x_i} v_j \tag{A.4-32}$$

the second form resulting from the symmetry of $\boldsymbol{\tau}$. Subtraction of Eq. A.4-31 from Eq. A.4-30 will give Eq. A.4-32.

Now that we have given all the vector and tensor operations, including the various ∇ operations, we want to point out that the dot and double dot operations can be written down at once by using the following simple rule: *a dot implies a summation on adjacent indices*. We illustrate the rule with several examples.

To interpret $(\mathbf{v} \cdot \mathbf{w})$, we note that $\mathbf{v}$ and $\mathbf{w}$ are vectors, whose components have one index. Since both symbols are adjacent to the dot, we make the indices for both of them the same and then sum on them: $(\mathbf{v} \cdot \mathbf{w}) = \Sigma_i v_i w_i$. For double dot operations such as $(\boldsymbol{\tau}:\nabla\mathbf{v})$, we proceed as follows. We note that $\boldsymbol{\tau}$, being a tensor, has two subscripts, whereas ∇ and $\mathbf{v}$ each have one. We therefore set the second subscript of $\boldsymbol{\tau}$ equal to the subscript on ∇ and sum; then we set the first subscript of $\boldsymbol{\tau}$ equal to the subscript on $\mathbf{v}$ and sum. Hence we get $(\boldsymbol{\tau}:\nabla\mathbf{v}) = \Sigma_i\Sigma_j \tau_{ji}(\partial/\partial x_i)v_j$. Similarly, $(\mathbf{v} \cdot [\nabla \cdot \boldsymbol{\tau}])$ can be written down at once as $\Sigma_i\Sigma_j v_j(\partial/\partial x_i)\tau_{ij}$ by performing the operation in the inner enclosure (the brackets) before the outer (the parentheses).

To get the ith component of a vector quantity, we proceed in exactly the same way. To evaluate $[\boldsymbol{\tau} \cdot \mathbf{v}]_i$ we set the second index of the tensor $\boldsymbol{\tau}$ equal to the index on $\mathbf{v}$ and sum to get $\Sigma_j \tau_{ij} v_j$. Similarly, the ith component of $[\nabla \cdot \rho\mathbf{vv}]$ is obtained as $\Sigma_j(\partial/\partial x_j)(\rho v_j v_i)$. Becoming skilled with this method can save a great deal of time in interpreting the dot and double dot operations in Cartesian coordinates.

EXERCISES

1. Perform all the operations in Eq. A.4-6 by writing out all the summations instead of using the $\sum$ notation.

2. A field $\mathbf{v}(x, y, z)$ is said to be *irrotational* if $[\nabla \times \mathbf{v}] = 0$. Which of the following fields are irrotational?
   (a) $v_x = by \quad v_y = 0 \quad v_z = 0$
   (b) $v_x = bx \quad v_y = 0 \quad v_z = 0$
   (c) $v_x = by \quad v_y = bx \quad v_z = 0$
   (d) $v_x = -by \quad v_y = bx \quad v_z = 0$

3. Evaluate $(\nabla \cdot \mathbf{v})$, $\nabla\mathbf{v}$, and $[\nabla \cdot \mathbf{vv}]$ for the four fields in Exercise 2.

4. A vector $\mathbf{v}$ has components

$$v_i = \sum_{j=1}^{3} \alpha_{ij} x_j$$

   with $\alpha_{ij} = \alpha_{ji}$ and $\sum_{i=1}^{3} \alpha_{ii} = 0$; the α_{ij} are constants. Evaluate $(\nabla \cdot \mathbf{v})$, $[\nabla \times \mathbf{v}]$, $\nabla\mathbf{v}$, $(\nabla\mathbf{v})^\dagger$, and $[\nabla \cdot \mathbf{vv}]$. (*Hint:* In connection with evaluating $[\nabla \times \mathbf{v}]$, see Exercise 5 in §A.2.)

5. Verify that $\nabla^2(\nabla \cdot \mathbf{v}) = (\nabla \cdot (\nabla^2\mathbf{v}))$, and that $[\nabla \cdot (\nabla\mathbf{v})^\dagger] = \nabla(\nabla \cdot \mathbf{v})$.

6. Verify that $(\nabla \cdot [\nabla \times \mathbf{v}]) = 0$ and $[\nabla \times \nabla s] = 0$.

7. If $\mathbf{r}$ is the position vector (with components x_1, x_2, x_3) and $\mathbf{v}$ is any vector, show that
   (a) $(\nabla \cdot \mathbf{r}) = 3$
   (b) $[\nabla \times \mathbf{r}] = 0$
   (c) $[\mathbf{r} \times [\nabla \cdot \mathbf{vv}]] = [\nabla \cdot \mathbf{v}[\mathbf{r} \times \mathbf{v}]]$ (where $\mathbf{v}$ is a function of position)

8. Develop an alternative expression for $[\nabla \times [\nabla \cdot s\mathbf{vv}]]$.

9. If $\mathbf{r}$ is the position vector and r is its magnitude, verify that
   (a) $\nabla\frac{1}{r} = -\frac{\mathbf{r}}{r^3}$ **(c)** $\nabla(\mathbf{a} \cdot \mathbf{r}) = \mathbf{a}$ if $\mathbf{a}$ is a constant vector
   (b) $\nabla f(r) = \frac{1}{r}\frac{df}{dr}\mathbf{r}$

10. Write out in full in Cartesian coordinates

(a) $\frac{\partial}{\partial t}\rho\mathbf{v} = -[\nabla\cdot\rho\mathbf{vv}] - \nabla p - [\nabla\cdot\boldsymbol{\tau}] + \rho g$

(b) $\boldsymbol{\tau} = -\mu\{\nabla\mathbf{v} + (\nabla\mathbf{v})^{\dagger} - \frac{2}{3}(\nabla\cdot\mathbf{v})\boldsymbol{\delta}\}$

§A.5 VECTOR AND TENSOR INTEGRAL THEOREMS

For performing general proofs in continuum physics, several integral theorems are extremely useful.

The Gauss–Ostrogradskii Divergence Theorem

If V is a closed region in space enclosed by a surface S, then

$$\int_V (\nabla\cdot\mathbf{v})dV = \int_S (\mathbf{n}\cdot\mathbf{v})dS \tag{A.5-1}$$

in which $\boldsymbol{n}$ is the outwardly directed unit normal vector. This is known as the *divergence theorem* of Gauss and Ostrogradskii. Two closely allied theorems for scalars and tensors are

$$\int_V \nabla s\, dV = \int_S \mathbf{n}s\, dS \tag{A.5-2}$$

$$\int_V [\nabla\cdot\boldsymbol{\tau}]\, dV = \int_S [\mathbf{n}\cdot\boldsymbol{\tau}]dS \tag{A.5-3}[1]$$

The last relation is also valid for dyadic products **vw**. Note that, in all three equations, ∇ in the volume integral is just replaced by $\boldsymbol{n}$ in the surface integral.

The Stokes Curl Theorem

If S is a surface bounded by the closed curve C, then

$$\int_S (\mathbf{n}\cdot[\nabla\times\mathbf{v}])\, dS = \oint_C (\mathbf{t}\cdot\mathbf{v})dC \tag{A.5-4}$$

in which $\boldsymbol{t}$ is a unit tangential vector in the direction of integration along C; $\boldsymbol{n}$ is the unit normal vector to S in the direction that a right-hand screw would move if its head were twisted in the direction of integration along C. There is a similar relation for tensors.[1]

The Leibniz Formula for Differentiating a Volume Integral[2]

Let V be a closed moving region in space enclosed by a surface S; let the velocity of any surface element be $\mathbf{v}_S$. Then, if $s(x, y, z, t)$ is a scalar function of position and time,

$$\frac{d}{dt}\int_V s\, dV = \int_V \frac{\partial s}{\partial t} dV + \int_S s(\mathbf{v}_S\cdot\mathbf{n})dS \tag{A.5-5}$$

---

[1] See P. M. Morse and H. Feshbach, *Methods of Theoretical Physics*, McGraw-Hill, New York (1953), p. 66.

[2] M. D. Greenberg, *Foundations of Applied Mathematics*, Prentice-Hall, Englewood Cliffs, N.J. (1978), pp. 163–164.

This is an extension of the *Leibniz formula* for differentiating a single integral (see Eq. C.3-2); keep in mind that $V = V(t)$ and $S = S(t)$. Equation A.5-5 also applies to vectors and tensors.

If the integral is over a volume, the surface of which is moving with the local fluid velocity (so that $\mathbf{v}_S = \mathbf{v}$), then use of the equation of continuity leads to the additional useful result:

$$\frac{d}{dt}\int_V \rho s\, dV = \int_V \rho \frac{Ds}{Dt}\, dV \tag{A.5-6}$$

in which ρ is the fluid density. Equation A.5-6 is sometimes called the *Reynolds transport theorem*.

EXERCISES

1. Consider the vector field

$$\mathbf{v} = \boldsymbol{\delta}_1 x_1 + \boldsymbol{\delta}_2 x_3 + \boldsymbol{\delta}_3 x_2$$

Evaluate both sides of Eq. A.5-1 over the region bounded by the planes $x_1 = 0$, $x_1 = 1$; $x_2 = 0$, $x_2 = 2$; $x_3 = 0$, $x_3 = 4$.

2. Use the same vector field to evaluate both sides of Eq. A.5-4 for the face $x_1 = 1$ in Exercise 1.

3. Consider the time-dependent scalar function:

$$s = x + y + zt$$

Evaluate both sides of Eq. A.5-5 over the volume bounded by the planes: $x = 0$, $x = t$; $y = 0$, $y = 2t$; $z = 0$, $z = 4t$. The quantities x, y, z, t are dimensionless.

4. Use Eq. A.5-4 (with $\mathbf{v}$ replaced by $\boldsymbol{\tau}$) to show that, when $\tau_{ki} = \sum_j \epsilon_{ijk} x_j$,

$$2\int_S \mathbf{n}\, dS = \oint_C [\mathbf{r} \times \mathbf{t}] dC$$

where $\boldsymbol{r}$ is the position vector locating a point on C with respect to the origin.

5. Evaluate both sides of Eq. A.5-2 for the function $s(x, y, z) = x^2 + y^2 + z^2$. The volume V is the triangular prism lying between the two triangles whose vertices are (2, 0, 0), (2, 1, 0), (2, 0, 3), and (−2, 0, 0), (−2, 1, 0), (−2, 0, 3).

§A.6 VECTOR AND TENSOR ALGEBRA IN CURVILINEAR COORDINATES

Thus far we have considered only Cartesian coordinates x, y, and z. Although formal derivations are usually made in Cartesian coordinates, for working problems it is often more natural to use curvilinear coordinates. The two most commonly occurring curvilinear coordinate systems are the *cylindrical* and the *spherical*. In the following we discuss only these two systems, but the method can also be applied to all *orthogonal* coordinate systems—that is, those in which the three families of coordinate surfaces are mutually perpendicular.

We are primarily interested in knowing how to write various differential operations, such as ∇s, $[\nabla \times \mathbf{v}]$, and $(\boldsymbol{\tau}:\nabla\mathbf{v})$ in curvilinear coordinates. It turns out that we can do this in a straightforward way if we know, for the coordinate system being used, two things: (a) the expression for ∇ in curvilinear coordinates; and (b) the spatial derivatives of the unit vectors in curvilinear coordinates. Hence, we want to focus our attention on these two points.

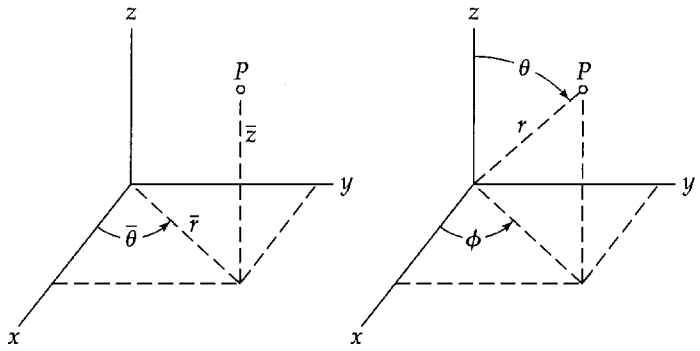

Fig. A.6-1. (*a*) Cylindrical coordinates[1] with $0 \le \bar{r} < \infty$, $0 \le \bar{\theta} < 2\pi$, $-\infty < \bar{z} < \infty$.
(*b*) Spherical coordinates with $0 \le r < \infty$, $0 \le \theta \le \pi$, $0 \le \phi < 2\pi$. Note that $\bar{r}$ and $\bar{\theta}$ in cylindrical coordinates are *not* the same as r and θ in spherical coordinates. Note carefully how the position vector $\mathbf{r}$ and its length r are written in the three coordinate systems:

Rectangular:	$\mathbf{r} = \boldsymbol{\delta}_x x + \boldsymbol{\delta}_y y + \boldsymbol{\delta}_z z;$	$r = \sqrt{x^2 + y^2 + z^2}$
Cylindrical:	$\mathbf{r} = \boldsymbol{\delta}_r \bar{r} + \boldsymbol{\delta}_z \bar{z};$	$r = \sqrt{\bar{r}^2 + \bar{z}^2}$
Spherical:	$\mathbf{r} = \boldsymbol{\delta}_r r;$	$r = r$

Cylindrical Coordinates

In cylindrical coordinates, instead of designating the coordinates of a point by x, y, z, we locate the point by giving the values of r, θ, z. These coordinates[1] are shown in Fig. A.6-1*a*. They are related to the Cartesian coordinates by

$$\begin{cases} x = r\cos\theta & \text{(A.6-1)} \\ y = r\sin\theta & \text{(A.6-2)} \\ z = z & \text{(A.6-3)} \end{cases} \qquad \begin{cases} r = +\sqrt{x^2 + y^2} & \text{(A.6-4)} \\ \theta = \arctan(y/x) & \text{(A.6-5)} \\ z = z & \text{(A.6-6)} \end{cases}$$

To convert derivatives of scalars with respect to x, y, z into derivatives with respect to r, θ, z, the "chain rule" of partial differentiation[2] is used. The derivative operators are readily found to be related thus:

$$\begin{cases} \dfrac{\partial}{\partial x} = (\cos\theta)\dfrac{\partial}{\partial r} + \left(-\dfrac{\sin\theta}{r}\right)\dfrac{\partial}{\partial \theta} + (0)\dfrac{\partial}{\partial z} & \text{(A.6-7)} \\ \dfrac{\partial}{\partial y} = (\sin\theta)\dfrac{\partial}{\partial r} + \left(\dfrac{\cos\theta}{r}\right)\dfrac{\partial}{\partial \theta} + (0)\dfrac{\partial}{\partial z} & \text{(A.6-8)} \\ \dfrac{\partial}{\partial z} = (0)\dfrac{\partial}{\partial r} + (0)\dfrac{\partial}{\partial \theta} + (1)\dfrac{\partial}{\partial z} & \text{(A.6-9)} \end{cases}$$

---

[1] *Caution:* We have chosen to use the familiar r, θ, z-notation for cylindrical coordinates rather than to switch to some less familiar symbols, even though there are two situations in which confusion can arise: (a) occasionally one has to use cylindrical and spherical coordinates in the same problem, and the symbols r and θ have different meanings in the two systems; (b) occasionally one deals with the position vector $\mathbf{r}$ in problems involving cylindrical coordinates, but then the magnitude of $\mathbf{r}$ is not the same as the coordinate r, but rather $\sqrt{r^2 + z^2}$. In such situations, as in Fig. A.6-1, we can use overbars for the cylindrical coordinates and write $\bar{r}, \bar{\theta}, \bar{z}$. For most discussions bars will not be needed.

[2] For example, for a scalar function $\chi(x, y, z) = \psi(r, \theta, z)$:

$$\left(\frac{\partial \chi}{\partial x}\right)_{y,z} = \left(\frac{\partial r}{\partial x}\right)_{y,z}\left(\frac{\partial \psi}{\partial r}\right)_{\theta,z} + \left(\frac{\partial \theta}{\partial x}\right)_{y,z}\left(\frac{\partial \psi}{\partial \theta}\right)_{r,z} + \left(\frac{\partial z}{\partial x}\right)_{y,z}\left(\frac{\partial \psi}{\partial z}\right)_{r,\theta}$$

Note that we are careful to use different symbols χ and ψ, since χ is a different function of x, y, z than ψ is of r, θ, and z!

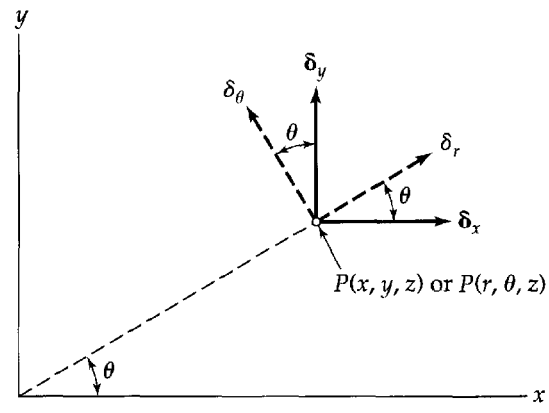

Fig. A.6-2. Unit vectors in rectangular and cylindrical coordinates. The z-axis and the unit vector $\boldsymbol{\delta}_z$ have been omitted for simplicity.

With these relations, derivatives of any scalar functions (including, of course, components of vectors and tensors) with respect to x, y, and z can be expressed in terms of derivatives with respect to r, θ, and z.

Having discussed the interrelationship of the coordinates and derivatives in the two coordinate systems, we now turn to the relation between the unit vectors. We begin by noting that the unit vectors $\boldsymbol{\delta}_x$, $\boldsymbol{\delta}_y$, $\boldsymbol{\delta}_z$ (or $\boldsymbol{\delta}_1$, $\boldsymbol{\delta}_2$, $\boldsymbol{\delta}_3$ as we have been calling them) are independent of position—that is, independent of x, y, z. In cylindrical coordinates the unit vectors $\boldsymbol{\delta}_r$ and $\boldsymbol{\delta}_\theta$ will depend on position, as we can see in Fig. A.6-2. The unit vector $\boldsymbol{\delta}_r$ is a vector of unit length in the direction of increasing r; the unit vector $\boldsymbol{\delta}_\theta$ is a vector of unit length in the direction of increasing θ. Clearly as the point P is moved around on the xy-plane, the directions of $\boldsymbol{\delta}_r$ and $\boldsymbol{\delta}_\theta$ change. Elementary trigonometrical arguments lead to the following relations:

$$\begin{cases} \boldsymbol{\delta}_r = (\cos\theta)\boldsymbol{\delta}_x + (\sin\theta)\boldsymbol{\delta}_y + (0)\boldsymbol{\delta}_z & \text{(A.6-10)} \\ \boldsymbol{\delta}_\theta = (-\sin\theta)\boldsymbol{\delta}_x + (\cos\theta)\boldsymbol{\delta}_y + (0)\boldsymbol{\delta}_z & \text{(A.6-11)} \\ \boldsymbol{\delta}_z = (0)\boldsymbol{\delta}_x + (0)\boldsymbol{\delta}_y + (1)\boldsymbol{\delta}_z & \text{(A.6-12)} \end{cases}$$

These may be solved for $\boldsymbol{\delta}_x$, $\boldsymbol{\delta}_y$, and $\boldsymbol{\delta}_z$ to give

$$\begin{cases} \boldsymbol{\delta}_x = (\cos\theta)\boldsymbol{\delta}_r + (-\sin\theta)\boldsymbol{\delta}_\theta + (0)\boldsymbol{\delta}_z & \text{(A.6-13)} \\ \boldsymbol{\delta}_y = (\sin\theta)\boldsymbol{\delta}_r + (\cos\theta)\boldsymbol{\delta}_\theta + (0)\boldsymbol{\delta}_z & \text{(A.6-14)} \\ \boldsymbol{\delta}_z = (0)\boldsymbol{\delta}_r + (0)\boldsymbol{\delta}_\theta + (1)\boldsymbol{\delta}_z & \text{(A.6-15)} \end{cases}$$

The utility of these two sets of relations will be made clear in the next section.

Vectors and tensors can be decomposed into components with respect to cylindrical coordinates as was done for Cartesian coordinates in Eqs. A.2-16 and A.3-7 (i.e., $\boldsymbol{v} = \boldsymbol{\delta}_r v_r + \boldsymbol{\delta}_\theta v_\theta + \boldsymbol{\delta}_z v_z$). Also, the multiplication rules for the unit vectors and unit dyads are the same as in Eqs. A.2-14 and 15 and A.3-1 to 6. Consequently the various dot and cross product operations (but *not* the differential operations!) are performed as described in §§A.2 and 3. For example,

$$(\mathbf{v}\cdot\mathbf{w}) = v_r w_r + v_\theta w_\theta + v_z w_z \qquad \text{(A.6-16)}$$

$$\begin{aligned}[\mathbf{v}\times\mathbf{w}] = {} & \boldsymbol{\delta}_r(v_\theta w_z - v_z w_\theta) + \boldsymbol{\delta}_\theta(v_z w_r - v_r w_z) \\ & + \boldsymbol{\delta}_z(v_r w_\theta - v_\theta w_r)\end{aligned} \qquad \text{(A.6-17)}$$

$$\begin{aligned}[\boldsymbol{\sigma}\cdot\boldsymbol{\tau}] = {} & \boldsymbol{\delta}_r\boldsymbol{\delta}_r(\sigma_{rr}\tau_{rr} + \sigma_{r\theta}\tau_{\theta r} + \sigma_{rz}\tau_{zr}) \\ & + \boldsymbol{\delta}_r\boldsymbol{\delta}_\theta(\sigma_{rr}\tau_{r\theta} + \sigma_{r\theta}\tau_{\theta\theta} + \sigma_{rz}\tau_{z\theta}) \\ & + \boldsymbol{\delta}_r\boldsymbol{\delta}_z(\sigma_{rr}\tau_{rz} + \sigma_{r\theta}\tau_{\theta z} + \sigma_{rz}\tau_{zz}) \\ & + \text{etc.}\end{aligned} \qquad \text{(A.6-18)}$$

Spherical Coordinates

We now tabulate for reference the same kind of information for spherical coordinates r, θ, ϕ. These coordinates are shown in Figure A.6-1*b*. They are related to the Cartesian coordinates by

$$\begin{cases} x = r\ \sin\ \theta\ \cos\ \phi & \text{(A.6-19)} \\ y = r\ \sin\ \theta\ \sin\ \phi & \text{(A.6-20)} \\ z = r\ \cos\ \theta & \text{(A.6-21)} \end{cases} \qquad \begin{cases} r = +\sqrt{x^2 + y^2 + z^2} & \text{(A.6-22)} \\ \theta = \arctan(\sqrt{x^2 + y^2}/z) & \text{(A.6-23)} \\ \phi = \arctan(y/x) & \text{(A.6-24)} \end{cases}$$

For the spherical coordinates we have the following relations for the derivative operators:

$$\begin{cases} \dfrac{\partial}{\partial x} = (\sin\theta\cos\phi)\dfrac{\partial}{\partial r} + \left(\dfrac{\cos\theta\cos\phi}{r}\right)\dfrac{\partial}{\partial\theta} + \left(-\dfrac{\sin\phi}{r\sin\theta}\right)\dfrac{\partial}{\partial\phi} & \text{(A.6-25)} \\ \dfrac{\partial}{\partial y} = (\sin\theta\sin\phi)\dfrac{\partial}{\partial r} + \left(\dfrac{\cos\theta\sin\phi}{r}\right)\dfrac{\partial}{\partial\theta} + \left(\dfrac{\cos\phi}{r\sin\theta}\right)\dfrac{\partial}{\partial\phi} & \text{(A.6-26)} \\ \dfrac{\partial}{\partial z} = (\cos\theta)\dfrac{\partial}{\partial r} + \left(-\dfrac{\sin\theta}{r}\right)\dfrac{\partial}{\partial\theta} + (0)\dfrac{\partial}{\partial\phi} & \text{(A.6-27)} \end{cases}$$

The relations between the unit vectors are

$$\begin{cases} \boldsymbol{\delta}_r = (\sin\ \theta\ \cos\ \phi)\boldsymbol{\delta}_x + (\sin\ \theta\ \sin\ \phi)\boldsymbol{\delta}_y + (\cos\ \theta)\boldsymbol{\delta}_z & \text{(A.6-28)} \\ \boldsymbol{\delta}_\theta = (\cos\ \theta\ \cos\ \phi)\boldsymbol{\delta}_x + (\cos\ \theta\ \sin\ \phi)\boldsymbol{\delta}_y + (-\sin\ \theta)\boldsymbol{\delta}_z & \text{(A.6-29)} \\ \boldsymbol{\delta}_\phi = (-\sin\ \phi)\boldsymbol{\delta}_x + (\cos\ \phi)\boldsymbol{\delta}_y + (0)\boldsymbol{\delta}_z & \text{(A.6-30)} \end{cases}$$

and

$$\begin{cases} \boldsymbol{\delta}_x = (\sin\ \theta\ \cos\ \phi)\boldsymbol{\delta}_r + (\cos\ \theta\ \cos\ \phi)\boldsymbol{\delta}_\theta + (-\sin\ \phi)\boldsymbol{\delta}_\phi & \text{(A.6-31)} \\ \boldsymbol{\delta}_y = (\sin\ \theta\ \sin\ \phi)\boldsymbol{\delta}_r + (\cos\ \theta\ \sin\ \phi)\boldsymbol{\delta}_\theta + (\cos\ \phi)\boldsymbol{\delta}_\phi & \text{(A.6-32)} \\ \boldsymbol{\delta}_z = (\cos\ \theta)\boldsymbol{\delta}_r + (-\sin\ \theta)\boldsymbol{\delta}_\theta + (0)\boldsymbol{\delta}_\phi & \text{(A.6-33)} \end{cases}$$

And, finally, some sample operations in spherical coordinates are

$$\begin{aligned} (\boldsymbol{\sigma}:\boldsymbol{\tau}) = {} & \sigma_{rr}\tau_{rr} + \sigma_{r\theta}\tau_{\theta r} + \sigma_{r\phi}\tau_{\phi r} \\ & + \sigma_{\theta r}\tau_{r\theta} + \sigma_{\theta\theta}\tau_{\theta\theta} + \sigma_{\theta\phi}\tau_{\phi\theta} \\ & + \sigma_{\phi r}\tau_{r\phi} + \sigma_{\phi\theta}\tau_{\theta\phi} + \sigma_{\phi\phi}\tau_{\phi\phi} \end{aligned} \qquad \text{(A.6-34)}$$

$$(\mathbf{u}\cdot[\mathbf{v}\times\mathbf{w}]) = \begin{vmatrix} u_r & u_\theta & u_\phi \\ v_r & v_\theta & v_\phi \\ w_r & w_\theta & w_\phi \end{vmatrix} \qquad \text{(A.6-35)}$$

That is, the relations (not involving ∇!) given in §§A.2 and 3 can be written directly in terms of spherical components.

EXERCISES

1. Show that

$$\int_0^{2\pi}\int_0^{\pi} \boldsymbol{\delta}_r\ \sin\ \theta\, d\theta\, d\phi = \mathbf{0}$$

$$\int_0^{2\pi}\int_0^{\pi} \boldsymbol{\delta}_r\boldsymbol{\delta}_r\ \sin\ \theta\, d\theta\, d\phi = \tfrac{4}{3}\pi\boldsymbol{\delta}$$

where $\boldsymbol{\delta}_r$ is the unit vector in the r direction in spherical coordinates.

2. Verify that in spherical coordinates $\boldsymbol{\delta} = \boldsymbol{\delta}_r\boldsymbol{\delta}_r + \boldsymbol{\delta}_\theta\boldsymbol{\delta}_\theta + \boldsymbol{\delta}_\phi\boldsymbol{\delta}_\phi$.

§A.7 DIFFERENTIAL OPERATIONS IN CURVILINEAR COORDINATES

We now turn to the use of the ∇-operator in curvilinear coordinates. As in the previous section, we work out in detail the results for cylindrical and spherical coordinates. Then we summarize the procedure for getting the ∇-operations for any orthogonal curvilinear coordinates.

Cylindrical Coordinates

From Eqs. A.6-10, 11, and 12 we can obtain expressions for the spatial derivatives of the unit vectors $\boldsymbol{\delta}_r$, $\boldsymbol{\delta}_\theta$, and $\boldsymbol{\delta}_z$:

$$\boxed{\frac{\partial}{\partial r}\boldsymbol{\delta}_r = 0 \qquad \frac{\partial}{\partial r}\boldsymbol{\delta}_\theta = 0 \qquad \frac{\partial}{\partial r}\boldsymbol{\delta}_z = 0} \tag{A.7-1}$$

$$\boxed{\frac{\partial}{\partial \theta}\boldsymbol{\delta}_r = \boldsymbol{\delta}_\theta \qquad \frac{\partial}{\partial \theta}\boldsymbol{\delta}_\theta = -\boldsymbol{\delta}_r \qquad \frac{\partial}{\partial \theta}\boldsymbol{\delta}_z = 0} \tag{A.7-2}$$

$$\boxed{\frac{\partial}{\partial z}\boldsymbol{\delta}_r = 0 \qquad \frac{\partial}{\partial z}\boldsymbol{\delta}_\theta = 0 \qquad \frac{\partial}{\partial z}\boldsymbol{\delta}_z = 0} \tag{A.7-3}$$

The reader would do well to interpret these derivatives geometrically by considering the way $\boldsymbol{\delta}_r$, $\boldsymbol{\delta}_\theta$, $\boldsymbol{\delta}_z$ change as the location of P is changed in Fig. A.6-2.

We now use the definition of the ∇-operator in Eq. A.4-1, the expressions in Eqs. A.6-13, 14, and 15, and the derivative operators in Eqs. A.6-7, 8, and 9 to obtain the formula for ∇ in cylindrical coordinates

$$\begin{aligned}\nabla &= \boldsymbol{\delta}_x\frac{\partial}{\partial x} + \boldsymbol{\delta}_y\frac{\partial}{\partial y} + \boldsymbol{\delta}_z\frac{\partial}{\partial z} \\ &= (\boldsymbol{\delta}_r\cos\theta - \boldsymbol{\delta}_\theta\sin\theta)\left(\cos\theta\frac{\partial}{\partial r} - \frac{\sin\theta}{r}\frac{\partial}{\partial\theta}\right) \\ &\quad + (\boldsymbol{\delta}_r\sin\theta + \boldsymbol{\delta}_\theta\cos\theta)\left(\sin\theta\frac{\partial}{\partial r} + \frac{\cos\theta}{r}\frac{\partial}{\partial\theta}\right) + \boldsymbol{\delta}_z\frac{\partial}{\partial z}\end{aligned} \tag{A.7-4}$$

When this is multiplied out, there is considerable simplification, and we get

$$\boxed{\nabla = \boldsymbol{\delta}_r\frac{\partial}{\partial r} + \boldsymbol{\delta}_\theta\frac{1}{r}\frac{\partial}{\partial\theta} + \boldsymbol{\delta}_z\frac{\partial}{\partial z}} \tag{A.7-5}$$

for *cylindrical* coordinates. This may be used for obtaining all differential operations in cylindrical coordinates, provided that Eqs. A.7-1, 2, and 3 are used to differentiate any unit vectors on which ∇ operates. This point will be made clear in the subsequent illustrative example.

Spherical Coordinates

The spatial derivatives of $\boldsymbol{\delta}_r$, $\boldsymbol{\delta}_\theta$, and $\boldsymbol{\delta}_\phi$ are obtained by differentiating Eqs. A.6-28, 29, and 30:

$$\boxed{\frac{\partial}{\partial r}\boldsymbol{\delta}_r = 0 \qquad \frac{\partial}{\partial r}\boldsymbol{\delta}_\theta = 0 \qquad \frac{\partial}{\partial r}\boldsymbol{\delta}_\phi = 0} \tag{A.7-6}$$

$$\boxed{\frac{\partial}{\partial \theta}\boldsymbol{\delta}_r = \boldsymbol{\delta}_\theta \qquad \frac{\partial}{\partial \theta}\boldsymbol{\delta}_\theta = -\boldsymbol{\delta}_r \qquad \frac{\partial}{\partial \theta}\boldsymbol{\delta}_\phi = 0} \tag{A.7-7}$$

$$\boxed{\frac{\partial}{\partial \phi}\boldsymbol{\delta}_r = \boldsymbol{\delta}_\phi\sin\theta \qquad \frac{\partial}{\partial \phi}\boldsymbol{\delta}_\theta = \boldsymbol{\delta}_\phi\cos\theta \qquad \frac{\partial}{\partial \phi}\boldsymbol{\delta}_\phi = -\boldsymbol{\delta}_r\sin\theta - \boldsymbol{\delta}_\theta\cos\theta} \tag{A.7-8}$$

Use of Eqs. A.6-31, 32, and 33 and Eqs. A.6-25, 26, and 27 in Eq. A.4-1 gives the following expression for the ∇-operator:

$$\boxed{\nabla = \boldsymbol{\delta}_r \frac{\partial}{\partial r} + \boldsymbol{\delta}_\theta \frac{1}{r}\frac{\partial}{\partial \theta} + \boldsymbol{\delta}_\phi \frac{1}{r \sin\theta}\frac{\partial}{\partial \phi}} \tag{A.7-9}$$

in *spherical* coordinates. This expression may be used for obtaining differential operations in spherical coordinates, provided that Eqs. A.7-6, 7, and 8 are used for differentiating the unit vectors.

General Orthogonal Coordinates

Thus far we have discussed the two most-used curvilinear coordinate systems. We now present without proof the relations for any orthogonal curvilinear coordinates. Let the relation between Cartesian coordinates x_i and the curvilinear coordinates q_α be given by

$$\begin{cases} x_1 = x_1(q_1, q_2, q_3) \\ x_2 = x_2(q_1, q_2, q_3) \\ x_3 = x_3(q_1, q_2, q_3) \end{cases} \quad \text{or} \quad x_i = x_i(q_\alpha) \tag{A.7-10}$$

These can be solved for the q_α to get the inverse relations $q_\alpha = q_\alpha(x_i)$. Then[1] the unit vectors $\boldsymbol{\delta}_i$ in rectangular coordinates and the $\boldsymbol{\delta}_\alpha$ in curvilinear coordinates are related thus:

$$\boldsymbol{\delta}_\alpha = \sum_i h_\alpha \left(\frac{\partial q_\alpha}{\partial x_i}\right)\boldsymbol{\delta}_i = \sum_i \frac{1}{h_\alpha}\left(\frac{\partial x_i}{\partial q_\alpha}\right)\boldsymbol{\delta}_i \tag{A.7-11}$$

$$\boldsymbol{\delta}_i = \sum_\alpha h_\alpha \left(\frac{\partial q_\alpha}{\partial x_i}\right)\boldsymbol{\delta}_\alpha = \sum_\alpha \frac{1}{h_\alpha}\left(\frac{\partial x_i}{\partial q_\alpha}\right)\boldsymbol{\delta}_\alpha \tag{A.7-12}$$

in which the "scale factors" h_α are given by

$$h_\alpha^2 = \sum_i \left(\frac{\partial x_i}{\partial q_\alpha}\right)^2 = \left[\sum_i \left(\frac{\partial q_\alpha}{\partial x_i}\right)^2\right]^{-1} \tag{A.7-13}$$

The spatial derivatives of the unit vectors $\boldsymbol{\delta}_\alpha$ can then be found to be

$$\boxed{\frac{\partial \boldsymbol{\delta}_\alpha}{\partial q_\beta} = \frac{\boldsymbol{\delta}_\beta}{h_\alpha}\frac{\partial h_\beta}{\partial q_\alpha} - \delta_{\alpha\beta}\sum_{\gamma=1}^{3}\frac{\boldsymbol{\delta}_\gamma}{h_\gamma}\frac{\partial h_\alpha}{\partial q_\gamma}} \tag{A.7-14}$$

and the ∇-operator is

$$\boxed{\nabla = \sum_\alpha \frac{\boldsymbol{\delta}_\alpha}{h_\alpha}\frac{\partial}{\partial q_\alpha}} \tag{A.7-15}$$

The reader should verify that Eqs. A.7-14 and 15 can be used to get Eqs. A.7-1 to 3, A.7-5 and A.7-6 to 9.

From Eqs. A.7-15 and 14 we can now get the following expressions for the simplest of the ∇-operations:

$$(\nabla \cdot \mathbf{v}) = \frac{1}{h_1 h_2 h_3}\sum_\alpha \frac{\partial}{\partial q_\alpha}\left(\frac{h_1 h_2 h_3}{h_\alpha} v_\alpha\right) \tag{A.7-16}$$

$$\nabla^2 s = \frac{1}{h_1 h_2 h_3}\sum_\alpha \frac{\partial}{\partial q_\alpha}\left(\frac{h_1 h_2 h_3}{h_\alpha^2}\frac{\partial s}{\partial q_\alpha}\right) \tag{A.7-17}$$

---

[1] P. Morse and H. Feshbach, *Methods of Theoretical Physics*, McGraw-Hill, New York (1953), p. 26 and p. 115.

$$[\nabla \times \mathbf{v}] = \frac{1}{h_1 h_2 h_3} \begin{vmatrix} h_1\boldsymbol{\delta}_1 & h_2\boldsymbol{\delta}_2 & h_3\boldsymbol{\delta}_3 \\ \dfrac{\partial}{\partial q_1} & \dfrac{\partial}{\partial q_2} & \dfrac{\partial}{\partial q_3} \\ h_1 v_1 & h_2 v_2 & h_3 v_3 \end{vmatrix} \tag{A.7-18}$$

In the last expression, the unit vectors are those belonging to the curvilinear coordinate system. Additional operations may be found in Morse and Feshbach.[1]

The scale factors introduced above also arise in the expressions for the volume and surface elements $dV = h_1 h_2 h_3 dq_1 dq_2 dq_3$ and $dS_{\alpha\beta} = h_\alpha h_\beta dq_\alpha dq_\beta (\alpha \neq \beta)$; here $dS_{\alpha\beta}$ is a surface element on a surface of constant γ, where $\gamma \neq \alpha$ and $\gamma \neq \beta$. The reader should verify that the volume elements and various surface elements in cylindrical and spherical coordinates can be found in this way.

In Tables A.7-1, 2, and 3 we summarize the differential operations most commonly encountered in Cartesian, cylindrical, and spherical coordinates.[2] The curvilinear coordinate expressions given can be obtained by the method illustrated in the following two examples.

EXAMPLE A.7-1

Differential Operations in Cylindrical Coordinates

Derive expressions for $(\nabla \cdot \boldsymbol{v})$ and $\nabla \boldsymbol{v}$ in cylindrical coordinates.

SOLUTION

(a) We begin by writing ∇ in cylindrical coordinates and decomposing $\boldsymbol{v}$ into its components

$$(\nabla \cdot \mathbf{v}) = \left(\left\{ \boldsymbol{\delta}_r \frac{\partial}{\partial r} + \boldsymbol{\delta}_\theta \frac{1}{r} \frac{\partial}{\partial \theta} + \boldsymbol{\delta}_z \frac{\partial}{\partial z} \right\} \cdot \{ \boldsymbol{\delta}_r v_r + \boldsymbol{\delta}_\theta v_\theta + \boldsymbol{\delta}_z v_z \} \right) \tag{A.7-19}$$

Expanding, we get

$$\begin{aligned} (\nabla \cdot \mathbf{v}) = {} & \left(\boldsymbol{\delta}_r \cdot \frac{\partial}{\partial r} \boldsymbol{\delta}_r v_r \right) + \left(\boldsymbol{\delta}_r \cdot \frac{\partial}{\partial r} \boldsymbol{\delta}_\theta v_\theta \right) + \left(\boldsymbol{\delta}_r \cdot \frac{\partial}{\partial r} \boldsymbol{\delta}_z v_z \right) \\ & + \left(\boldsymbol{\delta}_\theta \cdot \frac{1}{r} \frac{\partial}{\partial \theta} \boldsymbol{\delta}_r v_r \right) + \left(\boldsymbol{\delta}_\theta \cdot \frac{1}{r} \frac{\partial}{\partial \theta} \boldsymbol{\delta}_\theta v_\theta \right) + \left(\boldsymbol{\delta}_\theta \cdot \frac{1}{r} \frac{\partial}{\partial \theta} \boldsymbol{\delta}_z v_z \right) \\ & + \left(\boldsymbol{\delta}_z \cdot \frac{\partial}{\partial z} \boldsymbol{\delta}_r v_r \right) + \left(\boldsymbol{\delta}_z \cdot \frac{\partial}{\partial z} \boldsymbol{\delta}_\theta v_\theta \right) + \left(\boldsymbol{\delta}_z \cdot \frac{\partial}{\partial z} \boldsymbol{\delta}_z v_z \right) \end{aligned} \tag{A.7-20}$$

We now use the relations given in Eqs. A.7-1, 2, and 3 to evaluate the derivatives of the unit vectors. This gives

$$\begin{aligned} (\nabla \cdot \mathbf{v}) = {} & (\boldsymbol{\delta}_r \cdot \boldsymbol{\delta}_r) \frac{\partial v_r}{\partial r} + (\boldsymbol{\delta}_r \cdot \boldsymbol{\delta}_\theta) \frac{\partial v_\theta}{\partial r} + (\boldsymbol{\delta}_r \cdot \boldsymbol{\delta}_z) \frac{\partial v_z}{\partial r} + (\boldsymbol{\delta}_\theta \cdot \boldsymbol{\delta}_r) \frac{1}{r} \frac{\partial v_r}{\partial \theta} \\ & + (\boldsymbol{\delta}_\theta \cdot \boldsymbol{\delta}_\theta) \frac{1}{r} \frac{\partial v_\theta}{\partial \theta} + (\boldsymbol{\delta}_\theta \cdot \boldsymbol{\delta}_z) \frac{1}{r} \frac{\partial v_z}{\partial \theta} + \frac{v_r}{r} (\boldsymbol{\delta}_\theta \cdot \boldsymbol{\delta}_\theta) + \frac{v_\theta}{r} (\boldsymbol{\delta}_\theta \cdot \{-\boldsymbol{\delta}_r\}) \\ & + (\boldsymbol{\delta}_z \cdot \boldsymbol{\delta}_r) \frac{\partial v_r}{\partial z} + (\boldsymbol{\delta}_z \cdot \boldsymbol{\delta}_\theta) \frac{\partial v_\theta}{\partial z} + (\boldsymbol{\delta}_z \cdot \boldsymbol{\delta}_z) \frac{\partial v_z}{\partial z} \end{aligned} \tag{A.7-21}$$

Since $(\boldsymbol{\delta}_r \cdot \boldsymbol{\delta}_r) = 1$, $(\boldsymbol{\delta}_r \cdot \boldsymbol{\delta}_\theta) = 0$, and so on, the latter simplifies to

$$(\nabla \cdot \mathbf{v}) = \frac{\partial v_r}{\partial r} + \frac{1}{r} \frac{\partial v_\theta}{\partial \theta} + \frac{v_r}{r} + \frac{\partial v_z}{\partial z} \tag{A.7-22}$$

which is the same as Eq. A of Table A.7-2. The procedure is a bit tedious, but is *is* straightforward.

---

[2] For other coordinate systems see the extensive compilation of P. Moon and D. E. Spencer, *Field Theory Handbook*, Springer, Berlin (1961). In addition, an orthogonal coordinate system is available in which one of the three sets of coordinate surfaces is made up of coaxial cones (but with noncoincident apexes); all of the ∇-operations have been tabulated by the originators of this coordinate system, J. F. Dijksman and E. P. W. Savenije, *Rheol. Acta*, **24**, 105–118 (1985).

Table A.7-1 Summary of Differential Operations Involving the ∇-Operator in Cartesian Coordinates (x, y, z)

$$(\nabla \cdot \mathbf{v}) = \frac{\partial v_x}{\partial x} + \frac{\partial v_y}{\partial y} + \frac{\partial v_z}{\partial z} \tag{A}$$

$$(\nabla^2 s) = \frac{\partial^2 s}{\partial x^2} + \frac{\partial^2 s}{\partial y^2} + \frac{\partial^2 s}{\partial z^2} \tag{B}$$

$$\begin{aligned}(\boldsymbol{\tau}:\nabla\mathbf{v}) = {} & \tau_{xx}\left(\frac{\partial v_x}{\partial x}\right) + \tau_{xy}\left(\frac{\partial v_x}{\partial y}\right) + \tau_{xz}\left(\frac{\partial v_x}{\partial z}\right) \\ & + \tau_{yx}\left(\frac{\partial v_y}{\partial x}\right) + \tau_{yy}\left(\frac{\partial v_y}{\partial y}\right) + \tau_{yz}\left(\frac{\partial v_y}{\partial z}\right) \\ & + \tau_{zx}\left(\frac{\partial v_z}{\partial x}\right) + \tau_{zy}\left(\frac{\partial v_z}{\partial y}\right) + \tau_{zz}\left(\frac{\partial v_z}{\partial z}\right)\end{aligned} \tag{C}$$

$$[\nabla s]_x = \frac{\partial s}{\partial x} \tag{D}$$

$$[\nabla s]_y = \frac{\partial s}{\partial y} \tag{E}$$

$$[\nabla s]_z = \frac{\partial s}{\partial z} \tag{F}$$

$$[\nabla \times \mathbf{v}]_x = \frac{\partial v_z}{\partial y} - \frac{\partial v_y}{\partial z} \tag{G}$$

$$[\nabla \times \mathbf{v}]_y = \frac{\partial v_x}{\partial z} - \frac{\partial v_z}{\partial x} \tag{H}$$

$$[\nabla \times \mathbf{v}]_z = \frac{\partial v_y}{\partial x} - \frac{\partial v_x}{\partial y} \tag{I}$$

$$[\nabla \cdot \boldsymbol{\tau}]_x = \frac{\partial \tau_{xx}}{\partial x} + \frac{\partial \tau_{yx}}{\partial y} + \frac{\partial \tau_{zx}}{\partial z} \tag{J}$$

$$[\nabla \cdot \boldsymbol{\tau}]_y = \frac{\partial \tau_{xy}}{\partial x} + \frac{\partial \tau_{yy}}{\partial y} + \frac{\partial \tau_{zy}}{\partial z} \tag{K}$$

$$[\nabla \cdot \boldsymbol{\tau}]_z = \frac{\partial \tau_{xz}}{\partial x} + \frac{\partial \tau_{yz}}{\partial y} + \frac{\partial \tau_{zz}}{\partial z} \tag{L}$$

$$[\nabla^2 \mathbf{v}]_x = \frac{\partial^2 v_x}{\partial x^2} + \frac{\partial^2 v_x}{\partial y^2} + \frac{\partial^2 v_x}{\partial z^2} \tag{M}$$

$$[\nabla^2 \mathbf{v}]_y = \frac{\partial^2 v_y}{\partial x^2} + \frac{\partial^2 v_y}{\partial y^2} + \frac{\partial^2 v_y}{\partial z^2} \tag{N}$$

$$[\nabla^2 \mathbf{v}]_z = \frac{\partial^2 v_z}{\partial x^2} + \frac{\partial^2 v_z}{\partial y^2} + \frac{\partial^2 v_z}{\partial z^2} \tag{O}$$

$$[\mathbf{v} \cdot\cdot \nabla\mathbf{w}]_x = v_x\left(\frac{\partial w_x}{\partial x}\right) + v_y\left(\frac{\partial w_x}{\partial y}\right) + v_z\left(\frac{\partial w_x}{\partial z}\right) \tag{P}$$

$$[\mathbf{v} \cdot \nabla\mathbf{w}]_y = v_x\left(\frac{\partial w_y}{\partial x}\right) + v_y\left(\frac{\partial w_y}{\partial y}\right) + v_z\left(\frac{\partial w_y}{\partial z}\right) \tag{Q}$$

$$[\mathbf{v} \cdot \nabla\mathbf{w}]_z = v_x\left(\frac{\partial w_z}{\partial x}\right) + v_y\left(\frac{\partial w_z}{\partial y}\right) + v_z\left(\frac{\partial w_z}{\partial z}\right) \tag{R}$$

$$\{\nabla \mathbf{v}\}_{xx} = \frac{\partial v_x}{\partial x} \tag{S}$$

$$\{\nabla \mathbf{v}\}_{xy} = \frac{\partial v_y}{\partial x} \tag{T}$$

$$\{\nabla \mathbf{v}\}_{xz} = \frac{\partial v_z}{\partial x} \tag{U}$$

$$\{\nabla \mathbf{v}\}_{yx} = \frac{\partial v_x}{\partial y} \tag{V}$$

$$\{\nabla \mathbf{v}\}_{yy} = \frac{\partial v_y}{\partial y} \tag{W}$$

$$\{\nabla \mathbf{v}\}_{yz} = \frac{\partial v_z}{\partial y} \tag{X}$$

$$\{\nabla \mathbf{v}\}_{zx} = \frac{\partial v_x}{\partial z} \tag{Y}$$

$$\{\nabla \mathbf{v}\}_{zy} = \frac{\partial v_y}{\partial z} \tag{Z}$$

$$\{\nabla \mathbf{v}\}_{zz} = \frac{\partial v_z}{\partial z} \tag{AA}$$

$$\{\mathbf{v} \cdot \nabla \boldsymbol{\tau}\}_{xx} = (\mathbf{v} \cdot \nabla)\tau_{xx} \tag{BB}$$

$$\{\mathbf{v} \cdot \nabla \boldsymbol{\tau}\}_{xy} = (\mathbf{v} \cdot \nabla)\tau_{xy} \tag{CC}$$

$$\{\mathbf{v} \cdot \nabla \boldsymbol{\tau}\}_{xz} = (\mathbf{v} \cdot \nabla)\tau_{xz} \tag{DD}$$

$$\{\mathbf{v} \cdot \nabla \boldsymbol{\tau}\}_{yx} = (\mathbf{v} \cdot \nabla)\tau_{yx} \tag{EE}$$

$$\{\mathbf{v} \cdot \nabla \boldsymbol{\tau}\}_{yy} = (\mathbf{v} \cdot \nabla)\tau_{yy} \tag{FF}$$

$$\{\mathbf{v} \cdot \nabla \boldsymbol{\tau}\}_{yz} = (\mathbf{v} \cdot \nabla)\tau_{yz} \tag{GG}$$

$$\{\mathbf{v} \cdot \nabla \boldsymbol{\tau}\}_{zx} = (\mathbf{v} \cdot \nabla)\tau_{zx} \tag{HH}$$

$$\{\mathbf{v} \cdot \nabla \boldsymbol{\tau}\}_{zy} = (\mathbf{v} \cdot \nabla)\tau_{zy} \tag{II}$$

$$\{\mathbf{v} \cdot \nabla \boldsymbol{\tau}\}_{zz} = (\mathbf{v} \cdot \nabla)\tau_{zz} \tag{JJ}$$

where the operator $(\mathbf{v} \cdot \nabla) = v_x \frac{\partial}{\partial x} + v_y \frac{\partial}{\partial y} + v_z \frac{\partial}{\partial z}$

Table A.7-2 Summary of Differential Operations Involving the ∇-Operator in Cylindrical Coordinates (r, θ, z)

$$(\nabla \cdot \mathbf{v}) = \frac{1}{r}\frac{\partial}{\partial r}(rv_r) + \frac{1}{r}\frac{\partial v_\theta}{\partial \theta} + \frac{\partial v_z}{\partial z} \tag{A}$$

$$(\nabla^2 s) = \frac{1}{r}\frac{\partial}{\partial r}\left(r\frac{\partial s}{\partial r}\right) + \frac{1}{r^2}\frac{\partial^2 s}{\partial \theta^2} + \frac{\partial^2 s}{\partial z^2} \tag{B}$$

$$\begin{aligned}(\boldsymbol{\tau}:\nabla\mathbf{v}) = {} & \tau_{rr}\left(\frac{\partial v_r}{\partial r}\right) + \tau_{r\theta}\left(\frac{1}{r}\frac{\partial v_r}{\partial \theta} - \frac{v_\theta}{r}\right) + \tau_{rz}\left(\frac{\partial v_r}{\partial z}\right) \\ & + \tau_{\theta r}\left(\frac{\partial v_\theta}{\partial r}\right) + \tau_{\theta\theta}\left(\frac{1}{r}\frac{\partial v_\theta}{\partial \theta} + \frac{v_r}{r}\right) + \tau_{\theta z}\left(\frac{\partial v_\theta}{\partial z}\right) \\ & + \tau_{zr}\left(\frac{\partial v_z}{\partial r}\right) + \tau_{z\theta}\left(\frac{1}{r}\frac{\partial v_z}{\partial \theta}\right) + \tau_{zz}\left(\frac{\partial v_z}{\partial z}\right)\end{aligned} \tag{C}$$

$$[\nabla s]_r = \frac{\partial s}{\partial r} \tag{D}$$

$$[\nabla s]_\theta = \frac{1}{r}\frac{\partial s}{\partial \theta} \tag{E}$$

$$[\nabla s]_z = \frac{\partial s}{\partial z} \tag{F}$$

$$[\nabla \times \mathbf{v}]_r = \frac{1}{r}\frac{\partial v_z}{\partial \theta} - \frac{\partial v_\theta}{\partial z} \tag{G}$$

$$[\nabla \times \mathbf{v}]_\theta = \frac{\partial v_r}{\partial z} - \frac{\partial v_z}{\partial r} \tag{H}$$

$$[\nabla \times \mathbf{v}]_z = \frac{1}{r}\frac{\partial}{\partial r}(rv_\theta) - \frac{1}{r}\frac{\partial v_r}{\partial \theta} \tag{I}$$

$$[\nabla \cdot \boldsymbol{\tau}]_r = \frac{1}{r}\frac{\partial}{\partial r}(r\tau_{rr}) + \frac{1}{r}\frac{\partial}{\partial \theta}\tau_{\theta r} + \frac{\partial}{\partial z}\tau_{zr} - \frac{\tau_{\theta\theta}}{r} \tag{J}$$

$$[\nabla \cdot \boldsymbol{\tau}]_\theta = \frac{1}{r^2}\frac{\partial}{\partial r}(r^2\tau_{r\theta}) + \frac{1}{r}\frac{\partial}{\partial \theta}\tau_{\theta\theta} + \frac{\partial}{\partial z}\tau_{z\theta} + \frac{\tau_{\theta r} - \tau_{r\theta}}{r} \tag{K}$$

$$[\nabla \cdot \boldsymbol{\tau}]_z = \frac{1}{r}\frac{\partial}{\partial r}(r\tau_{rz}) + \frac{1}{r}\frac{\partial}{\partial \theta}\tau_{\theta z} + \frac{\partial}{\partial z}\tau_{zz} \tag{L}$$

$$[\nabla^2 \mathbf{v}]_r = \frac{\partial}{\partial r}\left(\frac{1}{r}\frac{\partial}{\partial r}(rv_r)\right) + \frac{1}{r^2}\frac{\partial^2 v_r}{\partial \theta^2} + \frac{\partial^2 v_r}{\partial z^2} - \frac{2}{r^2}\frac{\partial v_\theta}{\partial \theta} \tag{M}$$

$$[\nabla^2 \mathbf{v}]_\theta = \frac{\partial}{\partial r}\left(\frac{1}{r}\frac{\partial}{\partial r}(rv_\theta)\right) + \frac{1}{r^2}\frac{\partial^2 v_\theta}{\partial \theta^2} + \frac{\partial^2 v_\theta}{\partial z^2} + \frac{2}{r^2}\frac{\partial v_r}{\partial \theta} \tag{N}$$

$$[\nabla^2 \mathbf{v}]_z = \frac{1}{r}\frac{\partial}{\partial r}\left(r\frac{\partial v_z}{\partial r}\right) + \frac{1}{r^2}\frac{\partial^2 v_z}{\partial \theta^2} + \frac{\partial^2 v_z}{\partial z^2} \tag{O}$$

$$[\mathbf{v} \cdot \nabla\mathbf{w}]_r = v_r\left(\frac{\partial w_r}{\partial r}\right) + v_\theta\left(\frac{1}{r}\frac{\partial w_r}{\partial \theta} - \frac{w_\theta}{r}\right) + v_z\left(\frac{\partial w_r}{\partial z}\right) \tag{P}$$

$$[\mathbf{v} \cdot \nabla\mathbf{w}]_\theta = v_r\left(\frac{\partial w_\theta}{\partial r}\right) + v_\theta\left(\frac{1}{r}\frac{\partial w_\theta}{\partial \theta} + \frac{w_r}{r}\right) + v_z\left(\frac{\partial w_\theta}{\partial z}\right) \tag{Q}$$

$$[\mathbf{v} \cdot \nabla\mathbf{w}]_z = v_r\left(\frac{\partial w_z}{\partial r}\right) + v_\theta\left(\frac{1}{r}\frac{\partial w_z}{\partial \theta}\right) + v_z\left(\frac{\partial w_z}{\partial z}\right) \tag{R}$$

$$\{\nabla \mathbf{v}\}_{rr} = \frac{\partial v_r}{\partial r} \tag{S}$$

$$\{\nabla \mathbf{v}\}_{r\theta} = \frac{\partial v_\theta}{\partial r} \tag{T}$$

$$\{\nabla \mathbf{v}\}_{rz} = \frac{\partial v_z}{\partial r} \tag{U}$$

$$\{\nabla \mathbf{v}\}_{\theta r} = \frac{1}{r}\frac{\partial v_r}{\partial \theta} - \frac{v_\theta}{r} \tag{V}$$

$$\{\nabla \mathbf{v}\}_{\theta\theta} = \frac{1}{r}\frac{\partial v_\theta}{\partial \theta} + \frac{v_r}{r} \tag{W}$$

$$\{\nabla \mathbf{v}\}_{\theta z} = \frac{1}{r}\frac{\partial v_z}{\partial \theta} \tag{X}$$

$$\{\nabla \mathbf{v}\}_{zr} = \frac{\partial v_r}{\partial z} \tag{Y}$$

$$\{\nabla \mathbf{v}\}_{z\theta} = \frac{\partial v_\theta}{\partial z} \tag{Z}$$

$$\{\nabla \mathbf{v}\}_{zz} = \frac{\partial v_z}{\partial z} \tag{AA}$$

$$\{\mathbf{v}\cdot\nabla\boldsymbol{\tau}\}_{rr} = (\mathbf{v}\cdot\nabla)\tau_{rr} - \frac{v_\theta}{r}(\tau_{r\theta} + \tau_{\theta r}) \tag{BB}$$

$$\{\mathbf{v}\cdot\nabla\boldsymbol{\tau}\}_{r\theta} = (\mathbf{v}\cdot\nabla)\tau_{r\theta} + \frac{v_\theta}{r}(\tau_{rr} - \tau_{\theta\theta}) \tag{CC}$$

$$\{\mathbf{v}\cdot\nabla\boldsymbol{\tau}\}_{rz} = (\mathbf{v}\cdot\nabla)\tau_{rz} - \frac{v_\theta}{r}\tau_{\theta z} \tag{DD}$$

$$\{\mathbf{v}\cdot\nabla\boldsymbol{\tau}\}_{\theta r} = (\mathbf{v}\cdot\nabla)\tau_{\theta r} + \frac{v_\theta}{r}(\tau_{rr} - \tau_{\theta\theta}) \tag{EE}$$

$$\{\mathbf{v}\cdot\nabla\boldsymbol{\tau}\}_{\theta\theta} = (\mathbf{v}\cdot\nabla)\tau_{\theta\theta} + \frac{v_\theta}{r}(\tau_{r\theta} + \tau_{\theta r}) \tag{FF}$$

$$\{\mathbf{v}\cdot\nabla\boldsymbol{\tau}\}_{\theta z} = (\mathbf{v}\cdot\nabla)\tau_{\theta z} + \frac{v_\theta}{r}\tau_{rz} \tag{GG}$$

$$\{\mathbf{v}\cdot\nabla\boldsymbol{\tau}\}_{zr} = (\mathbf{v}\cdot\nabla)\tau_{zr} - \frac{v_\theta}{r}\tau_{z\theta} \tag{HH}$$

$$\{\mathbf{v}\cdot\nabla\boldsymbol{\tau}\}_{z\theta} = (\mathbf{v}\cdot\nabla)\tau_{z\theta} + \frac{v_\theta}{r}\tau_{zr} \tag{II}$$

$$\{\mathbf{v}\cdot\nabla\boldsymbol{\tau}\}_{zz} = (\mathbf{v}\cdot\nabla)\tau_{zz} \tag{JJ}$$

where the operator $(\mathbf{v}\cdot\nabla) = v_r\frac{\partial}{\partial r} + \frac{v_\theta}{r}\frac{\partial}{\partial \theta} + v_z\frac{\partial}{\partial z}$

Table A.7-3 Summary of Differential Operations Involving the ∇-Operator in Spherical Coordinates (r, θ, ϕ)

$$(\nabla \cdot \mathbf{v}) = \frac{1}{r^2}\frac{\partial}{\partial r}(r^2 v_r) + \frac{1}{r\ \sin\ \theta}\frac{\partial}{\partial \theta}(v_\theta\ \sin\ \theta) + \frac{1}{r\ \sin\ \theta}\frac{\partial v_\phi}{\partial \phi} \tag{A}$$

$$(\nabla^2 s) = \frac{1}{r^2}\frac{\partial}{\partial r}\left(r^2\frac{\partial s}{\partial r}\right) + \frac{1}{r^2 \sin\theta}\frac{\partial}{\partial \theta}\left(\sin\theta\frac{\partial s}{\partial \theta}\right) + \frac{1}{r^2 \sin^2\theta}\frac{\partial^2 s}{\partial \phi^2} \tag{B}$$

$$\begin{aligned}(\boldsymbol{\tau}:\nabla\mathbf{v}) = {} & \tau_{rr}\left(\frac{\partial v_r}{\partial r}\right) + \tau_{r\theta}\left(\frac{1}{r}\frac{\partial v_r}{\partial \theta} - \frac{v_\theta}{r}\right) + \tau_{r\phi}\left(\frac{1}{r\sin\theta}\frac{\partial v_r}{\partial \phi} - \frac{v_\phi}{r}\right) \\ & + \tau_{\theta r}\left(\frac{\partial v_\theta}{\partial r}\right) + \tau_{\theta\theta}\left(\frac{1}{r}\frac{\partial v_\theta}{\partial \theta} + \frac{v_r}{r}\right) + \tau_{\theta\phi}\left(\frac{1}{r\sin\theta}\frac{\partial v_\theta}{\partial \phi} - \frac{v_\phi}{r}\cot\theta\right) \\ & + \tau_{\phi r}\left(\frac{\partial v_\phi}{\partial r}\right) + \tau_{\phi\theta}\left(\frac{1}{r}\frac{\partial v_\phi}{\partial \theta}\right) + \tau_{\phi\phi}\left(\frac{1}{r\sin\theta}\frac{\partial v_\phi}{\partial \phi} + \frac{v_r}{r} + \frac{v_\theta}{r}\cot\theta\right)\end{aligned} \tag{C}$$

$$[\nabla s]_r = \frac{\partial s}{\partial r} \tag{D}$$

$$[\nabla s]_\theta = \frac{1}{r}\frac{\partial s}{\partial \theta} \tag{E}$$

$$[\nabla s]_\phi = \frac{1}{r\ \sin\ \theta}\frac{\partial s}{\partial \phi} \tag{F}$$

$$[\nabla \times \mathbf{v}]_r = \frac{1}{r\sin\theta}\frac{\partial}{\partial \theta}(v_\phi \sin\theta) - \frac{1}{r\sin\theta}\frac{\partial v_\theta}{\partial \phi} \tag{G}$$

$$[\nabla \times \mathbf{v}]_\theta = \frac{1}{r\sin\theta}\frac{\partial v_r}{\partial \phi} - \frac{1}{r}\frac{\partial}{\partial r}(r v_\phi) \tag{H}$$

$$[\nabla \times \mathbf{v}]_\phi = \frac{1}{r}\frac{\partial}{\partial r}(r v_\theta) - \frac{1}{r}\frac{\partial v_r}{\partial \theta} \tag{I}$$

$$[\nabla \cdot \boldsymbol{\tau}]_r = \frac{1}{r^2}\frac{\partial}{\partial r}(r^2\tau_{rr}) + \frac{1}{r\ \sin\ \theta}\frac{\partial}{\partial \theta}(\tau_{\theta r}\ \sin\ \theta) + \frac{1}{r\ \sin\ \theta}\frac{\partial}{\partial \phi}\tau_{\phi r} - \frac{\tau_{\theta\theta} + \tau_{\phi\phi}}{r} \tag{J}$$

$$[\nabla \cdot \boldsymbol{\tau}]_\theta = \frac{1}{r^3}\frac{\partial}{\partial r}(r^3\tau_{r\theta}) + \frac{1}{r\ \sin\ \theta}\frac{\partial}{\partial \theta}(\tau_{\theta\theta}\ \sin\ \theta) + \frac{1}{r\ \sin\ \theta}\frac{\partial}{\partial \phi}\tau_{\phi\theta} + \frac{(\tau_{\theta r} - \tau_{r\theta}) - \tau_{\phi\phi}\ \cot\ \theta}{r} \tag{K}$$

$$[\nabla \cdot \boldsymbol{\tau}]_\phi = \frac{1}{r^3}\frac{\partial}{\partial r}(r^3\tau_{r\phi}) + \frac{1}{r\ \sin\ \theta}\frac{\partial}{\partial \theta}(\tau_{\theta\phi}\ \sin\ \theta) + \frac{1}{r\ \sin\ \theta}\frac{\partial}{\partial \phi}\tau_{\phi\phi} + \frac{(\tau_{\phi r} - \tau_{r\phi}) + \tau_{\phi\theta}\ \cot\ \theta}{r} \tag{L}$$

$$[\nabla^2 \mathbf{v}]_r = \frac{\partial}{\partial r}\left(\frac{1}{r^2}\frac{\partial}{\partial r}(r^2 v_r)\right) + \frac{1}{r^2\ \sin\ \theta}\frac{\partial}{\partial \theta}\left(\sin\ \theta\frac{\partial v_r}{\partial \theta}\right) + \frac{1}{r^2\ \sin^2\theta}\frac{\partial^2 v_r}{\partial \phi^2} - \frac{2}{r^2\ \sin\ \theta}\frac{\partial}{\partial \theta}(v_\theta\ \sin\ \theta) - \frac{2}{r^2\ \sin\ \theta}\frac{\partial v_\phi}{\partial \phi} \tag{M}$$

$$[\nabla^2 \mathbf{v}]_\theta = \frac{1}{r^2}\frac{\partial}{\partial r}\left(r^2\frac{\partial v_\theta}{\partial r}\right) + \frac{1}{r^2}\frac{\partial}{\partial \theta}\left(\frac{1}{\sin\ \theta}\frac{\partial}{\partial \theta}(v_\theta\ \sin\ \theta)\right) + \frac{1}{r^2\ \sin^2\theta}\frac{\partial^2 v_\theta}{\partial \phi^2} + \frac{2}{r^2}\frac{\partial v_r}{\partial \theta} - \frac{2\ \cot\ \theta}{r^2\ \sin\ \theta}\frac{\partial v_\phi}{\partial \phi} \tag{N}$$

$$[\nabla^2 \mathbf{v}]_\phi = \frac{1}{r^2}\frac{\partial}{\partial r}\left(r^2\frac{\partial v_\phi}{\partial r}\right) + \frac{1}{r^2}\frac{\partial}{\partial \theta}\left(\frac{1}{\sin\ \theta}\frac{\partial}{\partial \theta}(v_\phi\ \sin\ \theta)\right) + \frac{1}{r^2\ \sin^2\theta}\frac{\partial^2 v_\phi}{\partial \phi^2} + \frac{2}{r^2\ \sin\ \theta}\frac{\partial v_r}{\partial \phi} + \frac{2\ \cot\ \theta}{r^2\ \sin\ \theta}\frac{\partial v_\theta}{\partial \phi} \tag{O}$$

$$[\mathbf{v} \cdot \nabla\mathbf{w}]_r = v_r\left(\frac{\partial w_r}{\partial r}\right) + v_\theta\left(\frac{1}{r}\frac{\partial w_r}{\partial \theta} - \frac{w_\theta}{r}\right) + v_\phi\left(\frac{1}{r\ \sin\ \theta}\frac{\partial w_r}{\partial \phi} - \frac{w_\phi}{r}\right) \tag{P}$$

$$[\mathbf{v} \cdot \nabla\mathbf{w}]_\theta = v_r\left(\frac{\partial w_\theta}{\partial r}\right) + v_\theta\left(\frac{1}{r}\frac{\partial w_\theta}{\partial \theta} + \frac{w_r}{r}\right) + v_\phi\left(\frac{1}{r\ \sin\ \theta}\frac{\partial w_\theta}{\partial \phi} - \frac{w_\phi}{r}\cot\ \theta\right) \tag{Q}$$

$$[\mathbf{v} \cdot \nabla\mathbf{w}]_\phi = v_r\left(\frac{\partial w_\phi}{\partial r}\right) + v_\theta\left(\frac{1}{r}\frac{\partial w_\phi}{\partial \theta}\right) + v_\phi\left(\frac{1}{r\ \sin\ \theta}\frac{\partial w_\phi}{\partial \phi} + \frac{w_r}{r} + \frac{w_\theta}{r}\cot\ \theta\right) \tag{R}$$

$$\{\nabla \mathbf{v}\}_{rr} = \frac{\partial v_r}{\partial r} \tag{S}$$

$$\{\nabla \mathbf{v}\}_{r\theta} = \frac{\partial v_\theta}{\partial r} \tag{T}$$

$$\{\nabla \mathbf{v}\}_{r\phi} = \frac{\partial v_\phi}{\partial r} \tag{U}$$

$$\{\nabla \mathbf{v}\}_{\theta r} = \frac{1}{r}\frac{\partial v_r}{\partial \theta} - \frac{v_\theta}{r} \tag{V}$$

$$\{\nabla \mathbf{v}\}_{\theta\theta} = \frac{1}{r}\frac{\partial v_\theta}{\partial \theta} + \frac{v_r}{r} \tag{W}$$

$$\{\nabla \mathbf{v}\}_{\theta\phi} = \frac{1}{r}\frac{\partial v_\phi}{\partial \theta} \tag{X}$$

$$\{\nabla \mathbf{v}\}_{\phi r} = \frac{1}{r \sin \theta}\frac{\partial v_r}{\partial \phi} - \frac{v_\phi}{r} \tag{Y}$$

$$\{\nabla \mathbf{v}\}_{\phi\theta} = \frac{1}{r \sin \theta}\frac{\partial v_\theta}{\partial \phi} - \frac{v_\phi}{r}\cot\theta \tag{Z}$$

$$\{\nabla \mathbf{v}\}_{\phi\phi} = \frac{1}{r \sin \theta}\frac{\partial v_\phi}{\partial \phi} + \frac{v_r}{r} + \frac{v_\theta}{r}\cot\theta \tag{AA}$$

$$\{\mathbf{v}\cdot\nabla\boldsymbol{\tau}\}_{rr} = (\mathbf{v}\cdot\nabla)\tau_{rr} - \left(\frac{v_\theta}{r}\right)(\tau_{r\theta} + \tau_{\theta r}) - \left(\frac{v_\phi}{r}\right)(\tau_{r\phi} + \tau_{\phi r}) \tag{BB}$$

$$\{\mathbf{v}\cdot\nabla\boldsymbol{\tau}\}_{r\theta} = (\mathbf{v}\cdot\nabla)\tau_{r\theta} + \left(\frac{v_\theta}{r}\right)(\tau_{rr} - \tau_{\theta\theta}) - \left(\frac{v_\phi}{r}\right)(\tau_{\phi\theta} + \tau_{r\phi}\cot\theta) \tag{CC}$$

$$\{\mathbf{v}\cdot\nabla\boldsymbol{\tau}\}_{r\phi} = (\mathbf{v}\cdot\nabla)\tau_{r\phi} - \left(\frac{v_\theta}{r}\right)\tau_{\theta\phi} + \left(\frac{v_\phi}{r}\right)[(\tau_{rr} - \tau_{\phi\phi}) + \tau_{r\theta}\cot\theta] \tag{DD}$$

$$\{\mathbf{v}\cdot\nabla\boldsymbol{\tau}\}_{\theta r} = (\mathbf{v}\cdot\nabla)\tau_{\theta r} + \left(\frac{v_\theta}{r}\right)(\tau_{rr} - \tau_{\theta\theta}) - \left(\frac{v_\phi}{r}\right)(\tau_{\theta\phi} + \tau_{\phi r}\cot\theta) \tag{EE}$$

$$\{\mathbf{v}\cdot\nabla\boldsymbol{\tau}\}_{\theta\theta} = (\mathbf{v}\cdot\nabla)\tau_{\theta\theta} + \left(\frac{v_\theta}{r}\right)(\tau_{r\theta} + \tau_{\theta r}) - \left(\frac{v_\phi}{r}\right)(\tau_{\theta\phi} + \tau_{\phi\theta})\cot\theta \tag{FF}$$

$$\{\mathbf{v}\cdot\nabla\boldsymbol{\tau}\}_{\theta\phi} = (\mathbf{v}\cdot\nabla)\tau_{\theta\phi} + \left(\frac{v_\theta}{r}\right)\tau_{r\phi} + \left(\frac{v_\phi}{r}\right)[\tau_{\theta r} + (\tau_{\theta\theta} - \tau_{\phi\phi})\cot\theta] \tag{GG}$$

$$\{\mathbf{v}\cdot\nabla\boldsymbol{\tau}\}_{\phi r} = (\mathbf{v}\cdot\nabla)\tau_{\phi r} - \left(\frac{v_\theta}{r}\right)\tau_{\phi\theta} + \left(\frac{v_\phi}{r}\right)[(\tau_{rr} - \tau_{\phi\phi}) + \tau_{\theta r}\cot\theta] \tag{HH}$$

$$\{\mathbf{v}\cdot\nabla\boldsymbol{\tau}\}_{\phi\theta} = (\mathbf{v}\cdot\nabla)\tau_{\phi\theta} + \left(\frac{v_\theta}{r}\right)\tau_{\phi r} + \left(\frac{v_\phi}{r}\right)[\tau_{r\theta} + (\tau_{\theta\theta} - \tau_{\phi\phi})\cot\theta] \tag{II}$$

$$\{\mathbf{v}\cdot\nabla\boldsymbol{\tau}\}_{\phi\phi} = (\mathbf{v}\cdot\nabla)\tau_{\phi\phi} + \left(\frac{v_\phi}{r}\right)[(\tau_{r\phi} + \tau_{\phi r}) + (\tau_{\theta\phi} + \tau_{\phi\theta})\cot\theta] \tag{JJ}$$

where the operator $(\mathbf{v}\cdot\nabla) = v_r\frac{\partial}{\partial r} + \frac{v_\theta}{r}\frac{\partial}{\partial\theta} + \frac{v_\phi}{r\sin\theta}\frac{\partial}{\partial\phi}$

(b) Next we examine the dyadic product ∇v:

$$\begin{aligned}\nabla\mathbf{v} &= \left\{\boldsymbol{\delta}_r\frac{\partial}{\partial r}+\boldsymbol{\delta}_\theta\frac{1}{r}\frac{\partial}{\partial\theta}+\boldsymbol{\delta}_z\frac{\partial}{\partial z}\right\}\{\boldsymbol{\delta}_r v_r+\boldsymbol{\delta}_\theta v_\theta+\boldsymbol{\delta}_z v_z\}\\ &= \boldsymbol{\delta}_r\boldsymbol{\delta}_r\frac{\partial v_r}{\partial r}+\boldsymbol{\delta}_r\boldsymbol{\delta}_\theta\frac{\partial v_\theta}{\partial r}+\boldsymbol{\delta}_r\boldsymbol{\delta}_z\frac{\partial v_z}{\partial r}+\boldsymbol{\delta}_\theta\boldsymbol{\delta}_r\frac{1}{r}\frac{\partial v_r}{\partial\theta}+\boldsymbol{\delta}_\theta\boldsymbol{\delta}_\theta\frac{1}{r}\frac{\partial v_\theta}{\partial\theta}+\boldsymbol{\delta}_\theta\boldsymbol{\delta}_z\frac{1}{r}\frac{\partial v_z}{\partial\theta}\\ &\quad+\boldsymbol{\delta}_\theta\boldsymbol{\delta}_\theta\frac{v_r}{r}-\boldsymbol{\delta}_\theta\boldsymbol{\delta}_r\frac{v_\theta}{r}+\boldsymbol{\delta}_z\boldsymbol{\delta}_r\frac{\partial v_r}{\partial z}+\boldsymbol{\delta}_z\boldsymbol{\delta}_\theta\frac{\partial v_\theta}{\partial z}+\boldsymbol{\delta}_z\boldsymbol{\delta}_z\frac{\partial v_z}{\partial z}\\ &= \boldsymbol{\delta}_r\boldsymbol{\delta}_r\frac{\partial v_r}{\partial r}+\boldsymbol{\delta}_r\boldsymbol{\delta}_\theta\frac{\partial v_\theta}{\partial r}+\boldsymbol{\delta}_r\boldsymbol{\delta}_z\frac{\partial v_z}{\partial r}+\boldsymbol{\delta}_\theta\boldsymbol{\delta}_r\left(\frac{1}{r}\frac{\partial v_r}{\partial\theta}-\frac{v_\theta}{r}\right)+\boldsymbol{\delta}_\theta\boldsymbol{\delta}_\theta\left(\frac{1}{r}\frac{\partial v_\theta}{\partial\theta}+\frac{v_r}{r}\right)\\ &\quad+\boldsymbol{\delta}_\theta\boldsymbol{\delta}_z\frac{1}{r}\frac{\partial v_z}{\partial\theta}+\boldsymbol{\delta}_z\boldsymbol{\delta}_r\frac{\partial v_r}{\partial z}+\boldsymbol{\delta}_z\boldsymbol{\delta}_\theta\frac{\partial v_\theta}{\partial z}+\boldsymbol{\delta}_z\boldsymbol{\delta}_z\frac{\partial v_z}{\partial z}\end{aligned}\tag{A.7-23}$$

Hence, the rr-component is $\partial v_r/\partial r$, the $r\theta$-component is $\partial v_\theta/\partial r$, and so on, as given in Table A.7-2.

EXAMPLE A.7-2

Differential Operations in Spherical Coordinates

Find the r-component of $[\nabla\cdot\boldsymbol{\tau}]$ in spherical coordinates.

SOLUTION

Using Eq. A.7-9 we have

$$\begin{aligned}[\nabla\cdot\boldsymbol{\tau}]_r = \Bigg[\left\{\boldsymbol{\delta}_r\frac{\partial}{\partial r}+\boldsymbol{\delta}_\theta\frac{1}{r}\frac{\partial}{\partial\theta}+\boldsymbol{\delta}_\phi\frac{1}{r\sin\theta}\frac{\partial}{\partial\phi}\right\}\cdot\{&\boldsymbol{\delta}_r\boldsymbol{\delta}_r\tau_{rr}+\boldsymbol{\delta}_r\boldsymbol{\delta}_\theta\tau_{r\theta}+\boldsymbol{\delta}_r\boldsymbol{\delta}_\phi\tau_{r\phi}\\ &+\boldsymbol{\delta}_\theta\boldsymbol{\delta}_r\tau_{\theta r}+\boldsymbol{\delta}_\theta\boldsymbol{\delta}_\theta\tau_{\theta\theta}+\boldsymbol{\delta}_\theta\boldsymbol{\delta}_\phi\tau_{\theta\phi}+\boldsymbol{\delta}_\phi\boldsymbol{\delta}_r\tau_{\phi r}+\boldsymbol{\delta}_\phi\boldsymbol{\delta}_\theta\tau_{\phi\theta}+\boldsymbol{\delta}_\phi\boldsymbol{\delta}_\phi\tau_{\phi\phi}\}\Bigg]\end{aligned}\tag{A.7-24}$$

We now use Eqs. A.7-6, 7, 8 and Eq. A.3-3. Since we want only the r-component, we select only those terms that contribute to the coefficient of $\boldsymbol{\delta}_r$:

$$\left[\boldsymbol{\delta}_r\frac{\partial}{\partial r}\cdot\boldsymbol{\delta}_r\boldsymbol{\delta}_r\tau_{rr}\right]=[\boldsymbol{\delta}_r\cdot\boldsymbol{\delta}_r\boldsymbol{\delta}_r]\frac{\partial\tau_{rr}}{\partial r}=\boldsymbol{\delta}_r\frac{\partial\tau_{rr}}{\partial r}\tag{A.7-25}$$

$$\left[\boldsymbol{\delta}_\theta\frac{1}{r}\frac{\partial}{\partial\theta}\cdot\boldsymbol{\delta}_\theta\boldsymbol{\delta}_r\tau_{\theta r}\right]=[\boldsymbol{\delta}_\theta\cdot\boldsymbol{\delta}_\theta\boldsymbol{\delta}_r]\frac{1}{r}\frac{\partial}{\partial\theta}\tau_{\theta r}+\text{other term}\tag{A.7-26}$$

$$\left[\boldsymbol{\delta}_\phi\frac{1}{r\sin\theta}\frac{\partial}{\partial\phi}\cdot\boldsymbol{\delta}_\phi\boldsymbol{\delta}_r\tau_{\phi r}\right]=[\boldsymbol{\delta}_\phi\cdot\boldsymbol{\delta}_\phi\boldsymbol{\delta}_r]\frac{1}{r\sin\phi}\frac{\partial}{\partial\phi}\tau_{\phi r}+\text{other term}\tag{A.7-27}$$

$$\begin{aligned}\left[\boldsymbol{\delta}_\theta\frac{1}{r}\frac{\partial}{\partial\theta}\cdot\boldsymbol{\delta}_r\boldsymbol{\delta}_r\tau_{rr}\right]&=\frac{\tau_{rr}}{r}\left[\boldsymbol{\delta}_\theta\cdot\left\{\frac{\partial}{\partial\theta}\boldsymbol{\delta}_r\right\}\boldsymbol{\delta}_r\right]+\frac{\tau_{rr}}{r}\left[\boldsymbol{\delta}_\theta\cdot\boldsymbol{\delta}_r\left\{\frac{\partial}{\partial\theta}\boldsymbol{\delta}_r\right\}\right]\\ &=\frac{\tau_{rr}}{r}[\boldsymbol{\delta}_\theta\cdot\boldsymbol{\delta}_\theta\boldsymbol{\delta}_r]=\boldsymbol{\delta}_r\frac{\tau_{rr}}{r}\end{aligned}\tag{A.7-28}$$

$$\begin{aligned}\left[\boldsymbol{\delta}_\phi\frac{1}{r\sin\theta}\frac{\partial}{\partial\phi}\cdot\boldsymbol{\delta}_r\boldsymbol{\delta}_r\tau_{rr}\right]&=\frac{\tau_{rr}}{r\sin\theta}\left[\boldsymbol{\delta}_\phi\cdot\left\{\frac{\partial}{\partial\phi}\boldsymbol{\delta}_r\right\}\boldsymbol{\delta}_r\right]\\ &=\frac{\tau_{rr}}{r\sin\theta}[\boldsymbol{\delta}_\phi\cdot\boldsymbol{\delta}_\phi\sin\theta\,\boldsymbol{\delta}_r]=\boldsymbol{\delta}_r\frac{\tau_{rr}}{r}\end{aligned}\tag{A.7-29}$$

$$\left[\boldsymbol{\delta}_\theta\frac{1}{r}\frac{\partial}{\partial\theta}\cdot\boldsymbol{\delta}_\theta\boldsymbol{\delta}_\theta\tau_{\theta\theta}\right]=\boldsymbol{\delta}_r\left(-\frac{\tau_{\theta\theta}}{r}\right)+\text{other term}\tag{A.7-30}$$

$$\left[\boldsymbol{\delta}_\phi\frac{1}{r\sin\theta}\frac{\partial}{\partial\phi}\cdot\boldsymbol{\delta}_\theta\boldsymbol{\delta}_r\tau_{\theta r}\right]=\boldsymbol{\delta}_r\frac{\tau_{\theta r}\cos\theta}{r\sin\theta}\tag{A.7-31}$$

$$\left[\boldsymbol{\delta}_\phi\frac{1}{r\sin\theta}\frac{\partial}{\partial\phi}\cdot\boldsymbol{\delta}_\phi\boldsymbol{\delta}_\phi\tau_{\phi\phi}\right]=\boldsymbol{\delta}_r\left(\frac{-\tau_{\phi\phi}}{r}\right)+\text{other terms}\tag{A.7-32}$$

Combining the above results we get

$$[\nabla \cdot \boldsymbol{\tau}]_r = \frac{1}{r^2}\frac{\partial}{\partial r}(r^2\tau_{rr}) + \frac{\tau_{\theta r}}{r}\cot\theta + \frac{1}{r}\frac{\partial}{\partial\theta}\tau_{\theta r} + \frac{1}{r\sin\theta}\frac{\partial\tau_{\phi r}}{\partial\phi} - \frac{\tau_{\theta\theta}+\tau_{\phi\phi}}{r} \tag{A.7-33}$$

Note that this expression is correct whether or not $\boldsymbol{\tau}$ is symmetric.

EXERCISES

1. If $\mathbf{r}$ is the instantaneous position vector for a particle, show that the velocity and acceleration of the particle are given by (use Eq. A.7-2):

$$\mathbf{v} = \frac{d}{dt}\mathbf{r} = \boldsymbol{\delta}_r\dot{r} + \boldsymbol{\delta}_\theta r\dot{\theta} + \boldsymbol{\delta}_z\dot{z} \tag{A.7-34}$$

$$\mathbf{a} = \boldsymbol{\delta}_r(\ddot{r} - r\dot{\theta}^2) + \boldsymbol{\delta}_\theta(r\ddot{\theta} + 2\dot{r}\dot{\theta}) + \boldsymbol{\delta}_z\ddot{z} \tag{A.7-35}$$

in cylindrical coordinates. The dots indicate time derivatives of the coordinates.

2. Obtain $(\nabla \cdot \mathbf{v})$, $[\nabla \times \mathbf{v}]$, and $\nabla\mathbf{v}$ in spherical coordinates, and $[\nabla \cdot \boldsymbol{\tau}]$ in cylindrical coordinates.

3. Use Table A.7-2 to write down directly the following quantities in cylindrical coordinates:
   (a) $(\nabla \cdot \rho\mathbf{v})$, where ρ is a scalar
   (b) $[\nabla \cdot \rho\mathbf{vv}]_r$, where ρ is a scalar
   (c) $[\nabla \cdot p\boldsymbol{\delta}]_\theta$, where p is a scalar
   (d) $(\nabla \cdot [\boldsymbol{\tau} \cdot \mathbf{v}])$
   (e) $[\mathbf{v} \cdot \nabla\mathbf{v}]_\theta$
   (f) $\nabla\mathbf{v} + (\nabla\mathbf{v})^\dagger$

4. Verify that the entries for $\nabla^2 v$ in Table A.7-2 can be obtained by any one of the following methods:
   (a) First verify that, in cylindrical coordinates the operator $(\nabla \cdot \nabla)$ is

$$(\nabla \cdot \nabla) = \frac{\partial^2}{\partial r^2} + \frac{1}{r}\frac{\partial}{\partial r} + \frac{1}{r^2}\frac{\partial^2}{\partial\theta^2} + \frac{\partial^2}{\partial z^2} \tag{A.7-36}$$

   and then apply the operator to $\mathbf{v}$.
   (b) Use the expression for $[\nabla \cdot \boldsymbol{\tau}]$ in Table A.7-2, but substitute the components for $\nabla\mathbf{v}$ in place of the components of $\boldsymbol{\tau}$, so as to obtain $[\nabla \cdot \nabla v]$.
   (c) Use Eq. A.4-22:

$$\nabla^2\mathbf{v} = \nabla(\nabla \cdot \mathbf{v}) - [\nabla \times [\nabla \times \mathbf{v}]] \tag{A.7-37}$$

   and use the gradient, divergence, and curl operations in Table A.7-2 to evaluate the operations on the right side.

§A.8 INTEGRAL OPERATIONS IN CURVILINEAR COORDINATES

In performing the integrations of §A.5 in curvilinear coordinates, it is important to understand the construction of the volume elements, as is shown for cylindrical coordinates in Fig. A.8-1 and for spherical coordinates in Fig. A.8-2.

In doing *volume integrals*, the simplest situations are those in which the bounding surfaces are surfaces of the coordinate system. For *cylindrical coordinates*, a typical volume integral of a function $f(r, \theta, z)$ would be of the form

$$\int_{z_1}^{z_2}\int_{\theta_1}^{\theta_2}\int_{r_1}^{r_2} f(r,\theta,z)\,r\,dr\,d\theta\,dz \tag{A.8-1}$$

and for *spherical coordinates* a typical volume integral of a function $g(r, \theta, \phi)$ would be

$$\int_{\phi_1}^{\phi_2}\int_{\theta_1}^{\theta_2}\int_{r_1}^{r_2} g(r,\theta,\phi)\,r^2\,dr\,\sin\theta\,d\theta\,d\phi \tag{A.8-2}$$

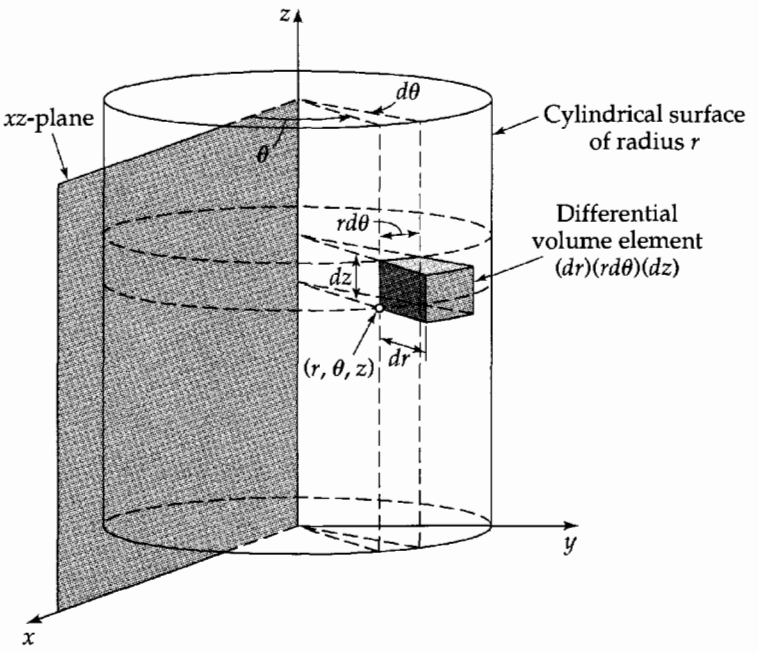

Fig. A.8-1. Differential volume element $r\,dr\,d\theta\,dz$ in cylindrical coordinates, and differential line elements dr, $r\,d\theta$, and dz. The differential surface elements are: $(r\,d\theta)(dz)$ perpendicular to the r direction (intermediate shading); $(dz)(dr)$ perpendicular to the θ direction (darkest shading); and $(dr)(r\,d\theta)$ perpendicular to the z direction (lightest shading).

Since the limits in these integrals (r_1, r_2, θ_1, θ_2, etc.) are constants, the order of the integration is immaterial.

In doing *surface integrals*, the simplest situations are those in which the integration is performed on one of the surfaces of the coordinate system. For *cylindrical coordinates* there are three possibilities:

On the surface $r = r_0$:
$$\int_{z_1}^{z_2}\int_{\theta_1}^{\theta_2} f(r_0, \theta, z) r_0\, d\theta\, dz \tag{A.8-3}$$

On the surface $\theta = \theta_0$:
$$\int_{z_1}^{z_2}\int_{r_1}^{r_2} f(r, \theta_0, z) r\, dr\, dz \tag{A.8-4}$$

On the surface $z = z_0$:
$$\int_{\theta_1}^{\theta_2}\int_{r_1}^{r_2} f(r, \theta, z_0) r\, dr\, d\theta \tag{A.8-5}$$

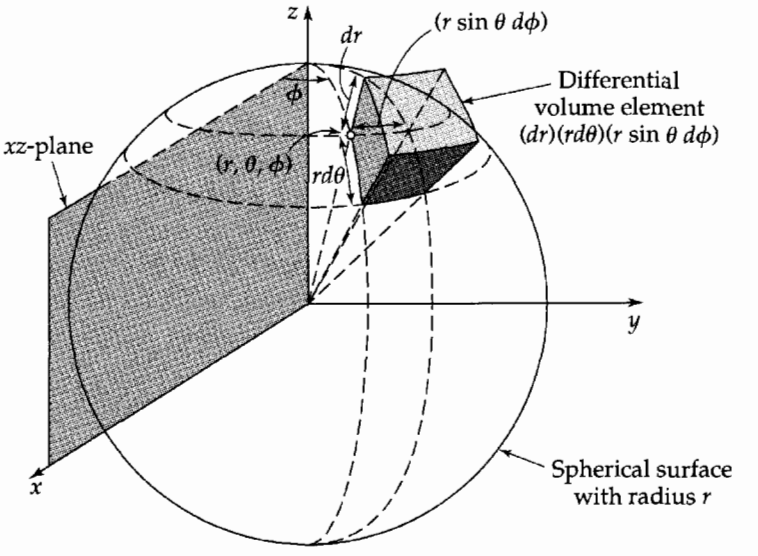

Fig. A.8-2. Differential volume element $r^2 \sin\theta\, dr\, d\theta\, d\phi$ in spherical coordinates, and the differential line elements dr, $r\,d\theta$, and $r \sin\theta\, d\phi$. The differential surface elements are: $(r\,d\theta)(r \sin\theta\, d\phi)$ perpendicular to the r direction (lightest shading); $(r \sin\theta\, d\phi)(dr)$ perpendicular to the θ direction (darkest shading); and $(dr)(r\,d\theta)$ perpendicular to the ϕ direction (intermediate shading).

Similarly, for *spherical coordinates*:

On the surface $r = r_0$: $$\int_{\phi_1}^{\phi_2}\int_{\theta_1}^{\theta_2} g(r_0, \theta, \phi) r_0^2 \sin\theta \, d\theta \, d\phi \tag{A.8-6}$$

On the surface $\theta = \theta_0$: $$\int_{\phi}^{\phi_2}\int_{r_1}^{r_2} g(r, \theta_0, \phi) \sin\theta_0 \, r^2 \, dr \, d\phi \tag{A.8-7}$$

On the surface $\phi = \phi_0$: $$\int_{\theta_1}^{\theta_2}\int_{r_1}^{r_2} g(r, \theta, \phi_0) r^2 \, dr \sin\theta \, d\theta \tag{A.8-8}$$

The reader should try making sketches to show exactly what areas are described by each of the above six surface integrals.

If the area of integration in a surface integral is not one of the surfaces of the coordinate system, then a book on differential and integral calculus should be consulted.

§A.9 FURTHER COMMENTS ON VECTOR–TENSOR NOTATION

The boldface notation used in this book is called *Gibbs notation*.[1] Also widely used is another notation referred to as Cartesian tensor notation.[2] As shown in Table A.9-1, a few examples suffice to compare the two systems. The two outer columns are just two different ways of abbreviating the operations described explicitly in the middle column in Cartesian coordinates. The rules for converting from one system to another are as follows.

To convert from expanded notation to Cartesian tensor notation:

1. Omit all summation signs (the "Einstein summation convention")
2. Omit all unit vectors and unit dyads.
3. Replace $\partial/\partial x_i$ by ∂_i.

Table A.9-1

Gibbs notation	Expanded notation in terms of unit vectors and unit dyads	Cartesian tensor notation
$(\mathbf{v}\cdot\mathbf{w})$	$\sum_i v_i w_i$	$v_i w_i$
$[\mathbf{v}\times\mathbf{w}]$	$\sum_i\sum_j\sum_k \varepsilon_{ijk}\boldsymbol{\delta}_i v_j w_k$	$\varepsilon_{ijk} v_j w_k$
$[\nabla\cdot\boldsymbol{\tau}]$	$\sum_i\sum_j \boldsymbol{\delta}_i \frac{\partial}{\partial x_j}\tau_{ji}$	$\partial_j \tau_{ji}$
$\nabla^2 s$	$\sum_i \frac{\partial^2}{\partial x_i^2} s$	$\partial_i\partial_i s$
$[\nabla\times[\nabla\times\mathbf{v}]]$	$\sum_i\sum_j\sum_k\sum_m\sum_n \boldsymbol{\delta}_i\varepsilon_{ijk}\varepsilon_{kmn}\frac{\partial}{\partial x_j}\frac{\partial}{\partial x_m} v_n$	$\varepsilon_{ijk}\varepsilon_{kmn}\partial_j\partial_m v_n$
$\{\boldsymbol{\tau}\times\mathbf{v}\}$	$\sum_i\sum_j\sum_k\sum_l \varepsilon_{jkl}\boldsymbol{\delta}_i\boldsymbol{\delta}_l\tau_{ij}v_k$	$\varepsilon_{jkl}\tau_{ij}v_k$

[1] J. W. Gibbs, *Vector Analysis*, Dover Reprint, New York (1960).
[2] W. Prager, *Mechanics of Continua*, Ginn, Boston (1961).

To convert from Cartesian tensor notation to expanded notation:

1. Supply summation signs for all repeated indices.
2. Supply unit vectors and unit dyads for all nonrepeated indices; in each term of a tensor equation the unit vectors must appear in the same order in the unit dyads.
3. Replace ∂_i by $\partial/\partial x_i$.

The Gibbs notation is compact, easy to read, and devoid of any reference to a particular coordinate system; however, one has to know the meaning of the dot and cross operations and the use of boldface symbols. The Cartesian tensor notation indicates the nature of the operations explicitly in Cartesian coordinates, but errors in reading or writing subscripts can be most aggravating. People who know both systems equally well prefer the Gibbs notation for general discussions and for presenting results, but revert to Cartesian tensor notation for doing proofs of identities.

Occasionally *matrix notation* is used to display the components of vectors and tensors with respect to designated coordinate systems. For example, when $v_x = \dot{\gamma}y$, $v_y = 0$, $v_z = 0$, $\nabla\mathbf{v}$ can be written in two ways:

$$\nabla\mathbf{v} = \boldsymbol{\delta}_y\boldsymbol{\delta}_x\dot{\gamma} = \begin{pmatrix} 0 & 0 & 0 \\ \dot{\gamma} & 0 & 0 \\ 0 & 0 & 0 \end{pmatrix} \tag{A.9-1}$$

The second "=" is not really an "equals" sign, but has to be interpreted as "may be displayed as." Note that this notation is somewhat dangerous since one has to infer the unit dyads that are to be multiplied by the matrix elements—in this case, $\boldsymbol{\delta}_x\boldsymbol{\delta}_x$, $\boldsymbol{\delta}_x\boldsymbol{\delta}_y$, and so on. If we had used cylindrical coordinates, $\nabla\mathbf{v}$ would be represented by the matrix

$$\nabla\mathbf{v} = \begin{pmatrix} \dot{\gamma}\sin\theta\cos\theta & -\dot{\gamma}\sin^2\theta & 0 \\ \dot{\gamma}\cos^2\theta & -\dot{\gamma}\sin\theta\cos\theta & 0 \\ 0 & 0 & 0 \end{pmatrix} \tag{A.9-2}$$

where the matrix elements are understood to be multiplied by $\boldsymbol{\delta}_r\boldsymbol{\delta}_r$, $\boldsymbol{\delta}_r\boldsymbol{\delta}_\theta$, and so on, and then added together.

Despite the hazard of misinterpretation and the loose use of "=," the matrix notation enjoys widespread use, the main reason being that the "dot" operations correspond to standard matrix multiplication rules. For example,

$$(\mathbf{v}\cdot\mathbf{w}) = (v_1 \quad v_2 \quad v_3)\begin{pmatrix} w_1 \\ w_2 \\ w_3 \end{pmatrix} = v_1w_1 + v_2w_2 + v_3w_3 \tag{A.9-3}$$

$$[\boldsymbol{\tau}\cdot\mathbf{v}] = \begin{pmatrix} \tau_{11} & \tau_{12} & \tau_{13} \\ \tau_{21} & \tau_{22} & \tau_{23} \\ \tau_{31} & \tau_{32} & \tau_{33} \end{pmatrix}\begin{pmatrix} v_1 \\ v_2 \\ v_3 \end{pmatrix} = \begin{pmatrix} \tau_{11}v_1 + \tau_{12}v_2 + \tau_{13}v_3 \\ \tau_{21}v_1 + \tau_{22}v_2 + \tau_{23}v_3 \\ \tau_{31}v_1 + \tau_{32}v_2 + \tau_{33}v_3 \end{pmatrix} \tag{A.9-4}$$

Of course such matrix multiplications are meaningful only when the components are referred to the same unit vectors.

Appendix B

The Fluxes and the Equations of Change

§B.1 NEWTON'S LAW OF VISCOSITY

$$[\boldsymbol{\tau} = -\mu(\nabla\mathbf{v} + (\nabla\mathbf{v})^\dagger) + (\tfrac{2}{3}\mu - \kappa)(\nabla\cdot\mathbf{v})\boldsymbol{\delta}]$$

Cartesian coordinates (x, y, z):

$$\tau_{xx} = -\mu\left[2\frac{\partial v_x}{\partial x}\right] + (\tfrac{2}{3}\mu - \kappa)(\nabla\cdot\mathbf{v}) \tag{B.1-1}^a$$

$$\tau_{yy} = -\mu\left[2\frac{\partial v_y}{\partial y}\right] + (\tfrac{2}{3}\mu - \kappa)(\nabla\cdot\mathbf{v}) \tag{B.1-2}^a$$

$$\tau_{zz} = -\mu\left[2\frac{\partial v_z}{\partial z}\right] + (\tfrac{2}{3}\mu - \kappa)(\nabla\cdot\mathbf{v}) \tag{B.1-3}^a$$

$$\tau_{xy} = \tau_{yx} = -\mu\left[\frac{\partial v_y}{\partial x} + \frac{\partial v_x}{\partial y}\right] \tag{B.1-4}$$

$$\tau_{yz} = \tau_{zy} = -\mu\left[\frac{\partial v_z}{\partial y} + \frac{\partial v_y}{\partial z}\right] \tag{B.1-5}$$

$$\tau_{zx} = \tau_{xz} = -\mu\left[\frac{\partial v_x}{\partial z} + \frac{\partial v_z}{\partial x}\right] \tag{B.1-6}$$

in which

$$(\nabla\cdot\mathbf{v}) = \frac{\partial v_x}{\partial x} + \frac{\partial v_y}{\partial y} + \frac{\partial v_z}{\partial z} \tag{B.1-7}$$

[a] When the fluid is assumed to have constant density, the term containing $(\nabla\cdot\mathbf{v})$ may be omitted. For monatomic gases at low density, the dilatational viscosity κ is zero.

§B.1 NEWTON'S LAW OF VISCOSITY (continued)

Cylindrical coordinates (r, θ, z):

$$\tau_{rr} = -\mu\left[2\frac{\partial v_r}{\partial r}\right] + (\tfrac{2}{3}\mu - \kappa)(\nabla \cdot \mathbf{v}) \tag{B.1-8}^a$$

$$\tau_{\theta\theta} = -\mu\left[2\left(\frac{1}{r}\frac{\partial v_\theta}{\partial \theta} + \frac{v_r}{r}\right)\right] + (\tfrac{2}{3}\mu - \kappa)(\nabla \cdot \mathbf{v}) \tag{B.1-9}^a$$

$$\tau_{zz} = -\mu\left[2\frac{\partial v_z}{\partial z}\right] + (\tfrac{2}{3}\mu - \kappa)(\nabla \cdot \mathbf{v}) \tag{B.1-10}^a$$

$$\tau_{r\theta} = \tau_{\theta r} = -\mu\left[r\frac{\partial}{\partial r}\left(\frac{v_\theta}{r}\right) + \frac{1}{r}\frac{\partial v_r}{\partial \theta}\right] \tag{B.1-11}$$

$$\tau_{\theta z} = \tau_{z\theta} = -\mu\left[\frac{1}{r}\frac{\partial v_z}{\partial \theta} + \frac{\partial v_\theta}{\partial z}\right] \tag{B.1-12}$$

$$\tau_{zr} = \tau_{rz} = -\mu\left[\frac{\partial v_r}{\partial z} + \frac{\partial v_z}{\partial r}\right] \tag{B.1-13}$$

in which

$$(\nabla \cdot \mathbf{v}) = \frac{1}{r}\frac{\partial}{\partial r}(rv_r) + \frac{1}{r}\frac{\partial v_\theta}{\partial \theta} + \frac{\partial v_z}{\partial z} \tag{B.1-14}$$

[a] When the fluid is assumed to have constant density, the term containing $(\nabla \cdot \mathbf{v})$ may be omitted. For monatomic gases at low density, the dilatational viscosity κ is zero.

Spherical coordinates (r, θ, φ):

$$\tau_{rr} = -\mu\left[2\frac{\partial v_r}{\partial r}\right] + (\tfrac{2}{3}\mu - \kappa)(\nabla \cdot \mathbf{v}) \tag{B.1-15}^a$$

$$\tau_{\theta\theta} = -\mu\left[2\left(\frac{1}{r}\frac{\partial v_\theta}{\partial \theta} + \frac{v_r}{r}\right)\right] + (\tfrac{2}{3}\mu - \kappa)(\nabla \cdot \mathbf{v}) \tag{B.1-16}^a$$

$$\tau_{\phi\phi} = -\mu\left[2\left(\frac{1}{r\sin\theta}\frac{\partial v_\phi}{\partial \phi} + \frac{v_r + v_\theta \cot\theta}{r}\right)\right] + (\tfrac{2}{3}\mu - \kappa)(\nabla \cdot \mathbf{v}) \tag{B.1-17}^a$$

$$\tau_{r\theta} = \tau_{\theta r} = -\mu\left[r\frac{\partial}{\partial r}\left(\frac{v_\theta}{r}\right) + \frac{1}{r}\frac{\partial v_r}{\partial \theta}\right] \tag{B.1-18}$$

$$\tau_{\theta\phi} = \tau_{\phi\theta} = -\mu\left[\frac{\sin\theta}{r}\frac{\partial}{\partial \theta}\left(\frac{v_\phi}{\sin\theta}\right) + \frac{1}{r\sin\theta}\frac{\partial v_\theta}{\partial \phi}\right] \tag{B.1-19}$$

$$\tau_{\phi r} = \tau_{r\phi} = -\mu\left[\frac{1}{r\sin\theta}\frac{\partial v_r}{\partial \phi} + r\frac{\partial}{\partial r}\left(\frac{v_\phi}{r}\right)\right] \tag{B.1-20}$$

in which

$$(\nabla \cdot \mathbf{v}) = \frac{1}{r^2}\frac{\partial}{\partial r}(r^2 v_r) + \frac{1}{r\sin\theta}\frac{\partial}{\partial \theta}(v_\theta \sin\theta) + \frac{1}{r\sin\theta}\frac{\partial v_\phi}{\partial \phi} \tag{B.1-21}$$

[a] When the fluid is assumed to have constant density, the term containing $(\nabla \cdot \mathbf{v})$ may be omitted. For monatomic gases at low density, the dilatational viscosity κ is zero.

§B.2 FOURIER'S LAW OF HEAT CONDUCTION[a]

$$[\mathbf{q} = -k\nabla T]$$

Cartesian coordinates (x, y, z):

$$q_x = -k\frac{\partial T}{\partial x} \tag{B.2-1}$$

$$q_y = -k\frac{\partial T}{\partial y} \tag{B.2-2}$$

$$q_z = -k\frac{\partial T}{\partial z} \tag{B.2-3}$$

Cylindrical coordinates (r, θ, z):

$$q_r = -k\frac{dT}{\partial r} \tag{B.2-4}$$

$$q_\theta = -k\frac{1}{r}\frac{\partial T}{\partial \theta} \tag{B.2-5}$$

$$q_z = -k\frac{\partial T}{\partial z} \tag{B.2-6}$$

Spherical coordinates (r, θ, φ):

$$q_r = -k\frac{\partial T}{\partial r} \tag{B.2-7}$$

$$q_\theta = -k\frac{1}{r}\frac{\partial T}{\partial \theta} \tag{B.2-8}$$

$$q_\phi = -k\frac{1}{r\sin\theta}\frac{\partial T}{\partial \phi} \tag{B.2-9}$$

[a] For mixtures, the term $\Sigma_\alpha(\bar{H}_\alpha/M_\alpha)\mathbf{j}_\alpha$ must be added to $\mathbf{q}$ (see Eq. 19.3-3).

§B.3 FICK'S (FIRST) LAW OF BINARY DIFFUSION[a]

$$[\mathbf{j}_A = -\rho\mathscr{D}_{AB}\nabla\omega_A]$$

Cartesian coordinates (x, y, z):

$$j_{Ax} = -\rho\mathscr{D}_{AB}\frac{\partial\omega_A}{\partial x} \tag{B.3-1}$$

$$j_{Ay} = -\rho\mathscr{D}_{AB}\frac{\partial\omega_A}{\partial y} \tag{B.3-2}$$

$$j_{Az} = -\rho\mathscr{D}_{AB}\frac{\partial\omega_A}{\partial z} \tag{B.3-3}$$

Cylindrical coordinates (r, θ, z):

$$j_{Ar} = -\rho\mathscr{D}_{AB}\frac{\partial\omega_A}{\partial r} \tag{B.3-4}$$

$$j_{A\theta} = -\rho\mathscr{D}_{AB}\frac{1}{r}\frac{\partial\omega_A}{\partial\theta} \tag{B.3-5}$$

$$j_{Az} = -\rho\mathscr{D}_{AB}\frac{\partial\omega_A}{\partial z} \tag{B.3-6}$$

Spherical coordinates (r, θ, φ):

$$j_{Ar} = -\rho\mathscr{D}_{AB}\frac{\partial\omega_A}{\partial r} \tag{B.3-7}$$

$$j_{A\theta} = -\rho\mathscr{D}_{AB}\frac{1}{r}\frac{\partial\omega_A}{\partial\theta} \tag{B.3-8}$$

$$j_{A\phi} = -\rho\mathscr{D}_{AB}\frac{1}{r\sin\theta}\frac{\partial\omega_A}{\partial\phi} \tag{B.3-9}$$

[a] To get the molar fluxes with respect to the molar average velocity, replace $\mathbf{j}_A$, ρ, and ω_A by $\mathbf{J}^*_A$, c, and x_A.

§B.4 THE EQUATION OF CONTINUITY[a]

$$[\partial\rho/\partial t + (\nabla\cdot\rho\mathbf{v}) = 0]$$

Cartesian coordinates (x, y, z):

$$\frac{\partial\rho}{\partial t} + \frac{\partial}{\partial x}(\rho v_x) + \frac{\partial}{\partial y}(\rho v_y) + \frac{\partial}{\partial z}(\rho v_z) = 0 \tag{B.4-1}$$

Cylindrical coordinates (r, θ, z):

$$\frac{\partial\rho}{\partial t} + \frac{1}{r}\frac{\partial}{\partial r}(\rho r v_r) + \frac{1}{r}\frac{\partial}{\partial\theta}(\rho v_\theta) + \frac{\partial}{\partial z}(\rho v_z) = 0 \tag{B.4-2}$$

Spherical coordinates (r, θ, φ):

$$\frac{\partial\rho}{\partial t} + \frac{1}{r^2}\frac{\partial}{\partial r}(\rho r^2 v_r) + \frac{1}{r\sin\theta}\frac{\partial}{\partial\theta}(\rho v_\theta\sin\theta) + \frac{1}{r\sin\theta}\frac{\partial}{\partial\phi}(\rho v_\phi) = 0 \tag{B.4-3}$$

[a] When the fluid is assumed to have constant mass density ρ, the equation simplifies to $(\nabla\cdot\mathbf{v}) = 0$.

§B.5 THE EQUATION OF MOTION IN TERMS OF τ

$$[\rho D\mathbf{v}/Dt = -\nabla p - [\nabla \cdot \boldsymbol{\tau}] + \rho \mathbf{g}]$$

Cartesian coordinates (x, y, z):[a]

$$\rho\left(\frac{\partial v_x}{\partial t} + v_x\frac{\partial v_x}{\partial x} + v_y\frac{\partial v_x}{\partial y} + v_z\frac{\partial v_x}{\partial z}\right) = -\frac{\partial p}{\partial x} - \left[\frac{\partial}{\partial x}\tau_{xx} + \frac{\partial}{\partial y}\tau_{yx} + \frac{\partial}{\partial z}\tau_{zx}\right] + \rho g_x \tag{B.5-1}$$

$$\rho\left(\frac{\partial v_y}{\partial t} + v_x\frac{\partial v_y}{\partial x} + v_y\frac{\partial v_y}{\partial y} + v_z\frac{\partial v_y}{\partial z}\right) = -\frac{\partial p}{\partial y} - \left[\frac{\partial}{\partial x}\tau_{xy} + \frac{\partial}{\partial y}\tau_{yy} + \frac{\partial}{\partial z}\tau_{zy}\right] + \rho g_y \tag{B.5-2}$$

$$\rho\left(\frac{\partial v_z}{\partial t} + v_x\frac{\partial v_z}{\partial x} + v_y\frac{\partial v_z}{\partial y} + v_z\frac{\partial v_z}{\partial z}\right) = -\frac{\partial p}{\partial z} - \left[\frac{\partial}{\partial x}\tau_{xz} + \frac{\partial}{\partial y}\tau_{yz} + \frac{\partial}{\partial z}\tau_{zz}\right] + \rho g_z \tag{B.5-3}$$

[a] These equations have been written without making the assumption that $\boldsymbol{\tau}$ is symmetric. This means, for example, that when the usual assumption is made that the stress tensor is symmetric, τ_{xy} and τ_{yx} may be interchanged.

Cylindrical coordinates (r, θ, z):[b]

$$\rho\left(\frac{\partial v_r}{\partial t} + v_r\frac{\partial v_r}{\partial r} + \frac{v_\theta}{r}\frac{\partial v_r}{\partial \theta} + v_z\frac{\partial v_r}{\partial z} - \frac{v_\theta^2}{r}\right) = -\frac{\partial p}{\partial r} - \left[\frac{1}{r}\frac{\partial}{\partial r}(r\tau_{rr}) + \frac{1}{r}\frac{\partial}{\partial \theta}\tau_{\theta r} + \frac{\partial}{\partial z}\tau_{zr} - \frac{\tau_{\theta\theta}}{r}\right] + \rho g_r \tag{B.5-4}$$

$$\rho\left(\frac{\partial v_\theta}{\partial t} + v_r\frac{\partial v_\theta}{\partial r} + \frac{v_\theta}{r}\frac{\partial v_\theta}{\partial \theta} + v_z\frac{\partial v_\theta}{\partial z} + \frac{v_r v_\theta}{r}\right) = -\frac{1}{r}\frac{\partial p}{\partial \theta} - \left[\frac{1}{r^2}\frac{\partial}{\partial r}(r^2\tau_{r\theta}) + \frac{1}{r}\frac{\partial}{\partial \theta}\tau_{\theta\theta} + \frac{\partial}{\partial z}\tau_{z\theta} + \frac{\tau_{\theta r} - \tau_{r\theta}}{r}\right] + \rho g_\theta \tag{B.5-5}$$

$$\rho\left(\frac{\partial v_z}{\partial t} + v_r\frac{\partial v_z}{\partial r} + \frac{v_\theta}{r}\frac{\partial v_z}{\partial \theta} + v_z\frac{\partial v_z}{\partial z}\right) = -\frac{\partial p}{\partial z} - \left[\frac{1}{r}\frac{\partial}{\partial r}(r\tau_{rz}) + \frac{1}{r}\frac{\partial}{\partial \theta}\tau_{\theta z} + \frac{\partial}{\partial z}\tau_{zz}\right] + \rho g_z \tag{B.5-6}$$

[b] These equations have been written without making the assumption that $\boldsymbol{\tau}$ is symmetric. This means, for example, that when the usual assumption is made that the stress tensor is symmetric, $\tau_{r\theta} - \tau_{\theta r} = 0$.

Spherical coordinates (r, θ, φ):[c]

$$\rho\left(\frac{\partial v_r}{\partial t} + v_r\frac{\partial v_r}{\partial r} + \frac{v_\theta}{r}\frac{\partial v_r}{\partial \theta} + \frac{v_\phi}{r\sin\theta}\frac{\partial v_r}{\partial \phi} - \frac{v_\theta^2 + v_\phi^2}{r}\right) = -\frac{\partial p}{\partial r}$$
$$- \left[\frac{1}{r^2}\frac{\partial}{\partial r}(r^2\tau_{rr}) + \frac{1}{r\sin\theta}\frac{\partial}{\partial \theta}(\tau_{\theta r}\sin\theta) + \frac{1}{r\sin\theta}\frac{\partial}{\partial \phi}\tau_{\phi r} - \frac{\tau_{\theta\theta} + \tau_{\phi\phi}}{r}\right] + \rho g_r \tag{B.5-7}$$

$$\rho\left(\frac{\partial v_\theta}{\partial t} + v_r\frac{\partial v_\theta}{\partial r} + \frac{v_\theta}{r}\frac{\partial v_\theta}{\partial \theta} + \frac{v_\phi}{r\sin\theta}\frac{\partial v_\theta}{\partial \phi} + \frac{v_r v_\theta - v_\phi^2\cot\theta}{r}\right) = -\frac{1}{r}\frac{\partial p}{\partial \theta}$$
$$- \left[\frac{1}{r^3}\frac{\partial}{\partial r}(r^3\tau_{r\theta}) + \frac{1}{r\sin\theta}\frac{\partial}{\partial \theta}(\tau_{\theta\theta}\sin\theta) + \frac{1}{r\sin\theta}\frac{\partial}{\partial \phi}\tau_{\phi\theta} + \frac{(\tau_{\theta r} - \tau_{r\theta}) - \tau_{\phi\phi}\cot\theta}{r}\right) + \rho g_\theta \tag{B.5-8}$$

$$\rho\left(\frac{\partial v_\phi}{\partial t} + v_r\frac{\partial v_\phi}{\partial r} + \frac{v_\theta}{r}\frac{\partial v_\phi}{\partial \theta} + \frac{v_\phi}{r\sin\theta}\frac{\partial v_\phi}{\partial \phi} + \frac{v_\phi v_r + v_\theta v_\phi\cot\theta}{r}\right) = -\frac{1}{r\sin\theta}\frac{\partial p}{\partial \phi}$$
$$- \left[\frac{1}{r^3}\frac{\partial}{\partial r}(r^3\tau_{r\phi}) + \frac{1}{r\sin\theta}\frac{\partial}{\partial \theta}(\tau_{\theta\phi}\sin\theta) + \frac{1}{r\sin\theta}\frac{\partial}{\partial \phi}\tau_{\phi\phi} + \frac{(\tau_{\phi r} - \tau_{r\phi}) + \tau_{\phi\theta}\cot\theta}{r}\right] + \rho g_\phi \tag{B.5-9}$$

[c] These equations have been written without making the assumption that $\boldsymbol{\tau}$ is symmetric. This means, for example, that when the usual assumption is made that the stress tensor is symmetric, $\tau_{r\theta} - \tau_{\theta r} = 0$.

§B.6 EQUATION OF MOTION FOR A NEWTONIAN FLUID WITH CONSTANT ρ AND μ

$$[\rho D\mathbf{v}/Dt = -\nabla p + \mu\nabla^2\mathbf{v} + \rho\mathbf{g}]$$

Cartesian coordinates (x, y, z):

$$\rho\left(\frac{\partial v_x}{\partial t} + v_x\frac{\partial v_x}{\partial x} + v_y\frac{\partial v_x}{\partial y} + v_z\frac{\partial v_x}{\partial z}\right) = -\frac{\partial p}{\partial x} + \mu\left[\frac{\partial^2 v_x}{\partial x^2} + \frac{\partial^2 v_x}{\partial y^2} + \frac{\partial^2 v_x}{\partial z^2}\right] + \rho g_x \tag{B.6-1}$$

$$\rho\left(\frac{\partial v_y}{\partial t} + v_x\frac{\partial v_y}{\partial x} + v_y\frac{\partial v_y}{\partial y} + v_z\frac{\partial v_y}{\partial z}\right) = -\frac{\partial p}{\partial y} + \mu\left[\frac{\partial^2 v_y}{\partial x^2} + \frac{\partial^2 v_y}{\partial y^2} + \frac{\partial^2 v_y}{\partial z^2}\right] + \rho g_y \tag{B.6-2}$$

$$\rho\left(\frac{\partial v_z}{\partial t} + v_x\frac{\partial v_z}{\partial x} + v_y\frac{\partial v_z}{\partial y} + v_z\frac{\partial v_z}{\partial z}\right) = -\frac{\partial p}{\partial z} + \mu\left[\frac{\partial^2 v_z}{\partial x^2} + \frac{\partial^2 v_z}{\partial y^2} + \frac{\partial^2 v_z}{\partial z^2}\right] + \rho g_z \tag{B.6-3}$$

Cylindrical coordinates (r, θ, z):

$$\rho\left(\frac{\partial v_r}{\partial t} + v_r\frac{\partial v_r}{\partial r} + \frac{v_\theta}{r}\frac{\partial v_r}{\partial \theta} + v_z\frac{\partial v_r}{\partial z} - \frac{v_\theta^2}{r}\right) = -\frac{\partial p}{\partial r} + \mu\left[\frac{\partial}{\partial r}\left(\frac{1}{r}\frac{\partial}{\partial r}(rv_r)\right) + \frac{1}{r^2}\frac{\partial^2 v_r}{\partial \theta^2} + \frac{\partial^2 v_r}{\partial z^2} - \frac{2}{r^2}\frac{\partial v_\theta}{\partial \theta}\right] + \rho g_r \tag{B.6-4}$$

$$\rho\left(\frac{\partial v_\theta}{\partial t} + v_r\frac{\partial v_\theta}{\partial r} + \frac{v_\theta}{r}\frac{\partial v_\theta}{\partial \theta} + v_z\frac{\partial v_\theta}{\partial z} + \frac{v_r v_\theta}{r}\right) = -\frac{1}{r}\frac{\partial p}{\partial \theta} + \mu\left[\frac{\partial}{\partial r}\left(\frac{1}{r}\frac{\partial}{\partial r}(rv_\theta)\right) + \frac{1}{r^2}\frac{\partial^2 v_\theta}{\partial \theta^2} + \frac{\partial^2 v_\theta}{\partial z^2} + \frac{2}{r^2}\frac{\partial v_r}{\partial \theta}\right] + \rho g_\theta \tag{B.6-5}$$

$$\rho\left(\frac{\partial v_z}{\partial t} + v_r\frac{\partial v_z}{\partial r} + \frac{v_\theta}{r}\frac{\partial v_z}{\partial \theta} + v_z\frac{\partial v_z}{\partial z}\right) = -\frac{\partial p}{\partial z} + \mu\left[\frac{1}{r}\frac{\partial}{\partial r}\left(r\frac{\partial v_z}{\partial r}\right) + \frac{1}{r^2}\frac{\partial^2 v_z}{\partial \theta^2} + \frac{\partial^2 v_z}{\partial z^2}\right] + \rho g_z \tag{B.6-6}$$

Spherical coordinates (r, θ, φ):

$$\rho\left(\frac{\partial v_r}{\partial t} + v_r\frac{\partial v_r}{\partial r} + \frac{v_\theta}{r}\frac{\partial v_r}{\partial \theta} + \frac{v_\phi}{r\sin\theta}\frac{\partial v_r}{\partial \phi} - \frac{v_\theta^2 + v_\phi^2}{r}\right) = -\frac{\partial p}{\partial r} + \mu\left[\frac{1}{r^2}\frac{\partial^2}{\partial r^2}(r^2 v_r) + \frac{1}{r^2\sin\theta}\frac{\partial}{\partial \theta}\left(\sin\theta\frac{\partial v_r}{\partial \theta}\right) + \frac{1}{r^2\sin^2\theta}\frac{\partial^2 v_r}{\partial \phi^2}\right] + \rho g_r \tag{B.6-7}[a]$$

$$\rho\left(\frac{\partial v_\theta}{\partial t} + v_r\frac{\partial v_\theta}{\partial r} + \frac{v_\theta}{r}\frac{\partial v_\theta}{\partial \theta} + \frac{v_\phi}{r\sin\theta}\frac{\partial v_\theta}{\partial \phi} + \frac{v_r v_\theta - v_\phi^2\cot\theta}{r}\right) = -\frac{1}{r}\frac{\partial p}{\partial \theta} + \mu\left[\frac{1}{r^2}\frac{\partial}{\partial r}\left(r^2\frac{\partial v_\theta}{\partial r}\right) + \frac{1}{r^2}\frac{\partial}{\partial \theta}\left(\frac{1}{\sin\theta}\frac{\partial}{\partial \theta}(v_\theta\sin\theta)\right) + \frac{1}{r^2\sin^2\theta}\frac{\partial^2 v_\theta}{\partial \phi^2} + \frac{2}{r^2}\frac{\partial v_r}{\partial \theta} - \frac{2\cot\theta}{r^2\sin\theta}\frac{\partial v_\phi}{\partial \phi}\right] + \rho g_\theta \tag{B.6-8}$$

$$\rho\left(\frac{\partial v_\phi}{\partial t} + v_r\frac{\partial v_\phi}{\partial r} + \frac{v_\theta}{r}\frac{\partial v_\phi}{\partial \theta} + \frac{v_\phi}{r\sin\theta}\frac{\partial v_\phi}{\partial \phi} + \frac{v_\phi v_r + v_\theta v_\phi\cot\theta}{r}\right) = -\frac{1}{r\sin\theta}\frac{\partial p}{\partial \phi} + \mu\left[\frac{1}{r^2}\frac{\partial}{\partial r}\left(r^2\frac{\partial v_\phi}{\partial r}\right) + \frac{1}{r^2}\frac{\partial}{\partial \theta}\left(\frac{1}{\sin\theta}\frac{\partial}{\partial \theta}(v_\phi\sin\theta)\right) + \frac{1}{r^2\sin^2\theta}\frac{\partial^2 v_\phi}{\partial \phi^2} + \frac{2}{r^2\sin\theta}\frac{\partial v_r}{\partial \phi} + \frac{2\cot\theta}{r^2\sin\theta}\frac{\partial v_\theta}{\partial \phi}\right] + \rho g_\phi \tag{B.6-9}$$

[a] The quantity in the brackets in Eq. B.6-7 is *not* what one would expect from Eq. (M) for $[\nabla\cdot\nabla\mathbf{v}]$ in Table A.7-3, because we have added to Eq. (M) the expression for $(2/r)(\nabla\cdot\mathbf{v})$, which is zero for fluids with constant ρ. This gives a much simpler equation.

§B.7 THE DISSIPATION FUNCTION Φv FOR NEWTONIAN FLUIDS (SEE EQ. 3.3-3)

Cartesian coordinates (x, y, z):

$$\Phi_v = 2\left[\left(\frac{\partial v_x}{\partial x}\right)^2 + \left(\frac{\partial v_y}{\partial y}\right)^2 + \left(\frac{\partial v_z}{\partial z}\right)^2\right] + \left[\frac{\partial v_y}{\partial x} + \frac{\partial v_x}{\partial y}\right]^2 + \left[\frac{\partial v_z}{\partial y} + \frac{\partial v_y}{\partial z}\right]^2 + \left[\frac{\partial v_x}{\partial z} + \frac{\partial v_z}{\partial x}\right]^2 - \frac{2}{3}\left[\frac{\partial v_x}{\partial x} + \frac{\partial v_y}{\partial y} + \frac{\partial v_z}{\partial z}\right]^2 \tag{B.7-1}$$

Cylindrical coordinates (r, θ, z):

$$\Phi_v = 2\left[\left(\frac{\partial v_r}{\partial r}\right)^2 + \left(\frac{1}{r}\frac{\partial v_\theta}{\partial \theta} + \frac{v_r}{r}\right)^2 + \left(\frac{\partial v_z}{\partial z}\right)^2\right] + \left[r\frac{\partial}{\partial r}\left(\frac{v_\theta}{r}\right) + \frac{1}{r}\frac{\partial v_r}{\partial \theta}\right]^2 + \left[\frac{1}{r}\frac{\partial v_z}{\partial \theta} + \frac{\partial v_\theta}{\partial z}\right]^2 + \left[\frac{\partial v_r}{\partial z} + \frac{\partial v_z}{\partial r}\right]^2$$

$$- \frac{2}{3}\left[\frac{1}{r}\frac{\partial}{\partial r}(rv_r) + \frac{1}{r}\frac{\partial v_\theta}{\partial \theta} + \frac{\partial v_z}{\partial z}\right]^2 \tag{B.7-2}$$

Spherical coordinates (r, θ, φ):

$$\Phi_v = 2\left[\left(\frac{\partial v_r}{\partial r}\right)^2 + \left(\frac{1}{r}\frac{\partial v_\theta}{\partial \theta} + \frac{v_r}{r}\right)^2 + \left(\frac{1}{r\sin\theta}\frac{\partial v_\phi}{\partial \phi} + \frac{v_r + v_\theta \cot\theta}{r}\right)^2\right]$$

$$+ \left[r\frac{\partial}{\partial r}\left(\frac{v_\theta}{r}\right) + \frac{1}{r}\frac{\partial v_r}{\partial \theta}\right]^2 + \left[\frac{\sin\theta}{r}\frac{\partial}{\partial \theta}\left(\frac{v_\phi}{\sin\theta}\right) + \frac{1}{r\sin\theta}\frac{\partial v_\theta}{\partial \phi}\right]^2 + \left[\frac{1}{r\sin\theta}\frac{\partial v_r}{\partial \phi} + r\frac{\partial}{\partial r}\left(\frac{v_\phi}{r}\right)\right]^2$$

$$- \frac{2}{3}\left[\frac{1}{r^2}\frac{\partial}{\partial r}(r^2 v_r) + \frac{1}{r\sin\theta}\frac{\partial}{\partial \theta}(v_\theta \sin\theta) + \frac{1}{r\sin\theta}\frac{\partial v_\phi}{\partial \phi}\right]^2 \tag{B.7-3}$$

§B.8 THE EQUATION OF ENERGY IN TERMS OF q

$$[\rho\hat{C}_p DT/Dt = -(\nabla \cdot \mathbf{q}) - (\partial \ln \rho/\partial \ln T)_p Dp/Dt - (\boldsymbol{\tau}:\nabla\mathbf{v})]$$

Cartesian coordinates (x, y, z):

$$\rho\hat{C}_p\left(\frac{\partial T}{\partial t} + v_x\frac{\partial T}{\partial x} + v_y\frac{\partial T}{\partial y} + v_z\frac{\partial T}{\partial z}\right) = -\left[\frac{\partial q_x}{\partial x} + \frac{\partial q_y}{\partial y} + \frac{\partial q_z}{\partial z}\right] - \left(\frac{\partial \ln \rho}{\partial \ln T}\right)_p \frac{Dp}{Dt} - (\boldsymbol{\tau}:\nabla\mathbf{v}) \tag{B.8-1}^a$$

Cylindrical coordinates (r, θ, z):

$$\rho\hat{C}_p\left(\frac{\partial T}{\partial t} + v_r\frac{\partial T}{\partial r} + \frac{v_\theta}{r}\frac{\partial T}{\partial \theta} + v_z\frac{\partial T}{\partial z}\right) = -\left[\frac{1}{r}\frac{\partial}{\partial r}(rq_r) + \frac{1}{r}\frac{\partial q_\theta}{\partial \theta} + \frac{\partial q_z}{\partial z}\right] - \left(\frac{\partial \ln \rho}{\partial \ln T}\right)_p \frac{Dp}{Dt} - (\boldsymbol{\tau}:\nabla\mathbf{v}) \tag{B.8-2}^a$$

Spherical coordinates (r, θ, φ):

$$\rho\hat{C}_p\left(\frac{\partial T}{\partial t} + v_r\frac{\partial T}{\partial r} + \frac{v_\theta}{r}\frac{\partial T}{\partial \theta} + \frac{v_\phi}{r\sin\theta}\frac{\partial T}{\partial \phi}\right) = \left[\frac{1}{r^2}\frac{\partial}{\partial r}(r^2 q_r) + \frac{1}{r\sin\theta}\frac{\partial}{\partial \theta}(q_\theta \sin\theta) + \frac{1}{r\sin\theta}\frac{\partial q_\phi}{\partial \phi}\right] - \left(\frac{\partial \ln \rho}{\partial \ln T}\right)_p \frac{Dp}{Dt} - (\boldsymbol{\tau}:\nabla\mathbf{v}) \tag{B.8-3}^a$$

[a] The viscous dissipation term, $-(\boldsymbol{\tau}:\nabla\mathbf{v})$, is given in Appendix A, Tables A.7-1, 2, 3. This term may usually be neglected, except for systems with very large velocity gradients. The term containing $(\partial \ln \rho/\partial \ln T)_p$ is zero for fluid with constant ρ.

§B.9 THE EQUATION OF ENERGY FOR PURE NEWTONIAN FLUIDS WITH CONSTANT[a] ρ AND k

$$[\rho\hat{C}_p DT/Dt = k\nabla^2 T + \mu\Phi_v]$$

Cartesian coordinates (x, y, z):

$$\rho\hat{C}_p\left(\frac{\partial T}{\partial t} + v_x\frac{\partial T}{\partial x} + v_y\frac{\partial T}{\partial y} + v_z\frac{\partial T}{\partial z}\right) = k\left[\frac{\partial^2 T}{\partial x^2} + \frac{\partial^2 T}{\partial y^2} + \frac{\partial^2 T}{\partial z^2}\right] + \mu\Phi_v \tag{B.9-1}[b]$$

Cylindrical coordinates (r, θ, z):

$$\rho\hat{C}_p\left(\frac{\partial T}{\partial t} + v_r\frac{\partial T}{\partial r} + \frac{v_\theta}{r}\frac{\partial T}{\partial \theta} + v_z\frac{\partial T}{\partial z}\right) = k\left[\frac{1}{r}\frac{\partial}{\partial r}\left(r\frac{\partial T}{\partial r}\right) + \frac{1}{r^2}\frac{\partial^2 T}{\partial \theta^2} + \frac{\partial^2 T}{\partial z^2}\right] + \mu\Phi_v \tag{B.9-2}[b]$$

Spherical coordinates (r, θ, φ):

$$\rho\hat{C}_p\left(\frac{\partial T}{\partial t} + v_r\frac{\partial T}{\partial r} + \frac{v_\theta}{r}\frac{\partial T}{\partial \theta} + \frac{v_\phi}{r\sin\theta}\frac{\partial T}{\partial \phi}\right) = k\left[\frac{1}{r^2}\frac{\partial}{\partial r}\left(r^2\frac{\partial T}{\partial r}\right) + \frac{1}{r^2\sin\theta}\frac{\partial}{\partial \theta}\left(\sin\theta\frac{\partial T}{\partial \theta}\right) + \frac{1}{r^2\sin^2\theta}\frac{\partial^2 T}{\partial \phi^2}\right] + \mu\Phi_v \tag{B.9-3}[b]$$

[a] This form of the energy equation is also valid under the less stringent assumptions k = constant and $(\partial \ln \rho/\partial \ln T)_p Dp/Dt = 0$. The assumption ρ = constant is given in the table heading because it is the assumption more often made.

[b] The function Φ_v is given in §B.7. The term $\mu\Phi_v$ is usually negligible, except in systems with large velocity gradients.

§B.10 THE EQUATION OF CONTINUITY FOR SPECIES α IN TERMS[a] OF $\mathbf{j}_\alpha$

$$[\rho D\omega_\alpha/Dt = -(\nabla\cdot\mathbf{j}_\alpha) + r_\alpha]$$

Cartesian coordinates (x, y, z):

$$\rho\left(\frac{\partial \omega_\alpha}{\partial t} + v_x\frac{\partial \omega_\alpha}{\partial x} + v_y\frac{\partial \omega_\alpha}{\partial y} + v_z\frac{\partial \omega_\alpha}{\partial z}\right) = -\left[\frac{\partial j_{\alpha x}}{\partial x} + \frac{\partial j_{\alpha y}}{\partial y} + \frac{\partial j_{\alpha z}}{\partial z}\right] + r_\alpha \tag{B.10-1}$$

Cylindrical coordinates (r, θ, z):

$$\rho\left(\frac{\partial \omega_\alpha}{\partial t} + v_r\frac{\partial \omega_\alpha}{\partial r} + \frac{v_\theta}{r}\frac{\partial \omega_\alpha}{\partial \theta} + v_z\frac{\partial \omega_\alpha}{\partial z}\right) = -\left[\frac{1}{r}\frac{\partial}{\partial r}(rj_{\alpha r}) + \frac{1}{r}\frac{\partial j_{\alpha\theta}}{\partial \theta} + \frac{\partial j_{\alpha z}}{\partial z}\right] + r_\alpha \tag{B.10-2}$$

Spherical coordinates (r, θ, φ):

$$\rho\left(\frac{\partial \omega_\alpha}{\partial t} + v_r\frac{\partial \omega_\alpha}{\partial r} + \frac{v_\theta}{r}\frac{\partial \omega_\alpha}{\partial \theta} + \frac{v_\phi}{r\sin\theta}\frac{\partial \omega_\alpha}{\partial \phi}\right) = \left[\frac{1}{r^2}\frac{\partial}{\partial r}(r^2 j_{\alpha r}) + \frac{1}{r\sin\theta}\frac{\partial}{\partial \theta}(j_{\alpha\theta}\sin\theta) + \frac{1}{r\sin\theta}\frac{\partial j_{\alpha\phi}}{\partial \phi}\right] + r_\alpha \tag{B.10-3}$$

[a] To obtain the corresponding equations in terms of $\mathbf{J}_\alpha^*$ make the following replacements:

Replace	ρ	ω_α	$\mathbf{j}_\alpha$	$\mathbf{v}$	r_α
by	c	x_α	$\mathbf{J}_\alpha^*$	$\mathbf{v}^*$	$R_\alpha - x_\alpha\sum_{\beta=1}^{N} R_\beta$

§B.11 THE EQUATION OF CONTINUITY FOR SPECIES A IN TERMS OF ω_A FOR CONSTANT[a] $\rho\mathscr{D}_{AB}$

$$[\rho D\omega_A/Dt = \rho\mathscr{D}_{AB}\nabla^2\omega_A + r_A]$$

Cartesian coordinates (x, y, z):

$$\rho\left(\frac{\partial\omega_A}{\partial t} + v_x\frac{\partial\omega_A}{\partial x} + v_y\frac{\partial\omega_A}{\partial y} + v_z\frac{\partial\omega_A}{\partial z}\right) = \rho\mathscr{D}_{AB}\left[\frac{\partial^2\omega_A}{\partial x^2} + \frac{\partial^2\omega_A}{\partial y^2} + \frac{\partial^2\omega_A}{\partial z^2}\right] + r_A \tag{B.11-1}$$

Cylindrical coordinates (r, θ, z):

$$\rho\left(\frac{\partial\omega_A}{\partial t} + v_r\frac{\partial\omega_A}{\partial r} + \frac{v_\theta}{r}\frac{\partial\omega_A}{\partial\theta} + v_z\frac{\partial\omega_A}{\partial z}\right) = \rho\mathscr{D}_{AB}\left[\frac{1}{r}\frac{\partial}{\partial r}\left(r\frac{\partial\omega_A}{\partial r}\right) + \frac{1}{r^2}\frac{\partial^2\omega_A}{\partial\theta^2} + \frac{\partial^2\omega_A}{\partial z^2}\right] + r_A \tag{B.11-2}$$

Spherical coordinates (r, θ, φ):

$$\rho\left(\frac{\partial\omega_A}{\partial t} + v_r\frac{\partial\omega_A}{\partial r} + \frac{v_\theta}{r}\frac{\partial\omega_A}{\partial\theta} + \frac{v_\phi}{r\sin\theta}\frac{\partial\omega_A}{\partial\phi}\right) = \rho\mathscr{D}_{AB}\left[\frac{1}{r^2}\frac{\partial}{\partial r}\left(r^2\frac{\partial\omega_A}{\partial r}\right) + \frac{1}{r^2\sin\theta}\frac{\partial}{\partial\theta}\left(\sin\theta\frac{\partial\omega_A}{\partial\theta}\right) + \frac{1}{r^2\sin^2\theta}\frac{\partial^2\omega_A}{\partial\phi^2}\right] + r_A \tag{B.11-3}$$

[a] To obtain the corresponding equations in terms of x_A, make the following replacements:

Replace	ρ	ω_α	**v**	r_α
by	c	x_α	**v***	$R_\alpha - x_\alpha\sum_{\beta=1}^{N} R_\beta$

Appendix C

Mathematical Topics

In this appendix we summarize information on mathematical topics (other than vectors and tensors) that are useful in the study of transport phenomena.[1]

§C.1 SOME ORDINARY DIFFERENTIAL EQUATIONS AND THEIR SOLUTIONS

We assemble here a short list of differential equations that arise frequently in transport phenomena. The reader is assumed to be familiar with these equations and how to solve them. The quantities a, b, and c are real constants and f and g are functions of x.

Equation	Solution	
$\frac{dy}{dx} = \frac{f(x)}{g(y)}$	$\int g\,dy = \int f\,dx + C_1$	(C.1-1)
$\frac{dy}{dx} + f(x)y = g(x)$	$y = e^{-\int f\,dx}(\int e^{\int f\,dx} g\,dx + C_1)$	(C.1-2)
$\frac{d^2y}{dx^2} + a^2y = 0$	$y = C_1 \cos ax + C_2 \sin ax$	(C.1-3)
$\frac{d^2y}{dx^2} - a^2y = 0$	$y = C_1 \cosh ax + C_2 \sinh ax$ or	(C.1-4a)
	$y = C_3e^{+ax} + C_4e^{-ax}$	(C.1-4b)
$\frac{1}{x^2}\frac{d}{dx}\left(x^2\frac{dy}{dx}\right) + a^2y = 0$	$y = \frac{C_1}{x}\cos ax + \frac{C_2}{x}\sin ax$	(C.1-5)

[1] Some useful reference books on applied mathematics are: M. Abramowitz and I. A. Stegun, *Handbook of Mathematical Functions*, Dover, New York, 9th printing (1973); G. M. Murphy, *Ordinary Differential Equations and Their Solutions*, Van Nostrand, Princeton, N.J. (1960); J. J. Tuma, *Engineering Mathematics Handbook*, 3rd edition, McGraw-Hill, New York (1987).

$\frac{1}{x^2}\frac{d}{dx}\left(x^2\frac{dy}{dx}\right) - a^2y = 0$	$y = \frac{C_1}{x}\cosh ax + \frac{C_2}{x}\sinh ax$ or	(C.1-6a)
	$y = \frac{C_3}{x}e^{+ax} + \frac{C_4}{x}e^{-ax}$	(C.1-6b)
$\frac{d^2y}{dx^2} + a\frac{dy}{dx} + by = 0$	Solve the equation $n^2 + an + b = 0$, and get the roots $n = n_+$ and $n = n_-$. Then (a) if n_+ and n_- are real and unequal, $y = C_1\exp(n_+x) + C_2\exp(n_-x)$	(C.1-7a)
	(b) if n_+ and n_- are real and equal to n, $y = e^{nx}(C_1x + C_2)$	(C.1-7b)
	(c) if n_+ and n_- are complex: $n_\pm = p \pm iq$, $y = e^{px}(C_1\cos qx + C_2\sin qx)$	(C.1-7c)
$\frac{d^2y}{dx^2} + 2x\frac{dy}{dx} = 0$	$y = C_1\int_0^x \exp(-\bar{x}^2)\,d\bar{x} + C_2$	(C.1-8)
$\frac{d^2y}{dx^2} + 3x^2\frac{dy}{dx} = 0$	$y = C_1\int_0^x \exp(-\bar{x}^3)\,d\bar{x} + C_2$	(C.1-9)
$\frac{d^2y}{dx^2} = f(x)$	$y = \int_0^x\int_0^{\bar{x}} f(\bar{\bar{x}})d\bar{\bar{x}}\,d\bar{x} + C_1x + C_2$	(C.1-10)
$\frac{1}{x}\frac{d}{dx}\left(x\frac{dy}{dx}\right) = f(x)$	$y = \int_0^x \frac{1}{\bar{\bar{x}}}\int_0^{\bar{x}} \bar{\bar{x}}f(\bar{\bar{x}})d\bar{\bar{x}}d\bar{x} + C_1\ln x + C_2$	(C.1-11)
$\frac{1}{x^2}\frac{d}{dx}\left(x^2\frac{dy}{dx}\right) = f(x)$	$y = \int_0^x \frac{1}{\bar{x}^2}\int_0^{\bar{x}} \bar{\bar{x}}^2f(\bar{\bar{x}})d\bar{\bar{x}}d\bar{x} - \frac{C_1}{x} + C_2$	(C.1-12)
$\frac{d^2y}{dx^2} = h(y)$	$x = \int_0^y \frac{d\bar{y}}{\sqrt{2\int_0^{\bar{y}} h(\bar{\bar{y}})d\bar{\bar{y}} + C_1}} + C_2$	(C.1-13)
$x^3\frac{d^3y}{dx^3} + ax^2\frac{d^2y}{dx^2} + bx\frac{dy}{dx} + cy = 0$		(C.1-14)
	$y = C_1x^{n_1} + C_2x^{n_2} + C_3x^{n_3}$, where the n_k are the roots of the equation $n(n-1)(n-2) + an(n-1) + bn + c = 0$, provided that all roots are distinct.	

Notes:

[a] In Eqs. C.1-4 and C.1-6 the decisions as to whether to use the exponential forms or the trigonometric (or hyperbolic) functions are usually made on the basis of the boundary conditions on the problem or the symmetry properties of the solution.

[b] Equations C.1-5 and C.1-6 are solved by making the substitution $y(x) = u(x)/x$ and then solving the resulting equation for $u(x)$.

[c] In Eqs. C.1-8 to C.1-13, it may be convenient or necessary to change the lower limits of the integrals to some value other than zero.

§C.2 EXPANSIONS OF FUNCTIONS IN TAYLOR SERIES

In physical problems we often need to describe a function $y(x)$ in the neighborhood of some point $x = x_0$. Then we expand the function $y(x)$ in a "Taylor series about the point $x = x_0$":

$$y(x) = y|_{x=x_0} + \frac{1}{1!}\left(\frac{dy}{dx}\bigg|_{x=x_0}\right)(x - x_0) + \frac{1}{2!}\left(\frac{d^2y}{dx^2}\bigg|_{x=x_0}\right)(x - x_0)^2$$

$$+ \frac{1}{3!}\left(\frac{d^3y}{dx^3}\bigg|_{x=x_0}\right)(x - x_0)^3 + \cdots \qquad \text{(C.2-1)}$$

The first term gives the value of the function at $x = x_0$. The first two terms give a straight-line fit of the curve at $x = x_0$. The first three terms give a parabolic fit of the curve at $x = x_0$, and so on. The Taylor series is often used when only the first several terms are needed to describe the function adequately.

Here are a few Taylor series expansions of standard functions about the point $x = 0$:

$$e^{\pm x} = 1 \pm \frac{x}{1!} + \frac{x^2}{2!} \pm \frac{x^3}{3!} + \cdots \tag{C.2-2}$$

$$\ln(1 + x) = x - \frac{x^2}{2} + \frac{x^3}{3} - \frac{x^4}{4} + \cdots \tag{C.2.3}$$

$$\operatorname{erf} x = \frac{2x}{\sqrt{\pi}}\left(1 - \frac{x^2}{1!3} + \frac{x^4}{2!5} - \frac{x^6}{3!7} + \cdots\right) \tag{C.2-4}$$

$$\sqrt{1 \pm x} = 1 \pm \frac{1}{2}x - \frac{1 \cdot 1}{2 \cdot 4}x^2 \pm \frac{1 \cdot 1 \cdot 3}{2 \cdot 4 \cdot 6}x^3 - \cdots \tag{C.2-5}$$

Further examples may be found in calculus textbooks and handbooks. Taylor series can also be written for functions of two or more variables.

§C.3 DIFFERENTIATION OF INTEGRALS (THE LEIBNIZ FORMULA)

Suppose we have a function $f(x, t)$ that depends on a space variable x and the time t. Then we can form the integral

$$I(t) = \int_{\alpha(t)}^{\beta(t)} f(x, t)\, dx \tag{C.3-1}$$

which is a function of t [see Fig. C.3-1(*a*)]. If we want to differentiate this function with respect to t without evaluating the integral, we can use the Leibniz formula

$$\frac{d}{dt}\int_{\alpha(t)}^{\beta(t)} f(x, t)\, dx = \int_{\alpha(t)}^{\beta(t)} \frac{\partial}{\partial t} f(x, t)\, dx + \left(f(\beta, t)\frac{d\beta}{dt} - f(\alpha, t)\frac{d\alpha}{dt}\right) \tag{C.3-2}$$

Figure C.3-1(*b*) shows the meanings of the operations performed here: the first term on the right side gives the change in the integral because the function itself is changing with

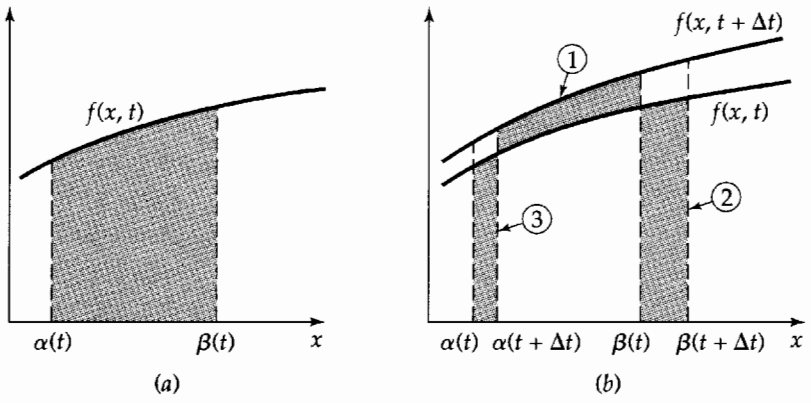

Fig. C.3-1. (*a*) The shaded area represents $I(t) = \int_{\alpha(t)}^{\beta(t)} f(x, t)dx$ at an instant t (Eq. C.3-1). (*b*) To get dI/dt, we form the difference $I(t + \Delta t) - I(t)$, divide by Δt, and then let $\Delta t \to 0$. The three shaded areas correspond to the three terms on the right side of Eq. C.3-2.

time; the second term accounts for the gain in area as the upper limit is moved to the right; and the third term shows the loss in area as the lower limit is moved to the right. This formula finds many uses in science and engineering. The three-dimensional analog is given in Eq. A.5-5.

§C.4 THE GAMMA FUNCTION

The gamma function appears frequently as the result of integrations:

$$\Gamma(n) = \int_0^\infty x^{n-1}e^{-x}dx \tag{C.4-1}$$

$$\Gamma(n) = \int_0^1 \left(\ln \frac{1}{x}\right)^{n-1} dx \tag{C.4-2}$$

$$\Gamma(n+1) = \int_0^\infty \exp(-x^{1/n})\, dx \tag{C.4-3}$$

Several formulas for gamma functions are important:

$$\Gamma(n+1) = n\Gamma(n) \qquad \text{(used to define } \Gamma(n) \text{ for negative } n) \tag{C.4-4}$$

$$\Gamma(n) = (n-1)! \qquad \text{(when } n \text{ is an integer greater than 0)} \tag{C.4-5}$$

Some special values of the gamma function are:

$$\Gamma(1) = \Gamma(2) = 1 \tag{C.4-6}$$

$$\Gamma(\tfrac{1}{2}) = \sqrt{\pi} = 1.77245\ldots \tag{C.4-7}$$

$$\Gamma(\tfrac{3}{2}) = \tfrac{1}{2}\Gamma(\tfrac{1}{2}) = \tfrac{1}{2}\sqrt{\pi} = 0.88622\ldots \tag{C.4-8}$$

$$\Gamma(\tfrac{1}{3}) = 2.67893\ldots \tag{C.4-9}$$

$$\Gamma(\tfrac{4}{3}) = \tfrac{1}{3}\Gamma(\tfrac{1}{3}) = 0.89297\ldots \tag{C.4-10}$$

$$\Gamma(\tfrac{7}{3}) = \tfrac{4}{3}\Gamma(\tfrac{4}{3}) = 1.19063\ldots \tag{C.4-11}$$

The gamma function is displayed in Fig. C.4-1.

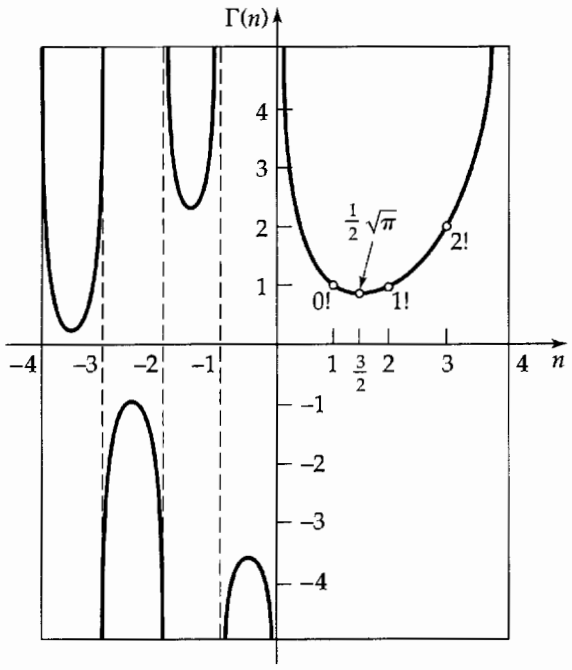

Fig. C.4-1. The gamma function.

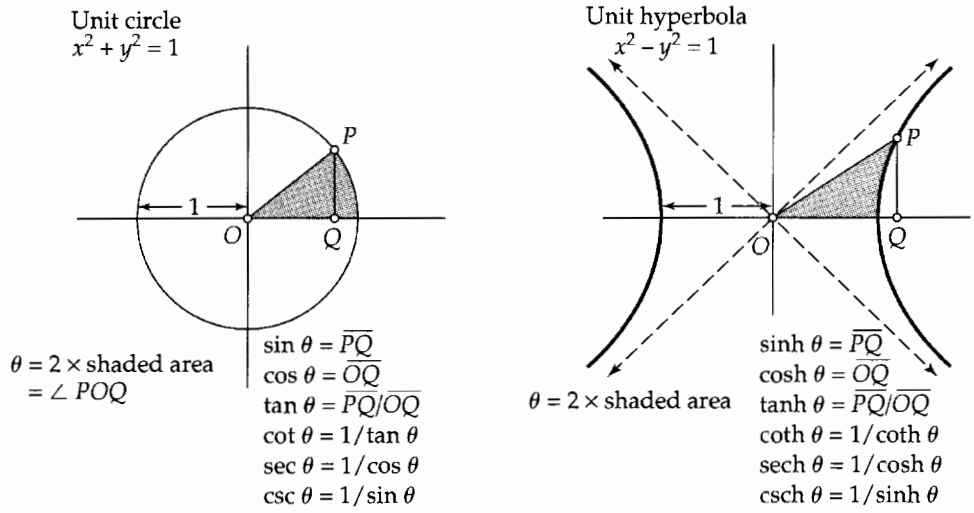

Fig. C.5-1. Comparison of circular and hyperbolic functions.

§C.5 THE HYPERBOLIC FUNCTIONS

The hyperbolic sine (sinh x), the hyperbolic cosine (cosh x), and the hyperbolic tangent (tanh x) arise frequently in science and engineering problems. They are related to the hyperbola in very much the same way that the circular functions are related to the circle (see Fig. C.5-1). The circular functions (sin x and cos x) are periodic, oscillating functions, whereas their hyperbolic analogs are not (see Fig. C.5-2).

The hyperbolic functions are related to the exponential function as follows:

$$\cosh x = \tfrac{1}{2}(e^x + e^{-x}); \qquad \sinh x = \tfrac{1}{2}(e^x - e^{-x}) \tag{C.5-1, 2}$$

The corresponding relations for the circular functions are:

$$\cos x = \tfrac{1}{2}(e^{ix} + e^{-ix}); \qquad \sin x = \tfrac{1}{2}(e^{ix} - e^{-ix}) \tag{C.5-3, 4}$$

One can derive a variety of standard relations for the hyperbolic functions, such as

$$\cosh^2 x - \sinh^2 x = 1 \tag{C.5-5}$$

$$\cosh(x \pm y) = \cosh x \cosh y \pm \sinh x \sinh y \tag{C.5-6}$$

$$\sinh(x \pm y) = \sinh x \cosh y \pm \cosh x \sinh y \tag{C.5-7}$$

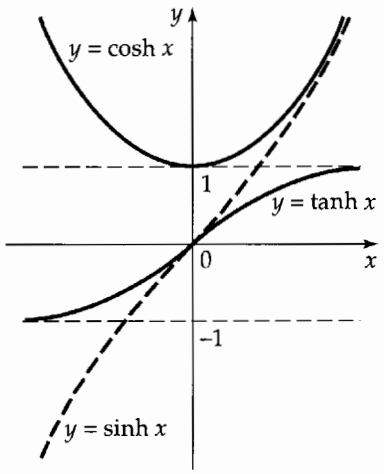

Fig. C.5-2. Comparison of the shapes of the hyperbolic functions.

$$\cosh ix = \cos x; \qquad \sinh ix = i \sin x \tag{C.5-8, 9}$$

$$\frac{d \cosh x}{dx} = \sinh x; \qquad \frac{d \sinh x}{dx} = \cosh x \tag{C.5-10, 11}$$

$$\int \cosh x \, dx = \sinh x; \qquad \int \sinh x \, dx = \cosh x \tag{C.5-12, 13}$$

It should be kept in mind that cosh x and cos x are both even functions of x, whereas sinh x and sin x are odd functions of x.

§C.6 THE ERROR FUNCTION

The error function is defined as

$$\operatorname{erf} x = \frac{\int_0^x \exp(-\bar{x}^2)\, d\bar{x}}{\int_0^\infty \exp(-\bar{x}^2)\, d\bar{x}} = \frac{2}{\sqrt{\pi}} \int_0^x \exp(-\bar{x}^2)\, d\bar{x} \tag{C.6-1}$$

This function, which arises naturally in numerous transport problems, is monotone increasing, going from erf 0 = 0 to erf ∞ = 1, and has the value of 0.99 at about $x = 2$. The Taylor series expansion for the error function about $x = 0$ is given in Eq. C.2-4. It is also worth noting that erf $(-x) = -\text{erf}\, x$, and that

$$\frac{d}{dx} \operatorname{erf} u = \frac{2}{\sqrt{\pi}} \exp(-u^2) \frac{du}{dx} \tag{C.6-2}$$

by applying the Leibniz formula to Eq. C.6-1.

The closely related function erfc $x = 1 - \text{erf}\, x$ is called the "complementary error function."

Appendix D

The Kinetic Theory of Gases

In Chapters 1, 9, and 17 we gave a brief account of the use of mean free path arguments to get approximate expressions for the transport properties. Then we gave the rigorous results from the Chapman–Enskog development for dilute monatomic gases. In this appendix we give a brief description of the Chapman–Enskog theory, just enough to show what the theory involves and to show how it gives a sense of unity to the subject of transport phenomena in gases. The reader who wishes to pursue the subject further can consult the standard references.[1]

§D.1 THE BOLTZMANN EQUATION[2]

The starting point for the kinetic theory of low-density, nonreacting mixtures of monatomic gases is the *Boltzmann equation* for the velocity distribution function $f_\alpha(\dot{\mathbf{r}}_\alpha, \mathbf{r}, t)$. The quantity $f_\alpha(\dot{\mathbf{r}}_\alpha, \mathbf{r}, t)\, d\dot{\mathbf{r}}_\alpha d\mathbf{r}$ is the probable number of molecules of species α, which at time t are located in the volume element $d\mathbf{r}$ at position $\mathbf{r}$, and have velocities within the range $d\dot{\mathbf{r}}_\alpha$ about $\dot{\mathbf{r}}_\alpha$. The Boltzmann equation, which describes how f_α evolves with time, is

$$\frac{\partial}{\partial t} f_\alpha = -\left(\frac{\partial}{\partial \mathbf{r}} \cdot \dot{\mathbf{r}}_\alpha f_\alpha\right) - \left(\frac{\partial}{\partial \dot{\mathbf{r}}_\alpha} \cdot \mathbf{g}_\alpha f_\alpha\right) + J_\alpha \tag{D.1-1}$$

[1] J. H. Ferziger and H. G. Kaper, *Mathematical Theory of Transport Processes in Gases*, North-Holland, Amsterdam (1972); S. Chapman and T. G. Cowling, *The Mathematical Theory of Non-Uniform Gases*, 3rd edition, Cambridge University Press (1970); J. O. Hirschfelder, C. F. Curtiss, and R. B. Bird, *Molecular Theory of Gases and Liquids*, 2nd corrected printing, Wiley, New York (1964), Chapter 7; E. M. Lifshitz and L. P. Pitaevskii, *Physical Kinetics*, Pergamon, Oxford (1981), Chapter 1.

[2] L. Boltzmann, *Sitzungsberichte Keiserl. Akad. der Wissenschaften*, **66** (2), 275–370 (1872); C. Cercignani, *The Boltzmann Equation and Its Applications*, Springer-Verlag, New York (1988). C. F. Curtiss, *J. Chem. Phys.*, **97**, 1416–1423, 7679–7686 (1992), found it necessary to modify the Boltzmann equation to account for the possibility of orbiting pairs of molecules; the modification, important only at very low temperatures, was found to give much better agreement with the limited low-temperature experimental data.

in which $\partial/\partial\mathbf{r}$ is identical to the ∇-operator, and $\partial/\partial\dot{\mathbf{r}}_\alpha$ is a similar operator involving velocities rather than positions. The quantity $\mathbf{g}_\alpha$ is the external force per unit mass acting on a molecule of species α, and J_α is a very complicated five-fold integral term accounting for the change in f_α because of molecular collisions. The J_α term involves the intermolecular potential energy function (e.g., the Lennard-Jones potential) and the details of the collision trajectories. The Boltzmann equation may be thought of as a continuity equation in the six-dimensional position-velocity space, and J_α serves as a source term. The velocity distribution function is "normalized" to the number density of species α; that is, $\int f_\alpha(\dot{\mathbf{r}}_\alpha, \mathbf{r}, t)d\dot{\mathbf{r}}_\alpha = n_\alpha(\mathbf{r}, t)$.

§D.2 THE EQUATIONS OF CHANGE

When the Boltzmann equation is multiplied by some molecular property $\psi_\alpha(\dot{\mathbf{r}}_\alpha)$ and then integrated over all molecular velocities, the *general equation of change* is obtained:

$$\frac{\partial}{\partial t}\int\psi_\alpha f_\alpha d\dot{\mathbf{r}}_\alpha = -\left(\frac{\partial}{\partial\mathbf{r}}\cdot\int\dot{\mathbf{r}}_\alpha\psi_\alpha f_\alpha d\dot{\mathbf{r}}_\alpha\right) + \int\left(\mathbf{g}_\alpha\cdot\frac{\partial\psi_\alpha}{\partial\dot{\mathbf{r}}_\alpha}\right)f_\alpha d\dot{\mathbf{r}}_\alpha + \int\psi_\alpha J_\alpha d\dot{\mathbf{r}}_\alpha \tag{D.2-1}$$

An integration by parts is performed to get this result, and use is made of the fact that f_α is zero at infinite velocities. If ψ_α is a quantity that is conserved during a collision (see §0.3), then the term containing J_α can be shown to be zero.[1]

Now let ψ_α be successively the conserved quantities for monatomic molecules: the mass m_α, the momentum $m_\alpha\dot{\mathbf{r}}_\alpha$, and the energy $\frac{1}{2}m_\alpha(\dot{\mathbf{r}}_\alpha\cdot\dot{\mathbf{r}}_\alpha)$. When these are substituted for ψ_α into Eq. D.2-1, and when a sum over all species α is performed for the second and third of these, we get the *equations of change* for mass of α, momentum, and energy as follows:

$$\frac{\partial}{\partial t}\rho_\alpha = -(\nabla\cdot\rho_\alpha\mathbf{v}) - (\nabla\cdot\mathbf{j}_\alpha) \tag{D.2-2}$$

$$\frac{\partial}{\partial t}\rho\mathbf{v} = -[\nabla\cdot\rho\mathbf{v}\mathbf{v}] - [\nabla\cdot\boldsymbol{\pi}] + \sum_\alpha\rho_\alpha\mathbf{g}_\alpha \tag{D.2-3}$$

$$\frac{\partial}{\partial t}(\tfrac{1}{2}\rho v^2 + \rho\hat{U}) = -(\nabla\cdot(\tfrac{1}{2}\rho v^2 + \rho\hat{U})\mathbf{v}) - (\nabla\cdot\mathbf{q}) - (\nabla\cdot[\boldsymbol{\pi}\cdot\mathbf{v}]) + \sum_\alpha((\mathbf{j}_\alpha + \rho_\alpha\mathbf{v})\cdot\mathbf{g}_\alpha) \tag{D.2-4}$$

In the last of these equations the internal energy per unit volume is defined to be

$$\rho\hat{U} = \tfrac{3}{2}nKT = \int\tfrac{1}{2}m_\alpha(\dot{\mathbf{r}}_\alpha - \mathbf{v})^2 f_\alpha d\dot{\mathbf{r}}_\alpha \tag{D.2-5}$$

Thus we see that the equations of continuity, motion, and energy are direct consequences of the conservation laws for mass, momentum, and energy discussed in Chapter 0. Equations D.2-2 to 4 should be compared with Eqs. 19.1-7, 3.2-9, and Eq. (B) and footnote (b) of Table 19.2-4, which were derived by continuum arguments.

§D.3 THE MOLECULAR EXPRESSIONS FOR THE FLUXES

At the same time the equations of change are obtained, the molecular expressions for the fluxes are generated as integrals over the distribution function:

$$\mathbf{j}_\alpha(\mathbf{r}, t) = m_\alpha\int(\dot{\mathbf{r}}_\alpha - \mathbf{v})f_\alpha d\dot{\mathbf{r}}_\alpha \xrightarrow{\text{at equilibrium}} 0 \tag{D.3-1}$$

$$\boldsymbol{\pi}(\mathbf{r}, t) = \sum_\alpha m_\alpha\int(\dot{\mathbf{r}}_\alpha - \mathbf{v})(\dot{\mathbf{r}}_\alpha - \mathbf{v})f_\alpha d\dot{\mathbf{r}}_\alpha \xrightarrow{\text{at equilibrium}} p\boldsymbol{\delta} \tag{D.3-2}$$

$$\mathbf{q}(\mathbf{r}, t) = \sum_\alpha\tfrac{1}{2}m_\alpha\int(\dot{\mathbf{r}}_\alpha - \mathbf{v})^2(\dot{\mathbf{r}}_\alpha - \mathbf{v})f_\alpha d\dot{\mathbf{r}}_\alpha \xrightarrow{\text{at equilibrium}} 0 \tag{D.3-3}$$

In these expressions the fluxes involve integrals over the products of mass, momentum, and energy with the "diffusion velocity" $(\dot{\mathbf{r}}_\alpha - \mathbf{v})$ of species α. Note the similarity between the structure of these *molecular fluxes* (or "diffusive fluxes") and that of the convective fluxes of mass $\rho_\alpha \mathbf{v}$, momentum $\rho\mathbf{vv}$, and kinetic energy $\frac{1}{2}\rho v^2\mathbf{v}$ appearing in the equations of change, where $\mathbf{v}$ is the local instantaneous mass average velocity of the gas mixture. Thus the molecular fluxes represent the diffusive movement of mass, momentum, and energy above and beyond that described by the convective fluxes. Note also that the molecular theory automatically generates the molecular work term $-(\nabla \cdot [\boldsymbol{\pi} \cdot \mathbf{v}])$ in the energy equation.

§D.4 THE SOLUTION TO THE BOLTZMANN EQUATION

If the gas mixture were at rest, the velocity distribution function would be given by the Maxwell–Boltzmann distribution function (known from equilibrium statistical mechanics). Then we would find, as shown in §D.3, that $\mathbf{j}_\alpha = 0$, that $\boldsymbol{\pi} = p\boldsymbol{\delta} = n\kappa T\boldsymbol{\delta}$, and that $\mathbf{q} = 0$. The derivation of $p = n\kappa T$ is given in Problem 1C.3.

On the other hand, when there are concentration, velocity, and temperature gradients, the distribution function is given as the Maxwell–Boltzmann distribution multiplied by a "correction factor":

$$f_\alpha(\dot{\mathbf{r}}_\alpha, \mathbf{r}, t) = n_\alpha\left(\frac{m_\alpha}{2\pi\kappa T}\right)^{3/2} \exp[-m_\alpha(\dot{\mathbf{r}} - \mathbf{v})^2/2\kappa T]\,(1 + \phi_\alpha(\dot{\mathbf{r}}_\alpha, \mathbf{r}, t) + \cdots) \quad \text{(D.4-1)}$$

where $\phi_\alpha << 1$. In this expression n_α, $\mathbf{v}$, and T are functions of position $\mathbf{r}$ and time t. Since the deviations from equilibrium result from the temperature, velocity, and concentration gradients, $\phi_\alpha(\dot{\mathbf{r}}_\alpha, \mathbf{r}, t)$ can be represented, near equilibrium, as a linear function of the various gradients,

$$\phi_\alpha = -(\mathbf{A}_\alpha \cdot \nabla \ln T) - (\mathbf{B}_\alpha : \nabla\mathbf{v}) + n\sum_\beta (\mathbf{C}_{\alpha\beta} \cdot \mathbf{d}_\beta) \quad \text{(D.4-2)}$$

in which the vector $\mathbf{A}_\alpha$, the tensor $\mathbf{B}_\alpha$, and the vectors $\mathbf{C}_{\alpha\beta}$, all functions of $\dot{\mathbf{r}}_\alpha$, $\mathbf{r}$, and t, are given as the solutions of integrodifferential equations.[1] The quantities $\mathbf{d}_\alpha$ are "generalized diffusional driving forces" that include concentration gradients, the pressure gradient, and external force differences, defined as

$$\begin{aligned}\mathbf{d}_\alpha &= \nabla x_\alpha + (x_\alpha - \omega_\alpha)\nabla \ln p - (\rho/p)\omega_\alpha(\mathbf{g}_\alpha - \Sigma_\beta \omega_\beta \mathbf{g}_\beta) \\ &= \frac{1}{cRT}\left[(\nabla p_\alpha - \rho_\alpha \mathbf{g}_\alpha) - \omega_\alpha\left(\nabla p - \sum_\beta \rho_\beta \mathbf{g}_\beta\right)\right]\end{aligned} \quad \text{(D.4-3)}$$

in which x_α, ω_α, and p_α are the mole fraction, mass fraction, and partial pressure, respectively. Equation D.4-3, valid only for a mixture of monatomic gases at low density, is generalized for other fluids in the discussion of the thermodynamics of irreversible processes in §24.1.

§D.5 THE FLUXES IN TERMS OF THE TRANSPORT PROPERTIES

When Eqs. D.4-1 to 3 are substituted into Eqs. D.3-1 to 3, we get the expressions for the fluxes in terms of $\mathbf{d}_\alpha$, $\nabla\mathbf{v}$, and ∇T:

$$\mathbf{j}_\alpha(\mathbf{r}, t) = +\rho_\alpha \sum_\beta \mathbb{D}_{\alpha\beta}\mathbf{d}_\beta - D_\alpha^T \nabla \ln T \quad \text{(D.5-1)}$$

$$\boldsymbol{\pi}(\mathbf{r}, t) = p\boldsymbol{\delta} - \mu[\nabla\mathbf{v} + (\nabla\mathbf{v})^\dagger - \tfrac{2}{3}(\nabla \cdot \mathbf{v})\boldsymbol{\delta}] \quad \text{(D.5-2)}$$

$$\mathbf{q}(\mathbf{r}, t) = -k\nabla T + \sum_\alpha \frac{\bar{H}_\alpha}{M_\alpha}\mathbf{j}_\alpha + \sum_\alpha \sum_\beta \frac{cRTx_\alpha x_\beta}{\rho_\alpha} \frac{D_\alpha^T}{\mathcal{D}_{\alpha\beta}}\left(\frac{\mathbf{j}_\alpha}{\rho_\alpha} - \frac{\mathbf{j}_\beta}{\rho_\beta}\right) \quad \text{(D.5-3)}$$

In these equations the transport properties appear: the viscosity μ, the thermal conductivity k, the multicomponent thermal diffusion coefficients D_α^T, and the multicomponent Fick diffusivities $\mathbb{D}_{\alpha\beta}$ (the $\mathcal{D}_{\alpha\beta}$ are the Maxwell–Stefan diffusivities, closely related to the $\mathbb{D}_{\alpha\beta}$). Thus the kinetic theory predicts the "cross effects": the transport of mass resulting from a temperature gradient (thermal diffusion) and the transport of energy resulting from a concentration gradient (the diffusion-thermo effect).

The pressure term in Eq. D.5-2 comes from the first term in the expansion in Eq. D.4-1 (that is, the Maxwell–Boltzmann distribution), and the viscosity term comes from the second term (that is, the ϕ_α term containing the gradients). The kinetic theory of monatomic gases at low density predicts that the dilatational viscosity will be zero.

§D.6 THE TRANSPORT PROPERTIES IN TERMS OF THE INTERMOLECULAR FORCES

The transport properties in Eqs. D.5-1 to 3 are given by the kinetic theory as complicated multiple integrals involving the intermolecular forces that describe binary collisions in the gas mixture. Once an expression has been chosen for the intermolecular force law (such as the Lennard-Jones (6–12) potential of Eq. 1.4-10), these integrals can be evaluated numerically. For a pure gas, the three transport properties—self-diffusivity, viscosity, and thermal conductivity—are then given by:

$$\mathscr{D} = \frac{3}{8}\frac{\sqrt{\pi m \kappa T}}{\pi\sigma^2\Omega_{\mathscr{D}}}\frac{1}{\rho}; \qquad \mu = \frac{5}{16}\frac{\sqrt{\pi m \kappa T}}{\pi\sigma^2\Omega_\mu}; \qquad k = \frac{25}{32}\frac{\sqrt{\pi m \kappa T}}{\pi\sigma^2\Omega_k}\hat{C}_V \quad \text{(D.6-1, 2, 3)}$$

The dimensionless "collision integrals" $\Omega_\mu = \Omega_k \approx 1.1\Omega_{\mathscr{D}}$ contain all the information about the intermolecular forces and the binary collision dynamics. They are given in Table E.2 as functions of $\kappa T/\varepsilon$. If we set the collision integrals equal to unity, we then get the transport properties for a gas composed of rigid spheres.

Thus the transport properties, needed in the equations of change, have been obtained from kinetic theory in terms of the two parameters σ and ε of the intermolecular potential energy function. From these expressions we get $\mathrm{Pr} = \hat{C}_p\mu/k = \frac{2}{5}(\hat{C}_p/\hat{C}_V) = \frac{2}{5}(\frac{5}{3}) = \frac{2}{3}$ and $\mathrm{Sc} = \mu/\rho\mathscr{D} = \frac{5}{6}(\Omega_{\mathscr{D}}/\Omega_\mu) \approx \frac{3}{4}$, these values being quite good for pure monatomic gases.

§D.7 CONCLUDING COMMENTS

The above discussion emphasizes the close connections among mass, momentum, and energy transport, and it is seen how all three transport phenomena can be explained in terms of a molecular theory for low-density, monatomic gases. It is also important to see that the continuum equations of continuity, motion, and energy can all be derived from one starting point—the Boltzmann equation—and that the molecular expressions for the fluxes and transport properties are generated in the process. In addition, the discussion of the dependence of the fluxes on the driving forces is very closely related to the irreversible thermodynamics approach in Chapter 24.

This appendix has dealt only with low-density, monatomic gases. Similar discus-

---

[3] C. F. Curtiss, *J. Chem. Phys.*, **24**, 225–241 (1956); C. Muckenfuss and C. F. Curtiss, *J. Chem. Phys.*, **29**, 1257–1277 (1958); L. A. Viehland and C. F. Curtiss, *J. Chem. Phys.*, **60**, 492–520 (1974); D. Russell and C. F. Curtiss, *J. Chem. Phys.*, **60**, 514–520 (1974).

[4] J. H. Irving and J. G. Kirkwood, *J. Chem. Phys.*, **18**, 817–829 (1950); R. J. Bearman and J. G. Kirkwood, *J. Chem. Phys.*, **28**, 136–145 (1958).

[5] C. F. Curtiss and R. B. Bird, *Adv. Polymer Sci.*, **125**, 1–101 (1996); *Proc. Nat. Acad. Sci.*, **93**, 7440–7445 (1996); *J. Chem. Phys.*, **106**, 9899–9921 (1997), **107**, 5254–5267 (1997), **111**, 10362–10370 (1999).

sions are available for polyatomic gases,[3] monatomic liquids,[4] and polymeric liquids.[5] In kinetic theories for monatomic liquids, the expressions for the momentum and heat fluxes contain terms similar to those in Eqs. D.3-2 and 3, but also contributions associated with forces between molecules; for polymers, one has the latter contribution, but also additional forces within the polymer chain. In all of these theories one can derive the equations of change from an equation for a distribution function and then get formal expressions for the transport properties.

Appendix E

Tables for Prediction of Transport Properties

Table E.1 Lennard-Jones (6–12) Potential Parameters and Critical Properties

		Lennard-Jones parameters			Critical properties[g,h]				
Substance	Molecular Weight M	σ (Å)	ε/κ (K)	Ref.	T_c (K)	p_c (atm)	$\tilde{V}_c$ (cm^3/g-mole)	μ_c (g/cm · s × 10^6)	k_c (cal/cm · s · K × 10^6)
Light elements:									
H_2	2.016	2.915	38.0	*a*	33.3	12.80	65.0	34.7	—
He	4.003	2.576	10.2	*a*	5.26	2.26	57.8	25.4	—
Noble gases:									
Ne	20.180	2.789	35.7	*a*	44.5	26.9	41.7	156.	79.2
Ar	39.948	3.432	122.4	*b*	150.7	48.0	75.2	264.	71.0
Kr	83.80	3.675	170.0	*b*	209.4	54.3	92.2	396.	49.4
Xe	131.29	4.009	234.7	*b*	289.8	58.0	118.8	490.	40.2
Simple polyatomic gases:									
Air	28.964[i]	3.617	97.0	*a*	132.4[i]	37.0[i]	86.7[i]	193.	90.8
N_2	28.013	3.667	99.8	*b*	126.2	33.5	90.1	180.	86.8
O_2	31.999	3.433	113.	*a*	154.4	49.7	74.4	250.	105.3
CO	28.010	3.590	110.	*a*	132.9	34.5	93.1	190.	86.5
CO_2	44.010	3.996	190.	*a*	304.2	72.8	94.1	343.	122.
NO	30.006	3.470	119.	*a*	180.	64.	57.	258.	118.2
N_2O	44.012	3.879	220.	*a*	309.7	71.7	96.3	332.	131.
SO_2	64.065	4.026	363.	*c*	430.7	77.8	122.	411.	98.6
F_2	37.997	3.653	112.	*a*	—	—	—	—	—
Cl_2	70.905	4.115	357.	*a*	417.	76.1	124.	420.	97.0
Br_2	159.808	4.268	520.	*a*	584.	102.	144.	—	—
I_2	253.809	4.982	550.	*a*	800.	—	—	—	—
Hydrocarbons:									
CH_4	16.04	3.780	154.	*b*	191.1	45.8	98.7	159.	158.
CH≡CH	26.04	4.114	212.	*d*	308.7	61.6	112.9	237.	—
CH_2=CH_2	28.05	4.228	216.	*b*	282.4	50.0	124.	215.	—
C_2H_6	30.07	4.388	232.	*b*	305.4	48.2	148.	210.	203.
CH_3C≡CH	40.06	4.742	261.	*d*	394.8	—	—	—	—
CH_3CH=CH_2	42.08	4.766	275.	*b*	365.0	45.5	181.	233.	—
C_3H_8	44.10	4.934	273.	*b*	369.8	41.9	200.	228.	—
n—C_4H_{10}	58.12	5.604	304.	*b*	425.2	37.5	255.	239.	—

i—C_4H_{10}	58.12	5.393	295.	*b*	408.1	36.0	263.	239.	—
n—C_5H_{12}	72.15	5.850	326.	*b*	469.5	33.2	311.	238.	—
i—C_5H_{12}	72.15	5.812	327.	*b*	460.4	33.7	306.	—	—
$C(CH_3)_4$	72.15	5.759	312.	*b*	433.8	31.6	303.	—	—
n—C_6H_{14}	86.18	6.264	342.	*b*	507.3	29.7	370.	248.	—
n—C_7H_{16}	100.20	6.663	352.	*b*	540.1	27.0	432.	254.	—
n—C_8H_{18}	114.23	7.035	361.	*b*	568.7	24.5	492	259.	—
n—C_9H_{20}	128.26	7.463	351.	*b*	594.6	22.6	548.	265.	—
Cyclohexane	84.16	6.143	313.	*d*	553.	40.0	308.	284.	—
Benzene	78.11	5.443	387.	*b*	562.6	48.6	260.	312.	—
Other organic compounds:									
CH_4	16.04	3.780	154.	*b*	191.1	45.8	98.7	159.	158.
CH_3Cl	50.49	4.151	355.	*c*	416.3	65.9	143.	338.	—
CH_2Cl_2	84.93	4.748	398.	*c*	510.	60.	—	—	—
$CHCl_3$	119.38	5.389	340.	*e*	536.6	54.	240.	410.	—
CCl_4	153.82	5.947	323.	*e*	556.4	45.0	276.	413.	—
C_2N_2	52.034	4.361	349.	*e*	400.	59.	—	—	—
COS	60.076	4.130	336.	*e*	378.	61.	—	—	—
CS_2	76.143	4.483	467.	*e*	552.	78.	170.	404.	—
CCl_2F_2	120.91	5.116	280.	*b*	384.7	39.6	218.	—	—

[a] J. O. Hirschfelder, C. F. Curtiss, and R. B. Bird, *Molecular Theory of Gases and Liquids*, corrected printing with notes added, Wiley, New York (1964).

[b] L. S. Tee, S. Gotoh, and W. E. Stewart, *Ind. Eng. Chem. Fundamentals*, **5**, 356–363 (1966). The values for benzene are from viscosity data on that substance. The values for other substances are computed from Correlation (iii) of the paper.

[c] L. Monchick and E. A. Mason, *J. Chem. Phys.*, **35**, 1676–1697 (1961); parameters obtained from viscosity.

[d] L. W. Flynn and G. Thodos, *AIChE Journal*, **8**, 362–365 (1962); parameters obtained from viscosity.

[e] R. A. Svehla, *NASA Tech. Report R-132* (1962); parameters obtained from viscosity. This report provides extensive tables of Lennard-Jones parameters, heat capacities, and calculated transport properties.

[f] Values of the critical constants for the pure substances are selected from K. A. Kobe and R. E. Lynn, Jr., *Chem. Rev.*, **52**, 117–236 (1962); *Amer. Petroleum Inst. Research Proj.* **44**, Thermodynamics Research Center, Texas A&M University, College Station, Texas (1966); and *Thermodynamic Functions of Gases*, F. Din (editor), Vols. 1–3, Butterworths, London (1956, 1961, 1962).

[g] Values of the critical viscosity are from O. A. Hougen and K. M. Watson, *Chemical Process Principles*, Vol. 3, Wiley, New York (1947), p. 873.

[h] Values of the critical thermal conductivity are from E. J. Owens and G. Thodos, *AIChE Journal*, **3**, 454–461 (1957).

[i] For air, the molecular weight M and the pseudocritical properties have been computed from the average composition of dry air as given in COESA, *U.S. Standard Atmosphere 1976*, U.S. Government Printing Office, Washington, D.C. (1976).

Table E.2 Collision Integrals for Use with the Lennard-Jones (6–12) Potential for the Prediction of Transport Properties of Gases at Low Densities[a,b,c]

$\kappa T/\varepsilon$ or $\kappa T/\varepsilon_{AB}$	$\Omega_\mu = \Omega_k$ (for viscosity and thermal conductivity)	$\Omega_{\mathcal{D},AB}$ (for diffusivity)	$\kappa T/\varepsilon$ or $\kappa T/\varepsilon_{AB}$	$\Omega_\mu = \Omega_k$ (for viscosity and thermal conductivity)	$\Omega_{\mathcal{D},AB}$ (for diffusivity)
0.30	2.840	2.649	2.7	1.0691	0.9782
0.35	2.676	2.468	2.8	1.0583	0.9682
0.40	2.531	2.314	2.9	1.0482	0.9588
0.45	2.401	2.182	3.0	1.0388	0.9500
0.50	2.284	2.066	3.1	1.0300	0.9418
0.55	2.178	1.965	3.2	1.0217	0.9340
0.60	2.084	1.877	3.3	1.0139	0.9267
0.65	1.999	1.799	3.4	1.0066	0.9197
0.70	1.922	1.729	3.5	0.9996	0.9131
0.75	1.853	1.667	3.6	0.9931	0.9068
0.80	1.790	1.612	3.7	0.9868	0.9008
0.85	1.734	1.562	3.8	0.9809	0.8952
0.90	1.682	1.517	3.9	0.9753	0.8897
0.95	1.636	1.477	4.0	0.9699	0.8845
1.00	1.593	1.440	4.1	0.9647	0.8796
1.05	1.554	1.406	4.2	0.9598	0.8748
1.10	1.518	1.375	4.3	0.9551	0.8703
1.15	1.485	1.347	4.4	0.9506	0.8659
1.20	1.455	1.320	4.5	0.9462	0.8617
1.25	1.427	1.296	4.6	0.9420	0.8576
1.30	1.401	1.274	4.7	0.9380	0.8537
1.35	1.377	1.253	4.8	0.9341	0.8499
1.40	1.355	1.234	4.9	0.9304	0.8463
1.45	1.334	1.216	5.0	0.9268	0.8428
1.50	1.315	1.199	6.0	0.8962	0.8129
1.55	1.297	1.183	7.0	0.8727	0.7898
1.60	1.280	1.168	8.0	0.8538	0.7711
1.65	1.264	1.154	9.0	0.8380	0.7555
1.70	1.249	1.141	10.0	0.8244	0.7422
1.75	1.235	1.128	12.0	0.8018	0.7202
1.80	1.222	1.117	14.0	0.7836	0.7025
1.85	1.209	1.105	16.0	0.7683	0.6878
1.90	1.198	1.095	18.0	0.7552	0.6751
1.95	1.186	1.085	20.0	0.7436	0.6640
2.00	1.176	1.075	25.0	0.7198	0.6414
2.10	1.156	1.058	30.0	0.7010	0.6235
2.20	1.138	1.042	35.0	0.6854	0.6088
2.30	1.122	1.027	40.0	0.6723	0.5964
2.40	1.107	1.013	50.0	0.6510	0.5763
2.50	1.0933	1.0006	75.0	0.6140	0.5415
2.60	1.0807	0.9890	100.0	0.5887	0.5180

[a] The values in this table, applicable for the Lennard-Jones (6–12) potential, are interpolated from the results of L. Monchick and E. A. Mason, *J. Chem. Phys.*, **35**, 1676–1697 (1961). The Monchick–Mason table is believed to be slightly better than the earlier table by J. O. Hirschfelder, R. B. Bird, and E. L. Spotz, *J. Chem. Phys.*, **16**, 968–981 (1948).

[b] This table has been extended to lower temperatures by C. F. Curtiss, *J. Chem. Phys.*, **97**, 7679–7686 (1992). Curtiss showed that at low temperatures, the Boltzmann equation needs to be modified to take into account "orbiting pairs" of molecules. Only by making this modification is it possible to get a smooth transition from quantum to classical behavior. The deviations are appreciable below dimensionless temperatures of 0.30.

[c] The collision integrals have been curve-fitted by P. D. Neufeld, A. R. Jansen, and R. A. Aziz, *J. Chem. Phys.*, **57**, 1100–1102 (1972), as follows:

$$\Omega_\mu = \Omega_k = \frac{1.16145}{T^{*0.14874}} + \frac{0.52487}{\exp(0.77320T^*)} + \frac{2.16178}{\exp(2.43787T^*)} \tag{E.2-1}$$

$$\Omega_{\mathcal{D},AB} = \frac{1.06036}{T^{*0.15610}} + \frac{0.19300}{\exp(0.47635T^*)} + \frac{1.03587}{\exp(1.52996T^*)} + \frac{1.76474}{\exp(3.89411T^*)} \tag{E.2-2}$$

where $T^* = \kappa T/\varepsilon$.

Appendix F

Constants and Conversion Factors

§F.1 MATHEMATICAL CONSTANTS

$$\pi = 3.14159\ldots$$
$$e = 2.71828\ldots$$
$$\ln 10 = 2.30259\ldots$$

§F.2 PHYSICAL CONSTANTS[1]

Gas law constant (R)	8.31451	J/g-mol · K
	8.31451×10^3	kg · m^2/s^2 · kg-mol · K
	8.31451×10^7	g · cm^2/s^2 · g-mol · K
	1.98721	cal/g-mol · K
	82.0578	cm^3 atm/g-mol · K
	4.9686×10^4	lb$_m$ ft^2/s^2 · lb-mol · R
	1.5443×10^3	ft · lb$_f$/lb-mol · R
Standard acceleration of gravity (g_0)	9.80665	m/s^2
	980.665	cm/s^2
	32.1740	ft/s^2
Joule's constant (J_c) (mechanical equivalent of heat)	4.1840	J/cal
	4.1840×10^7	erg/cal
	778.16	ft · lb$_f$/Btu
Avogadro's number ($\tilde{N}$)	6.02214×10^{23}	molecules/g-mol
Boltzmann's constant ($\kappa = R/\tilde{N}$)	1.38066×10^{-23}	J/K
	1.38066×10^{-16}	erg/K
Faraday's constant (F)	96485.3	C/g-equivalent
Planck's constant (h)	6.62608×10^{-34}	J · s
	6.62608×10^{-27}	erg · s
Stefan–Boltzmann constant (σ)	5.67051×10^{-8}	W/m^2 · K^4
	1.3553×10^{-12}	cal/s · cm^{2}K^4
	1.7124×10^{-9}	Btu/hr · ft^{2}R^4
Electron charge (e)	1.60218×10^{-19}	C
Speed of light in a vacuum (c)	2.99792×10^8	m/s

[1] E. R. Cohen and B. N. Taylor, *Physics Today* (August 1996), pp. BG9–BG13; R. A. Nelson, *Physics Today* (August 1996), pp. BG15–BG16.

§F.3 CONVERSION FACTORS

In the tables that follow, to convert any physical quantity from one set of units to another, multiply it by the appropriate table entry. For example, suppose that p is given as 10 $lb_f/in.^2$, and we wish to have p in poundals/ft^2. From Table F.3-2 the result is

$$p = (10)(4.6330 \times 10^3) = 4.6330 \times 10^4 \text{ poundals/ft}^2$$

The entries in the shaded rows and columns are those that are needed for converting from and to SI units.

In addition to the tables, we give a few of the commonly used conversion factors here:

Given a quantity in these units:	Multiply by:	To get quantity in these units:
Pounds	453.59	Grams
Kilograms	2.2046	Pounds
Inches	2.5400	Centimeters
Meters	39.370	Inches
Gallons (U.S.)	3.7853	Liters
Gallons (U.S.)	231.00	Cubic inches
Gallons (U.S.)	0.13368	Cubic feet
Cubic feet	28.316	Liters
Kelvins	1.800000	Degrees Rankine
Degrees Rankine	0.555556	Kelvins

Table F.3-1 Conversion Factors for Quantities Having Dimensions of F or ML/t^2

Given a quantity in these units ↓	Multiply by table value to convert to these units→	$N = kg \cdot m/s^2$ (Newtons)	$g \cdot cm/s^2$ (dynes)	$lb_m \cdot ft/s^2$ (poundals)	lb_f
$N = kg \cdot m/s^2$	(Newtons)	1	10^5	7.2330	2.24881×10^{-1}
$g \cdot cm/s^2$	(dynes)	10^{-5}	1	7.2330×10^{-5}	2.24881×10^{-6}
$lb_m \cdot ft/s^2$	(poundals)	1.3826×10^{-1}	1.3826×10^4	1	3.1081×10^{-2}
lb_f		4.4482	4.4482×10^5	32.1740	1

Table F.3-2 Conversion Factors for Quantities Having Dimensions of F/L^2 or M/Lt^2 (pressure, momentum flux)

Given a quantity in these units ↓ / Multiply by table value to convert to these units →	Pa (N/m^2) ($kg/m \cdot s^2$)	dyne/cm^2 ($g/cm \cdot s^2$)	poundals/ft^2 ($lb_m/ft \cdot s^2$)	lb_f/ft^2	lb_f/in^2 (psia)[a]	atm	mm Hg	in. Hg
$Pa = N/m^2 = kg/m \cdot s^2$	1	10	6.7197×10^{-1}	2.0886×10^{-2}	1.4504×10^{-4}	9.8692×10^{-6}	7.5006×10^{-3}	2.9530×10^{-4}
$dyne/cm^2 = g/cm \cdot s^2$	10^{-1}	1	6.7197×10^{-2}	2.0886×10^{-3}	1.4504×10^{-5}	9.8692×10^{-7}	7.5006×10^{-4}	2.9530×10^{-5}
$poundals/ft^2 = lb_m/ft \cdot s^2$	1.4882	1.4882×10^{1}	1	3.1081×10^{-2}	2.1584×10^{-4}	1.4687×10^{-5}	1.1162×10^{-2}	4.3945×10^{-4}
lb_f/ft^2	4.7880×10^{1}	4.7880×10^{2}	32.1740	1	6.9444×10^{-3}	4.7254×10^{-4}	3.5913×10^{-1}	1.4139×10^{-2}
$lb_f/in.^2$	6.8947×10^{3}	6.8947×10^{4}	4.6330×10^{3}	144	1	6.8046×10^{-2}	5.1715×10^{1}	2.0360
atm	1.0133×10^{5}	1.0133×10^{6}	6.8087×10^{4}	2.1162×10^{3}	14.696	1	760	29.921
mm Hg	1.3332×10^{2}	1.3332×10^{3}	8.9588×10^{1}	2.7845	1.9337×10^{-2}	1.3158×10^{-3}	1	3.9370×10^{-2}
in. Hg	3.3864×10^{3}	3.3864×10^{4}	2.2756×10^{3}	7.0727×10^{1}	4.9116×10^{-1}	3.3421×10^{-2}	25.400	1

[a] This unit is preferably abbreviated "psia" (pounds per square inch absolute) or "psig" (pounds per square inch gage). Gage pressure is absolute pressure minus the prevailing barometric pressure. Sometimes the pressure is reported in "bars"; to convert from bars to pascals, multiply by 10^5, and to convert from bars to atmospheres, multiply by 0.98692.

Table F.3-3 Conversion Factors for Quantities Having Dimensions of FL or ML^2/t^2 (energy, work, torque)

Given a quantity in these units ↓ / Multiply by table value to convert to these units →	J ($kg \cdot m^2/s^2$)	ergs ($g \cdot cm^2/s^2$)	foot poundals $lb_m\ ft^2/s^2$	$ft \cdot lb_f$	cal	Btu	hp-hr	kw-hr
$J = kg \cdot m^2/s^2$	1	10^7	2.3730×10^{1}	7.3756×10^{-1}	2.3901×10^{-1}	9.4783×10^{-4}	3.7251×10^{-7}	2.7778×10^{-7}
$ergs = g \cdot cm^2/s^2$	10^{-7}	1	2.3730×10^{-6}	7.3756×10^{-8}	2.3901×10^{-8}	9.4783×10^{-11}	3.7251×10^{-14}	2.7778×10^{-14}
foot poundals = $lb_m\ ft^2/s^2$	4.2140×10^{-2}	4.2140×10^{5}	1	3.1081×10^{-2}	1.0072×10^{-2}	3.9942×10^{-5}	1.5698×10^{-8}	1.1706×10^{-8}
$ft \cdot lb_f$	1.3558	1.3558×10^{7}	32.1740	1	3.2405×10^{-1}	1.2851×10^{-3}	5.0505×10^{-7}	3.7662×10^{-7}
thermochemical calories[a]	4.1840	4.1840×10^{7}	9.9287×10^{1}	3.0860	1	3.9657×10^{-3}	1.5586×10^{-6}	1.1622×10^{-6}
British thermal units	1.0550×10^{3}	1.0550×10^{10}	2.5036×10^{4}	778.16	2.5216×10^{2}	1	3.9301×10^{-4}	2.9307×10^{-4}
Horsepower hours	2.6845×10^{6}	2.6845×10^{13}	6.3705×10^{7}	1.9800×10^{6}	6.4162×10^{5}	2.5445×10^{3}	1	7.4570×10^{-1}
kilowatt hours	3.6000×10^{6}	3.6000×10^{13}	8.5429×10^{7}	2.6552×10^{6}	8.6042×10^{5}	3.4122×10^{3}	1.3410	1

[a] This unit, abbreviated "cal," is used in some chemical thermodynamic tables. To convert quantities expressed in International Steam Table calories (abbreviated "I. T. cal") to this unit, multiply by 1.000654.

Table F.3-4 Conversion Factors for Quantities Having dimensions[a] of M/Lt or Ft/L^2 (viscosity, density times diffusivity)

Given a quantity in these units ↓ / Multiply by table value to convert to these units →	Pa · s (kg/m · s)	g/cm · s (poises)	centipoises	lb_m/ft · s	lb_m/ft · hr	lb_f · s/ft^2
Pa · s = kg/m · s	1	10	10^3	6.7197×10^{-1}	2.4191×10^3	2.0886×10^{-2}
g/cm · s = (poises)	10^{-1}	1	10^2	6.7197×10^{-2}	2.4191×10^2	2.0886×10^{-3}
centipoises	10^{-3}	10^{-2}	1	6.7197×10^{-4}	2.4191	2.0886×10^{-5}
lb_m/ft · s	1.4882	1.4882×10^1	1.4882×10^3	1	3600	3.1081×10^{-2}
lb_m/ft · hr	4.1338×10^{-4}	4.1338×10^{-3}	4.1338×10^{-1}	2.7778×10^{-4}	1	8.6336×10^{-6}
lb_f · s/ft^2	4.7880×10^1	4.7880×10^2	4.7880×10^4	32.1740	1.1583×10^5	1

[a] When moles appear in the given and the desired units, the conversion factor is the same as for the corresponding mass units.

Table F.3-5 Conversion Factors for Quantities Having Dimensions of ML/t^3T or F/tT (thermal conductivity)

Given a quantity in these units ↓ / Multiply by table value to convert to these units →	W/m · K or kg · m/s^3 · K	g · cm/s^3 · K or erg/s · cm · K	lb_m ft/s^3 F	lb_f/s · F	cal/s · cm · K	Btu/hr · ft · F
W/m · K = kg · m/s^3 · K	1	10^5	4.0183	1.2489×10^{-1}	2.3901×10^{-3}	5.7780×10^{-1}
g · cm/s^3 · K	10^{-5}	1	4.0183×10^{-5}	1.2489×10^{-6}	2.3901×10^{-8}	5.7780×10^{-6}
lb_m ft/s^3 F	2.4886×10^{-1}	2.4886×10^4	1	3.1081×10^{-2}	5.9479×10^{-4}	1.4379×10^{-1}
lb_f/s · F	8.0068	8.0068×10^5	3.2174×10^1	1	1.9137×10^{-2}	4.6263
cal/s · cm · K	4.1840×10^2	4.1840×10^7	1.6813×10^3	5.2256×10^1	1	2.4175×10^2
Btu/hr · ft · F	1.7307	1.7307×10^5	6.9546	2.1616×10^{-1}	4.1365×10^{-3}	1

Table F.3-6 Conversion Factors for Quantities Having Dimensions of L^2/t (momentum diffusivity, thermal diffusivity, molecular diffusivity)

Given a quantity in these units ↓ / Multiply by table value to convert to these units →	m^2/s	cm^2/s	ft^2/hr	centistokes
m^2/s	1	10^4	3.8750×10^4	10^6
cm^2/s	10^{-4}	1	3.8750	10^2
ft^2/hr	2.5807×10^{-5}	2.5807×10^{-1}	1	2.5807×10^1
centistokes	10^{-6}	10^{-2}	3.8750×10^{-2}	1

Table F.3-7 Conversion Factors for Quantities Having Dimensions of M/t^3T or F/LtT (heat transfer coefficients)

Given a quantity in these units ↓ / Multiply by table value to convert to these units →	$W/m^2\,K$ ($J/m^2\,s \cdot K$) $kg/s^3\,K$	$W/cm^2\,K$	$g/s^3\,K$	$lb_m/s^3\,F$	$lb_f/ft \cdot s \cdot F$	$cal/cm^2\,s \cdot K$	Btu/ $ft^2\,hr \cdot F$
$W/m^2\,K = kg/s^3\,K$	1	10^{-4}	10^3	1.2248	3.8068×10^{-2}	2.3901×10^{-5}	1.7611×10^{-1}
$W/cm^2\,K$	10^4	1	10^7	1.2248×10^4	3.8068×10^2	2.3901×10^{-1}	1.7611×10^3
$g/s^3\,K$	10^{-3}	10^{-7}	1	1.2248×10^{-3}	3.8068×10^{-5}	2.3901×10^{-8}	1.7611×10^{-4}
$lb_m/s^3\,F$	8.1647×10^{-1}	8.1647×10^{-5}	8.1647×10^2	1	3.1081×10^{-2}	1.9514×10^{-5}	1.4379×10^{-1}
$lb_f/ft \cdot s \cdot F$	2.6269×10^1	2.6269×10^{-3}	2.6269×10^4	32.1740	1	6.2784×10^{-4}	4.6263
$cal/cm^2\,s \cdot K$	4.1840×10^4	4.1840	4.1840×10^7	5.1245×10^4	1.5928×10^3	1	7.3686×10^3
$Btu/ft^2\,hr \cdot F$	5.6782	5.6782×10^{-4}	5.6782×10^3	6.9546	2.1616×10^{-1}	1.3571×10^{-4}	1

Table F.3-8 Conversion Factors for Quantities Having Dimensions[a] of M/L^2t or Ft/L^3 (mass transfer coefficients k_x or k_ω)

Given a quantity in these units ↓ / Multiply by table value to convert to these units →	$kg/m^2\,s$	$g/cm^2\,s$	$lb_m/ft^2\,s$	$lb_m/ft^2\,hr$	$lb_f\,s/ft^3$
$kg/m^2\,s$	1	10^{-1}	2.0482×10^{-1}	7.3734×10^2	6.3659×10^{-3}
$g/cm^2\,s$	10^1	1	2.0482	7.3734×10^3	6.3659×10^{-2}
$lb_m/ft^2\,s$	4.8824	4.8824×10^{-1}	1	3600	3.1081×10^{-2}
$lb_m/ft^2\,hr$	1.3562×10^{-3}	1.3562×10^{-4}	2.7778×10^{-4}	1	8.6336×10^{-6}
$lb_f\,s/ft^3$	1.5709×10^2	1.5709×10^1	32.1740	1.1583×10^5	1

[a] When moles appear in the given and the desired units, the conversion factor is the same as for the corresponding mass units.

Notation

Numbers in parentheses refer to equations, sections, or tables in which the symbols are defined or first used. Dimensions are given in terms of mass (M), length (L), time (t), temperature (T), and dimensionless (—). Boldface symbols are vectors or tensors (see Appendix A). Symbols that appear infrequently are not listed.

A = area, L^2
a = absorptivity (16.2-1),—
a = interfacial area per unit volume of packed bed (6.4-4), L^{-1}
a_α = activity of species α (24.1-8),—
C_p = heat capacity at constant pressure (9.1-7), ML^2/t^2T
C_V = heat capacity at constant volume (9.3-6), ML^2/t^2T
c = speed of light (16.1-1), L/t
c = total molar concentration (§17.7), moles/L^3
c_α = molar concentration of species α, (§17.7), moles/L^3
D = diameter of cylinder or sphere, L
D_p = particle diameter in packed bed, (6.4-6), L
$\mathscr{D}_{AB}$ = binary diffusivity for system A–B (17.1-2), L^2/t
$\mathscr{D}_{\alpha\beta}$ = binary diffusivity for the pair α–β in a multicomponent system (17.9-1), L^2/t
$\mathscr{Đ}_{\alpha\beta}$ = Maxwell–Stefan multicomponent diffusivity (24.2-4), L^2/t
$\mathbb{D}_{\alpha\beta}$ = Fick multicomponent diffusivity (24.2-3), L^2/t
D_α^T = multicomponent thermal diffusion coefficient (24.2-3), M/Lt
d = molecular diameter (1.4-3), L
$\mathbf{d}_\alpha$ = diffusional driving force for species α (24.1-8), L^{-1}
E_{tot} = $U_{tot} + K_{tot} + \Phi_{tot}$ = total energy in a macroscopic system (15.1-2), ML^2/t^2
E_c = compression term in mechanical energy balance (7.4-3), ML^2/t^3
E_v = viscous dissipation term in mechanical energy balance (7.4-4), ML^2/t^3
e = 2.71828 . . .
e = emissivity (16.2-3),—
$\mathbf{e}$ = combined energy flux vector (9.8-5), M/t^3
F_{12}, $\overline{F}_{12}$ = direct, indirect view factor (16.4-9), (16.5-15),—
$\mathbf{F}_{s\to f}$ = force exerted by the solid on the fluid (7.2-1), ML/t^2
f = friction factor (or drag coefficient) (6.1-1),—
G = $H - TS$ = Gibbs free energy (24.1-2), ML^2/t^2
G = $\langle \rho v \rangle$ = mass velocity (6.4-8), M/L^2t
$\mathbf{g}$ = gravitational acceleration (3.2-8), L/t^2
$\mathbf{g}_\alpha$ = body force per unit mass acting on species α (Table 19.2-1), L/t^2
H = $U + pV$ = enthalpy (9.8-6), ML^2/t^2
h = Planck's constant (14.1-2), ML^2/t
h = elevation (2.3-10), L
h, h_1, h_{ln}, h_{loc}, h_a, h_m = heat transfer coefficients (14.1-1 to 6), M/t^3T
i = $\sqrt{-1}$ (4.1-43),—
$\mathbf{J}_\alpha$, $\mathbf{J}_\alpha^*$ = molar fluxes (Table 17.8-1), moles/L^2t
$\mathbf{j}_\alpha$, $\mathbf{j}_\alpha^*$ = mass fluxes (Table 17.8-1), M/L^2t
j_H, j_D = Chilton–Colburn j-factors (14.3-19, Table 22.2-1),—

K = kinetic energy (7.4-1), ML^2/t^2
K_x, K_y = two-phase mass transfer coefficients (22.4-4), moles/tL^2
κ = $R/\tilde{N}$ = Boltzmann's constant (1.4-1), ML^2/t^2T
k = thermal conductivity (9.1-1 and 24.2-6), ML/t^3T
k_x = single-phase mass transfer coefficients (22.1-7, 22.3-4, Table 22.2-1), moles/tL^2
k_x^0, k_y^0 = mass transfer coefficient for small mass-transfer rates and small species concentration (22.1-9, 22.4-2), moles/tL^2
$k_x^\bullet$ = mass transfer coefficient for high net mass-transfer rates (22.8-2a), moles/tL^2
k_T = thermal diffusion ratio (24.2-10),—
k_e = electrical conductivity (9.5-1), ohm^{-1} cm^{-1}
k_n'' = heterogeneous chemical reaction rate coefficient (18.0-3), moles$^{1-n}/L^{2-3n}t$
k_n''' = homogeneous chemical reaction rate coefficient (18.0-2), moles$^{1-n}/L^{3-3n}t$
L = length of film, tube, or slit (2.2-22), L
$\mathbf{L}_{\text{tot}}$ = total angular momentum within a macroscopic system (7.3-1), ML^2/t
l = mixing length (5.4-4), L
l_0 = characteristic length in dimensional analysis (3.7-3), L
M = molar mean molecular weight (Table 17.7-1), M/mole
M_α = molecular weight of species α (Table 17.7-1), M/mole
$M_{\alpha,\text{tot}}$ = total number of moles of species α in macroscopic system (23.1-3), moles
m = mass of a molecule (1.4-1), M
m, n = parameters in power law viscosity model (8.3-3), M/Lt^{2-n},—
$m_{\alpha,\text{tot}}$ = total mass of species α in macroscopic system (23.1-1), M
N = rate of shaft rotation (3.7-28), t^{-1}
N = number of species in a multicomponent mixture (17.7-1),—
$\tilde{N}$ = Avogadro's number, (g-mole)$^{-1}$
$\mathbf{N}_\alpha$ = combined molar flux vector for species α (17.8-2), moles/L^2t
$\mathbf{n}$ = unit normal vector (A.5-1),—
$\mathbf{n}_\alpha$ = combined mass flux vector for species α (17.8-1), M/L^2t
n = molecular concentration or number density (1.4-2), L^{-3}
$\mathbf{P}_{\text{tot}}$ = total momentum in a macroscopic flow system (7.2-1), ML/t
$\mathcal{P}$ = $p + \rho gh$ = modified pressure (for constant ρ and g) (2.3-10), M/Lt^2
$\mathcal{P}_0$ = characteristic pressure used in dimensional analysis (3.7-4), M/Lt^2
p = fluid pressure, M/Lt^2
Q = rate of heat flow across a surface (9.1-1, 15.1-1), ML^2/t^3
$Q_{\vec{12}}$ = radiant energy flow from surface 1 to surface 2 (16.4-5), ML^2/t^3
Q_{12} = net radiant energy interchange between surface 1 and surface 2 (16.4-8), ML^2/t^3
$\mathbf{q}$ = heat flux vector (9.1-4), M/t^3
q_0 = interfacial heat flux (10.8-14), M/t^3
R = gas constant (in $p\tilde{V} = RT$), ML^2/t^2T mole
R = radius of a cylinder or a sphere, L
R_α = molar rate of production of species α by homogeneous chemical reaction (18.0-2), moles/tL^3
R_h = mean hydraulic radius (6.2-16), L

$\Re$ = real part (of complex quantity) (4.1-43)
$\mathbf{r}$ = position vector (3.4-1), L
$r = \sqrt{x^2 + y^2}$ = radial coordinate in cylindrical coordinates, L
$r = \sqrt{x^2 + y^2 + z^2}$ = radial coordinate in spherical coordinates, L
r_α = mass rate of production of species α by homogeneous chemical reaction (19.1-5), M/tL^3
S_1, S_2 = cross-sectional area at planes 1 and 2 (7.1-1), L^2
S = entropy (11D.1-1, 24.1-1), ML^2/t^2T
T = absolute temperature, T
$\mathbf{T}_{s\to f}$ = torque exerted by a solid boundary on the fluid (7.3-1), ML^2/t^2
$\mathbf{T}_{\text{ext}}$ = external torque acting on system (7.3-1), ML^2/t^2
$T_1 - T_0$ = characteristic temperature difference used in dimensional analysis (11.5-5), T
t = time, t
U = internal energy (9.7-1), ML^2/t^2
U = overall heat-transfer coefficient (10.6-15), M/t^3T
$\bar{u}$ = arithmetic mean molecular speed (1.4-1), L/t
$\mathbf{u}$ = unit vector in direction of flow (7.2-1),—
V = volume, L^3
$\mathbf{v}$ = mass average velocity (17.7-1), L/t
$\mathbf{v}^*$ = molar average velocity (17.7-2), L/t
$\mathbf{v}_\alpha$ = velocity of species α (17.1-3, Table 17.7-1), L/t
v_0 = characteristic velocity in dimensional analysis (3.7-4), L/t
v_s = speed of sound (9.4-2, 11C.1-4), L/t
$v_* = \sqrt{\tau_0/\rho}$ = friction velocity (5.3-2), L/t
W = molar rate of flow across a surface, (23.1-4), moles/t
W_α = molar rate of flow of species α across a surface (23.1-3), moles/t
W_m = rate of doing work on a system by the surroundings via moving parts (7.4-1), ML^2/t^3
w = mass rate of flow across a surface (2.2-21), M/t
w_α = mass flow rate of species α across a surface (23.1-1), M/t
x_α = mole fraction of species α (Table 17.7-1),—
x, y, z = Cartesian coordinates
y = distance from wall (in boundary layer theory and turbulence) (§4.4), L
y_α = mole fraction of species α (22.4-2),—
Z = wall collision frequency (1.4-2), $L^{-2}t^{-1}$
z_α = ionic charge, (24.4-5), equiv/mole
alpha $\alpha = k/\rho\hat{C}_p$ = thermal diffusivity (9.1-7), L^2/t
beta β = thermal coefficient of volume expansion (10.9-6), T^{-1}
β = velocity gradient at a surface (12.4-6), s^{-1}
gamma $\gamma = C_p/C_V$ = heat capacity ratio (11.4-56),—
$\dot{\boldsymbol{\gamma}} = \nabla\mathbf{v} + (\nabla\mathbf{v})^\dagger$ = rate-of-deformation tensor (8.3-1), t^{-1}
delta $\Delta X = X_2 - X_1$ = difference between exit and entry values
δ = falling-film thickness (2.2-22), boundary layer thickness (4.4-14), L
$\boldsymbol{\delta}$ = unit tensor (1.2-2, A.3-10),—
$\boldsymbol{\delta}_i$ = unit vector in the i direction (A.2-9),—
δ_{ij} = Kronecker delta (A.2-1),—
epsilon ε = fractional void space (6.4-3),—
$\varepsilon, \varepsilon_{AB}$ = maximum attractive energy between two molecules (1.4-10, 17.3-13), ML^2/t^2
ε_{ijk} = permutation symbol (A.2-3),—

zeta ζ = composition coefficient of volume expansion (19.2-2 and Table 22.2-1),—

eta η = non-Newtonian viscosity (8.2-1), M/Lt

η', η'' = components of the complex viscosity (8.2-4), M/Lt

$\overline{\eta}$ = elongational viscosity (8.2-5), M/Lt

η_0 = zero shear rate viscosity (8.3-4), M/Lt

theta θ = $\arctan(y/x)$ = angle in cylindrical coordinates (A.6-5),—

θ = $\arctan(\sqrt{x^2 + y^2}/z)$ = angle in spherical coordinates (A.6-23),—

kappa κ = dilatational viscosity (1.2-6), M/Lt

κ, κ_0, κ_1, κ_2 = dimensionless constants used in turbulence (5.3-1, 5.4-3, 5.4-5, 5.4-6)

lambda Λ, Λ_v, Λ_T, Λ_ω = diffusivity ratios (20.2-29),—

λ = wavelength of electromagnetic radiation (16.1-1), L

λ = mean free path (1.4-3), L

λ, λ_1, λ_2, λ_k, λ_H = time constants in rheological models (§8.4 to §8.6), t

mu μ = viscosity (1.1-1), M/Lt

nu ν = μ/ρ = kinematic viscosity (1.1-3), L^2/t

ν = frequency of electromagnetic radiation (16.1-1), t^{-1}

xi ξ = composition coefficient of volume expansion (Table 22.2-1),—

pi Π, Π_v, Π_T, Π_ω = dimensionless profiles (4.4-25, 12.4-21, 20.2-28),—

π = 3.14159 . . .

$\boldsymbol{\pi}$ = $\boldsymbol{\tau} + p\boldsymbol{\delta}$ = molecular momentum flux tensor, molecular stress tensor (1.2-2, 1.7-1), M/Lt^2

rho ρ = density, M/L^3

ρ_α = mass of species α per unit volume of mixture (Table 17.7-1), M/L^3

sigma σ = Stefan–Boltzmann constant, M/t^3T^4

σ = surface tension (3.7-12), M/t^2

σ, σ_{AB} = collision diameter (1.4-10, 17.3-11), L

tau $\boldsymbol{\tau}$ = (viscous) momentum flux tensor, (viscous) stress tensor (1.2-2), M/Lt^2

τ_0 = magnitude of shear stress at fluid–solid interface (5.3-1), M/Lt^2

phi Φ = potential energy (3.3-2), ML^2/t^2

Φ_v = viscous dissipation function (3.3-3), t^{-2}

$\boldsymbol{\phi}$ = $\boldsymbol{\pi} + p\mathbf{vv}$ = combined momentum flux tensor (1.7-1), M/Lt^2

ϕ = arctan y/x = angle in spherical coordinates (A.6-24),—

ϕ = electrostatic potential (24.4-5), volts

φ = intermolecular potential energy (1.4-10), ML^2/t^2

psi Ψ_1, Ψ_2 = first, second normal stress coefficient (8.2-2, 3), M/L

Ψ_v = viscous dissipation function (3.3-3), t^{-2}

ψ = stream function (Table 4.2-1), dimensions depend on the coordinate system

omega Ω_μ, Ω_k, $\Omega_{\mathscr{D}}$ = collision integrals (1.4-14, 9.3-13, 17.3-11),—

ω_α = mass fraction of species α (17.1-2, Table 17.7-1),—

$\omega_{A1} - \omega_{A0}$ = characteristic mass fraction difference used in dimensional analysis (19.5-7),—

Overlines

$\tilde{X}$ = per mole

$\hat{X}$ = per unit mass

$\overline{X}$ = partial molar (19.3-3, 24.1-2)

$\overline{X}$ = time smoothed (5.1-4)

$\check{X}$ = dimensionless (3.7-3)

Brackets

$\langle X \rangle$ = average value over a flow cross section

(X), [X], {X} = used in vector–tensor operations when the brackets enclose dot or cross operations (Appendix A)

$[\![\ ]\!]$ = dimensionless groupings
$[=]$ = has the dimensions of

Superscripts

$X^{\dagger}$ = transpose of a tensor
$X^{(t)}$ = turbulent (5.2-8)
$X^{(v)}$ = viscous (5.2-9)
X' = fluctuating quantity (5.2-1)

Subscripts

A, B = species A and B in binary systems
$\alpha, \beta, \ldots$ = species in multicomponent systems
a = arithmetic-mean driving force or associated transfer coefficient (14.1-3)
b = bulk or "cup-mixing" value for an enclosed stream (10.8-33, 14.1-2)
c = evaluated at the critical point (1.3-1)
ln = logarithmic-mean driving force or associated transfer coefficient (14.1-4)
loc = local driving force or associated transfer coefficient (14.1-5)
m = mean transfer coefficient for a submerged object (14.1-6)
r = reduced, relative to critical value (§1.3)
tot = total amount of entity in a macroscopic system
0 = evaluated at a surface
1, 2 = evaluated at cross-sections 1 and 2 (7.1-1)

Named dimensionless groups designated with two letters

Br = Brinkman number (10.4-9, Table 11.5-2)
Ec = Eckert number (Table 11.5-2)
Fr = Froude number (3.7-11)
Gr = Grashof number (10.9-18, Table 11.5-2)
Gr_{ω}, Gr_{x} = Diffusional Grashof number (19.5-13, Table 22.2-1)
Ha = Hatta number (20.1-41)
Le = Lewis number (17.1-9)
Ma = Mach number (11.4-71)
Nu = Nusselt number (14.3-10 to 15)
Pé = Péclet number (Table 11.5-2)
Pr = Prandtl number (9.1-8, Table 11.5-2)
Ra = Rayleigh number (Table 11.5-2)
Re = Reynolds number (3.7-10)
Sc = Schmidt number (17.1-8)
Sh = Sherwood number (22.1-5)
We = Weber number (3.7-12)

Mathematical operations

D/Dt = substantial derivative (3.5-2), t^{-1}
$\mathfrak{D}/\mathfrak{D}t$ = corotational derivative (8.5-2), t^{-1}
∇ = del operator (A.4-1), L^{-1}
$\ln x$ = the logarithm of x to the base e
$\log_{10} x$ = the logarithm of x to the base 10
$\exp x$ = e^{x} = the exponential function of x
$\mathrm{erf}\, x$ = error function of x (4.1-14, §C.6)
$\Gamma(x)$ = the (complete) gamma function (12.2-24, §C.4)
$\Gamma(x, u)$ = the incomplete gamma function (12.2-24)
O(. . .) = "of the order of"

Author Index

(Bold-face page numbers indicate that biographical data are given)

Subject Index

•••MOLECULAR FLUX EXPRESSIONS (SEE APPENDIX B.1, B.2, AND B.3)

Momentum (ρ = constant, Newtonian fluid):

$$\boldsymbol{\pi} = p\boldsymbol{\delta} - \mu(\nabla\mathbf{v} + (\nabla\mathbf{v})^{\dagger}) \qquad \text{or} \qquad \pi_{ij} = p\delta_{ij} - \mu\left(\frac{\partial v_j}{\partial x_i} + \frac{\partial v_i}{\partial x_j}\right)$$

Heat (pure fluid only):

$$\mathbf{q} = -k\nabla T \qquad \text{or} \qquad q_i = -k\frac{\partial T}{\partial x_i}$$

Mass (for a binary mixture of A and B):

$$\mathbf{j}_A = -\rho\mathscr{D}_{AB}\nabla\omega_A \qquad \text{or} \qquad j_{Ai} = -\rho\mathscr{D}_{AB}\frac{\partial\omega_A}{\partial x_i}$$

•••CONVECTED FLUX EXPRESSIONS (SEE §§1.7, 9.7, 17.7)

Momentum:

$$\rho\mathbf{v}\mathbf{v} \qquad \text{or} \qquad \rho v_i v_j$$

Energy:

$$\rho(\hat{U} + \tfrac{1}{2}v^2)\mathbf{v} \qquad \text{or} \qquad \rho(\hat{U} + \tfrac{1}{2}v^2)v_i$$

Mass:

$$\rho\omega_A\mathbf{v} \qquad \text{or} \qquad \rho\omega_A v_i$$

•••COMBINED FLUX EXPRESSIONS

Momentum:

$$\boldsymbol{\phi} = \rho\mathbf{v}\mathbf{v} + \boldsymbol{\pi} = \rho\mathbf{v}\mathbf{v} + p\boldsymbol{\delta} + \boldsymbol{\tau} \qquad \text{(Eq. 1.7-2)}$$

Energy:

$$\mathbf{e} = \rho(\hat{U} + \tfrac{1}{2}v^2)\mathbf{v} + \mathbf{q} + [\boldsymbol{\pi}\cdot\mathbf{v}] \qquad \text{(Eq. 9.8-5)}$$

$$= \rho(\hat{H} + \tfrac{1}{2}v^2)\mathbf{v} + \mathbf{q} + [\boldsymbol{\tau}\cdot\mathbf{v}] \qquad \text{(Eq. 9.8-6)}$$

Mass:

$$\mathbf{n}_A = \rho\omega_A\mathbf{v} + \mathbf{j}_A \qquad \text{(Eq. 17.8-1)}$$

Note: The quantity $[\boldsymbol{\pi}\cdot\mathbf{v}]$ is the molecular work flux (see §9.8), and $\boldsymbol{\pi} = p\boldsymbol{\delta} + \boldsymbol{\tau}$ (see Table 1.2-21). All fluxes obey the same sign convention: they are positive when the entity being transported is moving from the negative side of a surface to the positive side.

•••EQUATIONS OF CHANGE IN TERMS OF THE COMBINED FLUXES

These equations are valid only for systems in which gravity is the only external force. More information may be found in §19.2.

Momentum:

$$\frac{\partial}{\partial t}\rho\mathbf{v} = -[\nabla\cdot\boldsymbol{\phi}] + \rho\mathbf{g} \qquad \text{(Eq. 3.2-8)}$$

Energy:

$$\frac{\partial}{\partial t}\rho(\hat{U} + \tfrac{1}{2}v^2) = -(\nabla\cdot\mathbf{e}) + \rho(\mathbf{v}\cdot\mathbf{g}) \qquad \text{(Eq. 11.1-6)}$$

Mass:

$$\frac{\partial}{\partial t}\rho\omega_A = -(\nabla\cdot\mathbf{n}_A) + r_A \qquad \text{(Eq. 19.1-6)}$$

•••EQUATIONS OF CHANGE (SPECIAL FORMS)

Momentum (for Newtonian fluids with constant ρ and μ): (§B.6)

$$\rho\frac{D\mathbf{v}}{Dt} \equiv \rho\left(\frac{\partial\mathbf{v}}{\partial t} + [\mathbf{v}\cdot\nabla\mathbf{v}]\right) = -\nabla p + \mu\nabla^2\mathbf{v} + \rho\mathbf{g}$$

Energy (for Newtonian fluids with constant ρ and k): (§B.9)

$$\rho\hat{C}_p\frac{DT}{Dt} \equiv \rho\hat{C}_p\left(\frac{\partial T}{\partial t} + (\mathbf{v}\cdot\nabla T)\right) = k\nabla^2 T + \mu\Phi_v$$

Mass (for binary mixtures of A and B with constant $\rho\mathscr{D}_{AB}$): (§B.11)

$$\rho\frac{D\omega_A}{Dt} \equiv \rho\left(\frac{\partial\omega_A}{\partial t} + (\mathbf{v}\cdot\nabla\omega_A)\right) = \rho\mathscr{D}_{AB}\nabla^2\omega_A + r_A$$

•••DIMENSIONLESS GROUPS

(l_0 and v_0 are a characteristic length and a characteristic velocity, respectively)

$\mathrm{Re} = l_0 v_0\rho/\mu$	$\mathrm{Pr} = \hat{C}_p\mu/k$	$\mathrm{Sc} = \mu/\rho\mathscr{D}_{AB}$
$\mathrm{Ra} = \mathrm{GrPr}$	$\mathrm{Gr} = g\beta l_0^3\Delta T/\nu^2$	$\mathrm{Gr}_\omega = g\zeta l_0^3\Delta\omega_A/\nu^2$
$\mathrm{Nu} = hl_0/k$	$\mathrm{Pé} = \mathrm{RePr}$	$\mathrm{Pé}_{AB} = \mathrm{ReSc}$
$\mathrm{Sh} = k_c l_0/\mathscr{D}_{AB}$	$j_H = \mathrm{Nu}/\mathrm{RePr}^{1/3}$	$j_D = \mathrm{Sh}/\mathrm{ReSc}^{1/3}$

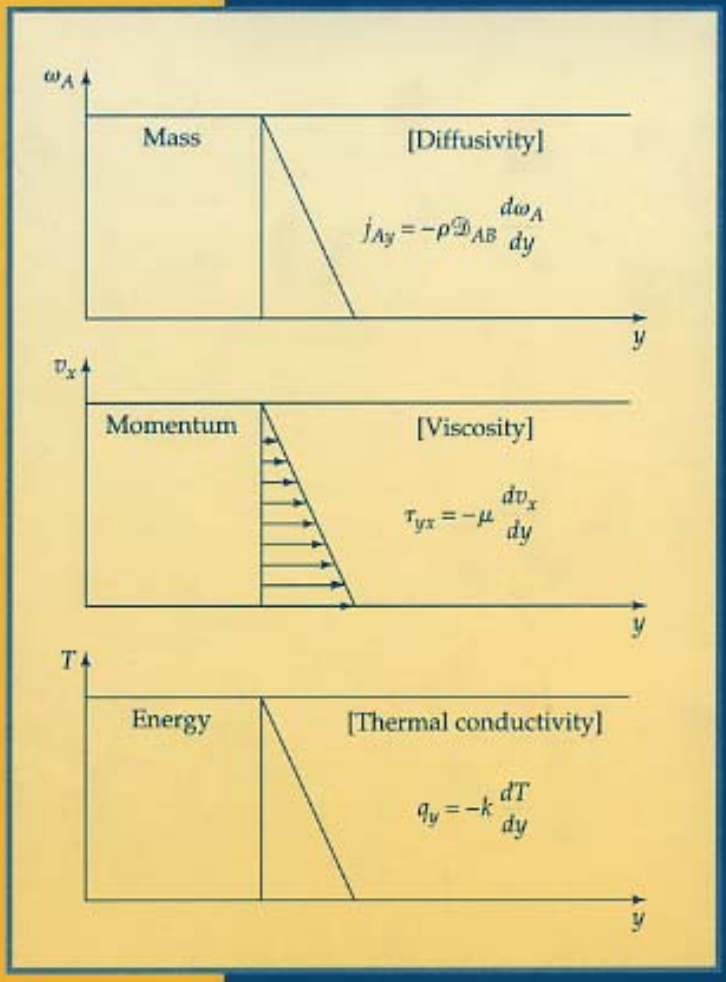

JOHN WILEY & SONS, INC.
New York Chichester Weinheim
Brisbane Singapore Toronto

http://www.wiley.com/college/bird

ISBN 0-471-41077-2

9 780471 410775 90000>